



Nottingham, UK  
Crowne Plaza Hotel  
13-14 September 2017

**38<sup>th</sup> AIVC Conference**  
**6<sup>th</sup> TightVent Conference**  
**4<sup>th</sup> venticool Conference**

**Ventilating healthy  
Low-energy buildings**

**PROCEEDINGS**

**In cooperation with:**



# Acknowledgments

The conference organisers gratefully acknowledge the support from:

**AIVC** with its member countries : Belgium, Czech Republic, Denmark, France, Germany, Italy, Japan, the Netherlands, New Zealand, Norway, Republic of Korea, Spain, Sweden, UK and USA.

Since 1980, the annual AIVC conferences have been the meeting point for presenting and discussing major developments and results regarding infiltration and ventilation in buildings. AIVC contributes to the programme development, selection of speakers and dissemination of the results. pdf files of the papers of older conferences can be found in AIRBASE. See [www.aivc.org](http://www.aivc.org).



## **TightVent Europe**

The TightVent Europe 'Building and Ductwork Airtightness Platform' was launched in January 2011.

It aims at facilitating exchanges and progress on building and ductwork airtightness issues, including the production and dissemination of policy oriented reference documents and the organization of conferences, workshops, webinars, etc. The platform has been initiated by INIVE EEIG (International Network for Information on Ventilation and Energy Performance) and receives active support from the following organisations: Buildings Performance Institute Europe, BlowerDoor GmbH, Covenant of Mayors for Climate & Energy, Eurima, IndustriasGonal, Lindab, Retrotec and Soudal. More information can be found on [www.tightvent.eu](http://www.tightvent.eu).



## **venticool**

The international ventilative cooling platform, venticool ([venticool.eu](http://venticool.eu)) was launched in October 2012 to accelerate the uptake of ventilative cooling by raising awareness, sharing experience and steering research and development efforts in the field of ventilative cooling. The platform supports better guidance for the appropriate implementation of ventilative cooling strategies as well as adequate credit for such strategies in building regulations. The platform philosophy is pull resources together and to avoid duplicating efforts to maximize the impact of existing and new initiatives. venticool collaborates with organizations with significant experience and/or well identified in the field of ventilation and thermal comfort like AIVC ([www.aivc.org](http://www.aivc.org)) and REHVA ([www.rehva.eu](http://www.rehva.eu)). Venticool has been initiated by INIVE EEIG (International Network for Information on Ventilation and Energy Performance) with the financial and/or technical support of the following partners: Agoria-NAVENTA, Covenant of Mayors for Climate & Energy, CIBSE Natural Ventilation Group, ES-SO, Velux, Wienerberger and WindowMaster



## **Brunel University London**

Brunel University London ([brunel.ac.uk](http://brunel.ac.uk)) is home to 13,500 students on a single campus at Uxbridge, West London, UK. Brunel is one of the top 25 universities worldwide founded in the last 50 years. Since the launch of the university in 1966, Brunel has offered undergraduate and postgraduate degrees that encourage invention, innovation and imaginative thinking.

Brunel University London is one of the UK's strongest research universities with a culture of high-quality research and a tradition of innovation and entrepreneurship and longstanding post-graduate courses in the built environment and energy efficiency. Brunel is firmly within the top quarter of research universities in the UK according to the [Research Excellence Framework 2014](#), with a number of areas of study including public health, sport science, art and design, politics, and environmental and earth sciences, recognised as world-leading or internationally excellent for research impact.

Ventilation research is carried out within the Institute of Energy Futures, established to tackle challenges in the areas of energy use efficiency, sustainable environmental development of buildings, power networks and automotive applications.



## **University Of Nottingham**

The University Of Nottingham has 43,000 students and is 'the nearest Britain has to a truly global university, with a "distinct" approach to internationalisation, which rests on those full-scale campuses in China and Malaysia, as well as a large presence in its home city.' (Times Good University Guide 2016). It is also one of the most popular universities in the UK among graduate employers and the winner of 'Outstanding Support for Early Career Researchers' at the Times Higher Education Awards 2015. It is ranked in the world's top 75 by the QS World University Rankings 2015/16, and 8th in the UK by research power according to the Research Excellence Framework 2014. It has been voted the world's greenest campus for three years running, according to Greenmetrics Ranking of World Universities.



## **CIBSE**

The Chartered Institution of Building Services Engineers (CIBSE) received its Royal Charter in 1976. It is the professional body that exists to:

'support the Science, Art and Practice of building services engineering, by providing our members and the public with first class information and education services and promoting the spirit of fellowship which guides our work.'

CIBSE promotes the career of building services engineers by accrediting courses of study in further and higher education, by approving workbased training programmes and providing routes to full professional Registration and Membership, including Chartered Engineer, Incorporated Engineer and Engineering Technician. Once qualified, CIBSE offers a range of services, all focussed on maintaining and enhancing professional excellence throughout a career.



## **INIVE EEIG (International Network for Information on Ventilation and Energy performance)**

INIVE was founded in 2001.

INIVE is a registered European Economic Interest Grouping (EEIG), whereby from a legal viewpoint its full members act together as a single organisation and bring together the best available knowledge from its member organisations. The present full members are all leading organisations in the building sector, with expertise in building technology, human sciences and dissemination/publishing of information. They also actively conduct research in this field - the development of new knowledge will always be important for INIVE members.

INIVE has multiple aims, including the collection and efficient storage of relevant information, providing guidance and identifying major trends, developing intelligent systems to provide the world of construction with useful knowledge in the area of energy efficiency, indoor climate and ventilation. Building energy-performance regulations are another major area of interest for the INIVE members, especially the implementation of the European Energy Performance of Buildings Directive.

With respect to the dissemination of information, INIVE EEIG aims for the widest possible distribution of information.

The following organisations are members of INIVE EEIG ([www.inive.org](http://www.inive.org)):

[BBRI](#) - Belgian Building Research Institute - Belgium

[CETIAT](#) - Centre Technique des Industries Aérauliques et Thermiques - France

[CSTB](#) - Centre Scientifique et Technique du Bâtiment - France

[IBP](#) - Fraunhofer Institute for Building Physics - Germany

[SINTEF](#) - SINTEF Building and Infrastructure - Norway

[NKUA](#) - National & Kapodistrian University of Athens - Greece

[TNO](#) - TNO Built Environment and Geosciences, business unit Building and Construction - Netherlands

The following organisations are associated members.

[eERG](#) - End-use Efficiency Research Group, Politecnico di Milano, Italy

[TMT US](#) - Grupo Termotecnia, Universidad de Sevilla, Spain

## **Table of contents**

Durability of building airtightness, review and analysis of existing studies.....	1
Long-time durability of passive house building airtightness.....	15
Assessment of the durability of the airtightness of building elements via laboratory tests.....	24
Will naturally ventilated dwellings still be safe under heatwaves?.....	26
Effectiveness of Ventilative Cooling Strategies in Hot and Dry and Temperate Climates of India.....	38
Hybrid ventilation in new and refurbished school buildings – the future of ventilation.....	49
Ventilative cooling potential based on climatic condition and building thermal characteristics....	61
The Reintroduction of Natural Ventilation to a 19th Century Opera House, Utilising Calibrated Computer Simulation and User Operation.....	70
Assessing Occupant and Outdoor Air Impacts on Indoor Air Quality in New California Homes...	80
From EN 779 to ISO 16890: a new worldwide reference test method for general ventilation filters..	91
Preventing condensation and frosting in an energy recovery ventilator using a preheat coil...97	
Characterising the actual performance of domestic mechanical ventilation and heat recovery systems.....	106
Comparing extracting and recirculating residential kitchen range hoods for the use in high energy efficient housing.....	117
How loud is too loud? Noise from domestic mechanical ventilation systems.....	129
Air leakage of defects in the vapour barrier of compact roofs.....	140
Air leakage variations due to changes in moisture content in wooden construction- magnitudes and consequences.....	148
Statistics, analysis and conclusions from 250,000 blower door tests, including ventilation types.....	160
A comparison study of the blower door and novel pulse technique on measuring enclosure airtightness in a controlled environment.....	168
Natural Pressure Differential – Infiltration Through Wind Results of a Long-Term Measurement...	180
Building and ductwork airtightness requirements in Europe – Comparison of 10 European countries.....	192

Ventilative Cooling on the test bench - Learnings and conclusions from practical design and performance evaluation.....	202
Bulk airflow measurements in a large naturally ventilated atrium in a mild climate.....	211
Delivery and performance of a ventilative cooling strategy: the demonstration case of a shopping centre in Trondheim, Norway.....	220
Ventilative cooling in a single-family active house from design stage to user experience.....	230
The future of hybrid ventilation in office buildings – energy simulations and lifecycle cost.....	238
Design and performance of ventilative cooling: a review of principals, strategies and components from International case studies.....	251
A New Approach to Estimating Carbon Dioxide Generation Rates from Building Occupants.....	263
Methodology for assessing the air-exchange performance of residential ventilation systems.....	270
Quantitative relationships between classroom CO2 concentration and learning in elementary schools.....	279
The impact of the quality of homes on indoor climate and health: an analysis of data from the EU-SILC database.....	288
Assessment of airflow measurement uncertainty at terminal devices.....	295
The industries vision and activities for better buildings in the future.....	306
About 1,000 ductwork airtightness measurements performed in new French buildings: database creation and first analyses.....	310
Impact of ductwork airtightness on fan energy use: calculation model and test case.....	319
Utilization of heat recovery ventilation: problem statement based on steady-state two-zone energy use analysis and field studies.....	333
Influence of the zoning, the climate, and the airtightness on the energy needs of a building with mechanical ventilation system with heat recovery.....	335
A ‘use factor’ for HRV in intermittently heated dwellings.....	337
Methodology for the characterization of the envelope airtightness of the existing housing stock in Spain.....	342
On the design and testing of Airtightness Modifier dedicated to the TIPEE IEQ House.....	352
Component leakage: potential improvement graphs and classification of airpaths.....	361

The effect of refurbishment and trickle vents on airtightness: the case of a 1930s semi-detached house.....	369
Impact of airtightness on the heat demand of passive houses in central European climate.....	381
Demand controlled ventilation in school and office buildings: lessons learnt from case studies.....	391
Experimental and Numerical Investigation of Air Distribution in a Large Space.....	400
Development of protocol for sub-metering for ventilation models and verification for shopping centres.....	410
Heat Recovery Hybrid Ventilation System With a Thermal Storage.....	422
A study of panel ridges effect on heat transfer and pressure drop in a ventilation duct.....	430
Development and measurement results of a compact Counterflow Heat Recovery Fan for single/double room ventilation.....	440
Full-scale experimental study of ceiling turbulent air jets in mechanically ventilated rooms.....	448
Technologies to overcome effects of condensation in exchangers of ventilation units - analysis of monitored field studies.....	458
A Method to Measure Emission Rates of PM2.5s from Cooking.....	463
An Experimental Validation of an Indoor Radon Model that examines Energy Retrofit Buildings.....	474
Evaluating natural ventilation cooling potentials during early building designs.....	482
Challenges of using passive ventilation to control the overheating of dwellings in noisy environments.....	491
Natural ventilation systems in Mediterranean schools. A prototype experience in Andalusia as an alternative to mechanical ventilation.....	504
Impact assessment of natural ventilation on thermal comfort levels in sustainable residential buildings.....	517
Inter-model comparison of indoor overheating risk prediction for English dwellings.....	527
Towards Real-Time Model-Based Monitoring and Adoptive Controlling of Indoor Thermal Comfort.....	536
Application of open-source CFD software to the indoor airflow simulation.....	544
Experimental study on the in-situ performance of a natural ventilation system with heat recovery..	554
An interface of night ventilation and mass structure for passive cooling design strategy in	

Ghadames traditional dwellings.....	565
Indoor Air Quality and Thermal Comfort, in Irish Retrofitted Energy Efficient Homes.....	572
Evaluation of thermal comfort in an office building served by a liquid desiccant-assisted evaporative cooling air conditioning system.....	578
Energy Efficiency in a Thermal Comfort Field Work in Spain.....	588
The influence of occupancy behaviour on the performance of mechanical ventilation systems regarding energy consumption and IAQ.....	594
Thermal performance of ventilated solar collector with energy storage containing phase change material.....	604
Energy performance prediction of thermoelectric ceiling radiant panels with a dedicated outdoor air system.....	614
Microorganism contaminants removal in a liquid desiccant dehumidification system.....	623
The Development of Archetypes to Represent the Chilean Housing Stock.....	631
The Cleanliness Classification of Air-handling Components- A success Story in Finland.....	642
Circadian House: a vision for homes designed to be healthy and human-centric.....	649
Contaminant stratification in displacement ventilated spaces - a two zone model approach. Model prediction compared to experimental data.....	657
Study of variants to classical mechanical exhaust ventilation systems by using mechanical exhaust in habitable rooms.....	666
The effectiveness of mechanical exhaust ventilation in dwellings.....	672
Investigation of future ventilation flow rate requirements for dwellings in Belgium: from the application of FprEN16798-1:2016 to proposed robust rules.....	682
Advanced airflow distribution methods for reducing exposure of indoor pollution.....	692
Towards the definition of an indoor air quality index for residential buildings based on long- and short-term exposure limit values.....	698
Pollutant exposure of the occupants of dwellings that complies with the Spanish indoor air quality regulations.....	710
Method development for measuring volatile organic compound (VOC) emission rates from spray foam insulation (SPF) and their interrelationship with indoor air quality (IAQ), human health and ventilation strategies.....	717

The effect of enhanced stove design on ‘real life’ exposure to PM2.5 and CO in rural dwellings in Salambu, Nepal.....	729
Field measurement of carbonyl compound and particles in South Korea residential spaces...	738
Indoor air quality in mechanically ventilated residential dwellings/low-rise buildings: A review of existing information.....	746
Reducing Uncertainty in Air Tightness Measurements.....	756
On the contribution of steady wind to uncertainties in building pressurisation tests.....	758
The impact of wind gusts on air infiltration in buildings.....	764
Airtightness of Buildings – Considerations regarding the Zero-Flow Pressure and the Weighted Line of Organic Correlation.....	770
Energy Performance Indicators for Ventilative Cooling.....	781
Experimental evidence of effective single sided natural ventilation beyond 20ft or 2.5 floor to ceiling heights in open plan office spaces.....	792
Automated window opening control system to address thermal discomfort risk in energy renovated dwellings. Summertime assessment.....	794
Experiences regarding draught effects for ventilative cooling in cold climate.....	796
Coupling night ventilative and active cooling to reduce energy use in supermarkets with high refrigeration loads.....	807
Mixed-mode ventilative cooling opportunity for an existing shopping mall retrofit.....	817
Defining the metrics to assess the Indoor Air Quality in low-energy residential buildings.....	828
On the use of co-simulating modelling tools to enhance our understanding and optimization of heat and mass flow effects in whole buildings.....	830
Design and operation of ventilation in low energy residences – A survey on code requirements and building reality from six European countries and China.....	832
Numerical analysis of the potential of using light radiant ceilings in combination with diffuse ventilation to achieve thermal comfort in NZEB buildings.....	843
Influence of night ventilation on the cooling demand of typical residential buildings in Germany.....	852
Affordable and replicable renovation of social housing fulfilling indoor climate and energy targets thanks to seven replicable renovation elements.....	862

Façade Improvements to Avoid Draught in Cold Climates – Laboratory Measurements.....	869
Cool materials in the urban built environment to mitigate heat islands: potential consequences for building ventilation.....	879
TVOC concentrations measured in Belgium dwellings and their potential for DCV control.....	890
Possible UK residential demand-controlled ventilation assessment methodology.....	898
A novel algorithm for demand-control of a single-room ventilation unit with a rotary heat exchanger.....	909
Evaluating the Performance of Island Kitchen Range Hoods.....	919
Efficiency of recirculation hoods.....	928
Emission source strength of cooking and reduction of a typical hood.....	935
The effect of adjustable cooling jet on thermal comfort and perception in warm office environment – a laboratory study.....	937
A Case Study assessing the impact of Shading Systems combined with Night-Time Ventilation strategies on Overheating within a Residential Property.....	944
The flow interaction of air distribution with thermal plumes and the effect on the air velocity fluctuation under increased heat load conditions.....	957
Determining the venting efficiency of simple chimneys for buoyant plumes.....	968
A comparison of line-sources of buoyancy placed near and far from a wall.....	975
Effect of human walking on air curtain sealing in the doorway of an airtight building.....	984
Pollutant loads from materials and assemblies in residential buildings.....	990

# Durability of building airtightness, review and analysis of existing studies

Valerie Leprince<sup>\*1</sup>, Bassam Moujalled<sup>2</sup> and Andrés Litvak<sup>3</sup>

*1 PLEIAQ  
84 C Avenue de la Libération  
69330 Meyzieu*

*2 CEREMA Centre-Est  
46, rue St Théobald - BP 128  
38081 L'Isle d'Abeau Cedex, France*

*\*Corresponding author: Valerie.leprince@pleiaq.net*

*3 CEREMA  
Rue Pierre RAMOND DAIT/GBAT  
33165 Saint Médard en Jalles, FRANCE*

## ABSTRACT

Mandatory building airtightness testing has come gradually into force in European countries mostly because of the increasing weight of building leakage energy impact on the overall energy performance of low-energy buildings. Therefore, airtightness level of new buildings has significantly improved in the last decade. However, until now, low expertise is available about the durability of building airtightness at mid- and long-term scales.

The Durabilit'air French research project aims at improving our knowledge on ageing of airtightness products onsite and in laboratory controlled conditions.

This paper is issued from the first task of the Durabilit'air project: the "state of the art". It presents a comprehensive review of studies that deal with building airtightness durability, using mostly as references the AIVC publications but also specific studies from UK, Germany, Sweden and France. It covers field measurements, accelerated ageing in laboratory, seasonal variations and also exposure loads of the air-barrier.

Regarding field measurement studies, it seems that the envelope airtightness decreases during the first years after achievement and then stabilises. The main result of this review is a list of key elements that may govern airtightness variations:

- Measurement uncertainty and how it could be reduced
- Structure movements
- Shrinks of mastics in the first weeks when the house gets heated for the first time
- Drilling of the air-barrier due to the installation of new equipment
- Ageing of assembly due to unsuitable association of products and bad implementation conditions
- And, of course, normal ageing of products.

Such information will be useful for future field measurement campaigns. Besides it is necessary to perform leakage detection together with measurements to be able to explain changes in airtightness level.

The analysis of laboratory ageing studies showed that there is actually no standardised protocol to characterise durability of product assemblies. However, due to the various natures of airtightness products, it seems difficult to define an accelerated ageing universal protocol that would be equivalent to a known amount of years of natural ageing. This paper gives pro and cons of various alternatives to assess the durability of airtightness products in laboratory.

## KEYWORDS

Airtightness durability, field measurement, laboratory testing, literature review, building envelope

## 1 INTRODUCTION

Over the last thirty years, much progress has been made to increase our knowledge about mechanisms governing building's airtightness and the impact of air infiltrations on energy

efficiency, health effects and construction quality related issues. As a matter of fact, since the early 2000's, regulations in many countries explicitly account for airtightness, sometimes with mandatory requirements, as a consequence of Europe's ambition to generalize nearly zero energy buildings by the end of 2020. Nevertheless, less expertise is available today about the durability of airtightness products, at mid- and long- term scales. Indeed, this subject remains very complex, since it covers in the meantime:

- the modelling of the mechanisms of building's and products' loads and deformations
- the accelerated ageing in laboratory controlled conditions and
- the performance characterization from field measurements results.

With the DURABILIT' AIR research project, Cerema, PLEIAQ, CETII and RESCOLL aim at improving knowledge on various questions related to residential buildings envelope airtightness durability. This 36-months project has 4 major objectives:

- 1) listing the major international research findings dealing with airtightness durability of building products, through a state of the art review;
- 2) characterizing the evolution over time in mid and long term scales (respectively of 1 to 3 and 5 to 10 years) of the airtightness of existing single family dwellings by on-site measurement campaigns;
- 3) understanding and modelling the physical mechanisms causing the airtightness performance degradation as a function of time with the purpose of developing a laboratory controlled method in order to test the accelerated ageing of airtightness sensitive products and systems;
- 4) disseminating the main results of this work, with tools and communications among professional of the building sector in order to promote best practices.

This paper is issued from the first task of the Durabilit'air project: the "state of the art". It presents a comprehensive review of studies that deal with building airtightness durability, using mostly as references the AIVC publications but also specific studies from UK, Germany, Sweden and France. It covers field measurements, accelerated ageing in laboratory, seasonal variations and also exposure loads of the air-barrier.

## **2 APPROACH**

We have made a comprehensive review of studies and existing standards on characterisation of building airtightness durability. The objective was to learn from previous studies to develop protocols for the next steps of the Durabilit'air project:

- characterizing the evolution over time of the airtightness of existing single family dwellings by field measurements;
- testing the accelerated ageing of airtightness products and systems in laboratory controlled conditions.

Therefore this review has focused on studies regarding:

- field measurement of building airtightness years after years;
- variability of airtightness test due to tester, measurement devices, external conditions, seasonal variations, etc;
- physical (and no chemical) stresses on the air barrier inducing its deterioration;
- experimental protocols to estimate ageing of the air barrier.

The long term performance of building airtightness has been a key subject of research in the second part of the 80's (mostly in the USA and Canada). Very few studies were published during the 90's and 2000 but since 2010, this subject has come back into focus in Europe.

The review has been done mostly on studies published from 1995 for two reasons:

- There were a lot of changes in building construction habits and products in the last 20 years.

- Airtightness tests in the 80's were not as reliable as now.

For practical reasons the review mostly includes publications in English or French.

### 3 RESULTS

#### 3.1 Field measurements

Table 1: Summary of field measurement studies

Country	Number of houses Green: new houses Blue: Refurbished houses	Year of const. or refurbish.	Ageing (year)	Average airtightness ( $n_{50}$ )	Main material	Airtightness evolution: Max / Average/ Min	Ref.
US	 17	2001	10-13	 6 ACH	Wood?	+140% <b>+15%</b> -25%	(Chan & Sherman, 2014)
US	 17	2007	5-7	 10 ACH	Wood?	+150% <b>0%</b> -40%	(Chan & Sherman, 2014)
Belgium	 15	2010	1-2	 0.6 ACH	Concrete blocks	+120% <b>+36%</b> -3%	(Bracke, Laverge, Van Den Bossche, & Janssens, 2016)
Sweden	 6	1990	10-20	  0.6-4 ACH	Wood?	+580% <b>+162%</b> -11%	(Hansen & Ylmén, 2012)
Canada	 17	1985	3 then 11	 1.5 ACH	Wood	+60% <b>+6%</b> <b>+11%</b> -16%	(Prowski, December 6-10, 1998)
France	 30	2009	5-6	 1.8 ACH	Concrete blocks	- <b>+50%</b> -	(ADEME, 2016)
Germany	2 	1990	25	 0.6 ACH	Concrete blocks	1 <sup>st</sup> house: <b>0%</b> 2 <sup>nd</sup> : <b>+34%</b>	(Feist, Ebel, Peper, Hasper, Pflugler, & Kirchmair, 2016)
UK	 23	2007	1-3	 4 ACH	Wood or concrete blocks	+154% <b>+25%</b> -33%	(Philips, Rogers, & Smith, 2011)

In every study, results show a significant difference between tested houses: in some houses, the permeability is multiplied by a factor of two while in other it decreases after few years. Most of studies come up with global averaged results and do not explain the variations between houses.

However, interesting results in studies provide clues to explain those variations.

In US, (Chan & Sherman, 2014) noticed that the air leakage increased in average by 15% in the new build homes while no increase in the air leakage was observed in the weatherized homes. It was noted that for the weatherized homes, the joints between building components, that were sealed, do not change their leakage characteristics with time. In new build homes, **the moist wood materials may have shrunk over the first several years, potentially causing leaks in the building envelope.**

In Belgium, (Bracke, Laverge, Van Den Bossche, & Janssens, 2016) have tested the durability on 15 nearly identical houses: build by the same craftsmen with the same products (air barrier done by plaster on the masonry). However, ageing results vary from -3% to +120%, therefore in this case the **main impact** is probably not due to the ageing of products but to other factors such as **asoccupant behaviour, measurement uncertainty**, etc.

In the Swedish study (Hansen, et al., 2012), conclusions were difficult to draw as the air leakage increased for half of tested houses (up to 6 times) and decreased for the other half. This was not correlated neither with changes made in the construction, nor with the year of construction.

In Canada, (Prowski, December 6-10, 1998) concludes that performance of polyethylene air barriers was unchanged over 8 to 11 years. Although three of houses became leakier, the leakage detection has shown that leakages were not occurring at locations associated with the polyethylene portions of the air barrier. Conversely houses built with the drywall approach degraded slightly over the 11-year monitoring period but there is no evidence that it was due to this approach.

In France, (ADEME, 2016), a case study of 30 tested houses showed that permeability of houses made of concrete blocks (air barrier made by plaster boards) deteriorates more than houses made of wood (air barrier made by membrane). However results are heterogeneous from one house to another. In this study, an important work has been performed to compare leakages locations before and after a few years. It has been noticed that **leakages** are mainly at:

- **Penetrations of the air barrier;**
- **Electrical appliances;**
- **New non-airtight appliances (hood, recessed lighting, etc.).**

However, no correlation has been made between value of airtightness and new leakages in houses.

In Germany, (Feist, Ebel, Peper, Hasper, Pfluger, & Kirchmair, 2016) have performed advanced leakage detection on the air barrier (made with plaster boards). They concluded that only windows and doors gaskets (on the openings) have deteriorated, they have been changed for the new test. **Acrylic mastics, set on backer rod, have not deteriorated at all.**

In UK, (Philips, Rogers, & Smith, 2011) showed on a 23 dwelling sample study that the air permeability of two thirds of the dwellings tested had increased while the air permeability of the remaining third had decreased. They observed that:

- Houses generally became more leaky than the flats.
- Timber frame dwellings showed the largest change in airtightness compared to plastered masonry.
- Six of the eight results that achieved a performance improvement were heated with electric panels rather than a gas and radiator (may be due to the reduced number of service penetrations).

In another project in UK, (Wingfield, Bell, Miles-Shenton, South, & Bob, 2009) have shown that **after few weeks of heating, mastics began to shrink**. On 3 houses, they performed tests before and few weeks after heating and observed up to 30% increase of permeability.

Finally, it is interesting to notice that, in almost every study, the air permeability of part of dwelling tested had decreased. There are few explanations, but apart from measurement uncertainty, it could be the result of settlement, the installation of carpets and floor finishes after the original test, and the presence of plugs in electrical sockets. (Philips, Rogers, & Smith, 2011)

### 3.2 Uncertainty in airtightness testing

Part of the difference between tests results may be due to airtightness test uncertainty. Deviations in airtightness testing are due to

- Tester behaviour (including building preparation),
- Reproducibility issues,
- Wind and thermal draft impact,
- Measurement device uncertainty,
- Seasonal variation of airtightness.

To limit the impact of tester behaviour, many countries have developed competent tester schemes and specific standards that among other things describe building preparation (Leprince & Carrié, 2014). However (Bracke, Laverge, Van Den Bossche, & Janssens, 2016), noticed that small changes in building preparation, such as locking or not a door, may have an important impact on results when it comes to very airtight buildings. Also for terraced houses, depending on where the air barrier is set, the status of openings in adjoining dwellings may have an impact on the measurement result.

Various studies of repeatability and reproducibility have been performed in the last 5 years (Delmotte, et al., 2011), (Bracke, et al., 2013), (Brennan, et al., 2013).

Main conclusions are:

- The average air leakage rate had a repeatability standard deviation ranging from 3.5% at 4 Pa to 1.4% at 50 Pa (Delmotte, et al., 2011), confirmed by (Bracke, et al., 2013), (Brennan, et al., 2013)). The average air leakage rate had a reproducibility standard deviation ranging from 5.9% at 4 Pa **to 2.4% at 50 Pa** (under favourable conditions: no wind, low temperature difference) (Delmotte, et al., 2011).
- The repeatability and reproducibility improve when tests are performed both in pressurization and depressurization (Delmotte, et al., 2011), (Bailly, et al., 2012).

The impact of wind on the uncertainty in airtightness testing was studied by (Carrié, et al., 2014). The study concludes that the model error due to the wind on the estimated airflow rate is relatively small for the high pressure point (12% for wind speeds up to 10 m/s at 50 Pa), but it can become very significant with a low pressure point (up to 60% at the low pressure point (10 Pa)). Therefore, when estimating airtightness at 4 Pa, wind could be responsible for significant errors (in some cases more than 35%) (Bailly, et al., 2012).

Seasonal variation of building airtightness is a pending question and has led to various publications with inhomogeneous results. In Sweden, two very tight wood structure houses were tested 10% tighter in summer than in winter during 2 years (Wahlgren, 2014). Study from the early 80's reported seasonal variations in the order of up to 100% (Kim & Shaw, 1986). This is not confirmed in recent studies. However most studies have been performed on very airtight building, therefore variations represent very small airflow rate.

On the other hand, studies of the French (Bailly, et al., 2015) and British (ATTMA website) database on average results for each month show no difference between summer and winter. However those two databases contain mostly houses made of concrete blocks and only few of wood structures. Further statistics shall be done per building type and per local climate to confirm this result.

### 3.3 Loads on air barrier and equivalent artificial ageing

Very few studies have been performed to quantify loads on the air barrier. (Ackermann, 2012) estimates that 60 to 75% of pressure loads reach the air barrier.

Pressure due to wind can be estimated with the following formula:

$$P_{wind} = \frac{1}{2} \rho C_p v^2 \quad (1)$$

With

v	m/s	Wind speed at building level
C <sub>p</sub>	-	Pressure coefficient (up to 0.5 according FprEN 16798-7)
ρ	kg/m <sup>3</sup>	Air density

The wind speed at building level can be calculated from meteorological wind speed according to ISO 15927-1.

When the maximum pressure on airbarrier is known, BRE digest 346 part 7 proposes pressure cycles that represent 50 years (equivalent to more than 6400 positive/negative pressures).

Estimating thermal and humidity loads is more difficult and depends on the air barrier position. Table 2 summarizes positions and constraints.

Table 2: Air barrier position and constraints

Nature of the air barrier	Membrane, adhesives and accessories			Plasters		Plaster boards, mastic and accessories	
	Position	Outside insulation (not possible in France)	In the insulation thickness (in France the rule of maximum 1/3 of insulation inside air barrier applies)	Inside	On masonry with insulation inside		Inside insulation
Constraints		It depends on its actual position may be expose to high temperature when used in roofing		Internal conditions	External conditions	Internal conditions	Internal condition

Internal and external conditions differ from one country to another.

(Lamoulie, et al., 22th-24th June 2015) have studied the hygrothermal conditions in use of bio-based material to assess their resistance to moulds. According to this study, the usual hygrothermal conditions of usual roof and wall configurations in France can be classified according to two use classes:

- a dry use class usually lower than 85% RH with laboratory test conditions of 85%RH and 26°C,
- a wet use class with a usual relative humidity that can be greater than 85% for more than 48 hours with laboratory test conditions of 95%RH and 26°C.

To perform artificial ageing due to temperature variations, "time-temperature superposition principle" can be used. For polymer, the principle is that translation factor can be found between time and temperature. Therefore chemical ageing can be performed rapidly by maintaining a polymer at high temperature (below its glass transition temperature). This translation factor is often computed using WLF model or Arrhenius law. However this translation factor depends on actual solicitations and on materials. It remains unclear for us how it can be applied to assembly.

Therefore literature, such as ASTM D3611-89 and SATAS give inconsistent information regarding equivalence between artificial and natural ageing.

The time-temperature superposition principle is a chemical ageing, it creates:

- neither physical ageing that can be induced by humidity variation
- nor mechanical ageing that can be induced by pressure variations.

However it is unclear for us whether chemical, mechanical or physical ageing predominates when it comes to airtightness products. Regarding mechanical constraints it is also unclear whether only the maximum pressure has an impact or if the number of cycle is also important.

### 3.4 Artificial aging

Table 3: Summary of artificial ageing studies

Country	Assembly			Scale		Constraints				Ageing criteria			Test duration	Ageing Equivalent	Ref
	Product alone	2 products	Complete wall	Reduced scale	Scale 1	Extreme loads	Cycles	Heat treatment	Details	Visual	Material properties	Airtightness			
Belgium		X		X		X			Water pressurisation			X	45-70 min	?	(Bracke, Van Den Bossche, & Janssens, 2014)
US(ductwork sealants)		X			X		X		93°C, 84 Pa	X		X	2 yr.	30 yr.	(Sherman & Walker, April 2004)
Sweden			X		X		X	X	80°C, HR cycles	X		X	1 yr.	50 yr.	(Ylmén, Hansén, & Romild, 2014)
Belgium		X		X			X		15/70°C Rain +frost UV+HR			X	8 wk.	?	(Langmans, Desta, Alderweireldt, & Roels, 2015)
Belgium			X		X	X	X		Pressure cycles(up to 1000Pa) 20/90% RH -10/70°C			X	Visual	?	(Michaux, Mees, Nguyen, & Loncour, 2014)
Sweden			X		X		X	X	-150/ 150 Pa 60°C/ 50%HR			X	7 days	?	(Antonsson, 2015)
French standard	X			X				X	50°C 70% HR		X		168 h	?	CSTB, cahier 3710

Michaux et al. in the context of the DREAM project, tested more than 50 buildings walls under pressure, humidity and temperature variations (Michaux, et al., 2014). The impact of each solicitation was different depending on the kind of air barrier: plasters were sensitive to humidity and temperature (cracks appeared if the plaster was too thin) while membranes were

sensitive to pressure variation (due to staples). Therefore if one wants to define a protocol that would apply to all kind of air barrier, all type of constraints shall be included in the protocol. SP (Ylmén, et al., 2014) tested both products properties alone and products assemblies implemented in a cell. **They observed no correlation between the durability of the product alone (in term of peeling, etc.) and the durability of the assembly airtightness.**

According to the research team involved, this was due to:

- compatibility problems between film and tapes,
- difference in the results for smaller and full scale specimens,
- air channel appearing during the heat treatment.

Therefore they concluded that it was required to develop durability tests of the complete airtightness systems on full-scale set-up.

According to results of this 1st research project, researchers from SP have decided to test products implemented at full-scale wall constructed on a steel frame of 3m\*3m (Antonsson, 2015). They applied heat treatment (60°C, 1 week) and pressure load (-150/+150 Pa) on the sample with a climatic chamber and a pressurisation device docked on the wall (not simultaneously). Two systems have been tested with this protocol and significant deviations were observed in the results. With the first system, a significant change in air leakage has been observed after the heat treatment, while with the second system very little change could be observed.

Another ongoing project in Sweden is testing the impact of implementing the air barrier either during cold and humid conditions or with artificial dust projected on the membrane before putting any kind of adhesives or sealants. It seems that the cold conditions (5°C, 90-95% RH) are very detrimental: even before applying the heat treatment the permeability is 5 times higher than the case implemented in ideal conditions and 6 times higher after heat treatment. The dusty environment approximately doubles the air permeability before and after heat treatment.



Figure 1: tested wall in SP (RISE)

## 4 DISCUSSION

### 4.1 On-site ageing

Regarding on-site measurements after few years, it seems that the airtightness decreases in the 3 first years after completion and then stabilises.

In literature there are various explanation factors for this phenomenon. In one hand, short term ageing may be due to:

- Heating houses for the first time may induce the shrink of mastics, if the first test was performed before the heating of the house the impact of mastic shrinking is not seen in the first test.

- Mastic shrinking when backer rod are not used
- Structure movements and packing may induce cracking in the junctions between air barrier and penetrations (ex. carpentry or ductwork and plaster board)
- Envelope drilling, lot of them occurs in the first years of life of a building (for kitchen furniture, hood, wood stove, etc.)
- Unsuitable implementation conditions for adhesives and mastic (cold and/or dusty conditions).

On another hand, it seems that some products do not deteriorate in long term (Feist, Ebel, Peper, Hasper, Pfluger, & Kirchmair, 2016) however the durability of assemblies can be deteriorated by the association of incompatible products.

Those explanations for short term ageing are relevant mostly when part of airtightness is made with mastic. When the air barrier is made with a membrane or with plaster on masonry it seems that airtightness durability mostly relies on occupants' behaviour rather than on products (Bracke, Laverge, Van Den Bossche, & Janssens, 2016) (Prowski, December 6-10, 1998).

Therefore it is relevant to couple future field measurements with:

- Questionnaires to occupants to find out drillings made in the air barrier after the first test and check with leakage detection consequences of drilling.
- Leakage detection and visual inspection at visible assemblies of air barrier with specific care on:
  - mastics,
  - penetrations of building structure inside the air barrier (ex. carpentry).
- Information about:
  - Products used for the air barrier including:
    - whether or not backer rod is used under mastics
    - compatibility of products
  - Construction details
  - Period when the air-barrier was laid-out (heating period or not)
  - Whether the air-barrier has been heated prior to the first test

Some of these have been done in field studies. Unfortunately, the correlation between airtightness results and outcome of these analysis were not investigated.

#### **4.2 Reduce measurement uncertainty**

The following recommendations would help to reduce the difference between the first and the second test that is due to measurement uncertainty rather than ageing:

- A qualified tester shall perform tests; if possible the same tester shall perform the first and the second test.
- The first test report shall precisely describe building preparation including locked and unlocked external doors.
- Measurement devices shall be calibrated according ISO 9972.
- Measurements shall be performed in low wind conditions.
- Airtightness shall be compared at 50 Pa rather than 4 or 10 Pa.
- The average of pressurisation and depressurisation shall be used for comparison.
- Even if the impact is unclear, tests shall be performed at the same season.

#### **4.3 Laboratory ageing**

Results of laboratory ageing studies differ from one to another. One of the reasons may be that the protocol is not standardised. Nevertheless, the following general conclusions can be drawn (Langmans, et al., 2015), (Michaux, et al., 2014), (Ylmén, et al., 2014) :

- ageing of assembly' airtightness cannot be correlated with ageing of material properties (peeling, etc.);
- the implementation has a great impact on the durability;
- every product does not have the same reaction under extreme conditions (extreme temperature, humidity or pressure);
- a standardised procedure for artificial ageing of airtightness products is missing to characterise products and assemblies.
- ageing strategy has to be consistent with solicitation on products, the strategy may differ for exterior, indoor or embedded air barrier.

### **The reproducibility issue**

A good reproducibility is, in our opinion, required for a protocol to be used in a certification context.

Most of projects have not tested the reproducibility of their protocols. A major limitation of testing a whole scale 1:1 system is the reproducibility of the protocol as:

- the quality of implementation may have an important impact on product results.
- it is too expensive to test several times the same system and use the average as the result.

Therefore the bigger the assembly (large with many products) is the more difficult it is to guarantee the reproducibility of the test.

### **The simultaneous load issue**

In most studies, the impact of wind load and heat load are tested one after the other. It seems appropriate for estimating the impact of each load separately. However, it seems interesting to characterize the behaviour of products/systems subjected to the following cycle:

- simultaneous heating over melting temperature and wind load;
- cooling under melting temperature with wind load.

This will allow to see if the melting under mechanical constraint has an impact or not on the performance of the system. Note that in this context, melting is a reversible transformation, i.e., if no mechanical constraint is applied to the product when melted, it comes back to its initial stage without deterioration when cooled under melting temperature. The ability of products to melt depends on their nature: for instance, thermoplastics products can melt, whereas thermosetting products cannot.

If the heat treatment is done over the melting temperature without a wind load, the product will soften during the treatment but get back to its initial state when cooled (reversible phenomenon). However, if the sample is pressurised during the heat treatment and then cooled according to the cycle proposed above, the product could remain distorted when cooled which may have an impact on its airtightness.

Practical limitations of an approach to these simultaneous loads include:

- the maximum pressure the air barrier may undergo simultaneously with the maximum temperature is unknown;
- it complicates the test apparatus and procedure.

### **Ageing issue**

Most of studies only include a heat treatment which is not an ageing protocol (they do not pretend to be equivalent to a certain amount of year).

Defining a chemical ageing protocol may be an objective to simulate realistic service lifetimes, for example, by using Arrhenius law based on the fact that chemistry reactions are accelerated at high temperature.

However, we are unsure if Arrhenius laws are applicable and yield the same equivalent ageing for all materials (thermosetting plastics, elastomer and thermoplastics). For thermoplastics, it

is important not to pass the glass transition temperature to avoid irreversible changes that would not occur in "real-life".

Moreover, chemical ageing is not suitable to account for physical and mechanical ageing. To consider mechanical ageing equivalent to 50 years, probably wind cycles should also be implemented.

Overall, we are unsure if it is possible to develop a protocol that could guarantee being equivalent to a 50 year ageing for every product.

### Steps to develop a protocol

The following table summarizes pro and cons of various options for a protocol

Table 4: Pro and cons of various options to define a protocol

Assembly	Product alone		Simple assembly (2 products)		Complete wall	
	Pro	Cons	Pro	Cons	Pro	Cons
Simple		No correlation between aging of product and aging of assemblies	Product implemented	1/ Impact of implementation 2/ Interaction between products	Product implemented	1/ Interaction between products 2/ Impact of implementation => Reproducibility? 3/ Cost of experimental set up
Scale	Scale 1			Reduced scale		
	Pro	Cons	Pro	Cons		
More representative		Cost of experimental set up	Lower cost (use of existing stove, etc.)	1/ Longest samples do not react as shortest (proved for adhesives by (Antonsson, 2015)) 2/ May be difficult to measure very low flowrates		
Constraints	Extreme load		Accelerated cycles		Heat and humidity treatment (chemical aging)	
	Pro	Cons	Pro	Cons	Pro	Cons
Guarantee resistance at normal constraints		Not representative of actual constraints, products not made to resist	Representative	1/Apart from pressure load difficult to defines cycles 2/ Takes long	Stoves already exist	Equivalent aging difficult to determine
Applying constraints	Simultaneously			One after the other		
	Pro	Cons		Pro	Cons	
More representative		Difficult to estimate the impact of each Complicate the apparatus		Impact of each	Impact of reversible phenomena not seen	
Aging evaluation	Visual		Properties of material		Airtightness	
	Pro	Cons	Pro	Cons	Pro	Cons
Simple, easy to communicate		1/Subjective 2/No correlation with airtightness	Standards exit	No correlation with airtightness	Objective of the study	Measure very small flowrate requires specific devices

Obviously, science is not fully mature to develop a test protocol and facility to characterise the performance of an air barrier system over time, but there are important steps to underline in such investigations:

- 1) Design the testing facility considering that:
  - a. reduced scales may not be representative,
  - b. tests have to be repeatable and reproducible.
- 2) Define implementation conditions (temperature, relative humidity, dusty area, etc.).
- 3) Specify the loads on clear bases and considering:
  - c. worst conditions the air barrier undergoes in the field (maximum and minimum temperature, relative humidity and pressure);
  - d. preliminary tests to evaluate of which impact between steady worst condition or cycling prevails.
- 4) Consider preconditioning samples focussing on the comparison of products, not on actual ageing. Ageing laws for chemical ageing can be considered bearing in mind that

these are applicable to specific product families and reversible effects. The influence of wind cycle loads on mechanical ageing still needs to be investigated.

- 5) Implement small scale preliminary tests to evaluate the feasibility and results. One should keep in mind that product characteristics (for example tape) can vary a lot depending on the sample size (e.g. tape can be good on a 50-cm but bad on a 3-m facility).

## **5 CONCLUSIONS**

Regarding field measurements studies, it seems that the envelope airtightness decreases during the first years after achievement and then stabilises. The main results of this review are a list of key elements that may govern airtightness variations:

- Measurement uncertainty and how it could be reduced;
- Structure movements;
- Shrinks of mastics in the first weeks when the house get heated for the first time and/or when backer rod are not implemented;
- Drilling of the air-barrier due to the installation of new equipment;
- Aging of assembly due to unsuitable association of product and bad implementation conditions;
- And of course normal ageing of products.

Such information will be useful for future field measurements campaigns. Besides it is necessary to perform leakage detection and some investigations together with measurements to be able to explain changes in airtightness level.

The analysis of laboratory ageing studies showed that there is actually no standardised protocol to characterise durability of product assemblies in term of airtightness. Moreover due to the various natures of airtightness products it seems difficult to define an accelerated ageing protocol that would be equivalent to a certain amount of years of natural ageing. This paper gives pro and cons of various alternatives to assess the durability of airtightness products in laboratory in particular it insists on two conflicting constraints on the tested sample:

- being large enough and realistically implemented to be representative
- being simple enough to ensure the reproducibility of the test.

In the context of the Durabilit'air project, we are moving toward testing simple assembly of maximum 3 products in a 1m\*1m frame that fits with existing stoves. Constraints applied would be both pressure cycles and heat treatment (under fix pressure constraint). The durability will be assessed by an airtightness test.

## **6 ACKNOWLEDGEMENTS**

This work was supported by ADEME and French ministry for construction. The views and opinions of the authors do not necessarily reflect those of ADEME and French ministry. The published material is being distributed without warranty of any kind, either expressed or implied. The responsibility for the interpretation and use of the material lies with the reader. In no event shall authors, ADEME or French ministry be liable for damages arising from its use. Any responsibility arising from the use of this report lies with the user.

Authors also thank Ulf Antonsson and Eva Sikander for their welcome in RISE (new name for SP) laboratories in Boras (Sweden).

## 7 REFERENCES

- ADEME. (2016). *Quelle pérennité de la perméabilité à l'air des maisons individuelles en Basse Normandie*.
- Bailly, A., Guyot, G., & Leprince, V. (2015). 6 years of envelope airtightness measurements performed by French certified operators: analyses of about 65,000 tests. *36th AIVC Conference "Effective ventilation in high performance buildings", Madrid, Spain, 23-24 September 2015*. (pp. 22-32). AIVC.
- Bailly, A., Leprince, V., Guyot, G., Carrié, F., & El Mankibi, M. (2012). Numerical evaluation of airtightness measurement protocols. *33rd AIVC Conference "Optimising Ventilative Cooling and Airtightness for [Nearly] Zero-Energy Buildings, IAQ and Comfort", Copenhagen, Denmark, 10-11 October 2012* (pp. 252-255). AIVC.
- Bracke, W., Laverge, J., Van Den Bossche, N., & Janssens, A. (2013). Durability and measurement uncertainty of airtightness in extremely airtight dwellings. *34th AIVC Conference "Energy conservation technologies for mitigation and adaptation in the built environment: the role of ventilation strategies and smart materials", Athens, Greece, 25-26 September 2013* (pp. 524-534). AIVC.
- Bracke, W., Laverge, J., Van Den Bossche, N., & Janssens, A. (2016). Durability and Measurement Uncertainty of Airtightness in Extremely Airtight Dwellings. *International Journal of Ventilation*, 383-393.
- Carrié, F., & Leprince, V. (2014). Model error due to steady wind in building pressurization tests. *35th AIVC Conference "Ventilation and airtightness in transforming the building stock to high performance", Poznań, Poland, 24-25 September 2014* (pp. 770-774). AIVC.
- Chan, W., & Sherman, M. (2014). Durable airtightness in single-family dwellings: field measurements and analysis. *35th AIVC Conference "Ventilation and airtightness in transforming the building stock to high performance", Poznań, Poland, 24-25 September 2014* (pp. 7-15). AIVC.
- Crowe, K. (1974). *A History of the Original Peoples of Northern Canada*. Montreal: McGill/Queen's University Press for the Arctic Institute of North America.
- Feist, W., Ebel, W., Peper, S., Hasper, W., Pfluger, R., & Kirchmair, M. (2016). *25 Jahre Passivhaus Darmstadt Kranichstein*. Darmstadt: PASSIVHAUS INSTITUT.
- Hansen, M., & Ylmén, P. (2012). Changes in airtightness for six single family houses after 10-20 years. *TightVent- AIVC International workshop: "Achieving relevant and durable airtightness levels: status, options and progress needed", Brussels, Belgium, 28-29 March 2012* (pp. 67-75). AIVC.
- Langmans, J., Desta, T., Alderweireldt, L., & Roels, S. (2015). Laboratory investigation on the durability of taped joints in exterior air barrier applications. *36th AIVC Conference "Effective ventilation in high performance buildings", Madrid, Spain, 23-24 September 2015* (pp. 615-623). AIVC.

- Liddament, M. (2012). UK experience with quality approaches for airtight constructions. *TightVent - AIVC International workshop: "Achieving relevant and durable airtightness levels: status, options and progress needed"*, Brussels, Belgium, 28-29 March 2012 , (pp. 103-110).
- Michaux, B., Mees, C., Nguyen, E., & Loncour, X. (2014). Assessment of the durability of the airtightness of building elements via laboratory tests. *35th AIVC Conference " Ventilation and airtightness in transforming the building stock to high performance"*, Poznań, Poland, 24-25 September 2014 (pp. 738-746). AIVC.
- Philips, T., Rogers, P., & Smith, N. (2011). *Ageing and airtightness How dwelling air permeability changes over time*. Milton Keynes: NHBC foundation.
- Prowski, G. (December 6-10, 1998). The variation of airtightness of wood-frame houses over an 11-year period.
- Wahlgren, P. (2014). Seasonal variation in airtightness. *35th AIVC Conference " Ventilation and airtightness in transforming the building stock to high performance"*, Poznań, Poland, 24-25 September 2014 (pp. 621-628). AIVC.
- Ylmén, P., Hansén , M., & Romild, J. (2014). Durability of airtightness solutions for. *35th AIVC Conference " Ventilation and airtightness in transforming the building stock to high performance"*, Poznań, Poland, 24-25 September 2014 (pp. 268-278). AIVC.

# Long-time durability of passive house building airtightness

Søren Peper<sup>1</sup>, Oliver Kah<sup>1</sup> and Wolfgang Feist<sup>1,2</sup>

*1 Passive House Institute  
Dr. Wolfgang Feist  
Rheinstr. 44/46  
64283 Darmstadt, Germany*

*2 University of Innsbruck  
Department of Energy Efficient, Konstruktion and  
Building Physics  
Technikerstrasse 15  
6020 Innsbruck, Austria*

## ABSTRACT

An airtight building envelope ensures not only the energy-efficiency of a building, but also a damage free construction. Important to achieve optimal airtightness are the planning, implementation and materials. Long-term airtightness requires efforts in all three aspects. Airtightness products are being tested under lab conditions but these results cannot be transferred one-on-one onto buildings. To gather more information regarding the durability of the airtightness 17 passive houses were re-measured as part of a research project of the International Energy Agency, "IEA Task 28, Annex 38". The re-measured buildings included various construction types, different building types, e.g. terrace houses and single family houses, and buildings aging from 1.4 to 10.5 years. As all buildings are passive houses, airtightness was a key aspect during the planning phase and the initially measured  $n_{50}$ -values were very low. For 16 out of 17 buildings the re-measured results were good to very good with an average  $n_{50}$ -value of 0.42 1/h. The re-measurements have shown, that it is rather the planning than the type of construction that has a significant impact on the long-term durability of the airtightness of buildings. In 2016 the first passive house in Darmstadt-Kranichstein, was re-measured again 25 years after it has been built. The two terrace buildings originally reached  $n_{50}$ -values ranging between 0.2 and 0.4 1/h, which experts thought not possible at the time. During the first re-measurement in 1999 the level of airtightness has not dropped significantly. After 25 years the sealants for windows and doors, that can be opened were identified as a possible cause for leakage and were replaced. Measurements before and after the replacement presented an improvement due to this very simple measure. Even though many materials were not yet available in 1991, when the passive house in Darmstadt-Kranichstein was built, it could still obtain a high airtightness. This proves the importance and impact of airtight design in early stages of the planning phase onto the long-time durability of passive house building airtightness.

## KEYWORDS

Durability, Passive House, Airtightness

## 1 INTRODUCTION

For damage-free and energy-efficient building, good airtightness of the building envelope is indispensable. Efforts in planning and implementation, and the control with an airtightness test aim at a high quality of the building envelope. It is subsequently assumed that the building airtightness implemented will remain the same throughout the building's life time. Considering this, the following aspects become important:

- **Planning:** airtightness design with detailed planning of all connections, joints, and penetrations
- **Material:** suitability or required characteristics of the products used
- **Implementation:** professional workmanship

Efforts in quality assurance and improvement have been made in all three areas. To test and guarantee the durability of airtightness products (adhesive tapes, foils, sealing tapes, and

gunning compounds, etc.), they are, among other things, artificially aged in climatic chambers. However, even the sometimes very long system guarantees given by the manufacturers cannot ensure building airtightness over periods from 30 to 50 years (depending on the building element), although the products themselves may cover such time spans. Together with manufacturers, the working group of the Association for Airtightness in Buildings (FachverbandLuftdichtheitimBauwesen e.V. / [www.flib.de](http://www.flib.de)) on adhesive tapes developed criteria for evaluating and testing adhesive tapes. Among other things, these results will be used for drafting the new standard regulating this issue (German Industrial Standard DIN 4108 Teil 11).

## 2 RE-MEASUREMENT OF AIRTIGHTNESS

Thus far, there is very little information available on the durability of building airtightness in general, that is not only for individual products. This is particularly true for the category of buildings with very good airtightness ( $n_{50} < 0.6 \text{ h}^{-1}$ ). Therefore, as part of a research project of the International Energy Agency, “IEA Task 28, Annex 38”, the airtightness of 17 passive houses was re-measured. In this context, the passive houses represent energy-efficient buildings, where airtightness has been planned before beginning construction – as it should be done in general. For the selected buildings, the airtightness design, as well as the first measurement or the final acceptance test had been well documented. During the re-measurements, this specifically allowed for checking the leakages found during the first measurements. The buildings were also selected so that all common types of structures like solid, lightweight, composite, and concrete formwork construction were represented.

Using this method, the durability of the designs could be tested 1.4 to 10.5 years after their implementation. The tests included terraced houses and single-family homes of the different types of construction at eight locations. Further measurements will be conducted in 2016, testing the first passive house in Darmstadt-Kranichstein 25 years after construction. This paper is a summary of the research report “On the durability of airtightness designs of passive houses. Field measurements.” [Peper/Kah/Feist 2005] published as part of the IEA project.



Figure 1: Exterior view of the buildings tested for airtightness during the study

Table 1: Passive houses, where re-measurements were conducted

#	Passive house project	Architects/		Passive house project
1	terraced houses, Darmstadt-Kranichstein	Bott / Ridder / Westermeyer	solid	2
2	single-family homes, Bretten	Oehler + archkom	lightweight wood-frame	2
3	housing development, Lindlar / Hohkeppel	M. Brausem	lightweight wood-frame (force-fitted)	5
4	single-family homes, Stegaurach / Mühlendorf and Bamberg	Ingenieurbüro Trykowski	lightweight wood-frame	2
5	terraced houses, Hanover-Kronsberg	F. Rasch / P. Grenz	composite	4
6	terraced houses, Rhein-münster and Bühl	Planungsbüro Früh	concrete formwork (solid)	2

For each of the buildings or projects tested, we first described the respective airtightness design with the connections that had been implemented. For a systematic overview, we also drew up a table with the corresponding connections between building components. This was done analog to the tabular overview of connection possibilities by [Peper/Feist 1999]. By way of example, we show the systematic of the passive-house development in Hanover-Kronsberg.

Table 2: Airtight connections of the passive-house development in Hanover-Kronsberg

connection of	base plate	sash	blind frame	AW lightweight	roof
<b>roof</b>				acrylic adhesive tape (connection with PE panel)	acrylic adhesive tape (connection with PE panel)
<b>AW lightweight</b>	PE panel with acrylic or butyl-rubber adhesive tape or butyl-rubber adhesive tape on primed concrete		butyl-rubber adhesive tape with fleece lamination connected to PE panel	acrylic adhesive tape (connection with PE panel)	
<b>blind frame</b>	butyl-rubber adhesive tape with fleece lamination	lip seal			
<b>sash</b>					
<b>base plate</b>	mortar plus smoothing				

In the following, the research report documents the first measurement for each project. To the extent possible, the re-measurements tested for the residual leakages found.

### 3 EXAMPLE: PASSIVE-HOUSE DEVELOPMENT IN HANOVER-KRONSBURG

In the housing development in Hanover-Kronsberg, four of the 32 terraced houses were re-measured after four years and two months and the measurements documented. In all four

houses, residual leakages were found in the following areas: front-door sealings, some window sealings, some glass-strip connections, integration of window and front-door frames in the light-weight wall, some connections of building components as of the exterior walls with the walls separating houses, with base plates, or roof elements, as well as some corners of window reveal/floor.

Most of the residual leakages from the first measurements could still be detected in the re-measurement. An exact allocation of the leakages to the actual leakage point is, however, difficult because of the wall panels and floor coverings. The actual leakage is frequently no longer accessible and only the outlet of the flow path into the room can be located. The leakages detected at front doors and windows can be significantly reduced by re-adjusting. The small leakages at various mitre joints of the glass strips seem to indicate a weakness in window production. However, the leakages are so insignificant that rework is not recommended because it is expensive and time-consuming. Further residual leakages were also tested and evaluated.

The measuring results of the re-measurement are always compared to the first measurements. The different levels of measuring accuracy between both measurements due to the devices used and particularly the effect of wind must be taken into consideration for the final evaluation. In general, having considered the measuring accuracy, the results of the first measurement and the re-measurement overlap. Since any changes range within the measurement uncertainty, neither improvement nor deterioration of the airtightness can be proved.

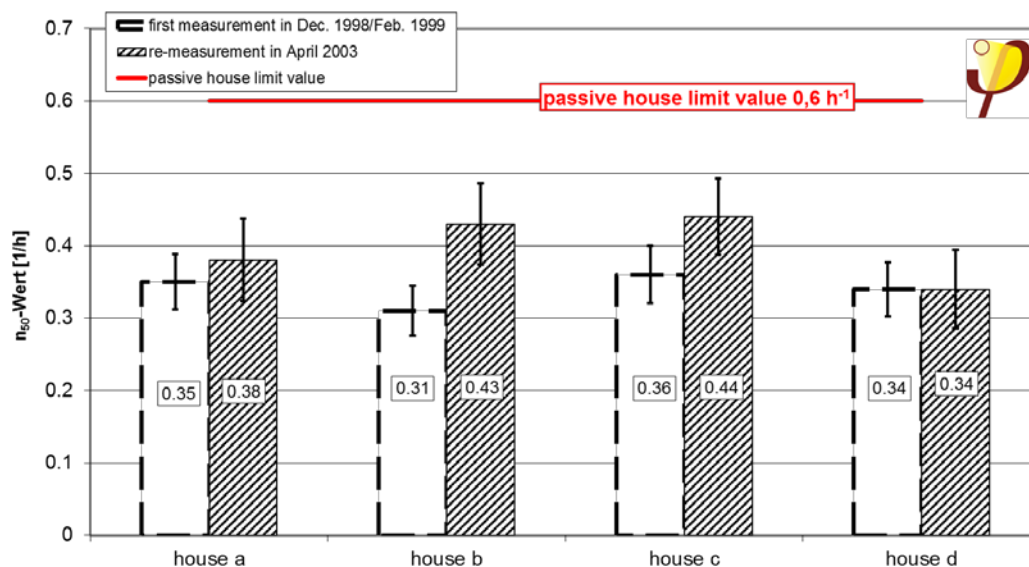


Figure 2: Example of the results of the four airtightness re-measurements in Hanover-Kronsberg in comparison to the results of the first measurements. The bars show the measuring uncertainty of each measurement.

The results of the four re-measurements show that all buildings tested have maintained a very high quality of airtightness. The mean of all four re-measurements is at  $n_{50}=0.4 \text{ h}^{-1}$ . For three of the four buildings, the measuring value has slightly increased, for the fourth, it has remained the same. However, the changes range within the area of the measuring accuracy of the tests. This makes it impossible to make a clear statement on an increase of the  $n_{50}$ -values. House B is the exception, because it shows a slight increase of the measuring value even after having considered the measuring accuracy. Overall, the four objects show very high airtightness in the first measurements as well as in the re-measurement.

The principal result of the re-measurements is the high airtightness of the terraced houses proven in the first measurement as well as in the re-measurement. If at all, partial “deteriorations” are mainly detected at windows or front doors and nondurable silicon rework. The airtightness design of these buildings with composite structure can be rated as durable – at least for the time span until the re-measurement. Further relevant reductions in airtightness are not to be expected. The success of this “airtightness in series” in the passive-house development is above all based on the explicit planning of the airtightness. Drawing up detailed models (up to a scale of 1:1) has proven to be useful and expedient for areas where an airtight connection of up to three panels had been planned. This shows that consistent theoretical planning is critical, but the possibilities of a more practical implementation do also have to be carefully considered.

#### 4 OVERALL RESULT

For 16 of the 17 buildings, the results of the re-measurement were good to very good – and that for the strict passive house requirements with a limit of  $n_{50}=0.6$  1/h. These 16 passive houses averaged at a  $n_{50}$ -value of 0.42 1/h. In the exception, the main leakages supersede the quality of the other connections. The  $n_{50}$ -value was 1.2 1/h. It was not possible to draw conclusions on long-term stability. The architect of the building indicated the lack of a sufficient airtightness design. For the structurally identical subsequent buildings, such a design was available leading to a positive result (see number 4 in Figure 3). For the 16 positive results, the changes between the first and the re-measurement were almost always within the measuring accuracy. Five buildings even showed a significant improvement of the measuring values due to rework following the first pressure test.

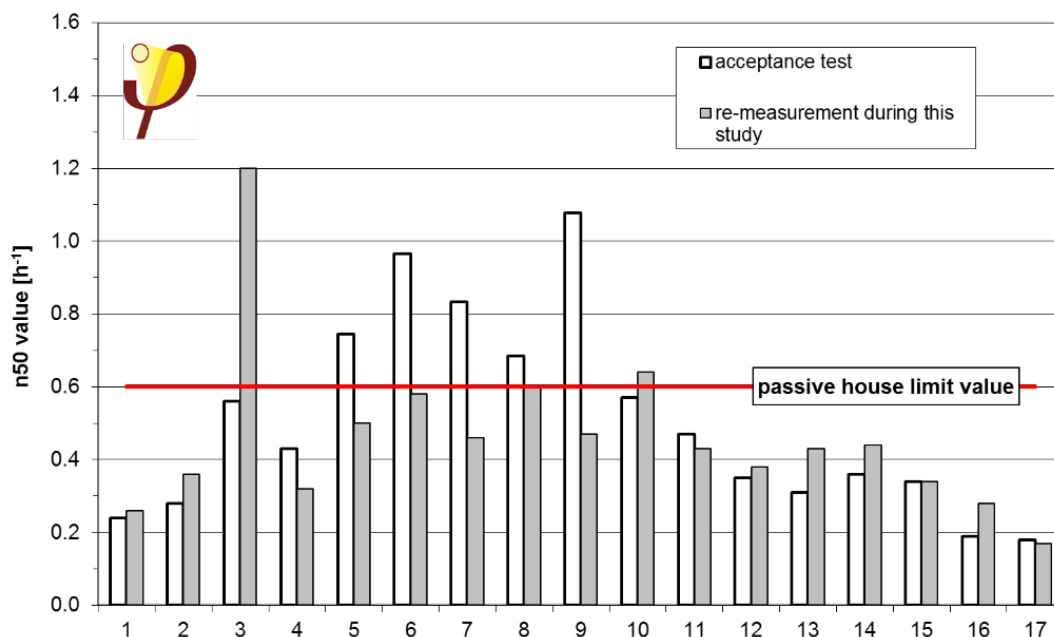


Figure 3: Overview of the measuring results of the airtightness tests of the 17 buildings analysed (acceptance test and re-measurement during this study).

Table 3: Overview of the re-measured buildings and evaluation of the durability of the airtightness in the period assessable

#	Type of construction	Airtight layer	Number of objects	Time span	Evaluation
1	solid	interior plaster / PE-panel / concrete	2	> 10,5 a	durable
2	wood-frame	intermittently bonded wood composite boards, PE-panel, concrete	2	> 3,6	cannot be evaluated
				> 2,8 a	durable
3	wood-frame (force-fitted)	force-locked, bonded wood composite boards, concrete	5	> 3,5 a	durable
4	wood frame	bonded wood composite boards	2	> 4 and > 4,3 a	durable
5	composite	PE-panel/ concrete	4	> 3,1 a	durable
6	concrete formwork	interior plaster / PE-panel / concrete	2	> 4,8 and > 1,4 a	durable

These measurements paint a positive picture of the durability of airtightness designs. The designs and connections selected by the respective planners and architects must be considered successful, at least for the time span between the acceptance test and the re-measurement. All types of structures are to be regarded as equally positive. **It is the quality of planning rather than the type of construction that is decisive for a successful implementation of high airtightness.** This obviously also requires a careful implementation of the plans and is the point when it becomes evident if the planning contains designs that allow for a successful implementation.

We do not assume that airtightness for the buildings analysed will deteriorate significantly over the next few years. They have, after all, been planned and implemented using suitable products and installing them according to recognized quality standards. Considering the respective time spans since construction, most of the expected movements of building components have already passed. According to the results on hand, it is to be expected that the airtightness in the category of buildings with excellent airtightness ( $n_{50} < 0,6 \text{ h}^{-1}$ ) tested here is durable. For the passive houses tested, a deterioration of airtightness during the first two years as it is described in some of the literature cannot be confirmed.

## 5 FOLLOW-UP ON THE PASSIVE HOUSE IN DARMSTADT-KRANICHSTEIN

The passive house in Darmstadt-Kranichstein was re-measured again in 2016, 25 years after it has been built (see Figure 4), 15 years after the previously described pressure tests in 1999.



Figure 4:Left: The first pressure test was conducted on 24/26 of May 1991 by Ingenieurbüro ebök once the airtight envelope had been finished.Right: The current BlowerDoor Test (here in House B) was conducted on 11/12 of February 2016 by the PHI 25 years after construction.

The only significant shortfalls in the two houses were detected at the sealants for windows and doors that can be opened. After 25 years, the sealants have become somewhat inelastic. Adjustments to the windows did not fix the issue sufficiently, so all of the windows and the front door were additionally sealed.

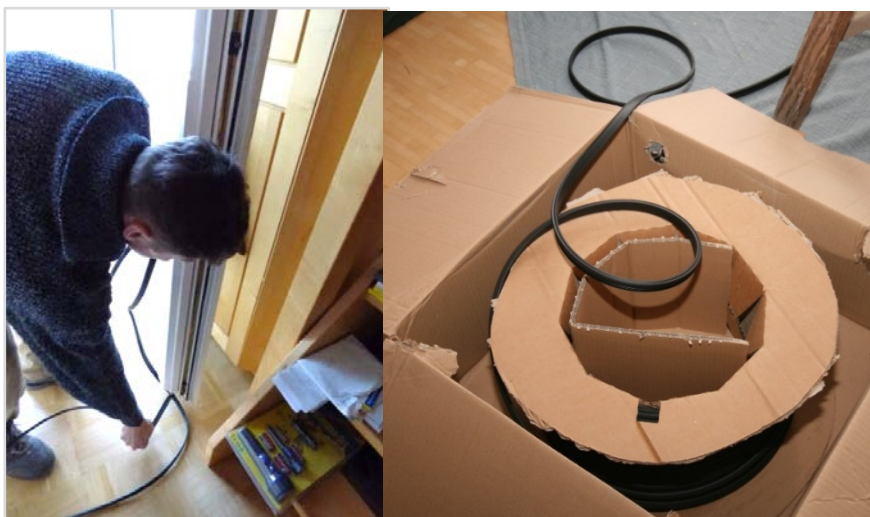


Figure 5:A qualified contractor replacing the window seals in House A on 12/02/2016 and the sealing material used (yard ware).

As a result, the original value has once again been reached in both houses: At  $n_{50} = 0.21$  and  $0.35 \text{ h}^{-1}$  (see Figure 6), respectively, the extremely good results of the preliminary measurements were reproduced. Detailed inspections of the building component connections revealed how durable they were although the materials available today were not yet on the market in 1991. For instance, the acrylic seals between the window frames and plaster end rails are nearly perfectly airtight everywhere, as is the connection between the airtightness foil in the

roof and the wall's interior plaster. For a lack of alternatives at the time, the windows that reach down to the floor slab have a wide silicon joint with backfill material. Aside from a few areas, even this suboptimal sealing is still perfectly airtight.

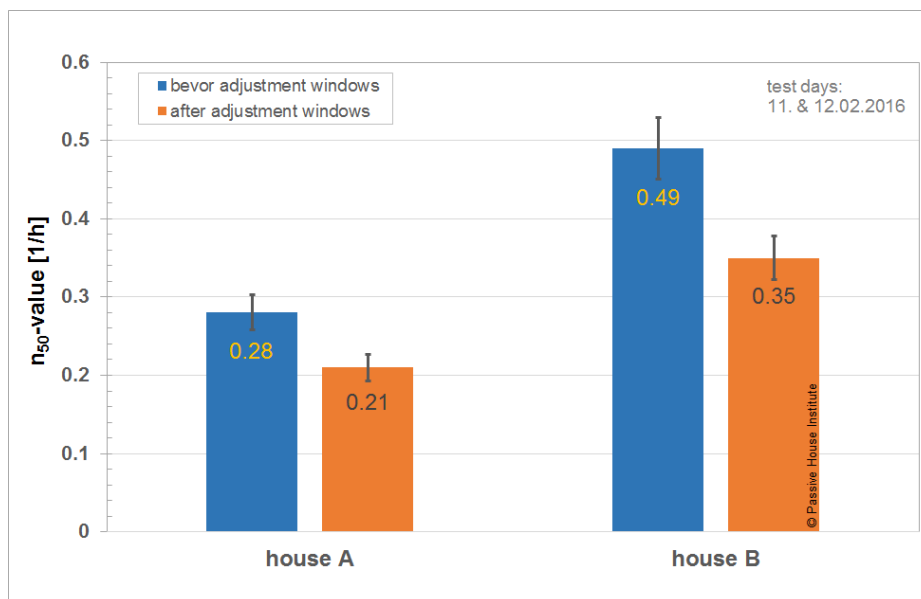


Figure 6: Airtightness tests of the passive house in Kranichstein (Houses A and B) in February 2016, 25 years after construction, before and after replacing the window and door seals.

The terrace houses in Darmstadt-Kranichstein originally had  $n_{50}$ -values ranging from 0.2 to  $0.4 \text{ h}^{-1}$ , which not even experts had previously thought possible. As shown in Figure 3 (buildings number 1 and 2) during the in previous chapter described tests in 1991, the  $n_{50}$ -values had not significantly gone down since then (see also Figure 7). The latest measurements in 2016 after 25 years once again revealed extremely good levels of airtightness.

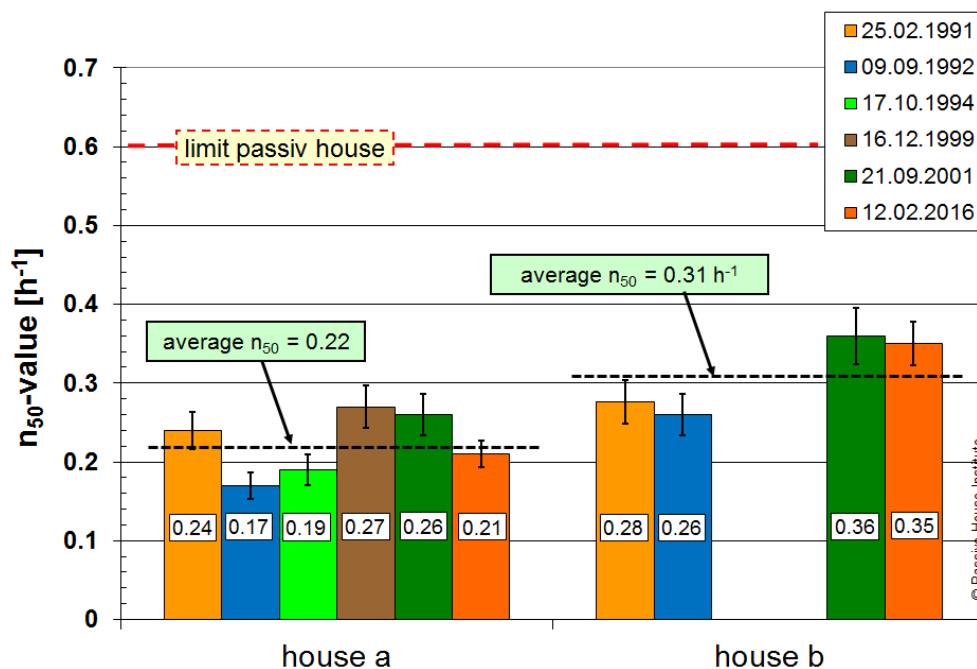


Figure 7: Overview of all pressure tests of two of the four units of the passive house in Kranichstein conducted over the years. The two measurements before replacing the seals are not included.

## 6 CONCLUSION

In general, it can be stated that the detailed analysis of the connections between building components shows their durability, even though in 1991 the number of materials and construction solutions available was much smaller than today. The very good airtightness results of the building were clearly below an  $n_{50} = 0.4 \text{ h}^{-1}$  and the data for this long period is secure. A durably airtight building envelope is, above all, a question of planning (see also [Peper/Feist 1999]). Everything depends on the connection of the airtight layers at the edges of building components. There are standard solutions that can be implemented easily, as for example the elastically filled joint (with anti-adhesion “round cord” to avoid three-flank adhesion) or the plastered sealing sheet. These procedures had already been implemented during the construction of the passive house in Darmstadt-Kranichstein and continue to be perfectly airtight even 25 years after construction

## 7 REFERENCES

[Peper/Kah/Feist 2005] Peper, S.; Kah, O.; Feist, W.: *On the durability of airtightness concepts in Passive Houses. Field measurements*. IEA SHC TASK 28 / ECBCS ANNEX 38. Research Project within the framework of national participation in the working group 'Sustainable Solar Housing' of the International Energy Agency IEA Subtask D: Monitoring and Evaluation, Darmstadt, June, 2005.

[Peper/Feist 1999] Peper, S., Feist, W.: *Airtight planning of Passive Houses*, CEPHEUS Project Information No. 7, Passive House Institute, Darmstadt 1999; Technical Information PHI-1999/6, 10th edition, October 2009.

[Feist et al.] Feist, W.; Ebel, W.; Peper, S.; Hasper, W.; Pfluger, R.; Kirchmair, M.: *25 Years Passive House Darmstadt Kranichstein*. Passivhaus Institut, Darmstadt, 2016

# Assessment of the durability of the airtightness of building elements via laboratory tests

Benoît Michaux<sup>\*</sup>, Clarisse Mees, Evelyne Nguyen, Xavier Loncour

*Belgian Building Research  
Institute  
Lombard Street, 42  
BE 1000 Brussels, Belgium  
\*Corresponding author:  
bmi@bbri.be*

The airtightness just after the end of a building phase is assumed to be relevant criteria for high energy performance. Testing on site the initial performance of the airtightness via the blower door test has become nowadays a common practice but generally implemented before the occupation of the building. But a lot of questions are still remaining targeting the sustainability of the performances. Even if retesting a building a few years after the initial test can provide a general view on the evolution of this performance, this could generate the adding cost and couldn't give information on the origin of potential changes. Another approach may be to validate technology and building technics as sustainable solutions. In order to quantitatively evaluate the durability of the airtightness of building elements as well as building technics, a research realized in Belgium has tested in laboratory the initial performance of more than 50 building walls and their materials.

The project called DREAM conducted from 2012 to 2013 by the Belgian Building Research Institute in partnership with the University of Liège has targeted the basic criteria and useful technologies insuring the sustainability of the airtightness.

DREAM aims to evaluate and improve the sustainability of the airtightness of buildings quantifying the air tightness performance of different materials before and after ageing for 46 different walls (divided into 4 families).

Four different families of system ensuring the airtightness have been targeted in this project.

- Walls of blocks / bricks whose airtightness is ensured by coatings/plastering (17 cases);
- Walls whose airtightness is ensured by wood panels (11 cases);
- Walls whose airtightness is ensured by a membrane (11 cases);
- Walls composed by industrialized systems (sandwich panels, architectural concrete panels, ...). (7 cases).

Note that the sample are representative of the existing building method in Belgium.

Air permeability and ageing process are done in laboratory. Three types of ageing were implemented successively on the samples.

- Ageing representing wind effects and storms.
- Ageing representing the variation of moisture
- Ageing representing the variation of temperature

These various types of ageing are organized into 7 phases. All the samples are tested before ageing (step 1) and after each phase.

The results are represented graphically ( $Q_{50}$ , Ageing test) for each case as example below. Graphics show the evolution of the air flow at 50Pa after each step of ageing.

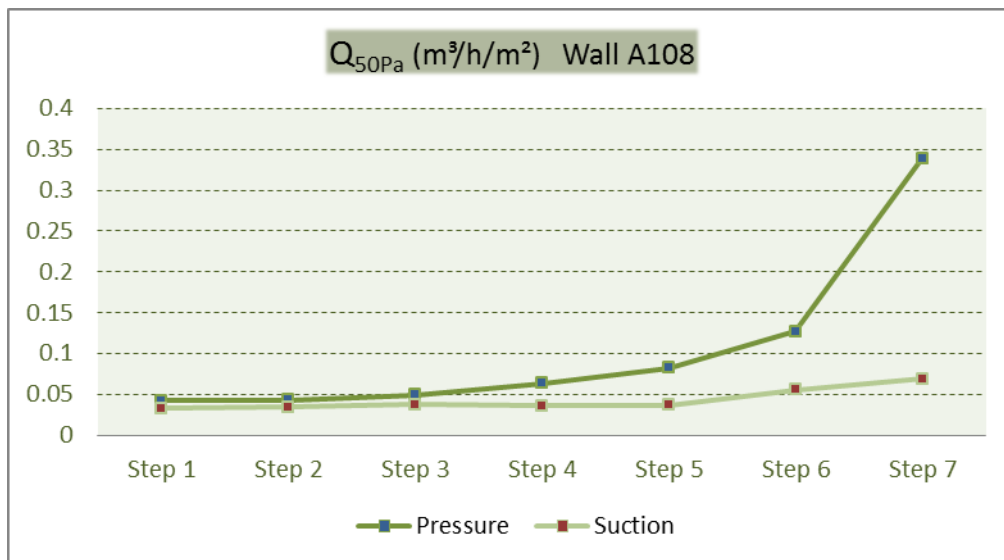


Figure 5: Evolution of the  $Q_{50Pa}$  (case of wood panel)

These results give:

- initial performance ;
- critical constraint according to the different system (for instance, only moisture and thermal ageing influence the airtightness of the walls of bricks whose airtightness is ensured by internal plastering) ;
- strengths and weaknesses of the different system

The results of this research are available in publications of the Belgian Building Research Institute in the form of implementation guidelines. These guidelines are given according to the constraints on the building such as wind exposure on the wall

# Will naturally ventilated dwellings still be safe under heatwaves?

Jean-Marie Alessandrini\*<sup>1</sup>, Jacques Ribéron<sup>2</sup>

*1 Energy&Environment Department  
Centre Scientifique et Technique du Bâtiment (CSTB)  
84 avenue Jean-Jaurès, Champs-sur-Marne,  
77447 Marne-la-Vallée cedex 2, France*

*2 Health & Comfort Department  
Centre Scientifique et Technique du Bâtiment (CSTB)  
84 avenue Jean-Jaurès, Champs-sur-Marne,  
77447 Marne-la-Vallée cedex 2, France*

*Corresponding author:  
jean-marie.alessandrini@cstb.fr*

## ABSTRACT

Heatwaves are often responsible for many deaths due to high temperature indoors. Energy savings is a key element in building design and refurbishment works to reduce the impact of climate change. Natural ventilation is often promoted as an indoor space cooling solution thanks to its energy saving potential.

The paper deals with prediction of heat-related health risks situations in naturally ventilated dwellings.

In these spaces, indoor thermal conditions depend on windows opening and on difference between outdoor and indoor temperatures. The efficiency of temperature control also depends on especially building thermal inertia, solar gains and occupants' behaviour. Yet, meteorological variability and occupants' behaviour are difficult to predict. Thus, operating limits of technical solutions using natural ventilation are not totally reliable because of uncertainties on the variability of these parameters.

In order to decrease uncertainties in prediction of heat-related health risks and to secure building design, the first step of a science-based methodology is proposed to help building sector professionals. It links consensual indicators, including ergonomics of the thermal environment standards, to distinguish between a moderately warm situation from heat stress causing unhealthy indoor environment for occupants. Simulations are performed for a dwelling with different air flow rates under contrasting meteorological conditions to illustrate the methodology and the potential limits of natural ventilative cooling, according to health risks.

In tested dwelling, natural ventilation can reduce indoor temperature but doubt remains about providing comfortable conditions. According to ergonomics standards scopes, a gap occurs between "moderate thermal environment" and "heat stress" areas. Further investigations are needed to bridge the observed gap.

## KEYWORDS

Thermal comfort, heat stress, natural ventilative cooling, health, climate change

## 1 INTRODUCTION

Once upon a time in Western Europe, during a conference about climate change<sup>1</sup>, a naturally ventilated school<sup>2</sup> was presented as the paragon of adapted building to climate change. Later, supplement to CEN Guide 32 (2016), about climate change adaptation in standards, recommends to "give[s] preference to equipment that is not weather sensitive". The contrast is striking between both comments.

Indeed, usually passive energy constructions, mixing high thermal mass and night cooling ventilation, are supported according to climate change mitigation policies. These constructions are known to significantly reduce indoor temperature, if outside temperature is low enough at night. Thus which way should be followed?

Climate projections warn us about the return of even hotter heatwaves with several hot days. Cautiously CEN GUIDE 32 (2016) invites to "ensure building can [...] provide thermal comfort in a changing climate." In practical terms, is natural ventilation reliable enough to avoid thermal stress and their dire consequences?

---

<sup>1</sup>11<sup>th</sup>, The international weather and climate forum, april 2014.

<sup>2</sup>Ecole Saint Exupéry, Pantin (Paris suburb), Ademe et vous, n°73-Mars 2014

The long term goal of this work is to help professional to establish the running limits of these bioclimatic solutions. Dedicated to professionals, most of references are international standards, and used numerical models are strongly linked to them.

In this paper, an overall view of the methodology in process is introduced, before studying how to bridge the gap between thermal comfort and thermal stress. A tested situation helps to draw standards limits and to provide reasonable values of disruptive threshold from comfort to stress. Finally, it gives an idea of natural ventilation efficiency to keep dwelling safety with high thermal mass under a heatwave. First of all, heatwave hazards and climate change context are outline in order to highlight a way to design buildings to achieve both objectives: adaptation and mitigation to climate change.

## **2 METHODOLOGY**

In this section are presented the health effects of heatwaves and the measures to limit their impacts. Then, the method is described step by step. Finally, it presents the results understanding keys as regards the question of mitigation and adaptation to climate change.

### **2.1 Heatwave hazards and climate change**

Long-duration heatwaves and prevailing warmth for annual conditions are becoming increasingly likely because of a warming planet. Heatwaves represent a real risk to vulnerable population. Significant increases in the risks of extreme heat are projected under all scenarios of climate change. There is a well-established relationship between extreme high temperatures and human morbidity and mortality (The Lancet Commission, 2015; Koppe et al. 2004).

The effects are worsened by the urban heat island effect, which results from greater heat retention of buildings and paved surfaces, compared with transpiring, shading, and air-flow promoting vegetation-covered surfaces. Today, a quarter of the French population is aged over 60, and three-quarters of the population live in urban areas. In next decades, ageing population and urban life will increase, leading to an increased risk of heat-related death.

The 2003 heatwave in Europe killed up to 70 000 people (Kovats and Hajat 2008). It is estimated that it caused 14 800 excess deaths in France (Hémon and Jouglu, 2004). The 2006 heatwave in France caused 2 000 excess deaths in a 18-day period, the 2015 heatwave caused 3 300 excess deaths in a 26-day period. Today, French people are better prepared to deal with significant heatwaves. Despite the prevention measures, the impact of heatwaves remains significant and demands the continuation of all the work achieved.

Five kinds of heat-related health factors are considered in literature (Laaidi et al., 2015): environmental factors (urban density, building construction quality,...), socio-demographic factors (age, specific population, ...), health factors, social factors, behaviour factors (inadequate clothing, reduced mobility,...).

Following the 2003 heatwave, a case-control study has shown that for people who lived at the top floor of an uninsulated block of flat, the risk factor was multiplied by 4 (Ribéron et al., 2006). Other factors, such as window number and the inability to create draughts by cross ventilation were associated with increased death rates (Vandentorren et al., 2006).

This history explains strong apprehensions about climate change. But to understand consequences on thermal comfort and heat stress in buildings, average annual temperature on a national or world scale is not comprehensive enough. Indeed, to estimate comfort or energy consumption, to design or to define operating limits, different weather sequences must be selected based on probability of occurrence. The following figure shows a probability distribution of outside daily temperatures during a nowadays typical year, called previous climate, and a projection of a future one, called new climate.

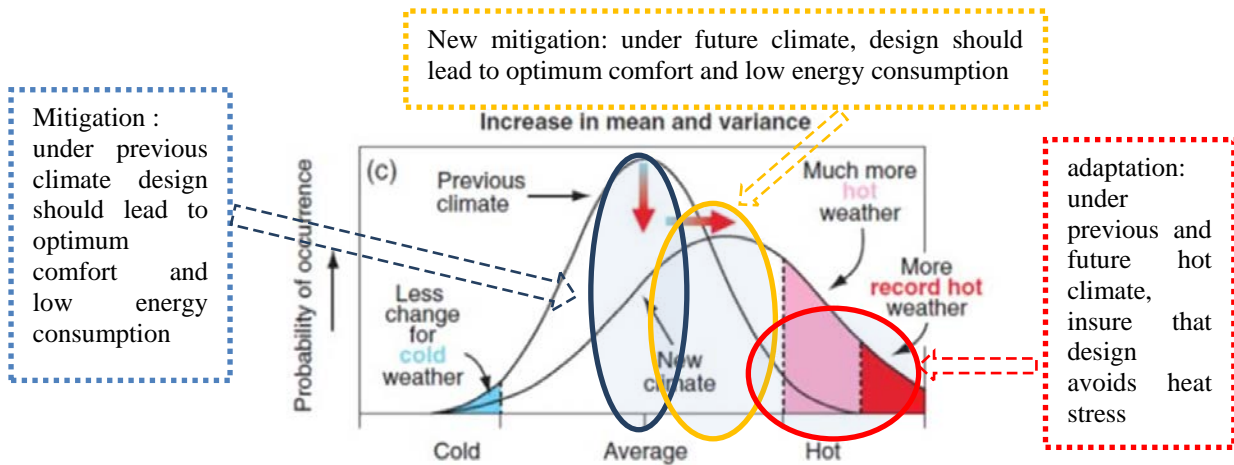


Figure 1: schematic showing the effect on extreme temperatures when both the mean and variance increase for a normal distribution of temperature (Folland, 2001)

Long term objective aim is to link two areas from average to hot weathers:

- The average one, with a high frequency, concerns notably mitigation. Indeed, buildings under it should lead to optimum indoor thermal comfort with low energy consumption.
- The hot one, with a low frequency, concerns mostly adaptation. It is too rare to be used for building design. Should these hot weathers happen, which occurs more often in urban heat islands, estimating indoor thermal conditions would be necessary to avoid danger.

Selected weather is previous extreme hot climate, in the pink area. It also gives an idea of future design conditions. As stakes, objectives and study boundaries are known; an overall overview of the methodology can be drawn.

## 2.2 Methodology main steps

They are introduced in figure below. According to the long term goal, available tools for building designs are mainly standards related to:

- energetically performant building for meteorological data and calculation methods,
- ergonomics of the thermal environment for comfort and heat stress.

ISO 15265 (2004), deals with risk assessment strategy for the prevention of stress or discomfort, but it cannot be used because, firstly, it concerns usual situations not designed ones. But recommendations from this standard are used when possible.

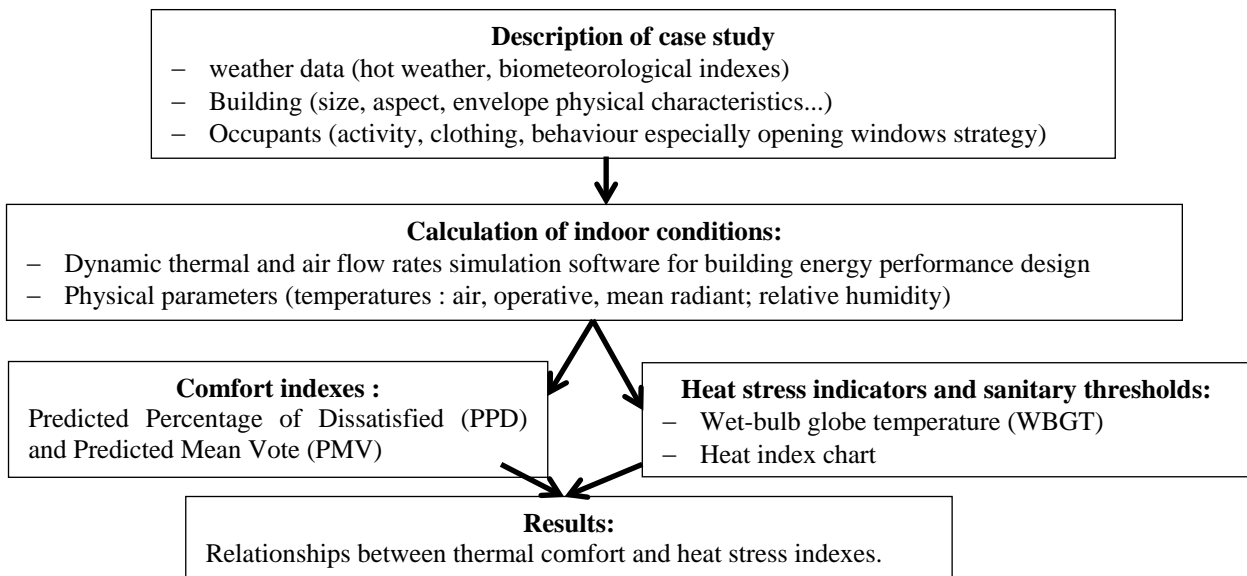


Figure 2: chronological sequence with basic steps of the methodology

### 2.3 Biometeorological indicators IBM

In order to improve the heatwave response, the French Minister of Health developed a National Heatwave Plan (NHP) in 2004. The NHP defines actions aimed at preventing the health impact in episodes of extreme heat. It includes recommendations for different stakeholders: health professionals, key actors in the social sphere, etc. The NHP includes a Heat Health Watch Warning System (HHWWS) (Laaidi et al., 2013). HHWWS has classified NHP actions according to four levels:

- Seasonal vigilance, continuously activated from 1<sup>st</sup> of June to 30<sup>th</sup> of September,
- Warning level, when the thresholds are to be reached within three days. Preparation for staggered implementation of the preventive measures detailed in the NHP,
- Heatwave alert, when the thresholds are reached. Implementation of the appropriate sanitary and social measures,
- Maximum mobilization level, when the thresholds are reached and when the heatwave tends to last or when exceptional conditions are met.

The HHWWS was developed on the basis of retrospective analysis of mortality and meteorological data in fourteen pilot cities representative of the different climates of mainland France (Laaidi et al., 2013). Several heatwave indicators were tested in relation to levels of excess mortality. An indicator that mixes minimum and maximum temperatures was chosen. Excess mortality levels were set at 50% for Paris, Lyon, Lille and Marseille and at 100% for the other smaller cities. The indicator is therefore the pair (IBMin, IBMax) where IBMin is the sliding mean over three days of minimum temperatures, and IBMax the sliding mean over three days of maximum temperatures. The HHWWS is regularly assessed, and updated annually (Pascal et al., 2006).

### 2.4 Occupants' behaviours

Indoor thermal environment is strongly impacted by occupants. Metabolic water vapour and heat production depend on activity. Moreover, opening window strategy, solar shading running and the way appliances are used are deeply linked to occupants' behaviours. Thus, building occupation is needed to predict indoor temperature and humidity. Behaviour scenarios are better reliable when done in cooperation with building project stakeholders. In this paper, given scenarios are close to those used in French thermal regulation (J.O., 2013).

### 2.5 Thermal and air flow rates models

Indoor environmental conditions are calculated with a dynamic thermal model linked with a mass air flow balance one, including large opening windows, so called COMETH (Videau et al., 2013). This integrated model is used by French thermal regulations since 2000 (Da Silva et al., 2016a; Da Silva et al., 2016b), first for summer thermal comfort then for heating, cooling, ventilation, sanitary hot water and lighting consumptions. It is acquainted to thermal design engineers at a national scale. COMETH can calculate indoor environment conditions for different occupants' behaviours and under different climates.

Thermal model has been successfully compared to EN 15265 standard (2008) and to ASHRAE 140 Standard (ASHRAE, 2001). Thermal balance is computed with a 5RC equivalent electric representation of the building components, similar to ISO 13790 (2013) simplified model. It gives air ( $T_a$ ), mean radiant ( $T_{rm}$ ) and operative temperatures ( $T_{op}$ ) at each hourly time step. Radiant internal heat exchanges are based in the Walton radiation model (Walton, 1980). Solar radiations are absorbed by walls, which is in accordance with black globe temperature. Then  $T_{op}$  is obtained with usual equation:

$$T_{op} = \frac{T_a + T_{rm}}{2} \quad (1)$$

The air change rate is calculated according to the De Gids and Phaff air flow model through large openings (De Gids and Phaff, 1982). It gives a general expression for the ventilation rate

Q through an open window as a function of,  $\Delta T$ , temperature difference between inside and outside,  $U_{wind}$ , wind velocity and fluctuating terms:

$$Q = \frac{A}{2} \times \sqrt{C_1 U_{wind}^2 + C_2 H \Delta T + C_3} \quad (2)$$

Where A is area of the window opening, H is height of the opening,  $C_1$  is a dimensionless coefficient depending on the wind,  $C_2$  is buoyancy constant and  $C_3$  is turbulence constant. This model has been used for the IEA Annex 20 research works especially for single-sided ventilation studies (IEA, 1992). It has been used in the calculation method for the French thermal regulation since 2000 (J.O., 2013) and in the European standard dealing with calculation methods for the determination of air flow rates in buildings EN 15242 (2007). For humidity balance, in and out dry air flow rates are supposed equal. Without cooling systems absolute humidity variation is given by next equation.

$$\frac{dw}{dt} = \frac{\sum Q_{in}(w_{in} - w_{ex}) + \text{internal Latent loads}}{V \rho_{indoor}} \quad (3)$$

$Q_{in}$  is incoming air flow rate,  $w_{in}$  is incoming air absolute humidity,  $w_{ex}$  is absolute humidity exhausting from dwelling, internal latent loads (kg/s), V is dwelling volume and  $\rho_{indoor}$  is indoor air density.  $w_{ex}$  is assumed to be equal to absolute humidity within dwelling.

A Cranck Nicholson method is used to link thermal and air flow models. Time step result is the average between end and beginning time step solutions. Solution at the end of previous time step is assigned to beginning of next time step. Thus temperature beginning value is used to calculate air flow rate through windows and humidity balance at time step end.

Models assume indoor temperature and humidity are spatially homogenous and each wall has isothermal surfaces. Radiation balance is done for a cube with same absorption and emissivity for walls. To linearize radiation equation inside wall temperatures must be close. According to these assumptions only whole thermal feeling can be assessed, effects of draught, vertical air temperature difference or radiant asymmetry are not checked.

## 2.6 Thermal comfort and thermal stress indexes

ISO11399(2001) is used to select two main standards with adjacent scopes:

- ISO 7730 (2006) for moderate thermal environment with predicted mean vote (PMV),
- ISO 7243 (1994) for hot thermal environment with wet bulb globe temperature (WBGT).

Both indexes are consistent with a hourly time step.

Predicted percentage of dissatisfied (PPD) can be obtained from the predicted mean vote (PMV). In this study  $T_a$ ,  $T_{rm}$  and relative humidity (RH) are calculated by the model, while air velocity ( $V_a$ ), metabolic rate, and clothing insulation are given data.

WBGT index is a weighted sum of natural wet-bulb temperature ( $t_{nw}$ ) and globe temperature ( $t_g$ ). For indoor conditions, WBGT formula, without sun loads, is used:

$$\text{WBGT} = 0.7 t_{nw} + 0.3 t_g \quad (4)$$

WBGT is to be measured. Thus ISO 7726 (2002) is used to establish the link with the thermal model.  $t_g$  can be assumed to be equal to  $T_{op}$  calculated with the model. To obtain  $t_{nw}$ , natural wet-bulb temperature, Malchaire (1976) formula is used:

$$(t_{nw} - t_{wb}) = \frac{0.16(t_g - t_a) + 0.8}{200} (560 - 2RH - 5t_a) - 0.8 \quad (5)$$

He specifies that a good accuracy is obtained for  $V_a$  below 0.15 m/s. As before,  $T_{op}$  is assumed to be equal to  $t_g$ . All parameters are calculated by the model except  $t_{wb}$ , psychrometric wet-bulb temperature. According to psychrometric chart,  $t_{wb}$  is the cross section of continuous enthalpy curve and air saturation one. Enthalpy is calculated with  $t_a$  and RH, given by the model.

## 2.7 How to read results

The aim is to find a design running the limits of naturally ventilated dwellings. It also includes balance between mitigation building design and solutions for adaptation to climate change. The figure below presents increasing health risk versus increasing discomfort. Safety indoor environment is on the left and unsafe one on the right. Blue arrows show the way proposed to design building in order to save energy and provide occupants health.

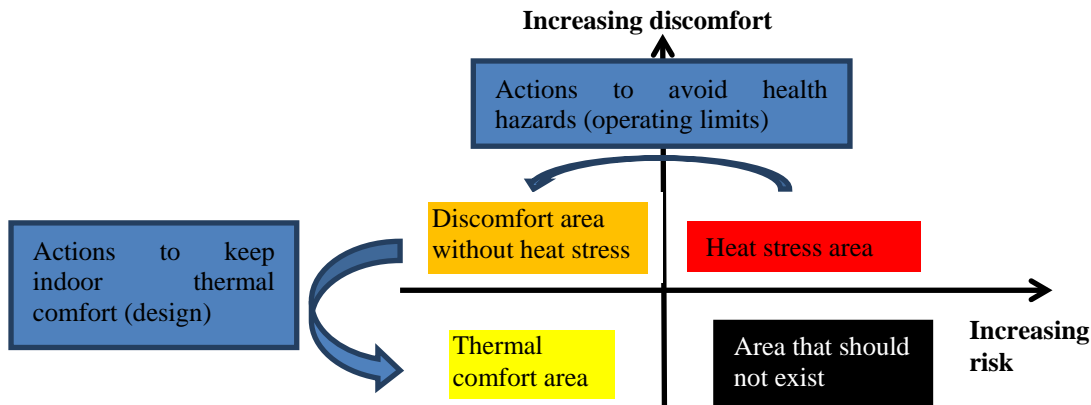


Figure 3: arbitration between thermal comfort and health risk

In reference to automotive segment, after a crash test occupants are expected to be safe. On the same idea, under a heat stress test, dwelling is supposed to protect people from health hazards. Thus attempted indoor thermal conditions are not the same under extreme and common weathers. Solutions, which guarantee comfort under usual circumstances – from the top left area to the bottom left one- should also protect occupants from health hazards under extreme events, from top right area to top left one. The crossing dot, at the border between thermal comfort and heat stress, is needed to apply the methodology. A practical approach through a specific situation is used to find it.

## 3 CASE STUDY AND RESULTS

Dwelling characteristics, climate conditions and occupants' behaviours selected for numerical simulations are given as following.

### 3.1 Simulation conditions

Without future climate data available for the numerical model (a set of 8 meteorological parameters with an hourly time step), a real heatwave episode is chosen according to HHWS (§2.3). The chosen 7-days period is during July 1999 in Hautes-Alpes district in France. Table below sums up IBM thresholds and daily values.

Table 1: IBM thresholds and daily values during selected heat wave

IBM	Thresholds	Day 1	Day 2	Day 3	Day 4	Day 5	Day 6	Day 7
IBMin (°C)	18	20	20	19	18	18	19	20
IBMax (°C)	33	33	33	33	33	33	34	36

Internal heat loads and humidity production are given according to people activity. Three occupants are supposed present in the dwelling all day long, awake from 8AM to 11PM. At each hourly time step, appliances loads range from 8 to 12 W/m<sup>2</sup> during waking time. Clothing insulation is equal to 0.6 clo. Metabolic data are selected in order to match with ISO 7730 (2006) and ISO 7243 (1994) scopes. A 1.2 met is selected for occupant assuming a sedentary activity. In the model, body's water vapor losses are not indoor temperature dependent. For each occupant, a 85 g/h metabolic vapor production is used. It matches with a sedentary activity under a 28°C (Recknagel, 1995).

A three-room middle floor dwelling, without air conditioning system, is selected. It has a 68 m<sup>2</sup> area and a 170 m<sup>3</sup> volume. It is a one single-sided ventilated dwelling mainly south orientated. Insulation and airtightness levels, recommended in Effnergie guidebooks (2008) are used. A 0.19 W/(m<sup>2</sup>.K) U value is used for walls and for stairwell partition wall a 0.3 factor is applied. External insulation and concrete structure lead to heavy inertia. Each wall thermal capacity is calculated with ISO 13786 (2008). Th-I, French professional rules (CSTB, 2012) is used to obtain dwelling thermal capacity, i.e. the C value of the thermal model. For a square meter living space it reaches 264 Kj/(K.m<sup>2</sup>). Windows characteristics are selected with Th-S French professional rules (CSTB, 2012). Solar shadings are always used. Details are presented in table below.

Table 2: walls size and thermal characteristics

Orientation	Area (m <sup>2</sup> )	Uw (W/(m <sup>2</sup> .K))	Solar factor		Description
			Sw1	Sw2	
South	8.26	1.6	0.08 short	0.05 long	4/16/4 double glaze, low emissivity glass, argon filled gap, outside clear color solar shading, 0,2 solar transmission rate
North	2.73		wave radiation	wave radiation	

The mechanical ventilation system provides an air renewal of 0.3 air change per hour (ach). Building envelope airtightness leads in calculation to an infiltration air flow rates lower than 0.1 ach. Southern windows are open when outside temperature is below indoor one, which is supposed to be cooling optimal strategy. Northern windows are never open. Air flow rates through windows are calculated according De Gids model (1982) with a 1.5m height of the opening and 3 opening windows areas of 0, 1 and 5 m<sup>2</sup>.

### 3.2 Results

Table below gives air flow rates and indoor temperatures during the last three days of the heatwave, when outside night temperature is above 20°C.

Table 3: indoor temperatures and air flow rate during the last three days of a heatwave

Opening windows airing	Opening windows area (m <sup>2</sup> )	ach max	Top min-max (°C)	Outside T min-max (°C)
No	0	0.4	39 - 41	20 - 37
Low	1	2	30 - 34	20 - 37
High	5	10	26 - 31	20 - 37

In these simulations, opening windows, at relevant time, is needed to avoid heat stress. Wide opening window increases ventilation rate. Then maximal and minimal Top can be lowered, respectively, by 10°C and 13°C. To understand better interaction between natural ventilation and indoor environment, indoor temperatures courses are represented in figure below. Green round spots represent Top for a high flow rate (black line) and purple crosses concern Top for a low flow rate (dotted purple line).

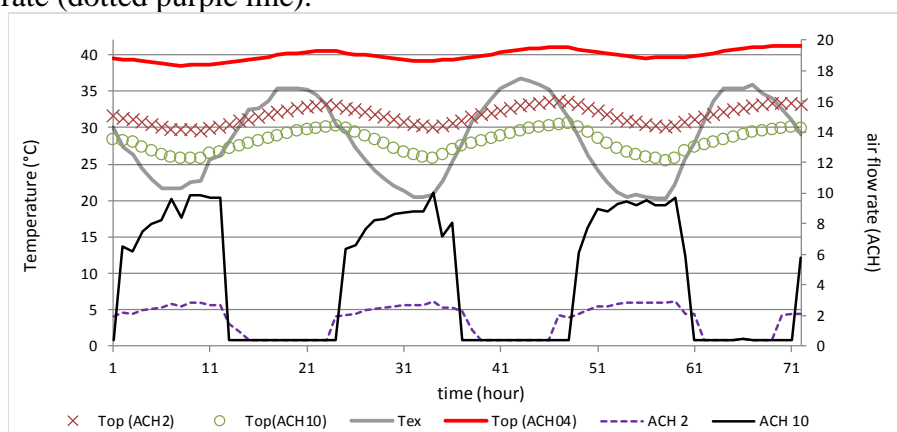


Figure 4: air change rate (ACH) and outside temperature impact on indoor temperatures under the last 3 days of a heatwave.

High and low ventilation rates, lead to the similar temperatures course. In tested situation, a 10ach air change rate reduces Top by about 4°C as compared to the one reached with 2ach. High ventilation reduces the gap between indoor and outside night temperatures (full grey line). Then heavy inertia sustains Top 6°C below outdoor maximal temperature. In this case, natural ventilation is efficient to reduce temperature. Nevertheless is indoor environment comfortable or does it cause a heat stress?

Main parameters run in recommended ranges of ISO 7730 (2006). Assumptions to calculate PMV are:  $V_a$  under 0.1 m/s, 1.2 met and 0.6 clo. A 0.1 m/s  $V_a$  may underestimate effective velocity in a high ventilated dwelling and thus over estimate PPD in this situation. This protective value is used, since indoor  $V_a$  profiles is not estimated. These assumptions are also used to select threshold proposed for WBGT; for not acclimated people ISO 7243 (1994) recommends not to exceed a 29°C WBGT. Each index is then calculated during waking period. Table below resumes main results relative to thermal comfort and heat stress. At several times,  $T_a$  and  $T_{rm}$  exceed comfort standard recommended limits. When it happens letters O.R. are added after concern PMV and PPD values in table below.

Table 4: indoor thermal comfort and heat stress indexes during last three days of a heatwave

ach	PMV		PPD (%)	WBGT (°C)	Globe T (°C)	$T_{nw}$ (°C)	RH (%)
	Min	Max	Min - Max	min-max	min-max	min-max	min-max
0.4	>2(O.R.)	>2(O.R.)	100(O.R.)-100(O.R.)	29-31	39-41	24-26	23-32
2	1.3->2(O.R.)		42-96 (O.R.)	23-26	29-34	19-24	25-47
10	0 - 1.7		5-60	20-25	24-31	17-23	32-57

For 0.4 ach, indoor environment conditions are strongly deteriorated and WBGT awareness limits are exceeded. With wide opening windows case (10 ach max), indoor conditions are kept, most of time, in moderate thermal environment according to standards. Calculated WBGT is significantly lower than standard proposed limits. In those both contrasted situations ergonomics standards indexes are reliable. In order to study boundaries between comfort and heat stress, PPD is plotted versus WBGT for the low ventilation test case on the figure below. Both indexes are calculated during the seven days heatwave.

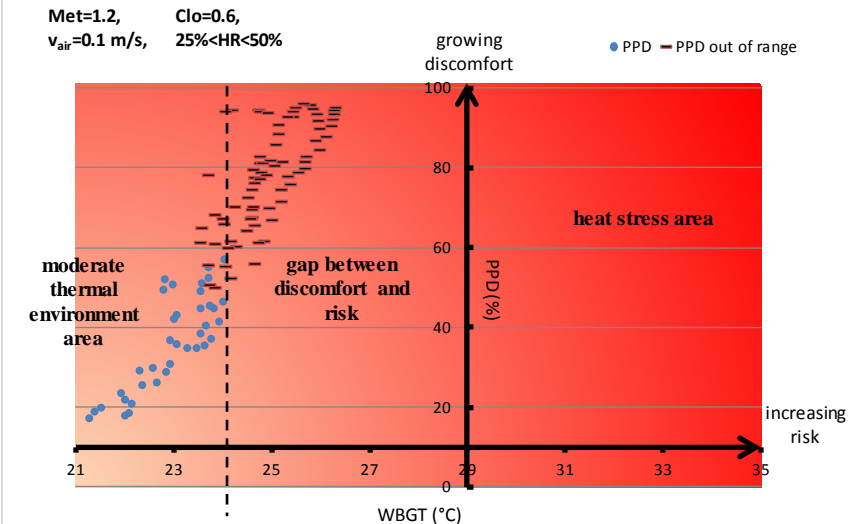


Figure 5: PPD versus WBGT calculated for a low natural ventilated building (2 ach) under a 7-day heatwave

Red dashes mean that PPD is calculated out of standard recommended range. According to ISO 7730 (2006), situation is never comfortable. Indeed, PMV is always above +0.5 with a percentage of dissatisfied over 10%. For a PPD above 50%, according to our assumptions, moderate thermal environmental area is exceeded. Numerous red dashes mean that indoor environment is often over moderate thermal environment limits. But it is also below heat stress according to 29°C WBGT limit and thus no specific supervision is required. There is a gap between areas for moderate environment and heat stress. With a 34 °C  $t_g$  (Table 4), it is

hopeful to say that situation is healthy. When 32°C is exceeded, ISO 15265 (2004), in its observation scale, recommends preventive steps. Thus in this particularly situation the gap, between both standard indexes, is too large to check if indoor environment is safe.

**3.3 How to bridge the gap between thermal comfort and heat stress?**

Excepted human factor- WBGT was invented in the 1950s to avoid heat illness in US Army (Budd, 2008)-, two physical parameters,  $V_a$  and RH, are striking. G.M. Budd (2008) explains that evaporation impact increases with temperature. Yet,  $t_{nw}$  weight factor is set at 0.7 in WBGT. Under quite dry environment (25-47% RH) studied, at the border of moderate thermal climate, dry temperature weight factor (set at 0.3) should increase and lead to increase WBGT in the tested situation. WBGT gives no indication of air velocity reduction effects. Because it was developed for outside environment,  $V_a$  that led to set WBGT safety thresholds were probably higher than those in our study. Yet, heat resilience is strongly reduced at low  $V_a$  because of reduction of air potential evaporation (Budd, 2008). For indoor environment without wind, existing WBGT limits might be reduced.

Many of detailed relationships between indoor thermal climate and human health are poorly understood in epidemiological terms. Goromosov (1968) investigated influence of indoor climate on human health. He proposed to use a combination of methods, including study of indoor climate, physiological investigations, and statistical study of thermal conditions. He carried out studies in apartments under hot climate (outdoor temperatures ranged from 35°C à 38°C). Outcomes suggested that people feel "comfortable" for 25°C indoor temperature associated to a 65 beats/min heart rate (HR). They feel "warm" for 27°C (HR=68 beats/min), "hot" for 31°C (HR=72 beats/min) and "hot and oppressive" for 34°C (HR=74 beats/min).

Weihe reviewed health impacts of adverse thermal conditions. A 17°C to 31°C acceptable range for thermal comfort neutrality without impacts on health is defined. Then symptoms of discomfort and health risks are listed; such as fatigue, inappetance, hyperthermia, for temperatures higher than 31°C, health effects are heat stroke and heart failure for temperatures significantly higher than 31°C. (WHO, 1987, WHO, 1990).

The Heat Index Chart (HIC) developed by the US, National Oceanographic and Atmospheric Administration (NOAA, 1985) gives, according to temperature and humidity, physiological disorders in case of prolonged exposure to heat. Health effects are classified in four levels: caution level (fatigue), extreme caution level (muscle cramps, physical exhaustion), danger level (heatstroke possible), extreme danger level (high risk of heat stroke). For a sedentary activity (circa 1.2 met) and a light clothing (circa 0.6 clo), thermal comfort indexes show that comfort requirement is met as far as Top does not exceed circa 26°C. Arrow below draws continuum from thermal comfortable area to severe conditions with adverse health effects.

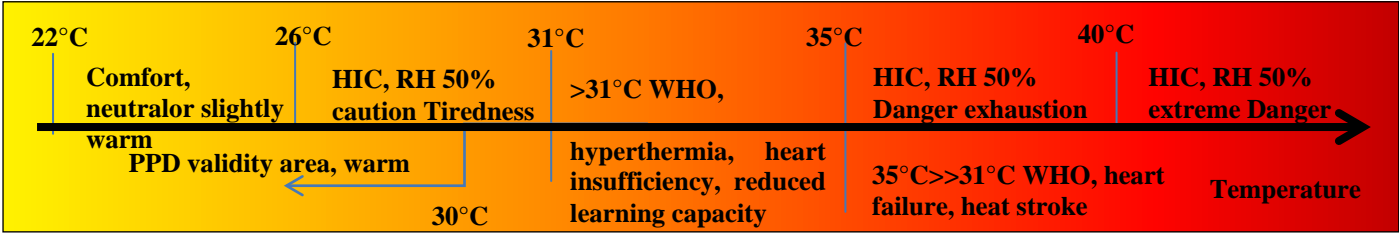


Figure 6: comfort and health continuum in warm and hot climates

For a given thermal stress physiological responses are variable, thus it is difficult to predict with accuracy an individual response.

**4 CONCLUSIONS**

Air temperature can be significantly reduced with natural ventilative cooling at relevant period, which occurs mostly at night, if outside temperature is below indoor one. In case study, natural ventilation avoids health risk upon ISO 7243 (1994), but doesn't meet moderate

comfort requirement upon ISO 7730 (2006). Strong air flow rate makes it possible to turn from hot to warm situation upon ISO 7730 (2006) with a PMV below 2. WBGT is attractive because it can be obtained with environment physical parameters. But a gap exists between ISO 7730 (2006) legitimate domain, for PPD calculation, and WBGT thresholds, proposed in ISO 7243 (1994). It can be explained by discrepancies between standard experimental conditions to quantify indexes. Indexes concern healthy people but WBGT was invented for US Army for probably more resistant people. Humidity weight given in WBGT seems too strong to match with moderate thermal environment limits. Moreover, WBGT thresholds appear too high for low air velocity. The observed gap attests difficulties to match indoor physical parameters and body physiological ones.

Standard indexes, consistent with building thermal models and literature thresholds, help to build a first step toward a continuum between thermal comfort and heat stress. But only healthy people under sedentary activity have been selected to bridge the gap. Investigations could be enlarged to vulnerable people and different metabolism. Moreover, situations could be tested under milder climate conditions at the HHWWS “warning level”, to check ability of naturally ventilated dwelling to protect people from thermal stress.

## 5 ACKNOWLEDGEMENTS

Authors thank S. Lacour (IRSTEA) for her help to compute wet bulb temperature, P. Delpech (CSTB) for his support, C. Cochet (CSTB) for his reviewing, K. Begredj (CSTB) for his help with COMETH model.

## 6 REFERENCES

ASHRAE 140.(2001). Method of Test for the Evaluation of Building Energy Analysis Computer Programs. ANSI/ASHRAE, Atlanta, 92p.

Budd, G. M. (2008). Wet-bulb globe temperature (WBGT)-its history and its limitations, *Journal of Science and Medicine in Sport*, 11, 20-32

CEN Guide 32 (2016), Guide for addressing climate change adaptation in standards, CEN 42p  
CSTB, (2012). Règles de calcul TH-I & S Guide réglementaire – R.T. 2012. CSTB éd. - 2012.

Da Silva, D. Alessandrini, J.M et al. (2016a). Evaluation et perspectives du modèle thermique de COMETH, le coeur de calcul de la RT des bâtiments neufs. IBPSA France.

Da Silva, D. Alessandrini et al. (2016b). International standards and thermal dynamic model for building regulation: validity and limits. IAQVEC, Songdo, Republic of Korea.

De Gids, W. Phaff, H. (1982). Ventilation Rate and Energy Consumption due to Open Windows. *Air Infiltration review*, 4 (1), 4-5.

Effinergie (2008) Le guide technique, "Réussir un projet Effinergie, des clés pour des logements neufs confortables et économes en énergie", 34 p.

EN 15242. (2007). NF EN 15242. Ventilation for buildings. Calculation methods for the determination of air flow rates in buildings including infiltration. AFNOR.

EN 15265.(2008). NF EN 15265. Energy performance of buildings - calculation of energy needs for space heating and cooling. AFNOR

- Folland, C.K., T.R. Karl, J.R. Christy, R.A. et al.(2001): Observed Climate Variability and Change. In: *Climate Change 2001: The Scientific Basis. Contribution of WG. I to the 3<sup>th</sup> Assessment Report of the IPCC* [Houghton, J.T. et al. (eds.)]. Cambridge University Press, 881pp.
- Goromosov, M.S. (1968). *The physiological basis of health standards for dwelling*. World Health Organization, Geneva. 100 pages.
- Hémon, D. Jougl, E. (2004). La canicule du mois d'août 2003 en France. *Rev. Epidémiol. Santé Publique*, 52 (1), 3-5.
- IEA. (1992). *Air flow through openings in buildings*. International Energy Agency; IEA/ECB-Annex 20 : *Air Flow Patterns Within Buildings. Subtask-2. Technical report*. (Ed) Jacobus van der Maas, EPFL, Lausanne, Switzerland, 163 pages.
- ISO 15265.(2004). NF EN ISO standard.Risk assessment strategy for the prevention of stress or discomfort in thermal working conditions, AFNOR, December 2004.
- ISO 11399.(2001). NF EN ISO Principles and application of relevant International Standards, AFNOR, March 2001.
- ISO 7730. (2006). NF EN ISO standard Analytical determination and interpretation of thermal comfort using calculation of the PMV and PPD indices and local thermal comfort criteria, AFNOR, March 2006.
- ISO 7243. (1994). NF EN ISO Hot environments-estimation of the heat stress on working man, based on the WBGT-index (wet bulb globe temperature), AFNOR.
- ISO 13790. (2013). NF EN ISO Energy performance of buildings — Calculation of energy use for space heating and cooling, AFNOR, September 2013.
- ISO 13786 (2008).NF EN ISO Thermal performance of building components Dynamic thermal characteristics Calculation methods, AFNOR July 2008.
- J.O. (2013). Arrêté du 30 avril 2013 portant approbation de la méthode de calcul Th-BCE 2012. *Journal Officiel de la République Française* du 7 mai 2013.
- Koppe, C. Kovats, S. Jendritzky, G. Menne, B. (2004). *Heat-waves: risk and response*. World Health Organization. *Health and Global Environmental Change Series*, n°2. 124 p.
- Kovats, S. Hajat, S. (2008). Heat Stress and Public Health: A critical Review. *Annu. Rev. Public Health*, (29), 41-55.
- Laaidi, K. Ung, A. Wagner, et al. (2013). *The French Heat and Health Watch Warning System: principles, fundamentals and assessment*. Saint-Maurice: InVS ; 17 pages.
- Laaidi, K. Ung, A. Pascal, M. Beaudeau, P. (2015). Vulnérabilité à la chaleur : actualisation des connaissances sur les facteurs de risque. *Bull Epidémiol Hebd.*(5), 76-82.

- The Lancet Commission. (2015). Health and climate change: policy responses to protect public health. *The Lancet*, vol 386 n°10006, 1861-1914.
- Malchaire, J.B. (1976), Evaluation of natural wet bulb and wet globe thermometers, *Ann. Occup. Hyg.* (19), 251-258.
- NOAA. (1985) Heat Index Chart. National Oceanic and Atmospheric Administration, Silver Spring, USA.[http://www.nws.noaa.gov/os/heat/heat\\_index.shtml](http://www.nws.noaa.gov/os/heat/heat_index.shtml)
- Pascal, M. Laaidi, K. Ledrans, M. et al.(2006). France's heat and health watch warning system. *Int J Biometeorol* 50, 144-153.
- Recknagel (1995). Le Recknagel. Manuel pratique du génie climatique, tome 1 Données fondamentales. PYC Ed,
- Ribéron, J. Vandentorren, S. Bretin, P. Zeghnoun, A., Salines, G. Cochet, et al.(2006). Building and Urban Factors in Heat-Related Deaths during the 2003 Heatwave in France. Healthy Buildings conference.Lisboa, Portugal 4-8 June 2006. (5), 323-326.
- Vandentorren, S. Bretin, P. Zeghnoun, A., Mandereau-Bruno, L. Croisier, A. Cochet, C. Ribéron, J. et al. (2006). August 2003 Heatwave in France: Risk factors for Death of Elderly People Living at Home. *Eur. J. Public Health*.(16), 583-591.
- Videau, J.B Alessandrini, J.M Haas, B. Pelé, C. et al. (2013), Bioclimatic design in the French regulation of buildings energy performance, CLIMA2013, Praha.
- Walton, G.N. (1980). A new algorithm for radiant interchange in room loads calculations. *ASHRAE Trans.* (86), 190-208
- WHO. (1987). Climate and Human Health. World Climate programme applications. World Health Organization Geneva, 18p.
- WHO. (1990). Indoor Environment: Health aspects of air quality, thermal environment, light and noise. World Health Organization. WHO/EHE/RUD/90.2. Geneva, 127 pages.

# Effectiveness of Ventilative Cooling Strategies in Hot and Dry and Temperate Climates of India

Devna Vyas<sup>1</sup>, Michael Apte<sup>1</sup>

*ICEPT University,  
K.L Campus, Navarangpura,  
Ahmedabad, Gujarat, India*

## ABSTRACT

Increasing use of air-conditioning in India is applying upward pressure on energy demand and may have implications on dependability. Electrical energy can be saved if favourable outdoor conditions are effectively utilized for cooling buildings with the minimum use of energy. This could be specifically applicable to residences where night-time use is more predominant for cooling by air conditioning systems but also aligns favourably with suitable outdoor conditions to be used as ventilative cooling. The potential of cooling with natural ventilation and mechanical ventilation remains an important topic to meet the needs of the larger section of the population who cannot afford to air-conditioning system as well as to reduce the energy consumption and greenhouse gas emission due to space cooling demands. This study evaluates the benefit of ventilative cooling techniques in Indian residences of hot and dry and temperate climates. The study first identifies typical residential plans in India based on past studies of residential surveys and existing literature. These plans are then simulated in DesignBuilder for modelling natural ventilation to understand baseline comfort and cooling needs. Further, ventilative cooling design strategies (single-side opening, cross-flow, stack ventilation with natural and mechanical ventilation) are designed using sizing methods described in IEA-Annex 62 and are incorporated in the residential plans to assess the ventilative cooling benefits. The effectiveness of ventilative cooling is investigated for two representative cities (Ahmedabad in hot and dry; Bangalore in temperate) located in two different climate zones of India to draw the comparison. The ventilative cooling benefits are quantified by percentage reduction in annual uncomfortable hours and cooling needs for various natural and mechanical ventilative cooling strategies in two the climate zones. Further, a novel method to continuously measure ventilation rate is developed for affordable yet accurate measurements. Short-term field measurements are conducted in an apartment building with continuous logging of surface temperatures, air temperature and air changes rates (using tracer gas method). The measurements are made to check if the input assumptions (such as ventilation rate or air velocity estimates) are realistic. These measurements are supported by physical model that calculates instantaneous ventilative cooling. The study provides scientific basis for building designers for incorporating ventilative cooling strategies. It also provides understanding of the benefits and limitations of natural and mechanical ventilative cooling in two different climates of India for residential application.

## KEYWORDS

Ventilative Cooling, Field Measurements, Simulation, Natural Ventilation, Mechanical Ventilation

## 1 INTRODUCTION

Increasing use of air-conditioning in India is exerting upward pressure on energy demand and may have implications on reliability (McNeil & Letschert, 2010). There have been situations when power supply in many of the metropolitan cities of India is not able to meet the energy demand and causes a large number of hours of power cut off and shutdowns (Central Statistics Office, 2016). Electrical energy can be saved if favourable outdoor conditions are effectively utilized for cooling buildings with the minimum use of energy. This could be specifically applicable to residences where night-time use is more predominant for cooling by air conditioning systems but also aligns favourably with suitable outdoor conditions to be used as ventilative cooling. The potential of cooling with natural ventilation and mechanical ventilation remains an important topic to meet the needs of the larger section of the population who cannot afford to air-conditioning system as well as to reduce the energy consumption and greenhouse gas emission due to space cooling demands. The effectiveness of

Ventilative cooling is dependent on the availability of suitable ambient conditions to provide cooling to the space and the comfort requirements.

## 2 LITERATURE REVIEW

Literature provides extensive guidance on theory, design and examples of ventilative cooling strategies (Axley, Emmerich, Dols, & Walton, 2002; Heiselberg, 2002; Jicha & Charvat, 2007; Kolokotroni & Heiselberg, 2015). Salcido et.al conducted an extensive literature review of the past work(1996-2016) on mixed-mode ventilation(Salcido, Raheem, & Issa, 2016). As shown in Figure 1, the study also documents percentage of energy saving potential by optimized window operation in mixed-mode buildings for various climate zones.

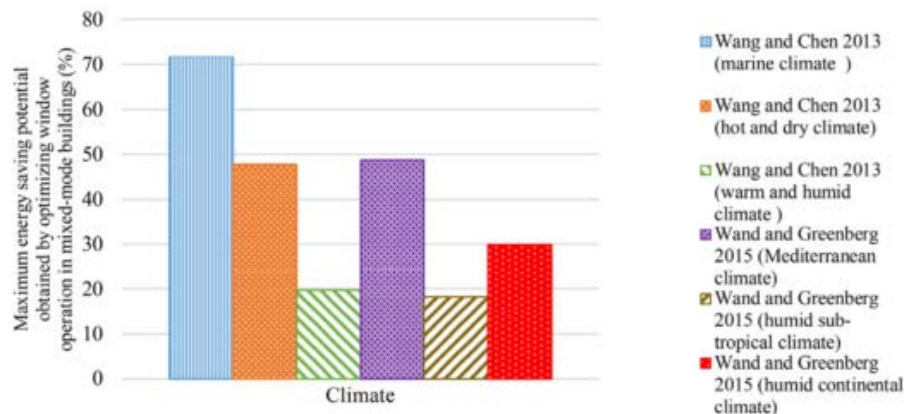


Figure 1: Overview of Research Methodology

Image Source: (Salcido et al., 2016)

Albadra and Lo(Albadra & Lo, 2014)performed short-term environmental monitoring and dynamic energy modeling of selected naturally ventilated domestic buildings in Lebanon and Jordan. Their initial results showed that computer modeling overestimates ventilation rates through windows with Venetian shutters. Aflaki et.al (Aflaki, Mahyuddin, & Baharum, 2016) demonstrated that the ventilation can vary a lot based on orientation and height.Both of these studies highlight the importance of field measurements of ventilation rates in buildings to avoid overestimation of ventilative cooling. Endurthy(Endurthy, 2011) studied in detail on how thermal mass can be coupled with night ventilation to maximize cooling benefits in the building and estimated about 12-13% reduction in electricity use can be achieved through night ventilation in Arizona.

Only a few studies have attempted to study free cooling benefits in buildings in India. Two studies have demonstrate good potential of free cooling and night purge in a commercial building in a temperate climate of Pune (Iddon & ParasuRaman, 2015; Thambidurai, Krishnamohan, Rajagopal, & Velraj, 2015). However, these studies looked at the potential of free cooling in a representative office building with air conditioning systems. Further, the study focused on a demonstration in a favorable climate and did not assess the benefits of different ventilative cooling strategies in the building.

Gradillas (Gradillas, 2015)studied the benefits of natural ventilative cooling in an 3 m by 3 m by 3 m cube located in Bhuj, Gujarat using DesignBuilder for single-side and cross ventilation strategies. However, the results are expected to be quite different for a complex residential building. Thomas (Thomas & Thomas, 2014)states that the significant energy savings potential can be achieved if the apartments in India are designed as per natural ventilation guidelines and principles mentioned in national building codes (NBC). While it provided suggestions on possible natural ventilation strategies for a residential plan and

suggested good potential of the same based on climate analysis, it has not simulated or calculated benefits of the approach.

This paper attempts to study the effectiveness of ventilative cooling in Indian residences first using simulation tools. Further, the study conducts periodic field measurement for one month in an apartment to compare the results with the simulation models.

### 3 METHODOLOGY

The approach of the study is to use the already available data of apartment typology in two climates of India, one which is considered favorable for ventilation (temperate) and one which is a harsh climate for ventilative cooling strategy (hot and dry). Simultaneously, conduct some actual measurement in hot and dry climate observe the difference to validate input assumptions for simulation models. Figure 2 shows the steps followed for simulation as well as measurement study.

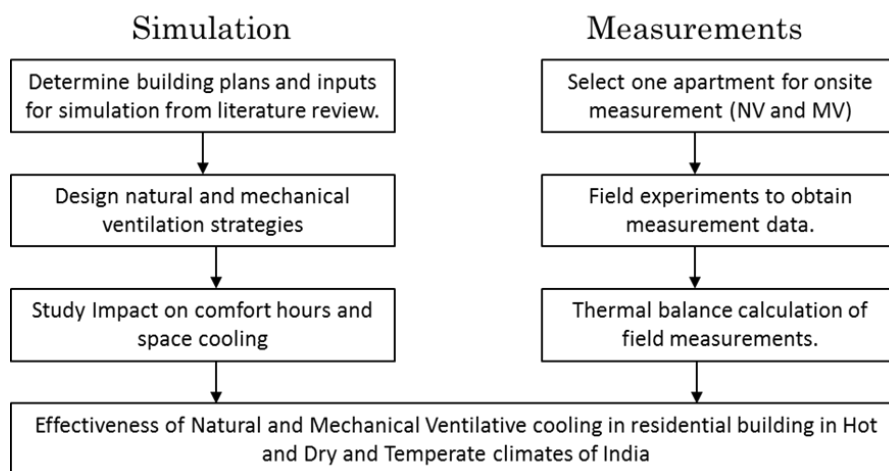


Figure 2: Overview of Research Methodology

#### 3.1 Simulation Models

To assess ventilative cooling potential in India, the study needs to first identify typical residential plans and constructions in India. Rawal and Shukla (Rawal & Shukla, 2014) selected five typical apartment layouts based on a survey of existing building plans and modeled them in DesignBuilder to estimate energy consumption of a typical residential apartment. They also surveyed eight hundred (800) residences in India to develop appropriate inputs on equipment penetration and simulation inputs. Hence, one bedroom, two bedroom, and three bedroom floor plans identified in the above study is used to model typical residential building in order to estimate benefits of ventilative cooling.

The study also highlight that the Indian residences are designed for zoned mixed mode where an air conditioning system is typically installed only in the bedrooms. Further, the air-conditioning system in the bedroom operates in change-over mixed mode where the system runs only during extreme weather periods. Manu (Manu, Shukla, Rawal, Thomas, & Dear, 2016) developed adaptive comfort model suitable for mixed-mode buildings in India known as IMAC (India Model of Adaptive Comfort). This model is primarily developed for commercial building operated in mixed-mode operation. In the lack of a perfect comfort model for this residential study, the IMAC has been used for set points as it is developed for Indian context and is applicable for mixed-mode buildings. This comfort model has recently been integrated into the revised National Building Code. IMAC is used as comfort criteria for

typical residences in India to determine the number of uncomfortable hours and to use the set points to estimate the flow rate.

Table 1 provides key simulation inputs in simulation model. Ahmedabad location is selected under hot and dry climate and Bangalore is selected under the temperate climate.

Table 1: Key Simulation Inputs

Envelope Construction and Thermal Properties	
Wall	12mm Outside Plaster + 230 mm brick wall + 12 mm Inside Plaster U-Value - 1.722 W/m <sup>2</sup> -K
Roof	10 mm Tiles + 12mm Plaster + 150 mm concrete roof + 12mm Plaster U-Value - 2.942 W/m <sup>2</sup> -K
Window	Single Glazing with Aluminium Frame 22% Window to Wall Ratio (as per plan) U-Value - 5.8 W/m <sup>2</sup> -K, SHGC - 0.82, VLT - 0.8
Floor	10 mm Tiles + 12mm Plaster + 150 mm concrete roof + 12mm Plaster U-Value - 2.942 W/m <sup>2</sup> -K
Zone Area, Operation Schedule, Occupancy and Internal Heat Gains	
Bedroom	Operation: 10 pm to 7 am, Internal Gains (lighting + equipment): 320 Watts, Occupancy: 2 people, Area: 9.6 m <sup>2</sup>
Living Area / Kitchen / Others	Operation: 7 am to 10 am and 7 pm - 10 pm, Internal Gains (lighting + equipment): 800 Watts, Occupancy: 2 people

The following natural and mechanical ventilative cooling strategies have been identified for evaluation in the simulation model (Figure 3):

- Natural ventilation - Single-side one opening, Cross-ventilation (openings in opposite direction of the room), Single-sided two openings, one on top of the other (stack)
- Mechanical Ventilation - Fan assisted cross-ventilation (openings in opposite directions), Fan assisted single sided two openings at different heights (stack)



Figure 3: Sectional sketch of Ventilative Cooling Strategies

These ventilative cooling strategies are designed using sizing methods described in IEA-Annex 62 and are incorporated in the residential plans to assess the ventilative cooling benefits. The initial aim of the paper was to use Coolvent to estimate ventilative cooling benefits. However, Coolvent could not model the detailed plan of the residential buildings especially zoned mixed-mode configurations. Hence, the typical residential apartments are modelled in DesignBuilder V4.5.1.178 (Designbuilder, 2017). This tool has a user-friendly interface with capability of whole-building energy simulation, load calculation and natural ventilation mode simulation.

### 3.2 Field Measurements

Past literature emphasized the importance of field measurement to avoid overestimation of ventilation rates. Hence, this research incorporates air changes per hour (ACH) as one of the important measurements during field measurements. The approach devised for field measurement was a variant of the continuous tracer gas injection method (Persily, 2016; Sherman, 1990). But here, the measured sublimation rate of dry ice was used as a tracer gas source for generating CO<sub>2</sub> inside the room. The intention was to be able to measure the continuous ventilation rates to quantify the ACH for calculation of the measured ventilative cooling effect.

An unoccupied two-bedroom apartment was selected for field measurements on the first floor (one floor above ground floor level) of an apartment complex. One bedroom with windows on East and South direction was the focus for monitoring purpose and was set up with measurement instruments to measure the ventilation rates (as explained below). Figure 4 shows the layout of the field measurement equipment at the monitoring site. The red dots represent the location of surface temperature sensors. The black dot represents the location of CO<sub>2</sub> logger. The blue dot represents the location of the air temperature and humidity logger. There is a ceiling fan situated in the centre of the room, which is operated at a low speed throughout the measurement period for proper mixing of the air inside the room.

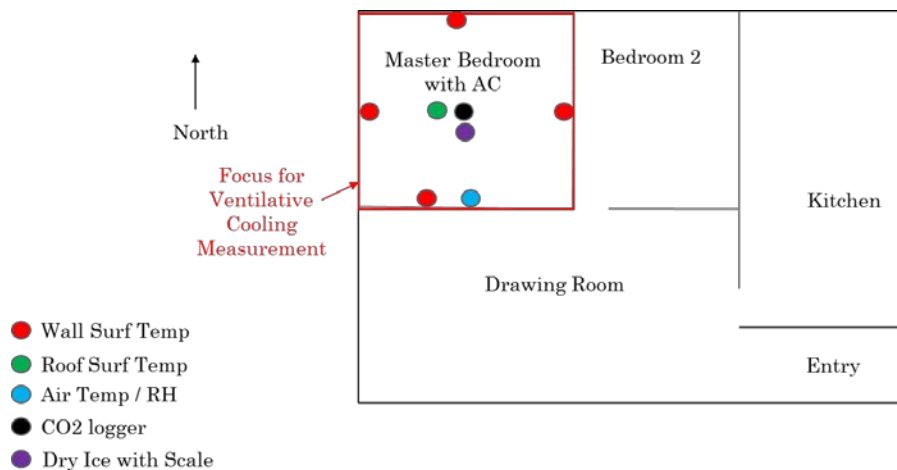


Figure 4: Apartment layout of field measurement

During field measurements of ventilative cooling, an important parameter to monitor in building is ventilation rate. A block of dry ice of around 10 kg is placed in an insulated box on a precision electronic weighing scale in the centre of the room and allowed to slowly release carbon dioxide (CO<sub>2</sub>) in the space. More dry ice is added daily to keep continuous generation. The weighing scale is connected to a laptop placed at the site and is given command through a Python code to continuously log the weight of the dry ice at 5 minutes' intervals. Concurrently, to measure the CO<sub>2</sub> concentration inside the space, a calibrated HOB0 MX 1102 logger is used (Onset, 2017) to continuously measure and store CO<sub>2</sub> levels in the space every 5 minutes. Once the CO<sub>2</sub> source strength (mass of dry ice sublimated into gaseous CO<sub>2</sub>) and the well-mixed indoor CO<sub>2</sub> concentration are measured, it is possible to calculate the air exchange rate using a mass balance model. The continuous ventilation rates are calculated for each measurement period using the mathematical expression for change in mass concentration of indoor CO<sub>2</sub> (Traynor, Aceti, Apte, Smith, & Green, 1989).

The inside surface temperatures of the six surfaces (four walls, floor and ceiling) were measured using thermistors in a circuit made with the help of Arduino Uno board (Arduino, 2017). The temperature data were recorded continuously for every time step of 5 minutes as per the code uploaded in the board, and were stored in the memory card inserted in the

Arduino circuit board. Outdoor weather data were obtained from online website (WorldWeatherOnline, 2017).

Simplified room thermal balance is used to understand the effectiveness of ventilative cooling in the monitored space. This calculation provides the difference in the temperature achieved with taking into consideration all the components adding to or removing the heat from the space. The field measurements were carried out in an unoccupied apartment; hence occupant gain was nil. Lighting, and equipment details were noted down from onsite visits and the cooling loads caused by them are calculated using 2009 ASHRAE fundamentals (American Society of Heating, Refrigerating, and Air Conditioning Engineers, 2009). Similarly, construction details of wall, roof, floor, and window were obtained for the measured apartment to calculate area, specific heat, and thermal conductivity of each envelope components.

## 4 RESULTS AND DISCUSSIONS

### 4.1 Simulation Results

The simulation results generated from the Design Builder software for the apartment models created for the study are compared using two metrics – uncomfortable hours and reduction in thermal cooling needs of the space. The simulation results are compared using the operation model described in Figure 5.

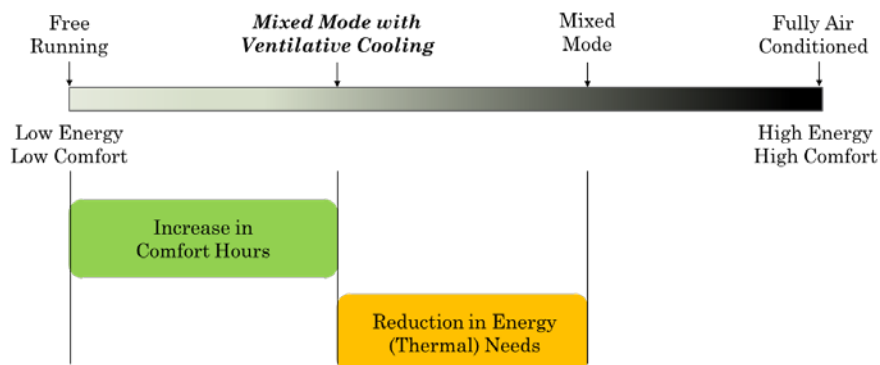


Figure 5: Parameters to quantify cooling benefits for various modes

As seen in Table 2, natural (NV) and mechanical ventilation (MV) can reduce annual uncomfortable hours by 10-12% and 21-40%, respectively, as compared to free-running mode.

Table 2: Percentage Reduction in Annual Comfortable Hours

% Reduction in annual discomfort Hours	Ahmedabad			Bangalore		
	1BHK	2BHK	3BHK	1BHK	2BHK	3BHK
Free Running	0%	0%	0%	0%	0%	0%
NV - Single Sided (One Opening)	5%	5%	6%	7%	7%	8%
NV - Cross Ventilation	14%	16%	13%	26%	11%	37%
NV - Single Sided (Two Openings- Stack)	12%	13%	10%	19%	8%	24%
MV - Fan Assisted Cross Ventilation	19%	21%	19%	27%	17%	35%
MV - Single Sided (Two Openings- Stack)	21%	23%	22%	28%	22%	43%

The ventilative cooling benefits are 2-10% higher in temperate climate as compared with hot and dry climate. The ventilative cooling benefits are slightly higher (3-5%) for cross-ventilation as compared to the single-sided ventilation.

Table 3: Percentage Reduction in Annual Thermal Cooling (kWh)

% Reduction in Thermal Cooling (kWh)	Ahmedabad			Bangalore		
	1BHK	2BHK	3BHK	1BHK	2BHK	3BHK
MM (No Ventilative Cooling)	0%	0%	0%	0%	0%	0%
NV - Single Sided (One Opening)	5%	4%	4%	7%	3%	5%
NV - Cross Ventilation	12%	12%	9%	14%	13%	12%
NV - Single Sided (Two Openings- Stack)	8%	9%	7%	13%	14%	10%
MV - Fan Assisted Cross Ventilation	29%	30%	27%	30%	27%	24%
MV - Single Sided (Two Openings- Stack)	31%	34%	30%	33%	31%	28%

## 4.2 Field Measurement Results

The measurements were done for a period of 30 days in the month of March and April. Data were recorded for three modes; free running, natural ventilation, and mechanical (fan-assisted) ventilation in random order during the course of measurement period. As explained in the methodology section, dry ice weight and CO<sub>2</sub> level are continuously measured in the room during field measurements. As an example, Figure 6 shows measured dry ice weight and CO<sub>2</sub> measurements for 25<sup>th</sup> – 26<sup>th</sup> March. Each dot in the figure shows measured value at every five-minute sampling interval. The total measurement period shown in the figure is approximately 11 hours (129 measurements at every five-minute intervals). As seen in the figure, CO<sub>2</sub> level (ppm) in the space increased from 480 to 2100 ppm. During the same period, dry ice weight reduced by 500 grams (from 6.4 to 5.9 Kilograms) during the measurements period. The dry ice weight in the graph also shows inherent noises due to scale accuracy and limitations of the manual measurement approach. Hence, to filter the noises and to find a mean dry weight for the measurements period for further calculations, the measurements were fit with exponential curve fit. Very good fit was obtained ( $R^2 > 0.95$ ) with exponential curve indicating the average weight change on scale are captured appropriately with exponential curve fit.

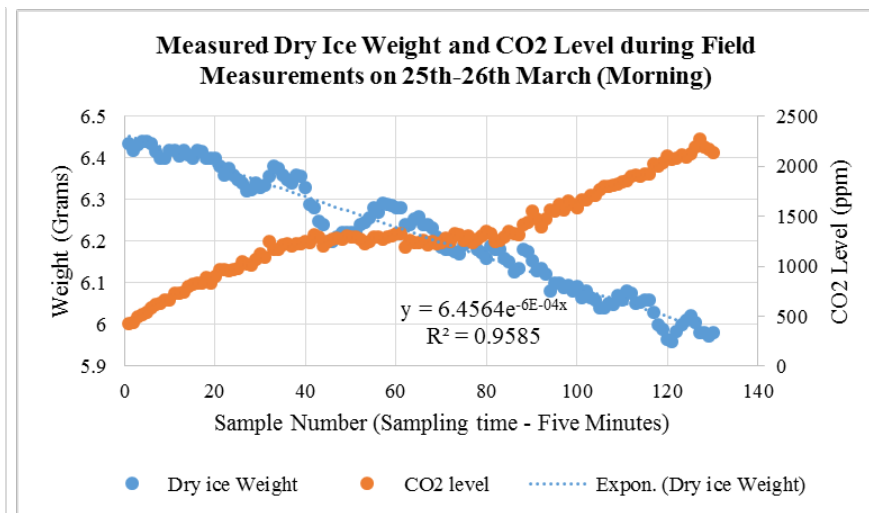


Figure 6: Measured CO<sub>2</sub>, dry ice weight

ACH values were calculated from the data collected for CO<sub>2</sub> ppm and dry ice weight. Figure 7 shows the summary of the entire measurement period of the ventilation rates observed in different modes of window operation. As can be seen Figure 7, the closed window mode or the free running mode where there is no natural ventilation happening, the air change as a result of infiltration shows the values of 0 to 2 ACH with the average value of 1 ACH. In the natural ventilation mode when the windows are open from morning to evening, the ACH values varies between 2.5 to 25 ACH and the average value is observed to be 5 to 7 ACH.

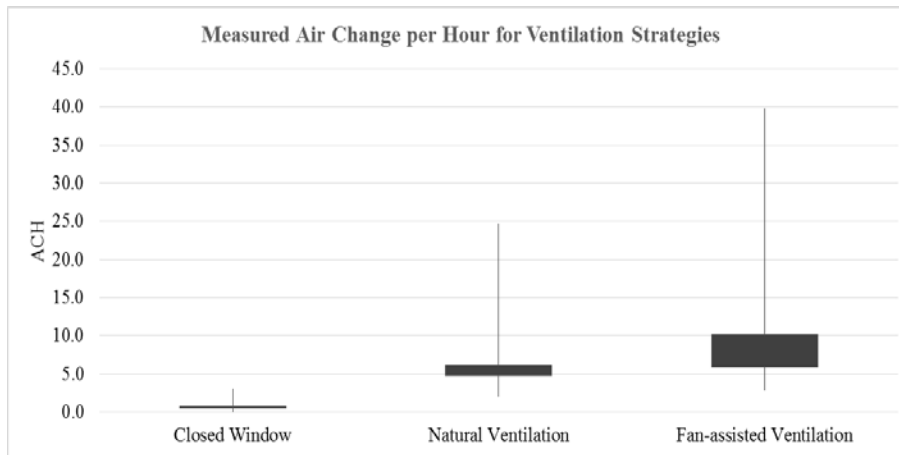


Figure 7: Summary of ACH in Different Window Operation Mode

For the fan-assisted mode, where a fan is kept on inside of the open window, the ACH values vary between 3 ACH to 40 ACH sometimes with an average value observed to be around 6-10 ACH. Once ACH is calculated, mass balance using air flow and temperature difference of indoor air and outdoor is used to calculate heat gain (heating) or heat loss (cooling) through ventilation.

Table 4: Summary of Ventilative Cooling during Field Measurements

Date	Minutes	Count	Cooling Needs (Watts)			Ventilative Cooling (Watts)			%Ventilative Cooling Possible			Operation Mode
			Average	Max	Min	Average	Max	Min	Average	Max	Min	
22nd Mar	85	17	101	158	69	-9	6	-50	100%	71%	-9%	Closed Window
23rd Mar	270	54	221	342	144	17	64	-10	-7%	7%	-19%	Closed Window
25th Mar	725	145	366	472	134	51	291	-125	-13%	30%	-72%	Closed Window
26th Mar	1370	274	271	534	32	220	2924	-95	-51%	100%	-100%	Closed Window
28th Mar	130	26	-85	0	-131	2	10	-9	4%	23%	-7%	Closed Window
29th Mar	745	149	-4	310	-212	-3	143	-84	-37%	100%	-100%	Closed Window
2nd Apr	830	166	396	483	185	65	471	-43	-16%	9%	-100%	Closed Window
17th Apr	1440	288	361	582	113	-24	459	-785	10%	100%	-96%	Closed Window
24th Mar	115	23	112	139	77	-125	-8	-405	100%	100%	6%	Open Window
26th Mar	1370	274	271	534	32	220	2924	-95	-51%	100%	-100%	Open Window
27th Mar	370	74	157	245	75	78	5728	-1090	21%	100%	-100%	Open Window
3rd Apr	1415	283	283	503	35	-18	519	-474	22%	100%	-100%	Open Window
4th Apr	1410	282	283	442	91	4988	97801	-315	-100%	100%	-100%	Open Window
7th Apr	145	29	152	180	117	-22	75	-152	18%	100%	-45%	Open Window
8th Apr	1440	288	268	450	38	367	3294	-432	-37%	100%	-100%	Open Window
9th Apr	835	167	240	573	41	121	2183	-550	76%	100%	-100%	Open Window
20th Apr	55	207	239	495	9	582	13649	-29542	100%	100%	-100%	Open Window
12th Apr	130	26	113	213	38	159	854	-53	-100%	38%	-100%	Open Window and Fan
13th Apr	1420	284	-1	131	-140	721	52599	-2663	-100%	100%	-100%	Open Window and Fan
14th Apr	885	177	-24	161	-219	1731	56475	-712	-100%	100%	-100%	Open Window and Fan
15th Apr	655	131	513	610	278	-1142	29047	-33529	100%	100%	-100%	Open Window and Fan
16th Apr	1430	286	341	570	34	63	6103	-2081	100%	100%	-100%	Open Window and Fan
17th Apr	1440	288	361	582	113	-24	459	-785	10%	100%	-96%	Open Window and Fan
18th Apr	145	29	216	317	147	70	3586	-2174	-22%	100%	-100%	Open Window and Fan
19th Apr	1440	288	235	449	-5	295	4238	-1195	100%	100%	-100%	Open Window and Fan
20th Apr	1035	207	239	495	9	582	13649	-29542	100%	100%	-100%	Open Window and Fan

Table 4 shows the calculated amount of cooling load (watts) requirement for the monitoring space through heat balance equation. It also shows the ventilative cooling contribution in watts and percentage as average, maximum and minimum value for each day of measurement. Further, using the inside surface temperature and air temperature measurements, a simplified room thermal balance is used to understand the effectiveness of ventilative cooling in the monitored space. The cooling ventilative cooling benefits are classified in 0-25%, 25-50%, 50-75%, >75% benefits throughout the measurement periods. Since the window is at one position, negative benefits are also achieved when outdoor conditions are not favourable. Table 5 provide summary of ventilative cooling benefits during the field measurements.

Table 5: Measured Ventilative Cooling Benefits

	Closed Window		Natural Ventilation		Fan Assisted Ventilation	
	Hours	% Monitored Hours	Hours	% Monitored Hours	Hours	% Monitored Hours
Not Measured	395		320		293	
0-25% Cooling Benefit	70	19%	60	11%	44	8%
25-50% Cooling Benefit	24	6%	39	7%	22	4%
50-75% Cooling Benefit	12	3%	16	3%	12	2%
>75% Cooling Benefit	3	1%	117	22%	128	22%
Negative Benefits	264	71%	312	57%	365	64%
Total Hours	768		864		864	
<b>Outdoor Air Temperature (deg C) - Only during Monitored Hours</b>						
Max	43		44		45	
Min	27		25		28	
Average	35.7		34.8		36.8	
Standard Deviation	0.5		0.52		0.55	

The period where ventilative cooling can meet more than 75% of space cooling needs increases from 1% in closed window (infiltration only) to 22% in natural and mechanical ventilation modes. Outdoor conditions during the monitoring period is similar between the three operation modes with slightly higher outdoor temperature during open mechanical (fan-assisted) ventilation modes. Natural and mechanical ventilation strategies performed very similar during the monitoring period.

## 5 CONCLUSIONS

The simulation results demonstrate good potential for natural and mechanical ventilation strategies to be effective for apartment residences in India. Adding ventilating cooling using natural ventilation in a typical residential apartment provides 5-43% increase in comfortable hours for two climate zones of India as compared with free running building. Ventilative cooling with mechanical ventilation provides significant comfort benefits (14-25% as compared to ventilative cooling with natural ventilation) and is beneficial to incorporate in residential apartment buildings. When compared to mixed mode buildings with no ventilative cooling, ventilative cooling can reduce thermal load of the apartment by 4-14% and 24-34%. While ventilative cooling is more effective in temperate climate, significant benefits can be achieved even in hot and dry climate of India during night periods. A novel method to continuously measure ventilation rate is developed for affordable yet accurate measurements. The measurements are performed for one month in a bedroom of apartment building where air change per hour and ventilative cooling benefits are calculated for one bedroom. The finding indicates significant savings benefits for natural and mechanical ventilation. Unlike simulation, the benefits measured in field indicated similar benefits between natural and mechanical ventilation. This could be due to slightly worse outdoor conditions during mechanical ventilation measurements or due to underestimation / overestimation of natural and mechanical ventilation savings in simulation models.

## 6 REFERENCES

- Aflaki, A., Mahyuddin, N., & Baharum, M. R. (2016). The influence of single-sided ventilation towards the indoor thermal performance of high-rise residential building: A field study. *Energy and Buildings*, 126, 146–158.  
<http://doi.org/http://dx.doi.org/10.1016/j.enbuild.2016.05.017>
- Albadra, D., & Lo, S. (2014). The Potential for Natural Ventilation as a viable Passive Cooling Strategy in Hot Developing Countries. *PLEA 2014 - 30th INTERNATIONAL PLEA CONFERENCE*, (December), 1–10.

- American Society of Heating, Refrigerating, and Air Conditioning Engineers, I. (2009). *2009 ASHRAE Handbook - Fundamentals*. (I. American Society of Heating, Refrigerating, and Air Conditioning Engineers, Ed.) (Vol. 30329). American Society of Heating, Refrigerating, and Air Conditioning Engineers, Inc.
- Arduino. (2017). Arduino UNO. Retrieved May 3, 2017, from <https://www.arduino.cc/en/main/arduinoBoardUno>
- Axley, J., Emmerich, S., Dols, S., & Walton, G. (2002). An Approach to the Design of Natural and Hybrid Ventilation Systems for Cooling Buildings. *Indoor Air*, 836–841.
- Central Statistics Office. (2016). *Energy statistics 2016. Ministry of Statistics and Programme Implementation Government of India*.
- Designbuilder. (2017). DesignBuilder. Retrieved from <http://www.designbuilder.co.uk/>
- Endurthy, A. R. (2011). *Coupling of Thermal Mass with Night Ventilation in buildings*. Arizona State University.
- Gradillas, M. (2015). Cooling Potential of Natural Ventilation for Affordable Housing in India.
- Heiselberg, P. (2002). Principles of hybrid ventilation. *IEA Annex 35: Hybrid Ventilation in New and Retrofitted Office Buildings*.
- Iddon, C. R., & ParasuRaman, N. (2015). Night purge as a means to reduce cooling load of an office in Pune, India. *Proceedings of Building Simulation 2015, Hyderabad, 7-9 December*, (Reid 1844).
- Jicha, M., & Charvat, P. (2007). Hybrid ventilation Guidelines, 1–6.
- Kolokotroni, M., & Heiselberg, P. (2015). Ventilative Cooling (State-of-the-art review). *IEA - EBC Programme, Annex 62*, 213. Retrieved from <http://venticool.eu/wp-content/uploads/2013/09/SOTAR-Annex-62-FINAL.pdf>
- Manu, S., Shukla, Y., Rawal, R., Thomas, L. E., & Dear, R. De. (2016). Field studies of thermal comfort across multiple climate zones for the subcontinent : India Model for Adaptive Comfort ( IMAC ). *Building and Environment*, 98, 55–70. <http://doi.org/10.1016/j.buildenv.2015.12.019>
- Onset. (2017). CO2 Logger MX1102. Retrieved May 3, 2017, from [www.onsetcomp.com](http://www.onsetcomp.com)
- Persily, A. K. (2016). Field measurement of ventilation rates. *Indoor Air*, 26(1), 97–111. <http://doi.org/10.1111/ina.12193>
- Rawal, R., & Shukla, Y. (2014). Residential Buildings in India : Energy Use Projections and Saving Potentials. *Gbpn*, (September).
- Salcido, J. C., Raheem, A. A., & Issa, R. R. A. (2016). From simulation to monitoring: Evaluating the potential of mixed-mode ventilation (MMV) systems for integrating natural ventilation in office buildings through a comprehensive literature review. *Energy*

*and Buildings*, 127, 1008–1018. <http://doi.org/10.1016/j.enbuild.2016.06.054>

Sherman, M. H. (1990). Tracer-gas techniques for measuring ventilation in a single zone. *Building and Environment*, 25(4), 365–374. [http://doi.org/10.1016/0360-1323\(90\)90010-O](http://doi.org/10.1016/0360-1323(90)90010-O)

Thambidurai, M., Krishnamohan, N., Rajagopal, M., & Velraj, R. (2015). Free cooling feasibility of a typical commercial building in Pune city, India. *International Journal of Applied Engineering Research*, 10(2), 4419–4435.

Thomas, P. C., & Thomas, L. E. (2014). Effective natural ventilation in modern apartment buildings, (December), 1–8.

Traynor, G., Aceti, J. C., Apte, M. G., Smith, B. V., & Green, L. L. (1989). Macromodel for Assessing Residential Concentrations of Combustion-Generated Pollutants : Model Development and Preliminary Predictions for CO , NO<sub>2</sub> , and Respirable Suspended Particles.

WorldWeatherOnline. (2017). WorldWeatherOnline. Retrieved May 3, 2017, from <https://developer.worldweatheronline.com/api/historical-weather-api.aspx>

# Hybrid ventilation in new and refurbished school buildings – the future of ventilation

Simone Steiger<sup>1</sup>, and Jannick Karsten Roth\*<sup>2</sup>

*1 Fraunhofer Institute for Building Physics  
Fraunhoferstraße 10  
83626 Valley, Germany*

*2 WindowMaster A/S  
Skelstedet 13  
Vedbæk, Denmark*

*\*Corresponding author: jkr.dk@windowmaster.com*

## ABSTRACT

More than 64 million pupils spend more time in school than in any other place except home in Europe (European Commission, 2014). The indoor air quality is often a challenge in existing school buildings and the lack of proper ventilation often leads to negative effects like increased absenteeism and sick building syndrome symptoms as well as lowered performance amongst students compared to new buildings.

For this study a comparison of automated Natural Ventilation (NV), balanced Mechanical Ventilation (MV) with heat recovery and Hybrid Ventilation (HV) with heat recovery has been made by means of detailed modelling applied to an existing school building using the simulation program IESVE. The energy demand for heating and ventilating the building using the three different ventilation methods was calculated for three key European cities; Munich, Copenhagen and London. Control strategies were set to achieve the same indoor climate for all three ventilation systems, and the indoor climate targets were set according to European Standard EN 15251 (EN15251, 2007).

The results show that the energy performance of the MV and NV systems are nearly the same in terms of primary energy, while demonstrating that HV enables energy savings of 44-52%.

Total costs of the different systems including capital expenditure (products and installation), operation (electricity and heating) and maintenance over the first year and a 20 year life cycle were calculated. This showed that in the first year MV was 2.5 to 4 times more expensive than NV. By selecting HV and taking advantage of NV reducing the load on the mechanical ventilation, 25% of the cost could be saved compared to a pure MV system, and this was similar over a 20 year life cycle.

## KEYWORDS

Hybrid ventilation; natural ventilation; mechanical ventilation; ventilation in schools; Indoor Air Quality (IAQ).

## 1 INTRODUCTION

Studies have shown that the combination of automatic NV and MV offers a promising opportunity to achieve significant energy savings in buildings while maintaining a comfortable indoor climate. HV might, as such, be a key technology to enable designers to fulfil ever stricter energy requirements while at the same time providing the user with a healthy and comfortable indoor climate.

The Reshyvent project (Reshyvent, 2004) investigated HV in residential buildings, while the Hybvent project (Heiselberg, 2006) studied the application for non-residential buildings. Several case studies investigated in the international project IEA ECBCS-Annex 35 (Heiselberg, 2006) show that significant energy savings can be achieved in hybrid ventilated

buildings, especially through reduction in fan and cooling energy demand. The case studies for school buildings show that the HV system saves 17-55 % in a year compared to a mechanical system alone. Examples also include Cron(Cron, 2003) who investigated classrooms and found the best results for HV (fan assisted stack ventilation) were in the warmer regions, saving up to 42% energy consumption compared to MV without heat recovery. Comparing HV with MV with heat recovery the results were only better in the warmest regions where there was no requirement for heat recovery. Emmerich (Emmerich, 2004) compared NV, MV and HV and found for HV that heating demand is reduced most in cold regions, and maximum reductions in fan electricity are realised in warm regions compared to purely NV and MV.Sowa (Sowa, 2007) found a reduction of about 60 % for heating demand and about 40 % for fan electricity in a HV simulation for a real school. Heikkinen et al. (Heikkinen, 2002) who investigated ventilation concepts for a school in Finland, found only a limited potential reduction in heating demand, but also a reduction of 70 % in fan electricity.

Thus, the literature contains several findings and in general, HV is demonstrated to result in significant energy savings. This study investigates whether this conclusion is also valid in schools, using state-of-the-art MV and NV systems and a school building fulfilling the performance requirements (in Denmark). This requires very low U-values for the building elements and a requirement for the total primary energy frame in kWh/m<sup>2</sup> per year of 41 + 1000/A (A is the gross floor area). The total primary energy use in the energy frame consists of heating, ventilation, cooling, hot water and lighting. In order to give a true comparison between the energy performances of the systems, nearly identical indoor air quality and thermal climates in the buildings have been established. The simulations are carried out for three large European cities with different climates; Copenhagen, London and Munich. The study also calculates the expected CO<sub>2</sub> emissions and the economical costs from selecting the different systems.

## 2 SCHOOL BUILDING GEOMETRY, PROPERIES AND LOCATION

### 2.1 Building layout

The one storey school building consists of eight classrooms, four on each side of the corridor and is oriented north/south. The floor to ceiling height varies from 2.8 to 4.5m no matter of ventilation principle and the floor area of one classroom is 76m<sup>2</sup>, which gives a total volume of 278m<sup>3</sup>. The building geometry can be seen in Figure 1.



Figure 1: Layout of the school building.

### 2.2 Construction properties

The main construction properties attached to the models are listed in Table 1.

Table 1: Construction properties

<b>Building element</b>	<b>U-Value [W/m<sup>2</sup>K]</b>
Ground Slab	0.08
Exterior Walls	0.12
Roof	0.08
Windows	0.9-1.1

Glass ratio of the outer façade is 45 % and the g-value is 0.63 and light transmittance is 0.74. Only the windows which aren't used for natural ventilation have an external sun screening with a shading coefficient of 0.2.

### **2.3 Internal heat loads**

There are 28 students and one teacher in each classroom, resulting in an occupancy density about 2.6 m<sup>2</sup>/person. The occupancy during lessons are 95 % from Monday to Friday from 8 am to 2:50 pm. Vacation time is 12 weeks per year in total (week 7, 14, 20, 26 - 31, 42 and 51 - 52). The occupancy during vacation is set to 10 % from 8:00 am to 2:50 pm from Monday to Friday, as summer courses or maintenance might occur. There is no occupancy during weekends.

Each person has a heat load of 75 W sensible heat and 50 W latent heat corresponding to an adult with an activity level of 1.2 met. This assumes a heat emission of 70 W/m<sup>2</sup> skin surface and a skin surface of 1.8 m<sup>2</sup>. Children with a lower body mass normally also have a higher level of activity of about 1.4 met(81 W/m<sup>2</sup>skin surface). Assuming a skin surface of 1.5 m<sup>2</sup> per child, the heat emission for all persons is quite the same.

Each student and teacher is expected to have a computer, which is switched on 50 % of the time during occupancy. As it is expected that the use of computers will increase in the future.

The lighting (fluorescent lighting) shall provide a luminance intensity of 300 lux at the desk and has a maximum heat load of 15 W/m<sup>2</sup>, which corresponds to an effective lighting system (a luminous efficacy of 20 lumens per watt).

### **2.4 Outdoor climatic conditions**

The locations chosen for the comparison are Copenhagen, Munich and London. These three cities are typical European cities with different climates and therefore different possible opportunities for HV. Copenhagen has a cold winter and a cool summer, whereas Munich has a colder winter and a warm summer. London, located near the sea, has a maritime climate with a mild winter and a cool summer.

## **3 REQUIREMENTS FOR INDOOR AIR QUALITY AND THERMAL COMFORT**

Several studies have shown that many of the existing schools have a poor indoor climate with CO<sub>2</sub> levels sometimes exceeding 2-4,000 ppm (Byg DTU, 2009). These levels are clearly adversely affecting the learning ability of the school children (Mendel, 2005. Wargocki, 2007. Wargocki, 2007) - and must be improved. However, general adoption of the current Category

II requirements in EN 15251 with a maximum CO<sub>2</sub> concentration of 900ppm seems unrealistic in schools for two key reasons: Firstly, the air exchange rate for a 60 m<sup>2</sup> classroom with a room height of 2.8m and 29 persons needs to be at least 6-7 air change per hour. This can create problems with air speeds in the comfort zone in the majority of existing schools. Secondly, it is also noted that the financial abilities of the public authorities in most countries does not support such strict requirements. In fact, they could prove to be a barrier against improving the indoor climate in existing schools simply because the systems become too expensive.

The classification of the thermal comfort and indoor air quality in the buildings are based on EN 15251. Category III is deemed an acceptable level of expectation and a target of 1200ppm is applied for the assessment of indoor climate.

## **4 DIMENSIONING OF VENTILATION SYSTEMS**

To maintain the air quality according to Category III of EN 15251 (EN 15251, 2007) the necessary air flow rate was calculated by the air flow rates per m<sup>2</sup> given in the standard for persons in a classroom and low emissions from the building. This results in a flow rate of 2.4 l/sm<sup>2</sup> and a total air flow rate of 180 l/s, 648 m<sup>3</sup>/h. The total flow rate for all 8 classrooms is 1,440 l/s or 5,148 m<sup>3</sup>/h. For maintaining temperature, different air change rates were tested in the simulation. Due to these results a maximum air exchange of 4.6 per hour was chosen for summer and night ventilation. This is a flow rate of 360 l/s or 1,296 m<sup>3</sup>/h for one classroom and 2,880 l/s or 10,368 m<sup>3</sup>/h for all eight classrooms.

### **4.1 Natural ventilation**

For the NV every second high level window on both sides of the room can be opened with motors to realize cross ventilation. The resulting openable window area for the automated windows is 4.1 m<sup>2</sup> representing 5.4 % of the room area.

A temperature difference of 1 K and 5 K between inside and outside results in almost 4 and 9-fold air exchange respectively. A wind speed of 0.5 m/s and 1 m/s results in a 5 and 10-fold air exchange rates respectively - calculated according to the British Standard Method (Allard, 1998). Outdoor conditions with 0.5 m/s wind speed and a temperature difference above 1 K should be available most of the time throughout the year for all three locations and would also be sufficient for delivering adequate ventilation to maintain temperatures in summer.

### **4.2 Mechanical ventilation**

For the MV in the school building, four smaller decentralized units are utilized. The system was dimensioned for the maximum air flow rate according to air quality and indoor temperature (10,368 m<sup>3</sup>/h). The specifications of the four units have been selected from those products currently available in the market place, resulting in a total flow rate of 15,680 m<sup>3</sup>/h.

The pressure loss for the supply and the exhaust ductwork of the system is only 80 Pa for the supply system and 80 Pa for the exhaust system. The filter classes were F7 for supply air and F5 for exhaust air causing an additional pressure of 40 Pa due to dirt. The Specific Fan Power (SFP) value for each of the four units is 993 J/m<sup>3</sup> - which is probably among the best currently available in the market. No additional heating or cooling units were utilised. As the 'Demand

Controlled Ventilation operates with a constant pressure loss in the main ductwork, the setting for the external pressure was held constant.

The heat recovery system is a state-of-the-art counter-flow plate heat exchanger with low-energy de-icing function, and the sensible heat effectiveness in the simulation was set to 92 %, which is the temperature efficiency including the effects of the motor heat at 1800 m<sup>3</sup>/h, 75 % of the design flow rate.

### **4.3 Hybrid ventilation**

For the HV two decentralized units are utilised and dimensioned for the air flow rate only according to air quality (5,148 m<sup>3</sup>/h). To maintain indoor temperature in summer NV is utilized with a flow rate of 10,368 m<sup>3</sup>/h. Hence the mechanical element of the system can be of significantly lower capacity than that used for pure MV.

The pressure loss in the MV element of the system for the supply and the exhaust ductwork is then about 132 Pa for the supply system and 143 Pa for the exhaust system. Pressure loss from filters, sensible heat effectiveness and heating/cooling unit is the same as the MV. SFP value for each of the two units is 1135 J/m<sup>3</sup>.

## **5 CALCULATION METHOD**

The energy demand and the indoor climate of the building were simulated in the widely recognised simulation program VE-Pro (version 6.4.0.7, Integrated Environmental Solutions Limited, Glasgow, UK). This program has a special function for calculating more complex HVAC systems (ApacheHVAC) and also a very reliable calculation tool for NV (MacroFlo), which is able to calculate NV and effects from wind turbulence on air exchange, considering special features like the aspect ratio and sash type of the opening. The calculation was done in 1 minute steps to achieve realistic results for natural and especially natural pulse ventilation. The results are derived from 6 minute averages of the calculation. This is mainly due to the pulse ventilation when using natural ventilation, which has to be controlled very precisely in order to avoid over cooling of the room during cold periods.

For the assessment of indoor climate, CO<sub>2</sub> levels inside the building were used as an indicator for indoor air quality, and operative room temperature was used as an indicator for thermal comfort. The values were obtained during occupancy in one representative room, and the requirements for thermal comfort and indoor air quality were based on EN 15251 (EN 15251, 2007).

## **6 CONTROL STRATEGIES**

The operational parameters of the control strategy for the simulation models were input to reflect as closely as possible WindowMaster's control strategy. Sometimes changes were necessary due to the restrictions of the simulation software or to obtain a similar thermal comfort and indoor quality.

## **6.1 Natural ventilation**

NV is defined as automated NV through high level windows on both sides of the rooms utilizing cross ventilation. The windows are opened and closed by a specific amount with small MotorLink™ chain drive actuators. The opening distance is defined by a controller, which uses indoor and outdoor climatic parameters to calculate the appropriate opening distance. This precise opening is necessary, because the resulting air flow rate is not only dependent on the climatic conditions, but also very much on the opening distance of the windows. A precise control of air flow is necessary to avoid too high ventilation rates, which cause additional heat loss or poor thermal comfort due to low temperatures or high draughts, while still providing good air quality at the same time.

Three different opening strategies were implemented; continuous ventilation with a varying opening degree, pulse ventilation with the maximum opening degree calculated due to weather for a short time, and night ventilation. The first strategy is utilized for control of air quality during the whole year and indoor temperature in summer. The second strategy is only for additional control of indoor air quality during winter and transient times, where the opening distance for continuous ventilation needs to be restricted for comfort reasons. The third strategy is utilized for additional cooling of the rooms in summer. In addition, the windows are opened to maximum after occupancy to purge ventilate the rooms completely with fresh air until outdoor air quality is reached.

## **6.2 Mechanical ventilation**

The flow volume of the MV is defined by the need to achieve the required improvement of indoor air quality and reduction of overheating. Therefore, the maximum flow volume is utilized when either the carbon dioxide level or the indoor air temperature rises above a certain point. Furthermore, night ventilation is only active during the warmer periods

## **6.3 Hybrid ventilation**

The HV control strategy is a combination of the natural and mechanical control strategies. The main strategy is to use the best aspects of both systems in order to reach the best possible values for energy consumption and indoor climate quality.

During winter season, only MV is activated as the heat recovery of the system helps save energy to heating. NV has best results during summer where good indoor air quality and temperatures can easily be reached. In addition, the motors of the windows need much less electricity than the fans for MV and the flow rate can be raised by simply increasing the window openings a little more without using further energy. This is also the benefit from NV during night time for ‘free cooling’.

During the transient season, it mainly depends on internal conditions as to whether MV or NV is the best solution. Therefore, the system automatically chooses between NV or MV depending on indoor temperature as an indicator of demand for heating or possible cooling.

## 6.4 Heating, shading and lighting

The heating is activated from October to May. The heating is set to avoid too low temperatures in accordance to Category III during occupancy (8 am - 2:50 pm). During hours with no occupants in the building the set-point is 18°C.

The operation of automated external blinds is according to outdoor and indoor parameters. This is done to avoid overheating, which may affect indoor temperature and thermal comfort for up to a few days later. The blind rises with a wind velocity above 12 m/s and/or an outdoor temperature below minus 6°C to avoid damage to the blinds. The blind lowers with a solar radiation above 100 W/m<sup>2</sup> and if the indoor temperature is above 23.5°C.

The dimming of artificial light is controlled due to occupancy and to maintain 300 lux in the rooms.

## 7 RESULTS

### 7.1 Temperature and CO<sub>2</sub>

The results of thermal comfort and indoor air quality were evaluated for one south facing classroom, as negligible differences were found between a north and south facing classroom. Figure 2 shows the percentage of occupied time where indoor temperature achieved the different performance categories according to EN 15251 (EN 15251, 2007). This is displayed for all three ventilation types in each location.

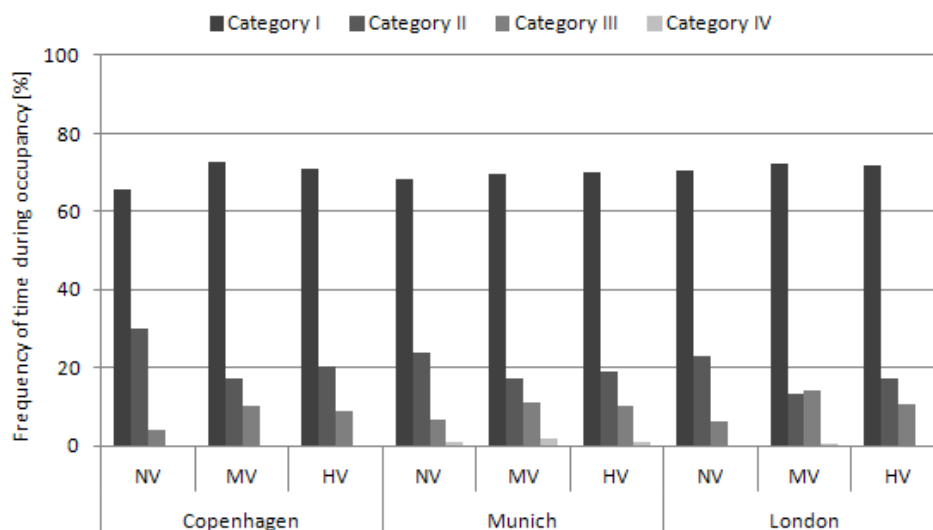


Figure 2. Percentage of occupied time where indoor temperatures achieved the different performance categories according to EN 15251

Only very small temperature variations were found for the different locations. This implies that each of the three ventilation systems would achieve similar levels of thermal comfort in each location. A similar picture was found when comparing the CO<sub>2</sub> levels. The result showed that Category II performance could be achieved 45-55% of the time depending on the ventilation system, while the remainder of the time fulfilled the requirements according to Category III.

## 7.2 Primary energy

For the calculation of the total primary energy consumed (sum of heating and fan electricity demand multiplied by the primary energy factors) the nationally adopted primary energy factors have been used for the different locations; Munich (district heating: 0.7; electricity 2.6), Copenhagen (0.8; 2.5) and London (1.2; 2.92).

Figure 3 shows the primary energy consumption. Comparing the primary energy consumption figures it can be seen that heating energy demand can be reduced by nearly 70 % for HV compared to NV. Fan electricity can be reduced by 75 % for HV compared to MV. Total primary energy is almost the same for MV and NV, but can be reduced by up to 50 % by utilising HV.

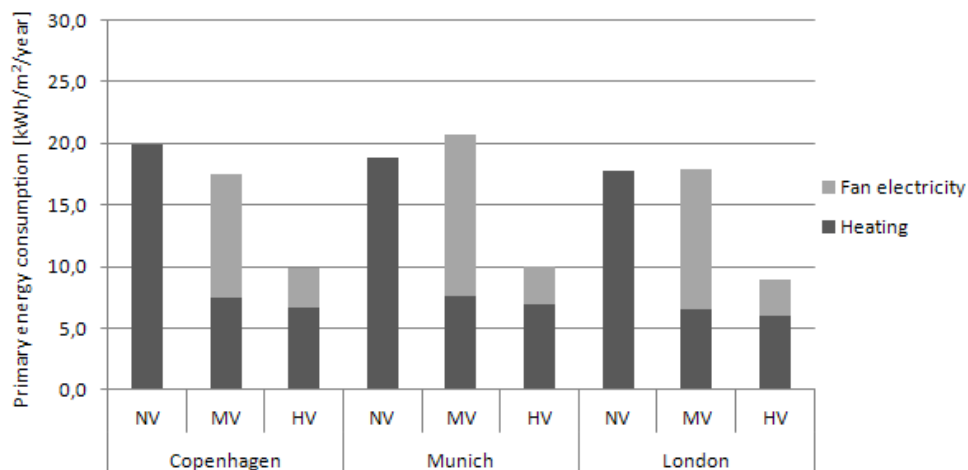


Figure 3. Primary energy consumption

## 8 CO<sub>2</sub> EMISSION

Calculation of CO<sub>2</sub> emissions are based on the following figures; Munich (district heating 200 g/kWh and electricity 606 g/kWh), Copenhagen (104; 425) and London (206; 517). CO<sub>2</sub> emissions due to electricity and heating are almost the same for NV and MV. Depending on the location the total CO<sub>2</sub> emission ranges from 2.6-5.4 kg CO<sub>2</sub>/m<sup>2</sup> per year. HV makes it possible to reduce this CO<sub>2</sub> emission by up to 50%.

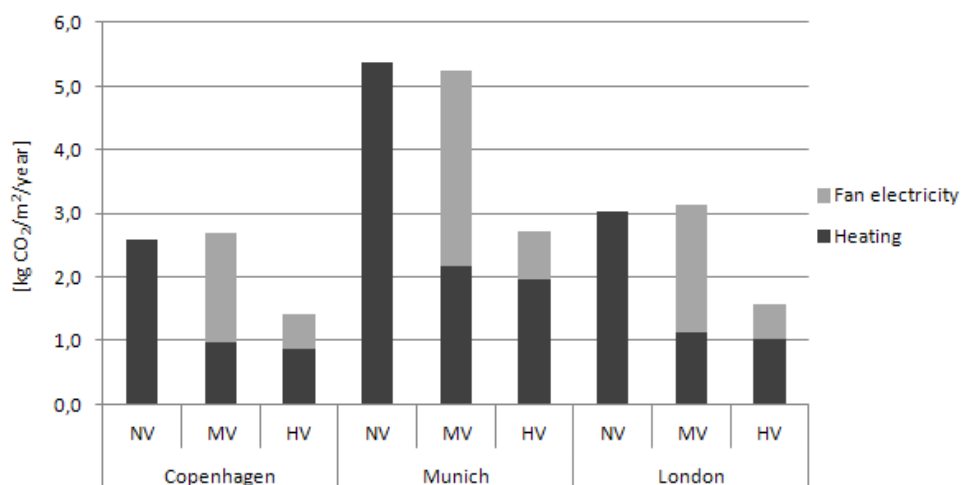


Figure 4. CO<sub>2</sub> emission

## 9 COST

The total investment required by the different systems has been evaluated including capital cost (products and installation), operation (electricity and heating), and maintenance costs for the first year of operation (Figure 5) and during a period of 20 years (Figure 6). The prices are calculated by WindowMaster in close collaboration with a Danish ventilation contractor (Roth, 2012). The maintenance cost for HV is almost the same as MV. Choosing NV this cost could be reduced by 70%. No significant difference was found between NV and MV for the operation cost during the first year. However, using HV the operational cost could be reduced by 50%.

One of the major differences of the three systems is the capital cost. Here it was found that a MV system is more than four times as expensive as a NV system. For HV this was only a factor of three. As a result of these large capital costs, the total investment for the first year is still in favour of NV by a factor of four compared to MV and a factor of three compared to HV. Accordingly, HV was found to be 25% cheaper than a full MV system.

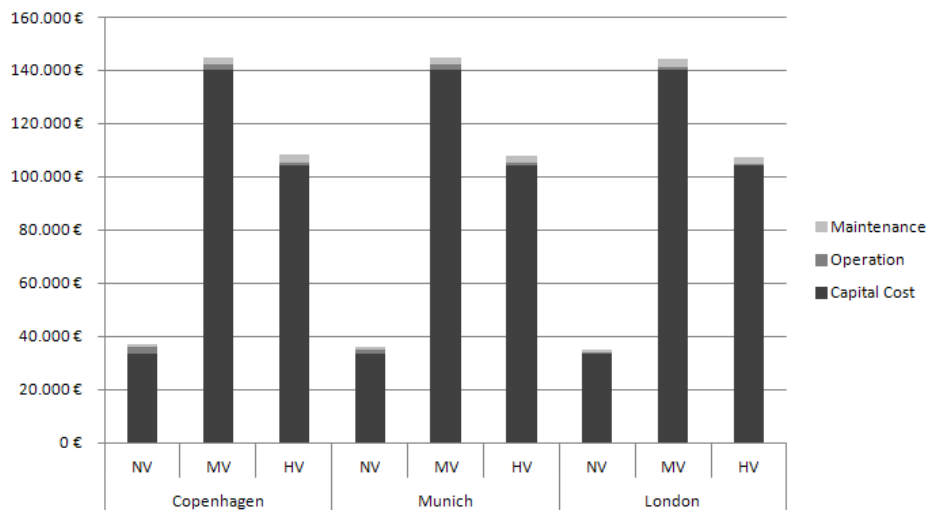


Figure 5. The total investment during the first year of operation

The total investment over a period of 20 years showed almost the same pattern as the first year of operation. MV was found to be 2.5 to 3 times more expensive than NV on the total investment during a 20 year period. 25% could be saved over 20 years by choosing a HV system compared to a MV system.

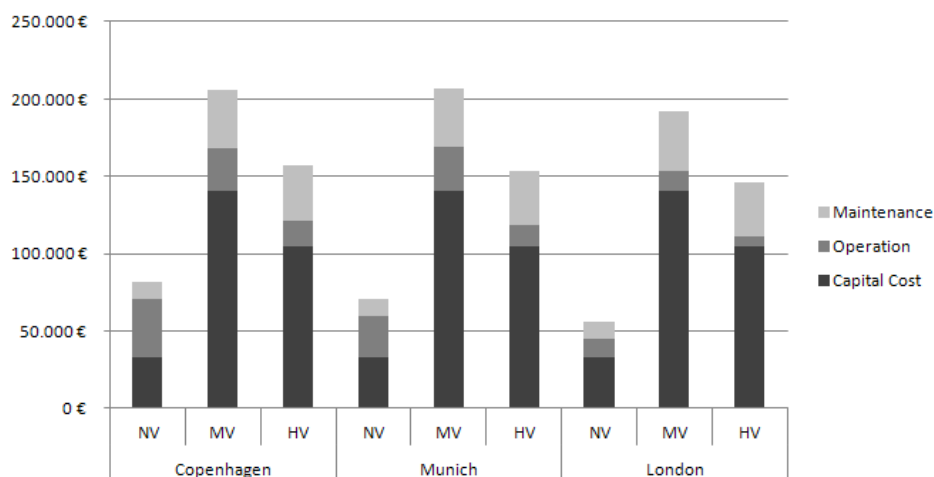


Figure 6. The total investment during a period of 20 years

## 10 DISCUSSION

The main ambition for the control strategies is to obtain the desired thermal comfort and indoor quality defined in EN 15251 Category III and to obtain very similar indoor air quality for all three ventilation types. This is necessary for a useful comparison of energy demand resulting from the different ventilation types. It should be noted that better relative indoor air quality and thermal comfort performance could have been achieved for all three ventilation systems if other benchmarks for CO<sub>2</sub> and temperature performance had been chosen.

To make the study as realistic as possible, it was decided to use real, commercially available products. Likewise, is the product specifications selected corresponding to these products. The approach avoids a discussion about whether the results can be transferred in practice. However, the actual products are only available in certain sizes, so it is not possible to select a product for all locations that just fits the exact requirements. Instead, we have chosen a product that can meet the requirements of the most heavily loaded location - and this product is used at all locations. It avoids that the choice of commercially available product affects energy calculations. The only effect can occur at the cost side, where the MV in London and Copenhagen could possibly be a more customized MV product.

The transfer of the control strategy to the simulation models was done as close as possible to WindowMaster's control strategy. Sometimes changes were necessary due to the restrictions of the simulation software or to obtain a similar thermal comfort and indoor quality. It is believed that these simulations still closely reflect the WindowMaster control system.

HV control strategy is a combination of the NV and MV control strategies. The overall objective is to use the best aspects of both systems, in order to optimise the balance between indoor climate and energy consumption. This is possibly the greatest challenge with HV and it is therefore necessary to have a control strategy that can take this into consideration.

During winter and summer the HV control strategy is almost straight forward; MV gives the best results during cold periods, when there is a heating demand. The heat recovery of the system helps save heat energy from the building. During the summer period, it is NV that has the best results. Good indoor air quality and thermal comfort can easily be reached without using any fan energy. The ventilation rate can be increased only by opening the windows a little more without using additional energy. NV also has the ability to benefit from night ventilation/cooling without using any additional energy.

The transient season is, however much more complicated and most of the time it depends on internal conditions to dictate whether MV or NV is the best solution. Therefore, it is very important to have an automatic system that can choose between the two systems depending on indoor temperatures as an indicator for heating or possible cooling demand. This is perhaps not that complicated. The complex part is to know, when, for instance, to make the MV stop and then start up the NV system due to the fact that the internal environment has changed throughout the period where MV has been used. This strategy has been developed in these calculations.

## 11 CONCLUSION

The total primary energy demand (sum of heating and fan electricity demand multiplied by the primary energy factors) for the NV and MV systems ranges from 18-21 kWh/m<sup>2</sup> per year in all three locations. For HV the total primary energy demand was only 9-10 kWh/m<sup>2</sup> per year.

The result shows that HV enables energy savings of 44-52% compared with MV. Compared to NV an energy saving of 46-50% could be achieved. The heating demand can be reduced by nearly 70% for HV compared to NV. Fan electricity usage can be reduced by 75% for HV compared to MV. Overall, total primary energy consumption is almost the same for MV and NV, but can be reduced by up to 50% using HV.

One of the major differences was to be found in the total investment of the different systems including capital cost (products and installation), operation (electricity and heating), and maintenance. Looking at both the first year of operation and during a period of 20 years, MV was found to be 2.5 to 4 times more expensive than automated NV. By selecting HV, 25% of the total investment could be saved compared to a MV system.

The results demonstrate clearly that effective automated NV can deliver similar indoor climates and energy performance to MV, but with significantly reduced capital costs. However, HV should be more widely considered for schools in addition to NV and MV. Overall HV makes it possible to save on capital costs compared with MV, and delivers ongoing savings for heating and electricity during operation while reducing CO<sub>2</sub> emissions by up to 50%.

## 12 ACKNOWLEDGEMENTS

First and foremost, we would like to thank WindowMaster for the valuable guidance, advice and knowledge sharing. Besides, we would like to thank the *Fraunhofer Institute for Building Physics* for providing a good environment and facilities to complete this project.

## 13 REFERENCES

- Allard, F. (1998). *Natural ventilation in buildings*. A design handbook. MPG Books Ltd, London
- Byg DTU (2009). *Elever undersøger indeklima i klasselokaler - rapport om resultater fra Masseeksperiment*.
- Cron, F. and Inard, C. (2003). *Analysis of hybrid ventilation performance in France*. Proceedings of Eighth International IBPSA Conference, Eindhoven, 243 - 250.
- EN 15251 (2007). *Indoor environmental input parameters for design and assessment of energy performance of buildings addressing indoor air quality, thermal environment, lighting and acoustics*.
- Emmerich, S. J (2006) *Ventilation Systems in an Office Building*. HVAC & Research 12, 4, 975 - 1004.

- European Commission (2014). *Guidelines for healthy environments within European schools*.
- Heikkinen, J. et al. (2002). *Performance simulation of hybrid ventilation concepts*. IEA - Technical report in Annex 35 Hybrid Ventilation.
- Heiselberg, P. (2006). *Design of Natural and Hybrid Ventilation*. DCE Lecture Notes, Aalborg University.
- Mendell M.J. and Heath G.A. (2005). “*Do indoor pollutants and thermal conditions in school’s influence student performance? A critical review of the literature*”, *Indoor Air*, Vol. 15, 27-52.
- Reshyvent (2004) *Demand controlled hybrid ventilation in residential buildings with specific emphasis on the integration of renewables*.
- Roth, J. (2012). *Cost calculation for the office investigated in the Fraunhofer study*.
- Sowa, J. and Karaś, A. (2007). *Whole year simulation of natural and hybrid ventilation performance and estimation indoor air quality for modernized school building*. Proceedings of Clima 2007 WellBeing Indoors, 1 - 8.
- Wargoeki, P. and Wyon, D.P. (2007). “*The effects of outdoor air supply rate and supply air filter condition in classrooms on the performance of schoolwork by children*”, *HVAC&R Research*, Vol. 13(2), 165-191.
- Wargoeki, P. et al. (2007) “*The effects of electrostatic filtration and supply air filter condition in classrooms on the performance of schoolwork by children*”, *HVAC&R Research*, submitted.

# Ventilative cooling potential based on climatic condition and building thermal characteristics

Haolia Rahman<sup>1</sup> and Hwataik Han<sup>\*2</sup>

*1 Graduate School, Kookmin University  
77 Jeungneung-ro, Seongbuk-gu  
Seoul 02707, Korea*

*2 Mechanical Engineering, Kookmin University  
77 Jeungneung-ro, Seongbuk-gu  
Seoul 02707, Korea*

*\*Corresponding author: [hhan@kookmin.ac.kr](mailto:hhan@kookmin.ac.kr)*

## ABSTRACT

We introduce a new method for defining ventilative cooling potential (VCP) for office buildings that depends not only on the climatic conditions but also on building thermal characteristics. The energy savings from ventilative cooling differs from building to building; therefore, VCP should be able to represent the actual energy savings—though not perfectly—in order to guide optimization of ventilative cooling parameters during the initial design stage.

In this paper, we proposed the VCP with temperature shift index representing building thermal characteristics. The temperature shift is based on the adaptive thermal comfort region shifted in the psychrometric chart. The index of temperature shift can be determined by the balance temperature difference of the building, which is defined as the heat gain in the building divided by the thermal loss characteristics of the building envelope.

To validate the concept, we conducted simulations using a model office building in four representative cities during summer climates: tropical, dry–semi-arid, Mediterranean, and continental. Using energy analysis software, we calculated the amount of energy consumed in each case of ventilative cooling whenever possible compared to the energy consumed by solely mechanical cooling during summer. Comparisons were made on a weekly basis. Results demonstrate a strong correlation between energy savings and VCP in cases when a proper balance temperature difference was applied.

## KEYWORDS

Building design, Ventilative cooling, Balance temperature difference, Cooling potential

## 1 INTRODUCTION

Ventilative cooling is an energy-efficient way of cooling a building using outdoor air through natural or mechanical ventilation (Kolokotroni and Heiselberg, 2015). It requires only fan power or minor power to control the system, which is usually much less than the power consumed by a mechanical cooling system's compressor. We cannot totally rely on ventilative cooling because of its dependence on climatic conditions but can take advantage of it as much as possible to reduce cooling energy consumption. It is necessary to quantify how much cooling energy can be saved using ventilative cooling.

In recent years, an index to quantify climatic potential has been introduced in several ways. Yao (2009) assesses an index of the natural ventilation cooling potential (NVCP) for an office building. The NVCP was described as the ratio of the number of hours within the comfort zone to the total occupied hours. Herein, building characteristics, ventilation type, and internal heat load should be defined in advance to match natural ventilation with the expected occupancy thermal comfort. Artmann (2007) introduced a concept to quantify the climatic cooling potential (CCP) for buildings due to night-time ventilation. The potential is defined as the sum of the product of the indoor–outdoor temperature difference and the time interval at night with acceptable outdoor conditions. Given that building temperature oscillates harmonically within the range of  $24.5^{\circ}\text{C} \pm 2.5^{\circ}\text{C}$ , the CCP does not consider any building-specific parameters. For night cooling purposes, the largest air temperature

differences are the most valuable benefit that can be extracted from the climate. Meanwhile, for direct cooling during the day, limitations should be made on outdoor air supplies to prevent overcooling of the indoor space.

Ghiaus and Allard (2006) addressed energy-saving potential based on temperature difference and free running temperature, and they considered the probability distribution of outdoor temperature and the applied degree-hour bin method to estimate energy savings. Without including the building model, Causone (2016) proposed an index of the climatic potential for natural ventilation (CPNV). The index is based on the number of hours that natural ventilation agrees with temperature and humidity constraints. The acceptable supply air conditions should be within the lower and upper temperature limits of 10°C and 3.5°C higher than the adaptive thermal comfort, respectively, and the humidity ratio ( $W$ ) uses a range within 30% RH and 70% RH. However, a wide acceptable temperature ranges in CPNV may create over capacity in the design of ventilation systems or cause occupant dissatisfaction.

This study introduces an index to evaluate ventilation cooling potential based on the shifted temperature from the adaptive thermal comfort zone. Lookup tables of VCPs at various temperature shifts are suggested to provide for various cities so that designers can look up corresponding building characteristics represented by the balance temperature difference. The VCP index introduced in this paper can be used to design ventilation systems in conjunction with thermal characteristics of a new building and to adjust ventilation system operation in an existing building to maximize energy savings by ventilative cooling during summer.

## 2 THEORY

### 2.1 Thermal comfort model

There are various thermal comfort models in the literature. In this study, we used the adaptive thermal comfort model of ASHRAE standard 55 (ASHRAE, 2004) for a naturally ventilated building, which was originally proposed by de Dear and Brager (2002). This is an optimum comfort temperature in a naturally conditioned space as a function of outdoor temperature as shown in Eq. (1). The criteria are differentiated into 80% and 90% occupant acceptability of  $\pm 3.5^\circ\text{C}$  and  $\pm 2.5^\circ\text{C}$  bands, respectively. This model assumes that occupants adapt their clothing to thermal conditions and are sedentary, with 1.0 to 1.3 met.

$$T_{comf} = 0.31T_{a,out} + 17.8 \quad . (1)$$

### 2.2 Balance temperature difference

When the total heat gain of an indoor space equals the heat losses through the building envelope, the indoor temperature is in equilibrium with outdoor temperature. The temperature difference can be defined as the balance temperature difference. The heat losses are composed of heat transmission through walls and heat infiltration by ventilation air exchange.

$$\widehat{U}A_{bldg} \Delta T_{bal} + \rho C_p Q \Delta T_{bal} = W_{IHG} \quad , (2)$$

$$\Delta T_{bal} = \frac{W_{IHG}}{\widehat{U}A_{bldg} + \rho C_p Q} = \frac{W_{IHG}}{\widehat{U}A_{bldg} (1 + \alpha)} \quad , (3)$$

where  $\alpha$  is defined as  $\frac{\rho C_p Q}{\widehat{U}A_{bldg}}$ , which means the ratio of infiltration loss to transmission loss. Building thermal characteristics include the UA value of the building walls and the air

exchange rate,  $Q$ , by either mechanical ventilation or natural ventilation through cracks and openings in the envelope. The balance temperature difference expresses the overall thermal characteristics of a building with a single parameter.  $\Delta T_{bal}$  is large for well-insulated and airtight buildings with large internal heat gains, whereas it is small for poorly insulated and leaky buildings with small internal gains. Modern buildings tend to move toward large balance temperature differences as they increase insulation thickness to achieve zero-energy buildings and use high-energy-density electronic equipment.

### 2.3 Ventilative cooling potential with temperature shift

VCP is defined as the number of satisfied hours for ventilative cooling over total hours as described in Eq. (2). The satisfied hours may differ from one author to another depending on applications, but they are chosen here as the daytime hours when outdoor conditions are within the shifted zone. As seen in Fig. 1, the lower limit of the comfort zone ( $T_{cl}$ ) is shifted by the balance temperature difference, and the upper limit ( $T_{cu}$ ) is shifted by half of the balance temperature difference. When outdoor temperature is in region B (enclosed by a dotted line), outdoor air can be fully used for ventilative cooling. In region C (enclosed by a solid gray line) outdoor air can be partially used for ventilative cooling, as the temperature difference is not large enough to completely cover the cooling load. Assuming that the outdoor temperature is equally distributed in the region statistically, half of the region C is added to the shifted zone for VCP calculation.

$$VCP = \frac{1}{H} \sum_{d=d_i}^{d_f} \sum_{h=h_i}^{h_f} h_{vc} \tag{4}$$

where  $H$  is the total number of hours considered,  $h_{vc}$  is the number of hours in the shifted comfort zone when ventilative cooling is possible,  $d$  and  $h$  are the standard time day and hour, and the subscripts  $i$  and  $f$  denote the initial and final time day and hour.

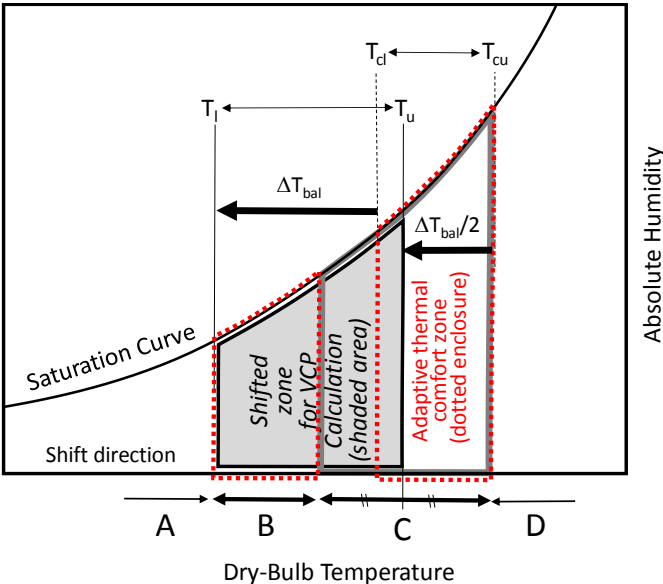


Figure 1: Thermal comfort zone shifted on psychrometric chart

### 3 METHOD

#### 3.1 Climatic data

We investigated four representative cities in our analysis. Those cities belong to one of the following four main groups: megathermal, dry, mesothermal, and microthermal zones. These groups are from the five main groups according to the Köppen climate classification (Peel, 2007). The fifth group, polar, is not considered here because ventilative cooling is not quite necessary therein. The cities and their climate summaries are shown in Table 1, which shows average summertime outdoor temperature and average wind speed.

Table 1: Representative cities of four main groups of Köppen climate (data source taken from Energyplus, 2007)

Climate zone	City	Location	Average outdoor temperature (°C)				Average wind speed (m/s)			
			Jun	Jul	Aug	Sep	Jun	Jul	Aug	Sep
Megathermal-tropical monsoon	Jakarta, Indonesia	6.13S, 106.75E	29.0	29.0	29.4	29.6	4.51	4.76	5.11	4.89
Dry semi-arid	Madrid, Spain	40.45N, 3.55W	23.2	27.0	20.6	25.5	2.73	3.26	3.61	3.46
Mesothermal-mediterranean	Los Angeles, USA	33.93N, 118.4W	24.7	20.1	21.9	21.6	4.54	5.00	5.10	4.49
Microthermal-hot summer continental	Seoul, Korea	37.57N, 126.97E	23.2	26.2	27.0	22.3	2.46	2.60	2.25	2.17

#### 3.2 Building and ventilation model

To verify our results, we performed an energy simulation for a sample building. The building is a medium sized office building (Deru, 2011) with 4,982 m<sup>2</sup> of total area. There are three stories and a 5-m central atrium lengthwise in between the building floors with a floor-to-ceiling height of 3 m as shown in Fig. 2. A simple input parameter of total heat gain density produced by occupants, lights, and equipment is given as 31.24 W/m<sup>2</sup> with the schedule of loads lasting from 8 a.m. to 8 p.m. (12 hours). There are 33% and 11% of glazing and opening areas, respectively, over wall ratio per floor area. The building terrain is located in a rural area with low buildings and faces 90° to the north.

The three ventilation schemes used for cooling the space inside the building are shown in Table 2. In the air conditioner (AC)-only scheme, the cooling system is handled by the AC only. The Fan-AC assist scheme uses fans as a main cooling device to replace indoor air with cool outdoor air and the air conditioner as a backup device in case ventilative cooling is not possible. In the natural ventilation-air conditioner (NV-AC) assist scheme, natural driving forces are used to entrain cool outdoor air when it is available. The AC is always on during the occupied hours when the indoor temperature above  $T_{cu}$ . The coefficient of performance of the AC is 3.0, and mechanical fans are on at a constant flow rate of 14 m<sup>3</sup>/s when the internal temperature is between 22°C and  $T_{cu}$ . The ACs and windows are independently controlled in each zone. Night ventilation based on thermal mass is not considered and is assumed to not affect cooling potential during the day. Energy consumption and indoor conditions are calculated using Coolvent software (Maria-Alexandra, 2008) from June till September on an hourly basis. The energy savings from utilizing a mechanical fan or natural ventilation are obtained based on the energy consumption by the reference case of the AC-only scheme.

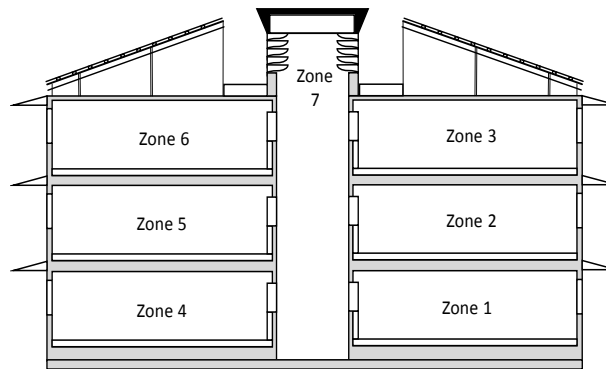


Figure 2: Building model for validation

Table 2: Air conditioner, fan, and window operations

Operation	Cooling scheme		
	Scheme 1 (AC-only)	Scheme 2 (Fan-AC assist)	Scheme 3 (NV-AC assist)
Air conditioner	On $T_{in} > T_{cu}$	On $T_{in} > T_{cu}$	On $T_{in} > T_{cu}$
Natural ventilation	No	No	Window opening
Mechanical fan	No	Fan operation	No

According to the given building model, the balance temperature difference,  $\Delta T_{bal}$ , is obtained manually by considering the energy balance between internal heat gain and building heat transfer. The UA value of the building is estimated to be 3600 W/K, and the internal heat generation is 16,800 W/K; solar radiation is not included in the calculation. The balance temperature difference is calculated to be approximately 7°C for this building.

## 4 RESULTS AND DISCUSSION

### 4.1 VCP with an index of temperature shift

Table 3 shows the VCPs obtained for four cities according to temperature shifts of 1°C–9°C for each summer month. It also gives the overall VCPs for the entire summer depending on the temperature shifts. The temperature shift for a given VCP can be selected by a designer to account for the balance temperature difference representing the thermal characteristics of the building.

For a tropical climate, such as that in Jakarta, where it is relatively hot and humid throughout the year, the VCP is as large as approximately 50%–60% for buildings with a zero-balance temperature difference, i.e., completely open space. However, VCP sharply decreases as the temperature shift increases. This means that it is very difficult to implement ventilative cooling for buildings with balance temperature differences greater than 4°C–5°C.

Madrid, which has a semi-arid climate, has a maximum VCP at temperature shifts between 3°C and 5°C from June till September. VCPs remain relatively large for a wide range of temperature shifts, which means most buildings with a wide range of thermal characteristics can benefit more or less from ventilative cooling. Los Angeles is typically not too hot during the day and cool at night during the summer season. This condition creates an excellent strategy for ventilative cooling during the day as well as at night. The peaks of VCP are between 4°C and 5°C, and the potential remains high until a temperature shift of around 9°C.

During the hot summer period in Seoul, VCP decreases almost linearly as the temperature shift increases. It would be beneficial for buildings to have a large balance temperature difference in terms of cooling energy savings. However, it is important to maintain building

insulation above a certain level to account for cold winters. To take advantage of ventilative cooling, building designers would need to be able to adjust ventilation systems instead of building envelope specifications.

Based on the balance temperature difference of the present building (7°C), the acceptable VCP from June to September for four representative locations is illustrated in Fig. 3. Empty circles in the figures show selected hourly outdoor temperatures when the buildings were occupied. From the figure, it can be seen that Jakarta only has a few potentials to use outdoor air for cooling the indoor space. Meanwhile, Los Angeles can take advantage of outdoor cooling, especially in early summer. Madrid and Seoul are similar, having fairly good cooling potential in June and September but less in July and August.

Table 3: Ventilative cooling potential of four representative cities during June to September

Cities	Month	Adaptive thermal comfort	Ventilative cooling potential (%) with temperature shift								
			1 °C	2 °C	3 °C	4 °C	5 °C	6 °C	7 °C	8 °C	9 °C
Jakarta	Jun	60.6	50.8	39.2	31.9	25.6	19.4	13.1	10.3	8.1	5.3
	Jul	58.3	49.5	40.3	32.5	27.4	21.8	16.9	10.8	7.8	5.6
	Aug	50.0	42.2	33.1	25.8	19.9	15.3	11.8	9.4	7.0	4.0
	Sep	51.4	40.0	33.3	26.1	21.4	16.9	11.9	8.3	5.8	4.4
	Ave	55.1	45.6	36.5	29.1	23.6	18.4	13.4	9.7	7.2	4.8
Madrid	Jun	42.5	46.1	46.9	52.8	50.8	52.2	49.4	49.7	49.7	48.9
	Jul	36.0	35.8	38.7	39.5	40.9	36.6	36.0	33.1	33.3	28.5
	Aug	32.8	36.0	35.8	37.6	37.1	37.1	34.7	33.6	33.6	32.8
	Sep	46.7	52.5	59.2	59.2	59.7	61.9	60.8	60.8	58.1	56.4
	Ave	39.5	42.6	45.1	47.3	47.1	47.0	45.2	44.3	43.7	41.6
Los Angeles	Jun	41.4	61.4	78.9	85.0	95.3	97.8	95.0	93.6	91.9	91.9
	Jul	65.6	75.3	89.5	96.5	97.0	95.4	95.4	89.8	86.0	80.6
	Aug	76.1	82.8	90.1	93.3	93.5	94.1	91.1	85.5	74.5	67.7
	Sep	57.8	67.5	80.3	89.4	90.6	88.1	88.1	85.8	81.9	77.5
	Ave	60.2	71.7	84.7	91.1	94.1	93.8	92.4	88.7	83.6	79.5
Seoul	Jun	63.9	70.3	73.9	75.8	73.3	70.3	67.2	60.6	55.0	51.9
	Jul	74.7	76.6	69.1	62.6	58.1	50.8	44.4	38.7	34.7	29.6
	Aug	69.1	65.9	59.7	55.6	49.5	43.3	36.6	29.3	23.9	20.4
	Sep	60.8	65.8	70.3	71.4	71.4	69.3	68.3	64.7	61.9	57.5
	Ave	67.1	69.6	68.2	66.4	63.1	58.4	54.1	48.3	43.9	39.9

## 4.2 Energy saving and correlation with VCP

Figure 4 shows the reduction of building energy consumption from using the Fan-AC assist and NV-AC assist schemes. The percentage of energy savings is calculated based on the ratio of energy consumption by Fan-AC assist or NV-AC assist schemes over the AC-only scheme. In other words, the energy savings represent how many hours outside air can replace AC operation hours. The monthly profiles of energy savings between the two distinguished schemes are typically similar. The NV-AC assist scheme has a greater effect on average energy savings than the Fan-AC assist scheme in Jakarta and LA because it has a higher wind speed that contributes to increase ventilation rate.

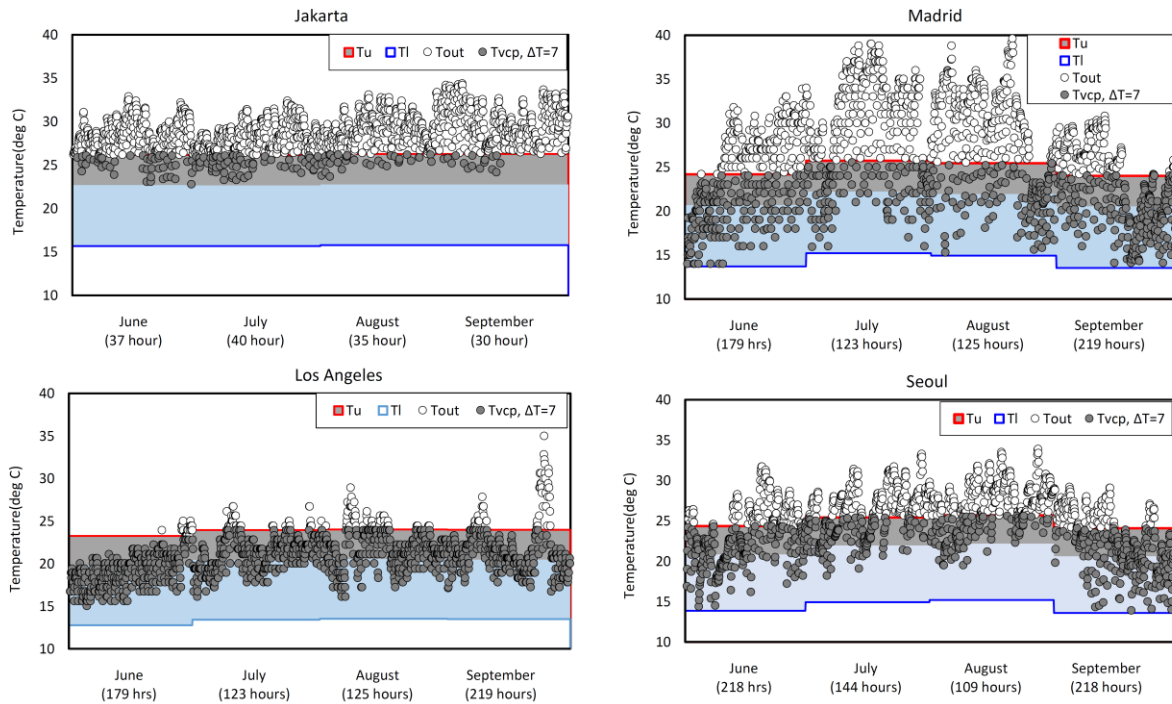


Figure 3: Selected VCP hours using 7°C temperature shift

The VCP discussed earlier should be able to represent the real energy saving even though they do not perfectly match. Figure 5 shows the correlations between calculated energy savings and the VCP obtained at a temperature shift of 7°C for the Fan-AC assist scheme and NV-AC scheme. The figure represents four cities from June till September on weekly basis. According to the given building model, energy savings strongly correlate with the VCP. That means the VCP can represent the energy savings estimation fairly well. The correlation between VCP and energy savings using the NV-AC scheme is found also to be strong but slightly weaker than using Fan-AC assist scheme because there are too many uncertainties involved in estimating energy consumption using climate data. The temperature shift at 7°C is not shown as the highest among VCPs at different temperature shifts, but it means that VCP with an appropriate temperature shift taking building thermal characteristics into account correlates well with the actual energy savings by adapting ventilative cooling.

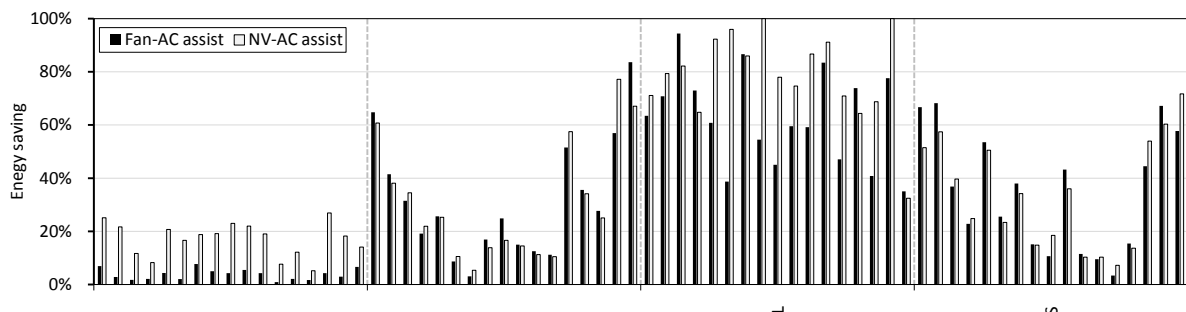


Figure 4: Energy savings by Fan-AC assist and NV-AC assist scheme

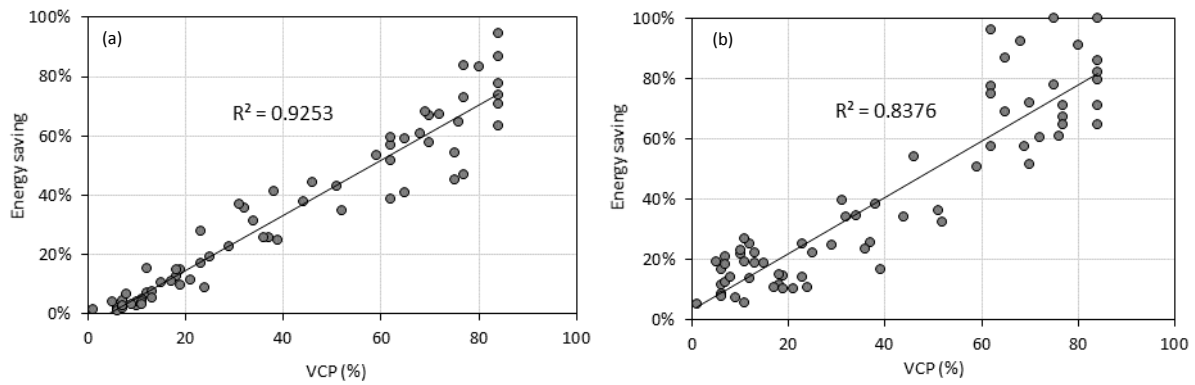


Figure 5: Correlation between weekly energy savings and VCP at 7°C during June to September in four representative cities (a) Fan-AC assist scheme (b) NV-AC assist scheme

## 5 CONCLUSIONS

The VCP with an index of temperature shift is introduced to account for building thermal characteristics for given climatic conditions. The temperature shift can be determined by a single parameter, balance temperature difference between indoors and outdoors. The following conclusions can be drawn:

1. The VCP distribution with respect to temperature shift shows different patterns depending on climatic zone. A tropical climate requires small temperature shifts for the maximum use of ventilative cooling. A similar conclusion can be made regarding a continental climate, but annual energy use should be addressed. Ventilative cooling is best applicable to a dry semi-arid climate where daily temperature fluctuations are large.
2. The VCP with temperature shift based on the balance temperature difference (lower limit by  $\Delta T_{bal}$ , upper limit by  $\Delta T_{bal}/2$ ) results in a good correlation with the actual energy savings of the building calculated on a weekly basis. We considered a simplified method to take into account the complicated probability distribution of outdoor temperature.
3. A lookup table can be provided for designers to easily estimate possible energy savings by adapting ventilative cooling in the initial design stage. The table shown in this paper can be modified further by optimizing the parameters appropriate for various applications.

Further research will be needed to investigate the effects of solar radiation, probability distribution of outdoor temperature, methods for estimating ventilation rate, applicability of the thermal comfort zone, and other factors.

## 6 ACKNOWLEDGMENTS

This work was supported by the Basic Science Research Program through the National Research Foundation of Korea (NRF) funded by the Ministry of Education (2016R1D1A1B01009625), and by the Industry-Academic Cooperation Program to support Industry Research Institute (C0340813).

## 7 REFERENCES

Artmann, N., Manz, H., and Heiselberg, P. (2007). Climatic potential for passive cooling of buildings by night-time ventilation in Europe. *Applied Energy*, 84(2), 187-201.

- ASHRAE. (2004). Thermal environmental conditions for human occupancy. ASHRAE Standard 55.
- Causone, F. (2016). Climatic potential for natural ventilation. *Architectural Science Review*, 59(3), 212-228.
- de Dear, R.J., Brager, G.S., and Artmann, N. (2002). Thermal comfort in naturally ventilated buildings: revisions to ASHRAE Standard 55. *Energy and Buildings*, 34, 549-561.
- Deru, M., Field, K., Studer, D., Benne, K., Griffith, B., Torcellini, P., Liu, B., Halverson, M., Winiarski, D., Rosenberg, M., Yazdani, M., Huang, J., and Crawley, D. (2011). U.S. Department of Energy Commercial Reference Building Models of the National Building Stock, NREL/TP-5500-46861, 1-118.
- Energyplus. (2016). *Weather Data*. Available from: <https://energyplus.net/weather>.
- Kolokotroni, M. and Heiselberg, P.(2015). Ventilative cooling state of the art review, Annex 62 Ventilative Cooling, Aalborg.
- Ghiaus, C. and Allard, F. (2006). Potential for free-cooling by ventilation. *Solar Energy*, 80, 402-413.
- Maria-Alenjandra, B.M. and Glicksman, L. (2008). Coolvent: A multizone airflow and thermal analysis simulator for natural ventilation in building, in 3rd National Conference of IBPSA-USA, Berkeley, California.
- Peel, M.C., Finlayson, B.L., and McMahon, T.A. (2007). Updated world map of the Köppen-Geiger climate classification. *Hydrology and Earth System Sciences Discussions*, 4, 439-473.
- Yao, R., Li, B., Steemers, K., and Short, A. (2009). Assessing the natural ventilation cooling potential of office buildings in different climate zones in China. *Renewable Energy*, 34(12), 2697-2705.

# The Reintroduction of Natural Ventilation to a 19<sup>th</sup> Century Opera House, Utilising Calibrated Computer Simulation and User Operation

Julia Thompson<sup>1\*</sup>, Michael Donn<sup>1</sup>, and George Baird<sup>1</sup>

*1 Victoria University of Wellington  
139 Vivian Street, TeAro  
Wellington, New Zealand  
\*juliasuzannethompson@gmail.com*

## ABSTRACT

The Royal Wanganui Opera House (RWOH), in Whanganui, New Zealand, was constructed in 1899, and now seats 830 people. This building was designed with a natural ventilation system; however, this system is no longer in operation and the RWOH has received regular complaints from patrons regarding indoor thermal comfort. Various options for mechanical systems to improve indoor comfort during summer performances have been considered, but have been deemed too costly. The RWOH is listed with Heritage New Zealand as a Category 1 heritage building. Without an effective ventilation scheme, the selection of the RWOH as a performance venue during peak summer months is threatened. The addition of a mechanical ventilation system will not only be costly, but also encounter issues complying with the building's heritage listing. The potential benefits of a natural ventilation scheme for the RWOH regarding initial cost, thermal comfort, and on-going maintenance costs for the local Council are key drivers of this investigation. An additional benefit is the functional heritage value: restoring the building technology to its original design.

A calibrated Computational Fluid Dynamics (CFD) software analysis of the RWOH has been completed. Temperature and humidity monitoring devices were placed throughout the auditorium, stage, and roof space to gain data to calibrate CFD modelling of the space. Because temperature monitoring devices are reliable, cheap and readily accessible, temperature, rather than airflow, was selected as the calibration medium at multiple points in the auditorium for the ventilation simulations. The CFD analysis investigated the building's potential for the reintroduction of a natural ventilation scheme in several incremental stages. Incremental changes to the operation of openings in the building have been completed: it saw reintroduction of natural ventilation airflows as tested through the CFD modelling. Staff at the RWOH were given an operation guide for the sold out performance of the New Zealand Opera School on Saturday the 21<sup>st</sup> January 2017, a performance that in previous years has sparked multiple complaints from the audience regarding comfort issues. No comfort complaints were received after this year's Opera School Performance. While the weather during this key performance was not as warm or detrimental to the indoor thermal comfort as it has been in previous years, the owners and operators of the RWOH are now aware of the benefits the changes to the operation of the building's ventilation openings has already achieved. The owners of the RWOH are interested in undertaking further stages of renovations in order to continue to improve the ventilation of the building for the future. The research team is currently devising a guide for the application of successful natural ventilation schemes to similar buildings throughout New Zealand.

## KEYWORDS

Natural ventilation, passive, CFD, simulation

## 1 INTRODUCTION

Of the many ways in which the internal environment can be improved in our buildings, the issue of providing fresh air to people in crowded situations such as auditoria and school classrooms is particularly challenging. Of these situations the large theatre is an extreme example. This paper explores the application of CFD analysis to the understanding of the

natural ventilation designed into a 100+ year old theatre; calibration of the CFD predictions against measured data; and observation of the efficacy of design and operation interventions suggested by the CFD analysis.

## **1.1 An Overview of the Royal Wanganui Opera House Project**

The Royal Wanganui Opera House (RWOH) is an 830 seat theatre in Wanganui, New Zealand. Due to its recent comfort complaints, seismic renovations, and a history of natural ventilation design, the RWOH became the major case study for this research. The owners of the RWOH, the Wanganui District Council, wish to find a cost effective solution to ensure the building's use as a performance space can continue.

The original design of the RWOH was explored, and changes through its life span that have affected the ventilation were identified. The basic geometry of the building was 3D computer modelled in Revit. Temperature and humidity sensors were placed throughout the auditorium itself to collect measured data regarding the building's existing operation. The measurements were taken at 5 minute intervals over a two week period during winter. The goal was to obtain sufficient data to build quickly a trustable analytical model, which would enable the modification of the building prior to an early summer performance that has had a full house in past seasons and has engendered significant overheating complaints.

The geometry was imported into Autodesk Simulation CFD (Autodesk Inc., 2015), and selected situations (weather conditions, occupancy numbers, known openings, use of equipment) of the building were simulated. The CFD model was calibrated against a series of observations of the performance of the existing building. CFD modelling to test the likely success of new or restored interventions to the ventilation scheme was then undertaken. The input data was taken from weather data measured in the area at the same time as the measurements. The results of the CFD models were compared with the measured temperature and humidity data from inside the auditoria, entrance area, roof space, and back of stage. Once the model's geometry, materiality, solar exposure, and internal heat loads produced results aligned with the measured temperature data, these modelling conditions were confirmed and the design option modelling process could begin.

Once calibrated, the model was used in a fully occupied state to analyse performance in summer weather conditions. The goal was to assess key problem areas for overheating in the occupied space. This knowledge acquired from the analysis of the existing building helped identify the proposed ventilation alterations. The designs were then discussed with the building owners for construction feasibility, and the underlying geometry model was altered to reflect the proposed designs. The CFD analysis helped form design and operation recommendations focused on potential comfort hours in summer. From these recommendations, the project to mitigate the RWOH's overheating issues in summer months was split into two stages. Stage one necessitated immediate operational changes for an imminent heavily occupied performance. Stage two is currently underway, and involves constructional changes to the building.

## **1.2 History of Naturally Ventilated Auditoria Design**

Bringing natural ventilation back into auditoria buildings restores the original operational approach for historic theatres. "Destruction or refurbishment of 19<sup>th</sup> Century theatres has meant that there are few remaining vestiges of the old natural ventilation systems to be found" (Kenton 2004). The design of naturally ventilated auditoria has had a resurgence due to the

global energy crisis (Kenton, 2004). Not only does natural ventilation hold biophilic significance and comfort improvements, but it also has the potential to save operational energy (Kellert, Heerwagen, & Mador, 2008).

According to the Chartered Institution of Building Services Engineers (CIBSE) Ventilation Guide B, in 2005 little data existed regarding natural ventilation in buildings where floor-to-ceiling height exceeded 3.5m. By studying history and modelling a complex and extreme case, the intention is to get closer to normalising this type of space. While natural ventilation is not without design challenges, the benefits include a reduction in headaches, and often more highly oxygenated air than would be provided by mechanical means (Kellert, Heerwagen, & Mador, 2008). The issue is how to achieve these qualitative improvements even in the crowded and difficult circumstances of an auditorium, and whether the answer lies in the historical methods of natural ventilation.

### **1.3 Use of Computational Fluid Dynamics (CFD) in Natural Ventilation Design**

As a design tool, CFD is unique as it can predict the air motion at all points in the flow. CFD modelling can be used to predict temperature and velocity fields inside buildings for steady-state problems (Allard, 1998). Due to the intensive nature of the computations, CFD is normally only used to generate ‘snapshots’ of how the design would work at a given point in time (CIBSE, 2005). Accordingly, this software can be used to test extreme or representative conditions at a single point in time. This is different from thermal analysis programs, which today generally calculate an energy balance for each hour of a typical year. This is a key limitation of CFD, as the modelling does not take into account what is happening in the space before and after the analysis, making the specification of boundary conditions to define the existing space extremely important.

With the addition of thermal equations, CFD can predict the effects of buoyancy and the temperature field, addressing questions of stratification and local air movement (CIBSE, 2007). This is particularly important in auditoria such as RWOH, as inlet and outlet levels as well as the height of an auditorium, affect the stratification levels of air. Warm stale air collects below the ceiling; CFD can be used to test whether this air will remain above the occupied zone (Short & Cook, 2005). Since indoor conditions of naturally ventilated spaces are difficult to predict using alternative building simulation tools, the use of CFD simulation becomes necessary (Hajdukiewicz, Geron & Keane, 2013).

## **2 ABOUT THE CASE STUDY: THE ROYAL WANGANUI OPERA HOUSE**

The Royal Wanganui Opera House (RWOH) was designed by Wellington architect, George Stevenson, in 1899. The building has a history of natural ventilation design, but the many alterations since the building’s construction have seen this system become obstructed. Having recently completed seismic strengthening work, the Whanganui District Council became interested in making the internal environment more comfortable for the audience during summer performances. Designed to ventilate without mechanical assistance, the RWOH in its existent state with an 830 person occupancy received numerous complaints regarding the internal air quality during performances during previous summer months.

The building has a large dome above the main seating area with a grille vent into the ceiling space, Figure 2. From the ceiling space, original plans show two penthouse louvres located above the stage space and seating area, seen in Figure 3. The large penthouse louver over the seating area has been replaced with a curved ridge vent with a smaller aperture, Figure 4. The

penthouse louvre over the stage has also been replaced with a ridge vent, however the opening was boarded up (seen as image 3 of Figure 9). Within the auditorium, multiple external openings are situated at the perimeter of the high level seating space, Figure 2. These openings appear to be the main exhaust air location for the higher level seating. Due to light and noise pollution, these openings are no longer opened, but are shut tight during performances. Despite comfort complaints, no mechanical system has been added. An upgrade to the system is urgently required.



Figure 1: The Royal Wanganui Opera House (Wanganui Opera Week, 2016).

Figure 2: The Dome above the Seating Area, and External Perimeter Openings (Author's Image, 2016).

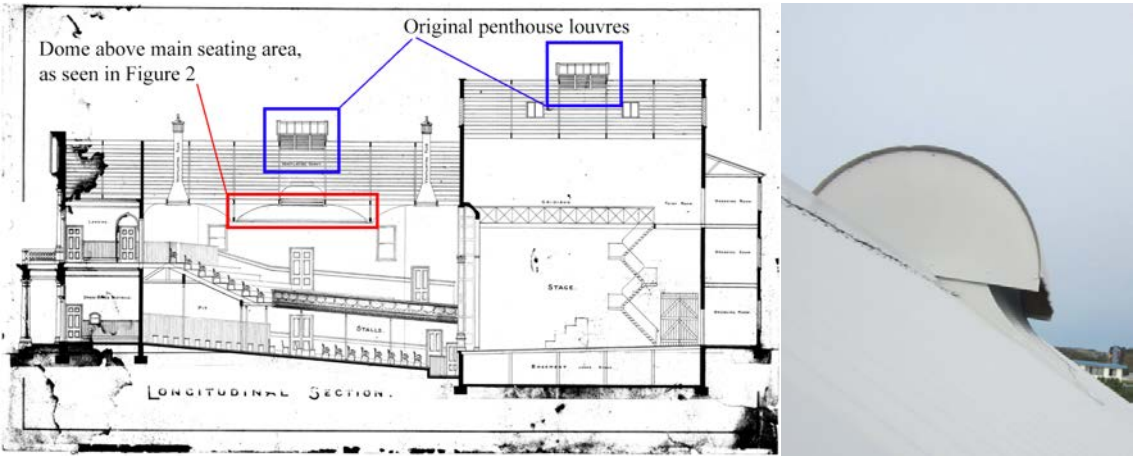


Figure 3: Longitudinal Section of the Wanganui Opera House, completed by architect George Stevenson, 1899.

Figure 4: Existing Ridge Vent Replacement of Penthouse Louvres (Author's Image, 2016).

### 3 3D COMPUTER GEOMETRY MODELLING

A combination of original plans, updated drawings from the recent seismic renovations, photographs, and measurements taken on site contributed to the 3D modelling of the RWOH in Autodesk Revit Software. In order to import a 3D model into Autodesk CFD (the air flow assessment software) the 3D model needs to be as simple as possible. A basic Revit model has been completed of the space, maintaining volume, wall area and the shell geometry. Due to the hierarchy of importance of elements and low complexity level required for a CFD model, ensuring the external shell and volume within the occupied space is as closely aligned with reality as possible was the main priority. Elements such as columns within the seating

area, individual seating and balustrades were not modelled due to their likely minimal effect on air flow. The operable area of openings has been modelled, and each external window and door has been modelled as a slot, even when closed, to account for air seepage. Detail has been incrementally added to the model to more closely align the simulated result with the measured data. The dome ceiling shape needed to be made more complex in order to reflect the pattern of air within the space, see Figure 5.

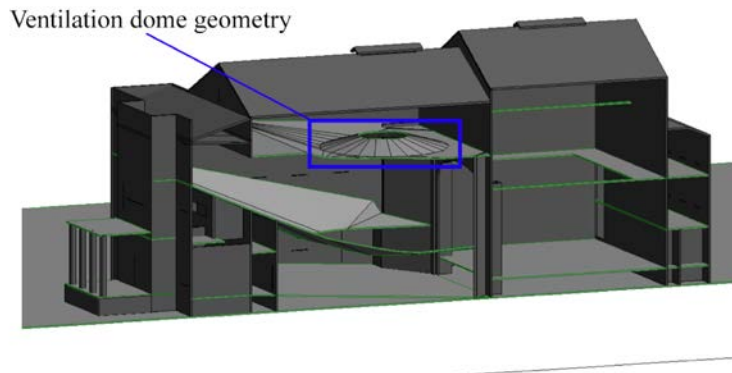


Figure 5: Longitudinal Section through the 3D Model of RWOH, showing the detail required for the dome ceiling in order to calibrate the CFD analysis.

#### 4 COLLECTION OF TEMPERATURE DATA

To calibrate the CFD simulation of the existing situation, thirteen calibrated Testo-175-H2 temperature and humidity recording devices were placed throughout the RWOH for a period of two weeks, set to record at 5-minute intervals. The Testo devices were themselves calibrated against an aspirated hygrometer temperature standard prior.

During the two-week period, several performances occurred including a local school production. While the Testo devices were largely left to run unattended, the day performance of the school production was attended in order to make operational alterations to the ventilation of the space during the interval. Due to the one-off nature of the CFD calculation, the calibration exercise was deliberately planned to test the model under as wide a range of operational and occupancy conditions as was feasible in the time available. The smoke exhaust bypass 'butterfly' dampers above the dome in the main seating area (image 2 in Figure 9), one of the vents above the high level seating (image 7 in Figure 9), the sliding shutters in the roof above the stage area (image 3 in Figure 9), and the roof access door above the stage area (image 6 in Figure 9) were opened for the second half of the performance.

Recordings from these performances, as well as when the building was empty, and real time external data from the Whanganui Weather Station provide the calibration data (NIWA, 2016). The recorded data of the temperature measurements taken during the two performances, in different weather conditions, show stratification in air temperature. The major test for the CFD simulations was to ensure it could re-create this stratification of air temperatures.

#### 5 CFD CALIBRATION

Calibration of the CFD modelling for the RWOH consisted of two stages. First, the model of the existing building was calibrated for the building's simplest situation: an unoccupied space during temperate weather conditions. Following a series of simulated iterations, incrementally altering the boundary conditions, turbulence equations, solar radiation inputs, wind speed

ratios, existing surface temperatures, assumed dimensions, and modelled materiality, the CFD outputs aligned with the measured data and fitted within the specified calibration tolerances and the limitations of the measuring devices.

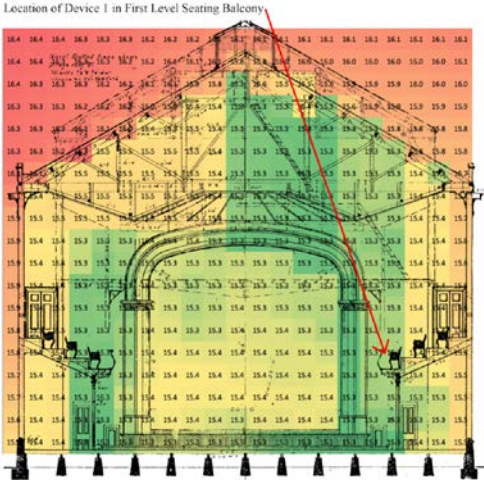
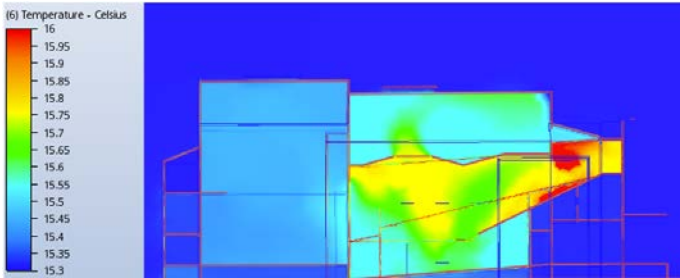


Figure 6. The Calibrated Occupied Model of 10.45am on the 20<sup>th</sup> September 2016, showing stratification of air and aligned results with measured data points.

Figure 7. A Cross Section of Exported Data from CFD, overlaid with architecture and device 1 location.

The second stage of the CFD modelling involved calibrating two models of the RWOH during an occupied time, when the number of occupants and state of the openings were known. One of the models depicted the space occupied as it is in usual operation with the majority of the openings closed; the second occupied model simulated the space when several high level openings had been opened. These models used the materiality, turbulence equations, solar radiation process, and assumed dimensions, that were confirmed in the stage one calibration. Following a series of simulated iterations, to determine the most effective way of modelling human heat gains within the space to decipher their influence on air temperature, the outputs from both models became aligned with the measured data and fitted within the specified calibration tolerances and the limitations of the measuring devices. The CFD output of a calibrated model of the occupied space can be seen in Figure 6, and Figure 7 shows the exported CFD data overlaid with the architectural drawings to identify the temperature measuring device location for numerical analysis.

**5.1 Calibration Conclusions**

While this study is based on CFD analysis, ultimately the measure of success for subsequent design alterations is the comfort of people within the RWOH. Accordingly, calibrating the CFD modelling by using temperature readings from within this space relates directly to the purpose of the CFD modelling process, and allows calibration utilising a measure that is more feasible to assess accurately across the full height of the auditorium than air movement. The value of calibrated CFD models is their potential for future application, examining the feasibility of reintroducing natural ventilation to modern buildings. This calibration process provided a Quality Assured level of trust in the design iterations that followed. Because the temperature recordings and subsequent calibration exercise was undertaken during spring rather than summer, when comfort issues occur, there is a degree of uncertainty as to whether the CFD modelling will reflect the summer scenario as accurately.

A further outcome of this process was the demonstration that the RWOH’s original natural ventilation system with penthouse louvres might have been successful. Successful naturally ventilated spaces not only have the ability to provide healthy and comfortable indoor

conditions, but also have the potential to reduce energy consumption. The demonstration of the success of the RWOH system adds strong support to the case that there is historical as well as functional value in the reinstatement of the system. It also suggests that the same process that has been applied to the RWOH could be replicated for many other large-scale historical buildings, which have most likely been designed to provide fresh air in a similar manner without fans or equipment. There is an added value of the calibration process for large-scale CFD models: demonstration of a consistency between prediction and reality. It suggests that CFD may reliably be used to study the feasibility of natural ventilation for modern buildings that house large crowds.

### 6 MODELLING PROPOSED DESIGN CHANGES

The CFD analysis of the summer performance identified several key areas of overheating concern. Potential changes to the RWOH were considered including: operational changes to air inlets, and air outlets; constructional changes to inlets, and outlets; and major alterations to the building. The first alterations tested were operational. These included reopening the ridge vent above the stage space (image 3 in Figure 9), opening the butterfly dampers above the dome (image 2 in Figure 9), and operating the perimeter windows that had been prohibited (image 4 in Figure 9). Allowing perimeter doors to be open during performances greatly improved the inlet air supply, but the operational issues of such a change restricted its uptake. Given the success of this last operational option, a construction change that was considered was operable louvres in these doors.

The major occupied area of concern noted in the CFD modelling, and confirmed by anecdotal evidence, was the high level seating at the back of the auditorium, shown in Figure 8. The shape of the ceiling rising above the high level seating creates a warm air trap. In the original design of the building, high level windows on the three perimeter walls surrounding this area were operable. Since the design of the building in 1899, the adjacent road has become significantly busier with motor vehicles. These windows are no longer opened during performances due to noise, as well as the light leak issues that will have existed from the outset. The constructional change agreed with the building owners was the addition of an airflow route from this high level seating space into the ceiling, by the way of a pelmet slot.

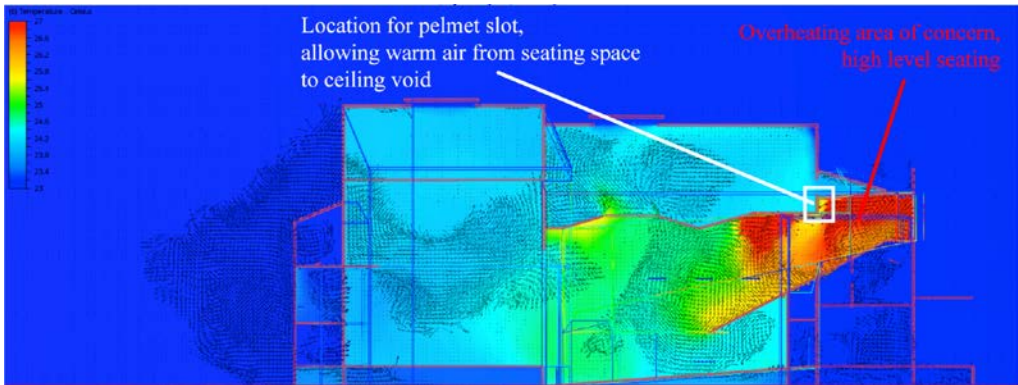


Figure 8. CFD Results from the Fully Occupied Summer Scenario, exposing the key problem area and potential solution.

Major constructional changes tested with CFD included removing the ridge vents (Figure 4), and reintroducing the original penthouse louvres above the stage and dome ceilings, as seen in the original section of Figure 3. The free area of these vents was far greater than their ridge vent replacements, and the height of the penthouse structures likely created a chimney effect. Restoration of the penthouse outlets would be a historical, as well as functional, feature.

## **7 STAGE ONE CHANGES FOR THE RWOH (OPERATIONAL)**

Given the restricted timeframe between the assessment of the building and an important performance, ventilation alterations were completed in two stages. The first stage involved ensuring the building was operated as successfully as possible during the New Zealand Opera School's performance in January 2017. A key member of the audience left the show part way through in a previous year, due to the heat and consequent fear of fainting. A repeat of this situation would likely see the building's use in future years becoming greatly reduced. Previously boarded up windows and the stage side ridge vent were rectified before the upcoming performance, but more intrusive construction changes were waitlisted for stage two. An operational user guide was created for this specific performance, Figure 9. This user guide was intended to guide the building management to operate the existing openings in a manner that allowed maximum airflow through the occupied spaces of the auditorium. Due to the importance of thermal comfort, previous restrictions due to traffic noise and light leaks were softened for this performance.

The weather in Whanganui during the Opera School's performance was cooler than previous years, a beneficial aspect for the ventilation. Feedback from the operational team was overwhelmingly positive; members of the audience reported no comfort complaints; temperatures in the space did not exceed 20°C.

## **8 STAGE TWO CHANGES FOR THE RWOH (CONSTRUCTION)**

Further work is being completed on the RWOH to safeguard the auditorium in future years, should the weather during summer performances not be as favourable as the night of the New Zealand Opera School's 2017 performance. Stage two changes are likely to occur incrementally as funds become available, with the priority of changes made being a reflection of their functional benefit, as well as their historic implication, constructional feasibility, and ultimately cost.

The major constructional alteration scheduled is the addition of a pelmet slot between the high level seating space and the ceiling void. The contract for this work is currently out to tender, along with the addition of thermostats throughout the auditorium, and louvres to the low level perimeter doors. Discussions are underway with Heritage New Zealand regarding the reintroduction of the penthouse louvres for functional and historical integrity.

## **9 CONCLUSIONS**

Natural ventilation systems often have a reduced cost in initial installation, as well as running and maintenance, over a fully mechanical heating, cooling and ventilation equivalent. Every town and city throughout New Zealand contains one, if not multiple, 100+ occupancy performance venues. Many are of similar historical value as the Royal Wanganui Opera House. Like the RWOH, as a result of recent severe earthquakes in New Zealand, many of these buildings are in the process of significant structural strengthening work. The RWOH experience has shown that the systems with which these buildings were originally designed have the potential to meet modern day standards of cooling and fresh air. The potential to restore not only the appearance but also the ventilation technology as a feature of historic preservation and earthquake strengthening is clear.

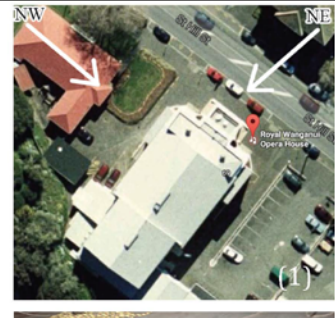
# Natural Ventilation Operation

Saturday 21<sup>st</sup> January 2017

Great Opera Moments 2017, 7.30pm – 10pm

## Predicted Weather for Sat:

Cloudy, temp begins increasing from 11°C at 7am, to 21°C at 2pm, and decreasing to 17°C at 7pm. NW winds turn NE from 5pm to 10pm (1).



## Day leading up to Performance:

### Flush the space

- Operate all openings Fri night; ensure they are closed by 7am Sat morning.
- Limit all openings after 7am to seal the building and keep cool night air in.
- If the internal air temp rises above the external air temp, open all openings.

### Limit heat gains

- Restrict all use of heaters, electrical equipment, number of occupants in the seating space, and use of stage lights where possible until the performance starts.

## Beginning of Performance:

If the space has remained cool, limit use of openings until performance starts.

- If the space has remained cool, limit use of openings until performance starts.
- If the space is already warm, and if it is cooler outside or there is perceivable wind, open all perimeter doors as occupants find their seats.
- If possible, place a member of staff in the high level seating space to monitor the temperature, and begin preventative ventilation before it is too late.

### Openings

- ☐ Ensure the butterfly dampers above the dome are in their held open position (2).
- ☐ Ensure the wooden slats to the vent above the high-level stage space are open (3).
- ☐ Ensure the windows at the back of the high-level seating space are fully

opened, including behind the stage space (4).

- ☐ If the NW/NE wind is not strong, or is cool, open all windows fully to their slid or held back position (5).
- ☐ Do not open the NE facing openings in the stage roof space and seating roof space if the wind is blowing directly in (this will push warm air in the ceiling down back into the space, (6)).
- ☐ In event of strong NE, open all southern facing windows only.
- ☐ Ensure the louvered vents to the ducts in the roof space above the high-level seating space are open (7).

## Performance Interval:

- Open all doors at low level, including fire doors, to flush the space. The more wind the better.

- If wind is occurring, open all openings to encourage cross ventilation.
- After the interval, maintain as many openings as possible depending on the success of flushing the space.

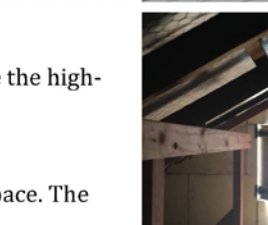
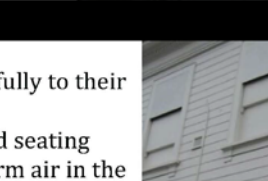
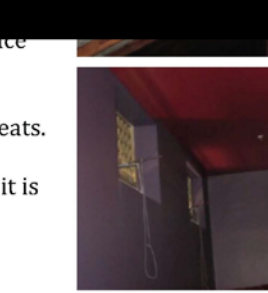
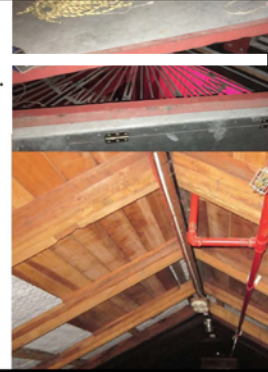


Figure 9: Ventilation Guide Supplied to the RWOH Operational Team, including images of existent operable ventilation.

This project is applying the same analysis to a large, 1380 seat, brick Opera House building constructed in 1913 in Wellington. Designed by Australian architect, William Pitt, the auditorium originally had a dome like the RWOH, but in place of the ridgeline vent it possessed a sliding roof opening of some 4m x 4m free area. Like the RWOH, the Opera House in Wellington has no contemporary description of how effective was its original system. Initial analysis suggests that its original design lacked the air inlets to bring cooling air into the auditorium to match the hot air exiting through the roof. Calibration studies have established a quality assured model. Design studies are exploring ways to restore the operation of the sliding roof and sliding ceiling during earthquake strengthening in a manner that restores this historical curiosity so visitors can see the building as designed, but ensures effective cooling and fresh air delivery for 1380 people on three levels in the auditorium.

The applicability of a similar process to assess the passive ventilation potential of similar buildings is vast in New Zealand. Ultimately, with these practical case study demonstrations of the potential of CFD analysis, the aim of this research is to produce a user guide for the investigation, analysis, and subsequent recommendations for the ventilation improvement of similar large audience buildings.

## 10 ACKNOWLEDGEMENTS

Whanganui District Council, Victoria University, BRANZ, and Norman Disney & Young.

## 11 REFERENCES

- Autodesk Inc. (2017). *Autodesk CFD: Computational fluid dynamics software*. Retrieved 2017 from Autodesk: <https://www.autodesk.com/products/cfd/overview>
- CIBSE. (2005). *Heating, Ventilating, Air Conditioning and Refrigeration CIBSE Guide B*. London: CIBSE Publications.
- CIBSE. (2007). *Natural Ventilation in Non-Domestic buildings AM10*. London: CIBSE Publications.
- Hajdukiewicz, M.; Geron, M.; Keane, MM. (2013). *Evaluation of Various Turbulence Models to Predict Indoor Conditions in Naturally Ventilated Room*. The 11<sup>th</sup> REHVA World Congress & 8<sup>th</sup> International Conference on IAQVEC, Prague.
- Kellert, S. R., Heerwagen, J., & Mador, M. (2008). *Biophilic Design: The Theory, Science, and Practice of Bringing Buildings to Life*. Hoboken, New Jersey: John Wiley & Sons, Inc.
- Kenton, A. G. (2004). Natural Ventilation in Auditorium Design; Strategies for Passive Environmental Control. *The 21st Conference on Passive and Low Energy Architecture* (pp. 19-22). Eindhoven: Martin Centre for Architectural and Urban Studies, University of Cambridge.
- Short, C., & Cook, M. (2005). Design guidance for naturally ventilated theatres. *Building Services Engineering Research and Technology*, 259-270.
- NIWA. (2016). *The National Climate Database*. Retrieved 2017 from CliFlo NIWA: <https://cliflo.niwa.co.nz>
- Wanganui Opera Week (2016). Tickets; Royal Wanganui Opera House. Retrieved from [wanganuioperaweek.co.nz/events/tickets](http://wanganuioperaweek.co.nz/events/tickets)

# Assessing Occupant and Outdoor Air Impacts on Indoor Air Quality in New California Homes

Iain S. Walker<sup>\*1</sup>, Yang-Seon Kim<sup>1</sup>, Brett C. Singer<sup>1</sup>, and W. Rengie Chan<sup>1</sup>

*1 Lawrence Berkeley National Laboratory  
MS 90-3074, 1 Cyclotron Road  
Berkeley, CA, USA  
Presenting author: Iain Walker  
\*Corresponding author: iswalker@lbl.gov*

## ABSTRACT

In 2008 the State of California adopted new building codes that required the use of mechanical ventilation systems in homes that meet the requirements of ASHRAE Standard 62.2. The standard requires both a dwelling unit mechanical ventilation system and exhaust fans in kitchens and bathrooms. A field study was undertaken to evaluate the IAQ and ventilation performance of homes built to these requirements. For ventilation system performance, the airflows of all mechanical ventilation systems were measured and their use was monitored for a one-week period. To evaluate IAQ, key pollutants were measured indoors and outdoors during the week, and occupants completed satisfaction surveys. The key pollutants included: formaldehyde, humidity, PM<sub>2.5</sub> and NO<sub>2</sub>. Passive samplers were used to determine average concentrations for the week. Active samplers were used to develop time-series results that can be used to correlate pollutant concentrations with occupant activities. Other ventilation/IAQ related parameters were also recorded, such as stove top temperatures to indicate cooking, exterior door contact switches to know when large openings were being used for ventilation and sensors to determine when clothes dryers were being used. The building envelope and duct leakage were measured to enable estimates of infiltration and duct leakage effects. This paper presents an overview of the test procedures and preliminary results from several homes. The results show that although average concentrations may be reasonable compared to available standards (with the exception of formaldehyde), occupants have a strong impact on pollutant variability and source strength and that outdoor concentrations cannot be ignored. Overall, these mechanically ventilated homes have reasonable IAQ. The homes and duct systems are moderately tight, though not excessively so, by US standards. Significant concerns have been expressed regarding compliance with the ventilation requirements in the California building code. However, almost all the ventilation systems in this study complied with the ventilation air flow requirements and on average were significantly higher than the minimum required air flow rates.

## KEYWORDS

ASHRAE 62.2, Pollutant measurement, Formaldehyde, Mechanical Ventilation, Compliance

## 1 INTRODUCTION

This paper presents methods and preliminary results from the Healthy Efficient New Gas Homes (HENGH) field study for the California Energy Commission. The field study is collecting data on ventilation systems and indoor air quality (IAQ) in California homes built since the 2008 update of the state's residential energy efficiency standards first required dwelling unit mechanical ventilation (CEC, 2008). Data are being collected on ventilation system designs and specifications, installed equipment performance and use, air contaminant concentrations and environmental parameters, and resident perceptions of indoor environmental quality. The focus of the study is on evaluation of IAQ when windows are closed and mechanical ventilation is operating. Measurements include one-time diagnostic testing of building and equipment performance and week-long monitoring of equipment use, pollutant concentrations, and pollutant-related activities. All the homes in the study are "new" and located in California. "New" homes for this study means homes that were built to meet Title 24 and be mechanically ventilated to meet ASHRAE Standard 62.2. The study

target is to collect data in about 70 homes in total. In this paper, we report results from the first 16 homes. The pollutant data are all from time-integrated measurements. Data from additional homes and analyses exploring time-resolved data to investigate associations of ventilation, pollutant concentrations and occupant activities will be presented in subsequent papers.

## **2 FIELD MEASUREMENT PROCEDURES**

More details regarding the field testing protocols can be found in Chan et al. (2016). The field test protocol was approved by the LBNL Human Subjects Committee.

The following general characteristics are determined for each home:

- Floor area, year of construction, number of stories, and number of occupants.
- Floor plan showing number and location of all bedrooms and bathrooms.
- Locations and rated airflows of all ventilation equipment (marked on floor plan).
- Number and location of all gas burning appliances, such as furnaces, water heaters, ovens, cooktops, and gas fireplaces.

### **2.1 Home Diagnostic Measurements**

The following diagnostic tests are performed at the beginning of the testing on each home in order to obtain information relevant for ventilation and IAQ assessments:

- Envelope air tightness is determined using multi-point blower door tests following the procedures and calculations in ASTM E779 (ASTM 2010). Envelope air tightness is expressed at Air Changes per Hour at 50 Pa (ACH50).
- Duct air tightness is determined using the “DeltaQ” approach that measures the duct leakage to outside for supply and return ducts under normal operating conditions following the procedures and calculations in ASTM E1554 (ASTM 3013).
- All mechanical system air flows: home ventilation system, kitchen and bathroom exhausts.

### **2.2 Indoor activity monitoring**

Many indoor pollutants are associated with occupant activities: moisture and VOCs from cooking, cleaning and bathing, CO<sub>2</sub> from metabolic activity, and CO<sub>2</sub>, NO<sub>2</sub>, moisture and particles from cooking. The following are continuously monitored during the test week and recorded using various devices:

- Cooktop and oven use using thermal sensors placed directly on the cooking surfaces
- Fireplace use using temperature sensors (no fireplace use was recorded in any of the current homes during our monitoring).
- Bathroom, kitchen and other exhaust fans using motor sensors or small data-logging anemometers to record when these fans operate and at which setting.
- Clothes dryer use using a motor on/off sensor and logger.
- Central forced air system operation from measuring air temperature at a supply register of the central forced air system.
- Opening/closing of doors using micro-switches. Only select doors and windows were monitored based on input from the occupants on those that were used most often. This information is critical because there are large ventilation air flows associated with these openings and estimating the impact of mechanical ventilation systems is very difficult if conflated with window or door opening.

### 2.3 IAQ Measurements

Temperature and relative humidity are measured outside the home and at multiple locations in the home, primarily in the main living area, bedrooms and bathrooms. Pollutants are measured using the instruments (and locations) listed in Table 1. The outdoor measurements are critical for pollutants whose outdoor levels can be significant – particularly PM<sub>2.5</sub> for which a major source can be outdoor air. The pollutants were chosen based on their potential health impact and ubiquity and include the major pollutants of concern determined from previous studies (Logue et al. (2012)). The multiple locations for some sensors provide some indication of the spatial variations of formaldehyde exposures inside the study homes. Temporal variations are evaluated using sensors with high time resolution. Because the real-time NO<sub>2</sub> and formaldehyde real-time sensors can have significant calibration issues passive samplers are also used, e.g., the performance of the real-time formaldehyde monitors (Carter et al., 2014) had been tested in laboratory setting but not in field applications. The results from the passive samplers are used as a calibration check for the real-time measurements.

Table 1 IAQ measurements during one-week sampling period

Parameter	Instrument	Indoor Location(s)	Outdoor
PM <sub>2.5</sub>	MetOne ES-642/ BT-645	Central location	Yes
CO <sub>2</sub>	Extech SD-800	Central location, master and other bedrooms	--
NO <sub>2</sub>	Aeroqual NO <sub>2</sub> monitor	Central location	--
	Passive Ogawa samplers	Central location	Yes
Formaldehyde	Shinyei formaldehyde monitor	Central location, master bedroom	--
Formaldehyde/ acetaldehyde	SKC UME <sub>x</sub> 100 passive sampler	Central location, master bedroom	Yes

PM<sub>2.5</sub> is monitored both indoors (MetOne BT-645) and outdoors (MetOne ES-642) in real-time. The light source and sensor of these two nephelometers are identical so that the measured concentrations can be compared. The ES-642 has a heated inlet to handle high humidity that may be encountered outdoors. PM<sub>2.5</sub> concentrations are recorded at a one-minute time interval.

CO<sub>2</sub> is monitored at multiple indoor locations as an indicator of bioeffluents. The Extech SD-800 is used to measure CO<sub>2</sub> concentrations, as well as temperature and relative humidity, at a one-minute time interval.

NO<sub>2</sub> is a combustion related air contaminant of interest. Real-time NO<sub>2</sub> concentrations are used to characterize contributions from cooking and other indoor sources. The Aeroqual monitor is used to measure NO<sub>2</sub> concentrations at a one-minute time interval. It is suitable for indoor use only. In addition, NO<sub>2</sub> is measured using passive samplers both indoors and outdoors to obtain a time-integrated NO<sub>2</sub> value that can be used to calibrate the Aeroqual measurements (from indoor results) and as a measure of outdoor concentrations.

Formaldehyde concentrations are measured at 30-minute time interval at the central indoor location and also in the master bedroom. Passive samples are collected using SKC UEM<sub>x</sub> 100 samplers in the same locations as the real-time monitors. The passive samplers are also used to measure formaldehyde concentrations outdoors.

### 3 SUMMARY AND RESULTS OF FIELD IAQ MEASUREMENTS AND HOME CHARACTERISTICS

The results of this study are compared to those of a prior study of ventilation and indoor air quality in new homes in California (Offermann, 2009). In that study, pollutant concentrations and air exchange rates were measured over a single day and window use was monitored over a week in 105 California homes that were built in 2002-2004 and measured in 2005-2007. The homes in the prior study were built and tested before the State of California required mechanical ventilation or limited the formaldehyde allowed in building products. We also compare the results to relevant guideline exposure limits.

Table 2 summarizes the home characteristics. Compared to state and US national averages these homes are fairly representative of new construction. The floor area is typical of new California homes but larger than the US average of about 200 m<sup>2</sup> (US Census Bureau). Analysis of blower door tests in California homes for the RESAVE project (Sherman et al. 2013) showed that homes built since 2000 have an average air leakage of 4-5 ACH<sub>50</sub>. Data from another recent California study (Proctor et al. 2011) showed a median of 4.7 ACH<sub>50</sub> for single-family homes. For comparison, the IECC (2013) that is used in many US states and energy programs would require most of these homes to be less than 3 ACH<sub>50</sub>. Only two of the sixteen homes tested so far in the HENGH study were below 3 ACH<sub>50</sub>.

Table 2 IAQ Home Characteristics and Diagnostic Test Results

	Mean	Range (Min- Max)
Size (m <sup>2</sup> )	252	156 – 390
# of Bedrooms	3.6	3 - 5
# of Full Bathrooms	2.9	2 - 5
Built Year	2014	2011- 2015
Number of Occupants	2.6	1 - 8
Envelope Tightness (ACH <sub>50</sub> )	5.0	1.8 - 7.8
Duct Leakage (%)	8	1.5 – 38
Min. required dwelling unit mech. ventilation (L/s)	29	22 - 41
Dwelling unit mech. ventilation ( % of min. required)	152	71- 218

Duct leakage is important in ventilation and IAQ studies because duct leaks act like mechanical ventilation and even a fairly small duct leak can have a much bigger effect on ventilation than the designed home ventilation system. For example, at a typical forced air system flow for these homes of 600 L/s, 6% leakage is an air flow of 36 L/s from outside; this is similar to the mechanical ventilation system flow, as noted in Table 2. In addition, if the duct leakage is from locations that may have higher pollutant levels than indoors (e.g., from chemical storage in a garage) then this duct leakage may draw pollutants into the home. In our study 13 homes had valid duct leakage test and nine homes meet the duct air tightness requirements for California homes, i.e., 6% of total system air flow. The average duct leakage is much higher than the median due to one outlier at 38%.

The dwelling unit mechanical ventilation systems are predominantly exhaust (13 out of 16 homes) extracting from a wet room, typically the laundry room. The other three homes had supply systems integrated into the central forced air duct system. California State Energy Code (Title 24) refers to ASHRAE 62.2-2008 fan sizing equation for its ventilation requirements. The California code does not allow for any infiltration credit (other than the 0.1 L/m<sup>2</sup> default infiltration credit assumed in the fan sizing equation). The individual home minimum flow requirements and installed flows are given in Table 3. On average the

mechanical systems are oversized compared to the fan size required by Title 24 by about 50%. This oversizing indicates that there is the potential for some energy savings. Two systems did not have sufficient air flow to meet the minimum requirements, one of which was more than 20% undersized. Similar oversizing was reported by Stratton et al. (2013) from measurements in 15 California homes in 2010: dwelling unit ventilation systems averaged 40% larger than the minimum requirements and 2 of the 15 systems had too little flow.

Table 3. IAQ Home Characteristics and Diagnostic Test Results

House	Min. required flow (L/s)	Dwelling unit mechanical ventilation (L/s)
3	32.0	47.0*
5	39.0	51.7
6	28.7	54.1
7	32.9	44.7
10	40.9	89.3*
15	24.0	33.4
16	31.5	27.7
8	28.7	47.9
9	32.0	47.0*
11	25.9	38.1
4	28.2	20.2
13	23.0	40.9
17	24.0	41.4
21	31.5	48.4
19	25.9	52.2
24	22.1	33.4
<b>Mean</b>	<b>29.4</b>	<b>44.8</b>
<b>STDEV</b>	<b>5.4</b>	<b>15.1</b>

\*Supply system, rated fan airflow (not measured)

Table 4 Range Hood Exhaust Flows

	Mean	Median	Range (Min- Max)
High setting (L/s)	167	101	48–493
Low setting (L/s)	69	54	27–170

Table 4 summarizes the range hood air flows. For kitchen ventilation, all of the homes met the minimum requirement of 50 L/s on the high setting and nine on the low setting. All of the homes used range hoods vented to outside. Half of the range hoods had an integrated microwave oven. For bathroom ventilation, all the exhaust fans met the 25 L/s minimum air flow requirement. For comparison, about 1/3 of the Stratton et al. (2013) homes had bathroom fans (48 total) that did not meet the minimum 25 L/s requirement of ASHRAE 62.2, but all four of the measurable kitchen range hoods did meet the minimum 50 L/s requirement. In general, these homes are meeting the requirements for installed exhaust fans in kitchens and bathrooms. A key issue with both kitchen and bathroom ventilation is how they are operated. For kitchen exhaust it is at the discretion of the occupants. For bathrooms there were humidity controls (whose setpoint is fixed by the installer) in 11 of the 16 master bathrooms and 29 of the 46 total bathroom fans. In future work we plan to compare estimates of cooking operation (using stove top temperatures) to range hood operation and measured bathroom temperatures and humidities to bath fan operation to see how often these fans are used as needed by occupants.

A key observation regarding the dwelling unit ventilation systems is that all but one of them were turned off when the field investigation teams first attended the homes. For the purposes of our study we turned these systems on. Note that in ASHRAE 62.2 and California Title 24 it

is a requirement to have a clearly labelled switch for this system that can be used by occupants to turn it off (or on) and there is little or no occupant education as to what this switch is doing to the home. However, ten of the homeowners claimed to know how to use the ventilation system (but had turned it off anyway).

Table 5 summarizes the results of the week-long, time-integrated measurementsofformaldehyde and NO<sub>2</sub>.The formaldehyde concentrations were similar in the master bedroom and common room of each home, but varied by more than a factor of three across homes. As a group, formaldehyde concentrations in the HENGH study are lower than those reported by Offermann(2009) for homes built 2002-2004, which had a median of 36 µg/m<sup>3</sup>, and range of 5–136µg/m<sup>3</sup>) and the 32 µg/m<sup>3</sup>from other studies quoted by Offermann.The meanformaldehyde concentrations fall somewhere between the 9 µg/m<sup>3</sup> chronic Reference Exposure Limit (REL) and 55 µg/m<sup>3</sup> acute REL from California’s Office of Environmental Health Hazard Assessment. One home in our study was at the acute formaldehyde REL in the bedroom.Time-integrated NO<sub>2</sub> concentrations in all homes were well below the California annual (i.e. long-term) air quality standard of 57 ug/m<sup>3</sup>. The average of 7.9 µg/m<sup>3</sup>across the first 16 HENGH homes is a little higher than the mean of 5.7 µg/m<sup>3</sup> reported by Offermann for the 29 homes in which it was measured in that study. NO<sub>2</sub> concentrations were much lower than the levels reported by Mullen et al. (2016) for California homes with gas appliances.

Table 5 Time Integrated results for Formaldehyde (HCHO) and NO<sub>2</sub>

House	HCHO Livingroom (µg/m <sup>3</sup> )	HCHO Bedroom (µg/m <sup>3</sup> )	HCHO Outdoor (µg/m <sup>3</sup> )	NO <sub>2</sub> Livingroom (µg/m <sup>3</sup> )	NO <sub>2</sub> Outdoor (µg/m <sup>3</sup> )
3	NA	NA	NA	3.8	1.9
5	NA	NA	NA	6.6	7.2
6	48	55	3.1	6.0	2.8
7	30	34	3.1	15.5	5.7
10	28	26	3.1	26.1	6.2
15	29	30	3.6	NA	NA
16	52	55	2.9	5.5	15.5
8	34	33	2.3	2.1	6.8
9	29	21	2.6	7.2	2.3
11	32	30	2.7	6.4	3.8
4	26	21	1.8	4.5	3.6
13	18	19	1.6	4.3	7.4
17	19	18	1	2.3	4.7
21	22	23	2	5.1	5.9
19	17	24	2.3	13.2	1.9
24	15	15	3	9.6	4.2
<b>Mean</b>	<b>28</b>	<b>29</b>	<b>2.5</b>	<b>7.9</b>	<b>5.3</b>
<b>STDEV</b>	<b>11</b>	<b>13</b>	<b>0.7</b>	<b>6.3</b>	<b>3.4</b>

The results in Table 6 show that on average the PM<sub>2.5</sub> levels are lower indoors than outdoors and only four homes had higher average indoor concentrations than outdoors. This implies that outdoor air is a significant source of indoor PM<sub>2.5</sub>. PM<sub>2.5</sub> indoors and outdoors is characterized by high periodic events (and minimums that are essentially zero) as shown by the extreme maximum values in some homes and outdoor conditions that are two orders of magnitude above the mean. Compared to WHO guidelines, the average PM<sub>2.5</sub> concentrations are below the annual level of 10 µg/m<sup>3</sup>. These are lower than the 24 hour time-integrated results averaged over 31 homes in Offermann, of 13 µg/m<sup>3</sup>indoors and 8 µg/m<sup>3</sup> outdoors. The

maximum levels exceed the 24 hour guideline level of 25  $\mu\text{g}/\text{m}^3$  but these maximum levels were for time periods much less than 24 hours.

Table 6 Summary of time-resolved indoor and outdoor PM<sub>2.5</sub>( $\mu\text{g}/\text{m}^3$ )

House	Living room				Outdoor		
	Mean	Minimum	Maximum	Minutes > 25 $\mu\text{g}/\text{m}^3$	Mean	Minimum	Maximum
3	5.9	1	27	15	2.4	0.6	13.2
5	1.1	0	8	X	3.3	0.7	15
6	NA	NA	NA	NA	4.8	0.7	48.2
7	2.3	0	9	X	4.5	0.7	51.4
10	4.2	0	112	113, 28, 32	2.5	0.02	82.5
15	2.3	0	32	5	3.8	0.01	53
16	1.7	0	50	1	8.3	1.6	63
8	1.5	0	26	1	2.2	0.01	65.1
9	2.6	0	14	X	3.6	0.7	25.9
11	0.1	0	3	X	1.7	0.7	10.9
4	11	0	493	367, 228 (oven cleaning)	5.1	0.01	63.5
13	0.9	0	12	X	15.7	0.7	82.4
17	4.5	0	98	42, 456, 3	15.5	0.7	315.8
21	10.6	5	65	92	8.2	0.7	77.9
19	3.0	0	298	40, 130	3.4	0.02	45.3
24	2.8	0	191	182	0.1	0.04	0.9
<b>Mean</b>	<b>3.6</b>				<b>5.3</b>		

Table 7 Summary of time-resolved CO<sub>2</sub> for the Living Room and Master Bedroom

House	Living Room CO <sub>2</sub> (ppm)		Master Bedroom CO <sub>2</sub> (ppm)	
	Average	Highest 1 hr	Average	Highest 1 hr
3	834	1176	849	1264
5	681	989	740	1024
6	608	820	686	1015
7	626	873	644	1030
10	638	974	760	1216
15	730	1345	751	1101
16	761	1008	706	918
8	555	650	610	821
9	569	690	643	965
11	578	859	568	694
4	520	818	607	785
13	618	1003	662	995
17	512	668	510	627
21	575	845	720	1163
19	564	963	665	1098
24	576	952	762	1280
<b>Mean</b>	<b>622</b>	<b>915</b>	<b>680</b>	<b>1000</b>
<b>STDEV</b>	<b>89</b>	<b>181</b>	<b>85</b>	<b>193</b>

Table 7 shows that the average and highest one-hour CO<sub>2</sub> in the common living space was lower than that in the master bedroom in almost all homes. This is consistent with other studies that have found higher CO<sub>2</sub> concentrations in bedrooms, owing to the extended period of occupancy in a room that commonly has a door closed overnight. The average of 622 ppm indoors is very close to the 610 ppm found by Offermann.

The mean indoor temperature in the test homes averaged 22.5°C, and varied from a low of 18°C to a high of 27°C. During the test week, indoor temperatures were relative constant; the mean of the standard deviations across homes was 0.8°C. There was more variability in relative humidity (RH). The mean over all homes was 46% with a standard deviation between homes of 8% RH. On average the range from minimum to maximum RH for each house was 15% RH. No home recorded a value above 70% RH, only one home had a maximum above 65% and three homes were above 60%.

The home ventilation rates were estimated by combining the known mechanical ventilation system air flows (including kitchen, bathroom and dryer exhaust operation) and their operating time with natural infiltration calculated from the measured air tightness using the enhanced infiltration model from the ASHRAE Handbook of Fundamentals, Chapter 16 (ASHRAE 2013). Table 8 summarizes the time-average air change rates combining infiltration and mechanical ventilation over the week of testing. We also calculated the effective ventilation rate that is required if average pollutant concentrations are to be calculated. For the HENGH homes, the standard deviation of the sample of individual home ventilation rates was about 30% of the mean. The mean difference between time-averaged and effective ventilation rates is only 0.02 ACH. The average of 0.37 ACH is close to historical US targets of 0.35 ACH for ventilation but lower than many European requirements. One home (19) had extremely high ventilation due to both master bathroom exhaust fan, and laundry room exhaust fan continuously running during the test period. One home (4) has a very low calculated ventilation rate due to inadequate dwelling unit mechanical ventilation fan flow.

Table 8 Mean and Effective Ventilation Rates

House	Time-averaged ventilation rate (Mechanical + Infiltration) (ACH)	STDEV	Effective Ventilation Rate (ACH)
3	0.20*	0.04	-
5	0.33*	0.09	-
6	0.08*	0.21	-
7	0.18	0.07	0.15
10	0.52	0.11	0.50
15	0.27	0.03	0.27
16	0.29	0.03	0.29
8	0.25	0.08	0.23
9	0.27	0.05	0.26
11	0.24	0.07	0.23
4	0.09	0.06	0.08
13	0.45	0.19	0.38
17	0.35	0.13	0.31
21	0.37	0.14	0.32
19	1.17	0.16	1.10
24	0.79	0.09	0.78
<b>Mean</b>	<b>0.37</b>	<b>0.10</b>	<b>0.36</b>
<b>STDEV</b>	<b>0.27</b>		

- leakage test data were not available – mechanical air flows only

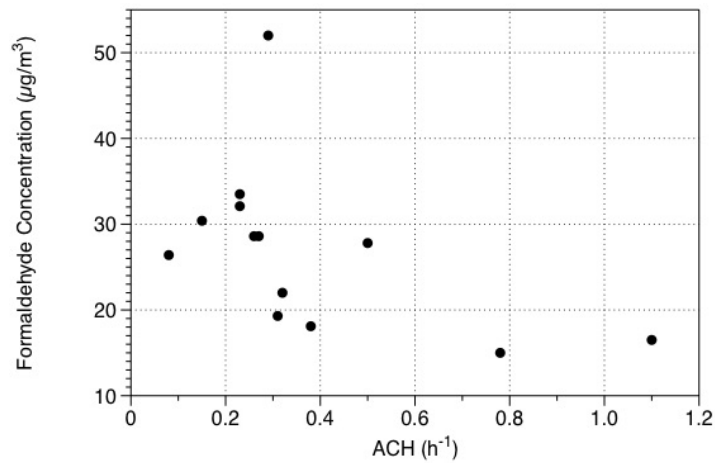


Figure 1. Dependence of Formaldehyde Concentration on Effective House Air Change Rate

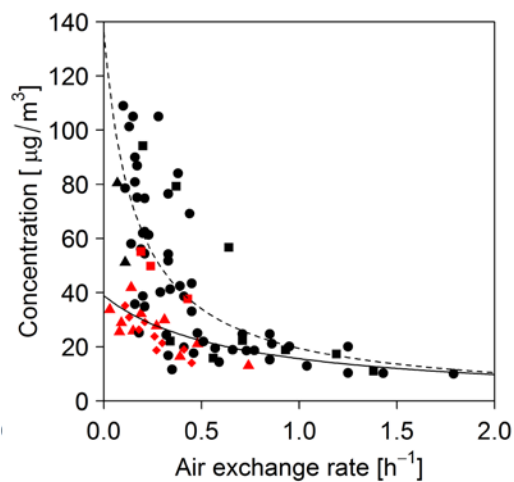


Figure 2. Dependence of Formaldehyde Concentration on House Air Change Rate from Hult et al. (2015).

Figure 1 shows how the average Formaldehyde concentration varies with the effective air change rate. A similar dependence of Formaldehyde concentration on air change rate was observed by Hult et al. (2015), as shown in Figure 2.

#### 4 CONCLUSIONS

Although these results are from a subset of study homes some preliminary conclusions can be drawn. Overall these homes showed good compliance with installed mechanical ventilation requirements. However, due to being turned off almost none of the dwelling unit ventilation systems were operating. It was not always clear who turned them off; but there is evidence that it was the occupants in at least some of the cases. The pollutant concentrations were similar to previous studies in California and the only levels of concern are for Formaldehyde. The results show that increasing ventilation rates would be a good method for reducing formaldehyde concentrations.

#### 5 ACKNOWLEDGEMENTS

The primary financial support for this research is provided by California Energy Commission Contract PIR-14-007. Financial, in-kind technical, and logistics support for the field study has been provided by the Pacific Gas and Electric Company and the Southern California

California Gas Company. Neil Leslie of the Gas Technology Institute and Max Sherman of LBNL were instrumental in initiating the project and obtaining funding. Luke Bingham (GTI) and Guy Lawrence (MistiBruceriand Associates) conducted the bulk of the data collection efforts for this paper. LBNL researchers Woody Delp helped with field data collection and Marion Russell assisted with aldehyde and NO<sub>2</sub> sample analysis. Rob Kamisky and Larry Brand of GTI provided project management support.

## 6 REFERENCES

ASTM (2010) E779-10 Standard Test Method for Determining Air Leakage Rate by Fan Pressurization, ASTM international.

ASTM (2013) E1554 / E1554M-13 Standard Test Methods for Determining Air Leakage of Distribution Systems by Fan Pressurization, ASTM International.

Carter, E.M., Jackson, M.C., Katz, L.E. and Speitel, G.E. (2014) A coupled sensor-spectrophotometric device for continuous measurement of formaldehyde in indoor environments, *Journal of Exposure Science and Environmental Epidemiology*. Vol. 24, pp. 305-310. Nature.

CEC (2008) 2008 Building Energy Efficiency Standards for Residential and Nonresidential Buildings, Sacramento, CA, California Energy Commission.

Chan, W.R., Kim, Y-S, Singer, B.C. Walker, I.S. and Sherman, M.H. 2016. Healthy Efficient New Gas Homes (HENGH) Field Study Protocol. Lawrence Berkeley National Laboratory, Berkeley CA, Report number LBNL-1005819.

Hult, E.L., Willem, H., Price, P.N., Hotchi, T., Russell, M.L. and Singer, B.C. (2015). Formaldehyde and acetaldehyde exposure mitigation in US residences: in-home measurements of ventilation control and source control. *Indoor Air*, 25, 523-535. doi:10.1111/ina.12160

IECC (2013). International Energy Conservation Code, International Code Council. Washington DC. USA.

Logue, J., Price, P., Sherman, M. and Singer, B. (2012). A method to estimate the chronic health impact of air pollutants in US residences. *Environmental Health Perspectives*. Vol. 120., No.2, February 2012. National Institute of Environmental Health Services, US Department of Health and Human Services, Washington DC. USA.

Mullen NA, Li J, Russell ML, Spears M, Less BD, Singer BC. 2016. Results of the California Healthy Homes Indoor Air Quality Study of 2011-13: Impact of natural gas appliances on air pollutant concentrations. *Indoor Air* 26(2): 231-245.

Offermann, F. (2009). Ventilation and Indoor Air Quality in New Homes. California Energy Commission Report CEC-500-2009-005.

Proctor, J., Chitwood, R., Wilcox, B., 2011, Energy Characteristics and Opportunities for New California Homes, CEC-500-21012-062. California Energy Commission, Sacramento, CA.

Sherman, M., B. Singer, J. Logue, I. Walker, C. Wray, W. Chan, E. Hult, W. Turner (Lawrence Berkeley National Laboratory), D. Stevens (Panasonic), T. Weston (DuPont), 2013, *Residential Energy Savings from Air-Tightness and Ventilation Excellence (RESAVE)*, California Energy Commission, publication number CEC-500-2013. <http://resave.lbl.gov>

Stratton, J.C., Walker, I.S. and Wray, C.P. (2013). Measuring airflows in residential mechanical ventilation systems: Part 2 - Field Evaluation of Commercially-Available Devices and System Flow Verification. Lawrence Berkeley National Laboratory, Berkeley CA, Report number LBNL 5982E.

# From EN 779 to ISO 16890: a new worldwide reference test method for general ventilation filters

Alain Ginestet<sup>1</sup>

*1 CETIAT*

*Centre Technique des Industries Aéronautiques et Thermiques  
Domaine scientifique de la Doua, 25 avenue des Arts  
69100 Villeurbanne, FRANCE*

*\*Corresponding author: alain.ginestet@cetiat.fr*

## ABSTRACT

For testing of general ventilation filters, a completely new standard is now available and is going to replace EN 779 (2012) since the parts 1 to 4 of ISO 16890 (2017) have been adopted in August 2016 and published in 2017 at both international and European levels. With this new standard, the fractional efficiency of the new and the conditioned (24 hours to isopropanol vapour) filters is measured between 0.3 and 10  $\mu\text{m}$ . The 2 fractional efficiency curves are combined to 2 different reference particle size distributions in order to obtain the efficiencies of the filter with reference to  $e\text{PM}_{1.0}$ ,  $e\text{PM}_{2.5}$  and  $e\text{PM}_{10.0}$ . This paper presents the content of the new ISO 16890 and highlights the main differences between EN 779 and ISO 16890. The adoption of the new ISO 16890 standard has a great impact on the filtration and ventilation industries.

## KEYWORDS

General ventilation filter, air filter testing, EN ISO 16890, EN 779, filter classification

## 1 INTRODUCTION

The reference standard for testing general ventilation filters (Figure 1) in Europe is EN 779 (2012).

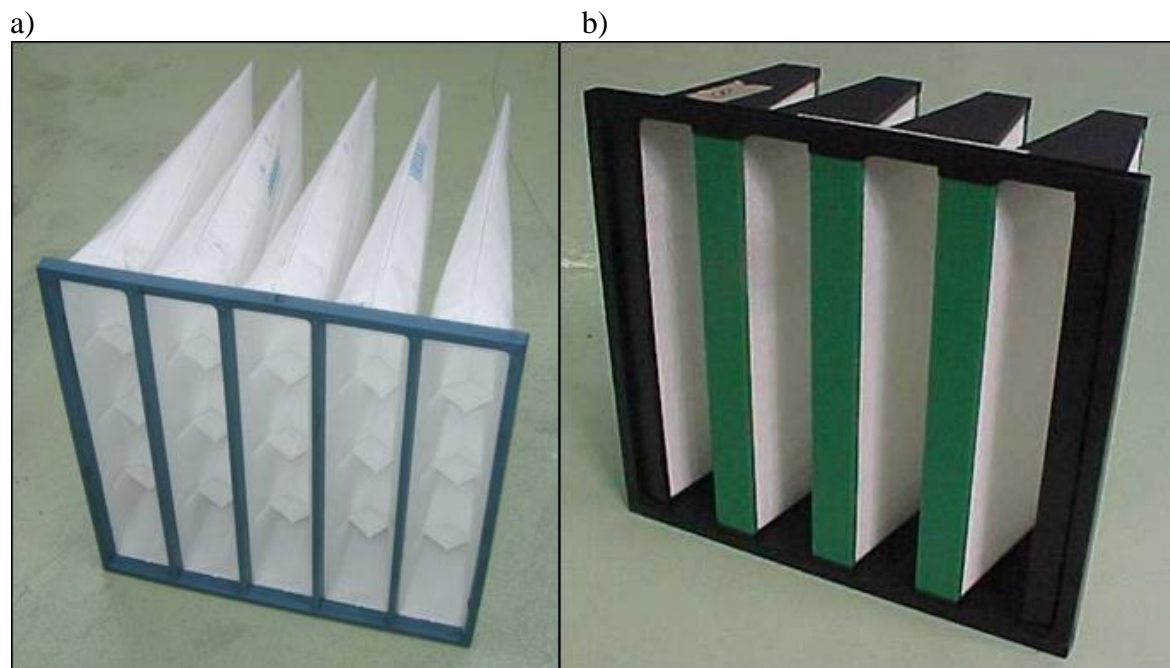


Figure 1: An example of general ventilation filters. a) Bag filter, b) Rigid filter

A completely new standard is now available and is going to replace EN 779 since the parts 1 to 4 of ISO 16890 standard (2017a, 2017b, 2017c, 2017d) have been adopted in August 2016 and published in 2017. Because this standard has also been adopted in Europe at the same time (2 votes in parallel according to the Vienna agreement), this ISO standard is also an EN standard and applies automatically in Europe in place of the existing EN 779 by mid-2018.

If the same parameters are measured with the use of both EN 779 and ISO 16890 standards – pressure drop as function of air flow, pressure drop as function of loading with an artificial dust, fractional efficiency, gravimetric efficiency, test dust holding capacity – there are some differences (test aerosol, loading dust, final pressure drop, etc.) and the filter ranking systems are completely different. So the objective of this paper is to present the content of the new standard and to explain the main differences between EN 779 and ISO 16890. The new filter ranking system is especially highlighted.

## **2 EN ISO 16890 VS. EN 779**

The ISO 16890 standard is applicable for an air flow rate between 900 m<sup>3</sup>/h and 5400 m<sup>3</sup>/h referring to a test rig with a nominal face area of 610 mm x 610 mm. The test rig used for filter testing according to ISO 16890 is the same as that used for filter testing according to EN 779 except of minor changes which are not described here (mainly a closer control of the temperature and the humidity of the test air and the use of an aerosol mixing device upstream of the downstream aerosol sampling line). The main differences between the ISO 16890 and EN 779 standard are listed in Table 1.

For both standards a test begins with the determination of the initial pressure drop / air flow characteristic and the resistance to air flow of the tested filter is measured at 50%, 75%, 100% and 125% of the rated air volume flow rate. The resistance to air flow data are corrected to an air density of 1.20 kg/m<sup>3</sup>.

For both standards the initial fractional efficiency (efficiency by particle size) of the tested filter is measured. Two different test aerosols are used with the ISO 16890 (DEHS (DiEthylHexylSebacate) liquid phase aerosol between 0.3 and 1.0 µm and KCl (Potassium chloride) solid phase aerosol between 1.0 and 10 µm) while DEHS (between 0.2 and 3.0 µm) only is used with EN 779. In ISO 16890 standard data are corrected with a correlation ratio which represents the efficiency measured with no filter within the test rig.

The choice of 2 different test aerosols has been driven by the need for an easy way to produce and to measure test aerosol for the fine particle size range (DEHS under 1 µm) and the importance to highlight the bouncing effects which concern the coarse particle size range (KCl over 1 µm).

Then the filter under test (ISO 16890) is conditioned for 24 hours within a chamber which air is saturated by isopropanol (IPA) vapours. This conditioning step is intended to completely remove the electrostatic charge of the filter medium (if any) with no compensating increase in mechanical efficiency (in EN 779 this conditioning step consists in the immersion for 2 minutes of flat filter sample media in liquid IPA). After this conditioning step the fractional efficiency of the tested filter is measured again on DEHS and KCl aerosols and this value is called the minimum efficiency of the filter. For each particle size (0.3 to 10 µm) the average efficiency is calculated taking into account the initial and the conditioned (minimum) values. To evaluate the air filters according to their ePM efficiencies (efficiencies with respect to particulate matter fractions), standardized volume distribution functions of the particle

sizes are used which globally represent the average ambient air of urban and rural areas (Table 2). So the efficiency of the filter is calculated on  $ePM_1$ ,  $ePM_{2.5}$  and  $ePM_{10}$  from the average fractional efficiencies and the 2 different standardized particle size distributions. The filters belong to a group depending on the values of the minimum efficiency on  $ePM$  except for  $ePM_{10}$  and coarse filter groups (Table 3). The  $ePM$  efficiency of the filter is the average of the initial ( $ePM_1$ , ini,  $ePM_{2.5}$ , ini,  $ePM_{10}$ , ini) and the minimum ( $ePM_1$ , min,  $ePM_{2.5}$ , min,  $ePM_{10}$ , min) efficiencies. The efficiency reported value ( $ePM_1$ ,  $ePM_{2.5}$ ,  $ePM_{10}$ ) is rounded downwards to the nearest multiple of 5% (Table 3). If the filter cannot belong to an  $ePM$  group then its initial gravimetric efficiency measured with the ISO 15957 L2 synthetic dust (Table 1) is used to express its performance (Table 3).

Finally, the loading curve of the filter under test is established. It consists in loading the filter with ISO 15957 L2 test dust (2015) (upstream concentration 140 mg/m<sup>3</sup>) step by step, at constant air flow rate, until its pressure drop reaches 200 Pa ( $ePM_{10} \geq 50\%$ ) or 300 Pa ( $ePM_{10} < 50\%$ ). The initial gravimetric efficiency as well as those after each loading step are measured. The average test dust holding capacity is calculated.

Table 1: Main differences between EN 779 and ISO 16890 standards

	EN 779	ISO 16890
<b>Test aerosol</b>	DEHS (0.2 to 3 $\mu\text{m}$ )	DEHS (0.3 to 1 $\mu\text{m}$ ) KCl (1 to 10 $\mu\text{m}$ )
<b>Loading dust</b>	ASHRAE dust	ISO 15957 (2015) L2 dust
<b>Final pressure drop</b>	250 Pa (G) 450 Pa (M, F)	200 Pa ( $ePM_{10} < 50\%$ ) 300 Pa ( $ePM_{10} \geq 50\%$ )
<b>Filter conditioning</b>	IPA liquid / filter media	IPA vapour / full size filter
<b>Filter classification / ranking</b>	G, M and F groups	$ePM$ group, coarse

Table 2: Particle parameters for  $ePM$  calculations

	Reference particle size distribution	Test aerosol	Particle size range
$ePM_1$	Urban	DEHS	0.3 – 1 $\mu\text{m}$
$ePM_{2.5}$	Urban	DEHS	0.3 – 1 $\mu\text{m}$
		KCl	1 – 2.5 $\mu\text{m}$
$ePM_{10}$	Rural	DEHS	0.3 – 1 $\mu\text{m}$
		KCl	1 – 10 $\mu\text{m}$
Coarse	Initial gravimetric efficiency on ISO 15957 L2 dust		

Table 3: Filter groups according to ISO 16890

Group designation	Requirement			Efficiency reported value
	$ePM_1$ , min	$ePM_{2.5}$ , min	$ePM_{10}$	
ISO coarse	-	-	< 50 %	Initial gravimetric arrestance
ISO $ePM_{10}$	-	-	$\geq 50$ %	$ePM_{10}$
ISO $ePM_{2.5}$	-	$\geq 50$ %		$ePM_{2.5}$
ISO $ePM_1$	$\geq 50$ %	-		$ePM_1$

An example of ISO 16890 test results is given in Figure 2 while an example of calculation and efficiency reported value is given in Table 4. In this example the filter is electrostatically charged (electret medium) and the minimum fractional efficiency (obtained after the conditioning step with isopropanol vapours) is for this reason much lower than the initial fractional efficiency. The  $ePM_{1, \text{min}}$  value is lower than 50% (49.5%) and for this reason the filter does not belong to the  $ePM_1$  group; it belongs to the  $ePM_{2.5}$  group because the  $ePM_{2.5, \text{min}}$  efficiency is greater than 50% (60.7%). The  $ePM_{2.5}$  efficiency equals 79.1% (average of 60.7 % and 97.5 %) and so it is rounded to 75% and this filter is declared 75%  $ePM_{2.5}$ .

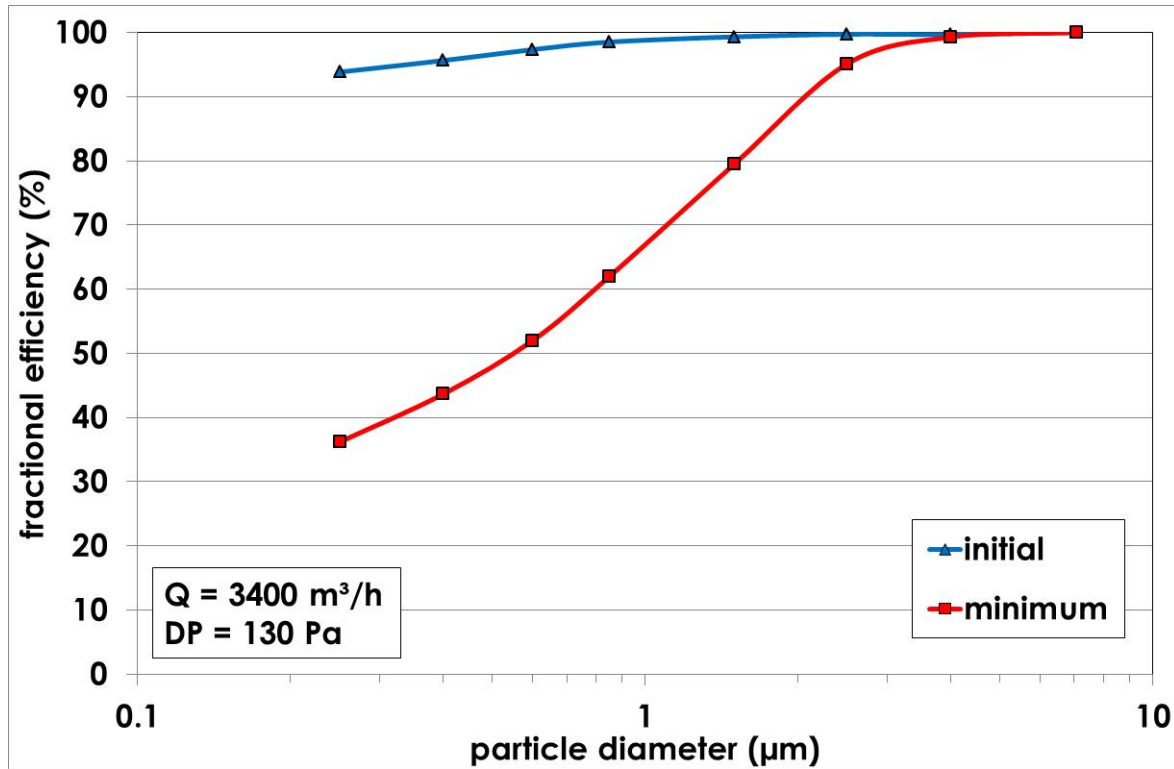


Figure 2: ISO 16890 fractional efficiency test results

Table 4: ePM values associated to test results presented in Figure 2

Calculated efficiency		$ePM_1$ (%)	$ePM_{2.5}$ (%)	$ePM_{10}$ (%)
$ePM_{1, \text{ini}}$ (%)	96.7	73.1		
$ePM_{1, \text{min}}$ (%)	49.5			
$ePM_{2.5, \text{ini}}$ (%)	97.5		79.1	
$ePM_{2.5, \text{min}}$ (%)	60.7			
$ePM_{10, \text{ini}}$ (%)	99.2			92.6
$ePM_{10, \text{min}}$ (%)	86.1			

### 3 DISCUSSION

The adoption of the ISO 16890 standard in 2016 represents a major change for general ventilation filters evaluation. The test method is not so different compared to that used in EN 779 but the use of the test results for filter ranking and/or classification is completely different. In ISO 16890 the efficiencies on ePM are calculated and the initial and conditioned (minimum) fractional efficiency values only are considered, combined to standardized particle size distributions. In EN 779, the class of the filters (groups M and F) depends on the average efficiency at 0.4  $\mu\text{m}$  which takes into account the initial efficiency at 0.4  $\mu\text{m}$  as well as those obtained after each loading phase with the ASHRAE synthetic dust. For EN 779, F group also takes into account the minimum efficiency at 0.4  $\mu\text{m}$  which is basically that obtained after the conditioning step with liquid IPA on the flat filter medium samples. Also, the loading dusts and the final pressure drop are different (see Table 1). For these reasons, there is no automatic link between the values obtained with the 2 standards.

But it is possible to use the EN 779 data to calculate the ePM<sub>1</sub> and ePM<sub>2.5</sub> efficiencies if we assume that the conditioned efficiencies obtained on the occasion of EN 779 testing represent the conditioned efficiencies of the full size filters that would be obtained according to the ISO 16890. Then it is possible to compare the average efficiency at 0.4  $\mu\text{m}$  (EN 779) and that on ePM<sub>1</sub> (ISO 16890) and examples for at least 50 filters are given in Figure 3.

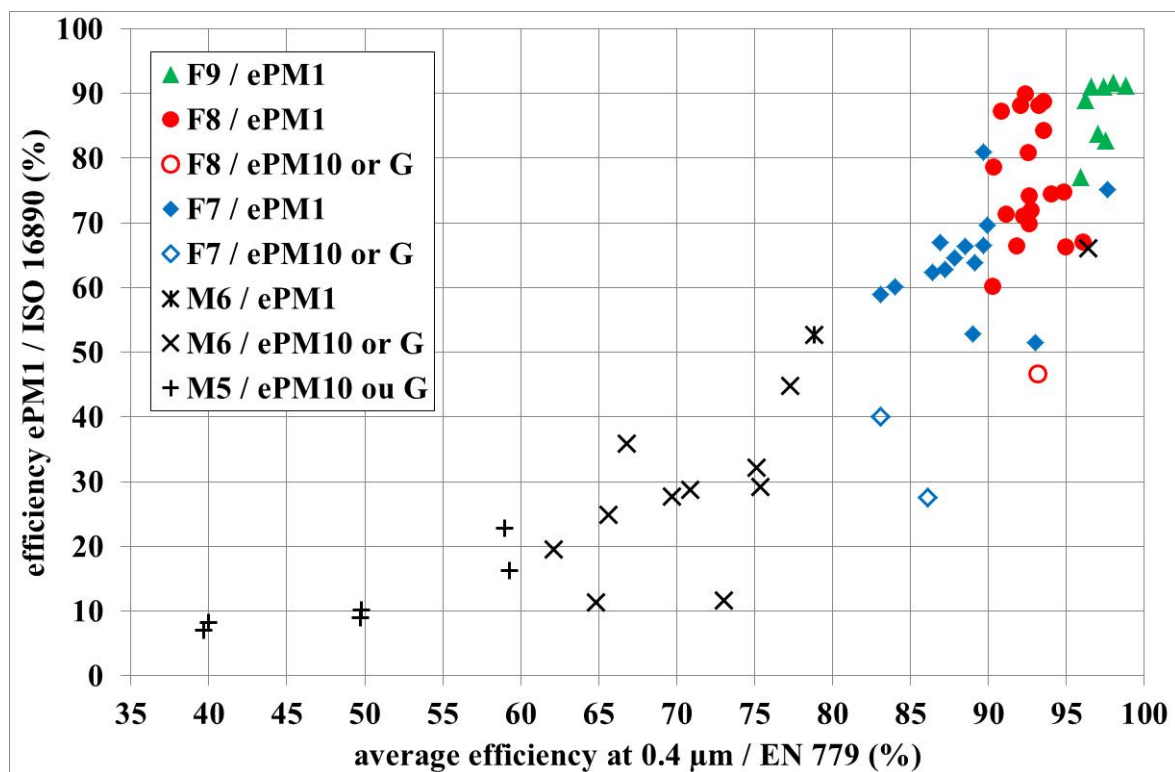


Figure 3: ePM<sub>1</sub> efficiency vs. average efficiency at 0.4  $\mu\text{m}$

It appears that F9 filters would correspond to ePM<sub>1</sub> filters with values mainly over 80 %, F8 filters would correspond to ePM<sub>1</sub> filters with values mainly between 60 % and 90 %, F7 filters would correspond to ePM<sub>1</sub> filters with values mainly between 50 % and 70 %; M6 and M5 filters would correspond to ePM<sub>10</sub> or coarse filters. Some few F8 and F7 filters would not correspond to ePM<sub>1</sub> filters and then would become ePM<sub>10</sub> or coarse filters (no calculation are available with reference to ePM<sub>10</sub> because EN 779 testing do not provides fractional efficiency data over 3  $\mu\text{m}$ ); this trend concern electret filters as well as filters with a low

initial efficiency and fast increase of the efficiency during loading. Surprisingly with this sample, no filter would correspond to ePM<sub>2.5</sub>.

Because of the differences between the 2 loading dusts, it is expected that the dust holding capacity with the ISO 16890 standard would probably be 3 to 5 times higher than that with EN 779 (at the same final pressure drop).

#### **4 CONCLUSIONS**

The adoption of the ISO 16890 standard in 2016 is of a great importance because this standard is also an EN standard and is going to replace the EN 779 by mid-2018 (EN 779 and ISO 16890 are used in parallel until mid-2018). The filter ranking system based on ePM is completely new and differs from that of EN 779 so that there is no automatic link between the efficiencies expressed according to the 2 standards. But the use of EN 779 data can help to imagine how the filters classified according to EN 779 could be efficient on ePM according to ISO 16890. Nevertheless, filter manufacturers, ventilation system manufacturers will probably need time to switch from a standard to the other, to adopt an other way to express and to deal with the performances of general ventilation filters according to ISO 16890. Also, many documents (standards, regulations, call for tenders, specifications, etc.) and activities (certification programs) referring to EN 779 must now be updated to refer to ISO 16890. For example, the energy classification system developed within the Eurovent Certification Scheme (ECP), which is now a reference in the industry, is being to change to take into account the new ISO 16890 standard.

Even if changes are often difficult to accept and to manage, it can be considered that the new filter ranking system will be easier to understand because the efficiency of filters is expressed according to ePM fraction which is a concept probably easier to understand than the average efficiency at 0.4 µm.

#### **5 ACKNOWLEDGEMENTS**

This study has been financially supported by the "Air Filtration" CETIAT working group.

#### **6 REFERENCES**

*NF EN 779:2012*, Particulate air filters for general ventilation – Determination of the filtration performance.

*NF EN ISO 16890-1:2017*, Air filters for general ventilation – Part 1: Technical specifications, requirements and classification system based upon particulate matter efficiency (ePM).

*NF EN ISO 16890-2:2017*, Air filters for general ventilation – Part 2: Measurement of fractional efficiency and air flow resistance.

*NF EN ISO 16890-3:2017*, Air filters for general ventilation – Part 3: Determination of the gravimetric efficiency and the air flow resistance versus the mass of test dust captured.

*NF EN ISO 16890-4:2017*, Air filters for general ventilation – Part 4: Conditioning method to determine the minimum fractional test efficiency.

*NF EN ISO 15957:2015*, Test dusts for evaluating air cleaning equipment.

# Preventing condensation and frosting in an energy recovery ventilator using a preheat coil

Won-Jun Kim<sup>1</sup>, Shiyong Li<sup>1</sup>, Min-suk Jo<sup>1</sup>, Eun-ji Choi<sup>1</sup>, Jae-Weon Jeong<sup>\*1</sup>

<sup>1</sup> Department of Architecture Engineering, College of Engineering, Hanyang University  
222 Wangsimni-Ro, Seungdong-Gu, Seoul, 04763, Republic of Korea

\*Corresponding author: [jjwarc@hanyang.ac.kr](mailto:jjwarc@hanyang.ac.kr)

## ABSTRACT

One of the problems presented by energy recovery ventilators (ERV) is the condensation/frosting problem that occurs during winter time. In order to prevent this problem, preheating outdoor air is the most common method used nowadays. The aim of this research is to evaluate preheat coil capacities according to different indoor/outdoor inlet air conditions (temperatures and humidities) and sensible/latent effectiveness of ERV ( $\epsilon_s$ ,  $\epsilon_L$ ). Considering all these factors, formulas for calculating a frost threshold temperature ( $T_{\text{Frost}}$ ) are suggested,  $T_{\text{Frost}}$  being the minimum inlet outdoor temperature at which condensation/frosting occurs under specific conditions. As a result, a control strategy for operating preheat coils for preventing condensation/frosting problems in ERVs is presented. For an ERV operating under outdoor inlet air conditions of  $-15^\circ\text{C}$  and 70% indoor inlet air conditions of  $22^\circ\text{C}$  and 50% humidity, and sensible effectiveness is 80%, latent effectiveness is 70%, the capacity needed for the preheat coil is 227 W. In addition, preheat coil capacities were calculated for the operation of an ERV in a few cities of AIVC countries.

## KEYWORDS

Energy recovery ventilator, Frosting, Condensation, Preheat coil

## 1 INTRODUCTION

Energy recovery ventilators (ERV) are mechanical ventilation devices that improve the indoor air quality (IAQ) and reduce cooling and heating load of an indoor area during ventilation in summer and winter times. The energy recovery is done by reusing the exhaust air's heat and moisture. However, when the ERV operates during the winter time, condensation can occur inside the total heat exchanger (THE) of the ERV while the sensible and latent heat is exchanged between the outdoor air and the exhaust air. If such condensation is exposed to freezing point, it may develop into frosting (ASHRAE, 2016). Both condensation and frosting phenomena can cause corrosion inside the ventilation system and/or increase microbial contaminants of the indoor air, what would threaten the health of building occupants (Jeon et al., 2013). In addition, condensation/frost may decrease the performance of the ERV, which may lead to the risk of cold air drafts as well as to the failure of the heat exchanger (Jang et al., 2008).

Various studies have been conducted to solve condensation and frosting problems in an ERV. Freund et al. (2011) compared the performance of various frosting control methods such as preheating outdoor air, reheating the exhaust air, controlling the wheel speed and bypassing the outdoor air using an enthalpy exchanger model. The results show that preheating outdoor air is the best method to prevent condensation/frosting in ERV. Nasr et al. (2013) explained the condensation and frosting process of the air-to-air heat/energy exchanger and compared the advantages and disadvantages of various methods that would be able to solve these problems. In the case of the HRV, condensation occurs when the temperature of the

exhaust air falls below the dew point temperature while exchanging sensible heat between the outdoor air and the exhaust air in the winter season.

Kim et al. (2016) confirmed the necessity of preventing condensation by calculating the time where condensation occur on the exhaust side of the HRV/ERV through a program for predicting the performance of the waste heat/energy recovery ventilation system.

## 2 CONDENSATION/FROSTING PROCESS IN ERV

During the winter, when the outdoor air and the exhaust air are exchanged through the total heat exchanger (THE) in ERVs, heat and moisture are transferred from the exhaust air side to the outdoor air side. Condensation or frosting occurs when the exhaust air temperature (Eq. (1)) drops below the dew point temperature of exhaust air during heat exchange (Eq. (2)). Condensation often occurs in most cases as the exhaust air is cooled and humidified.

$$T_{EA} = T_{RA} + \varepsilon_s(T_{OA} - T_{RA}) \quad (1)$$

$$T_{EA} < DPT_{EA} \quad (2)$$

Where  $T_{EA}$  is the outlet exhaust air temperature,  $T_{RA}$  is the inlet exhaust air temperature,  $T_{OA}$  is the outdoor air temperature,  $\varepsilon_s$  is the sensible effectiveness and  $DPT_{EA}$  is the dew point temperature of the outlet exhaust air.

## 3 PREVENTING CONDENSATION/FROSTING USING A PREHEAT COIL

Condensation or frosting is prevented by preheating the intake outdoor air at a temperature higher than a specific temperature (i.e., frost threshold temperature) and then performing heat exchange or more. In the following sections, present methods for predicting and preventing condensation/frosting using preheat coils at various effectiveness ratio in ERV.

### 3.1 Calculation of the frost threshold temperature of THE ( $\varepsilon_s = \varepsilon_L$ )

When the sensible and latent effectiveness are the same in the THE of the ERV, the state points of the exhaust process air and the inlet outdoor process air during the heat exchange, can be presented through a straight line (i.e., connect the OA & RA state points) in the temperature-humidity graph (T- $\omega$  graph).

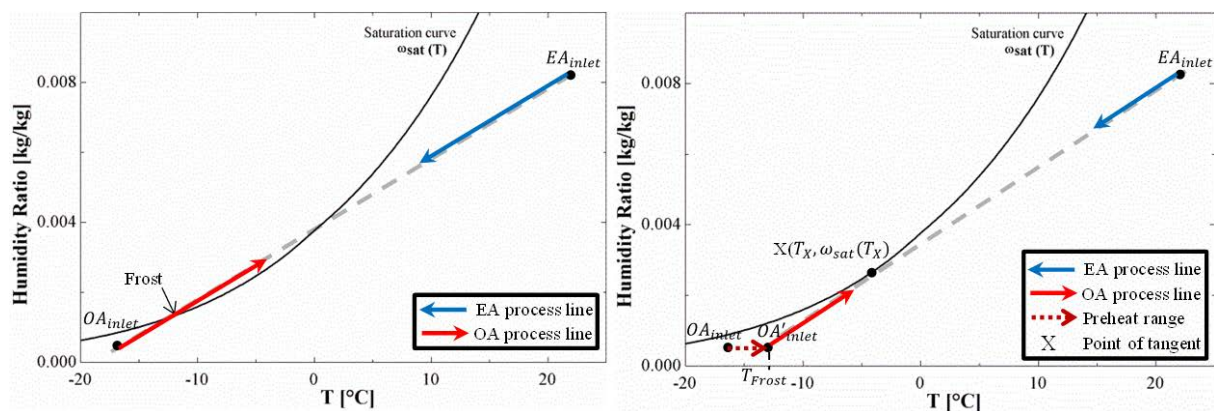


Figure 1. a) Condensation/frosting Process in THE ( $\varepsilon_s = \varepsilon_L$ ) b) Condensation/frosting prevention in THE ( $\varepsilon_s = \varepsilon_L$ )

Condensation or frosting may occur when the state point reaches the saturation curve while outdoor air is getting heat and moisture from the exhaust air as shown by Fig. 1a (Kim et al.,

2016). On the other hand, in fig. 1b, it can be observed that condensation does not occur when the introduced outdoor air is preheated to a temperature that is higher than the frost threshold temperature ( $T_{Frost}$ ). In this case, the straight line connecting the two state points (OA&RA) does not cross the saturation curve. The temperature at the point where a state point on the straight line in contact with the saturation curve from the state point of the indoor air is equal to the absolute humidity of the introduced outside air is the frost threshold temperature (Fig.1b). Consequently, for preventing condensation/frosting in the total heat exchanger (THE), the introduced outdoor air should be preheated to higher than the frost threshold temperature.

$$m_{OA-RA} = \frac{(\omega_{RA} - \omega_{OA})}{(T_{RA} - T_{OA})} \quad (3)$$

$$\omega_{Sat} = a + b * T + c * T^2 + d * T^3 + e * T^4 \quad (4)$$

$$\omega'_{Sat}(T_X) = \frac{(\omega_{RA} - \omega_X)}{(T_{RA} - T_X)} \quad (5)$$

$$\omega'_{Sat}(T_X) = \frac{(\omega_{RA} - \omega_{OA})}{(T_{RA} - T_{frost})} \quad (6)$$

$$T_{frost (\epsilon_S = \epsilon_L)} = \frac{1}{\omega'_{Sat}(T_X)} (\omega_{OA} - \omega_{RA}) + T_{RA} \quad (7)$$

where  $m_{OA-RA}$  represents the slope of the straight line indicating the state point during the heat exchange between the outdoor air and the indoor air in the T- $\omega$  graph;  $\omega_{RA}$  is the humidity of the exhaust air;  $\omega_{OA}$  is the humidity of the outdoor air;  $\omega_{sat}$  is the saturation curve (that depends on the absolute humidity,  $\omega$ , and temperature, T);  $\omega'_{sat}(T_X)$  is the slope of the straight line that connects the contact point X and the indoor air state point and  $T_{Frost (\epsilon_S = \epsilon_L)}$  is the frost threshold temperature. The coefficients of Eq. (4) can be found in Table 1.

Table 1: Coefficients of saturation curve

a	b	c	d	e
3.73292975E-03	2.85006859E-04	8.47353550E-06	1.62517930E-07	3.49040153E-09

### 3.2 Calculation of the frost threshold temperature of THE ( $\epsilon_S > \epsilon_L$ )

Most of the ERV present higher values for sensible effectiveness compared to latent effectiveness in the total heat exchanger. In order to prevent condensation, the same principle of preheating the outdoor air to a temperature that is higher than the frost threshold temperature can be used when  $\epsilon_S > \epsilon_L$ . However, the method used for calculating the frost threshold temperature is different from the method presented for a THE in which sensible and latent effectiveness have the same values. The state points of outdoor air and indoor air during the total heat exchange are represented by straight lines (i.e., OA & EA process lines) in fig. 2a and 2b, having a slope obtained by multiplying the slope of the straight line connecting the two state points (OA&RA) by the heat exchange efficiency ratio ( $\epsilon_L/\epsilon_S$ ) in the T- $\omega$  graph.

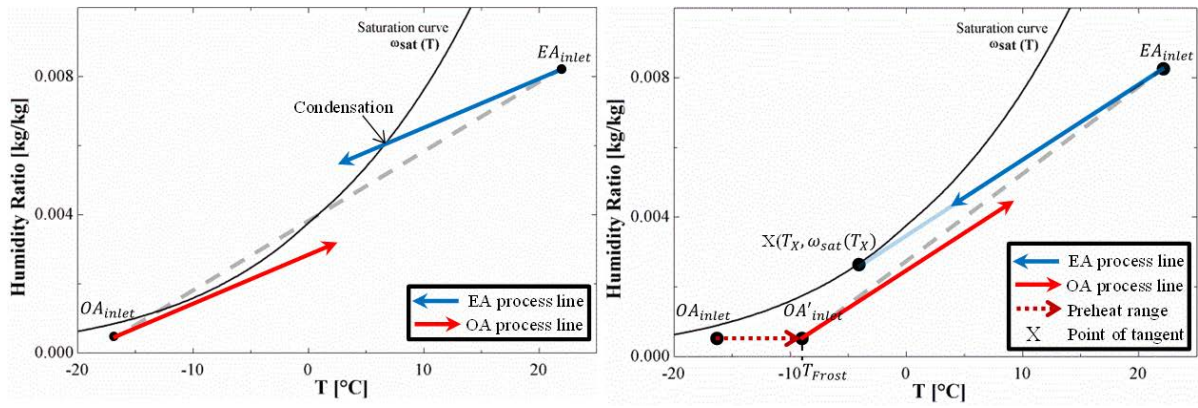


Figure 2.a) Condensation/frosting Process in THE( $\epsilon_S > \epsilon_L$ ) b) Condensation/frosting prevention in THE( $\epsilon_S > \epsilon_L$ )

In Fig. 2, the two colorful lines are straight lines that show the changes in the state of the inlet outdoor air and exhaust air during the heat and mass exchange. Two important conclusions can be drawn from fig. 2:(1) The lines showing the state change of the exhaust and process air are parallel;(2) the EA process line is located above the OA process line and is close to the saturation curve.

If the EA process line does not cross the saturation curve, the OA process line will not cross either and, consequently, condensation and frost will not occur. Therefore, the EA process line in the T- $\omega$  graph will be the baseline for determining whether or not condensation in the THE of the ERV will occur.

For calculating the preheat coil capacity needed to prevent condensation in a THE that has different sensible and latent effectiveness the following procedure is suggested:

- (1) Draw a tangent line to the saturation curve starting from one state point (RA). At this time, the contact point between the saturation curve and the tangent line is called  $X(T_X, \omega_{sat}(T_X))$ .
- (2) Using Eq.(5), the equation of the tangent line between contact point X and indoor air point can be obtained.
- (3) In the T- $\omega$  graph, the slope of the EA process line is the slope of the straight line between state points OA and RA multiplied by the heat effectiveness ratio ( $\epsilon_L/\epsilon_S$ ) (Eq.(8)).
- (4) If the slope of the EA process line is smaller than the slope of the tangent line, condensation will occur. Therefore, the frost threshold temperature is the outdoor temperature when the slope of the EA process line and the slope of the tangent line are the same.
- (5) Eq. (1), (8) and (9) can be summarized and an equation for the frost threshold temperature (Eq. (10)) is proposed.

$$\text{Slope of EA Process line} = \frac{\omega_{OA} - \omega_{RA}}{T_{OA} - T_{RA}} \times \frac{\omega_{EA} - \omega_{RA}}{\omega_{OA} - \omega_{RA}} \times \frac{\omega_{OA} - \omega_{RA}}{T_{EA} - T_{RA}} \quad (8)$$

$$\epsilon_L = \frac{\omega_{EA} - \omega_{RA}}{\omega_{OA} - \omega_{RA}} \quad (9)$$

$$T_{frost} (\epsilon_S > \epsilon_L) = (\omega_{OA} - \omega_{RA}) \times \frac{1}{\omega'_{sat}(T_X)} \times \frac{\epsilon_L}{\epsilon_S} + T_{RA} \quad (10)$$

$$Q = C_p \times \dot{m} \times (T_{Frost} - T_{OA}) \quad (11)$$

As can be seen from Eq. (10), the frost threshold temperature can be obtained by the indoor air temperature and humidity, the outdoor air temperature and absolute humidity, and the effectiveness ratio of heat exchange.

### 3.3 Control strategy for the preheating coil to prevent condensation/frosting

Through Eq. (10), it is possible to predict the state of the exhaust air and the occurrence of condensation or frosting in the total heat exchanger. Therefore, a control strategy for the operation of the preheating coil can be drawn based on both indoor and outdoor temperatures. It is important to mention that if the dry bulb temperature of EA process air is higher than the dew point temperature, the preheating coil will not operate because no condensation occurs. The following control strategy is presented for preventing condensation in a THE:

- (1) Enter the ventilation rate and the ventilation space size.
- (2) Obtain indoor & outdoor air condition data through temperature and humidity sensor.
- (3) The value of the sensible effectiveness and the latent effectiveness is calculated according to temperature and humidity data.
- (4) Determine the expected dry bulb temperature of the exhaust air through the sensible effectiveness equation (Eq. (1)). If the dry bulb temperature of the exhaust air is higher than the dew point temperature of the exhaust air, no condensation will occur and the preheat coil will not operate.
- (5) If the predicted dry bulb temperature of the exhaust air is less than or equal to the dew point temperature of the predicted exhaust air (which theoretically does not exist), then condensation may occur. Frost threshold temperature can be calculated by Eq.(7) or Eq. (10) depending on  $\epsilon_S$  and  $\epsilon_L$ .
- (6) Preheat coil capacity can be calculated by multiplying the specific heat of the air, the air flow rate, and the temperature difference between the outdoor air and the frost threshold temperature.

Process (2) to (6) can control the preheating coil operation according to indoor/outdoor temperature/humidity through the feedback process.

A diagram that presents the control strategy for the coil is shown on fig. 3.

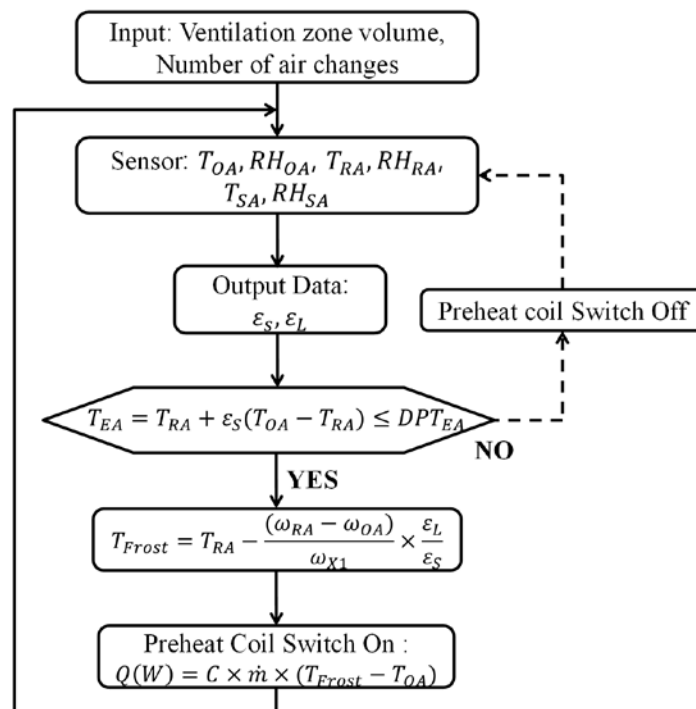


Figure 3. Preheat coil control strategy in ERV

## 4 SIMULATION RESULTS

### 4.1 Frost threshold temperature according to indoor air temperature and humidity

If the indoor air setpoint requires a lower temperature or requires a higher humidity, both temperature and humidity of the contact point  $X(T_X, \omega_{\text{sat}}(T_X))$  will be higher. Therefore, the frost threshold temperature becomes higher, and condensation is likely to occur during the heat exchange. Conversely, when the indoor air set point requires a higher temperature or a lower humidity, the frost threshold temperature is lower and the probability to occur condensation during heat exchange diminishes (Fig. 4a).

Fig. 4b shows the frost threshold temperature according to indoor air conditions under 80% of sensible effectiveness and 70% of latent effectiveness.

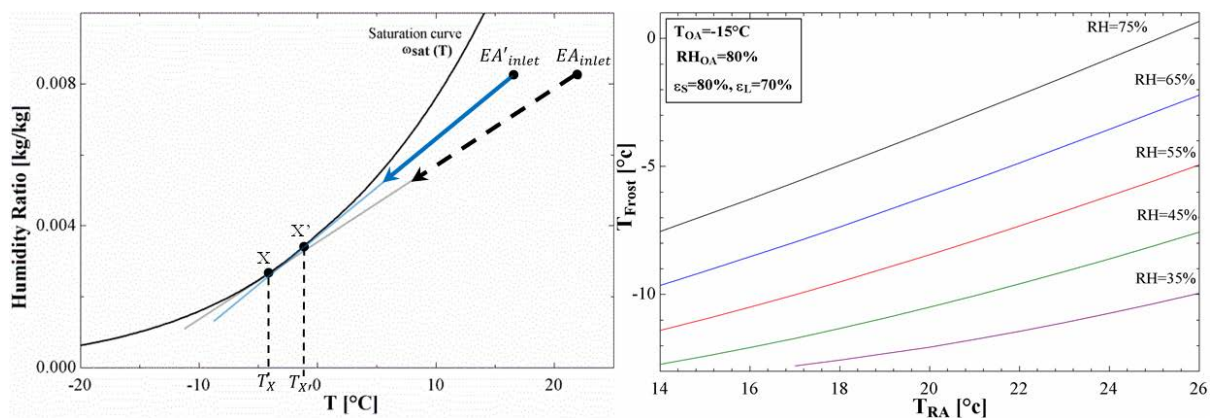


Figure 4. a) Change of contact point ( $X$ ) of saturation curve according to indoor air set temperature  
b) Frost threshold temperature for different outdoor air temperature and relative humidity

### 4.2 Frost threshold temperature according to outdoor air temperature and humidity

The Frost threshold temperature (Eq. (10)) calculation discussed in section 3 can be used to determine the frost threshold temperature according to the outdoor air temperature when indoor air condition is constant. Fig. 5 shows the frost threshold temperature according to various outdoor air conditions in the total heat exchanger. The values that were considered for heat exchanger effectiveness, indoor air temperature and relative humidity are  $\epsilon_S = 80\%$ ,  $\epsilon_L = 70\%$ ,  $22^\circ\text{C}$  and  $50\%$ , respectively.

When the relative humidity of the outdoor air is 40%, preheating is required when the dry bulb temperature of the outdoor air is below  $-12.7^\circ\text{C}$ . If the outdoor air temperature is higher than  $-12.7^\circ\text{C}$ , no condensation occurs during the heat exchange between the outdoor air and the exhaust air. Condensation occurs when temperatures inside the total heat exchanger reach  $-8.5^\circ\text{C}$  or lower. For an outdoor temperature range of  $-30^\circ\text{C}$  to  $5^\circ\text{C}$  and relative humidity range from 70 to 100%, the frost threshold temperature ranges from  $-11.2^\circ\text{C}$  to  $15^\circ\text{C}$  as shown in Fig. 5. It can be seen that the higher the temperature and the relative humidity of the introduced outdoor air, the higher the frost threshold temperature.

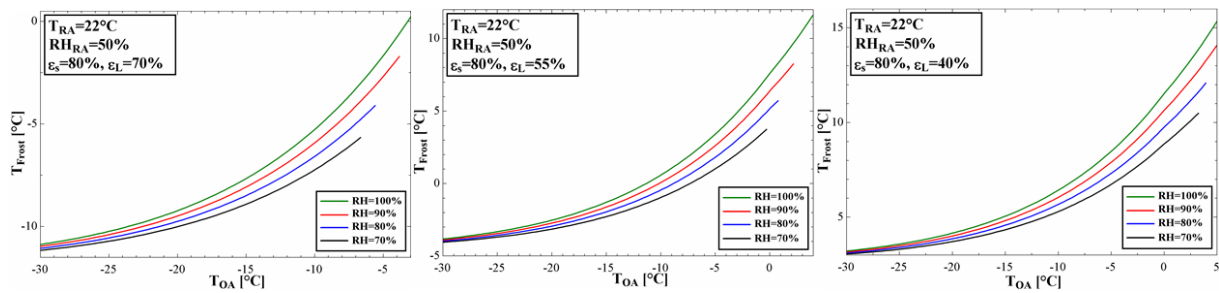


Figure 5. Frost threshold temperature according to outdoor air conditions and heat exchange effectiveness

As the heat exchange effectiveness ratio ( $\epsilon_L/\epsilon_S$ ) becomes smaller, the frost threshold temperature becomes relatively higher (Eq. (10)) and the interval of the introduced outdoor air, which requires preheating, becomes shorter.

### 4.3 Required preheat coil capacity by region

Table 2 shows the calculated required capacity of the preheating coil in major cities of Belgium, Czech Republic, Denmark, France, Germany, Italy, Japan, Netherlands, New Zealand, Norway, Republic of Korea, Spain, Sweden, and United Kingdom. Room condition was set at 22°C and 50% humidity, ventilation zone volume was set at 195.5m<sup>3</sup> and number of air changes was set at 0.5 times/hour. International Weather for Energy Calculations 2 (IWEC2) data was used for weather data.

Table 2. Frost threshold temperature and required capacity of preheating coils by region

Region	T <sub>Frost</sub> (°C) (min/Max)	Preheat coil capacity (W)	Preheating time (Hour/Year)	Region	T <sub>Frost</sub> (°C) (min/Max)	Preheat coil capacity (W)	Preheating time (Hour/Year)
London	-	-	-	Osaka	-	-	-
Birmingham	-3.1/1.6	118.6	29	Sapporo	-9/-1.8	168.8	328
Leeds	-0.5/1.0	108.5	7	Milano	-5.9/2.4	144.5	133
Stockholm	-9.1/2.4	316.2	876	Roma	-	-	-
Goteborg	-7.5/2.4	198.2	364	Torino	-0.6/2.4	122.2	18
Malmo	-8.9/2.4	335.4	364	Berlin	-6.8/2.4	192.9	333
Madrid	-3.3/2.4	122.2	37	Munich	-7.2/2.4	207.8	418
Barcelona	-	-	-	Frankfurt	-6.4/2.4	166.6	162
Valencia	-	-	-	Paris	-3.2/2.4	122.2	29
Seoul	-9.9/-2.1	211.2	177	Lyon	-6.5/2.4	125.2	108
Busan	-	-	-	Toulouse	-2.5/2.4	122.2	16
Incheon	-9.2/-1	176.4	145	Koebenhavn	-6.3/2.4	185.2	101
Oslo	-8.6/2.4	303.4	1082	Odense	-8.1/2.4	262.7	271
Bergen	-6.5/2.4	172.9	150	Aalborg	-5.3/2.4	166.8	232
Stavanger	-5.3/2.4	133.5	141	Praha	-7.8/1.5	232.9	322
Auckland	-	-	-	Brno	-8.9/2.4	377.3	646
Christchurch	-1.2/2.4	122.2	54	Ostrava	-9.1/2	359.7	450
Amsterdam	-5.9/2.4	137.3	169	Antwerpen	-4.9/2.1	120.5	57
Rotterdam	-6.5/2.4	170.5	149	Gent	-4.4/2.4	137.2	83
Eindhoven	-5.4/2.4	122.2	203	Charleroi	-5.4/1.4	115.6	198
Tokyo	-	-	-				

## 5 CONCLUSIONS

This study identifies possible condensation and frosting processes that may occur during winter in ERV and suggests preheating strategies that are able to prevent such problems. A

formula for calculating frost threshold temperature and the required preheat coil capacity to prevent condensation have been given.

Through this study, the following conclusions can be inferred:

- (1) Condensation occurs when the temperature of exhaust air (or introduced outdoor air) becomes lower than the dew point temperature during heat exchange. Therefore, it is possible to calculate the state of exhaust air in order to operate or not a preheating coil to prevent condensation.
- (2) In most ERVs, the sensible effectiveness is higher than the latent effectiveness. Therefore, condensation during heat exchange tends to occur on the exhaust side. When the outdoor air is preheated to a temperature higher than the frost threshold temperature to prevent condensation/frosting from occurring in the exhaust air, condensation does not occur in both the exhaust and the outdoor air.
- (3) When the sensible effectiveness and the latent effectiveness are the same ( $\epsilon_S = \epsilon_L$ ), the frost threshold temperature is obtained from Eq. (7). If the sensible effectiveness is higher than the latent effectiveness ( $\epsilon_S > \epsilon_L$ ), the frost threshold temperature is obtained from Eq. (10).
- (4) When indoor air and heat exchange effectiveness are constant, the frost threshold temperature increases in proportion to outdoor air and relative humidity. When the outdoor air temperature and the heat exchange effectiveness are constant, the frost threshold temperature increases in proportion to the indoor air temperature and the relative humidity.
- (5) IWEC2 weather data was used to calculate preheating coil capacity for several cities (Table 2). The capacity and preheating time of the preheating coil were the highest in Brno and Oslo. London, Barcelona, Valencia, Busan, Tokyo, Osaka and Roma are cities that do not need preheating coil.

## 6 ACKNOWLEDGEMENTS

This work was supported by the National Research Foundation (NRF) of Korea (No. 2015R1A2A1A05001726), the Korea Agency for Infrastructure Technology Advancement (KAIA) grant 16CTAP-C116268-01 and the Korea Institute of Energy Technology Evaluation and Planning (KETEP) (No. 20164010200860).

## 7 REFERENCES

- Alonso, M.J, 2015. Review of heat/energy recovery exchangers for use in ZEBs in cold climate countries. *Building and Environment*, 84, 228-237.
- ASHRAE. 2016. *ASHRAE Handbook: HVAC systems and equipment*, Chapter 26 SI: AIR-TO-AIR ENERGY RECOVERY EQUIPMENT.
- ASHRAE. 2012. *International Weather for Energy Calculations 2.0 (IWEC Weather Files) DVD*, American Society of Heating, Refrigerating and Air-Conditioning Engineers Inc., Atlanta.
- Freund, S. 2011. A Semi-Empirical Method to Estimate Enthalpy Exchanger Performance and a Comparison of Alternative Frost Control Strategies. *HVAC&R Research*, 9:4, 493-508.

- Jang, H. 2008. A Study on the Performance of Heat Recovery Ventilator for Apartment Houses. *Korean Journal of Air-Conditioning and Refrigeration Engineering*, 20(1), 26-34.
- Jeon, B. 2013. A Study on Dew Condensation According to the Operatinal Conditions of a Heat-Recovery Ventilator, *Korean Journal of Air-Conditioning and Refrigeration Engineering*, 25(10), 529-533.
- Kim, W. 2016. Region Preheat Coil Capacity Estimate for Preventing Condensation in Sensible Heat or Energy Recovery Ventilators. *Architectural Institute of Korea*, 32(10), 105-112.
- Liu, P. 2016. Performance of a quasi-counter-flow air-to-air membrane energy exchanger in cold climates. *Energy and Buildings*, 119, 129-142.
- Min, J. 2011. Performance analysis of a membrane-based energy recovery ventilator: Effects of outdoor air state. *Applied Thermal Engineering*, 31, 4036-4043.
- Nasif, M. 2005. Heat and Mass Transfer in Air to Air Enthalpy Heat Exchanger. Presented at the 6th World Conference on Experimental Heat Transfer, Fluid Mechanics, and Thermodynamics Matsushima, Miyagi, Japan.
- Nasif, M. 2010. Membrane heat exchanger in HVAC energy recovery systems, systems energy analysis. *Energy and buildings*, 42, 1833-1840.
- Nasr, M. 2013. A review of frosting in air-to-air energy exchangers, *Renewable and Sustainable Energy Reviews*, 30, 538-554.
- Yaïci, W. 2013. Numerical analysis of heat and energy recovery ventilators performance based on CFD for detailed design. *Applied Thermal Engineering*, 51, 770-780.
- Zhnag, L. 2001. Energy requirements for conditioning fresh air and the long-term savings with a membrane-based energy recovery ventilator in Hong Kong. *ENERGY*, 26, 119-135.

# Characterising the actual performance of domestic mechanical ventilation and heat recovery systems

Rajat Gupta<sup>\*1</sup>, Matt Gregg<sup>1</sup>, Tim Sharpe<sup>2</sup>, Grainne McGill<sup>2</sup>, and Ian Mawditt<sup>3</sup>

*1 Oxford Brookes University  
Gipsy Ln, Oxford OX3 0BP, UK*

*\*Corresponding author: rgupta@brookes.ac.uk  
Presenting author underlined*

*2 The Glasgow School of Art  
167 Renfrew Street  
Glasgow G3 6RQ, UK*

*3 Four Walls  
5 Pitchcombe Gardens, Bristol BS9 2RH, UK*

## ABSTRACT

This paper describes the findings and recommendations of a meta-study examining the actual in-use performance of whole-house mechanical ventilation heat recovery systems (MVHR) installed in 54 low energy dwellings in the UK, as part of a national research programme. The performance of the systems is assessed using monitored data on indoor air quality (temperature, relative humidity, CO<sub>2</sub>) and energy use, cross-related with actual experiences of operating these systems through resident surveys. Design/research team interviews were also used to ascertain the reasons for selecting MVHR as a ventilation strategy for a housing development. Cross-analysis of the quantitative and qualitative data helps to identify the key features of MVHR systems with respect to quality of design, installation and commissioning procedures.

Overall the study indicates that the rationale behind the use of MVHR systems is borne out – the rates of ventilation as evidenced very generally by CO<sub>2</sub> levels are better, and the energy use overall is lower. However the study also highlights the prevalence of sub-optimal systems and the possible implications on both energy efficiency and indoor air quality. This would lead to houses being naturally ventilated, but relying entirely on opening windows where there is no provision for background ventilation. In some spaces where this is not possible (for example due to external factors such as noise or security), or where there is less adaptive behaviour (for example bedrooms overnight), very poor levels of ventilation are experienced.

In general the energy consumption in houses with MVHR systems was lower, but this needs to be contextualised – 77% of the MVHR dwellings with energy data were of Passivhaus construction, which in general have lower consumption within the domestic sample (albeit with MVHR as a key component). In some cases it was found that MVHR systems were selected to achieve compliance with the Code for Sustainable Homes, without much understanding of required air-tightness of the building envelope or the maintenance requirements of these systems. Key recommendations include better understanding of the design issues to ensure good airflow and avoid installation problems associated with ductwork; designing in maintenance requirements including unit location, filter cleaning and replacement; ensuring good communication of the design details with installers and commissioners in conjunction with better quality control onsite; along with improved handover processes and occupant guidance.

## KEYWORDS

MVHR, indoor air quality, Passivhaus, meta-study, building performance evaluation

## 1 INTRODUCTION

There is growing evidence that decarbonisation strategies aimed at the housing sector do not always achieve intended results and this performance gap between ‘as designed’ and ‘as built’ is increasingly common in findings (McGill et al., 2017, Gupta and Kapsali, 2014). To address this, Innovate UK (formerly the Technology Strategy Board) commissioned the Building Performance Evaluation (BPE) programme in 2010. A key aim of the programme was to identify the causes and scope of performance gaps across a wide range of high-

performance buildings. This was a 4-year programme to support a range of BPE studies across the UK in both domestic and non-domestic buildings. There were two phases to the programme. Phase 1 studies looked at post-construction and early occupation only; Phase 2 studies undertook Phase 1 evaluation but also in-use and post-occupancy monitoring and evaluation over a 2-year period.

With improved fabric-thermal performance, ventilation losses become more significant and strategies that can reduce these may carry considerable weight when evaluating proposed performance. As a result, mechanical ventilation with heat recovery (MVHR) is an attractive option for improved performance standards. Consequently, the uptake of MVHR systems is on the rise, with these systems expected to become a common form of ventilation in the coming years. Therefore, considering the high-performance standards (such as Code for Sustainable Homes (CSH) and Passivhaus) of the BPE dwellings, it was apparent from the start of the programme that a significant number of dwellings were using MVHR systems. The ability to provide requisite levels of ventilation, whilst maintaining energy efficiency is a highly desirable goal, but a move away from traditional and familiar forms of ventilation is a step-change in UK housing design. These systems (combined with appropriate air tightness) are expected to reduce space heating demand, improve indoor air quality (IAQ), and improve thermal comfort (AECB, 2009, Banfill et al., 2011); however, with increasingly mainstream use, a series of studies have also highlighted significant concerns regarding the specification, installation, commissioning, performance, operation and maintenance of MVHR systems in a domestic context (Gupta et al., 2013). Appropriately therefore, among the many requirements under the BPE programme, the review of systems design and implementation included the review of installation, commissioning and measurement of performance and energy use of MVHR systems.

This paper describes the findings and recommendations of a meta-study examining the actual in-use performance of MVHR installed in low energy dwellings in the UK, as part of the national BPE research programme. This meta-study was commissioned by Innovate UK to undertake a broad assessment of domestic projects that utilised MVHR systems. The aims of the study were to identify the nature of MVHR systems, to analyse the available performance data, to gather information and insights from projects about the issues affecting the use and performance of these systems, and to share this information, experience and knowledge both within projects and to the wider construction industry. Whilst projects have undertaken individual assessments of performance, this study provided an opportunity to make a broad comparison across a range of projects, to identify common issues and to make a comparative analysis of the use of these systems.

## **1.1 MVHR in practice**

Several studies have been published on the expected and resultant performance of MVHR systems in new and retrofit dwellings across a number of countries. Common faults among dwellings with MVHR appear to be oversupply of heat, unacceptable noise levels, dirty systems, etc. stemming from poor planning, lacking design support, poor installation and commissioning. In addition, poor or non-existent occupant support for optimal use results in negative impacts on the energy and IAQ against design expectations. Gupta and Kapsali (2014) showed through BPE results that six dwellings in three different developments in the UK were built with final air permeability above that which warrants the need for MVHR. Poor installation and commissioning of the systems were also found to be highly problematic in all six dwellings due to lack of experience with the systems. These failures led to increased heat loss and heat loads, increased energy consumption, unacceptable noise, and cold draughts. Lack of knowledge regarding the systems also resulted in inaccessible controls, where most negative feedback from occupants related to operation and control of the

systems. Balvers et al. (2012) also demonstrated installation and commissioning failures in 150 homes in the Netherlands: half of homes had unintentional recirculation of exhaust air; many systems internally polluted with dust and dirt found in the air supply ducts of about 66% of the homes; half of the homes had no bypass on the heat exchanger; and more than half of the homes had noise levels from the systems that exceeded the reference value, especially in bedrooms.

McGill et al. (2015) demonstrated occupant lack of knowledge on how to operate the system and change filters. Likewise, Sodagar and Starkey (2016) concluded through monitoring and evaluation of MVHR systems in social housing designed to CSH Level 5 that occupant misunderstanding of how to operate controls of the MVHR system can undermine the energy benefit and purpose of the system. In response to the many issues with MVHR demonstrated in research, White et al. (2016) recommend education and training throughout the supply chain to ensure high quality MVHR installation which is critical for optimum system performance. In addition, Gupta et al. (2013) recommend well timed, phased training with hands on demonstration and visual and simple yet comprehensive guides to help occupants understand these complex systems. Also with regard to whole-system design, management and delivery of thermal comfort, Berge et al. (2016) showed through simulation and POE, of Passivhaus apartments in Bergen, Norway, that a uniform supply of heat recovery temperature throughout a dwelling using single-zone MVHR resulted in oversupply of heat in bedrooms. In addition, the observed response of increased window ventilation to lower the temperature in bedrooms did not completely resolve thermal comfort concerns and lead to an overall increase in space-heating demand. Toledo et al. (2016) demonstrated that the greatest propensity to overheat was in dwellings with MVHR. These findings show that much improvement is needed to deliver the expected benefits of MVHR systems in dwellings.

## 2 METHODOLOGY

From the 3000+ dwellings funded and built through the BPE programme, there were a total of 237 MVHR ventilated dwellings. The dwellings come from a range of development sizes, one-off through to major developments (largest ~790 dwellings). There was wide geographical spread of MVHR ventilated dwellings (from Edinburgh to Exeter and Northern Ireland to the east of Greater London) that are included within this study. Detailed investigations were only typically performed on a few dwelling from each development. This study involves 54 dwellings (54 MVHR systems); located in 29 developments (i.e. domestic BPE projects). Care was taken to ensure that both mainstream low energy housing and Passivhaus projects were represented in the sample. Out of all the dwellings assessed in this meta-study, 20 are certified Passivhaus properties. To enrich the study, a further 15 non-MVHR (MEV or naturally ventilated) dwellings have been assessed for environmental performance, and this has been used to benchmark performance against these two principle ventilation strategies. The meta-study involved both quantitative and qualitative data. Quantitative data included air flow rates, commissioning data, temperature, relative humidity (RH), CO<sub>2</sub>, and energy consumption. Qualitative data covered resident satisfaction, comfort, control, etc. from the Building Use Survey (BUS)<sup>1</sup> Methodology©(27 projects) and surveys and interviews with design team or BPE research team (from this point 'BPE team') representatives (15 projects) selected based on the willingness to get involved with qualitative review. A summary of data features and properties reviewed is provided in Table 1.

---

<sup>1</sup> The BUS methodology is an established way of benchmarking levels of occupant satisfaction within buildings using a structured questionnaire where respondents rate various aspects of performance on a scale of 1-7.

Table 1: Summary of properties reviewed

Dwelling types	Performance characteristics	BPE team interviews	Temp / RH data	BUS survey	CO <sub>2</sub> data	Energy
MVHR	54 homes	15 projects (163 homes)	35 / 36 living rooms 39 / 45 bedrooms	27 projects (211 homes)	22 living rooms 23 bedrooms	39 homes
Non-MVHR (source)	n/a BPE reports	n/a Primary	17 / 17 living rooms 24 / 24 bedrooms EMBED	15 homes Innovate UK	15 living rooms 24 bedrooms EMBED	20 homes DomEARM

Final reports and detail sheets were reviewed to create standardized characteristics forms identifying system and dwelling data characteristics (e.g. system balance). The original commissioning data was available for 38 out of the 54 systems reviewed. Design air flow rates were available for 43 systems and measured air flow rates were available for 52. Assessments have been made for each system to determine their success for meeting both their original design air flow values, and for meeting the design specification published in Approved Document F – Ventilation (AD F: Part F of the Building Regulations for England and Wales). Some dwellings within the portfolio are located in Scotland and Northern Ireland, where different regulations are used. However, for the purpose of this meta-study, comparisons have been made with the design guidance published in AD F, irrespective of dwelling location. AD F, which carries the same specification as Technical Booklet K (Building Regulations (Northern Ireland)), and Building (Scotland) Regulations (Technical Handbook - Domestic Section 3 Environment), does not contain any performance specification for dwelling air flow rates.

Environmental data (max, min, mean and range) generated within the EMBED<sup>2</sup> platform formed the basis of the indoor environmental analysis. Cleaning of the data was performed within the EMBED platform, where data greater than two standard deviations from the median was classified as ‘in error’ and was not used in the calculations. Analysis of environmental data was limited to three months (February, April and August), representative of winter, spring and summer conditions. This provided the opportunity to explore seasonal variations. The analysis was further limited to the year 2013, to reduce the impact of yearly climate variations. Monitoring sites were limited to living rooms and bedrooms, as these tend to have the greatest levels of occupancy. Although energy data was available on the EMBED platform, this was significantly limited and there were a number of caveats pertaining to the validity of the available information. Therefore, energy data (annual space heating, electricity consumption and non-electricity consumption) was instead extracted from the available Domestic energy assessment and reporting methodology (DomEARM) datasheets. Unfortunately, it was not possible to accurately evaluate the electrical consumption or heat recovery efficiency across the range of MVHR systems in practice due to a lack of data.

The purpose of the reanalysis of BUS surveys, surveys and interviews by the BPE teams was to contextualise the physical data; understand the design intention and expectation of the MVHR systems; identify problems and good practices in terms of specification, maintenance or operation; and to evaluate how occupants interact with MVHR systems and how this may impact on their performance. Feedback from occupants was assessed by undertaking a re-analysis of BUS survey results (n: 27 projects covering 211 dwellings) along with primary data collection using online survey questionnaire and/or telephone interviews with BPE teams (n: 15 projects covering 163 dwellings). Nearly half of the projects subject to survey were Passivhaus projects. The remaining projects were split between UK, Northern Ireland, and Scottish building regulations, and CSH 4 & 5.

<sup>2</sup>Monitoring data recorded by sensors and meters in each Phase 2 dwellings has been uploaded onto an online central data repository, owned and operated by Innovate UK, known as EMBED ([www.getembed.com/](http://www.getembed.com/)).



With regard to air flow rate requirements 23 of 34 systems (68%) designed under AD F (2006) met the minimum requirement in reality and six of 18 systems (33%) designed under AD F (2010) met the minimum requirement. The original commissioning data was available for 38 out of the 54 systems reviewed. Of these, only 19 were reported to be commissioned at both normal and boost speeds. Thus, 50% of the systems can be judged to be only partially commissioned with respect to air flow. Out of the 38 sets of commissioning data reviewed, only 6 (16%) systems have provided sufficient evidence to demonstrate that they have been satisfactorily commissioned with respect to minimum air flow rates and balancing. Likewise as per design interviews, the most common problems at the installation or commissioning stages include imbalance between supply and extract airflows, poor installation and (likely as a result of the former problems) the system had to be recommissioned in one-third of the projects. Interviewees specifically described installation and commissioning issues including: system imbalance (n. 3), no airflow in some supply lines (n. 1), blockage/restricted/crushed ducts (n. 2), uninsulated ducts (n. 1), and development with dwellings ranging from flats to three bedroom homes found to have identical fan speeds (n. 1).

### **3.2 Handover and use**

According to the BPE teams, the dissatisfaction among occupants with the MVHR system is mainly due to inadequate understanding of how to use, operate and control the system, indicating inadequate handover, training and/or guidance. Furthermore the respondents felt that although the majority of the occupants were aware of the purpose of the MVHR and where the essential controls and displays of these systems were located, there was a lack of understanding of what the controls and displays are meant for and actually do. According to the BUS results, the occupants felt that they had a higher level of control over ventilation than the BPE team perceived them to have. The BUS response can however, include the ability to open windows and from the point of view of the respondent they may not consider the MVHR system alone as a source for ventilation control.

The design/research respondents felt that the most common operational issue with the MVHR systems for occupants was maintenance of the system. As an example, in a number of cases, the MVHR system is not easily accessible for occupants, precluding occupant led maintenance in most cases. Evidence of occupants disabling the system was split down the middle. Half of the sampled projects had occupants that did not disable the system and of the half that did, the most common reason was out of concern for the operating cost of the MVHR. There appeared to be a lack of trust and understanding in the need for the system. Most often the assumption that the MVHR system was the highest consumer of electricity was also wrong. Other reasons included draughts, noise, and misunderstanding appropriate management of the system. It is apparent however from the interviews that the Passivhaus projects investigated had fewer performance issues than the non-Passivhaus dwellings, particularly with regard to draughts or other discomfort and high temperatures (figure 2). This difference in performance between the Passivhaus and non-Passivhaus dwellings may be in part to the level of detail and planning required for a Passivhaus as a whole system.

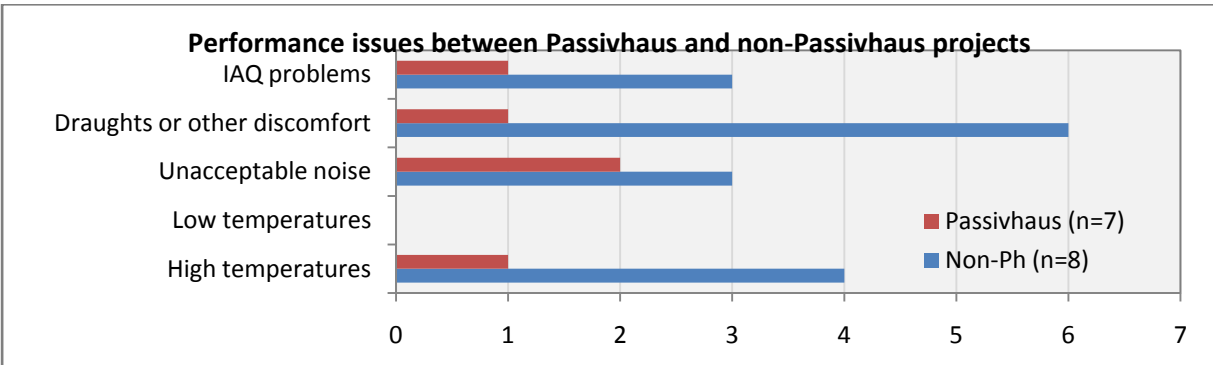


Figure 2. Performance issues

### 3.3 Energy and indoor environment

Metered data indicates that the space heating demand was generally lower in dwellings with MVHR systems. There were of course a few exceptions to this. Table 2 shows the mean annual energy consumption among the MVHR and non-MVHR dwellings analysed. It is important to note that airtightness levels, construction type and space heating strategies are likely to have significantly influenced these results. The findings show that homes with MVHR systems generally consumed less energy than homes without MVHR systems; however, it is important to emphasise that the majority of monitored MVHR dwellings were Passivhaus certified and given the stringent energy requirements of the Passivhaus certification method, this is likely to have had a significant impact on the results.

Table 2: Annual energy consumption (MVHR vs Non-MVHR)

	Electricity (kWh/a)	Electricity (kWh/m2/a)	Non-Electricity (kWh/a)	Non-Electricity (kWh/m2/a)	Total Consumption (kWh/a)	Total Consumption (kWh/m2/a)
<b>MVHR (n=39)</b>	3320.6	40.3	3689.8	46.5	6918.2	85.6
<b>Non-MVHR (n=20)</b>	3025.0	38.2	8611.2	113.3	10201.0	132.6

There is a clear differentiation in CO<sub>2</sub> levels between the dwellings with and without MVHR systems, with MVHR systems in general having lower levels of CO<sub>2</sub>. The difference is more marked when comparing peak CO<sub>2</sub> levels in living rooms and bedrooms, which were noticeably higher in the non-MVHR dwellings (Figure 3).

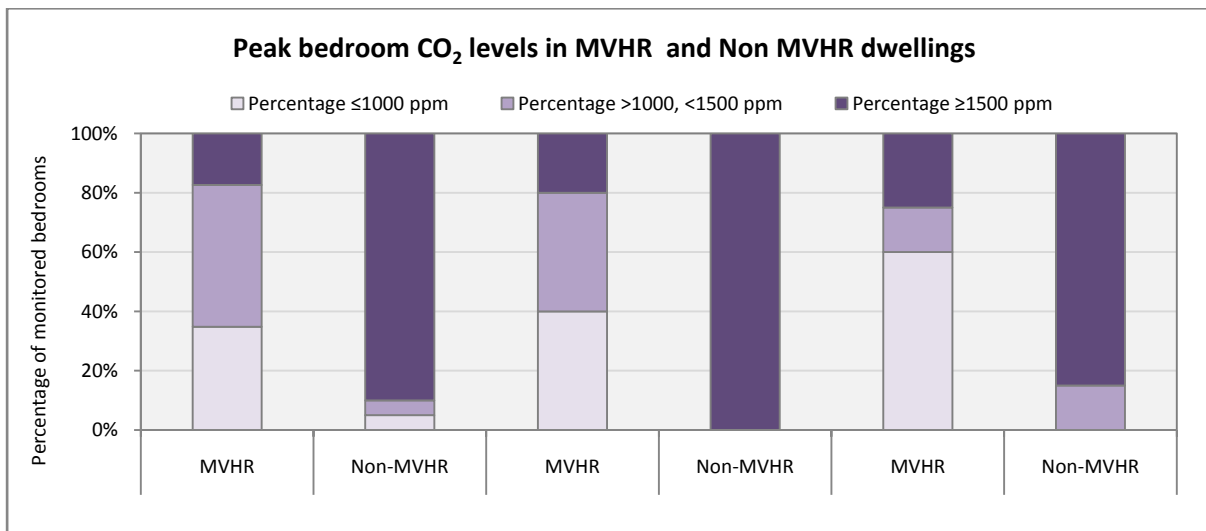


Figure 3. Peak Bedroom CO<sub>2</sub> levels in MVHR and Non-MVHR homes

Both peak and average levels were higher in the bedrooms and in these spaces the difference was much greater in non-MVHR houses. According to the mean BUS results from 10 of the 15 projects, satisfactory levels of IAQ were achieved both in summer and winter. This supports the fact that occupants in only four of the 15 projects (27%) reported IAQ problems to the BPE teams interviewed. The impact of ventilation provision on indoor CO<sub>2</sub> levels was most evident during February, which is likely due to a lower prevalence of window opening during the winter season. However higher CO<sub>2</sub> levels were also found in general in non-MVHR compared to MVHR dwellings during both April and August months, but in the summer the picture is more mixed, with more MVHR houses with higher CO<sub>2</sub> levels. This may be due to a shift toward natural ventilation strategies in summer with greater window opening, but may also be due in some cases to MVHR systems being turned off in summer. This comparison may indicate that the homes with MVHR systems achieved a better ventilation outcome compared to non-MVHR homes and, specifically, that the use of an MVHR system may have attributed to improvements of ventilation levels in these homes.

One of the potential consequences of ventilation performance is the impact on moisture in the buildings. Ventilation rates set in regulations are primarily designed to control moisture (rather than a more general requirement of IAQ) so a comparison may be made of RH levels in MVHR and Non-MVHR dwellings. In general RH levels were within reasonable ranges, tending toward the lower end. The average and minimum living room and bedroom RH levels (during February, April and August) were generally higher in dwellings with MVHR systems but were not at unduly extreme levels. In general, RH levels were more stable during all monitored seasons in the MVHR houses and this trend was particularly evident during winter. Highest RH levels were seen in August with 35% of MVHR dwellings recording peaks > 60% RH. As indicated by the CO<sub>2</sub> data this suggests high rates of window opening. On the other hand, it is apparent that low RH is common in MVHR dwellings during the heating season.

An observation of temperature data is that, in general, average temperatures were higher in Non-MVHR dwellings during February and April, but higher in MVHR dwellings during summer. As with the data on RH, an apparent trend is for houses with MVHR systems to have greater temperature stability, with a greater dispersion of indoor hygrothermal conditions found in dwellings without MVHR systems. The temperatures observed in the MVHR dwellings were closer to optimal conditions. This may be affected by the prevalence of Passivhaus dwellings in this cohort, but may also be due to poor performance in non-MVHR houses which may have oversized and poorly controlled heating systems. In summer a differentiation between MVHR and non-MVHR was less clear, with some MVHR houses

having very high peak temperatures. Whilst the overall trend for MVHR houses is positive, there are outliers where conditions are poorer. Without detailed occupancy data and external weather data, it may not be applicable to compare measured indoor temperatures with comfort criteria. Nevertheless, it is important to highlight that average temperatures exceeded 25°C (Passivhaus overheating criteria) during August in 18% of MVHR bedrooms, with peak levels exceeding 28°C in 11%. Correspondingly, in the monitored living rooms, average temperatures exceeded 25°C in 31% of MVHR dwellings during August, with levels peaking above 28°C in 16%. These results suggest issues with summertime overheating in a number of the MVHR dwellings. This may be attributed to a lack of summer by-pass capabilities in some homes, or systems being disabled in the summer, which is also suggested by the CO<sub>2</sub> and RH data. Whilst this may be expected, or indeed planned, it raises questions about the effectiveness of this in certain rooms which may be less tolerant of window opening due to issues of noise or security.

#### **4 DISCUSSION**

The paper has described a number of problems and issues encountered, evidenced both from the characteristic data and feedback from designers and occupants. These included lack of complete commissioning, poor air flow and extract rates (and associated lack of compliance with regulatory standards), lack of balance and inappropriate duct types. There was also a lack of consideration of key issues at design and construction stages, including the function of the system, integration into the design, quality of installation and commissioning, control systems, and occupant guidance and understanding. Poorly conceived and designed systems are difficult to install, difficult to maintain and difficult to use. The need for systems to be correctly selected, specified and designed could reduce many subsequent issues. Particular considerations include: unit location in terms of ease of installation and subsequent maintenance regime.

The study found a lack of Building Regulation compliance to be commonplace, and this is a cause for concern, particularly given the potential health impacts of under-ventilation. It is clear that a more rigorous commissioning and compliance checking regime is needed which may lead to increased onsite inspections by building control, but also warranty providers. There is a need for improved skills in the construction industry. One of the observations is the different trades that might be involved in the installation of a system, including plumbers, joiners and electricians, and there is a lack of oversight at installation stages. Although some improved guidance is available (for example NHBC Standards Chapter 3.2 'Mechanical ventilation with heat recovery', further improvement is needed, for example protection of ductwork during construction and on-site inspection to ensure compliance with these standards. The study found some issue with commissioning tests, and more rigour is required to ensure that such tests are undertaken to required standards. An issue arising with commissioning is subsequent interference with room supply air terminals, for example to reduce air movement. This may be addressed by having vents which can be locked or marked in place; better occupant guidance about the nature of the vents; or alternative (or variable) flow regulation systems. This may be important when considering variable flows such as demand led systems relying on CO<sub>2</sub> or RH sensors.

It is clear that MVHR are not fit-and-forget systems. For any domestic system, the proper understanding and interaction of occupants is critical. Lack of knowledge about the nature and control of MVHR systems is likely to lead to poorly used or disabled systems. Whilst there are examples of good handover processes, this is not yet commonplace, in part at least because the understanding of the nature and performance of the system is not clear amongst designers, landlords and contractors. The system also needs to not cause nuisance to occupants in the form of noise or draughts. A critical element is ensuring firstly that there is

clear understanding of the nature of the system and how it is supposed to be used by the procurement team, and secondly that robust mechanisms are in place for ensuring that occupants are given clear guidance in how to operate the system. Processes need to be available not just at early occupancy, but during changes in ownership or tenancy. Finally, a planned, legible maintenance regime will be needed for any house that has an MVHR system. For home owners this is an important aspect of the handover process. For tenanted properties, the landlord will need to evaluate who will be undertaking this maintenance, how frequent it will be, what access requirements are, and what the costs of this will be.

## 5 CONCLUSION

From this work and other literature it is clear that MVHR is becoming an increasingly widespread system in new energy efficient homes. For some construction approaches, particularly Passivhaus, it is standard practice. For houses built to the CSH standard, MVHR is also frequently used. Given the existing drivers for reducing energy and increasing airtightness, and emerging issues such as IAQ, it would seem likely that a solution that can provide good levels of ventilation, whilst providing heat recovery will continue to be an important component in contemporary low energy homes. Despite the issues outlined in the discussion, the performance data suggests that overall the use of MVHR systems can result in better levels of ventilation in comparison to naturally ventilated houses. The average CO<sub>2</sub> levels were reasonable; both average and peak levels were lower; and the environmental data suggests that more consistent temperature and relative humidity was achieved in dwellings with MVHR systems.

The overall picture that emerges from this study is that whilst there are some demonstrable benefits of MVHR systems, both in terms of ventilation and energy use, there are a number of significant risks. The tendency in the construction industry is to take a low risk approach and to avoid, rather than to solve problems. In the context of the removal of CSH and Zero Carbon targets, it would be tempting to conclude that the risks outweigh the benefits. However the ability to provide good ventilation without consequential heat loss is an important goal in modern housing and its use in high performing standards such as Passivhaus require continual development and improvement. There are emerging issues, for example urban locations where pollution or noise may mitigate against window opening, where MVHR systems could have important benefits for health and well-being. It is therefore important that the insights gained from this study are used to improve standards and practice.

## 6 ACKNOWLEDGEMENTS

The authors would like to thank Innovate UK, all the BPE teams for sharing data and participating in the interviews.

## 7 REFERENCES

- Aecb (2009). Comparing energy use and CO<sub>2</sub> emissions from natural ventilation and MVHR in a Passivhaus house. *In: AECB (ed.) Carbon Lite*. Association for Environment Conscious Building.
- Balvers, J., Bogers, R., Jongeneel, R., Van Kamp, I., Boerstra, A. & Van Dijken, F. (2012). Mechanical ventilation in recently built Dutch homes: technical shortcomings, possibilities for improvement, perceived indoor environment and health effects. *Architectural Science Review*, 55(1), pp.4-14.

- Banfill, P. F., Simpson, S. A., Gillott, M. C. & White, J. Mechanical ventilation and heat recovery for low carbon retrofitting in dwellings. World Renewable Energy Congress-Sweden; 8-13 May; 2011; Linköping; Sweden, 2011. Linköping University Electronic Press, pp.1102-1109.
- Berge, M., Georges, L. & Mathisen, H. M. (2016). On the oversupply of heat to bedrooms during winter in highly insulated dwellings with heat recovery ventilation. *Building and Environment*, 106389-401.
- Gupta, R., Gregg, M. & Cherian, R. Tackling the performance gap between design intent and actual outcomes of new low/zero carbon housing. ECEEE Summer study proceedings, 2013.
- Gupta, R. & Kapsali, M. How effective are 'close to zero' carbon new dwellings in reducing actual energy demand: Insights from UK. 30th International PLEA Conference, 2014. pp.16-18.
- Mcgill, G., Oyedele, L. O. & Keeffe, G. (2015). Indoor air-quality investigation in code for sustainable homes and passivhaus dwellings: A case study. *World Journal of Science, Technology and Sustainable Development*, 12(1), pp.39-60.
- Mcgill, G., Sharpe, T., Robertson, L., Gupta, R. & Mawditt, I. (2017). Meta-analysis of indoor temperatures in new-build housing. *Building Research & Information*, 45(1-2), pp.19-39.
- Sodagar, B. & Starkey, D. (2016). The monitored performance of four social houses certified to the Code for Sustainable Homes Level 5. *Energy and Buildings*, 110245-256.
- Toledo, L., Cropper, P. & Wright, A. J. Unintended consequences of sustainable architecture: Evaluating overheating risks in new dwellings. 2016. PLEA (Passive and Low Energy Architecture) Conference 2016.
- White, J., Gillott, M., Wood, C., Loveday, D. L. & Vadodaria, K. (2016). Performance evaluation of a mechanically ventilated heat recovery (MVHR) system as part of a series of UK residential energy retrofit measures. *Energy and Buildings*, 110220-228.

# Comparing extracting and recirculating residential kitchen range hoods for the use in high energy efficient housing

Gabriel Rojas\*<sup>1</sup>, Iain Walker<sup>1</sup>, Brett Singer<sup>1</sup>

*1 Lawrence Berkeley National Laboratory  
MS 90-3074, 1 Cyclotron Road  
Berkeley, CA, USA*

*\*Corresponding author: gabrielrojas@lbl.gov*

## ABSTRACT

Residential cooking can be a significant indoor source of odour, pollutants and particulate matter. Conventionally, range hoods expel the air into the ambient. A number of studies have investigated their contaminant capture performance. However, for highly energy efficient houses the installation of extracting range hoods can pose certain challenges, e.g. high ventilation losses, additional thermal bridges and potential air leakage sites. Therefore, the use of recirculation range hoods has become standard for highly energy efficient housing with mechanical ventilation with heat recovery in Central Europe.

Open questions remain regarding their capture and filtration efficiency as a function of filter age, especially for particles and odours. But also, the actual energy savings potential when using recirculating instead of extracting devices in a highly energy efficient housing had not been documented yet. This paper addresses these questions with a literature review and an energetic comparison.

The review identified a good number of studies which have investigated the capture performance of extracting range hoods with a focus on pollutants resulting from gas combustion and/or the cooking generated particles. These studies show that capture efficiency, in particular for front burner use, can vary drastically for different designs and that particle capture does not necessarily match capture efficiency for gaseous contaminants. No scientific study investigating the performance of recirculating range hoods was found. Tests for consumer magazines as well as surveys indicate notably lower performance compared to extracting hoods. In summary one can say that performance tests are urgently needed to quantify the capture and filter efficiency for particles and (odorous) organic compounds as a function of filter age.

## KEYWORDS

Kitchen ventilation, Extracting range hood, Recirculating range hood, Capture Efficiency

## 1 INTRODUCTION

Residential cooking can be a significant indoor source of odour, pollutants and particulate matter (PM). Range hoods are intended to remove the majority of cooking generated contaminants directly at the source before mixing with the rest of the air in the room. Conventionally, range hoods expel the air into the ambient. Usually these range hoods run at a volume flow of around 200-500 m<sup>3</sup>/h (50-150 l/s) and this contributes to additional home heating and cooling load. At higher air flows, there is the possibility that the resulting increase in envelope pressures may reduce the air flow through exhaust air system in other rooms (e.g., bathrooms and toilets) (Huber & Pluess, 2004). The required airflow openings penetrating the building envelope create additional thermal bridges and potential air leakage sites. For low-energy housing, such as Passive Houses (PH), these issues are considered problematic. Therefore, the use of recirculation range hoods has become standard for highly energy efficient housing with mechanical ventilation with heat recovery (MVHR) in Central Europe. They do not expel the extract air to the ambient, but release the filtered air back into the kitchen. The filtration typically consists of a grease removal screen followed by an activated carbon (AC) filter. Open questions remain regarding their capture and filtration efficiency as a

function of filter age, especially for PM and odours. Even if one assumes a sufficiently good contaminant removal performance, the question arises on how much energy can actually be saved with a recirculating compared to an extracting range hood? A study on the energy impacts of using extracting range hoods in US homes concludes that reducing the required airflow to obtain adequate pollutant capture would have the largest energy savings potential (Logue & Singer, 2014).

This paper addresses these questions with a literature review on capture efficiency of extracting and recirculating range hoods, looking at metrics, available standards and existing studies where capture performance has been measured. Finally, both range hood concepts are compared in terms of their energy use.

## 2 PERFORMANCE TESTING OF RESIDENTIAL KITCHEN RANGE HOODS

How effectively a kitchen range hood removes the pollutants depends on a number of variables. Besides obvious parameters like flow rate, hood design and position, there are less obvious influencing variable like the air currents in the room (Rong Fung Huang et al. 2015; Rong Fung Huang et al. 2010; Kim et al. 2017) and the cooking-generated thermal plume, which in turn depends on the heat input, the type of cooking, etc. (Walker et al. 2017). The removal of contaminants is quantified by the capture efficiency (CE), i.e., the fraction of the cooking pollutants that are removed and not allowed to mix with the air in the kitchen (and the rest of the home). CE has been used in previous studies and the new ASTM (ASTM 2017) test method based on the exhausting the pollutants to outside, but could also be used for recirculating hoods to represent the fraction of pollutants removed by the hood before the air returns to the kitchen.

### 2.1 Definitions of Capture Efficiency

The general definition of CE is the ratio of mass of contaminant removed to the mass of contaminant produced at the source. Both can be challenging to measure directly, so the following simple equation is widely used because its simplicity and the fact that it involves input values that are easy to measure (Wolbrink et al., 1992).

$$\varepsilon = 1 - \frac{c_R - c_A}{c_{RH} - c_A} = \frac{c_{RH} - c_R}{c_{RH} - c_A} \quad (1)$$

Here  $c_R$ ,  $c_{RH}$  and  $c_A$  are the concentrations in the room, in the range hood extract and in ambient. For recirculating range hoods this derivation for CE is not applicable. A corresponding model for recirculating hoods is proposed in Figure 1(b). It has three zones and splits the total contaminant removal efficiency  $\varepsilon_{Total}$  into the “fluid-dynamic” CE ( $\varepsilon_{CE}$ ) and the filter removal efficiency ( $\varepsilon_{Filter}$ ). To solve the corresponding set of mass balance equations either  $S$  or  $\dot{m}_{Fil}$  needs to be known. Depending on the pollutants, these could be hard to measure, e.g. the particle source term. Instead a method based on measuring the room contaminant concentration with and without the range hood in operation can be used:

$$\varepsilon = 1 - \frac{\int (c_R - c_A) dt}{\int (c_{R\_noRH} - c_{A\_noRH}) dt} \quad (2)$$

The subscript “noRH” stands for “no range hood”, indicating the concentrations measured with the range hood not being operated. This method can also be applied to non-continuous sources, like real cooking. It has also been applied for determining the CE for PM of extracting range hoods (Lunden, Delp, & Singer, 2015), since measuring the PM concentration of the extracted cooking fumes is problematic. Here the challenge is providing identical experimental conditions, including the source emission rate, for the set of runs needed to determine the CE. For steady state emission sources and non-contaminated ambient air, Eqn. 2 simplifies to Eqn. 3. This approach is also used within ISO 61591. Note all presented definitions apply the concept of “first pass” or “direct” CE.

$$\varepsilon = 1 - \frac{c_R}{c_{R\_noRH}}. \quad (3)$$

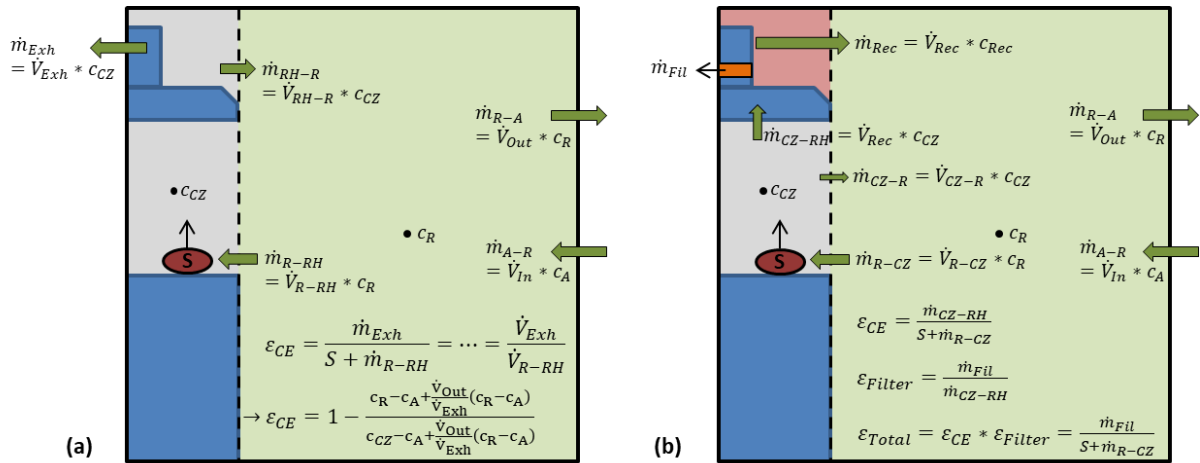


Figure 1: Schematic showing the conceptual models for deriving the capture efficiency  $\varepsilon_{CE}$  (a) for extracting range hoods and (b) for recirculating range hoods. See text for more details.

## 2.2 Standards covering residential range hood performance

Residential ventilation standards have usually no specific requirement on the kitchen range hood. However they usually have general kitchen ventilation requirements, e.g. the ASHRAE Standard 62.2 requires either an intermittent ventilation rate of 50 L/s (100 cfm) or a continuous air exchange rate of 5 Air Changes per Hour (ACH) for the kitchen. The Austrian standard applicable to residential mechanical ventilation ÖNORM H 6038 (2004) requires a minimal extract air flow of 30 m<sup>3</sup>/h (8 L/s) for the kitchen.

Whereas there are a number of standards addressing commercial kitchen range hoods (ASHRAE 154, ASTM F1704-09, VDI 2052, EN 16282-2 through -9), there are only a few standards addressing the performance of residential kitchen range hoods. The guideline from the Home Ventilating Institute (HVI) requires a minimal air flow of 40 cfm/foot of cooktop length, so 100 cfm (170 m<sup>3</sup>/h = 47 l/s) for a typical US range width of 30 inches (76 cm). The **Energy star** label addresses energy efficiency by requiring the fan efficacy to be  $\geq 2.8$  cfm/W (0.21 Wh/m<sup>3</sup>). It also limits the maximal air flow to 500 cfm and the sound to  $\leq 2$  sone.

**ISO 61591** covers methods to measure grease and odour removal performance. It can be applied to either extracting or recirculating range hoods. The odour extraction test is to be done in a symmetrically arranged test room with a volume of 22 m<sup>3</sup>  $\pm$  2 m<sup>3</sup> (3.5x2.5x2.5 m). A mix of 12 g methyl-ethyl ketone (MEK) and 300 g distilled water is dripped into a pan having a temperature of 170°C. The dripping rate should be adjusted so that this evaporation process takes 30 minutes. After that, the air in the test room is mixed with a room ventilator and the MEK concentration is measured in a certain position in the room at four different heights. The odour reduction factor  $O_f$  is determined as the relative difference of concentration  $C$  with and without use of range hood:

$$O_f = \frac{c_{wit\ h\ out} - c_{wit\ h}}{c_{wit\ h\ out}}. \quad (4)$$

Extracting range hoods are turned off directly after the evaporation process. The test room is otherwise not ventilated throughout the experiment. Recirculating range hoods are operated continuously even after the source has been removed. Besides  $O_f$ , the odour dispersion time is determined as the time it takes for the MEK concentration to reach 15% of its peak value without range hood use. Odour extraction filters are to be conditioned at 50°C for 16 hours prior to the test. For the grease absorption test, 48 g of corn oil and 69 g of water are dripped into a pan in 30 minutes, the pan having a temperature of 250°C. The grease absorption factor

is determined as the ratio of mass of grease retained in the grease filter and total mass of grease removed by ventilation equipment, i.e. in the range hood (including filter and -airways) and in a filter (placed at the hood outlet). It is interesting to note that **EN13141-3** which covers residential cooking hoods without fan requires the use of a “disturbing element” in front of the range when performing the odour extraction test. This disturbing element is to be moved periodically left and right to simulate air movements produced by a person. Otherwise the test method in EN13141-3 is very similar to ISO 61591.

A new ASTM standard (ASTM, 2017) has been developed to measure CE using tracer gas techniques for wall mount hoods. Further information on the development of this test method can be found in (I S Walker, Stratton, Delp, & Sherman, 2016). A standardized test method for island and downdraft range hoods is also being developed (Iain S Walker et al., 2017). The principle of both test methods is to determine the CE using tracer gas (e.g. CO<sub>2</sub>) emitted through specifically designed emitters. These emitter plates are to be heated to a certain temperature and/or by a given heat input and positioned at the front and/or rear burners of the range. The steady state tracer gas concentration is measured in three positions: at the test room inlet(s), at the extract air outlet and in the test room 0.5 m in front of the range at mid-height between range surface and hood. The CE can be determined with Eqn.1.

### **2.3 Actual range hood performance tests**

Besides reviewing recommended or previously known literature, a more systematic search using the phrases “range hood”, “kitchen ventilation” and “cooking exhaust” was performed within Web of Science. Publications older than 20 years, were excluded from a thorough review. There are a number of interesting publications from the National Taiwan University of Science and Technology investigating the performance of conventional, “air curtain”, “jet-isolated” and “quad-vortex” range hoods with the aid of tracer gas (SF<sub>6</sub>) measurements and flow visualization using oil fumes (J. Chen, 2015; J. K. Chen, Huang, & Dai, 2010; R.F. Huang, Nian, & Chen, 2010; Rong Fung Huang et al., 2015, 2010; Liu, Wang, & Xi, 2014). They document the effects of potential range hood improvements and the influence of disturbing air flows or even the presence of a cook. Besides the analysis of the laser-sheet visualized flow patterns, the local tracer gas spillage concentrations are presented. However, global CE is mostly not provided. In summary, these experimental studies give very valuable insights on flow characteristics and potential measures to improve contaminant capture. Experimental studies where the CE of commercially available range hoods was measured are summarized in Table 1. It lists: used performance metrics, number of tested devices and major results.

The main results of these studies are in good agreement and confirm what one would intuitively expect: higher CE for back burner use, for higher flow rates and for hoods with a big “sump”. These studies also show that CE, in particular for front burner use, can vary drastically for different designs and that particle capture does not necessarily match CE efficiency for gaseous contaminants. Note that the later conclusion somewhat contradicts conclusions derived in (Beamer, Muller, & Dessagne, 1998). High potential for improvement was identified in terms of sound performance. For the tested models higher CE performance seemed to always correlate with high noise levels, seemingly a reason for occupants to not use the range hood (see 2.4).

Unfortunately, no scientific study was found that investigated the performance of recirculating range hoods. However, the leading German consumer magazine has recently tested 21 different range hoods in their extracting and recirculating configuration (Stiftung Warentest, 2016). Besides evaluating functionality, which included grease and odour removal performance tests based on ISO 61591 (and humidity removal in extracting mode), the assessment encompassed test criteria for sound, handling, energy consumption, versatility and safety. The results of the tests are categorized in five levels ranging from “very good” to

“insufficient”. The results for grease removal in recirculation mode were either the same or dropped by one level compared to the extraction mode. However, the odour removal performance rating ranged mostly from “medium” to “insufficient” for recirculation, only one model was rated with “very good” and another model with “good”. In comparison, all models were rated “very good” for odour removal in extraction mode. Similar results can be observed in two older consumer tests by the same institution.

Table 1: Overview of publications on CE of commercially available range hoods

Study	Performance Metric	Test location, Type and Nr.	Results / Comments
B. C. Singer, Delp, Price, & Apte, 2012	CE (combustion product when heating pot of water) Airflow Sound	Field (15): Flat (5) Open Bowl (6) Hybrid (2) Downdraft (2)	Devices with flat bottom (no capture hood) have much lower CE CE is substantially higher for back burner use Flow rate and geometric coverage have also a large impact on CE A model to estimate CE from these parameters is derived
Rim, Wallace, Nabinger, & Persily, 2012	Whole house particle reduction effectiveness equivalent to CE (UFP produced by gas stove)	Field (2):	Higher flow rates generally increase UFP reduction Less reduction for smaller particles UFP reduction smaller for front burner, particle reduction 31% to 94%
Delp & Singer, 2012	CE (combustion product when heating pot of water) Airflow Sound	Lab (7): Basic (2) Compliant (1) Energy star (2) Microwave (1) Premium (1)	CE ranged from <15 to >98% Large open hoods perform best Front burner with CE>80% had sound levels too high for conversation Energy Star Hood had CE<30% for front burner
Yi et al. 2014	CE (Heat) CE (SF6 injected above pan with hot oil) CE not determined as “first pass” CE.	Lab (1)	CE for the combined use of kitchen ventilation (supply and extract) and extracting range hood CE of hood only around 50% Test chamber open on one side, concentration of entering air not recorded
Lunden et al., 2015	CE (PM from cooking) CE (combustion product)	Lab (4)	CE for back burner pan-frying (medium heat) mostly >80% and similar for PM and CO <sub>2</sub> CE for front burner stir-frying (high heat) varied by hood and airflow and were generally lower for PM capture
Claeys et al., 2015	CE (CO <sub>2</sub> injected above pot of boiling water)	Lab (1): Air curtain	CE reaches 77% at end of cooking event, but decreases after thermal plume of boiling water disappears Time-integrated CE is only 30%
Walker et al. 2016b	CE	Lab (8), Flat (4) Sump (4)	CE higher for lower mounting and greater depth from the wall
Simone et al. 2015	CE	Lab (1) Microwave	CE higher for back burners and lower temperatures
Farnsworth et al. 1989	NO <sub>2</sub> capture, H <sub>2</sub> O capture,	Lab (7)	CE increases with air flow, and with use of side curtains. Separate capture of combustion products from cooking contaminants using special vented cooktop.

For evaluation of recirculating hoods, a different approach to the tracer gas CE discussed above is required. Instead we need to look at how well particular contaminants are removed, provide a controlled source for these contaminants and then design an experimental apparatus for laboratory evaluation. One possible approach is to use the technique used in previous studies where the cooking event is performed with and without the hood operating and the difference in room concentrations is used to estimate the removal by the range hood that could be converted into an equivalent capture efficiency.

## 2.4 Results from surveys

A number of surveys have been performed that give insights into characteristics of residential kitchen range hoods and/or the associated user-perceived performance (Chan, Kim, Singer, Walker, & Sherman, 2016; Klug, Lobscheid, & Singer, 2011; Klug, Singer, Bedrosian, & D’Cruz, 2011; Mullen, Li, & Singer, 2014; Singer, 2015). Figure 2 shows the answers to the questions “How often do you use range hood when cooking with cooktop?” and “What are the reasons for not using the kitchen range hood or exhaust fan?” from a study performed in California (Chan et al., 2016).

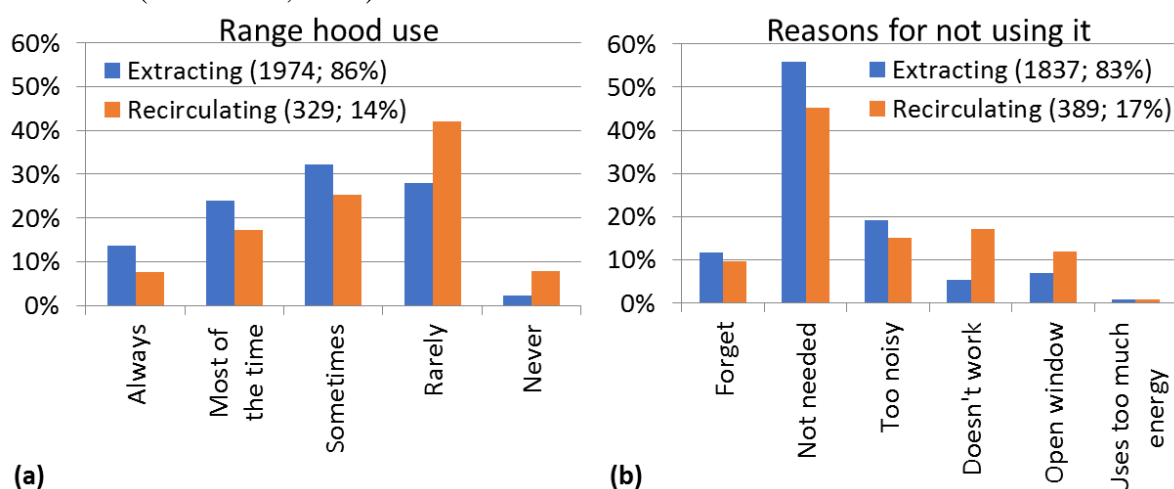


Figure 2: Survey results from (Chan et al., 2016) for the question “How often do you use range hood when cooking with cooktop?” (a) and “What are the reasons for not using the kitchen range hood or exhaust fan?” (b), segregated into households with extracting and recirculating cooking ventilation devices. The numbers in the legend refer to number and percentage of respondents in the respective category.

The results are segregated into households that had an extracting range hood or an extracting over-the-range microwave and households using a recirculating range hood or over-the-range microwave. Note that roughly 85% of respondents in this study used an extracting device. These data show a clear trend towards less usage for households with recirculating devices. And while both groups most frequently cite “not needed” as the reason for not using the hood, “Doesn’t work” was cited by only 5% of respondents with an extracting device but cited by 17% of respondents with a recirculating device. This answer could refer to devices not operating at all, but some respondents might have chosen this answer to express “Doesn’t work for removing odours/moisture”. This hypothesis is strengthened by looking at the preliminary results from another online survey performed in 2014/15 (Singer, 2015). Herein the question “In your opinion, how effective is your kitchen fan?” was asked. Again, when segregated into groups with extracting and recirculating devices, 94% and 38% respectively, responded with “Very effective” or “Moderately effective”. Only 6% of the households with extracting devices, but 58% of the group using a recirculating range hood chose “Not effective” as an answer. The small remainder of the respondents selected either “Fan is broken and does not work at all” or “No kitchen fan”.

### 3 ENERGETIC COMPARISON

Based on the previous section one can say that further research is needed to be able to evaluate the IAQ performance of recirculating range hoods. But what is the energetic benefit of installing a recirculating range hood in comparison to an extracting device? To answer that question a set of simple calculations were performed to estimate the difference in Primary Energy (PE) use for each of these two systems. The ventilation heat losses and the energetic impact of the required airflow openings were determined for an **extracting hood system**. The annual ventilation losses were calculated based on range hood airflow, heating degree hours and the estimated time the hood was in operation. Note that this estimation is conservative as it does not account that the extracted air will be somewhat above room temperature. This assumes that the operation of the hood is evenly spread out throughout the year. The average infiltration air flow through the “unused” air openings was estimated using the empirical formula and data provided in (ASHRAE, 1993) for the effective leakage area  $L$  of a kitchen ventilation with closed damper:

$$\dot{V}_{inf} = L \sqrt{A \Delta T + B v^2} \quad (5)$$

The average temperature difference  $\Delta T$  used to account for stack effects was determined for the months with an average ambient temperature  $<15^\circ\text{C}$  and for an indoor temperature of  $20^\circ\text{C}$ . The average wind speed  $v$  was estimated to be 3 m/s for the reference case, 1 m/s for the “min” case and 5 m/s for the “max” case. The stack and wind coefficient  $A$  and  $B$  for the “best estimate” reflect a two story house in moderate local shielding. The plausibility of the air flow results was compared to the calculated airflow of the effective leakage area model at 50 Pa using CONTAM and multiplied with the shielding coefficient  $e=0.07$  from EN 832 (average shielding,  $>1$  exposed façades). Both results were in good agreement. Recently, some manufacturers of air openings claim to have products specifically designed for low energy housing, e.g. (Naber, n.d.), which close airtight when the range hood is not in use. Therefore, no infiltrating airflow through the unused opening was applied as lower bound. The additional transmission losses due to the air openings were estimated as being the difference in heat transfer between a sheet metal plate and a wall with a  $U$ -value of  $0.1 \text{ W/m}^2\text{K}$  (typical for PH) for an area corresponding to a  $\text{Ø} 150 \text{ mm}$  opening. The  $U$ -value of the 1 mm thick sheet metal was increased by 20% to account for thermal bridge effects. The transmission losses turn out to be of minor relevance compared to the ventilation losses, justifying this simplified approach.

For the **recirculating system** aspects like, increased ventilation losses and fan power consumption for moisture (and possibly odour) removal via the MVHR, increased fan power consumption due to the increased pressure drop over the charcoal filter and embodied energy of the activated carbon were estimated. The increase in power consumption due to the carbon filter was determined based on the test results from a testing report (Stiftung Warentest, 2007). All 12 models were tested in extracting and recirculating mode, allowing the calculation of the difference in specific fan power (SFP) at highest setting. This difference in SFP multiplied by the assumed air flow and the time of operation gives the additional electricity consumption while assuming the same air flow. When the hoods are configured for recirculation they will not remove humidity generated during cooking. Additionally, the odour removal might not be sufficient and some occupants might want additional ventilation. This might be done by running the MVHR at a higher setting (or by opening a window). To account for this, the “best estimate” case assumes that one additional air exchange of the kitchen volume ( $35 \text{ m}^2 \times 2.5 \text{ m}$ ) is ventilated with a system having a heat recovery rate of 80% and a constant SFP of  $0.45 \text{ Wh/m}^3$ . Note that non-linear increase of the power consumption due to increase in pressure drop at higher flows is not accounted for. The “min” / “max” case assume that only 0.5 / 2 air exchange(s) are needed by the occupant and that the kitchen volume has  $38 \text{ m}^3 / 150 \text{ m}^3$ . The embodied primary energy contained in activated carbon is in the order of

20MJ/kg, e.g. (Zanoletti et al., 2017). Assuming that the filters contain 150 g / 300 g and 4000 g (as one of the models in the fore mentioned test) of activated carbon with a proposed change interval of 3 / 2 / 1 time(s) per year, the embodied energy is calculated for the three scenarios “min” / “best estimate” / “max”. For all of the described calculations a Primary Energy (PE) factor of 1.1 is used for thermal energy and a factor of 2 is used for electric energy.

**Figure 3** shows the calculated PE for the described aspects for extracting and recirculating range hoods. The “best estimate”, minimum and maximum scenarios are depicted for each category. Depending on range hood use, ventilation losses from extraction clearly dominate the other loss mechanisms and could be problematic when trying to reach the PH heating demand criteria of 15 kWh/m<sup>2</sup>a. The use of tightly sealing air openings would help reduce the PE use associated with the extraction hood by around 30% for the “best estimate” case. If users of a recirculating range hood end up needing a lot of extra ventilation, the energy use could in theory end up being higher than with an effective extracting system. The subjective need for additional ventilation will strongly depend on the occupants and their odour perception and the effectiveness of the recirculating range hood in removing odours. The need for humidity removal will depend on climates, but should not be an issue in houses with continuously running mechanical ventilation, as the relative humidity tends to be rather low for those located in heating dominated climates, e.g. in Central Europe (Rojas, 2015). The question remains on how well recirculating range hoods remove health related contaminants, like particles generated through cooking. These calculations also show that the embodied energy and the additional pressure drop of the AC filter, as well as the transmission losses of the air openings of an extracting solution will typically not strongly impact the PE balance.

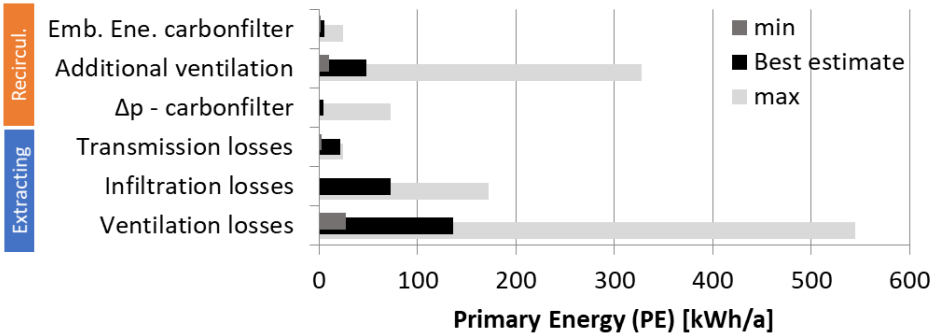


Figure 3: Differences in Primary Energy use for various aspects related to the use of extracting and recirculating range hoods.

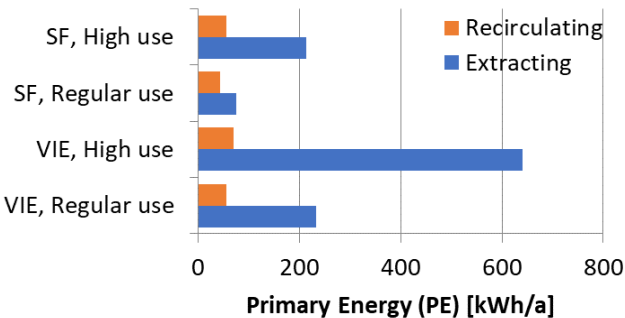


Figure 4: Differences in Primary Energy use related to the use of extracting and recirculating range hoods. The four scenarios represent the climate of San Francisco (SF) and Vienna (VIE) and regular and high usage of the range hood (time per day and flow setting).

**Figure 4** shows the total PE when the “best estimate” scenario is applied for the representative climate of Vienna and San Francisco (taken from PHPP (Passive House Institute, 2013)) assuming a regular use (30 min/day at 250 m<sup>3</sup>/h) and a high use (60 min/day

at 500m<sup>3</sup>/h). It shows that for regular use and climates with moderate heating demand there is no reason to install a recirculating range hood from an energetic point of view. This differs for colder climates and in particular for high use scenarios. Here, the reduction in heating demand could be substantial for low-energy housing.

#### 4 CONCLUSIONS

A good number of studies exist which have investigated the performance of extracting range hoods in residential settings and the associated exposure to cooking contaminants. The focus has been on pollutants resulting from gas combusting ranges and/or the cooking generated particles. However no scientific study investigating the performance of recirculating range hoods, as often installed in highly energy efficient homes, was found. Open questions remain on their effectiveness in removing cooking generated particles and organic (odorous) contaminants. Results from user surveys in the US indicate that low performance is, amongst others, a reason why people don't use their recirculating kitchen ventilation.

The existing test standard (ISO) applicable to recirculating devices covers grease adsorption and removal of a certain chemical (MEK). However performance test are needed to characterize effectiveness in reducing exposure to cooking generated PM and VOC's, in particular as the AC filter ages. A simple energetic comparison shows that for climates with distinct heating demand and for scenarios of high use (time and air flow) recirculating range hoods can substantially reduce energy use associated with cooking ventilation.

The main conclusion is that further research on the performance of recirculating range hoods in terms of IAQ is urgently needed.

#### 5 ACKNOWLEDGEMENTS

The authors would like to acknowledge the financial support by the Max Kade Foundation.

#### 6 REFERENCES

- ASHRAE. (1993). Calculating Air Exchange. In *ASHRAE Fundamentals* (1993, SI E ed., p. 23.18-23.19). Atlanta, GA: ASHRAE.
- ASTM. (2017). Standard Test Method for Capture Efficiency of Domestic Range Hoods (Draft). American Society of Testing and Materials.
- Beamer, D., Muller, J. P., & Dessagne, J. M. (1998). Comparison of Capture Efficiencies Measured by Tracer Gas and Aerosol Tracer Techniques. *Indoor Air*, 8(1), 47–60. <https://doi.org/10.1111/j.1600-0668.1998.t01-3-00007.x>
- Chan, W. R., Kim, Y., Singer, B. C., Walker, I., & Sherman, M. H. (2016). *Healthy Efficient New Gas Homes (HENGH) Field Study Protocol*. Retrieved from <https://eta.lbl.gov/sites/all/files/publications/1005819.pdf>
- Chen, J. (2015). Flow characteristics of an inclined air-curtain range hood in a draft, 346–353.
- Chen, J. K., Huang, R. F., & Dai, G. Z. (2010). Flow characteristics and spillage mechanisms of wall-mounted and jet-isolated range hoods. *Journal of Occupational and Environmental Hygiene*, 7(11), 651–661. <https://doi.org/10.1080/15459624.2012.635128>
- Claeys, B., Laverge, J., Pollet, I., & Bryuneel, G. (2015). Performance Testing of Air Curtains

- in Residential Range Hoods. *Procedia Engineering*, 121, 199–202.  
<https://doi.org/10.1016/j.proeng.2015.08.1052>
- Delp, W. W., & Singer, B. C. (2012). Performance assessment of U.S. residential cooking exhaust hoods. *Environmental Science and Technology*, 46(11), 6167–6173.  
<https://doi.org/10.1021/es3001079>
- Farnsworth, C., Waters, A., Kelso, R.M and Fritzsche, D. (1989) Development of a Fully Vented Gas Range. ASHRAE Transactions 1989, Vol. 95, Part 1, pp. 759-768.
- Honda, Y., H. Kotani, Y. Toshio, S. Kazunobu, and Y. Momoi. 2012. Modeling the thermal plume around cooking pot for prediction of thermal plume above residential gas cooking stove. proceedings of the 5<sup>th</sup> international building physics conference, pp. 1083 – 1091.
- Huang, R. F., Chen, J.-K., & Lin, J.-H. (2015). Flow Characteristics and Spillage Mechanisms of an Inclined Quad-Vortex Range Hood Subject to Influence from Draft. *Journal of Occupational and Environmental Hygiene*, 12(4), 235–244.  
<https://doi.org/10.1080/15459624.2014.987383>
- Huang, R. F., Dai, G. Z., & Chen, J. K. (2010). Effects of mannequin and walk-by motion on flow and spillage characteristics of wall-mounted and jet-isolated range hoods. *Annals of Occupational Hygiene*, 54(6), 625–639. <https://doi.org/10.1093/annhyg/meq030>
- Huang, R. F., Nian, Y.-C., & Chen, J.-K. (2010). Static condition differences in conventional and inclined air-curtain range hood flow and spillage characteristics. *Environmental Engineering Science*, 27(6), 513–522. <https://doi.org/10.1089/ees.2010.0059>
- Huber, H., & Pluess, I. (2004). *Küchenabluft in Wohnungen*. Zurich. Retrieved from [https://www.researchgate.net/profile/Heinrich\\_Huber3/publication/303519419\\_Kuchena\\_bluft\\_in\\_Wohnungen/links/5745f69a08ae9f741b43119c/Kuechenabluft-in-Wohnungen.pdf](https://www.researchgate.net/profile/Heinrich_Huber3/publication/303519419_Kuchena_bluft_in_Wohnungen/links/5745f69a08ae9f741b43119c/Kuechenabluft-in-Wohnungen.pdf)
- Kim, Y., Walker, I. S., & Delp, W. W. (2017). *Development of Standard Test Method for Reducing the Uncertainties in Measuring the Capture Efficiency of Range Hoods (to be published)*.
- Klug, V. L., Lobscheid, a B., & Singer, B. C. (2011). Cooking Appliance Use in California Homes – Data Collected from a Web-Based Survey. *Lbnl-5028E*, (August). Retrieved from <http://homes.lbl.gov/sites/all/files/lbnl-5028e-cooking-appliance.pdf>
- Klug, V. L., Singer, B. C., Bedrosian, T., & D’Cruz, C. (2011). Characteristics of Range Hoods in California Homes – Data Collected from a Real Estate Web Site. *Lbnl-5067E*, (August). Retrieved from <http://homes.lbl.gov/sites/all/files/lbnl-5067e.pdf>
- Kosonen, R., H. Koskela, and P. Saarinen. 2016. Thermal Plumes of kitchen appliances : Idle mode. *Energy and Buildings*.38(9): 1130-1139.
- Kosonen, R., H. Koskela, and P. Saarinen. 2006. Thermal Plumes of kitchen appliances : Cooking mode. *Energy and Buildings*. 38(9): 1141-1148.
- Liu, X., Wang, X., & Xi, G. (2014). Orthogonal Design on Range Hood with Air Curtain and

- Its Effects on Kitchen Environment. *Journal of Occupational and Environmental Hygiene*, 11(3), 186–199. <https://doi.org/10.1080/15459624.2013.848036>
- Logue, J. M., & Singer, B. C. (2014). Energy impacts of effective range hood use for all U.S. residential cooking. *HVAC and R Research*, 20(2), 264–275. <https://doi.org/10.1080/10789669.2013.869104>
- Lunden, M. M., Delp, W. W., & Singer, B. C. (2015). Capture efficiency of cooking-related fine and ultrafine particles by residential exhaust hoods. *Indoor Air*, 25(1), 45–58. <https://doi.org/10.1111/ina.12118>
- Mullen, N. A., Li, J., & Singer, B. C. (2014). Participant Assisted Data Collection Methods in the California Healthy Homes Indoor Air Quality Study of 2011-13, (August).
- Naber. (n.d.). Thermobox. Retrieved from <https://www.naber.de/de-thermobox-150-s13027/>
- Passive House Institute. (2013). *Passive House Planning Package - PHPP Version 8*. (W. Feist, Ed.) (8th ed.). Darmstadt, Germany: Passive House Institute. Retrieved from [http://www.passiv.de/de/04\\_phpp/04\\_phpp.htm](http://www.passiv.de/de/04_phpp/04_phpp.htm)
- Rim, D., Wallace, L., Nabinger, S., & Persily, A. (2012). Reduction of exposure to ultrafine particles by kitchen exhaust hoods: The effects of exhaust flow rates, particle size, and burner position. *Science of the Total Environment*, 432, 350–356. <https://doi.org/10.1016/j.scitotenv.2012.06.015>
- Rojas, G. (2015). *Optimization potentials for mechanical ventilation of energy efficient housing - Simulation and evaluation methods*. University of Innsbruck. Retrieved from <https://resolver.obvsg.at/urn:nbn:at:at-ubi:1-3370>
- Simone, A., Sherman, M.H., Walker, I.S., Singer, B.C., Delp, W.W. and Stratton, J.C. (2015). Measurements of Capture Efficiency of Range Hoods in Homes. Proc. Healthy Buildings 2015.
- Singer, B. (2015). Range Hood Roundup - Kitchen Ventilation Survey. Retrieved October 6, 2017, from <http://indoorair.lbl.gov/range-hood-roundup/>
- Singer, B. C., Delp, W. W., Price, P. N., & Apte, M. G. (2012). Performance of installed cooking exhaust devices. *Indoor Air*, 22(3), 224–234. <https://doi.org/10.1111/j.1600-0668.2011.00756.x>
- Stiftung Warentest. (2007, August). Stark und schick - Dunstabzugshauben. *Stiftung Warentest*, 66–72. Retrieved from <https://www.test.de/Dunstabzugshauben-Stark-und-schick-fuer-Ihre-Kueche-1558021-0/>
- Stiftung Warentest. (2016, March). Frische Luft in der Küche. *Stiftung Warentest*, 64–73. Retrieved from <https://www.test.de/Dunstabzugshauben-Die-besten-gegen-Dampf-Geruch-und-Fett-4980444-0/>
- Walker, I. S., Rojas, G., Clark, J., & Sherman, M. H. (2017). Evaluating the Performance of Island Kitchen Range Hoods. In *AIVC Proceedings*. AIVC.

- Walker, I. S., Stratton, J. C., Delp, W. W., & Sherman, M. H. (2016a). *Development of a Tracer Gas Capture Efficiency Test Method for Residential Kitchen Ventilation*. LBNL 1004365.
- Walker, I.S., Sherman, M.H, Singer, B.C. and Delp, W.W., (2016b) Development of a Tracer Gas Capture Efficiency Test Method for Residential Kitchen Ventilation. Proc. IAQ 2016. Wolbrink, D. W., & Sarnosky, J. R. (1992). Residential kitchen ventilation - a guide for the specifying engineer. *ASHRAE Transactions*, 98, 1187–1198.
- Yi, K. W., Kim, Y. I., & Bae, G.-N. (2014). Effect of air flow rates on concurrent supply and exhaust kitchen ventilation system. *Indoor and Built Environment*, 0(0), 1–11.  
<https://doi.org/10.1177/1420326X14541558>
- Zanoletti, A., Federici, S., Borgese, L., Bergese, P., Ferroni, M., Depero, L. E., & Bontempi, E. (2017). Embodied energy as key parameter for sustainable materials selection: The case of reusing coal fly ash for removing anionic surfactants. *Journal of Cleaner Production*, 141, 230–236.

# How loud is too loud?

## Noise from domestic mechanical ventilation systems

Jack Harvie-Clark<sup>\*1</sup>, Nick Conlan<sup>1</sup>, Weigang Wei<sup>1</sup>, and Mark Siddall<sup>2</sup>

*1 Apex Acoustics Ltd  
William Street  
Gateshead, UK*

*2 LEAP  
3 Toll House Road  
Durham, UK*

*\*jack.harvie-clark@apexacoustics.co.uk*

### ABSTRACT

Noise from domestic ventilation systems is currently a little understood problem in the UK. Other European countries that have a longer history of using mechanical domestic ventilation systems have introduced noise limits for these systems. Without mandatory limits for noise in UK, noise is not a factor that is often considered during the design. However, noise can be a significant constraint to the use of ventilation systems. Research is reviewed from across Europe and North America that indicates residents turn off ventilation equipment with objectionable noise. Without adequate ventilation in modern airtight dwellings, poor air quality can have a significantly adverse effect on the health of the occupants. There is a lack of evidence in the literature and performance standards for appropriate noise metrics and values that occupants find acceptable: this research is urgently required, and the steps to realise this are outlined. Causes of excessive noise are found to originate due to problems during the design, procurement, installation, commissioning and operation of ventilation systems. A suitable metric is required along with regulatory control to ensure that residents are not forced to choose between intolerable noise or inadequate air quality.

### KEYWORDS

Noise, domestic, mechanical ventilation

## 1 INTRODUCTION

Noise can be a significant constraint to the use of domestic ventilation systems. Almost every study on domestic mechanical ventilation, in countries where there are problems with mechanical ventilation, refers to noise as a reason that the systems are not used as intended by the designers (REHVA, 2012; Sharpe et al, 2016; McGill et al, 2015; Brown & Gorgolewski, 2015; Balvers et al, 2012; Hady et al, 2008; Kurnitski et al, 2007). Some of these studies detail how occupants turn down their ventilation systems to a level of noise that is tolerable, or disable them entirely to prevent the perceived noise nuisance. In modern airtight dwellings, effective ventilation is vital to ensure adequate Indoor Air Quality (IAQ), and prevent adverse health effects of inadequate ventilation (Dimitroulopoulou, 2012). The noise problem in domestic ventilation is not ubiquitous – van der Pluijm (2010) notes that there are no reports of this problem from Germany and Sweden, for example. While the potential causes of excessive noise are documented (Harvie-Clark et al, 2014), the levels and character of noise that are unacceptable to residents are not well researched.

A complication when reviewing the literature is that there are other reasons that people also often cite for turning their ventilation systems off, such as to avoid the cost of electricity, or to avoid draughts (Sharpe et al, 2016), and therefore resident's reports may not always be candid. For example, McGill (McGill et al, 2015) reports:

*... at the initial interview occupants stated that they did not have any problems with the system; however, during the building survey they mentioned they had turned the ventilation system off as it was making a loud noise.*

A larger body of noise research focuses on annoyance in office environments, seeking to detail noise levels that interfere with task performance, linking to productivity and hence financial performance of staff (Leventhall, 1998; Ayr, 2002; Wang & Novak, 2010). Another body of evidence concerns the effects of noise on sleep (see Marquis-Favre et al, 2005 for a review), mainly focussing on the effects of environmental noise on people sleeping. There is a marked absence of study of noise tolerance of people to their own ventilation systems.

The situation for occupants is different to the effects of environmental noise; the period when people are getting to sleep may be the most critical. At this time background noise from both internal and external sources is likely to be lower than at other times, and the activity of falling asleep is one of inactivity and hence little self-generated noise. Under these conditions, noise from mechanical ventilation systems is likely to be more noticeable than at other times. Any particular source of noise that is noticeable has the potential to be annoying. This may be because of the perceived interference with the need for quiet, in the sense of freedom from interruption as well as low noise level, described by Andringa&Lanser (Andringa&Lanser, 2013). The context is also important: in a rural setting with little environmental noise, or in modern dwellings with well-sealed façade elements in a range of settings, the background noise may be low. In these circumstances, any noise from the mechanical ventilation may be more prominent than other sources, and therefore attract attention.

How can noise from domestic mechanical systems be assessed to capture the range of tolerances that different people may exhibit? The purpose of a suitable metric would be to ensure that only very few people – or possibly nobody – would be motivated to restrict the use of the ventilation system due to noise. The purpose of this paper is to explore these questions and identify research that is required where there are gaps in the literature.

## **2 NOISE MODELS AND METRICS**

### **2.1 Noise response models**

A simple response model to noise is illustrated by Leventhall (Leventhall, 1998), and identifies three stages, namely *detection*, *perception*, and *response*. Leventhall notes that: *the response is conditioned by parameters in addition to the physical attributes of the noise alone, including personal and situational elements...*

Although Leventhall's 1998 research concerns noise in offices, most of the concepts are relevant for residents responding to noise from domestic ventilation systems. He studies the spectrum balance, frequency composition, and fluctuations, which are features that are not currently used to consider noise from domestic ventilation systems in the UK. The Qaulaity Assessment Index (QAI) methodology described by ASHRAE does address spectrum balance, see below. Further investigations of fluctuating noise tolerance typically concern the effect of people in office environments, such as that by Wang and Novak (Wang and Novak, 2010).

A more complex response model to indoor environmental conditions is discussed by Boerstra (Boerstra, 2016); central to this thesis is that control over the personal indoor environment can significantly affect the response to indoor climate conditions. This idea has been espoused by many people investigating conditions in offices, notably Leaman et al (Leaman et al, 1999). It is not currently known whether people may be more tolerant of noise from domestic ventilation systems where they have control over the systems, where they perceive a benefit from operation of the system. Researchers' comments suggest that the opposite may be true – that there is next to no tolerance of noise from these sources, especially as the level of knowledge of the purpose of ventilation is low (Baborska-Narozny & Stevenson, 2017),

(Brown & Gorgolewski, 2015) and there is little perceived benefit in their operation. According to Brown & Gorgolewski:  
*all 27% of respondents who had disabled their HRV did so because of its objectionable noise*

## **2.2 Noise metrics**

Noise metrics have been developed to correlate with human response to sound in many different contexts. It is worth remembering that sensitivity to different frequencies of sound varies with sound level, as illustrated by the equal loudness contours of ISO 226. This means that one fixed set of frequency weightings may be a good indicator of loudness at one sound level, but at different sound levels it will not. A large number of noise metrics are reviewed by Marquis-Favre et al (Marquis-Favre et al, 2005). Factors affecting noise annoyance are considered, along with the noise source, characteristics of the sound and non-acoustic factors.

Pearsons & Bennett (Pearsons & Bennett, 1974) classify noise metrics into categories including speech interference and annoyance. Although this publication pre-dates many more recent metrics, it illustrates the point that the metrics designed to describe building services noise levels are categorised for speech interference, rather than annoyance. Even though the concept for comfortable noise in offices may be considered in terms of effect on productivity, this is very different from relaxing in one's home, or falling asleep.

The A-weighted scale is widely acknowledged to under-represent the loudness of sounds with a strong low frequency content. For example, the WHO Community Noise Guidelines (Berglund et al, 1999) indicates that:

*Where noise is continuous, the equivalent sound pressure level should not exceed 30 dBA indoors, if negative effects on sleep are to be avoided. When the noise is composed of a large proportion of low-frequency sounds a still lower guideline value is recommended, because low-frequency noise (e.g. from ventilation systems) can disturb rest and sleep even at low sound pressure levels.*

The A-weighted sound level has become the default metric to indicate noise levels in many scenarios; it is often tested and found to be the indicator that correlates best with perception of noise levels (e.g. Ayr, 2003) in particular circumstances.

## **3 NATIONAL STANDARDS AND EXPERIENCE**

A systematic review of national guidelines for noise from mechanical services in a domestic setting has not been carried out, although some of the references below have undertaken this in some parts of the world.

### **3.1 UK**

In the UK, noise from domestic building services is not currently regulated. There is guidance in the standards for ventilation (Approved Document F, 2010) that noise from continuously running systems should not exceed 30 dB(A) in living rooms and bedrooms, with a reference to a previous version of BS 8233 (BSI, 1999). It appears that the 30 dB(A) value is simply taken from environmental noise studies as the threshold above which adverse effects of noise on sleep become apparent – ie the LOAEL (Lowest Observable Adverse Effect Level), rather than correlated with occupant response to ventilation systems.

The Chartered Institute of Building Services Engineers (CIBSE, 2015) offers three metrics for mechanical services noise limits in its Guide A: Environmental design. These are NR 25, 30 dB(A), and 55 dB(C) for bedrooms. The authors have indicated that the dB(C) values are based on experience with sound level meters prior to the modern day, when real time

analysers can log in frequency bands and overall weighted values simultaneously. The C-weighted limit is intended to highlight excessive low-frequency noise.

The effectiveness of ventilation systems in the UK has been investigated by the Zero Carbon Hub (ZCH, 2016), which found that:

*In summary, the Hub team found things going wrong at multiple stages of the construction process at every site... At 5 of the 6 sites, fans were operating at only half the required duty or lower, i.e. flow rates were far too low. The end result was that nearly all of the 13 occupants interviewed by the team across the sites had turned off their ventilation systems, finding them too noisy, especially at night.*

Failings in the design, specification, procurement, installation, commissioning and maintenance are detailed in the ZCH report. The National House Building Council (NHBC) introduced its Chapter 8.3 “Mechanical Ventilation with heat recovery” into its Standards 2014, in response to observations of poor practice. In April 2017 the NHBC produced a review of compliance with its own standards. The Technical Extra report (NHBC, 2017) follows investigations at over 200 sites, looking at six key areas of design and drawings, installation, ducting, air transfer, testing and commissioning, and handover to the homeowner. The report details significant findings of non-compliance, repeating many of the findings of the ZCH report, and reminds readers of what compliant practice would look like.

McGill et al (2015) list common MVHR shortcomings, and include noise as a problem. Baborska-Narozny&Stevenson (Baborska-Narozny&Stevenson,2016) evaluate 40 low carbon homes, and finding that noise is frequently a problem for occupants, with 30% of occupants switching fans off due to the noise.

**3.2 Sweden**

Sweden has a well-established acoustic classification system, documented in Swedish Standard SS 25267 (Svensk Standard 2015). This has four Classes for noise from mechanical ventilation, reproduced in Table 1.

Table 1: Class limits under the Swedish Classification system

Type of space and source	Class / L <sub>eq</sub> ,dB(A)			
	A	B	C	D
In spaces for sleep, rest or everyday social contact	≤ 22	≤ 26	*	≤ 30

Requirements for sound class C are described in National Board of Building, Planning and Housing building regulations BBR Section 7:21, and therefore omitted from the classification system. Reports from the authors of the standard indicate that:

*For sound class B the experience is massive in Sweden, and for sound class A it's a clear consensus that the values are adequate.*

**3.3 Finland**

A Finnish study by Kurnitski (Kurnitski,2007) describes measurements of not just ventilation performance, but also of measured noise levels, in 102 homes. This study is unique, as noted in Existing Buildings, Building Codes, Ventilation Standards and Ventilation in Europe: The Final Report (REHVA, 2012) that it is the only study that documents the noise levels and also compares the occupant-controlled point of operation with the noise levels. The study found a dependency between the maximum noise level in bedrooms and ventilation noise complaints. An upper limit threshold of 22 dB(A) resulted in < 10 % complaints and an upper limit threshold of 25 dB(A) resulted in < 20 % complaints. A significant dependency was

found between the maximum fan speed of the ventilation unit and complaints, rather than the whole dwelling ventilation rate. This study was one of the first to note that people operated their ventilation systems at the level at which they could tolerate the noise, rather than at the level that provided the minimum suggested ventilation rates. This finding is repeated in many other subsequent studies.

**3.4 Netherlands**

The experience of the Netherlands appears to be similar to that subsequently experienced in the UK. Problems with mechanical ventilation systems have been noted and adverse media coverage has resulted for modern air-tight homes. Hady et al (Hady et al, 2008) report on the characteristics and associated adverse health effects in under-ventilated homes, reporting noise and draughts being the biggest causes for dissatisfaction. Noise is reported as a barrier for occupants’ use at the ventilation set point.

Balvers et al (Balvers et al,2012) investigated 299 homes, and notes that:  
*Noise annoyance results in occupants setting the system in a low setting or turning it completely off, leading to insufficient ventilation... The most common shortcomings related to high noise levels(wher >30% of the homes did not comply with the reference level) ... Noise levels are higher than 30 dB(A) in one or more bedrooms in 86% of homes with MVHR in the setting in which the ventilation system is providing a sufficient ventilation rate.*

**3.5 Europe**

A pan-European acoustic collaboration, COST Action TU-0901, concluded in 2014 (Rasmussen, 2014). Although focussed on producing a classification system for sound insulation, noise from building services was included; the Classes for noise from building services are shown in Table 2. There is a reference to ISO 16023 for the measurement of sound levels.

Table 2: Class limits for service equipment noise proposed in COST Action 0901

Type of space and source	Class / L <sub>eq</sub> ,dB(A), and dissatisfaction, %					
	A	B	C	D	E	F
Rooms in dwellings; ventilation / heating installation	≤ 20	≤ 24	≤ 28	≤ 32	≤ 36	≤ 40
Guide to occupant dissatisfaction, %	≤ 5 %	≈ 5 %	≈ 10 %	≈ 20 %	≈ 35 %	≥ 50 %

This does not distinguish between different room types, and has much lower limits for the highest performance, Class A than may be anticipated by designers in the UK. The information about Classes suggests occupant dissatisfaction levels as shown in Table 2 with around 20 % dissatisfaction for noise levels not exceeding 32 dB(A).

Taken from a ventilation rather than acoustic point of view, REHVA (REHVA,2012) notes, in reviewing noise guideline levels across Europe, that:

*Many of the noise limit levels seem quite high, which is especially the case for bedrooms. A common European regulation is required. It should define noise levels in only one type of units to avoid confusion.*

And further comments that echo those made by many other investigators:  
*The reviewed studies show that ventilation rates, indoor environmental parameters and noise do not comply with regulations. Deviations between measured and required values are considerable and actions need to be taken. A new European guideline is needed, which would serve as a base document for legislators in EU countries or in the European Commission. The guideline should provide guidance on suitable design, construction,*

*maintenance and inspections of ventilation systems. For improved efficiency, the inspection of ventilation systems should be merged with the inspection of air-conditioning systems and energy auditing. More effort should be put into education of all parties involved in design, construction and operation of ventilation systems.*

Furthermore, in dwellings:

*Noise in mechanical ventilation systems is a common problem. Even though systems are often able to provide the required ventilation rate, the occupants lower fan speed setting because of the noise disturbance. Too little attention is paid to noise during the design and construction phases. Surveys report that almost all regulated noise levels are too high in practice.*

### **3.6 USA**

A large body of work has been undertaken by ASHRAE to determine the acceptability of noise levels. The 2015 ASHRAE Fundamentals Handbook (ASHRAE, 2015) includes a detailed discussion of a range of parameters for assessing noise from building services. The preferred criterion identified is the RC Mk II, which includes the Quality Assessment Index (QAI) proposed by Blazier (Blazier, 1995, 1997). The QAI is a measure of the spectral imbalance of sound levels, and it is claimed that more imbalanced sounds lead to greater dissatisfaction and complaints. Excessive high-frequency sound is described as a “hiss”, mid-frequency excess as “roar”, and low frequency excess a “rumble”. Interestingly, the ASHRAE Handbook indicates that a level of NC / RC 30 for “Living areas”, and indicates “Approximate Overall Sound Pressure Levels of 35 dB(A) and 60 dB(C). These values are conspicuously 5 dB higher than the WHO Guidelines (WHO, 1999), and the Handbook comments:

*It is recommended that when specifying background sound levels in dBA, the dBC is also included in the specification and does not exceed the dBA reading by more than 20 dB.*

It is speculated that a possible reason for the higher permissible sound levels from mechanical services is due to the greater cultural acceptance of this type of noise, with mechanical services having greater penetration in North America.

When investigating inhabitants use of ventilation in Toronto (Brown & Gorgolewski, 2015), the researchers reported the QAI values but not the overall sound pressure levels. They noted that:

*... QAI values were high and where the noise caused by continuously running bathroom fans prompted 27% of respondents to disable their fan...*

Thus the actions of the inhabitants are attributed to the quality of the sound rather than the overall level. This study is unique in the literature reviewed to conclude that the sound quality is unacceptable, rather than the sound level. The fact that this is due to noise in the bathroom rather than bedroom or living room is also significant.

## **4 OTHER SOURCES OF INFORMATION**

### **4.1 Sleep in hotels**

A fundamental purpose of a hotel is to provide a place to go to sleep. Some hotels place more emphasis on the acoustic performance of their brands than others, even making it a unique selling point. It is interesting to compare the range of noise levels that hoteliers provide in their brand standards when new developments are constructed. Some well-known four-star global hotel brands adopt a standard of NR 30 in guestrooms for mechanical services noise, which typically equates to noise levels in the range 33 – 36 dB(A). Comparison with the values in in Table 2 would suggest that a high proportion of people may well be dissatisfied with noise levels as high as these.

Conversely, a large value-range UK hotel chain that places great emphasis on acoustics has a limit of NR 20 for noise from the mechanical ventilation heat recovery system – which are

installed in a per-room arrangement. The hotel chain has a money-back guarantee if residents do not have a good night's sleep; the performance specification for new developments continually evolves in response to complaints received. This represents an effective quality system for meeting residents' expectations for noise, amongst other factors. Typical installed noise levels have been measured by the authors between NR 18 – 20, equating to 22 – 24 dB(A). It may be considered that these values represent noise levels at which people do not feel they have any valid cause for complaint, as there is a financial incentive to do so. It is also interesting to consider that comfort cooling systems in hotels almost always operate at noise levels that are unlikely to be compatible with undisturbed sleep; they are likely to only be used during the sleeping period if the need for thermal comfort is considered to be greater than the need for acoustic comfort, such that occupants may accept elevated noise levels over which they have control. There appears to be a general cultural acceptance that this is the case; clearly it need not be so from an engineering perspective, but it is cheaper for hotel developers to permit higher noise levels from comfort cooling systems.

#### **4.2 Passivhaus standards**

The Passivhaus standard for noise from the ventilation system is  $\leq 25$  dB(A). The authors have not been able to determine how this value was determined, and are not aware of any noise complaints from ventilation system in Passivhauses in the UK.

### **5 SOURCES OF NOISE FROM DOMESTIC VENTILATION SYSTEMS**

Excessive noise from domestic ventilation is typically symptomatic of other problems, and highlights one or more failings in the design, specification, procurement, installation or operation of mechanical ventilation systems. The knowledge and experience to mitigate noise from mechanical ventilation systems is well established, but is rarely employed in the residential construction sector in the UK.

There are many different typologies for the implementation of domestic ventilation. In some countries, such as Sweden, in blocks of flats it is common to have a centralised ventilation system. In the UK, each dwelling usually has its own ventilation system; the choice of system is usually determined by speculative housebuilding companies on the basis of thermal performance requirements. Particular sources of noise are likely to be dependent on local building customs and ventilation systems adopted.

Problems that can lead to excessive noise are presented by Harvie-Clark et al (Harvie-Clark et al, 2014), for example. Typical problems and the actions to avoid them in the UK are well documented by NHBC (NHBC, 2017), Zero Carbon Hub (ZCH, 2016), McGill et al (McGill et al, 2015), Dengel&Swainson (Dengel&Swainson, 2013), amongst others. Some studies note that ventilation systems are frequently commissioned “by ear”, rather than by flow measurement e.g. (ZCH, 2016). While this practice acknowledges the importance of the noise from these systems, it does nothing to ensure that sufficient ventilation is also provided.

### **6 FUTURE WORK REQUIRED**

The content in this section was developed at the HEMAC workshop (HEMAC, 2017). The future work required may be broken down into several categories. Most importantly, the question of what noise characteristics are best suited for ventilation systems for sleep and for relaxation should be addressed. Guidance is required for stakeholders to illustrate this, and government policy should be informed by the results. This may be achieved through the following research objectives:

- i.. Identify acoustic triggers and mitigating action by occupants on their MV systems
- ii. Diagnose problem noise sources and characteristics

- iii. Determine the ranges of ventilation system noise characteristics best-suited for bedrooms for sleep, living rooms, and bathrooms.
- iv. Inform policy and practice through guidance

It is suggested that these objectives may be achieved through the following actions:

Table 3: Potential work packages to determine sound levels that avoid causing occupants to curtail ventilation

Workpackage	WP overview
1	Occupant perception survey of installed systems, including measurements of the noise levels and recording of noise signal for laboratory studies.
2	Larger-scale survey of as-built mechanical ventilation noise levels, to characterise the potential extent of the problem when correlated with data from occupant perception survey and lab tests.
3	Physical survey of problem sources and resultant noise characteristics: design, installation, operation and maintenance.
4	Laboratory study of subjective testing and optimisation of MV noise characteristics for sleep, and for relaxation, using measured source data.
5	Mapping pathways to impact - implications for policy and practice

As with other aspects of new-build dwellings, the author’s experience is that many contractors in the UK seek to minimise costs by simply providing the minimum requirements of the regulations. Where noise levels remain unregulated, there is little incentive to take appropriate steps during the design, specification, procurement, installation and commissioning to ensure that suitable levels are achieved.

## 7 CONCLUSIONS

Many residents in parts of Europe and beyond are dissatisfied with their ventilation systems due to the noise. This dissatisfaction causes them to reduce or disable entirely the operation of those ventilation systems. This represents a potential health hazard in modern air-tight homes, as infiltration cannot be relied upon to achieve adequate IAQ. Excessive noise levels and unacceptable quality of noise are separately reported as issues leading to interference with ventilation systems.

The particular characteristics of ventilation system noise that cause occupants to interfere with the operation of their systems are not well researched; there is little evidence in the literature about people’s tolerance to noise from their own ventilation systems. Research is urgently needed to identify a suitable metric for ventilation system noise, and determine appropriate guideline values for different rooms. The Swedish and COST Action TU 0901 classification schemes emphasise the value of noise levels well below 30 dB(A).

In the interim, the highest limit that could be proposed for mechanical services noise in bedrooms is 30 dB(A), to avoid adverse effects on sleep. Where there is anticipated to be significant external noise ingress, a lower limit should be proposed such that the combined internal level does not exceed 30 dB(A). The literature suggests that a more prudent limit for mechanical services around 24 - 26 dB(A) is unlikely to cause an adverse reaction from most occupants while falling asleep, noting that 20 % of Finnish respondents found this too noisy. This may be an unnecessarily onerous target, depending on the characteristics of the

noise. There is insufficient evidence to propose limits in living spaces and bathrooms without suitable research.

In the absence of this work there is an ongoing risk that noise will continue to be cited as a reason that people chose to curtail the operation of their mechanical ventilation systems, and suffer the effects of poor IAQ as a result. People should not be forced to choose between intolerable noise or poor IAQ in their homes.

## 8 ACKNOWLEDGEMENTS

Thanks are due to the work of everyone at Apex Acoustics: you make this work possible.

## 9 REFERENCES

- Andringa, T. C., & Lanser, J. J. (2013). How Pleasant Sounds Promote and Annoying Sounds Impede Health: A Cognitive Approach. *Int. J. Environ. Res. Public Health*, 10(4), 1439-1461. doi:doi:10.3390/ijerph10041439
- ASHRAE. (2015). *2015 ASHRAE Handbook Heating, Ventilating, and Air-Conditioning Applications. SI Edition.*
- Ayr, U., Cirillo, E., & Martellotta, F. (2002). Further investigations of a new parameter to assess noise annoyance in air-conditioned buildings. *Energy and Buildings*, 765-774.
- Ayr, U., Cirillo, E., Fato, I., & Martellotta, F. (2003). A new approach to assessing the performance of noise indices in buildings. *Applied Acoustics*, 64, 129-145.
- Baborska-Narozny, M., & Stevenson, F. (2017). Mechanical ventilation in housing: understanding in-use issues. *Proceedings Institute of Civil Engineers - Engineering Sustainability*, 170, pp. 33-46. doi:doi.org/10.1680/jensu.15.00053
- Balvers, J., Bogers, R., Jongeneel, R., van Kamp, I., Boerstra, A., & van Dijken, F. (2012). Mechanical ventilation in recently built Dutch homes: technical shortcomings, possibilities for improvement, perceived indoor environment and health effects. *Architectural Science Review*, 4-14. doi:dx.doi.org/10.1080/00038628.2011.641736
- Blazier, W. E. (1995). Sound quality considerations in rating noise from heating, ventilating, and air-conditioning(HVAC) systems in buildings. *Noise Control Engineering Journal*, 53-63.
- Blazier, W. E. (1997). RC Mark II: A refined procedure for rating the noise of heating, ventilating, and air-conditioning (HVAC) systems in buildings. *Noise Control Engineering*, 243-250.
- Boerstra, A. C. (2016). *Personal control over indoor climate in offices : impact on comfort, health and productivity.* Eindhoven, Netherlands: Technische Universiteit Eindhoven. Retrieved from <http://repository.tue.nl/079d4ef4-04d3-4789-8101-8f0fdd7ca3a5>
- Brown, C., & Gorgolewski, M. (2015). Understanding the role of inhabitants in. *Building Research & Information*, 43(2), 210-221. doi:dx.doi.org/10.1080/09613218.2015.963350

- BSI. (2014). *BS 8233:1999, Sound insulation and noise reduction for buildings. Code of practice.*
- CIBSE. (2015). *CIBSE Guide A: Environmental Design.* Chartered Institute of Building Services Engineers.
- Crowe, K. (1974). *A History of the Original Peoples of Northern Canada.* Montreal: McGill/Queen's University Press for the Arctic Institute of North America.
- Dengel, A., & Swainson, M. (2013). *Assessment of MVHR Systems and air quality in zero carbon homes.* NHBC Foundation Research.
- Dimitroulopoulou, C. (2012). Ventilation in European dwellings: A review. *Building and Environment*, 109-125.
- Hady, M., van Ginkel, J., Hasselaar, E., & Schrijvers, G. (2008). The relationship between health complaints, the quality of indoor air and housing characteristics. *Indoor Air.*
- Harvie-Clark, J., Siddall, M. J., & Hunter, D. (2014). Noise from domestic ventilation systems. *Institute of Acoustics Conference Proceedings.* IOA. Retrieved from [www.apexacoustics.co.uk/wp-content/uploads/2015/07/Apex-Acoustics-MVHR-design-poster.pdf](http://www.apexacoustics.co.uk/wp-content/uploads/2015/07/Apex-Acoustics-MVHR-design-poster.pdf)
- HEMAC Sandpit. (2017, April 25). Health Effects of Modern Airtight Construction. *Noise effects.* (J. Harvie-Clark, D. Waddington, J. Laverge, M. Marinho, R. Gupta, R. Menon, & W. Swan, Eds.) Glasgow. Retrieved from <https://hemacnetwork.com/sandpit/>
- Kurnitski, J., Eskola, L., Palonen, J., & Seppänen, O. (2007). Use of mechanical ventilation in Finnish houses. *European BlowerDoor Symposium.*
- Leaman, A., & Bordass, B. (1999). Productivity in buildings: the 'killer' variables. *Building Research & Information*, 27(1). doi:dx.doi.org/10.1080/096132199369615
- Leventhall, H. G., & Wise, S. S. (1998). Making noise comfortable for people. *ASHRAE Transactions*, 104.
- Marquis-Favre, C., Premat, E., Aubree, D., & Vallet, M. (2005). Noise and its Effects – A Review on Qualitative Aspects of Sound. Part I: Notions and Acoustic Ratings. *Acta Acustica United with Acustica*, 91, 613-625.
- McGill, G., Oyedele, L., & Keeffe, G. (2015). Indoor air-quality investigation in code for sustainable homes and passivhaus dwellings: A case study. *World Journal of Science*, 12(1), 39-60. doi:10.1108/WJSTSD-08-2014-0021
- NHBC. (2017). *NHBC Technical Extra Issue 22.* NHBC. Retrieved from [www.nhbc.co.uk/NHBCpublications/LiteratureLibrary/Technical/TechnicalExtra/filedownload,71937,en.pdf](http://www.nhbc.co.uk/NHBCpublications/LiteratureLibrary/Technical/TechnicalExtra/filedownload,71937,en.pdf)

- Pearsons, K. S., & Bennett, R. L. (1974). *Handbook Of Noise Ratings*. National Aeronautics And Space Administration. Retrieved from [https://archive.org/stream/nasa\\_techdoc\\_19740015162/19740015162\\_djvu.txt](https://archive.org/stream/nasa_techdoc_19740015162/19740015162_djvu.txt)
- Rasmussen, B., & Machimbarrena, M. (2014). *Integrating and Harmonizing Sound Insulation Aspects in Sustainable Urban Housing Constructions*. COST Action TU0901.
- REHVA. (2012). *Work Package 5: Existing Buildings, Building Codes, Ventilation Standards and Ventilation in Europe*. Healthvent: Health-Based Ventilation Guidelines for Europe.
- Sharpe, T., McGill, G., Gupta, R., Gregg, M., & Mawditt, I. (2016). Characteristics and performance of MVHR systems: a meta study of MVHR systems used in the Innovate UK Building Performance Evaluation Programme.
- Svensk Standard. (2015). *Svensk Standard SS 25267:2015, Acoustics – Sound classification of spaces in buildings – Dwellings*.
- Van der Pluijm, W. M. (2010). *The robustness and effectiveness of mechanical ventilation in airtight dwellings. A study to the residential application of mechanical ventilation with heat recovery in the Netherlands*. Eindhoven, Netherlands: Eindhoven University of Technology.
- Wang, L. M., & Novak, C. C. (2010). Human performance and perception-based evaluations of indoor noise criteria for rating mechanical system noise with time-varying fluctuations. *ASHRAE Transactions*, 116(2). Retrieved from [http://digitalcommons.unl.edu/archengfacpub/41/?utm\\_source=digitalcommons.unl.edu%2Farchengfacpub%2F41&utm\\_medium=PDF&utm\\_campaign=PDFCoverPages](http://digitalcommons.unl.edu/archengfacpub/41/?utm_source=digitalcommons.unl.edu%2Farchengfacpub%2F41&utm_medium=PDF&utm_campaign=PDFCoverPages)
- ZCH. (2016). Retrieved from [www.zerocarbonhub.org](http://www.zerocarbonhub.org): [www.zerocarbonhub.org/sites/default/files/resources/reports/ZCH\\_Ventilation.pdf](http://www.zerocarbonhub.org/sites/default/files/resources/reports/ZCH_Ventilation.pdf)

# Air leakage of defects in the vapour barrier of compact roofs

Lars Gullbrekken<sup>\*1</sup>, Petra R  ther<sup>\*1</sup> and Tore Kvande<sup>2</sup>

<sup>1</sup> SINTEF Building and Infrastructure  
H  skoleringen 7B  
7046 Trondheim, Norway

<sup>2</sup> Norwegian University of Science and Technology  
Dep. of Civil and Environmental Engineering 7491  
Trondheim, Norway

\*Corresponding author: lars.gullbrekken@sintef.no

## ABSTRACT

The harsh Norwegian climate requires buildings designed according to high standards. The airtightness of the building envelope is crucial to attain an energy efficient building and to avoid moisture problems. A considerable part of building defects registered in the SINTEF Building defects archive are related to compact roofs.

Flat compact roofs with insulation of EPS or high-density mineral wool between the vapour barrier and the membrane roofing are a common solution particularly in large buildings. In order to retain the membrane roofing from wind forces, the membrane roofing is fastened to the load bearing construction beneath the insulation by use of long screws that penetrate the vapour barrier. Increased requirements related to the airtightness of buildings in the Norwegian building design codes has drawn the focus on airtightness also for compact roof constructions. In the recent years, it has become common to use adhesive tapes to ensure increased airtightness of joints and penetrations in the vapour barrier. However, practitioners have questioned the use of adhesive tape to ensure airtightness, as the vapour barrier at the same time is penetrated by screws. The presented study is trying to provide some answers to the matter.

A laboratory investigation using a special test rig has been conducted in order to measure the air leakage of screw holes and overlapping joints in the PE foil. Different screws and load bearing materials were investigated. Additionally, the air leakage of an overlapping joint was tested for different overlapping widths.

The results of the measurements are used to calculate the air leakage through compact roofs of two model buildings of different size. The calculations show that air leakages through the screw holes and overlapping joints in the vapour barrier had a minor effect on the airtightness ( $n_{50}$ ) of the model buildings.

The results from the study imply that a given a vapour barrier clamped between two plane materials it is unnecessary to use adhesive tapes in overlapping joints of the vapour barrier. However, the application of adhesive tape is advisable in order to avoid air leakages between the vapour barrier and other building components, e.g. transition between roof and cornice or penetrations in the vapour barrier such as ventilation channels.

## KEYWORDS

Compact roofs, vapour barrier defects, air leakage, laboratory investigation

## 1 INTRODUCTION

The latest revision of the Norwegian building code (DIBK, 2016) as well as a growing number of passive houses increased the importance of energy savings of buildings. An energy efficient building requires high performance airtightness of both the wind and the vapour barrier of the construction. The harsh Norwegian climate demands buildings designed according to high standards. The airtightness of the building envelope is crucial to attain an

energy efficient building and to avoid moisture problems. During the heating season, there is typically an overpressure in the upper parts of the building caused by the density differences of the indoor and outdoor air. Therefore, there is an increased chance for moisture transport by exfiltration through the roof construction. Previously (Hagentoft and Harderup, 1995) have shown that air leakages can carry moisture into the construction causing unacceptably large moisture levels even at moderate indoor moisture levels. A considerable part of building defects registered in the SINTEF building defects archive are related to compact roofs (Gullbrekken et al., 2016). Moisture problems related to air leakages in the joint between the roof and the wall are a known sources to building defect (Silseth et al., 2012).

Flat compact roofs with insulation of EPS or high-density mineral wool between the vapour barrier and the membrane roofing are a common solution particularly in large buildings. In order to retain the membrane roofing from wind forces, the membrane roofing is fixed to the load bearing construction beneath the insulation by use of long screws that penetrate the vapour barrier. Stricter demands related to airtightness of buildings in the Norwegian building design code has increased the focus on airtightness also for compact roof constructions. In the recent years, it has become common to use adhesive tapes to ensure increased airtightness of joints and penetrations in the vapour barrier. However, practitioners have questioned the use of adhesive tape to ensure airtightness, as the vapour barrier at the same time is penetrated by screws. The presented study is trying to provide some answers to the matter.

Typical leakage paths of Norwegian houses have previously been studied by (Brunsell and Uvsløkk, 1980) and (Relander et al., 2009). They found that junctions by walls and floors as well as joints around windows are typical air leakage paths. In detached houses (Kalamees et al 2008) found that the junction between the roof and wall was one of the most typical leakage paths (Kalamees et al., 2008).

This work is based on measurements performed by Askeland in 1992 (Askeland, 1992). The work was partly published previously in a Norwegian project report (Askeland1992). However, the scope of (Askeland1992) was limited to solely reporting the air leakages and not to evaluate their practical consequences. Raw data from the measurements have been used in the current work.

In order to address the effect of vapour barrier leakages of compact roofs, the following research questions are outlined:

- 1) How large is the air leakage caused by fasteners (screw penetration) through the vapour barrier (PE-foil)?
- 2) How large is the air leakage caused by loose clamped joints of the vapour barrier (PE-foil)?
- 3) How do the sum of local leakages in the vapour barrier layer influence the leakages on the air change rate of two model buildings.

## **2 METHOD**

### **2.1 Laboratory measurements**

The measurement device consists of a dividable airtight aluminium box with a metering area of 715 mm x 715 mm (approximately 0.5m<sup>2</sup>). The sample was fixed to the airtight measurement box by special clamps and gaskets to ensure an airtight joint.

The airflow was measured by use of a gas meter. It was coupled in series with a fan. A micromanometer was used to measure the pressure difference over the sample. Accuracy and

measuring range of the applied measuring equipment are given in Table 1. A vapour barrier of PE foil with a thickness of 0.2 mm was used. A 100 mm thick layer of rock wool hard mineral wool insulation was included to provide underlayer for the installed penetrations, see Figure 1 and 2.

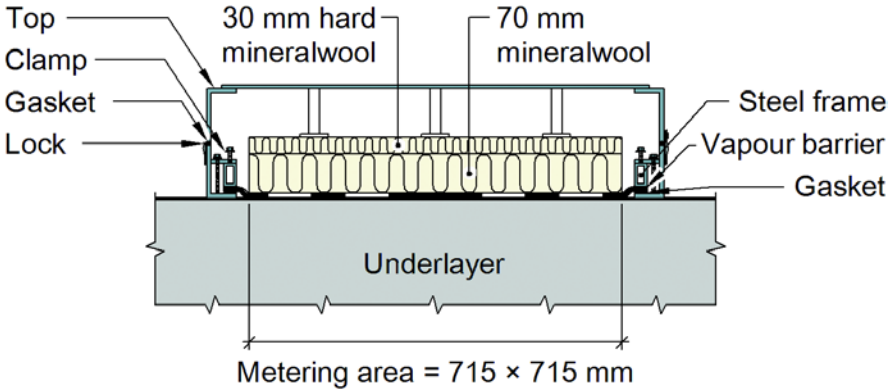


Figure 1. The measurement device for testing air leakage of vapour barrier joints.

Table 1. Accuracy and measuring range of applied sensors

Sensor	Manufacturer	Type	Resolution	Range
Pressure gauge	Furness	FCO 12	±1 Pa	±100 Pa
Gas meter	Elster	-	0.1 l	-

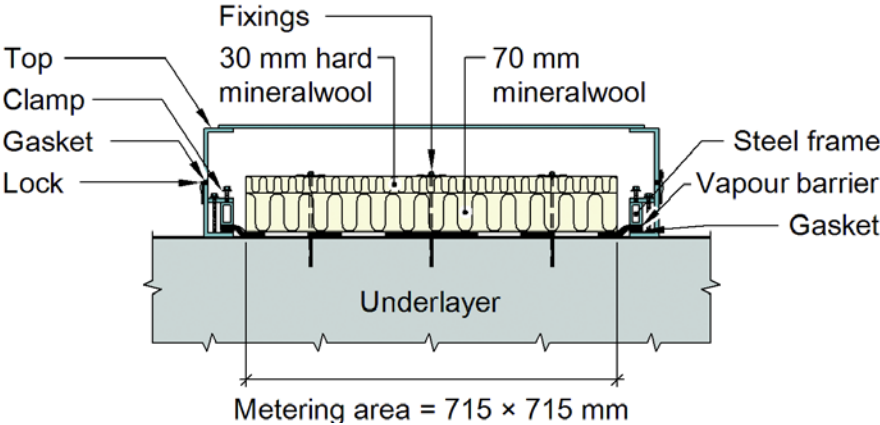


Figure 2. The measuring device for the testing of air leakage of fasteners.

The measuring procedure is given by 1) and 2).

- 1) Three pressure pulses of 500 Pa
- 2) Airtightness measurements at following the pressures: -10, -50, -400, -50, -10 Pa

In this paper the measurements of 50 Pa pressure difference is reported. An overview of the underlying materials and fasteners included in the measurements are shown in Table 2.

Table 2. The different underlying materials and fasteners included in the measurements

Underlay	Fastener
0.65 mm steel plate	Self-drilling screws (4.5 mm)
60 mm concrete	Telescope 4 (5.5 mm) (5.0 mm predrilled hole)
	Bifit (4.8 mm) (6.5 mm predrilled hole) (37 mm long nylonpipe)

Air leakages through the loose clamped joints in the PE-foil were tested with an overlap of the PE-foils of 175 mm, 350 mm and 700 mm.

## 2.2 Study on different building models

Two different building models were analysed:

- 1) A dwelling with a base area of 100 m<sup>2</sup> (10 m x 10 m), a total floor area of 200 m<sup>2</sup> and a building volume of 600 m<sup>3</sup>. The airtightness rate  $n_{50}$  was set to 1.5 h<sup>-1</sup>, the minimum requirement according to the current Norwegian building design rules.
- 2) A large shopping centre with a base area of 900 m<sup>2</sup> (30 m x 30 m), a total floor area of 1800 m<sup>2</sup> and a building volume of 7200 m<sup>3</sup>. The airtightness rate  $n_{50}$  was set to 1.5 h<sup>-1</sup>.

The input for the calculations are given in Table 3. Incorrect fastener means that the screw or fastener is positioned in an incorrect manner causing an extraordinary air leakage. Different incorrect fasteners have been tested and reported as part of section 3.2. A compact roof with an underlayer of concrete and a fastener of type Telescope 4 was assumed for the calculations.

Table 3. Input data for the roof calculations.

<b>Input for the calculations</b>	
Number of fasteners	3 screws per m <sup>2</sup>
Joint length	4 meter width of the PE-foil
Number of incorrect fasteners	1 mistake per 10 m <sup>2</sup> roof area

## 3 RESULTS

### 3.1 Airtightness of the laboratory equipment

Air leakages through the measuring equipment were determined by installing an airtight metal-plate in the metering area. The air leakages of the measuring equipment was determined in advance of each of the measurement set-ups. In most of the set ups the measuring equipment was highly airtight.

### 3.2 Air leakages through the fastening screws

Figure 3 shows the air leakages through the different fastening screws and underlays.

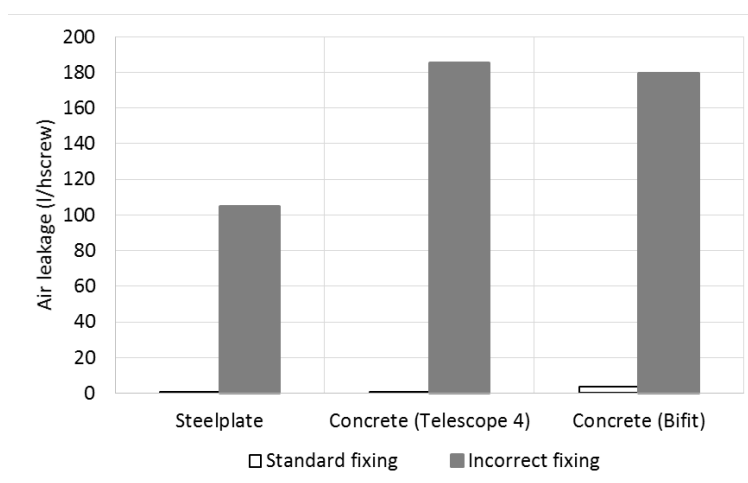


Figure 3. Air leakage of different fastening screws and underlays of 0.65 mm thick steel plate and 60 mm thick concrete.

### 3.3 Air leakages of loose joints in the PE-foil.

Figure 4 shows the air leakage through a clamped joint in the PE-foil.

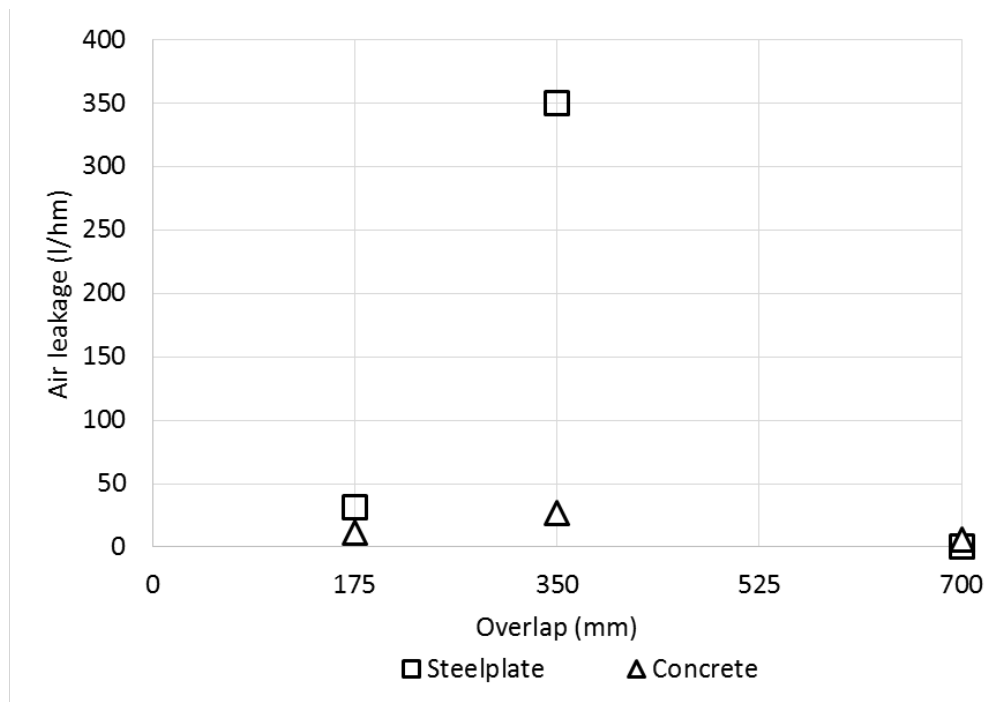


Figure 4. Air leakage of loose joints in the PE-foil.

### 3.4 Building model calculations

The joint length of the roof was calculated by assuming 4 m width of the PE-foil. A compact roof with an underlayer of concrete and a fastener of type Telescope 4 was assumed. The air leakages of the fasteners, the joints in the PE-foil and incorrectly applied fasteners were calculated using of the results from Table 3 and Figures 3 and 4.

Table 4. Results from the calculation of the two model buildings.

		Model 1	Model 2
<b>Air leakage limit at 50 Pa</b>	<b>m<sup>3</sup>/h</b>	<b>900</b>	<b>10800</b>
<b>Air leaking through roof</b>	<b>m<sup>3</sup>/h</b>	<b>3.2</b>	<b>29.4</b>
Air leakage joints	m <sup>3</sup> /h	0.38	3.99
Air leakage screws	m <sup>3</sup> /h	1.02	9.18
Air leakage incorrectness	m <sup>3</sup> /h	1.80	16.2

## 4 DISCUSSION

### 4.1 Airtightness of fastening screws

Regardless of the underlay the measurements show a small air leakage through a correctly fitted fastener. As expected, an incorrect fastener represents a considerable larger air leakage.

### 4.2 Loose clamped joints

The tests were performed under ideal conditions and on a limited sample size. Especially regarding the air leakages through the joints of the vapour barrier care should be taken when

evaluating the results. As the results show, the underlayer below the PE-foil is influencing the results to a large extent. The steel plate measurements was performed with the PE-foil directly on top of the corrugated steel plate. The vapour barrier was oriented perpendicular to the corrugations. As the results show this design gives large uncertainties regarding the airtightness performance because the lacking continuous pressure between two plane materials. Therefore, the SINTEF Design Guidelines recommend that the vapour barrier is positioned between a mineral wool layer of 50 mm and the rest of the roof insulation. Compared to the steelplate underlay the concrete underlay gives considerable lower air leakages. An underlayer of concrete results in a rather even surface. Given an underlayer of concrete, there are small differences between the different overlap lengths. However, the lowest air leakage was measured for the 700 mm overlap.

### 4.3 Two building models

The calculations of both building models showed that air leakages through loose clamped joints and screws amounted to less than 0.5 % of the air leakage limit at 50 Pa pressure difference. Given ideal conditions, this indicates that air leakages through screw holes, both correct and incorrectly installed, and joints in the vapour barrier of compact roofs represent minor air leakages. The results indicate that, given ideal conditions where it is possible to ensure clamping of the joint between two plane materials, the use of adhesive sealing may be unnecessary.

However, adhesive sealing can be useful to ensure airtight joints in and between building parts. Previously (Brunsell and Uvsløkk 1980), (Relander et al. 2009) and (Kalamees et al. 2008) found that joints between the wall and roof are typical air leakage paths. Experience from e.g. building damages also show that it is challenging to ensure an airtight joint between the roof and the wall of a flat roof, see Figure 6. Pictures from a compact roof where moisture transport caused by large air leakages through the air open joint in the vapour barrier between the roof and the wall are given in Figure 5.



Figure 5. Lacking airtightness of the joint between the vapour barrier of a compact roof and the sandwich wall-element of a large building. Bloating vapour barrier caused by internal overpressure given in the picture to the right (Pictures: T. Bøhlerengen).

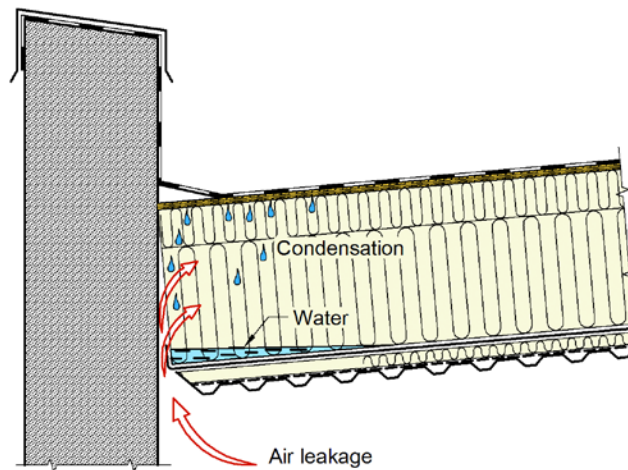


Figure 6. Moist air leaking into the construction causing moisture accumulation.

## 5 CONCLUSIONS

Calculations of two building models showed that air leakages through loose clamped joints in the vapour barrier and standard and incorrect fasteners had a minor effect on the air leakage rate,  $n_{50}$ .

Clamped joints with continuous pressure between two plane materials is considered a safe way to ensure the airtightness of joints in the vapour barrier. However, in cases where the conditions are less ideal the measurements show that taping of loose clamped joints may be necessary. Adhesive sealing was found to be useful to ensure airtight joints in and between building parts.

## 6 REFERENCES

- Askeland A. (1992) *Vapour barrier penetrated by mechanical fixings Measurement of air leakage* (In Norwegian). In: Norwegian Building and research Institute O, Norway (ed).
- Brunsell JT and Uvsløkk S. (1980) *The Airtightness of Norwegian Dwellings. Working Report 31*. Norwegian Building Research Institute (now SINTEF Building and Infrastructure),.
- DIBK. (2016) TEK 10. Directorate for building quality, Norway.
- Gullbrekken L, Kvande T, Jelle B, et al. (2016) Norwegian Pitched Roof Defects. *Buildings* 6: 24.
- Hagentoft C-E and Harderup E. (1995) Moisture conditions in a north-facing wall with cellulose loose-fill insulation: construction with and without a vapor retarder and air leakage. *ASHRAE Transactions*. 1 ed., 639-646.
- Kalamees T, Korpi M, Eskola L, et al. (2008) The distribution of the air leakage places and thermal bridges in Finnish detached houses and apartments. *Proceedings of Nordic Symposium on Building Physics, Copenhagen, Denmark*.

Relander TO, Thue JV, Aurlien T, et al. (2009) Airtightness and air leakages of Norwegian wood-frame houses. *4th International Building Physics Conference, Istanbul, Turkey.*

Silseth MK, Gåsbak J and Bøhlerengen T. (2012) 725.118 Damages in compact roofs. Causes and renovation (In Norwegian). *SINTEF Design Guidelines*. SINTEF Byggforsk, Oslo.s.

# Air leakage variations due to changes in moisture content in wooden construction- magnitudes and consequences

Fredrik Domhagen<sup>\*1</sup>, Paula Wahlgren<sup>1</sup>

*1 Division of Building Technology  
Chalmers University of Technology  
SE- 412 96 Gothenburg, Sweden*

*\*Corresponding author:*

[Fredrik.Domhagen@chalmers.se](mailto:Fredrik.Domhagen@chalmers.se)

## ABSTRACT

The airtightness of buildings is important for several reasons, such as being a prerequisite for low-energy buildings and for a healthy indoor air quality (without i.e. mould or radon). The airtightness of buildings can vary over time and investigations are made on these variations due to moisture induced movements in wooden constructions, and subsequent consequences, using both measurements and numerical simulations.

Measurements were performed in a wooden guest house that was built in a laboratory hall with an approximate relative humidity of 30 %. The guest house was designed with a wind barrier but without a moisture barrier, and with a majority of the leakages situated in the wall/floor connection. The relative humidity in the guest house was varied so that the indoor relative humidity was kept at 90 % during 8 days and then decreased to 25 % during 7 days. This variation in moisture content in the wooden part can also illustrate the built in moisture in construction timber (starting at a moisture content of 16%). The air permeability was measured frequently during both periods and showed a change in air permeability from 0.74 l/sm<sup>2</sup> to 1.21 l/sm<sup>2</sup> at 50 Pa pressure difference. Consequently, for a wooden construction with a moisture dependent air permeability, it is easier to fulfill airtightness demands (checked by measurements), when the building is just erected, compared to a couple of months later.

Numerical simulations on the moisture induced leakage variations and the impact of the resulting variation in air permeability are performed in Simulink and MATLAB. Air leakage is calculated using a set of object oriented functions within the MATLAB environment. These functions follow the same mathematical principle as presented in the airflow simulation software CONTAM. The simulations are made for the climate of Gothenburg in south-west part of Sweden. Results show, among other things, that the orientation of the building is decisive for the magnitude of the total exfiltration rate and that air leakage from the indoor environment up to the cold attic is higher during winter months compared to summer months.

## KEYWORDS

Air tightness, air permeability, air leakage

## 1 INTRODUCTION

The air permeability of a wooden frame building can vary over time. In a study by Wahlgren et al. (2015), the air permeability in two wooden buildings was measured during one year, resulting in variations up to 10 %, considering the total airflow through leakages at a pressure difference of 50 Pa. The variations correlated with fluctuations in relative humidity indoors, resulting in higher air permeability airtightness during winter and lower air permeability during summer. The fact that buildings often are less airtight during winter months has also previously been shown (Kim, 1986; Persily, 1982). Skogstad et al. (2011) show a substantial increase in air permeability with the drying of wood in cross laminated timber structures.

A varying airtightness raises a number of questions. For example, how the moisture safety is affected if air is allowed to move from the inside towards the outside of the thermal envelope (exfiltration) and possibly condensate inside the construction, and if there is an increase in leakage in wintertime? Normally this exfiltration is inhibited by adjusting the ventilation in a way that ensures negative internal pressure and thus forcing the air to move from the outside towards the inside. However, if the airtightness decreases, the negative pressure caused by the ventilation system might also be reduced. Moisture condensation and mould growth in cold attics is a problem that relates to air that leaks from the interior of the building up to the attic (Hagentoft and Sasic Kalagasidis, 2014). It is likely that the infiltration of air to the attic changes with changes in airtightness, but to what extent? In the following, the variation in air permeability and subsequent effects is investigated.

## **2 LABORATORY MEASUREMENTS ON A SMALL GUEST HOUSE**

In order to investigate the correlation between indoor relative humidity and airtightness of a wooden building, laboratory measurements are performed on a small guest house in a controlled environment. The guest house is built in a storage hall with an approximate relative humidity of 30 %. It is for example designed with a wind barrier but without a moisture/air barrier. There are some differences between the guest house and a conventional residential building.

It is likely that the way the airtightness of the guest house reacts to changes in humidity is somewhat different from that of an ordinary wooden building. For instance, since there is no moisture barrier, the timber parts will react faster to changes in indoor humidity compared to with the moisture barrier. Without the moisture/air barrier, the airtightness of the guest house will react faster to changes in indoor humidity compared to a building with moisture/air barrier. A leakage search of the guest house showed that the majority of the leakages were situated in the connection between the wall and the floor. This means that the majority of changes in airtightness is caused by swelling and shrinkage in that particular leakage. However in an ordinary building, air leakage typically occurs at many different locations.

### **2.1 Experimental Setup**

In order to test how the airtightness changes with changes in relative humidity, air permeability measurements are performed on the guest house. The measurement periods are divided into two phases, moistening phase and drying phase. In the moistening phase, the relative humidity in the air inside the guest house is increased and kept steady at around 90 % with the use of a humidifier. Blower door measurements are then performed at intervals of one to two days. During the drying phase, the indoor relative humidity decreased by heating the indoor environment and ventilation of the guest house. Blower door measurements are performed at intervals of one to two days. Throughout the entire test period, temperatures and humidities are continuously measured both inside the guest house and inside the storage hall outside the guest house.

## 2.2 Results from Measurements

The results from the measurements of relative humidity and airtightness can be seen in

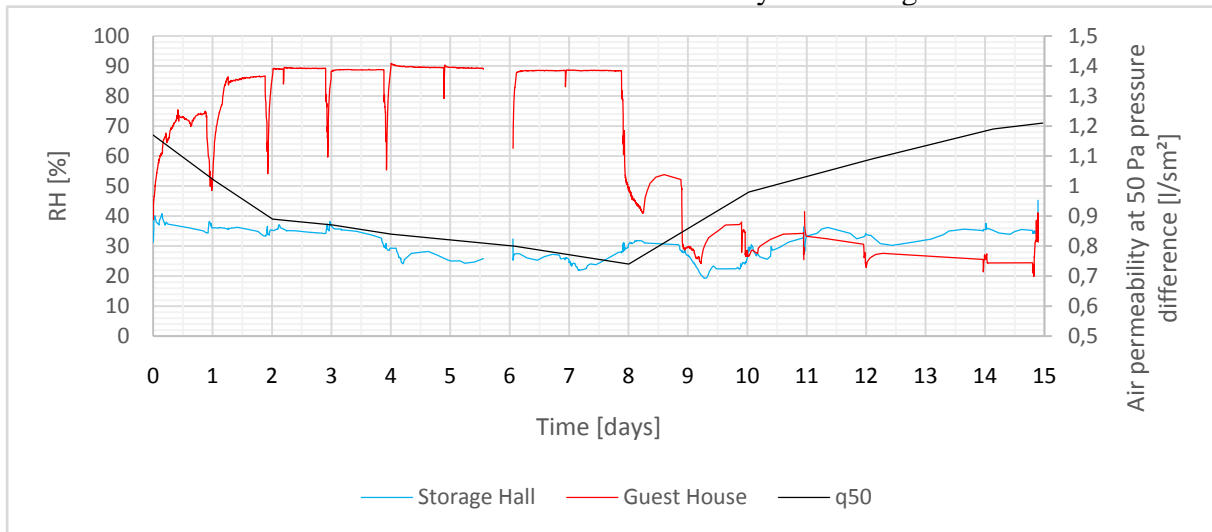


Figure 1. The airtightness changed from  $0.74 \text{ l/sm}^2$  to  $1.21 \text{ l/sm}^2$  at 50 Pa pressure difference during the measurement period. The measured relative humidity varied from about 90 % during the 8 days in the moistening phase to about 25 % during the 7 days in the drying phase. The moisture scenario can as a comparison be related to common levels of inbuilt moisture. For instance, a relative humidity of 80 % corresponds to moisture content of 16 % in wood, which is often found in construction timber (Olsson, 2014).

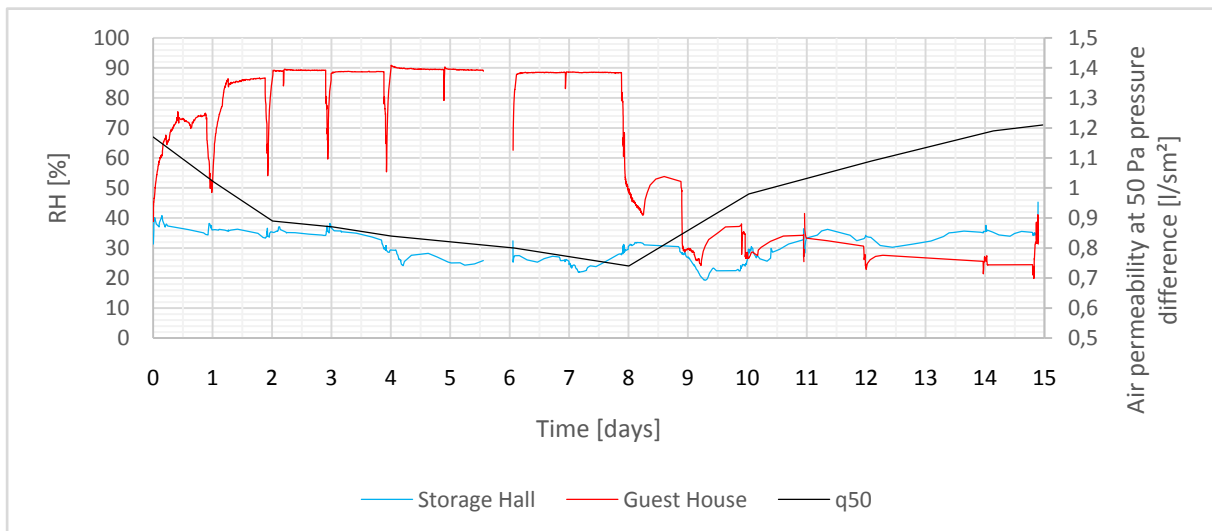


Figure 1. Shows the air permeability, relative humidity inside the guest house and relative humidity in the storage hall throughout the test period.

It is also of interest to couple these results to airtightness demands. As a result of the drying of the wooden parts, airtightness demands (checked by measurements) can be easier to fulfill when the building is erected with inbuilt moisture, compared to a couple of months later.

## 3 NUMERICAL SIMULATIONS

In order to study the impact of varying airtightness on the airflows in a building, numerical simulations are performed in Simulink and MATLAB. Airleakage is calculated using a set of object oriented functions within the MATLAB environment. These functions follow the same

mathematical principle as presented in the airflow simulation software CONTAM (Walton, 2003). Simulink is used to couple the step-wise air leakage calculations in MATLAB to input weather data and to determine the indoor relative humidity.

Previous research(Wahlgren, 2014) has shown that the air permeability variation follows the indoor two- to three-day mean relative humidity in a residential building. In order to take this moisture inertia into account, the relative humidity of the building is simulated as a function of outdoor humidity, indoor moisture production, indoor moisture buffer capacity and the total air-exchange rate. Furthermore, the airtightness follows the relative humidity with a dampening factor which is adjusted to make the airtightness follow the two-day mean relative humidity. The program flow structure for one time step is illustrated in Figure2.

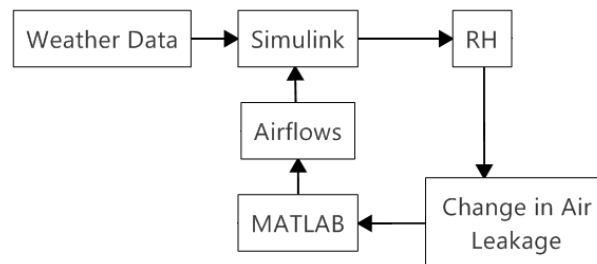


Figure2. Flow chart over the calculations performed during one time step.

The airflow model takes into account the airflow at pointwise defined leakages where the driving force is the total pressure difference caused by stack-effect, wind and mechanical ventilation. Terrain characteristics are taken into account with by tabled pressure coefficients(Orme, 1998), pressure coefficients for intermediate wind angles are found by linear interpolation.

### 3.1 Climate Data

Airflows are simulated for a building situated in Gothenburg. Climate data is taken from the Swedish Meteorological and Hydrological Institute, SMHI, where all data is collected from year 2016. Figure 3 shows the outdoor temperature and wind speed throughout the year.



Figure 3. Climate data for Gothenburg, 2016 (SMHI Öppna data, 2017).

Figure 4 shows a wind rose with the distribution of wind speeds at different wind directions. It is clear from the wind rose that wind speeds higher than 4 m/s dominate the south-westward direction while wind speeds lower than 4 m/s are mainly from north-east.

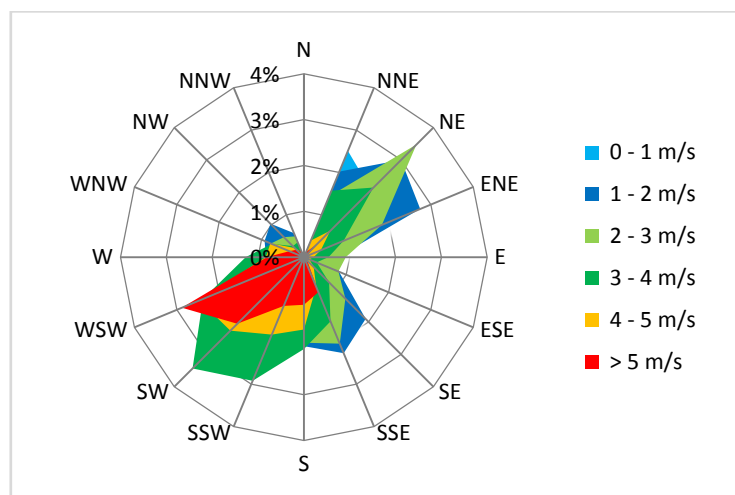


Figure 4. Wind rose showing wind speeds for different wind directions in Gothenburg, 2016 (SMHI Öppna data, 2017).

### 3.2 Model Description

The simulated building is a wooden detached building, with two floors and a concrete ground slab. The roof is a pitched gable roof with a cold attic and the attic is ventilated through two horizontal air gaps along the roof eaves. The total envelope area of the building is 300 m<sup>2</sup>. For a more thorough description see (Domhagen, 2016).

The indoor moisture production is simulated according to (Pallin, 2013). Here, the moisture production increases during the morning until 12.00 AM and decreases slightly before it increases again and peaks at around 18.00 PM. The moisture production has its minimum during night time. Indoor air temperature is 20°C.

The ventilation rate of the building is constant throughout the entire simulation and is adjusted to agree with the requirements set up by the Swedish National Board of Housing, Building and Planning (Boverket). The building has both a supply and an exhaust fan which are balanced so that a negative indoor pressure of 3.5 Pa is achieved. The purpose of the imbalance between the fans is to reduce air-exfiltration from the building. The ventilation rates in the simulation are handled as constant mass flows and are therefore independent of pressure.

Figure 5 shows three orientation scenarios for which airflows are simulated. The dashed lines mark the side with attic ventilation gaps.

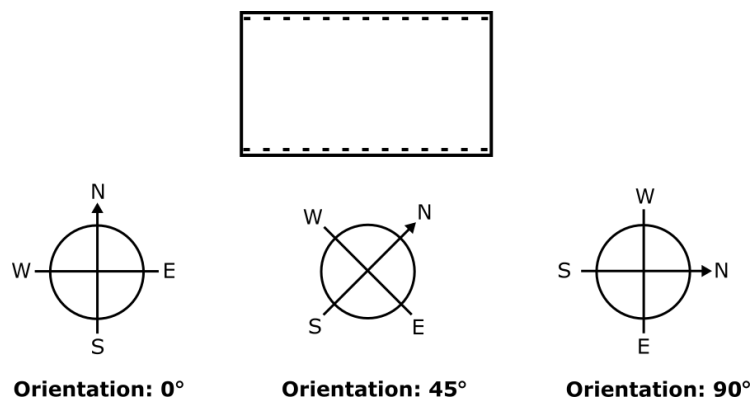


Figure 5. Orientation of building in relation to the cardinal direction of north. Dashed lines mark the sides with attic ventilation gaps.

Output from the simulations is pressure conditions, infiltration and exfiltration, over the whole building as well as for individual leakages. In the following, exfiltration is shown since it has a strong impact on moisture safety and also on energy efficiency.

### 3.3 Results of Numerical Simulations

Exfiltration from the simulations performed for three building orientations, 0°, 45° and 90° with wind, stack effect and mechanical ventilation can be seen in Figure 6. Simulations are performed for a scenario where the airtightness follows the indoor relative humidity with a dampening factor, as described earlier in Chapter 3. Variations are between 0.58 [l/sm<sup>2</sup>] and 0.52 [l/sm<sup>2</sup>]. Where the building is more airtight during summer which is also the period when indoor relative humidity reaches its maximum.

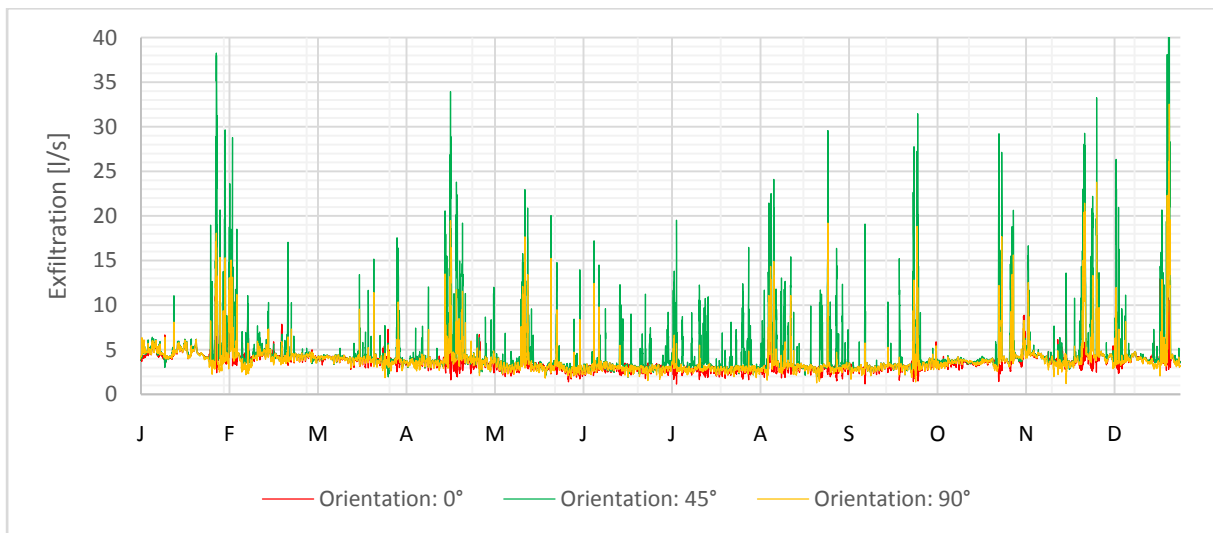


Figure 6. Exfiltration rates for three building orientations with airtightness variation between  $0.58 \text{ [l/sm}^2\text{]}$  and  $0.52 \text{ [l/sm}^2\text{]}$ .

Results also show a higher exfiltration rate with the  $45^\circ$  orientation. The reason is that at this orientation wind blows alongside the attic ventilation gaps during windy periods of the year (see wind direction in Figure 4) which in turn causes a negative pressure in the attic which draws air out from the indoor environment.

As a comparison exfiltration is also simulated for a scenario where stack effect is deleted by setting the indoor temperature to the same as outdoors. It is clear from the results that wind is the major driving force for exfiltration. When stack effect is included, it results typically in exfiltration of about  $2 \text{ l/s}$  during colder winter days, whereas exfiltration caused by wind may account for  $30 \text{ l/s}$ , or more, for windy periods (see Figure 7).

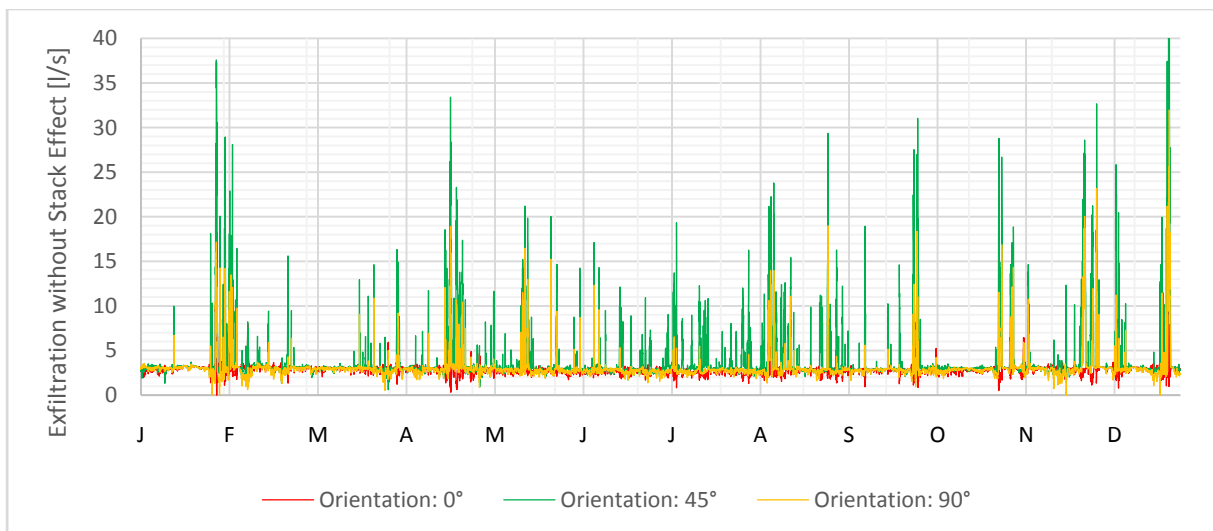


Figure 7. Exfiltration rates without stack effect for three building orientations with airtightness variation between  $0.58 \text{ [l/sm}^2\text{]}$  and  $0.52 \text{ [l/sm}^2\text{]}$ .

In contrast to varying airtightness due to moisture variations, the exfiltration is also simulated for constant airtightness calculated as the average of the varying airtightness which is  $0.56 \text{ l/sm}^2$  at a pressure difference of  $50 \text{ Pa}$ . The difference between the exfiltration for the case with varying airtightness and the case with constant airtightness is shown in Figure 8.

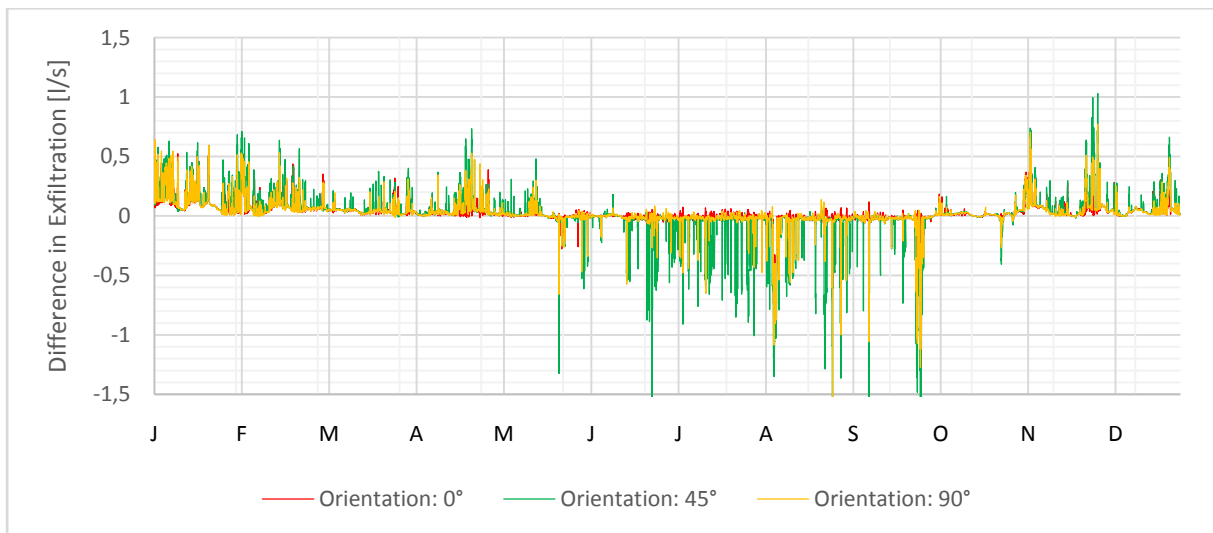


Figure 8. Difference between exfiltration for the case with varying airtightness (variation between  $0.58 \text{ [l/sm}^2\text{]}$  and  $0.52 \text{ [l/sm}^2\text{]}$ ) and a case where the airtightness is constant at the average of the varying airtightness.

The graphs show that the exfiltration is slightly increased during colder months and slightly decreased during summer, due to variations in air permeability.

Figure 9 shows exfiltration for January (same simulation as in Figure 6 and Figure 8). There are some climatic differences during the month which are reflected in the exfiltration rates. The first half of the month is slightly colder than the second half which increases exfiltration caused by stack effect. The last couple of days of the month are windier than the rest of the month which is why there is more exfiltration in the end of the month. A comparison shows that during the first 10 days of January the exfiltration is in average 4 %, 5 % and 5 % (for orientations:  $0^\circ$ ,  $45^\circ$  and  $90^\circ$  respectively) higher with varying airtightness compared to constant airtightness. During the last 6 days of January exfiltration is in average 2 % higher for all orientations (orientations:  $0^\circ$ ,  $45^\circ$  and  $90^\circ$ ) with varying airtightness compared to constant airtightness.

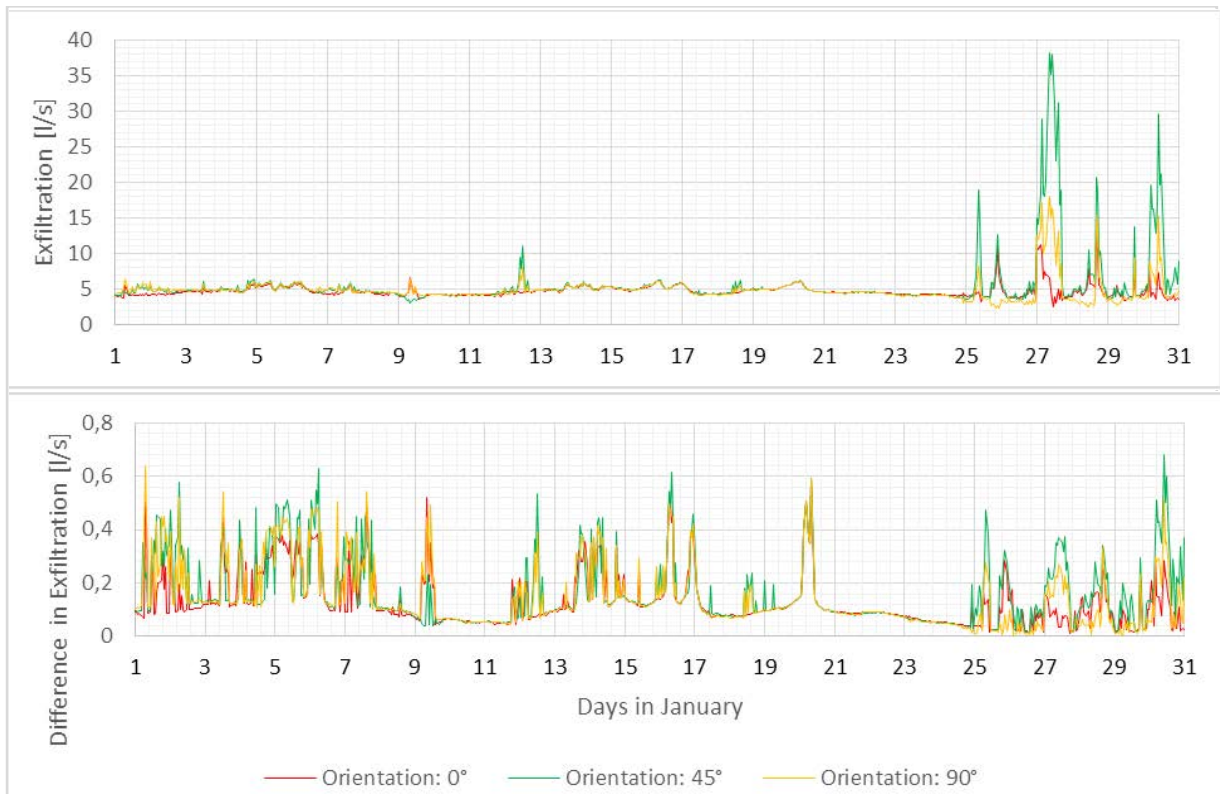


Figure 9. Shows exfiltration for January.

Airflow up to the cold attic is of interest since problems with mould growth in cold attics is common in Sweden (Hagentoft, 2014). A main cause of mould growth in attics is increased relative humidity due to airleakage from the indoor environment. The situation is worsened by night sky radiation during cloud free nights that lower the attic temperature. Simulations show that the airflow to the attic increases during winter months. Airflow to the attic also increases if the building is oriented with the long side of the building in south-western direction, same direction as the wind direction of the majority of the strong winds in Gothenburg, see Figure 4. Wind direction along the ventilation gaps of the attic will draw air out from the attic and cause a negative pressure difference between the attic and the indoor environment.

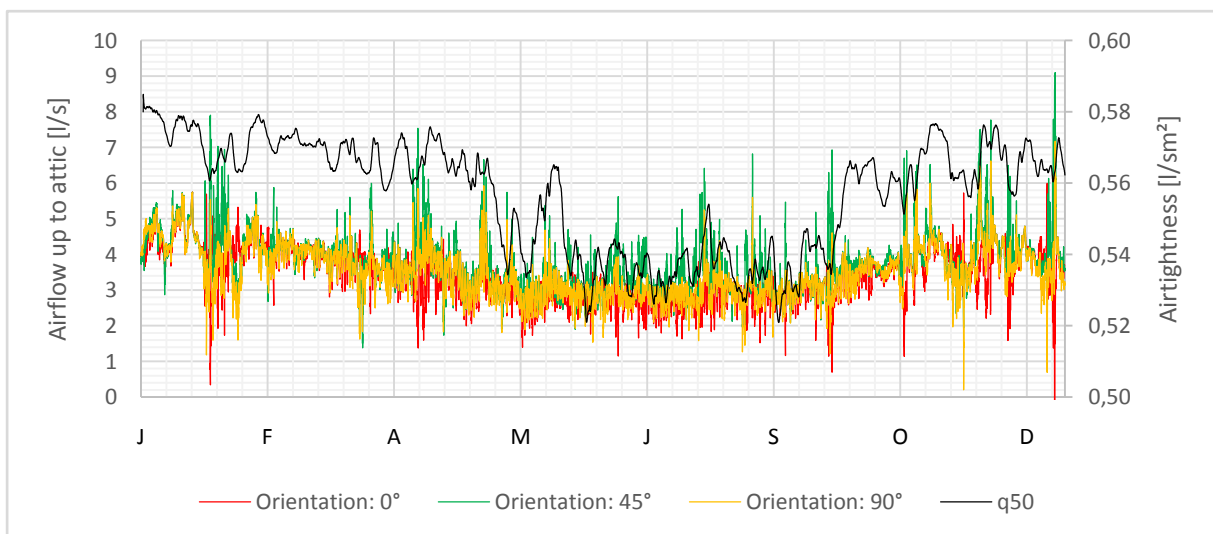


Figure 10. Airflow up to the attic cold space from the indoor environment together with moisture dependent airtightness. Airflows are shown for three different building orientations.

From the results, it becomes clear that a negative pressure caused by the imbalance between supply- and exhaust fans is not enough to eliminate the exfiltration. In fact, there is exfiltration through the thermal envelope during most times of the year.

Figure 11 shows an example of a building with greater variation in airtightness in comparison to the previously described building. The airtightness for this building varies between 0.95 [l/sm<sup>2</sup>] and 0.80 [l/sm<sup>2</sup>].

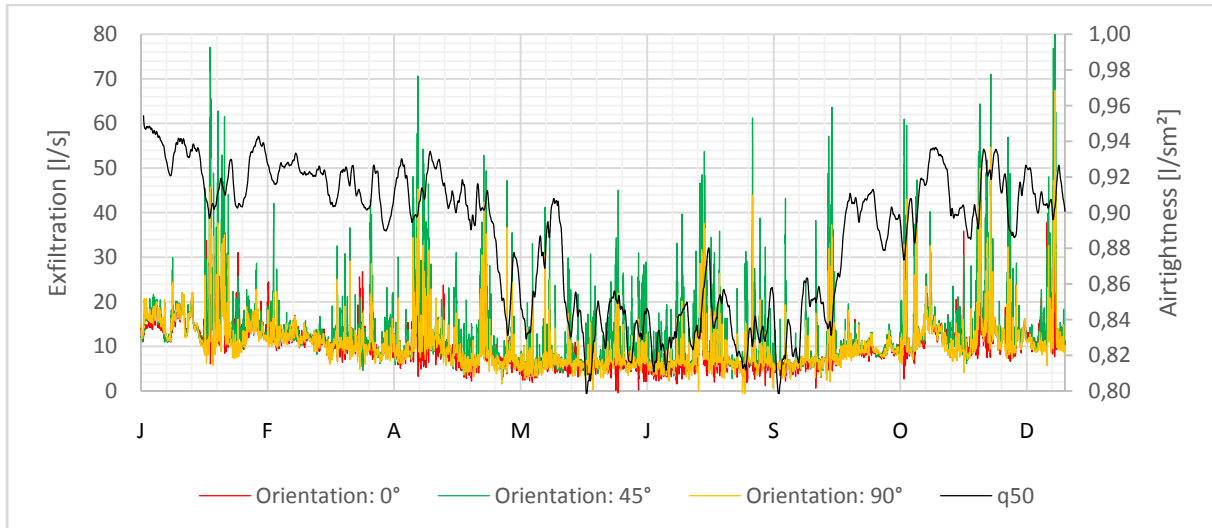


Figure 11. Exfiltration for building with an air permeability that varies between 0.95 [l/sm<sup>2</sup>] to 0.80 [l/sm<sup>2</sup>] at a pressure difference of 50 Pa.

For this building, the exfiltration is almost doubled during winter months in comparison with summer months. The increase in air permeability is nearly 19 % which is in agreement with previous findings. For example (Persily, 1982) found that the air permeability can vary with as much as 25 % in a year.

#### 4 CONCLUSIONS AND DISCUSSIONS

Laboratory measurements further strengthens the claim that the airtightness of a timber building is affected by the indoor relative humidity. However, since the investigated guest house is different from a conventional residential timber building more measurements need to be done on conventional residential buildings in order to better understand the extent of these variations.

The levels of relative humidity may also be related to levels of inbuilt moisture in the construction. If a building is constructed when timber components has a moisture content of 16 % it is likely that the measured air permeability will be lower than at a later stage when the moisture content of the timber components is lower. It might therefore be important to let inbuilt moisture dry out before measuring the air permeability or that the air permeability of the building is created so that it is independent of swelling and shrinkage of timber components.

Numerical simulations show a number of effects from moisture induced airtightness. For instance, when looking at the coldest month, January, the exfiltration is 5 % higher during cold days with little wind when comparing varying airtightness with average airtightness.

The driving forces for exfiltration is somewhat different, depending on the orientation of the building. The building with 0° orientation, has slightly more exfiltration at low wind speeds than 45° orientation, while the building with 45° orientation has more (at times twice as much) exfiltration at higher wind speeds. This fact is also true for the airflows up to the cold attic from the indoor environment. Here, the 45° orientation has more airflow up to the cold attic in comparison with 0° and 90° orientations. This is of importance since it will

increase the moisture transport up to the attic, which in turn leads to increased risk of moisture related hazards.

When comparing the exfiltration driven by wind with exfiltration driven by stack effect, results show that wind may account for more than ten times the airflow from stack effect.

An imbalance between supply- and exhaust ventilation is often applied with the purpose of reducing exfiltration. In this study, the imbalance was adjusted to achieve a negative pressure inside the building of 3.5 Pa. However, it is clear from the simulation results, that exfiltration occurred most of the time during the year. Since the level of imbalance in order to reduce exfiltration is dependent on the airtightness of the building, as well as exfiltration rates, more work is needed to determine an appropriate imbalance and how it is affected by variations in airtightness.

## 5 FUTURE WORK

In the near future, more measurements of air permeability in residential buildings over time will be made, in order to study the variations in airtightness, in particular the first time after construction.

The model will be further developed to include pressure-dependency in ventilation-systems and a more detailed description of cold attics in order to investigate risk of mould growth.

## 6 REFERENCES

- Domhagen, F. (2016). *Yearly Variations in Airtightness of Detached Wooden Houses: Simulations and Laboratory Measurements to Investigate Causes and Consequences*. Gothenburg, Sweden: Chalmers University of Technology.
- Hagentoft, C. E., Sasic Kalagasidis (2014). Moisture safe cold attics-Assessment based on risk analyses of performance and cost, *Proceedings of 10th Nordic Symposium on Building Physics*, Lund, Sweden, 2014.
- Kim, A. K. (1986). Seasonal variation in airtightness of two detached houses. *Measured air leakage of buildings*. ASTM International.
- Olsson, L. (2014). *Moisture Conditions in Exterior Wooden Walls and Timber During Production and Use*. Gothenburg: Chalmers University of Technology.
- Orme, M. M. (1998). *Numerical data for air infiltration and natural ventilation calculations*. Air Infiltration and Ventilation Centre.
- Pallin, S. (2013). *Risk Assessment of Hygrothermal Performance - Building Envelope Retrofit*. Gothenburg: Chalmers University of Technology.
- Persily, A. (1982). Repeatability and accuracy of pressurization testing. *Thermal Performance of the Exterior Envelope of Buildings, Procedures of ASHRAE/DOE Conference*. ASHRAE SP.
- Skogstad, H B., Gullbrekken L., Nore K. (2011). Air leakages through cross laminated timber (CLT) constructions, *Proceedings of the 9th Nordic symposium on Building Physics*, NSB 2011, Tampere, Finland, 2011.

*SMHI Öppna data.* (3 de April de 2017). Obtido de SMHI: <https://opendata-catalog.smhi.se/explore>

Wahlgren, P. (2014). Seasonal variation in airtightness. *35th AIVC Conference*. Poznan, Poland.

Walton, G. N. (2003). *NISTIR 7251 CONTAM 2.4 User Guide and Program Documentation*.

# Statistics, analysis and conclusions from 250,000 blower door tests, including ventilation types.

Barry Cope – ATTMA Scheme Manager

*The Air Tightness Testing & Measurement Association (ATTMA)  
St Mary's Court  
The Broadway  
Amersham  
Buckinghamshire  
HP7 0UT*

## ABSTRACT

With lower air leakage in modern homes, ventilation of homes has become more important than ever before. It seems however that we are getting it very wrong. A lack of ventilation can cause building sickness, with degradation of the physical building and also poor air quality which has a big impact on the occupants themselves. Our statistics show that designers and contractors are still not getting it right, leaving us with a generation of poorly ventilated housing stock.

The Air Tightness Testing and Measurement Association (ATTMA) introduced a lodgement system in September of 2015 that records results of approximately 85% of all air leakage tests in the United Kingdom. The Lodgement system also records the type of ventilation installed plus another 25 fields that allow us to study statistics in depth.

The ATTMA is able to therefore demonstrate that the average home is not adapted for the ventilation system installed. From the 200,000 tests, the average result between a System 1 (Trickle ventilators and intermittent extractors) and a System 4 (Whole house heat recovery ventilation) is only 0.39 m<sup>3</sup>.h-1.m-2@50Pa, the equivalent of a leaky letterbox. A System 4 ventilation type is usually designed to work with very low air leakage homes, yet the same building type and build quality is observed regardless of the ventilation strategy.

From the same data, we can also see that a staggering 58% of dwellings are still built using traditional ventilation strategy, System 1. Perhaps more concerning is the number of properties using a System 1 ventilation type but scoring a very low air leakage (less than 3.00 m<sup>3</sup>.h-1.m-2@50Pa), an estimated 10,000 dwellings a year. The percentage of System 4 ventilation types in comparison is 29%. Perhaps the scariest statistic of all is 85% of all dwellings tested with a System 4 ventilation type achieve greater than 3.00 m<sup>3</sup>.h-1.m-2@50Pa which could lead to inefficient heating because of the level of uncontrolled ventilation.

So what can we do to put this right? The legislation makes reference to the ventilation and infiltration needing to be matched but this is not regularly enforced by Building Control or Approved Inspectors. Contractors need to take the issue seriously. This may not happen until the poorly ventilated homes are exposed and building warranty providers are left with millions of pounds of claims.

## KEYWORDS

Air Tightness, Lodgement, Data,

## 1 INTRODUCTION

The Air Tightness Testing and Measurement Association (ATTMA) introduced a lodgement system in September of 2015 that records results of approximately 85% of all air leakage tests in the United Kingdom. The Lodgement system also records the type of ventilation installed plus another 25 fields that allow us to study statistics in depth.

The data recorded has now surpassed 250,000 tests which is one of, if not the, biggest collections of air tightness test data in the world. This paper looks at the conclusions we can draw from the data and how we can use this data to shape building regulations going forward.

## 2 BACKGROUND

### 2.1 Who is ATTMA?

ATTMA is both a UK based trade association and a government appointed Competent Persons Scheme. ATTMA exists to promote the value of air tightness testing to both the construction industry and to vendors that eventually purchase the buildings.

ATTMA run a not-for-profit competent person's scheme which means it reinvests all money made back into the industry which happens in a myriad of ways, from promotion in magazines through to industry research projects.

## 3 LODGEMENT

### 3.1 What is Lodgement?

Lodgement is the process of sending information from a test to an independent body and in return, receiving an authorised certificate.

From the 1<sup>st</sup> September 2015 this became a mandatory requirement for all members of the ATTMA scheme.

### 3.2 Introducing Lodgement into the Industry

Introducing lodgement to the air tightness industry was arguably the biggest challenge of all. The industry at the time was fragmented, with some testers providing lengthy reports for each air tightness test and some testers providing a single page certificate. The ATTMA sought to unify the industry and have all members produce the same output to make judging the validity of a test a faster, more simple process. The ATTMA were able to step in and reject certificates that are not valid and stop them being used for compliance.

### 3.3 The Process

In order for lodgement to be successful, it had to:

- a) Not be time consuming for the members
- b) Be simple and easy to understand

We set about trying to develop a process that worked for all members. We grouped the industry into three categories:

- 1) **Occasional tester** – tester that would normally conduct less than 50 tests a year, would generally handwrite results onto pre-printed certificates
- 2) **Medium sized testers** – tester that would normally conduct between 50 and 500 tests per year. Testers would normally provide a copy of the proprietary software output as evidence of the test.
- 3) **Large testers** – Would conduct more than 500 tests per year, would generally use their own test software and output, typically written on Microsoft Excel.

We looked at the list and came up with a simple solution for each:

- 1) **Occasional tester** – we could have them manually fill out information on a 'web based program'
- 2) **Medium tester** – we could work with the proprietary software manufacturers to introduce a 'lodge' button directly into the software

- 3) **Large tester** – we could, within the ‘web based program’ have a csv upload function which would allow large batches of testers to upload information.

From the thought process, we realised our lodgement system would add benefits to the members, which include:

- a) Significantly reduced administration time
- b) Records of all tests
- c) Records of calibration details
- d) Third party checking of data in real time

### **3.4 The Developer**

Once we had realised what we needed we had to have the system built. Unfortunately, ATTMA at the time was not cash rich but convinced a developer to take on the project on the basis that we would pay them each time we had a lodgement. The advantage for ATTMA was that we would not need to pay large amounts of money for a developer and the incentive for the developer was that, the better the system, the more members we would attract and therefore the more money they would make in the meantime.

### **3.5 Proprietary test Software**

The hardest part of our development was ensuring our newly created database would work seamlessly with the current software provided by both Retrotec and The Energy Conservatory. Both companies saw the bigger picture and agreed to work with us to complete the automatic lodgement process.

## **4 DATA**

### **4.1 Fields**

The data collected consists of the following fields:

- Test Date
- Plot Number
- Address
- Town / City
- County
- Postcode
- Country
- Dwelling or Non-Dwelling
- Envelope Area
- Footprint Area
- Ventilation Type
- Temporary Sealing
- Deviations
- Result
- Design Air Permeability
- Correlation of Results
- Flow Exponent
- Air Flow Coefficient
- Mastic Sealing Status
- Customer References
- Test Type
- Lodgement Type
- UKAS Registered
- Retested

The following fields were added in May 2017

- Building Type
- Construction Type
- Heating Type
- Air Conditioning
- No of Storeys
- Warm Roof Construction
- Pressurisation (Positive or Negative)
- Method (Manual or Auto)
- Q50
- Volume
- Calibration Exponent
- Calibration Coefficient

## 4.2 Numbers

We were amazed to see the number of lodgements made through our system. Table 1 shows the number of lodged tests received in our system within the end of the 2015 until 31 May 2017

Table 1: Table Caption

2015*	2016	2017**
40,826	133,599	67,294

\*2015 data between 1<sup>st</sup> September 2015 and 31 December 2015

\*\*2017 data between 1<sup>st</sup> January 2017 and 31 May 2017

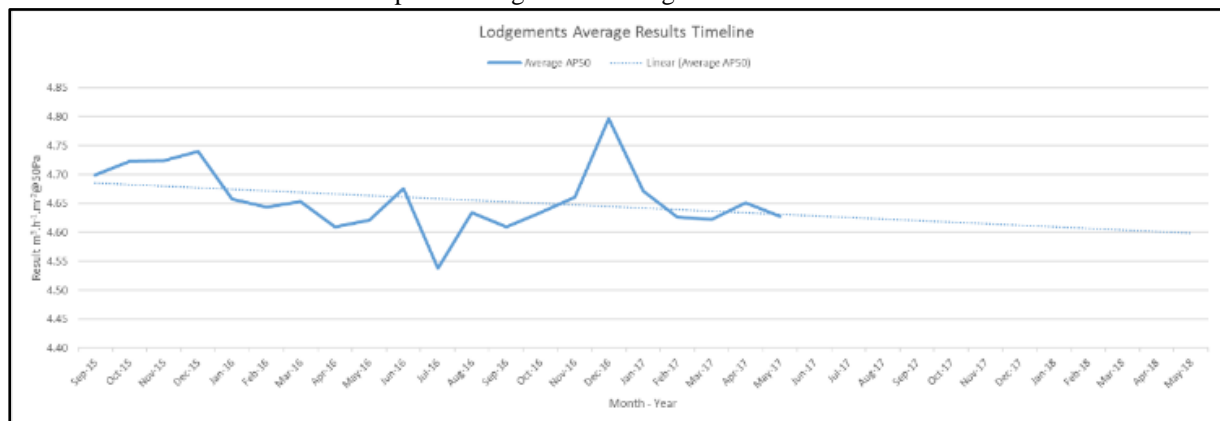
## 5 STATISTICS

With the large volume of data, we are able to identify trends that, perhaps were always known but never proven. Below is a series of data graphs and tables that highlight this information.

### 5.1 Average results over time

The data in Graph 1 shows that the average air permeability result is only very slowly decreasing. Between 1 September 2015 and 31 May 2017 the average result has only decreased by 0.07 m<sup>3</sup>.h.m<sup>2</sup>@50Pa.

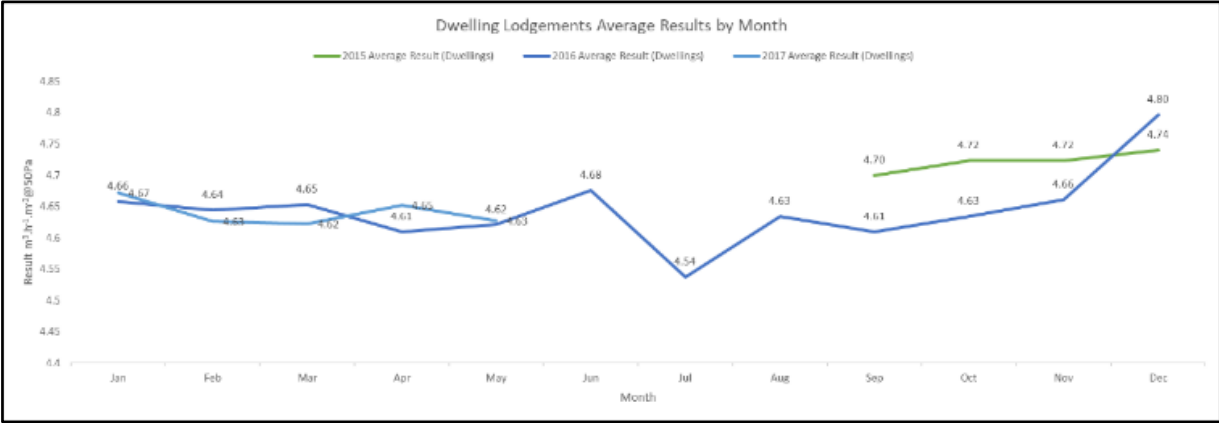
Graph 1 – Lodgement Average Results Timeline



The UK had a target to achieve Near Zero Energy Building status by 2020, but at this rate it will take more than 80 years! Without further input from the UK government it is likely the industry will never achieve NZEB status.

Graph 2 shows the same data but overlaid to give an indication by month.

Graph 2 – Lodgements Average Results by Month

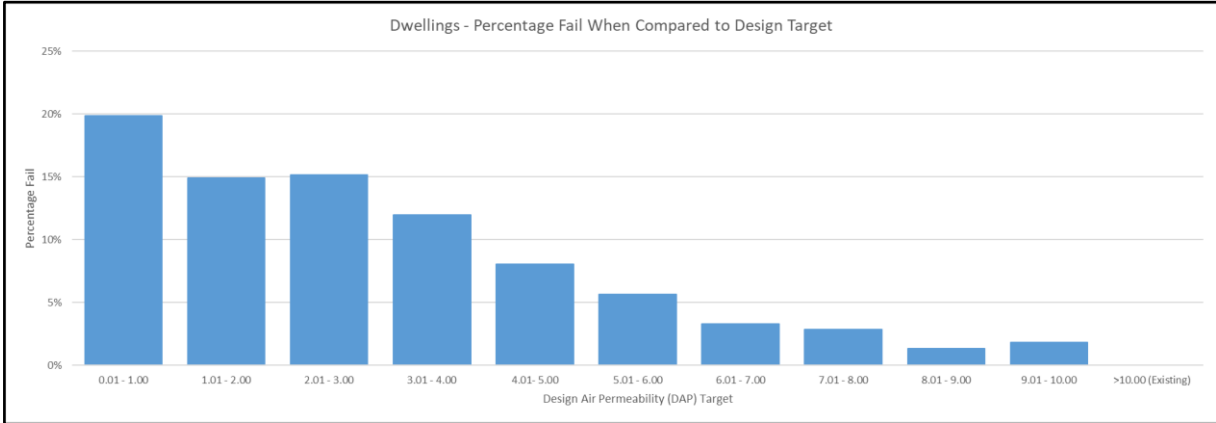


We had initially expected that the fall in air permeability would be much sharper, as the average results appeared to be reducing quickly between 1 September 2015 and 30 April 2016.

**5.2 Failure Rates Compared to Design Target**

One of the more obvious statistics was the failure rates when compared to design target, as identified in Graph 3.

Graph 3 – Failure rates when compared to Design Target

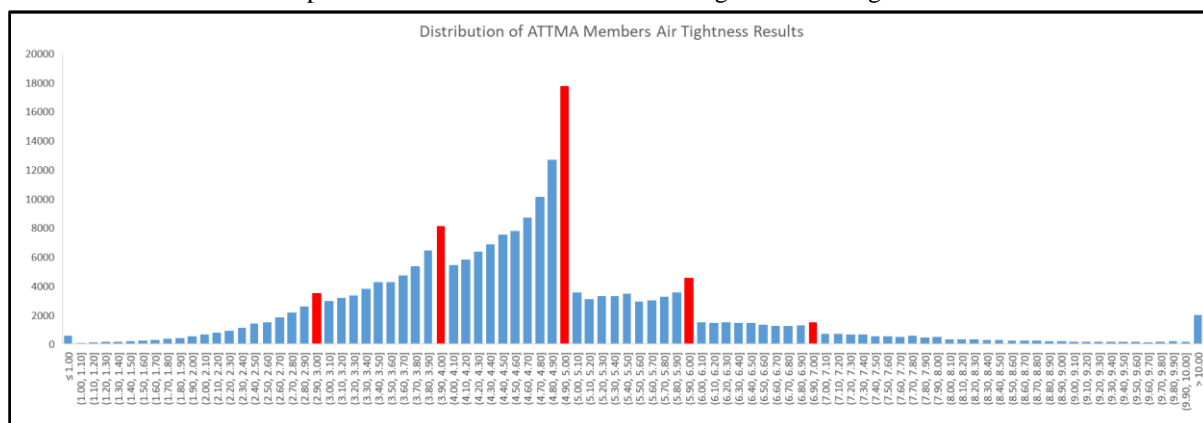


In short, the lower you set your target, the more likely you are to fail to meet your target.

**5.3 Distribution of Data**

We took the results for all tests and created a distribution graph, as shown in Graph 4, which raises some very serious concerns.

Graph 4 – Distribution of members Air Tightness Testing Results



The columns highlighted in red show the typical targets set by the energy modellers for air tightness testers.

Perhaps the most striking part of this graph is the drop between the number of results that achieve between 4.90 and 5.00 compared to the number of tests that achieve between 5.01 and 5.10.

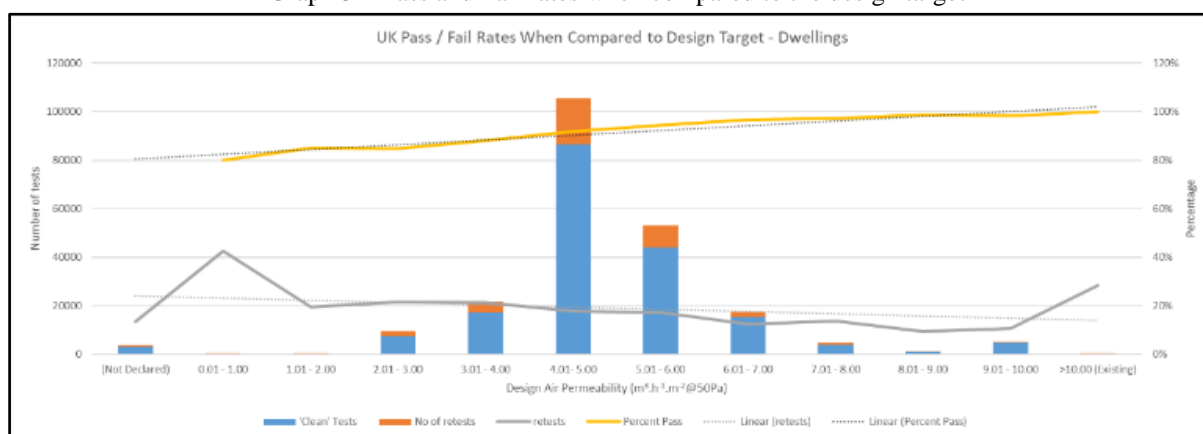
We can conclude that, as a country, we are not comfortably meeting air tightness targets but scraping through each test, relying on final finishes to ensure we achieve the desired targets.

Perhaps the second most interesting part of the graph for me is that the drops from the target change when the target is reduced. When contractors need to achieve a low target they react accordingly and design the building to be air tight. This means testers will regularly achieve between 2.5 and 2.9 when aiming for less than 3.00m<sup>3</sup>.h.m<sup>2</sup>@50Pa.

#### 5.4 Buildings that require testing multiple times.

Another striking statistic is the number of dwellings that need to be tested multiple times in order to achieve an air permeability lower than the target set by the energy modellers. Graph 5 shows this in more detail.

Graph 5 – Pass and Fail rates when compared to the design target



The area in red at the top of each column shows the number of retests conducted in order to achieve a pass. This represents about 18% of the tests conducted, which can be loosely described as 1 in 5 buildings tested require a second or third test before it met the target.

## 5.5 Ventilation

As part of the lodgement process, members are required to describe the ventilation system as part of the test. From this, we can compare the ventilation against average results which throws up perhaps the most concerning statistics of all. Table 2 shows the breakdown.

Table 2: Ventilation Statistics

Ventilation System	Ratio	Average Result	Concerns
<b>System 1</b> - Background ventilators with intermittent extractors	60.80%	4.80	25% of tests using System 1 ventilation achieve less than 4.00. This could lead to air quality issues.
<b>System 2</b> - Passive Stack Ventilation	0.59%	4.62	36% of tests using System 2 ventilation achieve less than 4.00. This could lead to air quality issues.
<b>System 3</b> - Continuous Mechanical Extraction	12.78%	4.51	24% of tests using System 3 achieve greater than 5.00 which could cause inefficient ventilation.
<b>System 4</b> - Continuous Mechanical Ventilation with Heat Recovery	25.21%	4.38	85% of tests using System 4 achieve greater than 3.00 which is against the majority of design specifications. This could lead to inefficient ventilation
<b>System 5</b> - Other	0.64%	4.75	

The concerns raised with ventilation in dwellings are plentiful.

1. System 1 – 25% of tests using a system 1 ventilation system achieve results below 4.00 m<sup>3</sup>.h.m<sup>2</sup>@50Pa which is circa 35,000 tests in 20 months, and could mean as many as 30,000 homes a year are being constructed with inadequate ventilation which could cause occupant sickness.

It should be noted however that some plots with a low air tightness score will, in theory, comply with the regulations due to an increased level of trickle ventilation. In the same token we can say that some ventilation systems for plots with higher air permeabilities could be ineffective and there are no figures available to back up these findings.

2. System 4 – Continuous mechanical ventilation with heat recovery systems show that 85% of all dwellings tested achieve greater than 3.00 m<sup>3</sup>.h.m<sup>2</sup>@50Pa which is greater than almost all manufacturers specifications and will lead to ineffective heating of the building over time.

## 6 CONCLUSIONS

In conclusion, the Lodgement system allows us to look at air tightness results in ways we have never been able to in the past.

Data shows that the construction industry is not taking air tightness seriously, as around 18% of dwellings tested fail to meet the criteria on the first attempt.

The spread of data shows that many plots are only just achieving the targets, some by the smallest of margins which raises concerns about the validity and longevity of the air permeability in these plots.

We, as the ATTMA, believe that regulation plays a strong part in delivering performance and reducing the performance gap in the UK. The current regulations are not stringent enough and are littered with loopholes that allow the construction industry to make small adjustments in order to achieve Building Regulations compliance. We must look to our Government to change the regulations in both air tightness and ventilation to avoid a generation of poor quality construction.

# A comparison study of the blower door and novel pulse technique on measuring enclosure airtightness in a controlled environment

Xiaofeng Zheng<sup>\*1</sup>, Edward Cooper<sup>1</sup>, Joe Mazzon<sup>2</sup>, Ian Wallis<sup>2</sup>, Christopher J Wood<sup>1</sup>

*1 Architecture, Energy and Environment Research Group, Faculty of Engineering, University of Nottingham  
University Park, Nottingham NG7 2RD, UK*

*2 BSRIA Limited  
Old Bracknell Lane West  
Bracknell, Berkshire, RG12 7AH,  
UK\*Corresponding author:  
[xiaofeng.zheng@nottingham.ac.uk](mailto:xiaofeng.zheng@nottingham.ac.uk)*

## ABSTRACT

This paper introduces a comparison study of measuring the airtightness of a house sized test chamber using the novel pulse technique and the standard blower door method in a controlled environment. Eight different testing plates have been applied to the improvised envelope of the chamber to establish different leakage characteristics. Each testing plate has a unique opening in the centre of the plate, achieved by obtaining a different combination of shape and thickness of the opening. By using the controlled environment, the vagaries of the natural condition when testing within buildings have been reduced providing a more robust testing environment. This investigation focuses on how the air leakage rate calculated from the measurements made by both techniques compare with each other. Comparable results ( $\pm 3\%$ ) under most scenarios have been obtained. Additionally, other aspects such as usability of the equipment used for the pulse testing have also been appraised.

## KEYWORDS

Building airtightness, Blower door, PULSE unit, Controlled environment

## 1. INTRODUCTION

### 1.1. Context

One of the main challenges in the measurement of building airtightness lies in accurately measuring low pressures that a building experiences under natural conditions. This pressure is typically in a range of 1-4 Pa and difficulties in measurement exist at this level due to the uncertain nature of external wind and buoyancy effects. Pressure changes due to external influences need to be accounted for in the measured pressure difference across the building envelope in order to obtain the actual pressure difference that the building is subjected to. One of the approaches to overcome this issue is to perform the test at high pressures in order to negate the wind and buoyancy effects; as with the steady state, *alias* blower door test at 50 Pa. However, this approach has its own shortcomings, which have been discussed in scientific studies and practical uses (Cooper 2007, Cooper 2014, Cooper 2016, Zero Carbon Hub 2014, Sherman 1994, Sherman 2002, Sherman 2009). It can be understood by performing the blower door test at 50 Pa it will reduce the impact of the natural vagaries of wind and buoyancy; however this does not preclude the use of such a test at 4 Pa. Nevertheless, one must consider the increasing impact of such influences upon the accuracy of the final result at 4 Pa. In fact in a number of countries, including the UK the test measurement must be

recorded at 50Pa for regulatory requirements. In this study, the difference in error between the 4Pa and 50Pa blowerdoor test is not investigated explicitly in terms of causation, but both measures are used to compare against the novel airtightness testing process known as the pulse technique. The pulse technique is a low pressure process (typically around 4Pa) whereby the airtightness of a building is determined through the release of a 1.5second pulse of air from a pressurised vessel. The rapid measurement of the consequential change in internal pressure of the building can be used to calculate a flow rate through the building envelope at 4Pa. The underlying principle is that of a quasi-steady flow, which can be shown to exist via the temporal inertial model and further detail is given by Cooper (Cooper 2007 and Cooper 2014).

A recent study by Remi (Remi 2016) using the blower door method shows an uncertainty of 6%-12% can be caused by steady wind in a range of 6-10 m/s combined with other sources of error in a steady state test at 50 Pa. Given the low operating pressure (around 4 Pa) of the pulse technique the wind could be considered the foremost important environmental factor due to its direct impact on the building pressure. In this study, the pulse and blower door units are used to measure the air leakage rates of an environmental chamber installed with 8 different testing plates, which provide 11 testing scenarios. The test chamber is housed inside another large building and therefore the ambient external condition is more stable than that of real houses. This test arrangement allows both the blower door and the pulse technique to measure leakage at low pressures. The objective of this comparative testing is to find out how these two techniques perform under different building leakage scenarios in a controlled environment.

## **1.2. Equipment**

The blower door unit that is used in this study is a Duct Blaster B (DBB), manufactured by 'The Energy Conservatory' in the United States. It consists of an adjustable door frame, flexible canvas panel, a variable-speed fan, and a DG700 pressure and flow gauge, as shown in Figure 1. The DBB is calibrated to take reliable readings at lower pressures than the larger blower door units and is therefore used to carry out the comparative tests alongside the PULSE-80 unit in this investigation.

The PULSE-80 unit incorporates an 80 litre light weight composite tank and oil free double piston compressor as shown in Figure 2. The outlet utilises a  $\frac{3}{4}$  inch (BSP) solenoid valve to release compressed air from the air tank into the test space, which delivers the 1.5second pressure rise. The data is recorded and analysed by the control box and results are displayed on the LCD screen of the control box.



Figure 1 Energy Conservatory Duct blaster B (DBB) Figure 2 PULSE-80 and associated control box

## 2. METHODOLOGY

### 2.1. Chamber

The tests were carried out in environmental chamber (No.4) at the testing laboratories of BSRIA Ltd, UK. The chamber, built inside a building, is made of insulated cold-store panels. The dimensions of the chamber are 6.01 m×4.64 m×7.20 m (L×W×H) with a 50 mm wall thickness, which give an envelope area and internal volume of 209m<sup>2</sup> and 200 m<sup>3</sup> respectively. The spaces surrounding the chamber were left open during the tests. The chamber's air supply, extract and instrumentation holes were all sealed during the course of testing.

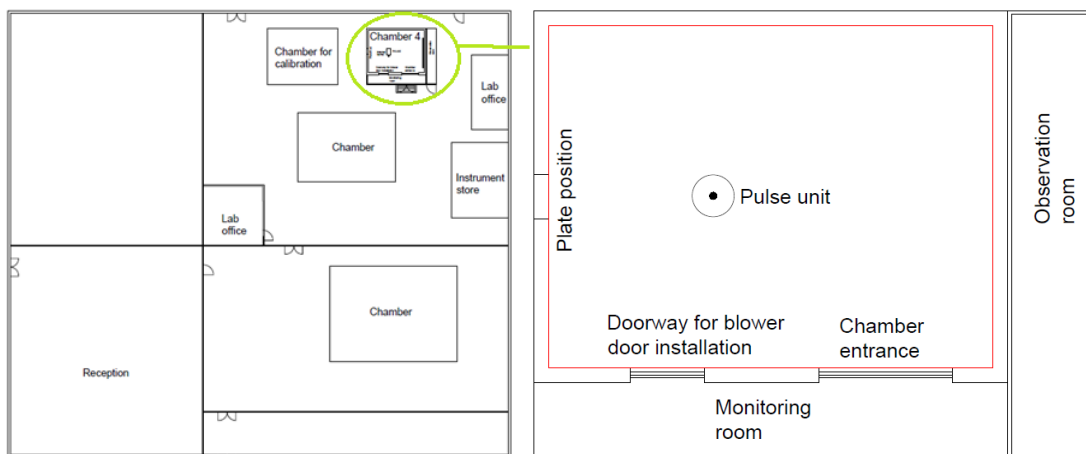


Figure 3 Environmental chamber for testing inside outer building (left) and test enclosure inside the chamber (right)

As shown in Figure 3, the chamber has a main entrance door and two smaller doors. One of them was used to install the DBB and the other was replaced by a compressed-fibreboard (MDF) sheet where plates with different openings were installed. The setup of the pulse unit in the environmental chamber is shown in Figure 3, in which the red rectangle represents the test space. Table 1 shows the details for the three tests conducted, with the aim to investigate the following:

- The difference between the  $Q_4$  (air permeability at 4 Pa, m<sup>3</sup>/hm<sup>2</sup>) measured by DBB using standard and Non-standard approach (see Table 1).
- The measurement of  $Q_4$  using DBB and PULSE-80 under various testing scenarios.

Table 1 Three testing approach

Equipment	DBB		PULSE
Test approach	Standard	Non-standard	PULSE-80

**Standard** test: carried out in accordance to ATTMA technical standard L1, typically in 10-60 Pa;

**Non-standard** test: carried out mainly in accordance to ATTMA technical standard L1, but in 4-60 Pa.

## 2.2. Plates

8 fibre-board plates of two thicknesses were cut to provide various openings of known geometric area as shown together with their associated photograph in Table 2. Plates 2 and 6 were also modified to make three more testing plates, the details are listed in Table 3, therefore giving 11 plate test scenarios overall.

Table 2 Details of the testing plates

Test	Plate No.	Thickness	Description	Measured Area
1	1	18mm	Blank plate	0 cm <sup>2</sup>
2	2	18mm	Circle	318.10 cm <sup>2</sup>
3	3	18mm	Four squares	314.76 cm <sup>2</sup>
4	4	18mm	Slots	230.04 cm <sup>2</sup>
5	5	50mm	Circle	307.91 cm <sup>2</sup>
6	6	50mm	Four squares	306.56 cm <sup>2</sup>
7	7	50mm	Slots	328.73 cm <sup>2</sup>
8	8	50mm	Angled circle	381.44 cm <sup>2</sup>

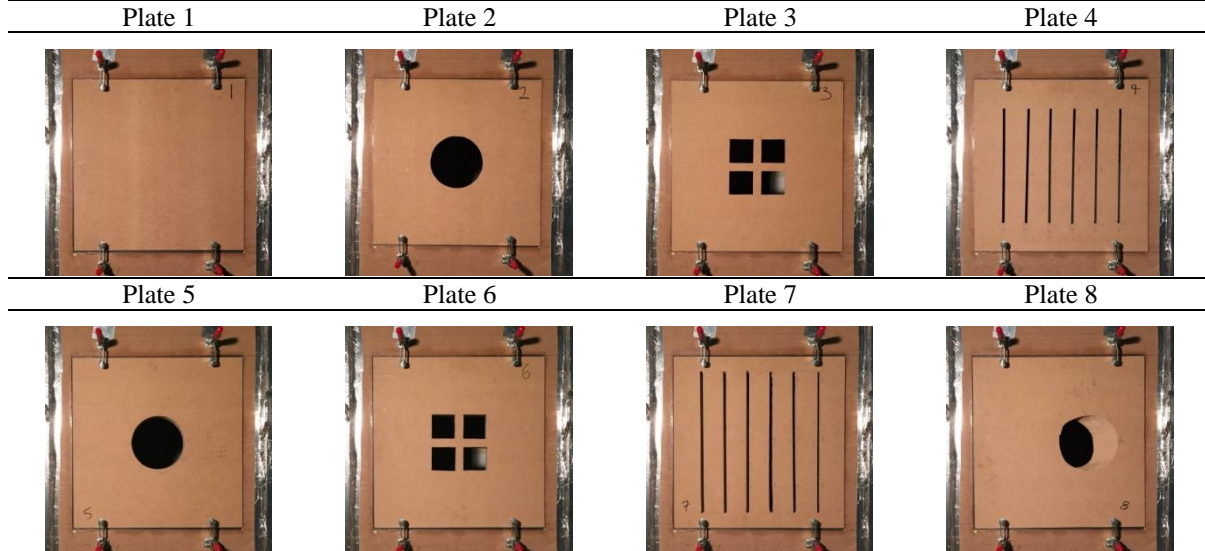
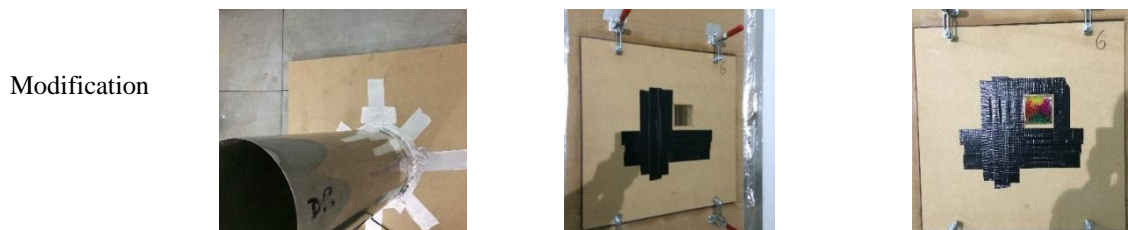


Table 3 Additional testing arrangements with modifications made to plates 2 and 6

Plate No.	9	10	11
Test	9	10	11
	A 410 mm circular duct is added	Three squares were sealed	Straws in one square with others sealed



### 2.3. Basic testing process

The comparison tests were carried out under the assumption that any difference in environmental conditions over the course of testing is insignificant. The DBB tests were conducted by a qualified BSRIA compliance engineer and the testing procedure followed the ATTMA (the Air Tightness Testing & Measurement Association) technical standard L1. The tests were performed in the pressurisation state. The pulse tests were conducted under the same experimental conditions as the DBB tests. In this paper the air permeability measured by both the DBB and PULSE-80 is compared at 4 Pa, but a discussion to the comparison at 50 Pa is also made. In order to predict  $Q_4$  and  $Q_{50}$  (air permeability at 4 Pa and 50 Pa,  $m^3/hm^2$ ), the power law equation  $V = C\Delta P^n$  is used, where  $V$  is the air leakage rate ( $m^3/s$ ),  $C$  is the flow coefficient ( $m^3/s \cdot Pa^n$ ),  $\Delta P$  is the building pressure (Pa) and  $n$  is the pressure exponent.

## 3. RESULTS AND ANALYSIS

### 3.1. Tested plates

$Q_4$  of the 11 testing plates are shown in Table 4 with achieved pressure range ( $\Delta P$ ). All the plates were tested by each approach consecutively. For the pulse tests, ideally the  $\Delta P$  needs to cover 4 Pa so as to avoid any extrapolation, however, in some of the pulse tests, the  $\Delta P$  doesn't cover 4 Pa but is in close proximity. Considering the hydraulic similarity at low pressures, minor extrapolations are made to the results close to 4 Pa in order to calculate  $Q_4$ , all the pulse tests that cover or are in close proximity of 4 Pa are used for comparison.

Table 4 Air permeability at 4 Pa of pulse and DBB tests ( $m^3/h \cdot m^2$ )

Test	1	2	3	4	5	6	7	8	9	10	11
Standard (DBB)	0.50	1.24	1.27	1.10	1.28	1.33	1.48	1.01	1.51	0.79	0.57
$\Delta P$ range (Pa)	25-60	25-61	25-57	26-59	27-57	27-57	25-56	29-63	27-55	23-60	26-50
Non-standard (DBB)	0.48	1.31	1.34	1.23	1.34	1.36	1.51	1.08	1.59	0.73	0.55
$\Delta P$ range (Pa)	4.5-60	4.0-61	4.2-57	4.2-59	4.0-57	4.0-57	4.0-56	4.0-63	4-55	4.4-60	4.4-54
PULSE-80	0.51	N/A	1.37	1.24	1.37	1.40	1.51	1.06	1.38	0.71	0.72
$\Delta P$ range (Pa)	4.6-6.7	N/A	3.3-4.9	2.8-4.5	3.2-4.1	3.1-4.1	2.6-4.3	4.9-8.5	3.0-4.6	5.7-9.3	5.9-6.9

$\Delta P$  range stands for the achieved pressure range in which the leakage is measured.

N/A stands for the fact that the test was not carried out due to the time constraint.

The air leakage vs building pressure of all tests measured by DBB and PULSE-80 is plotted in log-log scale graph, as shown in Figure 5. The pulse and DBB tests of the same plate are plotted in the same colour with a trend line added to each DBB test. It can be seen that the pulse measurement of tests 1 to 8 lie closely to the trend line of each corresponding DBB measurement, however this is not the case for tests 9, 10 and 11.

#### 3.1.1. Comparison between DBB Standard and Non-standard

Two testing approaches, including the Standard and Non-standard DBB tests, are compared to see the impact of extrapolation to the prediction of  $Q_4$ . Assuming the influence of wind and buoyancy is insignificant due to the experimental arrangement then, theoretically,  $Q_4$  given by the Non-standard approach should be more reliable than the Standard approach

considering it doesn't involve any extrapolation. In the analysis, the  $Q_4$  given by the Non-standard approach is used as the baseline to present the percentage difference of  $Q_4$  given by both approaches, as shown in Figure 4. Hence, it is seen that by measuring the building leakage according to the standard procedure in a controlled environment, the DBB test produces a deviation of between 2.2% and 10.6% when predicting  $Q_4$ .

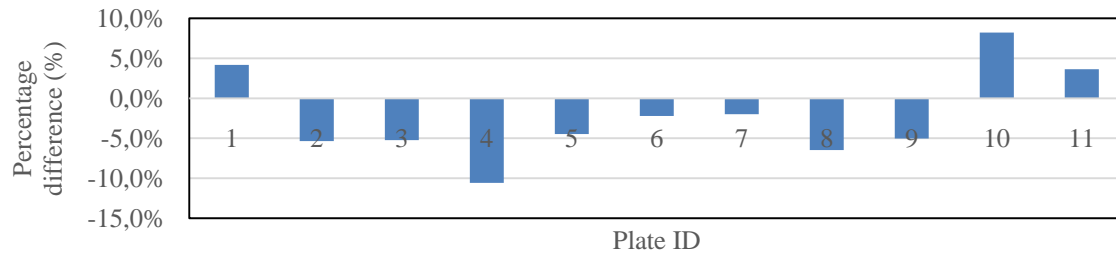


Figure 4 Percentage difference of  $Q_4$  measured by DBB in Standard and Non-standard approach

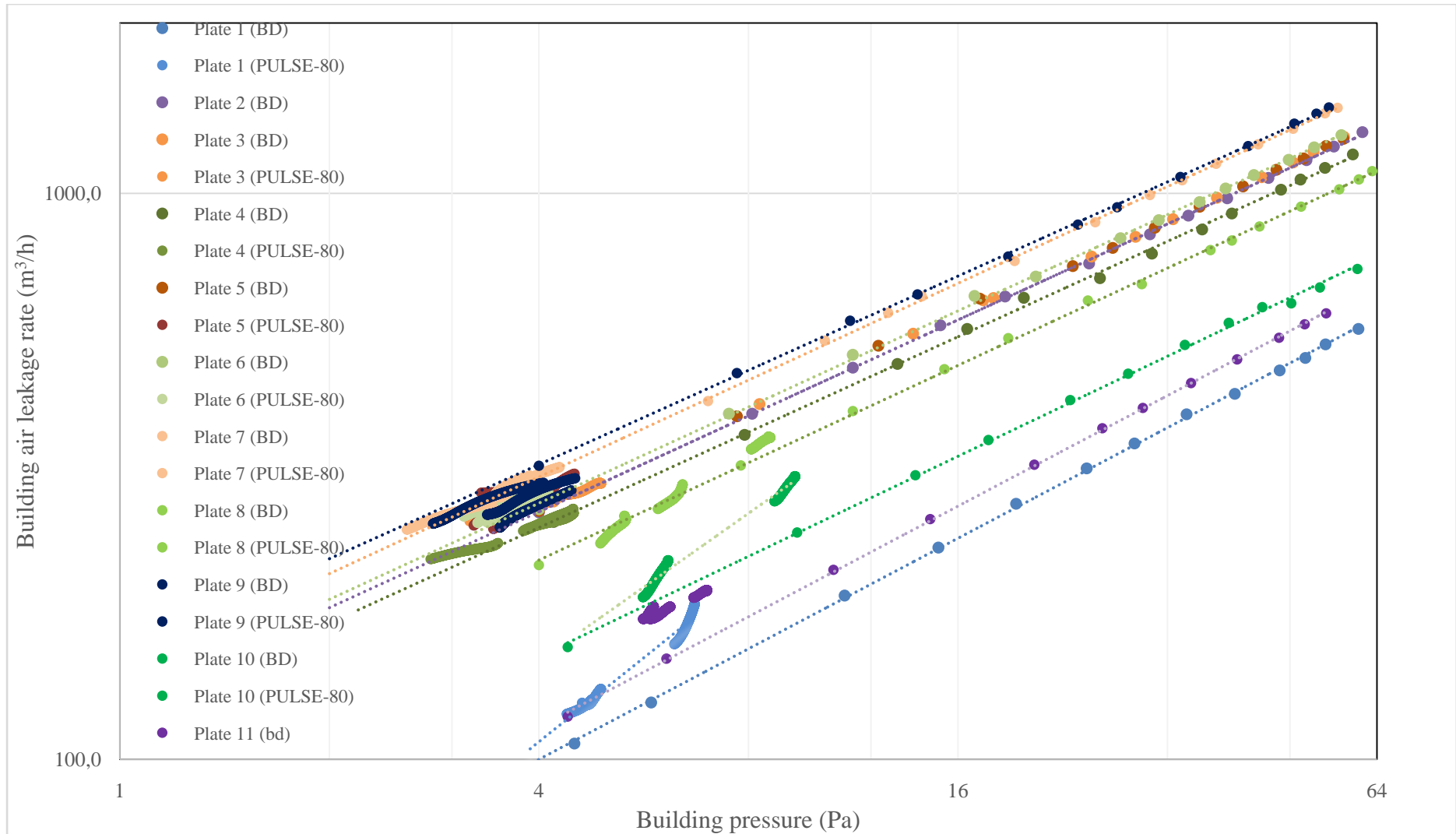


Figure 5 Log-log scale graph of leakage-pressure measured by DBB and PULSE-80

### 3.1.2. Comparison between the DBB and PULSE-80

Tests using PULSE-80 are compared with those done in Standard and Non-standard approach using DBB. The percentage difference of  $Q_4$  measured by PULSE-80 against that given by the Standard DBB test lies in 2.0%-26.3%, and 0%-30.9% for the Non-standard DBB test, as shown in Figure 6.

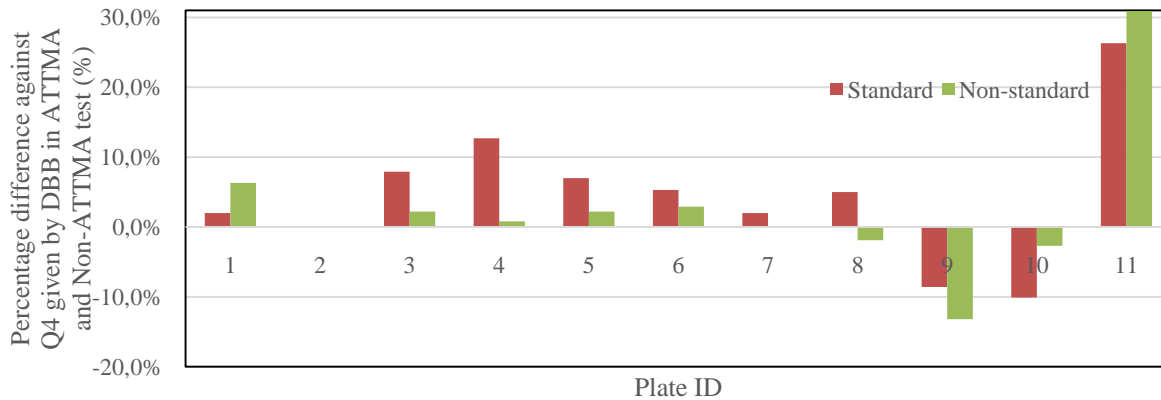


Figure 6 Percentage difference of  $Q_4$  measured by pulse units against that measured by DBB in two approaches

The percentage difference of  $Q_4$  measured by PULSE-80 against that given by DBB falls into a wider range, from 0% to 31%. But when tests 9 and 11 are excluded, the percentage difference of  $Q_4$  given by PULSE-80 and DBB (Standard) comes down to 2.0%-12.7% and 0%-6.3% for DBB (Non-standard). Tests 9 and 11 are excluded on the basis that the openings in the modified plates are of long duct (s) and are therefore significantly unrepresentative of the flow conditions of the other plate openings. Therefore, in most of the testing scenarios, a good agreement has been achieved in the measurement of  $Q_4$  using PULSE-80 and DBB. It is also seen that PULSE-80 has closer agreement with the non-standard DBB than the standard approach. This may suggest that the extrapolation error with the  $Q_4$  obtained from the standard DBB could be responsible for this greater difference when compared to the PULSE-80 and non-standard DBB results.

Using the results of the tests described above and assuming all openings being sharp edged with a discharge coefficient of 0.61, the geometric area of each test plate was calculated by using eq.(1).

$$GA = V \sqrt{\rho / 2P} / 0.61 \quad (1)$$

Where GA stands for the geometric area of the opening ( $m^2$ ), V is the air leakage rate ( $m^3/s$ ),  $\rho$  is the air density ( $kg/m^3$ ), and P is the building pressure (Pa). Table 5 shows the geometric areas of the openings from plate 2 to plate 8 measured by PULSE-80 and DBB with the relative percentage difference of them to the actual measured areas given in Table 2. The GA of the opening in plate 3, 5 and 6 measured by both methods differs from the manually measured one by from 0.38% to 7.63%. For the plate 4, 7 and 8, the percentage difference is much larger. This could be caused by the fact that plate 8 has an angled opening and that plate 4 and 7 have six long slots fabricated with uneven edges and finishes, both of which are difficult to quantify accurately. This could contribute to the difference between the manually measured GA and the actual one. However, both methods have shown similar percentage difference from the manually measured GA. The assumed discharge coefficient

0.61 is for sharp edged orifice and hence not applicable for some of the openings, especially plate 8. This calculation of GA should only be treated as an approximation.

Table 5 Comparison of  $Q_{50}$  predicted by the pulse test using various methods

Plate ID	1	2	3	4	5	6	7	8
Measured GA (m <sup>2</sup> )	0	0.0318	0.0315	0.0230	0.0308	0.0307	0.0329	0.0381
GA by PULSE-80 (m <sup>2</sup> )	N/A	N/A	0.0314	0.0265	0.0316	0.0325	0.0365	0.0201
RPD (%)	N/A	N/A	-0.38%	15.09%	2.65%	6.04%	10.99%	-47.30%
GA by DBB (Standard) (m <sup>2</sup> )	N/A	0.031	0.032	0.027	0.032	0.033	0.040	0.022
RPD (%)	N/A	-2.55%	1.65%	17.39%	3.93%	7.63%	21.69%	-42.32%

**GA:** geometric area of the openings in test plates, as listed in Table 2. **RPD:** the relative percentage difference of GA measured by PULSE-80 or DBB to the manually measured GA. **N/A** means either the test is not carried out due to time constraint or not applicable.

Although the pulse test is designed to resolve the issues existing in the measurement of building air leakage at low pressures, it is frequently asked how it is compared with the blower door test at 50 Pa. The flow regimes at low pressure and high pressure levels are hydraulically dissimilar and therefore significant errors will occur in the prediction of air leakage rate from one level to the other. One of the issues with extrapolating a low pressure reading to a high pressure level is the absence of a higher data point, whereas an extrapolation downwards (as with the DBB tests) at least has the presence of the origin at the lowest point. Nevertheless,  $Q_{50}$  is predicted by using the pulse test data in various ways and compared with the DBB test, as listed in Table 6.

Table 6 Comparison of  $Q_{50}$  predicted by the pulse test using various methods against  $Q_{50}$  (standard method by DBB)

Plate	1	2	3	4	5	6	7	8	9	10	11
n	0.627	0.588	0.583	0.606	0.582	0.576	0.578	0.595	0.576	0.548	0.631
(DBB) $Q_{50}$	2.45	5.45	5.56	5.08	5.54	5.7	6.37	4.56	6.45	3.17	2.80
(Pulse) $Q_{50}$ (n)	2.49	N/A	5.97	5.73	5.96	6.00	6.50	4.76	5.91	2.83	3.54
RPD (%)	1.6%	N/A	7.4%	12.8%	7.6%	5.3%	2.0%	4.4%	-8.4%	-11%	26%
(Pulse) $Q_{50}$ (0.66)	2.70	N/A	7.26	6.57	7.26	7.42	8.00	5.62	7.31	3.76	3.82
RPD (%)	10.2%	N/A	30.6%	29.3%	31.0%	30.2%	25.6%	23.2%	13.3%	18.6%	36.4%
(Pulse) $Q_{50}$ (Qua)	7.88	N/A	3.85	4.13	8.39	5.67	6.08	5.56	6.50	5.27	2.70
RPD (%)	222%	N/A	-31%	-19%	51%	-0.5%	-4.6%	21.9%	0.8%	66.2%	-3.6%
(Pulse) $Q_{50}$ (Pow)	6.18	N/A	3.10	3.75	5.05	4.25	5.75	7.35	2.89	6.37	2.56
RPD (%)	152%	N/A	-44%	-26%	-8.8%	-25%	-9.7%	61%	-55%	101%	-8.6%

**RPD (%)**: relative percentage difference of  $Q_{50}$  predicted by using various methods using the  $Q_4$  measured by PULSE-80 against the **(DBB)  $Q_{50}$**  measurement. **(Pulse)  $Q_{50}$  (n)** stands for the air permeability at 50 Pa predicted by the pulse test using the pressure exponent n given by DBB test. **(Pulse)  $Q_{50}$  (0.66)** stands for the air permeability at 50 Pa predicted by the pulse test using the empirical n value (Orme 1994). **(Pulse)  $Q_{50}$  (Qua)** stands for the predicted air permeability at 50 Pa using quadratic equation based on the pulse test. **(Pulse)  $Q_{50}$  (Pow)** stands for the predicted air permeability at 50 Pa using power law equation based on the pulse test.

Compared with the  $Q_{50}$  measured by the DBB in the Standard tests, the percentage difference of  $Q_{50}$  predicted by PULSE-80 lies in 1.6%-26%, 10.2%-36.4%, 0.5%-222% and 8.6%-152% when 'n' value measured by DBB, the empirical n value 0.66, quadratic equation based on the pulse test and power law equation based on the pulse test is used, respectively. The best prediction is the one using the n value measured by DBB, which gives predictions of  $Q_{50}$  within 13% difference excluding plate 11. However, this wouldn't fit the practical purpose because a DBB test wouldn't be available when a pulse test is carried out as an alternative. For the predictions using the empirical n value obtained by Orme (Orme 1994), the percentage difference generally lies in the range of 20%-40%. It indicates the empirical n value is not representative of that of most testing scenarios. This could also be explained

roughly by the fact the test environmental chamber is a single cell enclosure without the adventitious openings that are present in typical dwellings. For the predictions using either quadratic or power law equation based on the pulse test, there is lack of accuracy in most predictions although for a few reasonable accuracy is seen. Therefore, similar with the findings reported by Cooper and Zheng (Cooper 2016) the low pressure pulse test doesn't always provide accurate indication of  $Q_{50}$ . The measurement needs to be made over a wider pressure range in order to reduce the error in extrapolation if  $Q_{50}$  is calculated using the pulse test.

### **3. 2. Observations and discussions**

In addition to the above comparison testing, there are a number of notable observations from the testing, which are worthy of discussion. Firstly it is interesting to observe that  $Q_4$  of tests 9 and 11 measured by PULSE-80 and DBB don't agree with each other well. The similarity of the arrangement of both tests is the use of an extended opening; test 9 the addition of a single duct and test 11 a collection of tightly packed of straws.

For a well-developed flow in a steady test, the discharge coefficient of the openings changes when they are extended. In a pulse test, the air flow through the extended openings occurs in a short time and might behave in a different way to that of a steady state test. This may explain why the measurements by the two methods are different in this case. It is therefore considered that further investigative work needs to be performed to not only understand the difference between the airflow through an extended opening produced by a DBB and a pulse test but also how these flows relate to that of natural building infiltration. Future work, will also report on other findings, such as the impact of the location of pulse unit in relation to internal barriers, artificial cross wind outside the opening and vibration effects upon the pulse test readings.

Observations were also made in regards to the practical aspects of both the PULSE-80 and the DBB. Due to the fact the weight of PULSE-80 used in this study is 40.4kg, setup of the pulse unit in the chamber relied on two people lifting between different levels, while the DBB showed a big advantage in the portability due to smaller weight, 19.2 kg. This advantage would be weakened when a model of blower door with larger capacity is needed, such as Minneapolis blower door model 4 with a 25 kg door fan. It must also be noted however that the PULSE-80 unit is a prototype system and in fact in terms of capacity is much larger than that which would be required for testing an enclosure of this size and airtightness. Hence it could be considered that in future testing, smaller units of reduced size and weight would be available.

The PULSE-80 did not require any complex assembly on site apart from the connection of control plugs and therefore it is seen to be quick and efficient in terms of setup, implementation and disassembly. However, as discussed above the PULSE-80 in terms of stored air capacity was much larger than required for the testing and therefore extra time was required to adjust tank pressure prior to testing. This adjustment required computer based data analysis to ensure a suitable  $\Delta P$  was being achieved. This finding of 'required adjustment' has subsequently been used to direct the development of PULSE, whereby the LCD screen now incorporates achieved pressure difference and the unit is able to perform a step process of 3 separate tests using different starting tank pressures. Hence this ensures that the correct range of  $\Delta P$  can be captured without the need for post-test analysis.

#### 4. CONCLUSION

The experimental study, using PULSE-80 and DBB to measure the airtightness of a house size chamber in a controlled condition, has allowed us to compare two methods from a different perspective. For 9 out of 11 plates, the pulse tests using PULSE-80 and the Non-standard DBB tests have given  $Q_4$  that are in close agreement, with a percentage difference ranging in 0%-6.2%, whereas the Standard DBB tests have given a percentage difference up to 12.7%. This may suggest that extrapolation error in Standard DBB test may be contributing to the greater deviation. The tests of plates with extended openings did not provide good agreement and further investigation on the flow dynamics of the air flow through extended opening under two testing methods is required. This study has also led to a question on how these two particular test units compare in a real life scenario, i.e. uncontrolled environment. It was previously reported by Cooper and Zheng (Cooper 2016) that it is unreliable for both methods to make extrapolations between low pressure and high pressure, which was based on the tests done in a number of dwellings using Minneapolis blower door model 4. Following this comparison study in a controlled environment, continued comparison study in an external chamber using the same units has been carried out and will be reported in future.

#### 5. REFERENCES

- Cooper EW, Etheridge DW (2007). Determining the adventitious leakage of buildings at low pressure. Part 1: uncertainties. *Building Serv. Eng. Res. Technol.* 2007; 28: 71-80.
- Cooper EW, Etheridge DW. (2007). Determining the adventitious leakage of buildings at low pressure. Part 2: pulse technique. *Building Serv. Eng. Res. Technol.*; 28: 81-96.
- Cooper E., Zheng X.F., Gillot M., Riffat S., Zu Y.Q. (2014). A nozzle pulse pressurisation technique for measurement of building leakage at low pressure. *35th AIVC Conference "Ventilation and airtightness in transforming the building stock to high performance"*, Poznan, Poland, 24-25 September 2014.
- Cooper E., Zheng X.F., Wood C., Gillott M., Tetlow D., Riffat. S, Simon L. (2016) . Field trialling of a new airtightness tester in a range of UK homes. *International Journal of Ventilation*. <http://dx.doi.org/10.1080/14733315.2016.1252155>
- Zero Carbon Hub (2014). Closing the gap between design and as-built performance: End of term report, July 2014. Available from: [http://www.zerocarbonhub.org/sites/default/files/resources/reports/Design\\_vs\\_As\\_Built\\_Performance\\_Gap\\_End\\_of\\_Term\\_Report\\_0.pdf](http://www.zerocarbonhub.org/sites/default/files/resources/reports/Design_vs_As_Built_Performance_Gap_End_of_Term_Report_0.pdf)
- Sherman M.H. and Matson N.E., 2002. "Air Tightness of New U.S. Houses: A Preliminary Report", Lawrence Berkeley National Laboratory, LBNL 48671. Lawrence Berkeley National Laboratory, Berkeley, CA.
- Sherman M.H. and Dickerhoff D., 1994 "Air-Tightness of U.S. Dwellings" In Proceedings, 15th AIVC Conference: The Role of Ventilation, Vol. 1, Coventry, Great Britain: *Air Infiltration and Ventilation Centre*, pp. 225-234. (LBNL-35700).

Sherman M. H., 2009 Infiltration in ASHRAE's residential ventilation standards, Lawrence Berkeley National Laboratory, LBNL-1220E. Lawrence Berkeley National Laboratory, Berkeley, CA.

Remi C.F., Leprince V, 2016. Uncertainties in building pressurisation tests due to steady wind. Energy and Buildings. Vol.116, 15th March 2016, pp 656-665.

Orme M., Liddament M. and Wilson A., 1994 "An Analysis and Data Summary of the AIVC's Numerical Database", Technical Note 44, Air Infiltration and Ventilation Centre, Coventry, 1994.

# Natural Pressure Differential – Infiltration Through Wind

## Results of a Long-Term Measurement

Dipl.-Ing. (FH) Oliver Solcher<sup>1</sup>, Dipl. Ing. Stefanie Rolfsmeier<sup>2</sup>, Dipl.-Ing. Paul Simons<sup>3</sup>

*1 Ingenieurbüro für Wärmetechnik  
Dipl.-Ing. (FH) Oliver Solcher  
Friedenstraße 17  
10249 Berlin, Germany*

*2 Ingenieurgemeinschaft Bau + Energie + Umwelt  
GmbH  
Zum Energie- und Umweltzentrum 1  
D-31832 Springe-Eldagsen*

*3 BlowerDoor GmbH  
Zum Energie- und Umweltzentrum 1  
D-31832 Springe-Eldagsen*

### ABSTRACT

#### Topic

Wind pressure and thermal forces are driving forces for pressure difference on the building envelope. In European and German standards infiltration is calculated using wind speed, temperature difference and wind pressure coefficients resulting from upstream and downstream flow on the building envelope. This long term measurements shall present measured pressure differences on the building envelope in comparison to those calculations.

#### Approach

Measurement of pressure differences over the building envelope over a year. Samples are a dwelling in a multi-family-house in Berlin-Friedrichshain and a dwelling in a multi-family-house on the island Helgoland. Pressure was logged for one year with capillary pipes over the gate folds of several windows. Wind speed was measured close to the building.

#### Results

The recorded pressure differences show a great dependence on the wind speed and the direction of flow on the building. Pressure differences fluctuate strongly at very short intervals. A constant pressure over a certain time could not be observed. The temperature differences play a subordinate role or no role in these measurement objects.

### KEYWORDS

Infiltration, wind pressure, leakage, differential pressure

## 1 INTRODUCTION

The purpose of this long-term study is to record pressure differences on the building envelope. On the one hand, the influences of wind, temperature difference and ventilation systems as well as the user behavior can be made visible, and on the other hand there is the idea that the measured values can be matched with theoretical assumptions. At present we are still in the evaluation of the measured data and present an interim work.

## 2 INFILTRATION CALCULATION

The differential pressure on the building envelope is the result of wind pressure and thermal buoyancy. In European and German standards, infiltration calculations include figures on wind speed, temperature difference and wind pressure coefficients from upstream and downstream flow on the building envelope.

Together with the air permeability measurement of the building envelope, the differential pressure can then be used to derive a flow rate under environmental conditions that is applied toward determining energy requirement and ventilation needs.

### 3 BOUNDARY CONDITIONS – OBJECT 1

#### 3.1 Measurement Object: Berlin

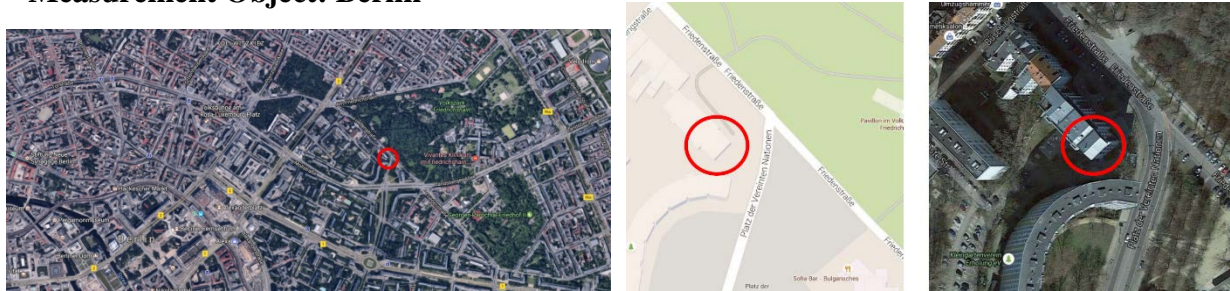


Figure 1: Location of measurement object, Berlin Source: Google Maps

Address:	Friedenstrasse 17, 10249 Berlin, Germany
Apartment location:	2nd story, finished floor level 11m above the ground
	three faces: NE park, SE open, SW prefab building around 30m high, 10 to 15m away
Ventilation style:	Apartment-central, humidity-controlled ventilation system with outside air apertures in the window, ventilation fans switches off every 1.5 hours for a duration of 1.5 hours
Airtightness of apartment:	$n_{50} = 1.3$ 1/h Leakages at the balcony door, at penetration of the outgoing duct, at penetration of incoming duct of the fireplace, and at all installation shafts
Wind measurement:	logicenergy LeWL Windlogger Speed kit Measurement point: bedroom balcony to the northeast The log interval is 1 minute. The values measured continuously over this interval are added up each minute and saved as an averaged value called Wind_mittel. The maximum wind speed during this interval is also saved as a value called Wind_max.
Outside temperature:	logicenergy LeWL Windlogger Speed kit Measurement point: bedroom balcony to the northeast The log interval is 1 minute. The values measured continuously over this interval are added up each minute and saved as one value.
Inside temperature:	Not recorded; room temperature during heating period at 20–22°C
Differential pressure:	Two measurements using TEC DG-700 with TEC Wifi Link Office, located to the northeast Combined living/kitchen area, located to the southeast, southwest Analysis conducted using Teclog3 The log interval is 1 second for Measurement Configuration 1 and 5 seconds for Measurement Configuration 2. The values measured continuously over these intervals are added up and saved every 1 second for Measurement Configuration 1 and every 5 seconds for Measurement Configuration 2.
Measurement period:	February 2016 to February 2017

### 3.2 Measurement Configuration

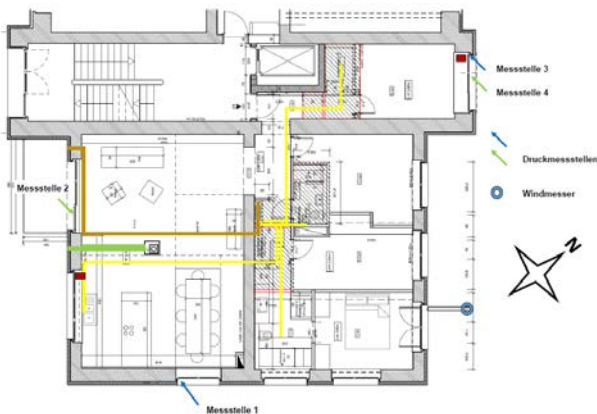


Figure 2: Measurement Configuration 1  
(Key: *Messstelle* = measuring point;  
*Druckmessstellen* = pressure measuring points;  
*Windmesser* = wind gauge)



Figure 3: Measurement Configuration 1, pressure recording

Figures 2 and 3 show the first measurement configuration. At differential pressure gauge 1, channel A records the differential pressure between measuring point 1 and the reference pressure inside, while channel B records that between measuring point 2 and the reference pressure inside. At differential pressure gauge 2, channel A is used to record the differential pressure between measuring point 3 and the reference pressure inside while channel B is used to record that between measuring point 4 and the reference pressure inside. Measuring points 3 and 4 are situated at the window door at 1.6 m height. Measuring point 3 is ap. 10 cm away of the window reveal, Measuring points 3 and 4 are ap. 0.8 m apart.

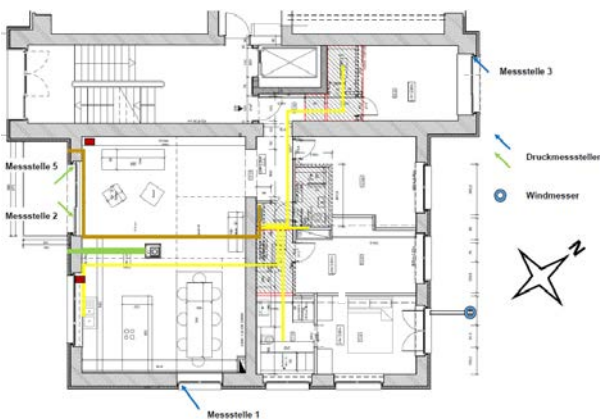


Figure 4: Measurement Configuration 2  
(Key: *Messstelle* = measuring point;  
*Druckmessstellen* = pressure measuring points;  
*Windmesser* = wind gauge)



Figure 5: Measurement Configuration 2, pressure recording

Figures 4 and 5 show the slightly altered second measurement configuration. Compared to the first configuration, measurement at the differential pressure gauge 2 has been changed so that channel A measures the differential pressure between measuring point 5 and the reference pressure inside while channel B measures that between measuring point 3 and the reference pressure inside.

Recording pressure at the windows takes place in the upper windows through capillary tubes threaded through the window reveal to the outside. Wind pressure on the façade is recorded as positive pressure. When the ventilation system is activated, the apartment will be under negative pressure, but the pressure recorded at the measuring points will nonetheless show positive.

Because the apartment is equipped with demand controlled residential ventilation in the form of an exhaust system regulated by room air humidity, and this system cannot be shut off during the measuring period, the central apartment exhaust fan is turned off in 1.5-hour intervals using an automatic timer. The exhaust system therefore runs for 8 x 1.5 hours a day and is switched off for 8 x 1.5 hours a day. For the periods when it is off, differential pressures at the measuring points are affected only by wind and thermal buoyancy.

Measurement Configuration 1 aims to use the first differential pressure gauge to determine how wind inflow behaves in a room. The second differential pressure gauge aims to discover whether a difference can be shown between the pressure recorded at the window reveal and the window surface. Using the modified Measurement Configuration 2, the second differential pressure gauge attempts to record a two-sided pressure situation through the apartment.

## 4 MEASUREMENT RESULTS: BERLIN

### 4.1 Influence of Exhaust System

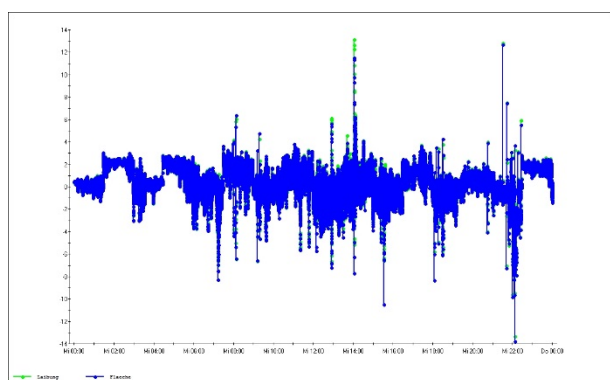


Figure 6: Measuring points 3 and 4, differential pressure Pa, March 23, 2016

The effect of the exhaust system on the pressure ratios in the apartment is clearly visible in Figure 6. The exhaust system is on at the following times:

#### Winter time

- 1:30 a.m. to 3:00 a.m.
- 4:30 a.m. to 6:00 a.m.
- 7:30 a.m. to 9:00 a.m.
- 10:30 a.m. to 12:00 noon
- 1:30 p.m. to 3:00 p.m.
- 4:30 p.m. to 6:00 p.m.
- 7:30 p.m. to 9:00 p.m.
- 10:30 p.m. to 12:00 midnight

#### Summer time (Mar. 27<sup>th</sup> to Oct. 30<sup>th</sup> 2016)

- 2:30 a.m. to 4:00 a.m.
- 5:30 a.m. to 7:00 a.m.
- 8:30 a.m. to 10:00 a.m.
- 11:30 a.m. to 13:00 p.m.
- 2:30 p.m. to 4:00 p.m.
- 5:30 p.m. to 7:00 p.m.
- 8:30 p.m. to 10:00 p.m.
- 11:30 p.m. to 1:00 a.m.

Figure 7 shows a low wind speed between midnight and 8:00 a.m. By 4:00 a.m., its maximum speed was 0.5 m/s. By 8:00 a.m., the wind speed had not exceeded 1 m/s. Excluding the effects of the exhaust system, the differential pressure fluctuates by  $-1$  Pa to  $+1$  Pa. When the exhaust system is on, the differential pressure fluctuates by  $+2$  Pa, up to  $+3$  Pa.

After 8:00 a.m., local wind speed is measured at 1 to 2 m/s. The diagram levels “ventilation system on/off” are no longer clearly recognizable and are obscured by the effects of wind. Differential pressures are measured from  $-4$  to  $+4$  Pa. Higher peaks are visible up to  $\pm 14$  Pa. A relation from measured pressure difference to high wind speed is visible, though due to the measuring interval from 1 Minute not all wind peaks are recorded. It is only visible the largest

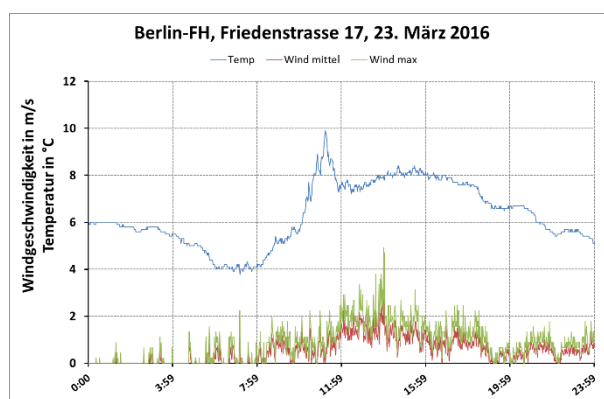


Figure 7: Local wind speed (*Windgeschwindigkeit*) m/s and temperature °C, March 23, 2016

wind speed within that interval. Measuring interval of pressure at this configuration is 1 second. A specific comparison between peaks of pressure difference and wind speed is not possible.

The influence of the ventilation system on the measured differential pressure is visible at low wind speeds and accounts for around 2 to 3 Pa. Since the flow rate of the exhaust system was not measured, however, there is still uncertainty here. The humidity regulation adapts the exhaust flow according to its needs: should high humidity levels be emitted, more air is expelled. Varying differential pressure occurs inside the apartment depending on the exhaust flow rate. This connection was not recorded, however.

Exhaust ventilation system was designed for maximum pressure difference of 8 Pa at maximum exhaust air flow. Nevertheless externally mounted air transfer devices are mounted without internal façade yet, leading to a lower pressure drop at same air flow. This can be recognized in measured values.

#### 4.2 Pressure Recording at Window Reveal / Window Surface

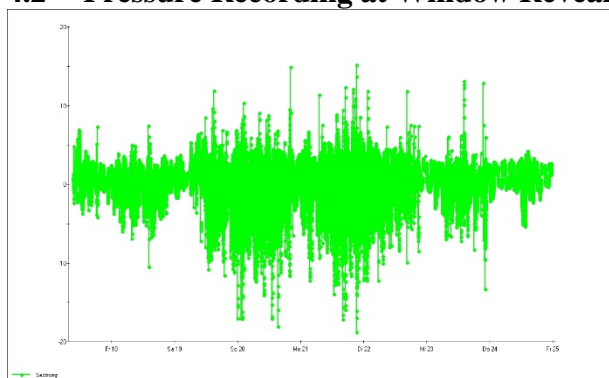


Figure 8: Measuring point 3 (reveal), differential pressure Pa, March 18 to 25, 2016

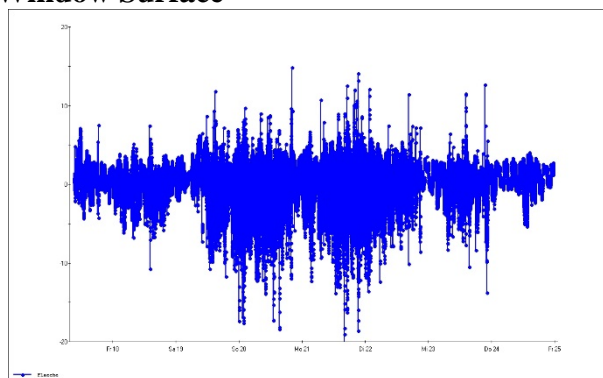


Figure 9: Measuring point 4 (surface), differential pressure Pa, March 18 to 25, 2016

	Avg [Pa]	Min [Pa]	Max [Pa]
Laibung	0,49	-18,76	15,18
Flaeche	0,44	-22,26	14,87

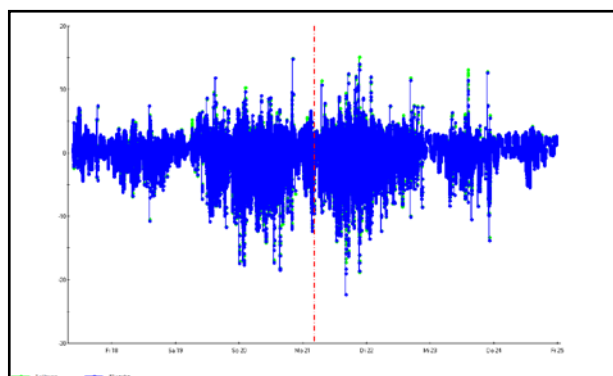


Figure 10: Measuring points 3 and 4, differential pressure Pa, March 18 to 25, 2016 (Laibung = reveal; Flaeche = surface)

	Avg [Pa]	Min [Pa]	Max [Pa]
Laibung	0,94	-13,96	3,72
Flaeche	-1,01	-13,8	4,1

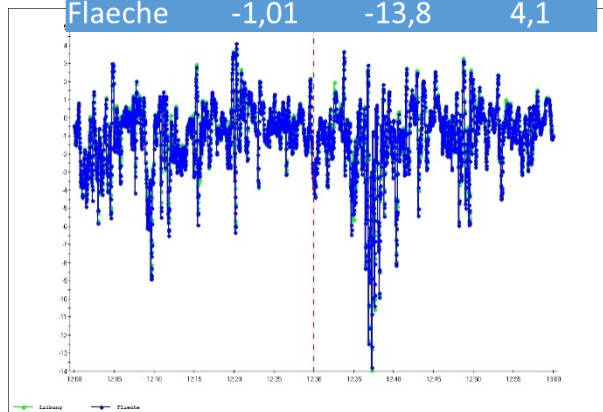


Figure 11: Measuring points 3 and 4, differential pressure Pa, March 21, 2016, noon to 1:00 p.m. (Laibung = reveal; Flaeche = surface)

The measurement between measuring points 3 and 4 aims to calculate whether a difference arises between the window reveal and the window surface. No significant pressure difference was discovered.

### 4.3 Two-sided pressure recording

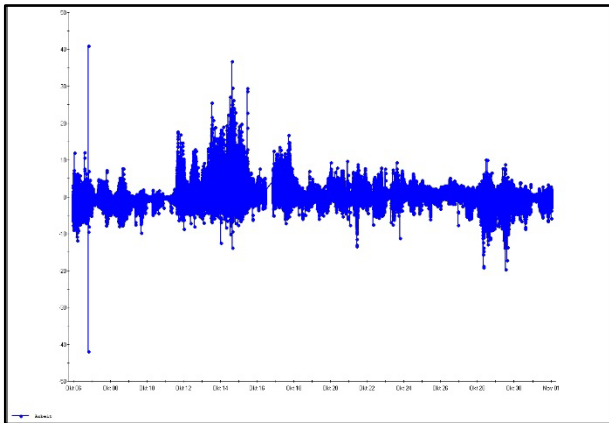


Figure 12: Measuring point 3, differential pressure Pa, October 6 to 31, 2016

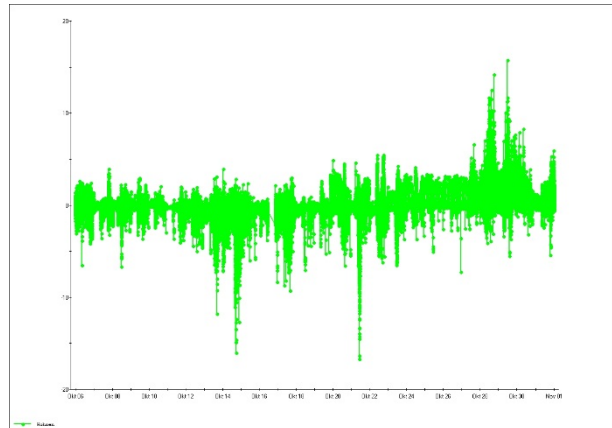


Figure 13: Measuring point 5, differential pressure Pa, October 6 to 31, 2016

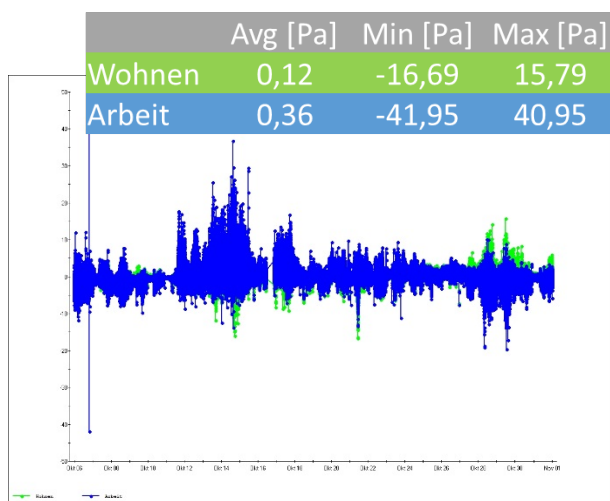


Figure 14: Measuring points 3 and 5, differential pressure Pa, October 6 to 31, 2016

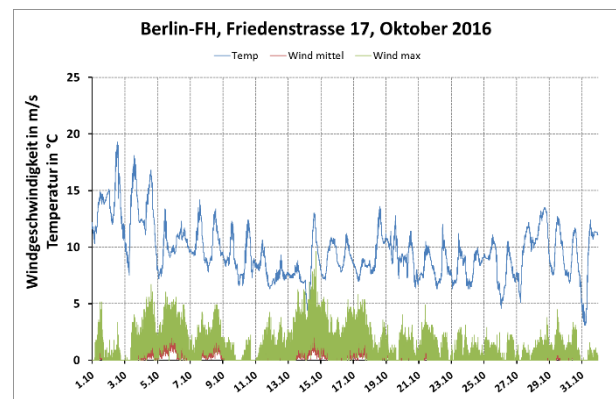


Figure 15: Local wind speed (Windgeschwindigkeit) in m/s and temperature in °C, Oktober 2016

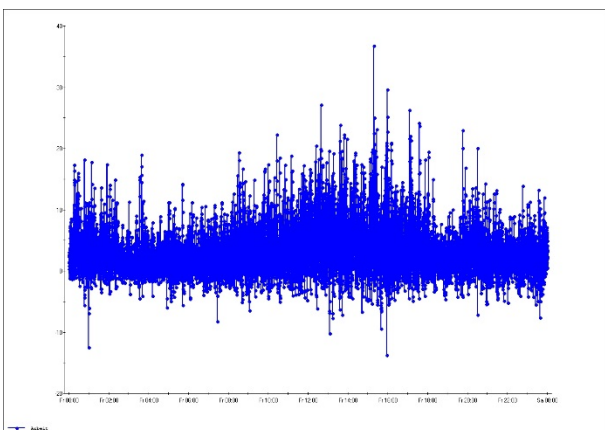


Figure 16: Measuring point 3, differential pressure Pa, October 14, 2016

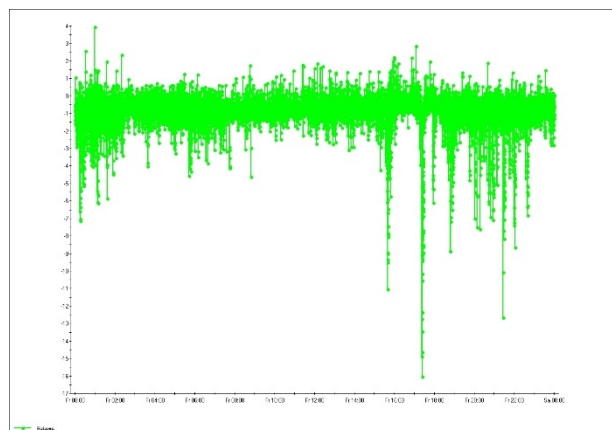


Figure 17: Measuring point 5, differential pressure Pa, October 14, 2016

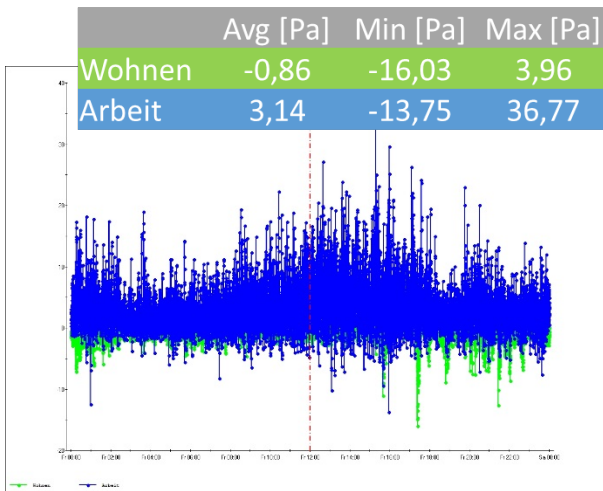


Figure 18: Measuring points 3 and 5, differential pressure Pa, 14.10.2016

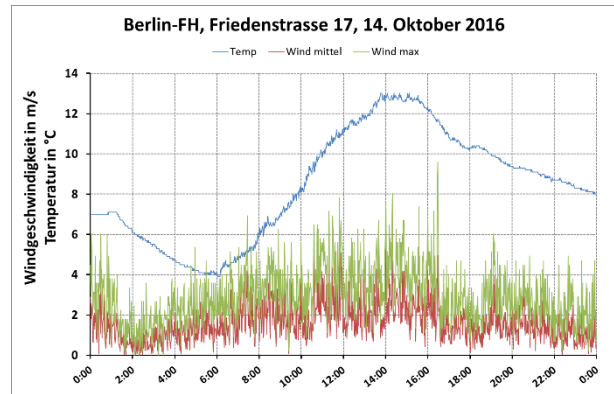


Figure 19: lokale Windgeschwindigkeit m/s and Temperatur °C, 14.10.2016

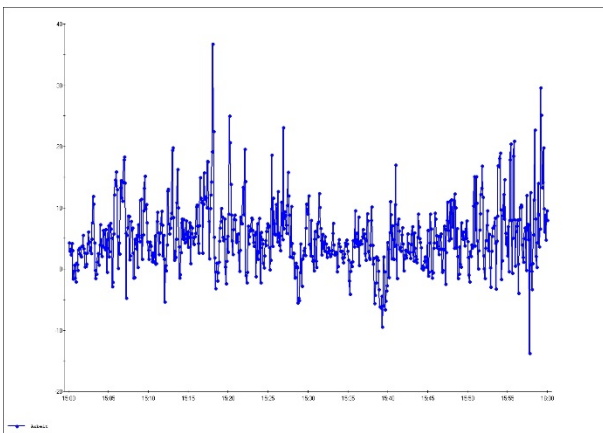


Figure 20: Measuring point 3, Differential pressure Pa, 14.10.2016, 3:00 to 4:00 p.m.

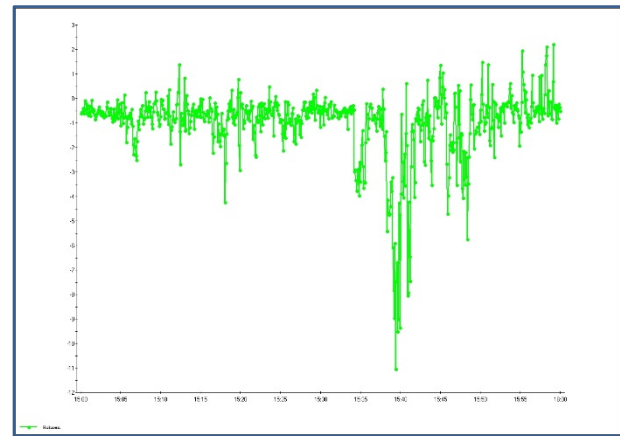


Figure 21: Measuring point 5, Differential pressure Pa, 14.10.2016, 3:00 to 4:00 p.m.

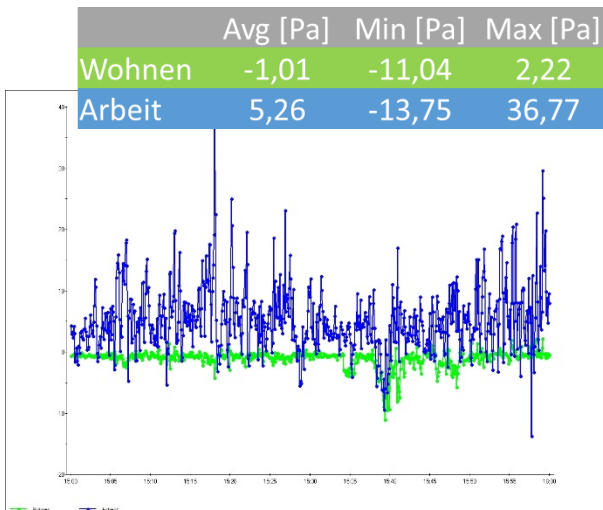


Figure 22: Measuring points 3 and 5, differential pressure Pa, October 14, 2016, 3 p.m. to 4 p.m.

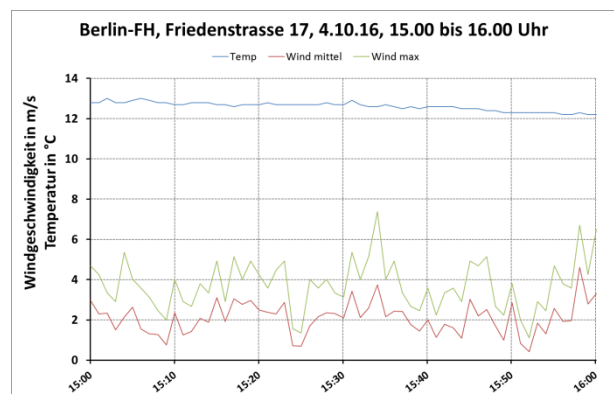


Figure 23: Local wind speed (*Windgeschwindigkeit*) in m/s and temperature in °C, October 14, 2016, 3 p.m. to 4 p.m

Figures 12 to 16 show the increased effect of the wind on measuring point 3 of the façade facing the park. Here, differential pressures are measured from  $\pm 5$  to  $\pm 10$  Pa, while at measuring point 5, which faces a neighboring building, differential pressures are shown from  $\pm 2$  to  $\pm 5$  Pa. The extremes are also much lower:  $-16$  Pa at the courtyard side (measuring point 5) compared with  $+36$  Pa at the park-facing side (measuring point 3). Maximum local wind speed is at 5 to 10 m/s.

A somewhat more precise observation can be seen in the example day of October 14, 2016, and Figures 17 to 23. Figure 16 shows substantially stronger positive wind pressure on the park-facing side (measuring point 3) while Figure 17 shows a slighter, negative pressure at the courtyard side (measuring point 5). Maximum local wind speed is at 5 to 10 m/s.

The hourly diagram in Figure 22 clearly shows the strong influence of the wind on the park-facing side: An average of +5.26 Pa (minimum -13.75; maximum +36.77 Pa) was recorded here. On the courtyard side, the average differential pressure during this hour was -1 Pa (minimum -11.04 Pa; maximum +2.22 Pa).

Because only local wind speed was recorded, however, information is missing on the direction from which the wind approached the building.

Influence of exhaust ventilation system (in operation from 2:30 p.m. till 4:00 p.m.) can not be recognized in the recorded pressure differences.

#### 4.4 Frequency and Average Differential Pressure

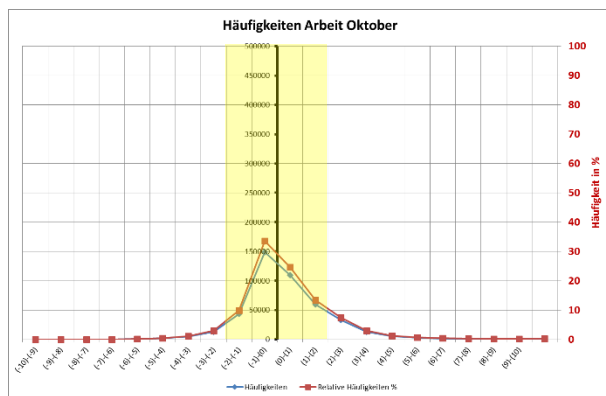


Table 24: October 2016, measuring point 3, frequency of differential pressures



Table 25: October 2016, measuring point 5, frequency of differential pressures

		Avg [Pa]	Min [Pa]	Max [Pa]
<b>October 2016</b>	Living	0.12	-16.69	15.79
	Working	0.36	-41.95	40.95
<b>October 9–15, 2016</b>	Living	-0.4	-16.03	3.96
	Working	0.75	-13.75	36.77
<b>October 14, 2016</b>	Living	-0.86	-16.03	3.96
	Working	3.14	-13.75	36.77
<b>Oct. 14, 2016, 3:00–4:00 p.m.</b>	Living	-1.01	-11.04	2.22
	Working	5.26	-13.75	36.77

Table 1: October 2016, average, minimum and maximum differential pressure

It makes sense to calculate an average differential pressure over a period of time. Nevertheless the smaller this period, the higher the influence of individual values. Table 1 displays this clearly.

When the frequency is added up of values occurring within the range of -2 Pa to +2 Pa (area shaded yellow in Figures 24 and 25), measuring point 3 (work) produces a value of 81% and measuring point 5 (living) a value of 92%.

Largest frequency was recorded for negative pressure differences between 0 to -1 Pa. Due to the exhaust ventilation system and having the internal pressure as reference pressure highest frequency would be expected at positive pressure differences.

Any calculation of frequency or averages, however, includes the constant, intermittent, substantially stronger wind pressures to an only marginal extent, given their lower frequency of occurrence. The

fluctuation between positive and negative differential pressures also results in the pressures offsetting each other. Although strong fluctuations were shown between differential pressures, the average appears quite low.

Pressure extremes nevertheless result in infiltration/exfiltration over the building envelope that is well above the average differential pressure. They generate additional outflow/exhaust flow at ventilation system components. In this respect, it is insufficient to view averages alone without consideration of the pressure extremes. It is necessary to look more closely at the effects of these pressure peaks on the airflow over the building envelope.

## 5 BOUNDARY CONDITIONS – OBJECT 2

### 5.1 Measurement Object: Helgoland



Figure 1: Location of measurement object, Helgoland Source: Google Maps and Earthstar Geographics SIO

Address:	Helgoland, Germany
Apartment location:	1 <sup>st</sup> floor of a 3-storey more family house. The Southeast side faces to a place and a 2-storey building, the Northeast side to a 2.5-storey building, the Northwest side to a court and the Southwest side to a neighbor apartment.
Ventilation style:	Natural ventilation
Wind measurement:	logicenergy LeWL Windlogger Speed kit Measurement point: SE side of the building (balcony)
Outside temperature:	logicenergy LeWL Windlogger Speed kit Measurement point: SE side of the building (balcony)
Inside temperature:	Device: TEC APT and temperature sensor. Recording with TECLOG3
Differential pressure:	Devices: DG-700 with TEC WiFi Link and TEC APT. Recording and analyses with TECLOG3. Sample interval: 1 second Resample interval for this study: 5 seconds
Measurement period:	March 2016 to February 2017

## 5.2 Measurement Configuration

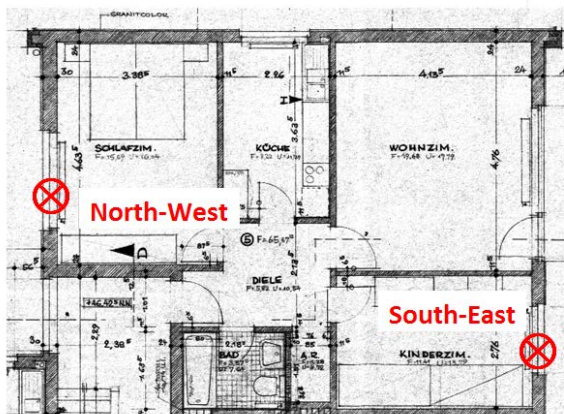


Figure 2: Location of Test Points for measuring the pressure differences



Figure 3: Test Point of Northwest-Side (left), Test Point of Southeast-Side (right)

Figures 2 and 3 show the locations of the two test points. One test point is located on the northwest side and the other on the southeast side of the apartment. At each side a differential pressure gauge measures the pressure difference between inside and outside at a window. Each gauge has two channels A and B that both are used in order to have a backup, if one channel shows problems (for example: water in a tube because of rain).

A capillary tube is placed between the window wing and window frame to get the outside pressure. In these tests the reference pressure is outside of the building. If the gauge or the graph shows a negative pressure inside of the room is a depression and outside of the façade an overpressure. A positive pressure means outside of the façade is depression and inside is an overpressure.

## 6 MEASUREMENT RESULTS: HELGOLAND

### 6.1 Wind Pressure

The diagrams in figure 4 show the building pressure differences of one apartment (1. floor) in a more family building on the island Helgoland in October 2016. The red graph shows the pressure differences of the room on the northwest side, the blue graph of the room on the southeast side. The sample interval is one second.

Figure 5 shows the wind speed in m/s (average per hour) for October 2016 from the DWD (Deutschen Wetterdienst) on Helgoland.

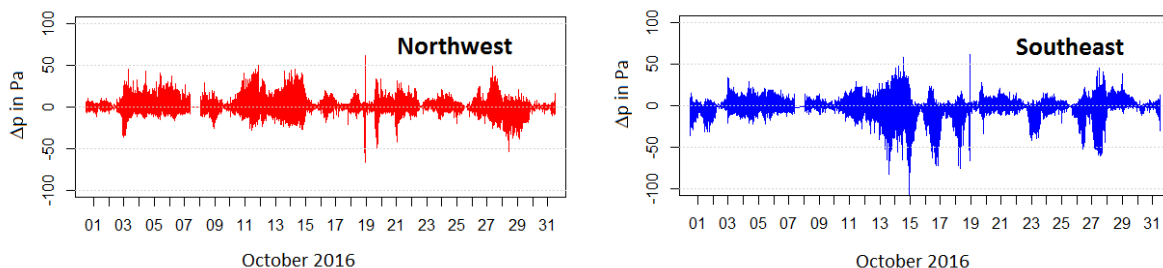


Figure 4: Pressure differences caused by wind on the façade of the building. Negative pressure differences = depression inside and overpressure outside. Positive pressure difference = overpressure inside and depression outside.

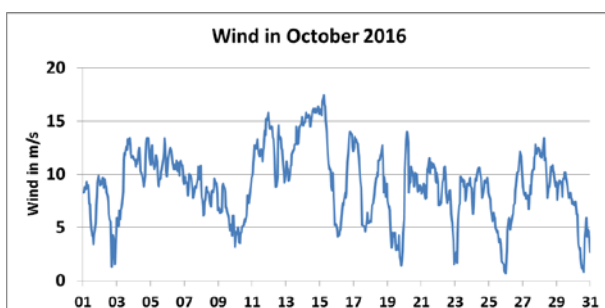


Figure 5: Wind on Helgoland in October 2016 (average per hour) (Source: DWD)

The pressure differences at the façade are mainly caused by the wind. As expected the pressure difference (figure 4) increases with increasing wind speed (figure 5).

On the northwest side the average of the pressure differences in October 2016 is 0 Pa. The maximum wind pressure on the façade is 66 Pa; the highest wind suction is -62 Pa. The average wind pressure is 2 Pa and wind suction is -2 Pa.

The southeast façade shows an average of 1.5 Pa wind pressure on the façade. The maximum wind suction is -62 Pa and the maximum wind pressure is 121 Pa. The averages for wind pressure are 4.3 Pa and wind suction -2.6 Pa.

It is obvious that the average of the wind speed in figure 5 doesn't explain all pressure differences in the diagrams. What is the reason? In this study the maximum wind speeds are missing and smaller intervals than an average over one hour could be helpful, in order to understand the peaks in the pressure differences. Additionally it is necessary to record the wind direction, because the pressure differences are depending on the direction of the flow on the façade, too.

An unexpected observation is the high fluctuation in a very short time of the pressure differences around more or less 0 Pa. It seems to be no steady wind on a certain level. The next chapter will show this in detail.

## 6.2 Wind Fluctuation

Figure 6 shows the pressure differences of 14<sup>th</sup> October 2016 and figure 7 the wind.

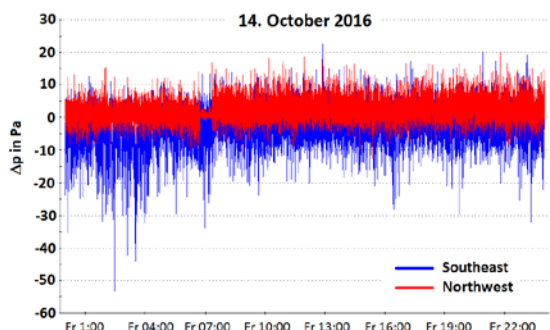


Figure 6: Pressure differences caused by wind 14<sup>th</sup> October 2016

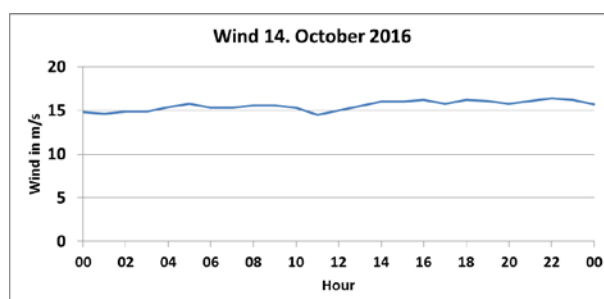


Figure 7: Wind on Helgoland 14<sup>th</sup> October 2016 (source: DWD)

The graph in figure 7 shows an almost steady wind of ca. 15 m/s (7 Beaufort) over the day. But the pressure differences in figure 6 (Northwest) vary over a range of 15 Pa between 5 Pa wind pressure on the façade and 10 Pa wind suction. The fluctuation on the Southeast side is even 30 Pa and higher. Also in this case it would be helpful to have a smaller resolution of the wind measurements.

Around 7 am the pressure differences on the Northwest side are much lower than on the Southwest Side. This is caused by an open window in the room on the Northwest side. It is interesting to see that this has more or less no effect on the other side of the apartment.

In figure 8 the graph shows the pressure differences over one hour between 3 pm and 4 pm of 14<sup>th</sup> October. Also here is the fluctuation visible.

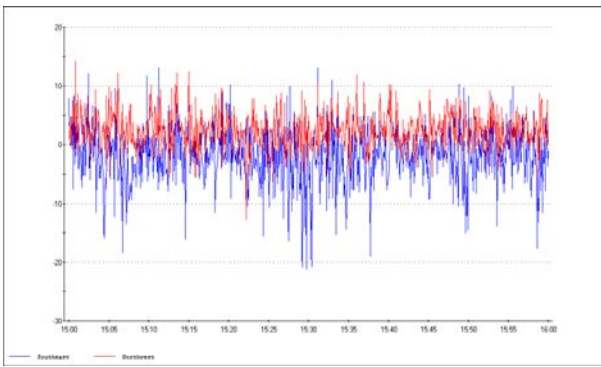


Figure 8: Pressure difference over one hour caused by wind of around 15 m/s

## 7 CONCLUSIONS

The recorded pressure differences show a great dependence on the wind speed and the direction of flow on the building. It is interesting that the pressure differences fluctuate strongly at very short intervals. A constant pressure over a certain time could not be observed. The temperature differences play a subordinate role or no role in these measurement objects.

The influence of the exhaust ventilation system on the measured differential pressure is visible at low wind speeds and is about 2 to 3 Pa. However, since a measurement of the exhaust airflow did not take place, it is not clear how high the exhaust airflow was at the measurement time point. Depending on the exhaust airflow, a differently high differential pressure in the dwelling will occur. However, this connection has not been included.

A reference of the measured differential pressure to the maximum wind speed is achievable, due to the measuring interval of the local wind speed measurement of 1 minute, not all wind peaks are recorded. Visible is only the greatest wind speed in the respective minute interval. The recording interval during the pressure measurement during those recordings is 1 or 5 seconds. A direct comparison between the differential pressure tip and the wind speed peak is thus not possible.

A difference in pressure between the positioning of the pressure receptacle on the window reveal and the window surface is not detectable.

On the facade of the park, higher differential pressures can be measured than on the courtyard side oriented towards neighboring buildings. However, since only the local wind speed has been recorded, the wind direction from is missing.

With a frequency consideration or averaging, the constantly occurring alternating wind loads, which reach significantly higher values, enter into the result only with a low value due to the lower frequency. The pressure fluctuations between the positive and the negative pressure also cancel one another in the mean value. Although strong fluctuations in the differential pressure are recorded, the average value is very low. In this respect, an average consideration without appreciation of the pressure peaks is not sufficient. In addition, a more detailed consideration of the effects of these pressure peaks on the volume flows over the building envelope is required.

# Building and ductwork airtightness requirements in Europe – Comparison of 10 European countries

Valérie Leprince<sup>\*1</sup>, François Rémi Carrié<sup>2</sup>, Maria Kapsalaki<sup>2</sup>

1 PLEIAQ  
84 C Avenue de la Libération  
69330 Meyzieu, FRANCE

2 INIVE  
Lozenberg 7  
BE-1932 Sint-Steven-Woluwe, BELGIUM

\*Corresponding author: [Valerie.leprince@pleiaq.net](mailto:Valerie.leprince@pleiaq.net)

## ABSTRACT

Mandatory building airtightness testing has come gradually into force in the UK, France, Ireland and Denmark. It is considered in many other European countries because of the increasing weight of the energy impact of building leakage on the overall energy performance of low-energy buildings.

This study analyses recent developments in 10 European countries on the following aspects:

- requirements regarding building airtightness in EP- regulation
- requirements in specific energy programmes
- airtightness testers schemes
- field airtightness measurement databases
- increasing awareness regarding building airtightness, main motivations and progress needed.

The same type of analyses has been done with ductwork airtightness. Information has been collected through a questionnaire sent to TAAC (TightVent Airtightness Associations Committee) members.

Regarding building airtightness, we found that 7 out of the 10 countries have minimum requirements that have to be justified by testing or another mean, either in the context of the EP-regulation (for 3 of them) or in specific energy performance programmes. Minimum requirements mostly apply to new buildings, only three countries have a regulation or programme dealing with the airtightness of refurbished buildings. 7 countries out of 10 now have a quality framework for building airtightness testers; the number of qualified testers in Europe has almost doubled in 4 years. Field measurement data are available in 6 countries out of 10. Most of the time, databases are managed by testers' qualification bodies and contain mainly data of new residential buildings. All respondents acknowledge that awareness regarding, building airtightness has grown in their country in the last 5 years. The main motivation remains energy use, however, work on this topic is still needed to better quantify the impact of airtightness on energy use.

Conversely, ductwork airtightness does not seem to be taken into account (neither in regulation nor in energy performance programmes) in most European countries. In our survey, only France and Belgium take into account ductwork airtightness in their energy performance calculation. Progress is needed to better understand the impact of ductwork airtightness on energy use (fan, cooling and heating) and indoor air quality.

## KEYWORDS

Airtightness measurement, Regulation, European comparison, competent tester schemes

## 1 INTRODUCTION

Building airtightness is a key issue to achieve low- and very low-energy targets. Therefore, an increasing number of tests are performed in European countries for various reasons: compliance to the energy performance regulation; compliance to a specific energy programme; or will of the building owner. For instance, to our knowledge, measuring the airtightness of all new buildings or at least part of them is required by the energy performance regulation in UK, France, Ireland and Denmark. Besides, specific energy programmes (such as Passivhaus or Minergie) that require or encourage building airtightness testing are

increasingly popular in many other countries. Likely, within a few years, over a million tests will be performed every year in Europe.

This study analyses recent developments in 10 European countries on the following aspects:

- requirements regarding building airtightness in EP- regulation;
- requirements in specific energy programmes;
- airtightness testers schemes;
- field airtightness measurement databases;
- increasing awareness regarding building airtightness, main motivations and progress needed.

The same type of analyses has been done with ductwork airtightness.

## **2 APPROACH**

This work has been done in the context of the Tight Vent Airtightness Associations Committee (TAAC). TAAC is a European working group, set up and hosted within Tight Vent Europe. The scope of this working group includes various aspects such as:

- airtightness requirements in the countries involved;
- competent tester schemes in the countries involved;
- applicable standards and guidelines for testing;
- collection of relevant guidance and training documents.

At present, the participants are from Belgium, Czech Republic, Estonia, France, Germany, Latvia, Ireland, Poland, Sweden, UK and Spain (Spain has not provided feedback in the questionnaire).

A questionnaire has been developed within the committee to compare building and ductwork airtightness awareness in a broad manner, ranging from requirements to progress needed to promote building airtightness. One or two representative(s) from each country has kindly accepted to answer the questionnaire. This document summarizes their answers.

Other comparison surveys have been done within the TAAC working groups and results have been published in (Leprince & Carrié, 2014), (Leprince & Carrié, 2014).

## **3 RESULTS OF THE STUDY**

### **3.1 Airtightness reference value**

To compare requirements between countries, it is useful to know which airtightness indicators are used. It is interesting to note that the air change rate at 50 Pa,  $n_{50}$ , is no longer the primary indicator: 8 out of 10 countries have at least one indicator that uses the envelope area as reference value. However, the envelope area is not always calculated as defined in ISO 9972; for example in France the reference area excludes the lowest floor and is calculated according to Energy Performance (EP-) calculation. In Germany two reference values are used: either the internal volume for small buildings (below 1500m<sup>3</sup>) or the envelope area for bigger ones. 9 out of 10 countries have a reference pressure value at 50 Pa; only France has an indicator at 4 Pa.

### **3.2 Airtightness in EP-regulation**

In 3 countries (Czech Republic, Sweden, and Latvia) out of 10, building airtightness is not taken into account in the EP-calculation; however, in one of these countries (Czech Republic) there exist minimum requirements on airtightness.

In 6 countries out of 10 (Czech Republic, Estonia, France, Germany, Ireland and UK) there are minimum requirements for building airtightness in EP-regulation. However, those minimum requirements do not necessarily need to be justified. Only France, Ireland and UK require systematic justification of airtightness level either by testing or by applying a certified approach. Table 1 summarizes requirements regarding building airtightness in European regulations. Names and details about regulations are given in Table 3.

In Belgium, there is no minimum requirement but the default value for airtightness is so high that 30-50% of new buildings are tested in order to improve the result in EP calculations. In Germany, even if the test is not required, it is done in most new buildings.

Table 1: Comparison of requirements on building airtightness in European countries

			$< 10 \text{ m}^3/\text{h}\cdot\text{m}^2 @ 50 \text{ Pa}$		
		$< 1500 \text{ m}^3 : n_{50}$		$< 3 \text{ l/h}$	
		$> 1500 \text{ m}^3 : q_{50}$		$< 4.5 \text{ m}^3/\text{h}/\text{m}^2$	
					$< 2.5 \text{ m}^3/\text{h}/\text{m}^2$
		$n_{50}$		$4.5 \text{ l/h}$	
				$1.5 \text{ l/h}$	
					$1 \text{ l/h}$
					$0.6 \text{ l/h}$
		Recommendations: $n_{50}$		$3 \text{ l/h}$	
					$1.5 \text{ l/h}$
	The measured building airtightness should not be higher than the value used in EP-calculation				
				$q_{50} \leq 7 \text{ m}^3/\text{h}/\text{m}^2$	
					
		$q_{4\text{Pa\_surf}}$		$0.6 \text{ m}^3/\text{h}/\text{m}^2$	
					$1 \text{ m}^3/\text{h}/\text{m}^2$
		Recommendations: $q_{50}$		$3 \text{ m}^3/\text{h}/\text{m}^2$	
					$2 \text{ m}^3/\text{h}/\text{m}^2$
					$1.5 \text{ m}^3/\text{h}/\text{m}^2$
	Single-family house/multi-family building/ non-residential building				Relative area. Proportional to the $q_{50}$ or calculated $q_{50}$ if the requirement is not expressed in $q_{50}$ (assuming $V/S=1.1\text{m}$ ).
	Blue: Retrofitted; Green: New				
		Without mechanical ventilation			Countries for which EP-regulation require a minimum airtightness level that has to be justified
		/With mechanical ventilation /			
		With heat recovery			
	Passive house				

### 3.3 Airtightness in EP-programmes

In 8 countries out of 10, EP-calculation for specific programmes depends on airtightness; in the Czech Republic, airtightness is not taken into account in regulatory EP-calculation but is in the programme calculation.

In 7 out of the 10 countries, a programme with requirements on building airtightness exists. For all of them, the airtightness value has to be justified:

- either by systematic testing (in Belgium, Czech Republic, Ireland, Germany and UK);
- or by systematic testing or by applying a certified approach (France);
- or by testing some buildings selected by a third party (Poland).

Table 2 summarizes requirements regarding building airtightness in European energy performance programmes. Names and details about programmes are given in Table 3.

Table 2: Comparison of requirements on building airtightness in programmes in European countries

			$q_{50} < 10 \text{ m}^3/\text{h}\cdot\text{m}^2$		
					
		$< 1500 \text{ m}^3 n_{50}$		$< 3 \text{ l/h}$	
		$> 1500 \text{ m}^3 q_{50}$		$< 4.5 \text{ m}^3/\text{h}/\text{m}^2$	
					$< 1.5 \text{ l/h}$
					$< 2.5 \text{ m}^3/\text{h}/\text{m}^2$
					
		$n_{50}$		$2.5 \text{ l/h}$	
					$0.6 \text{ l/h}$
			NF40	NF 15	
		$n_{50}$		$1 \text{ l/h}$	
					$0.6 \text{ l/h}$
				$0.6 \text{ l/h}$	
				$q_{50} \leq 7 \text{ m}^3/\text{h}/\text{m}^2$	
					
		$q_{4Pa\_surf}$		$0.4 \text{ m}^3/\text{h}/\text{m}^2$	
					$0.8 \text{ m}^3/\text{h}/\text{m}^2$
	Single-family house/multi-family building/ non-residential building		 Relative area. Proportional to the $q_{50}$ or calculated $q_{50}$ if the requirement is not expressed in $q_{50}$ (assuming $V/S=1.1\text{m}$ ).		
	Blue: Retrofitted; Green: New				
	Without mechanical ventilation		With mechanical ventilation		

### 3.4 Airtightness tester schemes

7 countries out of 10 have now a quality framework for building airtightness testers (excluding Estonia, Latvia and Poland). In 4 countries out of the 7, this qualification is required for testing either in the context of the regulation (Belgium Ireland and France) or in the context of a programme (Ireland, France and Poland). In the UK, the qualification is not required by the regulation, however, if a test is performed by a qualified tester a "standardised certificate" is automatically issued and the tester does not need to write a full report.

The evolution of number of testers per countries is given in Figure 1. For Germany, the figure only includes Flib testers, however, other qualifications exist.

As regards the Czech Republic, it is not exactly a qualification, but there exists an association with an ethical code; rules to become a member of the association have tightened in the last 4 years and hence some testers have decided to quit the association.

Names and details about qualifications are given in Table 3.

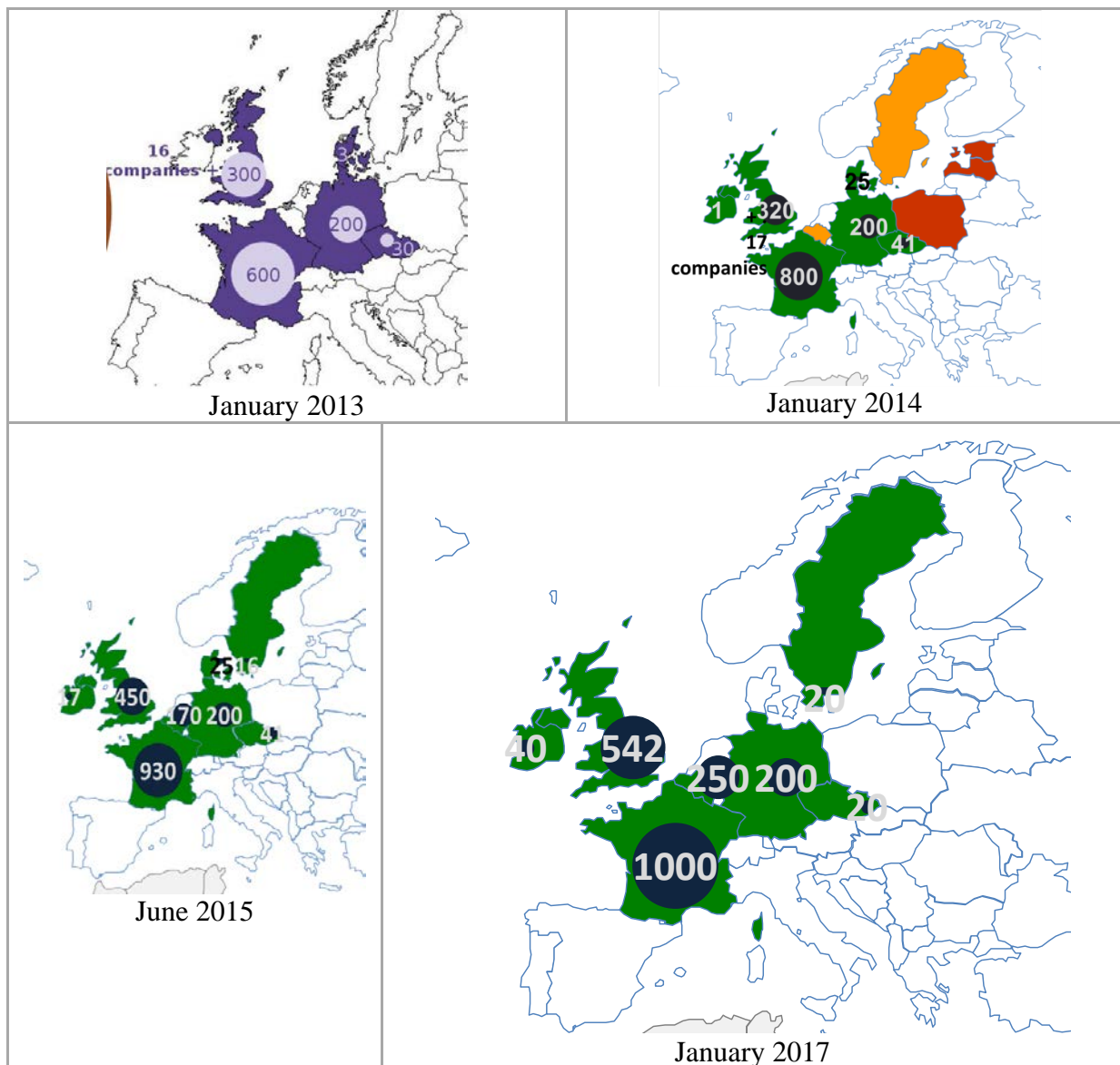


Figure 1: Increase of qualified airtightness testers in Europe in the the last 4 years

### 3.5 Guidelines for airtightness testing

4 countries out of 10 have issued guidelines for airtightness testing in addition to test standard ISO 9972 (Belgium, France, Germany, and UK). Names and details about guidelines are given in Table 3.

### 3.6 Databases

6 countries out of 10 have databases. They mainly contain data for new residential buildings tested by qualified testers. Figure 2 summarizes whether or not countries have a database available and the amount of measured data it represents. Details about databases are given in Table 3.

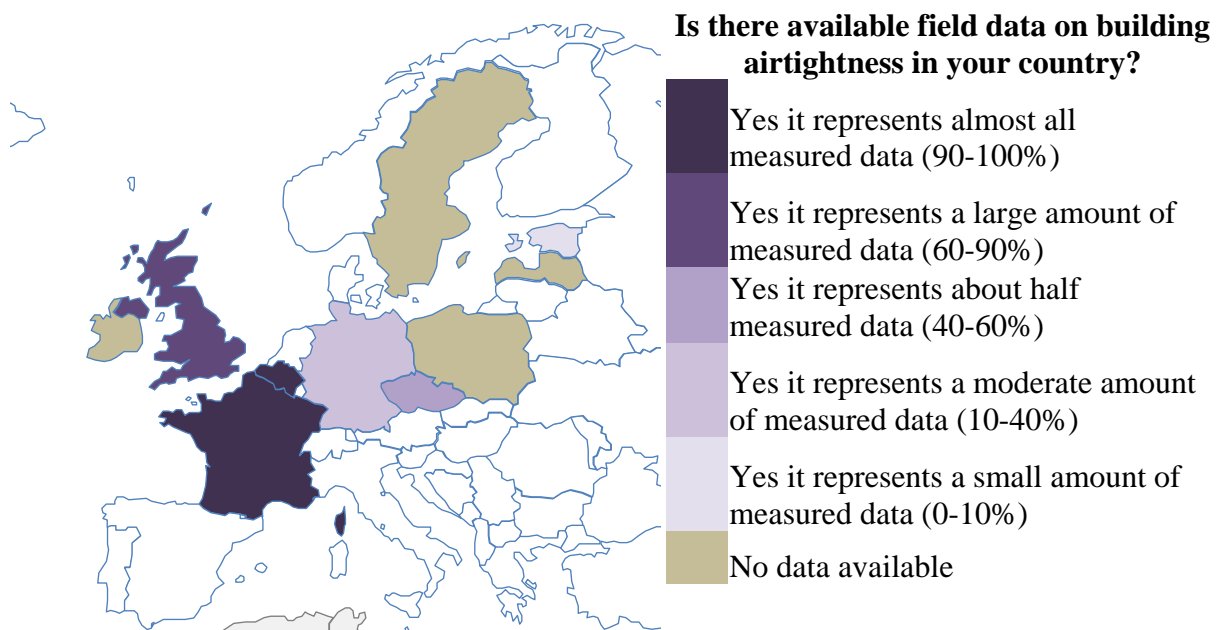


Figure 2: Database in countries and representativeness of measured data

### 3.7 Building airtightness awareness

In all countries, things have changed regarding building airtightness in the last five years. There has been either a significant or a moderate increase of awareness. There has been a new energy performance regulation in 6 out of the 10 countries (Belgium, Estonia, France, Germany, Poland and UK).

According to the respondents, energy use and national policy are the main drivers for change, building damages and European directives are secondary drivers, indoor air quality came last. According to respondents progress needed to promote building airtightness include (by order of priority):

1. Quantified impact in terms of energy use
2. Long-term performance
3. Impact of poor envelope airtightness in mild/hot climates inc. mould issues
4. Quantified impacts in terms of indoor environmental quality

Table 3: Summary of EP-regulations, programmes, qualification schemes, guidelines and database in Europe

EP-regulation	Name	UK	Germany	Belgium	Czech Republic	Poland	Estonia	Ireland	France	Sweden
	Approved Document L of the Building Regulations in England and Wales. Technical Handbook 6 in Scotland.		EnergieeinsparverordnungEnEV 2014	EPB	ČSN 73 0540-2 Thermal performance of buildings - Part 2 – Requirements	Regulation of the Minister of Infrastructure on the technical conditions that should be met by buildings and their location	Methodology for calculating the EP of buildings, regulation of Minister of Economic Affairs and Communications. Minimum requirements for energy performance, regulation of Government	EPBD -->Ireland 2011 Part (L) --> verified via DEAP software programme from government body SEAI	RT2012	

Database		Qualification and Guidelines			Programmes
Access to this database or studies	Database source	Guidelines beyond ISO 9972	Qualification tester schemes	Name	
For ATTMA: A case must be made to explain why you want the data, who you are and what you intend to do with it. For iATS: Access would have to be arranged with co-operation from iATS directors. Please contact manager@iats-uk.org	Both iATS and ATTMA maintain a lodgement scheme for completion results.	ATTMA TSL1 2016 (Dwellings), ATTMA TSL2 (Non-Dwellings) 2010 (currently under revision)	Air Tightness Testing & Measurement Associations (ATTMA) The Independent Airtightness Testing Scheme (iATS)	SAP - Standard Assessment Procedure	UK
<a href="http://www.flib.de/presse/2015/05/2015_05_Meld_Statistik15_Lpdf">http://www.flib.de/presse/2015/05/2015_05_Meld_Statistik15_Lpdf</a>	Flib asks its members for rough figures	EnEV 2014	There are some certification schemes. I.e. FLiB-certification.	DIN V 4108-6/ DIN V 4701-10; DIN V 18599	Germany
databases are not public	BCCA database, EPBD database	STS-P 71-3 2014	KwaliteitskaderLuchtdichtheid	Passiefhuis	Belgium
contact person: Jiri Novak, <a href="mailto:jiri.novak.4@fsv.cvut.cz">jiri.novak.4@fsv.cvut.cz</a>	Database of test results collected by the members of Association Blower Door CZ		Membership in the Association Blower Door CZ	New Green Savings Programme (state subsidies programme for construction of energy efficient	Czech Republic
				NF15 and NF40 by National Fund for Environmental Protection and Water Management	Poland
<a href="https://www.etis.ee/File/DownloadPublic/3cf0f211-274f-4bcf-a63a-6f01651e48b9?name=Fail_Raport.pdf&amp;type=application/pdf">https://www.etis.ee/File/DownloadPublic/3cf0f211-274f-4bcf-a63a-6f01651e48b9?name=Fail_Raport.pdf&amp;type=application/pdf</a> <a href="http://dx.doi.org/10.1016/j.buildenv.2006.06.001">http://dx.doi.org/10.1016/j.buildenv.2006.06.001</a>	Overview of measurements, 2008.				Estonia
	Only via individual testers		The National Standards Authority of Ireland- NSAI (95% of testers), The Irish National Accreditation Board - INAB and we also recognise the British ATTMA	Irish Building Regulations Technical Guidance Document Part (L) - Conservation of	Ireland
Various articles available on airbase (AIVC database): key authors are Mélois, Bailly, Guyot, Carrié, and Leprince.	Data collection via Qualibat qualification	FD 50-784, 2016	Qualibat 8711	Effnergie +, BEFOS Effnergie	France
	"Bygggal "(to be published in 2017)		Diplomeradlufttätthetsprovare (diplomaedairtightnester)		Sweden

### 3.8 Ductwork airtightness

Only 4 respondents have answered the ductwork airtightness questionnaire (Belgium, France, Latvia and Germany). The Czech Republic and Poland have answered that ductwork airtightness was not really considered in their country.

Among the respondents only France (RT2012) and Belgium EPB consider ductwork airtightness as an input in the EP-regulation but there are no minimum requirements. In France, if a value better than the default value is used then it has to be justified (either by test performed by a qualified tester or by certified quality approach). In France, the programmes Effinergie + and Effinergie BEPOS require a justified class A for ductwork airtightness.

In Belgium, the leakage flow according to EN 14134 is used as an airtightness indicator whereas, in France, it is the airtightness class according to EN 12237 (ductwork area is estimated with flat rate based on building area or ventilation flowrates).

Among the respondents, only France has a qualification for ductwork testers (Qualibat 8721) with 35 qualified testers. A specific guideline for testing has been set (FD E 51-767, 2014). There are no field data available in France yet but there should be by the end of 2017.

Among the respondents, only France has had changes regarding ductwork airtightness in the last 5 years with a new regulation, a new programme, a new qualification, an increase in the number of tests, and an increase of awareness.

The awareness on ductwork airtightness has increased moderately in France, Belgium and Germany. In Belgium, this is likely to happen in the near future because of the mandatory control of every ventilation system in new buildings and extensive renovation projects; there is broader awareness regarding the efficiency of ventilation system.

As for building airtightness the main driver for change will probably be the impact on energy use therefore progress is needed to quantify the impact of ductwork airtightness on cooling, heating and fan energy use. Studies on the impact of ductwork airtightness on indoor air quality were also requested.

## 4 DISCUSSION

In most countries building airtightness is now taken into account in the EP- calculation. The number of tests in Europe is increasing (Leprince, Carrié, & Kapsalaki, 2017) either due to:

- requirements on building airtightness with mandatory justification;
- programmes; or
- incentive rewards

Required values are most of the time much easier to achieve than the famous  $n_{50}=0.6$  vol/h. The objective seems to be the growth of awareness rather than the hardness of the constraint. However, in 3 countries the building airtightness is not taken into account in the EP-calculation; in those cases it may be hard to promote it.

Airtightness tester schemes now exist in 7 out of the 10 countries. The number of testers in Europe has almost doubled in 4 years and is increasing rapidly in Belgium, Ireland, France and UK, either because they are requiring airtightness testing (FR, UK, IE) or because they are promoting airtightness by rewarding the EP-calculation if a test is performed (BE).

The development of airtightness testers' schemes goes together with the development of databases; in 5 out of the 7 countries with tester schemes the qualification bodies manage a database. In the UK, qualification bodies provide tools for automatic lodgement of data which automatically collect data from more than 500 tests per working day.

The benefits of a database managed by qualification bodies are:

- collecting reliable data as they are provided by qualified testers
- representing a large amount of measured data if the qualification is required by regulation or programmes.

It is interesting to notice that having a quality framework for testers' qualification does not require specific guidelines for airtightness tests: the Czech Republic and Ireland have a quality framework but no specific guidelines. However guidelines have been developed only in countries where quality framework exist.

Every country agreed that things have changed in the last 5 years regarding building airtightness. The main driver is energy and more work is needed on the field to better:

- quantify the impact of airtightness on energy use; and
- take into account airtightness in the EP regulation.

The durability of airtightness is also a pending question that needs to be further studied. There is a little past and ongoing research on this subject but it gives heterogeneous results (Leprince, Carrié, & Kapsalaki, 2017).

Regarding ductwork airtightness, concern is still low in the field. Progress is needed to better understand the impact of ductwork airtightness on the energy use (fan, cooling and heating) to promote it and include its impact on the energy performance calculation.

## 5 CONCLUSIONS

Regarding building airtightness, we found that 7 out of the 10 countries have minimum requirements that have to be justified by testing or another mean, either in the context of the EP-regulation (for 3 of them) or in specific energy performance programmes. Minimum requirements mostly apply to new buildings and only three countries have a regulation or programme dealing with airtightness of refurbished buildings. 7 countries out of 10 now have a quality framework for building airtightness testers; the number of qualified testers in Europe has almost doubled in 4 years. The development of qualification has induced the development of databases. Field measurement data are now available in 6 countries out of 10. Most of the time, databases are managed by testers' qualification bodies and contain mainly data of new residential buildings.

All respondents acknowledge that awareness regarding, building airtightness has grown in their country in the last 5 years. The main motivation remains energy use, however work on this topic is still needed to better quantify the impact of airtightness on energy use.

Conversely, ductwork airtightness does not seem to be taken into account (neither in regulation nor in energy performance programmes) in most European countries. In our survey; only France and Belgium take into account ductwork airtightness in their energy performance calculation. And only France has an EP- programme with requirements on ductwork airtightness and a qualification for testers. Progress is needed to better understand the impact of ductwork airtightness on energy use (fan, cooling and heating) and indoor air quality.

## 6 ACKNOWLEDGEMENTS

The authors would like to acknowledge the support of TightVent Europe and AIVC to conduct this review. The authors also would like to thank the Belgian Construction Certification Association for its support.

The authors wish to express special thanks to the TAAC members who have kindly accepted to answer the questionnaire.

## 7 REFERENCES

- Leprince, V., Carrié, F., & Kapsalaki, M. (2017). Impact of Energy Policies on Building and Ductwork Airtightness. *Proceedings of the 10th International BUILDAIR-Symposium*. Hannover: BUILDAIR.
- Leprince, V., & Carrié, F. (2014). Reasons behind and lessons learnt with the development of airtightness testers schemes. *International Workshop: Quality of Methods for Measuring Ventilation and Air Infiltration in Buildings / Brussels, Belgium 18-19 March 2014* (pp. 103-107). AIVC.
- Leprince, V., & Carrié, F.-R. (2014). Comparison of building preparation rules for airtightness testing in 11 European countries. *35th AIVC Conference " Ventilation and airtightness in transforming the building stock to high performance"*, Poznań, Poland, 24-25 September 2014 (pp. 501-510). AIVC.

# Ventilative Cooling on the test bench - Learnings and conclusions from practical design and performance evaluation

Holzer Peter<sup>\*1</sup>, Moherndl Philipp<sup>2</sup> and Psomas Theofanis<sup>3</sup>

1 Institute of Building Research & Innovation  
Wipplingerstraße 23/3  
1010 Vienna, Austria  
peter.holzer@building-research.at

2 Institute of Building Research & Innovation  
Wipplingerstraße 23/3  
1010 Vienna, Austria

3 Aalborg University  
Department of Civil Engineering  
Thomas Manns Vej 23  
9220 Aalborg, Denmark

## ABSTRACT

Based on 3 short time performance measurements, 4 visits together with user-interviews, 3 involvements in Ventilative Cooling (VC)-building-design, 2 long-term case studies and 11 expert interviews the paper presents a list of key performance-indicators of successful Ventilative-Cooling solutions as well as challenges together with examples of their successful overcoming.

Information has been collected from projects located in Austria, using Ventilative Cooling, both natural and mechanical ventilation, in both residential and office buildings, mainly in urban surroundings.

The list of key-performance indicators is:

1. Design for very low pressure drop in the VC-system.
2. Design for significant air change rates in the VC-system.
3. Limit the operating time of automated VC to periods that physically make sense.
4. Keep the VC-System free from Influences from AC-Components.
5. Enhance VC-effects by heat transmission from adjacent rooms
6. Design the VC-system for summer comfort at elevated air temperatures
7. Strictly emphasise Operability and Reliability of VC Components because the challenges hide behind details:
  - Safety & security aspects dealing with injury, burglary and vandalism
  - Thermal Performance limitations
  - Comfort aspects dealing with noise, dust and humidity
  - Operational aspects dealing with (mis)adjustments in the control systems
  - Economic aspects dealing with investment and maintenance

## KEYWORDS

Ventilative Cooling performance indicators, Ventilative Cooling challenges

## 1 INTRODUCTION

Based on short time performance measurements, visits together with user-interviews, involvements in VC-building-design, long-term case studies and expert interviews the paper presents a list of key performance-indicators of successful Ventilative Cooling solutions and a list of major challenges together with examples of their successful overcoming.

## 2 KEY-PERFORMANCE INDICATORS

### 2.1 Design for very low pressure drop in the VC-system

A very low pressure drop is mandatory for successful VC application.

If the air driving force is buoyancy, typically design for less than 5 Pa.

If the air driving force is mechanical ventilation, design for less than 100 Pa.

Driving force by buoyancy equals:<sup>1</sup>

$$\Delta p = \left(\frac{1}{30}\right) \times \Delta T \times h \quad (1)$$

$\Delta p$ : pressure difference [Pa],  $\Delta T$ : temperature difference [K],  $h$ : height [m]

This leads to driving forces in the range of 5 Pa, rarely more. Wind pressure might help with another 5 Pa, equalling the dynamic pressure at a wind speed of  $\approx 3$  m/s.

Driving force by mechanical ventilation technically can be raised to some hundred Pa, but economically and ecologically is limited by the call for high power efficiency (COP), given by the ratio of  $P_{\text{thermal}} / P_{\text{electrical}}$ . A total pressure drop of 100 Pa will lead to a power efficiency (COP) of  $\approx 20$ , which is a reasonable benchmark, compared to a mechanical chiller. EN 13779 defines the best category of Specific Fan Power (SFP) lower than 500 W/(m<sup>3</sup>.s), equalling a pressure drop of 250 Pa. In Ventilative Cooling this is still too much. VC applications have to be designed within the non-existing category “SFP 1+” with a specific fan power of lower than 200 W/(m<sup>3</sup>.s), equalling a pressure drop of 100 Pa.<sup>2</sup>

A well performing example of a VC exhaust ventilation was monitored in a recent Viennese social housing project. The air is (1) drawn in via automated staircase windows, (2) guided through the central aisles, (3) drawn out via <10 m duct length by a central exhaust ventilator. The monitoring proofed a Specific Fan Power (SFP) lower than 170 W/(m<sup>3</sup>.s), equalling a total pressure drop of 85 Pa, resulting in COP = 24 at an extract air flow of 22.000 m<sup>3</sup>/h.<sup>3</sup>



Figure 1: Air inlet window with chain actuator (left) Exhaust ventilator on roof (right)

<sup>1</sup>Kolokotroni, M., Heiselberg, P. (2015).

<sup>2</sup> Calculations based on an average ventilator efficiency ratio of 50% and air temperature rising by 3 K.

<sup>3</sup>Holzer, P. et al. (2016)

## 2.2 Design for significant air change rates in the VC-system

ACH > 3 h<sup>-1</sup> is mandatory, ACH > 5 h<sup>-1</sup> is desirable to achieve substantial heat removal and justify noteworthy investments.

In VC applications, the nightly air change rate very often is the bottleneck. The following picture shows the balance of temperature and energy flow in a standard room within a characteristic Central European summer.

A massive wall, ceiling or floor may store up to 70 Wh/m<sup>2</sup> within one day. To release this heat by night ventilation, seven hour duration of specific heat flow of 10 W/m<sup>2</sup> is necessary. In a 24 m<sup>2</sup> room, under realistic circumstances this leads to the need of at least ACH 8,0 h<sup>-1</sup>, better ACH 10,0 h<sup>-1</sup>. ACH 5 is five to ten times more than needed for hygienic aspects only. Thus, unlink the function of Night Ventilation from the function of hygienic ventilation. Besides, trust windows. In the worst case of single sided ventilation in still air at only 3 K temperature difference a fully opened window of 2 m height and 0,5 m width will already provide an air exchange of approx. ≈300 m<sup>3</sup>/h.<sup>4</sup>

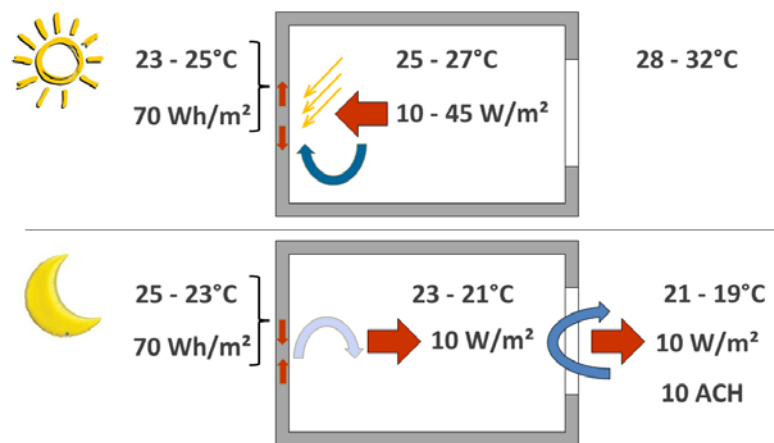


Figure 2: Scheme of typical VC temperatures, loads and airchangerates

## 2.3 Limit the operating time of automated VC to periods that physically make sense

If automated, run the VC system only at a temperature difference potential of 2 K or higher. Do not shoulder the challenges of VC during periods of weak performance.

Automated VC always consumes resources, such as energy and maintenance. Sometimes it interferes with the expectations of occupants, e.g. in case of noise.

Note: 1.000 m<sup>3</sup>/h at 1 K rise in temperature carry the thermal load of 340 W. If driven mechanically at “SFP 1” at 500 W<sub>el</sub>/(m<sup>3</sup>.s) this will cause an electrical load of 140 W. Thus, running automated Ventilative cooling at low indoor-outdoor temperature differences is only effective in naturally driven systems. Even there, 2 K seem to be a recommendable threshold.

The following figure shows short time monitoring results from mechanical ventilative cooling in a Viennese office during a mild summer period. Outdoor Air Temperature (green)

<sup>4</sup> According to formula I.14 from ISO 13791:2012 
$$m_{a,T} = c_d \rho \frac{A_T}{3} \left( \frac{\Delta\theta g H}{T_m} \right)^{0,5}$$

undergoes the extract air temperature (yellow) at 22:00. Ventilation runs from 22:00 to 06:00, which turns out to be a good choice regarding the start, but could have been extended regarding the end.<sup>5</sup>

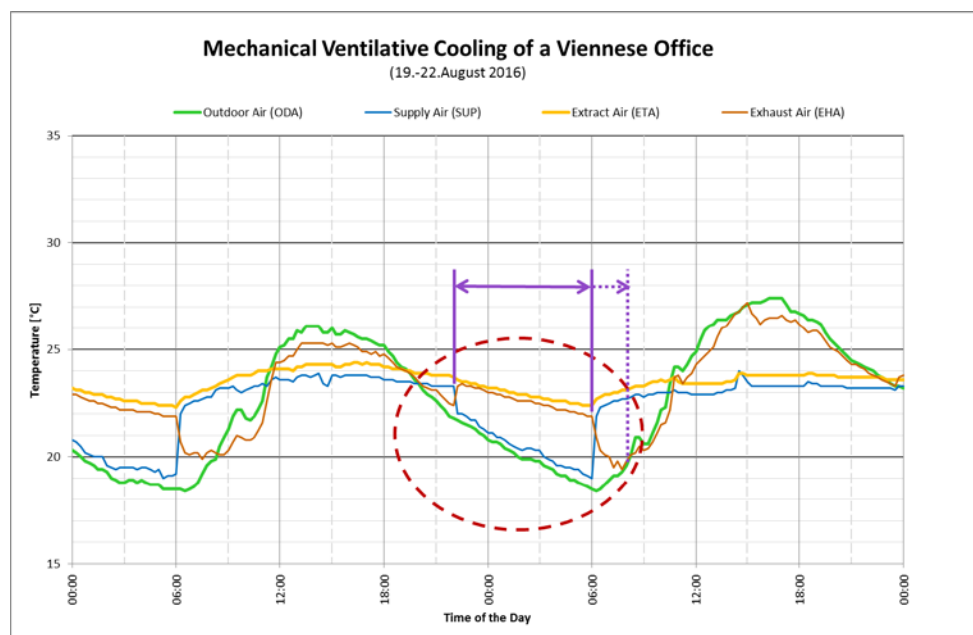


Figure 3: Temperature profile of mechanical Ventilative Cooling system in an office

## 2.4 Keep the VC-System free from Influences from AC-Components

Sometimes there are good reasons, to add some AC-components even within Ventilative Cooling concepts. If doing so, make sure that within the same building zone the AC components are strictly shut off during operation of Ventilative Cooling. A parallel operation of VC and AC has to be safely avoided.

An exemplary case has been observed during Annex 62 in one of the case study buildings: In an atrium of an office building a mechanical ventilation system automatically started into operation for dehumidification parallel to buoyancy driven night ventilation. The mistake was observed and fixed during the monitoring.<sup>6</sup>

Another case has been observed in a single family home with both mechanical crossflow ventilation with heat recovery and automated window ventilation: The balance between these two systems was highly problematic until there has been agreed upon a strict alternative-bivalent approach: The mechanical system now operates only up to an outdoor temperature of 12°C. The automated window ventilation fully takes over if outdoor temperature rises further. The switching point was defined upon consideration of energy efficiency and draft risk.

Finally, we found ongoing discussion, if Ventilative Cooling still is a good option, as soon as Air-conditioning is applied. And, furthermore, if Ventilative Cooling still is a good option, when climate change or urban heat island effect raise the ambient temperatures: The answer is

<sup>5</sup> Holzer, P. et al. (2016)

<sup>6</sup> Holzer, P. et al. (2016)

two time: Yes, it is, as long as air-conditioning is limited to moderate set point temperatures, e.g. 26°C and as long AC and VC are run strictly in alternative mode.

For one of our short time case studies we extrapolated the following scenarios of hybrid cooling: Figure one by green columns illustrates the days within a year with Ventilative Cooling being appropriate to keep the indoor set point temperature of 26°C. Sometimes VC won't be sufficient. If so, AC has to take over. Figure two illustrated the same, but against an outdoor temperature dataset with constantly plus 3 K. The figure shows, that the periods of necessarily running the AC are rising during summer, but cooling need also extends to early summer and late summer when, VC will take over. In fact, both the number of VC-days and the sum of thermal load being removed by VC stays constant.<sup>7</sup>

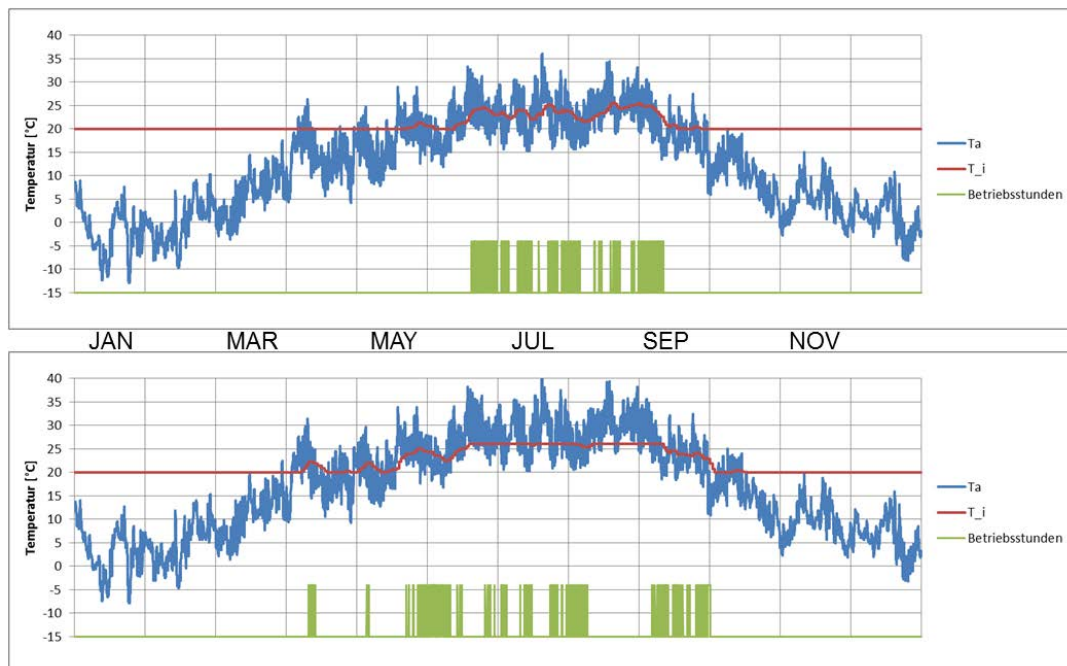


Figure 4: Days with climatic VC potential before and after a 3K outdoor climate change

## 2.5 Enhance VC-effects by heat transmission from adjacent rooms

There are promising examples for enhancing the effect of ventilative cooling by connecting adjacent rooms with deliberately high thermal conductivity.

We found examples of both residential and University buildings, with the central staircases and hallways being used for VC, while the adjacent rooms are thermally connected with building-elements of deliberate poor insulation quality.

This may be a very cost effective solution. It's comparably easy to effectively ventilate staircases and hallways, while it is costly and technically challenging to apply automated night ventilation to flats or to numerous single offices.

The following figure shows an example from a 1960's high-rise office building of Vienna's Technical University which has recently been refurbished to Plus-Energy-Standard, including

<sup>7</sup>Holzer (2016)

buoyancy driven Night Ventilation of the staircases and hallways. The offices and seminar rooms are separated from the hallway by single-pane laminated safety glass. The overflow orifice for night ventilation is situated above the lockable hallway door.<sup>8</sup>

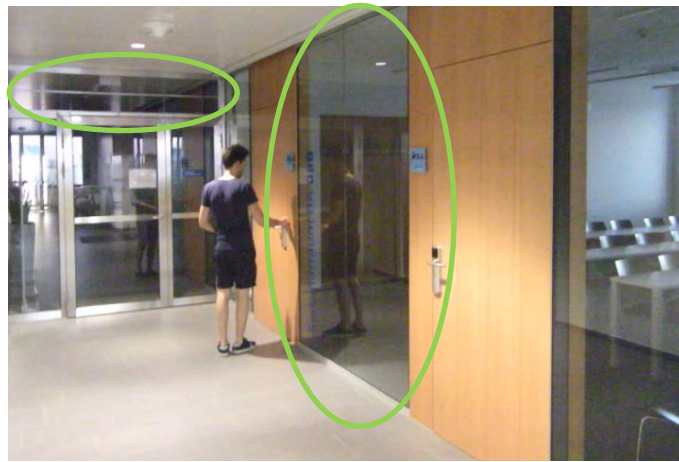


Figure 5 Glazed partition walls with high U-values and overflow orifice

## 2.6 Design the VC-system for summer comfort at elevated air temperatures

Good VC performance needs elevated indoor air temperatures.

Thus, both architecture and building technology have to support the VC-system by designing for summer comfort at elevated indoor air temperatures, e.g. by offering additional technical devices for personal comfort control or by encouraging people to let go strict dress codes.

Ventilative Cooling will not work, if daytime indoor temperatures are kept already at “modern” HVAC-standards.

Encourage your client based upon findings of adaptive comfort research as well as upon findings of resultant temperature at elevated air movement (both to be found in ISO 7730:2005).

The following figure, taken from ISO 7730:2005 illustrates the medium airspeed necessary to elevate the comfort temperature from 26°C for standard summer clothing (0,5 clo) and for standard sitting tasks (1,2 met). Note: Airspeed of only 1 m/s without any technical cooling already elevates the comfort temperature by 3 K.

---

<sup>8</sup> Holzer, P. et al. (2016)

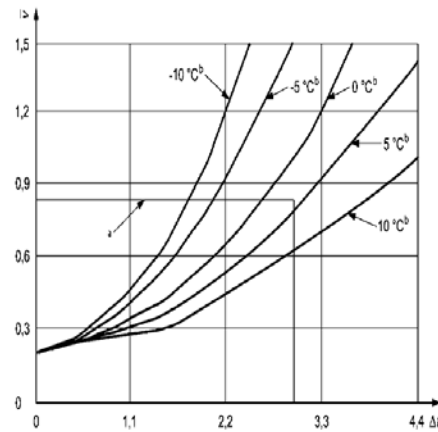


Figure 6: Mean air speed over elevation of comfort temperature

## 2.7 Strictly emphasise Operability and Reliability of VC-Components

In manually controlled as well as in automated systems the operability of Ventilative Cooling Components, especially of the airflow guiding and airflow enhancing components, turns out to be a key success criteria.

Within Annex 62 we identified these aspects as challenges of Ventilative Cooling in an operational context:<sup>9</sup>

- Safety & security aspects dealing with injury, burglary and vandalism
- Thermal Performance limitations
- Comfort aspects dealing with noise, dust and humidity
- Operational aspects dealing with (mis)adjustments in the control systems
- Economic aspects dealing with investment and maintenance

We learned: Keep operation strictly simple!

If VC is manually controlled, design ventilation openings free from interference with storage area and furniture, place opening handles very ergonomically, chose robust and long lasting mechanisms, always include anti-slam devices which prevent the ventilation openings slamming in case of draught.

If mechanical, put very intuitive operating devices at very intuitive places, be aware of stand by energy-consumption, operating noise levels, life cycles and maintenance; and find smart answers to questions relating to injury and vandalism.

Furthermore: Ensure strict rain protection: better by architecture than by rain sensors. Ensure burglary protection and consider needs for intimacy.

The next figure illustrates an example of a window, meant for manually operated night ventilation in an Austrian school, which was analysed within Annex 62: Protection against rain, burglary and fall is secured by a fixed metal grill in front of the window. But everyday operation of the window is handicapped by the exceptional deep windowsill, which invites users to use it as a shelf board, in fact blocking the window.

<sup>9</sup>Holzer, P. et al. (2015)



Figure 7 Window for manual night ventilation secured against rain burglary and fall but blocked by books

In our field research we found many examples how to deal with the risk of getting injured by automated ventilation openings, simple ones and sophisticated ones.

A high-tech example is shown in the next figure: A window which can be operated both manually and automated. The window handle is combined with an electro-mechanical device that disconnects the chain actuator from the window-frame, such allowing manual operation. Furthermore, the window gaskets are equipped with internal electronic sensors, ensuring an immediate interruption of the closing process if detecting an unexpected resistance. The windows are installed in a Viennese school. The flipside of the coin is the higher costs for this level of function, and the notable need for maintenance.



Figure 8 Automated window, with optional manual operation and resistance sensitive gasket

Another example showing the challenges of protecting against injuries was found at HCU “HafenCity University Hamburg”: Pictograms tell users not to interfere with the automated bottom hung ventilation windows, mounted already at elevations of > 2 m above floor level. Furthermore, protective grids secure ventilation flaps.



Figure 9: Ventilation flaps with additional warning pictogram and protective grid against finger injury

### 3 CONCLUSIONS

Ventilative Cooling proofs to be a robust and highly energy efficient solution to support summer comfort in buildings, not at justin NZEB's. Ventilative Cooling furthermore proofs being applicable in both cool and warm temperate climate. An International VC Building Database has been elaborated within Annex 62, so far documenting 99 buildings using Ventilative Cooling from 8 European Countries.<sup>10</sup>

### 4 ACKNOWLEDGEMENTS

This paper is based upon the findings of Annex 62 Ventilative Cooling, within IEA EBC programme. The authors express their thanks to their colleagues within Annex 62 and to their national funding authorities: In Austria the Federal Ministry for Transport, Innovation and Technology. In Denmark the EUDP (Energy Technology Development and Demonstration Program) together with VELUX A/S, DOVISTA A/S and VISILITY ApS.

### 5 REFERENCES

Kolokotroni, M., Heiselberg, P. (2015). Ventilative Cooling State-of-the-Art Review. Published via Internet: <http://venticool.eu/annex-62-publications/deliverables/>

Holzer, P. et al. (2015). Austrian Annex 62 Report Work Package 2. Currently unpublished.

Holzer, P. et al. (2016). Austrian Annex 62 Report Work Package 3. Currently unpublished.

Holzer, P. (2016). Presentation at IEA cross-linking workshop 20.10.2016. Published at <https://nachhaltigwirtschaften.at/de/iea/technologieprogramme/ebc/iea-ebc-annex-62.php>

Holzer, P., Moherndl, P., Psomas, T., O'Sullivan, P. (2016). International Ventilative Cooling Application Database. Published at <http://venticool.eu/annex-62-publications/ventilative-cooling-application-database/>

<sup>10</sup>Holzer, P., Moherndl, P., Psomas, T., O'Sullivan, P. (2016)

# Bulk airflow measurements in a large naturally ventilated atrium in a mild climate

Marta Avantaggiato<sup>\*1,2</sup>, Nuno Mateus<sup>3</sup>, Annamaria Belleri<sup>1</sup>, Wilmer Pasut<sup>1</sup>,  
Guillherme Carrilho da Graça<sup>3</sup>

*1 EURAC Research  
Viale Druso 1  
Bolzano, Italy*

*2 Department Industrial Engineering, University of  
Padua  
Street address  
Padova, Italy*

*3 Instituto Dom Luiz, Faculdade de Ciências,  
Universidade de Lisboa, 1749-016, Lisboa, Portugal*

*\*Corresponding author:  
marta.avantaggiato@eruc.edu*

## ABSTRACT

In recent years, concerns about global warming and greenhouse gas emissions have motivated designers to reduce building energy consumption through the implementation of passive solutions without compromising users' thermal comfort. This evidence has stimulated a renewed interest in designers for the exploitation of natural ventilation as means of passive cooling solutions. The adoption of ventilative cooling is particularly suitable for large spaces (non-residential buildings) as a measure to reduce the HVAC system high cooling loads. Due to the inability to control and ensure a constant airflow rate through natural ventilation most of the times designers choice goes towards mixed-mode buildings. Mixed-mode buildings are designed in such a way that the HVAC system acts as backup to prevent uncomfortable conditions when natural ventilation is not sufficient to guarantee a comfortable environment. Unfortunately, information about the actual performance of mixed-mode buildings is difficult to obtain due to the difficulties to set up measurements in naturally ventilated buildings that highly depend on building geometry and outdoor conditions (weather, pollution and noise). This limitation leads designers to follow a traditional design approach based on mechanical air conditioned systems.

With the aim of reducing the lack of information about the actual performance of mixed-mode non-residential buildings, this paper presents a full-scale bulk air flow measurements for a large naturally ventilated atrium in a mild climate. The methodology and the results presented in this paper refers to the first step of a more complete and complex work which aims at assessing the performance of the large mixed-mode atrium. The general performance of the atrium are tested through a long term measurement campaign which is indeed ongoing. The final aim is to quantify the effect of ventilative night cooling in terms of cooling energy reduction and indoor thermal environment.

## KEYWORDS

Full-scale bulk airflow measurement, tracer gas technique, large naturally ventilated atrium

## 1 INTRODUCTION

In recent years, concerns about global warming and greenhouse gas emissions have motivated designers to reduce building energy consumption through the implementation of passive solutions without compromising users' thermal comfort. The continuous improvements of building thermal envelope properties combined with the increased level of internal gains changed the non-residential building energy balance. These effects led to a lower heating demand while raising the problem of increased cooling demand during the whole year. This evidence has stimulated a renewed interest in designers for the exploitation of natural ventilation as means of passive cooling solutions.

The presence of large open spaces, such as lobbies and atria, in non-residential buildings architecture helps the implementation of passive cooling solutions through natural ventilation strategies. Before the uptake of air conditioning, especially in Eastern countries, indeed, large open atria property of air stratification were used to remove warm air from top allowing colder air entering from lower level providing comfortable conditions (Kuppaswamy I., 2015). In the case of large spaces, the adoption of passive cooling systems is further justified by the higher users' tolerance to warmer thermal environment under summer conditions, as proved by (Chun C., 2004 ; Pitts A., 2008).

Nowadays, the practise of using natural ventilation for cooling purpose is named Ventilative cooling. The international research project Annex 62 of the International Energy Agency (IEA), (IEA EBC Annex 62, 2014-2017), focuses its research activity on solutions and design methods for ventilative cooling.

Due the inability to control and ensure a constant airflow rate through natural ventilation most of the times designers choice goes towards mixed-mode buildings. Mixed-mode buildings are indeed designed in such way that the HVAC system helps to prevent uncomfortable conditions when natural ventilation is not sufficient to guarantee a comfortable environment. Information about ventilation design strategies, controls and integration between natural ventilation and HVAC systems can be found in literature. For example, within the Annex 62 this typology of information for different case studies among Europe have been collected in a database. Information can be retrieved on the project webpage (Annex 62, 2014-2017).

Nevertheless, information about the actual performances of mixed-mode buildings is difficult to source. This lack of information is keeping designers and building owners to follow a traditional design based on reliable mechanical and air conditioned systems.

The lack of information is justified by the objective measurements difficulties of assessing the actual performance of naturally ventilated spaces. Full-scale investigation of ventilation performances are mostly assessed by trace gas techniques. When the size of the internal volume involved is greater than 5000 m<sup>3</sup> measurement difficulties becomes progressively more considerable (IEA EBC Annex 26, 1998).

Difficulties go from technical to economic aspects. Because of the big volume, reaching a perfect air/gas mixing is really challenging and large quantity of traceable gas and time for the experiment are required. Large spaces implicate the need of a high number of sensors to track the evolution of the conditions inside the space. It has also to be considered the variability of outdoor weather condition to which the observer has no control. The quantification of the bulk airflow rate is also a requirement when performing the validation of thermal simulation models (Mateus et al., 2016).

This paper presents the methodology and the results of full-scale bulk air flow measurements in the naturally ventilated atrium of a mixed-mode multi-service building located in a mild climate. A first full-scale bulk airflow measurement is necessary in order to derive a correlation factor between the bulk air flow rate and the air velocity through the inlet windows. The correlation can be later used to quantify the airflow through openings at night measuring air velocity at inlet level during a long term measurements campaign.

The methodology and the results presented in this paper refers at the first step of a more complete and complex work which aims at assessing the performance of the large mixed-mode atrium. The general performance of the atrium are tested through a long term measurement campaign which is indeed ongoing. The final aim is to quantify the effect of ventilative night cooling in term of cooling energy reduction and indoor thermal environment.

## **2 CASE STUDY**

The building is located in the mild climate of Seixal, in the south bay area of Lisbon, Portugal (see Figure 1). It is a multi-service building consisting of two main blocks with 3-floors connected by a central atrium. Each block is equipped with both single and open space

offices. On its north–west orientation the building faces an Auditorium which is physically separated from the main building. The ground floor is occupied by the atrium and a cafeteria. In the basement there are a parking, the technical room and an archive. The two offices blocks face North and South orientation.

The central atrium (volume  $\approx 16244 \text{ m}^3$ ) is a transitional space for temporary users and people working in the adjacent offices as well as a working area for internal employees. The space is conditioned by means of a radiative floor system, which is supported, during mid-season and summer, by a night-time ventilative cooling strategy. The nighttime ventilative cooling strategy involve different openings located at different oriented façades.



Figure 1 Building view from the outside (left), an internal view of the central atrium (middle) and night ventilation strategy (right)

Wind and stack-driven ventilation runs during night circulating airflows from West to East side of the atrium through top hung openings located at different heights. The strategy was designed considering the prevailing wind direction on the site which at night usually comes from the ocean, namely from North-West orientation.

On the inlet side (West façade) there are two row of windows consisting of 8 openable module each. On the outlet side (East façade) there is one row of 12 windows and just 5 of them can be operated. All the windows have two positions, totally closed or  $25^\circ$  opening angle. No modulation is applied. Windows features are reported in Table 1.

Table 1 Features of the windows used in the ventilation strategy

Façade Orientation	Dimension	Typology	Maximum opening angle	Number of Module	Reference height of the middle plane from the ground
West	130 cm x 95 cm	Top hung tilted	$25^\circ$	14 (7 mod/row)	2.12 m (first row) 3.1 m (second row)
	85 cm x 95 cm	Top hung tilted	$25^\circ$	2 (1 mod/row)	2.12 m (first row) 3.1 m (second row)
Est	124 x 145 cm	Top-hung tilted	$25^\circ$	5	13.8 m

The windows are equipped with electric actuators which are connected to the general Building Management System (BMS) of the building. The control strategy is manual which means that the technical engineer of the building, based on outdoor and indoor climatic conditions, decides between two different modes. When mode A is selected, on inlet side only the second row of windows is opened while on outlet side 3 windows are operated. Under mode B, all openable windows on both inlet and outlet are operated. Information about the two modes are shown in Table 2.

Table 2 Control modes for windows operations

Mode	Inlet Openings	Outlet Openings	Opening Area [ $\text{m}^2$ ]	Opening Area/Floor Area
A	Second row	3 modules	9.7	1%

B	First&Second row	5 modules	18.7	2%
---	------------------	-----------	------	----

When night ventilation is applied, the windows are kept opened for all night starting from closing hours till the morning after.

The ventilation strategy was tested by the technical engineer also during working hours. Because of complains about draught from the people working in the atrium, he decided to operate windows only at night.

### 3 METHODOLOGY

Full-scale measurements of airflow in buildings are commonly performed by using tracer gas technique. This technique is based on the injection of gas into the space which concentration response is then measured. Carbene dioxide was used as tracer and two different tracer gas methods were tested. The first method, *Constant release method*, consists in a continuous release of a traceable gas into the space with a constant flow during the entire measuring period. When stabilized indoor conditions are reached the bulk airflow can be calculated by solving the mass balance described in equation (1) (Mateus et al.,2016).

$$F\left(\frac{m^3}{h}\right) = \frac{CO_{2,released} \left(\frac{mg}{s}\right)}{[CO_{2,outlet}] - [CO_{2,inlet}] \left(\frac{mg}{m^3}\right)} * \frac{1}{3600} \quad (1)$$

After reaching stabilized indoor conditions the release of the CO<sub>2</sub> is stopped and a natural decay of its concentration begins. By knowing the CO<sub>2</sub> concentration at multiple point during the decay it is possible to calculate the airflow through the equation (2) (Cui et al.,2015).

$$F\left(\frac{m^3}{h}\right) = \frac{(\sum_{j=1}^n t_j) * \sum_{j=1}^n \ln[C(t_j) - C_{bg}] - n * \sum_{j=1}^n \ln[C(t_j) - C_{bg}]}{n * \sum_{j=1}^n t_j^2 - (\sum_{j=1}^n t_j)^2} * V_{atrium} \quad (2)$$

The bulk air flow rate is calculated with both methods and then the average value is used to calculate the correlation constant *k* through equation (3).

$$k = \frac{F}{v_{air\_in}} \quad (3)$$

### 4 EXPERIMENTAL SET-UP

The experiment is conducted under control mode A (see Table 2). Figure 2 shows the measurement setup. The CO<sub>2</sub> injection took place at 3.1 m from ground, close to the inlet in two different positions. The air velocity of the air entering the atrium is monitored at the same level. A central row of CO<sub>2</sub> and air temperature sensors is used to track the development of the conditions (air temperature and CO<sub>2</sub> concentration) inside the atrium as well at the outlet level. Sensors characteristics are collected in Table 3.

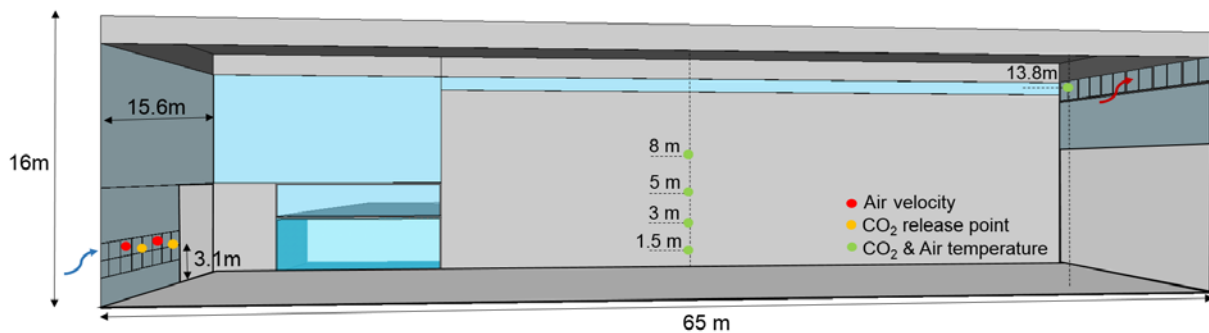


Figure 2 Location of the sensors used for the experiment and CO<sub>2</sub> release point location

Natural ventilation relies on natural forces. For this reason information about the actual climatic conditions of the building site are important for the assessment of the ventilation performance. Therefore a dedicated weather station was positioned close to the building in an open free area at 5 m above ground level. It consists of a wind speed and direction sensors, a pyranometer to measure global and diffuse radiation and a temperature and humidity sensor. The sensors specification are collected in Table 3.

The experiment was performed at the end of May 2017, after public opening hours, once the building was not occupied. Starting from 6:30 p.m. 2 CO<sub>2</sub> canisters released CO<sub>2</sub> in the atrium for two hours and a half before reaching stabilized conditions at around 9:15 p.m. During this time the CO<sub>2</sub> release rate was monitored in order to assure it was a constant rate. Once the stability was reached the release of CO<sub>2</sub> was stopped and a natural decay process started and lasted about 45 minutes. The experiment concluded at 22:00 p.m..

Table 3 Specification of the measurement equipment used

Sensor	Measurement	Specification	
F900 S-P Airflow Sensor, ONSET	Air velocity ( indoor)	Range	0.15 to 10 m/s
		Accuracy	10% ± 0.05 m/s
CO2 Meter (K-33 ELG)	Carbon dioxide ( indoor)	Range	0-10000 ppm
		Accuracy	± 30 ppm + 3%
	Temperature( indoor)	Range	-40 to + 60°C
		Accuracy	±0.4 °C at 25 °C
Wind Monitor 05103 Campbell Scientific	Wind speed(outdoor)	Range	0-100 m/s
		Accuracy	± 0.3 m/s or 1% reading
	Wind Direction(outdoor)	Range	0 to 360 °
		Accuracy	±3 °
Pyranometer SPN1 Delta-T Devices	Solar radiation ( global and diffuse)	Range	1 to 2000W/m <sup>2</sup>
		Accuracy	±5% ±10 W/m <sup>2</sup>
HOBO (U12-013)	Temperature (outdoor)	Range	-20.0 to 70.0 °C
		Accuracy	±0.35 °C from 0 to 50.0 °C

## 5 EXPERIMENTAL RESULTS

Pressure differences drive the circulation of airflow within building. The pressure difference can be either generated by wind or by the thermal stratification inside the building, named buoyancy. Starting from the measured data, we first calculated the pressure differences due to wind and buoyancy, in order to understand the main driving forces during the experiment. The pressure force due to wind is calculated according to equation (4) while the one produced by buoyancy according to equation (5). The combined effect can be calculated with equation (6).

$$\Delta P_{,w} = \frac{1}{2} \Delta C_p \rho W_s^2 \quad (4)$$

$$\Delta P_{,b} = \rho g (H_{out} - H_{in}) \left( \frac{T_{out} - T_{outlet}}{T_{outlet} + 273.15} \right) \quad (5)$$

$$\Delta P_{,tot} = \sqrt{\Delta P_{,w}^2 + \Delta P_{,b}^2} \quad (6)$$

The pressure coefficient is the ratio of the local wind driven static pressure and the incoming wind pressure express by equation (7)

$$C_p = \frac{P_{local}}{\frac{1}{2}\rho U_{ref}^2} \quad (7)$$

The pressure coefficient difference,  $\Delta C_p$ , used in equation (4), is the difference between the average pressure coefficient at inlet and the one at outlet calculated according to equation (7). By means of a CFD simulation model we calculated the local pressure,  $P_{local}$ , generated by the wind at inlet and outlet level for eight different wind orientations. The simulation have been run with the commercial CFD code Ansys Fluent 15 (Ansys, 2017) and the results are collected in Table 4.

Table 4 Pressure coefficient at inlet, outlet and difference

	N	NE	E	SE	S	SW	W	NW
$C_{p_{in}}$	-0.73	-0.27	-0.18	-0.54	0.00	0.46	0.97	0.31
$C_{p_{out}}$	-0.64	0.07	0.19	0.33	-0.58	-0.72	-0.42	-0.82
$\Delta C_p$	-0.09	-0.35	-0.37	-0.86	0.58	1.18	1.39	1.13

Minute by minute, depending on the wind direction we calculate the  $\Delta P_w$  by using the associated  $\Delta C_p$ . The analysis of the pressure trend during the experiment is essential to have a picture of the behaviour of the atrium during the whole experiment.

The graph in Figure 3 shows the distribution of the wind direction, the wind speed and the pressure generated by wind during the experiment. The prevailing wind direction was from north and north-west orientation. It is also observed a progressive decrease of the wind speed along the duration of the experiment. While the pressure due to wind decrease with time, the difference between indoor and outdoor temperature increase resulting in an increase buoyancy pressure (Figure 4). For the first half of the experiment the main driving force is the wind pressure which is very variable and unstable as shown in Figure 5. In the second half, the airflow is mainly driven by the buoyancy resulting in more stabilized conditions.

With reference to the  $CO_2$  concentration variation, three different phases during the experiment can be identified as showed in Figure 6.

The first phase is the *mixing phase*, where the total pressure conditions are unstable and the  $CO_2$  concentration progressively increases. This phase lasts around one hour and a half until a stable concentration of  $CO_2$  is reached. At this point we enter in the second phase, named *stabilized phase*, where we observe stable conditions for both the  $CO_2$  concentration and the total pressure for around one hour inside the atrium. The stabilized conditions allow us to calculate the average airflow. Considering a total  $CO_2$  release of 1720 mg/s and a  $CO_2$  concentration difference between inlet and outlet of around 330 ppm (600 mg/m<sup>3</sup>), the airflow calculated through equation (1) is equal to 10306 m<sup>3</sup>/h.

For both calculations the  $CO_{2,inlet}$  and the  $C_{bg}$  are equal and assumed to 400 ppm, measured value of the outdoor  $CO_2$  concentration.

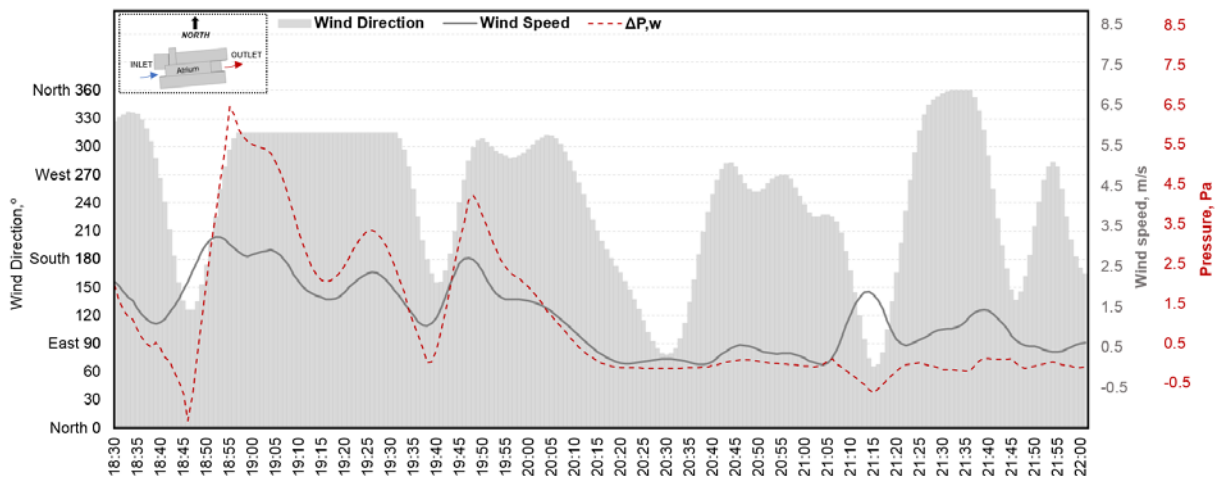


Figure 3 Wind distribution, wind speed and pressure generated by the wind

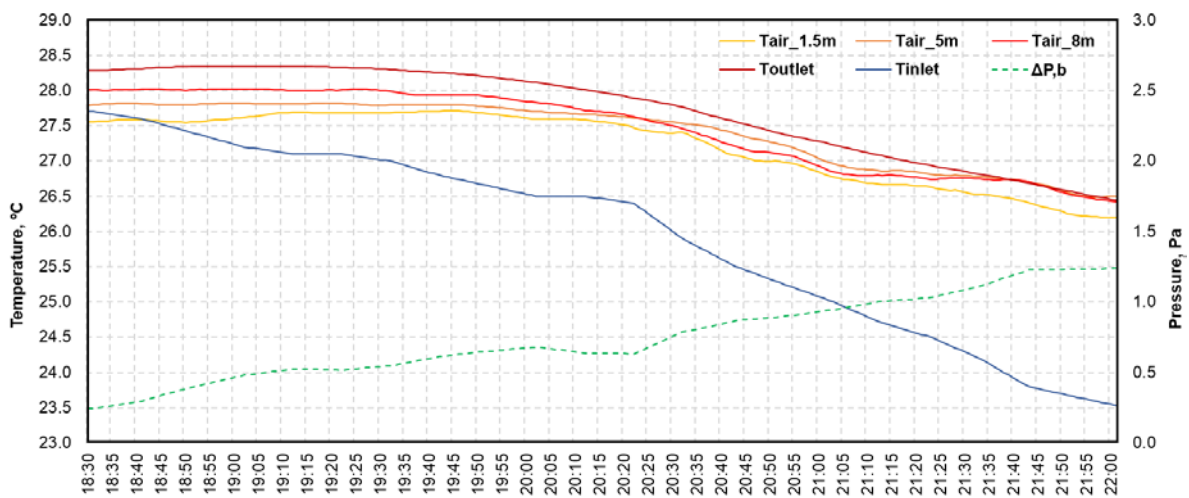


Figure 4 Temperature distribution during the experiment and buoyancy pressure

The last phase, named *decay phase*, starts when the  $\text{CO}_2$  release is stopped and the  $\text{CO}_2$  indoor concentration begins its natural decay. During this last phase we also observe stabilized condition of total pressure. The decay time was about 35 minutes until the initial conditions inside the atrium were reached again. The airflow calculated during the decay, through equation (2), it is equal to  $9668 \text{ m}^3/\text{h}$ . The error between the two methods is 6%. For the calculation of the constant correlation  $k$  we use the average of the two airflow values which is equal to  $9987 \text{ m}^3/\text{h}$ .

Considering an average air velocity at inlet of  $0.36 \text{ m/s}$  for the stabilized phase, the velocity constant, calculated though equation (3), is equal to  $7.62$ .

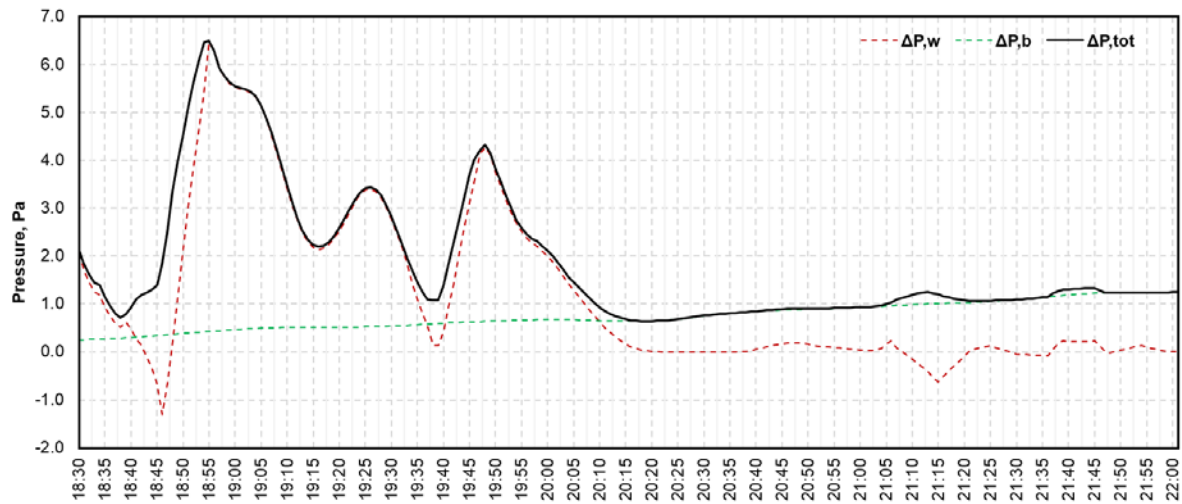


Figure 5 Physics of the pressure during the experiment

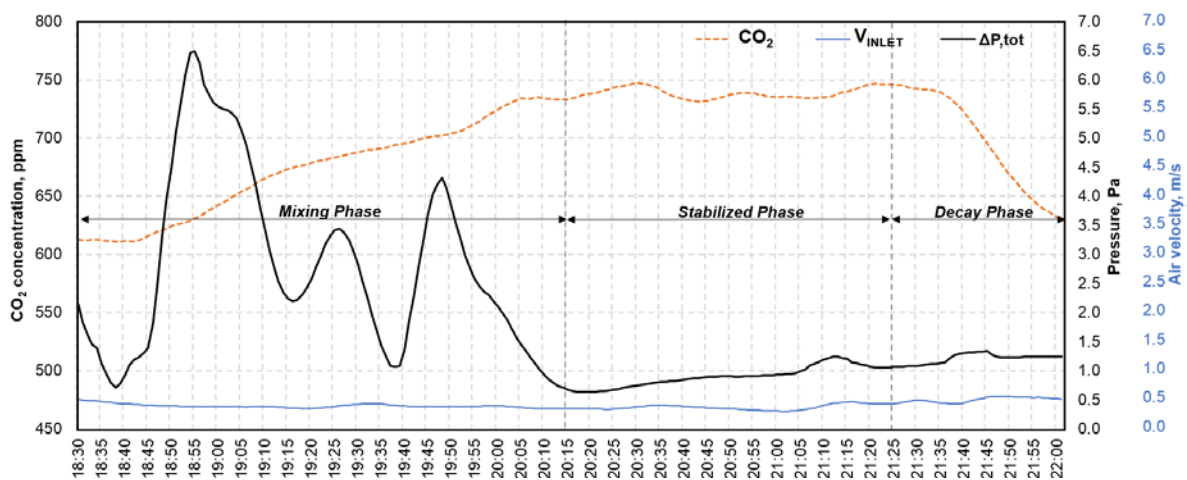


Figure 6 Phase of the experiment on the bases of CO<sub>2</sub> distribution

## 6 CONCLUSIONS

This paper presents the results of a full-scale bulk airflow measurements in a large atrium naturally ventilated. This measurement is the first step of a more complete research work. The finale objective is to quantify the effect of a wind and stack-driven night ventilation over the total cooling consumption of the radiant floor cooling system and the resulted indoor thermal environment of a large atrium. This quantification is possible through a long term measurements campaign comparing the performance with and without the use of the night ventilation.

In order to calculate the bulk airflow, two different tracer gas techniques were used during the experiment. A constant release technique followed by a natural decay. The tracer gas used is Carbon dioxide. The error in the bulk air flow prediction between the two methods is less than 10% and the average value is equal to 9987 m<sup>3</sup>/h. An effective opening area of 9.7 m<sup>2</sup> with a temperature difference between indoor and outdoor of about 2 K, have generated during the experiment an average airflow of 0.61 vol/h.

The average value was used for the definition of a correlation constant between the average bulk air flow and the average air velocity of the air at inlet level. This correlation constant characterized the openings behaviour and it can be used to calculate the airflow rates during the long term measurement just tracking the air velocity at inlet level.

The work has shown the possibility of the application of tracer gas techniques also for large volume where the difficulties of application are wider.

The analysis of the pressure conditions during the experiment was a useful tool to understand whether or not stable condition were favourable for the direct calculation of the airflow rate.

## 7 NOMENCLATURE

F airflow rate [ $\text{m}^3/\text{s}$ ]

$\text{CO}_{2,\text{inlet}}$  Carbon dioxide concentration at inlet level which equal to the  $C_{bg}$  [ $\text{mg}/\text{m}^3$ ]

$\text{CO}_{2,\text{outlet}}$  Carbon dioxide concentration measured at outlet level [ $\text{mg}/\text{m}^3$ ]

$\text{CO}_{2,\text{released}}$  Carbon dioxide released during the experiment [ $\text{mg}/\text{s}$ ]

n number of measurements points considered during the decay

$t_j$  j-th elapsed time from the decay process starting  $t_1 = 0$

$C(t_j)$  measured gas concentration at time ( $t_j$ )

$C_{bg}$  background tracer gas concentration which is the outdoor concentration of Carbon dioxide [ppm]

$V_{\text{atrium}}$  volume of the atrium [ $\text{m}^3$ ]

$v_{\text{air\_in}}$  average air velocity at inlet openings [m/s]

k correlation constant between average airflow rate and  $v_{\text{air\_in}}$

$P_{\text{local}}$  local pressure generated by wind on a building façade

$C_{p_{\text{in}}}$  pressure coefficient at inlet

$C_{p_{\text{out}}}$  pressure coefficient at outlet

$\Delta C_p$  difference between the pressure coefficient at inlet and outlet

$\rho$  air density [ $\text{kg}/\text{m}^3$ ]

g gravitational acceleration [ $\text{m}^2/\text{s}$ ]

$W_s$  wind speed [m/s]

$W_d$  wind direction [ $^\circ$ ]

$U_{\text{ref}}$  wind speed reference at weather station level (5m above the ground) [m/s]

$H_{\text{inlet}}$  distance between the middle plane of inlet windows and the floor

$H_{\text{outlet}}$  distance between the middle plane of outlet windows and the floor

$T_{\text{out}}$  outdoor temperature [ $^\circ\text{C}$ ]

$T_{\text{air\_1.5m}}$  temperature measured at 1.5 meters from the floor [ $^\circ\text{C}$ ]

$T_{\text{air\_5m}}$  temperature measured at 5 meters from the floor [ $^\circ\text{C}$ ]

$T_{\text{air\_8m}}$  temperature measured at 8 meters from the floor [ $^\circ\text{C}$ ]

$T_{\text{outlet}}$  temperature measured at 13.8 meters from the floor [ $^\circ\text{C}$ ]

$T_{\text{inlet}}$  temperature at inlet level which correspond to the  $T_{\text{out}}$  [ $^\circ\text{C}$ ]

## 8 REFERENCES

Annex 62, I. E. (2014-2017). *Ventilative cooling application database*. Retrieved from venticool.eu: <http://venticool.eu/annex-62-publications/ventilative-cooling-application-database/>

Ansys, F. (2017). *Release 18.0.Theory Guide*. Ansys Inc.

Chun C., K. A. (2004). Thermal comfort in transitional spaces-basic concepts: literature review and trial measurement. *Building and Environment*, 1187-1192.

Cui S., Cohen M., Stabat P., & Marchio D. (2015). CO2 tracer gas concentration decay method for measuring air change rate. *Building and Environment*, 84, 162-169.

IEA EBC Annex 26. (1998). *Technical Synthesis Report Energy Efficient Ventilation of Large Enclosures*.

IEA EBC Annex 62. (2014-2017). *Ventilative cooling*. <http://venticool.eu/annex-62-home/>.

Kuppaswany I. (2015). *Sustainable architectural desing: An overview*. Taylor & Francis.

Mateus, N. M., Nunes Simões, G., Lúcio, C., & Carrilho da Graça, G. (2016). Comparison of measured and simulated performance of natural displacement ventilation systems for classrooms. *Energy and Buildings*, 133, 185-196.

Pitts A., S. J. (2008). *Building transition spaces, comfort and energy use*. Dublin: 25th Conference on Passive and Low Energy Architecture.

# Delivery and performance of a ventilative cooling strategy: the demonstration case of a shopping centre in Trondheim, Norway

Annamaria Belleri\*<sup>1</sup>, Matthias Haase<sup>2</sup>, Sotirios Papantoniou<sup>3</sup>, and Roberto Lollini<sup>1</sup>

*1 Eurac Research – Institute for renewable energy  
viale Druso 1  
Bolzano, Italy*

*\*Corresponding author:  
annamaria.belleri@eurac.edu*

*2 SINTEF Building and Infrastructure  
Høyskoleringen 7b  
Trondheim, Norway*

*3 Schneider electric  
Via Giorgio Stephenson 73  
Milan, Italy*

## ABSTRACT

Nearly all retail locations use mechanical cooling systems to ensure indoor comfort temperatures and mechanical ventilation to ensure adequate air exchange, primarily for hygienic reasons. Because of the big volumes involved and the lack of knowledge in natural ventilation design, shopping centres designers have been relying on basic HVAC equipment, without considering the potential of ventilative cooling to reduce cooling needs and to maintain an acceptable indoor environmental quality.

The CommONEnergy FP7 project investigated the retrofit opportunities to exploit ventilative cooling in shopping centres' common areas (shop galleries and atria) considering external climate conditions and architectural features. The paper presents the development and demonstration of a ventilative cooling strategy in the demo case located in Trondheim (Norway). The strategy combines the effect of opened sliding doors and skylight openings to enhance stack ventilation and ventilate/cool the common areas and thus to reduce fan operation time. In order to prevent cold draughts, skylights windows groups are controlled separately and the opening angle of the skylight windows is modulated according to the outdoor temperature and the indoor temperatures as measured by sensors distributed within the common areas. The control strategy was first tested on the building energy simulation model coupled with an airflow model, then implemented in the integrated Building Energy Management System (iBEMS). The building energy model supported the monitoring based-commissioning phase by providing a set of benchmarking scenarios.

Thanks to the ventilative cooling solution, the total electricity consumption for heating, cooling and ventilation of the common areas over the whole reference year is predicted to reduce by an 11%. Simulation results also showed that, with the defined control strategy, natural ventilation is effective in providing the minimum required air change rates for 98% of its activation time and to provide acceptable indoor environmental quality.

The proposed solution is active in the shopping centre since summer 2016. First monitored data showed that, when natural ventilation is activated, indoor temperatures stay below 26°C. When natural ventilation is not activated, indoor temperatures can increase up to 28°C. The first measured data clearly highlighted room for improvement of the implemented control strategy and continuous commissioning is ongoing.

## KEYWORDS

Ventilative cooling; shopping centres; commissioning; natural ventilation; control strategy

## 1 INTRODUCTION

Data collected from several European retailers' sustainability reports show that on average heating, cooling and ventilation energy consumption account for 20% of the total energy

consumption in food retailers and up to 40% in non-food retailers (Schönberger, Galvez Martos & Styles 2013).

Nearly all retail locations use mechanical cooling systems to ensure indoor comfort temperatures and mechanical ventilation to ensure adequate air exchange, primarily for hygienic reasons (Retail forum for sustainability, 2009). Because of the big volumes involved and the lack of knowledge in natural ventilation design, shopping centres designers have been relying on basic HVAC equipment, without considering the potential of ventilative cooling to reduce cooling needs and to maintain an acceptable indoor environmental quality.

Despite their higher energy consumption, mechanical ventilation systems are preferred to natural ventilation strategies because more easy to control and reliable, since they are not affected by the uncertainty of natural forces. Thereby, within the design process the team never focused neither on opening sizing nor on control strategies definition for natural or hybrid ventilative cooling systems. So far, shopping centres' design has included a small proportion of automated windows, sized for smoke ventilation only.

The EU FP7 CommONEnergy project investigated the retrofit opportunities to exploit ventilative cooling in shopping centres' common areas (shop galleries and atria) considering external climate conditions and architectural features. The paper presents the development and demonstration of a ventilative cooling strategy in the demo case located in Trondheim (Norway). The strategy combines the effect of opened sliding doors and skylight openings to enhance stack ventilation and ventilate/cool the common areas and thus to reduce air-handling unit (AHU) operation time.

## **2 DEMO CASE DESCRIPTION**

The demo case is a suburban shopping centre, built on the outskirts of Trondheim in Norway. Opened in 1987 and covering an area of 38,000 m<sup>2</sup>, it houses 70 shops on three floors, with 1,000 outdoor parking spaces.

All the shops face the common areas, which have a circular layout. This circulation space surrounds a central atrium with escalators and shops. Cafeterias or restaurants are located in two intermediate floors in the atrium.

The heating and cooling needs are covered by two air to water heat pumps (AWHP), supplemented by district heating and two additional cooling machines when needed. The dual AWHPs provide heating/cooling to the main ventilation units, and they are manually switched from heating to cooling mode in the mid-season.

An air-handling unit with heat recovery and a capacity of 20,000 m<sup>3</sup>/hr supplies treated air to the common areas. The ventilation system is central damped and there are no automatic dampers. The air intake is on the building roof.

The ventilation unit operates 15 hours/day (from h 06:30 to 21:30) from Monday to Friday and 14 hours on Saturday (from h 06:30 to 20:30). On Sundays, when shopping centre is closed, the system is off. Temperature set points vary between 14°C and 19°C depending on the outside temperature and on exhaust temperature from the atrium/ common area.

The main entrance is a full height glazed atrium with four sliding doors (1.56m x 2.30m each), two entrance doors are located at ground floor (DR1 and DR2) and the other two at first floor (DR3 and DR4), as shown in Figure 1. The doors are controlled by motion sensors or by manual on/off switch, which are eventually overridden in case of fire.

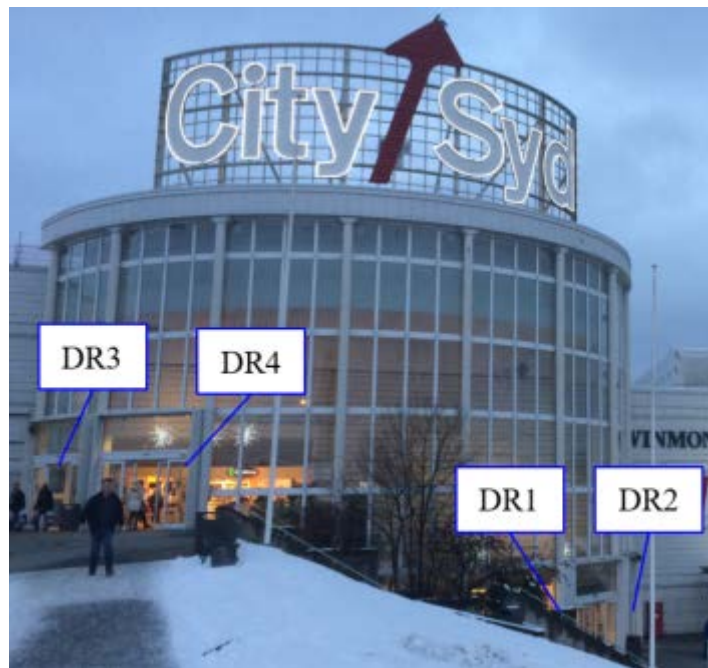


Figure 1: Main entrance of the shopping centre.

Main atrium (Figure 2) has 20 skylight openings equipped with linear actuators and a 3-phase gear motor with 180 cm railway. Among the 20 skylight openings, 10 are located on the west side (SK2) and the other 10 on the east side (SK1) of the skylight. Each opening is 1.2 m wide and 2.0 m high. The skylight windows are top hinged with an outward motion for approximately 45° opening angle off the sloping windows.

Natural ventilation through openable windows in the central atrium skylights helps vent out stale air in the summer.

The skylight windows are currently operated by a window automation system. The opening of the windows can be modulated (5 steps), but the algorithm that controls this practice is propriety from the manufacturer and the building manager cannot modify the control strategy.



Figure 2: Skylights in the central atrium and the cafeteria located on the mezzanine below. Openable windows are present on both sides of the skylight.

Several inefficiencies have been identified in the common areas ventilation:

- Mechanical ventilation system and window automation control are not integrated. Therefore, mechanical ventilation in the common areas cannot be switched off when natural ventilation is activated;
- The control protocol of skylight openings is encrypted in the window automation system and therefore, in case of complaints about natural ventilation operation, the energy manager manually shuts off the system and closes the openings;
- Cold draughts problems occur mainly in the cafeteria area, located in the atrium at the second mezzanine floor;

- Overheating problems are occurring in the main entrance due to the extensive glazed façade. Therefore, doors are kept open to cool down the entrance area.

### 3 NATURAL VENTILATION STRATEGY

The proposed natural ventilation strategy combines the effect of existing sliding doors and skylight openings to enhance stack ventilation and ventilate/cool the common areas.

The integration of natural ventilation together with mechanical ventilation allows exploiting the benefits of windows opening and stack effect for ventilating/cooling the common areas. Although some shopping centres have automated windows for natural ventilation, their controls often not linked to the HVAC system control. Therefore, the advantages obtained by ventilative cooling are neglected with an additional energy consumption from the HVAC system.

The flow chart in Figure 3 represents the control logic, which is described in detail in (Belleri, Avantaggiato 2017). The control scheme activates natural ventilation during opening time if it does not rain and the wind velocity does not exceed 7m/s (WS\_MAX) and the outdoor temperature is within the comfort range and the measured indoor temperature exceeds the heating set point. The skylight windows on east (SK1) and west (SK2) side are controlled separately and depending on indoor temperature measured in the cafeteria and the common areas at first and ground floor.

Additionally, as required by the window manufacturer, if wind speed is above 4 m/s (WSn\_MAX) and prevails from the opposite direction of east/west window row, that window row will stay close.

This results in 9 possible different configurations of windows and doors opening. Table 1 reports the possible openings configurations according to the defined control schemes. The AHU is turned off whenever doors or skylights are opened.

Table 2 reports the list of input for the control rules. Some inputs are monitored variables and some other are constant values that can be pre-defined and optimized in the commissioning phase.

Table 1: Configuration of control rules' output signals as defined in the control schemes (for windows/doors: 0 means the opening is closed, 1 means the opening is opened; for the AHU: 0 means the AHU is off, 1 means the AHU is on)

Control scheme	Skylight windows group 1 (OF_SK1)	Skylight windows group 2 (OF_SK2)	Door 1 (OF_DR1)	Door 2 (OF_DR2)	Door 3 (OF_DR3)	Door 4 (OF_DR4)	AHU
Sc_1a	1	0	0	0	1	1	0
Sc_1b	1	0	1	1	1	1	0
Sc_1c	0	1	1	1	0	0	0
Sc_1d	1	1	0	0	1	1	0
Sc_1e	1	1	1	1	1	1	0
Sc_1f	0	1	1	1	1	1	0
Sc_1g	1	0	1	1	0	0	0
Sc_1h	0	1	0	0	1	1	0
Sc_1i	1	1	1	1	0	0	0
Sc_2	0	0	0	0	0	0	1
Sc_3	0	0	0	0	0	0	0

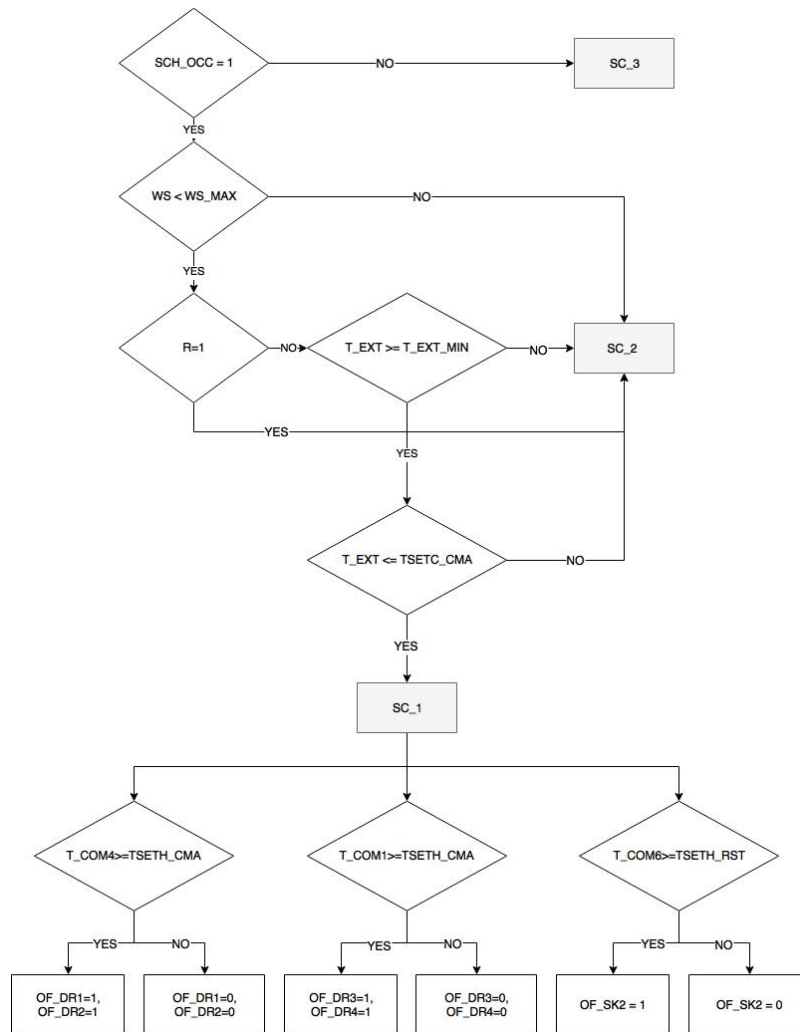


Figure 3: Control strategy scheme.

Table 2: Control rules input list.

Input ID	Unit	Description	Type
SCH_OCC	-	Occupancy schedule [0;1]	Scheduled
T_EXT	°C	Outdoor air temperature	Monitored
WS	m/s	Wind speed	Monitored
WD	°	Wind direction	Monitored
R	-	Precipitation sensor [0;1]	Monitored
T_COM4	°C	Indoor air temperature of the common area at ground floor	Monitored
T_COM1	°C	Indoor air temperature of the common area at first floor	Monitored
T_COM6	°C	Indoor air temperature of the cafeteria	Monitored
WS_MAX	m/s	Maximum wind speed	Setpoint
WSn_MAX	m/s	Maximum wind speed in the direction opposite to the normal of the window plane	Setpoint
T_EXT_MIN	°C	Minimum outdoor temperature for the activation of natural ventilation	Setpoint
T_EXT_MAX	°C	Maximum outdoor temperature for the activation of natural ventilation	Setpoint
TSETH_CMA	°C	Lower temperature limit of the comfort zone for common areas	Setpoint
TSETH_RST	°C	Lower temperature limit of the comfort zone for cafeteria	Setpoint
TSETC_CMA	°C	Higher temperature limit of the comfort zone for common areas	Setpoint

In order to prevent cold draughts, the opening angle of the skylight windows is modulated on 5 steps (0.2 - 0.4 - 0.6 - 0.8 - 1) depending on the outdoor temperature and the indoor

temperatures measured by sensors distributed within the common areas, as the function shown in Figure 4.

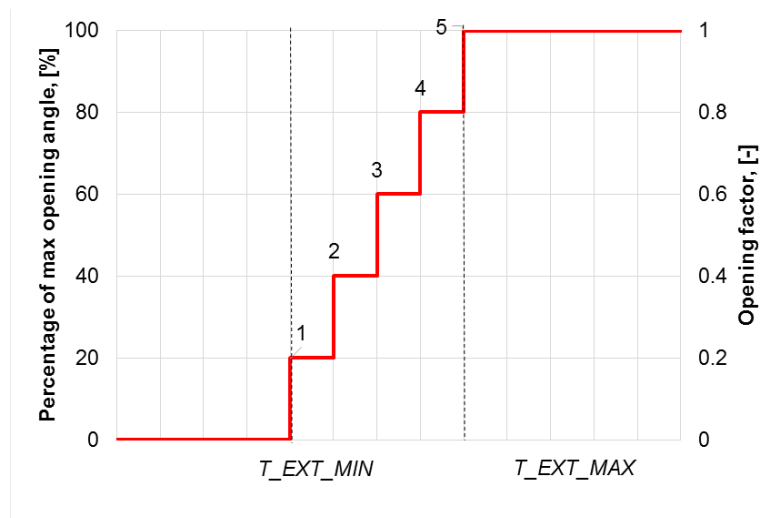


Figure 4: Skylight opening angle modulation depending on outdoor temperature.

## 4 IMPLEMENTATION AND COMMISSIONING

Since the ventilative cooling strategy involves different building systems (i.e. door and window actuators and air-handling unit), building energy simulations within a structured modelling environment supported the development and test of control strategies, the tuning of set-points, as well as the prediction of system performance improvement.

Input/output and control schemes are described using a predefined format agreed between the energy modeller and the system integrator so that we can manage control rules both in the Integrated Modelling Environment (IME) and in the intelligent Building Energy Management System (iBEMS) in a synergic way. Each input and output is identified by the same variable name in the IME, the iBEMS and the monitoring plan.

### 4.1 iBEMS architecture

Thanks to its integrated approach, the iBEMS architecture leverages the information and synergy between each of the systems and is able to provide a truly integrated function to the building. The system architecture foresees at least one automation server to which are potentially connected different subsystems for lighting, refrigeration, HVAC, energy storage and renewable energy technologies control.

In the demo case, the iBEMS is controlling directly the motors of the windows using a dedicated control for activating the motors. Figure 5 shows the architecture for the control of this sub-system. The sub-system communicates with the iBEMS hardware using the available open protocol (LonWorks).

The operation of the motors for natural ventilation uses information from sensors located in the common area. Thus, the information required for the operation of this sub-system are under the same hardware installation.

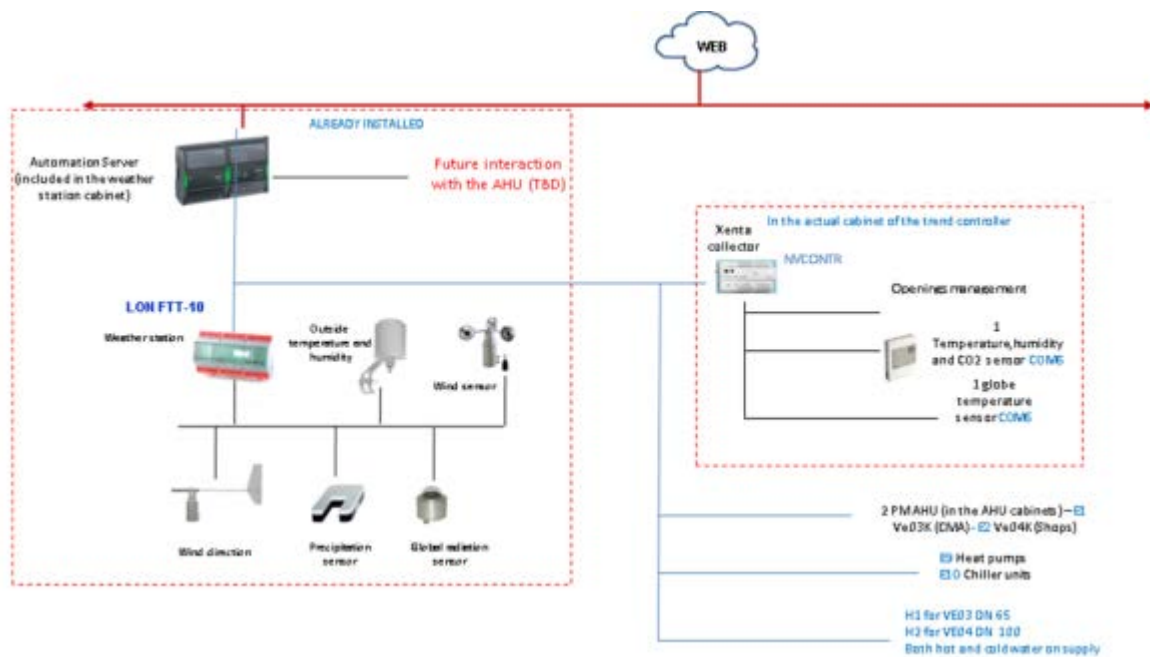


Figure 5: iBEMS architecture for openings automation.

## 4.2 Monitoring layout

Besides its role in the natural ventilation control rules, the common area monitoring aims at evaluating the overall performance of the natural ventilation.

Indoor air temperature, radiant temperature, relative humidity and CO<sub>2</sub> concentration sensors are installed in seven positions within the two floors of the common areas, as shown in Figure 6. Point 6 is located in the cafeteria in the mezzanine floor. The signals collected in the building are being saved in the iBEMS.

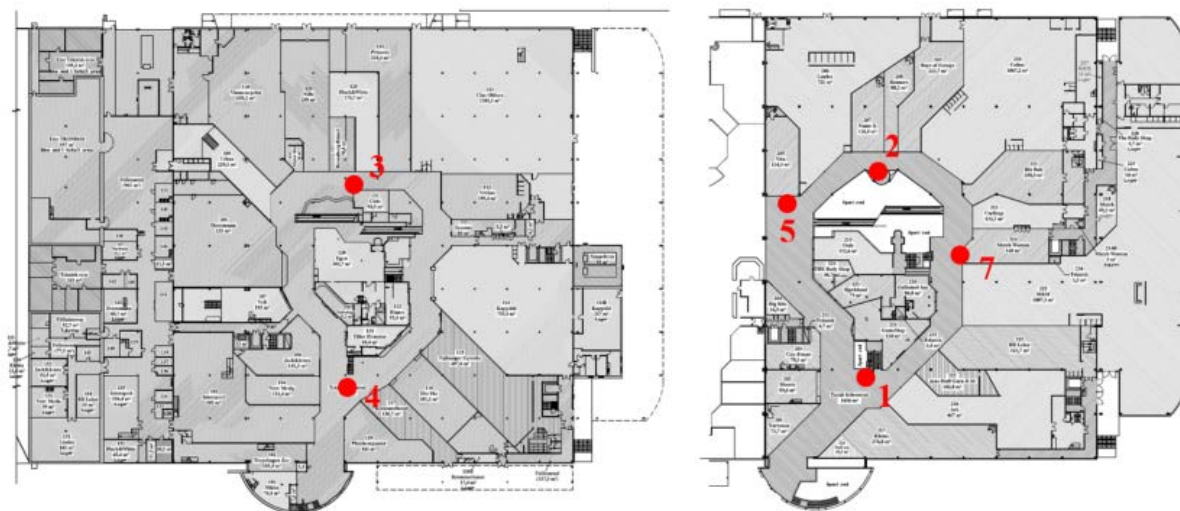


Figure 6: Sensors position in the common areas

## 4.3 Interaction between simulation model and iBEMS

The energy model of the building was developed within the Integrated Modelling Environment (Dipasquale, Belleri & Lollini 2016), a pre-casted simulation environment representing the building and its subsystems in a modular structure making more effective the development of a shopping mall model. We set up an airflow network model and coupled it with the energy model of the building (Haase et al. 2015).

Baseline simulations were run in unlimited power mode, where the generation system is assumed to always have the power necessary to keep indoor temperatures within 20°C (heating setpoint) and 25°C (cooling setpoint) during the opening time of the shopping centre (h 09:00-19:00). The mechanical ventilation is always on during opening time and provides the minimum required air change rates, which are assumed 20'835 m<sup>3</sup>/hr (circa 1 ach).

Then, we compared the baseline simulation results with the results of the energy simulation model where we implemented the natural ventilation strategy. The graph in Figure 7 shows the percentage of opening time when natural ventilation is activated and effective (MODE 1), when natural ventilation is activated but the minimum airflow rates are not met (MODE 2) and when mechanical ventilation is needed (MODE 3). Due to the low outdoor temperatures, natural ventilation is activated mainly during the summer season.

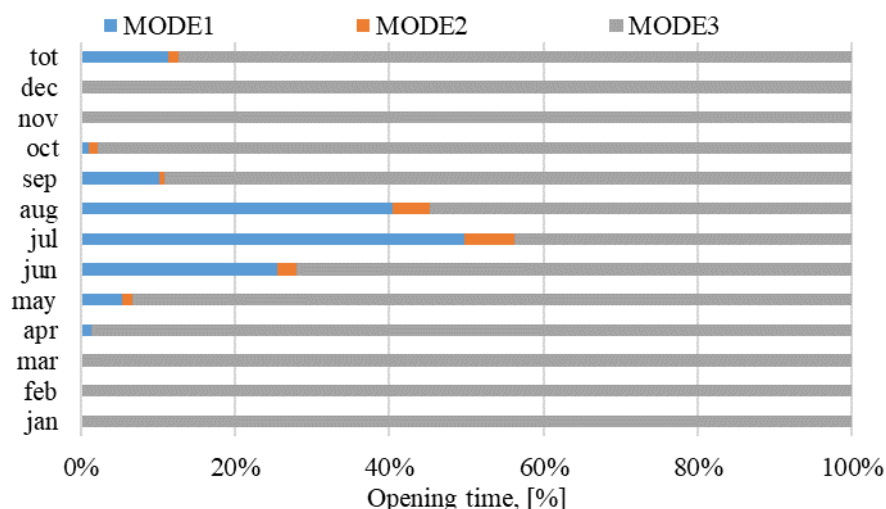


Figure 7: Percentage of opening time when natural ventilation is activated and minimum required airflow rates are met (MODE 1), minimum required airflow rates are not met (MODE 2) and mechanical ventilation is needed (MODE 3).

Since the HVAC model is ideal, the following efficiencies were considered for the estimation of the electricity consumption due to heating, cooling and ventilation: COP = 2.36; SPF = 0.45 Wh/m<sup>3</sup>.

Table 3: Estimated energy consumption and cost savings for the mixed mode ventilation strategy (natural and mechanical ventilation) compared to the energy performance of the building with mechanical ventilation only.

		Mechanical ventilation only	Mixed mode ventilation
Daytime natural ventilation operating hours	[hr/y]	0	513
Mechanical ventilation operating hours	[hr/y]	4,538	4,025
Electric energy consumed for ventilation	[MWh/y]	43	38
Electric energy consumed for cooling	[MWh/y]	28	19
Tot electric energy consumption	[MWh/y]	71	57
Operating costs saving <sup>1</sup>	[€y]	-	1,748

Table 3 summarizes the outcomes of the building energy simulation. The total electricity consumption for cooling and ventilation of the common areas over the whole reference year decreases by an 11% thanks to the exploitation of natural ventilation. Simulation results also showed that natural ventilation is effective in providing the minimum required air change rates for 98% of its activation time. The operating cost savings are approximately 1,750 €

<sup>1</sup> The cost of electricity in Norway is 0.12 €/kWh.

The building energy model also supported the monitoring based-commissioning phase by providing a set of benchmarking scenarios. The control output of the benchmarking scenarios was then compared to the iBEMS control output by setting the same boundary conditions.

**5 MEASURED PERFORMANCE**

The proposed solution is active in the demo case since summer 2016. The graphs in Figure 8 and Figure 9 report the monitored data recorded in August 2016 about outdoor (T\_EXT) and indoor (T\_IN) temperatures and doors and windows position (OF\_DR = opening factor of doors, OF\_SK = opening factor of skylight windows).

The graphs show that, when natural ventilation is activated, indoor temperatures stay below 26°C. Indoor temperatures can increase up to 28°C in the cafeteria area (T\_IN\_6) when natural ventilation is not activated (e.g. on 07.08.2016 or 21.08.2016 or 28.08.2016).

The data clearly highlights room for improvement of the implemented control strategy. Indoor temperature peaks in the cafeteria could be reduced by exploiting ventilative cooling.

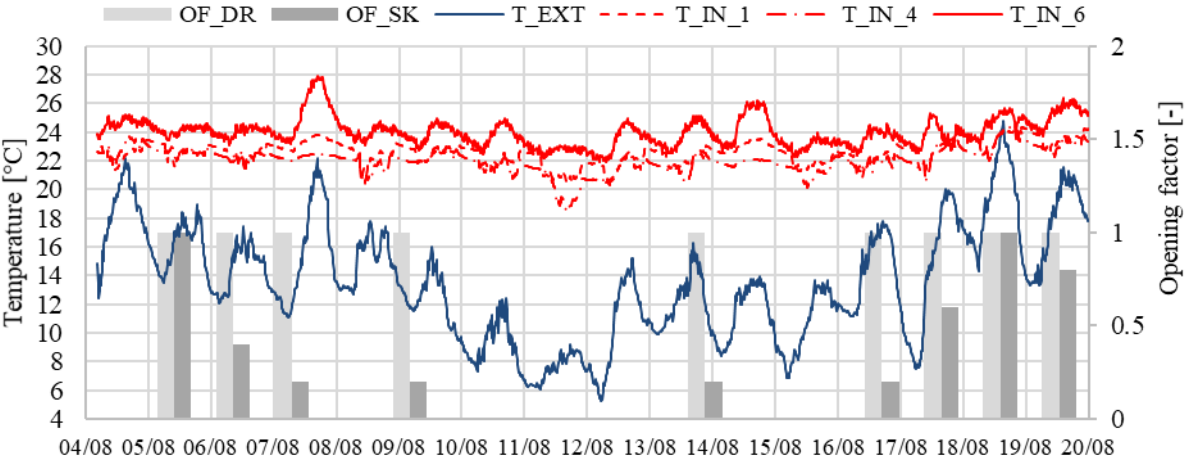


Figure 8: Monitored indoor and outdoor temperatures and opening factors from August 4<sup>th</sup> until August 20<sup>th</sup> 2016.

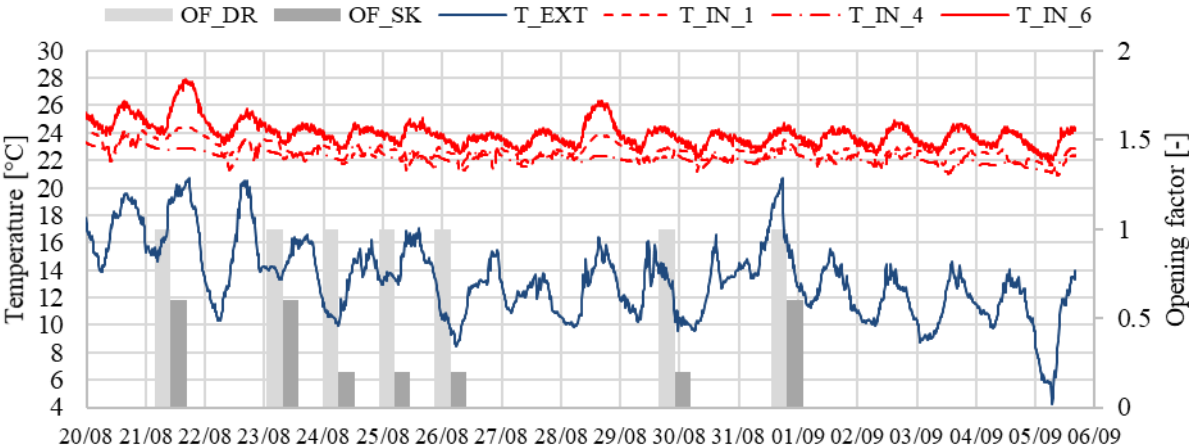


Figure 9: Monitored indoor and outdoor temperatures and opening factors from August 20<sup>th</sup> until September 6<sup>th</sup> 2016.

## 6 CONCLUSIONS

The demo case is suitable for the application of enhanced stack ventilation through the atrium. The natural ventilation strategy combines the effect of opened sliding doors and skylight openings to enhance stack ventilation and ventilate/cool the common areas. In order to prevent cold draughts, skylights windows groups are controlled separately and the opening angle of the skylight windows is modulated according to the outdoor temperature and the indoor temperatures measured by sensors distributed within the common areas.

Potential energy savings are estimated by building energy simulations. The total electricity consumption for heating, cooling and ventilation of the common areas over the whole reference year is reduced by an 11% thanks to the exploitation of natural ventilation. Simulation results also showed that, with the control strategy defined, natural ventilation is effective in providing the minimum required air change rates for 98% of its activation time.

The energy savings predicted by the simulation models are going to be validated by calibrating the building energy simulation models with dedicated measurements.

The proposed solution is active in the shopping centre since summer 2016. First monitored data showed that, when natural ventilation is activated, indoor temperatures stay below 26°C. When natural ventilation is not activated, indoor temperatures can increase up to 28°C. The first measured data clearly highlighted room for improvement of the implemented control strategy and continuous commissioning is ongoing.

## 7 ACKNOWLEDGEMENTS

The research leading to these results has received funding from the European Community Seventh Framework Programme (FP7/2007-2013) under grant agreement n. 608678.

## 8 REFERENCES

Belleri, A. & Avantaggiato, M. 2017, Deliverable 3.3: Ventilative cooling, CommONEnergy FP7 project.

Dipasquale, C., Belleri, A. & Lollini, R. 2016, Deliverable 4.1: Integrative Modelling Environment, CommONEnergy FP7 project.

Haase, M., Stenerud Skeie, K., Belleri, A. & Dipasquale, C. 2015, "Modelling of a complex shopping mall in Norway", Proceedings of BS2015: 14th Conference of International Building Performance Simulation Association, pp. 2264.

Retail forum for sustainability. 2009. Issue paper No1 on the energy efficiency of stores. s.l. : [http://ec.europa.eu/environment/industry/retail/pdf/issue\\_paper\\_1/Energy\\_Efficiency\\_en.pdf](http://ec.europa.eu/environment/industry/retail/pdf/issue_paper_1/Energy_Efficiency_en.pdf), 2009.

Schönberger, H., Galvez Martos, J.L. & Styles, D. 2013, Best Environmental Management Practice in the Retail Trade Sector, European Commission Joint Research Centre, European Union.

# Ventilative cooling in a single-family active house from design stage to user experience

Christoffer Plesner<sup>\*1</sup>, Nicolas Dupin<sup>2</sup>

*1 VELUX A/S  
Ådalsvej 99  
2970 Hørsholm, Denmark*

*2 VELUX  
1. rue Paul Cézanne B.P. 20, 91421  
Morangis Cedex, France*

*\*Corresponding author:  
christoffer.plesner@velux.com*

## ABSTRACT

Ventilative cooling through window airing presents a promising potential for low energy houses in order to avoid overheating risks and to reduce energy consumption of air conditioners. This case study aims at describing how ventilative cooling has been taken into account as from the design stage of a low-energy single-family active house located near Paris. Its performance on thermal comfort and air renewal, monitored from both sociological (feedback from a family) and scientific approach, is described and compares these two qualitative and quantitative approaches.

Key learnings from the sociological survey are presented and compared to the data monitored by environment sensors installed inside and outside the house.

Results from a research project carried out on the same house are presenting the accuracy of natural ventilation evaluation for design tools. Simulation tool were used to evaluate the potential of natural ventilation for its contribution to both air change and passive cooling of houses.

## KEYWORDS

Ventilative cooling, active house, design stage, passive cooling, natural ventilation

## 1 INTRODUCTION

Ventilative cooling of indoor spaces, including both natural and mechanical ventilation strategies, shows high energy savings and comfort improvement potential, especially for new and upcoming residential buildings with high standards for the envelope performance – making these subjects to overheating risks.

As a matter of fact, residential buildings such as single-family houses or apartments are originally designed to provide a comfortable, safe and healthy indoor environment to their occupants, whereas energy efficiency recently became an additional requirement to reach environmental and primary resources safeguarding.

One of the biggest drawbacks to the development of ventilative cooling is mainly the complex air flows passing through open windows, which requires detailed models for assessing indoor comfort with sufficient accuracy.

The case study presented here aims at describing how natural ventilation through window openings has been considered in the design process of a low-energy single-family active house - Maison Air et Lumière, part of the Model Home 2020 project - in order to reach simultaneous high targets on energy performance, summer comfort, indoor air quality and visual comfort. Furthermore, Maison Air et Lumière is to be found as 1 of initially 14 cases (5

more to come), in the upcoming IEA EBC Annex 62 “case study brochure” showcasing documented case studies of recent buildings with effective ventilative cooling systems.

In previous articles published for AIVC Conferences 2012 and 2013, Maison Air et Lumière has been presented with different focuses on key learnings of the quantitative monitoring of the house. This paper focuses on the global approach, presented through 3 main stages: the design stage, the occupancy stage (during which a family of 4 lived in the house for one year from September 2012 to August 2013) and the key learnings.

**2 RESULTS**

The results in this section are based on the data and information extracted from the various stages Maison Air et Lumière (MAL) has gone through, from the initial design stage to the occupancy stage. Finally, the key learnings stage is evaluated encompassing the user experience from the occupants (via a sociological survey) and the quantitative monitoring. Each stage serves specific purposes with its corresponding tools and methods, adapted for the needed evaluation.

The 3 main stages are shown below in Figure 1.

Design stage	Occupancy stage	Key Learnings
<ul style="list-style-type: none"> <li>- Scope development</li> <li>- Concept design</li> <li>- Detailed design</li> <li>- Construction design</li> </ul>	<ul style="list-style-type: none"> <li>- Sociological survey:               <ul style="list-style-type: none"> <li>- What people experience about living in the house (seasonal interviews)</li> </ul> </li> <li>- Quantitative monitoring:               <ul style="list-style-type: none"> <li>- Evaluation of the indoor climate and house behaviour</li> </ul> </li> <li>- Evaluate sensor data to e.g. make setpoint adjustments</li> </ul>	<ul style="list-style-type: none"> <li>- Learnings on the qualitative aspects of the indoor climate in new buildings</li> <li>- Learnings on how to design and operate future buildings</li> <li>- Learnings on the user experience of the occupants</li> </ul>

Figure 1 - The 3 main stages of Maison Air et Lumière

**2.1 Stage 1: Design stage**

The design stage consists of 4 sub-stages; Scope development, concept design, detailed design and construction design which all are part of the preliminary building phase as seen in Table 1.

In this design stage, potential overheating issues may become visible through continuous evaluations from simulations and therefore improvements in the design is an important aspect here. These design evaluations are essentially what makes the difference between buildings with good thermal comfort with no or limited overheating issues and buildings with overheating issues. In this case overheating was a focal point in the design stage and this has a significant impact on the positive results achieved from the “occupancy stage” shown in section 2.3.

Table 1 - Description of the design stage

Stage	Tool	Function
Scope Development	Perrenoud (RT 2005)	Define building features of materials/systems
Concept Design	VELUX Daylight Visualizer	Initial Daylight Check
Detailed Design	BSim (DK)	Thermal Comfort analysis & ACR
Construction Design	U21/U22 Perrenoud (RT2012)	Check compliance with RT 2012 regulation and evaluate future nZEBtarget level

At the very start of the scope development sub-stage, meetings were held between the various stakeholders of the upcoming Model Home 2020 project, where one of the homes were to be built in France. The aim was to agree on a set of building requirements for Maison Air et Lumière which would enable the building at that time to comply with first the minimum demands as set in the existing French thermal regulation, RT 2005 and also the future French thermal regulations at that time RT 2012 and nZEB 2020 (Near Zero Energy Building). From the start of this project the bar was set very high, as the target was to end up with a requirement specification that did not only comply with the existing French thermal regulation, RT 2005 - but requirements that were set even higher than the future, RT2012. The targets for the requirement specification were even set to comply with the future demands, of the upcoming nZEB regulation in 2020.

One of the tasks of this stage was to define building features of materials and systems, and here the choice of the ventilation system is important. This was to see what would work and what wouldn't work regarding building design. One of the tools used was Perrenoud to continuously check if the proposed design would comply with at least the existing regulations, RT2005 and future nZEB targets. For this, simulations were carried out by French consulting engineers, Cardonnel Ingénierie. The Perrenoud tool continuously enabled the stakeholder group to see what features worked or didn't work according to the design, hence looking at the energy consumption of the building.

Topics such as indoor climate and connection to outside were discussed as being important parameters to make the occupants in the building satisfied. It was important that there would be a balance between the different indoor climate parameters such as ventilation, daylight and connection to the outside. It was especially important to demonstrate a good indoor climate in combination with good energy performance, for good summer comfort. The energy consumption was of course always kept in mind continuously verified using the Perrenoud tool. As the project's target was set to nZEB 2020 foreseen level, one could say this specification was a contributing factor to specifying the later Active House specifications (Active House/).

The final requirement specification ended up satisfying the demands of future nZEB 2020 buildings.

### 2.1.1 Concept design

In the concept design sub-stage, more evaluations were made to e.g. evaluate the preliminary daylight levels in the MAL. This is important to focus on, as daylight is a valuable aspect to

the indoor climate, both regarding the visual aspects as well as the free solar gains entering the building. Furthermore, daylight apertures are bringing a connection to the outside. Daylight levels were evaluated using the software VELUX Daylight Visualizer, to check illuminance levels at specified locations as seen in Figure 2. Daylight simulations and concept design illustrations were carried out by French architects, Nomade Architectes. This stage is important as the initial daylight levels found had an impact on the further building design and structure of MAL, enabling to optimize the daylight levels both on room and building level.

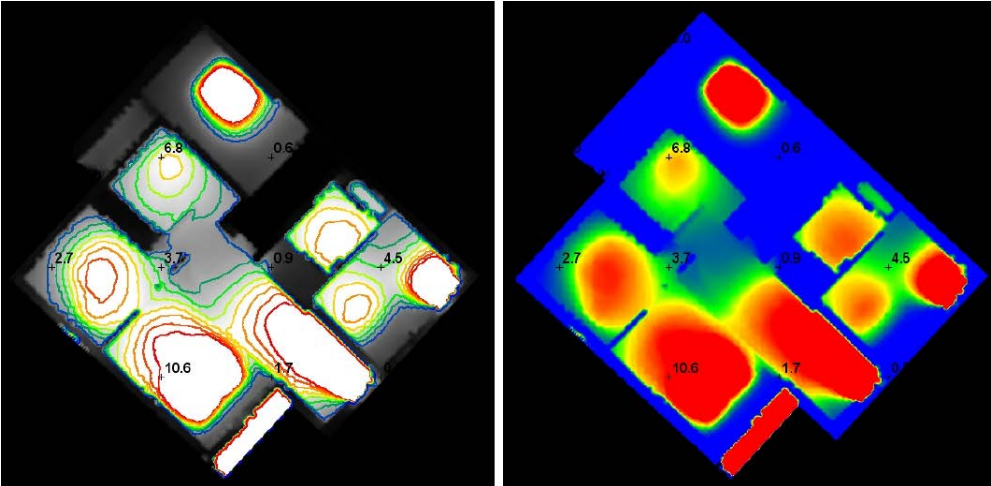


Figure 2 – Daylight factor simulations made in VELUX Daylight Visualizer

2.1.2 Detailed design

In the detailed design sub-stage, a thermal comfort and air change rate evaluation was made in order to evaluate the scoped design further, by making more detailed analysis through e.g. computer simulations. The simulations initially checked thermal comfort performance in Maison Air et Lumière. The tool used in this stage is BSim, which is an integrated tool for analysing buildings and installations (Danish building research institute). This simulation was carried out by a Danish consulting engineering firm, Esbensen consulting engineers. The basic BSim model is shown in Figure 3.

The air change rate analysis was also made using BSim as seen in Figure 5 which shows the average air change rates for all non-winter hours, while the lighter column shows the average air change rate of when the operative temperature is above 25 °C.

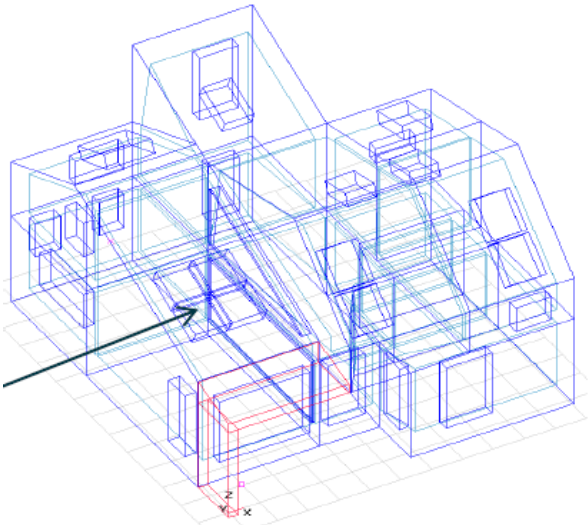


Figure 3 – Simulation model setup in BSim

In Figure 4, the operative temperatures are plotted as a function of the running mean temperature for the Living room of MAL, as e.g. found in the European standard, EN 15251 called the “adaptive comfort model”. This shows that the operative temperature in the living room is within the acceptance range.

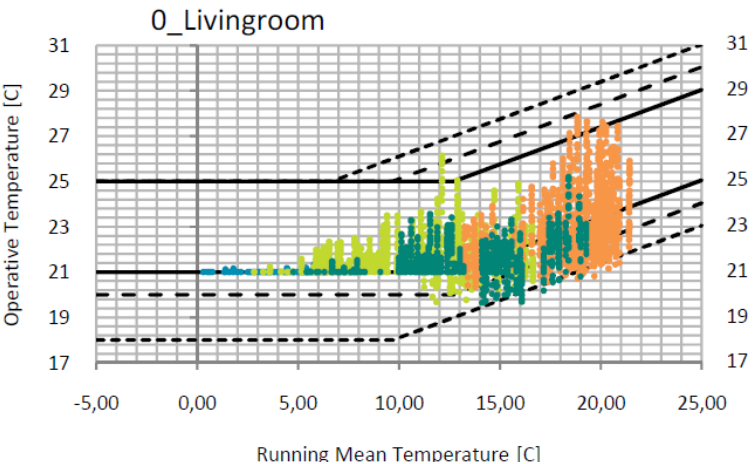


Figure 4 – Overheating evaluation based on EN 15251

In Figure 5 the lighter column is of particular importance as it indicates if there is sufficient natural ventilation in the zone. BSim maximizes the air change rate to cool the zone because the operative temperature is above 25°C. The maximum air change rate is 5 h<sup>-1</sup>. The average air change rate is lower due to days with low wind velocities. However, the closer the average air change is to 5 h<sup>-1</sup>, the better the natural ventilation works, where the bedrooms in MAL seems to perform best as they have the highest air change rates.

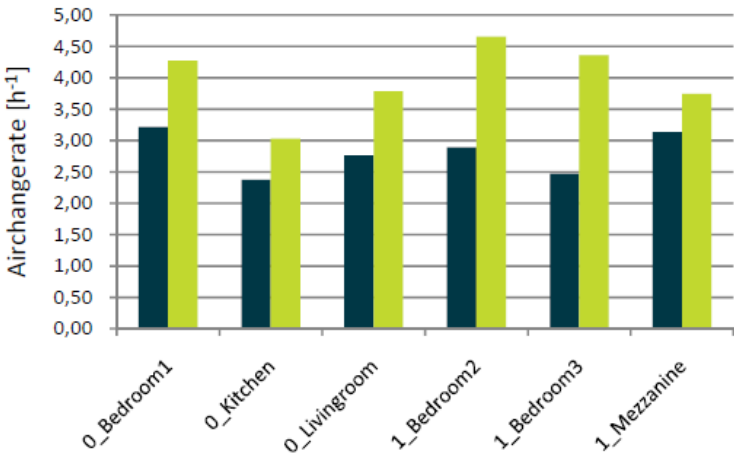


Figure 5 – Air change evaluation from BSim results

2.1.3 Construction design

The construction design sub-stage is the final sub-stage of the “design stage” where it is evaluated if the proposed building design complies with the regulation set in the requirement specification. To evaluate the energy performance of MAL, the Perrenoud tool was used to check if the proposed construction design would comply with the future French thermal regulation RT2012 and nZEB 2020 targets. This stage was also carried out by French consulting engineers, Cardonnel Ingénierie, like in the scope development stage.

Maison Air et Lumière complied with energy performance of the upcoming RT2012 regulation, showing high energy performance (below 50 kWh<sub>PE</sub>/(m<sup>2</sup>.yr).

## **2.2 Stage 2: Occupancy stage (methodology for monitoring)**

As the project was strongly focusing on the occupant's comfort, a double monitoring process was set up to track both scientific and sociologic achievements for the indoor comfort targets. The processes are:

- Sociological survey:
  - A sociologist carried out seasonal interviews with the family to get their feedback on the perceived indoor comfort while living in the house. Specific attention was paid to the summer comfort, indoor air quality and the automation of the natural ventilation system
- Quantitative monitoring:
  - A scientific monitoring was carried out thanks to built-in sensors in each room analysing both the indoor and outdoor environments and monthly reports were released to follow, inter alia, indoor air temperature, relative humidity, CO<sub>2</sub> concentration, illuminance, energy consumption, energy production, and outdoor weather conditions incl. solar radiation, wind speed and wind direction

Cross comparisons were carried out between these two monitoring processes to confirm the interpretation of sociological and quantitative results provided by the monitoring systems. Scientific indicators such as thermal comfort were evaluated to establish their relevancy towards end-users' perception. The feedback from the interviews were also used to adapt and adjust the home automation along the way, and increase users' acceptance and satisfaction (e.g. by windows opening frequency, actions on awning blinds, etc.).

## **2.3 Stage 3: Learnings of operation stage**

The operation stage has shown good results regarding summer thermal comfort, with a good correlation between measurements and perceived comfort.

From the sociological survey one key feedback given by the family was the perception of indoor temperature during a heat wave in the summer period: "When we were arriving inside the house, the heatwave still was present and the exterior air was above 30°C, and the temperature was 24 to 25°C inside the house without any other cooling system than natural cooling" (Quote from inhabitant of Maison Air et Lumière).

This statement was supported by the quantitative monitoring via the measurements carried out during both the unoccupied and occupied period (as shown in Figure 6).

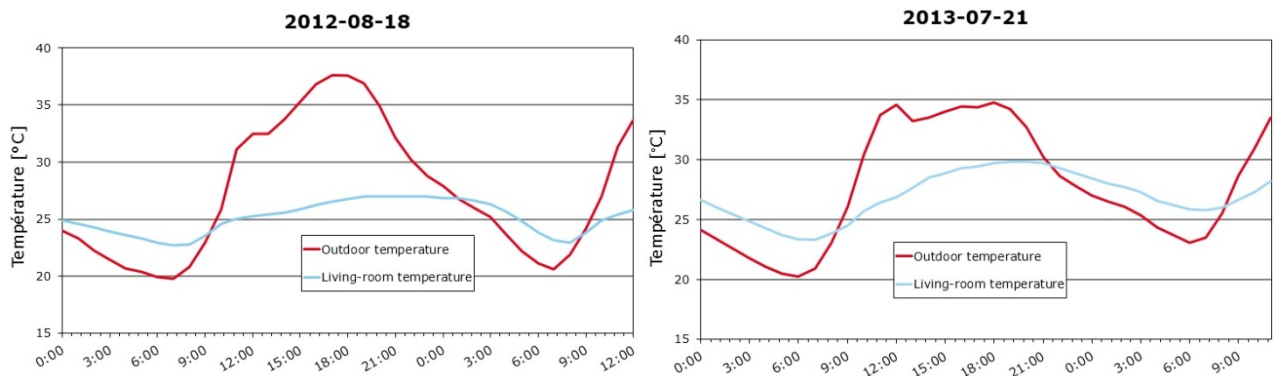


Figure 6 - Comparison of ventilative cooling benefits during a heat wave in unoccupied (left) and occupied periods (right). Blue: indoor temperature. Red: outdoor temperature

Another key learning from the operation stage was the acceptance of the home automation system inside the house, especially the system in charge of managing the motorized windows and blinds.

The family was indeed disturbed during the beginning of the experience by the frequent movements of the solar shadings and windows, which were automated and sensor controlled. After a short period, and as the family had the possibility to shut down the automation in the different rooms, interviews have shown that they were often switching the system into manual mode, due to the systems swift reaction to the temperature sensors making it complex to be understood.

After a short period, the decision was taken to change the automation principle by adapting the ventilative cooling algorithm to the family's daily and weekly habits instead. An hourly-based schedule was then implemented to be aligned with the family's presence and sleeping hours.

The results shown on Figure 6 during the occupancy period have been monitored with the hourly-based schedule.

Furthermore, from the quantitative monitoring an assessment showing the accuracy of the air flow rate passing through windows based on both laboratory measurements, simulated values using CONTAM software and from actual tracer gas measurements performed in the house, for in this case the Living room in Maison Air et Lumière. This generally shows a close correlation between the different methods.

Below in Table 2 the aeratic and thermal performance of ventilative cooling for the living room comparing actual tracer gas measurements and simulated values using CONTAM software for the Living room. As seen in Table 2a good correlation is shown between actual measurements compared with the simulations, e.g. for the morning case.

Furthermore, the table shows that high air change rates up to 14 ACH could be achieved in the living room with even limited wind velocities ( $< 3$  m/s) and low temperature difference between outside and inside ( $< 3^{\circ}\text{C}$ ), showing the high potential of ventilative cooling via elevated air change rates for cooling (K. Duer et al., 2013).

Table 2 - Aeraulic and thermal performance of ventilative cooling for the Living room

	Representative air flows in ACH [h <sup>-1</sup> ]		Representative average temperature difference (T <sub>int</sub> – T <sub>ext</sub> )		
	Morning	Afternoon	No ventilation	Full-time ventilation	Control ventilation
Simulation value	14 ACH	13,2 ACH	6 °C	1,5 °C	0 °C
Measurement value	13,4 ACH	10,6 ACH	4,8 °C	0,2 °C	-0,3 °C

The close correlations between measured and simulated values support the global evaluation of natural ventilation performance by using simulation tools to evaluate the air flow rate when dimensioning windows. Thereafter the performance of the natural ventilation and ventilative cooling may be sufficiently known, in order to successfully make a ventilative cooling strategy that may work for the whole house, as shown in Maison Air et Lumière.

### 3 CONCLUSIONS

#### 3.1 Characterization of natural ventilation through windows

Distinct laboratory measurements carried out for the project has shown that aeraulic features of windows available in the literature are giving relevant characterization for air flow evaluation (N. Dupin et al., 2014).

These aeraulic features can be used for evaluating air flow rates passing through windows thanks to natural ventilation with a good accuracy.

#### 3.2 Evaluation of natural ventilation performance on a single family house (air flow rates and air change per hour)

Generally, it is thought that natural ventilation only works in very favourable conditions with high temperature difference(e.g. during night) and with high wind speeds. Though, this has been refuted here,thanks to this project showing that ventilative cooling also works during very reasonable weather conditions.

An analysis carried out by French research institute, Armines - Mines ParisTech has shown that even withlimited wind velocities (< 3 m/s) and low temperature difference between outside and inside (< 3°C), elevated air change rates for cooling up to 14 ACH in the Living room, could be achieved during summer, showing the high potential of ventilative cooling.

#### 3.3 Temperature reduction potential of ventilative cooling in a single family house

Thanks to the accuracy of the numerical simulations – which were confirmed by on-site measurements – the potential for temperature reduction inside MAL using natural ventilation has been evaluated by comparing indoor air temperatures with and without ventilative cooling.

These results show that natural ventilation using ventilative cooling has a cooling potential of around 5°C with reasonable weather conditions, to which the benefits of solar shadings should be added.

### 3.4 Explain the overall ventilation strategy in Maison air et Lumière

It was found throughout the process of designing, occupying and evaluating the active house, Maison air et Lumière that the prescribed ventilation system, namely the hybrid ventilation system installed in the house combining the best of both worlds, from energy neutral ventilation during summer using ventilative cooling, to the mechanical ventilation with heat recovery used during colder periods worked well, proven in the both the sociological and quantitative monitoring. Especially the open rooms and floor plans in MAL combined with many well placed windows helped to utilize the stack effect in MAL, thereby increasing the potential air change rates to finally enable a good indoor air quality and thermal comfort. This is in good correlation with the actual found elevated air change rates found from the tracer gas measurements.

## 4 ACKNOWLEDGEMENTS

Armines – Mines ParisTech, France ([www.armines.net](http://www.armines.net))

## 5 REFERENCES

B. Peuportier, B. Favre, E. Vorger, N. Dupin (2012), *Towards the aeraulic characterization of roof windows*, 33rd AIVC Conference (Copenhagen, Denmark, 2012)

K. Duer, B. Peuportier, C. Plesner, N. Dupin (2013), *Evaluation of ventilative cooling in a single family house*, Proceedings of AIVC conference (Athens, Greece, 2013)

N. Dupin, B. Peuportier, M. Cohen, B. Favre, E. Vorger (2014), *Evaluation of ventilative cooling in a single family house - Characterization and modelling of natural ventilation*, World Sustainable Buildings Conference (Barcelona, Spain, 2014)

Danish building research institute, *Bsim (Building simulation) computer tool*, Dr. Neergaards Vej 15, DK-2970 Hørsholm, <http://sbi.dk/bsim/Pages/Start.aspx>

Active House, <https://www.activehouse.info/>

Quote from inhabitant of Maison Air et Lumière (2013), (L'habitat de demain: au-delà des expériences. Retour sur l'expérience Maison Air et Lumière VELUX MODEL HOME 2020, Final conference, December 2013)

# The future of hybrid ventilation in office buildings – energy simulations and lifecycle cost

Simone Steiger<sup>1</sup>, and Jannick Karsten Roth<sup>\*2</sup>

*1 Fraunhofer Institute for Building Physics  
Fraunhoferstraße 10  
83626 Valley, Germany*

*2 WindowMaster A/S  
Skelstedet 13  
Vedbæk, Denmark*

*\*Corresponding author: jkr.dk@windowmaster.com*

## ABSTRACT

This study presents a comparison of three ventilation systems; automated Natural Ventilation (NV), balanced Mechanical Ventilation (MV) with heat recovery and Hybrid Ventilation (HV) with heat recovery for a new build office building.

The energy demand for heating and electricity as well as the indoor climate of the building were simulated using IESVE. Three key European cities were selected (Copenhagen, Munich and London) in order to investigate the applicability of the principles to different climatic conditions in Europe.

Ventilation control strategies were set to achieve identical indoor climate for all three ventilation system. Thermal comfort and indoor air quality targets were set according to Category II of the European Standard EN 15251 (EN 15251, 2007).

The results show that the total primary energy demand (sum of heating and fan electricity demand multiplied by the primary energy factors) for NV was 9-11 kWh/m<sup>2</sup>/year, MV 20-25 kWh/m<sup>2</sup>/year and HV 7-8.5 kWh/m<sup>2</sup>/year. HV enables energy savings of 20-25% compared with NV and 60-70% compared with MV.

The total investment of the different systems including capital cost (products and installation), operation (electricity and heating), and maintenance was investigated for a 20 year period. Overall NV was found 4 to 5 times cheaper compared to MV and HV was found 2.5 times cheaper than the MV system.

The results demonstrate that HV should be considered for offices in addition to NV and MV. Overall the HV solution reduced the energy demand for heating and electricity and saved up to 60% of the CO<sub>2</sub> emissions compared to the NV and MV.

## KEYWORDS

Hybrid ventilation; natural ventilation; mechanical ventilation; ventilation in offices; Indoor Air Quality (IAQ).

## 1 INTRODUCTION

Many studies have shown that HV, combination of automatic NV and MV, offers a promising opportunity to maintaining a comfortable indoor climate and at the same time achieve significant energy savings. HV might, be the key technology to enable designers to fulfil ever stricter energy requirements and provide the user with a healthy and comfortable indoor climate.

The Reshyvent project (Reshyvent, 2004) investigated HV in residential buildings, while the Hybvent project (Heiselberg, 2006) studied the application for non-residential buildings.

Several case studies investigated in the international project IEA ECBCS-Annex 35 (Heiselberg, 2006) showed that significant energy savings can be achieved in hybrid ventilated buildings, especially through reduction in fan and cooling energy demand. The case studies for school buildings show that the HV system saves 17-55 % in a year compared to a mechanical system.

Dong (Dong, 2010) compared a MV system with a combination of NV and MV supply an office building in Scotland (Glasgow). The calculated energy savings for HV was found to about 12% utilising NV for 69% of the time. Heikkinen(Heikkinen, 2002) did a simulation for a comparison of two balanced MV systems with three types of HV for an office building. The result shows that the net energy consumption during one year for the cooling load and fan electricity could be reduced from an index 100 using MV to an index 82% and 8%, respectively, for a HV system. Ji (Ji, 2009) investigated the potential of HV for an office building in a very humid region in China. The study concluded that HV could enable 30 to 35% of the energy savings for fan power compared to the MV system.

Thus, the literature contains several findings and in general, HV is demonstrated to result in significant energy savings. This current study investigates if this conclusion is valid for an office building using state-of-the-art MV and NV systems. Identical indoor climate was realised for all three ventilation systems, as this would give a true comparison between the energy performance of the systems. The simulation was performed for three large European cities with different climates; Copenhagen, London and Munich. CO<sub>2</sub> emissions and the economical costs from selecting the different systems was also investigated from selecting the different systems.

## 2 OFFICE BUILDING GEOMETRY, PROPERTIES AND LOCATION

### 2.1 Building layout

The simulated office has three storeys with each three open-space-offices. The building is oriented East-West. Each office has windows in both directions and no openings or transparent façade elements to the north or south. Two meeting rooms, a kitchenette and a printing room are arranged along the main façade of each storey. Toilettes and stairways are placed in the two building cores.

The floor to ceiling height of each storey for the simulation with MV and MV is 2.8m below the suspended ceilings. For the simulation with NV the ceilings are less suspended, resulting in a room height of 3.0m. The gross room height is the same for all ventilation types. The net area is 233m<sup>2</sup> for the corner offices, 287m<sup>2</sup> for the middle offices and 17m<sup>2</sup> for the meeting rooms. The geometry of the building can be seen in Figure 1.

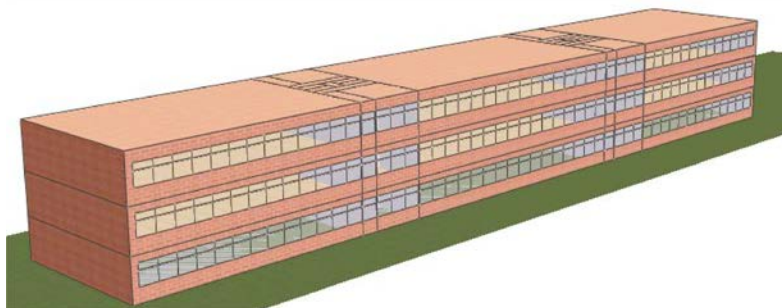


Figure 1: Layout of the building

## 2.2 Construction properties

The main construction properties attached to the models are listed in Table 1.

Glass ratio of the east/west façade is 42% and 41% in the meeting rooms. The glass selected have a g-value of 0.63 and light transmittance of 0.74.

External solar shading is provided for all three ventilation types. The lower level windows, which aren't used for natural ventilation, have an external sun screening with a shading coefficient of 0.1. In Munich, all windows were equipped with solar shading.

Table 1: Construction properties

Building element	U-Value [W/m <sup>2</sup> K]
Ground Slab	0.08
Exterior Walls	0.12
Roof	0.07
Windows	0.9-1.07

## 2.3 Internal heat loads

The occupant density in the office rooms is set to 10m<sup>2</sup> floor space and in the meeting rooms 2.25m<sup>2</sup> per employee.

The maximum occupant density during the day is 90% from Monday to Friday from 7 am to 18pm, see Figure 2.

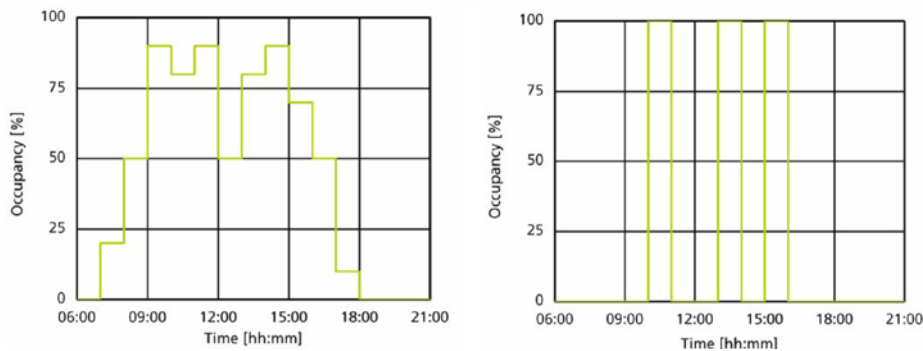


Figure 2: Occupant schedule for the open-plan-offices (left) and meeting rooms (right)

Vacation time is 7 weeks per year in total (week 14, 20, 27 - 29, and 51 - 52). The occupancy during vacation is set to 35 % adopting the same daily profiles as for the rest of the year. No occupancy is assumed during weekend.

Each person has a heat load of 75 W sensible heat and 50 W latent heat corresponding to an adult with an activity level of 1.2 met. This assumes a heat emission of 70 W/m<sup>2</sup> skin surface and a skin surface of 1.8 m<sup>2</sup>.

Each employee is expected to have technical equipment (computers etc.) with 100 W heat load. This is a typical heat load by equipment in offices according to EN 13779 (EN 13779,

2007).The lighting (fluorescent lighting) shall provide a luminance intensity of 500 lux at the table and has a maximum heat load of 8 W/m<sup>2</sup> including a desk lamp for each person.

The variation of the heat loads is adopted to the occupancy schedule.

## **2.4 Outdoor climatic conditions**

The locations chosen for the comparison are Copenhagen, Munich and London. These three cities are typical European cities with different climates and therefore different possible opportunities for HV. Copenhagen has a cold winter and a cool summer, whereas Munich has a colder winter and a warm summer. London, located near the sea, has a maritime climate with a mild winter and a cool summer.

## **3 REQUIREMENTS FOR INDOOR AIR QUALITY AND THERMAL COMFORT**

The requirements for thermal comfort and indoor air quality are based on EN 15251 (EN 15251, 2007) and Category II was applied to assessment of the indoor climate. The values might exceed the category up to 5% of the occupied hours. Category II is deemed an acceptable level of expectation and a target of 900ppm is applied for the assessment of indoor air quality.

## **4 DIMENSIONING OF VENTILATION SYSTEMS**

To maintain the air quality according to Category II of EN 15251 (EN 15251, 2007) the necessary air flow rate was calculated by the mass balance of the target carbon dioxide level of 900 ppm and a carbon dioxide emission per person of 18 l/h. This results in a total air flow rate of 230 l/s (828 m<sup>3</sup>/h) for the corner offices, 280 l/s (1008 m<sup>3</sup>/h) for the middle office and 80 l/s (288 m<sup>3</sup>/h) for the meeting rooms. The total flow rate for all meeting and office rooms is 3180 l/s (11,448 m<sup>3</sup>/h).

For maintaining temperature in summer different air change rates were tested. Due to these results a ventilation rate of 5 air times the air quality rate was selected for the summer and night ventilation. The total flow rate for all meeting and office rooms is 15,900 l/s (57,240 m<sup>3</sup>/h).

### **4.1 Natural ventilation**

For the NV every second high level window on both sides of the offices can be opened with chain drive actuators to realise cross ventilation for Copenhagen and London. For Munich, every high level window on both sides can be opened. In the meeting rooms, every high level window was set automated for all simulated locations with regard to the single-sided ventilation.

The resulting openable window area for the automated windows is 4.3 m<sup>2</sup> representing 1.8% of the floor area for the corner rooms and 4.9m<sup>2</sup> corresponding to 1.7% of the floor area (both doubled for Munich).

A wind speed of 0.5 m/s and 1 m/s results in a 2 and 4-fold air exchange rates respectively - calculated according to the British Standard Method (Allard, F., 1998) for open plan office

space. Outdoor conditions with 1 m/s wind speed should be available most of the time throughout the year for all three locations and would also be sufficient for delivering adequate ventilation.

## **4.2 Mechanical ventilation**

One centralised unit is utilised for the MV in the office building. The system was dimensioned for the maximum air flow rate according to air quality and indoor temperature (57,240 m<sup>3</sup>/h). The specification of the unit has been selected from those products currently available in the market place, resulting in a total flow rate of 70,200 m<sup>3</sup>/h.

The Specific Fan Power (SFP) value is 1814 J/m<sup>3</sup> and no heating or cooling units were assumed. The pressure loss for the ductwork of the system is 235 Pa for the supply and 170 Pa for the exhaust system. The filter classes were F7 for supply air and F5 for exhaust air causing an additional pressure of 40 Pa due to dirt. As the 'Demand Controlled Ventilation operates with a constant pressure loss in the main ductwork, the setting for the external pressure was held constant.

The sensible heat effectiveness in the simulation was set to 80 %, which is the temperature effectiveness including the effects of the motor heat.

## **4.3 Hybrid ventilation**

The HV combines a smaller decentralised MV system with automated NV.

The NV system is mainly utilised to maintain indoor temperature during summer and the transient seasons (57,240 m<sup>3</sup>/h), whereas the MV system is dimensioned solely to maintain air quality (11,480 m<sup>3</sup>/h). Hence the mechanical element has a significantly lower capacity compared to the pure MV.

The pressure loss in the MV element of the system for the supply and the exhaust ductwork is then about 235 Pa for the supply system and 170 Pa for the exhaust system. Pressure loss from filters, sensible heat effectiveness and heating/cooling unit is the same as the MV. SFP value for the system is 1814 J/m<sup>3</sup>.

## **5 CALCULATION METHOD**

The simulation program IESVE-Pro (version 6.4.0.7, Integrated Environmental Solutions Limited, Glasgow, UK) was used to simulate the energy demand and the indoor climate of the office building. The program has a special function for calculating more complex HVAC systems (ApacheHVAC) and a very reliable calculation tool for NV (MacroFlo), which can calculate NV and effects from wind turbulence on air exchange, considering special features like the aspect ratio and sash type of the opening. The calculation was done in 1 minute steps to achieve realistic results for natural and especially natural pulse ventilation. The results are derived from 6 minute averages of the calculation. This is mainly due to the pulse ventilation

when using natural ventilation, which should be controlled very precisely to avoid over cooling of the room during cold periods.

For the assessment of indoor climate, CO<sub>2</sub> levels inside the building were used as an indicator for indoor air quality, and operative room temperature was used as an indicator for thermal comfort. The values were obtained during occupancy in one representative room, and the requirements for thermal comfort and indoor air quality were based on EN 15251 (EN 15251, 2007)

## **6 CONTROL STRATEGIES**

The operational parameters of the control strategy for the simulation models were input to reflect as closely as possible WindowMaster's control strategy. Sometimes changes were necessary due to the restrictions of the simulation software or to obtain a similar thermal comfort and indoor quality.

### **6.1 Natural ventilation**

The definition of NV is automated windows on both sides of the rooms utilizing cross ventilation. Small MotorLink™ chain drive actuators are used to open and close the windows by a specific amount. The opening distance is defined by a controller, which uses indoor and outdoor climatic parameters to calculate the appropriate opening distance. This precise opening is necessary, because the resulting air flow rate is not only dependent on the climatic conditions, but also very much on the opening distance of the windows. A precise control of air flow is necessary to avoid too high ventilation rates, which cause additional heat loss or poor thermal comfort due to low temperatures or high draughts, while still providing good air quality at the same time.

Three different opening strategies were implemented; continuous ventilation, pulse ventilation, and night ventilation. Continuous ventilation with a varying opening degree is utilized for control of air quality during the whole year and indoor temperature in summer. The opening distance for continuous ventilation is restricted for comfort reasons. Pulse ventilation with the maximum opening degree calculated due to weather for a short time for additional control of indoor air quality during winter and transient times. Night ventilation is utilized for additional cooling of the rooms in summer. In addition, the windows are opened to maximum after occupancy to purge ventilate the rooms completely with fresh air until outdoor air quality is reached.

### **6.2 Mechanical ventilation**

The air flow rate of the MV is defined due to improvement of the indoor air quality and reduction of overheating. Hence, the maximum air flow rate is utilized, when either the air flow rate due to carbon dioxide level or due to indoor air temperature raise above a certain set point. Night ventilation is activated during warmer periods.

### **6.3 Hybrid ventilation**

Combining the natural and the mechanical control strategies leads to the HV control strategy. The overall strategy is to use the best aspects of both systems to achieve the best indoor climate at the lowest energy consumption.

MV is activated during the winter season, as the heat recovery of the system helps save energy to heating. NV is enabled during summer time to secure a good and stable indoor air quality and temperatures. Additionally, the chain drive actuators of the windows need much less electricity compared to the fans for MV and the flow rate can easily be increased by simply increasing the openings of the windows. Same benefit applies for NV during night time - exploiting the 'free cooling' potential.

In the transient season, most of the time the internal conditions determine, whether MV or NV is the best solution. The indoor temperature is used as an indicator of whether there is a heating or cooling demand and based on this the system automatically chooses between NV or MV.

### **6.4 Heating, shading and lighting**

The heating is enabled from October to May and if the outdoor temperature is below 12°C. The heating is set to avoid too low temperatures in accordance to Category II during occupancy (7 am - 6 pm). During occupancy, the set-point is 21°C and in times with no occupants the set-point is 19°C.

The operation of automated external blinds is according to outdoor and indoor parameters. This is done to avoid overheating, which may affect indoor temperature and thermal comfort for up to a few days later. The blind rises with a wind velocity above 12 m/s and/or an outdoor temperature below minus 6°C to avoid damage to the blinds. The blind lowers with a solar radiation above 100 W/m<sup>2</sup> and if the indoor temperature is above 24°C.

The dimming of artificial light is controlled due to occupancy and to maintain 500 lux in the rooms.

## **7 RESULTS**

### **7.1 Temperature and CO<sub>2</sub>**

The results of thermal comfort and indoor air quality were evaluated for a middle office space on the upper floor, as this was found to be the worst-case office space. Figure 3 shows the percentage of occupied hours where indoor temperature achieved the different performance categories according to EN 15251 (EN 15251 2007). This is displayed for the three ventilation types in each of the three locations.

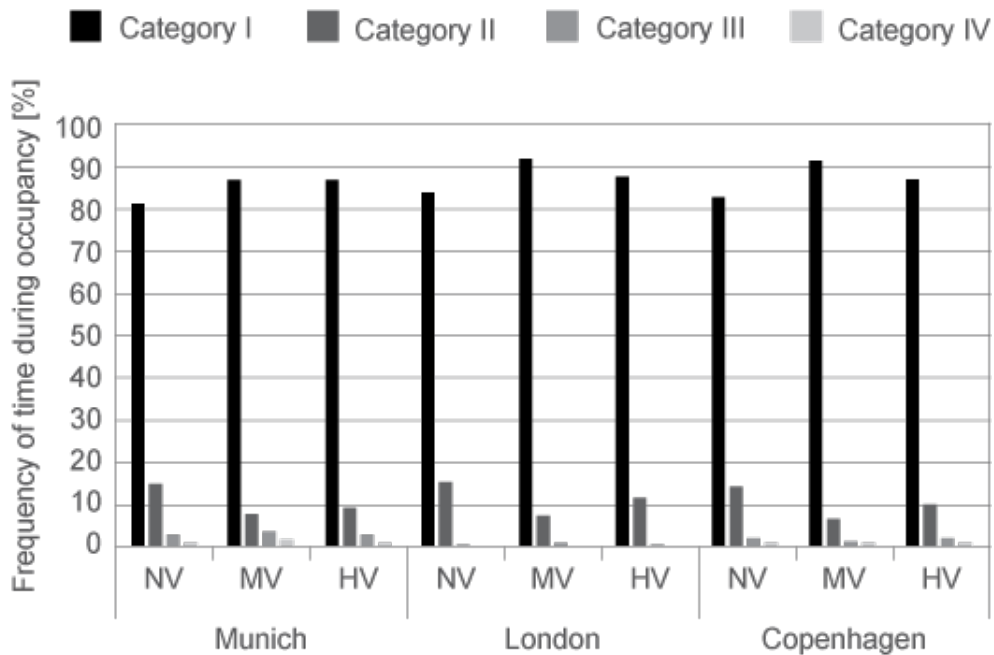


Figure 3: Percentage of occupied hours where indoor temperatures achieved the different performance categories according to EN 15251

Thermal comfort levels were found almost to be identical for the three ventilation types and at the different locations. This implies that each ventilation systems would achieve similar levels of thermal comfort in each location.

The results for the indoor air quality showed comparable figures for the three investigated ventilation types. The result demonstrated that Category II performance could be achieved 98.4-100% of the time depending on the ventilation system.

## 7.2 Primary energy

The total primary energy (sum of heating and fan electricity demand multiplied by the primary energy factors) was derived from the detailed energy modelling of the net energy. The nationally primary energy factors have been used for the different locations; Munich (district heating: 0.7; electricity 2.6), Copenhagen (0.8; 2.5) and London (1.2; 2.92).

The primary energy consumption is shown on Figure 4. The result shows that NV uses 9-11 kWh/m<sup>2</sup>/year, MV 20-25 kWh/m<sup>2</sup>/year and HV 7-8.5 kWh/m<sup>2</sup>/year. HV enables energy savings of 20-25% compared with NV and 60-70% compared with MV.

The energy performance for the HV was calculated based upon the calculations and following improvements suggested by Fraunhofer.

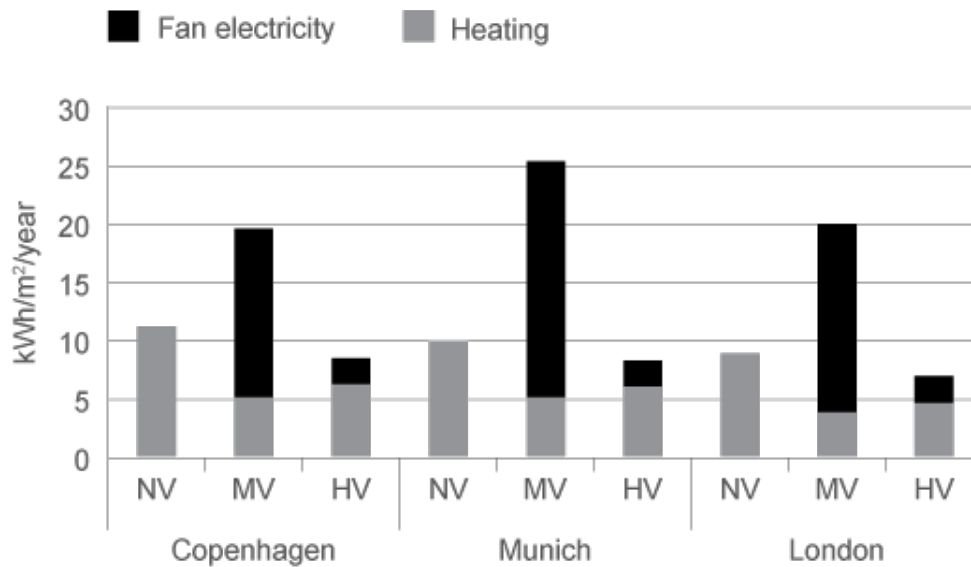


Figure 4: Primary energy consumption

## 8 CO<sub>2</sub> EMISSION

Calculation of CO<sub>2</sub> emissions are based on the following figures; Munich (district heating 200 g/kWh and electricity 606 g/kWh), Copenhagen (104; 425) and London (206; 517). CO<sub>2</sub> emissions due to electricity and heating ranges from 1.6-6.2 kg CO<sub>2</sub>/m<sup>2</sup> per year depending on location. The CO<sub>2</sub> emissions are much less for NV and HV compared to the MV system. HV emits approximately 20% than NV.

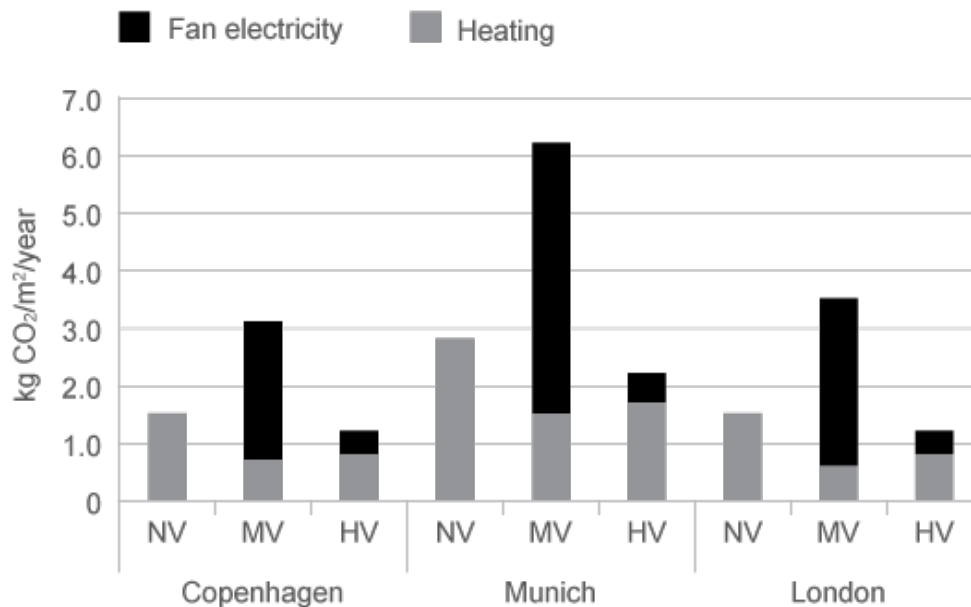


Figure 5: CO<sub>2</sub> emission

## 9 COST

The total investment required by the different systems has been evaluated including capital cost (products and installation), operation (electricity and heating), and maintenance costs for

during a period of 20 years (Figure 6). The prices are calculated by WindowMaster in close collaboration with a Danish ventilation contractor (Roth, 2012).

The maintenance cost for HV is around 40% lower compared to the pure MV system. Choosing NV this cost could be reduced by 75%. For the operation cost NV was found in the range of 30-60% cheaper compared to MV depending on location. Using HV the operation cost could be reduced in the range of 50-70% compared to MV.

One of the major differences of the three systems is the capital cost. Here it was found that a MV system is 4 to 5 times as expensive as a NV system. For HV this was a factor of 2.5.

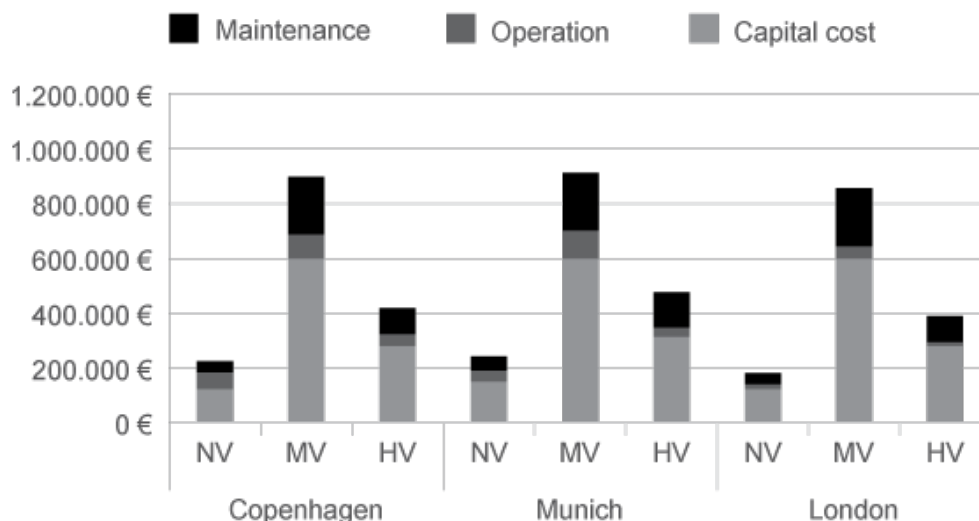


Figure 6: The total investment during a period of 20 years

## 10 DISCUSSION

The main goal was to have almost identical indoor environment for all three ventilation types in order to compare the energy demand. It should be noted that the indoor environment could have been improved for all three ventilation systems if other benchmarks for CO<sub>2</sub> and temperature performance had been chosen. The requirements for thermal comfort and indoor air quality are based on the Category II of EN 15251 with the possibility to exceed the criteria with 5% of the occupied hours. It was chosen not to use the adaptive comfort model, as it was found more easy to compare the results to fixed temperature levels.

Real, commercially available products and their specifications was chosen to make the study as realistic as possible. This method avoids a discussion about whether the results can be transferred in practice. Nevertheless, the actual products are only available in certain sizes, so it is not possible to select a product for all locations that just fits the exact requirements. Instead, it was chosen to use a product that can meet the requirements of the most heavily loaded location – which was used at all locations. The only effect can occur at the cost side, where the MV in London and Copenhagen could possibly be a more customized MV product.

WindowMaster's control strategy was adopted to a large extent as possible for the simulated models. It was to a minor degree necessary to do smaller restrictions of the simulation software or to obtain a similar thermal comfort and indoor quality. It is believed that these simulations still reflect the WindowMaster control system.

The overall objective of HV is to use the best aspects of NV and MV, in order to optimise the balance between indoor climate and energy consumption. The control strategy of HV is one of the greatest challenges, as it is a combination of the NV and MV control strategies. During winter and summer the HV control strategy is straight forward; MV gives the best results during winter, and NV gives the best results during summer period.

The transient season is, much more complex and most of the time it depends on internal conditions to dictate whether MV or NV is the best solution. Therefore, it is essential to have a control strategy that can choose between the two systems depending on indoor temperatures as an indicator for heating or possible cooling demand. This is, however not the most complicated part. The complex part is to know, when, for instance, to make the MV stop and then start up the NV system since the internal environment has changed throughout the period where MV has been used. This strategy has been developed and applied in the present study.

Even though it was out of the scope of these calculations, it was investigated if a mechanical cooling system would be more energy efficient compared to the relatively high air flow rates for the MV system especially during summer time. The following was based on basic hand calculation based on the previous results. The additional energy demand for electricity for Copenhagen and London is expected to be about 20-25% higher by using mechanical cooling compared to free cooling. For Munich, however, it would have been more effective to use mechanical cooling with the minimum flow rate, due to air quality, which would have saved 10-15% of fan energy. However, it is usually necessary to have higher flow rate with mechanical cooling to avoid too low supply air temperature.

## 11 CONCLUSION

The aim of this study was to compare the energy demand for heating and electricity for an office building located in one of the three key European cities; Munich, Copenhagen and London using either NV, MV or HV by the means of the simulation program IESVE. Identical indoor climate was realised for all three ventilation systems in accordance to European Standard EN 15251 (EN 15251, 2007).

The total primary energy demand (sum of heating and fan electricity demand multiplied by the primary energy factors) for the NV uses 9-11 kWh/m<sup>2</sup>/year, MV 20-25 kWh/m<sup>2</sup>/year and HV 7-8.5 kWh/m<sup>2</sup>/year. The result shows that HV enables energy savings of 20-25% compared with NV and 60-70% compared with MV.

One of the major differences was to be found in the total investment of the different systems including capital cost (products and installation), operation (electricity and heating), and maintenance. During a 20 year period the NV was found 4 to 5 times cheaper compared to MV. The HV was found 2.5 times cheaper than the MV system.

The results demonstrate clearly that effective automated NV can deliver similar indoor climates compared to MV, but with significantly reduced energy consumption and capital costs. However, HV should be considered for offices in addition to NV and MV. Overall the HV makes it possible to reduce the energy demand for heating and electricity and to save up to 60% of the CO<sub>2</sub> emissions.

## 12 ACKNOWLEDGEMENTS

First and foremost, we would like to thank WindowMaster for the valuable guidance, advice and knowledge sharing. Besides, we would like to thank the *Fraunhofer Institute for Building Physics* for providing a good environment and facilities to complete this project.

## 13 REFERENCES

- Allard, F. (1998). *Natural ventilation in buildings*. A design handbook. MPG Books Ltd, London
- Cron, F. and Inard, C. (2003). *Analysis of hybrid ventilation performance in France*. Proceedings of Eighth International IBPSA Conference, Eindhoven, 243 - 250.
- Dong et al. (2010). Simulation-based Hybrid Ventilation System Design and Evaluation. Proceeding of International High Performance Buildings Conference, Purdue, paper 3409, 1-7.
- EN 13779 (2007). Ventilation for non-residential buildings. Performance requirements for ventilation and room-conditioning systems
- EN 15251 (2007). *Indoor environmental input parameters for design and assessment of energy performance of buildings addressing indoor air quality, thermal environment, lighting and acoustics*.
- Emmerich, S. J (2006) *Ventilation Systems in an Office Building*. HVAC & Research 12, 4, 975 - 1004.
- Heikkinen, J. et al. (2002). *Performance simulation of hybrid ventilation concepts*. IEA - Technical report in Annex 35 Hybrid Ventilation.
- Heiselberg, P. (2006). *Design of Natural and Hybrid Ventilation*. DCE Lecture Notes, Aalborg University.
- Ji et al. (2009). Hybrid ventilation for low energy building design in south China. *Building and Environment* 44, 2245-2255.
- Reshyvent (2004) *Demand controlled hybrid ventilation in residential buildings with specific emphasis on the integration of renewables*.
- Roth, J. (2012). *Cost calculation for the office investigated in the Fraunhofer study*.

# Design and performance of ventilative cooling: a review of principals, strategies and components from International case studies

Paul D O'Sullivan<sup>\*1</sup>, Adam O'Donovan<sup>1</sup>, Guoqiang Zhang<sup>2</sup>, Guilherme Carrilho da Graca<sup>3</sup>

1. Cork Institute of Technology  
Rossa Avenue, Bishopstown, Cork,  
Ireland

\*Corresponding author:  
paul.osullivan@cit.ie

2. College of Civil Engineering,  
Hunan University, Yuelushan,  
Changsha, Hunan, 410082,  
P.R.China

3. DEGGE, University of  
Lisbon,  
Campo Grande,  
Lisbon, Portugal

## ABSTRACT

Overheating is an unwanted consequence of modern building designs and internal gains that will be aggravated by the effects of climate change on local climates within urban and suburban areas. To minimise the energy cost of limiting overheating several different approaches exist for passive cooling dissipation techniques. Free cooling by ventilation, or Ventilative Cooling,(VC), is a generally accepted effective, energy efficient, mitigation strategy to building overheating. There are many factors that influence the design and selection of suitable VC strategies. Obtaining quantitative data about the spectrum of solutions employed across the range of suitable VC applications can be difficult and high in collaborative effort. A recent International Energy Agency project gathered information about well documented case studies of buildings with VC and investigated the existence of synergies in design, selection and simulation of solutions as well as any heterogeneous patterns in the adoption of VC principles and VC system component characteristics. This paper presents the aggregated data for 14 international case studies, provides a review of the VC systems adopted and design methods applied to ensure successful performance for different building types and climates. Various methods for VC system sizing at each stage of the design process are discussed along with the design criteria adopted in each case. Values for the percentage opening area to floor area ratio, a key metric for benchmarking the sizing of ventilation openings are presented and discussed. Further, a recommended range for this fundamental design parameter is suggested. Demonstrated implementation of control strategies for different types of VC solutions is also reviewed and discussed. Similarities in lessons learned were found to exist across multiple case studies. Finally, a synopsis of the key lessons learned during the design and operation phases of the case studies is also presented and reviewed.

## KEYWORDS

Natural ventilation, ventilative cooling, case studies, thermal simulation

## 1 INTRODUCTION AND BACKGROUND

With 1983-2012 likely the warmest 30 year period of the last 1400 years in the Northern Hemisphere, Europe's human and managed systems, which include the built environment and urban infrastructure, are providing a major contribution to accelerating global climate change(IPCC 2014). Along with factors such as urban densification, a warming world is leading to increasingly hostile internal thermal environments in buildings. Evidence exists that current ambitious envelope and fabric oriented heating demand reduction strategies might result in an increased risk of extended periods of overheating in new buildings as well as in building retrofits(McLeod, Hopfe, and Kwan 2013; Psomas et al. 2016). A number of studies, both residential and non-residential have investigated the occurrence of overheating in buildings and found that a range of factors contribute to unacceptable levels of overheating (Beizaee, Lomas, and Firth 2013; Lomas and Kane 2013; Mavrogianni et al. 2012). Passive and hybrid cooling through the integration of natural and mechanical ventilation principles

with the building morphology and materials has long been championed as a viable alternative to mechanical cooling. However, the basic premises under which mechanical and natural approaches operate are fundamentally different and this has led to a scepticism from building owners regarding the ability of a natural ventilation system to adequately deliver acceptable internal conditions in buildings during the warmer months of the year. The criteria by which natural ventilation is assessed is often one suited only to mechanically controlled environments and this is diametrically opposed to the basic principles of the concept. However, there are still many barriers to the effective adoption of natural ventilation for cooling (Carrilho da Graça and Linden 2016). Passive cooling techniques can be organised into a three-step framework: 1. prevention of heat gains, 2. modulation of heat gains and 3. heat dissipation (Santamouris and Kolokotsa 2013). When implemented correctly in this way, ventilative cooling (VC) solutions, properly integrated with the building design, are generally accepted as effective, energy efficient, mitigation strategies to building overheating. The ongoing international project IEA-EBC Annex 62 on VC deals with improving the suitability of VC for buildings. This project addresses the existing challenges for VC application and devises recommendations through development of design methods and compliance tools related to predicting, evaluating and eliminating the cooling need and the risk of overheating in buildings and through the development of new attractive energy efficient VC solutions (Kolokotroni et al. 2015). IEA-EBC annex 62 State of the Art Review report recently defined VC as, *'The application of ventilation flow rates to reduce the cooling loads in buildings. VC utilizes the cooling and thermal perception potential of outdoor air. The air driving force can be natural, mechanical or a combination'* (Kolokotroni et al. 2015). This project included a subtask to analyse and evaluate the performance of real VC solutions and of used design methods and tools using similar criteria and methods. In doing this the objective was to identify lessons learned and develop recommendations for design and operation of VC as well as identifying barriers for application and functioning of ventilative cooling. To achieve this, well-documented case studies in their operational phase at various international locations were studied. The benefit of real buildings and field study measurements is the realistic nature of the boundary conditions and thermal gains. In total 19 case studies are proposed for the project, with the results of their performance evaluations due to be published in an IEA report in January 2018. This paper gives an initial overview of the characteristics and lessons learned of investigated case studies in Annex 62. It summarises the features of the various case studies including the building characteristics, VC strategies and systems, design criteria and approach and lessons learned. It presents results from performance evaluations for selected case studies.

## **2 OVERVIEW OF CASE STUDIES**

The 14 case studies of Annex 62 that will be analysed in this paper are located in 10 participant countries. Of the 14 case studies, three were completed in 2014, three in 2013, two in 2012, four in 2011 with the two remaining case studies in 2003 and 2007. Over 85% of case studies were built after 2010. There are three office buildings, five educational buildings, four residential, one mixed use and one kindergarten. Eight of the case studies have rural surroundings and six have urban surroundings. Four case studies were refurbishment projects. Table 1 shows the range of climate regions represented within the case studies while Table 2 summarises key categorical information about the case study buildings.

## **3 BUILDING DESIGN**

What are the typical characteristics of buildings that utilise ventilative cooling? Some of these characteristics are developed in response to the decision to use VC while others are the reason VC was adopted.

Table 1: Variation in climate regions for all case study buildings. (Please refer to the Koppen-Geiger climate classification system for details on KG abbreviations in column 1)

KG	General Description	Qty	Locations
Cfb	Temperate with warm summers and no dry season	6	Cork, IE; Ernstbrunn, AT; Waregem and Ghent, BE; Verrieres-le-Buisson, FR; Bristol, UK
Cfa	Temperate, hot summers and no dry season	2	Changsha, CN; Hayama, JP
Dfb	Cold with warm summers and no dry season	3	Stavern, NO; Trondheim, NO; Innsbruck, AT
Dfc	Cold with no dry season and cold summer	1	Larvik, NO
Csa	Temperate with dry, hot summers	2	Sicily, IT; Lisbon PT

Table 2: Building Type, size and year of completion for all case studies

Country	Building	Type	Year (New or Refurb)	Floor Area m <sup>2</sup>	Strategy
IE	zero2020	Office	2012 <sup>(R)</sup>	223	Natural
NO.1	Brunla Primary school	Education	2011 <sup>(R)</sup>	2500	Hybrid
NO.2	Solstadbarnehage	Kindergarten	2011 <sup>(N)</sup>	788	Hybrid
CN	Wanguo MOMA	Residential	2007 <sup>(N)</sup>	1109	Mechanical
AT.1	UNI Innsbruck	Education	2014 <sup>(R)</sup>	12530	Hybrid
AT.2	wkSimonsfeld	Office	2014 <sup>(N)</sup>	967	Hybrid
BE.1	Renson	Office	2003 <sup>(N)</sup>	2107	Natural
BE.2	KU Leuven Ghent	Education	2012 <sup>(N)</sup>	278	Hybrid
FR	Maison Air et Lumiere	House	2011 <sup>(N)</sup>	173	Natural
IT	Mascalucia ZEB	House	2013 <sup>(N)</sup>	144	Hybrid
JP	Nexus Hayama	Mixed Use	2011 <sup>(N)</sup>	12836	Natural
PT	CML Kindergarten	Education	2013 <sup>(N)</sup>	680	Natural
UK	Bristol University	Education	2013 <sup>(R)</sup>	117	Mechanical
NO.3	Living Lab	Residential	2014 <sup>(N)</sup>	100	Hybrid

### 3.1 Design Influences

What influences the design of a building that aims to adopt ventilative cooling? A range of factors can have varying levels of influence on building design. A list of those deemed as having properties that will affect the type of strategies and components adopted for cooling is presented in Table 3. For each case study, the relative importance of different factors on the design of the building was ranked qualitatively using High, Medium or Low classifications. In this table we can see that initial costs and energy costs were consistently important design influences across most case studies. Solar loads and air leakage were also important factors for most case studies. However, even in urban case studies external and internal noise did not appear to influence the building and ventilation designs. Rain ingress was however, relatively important in many locations. Finally, internal loads were important in about half of the case designs. It is difficult to draw global conclusions from the matrix in Table 3 but energy and initial costs along with internal and solar loads are key factors when considering design solutions.

### 3.2 Morphology

Some of the case studies are small, dedicated research spaces or studies using small isolated parts of a building such as the lecture rooms in KU Leuven, Bristol University computer room and the zero2020 testbed in Ireland.

Table 3: Design Influences (R denotes Rural; U denotes Urban; \*denotes residential)

Country	Building	Surroundings	Design Influences												
			Initial costs	Maintenance Costs	Energy Costs	Solar Loads	Internal Loads	External Noise	Internal Noise Propagation	Air Pollution	Rain Ingress	Insect Prevention	Burglary Prevention	Privacy	Air Leakage
IE	zero2020	R	H	M	H	H	L	L	L	L	M	L	H	M	M
NO.1	Brunla Primary school	R	H	H	H	L	M	L	L	H	M	L	L	L	H
NO.2	Solstadbarnehage	R	L	L	H	L	L	L	M	H	L	L	L	L	H
AT.2	wkSimonsfeld	R	H	H	H	M	L	L	L	L	L	L	L	L	M
BE.1	Renson	R	L	M	L	H	H	H	L	L	L	L	L	L	L
IT	Mascalucia ZEB*	R	H	M	H	H	L	L	L	L	L	L	M	L	M
JP	Nexus Hayama	R	M	M	H	H	L	L	L	L	M	H	H	M	M
UK	Bristol University	R	H	H	H	L	H	L	M	L	M	M	H	L	L
CN	Wanguo MOMA*	U	H	M	H	H	L	L	L	L	M	L	M	L	H
AT.1	UNI Innsbruck	U	H	H	H	M	L	M	L	L	M	L	L	L	H
BE.2	KU Leuven Ghent	U	H	L	H	H	H	L	L	L	M	L	L	L	H
FR	Maison Air et Lumiere*	U	M	M	L	H	M	L	L	H	L	L	M	L	M
PT	CML Kindergarden	U	H	L	L	M	M	L	L	L	M	M	M	M	L
NO.3	Living Lab*	U	L	L	H	H	M	L	M	L	H	L	L	L	H

Others are grand in scale such as Nexus Hayama in Japan and The University of Innsbruck. In almost all cases, except arguably the Chinese case study in Changsha, the buildings can be classified as low rise with typically 2-4 floors. The average floor area for the buildings is 2,468m<sup>2</sup>. However, when we remove Nexus Hayama in Japan (the largest case study at 12,836m<sup>2</sup>) and University of Innsbruck this reduces to 765m<sup>2</sup>. The smallest case study is the living lab in Trondheim at 100m<sup>2</sup>, this is a research test facility for residential dwellings in cold climates. The shape coefficient, a measure of the building shape and efficiency of external building surface to floor area, is shown in Figure 1. We can see that the small Italian zero energy home has a disproportionately high shape coefficient compared with the other values. Excluding this we have a minimum shape coefficient of 0.18 and a maximum shape coefficient of 0.96, still a good spread. Figure 2 shows the window to wall area ratios for each case study. Four of the case studies have relatively high window to wall area ratios at or greater than 50% while the average is 34%.

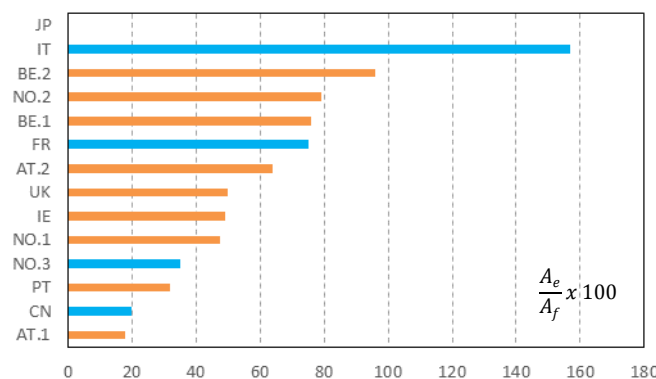


Figure 1: Building Shape Co-efficient for all Case Studies. (Residential shown in Blue)

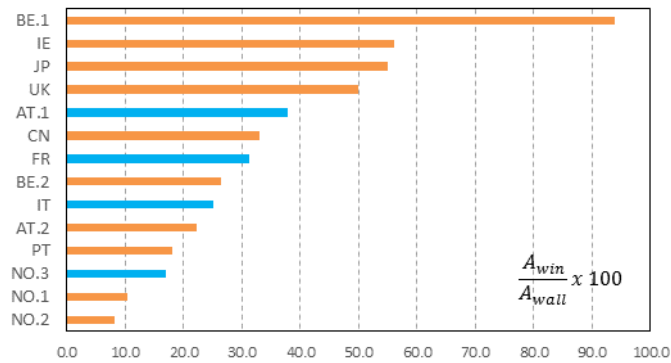


Figure 2: Window to Wall area ratio for all Case Studies. (Residential shown in Blue)

### 3.3 Thermal Properties

The case study buildings overall can be classified as high performance. Most buildings were designed as low energy or sustainable buildings. The average elemental U-value for all 14 case studies is  $0.41 \text{ W/m}^2\text{K}$ , which appears high but there is a large spread in individual values, with an average standard deviation across all elements of  $0.34 \text{ W/m}^2\text{K}$ . Some buildings such as the zero2020 testbed in Cork, have very high fabric performance (Wall U-value of  $0.09 \text{ W/m}^2\text{K}$ ) while other buildings have lower performance, in part due to their respective national building regulations, such as the Nexus Hayama (wall U-value of  $0.86 \text{ W/m}^2\text{K}$ ). This variation is in some part due to the different performance requirements and construction types for different climates. Six of the case studies can be classified as having heavy or very heavy thermal mass according to ISO13790. Good air tightness is a recurring feature of most case studies with the average Air Change Rate (ACR) from infiltration at  $1.13 \text{ h}^{-1}$ , ranging from  $0.51$  to  $1.85 \text{ h}^{-1}$ .

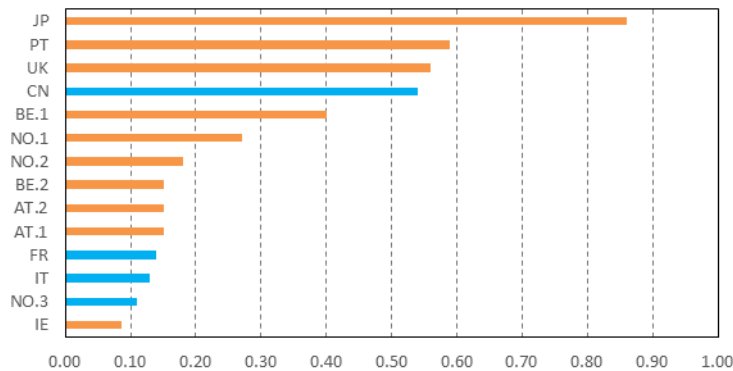


Figure 3: External Wall U-values for all Case Studies. ( $\text{W/m}^2\text{K}$ ) (Residential shown in Blue)

## 4 VC STRATEGIES, COMPONENTS & CONTROL

### 4.1 Strategies & components

The case studies present a rich variety of VC solutions across a range of building types, morphologies and climates. Table 4 summarises VC concepts used in the case studies. The large majority, 86%, of the case studies use natural ventilation for VC strategies. The sensible internal loads for these case studies are all below  $30 \text{ Wm}^{-2}$  except for the Kindergarten in Portugal. The average is  $25 \text{ Wm}^{-2}$ . All the climates were temperate. The number of days with the maximum daily external temperature greater than  $25^\circ\text{C}$  was less than 30 in all cases except Portugal and the cooling season humidity is also low throughout except in Japan. The most prevalent strategy was hybrid ventilation with 50% of buildings using this approach for ventilative cooling. Many of these systems used mechanical exhaust ventilation when conditions required an increased airflow through the building.

Table 4: VC Strategies in all Case Studies

Country	Building	VC Strategies								
		Natural driven	Mech. Supply Driven	Mech. exhaust driven	Natural night ventilation	Mech. night ventilation	Air conditioning	Indirect Evap. Cooling	Earth to Air Heat Exch.	Phase Change Materials
IE	Zero2020	X			X					
NO.1	Brunla Primary school	X			X					
NO.2	Solstadbarnehage	X		X	X	X				
CN	Wanguo MOMA		X	X		X	X			
AT.1	UNI Innsbruck	X		X	X					
AT.2	WkSimonsfeld	X		X						
BE.1	Renson	X			X					
BE.2	KU Leuven Ghent	X		X			X			
FR	Maison Air et Lumiere	X								
IT	Mascalucia ZEB	X			X				X	
JP	Nexus Hayama	X					X			
PT	CML Kindergarden	X			X					
UK	Bristol University					X	X			X
NO.3	Living Lab	X								

The internal loads in these spaces were greater than  $40 \text{ Wm}^{-2}$  in Norway and Belgium, while in Austria and Italy there were less than  $10 \text{ Wm}^{-2}$ . Two out of the 14 case studies use mechanical ventilation as a VC strategy.

A number of unique systems are employed in particular case studies such as the integrated manual and automated slot louvres at zero2020 in Ireland (O'Donovan, O'Sullivan, and Murphy 2017; O'Sullivan and Kolokotroni 2014, 2016), the displacement ventilation system at CML Kindergarten in Portugal (Mateus et al. 2016); the earth to air heat exchanger at the ZEB Home in Italy (Causone et al. 2014) and the PCM mechanical ventilation system in the UK (Santos, Hopper, and Kolokotroni 2016).

#### 4.2 VC system control

The control strategies used varied depending on the ventilation strategy of each case study building. Figure 4 conveys which parameters were used depending on the ventilation strategy as a percentage of all case studies. Thermal comfort was the main driver for controlling all ventilation systems. Temperatures and relative humidity were the main parameters considered by control systems for comfort, while  $\text{CO}_2$  was main parameter considered when controlling for air quality. Internal temperature was used by all cases studies with set-point control, one case study had a purely manual system. In addition, over 60% of case studies used an external temperature as part of their control strategy, this was typically a low temperature limit where the outside air was to be below the zone internal air temperature. Another point to note is the fact that exclusively mechanical systems did not consider precipitation or wind, while natural and hybrid systems did not incorporate external relative humidity levels into their control strategies.

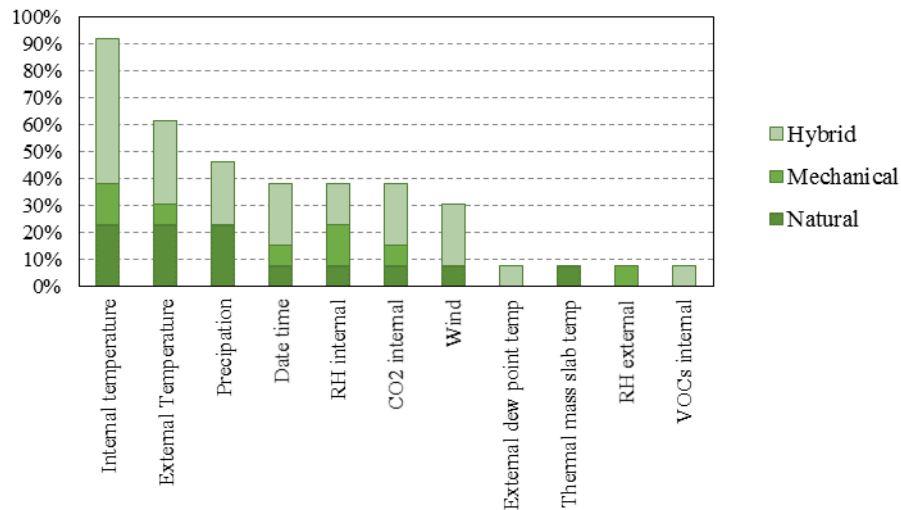


Figure 4: Summary of parameters used in VC control strategies for all case studies

Most control strategies for occupied periods used the internal zone temperature and an external temperature low limit as controlling parameters in ventilation strategies. There was no major correlation between the set-point used and the climate. The overall range of set-point temperatures were observed to be between 20-24°C where the mean internal air temperature set-point was around 22°C. The range of low temperature limits for outside air was between 10-18°C, with a mean external low temperature limit set-point of around 14°C. Around 54% of the case study buildings had a manual override switch or allowed occupant controlled ventilation during occupied hours as part of their typical occupied control strategies. All natural ventilation case studies allowed a form of occupant interaction with the ventilation system while 60% of hybrid systems allowed occupant interaction with the ventilation system. For systems that controlled depending on relative humidity an average set-point of 60% was observed. There were differing ranges of acceptability depending on whether the VC system was mechanical or natural. 69% of the case studies investigated incorporated a night ventilation strategy as well as an occupied ventilation control strategy. Typically, night ventilation strategies had different control parameters than ventilation strategies during occupied hours. The night ventilation strategies incorporated typically had a set-point for the zone as well as a limit on the properties of the air brought into the building also. The mechanical night ventilation strategies observed only used a combination of internal and external air temperature. The range of internal temperatures used for night ventilation strategies was between 15-23°C while the low limits on the external air temperature were between 10-18°C. Night ventilation was also dependant on the presence or absence of rain and wind speeds above a certain value. Typically, the wind speed had to be below 14m/s or 10m/s respectively and with no rain for night ventilation systems to operate. In cases where relative humidity was the control parameter night ventilation would not be activated unless the relative humidity was below 70% for a given zone. Parameters specifically related to indoor air quality were not considered in any of the night ventilation strategies.

## 5 SIZING AND SIMULATION OF VC

### 5.1 Sizing of VC systems

Information on the recommended aperture areas when sizing a VC systems is critical for the building designer. For almost all case studies, natural ventilation was adopted as either the sole source of VC or as part of a wider strategy, with, for example, natural supply and mechanical exhaust. It is generally beneficial to identify possible dimensionless parameters

that provide a characterisation of the system, thus allowing for similarity investigations across multiple different systems. Owing to this and the inherent importance of the ventilation opening geometry to the delivered airflow rate, a parameter calculated as the percentage opening area to floor area ratio, or POF, was obtained for each case study. The opening area used is the maximum available geometric opening area and does not incorporate the flow effects of the opening. Figure 5 presents POF values for all cases where this was relevant.

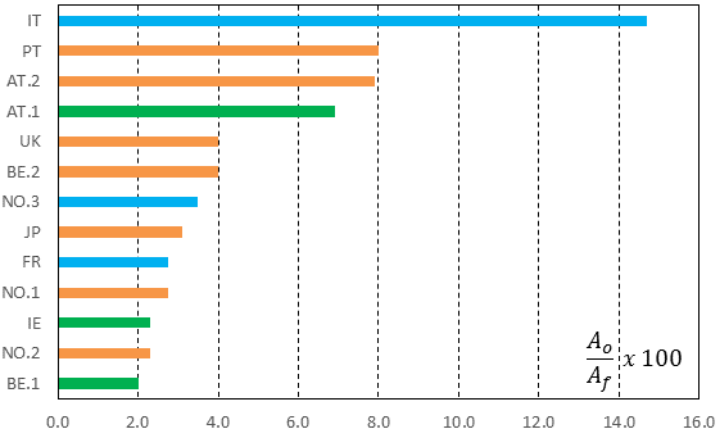


Figure 5: Percentage openable area to floor area for selected case studies. (Residential shown in blue, offices shown in green)

We can see a large spread of values for the case studies. 65% of buildings had POF values less than 4%. There seems to be no correlation with building category. The two highest values are from Csa climates. Two of the lowest three values are from fully naturally ventilated offices. Natural ventilated buildings had a POF of 3.6% while hybrid buildings had a POF of 4.6%, or 6.0% when the Italian case study is included. Although several building regulations impose a minimum floor to opening area ratio of 5% there is a generally accepted rule of thumb for designers when sizing openings at the concept stage of 1-3%. The low end of this range appears inadequate when compared with these case studies. A range of 2-4% seems more reasonable. Discharge coefficients range from 0.25 to 0.7 across the case studies although these were only measured in a few cases with many estimated.

**5.2 Simulation of VC systems**

Both the airflow performance and capacity sizing of the VC strategies and components, along with the building thermal performance, was investigated at various stages of the design using appropriate simulation tools. At the scope development stages national standards and engineering guidance documents, such as those published by CIBSE in the UK, were used by some countries. Some countries began to develop models in different design packages such as PHPP and TAS while the Portugal case study used EnergyPlus from the initial stage right through to the operational performance evaluation stage. There was no single dominant tool for modelling VC across all case studies. For example, at the detailed design BSim was used for the naturally ventilated house in France, WindmasterSIMIEN was for all three cases in Norway, EnergyPlus was used in Portugal and in Italy. IES Apache was used in Ireland and the UK for the detailed design but TRNSYS was adopted for the Irish case study for operational performance evaluations. Only in Japan was CFD used. IDA Ice was adopted in Norway for all operational performance evaluations. A more thorough analysis of feedback from the use of the tools is underway but currently unavailable.

## 6 PERFORMANCE EVALUATION

All case studies completed performance evaluations involving various measurement campaigns. Each case study adopted different approaches and investigated different phenomena, including ventilation rate measurements, thermal comfort studies, analysis of internal thermal environments, investigation of the performance of specific solutions such as displacement ventilation, chimney-stacks, hybrid systems, cross flow ventilation etc. It is not possible to present in this paper the individual findings from these campaigns.

The Annex research project identified that, in order to assess the minimum performance of the VCstrategy, one cooling season of internal air temperatures data should be obtained. This data should then be compared with a previously defined overheating risk criteria based on two static thresholds. Table 5 presents a selection of results from the case studies. There are some measuring campaigns still under way and as such results are unavailable for these. Overall there is very good performance from the VC solutions adopted in all case studies.

Table 5: Preliminary results of VC performance evaluation

Country	Building	Summer Design Values		overheating criteria	% Occ hrs above threshold		Occ hrs
		T <sub>e</sub>	T <sub>i,o</sub>		28°C	25°C	
IE	zero2020	26.0	25.0	T <sub>i</sub> <28°C for 99% occ hrs	0.7	5.5	2600
NO.1	BrunlaSchool	25.0	26.0	T <sub>i</sub> > 26°C	0.0	0.0	2600
NO.2	Solstad	25.0	24.0	T <sub>i</sub> > 26	0.0	0.0	2860
AT.1	UNI Innsbruck	34.0	27.0	T <sub>i</sub> < 26 for 95% occ hrs	1.1	16.2	2600
AT.2	wkSimonsfeld	34.5	24.0	T <sub>i</sub> > 26 zone / T > 29 gallery	0.0	5.0	3250
JP	Nexus Hayama	26.0	26.0	T <sub>i</sub> < 28 for 99% occ hrs (check)	1.0	40.0	8736
PT	Kindergarden	30.0	26.0	80% acceptability for 99% hr occ	2.6	16.0	3640

## 7 LESSONS LEARNED

The case studies analysed in this project yielded over sixty four key lessons learned, the majority of which were considered important. Thirty one lessons were contributed based on the design and construction and 33 lessons contributed from case studies buildings during operation and post occupancy. These are summarised separately.

### 7.1 Lessons from design and construction

Designing a building to incorporate VC can be challenging and may require a lot of detailed building information. While each challenge was different the main key lessons were as follows:

- Detailed building simulation is important when simulating VC strategies. Most case studies analysed highlighted the need for reliable building simulations in the design phase of a VC system. This was considered most important when designing for hybrid ventilation strategies where multiple mechanical systems need harmonization. Some studies also said that simulating the window opening in detail was important.
- Customisation may be an important factor in designing a VC system. In order to ventilate certain buildings it may be necessary to design custom components. Some case studies highlighted the need to have custom design systems that were specific to country

regulations and the use of a building or space. Some consideration should also be given to the clients expectations around specific issues like rain ingress and insect prevention.

- VC systems were considered a cost-effective and energy efficient in design by most case studies, but particularly with naturally ventilated systems. It was indicated that designing with the integration of manual operation and control was important, particularly in a domestic setting.

## **7.2 Operation and Post Occupancy**

While systems may be designed to have high levels of comfort, IAQ and energy performance, achieving this was difficult. All case studies emphasised that monitoring a buildings performance post occupancy is important if not essential in building performance optimisation. While some key lessons were more specific than others the following general observations were made;

- Engaging with the building owners or operators as soon as possible is integral to guaranteeing building performance for IAQ, comfort or energy savings. For some case studies this specifically meant educating or working with the facilities operator or manager for the building, for others it meant educating the building occupiers themselves.
- It was suggested by some that this engagement should occur already in the design stage.
- VC in operation is generally a good option. Case studies comment on the reduction of overheating and improvement of comfort conditions in the buildings that used outside air. However, correct maintenance and calibration of the systems is integral to maintaining performance.
- Some case studies highlighted the need to exploit the outside air more with lower external air control limits during typical and night-time operation. Others suggested that exploiting the thermal mass of a building was key. However, it was noted that care must be taken with considering these low temperatures as some case studies, particularly in cold climates observed more incidences of overcooling than overheating.

## **8 CONCLUSIONS**

In the last two decades, the use of VC has been slowly increasing. The best contemporary designs combine natural ventilation with conventional mechanical cooling. When properly designed, and implemented, these hybrid approaches maximize the VC potential while avoiding overheating during the warmer months. Yet, despite the potential shown in the case studies analysed in this study, and other existing examples, the potential of VC cooling remains largely untapped. This study showed that a lot can be learned from collecting information about VC case studies that have demonstrated through measurement that they perform well and their internal environments are comfortable for an acceptable period of the occupied time. However, due to the heterogeneity of the cases analysed, it is difficult to draw general conclusions regarding recommendations for designers. The characteristics of each case study appeared unique due to the need for the approach to respond to a specific climate, the building usage, morphology and client criteria. Hybrid systems are the most common type of system for VC and the use of mechanical fans to compliment a passive system should be strongly considered where possible. The use of simulation in the VC system design phase can reduce the uncertainties that are usually associated with natural ventilation systems. A POF value in the region of 2 – 8% was recorded and choosing a value on the larger end of this range at the concept design stage may be appropriate.

## 9 ACKNOWLEDGEMENTS

The authors would like to acknowledge all IEA Annex 62 participants that provided a case study for the project, namely: NO – Maria Justo Alonso; UK – M. Kolokotroni and T. Santos; IT – M. Peitrebbon, G. Cattarin & L. Pagaliano; IE – P. O’Sullivan & A. O’Donovan; FR – C. Plesner; AT – P. Holzer; PT – G. Carrilho da Graça & Nuno Mateus; CN – G Zhang & J Han; JP – T Nonoka & H Kotani; BE – H Breesch.

## 10 REFERENCES

- Beizaee, A., K. J. Lomas, and S. K. Firth. 2013. “National Survey of Summertime Temperatures and Overheating Risk in English Homes.” *Building and Environment* 65:1–17. Retrieved (<http://dx.doi.org/10.1016/j.buildenv.2013.03.011>).
- Carrilho da Graça, Guilherme and Paul Linden. 2016. “Ten Questions about Natural Ventilation of Non-Domestic Buildings.” *Building and Environment* 107:263–73. Retrieved (<http://dx.doi.org/10.1016/j.buildenv.2016.08.007>).
- Causone, Francesco, Salvatore Carlucci, Lorenzo Pagliano, and Marco Pietrobon. 2014. “A Zero Energy Concept Building for the Mediterranean Climate.” *Energy Procedia* 62:280–88. Retrieved (<http://dx.doi.org/10.1016/j.egypro.2014.12.389>).
- IPCC. 2014. *Climate Change 2014 Synthesis Report Summary Chapter for Policymakers*.
- Kolokotroni, Maria et al. 2015. *IEA EBC Annex 62 VC- State of the Art Review*. Retrieved ([venticool.eu/wp-content/uploads/2013/09/SOTAR-Annex-62-FINAL.pdf](http://venticool.eu/wp-content/uploads/2013/09/SOTAR-Annex-62-FINAL.pdf)).
- Lomas, Kevin and T. Kane. 2013. “Summertime Temperatures and Thermal Comfort in UK Homes.” *Building Research and Information* 41(3):259–80. Retrieved (<http://www.scopus.com/inward/record.url?eid=2-s2.0-84876211342&partnerID=40&md5=689ba31d894e461c921725e56066eeaa>).
- Mateus, Nuno M., Goncalo Nunes Simoes, Cristiano Lucio, and Guilherme Carrilho da Graça. 2016. “Comparison of Measured and Simulated Performance of Natural Displacement Ventilation Systems for Classrooms.” *Energy and Buildings* 133:185–96.
- Mavrogianni, Anna, Paul Wilkinson, Michael Davies, Phillip Biddulph, and Eleni Oikonomou. 2012. “Building Characteristics as Determinants of Propensity to High Indoor Summer Temperatures in London Dwellings.” *Building and Environment* 55:117–30. Retrieved (<http://dx.doi.org/10.1016/j.buildenv.2011.12.003>).
- McLeod, Robert S., Christina J. Hopfe, and Alan Kwan. 2013. “An Investigation into Future Performance and Overheating Risks in Passivhaus Dwellings.” *Building and Environment* 70:189–209. Retrieved April 30, 2014 (<http://linkinghub.elsevier.com/retrieve/pii/S0360132313002503>).
- O’Donovan, Adam, P. D. O’Sullivan, and Michael D. Murphy. 2017. “A Field Study of Thermal Comfort Performance for a Slotted Louvre Ventilation System in a Low Energy Retrofit.” *Energy and Buildings* 135:312–23. Retrieved (<http://dx.doi.org/10.1016/j.enbuild.2016.11.049>).
- O’Sullivan, Paul D. and Maria Kolokotroni. 2014. “Time-Averaged Single Sided Ventilation Rates and Thermal Environment in Cooling Mode for a Low Energy Retrofit Envelope.” *International Journal of Ventilation* 13(2):153–68. Retrieved (<http://ijvent.org/doi/abs/10.5555/2044-4044-13.2.153>).
- O’Sullivan, Paul D. and Maria Kolokotroni. 2016. “A Field Study of Wind Dominant Single Sided Ventilation through a Narrow Slotted Architectural Louvre System.” *Energy and Buildings* 138:733–47. Retrieved (<http://linkinghub.elsevier.com/retrieve/pii/S0378778816315614>).
- Psomas, Theofanis, Per Heiselberg, Karsten Duer, and Eirik Bjørn. 2016. “Overheating Risk Barriers to Energy Renovations of Single Family Houses: Multicriteria Analysis and Assessment.” *Energy and Buildings* 117:138–48. Retrieved (<http://linkinghub.elsevier.com/retrieve/pii/S0378778816300883>).

- Santamouris, Mattheos and Dionysia Kolokotsa. 2013. "Passive Cooling Dissipation Techniques for Buildings and Other Structures: The State of the Art." *Energy and Buildings* 57:74–94. Retrieved March 3, 2013 (<http://linkinghub.elsevier.com/retrieve/pii/S0378778812005762>).
- Santos, Thiago, Nick Hopper, and Maria Kolokotroni. 2016. "Performance in Practice of a Ventilation System with Thermal Storage in a Computer Seminar Room." *12th CLIMA REHVA World Congress* (May):11. Retrieved ([http://vbn.aau.dk/files/233719310/paper\\_142.pdf](http://vbn.aau.dk/files/233719310/paper_142.pdf)).

# A New Approach to Estimating Carbon Dioxide Generation Rates from Building Occupants

Andrew Persily<sup>\*1</sup>, Lilian de Jonge<sup>2</sup>

*1 National Institute of Standards and Technology  
100 Bureau Drive, MS8600  
Gaithersburg, MD 20899 USA*

*\*Corresponding author: andyp@nist.gov*

*2 George Mason University  
Department of Nutrition and Food Studies  
4400 University Drive, MS: 1F8  
Fairfax, VA 22031 USA*

## ABSTRACT

Indoor carbon dioxide (CO<sub>2</sub>) concentrations have been used in the fields of building ventilation and indoor air quality (IAQ) for decades. Specific applications include the estimation of ventilation rates, control of outdoor air ventilation rates based on indoor CO<sub>2</sub> as an indicator of occupancy, and use of CO<sub>2</sub> as an IAQ performance metric. All of these applications require values for the CO<sub>2</sub> generation rates of the occupants of the space or building being considered. Human CO<sub>2</sub> generation rates depend on their level of physical activity as well as their sex, age, and body size. Historically and currently, these rates have been based on formula and data from the literature that are many decades old. In many cases, a single value for an adult on the order of 0.3 L/min is used independent of individual characteristics that are known to impact CO<sub>2</sub> generation rates. While the fields of human metabolism and exercise physiology have been studying human energy use, oxygen consumption and CO<sub>2</sub> generation for many decades, that knowledge has not been incorporated by the ventilation and IAQ communities. This paper describes the known dependencies of CO<sub>2</sub> generation rates on occupant characteristics and presents a calculation method for estimating these generation rates based on these concepts. This method is more robust and up-to-date than previously-established calculation procedures and will support more accurate values of CO<sub>2</sub> generation rates for use in ventilation and IAQ applications. The paper also compares the CO<sub>2</sub> generation rates using the new approach to those from the approach commonly used today as well as the resulting steady-state concentrations for different space types.

## KEYWORDS

*Carbon dioxide; human metabolism; physical activity*

## 1 INTRODUCTION

Indoor CO<sub>2</sub> concentrations have been prominent in discussions of building ventilation and indoor air quality (IAQ) since the 18<sup>th</sup> century. More recent discussions have focused on the impacts of CO<sub>2</sub> on building occupants as well as the use of indoor CO<sub>2</sub> to estimate ventilation rates and to control outdoor air ventilation (Persily 2015). While the rates at which building occupants generate CO<sub>2</sub> are key to these applications, the rates currently in use are not based on recent references or a thorough consideration of the impacts of occupant characteristics.

The fields of human metabolism and exercise physiology have studied human activity for many decades, focusing on rates of energy expenditure, oxygen consumption and CO<sub>2</sub> generation, as well as the individual factors that affect these rates. These factors include sex, age, height, weight and body composition, with fitness level and diet composition also affecting energy expenditure and the ratio of O<sub>2</sub> consumed to CO<sub>2</sub> produced. This paper applies the principles of these fields to yield an updated approach to estimating CO<sub>2</sub> generation rates from building occupants.

## 2 CURRENT APPROACH TO ESTIMATE CO<sub>2</sub> GENERATION RATES

The ventilation and IAQ fields have long used the following equation to estimate CO<sub>2</sub> generation rates from building occupants (ASHRAE 2017):

$$V_{CO_2} = \frac{0.00276 A_D M RQ}{(0.23RQ + 0.77)} \quad (1)$$

where  $V_{CO_2}$  is the CO<sub>2</sub> generation rate per person (L/s);  $A_D$  is the DuBois surface area of the individual (m<sup>2</sup>);  $M$  is the level of physical activity, sometimes referred to as the metabolic rate (met); and  $RQ$  is the respiratory quotient.  $A_D$  is estimated from height  $H$  in m and body mass  $W$  in kg as follows:

$$A_D = 0.203H^{0.725}W^{0.425} \quad (2)$$

The respiratory quotient,  $RQ$ , is the ratio of the volumetric rate at which CO<sub>2</sub> is produced to the rate at which oxygen is consumed, and its value depends primarily on diet (Black et al., 1986). Based on data on human nutrition in the U.S, specifically the ratios of fat, protein and carbohydrate intake (Wright and Wang, 2010),  $RQ$  equals about 0.85.

Equation 1 first appeared in the Thermal Comfort chapter of the ASHRAE Fundamentals Handbook in 1989. That discussion, as well as the current discussion in the handbook, references Nishi (1981), which presents that equation as a means of measuring the metabolic rate of an individual. Nishi does not discuss the basis of this equation nor provide references. The ASHRAE Fundamentals Handbook also contains a table of metabolic rates for various activities, which has remained unchanged since the 1977 edition. These values are based on references predominantly from the 1960s, though some are even older. The same metabolic rate values are contained in the ASHRAE thermal comfort standard ASHRAE 2013), with similar data contained in ISO standard 8996 (ISO, 2004). As noted later in this paper, there are more recent and comprehensive sources of metabolic rate data.

The above equations and data are currently being used to estimate CO<sub>2</sub> generation rates within the field of ventilation and IAQ. For example, ASTM D6245 presents these equations and notes that for an average-sized adult ( $A_D = 1.8 \text{ m}^2$ ) engaged in office work at 1.2 met, the corresponding CO<sub>2</sub> generation rate is 0.0052 L/s (ASTM 2012). For a child ( $A_D = 1 \text{ m}^2$ ) at the same level of physical activity, the corresponding CO<sub>2</sub> generation rate is 0.0029 L/s. Note that discussions of the application of Equation 1 to ventilation and IAQ do not generally consider effects of air density on CO<sub>2</sub> generation rates, simply presenting these rates in volumetric units without specifying the air temperature or pressure.

## 3 ESTIMATION OF CO<sub>2</sub> GENERATION RATES

This section describes a new approach to estimating CO<sub>2</sub> generation rates from building occupants based on concepts from the fields of human metabolism and exercise physiology, as described in more detail in Persily and de Jonge (2017). This approach uses the basal metabolic rate ( $BMR$ ) of the individual(s) of interest combined with their level of physical activity. This approach contrasts with Equation 1, which only considers body surface area and level of physical activity.

The first step in this new approach is to estimate the  $BMR$  of the individuals of interest. Equations for estimating  $BMR$  values as a function of sex, age and body mass are presented in Schofield (1985) and shown in Table 1. For example, the  $BMR$  of an 85 kg male between 30 y

and 60 y old is 7.73 MJ/day and 6.09 MJ/day for a 75 kg female in this same age range.

Table 1. *BMR* values (Schofield 1985). (*m* is body mass in units of kg)

Age (y)	<b>BMR (MJ/day)</b>	
	Males	Females
< 3	0.249 m – 0.127	0.244 m – 0.130
3 to 10	0.095 m + 2.110	0.085 m + 2.033
10 to 18	0.074 m + 2.754	0.056 m + 2.898
18 to 30	0.063 m + 2.896	0.062 m + 2.036
30 to 60	0.048 m + 3.653	0.034 m + 3.538
>= 60	0.049 m + 2.459	0.038 m + 2.755

After estimating the value of *BMR*, the next step is to estimate their level of physical activity in terms of the value of *M* that corresponds to the activities in which they are involved. There are two primary references for obtaining information on energy requirements for different physical activities. The first is a report prepared by the Food and Agriculture Organization of the United Nations (FAO), the World Health Organization (WHO) and the United Nations University (UNU), which discusses human energy requirements as a function of age and other individual characteristics (FAO, 2001). The second is a web-based compendium of physical activities (Ainsworth et al., 2011a; Ainsworth et al., 2011b). The rate of energy use of an individual, or group of individuals, engaged in a specific activity is estimated by multiplying the *BMR* value for that individual or group by a factor that characterizes the specific activity. The FAO report refers to this factor as the physical activity ratio (*PAR*), while the web-based compendium refers to it as the metabolic equivalent using the term *MET*. In this paper, the variable *M* (in dimensionless units of met) is used to describe the ratio of the human energy use associated with a particular physical activity to the *BMR* of that individual. Persily and de Jonge (2017) contains tables of values of *M* for various activities from the FAO report and the web-based compendium.

Once the *BMR* value and the value of *M* for the relevant activity have been determined, their product in units of MJ/day is converted to L of oxygen consumed per unit time. This conversion is based on the conversion of 1 kcal (0.0042 MJ) of energy use to 0.206 L of oxygen consumption (Lusk, 1924). The exact conversion depends on the relative oxidation of carbohydrates and fat, but given the variation in the other factors used to calculate CO<sub>2</sub> generation rates, a value of 0.206 L is a reasonable approximation. This conversion results in 1 MJ/day of energy use corresponding to 0.00057 L/s of oxygen consumption, which based on a respiratory quotient *RQ* of 0.85 (discussed above), corresponds to 0.00048 L/s of CO<sub>2</sub> production. A *BMR* value of 7.73 MJ/day, mentioned above for an 85 kg male between 30 y and 60 y of age, therefore corresponds to 0.0037 L/s of CO<sub>2</sub> production. Using a physical activity level of 1.5 met for sitting tasks, light effort (e.g. office work) results in a CO<sub>2</sub> generation rate of 0.0056 L/s, which is close to the value of 0.0052 L/s cited in ASHRAE Standard 62.1 and ASTM D6245 for an adult.

Based on the approach just described, the CO<sub>2</sub> generation rate can be expressed in L/s at an air pressure of 101 kPa and a temperature of 273 K, with *BMR* in units of MJ/day and *M* in met, using Equations (3) and (4).

$$V_{CO_2} = RQ BMR M 0.000569 \quad (3)$$

Assuming *RQ* equals 0.85, Equation 3 can be expressed as:

$$V_{CO_2} = BMR M 0.000484 \quad (4)$$

Adjustments to other values of air pressure and temperature are described in Persily and de Jonge (2017), with Equation (5) showing the CO<sub>2</sub> generation rate for other values of T and P.

$$V_{CO_2} = RQ BMR M \left(\frac{T}{P}\right) 0.000211 \quad (5)$$

In order to facilitate use of these calculations, Table 2 contains CO<sub>2</sub> generation rates for a number of *M* values over a range of ages for both males and females. The mean body mass values are based on data in the EPA Exposure Factors Handbook, specifically the values in Tables 8-4 for males and 8-5 for females (EPA, 2011). These values are most accurate, but still inherently approximate, when applied to a group of individuals and will not generally be accurate for a single individual.

Table 2. CO<sub>2</sub> generation rates for ranges of ages and level of physical activity

Age (y)	Mean mass (kg)	BMR (MJ/day)	CO <sub>2</sub> generation rate (L/s)						
			Level of physical activity (met)						
			1.0	1.2	1.4	1.6	2.0	3.0	4.0
<b>Males</b>									
< 1	8.0	1.86	0.0009	0.0011	0.0013	0.0014	0.0018	0.0027	0.0036
1 to <3	12.8	3.05	0.0015	0.0018	0.0021	0.0024	0.0030	0.0044	0.0059
3 to <6	18.8	3.90	0.0019	0.0023	0.0026	0.0030	0.0038	0.0057	0.0075
6 to <11	31.9	5.14	0.0025	0.0030	0.0035	0.0040	0.0050	0.0075	0.0100
11 to <16	57.6	7.02	0.0034	0.0041	0.0048	0.0054	0.0068	0.0102	0.0136
16 to <21	77.3	7.77	0.0037	0.0045	0.0053	0.0060	0.0075	0.0113	0.0150
21 to <30	84.9	8.24	0.0039	0.0048	0.0056	0.0064	0.0080	0.0120	0.0160
30 to <40	87.0	7.83	0.0037	0.0046	0.0053	0.0061	0.0076	0.0114	0.0152
40 to <50	90.5	8.00	0.0038	0.0046	0.0054	0.0062	0.0077	0.0116	0.0155
50 to <60	89.5	7.95	0.0038	0.0046	0.0054	0.0062	0.0077	0.0116	0.0154
60 to <70	89.5	6.84	0.0033	0.0040	0.0046	0.0053	0.0066	0.0099	0.0133
70 to <80	83.9	6.57	0.0031	0.0038	0.0045	0.0051	0.0064	0.0095	0.0127
>= 80	76.1	6.19	0.0030	0.0036	0.0042	0.0048	0.0060	0.0090	0.0120
<b>Females</b>									
< 1	7.7	1.75	0.0008	0.0010	0.0012	0.0014	0.0017	0.0025	0.0034
1 to <3	12.3	2.88	0.0014	0.0017	0.0020	0.0022	0.0028	0.0042	0.0056
3 to <6	18.3	3.59	0.0017	0.0021	0.0024	0.0028	0.0035	0.0052	0.0070
6 to <11	31.7	4.73	0.0023	0.0027	0.0032	0.0037	0.0046	0.0069	0.0092
11 to <16	55.9	6.03	0.0029	0.0035	0.0041	0.0047	0.0058	0.0088	0.0117
16 to <21	65.9	6.12	0.0029	0.0036	0.0042	0.0047	0.0059	0.0089	0.0119
21 to <30	71.9	6.49	0.0031	0.0038	0.0044	0.0050	0.0063	0.0094	0.0126
30 to <40	74.8	6.08	0.0029	0.0035	0.0041	0.0047	0.0059	0.0088	0.0118
40 to <50	77.1	6.16	0.0029	0.0036	0.0042	0.0048	0.0060	0.0090	0.0119
50 to <60	77.5	6.17	0.0030	0.0036	0.0042	0.0048	0.0060	0.0090	0.0120
60 to <70	76.8	5.67	0.0027	0.0033	0.0038	0.0044	0.0055	0.0082	0.0110
70 to <80	70.8	5.45	0.0026	0.0032	0.0037	0.0042	0.0053	0.0079	0.0106
>= 80	64.1	5.19	0.0025	0.0030	0.0035	0.0040	0.0050	0.0075	0.0101

## 4 DISCUSSION

While the approach described in this paper for estimating CO<sub>2</sub> generation rates from individuals has the advantages that it is based on principles of human metabolism and exercise physiology, as well as using more recent data on levels of physical activity, it is not yet clear how much it will impact applications of indoor CO<sub>2</sub> to building ventilation and IAQ. Analyses are needed to understand the impact on CO<sub>2</sub> demand control ventilation

system setpoints, as well as the associated energy use. Other analyses are also needed to investigate how these updated CO<sub>2</sub> generation rates will impact the use of CO<sub>2</sub> as an IAQ metric. As an initial step in those analyses, CO<sub>2</sub> generation rates using the new approach are compared to those from the approaches commonly used today, as well as the resulting steady-state concentrations, for different space types.

Table 3 presents values of CO<sub>2</sub> generation rates and steady state indoor CO<sub>2</sub> concentrations (above outdoor) for three different space types, calculated three different ways. The columns labelled “Standard values” employ the default CO<sub>2</sub> generation rates provided in ASTM D6245, 0.0052 L/s for adults and 0.0029 L/s for children, both assuming 1.2 met of physical activity. Ideally, a user of that standard would not rely on these typical values but would instead calculate them for the spaces they are considering, using an appropriate body surface area and met level. However, it is also possible that some use these average values without considering the occupants in their specific situation. The values labelled “Equation 1 (Nishi)” use equation 1 in this paper, which accounts for surface area  $A_D$  and met level  $M$ . For the Office and Conference room,  $M$  is assumed to equal 1.4, based on the more recent physical activity data referenced in this paper. The body surface area  $A_D$  is assumed to equal 2.0 m<sup>2</sup>, based on mean values for adult males and females (EPA 2011). The classroom values are assume an occupancy of 24 students (1.2 met, 0.8 m<sup>2</sup>) and 1 teacher (1.6 met, 2 m<sup>2</sup>). The values labelled “Equation 4” use the values in Table 2 of this paper for the occupants as just described. The last three columns of Table 3 present steady-state values of the indoor minus outdoor CO<sub>2</sub> concentration, using the average CO<sub>2</sub> generation rates for each space and assuming they are ventilated in accordance with ASHRAE Standard 62.1 (ASHRAE 2016), per the values in the second column of the table.

Table 3. Comparison of CO<sub>2</sub> Generation Rates and Steady-State Indoor Concentrations

Space type	Outdoor air ventilation per Standard 62.1 (L/s per person)	Average CO <sub>2</sub> Generation Rate (L/s per person)			Steady-State Indoor – Outdoor CO <sub>2</sub> Concentration (mg/m <sup>3</sup> )		
		“Standard” values	Equation 1 (Nishi)	Equation 4 in this paper	“Standard” values	Nishi Equation	Equation 4
Office	8.5	0.0052	0.0068	0.0048	1120	1465	1039
Conference room	3.1	0.0052	0.0068	0.0048	3071	4018	2850
Classroom (5 to 8 y)	7.4	0.0030	0.0026	0.0030	740	631	746

In comparing the CO<sub>2</sub> generation rates in Table 3, the values calculated using Equation 4 of this paper are about 8 % lower than the “Standard values” for the Office and Conference room and the same for the Classroom. However, they are close to 40 % less than the value from the Nishi equation for the Office and Conference room and about 15 % higher for Classroom. The steady-state concentrations using Equation 4 are about 7 % lower than the “Standard values” in the Office and Conference room and very close in the Classroom. Compared to the Nishi equation, the concentrations using Equation 4 are about 30 % less in the Office and Conference room. The values using Equation 4 are close to 20 % higher than the Nishi values in the Classroom. Based on this very limited analysis, the use of the new method embodied in Equation 4 and the new physical activity data can yield differences CO<sub>2</sub> generation rates and steady-state concentrations, in some cases higher and in others lower. More space types and occupancy characteristics need to be investigated before any general trends are revealed, but it seems clear that the new method will yield significantly different results in many cases.

## 5 CONCLUSIONS

The approach described in this paper for estimating CO<sub>2</sub> generation rates from individuals is based on concepts from the fields of human metabolism and exercise physiology, as well as more recent data than those currently used in the fields of ventilation and IAQ. It is intended to replace the equation that has been used for decades within the ventilation and IAQ communities (Equation 1 in this paper) and offers important advantages. First, the previous equation is based on a 1981 reference that provides no explanation of its basis, while the new approach is derived using principles of human metabolism and energy expenditure. Also, the new approach characterizes body size using mass rather than surface area, which in practice is estimated not measured. Body mass is easily measured and data on body mass distributions are readily available. The new approach also explicitly accounts for the sex and age of the individuals being considered, which is not the case with Equation 1. As new data on body mass become available, these data can be used to adjust CO<sub>2</sub> generation rates accordingly. Similarly, new information on *BMR* values and approaches to their estimation can also be easily applied to these calculations.

The CO<sub>2</sub> generation rate estimation method described here is applicable to groups of individuals, as the theory behind the method and the data are based on groups, not single individuals. If the rate of energy consumption or CO<sub>2</sub> generation of a specific individual is needed, it must be measured for that individual to account for differences that can exist due to body composition, diet, genetics and other factors. When considering a population of individuals in a building or space, the average values derived using the described approach will be more reliable than for a single individual. However, that reliability should be increased by characterizing the specific population of interest in terms of sex, age, body mass and activity level. Methods for performing such characterizations in a standardized fashion are not described in this paper. The increased accuracy of CO<sub>2</sub> generation estimates that may be achieved by doing so have not been studied, but additional research would be useful to demonstrate their value.

Based on the initial and limited analysis presented in this paper, the use of the new method embodied in Equation 4 and the new physical activity data, can yield differences in CO<sub>2</sub> generation rates and resulting steady-state concentrations in some circumstances, in some cases higher and in others lower. More space types and occupancy characteristics need to be investigated before any general trends are revealed, but it seems clear that the new method will yield significantly different results in many cases.

The approach presented in this paper for estimating CO<sub>2</sub> generation rates from building occupants constitutes a significant advance in the analysis of IAQ and ventilation and should be considered in future applications of CO<sub>2</sub> in ventilation and IAQ studies and standards. In addition, the sources of physical activity data identified should be incorporated into the references that currently use older and much more limited data sources, i.e., ASHRAE Standard 55, the ASHRAE Fundamentals Handbook, ISO Standard 8996, and ASTM D6245 (ASHRE 2013, ASHRAE 2017, ISO 2004, ASTM 2012).

## 6 REFERENCES

- Ainsworth, B., Haskell, W., Herrmann, S., Meckes, N., Bassett Jr, D., Tudor-Locke, C., Greer, J., Vezina, J., Whitt-Glover, M. and Leon, A. (2011a) The Compendium of Physical Activities Tracking Guide, Healthy Lifestyles Research Center, College of Nursing & Health Innovation, Arizona State University: <https://sites.google.com/site/compendiumofphysicalactivities/>.
- Ainsworth, B., Haskell, W., Herrmann, S., Meckes, N., Bassett Jr, D., Tudor-Locke, C., Greer, J., Vezina, J., Whitt-Glover, M. and Leon, A. (2011b). Compendium of Physical Activities: a second update of codes and MET values. *Medicine and Science in Sports and Exercise*, 43(8), 1575-1581.
- ASHRAE. (2017). *Fundamentals Handbook*, Atlanta, GA, American Society of Heating, Refrigerating and Air-Conditioning Engineers, Inc.
- ASHRAE. (2013). *ANSI/ASHRAE Standard 55-2013, Thermal Environmental Conditions for Human Occupancy*, American Society of Heating, Refrigerating, and Air-Conditioning Engineers, Inc.
- ASHRAE. (2016). *ANSI/ASHRAE Standard 62.1-2016, Ventilation for Acceptable Indoor Air Quality*, American Society of Heating, Refrigerating, and Air-Conditioning Engineers, Inc.
- ASTM. (2012). *Standard Guide for Using Indoor Carbon Dioxide Concentrations to Evaluate Indoor Air Quality and Ventilation*, West Conshohocken, PA, American Society for Testing and Materials, (D6245-12).
- Black, A.E., Prentice, A.M. and Coward, W.A. (1986). Use of Food Quotients to Predict Respiratory Quotients for the Double-Labelled Water Method of Measuring Energy Expenditure. *Human Nutrition: Clinical Nutrition*, 40C, 381-391.
- EPA. (2011). *Exposure Factors Handbook*, Washington DC, U.S. Environmental Protection Agency, EPA/600/R-09/052F.
- FAO. (2001). *Human Energy Requirements. Report of a Joint FAO/WHO/UNU Expert Consultation*, Geneva, Food and Agriculture Organization of the United Nations, Food and Nutrition Technical Report Series 1.
- ISO. (2004). *Ergonomics of the thermal environment — Determination of Metabolic Rate*, Brussels, International Organization for Standardization, (EN ISO 8996).
- Lusk, G. 1924. Analysis of the Oxidation of Mixtures of Carbohydrate and Fat. *Journal of Biological Chemistry*, 59, 41-42.
- Nishi, Y. (1981) Measurement of the Thermal Balance of Man, In: Cena, K. and Clark, J. A. (eds) *Bioengineering Thermal Physiology and Comfort*, New York, Elsevier, 29-39.
- Persily, A. (2015). Challenges in developing ventilation and indoor air quality standards: The story of ASHRAE Standard 62. *Building and Environment*, 91, 61-69.
- Persily, A.K. and de Jonge, L. (2017). Carbon Dioxide Generation Rates of Building Occupants. *Indoor Air*, Accepted: 14 March 2017. 10.1111/ina.12383.
- Schofield, W.N. (1985). Predicting Basal Metabolic Rate, New Standards and Review of Previous Work. *Human Nutrition: Clinical Nutrition*, 39C (Supplement 1), 5-41.
- Wright, J.D. and Wang, C.-Y. (2010). *Trends in Intake of Energy and Macronutrients in Adults From 1999-2000 Through 2007-2008*, Hyattsville MD, Centers for Disease Control and Prevention, National Center for Health Statistics.

# Methodology for assessing the air-exchange performance of residential ventilation systems

Rob C.A. van Holsteijn<sup>\*1</sup>, Jelle Laverge<sup>2</sup>, and William L.K. Li<sup>1</sup>

*1 VHK BV  
Elektronicaweg 14  
2628 XG Delft, Netherlands*

*\*Corresponding author: r.van.holsteijn@vhk.nl*

*2 Ghent University  
Building Physics, Construction and Services Group  
Sint-Pietersnieuwstraat 41, B4  
B-9000 Ghent, Belgium*

## ABSTRACT

Residential ventilation standards, especially in Europe are slowly but substantially moving away from their usual prescriptive approach towards performance based specifications. While academics and policy makers argue about the relevant IAQ indicators, housing developers and end users need to make a choice between the different ventilation system options they are faced with in the market. Although several IAQ rating systems have emerged, a comprehensive assessment method to rate the inherent qualities of the ventilation system itself is not available [6]. In this paper, we propose a methodology for such a rating system based on the ability of the system to deliver the requested amount of air at the right place and time, issued from a project commissioned by the European Ventilation Industry Association (EVIA). The proposed method makes a distinction between the performance in habitable and wet spaces in dwellings and includes technical aspects such as mechanical support of the airflow, automatic control and (where applicable) filtration. The label proposed to communicate the results of the assessment specifies the design flow rate, the performance in each of the space types and a filtration rating separately, allowing end users to objectively compare products that are suited for their particular needs rather than lumping these aspects together in a rating for the ‘average’ dwelling. This paper is intended as a solicitation of comments from the broader field of ventilation stakeholders on the fundamental structure of the rating system.

## KEYWORDS

Performance indicators, residential ventilation systems

## 1 INTRODUCTION

Until today, differences in the performance of residential ventilation systems remain unaddressed. It is generally assumed that compliance with building codes also implies that the ventilation performance of the various systems is comparable. Existing EPBD and Ecodesign legislation is also based on this assumption and compare ventilation systems only on the basis of their energy performance. The result is a market in which the main reasons for selecting a ventilation system are limited to *energy performance* and *installed costs*. The performance of its primary function ‘*exchanging air*’ for the purpose of achieving acceptable IAQ-levels in all rooms is not a selection criterion.

Various recent field research projects however indicate that there are substantial differences among ventilation systems in the extent in which the requested air exchanges are achieved in the various rooms, resulting in large differences in IAQ-levels, especially in habitable rooms [1,2,3,4,5].

Field research shows that on a dwelling level, the total number of air changes per hour (ach) may be sufficient, but at room level the air exchanges do not always occur in the right place at

the right time [1] . A significant share of the air exchanged by these ventilation systems is therefore in vain and only contributes to a higher energy bill.

In addition there is the fact that occupants cannot properly assess the resulting IAQ-levels. Various pollutants are odourless (radon, CO, various VOC's) and occupants gradually adapt to changing IAQ-levels and simply do not possess the required sensory capacities to accurately perceive the IAQ-levels. In other words, there is no useful feedback as to whether the ventilation system performs adequately (e.g. field studies show that inhabitants can be fairly content with CO<sub>2</sub>-concentrations that are far above 2500 ppm) [1,2]. The inhabitant can therefore not be held accountable for his choice of ventilation system, nor for an incorrect (manual) operation of the ventilation systems on the basis of perceived IAQ-levels. In practice the technical system parameters are dominant where the air exchange performance is concerned. And there is a serious need to provide people with objective information concerning the air exchange performance of ventilation systems and their impact on the IAQ-levels in a dwelling.

This blind spot in ventilation system performance has manoeuvred the market into an unintended situation where the energy performance of ventilation systems is assessed without knowing its ventilation performance. Low cost ventilation systems with lower ventilation performance unduly benefit from this situation and burden households with questionable IAQ-levels.

The Residential Working Group of EVIA (European Ventilation Industry Association) initiated a project to investigate whether an effective and transparent method can be constructed to assess the ventilation performance of ventilation systems in residential dwellings. This paper presents the methodological basis for such an assessment method.

## **2 SCOPE OF THE ASSESSMENT METHOD**

### **2.1 Delimitation of the scope**

The initial focus of the assessment method will be on residential ventilation systems. It will only be applicable to ventilation systems that are properly installed according to prevailing building codes and manufacturer guidelines.

Air exchanges for the purpose of extracting cooking fumes are excluded from the assessment method, emphasizing the view of the EVIA Working Group that cooking fumes can better be removed with dedicated cooker hoods. Ventilation systems that use alternating flow directions (supply provision becomes exhaust provision and vice versa) are also excluded from the scope, since representative field research related to their ventilation performance is lacking. Future field research into these types of ventilation systems may lead to further extension of the scope.

Finally ventilation system solutions, that are added for the purpose of filtering or cleaning recirculated indoor air, are excluded from the scope. On the other hand ventilation system solutions that are used for cleaning the outdoor air are included.

### **2.2 Defining Ventilation Performance**

Pollutant emissions from building- and finishing products, from furniture and from humans activities are the main cause for a deteriorating indoor air quality. The best starting point for

improving IAQ in dwellings obviously is to reduce these source emissions. Selecting proper building materials and interior products is therefore the key strategy.

The second strategy for improving IAQ-levels is ventilation, or exchanging air for the purpose of achieving acceptable IAQ-levels in all rooms. This primary function of a ventilation system can be assessed separately. Occurring IAQ-levels are after all the end result of both source emission strength and air exchange rates in a specific room. Ventilation systems cannot control the source emission strength. In principle, ventilation systems can only control the air exchange rates that occur in specific rooms, and it is this specific function where systems show large differences in performance.

Academic discussions on what the proper metrics are for assessing the overall performance of ventilation systems are ongoing. In specific forums such as AIVC workshops, ASHRAE IAQ and IEA EBC Annex 68 it is stated that ‘as of today, there is no clear set of metrics that can be used to assess the overall ventilation performance of a building with regard to its indoor air quality’. It is expected that it will take another 5 to 10 years before this topic can be properly addressed.

For the interim period this paper proposes to use a more pragmatic approach, and to relate the ventilation performance solely to its primary function: *exchanging air for the purpose of achieving acceptable IAQ-levels in all rooms of a dwelling*.

For the envisaged assessment method the following definition is proposed for the air-exchange performance of residential ventilation systems: *‘the ability to achieve requested air exchanges in each room of a dwelling for the purpose of extracting and/or diluting concentrations of all hazardous and annoying substances’*.

The adjective ‘*requested*’ that is used in this definition, refers to the air exchange rates as defined in building codes and will be used as initial reference value. Since field research shows that code compliant ventilation rates in individual rooms are not always achieved [1,2,3,4,5] - especially during presence in habitable rooms – a logical first step should be to assess the air-exchange performance vis-à-vis its design air exchange rates. These design air exchange rates are generally selected to comply with building codes that often reflect the minimal required air exchange capacity. Because higher air exchange rates automatically lead to improved IAQ-levels, the proposed methodology will also appreciate ventilation rates that exceed these reference values [8].

### **2.3 Different room types, different ventilation strategy**

Dwellings are a series of connected rooms. These rooms can be grouped into two types, both with their own specific requirements concerning ventilation strategy:

- Habitable rooms (living room, bedrooms, study)
- Wet rooms (kitchen, bathroom, toilets, laundry room)

#### **Habitable rooms**

In habitable rooms, the main type of pollutants are bio-effluents, building material emissions, emissions from interior products and pollutants from human activities.

Exposure to these emissions occur during presence in these rooms, and because occupancy time typically is long, especially in bedrooms, the risk of exposure is highest in these type of rooms. A good ventilation strategy must therefore be based on the principle that requested ventilation rates are primarily achieved during presence. In these rooms the requested air exchanges must be achieved with air supply provisions that supply clean and fresh outdoor

air. In certain environments this could mean that filtration of the outside air is recommended before feeding the air into the habitable rooms. During absence, a minimum basic ventilation rates should be applied.

### **Wet rooms**

In contrast to the habitable rooms, the main pollutants in wet rooms are moisture, odour, material emissions and pollutants from human activities. Occupancy times are short, as is the exposure to the emissions in these rooms.

Main ventilation strategy in these rooms relates to the extraction of moisture starting at the moment it is produced, until humidity levels are below threshold levels and continue the extraction for a certain period of time to ensure that also the humidity that is accumulated in building materials is removed. The risk of mould and moisture related building problems can thus be reduced. After that, minimum basic ventilation rates can be applied. For wet rooms there are no specific demands regarding the quality of the supplied air, so for energy saving purposes, (used) indoor air is usually supplied.

Most ventilation standards, including the new draft EN16798-1, differentiate between these two type of rooms. Some standards also mention non-occupied spaces like connecting spaces (hall, staircase, etc.). As the name suggest there is no occupancy and a minimum risk of exposure in these spaces. Basic ventilation rates can be applied here, which will be achieved anyhow since these spaces are passageways for the supply air of the wet rooms.

The proposed assessment method will be based on those technical features of a ventilation system that have an influence on the ability of the ventilation system to achieve the requested air exchanges following the ventilation strategy described above for both the habitable rooms and the wet rooms.

## **3 TECHNICAL SYSTEM PARAMETERS**

The following system parameters are considered relevant for the air-exchange performance in habitable rooms and wet rooms. For the proposed assessment method it is essential that these technical parameters are assessed on room level.

Primary system parameters (to be assessed per room)

- Type of air exchange provision (direct/indirect, driving forces: natural/mechanical)
- Maximum installed air flow capacity
- Type of operation and controls
- Filtration method

Secondary parameters, like thermal comfort and noise production are kept out of this initial assessment because they are generally adequately described in building codes, related standards and guidelines. Furthermore, installers have a large influence on these aspects that are often not system related but installation-quality related. These topics can however be handled separately in a technical sheet in a more qualitative manner.

### **3.1 Type of air exchange provisions**

Code compliant ventilation systems require an air supply and an air exhaust provision in every room of a dwelling. The type of these supply and exhaust provision play a very

important role in determining the ability of the ventilation system to achieve the requested air exchanges in that room. A distinction will be made in the forces driving the air exchanges (natural or mechanical) and in the connection the supply or exhaust provision has with the outside (direct or indirect). An indirect connection means that the air is supplied or exhausted through one (or more) intermediate spaces. Both parameters will influence the ability of the ventilation system to achieve requested air exchanges in the room concerned. Natural and indirect provisions are subject to larger uncertainties than mechanical and direct ones.

### **3.2 Maximum installed air flow capacity**

The maximum installed air flow capacity limits the air exchange rate that can be achieved in the room concerned and as such limits the influence the ventilation system can have on the IAQ-levels in that room.

### **3.3 Type of operation and controls**

Extremely important for assessing the ability of the ventilation system to achieve the requested air exchanges at the right time is the type of operation and control methods that are selected. The range of options varies from no, to manual to automatic operation and if automatic operation is available, there is a large range of technical options. Apart from the control parameter (time, RH, CO<sub>2</sub>, VOC, presence, etc.) that is used, various other aspects may also influence the air-exchange performance, like e.g. the sample room (which is not always the room considered), the limit values (set points) of the selected control parameter, the modulation type and the modulation range.

### **3.4 Filtration method**

Finally the quality of the supplied outdoor air will influence the ventilation performance. Although outdoor air in general is cleaner than the indoor air [9], in specific regions and for pollutant sensitive inhabitants it can be necessary to apply filters to clean the outdoor air. If such is the case the filter type according to EN-ISO 16890 will be used for assessing the filtration quality.

## **4 ASSESSMENT AND CALCULATION PRINCIPLE**

The influence these technical system parameters will have on the occurring air exchange rates in the individual habitable rooms and wet rooms and their respective weights in the assessment will be based on several sources and methods, amongst which:

- Existing standards and building codes
- Results of real life monitoring studies
- Simulation studies
- Scientific literature

For all assessment values for which no existing valid source can be found and used, a logical and transparent line of reasoning will be communicated for consultation.

### **4.1 Basic score for air exchange provisions**

Core of the assessment method is the valuation of the various types of air exchange provisions with regards to the probability that installed air exchange rates are actually achieved in both

the habitable rooms and wet rooms. This assessment will primarily be based on real life monitoring results and simulation studies. The effect of operating mechanisms and controls will be excluded from this assessment. The result is a basic score reflecting the probability that the installed air exchange rates are achieved, given the selected air exchange provisions for the habitable and the wet room.

**4.2 Multiplier for operation and control method**

In a next step, the influence of the operating and control methods are assessed. Depending on the type of room and related ventilation strategy, the operating and control methods used can have different values. For habitable rooms, the criterion is to achieve requested air exchanges with clean outdoor air during presence and apply basic ventilation rates during absence. For wet rooms the criterion is to extract moisture and odours when generated and continue these air exchanges until humidity is sufficiently removed including accumulated humidity in rendering and building materials; after that basic ventilation rates are sufficient. Operating and control types will be assessed in the light of these criteria and will be expressed as multiplier/modifier for basic scores that are determined on the basis of the applied air exchange provisions.

Values reflecting the influence that various operating methods have, will be based on the typical use of these operating methods and are acquired from available field research regarding this topic. The influence that controls have on the basic score for the air exchange provisions will be based on simulations, type and quality of the sensors used and a clear understanding of the control mechanism and its relation to the reference ventilation strategy for the room type.

The multipliers that are determined here can either increase or decrease the basic score for the air exchange provisions.

**4.3 Proposed calculation principle**

The envisaged calculation principle for determining the air-exchange performance of a ventilation system in a specific dwelling is as follows:

**INPUT DATA**

- a) Specification of dwelling characteristics  
Notification of number, type and surface of the habitable rooms and number and type of the wet rooms.
  
- b) Selection of ventilation system type  
To be based on the air-exchange provisions in the habitable rooms and wet rooms (see table 1. below)

Table 1. Ventilation system types

	habitable rooms		wet rooms	
System 1	supply	exhaust	supply	exhaust
	natural direct	natural indirect		natural direct
System 2	exhaust	supply	supply	exhaust
	natural direct	mechanical indirect		natural direct

System 3	supply	exhaust	supply	exhaust
	natural direct	mechanical indirect		mechanical direct
System 4	supply	exhaust	supply	exhaust
	natural direct	mechanical direct	mechanical indirect	mechanical direct
System 5	supply	exhaust	supply	exhaust
	mechanical direct	mechanical indirect		mechanical direct
System 6	exhaust	supply	supply	exhaust
	mechanical direct	mechanical indirect		mechanical direct
System 7	supply	exhaust	supply	exhaust
	mechanical direct	mechanical direct	mechanical direct	mechanical direct
Combination of systems*				

\* In case a combination of systems is selected, the dwelling is split up in sections with their own ventilation system type. For each system the air-exchange performance is calculated for all the rooms that are served.

- c) Selection of maximum design air exchange rates per room:  $Q_{design}$   
Depending on ventilation system type, selected air-exchange rates for habitable rooms may be linked with the air-exchange rates of the wet rooms.

Because the principles for dimensioning the air-exchange provisions - especially the provisions using natural driving forces - may differ per member state, a uniform and EU-wide applicable convention will be needed here.

- d) Selection and specification operating and control methods  
After selection of the ventilation system type a pre-set of possible control options are presented with default values.
- e) Selection of type of filters used for cleaning the outdoor air before the supply to habitable rooms

## OUTPUT DATA

- f) Specification of probability that installed air-exchange rates are achieved (i.e. basic score per room) based on selected air-exchange provisions:  $P_{basic}$
- g) Specification of multipliers for selected operating and control methods per room:  $f_{control}$   
For habitable rooms multipliers are determined both for periods of absence and presence.
- h) Calculation of the air-exchange performance per room:  $Q_{design} * P_{basic} * f_{control}$
- i) Calculation of the combined air-exchange performance for all habitable rooms; weight factors for specific habitable rooms on the basis of occupation time may be used here.
- j) Calculation of the combined air-exchange performance for all wet rooms.
- k) Specification of filtration performance.

Filtration performance is determined for each habitable room based on the type of filter that is used. Overall filtration performance is determined by combining and weighing the performance of individual rooms.

#### 4.4 Presentation

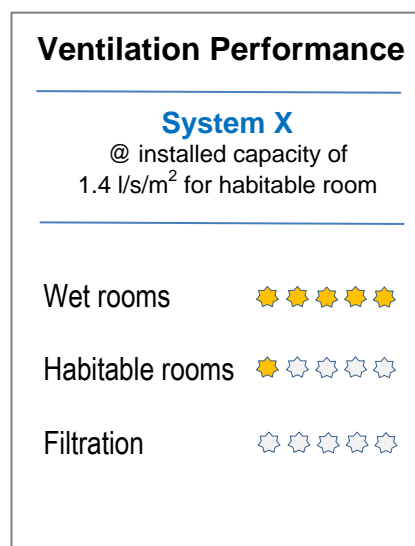
Apart from a technical sheet in which all relevant system specifications and corresponding valuation is explained, it is proposed to use a simple and clear representation of the final result of the assessment in a ventilation performance label.

The information such a label should contain must be clear and understandable for the average customer and contain those items that are relevant for system evaluation. It is proposed that the label contains the following information:

- 1) Ventilation system type and installed capacity in [l/s/m<sup>2</sup>] in habitable rooms.
- 2) Ventilation performance wet rooms, indicated with a 5 star ranking
- 3) Ventilation performance habitable rooms, indicated with a 5 star ranking
- 4) Filtration performance, indicated with a 5 star ranking

In anticipation of a final design of such a Ventilation Performance Label, a preliminary presentation of the presentation principle is given in figure 1 below.

Figure 1.  
Content Ventilation Performance Label



## 5 ACKNOWLEDGEMENTS

This paper was supported by the Residential Working Group of EVIA, the European Ventilation Industry Association.

## 6 REFERENCES

- [1] Van Holsteijn, R.C.A., Li, W.L., Valk, H.J.J., Kornaat, W., (2016), Improving the IAQ- & Energy Performance of Ventilation Systems in Dutch Residential Dwellings, *International Journal of Ventilation*, Vol. 14, No.4, p.363-370
- [2] Tappler, P., Hutter, H.P., Hengsberger, H., Ringer, W. (2014), *Lüftung 3.0 – Bewohnergesundheit und Raumluftqualität in neu errichteten energieeffizienten Wohnhäusern*, Österreichisches Institut für Baubiologie und Bauökologie (IBO), Wien, Austria
- [3] McGill, G.M., Oyedele, L.O., Keeffe, G.K., McAllister, K.M., Sharpe, T. (2015), Bedroom Environmental Conditions in Airtight Mechanically Ventilated Dwellings, *Conference Proceedings Healthy Buildings Europe May 2015*, The Netherlands, Paper ID548.
- [4] Sharpe, T., McGill, G., Gupta, R., Gregg, M., Mawditt, I., (2016), Characteristics and Performance of MVHR Systems, A meta study of MVHR systems used in the Innovative UK Building Performance Evaluation Programme, Report published by Fourwalls Consultants, MEARU and Oxford Brookes University.
- [5] Laverge, J., Delghust, M., Janssens, A., (2015) Carbon dioxide concentrations and humidity levels measured in Belgian standard and low energy dwellings with common ventilation strategies, *International Journal of Ventilation*, 14(2) p.165-180.
- [6] Van Holsteijn, R.C.A., Knoll, B., Valk, H.J.J., Hofman, M.C. (2015), Reviewing Legal Framework and Performance Assessment Tools for Residential Ventilation Systems, *Proceedings of the 36<sup>th</sup> AIVC Conference*, Madrid, Spain.
- [7] Laverge, J., Janssens, A., (2009), Evaluation of a prescriptive ventilation standard with regard to 3 different performance indicators, 11<sup>th</sup> International IBPSA Conference, Glasgow, Scotland.
- [8] Energy performance of buildings – Part 1: Indoor environmental input parameters for design and assessment of energy performance of buildings addressing indoor air quality, thermal environment, lighting and acoustics – Module M1-6, Final Draft prEN 16798-1: 2016
- [9] Various publications from WHO and EPA

# Quantitative relationships between classroom CO<sub>2</sub> concentration and learning in elementary schools

Pawel Wargocki<sup>1,\*</sup>, José Alí Porras-Salazar<sup>1,2</sup>, and William P. Bahnfleth<sup>1,3</sup>

*1 International Centre for Indoor Environment and Energy, DTU Civil Engineering, Technical University of Denmark,*

*\*Corresponding email: paw@byg.dtu.dk*

*2 Department of Design and Theory of Architecture, University of Bio-Bio, Chile*

*3 Indoor Environment Center, Department of Architectural Engineering, The Pennsylvania State University, USA*

## ABSTRACT

The data from published studies were used to build relationships between learning outcomes and air quality in classrooms. Psychological tests measuring cognitive abilities and skills, school tasks including mathematical and language-based tasks, ratings schemes and tests used to assess progress in learning including end-of-year grades and exam scores were considered to represent learning outcomes. Indoor air quality was characterized by concentrations of carbon dioxide (CO<sub>2</sub>). Short-term sick leave was included as well because it can influence learning. For psychological tests and school tasks, fractional changes in performance were regressed against the average concentrations of CO<sub>2</sub> at which the changes were recorded; all reported data were used regardless of whether the change was statistically significant. For other learning outcomes and absence rates, the relationships created by original studies were used. The results predict that reducing CO<sub>2</sub> concentration from 2,000 ppm to 1,000 ppm (equivalent to about 2.5 times higher outdoor air supply rate) would improve performance on psychological tests and school tasks on average by 12% (as regards the speed at which the tasks are performed) and by 3% (as regards errors made while performing the task). The performance on rating schemes will be improved by 1.3%. This change will increase the number of pupils passing exams by 12% and is further estimated to result in about 6 out of 100 pupils improving their performance and to reduce absence by 0.5 day per student in a 200 days long school year.

## KEYWORDS

Learning; Cognitive performance; Elementary schools; Carbon dioxide; Pupils

## 1 INTRODUCTION

Research has documented that classroom environmental quality in elementary schools, where children spend large part of their waking hours (ca. 14%), is often inadequate (Daisey et al., 2003; Toftum et al., 2015), and that this has significant consequences for learning process (Wargocki and Wyon, 2013; 2016). When air quality is suboptimal in classrooms, cognitive skills and abilities of pupils are compromised as, among others, they cannot concentrate and/or are distracted from the work that they are supposed to do (Myhrvold et al., 1996; Myhrvold and Olsen, 1997; Coley et al., 2007; Ribic, 2008; Bako-Biro et al., 2012). As a result, the optimal and

effective learning process is disturbed, which has consequences for learning performance outcomes, teachers work in suboptimal environment that do not support learning, and parents are distressed, troubled or must take the leave from work because children have stay home, all having significant socio-economic implications (Wargoeki et al., 2014).

A quantitative relationship showing the potential size of the effect of changes in indoor air quality on cognitive performance exists, but it was not developed specifically for the effects on learning performance; it integrates data from studies investigating the quality of indoor environment on primarily office-type work (Seppänen et al., 2006). The relationship shows that performance would improve by 1-3% for each 10 L/s per person increase in outdoor air supply rate (over the range of ventilation rates that were on average between 7 and 55 L/s per person).

Fisk et al. (2003) used the available and rather limited data on the link between absence rates and ventilation to develop a relationship predicting illness or sick leave prevalence as a function of air change rate. They showed that doubling ventilation rate would produce roughly a 10% reduction in the absence rate.

A few studies performed in schools that measured performance outcomes relevant for learning have attempted to create a relationship between temperature or air quality in classrooms to the performance of school work (Wargoeki and Wyon, 2012; Haverinnen-Shaughnessy et al., 2015; Mendell et al., 2013). These studies indicated that improvement in learning outcomes was about 5-15%, but unlike the analyses of Seppänen et al. (2006), they used only the results that had been obtained in their own measuring campaigns. Integration of results from a few studies in an attempt to create a relationship between school performance and ventilation was reported in the REHVA Guidebook (Alfano and Bellia, 2010). They showed that the effect of doubling ventilation rate would result in about 7-8% higher performance.

It is fair to say that no dedicated quantitative relationships between air quality and learning performance outcomes have yet been developed that systematically analyze and integrate the results obtained in many studies. The present work was consequently undertaken to fill this gap. The specific objective was to develop quantitative relationships that associate carbon dioxide (CO<sub>2</sub>) as a proxy of air quality with learning performance outcomes and absence rates in elementary schools using all available information in the published archival literature. CO<sub>2</sub> concentration was used rather than the other measures of air quality or ventilation rates as it was frequently measured to describe air quality or ventilation efficiency in classrooms.

## **2 RESULTS**

The archival literature was surveyed to find the articles reporting studies on learning performance outcomes and classroom conditions. Articles published from 1996 until the end of 2016 were included, i.e. covering and summarizing half a century of research on this topic. To be selected, the articles had to report both measurements of

air quality in classrooms and measurements of cognitive performance of pupils. Only studies performed in elementary schools (primary, middle and/or secondary schools) were accepted.

Diverse measures of cognitive performance were accepted including psychological tests measuring cognitive skills and abilities to perform school work, the tasks typical of schoolwork, results of aptitude and national tests examining progress in learning, and the results of midterm and final exams, as well as end-of-the year grades. Studies reporting absence rates in relation to classroom conditions were included as well. Papers reporting cross-sectional and intervention studies were included.

Altogether 16 studies were identified (Table 1). Five studies measured performance using psychological tests, four measured performance of schoolwork, five reported the results of aptitude and national tests or exams, and three studies reported absence rates as a function of classroom air quality. Classroom air quality was approximated by measuring carbon dioxide (CO<sub>2</sub>) concentrations and in few cases also outdoor air supply rates achieved by controlling the dedicated ventilation systems or by calculating them using the measured CO<sub>2</sub> levels (peak concentrations were used or the mass-balance model was fitted). Average daily, weekly or peak levels of CO<sub>2</sub> in ppm were reported. All measurements were performed in classrooms normally used by pupils during regular lessons. No study was performed in the tropical or subtropical climatic zones although air conditioning was part of the systems used to support classroom conditions in some schools. All studies were performed with elementary school children typically in the 4<sup>th</sup> to 6<sup>th</sup> grade (primary school children).

Table 1. Studies included to develop the relationship and the measures used to examine the effect on cognitive performance

Psychological tests	Myhrvold et al. (1996)
	Myhrvold and Olsen (1997)
	Coley et al. (2007)
	Ribic (2008)
	Bakó-Biró et al. (2012)
School tasks	Bakó-Biró et al. (2007)
	Wargocki and Wyon (2007a)
	Wargocki and Wyon (2007b)
	Petersen et al. (2015)
Standard tests and rating schemes	Shaughnessy et al. (2006)
	Haverinen-Shaughnessy et al. (2011)

---

	Gaihre et al. (2014)
	Haverinen-Shaughnessy et al. (2015)
	Mendell et al. (2015)
Absence rates	Shendell et al. (2004)
	Mendell et al. (2013)
	Gaihre et al. (2014)

---

Following the analytical approach used by Seppänen et al. (2006), for each individual task and test, the fractional change in performance was calculated per 100 ppm change in CO<sub>2</sub> concentration for the examined range of CO<sub>2</sub> concentrations. The fractional changes were calculated separately for the speed at which the tests were performed or the reaction time, if it was reported, and accuracy describing the percentage of errors committed; all data were included independently of whether the changes reached statistical significance in the original studies. The mid-range fractional changes in performance of psychological tests and the performance of school tasks were regressed against the average CO<sub>2</sub> concentration calculated based on the range of CO<sub>2</sub> concentrations for which they were calculated; linear regression was used. Using this fit, the relationships were produced between CO<sub>2</sub> and the performance metric. The developed relationships show thus diminution in performance from what is assumed to be the optimal performance.

To derive the relationship between CO<sub>2</sub> and the performance of tests examining progress in learning, the relationships developed in original studies were used: the median slope was calculated to determine the mean effect of changes in ventilation rate.

The relationship between absence rate and classroom conditions was derived using the change in absence rates as a function of CO<sub>2</sub> reported in the original studies. The median reported change was used to develop the final relationship. Using the relationship between absence rate and classroom CO<sub>2</sub> concentration the number of days absent from school per pupil was estimated. It was assumed that there are 200 schooldays in a school year, which is the length of school year in Denmark.

In case the data on means and standard deviations were reported by the studies included in the present analyses, Cohen's effect size *d* was calculated, as well (Cohen, 1988). Cohen's *d* provides a standardized difference; therefore, it allows comparison of effects obtained in different studies with diverse populations having different size of populations even when measuring scales are not the same. Cohen's *d* provides additional and supplementary information on the magnitude of effect on performance not in form of the effect size expressed as percentage loss in performance but in form of number of pupils that would be affected by the change in classroom CO<sub>2</sub> concentration.

### 3 RESULTS

#### 3.1 Effects on performance of psychological tests and school tasks

Figures 1 and 2 show the relationships between the concentration of CO<sub>2</sub> and the performance on psychological tests and school tasks. Since the highest average CO<sub>2</sub> concentration based on which the relationships were established was 889 ppm, it was decided not to extend the relationship to lower CO<sub>2</sub> concentrations. It was admitted that with the proposed analytical approach the shape of the relationship in this range cannot be validated and justified and simply will not be credible. The highest average concentration was around 2,000 ppm. Cohen's d could be calculated based on the data from the studies of Coley et al. (2007) and Wargocki et al. (2007a,b). Median d for the effects on speed at which the tasks were performed was 0.21. This corresponds to 6 pupils performing less well out of 100.

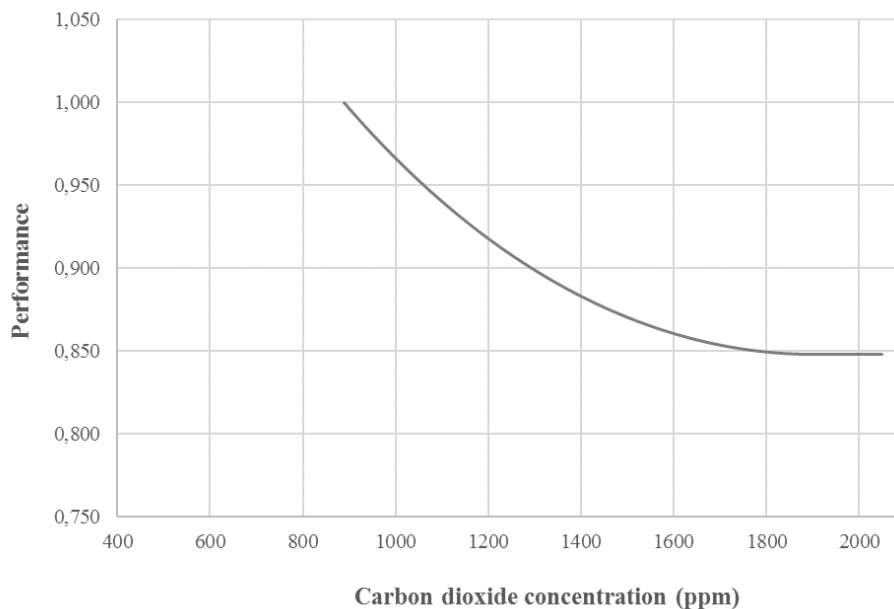


Figure 1: The performance of psychological tests and school tasks as a function of classroom CO<sub>2</sub> concentration; the performance was calculated based on the data showing speed and reaction time, at which the tests and tasks were performed by pupils.

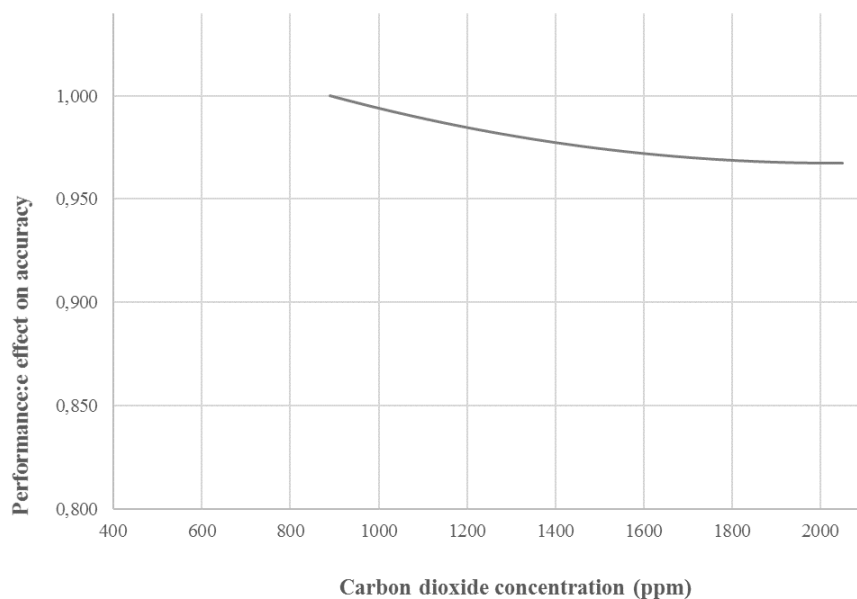


Figure 2: The performance of psychological tests and school tasks as a function of classroom CO<sub>2</sub> concentration; the performance was calculated based on the data showing accuracy, at which the tests and tasks were performed by pupils.

### 3.2 Effects on performance of standard rating schemes and final exams

Previous studies showed that the scores in math and English-art can be improved from 0.15% to 0.6% (median 0.375%) for each 1 L/s per person increase in classroom ventilation and that the percentage of students scoring satisfactorily or above (passing the tests) can increase by 2.7-2.9% for each 1 L/s per person higher classroom ventilation.

### 3.3 Absence rates

Three studies reported measurements of absence rates in relation to classroom ventilation. They show that 100 ppm lower concentration of CO<sub>2</sub> will reduce annual absence by 0.016% to 0.2% (median 0.07%) which corresponds to 0.03 to 0.4 days (median 0.14) per pupil per year with 200-day long school year.

## 4 DISCUSSION AND CONCLUSIONS

The present work is the first attempt to systematically summarize and compare current evidence on the effects of indoor environment in school classrooms on learning outcomes obtained in different studies using diverse methods. They show that there are significant economic benefits to gain if forceful actions for improving classroom environment and teaching conditions are executed.

The relationships developed in the present work can be used in cost-benefit analyses when seeking affordable and economically valid solutions that secure optimal

conditions in elementary school classrooms. The results provide a powerful argument for decision makers and regulators to revise requirements in codes and standards so that the pupil, the teacher and the optimal learning environment will always remain in the center of attention independently of whether the aim is to design, renovate or operate the school buildings.

## 5 ACKNOWLEDGMENTS

Velux A/S is cordially acknowledged for partially supporting the work. The work was additionally supported by the funding from sponsors supporting the International Centre for Indoor Environment and Energy at the Technical University of Denmark.

## 6 REFERENCES

Alfano, F.R. d'Ambrosio, & Bellia, L. (2010) *Indoor environment and energy efficiency in schools. Part 1*. Brussels, Belgium: REHVA, Federation of European Heating, Ventilation and Air-conditioning Associations.

Bakó-Biró, Z., Kochhar, N., et al. (2007) Ventilation rates in schools and learning performance. In *Proceedings of CLIMA* (pp. 1434-1440).

Bakó-Biró, Z., Clements-Croome, et al. (2012) Ventilation rates in schools and pupils' performance. *Building and Environment*, 48, pp.215-223.

Cohen J. (1988) *Statistical Power Analysis for the Behavioral Sciences*. New York, NY: Routledge Academic

Coley, D.A., Greeves, R. et al. (2007) The effect of low ventilation rates on the cognitive function of a primary school class. *International Journal of Ventilation*, 6(2), pp.107-112.

Daisey, J. M., Angell, W. J., & Apte, M. G. (2003). Indoor air quality, ventilation and health symptoms in schools: an analysis of existing information. *Indoor Air*, 13(1), 53-64.

Gaihre, S., Semple, S. et al. (2014) Classroom carbon dioxide concentration, school attendance, and educational attainment. *Journal of School Health*, 84(9), pp.569-574.

Haverinen-Shaughnessy, U., Moschandreas, D.J et al. (2011) Association between substandard classroom ventilation rates and students' academic achievement. *Indoor Air*, 21(2), pp.121-131.

Haverinen-Shaughnessy, U., Shaughnessy, R.J. et al. (2015) An assessment of indoor environmental quality in schools and its association with health and performance. *Building and Environment*, 93, pp.35-40.

Mendell, M.J., Eliseeva, E.A. et al. (2013) Association of classroom ventilation with reduced illness absence: a prospective study in California elementary schools. *Indoor Air*, 23(6), pp.515-528.

Mendell, M.J., Eliseeva, E.A. et al. (2015) Do classroom ventilation rates in California elementary schools influence standardized test scores? Results from a prospective study. *Indoor Air*.

Myhrvold, A.N., Olsen, E., et al. (1996) Indoor environment in schools—pupils health and performance in regard to CO<sub>2</sub> concentrations. Proc. *Indoor Air'96*, Vol. 4, pp.369-371.

Myhrvold, A.N. and Olsen, E. (1997) Pupil's health and performance due to renovation of schools. In: *Proceedings of Healthy Buildings/IAQ 1997*. Vol. 1, Washington, DC, 81–86.

Petersen, S., Jensen, K.L. et al. (2016). The effect of increased classroom ventilation rate indicated by reduced CO<sub>2</sub> concentration on the performance of schoolwork by children. *Indoor Air*, 26(3), pp.366-379.

Ribic W. (2008) Nachweis des Zusammenhangs zwischen Leistungsfähigkeit und Luftqualität. *Gesundheitsingenieur*, 129, 88-91.

Shaughnessy, R.J., Haverinen-Shaughnessy, U. et al. (2006) A preliminary study on the association between ventilation rates in classrooms and student performance. *Indoor Air*, 16(6), pp.465-468.

Shendell, D.G., Prill, R. et al. (2004) Associations between classroom CO<sub>2</sub> concentrations and student attendance in Washington and Idaho. *Indoor Air*, 14(5), pp.333-341.

Seppänen, O., Fisk, W.J. et al. (2006) Ventilation and performance in office work. *Indoor Air*, 16(1), pp.28-36.

Toftum, J., Kjeldsen, B. U., Wargocki, P., et al. (2015). Association between classroom ventilation mode and learning outcome in Danish schools. *Building and Environment*, 92, 494-503.

Wargocki, P. and Wyon, D.P., (2007a) The effects of moderately raised classroom temperatures and classroom ventilation rate on the performance of schoolwork by children (RP-1257). *HVAC&R Research*, 13(2), pp.193-220.

Wargocki, P. and Wyon, D.P., (2007b) The effects of outdoor air supply rate and supply air filter condition in classrooms on the performance of schoolwork by children (RP-1257). *HVAC&R Research*, 13(2), pp.165-191.

Wargoeki, P., &Wyon, D. P. (2013)Providing better thermal and air quality conditions in school classrooms would be cost-effective. *Building and Environment*, 59, 581-589.

Wargoeki, P., &Wyon, D. P. (2017) Ten questions concerning thermal and indoor air quality effects on the performance of office work and schoolwork, *Building and Environment*, 112.

Wargoeki, P., Foldbjerg, P., Eriksen, K. E., & Eriksen Videbæk, L. (2014). Socio-Economic Consequences of Improved Indoor Air Quality in Danish Primary Schools. In Proceedings of Indoor Air 2014 International Society of Indoor Air Quality and Climate.

# The impact of the quality of homes on indoor climate and health: an analysis of data from the EU-SILC database

AshokJohn<sup>\*1</sup>, Nicolas Galiotto<sup>2</sup>, Peter Foldbjerg<sup>2</sup>, Katrine Bjerre Milling Eriksen<sup>2</sup>, Jens Christoffersen<sup>2</sup> and Andreas Hermelink<sup>3</sup>

*1 Ecofys Germany GmbH  
Am Wassermann 36  
50829 Cologne, Germany*

*\*Corresponding author: a.john@ecofys.com*

*2 VELUX A/S  
Ådalsvej 99  
2970 Hørsholm, Denmark*

*Presenting author: underline First & Last name*

*3 Ecofys Germany GmbH  
Albrechtstr. 10c  
10117 Berlin, Germany*

## ABSTRACT

Today one out of six Europeans (84 million Europeans, or the equivalent of Germany's population), report deficiencies regarding the building status. In some countries, that number is as high as one out of three. This puts these buildings in the 'Unhealthy Buildings' category, which is defined as buildings that have damp (leaking roof or damp floor, walls or foundation), a lack of daylight, inadequate heating during the winter or overheating problems.

10% of Europeans report having poor perceived general health. And the probability that a person reports poor health increase up to 70% if that person also lives in an unhealthy building vs. a healthy one. The results of this study show a correlation between poor health and the specific unhealthy building factors:

- 1.7 times report poor health in a damp building
- 1.5 times report poor health when living in a building with insufficient daylight
- 1.3 times report poor health when perceiving overheating
- 1.7 times report poor health when living in uncomfortably cold temperatures

The paper is based on an analysis of the correlation between health and buildings in 27 EU member states using the Eurostat database EU-SILC (Survey on Income and Living Conditions). The presented research is based on EU-SILC raw data. For the purpose of the study, Eurostat approved the research proposal behind the analysis and gave access to the data to Ecofys Germany GmbH.

## KEYWORDS

Health, building, indoor climate, EU-SILC, European Union

## 1 INTRODUCTION

Around 508 million European citizens (EUROSTAT, 2015) spend about 90% of their time indoors (living and working) (NEST, 2004). Therefore Europe's buildings have a major impact on Europeans' health. According to WHO's definition (since 1948) "Health is a state of complete physical, mental and social well-being and not merely the absence of disease or infirmity."

Yet, research assessing the statistical links between health and housing conditions is largely missing. Considering that building renovation is a huge intervention into the whole building system – cross-cutting technical aspects of the building itself and social as well as economic

issues of the dwellers– it is necessary to fully grasp the implications, risks and chances. Therefore, a main research objective is to identify these links and to highlight which part of Europe's and MS's population is most in need of building renovation.

This insight triggered a detailed study on the relation between health and housing conditions across EU28 and its Member States. The results described here have been presented in the scientific report “The relation between quality of dwelling, socio-economic status and health in EU28 and its Member States” (Hermelink&John, 2017).

## **2 METHODOLOGY**

The research is based on analysing Eurostat microdata from the EU-wide survey „Income and Living Conditions in Europe“.(EU-SILC). EU-SILC is a Eurostat Survey, which is conducted in a European-wide household panel, to assess the status and development of Income and Living Conditions in Europe. The EU SILC survey covers amongst others the domains housing including economic issues and health. Data in EU-SILC are collected either on household or individual level. For this research, anonymised results for more than 100,000 individual households and more than 250,000 adults (16 +) across all EU Member States – except Germany - were made available by Eurostat. The focus of this study lies on data from 2012, where more detailed information on housing conditions was collected. To handle the massive amount of data the statistical computing program R (version 3.3.0) was used for statistical analyses of the microdata.

## **3 RESULTS**

The research reveals that around 16% of Europeans report deficiencies regarding the building status; either because of dampness (leaking roof or damp floor, walls or foundation), lack of daylight, inadequate heating during the winter or overheating problems. The analysis also shows that around 44 Mio adults report poor perceived general health; this is equivalent to nearly 10% of the European population. As described above, the results will focus on the linkage between building status and health. Accordingly, the focal point of analysis described here are

- health in damp buildings.
- health in dark buildings.
- health in overheated buildings.
- health in building with uncomfortably cold temperatures

Detailed results of each of the mentioned topics will be described in the following subsections.

### **3.1 Health in damp buildings**

15% of EU households (more than 30 Mio; or more than 60 Mio adults) report to live in damp buildings (leaking roof, damp floor/walls /roof/ foundation etc.).

- When adults report no dampness 9% report poor health
- When adults report dampness 16% report poor health

The probability that adults report poor health is significantly higher in homes with reported dampness; across the EU the probability is 1.7 times higher than with no dampness.

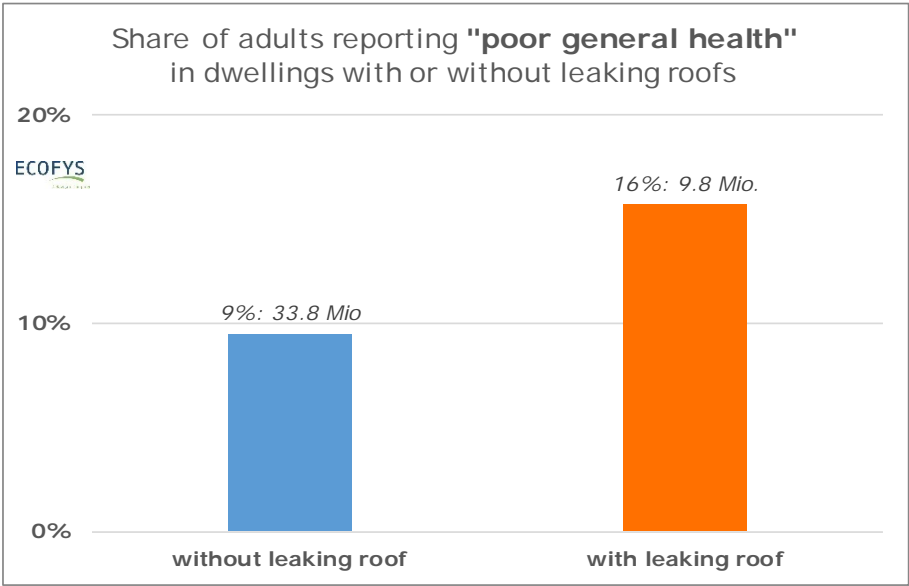


Figure 1: Health status in damp buildings for EU28(share within subset and number of adults)

### 3.2 Health in dark buildings

Approx. 6% of all EU households (14 million; or approx. 30 Mio adults) report a lack of daylight

- When adults report no lack of daylight 10% report poor health
- When adults report lack of daylight 15% report poor health

The probability that adults report bad health is significantly higher when a lack of daylight is perceived; across the EU this probability is 1.5 times the one when no lack of daylight is perceived. Altogether approx. 10% of all adults reporting poor health live in buildings lacking daylight, where only 7% of all adults live.

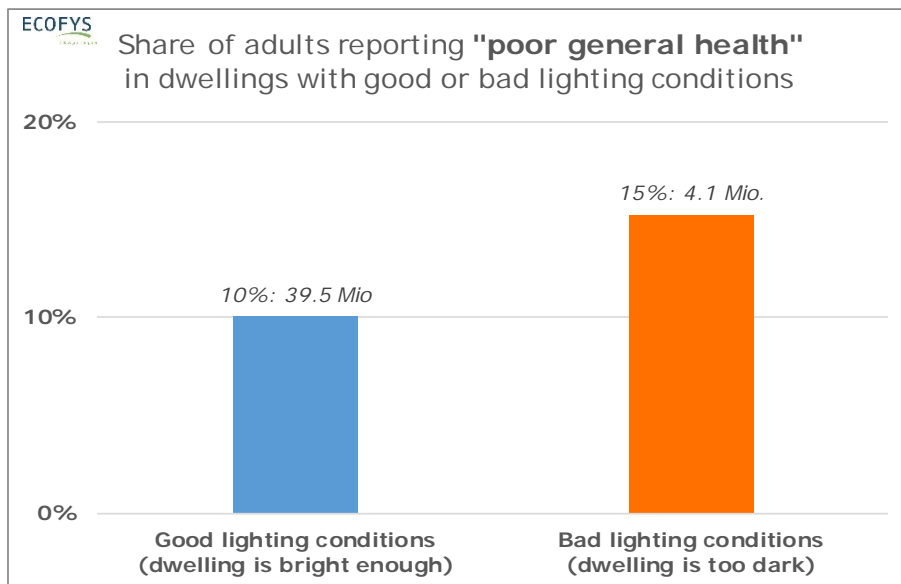


Figure 2: Health status in dark building for EU28 (share within subset and number of adults)

### 3.3 Health in overheated buildings

Approx. 20% of all EU households (40million; or approx. 84 Mio adults) report bad thermal comfort in summer.

- When adults report good thermal comfort (cool dwelling) in summer 10% report poor health
- When adults report bad thermal comfort (too hot dwellings) in summer 13% report poor health

The probability that adults report bad health is significantly higher when bad thermal comfort is perceived; across the EU this probability is 1.3 times the one when good thermal comfort is perceived.

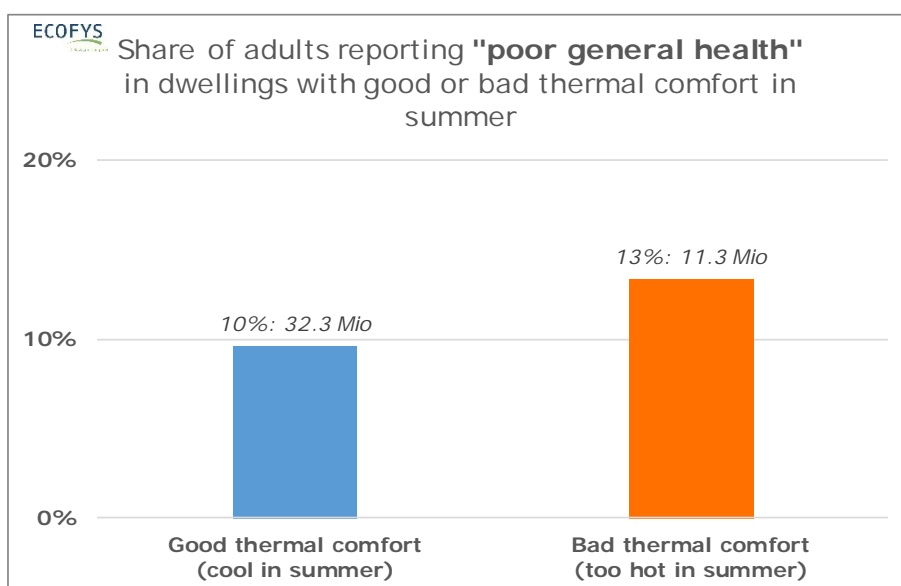


Figure 3: Health in overheated buildings for EU28 status (share within subset and number of adults)

### 3.4 Health in too cold buildings during winter

Approx. 15% of all EU households (more than 30 Mio; or more than 60 Mio adults) had thermal comfort in winter

- When adults report good thermal comfort (warm dwellings) in winter 9% report poor health
- When adults report bad thermal comfort (too cold dwellings) in winter 16% report poor health

The probability that adults report bad health is significantly higher when bad thermal comfort is perceived; across the EU this probability is 1.7 times the one when good thermal comfort is perceived.

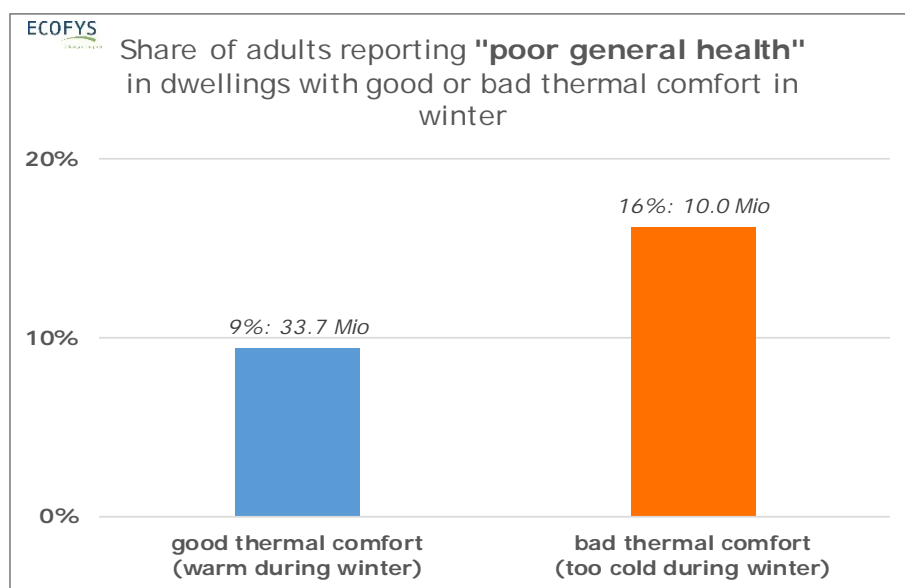


Figure 4: Health in too cold buildings for EU28 status (share within subset and number of adults)

## 4 CONCLUSION AND DISCUSSION

The results described in this paper based on EU-SILC variables on quality of buildings and general health show statistically significant interdependencies. However, additional analysis are needed to understand for example the influence of economic issues of households and individuals, regional patterns or energy poverty on health. Based on the results shown here, we observed that structural problems of the building like leaking roofs, damp walls (etc.), buildings' ability to provide comfortable temperatures in winter, lack of daylight seem to act as similarly strong accelerators and/or indicators for health problems. On average the relative share of adults reporting poor health increases 30 to 70% when at least one of the above-mentioned deficiencies is reported compared to the group of people who do not perceive such deficiencies.

However, as indicated above this study so far focused on a small selected sample of relevant variables influencing health. On the other hand like in the analyses of Thomson and Snell (2012) who focused their EU SILC analyses on energy poverty, the strengths of the correlations are moderate. This is why on the one hand we found statistically highly significant correlations between the presented variables. This means, that there are many other

variables apart from the ones analyzed in this study, also having a very significant impact on a person's perceived general health. Obviously personal and environmental variables determine health. Yet, we feel that buildings, which in this equation at least in Europe occupy 90% of the environmental variables' time are very much under-represented in today's overarching discussion about sustainability, which eventually is about shaping the world in a way that leads to sustained individual and societal health.

Above mentioned problems like dampness, darkness, too cold in winter or overheating in summer clearly hint at buildings in need of renovation. According to EUROSTAT (2012), ca. 58% of EU's population live in detached and semi-detached single family homes; our results also show that around 4 out of 5 of these dwelling types are owned by private owners. This means, that this group is crucial to successfully increase the renovation rate as implicated in the proposal for the amending directive on energy performance of buildings (European Commission, 2016) and needs to be addressed by incentives, renovation policies and awareness raising as well as information campaigns.

To reveal more insights, further research is ongoing to examine the linkage between health and building status, but also considering the economic status of building's occupants. This analysis considers additional variables such as health prevalence of building occupants for example due to age, occupancy status and, economic status, income level, existing chronic illnesses, medical care system of respective country, etc. In this sense, a prediction model and additional multiple correlations for health considering selected variables of building and economic status and previous mentioned variables could reveal insights on the impact on health, but also more general insights into causes and effects within the triangle of clusters of variables described above. Furthermore, analysis shall evaluate the development of the building and economic status as well as general health aspects over time to observe the impact of policy measures and to derive recommendations for priority areas for action. This can also reveal insights on causal chains between building status, economic situation and health aspects explaining energy poverty.

## **5 ACKNOWLEDGEMENTS**

This research was supported by VELUX A/S. The research was conducted by experts from Ecofys Germany GmbH, with assistance of experts from VELUX A/S.

## **6 REFERENCES**

EUROSTAT (2012): *Description of Target Variables: Cross-sectional and longitudinal. 2012 operation (Version May 2013)*. Ed. European Commission. Brussels.

EUROSTAT (2012). *Distribution of population by dwelling type*. (online data code: ilc\_lvho01), accessed 04.06.2017.

European Commission (2016). *Proposal for a Directive of the European Parliament and of the Council amending Directive 2010/31/EU on the energy performance of buildings*.

EUROSTAT (2015). *Population on 1 January by age and sex*. (online data code: demo\_pjan). accessed 04.06.2017.

European Commission (2017): *EU Building Stock Observatory*. Online: <https://ec.europa.eu/energy/en/eubuildings>, accessed 01.06.2017.

Gruen, G. and Urlaub, S. (2014): *White Paper: Towards an Identification of European indoor environment' impact on health and performance – homes and schools*. Fraunhofer IBP. Holzkirchen.  
Online: [https://www.ibp.fraunhofer.de/content/dam/ibp/de/documents/Presseinformationen/Velux-Prestudy\\_WhitePaper\\_141205\\_amended.pdf](https://www.ibp.fraunhofer.de/content/dam/ibp/de/documents/Presseinformationen/Velux-Prestudy_WhitePaper_141205_amended.pdf), accessed 04.06.2017.

Hermelink, A. and John, A. (2017). *The relation between quality of dwelling, socio-economic status and health in EU28 and its Member States. Scientific report as input for Healthy Home Barometer 2017*. Cologne. Ecofys by order of VELUX A/S. Online: <http://www.ecofys.com/files/files/ecofys-2017-relation-between-quality-of-dwelling-and-health-final.pdf>, accessed 01.06.2017.

NEST (2004): *NEST project, Technical University of Berlin, European Commission 2004*. quoted from Velux (2015). *Healthy Home Barometer 2015*.

Thomson, H. and Snell, C. (2012). Quantifying the prevalence of fuel poverty across European Union. *Energy Policy*, 52 (2013), 563-572

Velux (2015): *Healthy Homes Barometer 2015*. Online: [http://www.velux.dk/~media/marketing/master/documents/pdf/brochures/velux\\_hhb\\_18032015.pdf](http://www.velux.dk/~media/marketing/master/documents/pdf/brochures/velux_hhb_18032015.pdf), accessed 01.06.2017.

Velux (2016): *Healthy Homes Barometer 2016*. Online: <http://www.velux.com/article/2016/europeans-on-healthy-living-the-healthy-homes-barometer-2016>, accessed 01.06.2017.

Velux (2017): *Healthy Homes Barometer 2017*. Online: [http://velcdn.azureedge.net/~media/com/health/healthy-home-barometer/507505-01%20barometer\\_2017.pdf](http://velcdn.azureedge.net/~media/com/health/healthy-home-barometer/507505-01%20barometer_2017.pdf), accessed 01.06.2017.

WHO (1946): *Constitution of the World Health Organization*. Online: <http://apps.who.int/gb/bd/PDF/bd47/EN/constitution-en.pdf?ua=1>, accessed 04.06.2017.

# Assessment of airflow measurement uncertainty at terminal devices

Adeline Bailly Mélois<sup>\*1</sup>, Elodie Rousseuw<sup>1</sup>, Isabelle Caré<sup>2</sup>, and François Rémi Carrié<sup>3</sup>

*1 Cerema*

*48 rue Saint Théobald  
38081 L'Isle d'Abeau FRANCE*

*\*Corresponding author: [adeline.melois@cerema.fr](mailto:adeline.melois@cerema.fr)*

*2 CETIAT*

*25 avenue des Arts  
69603 Villeurbanne FRANCE*

*3 ICEE*

*93 rue Molière  
69003 Lyon FRANCE*

## ABSTRACT

Existing protocols for the inspection of mechanical residential systems poorly address both the assessment of uncertainties and recommendations or specifications for measurement methods and devices to be used to guarantee low measurement uncertainties. This paper gives the major elements of a new protocol developed within the Promevent project to overcome this problem. We have analyzed results from 180 airflow measurements performed in laboratory conditions in accordance with this protocol. The methodology developed to analyze uncertainties addresses errors due to repeatability, reproducibility and measurement method consistently with standard error propagation methods. Our analyses of laboratory results show that the measurement method often dominates the overall uncertainty. To contain the overall uncertainty within certain limits, several tables give the Maximum Permissible Error (MPE) of the measurement device as a function of the measurement technique and the geometry of the air terminal devices. These results show that in 6 out of 15 tested configurations, the measurement uncertainty cannot be contained within 15%. For the other tested configurations, the MPE must stay below 9-13% to contain the overall uncertainty below 15%.

## KEYWORDS

Ventilation, airflow rate, measurement, uncertainty

## 1 INTRODUCTION

One major challenge of the ventilation industry is to develop systems that both provide good indoor air quality and ensure high energy performance. However, several field studies in different countries have shown many important issues regarding the quality of the residential ventilation systems (Janssens et al., 2013). For instance, the analysis of regulatory compliance checks on 1,287 dwellings in France has shown that over one new dwelling out of two has a ventilation system that does not meet regulatory requirements (Jobert&Guyot, 2013), 46% and 33% of the problems being due to poor installation and poor design, respectively. Several field studies in Estonia, Austria, and The Netherlands report frequently malfunctioning mechanical systems in these countries (Carrié, 2016).

Requiring functional and performance checks at commissioning appears to be one effective means to overcome these problems. In France, the effinergie+ label (Effinergie, 2015) requires that the ductwork airtightness complies with airtightness class A (the levels are

defined in EN 12237 or EN 1507) and that the ventilation system is commissioned with a protocol specified by Effinergie (Effinergie, 2014).

While the Effinergie protocol requires a visual check of the system and gives recommendations for the measurements of airflow rates, it did not require the measurement of airflow rates until the recent publication of the results of the Promevent project. This is due to the lack of knowledge on the uncertainties obtained when measuring airflow rates at air terminal devices when the label was developed. Different technologies exist for measuring airflow rates at terminal devices, and some studies from Walker and collaborators (Walker et al., 2001), (Walker et al., 2003) and (Wray, 2002) have pointed out that the uncertainties of those measurements vary a lot from one device to another. Moreover, Caillou (Caillou, 2014) has shown that the type of air terminal device has a significant impact on those uncertainties. Depending on on-site conditions, Caré (Caré, 2013) has shown measurement uncertainties ranging from 10% to over 50%.

The objective of the Promevent project (Bailly&Lentillon, 2014) was to propose a protocol to assess the quality of the residential ventilation system including specifications for the measurement of airflow rates at air terminal device with acceptable uncertainties. This paper proposes a methodology to evaluate those uncertainties for measuring devices and air terminal devices commonly used in mechanical residential ventilation systems in France.

## 2 UNCERTAINTY CALCULATION METHOD

The proposed uncertainty analysis, in accordance with JCGM 100 (BIPM, 2008), also known as GUM, considers four main uncertainty sources, for which the following standard uncertainties have been identified:

- $u_{Q,1}$  pertaining to the contribution of the instrument, as a result of its characteristics;
- $u_{Q,2}$  pertaining to the contribution of the method, which is in our case a combination between the measurement principle of the instrument (array of hot wire anemometry, vane anemometer, (un)powered flow hood with Pitot tube, etc.), its use, including centering, airtightness, and (if applicable) alignment of the thermal anemometer, and the flow pattern generated by the air terminal device;
- $u_{Q,3}$  pertaining to the repeatability of the measurements;
- $u_{Q,4}$  pertaining to reproducibility of the measurements.

Assuming these components are uncorrelated, the combined expanded uncertainty,  $U_c$ , is calculated as shown in Equation 1:

$$U_c = 2 * u_c = 2 \sqrt{u_{Q,1}^2 + u_{Q,2}^2 + u_{Q,3}^2 + u_{Q,4}^2} \quad (1)$$

where

$u_c$  is the combined standard uncertainty;

$U_c$  is the expanded uncertainty with a 95% confidence level;

$u_{Q,i}$  are the standard uncertainties defined above.

We performed a series of experiments to:

1. evaluate the minimum instrument uncertainty component available instruments can meet;
2. evaluate the standard uncertainties  $u_{Q,2}$ ,  $u_{Q,3}$  and  $u_{Q,4}$  for different types of measuring instrument used to measure the flow rate at the level of different types of terminal device;
3. evaluate, for different values of the overall uncertainty, the maximum permissible instrument uncertainty;

4. define requirements for the maximum permissible instrument uncertainty depending on the overall uncertainty target.

### 2.1 Instrument uncertainty component ( $u_{Q,1}$ )

For each measuring device, the instrument standard uncertainty  $u_{Q,1}$  can be calculated according to JCGM 100, after evaluation of the several components. This procedure needs certain knowledge of uncertainty calculation and should be applied separately to all the used instruments.

A simpler method, also in accordance with JCGM 100, is to check after each calibration that the error of the instrument used (the difference between the value the instrument gives and the value the standard measurement gives) is lower than a target value named Maximum Permissible Error, MPE. Equation 2 gives the instrument standard uncertainty:

$$u_{Q,1} = \frac{MPE}{\sqrt{3}} \quad (2)$$

where MPE is the Maximum Permissible Error of the measuring device.

Combining Equation 1 and 2 leads to Equation 3:

$$MPE = \sqrt{3 * \left[ \left( \frac{U_c}{2} \right)^2 - (u_{Q,2}^2 + u_{Q,3}^2 + u_{Q,4}^2) \right]} \quad (3)$$

Therefore, we need to assess the other uncertainty components ( $u_{Q,2}$ ,  $u_{Q,3}$  and  $u_{Q,4}$ ) to obtain the MPE to remain within a given expanded combined uncertainty  $U_c$  found reasonable for the protocol.

### 2.2 Measurement method uncertainty ( $u_{Q,2}$ )

The aim of this study is to evaluate the uncertainties of the measurements performed according to the Promevent protocol. We thus consider that the instrument is correctly placed. Then, the measurement method standard uncertainty,  $u_{Q,2}$ , linked to the use of a measuring device on an air terminal device, can be determined according to Equation 4.

$$u_{Q,2} = u_{Q,p} \quad (4)$$

where:

$u_{Q,p}$  is the standard uncertainty due to the interaction of the instrument and the terminal device.

### 2.3 Repeatability measurement uncertainty ( $u_{Q,3}$ )

According to the JCGM 200 (BIPM, 2012), also known as VIM, the measurement repeatability is the “measurement precision under a set of repeatability conditions of measurement”. This set of conditions “includes the same measurement procedure, same operators, same measuring system, same operating conditions and same location, and replicate measurements on the same or similar objects over a short period of time”. This uncertainty component is estimated from results of measurements performed in repeatability conditions as defined here.

### 2.4 Reproducibility measurement uncertainty ( $u_{Q,4}$ )

According to the JCGM 200, the measurement reproducibility is the “measurement precision under reproducibility conditions of measurement”. These conditions are “out of a set of

conditions that includes different locations, operators, measuring systems, and replicate measurements on the same or similar objects”. In our case, the condition which has been considered is the operator and the uncertainty component is estimated from results of several measurements performed with the same measuring instrument, on the same terminal device but by different operators.

### 3 EXPERIMENTAL SETUP

To evaluate the different standard uncertainties ( $u_{Q,2}$ ,  $u_{Q,3}$  and  $u_{Q,4}$ ), we performed about 180 airflow measurements in laboratory conditions reflecting the following key requirements of the Promevent protocol:

- the air terminal device is connected to an airtight plenum;
- the measuring instrument is placed around the air terminal device in such a way that:
  - there is no leakage between the measurement device and the wall or the ceiling,
  - it is centered relative to the aperture,
  - the measurement is performed during stable conditions: when for 30 seconds, the flow rate does not vary by more than 10%. The result is the average of the airflows measured during that time;
- The measured airflow is corrected for:
  - the error of the used instrument,
  - on-site temperature and pressure conditions, according to the recommendations of the manufacturer.

#### 3.1 Description of the facility

The measurements are performed in a lab with a facility shown in figure 1 below.

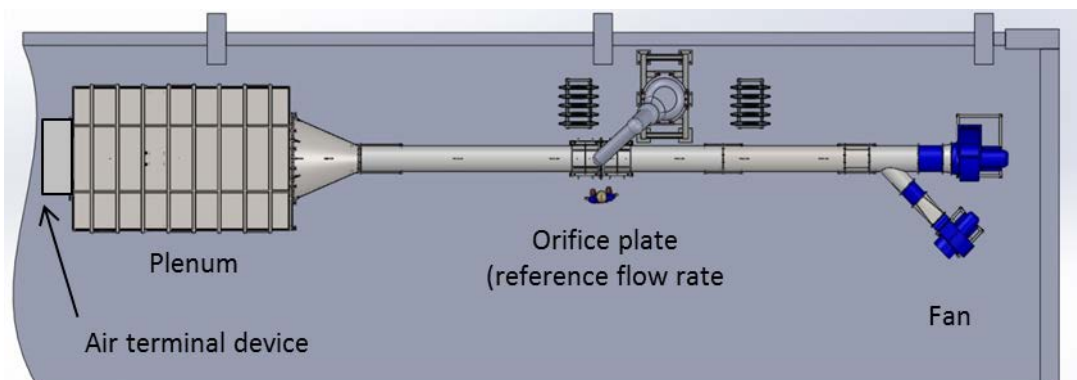


Figure 1: Facility used for the tests performed in lab

The flow rate is generated by changing the rotation frequency of a fan. The mass flow rate is then calculated by measuring the differential pressure at an orifice plate. Pressure and temperature sensors at the level of the terminal device are used to convert it to volume flow rate.

The flow range of the test rig is:

- in exhaust mode, from 5 to 17000 m<sup>3</sup>/h;
- in supply mode, from 5 to 5000 m<sup>3</sup>/h.

### 3.2 Description of the tests

The measurements were performed in supply mode, considering that the measurement method uncertainty is higher than in exhaust mode because of the impact of the distorted flow pattern on the measuring instrument (Mélois&Berthault, 2016).

Measurements were performed by 4 operators, with 4 measuring devices (4 different technologies commonly used in France, see Figure 2).

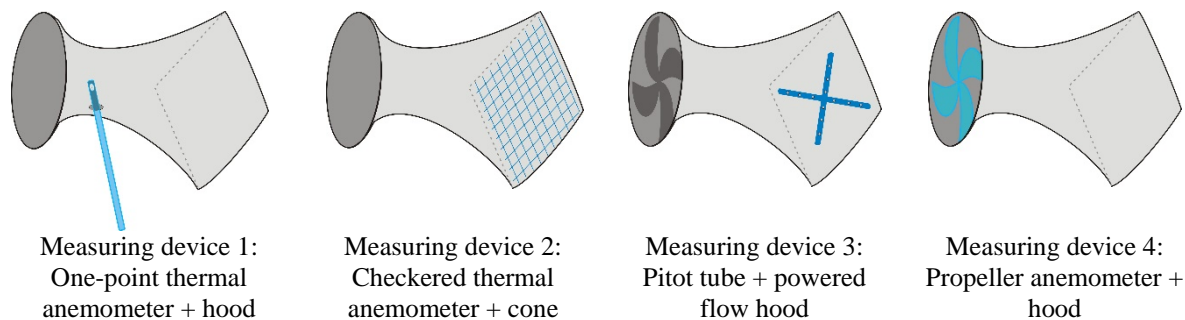


Figure 2: Measuring instruments used

In the cases of devices 1 and 4, an anemometer at the smallest section of a hood measures the air speed which is converted into volume flow rate. In the case of device 2, an array of small hot wires in a cross-section of the hood gives the flow rate. In device 3, the flow rate measurement is based on an array Pitot tubes. Moreover, the device 3 includes a fan which compensates the pressure drop induced by the positioning of the device on the terminal device.

Generally, the range of airflow rates at residential supply terminal devices in France is around  $30 \text{ m}^3 \cdot \text{h}^{-1}$ . We thus performed all laboratory tests at  $30 \text{ m}^3 \cdot \text{h}^{-1}$ . The measurements were performed at the facility for 3 supply air terminal devices representing 3 of the different geometries most used in France (Figure 3).

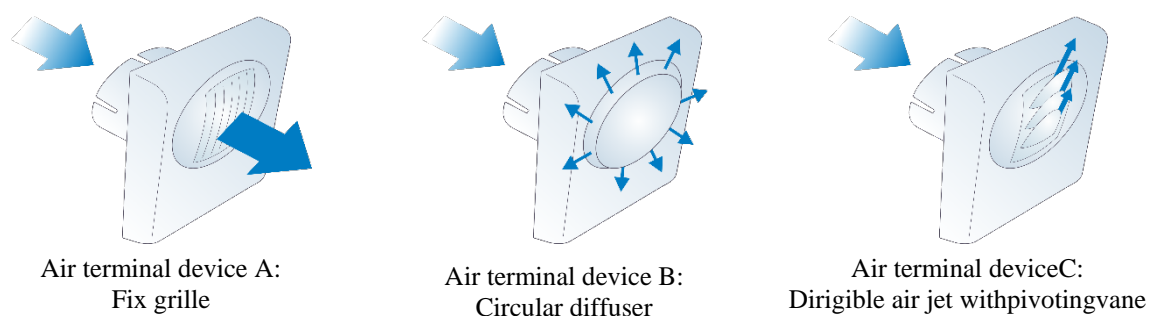


Figure 3: Supply air terminal devices tested

The airflow pattern generated by each of these air terminal devices has specificities:

- the fix grille (A) is perpendicular to the wall, so the direction of the airflow is consistent with the axis of the measurement device;
- the airflow induced by the circular diffuser (B) is omnidirectional: very close to the terminal device, there is no airflow along the axis of the measurement device (perpendicular to the wall);

- the airflow induced by the dirigible air jet with pivoting vane (C) follows a direction governed by the movable vanes, which can significantly deviate from the axis of the measurement device. This terminal device has been used with the vanes in the closed position which generates the most distorted flow.

We conducted analyses for each pair of measuring device/terminal device. Table 1 gives the matrix of our experiments.

Table 1: Number of measurements performed by each operator depending on the measuring instrument and the air terminal device

Air terminal device	Number of measurements											
	Fix grille				Circular diffuser				dirigible air jet with pivoting vane			
	1	2	3	4	1	2	3	4	1	2	3	4
Punctual thermal anemometer + cone	3	3	3	3	3	3	3	3	3	3	3	3
Checked thermal anemometer + cone	3	3	3	3	3	3	3	3	3	3	3	3
Pitot tube + cone with compensation	3	3	3	3	3	3	3	3	3	3	3	3
Propeller anemometer + cone (without extension)	3	3	3	3	3	3	3	3	3	3	3	3
Propeller anemometer + cone (with extension)	3	3	3	3	3	3	3	3	3	3	3	3

### 3.3 Preliminary tests

Before measuring flow rates at the air terminal devices, we performed a first test to estimate the measurement error of the instruments. We placed the instruments on the plenum with no terminal device and a reference flow rate of 30 m<sup>3</sup>/h was generated. Figure 4 represents this preliminary measurement.

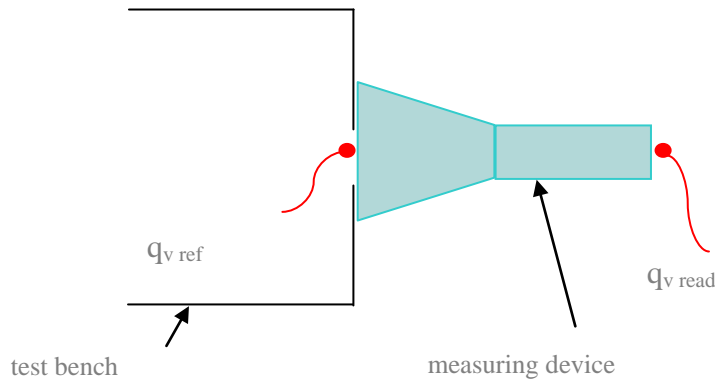


Figure 4: Measurement method in laboratory

The observed difference between the reading of the meter and the reference flow rate was used during experiments to correct the measurement of the meter from the instrument error. This preliminary experiment allowed to know the measurement error of each instrument to correct it in the following tests using Equation 5:

$$q_{v \text{ read, corrected}} = q_{v \text{ read}} + C_{\text{calibration}} \quad (5)$$

The relative errors between the “read, corrected” airflow  $q_{v \text{ read, corrected}}$  and the design rate  $q_{v \text{ ref}}$  have been considered in the analyses. This method allowed us to calculate the uncertainties considering the actual airflow rate generated by the test bench.

We defined  $q_{v \text{ ref, ij}}$  the result of the measurement number with:

- i the number of the measurement performed by on operator (i=1 for the first measurement, i=2 for the second and i=3 for the last one);
- j is the identification of the operator (from j=1 for the first operator to j=4 for the fourth operator).

#### 4 RESULTS OF LABORATORY MEASUREMENTS

##### 4.1 Evaluation of the measurement method uncertainty $u_{Q,2}$

For each pair of measuring device and terminal device, 3 measurements were performed by each of the 4 operators, therefore, 12 measurements in total. Assuming the errors follow a rectangular distribution, we assessed the uncertainty due to the method using Equation 6:

$$u_{Q,p} = \frac{\text{average}_{j=\{1,4\}} \text{average}_{i=\{1,3\}} \left( \frac{q_{v \text{ ref },ij} - q_{v \text{ read },corrected ,ij}}{q_{v \text{ ref },ij}} \right)}{\sqrt{3}} \quad (6)$$

Table 1: Measurement method uncertainty results for 3 air terminal devices and 4 technologies of measuring devices

Type of measuring device \ Type of terminal device	Fix grille	Circular diffuser	Dirigible air jet with pivoting vane
Punctual thermal anemometer + cone	3%	9%	14%
Checked thermal anemometer + cone	7%	32%	29%
Pitot tube + cone with compensation	2%	5%	2%
Propeller anemometer + cone (without extension)	0%	1%	15%

Table 2 gives results of the association air terminal device together with a measuring instrument.

They support that the uncertainty due to the method significantly depends on the type of air terminal device (up to 25% from one measuring device to another with the checked thermal anemometer + cone) and on the type of measuring device (up to 32% for the circular diffuser). These results confirm the need to conduct an error analysis for each pair of measuring device/terminal device.

##### 4.2 Evaluation of the repeatability uncertainty $u_{Q,3}$

For each pair of measuring device and air terminal device, we first analyzed the distribution of the results of the 3 measurements performed by the same operator. We obtained an evaluation of the repeatability for each operator. Then, we have evaluated the repeatability uncertainty component for each pair of measuring device/terminal device regardless of operators, according to the Equation 7.

$$u_{Q,3} = \text{average}_{j=\{1,4\}} \left( \sigma_j \left( \frac{q_{v \text{ ref },ij} - q_{v \text{ read },corrected ,ij}}{q_{v \text{ ref },ij}} \right)_{i=\{1,3\}} \right) \quad (7)$$

where  $\sigma_j$  is the standard deviation between the 3 measurements performed by the operator j.

Table 3 presents the uncertainties due to repeatability for each tested case. Most values of repeatability uncertainties lie between 1% and 3%, which is good. They are higher for few particular cases, especially for the movable vanes grilles (the grilles were half opened during

the whole series of measurements). The geometry of such air terminal devices induces difficulties to repeat the measurement.

Table 2: Repeatability uncertainties results for 3 air terminal devices and 4 technologies of measuring devices

Type of measuring device \ Type of terminal device	Fix grille	Circular diffuser	Dirigible air jet with pivoting vane
Punctual thermal anemometer + cone	2%	2%	9%
Checked thermal anemometer + cone	6%	3%	6%
Pitot tube + cone with compensation	1%	2%	1%
Propeller anemometer + cone (without extension)	0%	1%	5 %

### 4.3 Reproducibility measurement uncertainty

For each pair of measuring device and terminal device, the objective was to evaluate the impact of the operator. We thus characterized the operator results with his average error for each pair of measuring device/terminal device. Then, we analyzed the distribution of those average errors in order to compare the 4 operator results. We defined the reproducibility uncertainty component according to the Equation 8.

$$u_{Q,4} = \sigma_{j=\{1;4\}}(\text{average}_{i=\{1;3\}}\left(\frac{q_{v\text{ref},ij} - q_{v\text{read,corrected},ij}}{q_{v\text{ref},ij}}\right)) \quad (8)$$

where  $\sigma$  is the standard deviation between the 4 average results, one average is calculated for each of the 4 operators, from his 3 measurement results.

Table 3: Reproducibility uncertainties results for 3 air terminal devices and 4 technologies of measuring devices

Type of measuring device \ Type of terminal device	Fix grille	Circular diffuser	Dirigible air jet with pivoting vane
Punctual thermal anemometer + cone	3%	3%	11%
Checked thermal anemometer + cone	4%	5%	10%
Pitot tube + cone with compensation	1%	1%	1%
Propeller anemometer + cone (without extension)	0%	2%	7%

Table 4 presents the uncertainties due to repeatability for each tested case. The results of the reproducibility tests are similar to those for repeatability. Few values are higher than 3%, due to the geometry of the air terminal device

### 4.4 Comparison of the three uncertainties: method, repeatability, and reproducibility

Figure 4 shows that, in the case of a dirigible air jet with pivoting vane, the uncertainty due to the method ( $u_{Q,2}$ ) is higher than uncertainties due to repeatability ( $u_{Q,3}$ ) and reproducibility ( $u_{Q,4}$ ). We observed the same tendency for the fix grille and the circular diffuser.

The range of uncertainties (from nearly 0% up to 32%) is very large and depends significantly both on the type of measuring device and the type of terminal device. This conclusion confirms the need to formulate different conclusions depending on each combination.

## Evaluation of uncertainties for dirigible air jet with pivoting vane

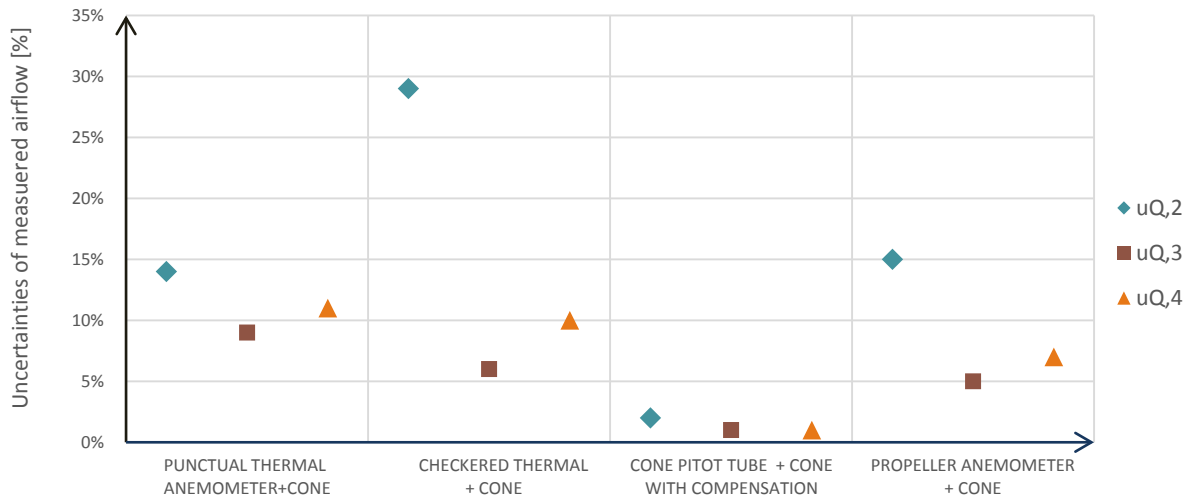


Figure 1: Evaluation of uncertainties from measurements performed on the test bench with a dirigible air jet with pivoting vane

## 5 CONCLUSION: DISCUSSION AND APPLICATION TO LARGE-SCALE FIELD MEASUREMENTS

The first result of this study is that the airflow measurement uncertainty depends very significantly on both the type of terminal device and measuring device. Therefore, the operator has to choose his measuring device to contain the uncertainty within acceptable limits.

The second result is the determination of Maximum Permissible Errors to respect an overall measurement uncertainty. We calculated MPEs to comply with several overall measurement uncertainties. Table 5 gives MPEs for a 15% overall measurement uncertainty. Cells with an “X” represent the incompatibility between the couple air terminal device/measuring device. In those cases, the combined uncertainties  $u_{Q,2}$ ,  $u_{Q,3}$  and  $u_{Q,4}$  are already higher than the acceptable limit. That means that there is no possibility of MPE which can allow making the measurement within the acceptable limit.

Table 5: MPE<sub>max</sub> for a 15% overall uncertainty

Type of measuring device \ Type of terminal device	Fix grille	Circular diffuser	Dirigible air jet with pivoting vane
Punctual thermal anemometer + cone	11	X	X
Checked thermal anemometer + cone	X	X	X
Pitot tube + cone with compensation	13	9	12
Propeller anemometer + cone	13	12	X

\*An “X” means that the 15% limit cannot be met given the other uncertainty components (measurement method, repeatability, and reproducibility)

With a 15% limit, the measurement can be performed in 6 cases out of 12, yet with reasonable MPEs. Setting the limit up to 20% or even 25% does not help: some cases remain impossible given other uncertainty components or the resulting MPE is too low. Therefore, 15% appeared to be a reasonable target for the overall combined expanded uncertainty. In this case, the MPEs of the eligible measuring devices have to be lower than 9% to 13% depending on the type of measuring device and air terminal device.

For practical large-scale applications, however, we preferred defining a unique MPE applicable to all types of the eligible measuring device. We chose to set 10% as the limit for the MPE, which is close to the most stringent requirement that can be inferred from table 5. These requirements are now part of the Promevent protocol which has been discussed with stakeholders at French level. The protocol requires ensuring a combined expanded measurement uncertainty below 15% and states that a calibration certificate proving that the measuring device has an MPE lower than or equal to 10% is sufficient to meet this requirement provided that the measurement device is used on a compatible terminal device, as shown in table 6.

## 6 ACKNOWLEDGEMENTS

Cerema, CETIAT, Allie' Air, CETii, PBC, Effinergie, ICEE and PLEIAQ have contributed to the Promevent project.

The Promevent project received funding from the French Environment and Energy Management Agency (ADEME) and had support from the French Ministry in charge of Construction.

The sole responsibility for the content of this publication lies with the authors.

## 7 REFERENCES

Bailly, A., & Lentillon, C. (2014). PROMEVENT: Improvement of protocols measurements used to characterize ventilation systems performance. 35th AIVC Conference. Poznan.

BIPM et al. 2008. Evaluation of measurement data — Guide to the expression of uncertainty in measurement. JCGM 100:2008. 120 pp.

BIPM et al. 2012. International vocabulary of metrology – Basic and general concepts and associated terms (VIM) 3rd edition. JCGM 200:2012. 108 pp.

Caillou, S. (2014). Mesurer les débits de ventilation mécanique. Les dossiers du CSTC.

Caré, I. (2013). Guide des bonnes pratiques des mesures de débit d'air sur site pour les installations de ventilation. CETIAT. 52 pp.

Carrié, F. R. et al. (2016). Improving the compliance of Energy Performance Certificates and the quality of building works. Qualicheck Booklet.

Effinergie (2014). Protocole de contrôle des systèmes de ventilation des bâtiments demandant le label effinergie+. Effinergie website [www.effinergie.org](http://www.effinergie.org)

Effinergie (2015). Règles Techniques label Effinergie+. Effinergie website [www.effinergie.org](http://www.effinergie.org)

Janssens, A., Durier, F., & Carrié, F. R. (2013). Securing the quality of ventilation systems in residential buildings: existing approaches in various countries. Proceedings of the AIVC TightVent International Workshop. Brussels.

Jobert, R., & Guyot, G. (2013). Detailed analysis of regulatory compliance controls of 1287 dwellings ventilation systems. Proceedings of the 34<sup>th</sup> AIVC Conference. Athens.

- Mélois, A. B., & Berthault, S. (2016) Reliability of ventilation system inspection for dwellings: comparisons of measurements and checks protocols tested during on-site campaign of the Promevent project. Proceedings of the ASHRAE and 37th AIVC Conference. Alexandria.
- Walker, I., Wray, C., Dickerhoff, D., & Sherman, M. (2001). Evaluation of flow hood measurements for residential register flows. Lawrence Berkeley National Laboratory, LBNL-47382.
- Walker, I., Wray, C., Guillot, C., & Masson, S. (2003). Evaluation of Commercially Available Techniques and Development of Simplified Methods for Measuring Grille Airflows in HVAC Systems. Lawrence Berkeley National Laboratory, LBNL-51551.
- Wray, C., Walker, I., & Sherman, M. (2002). Accuracy of flow hoods in residential applications. Lawrence Berkeley National Laboratory, LBNL-49697.

# The industries vision and activities for better buildings in the future.

Lars-Åke Mattsson, Kirk Bracey<sup>\*2</sup>

*1 Lindab Ventilation AB  
Stålhögavägen 115  
26982 Båstad, Sweden*

*2 Lindab Ltd.  
Units 6 & 7, Linkmel Close, Queens Drive Ind Est,  
Nottingham, NG2 1NA, UK  
\*Corresponding author: kirk.bracey@lindab.com*

## ABSTRACT

The industry is now focusing in system solutions and the goal is to be able to deliver complete reliable, energy efficient solutions that is understandable and easy to maintain by the normal service personal. In order to do this the basic products have to perform exactly as they are described in the technical documentation. The documentation have to help the designer and the installer to actually build the system in the correct way without compromises from other stakeholders. The system integration must also be simple and with a plug and play vision in order to have the correct function including demand controlled ventilation, the function in a fire situation and be able to maintain the system by a smart diagnostic tool, helping the service personal and enlighten the building owner with usable graphs and information to be able to follow up on the performance. All these issues is one by one not technically not very difficult but when it comes to reality it often fails due to the complexity of a building and the responsibility chain that is used in our business. We can today see that many systems is performing poorly and the end user have no chance of communicating the problem to the right responsible stakeholder. The solution is that the suppliers have to take a bigger responsibility and actually see and provide guaranteed functions instead of the cheapest product just like the car industry. One real technically difficult issue that will be highlighted in this presentation is to be able to measure the airflow very accurate in a world were space is not available and the flows are going to very low levels and that we are not allowed to create extra pressure drop. The modern way of measuring airflow will probably be with ultrasonic sound which allows very low flows and no pressure drop and high accuracy. This smart and accurate devices can also be the basis for a diagnostic tool that can provide indication of the:

- Controlling and monitoring of the system
- Status of the system
- Where to look for failure
- Costs follow-up
- Accurate payment of IAQ to the tenants

## KEYWORDS

Better IAQ, Accurate flow measurement, Better performing ventilation systems.

## 1 INTRODUCTION

Flow measurements has always been difficult to do in lab environment and even worse in a real building so the result is often bad and perhaps not constant over time due to contaminations in the ducts. At the handing over process the designed flows should be measured and documented and then verified by the inspector. If the flows mismatches the system have to be re-commissioned and verified again. This procedure seldom works and the customer receives a system balanced the best possible way but perhaps not the most effective way according to energy and IAQ. Lindab has developed a new flow measuring device based

on ultrasonic sensors that is very accurate in the whole flow range and is easy to use both for persons and superior control system. With this it will be easy to see and regulate the design values until they are accomplished and the design is thoroughly tested.

## 2 FLOW MEASUREMENT IN DUCTS

### 2.1 The K factor principle

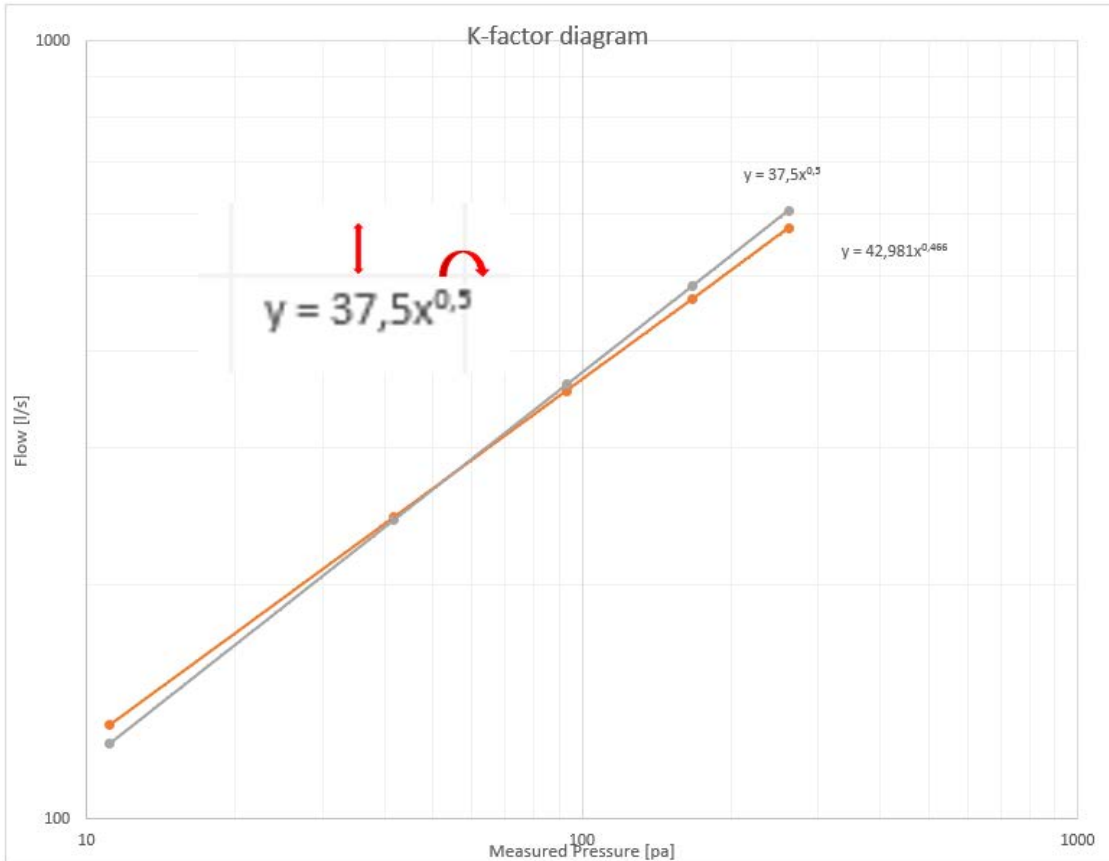
The flow can be measured using some kind of obstacle to create a predefined pressure drop and then measure the pressure difference over the obstacle.



This procedure is called k-factor measurements because the equation follows a straight line in a log-log diagram with the direction of 0,5.

$$Q = K * P_m^{0,5}$$

- Q is the flow in the duct.
- K is a factor found in measurements
- Pm is the measurement pressure over the predefined obstacle.
- 0,5 is the direction of the line.



- To make it easy to use there is an approximation using the direction 0,5 which is the same as square root that everybody know and can use even though the real result with better accuracy can be 0,48.
- The small holes to measure the pressure can easily be filled with dirt and change over time.
- The producers chose the highest pressure difference in order to measure it as correctly as possible. However to measure a pressure lower than 5-10 Pa is often very difficult and this ends up with a bad accuracy lower than 3 m/s.
- The K factor measurements are quite good in a defined steady state obstacle but to measure over some moving parts like a damper is very difficult and the K factors differs from individual to individual and also moving from closed to open or open to close due to hysteresis.



- The error is depending on the flow profile and is only correct with a non-disturbed. The flow profile and the measure pressure is very difficult to align.

## 2.2 The ultra-sonic principle

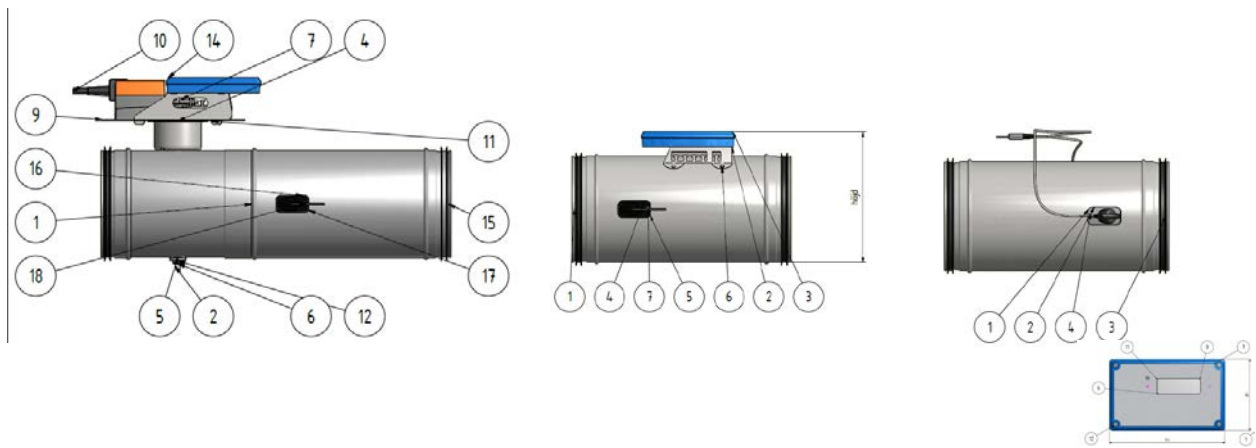
To measure with ultrasonic sound is in principal very easy. Only to use the time difference between upstream and downstream time for the ultrasonic sound. However to do it in a correct way there is a lot of traps to fall down in that we didn't know when we started. Millions of measurement wiser we know how to interpret the result and present it as the ultimate truth. The ultra-sonic sound is following the technique in a very straight forward manner and can be used to an accurate result. However all other old technology have problems and when we now see the result of the ultrasound it is easy to be misled and involve all this old errors into the new technology. The ultrasound is influenced mostly on the temperature but also a little bit by pressure, humidity and the shape of the flow profile. The flow shape can be to one side, which is the easiest part, swirled and divided to several componants. This errors will be in the result and has to be dealt with to present the right value.

## 2.3 The solution

Controller  
FTCU

Monitor  
FTMU

Sensor/display  
FTSU/FTD



The Lindab solution is an ultrasonic measuring device with three features depending on usage. The simplest is the sensor which only contains the transmitter and receiver and has to be read by a display that is like a handheld measuring device via a USB or radio. This is mostly to be used at a commissioning and service phase.

The second is the monitor that continuously monitors the flow and temperature and can communicate the result to a superior computer using the RS485 with Modbus. This product is very usable to advanced systems to measure the flow and the superior system can control the flow with the fan and dampers.

The third and most advanced product has its own damper and can be used as a standalone regulator controlling its own flow via analogue or digital inputs/outputs.

## 2.4 The accuracy

The accuracy is very good and very reliable all the way down to 0,5 m/s up to 15 m/s. The biggest problem today is that there are several measuring units with the same bad performance which does not add up to the correct decisions. With the UltraLink and its high accuracy and high reliability it is very easy to make the correct decision and it can also be a base for a diagnose tool for the whole system.

## 3 CONCLUSIONS

Lindab thinks we have a technology that is way better than common flow measuring and will in the future lift the ventilation business to a higher level being able to maintain a good IAQ and save energy by not over dimension and by being able to control the flows all the way down to 0,5 m/s when no one is in the room. Also being able to diagnose the system and guide the owner, service personnel and tenants to smart usage and operation.

## 4 ACKNOWLEDGEMENTS

Ola Berg Lindab Ventilation AB for flow measurement knowledge.

Niclas Ivarsson Lindab AB for mathematical and programming skills

Klemen Rupnik Lindab AS for mathematical and programming skills

Daniel Vidal de Ventos Lindab IMP Klima for CFD calculations.

Johnny Denh-Kien Nguyen Lindab Ventilation AB for millions of measurements.

# About 1,000 ductwork airtightness measurements performed in new French buildings: database creation and first analyses

Adeline Bailly Mélois<sup>\*1</sup>, Bassam Moujalled<sup>\*1</sup>

*1 Cerema Centre-Est  
46 rue Saint-Théobald  
38081 l'Isle d'Abeau, FRANCE*

*\*Corresponding author: [adeline.melois@cerema.fr](mailto:adeline.melois@cerema.fr)*

## ABSTRACT

In France, the current regulation on the energy performance of buildings (RT 2012) does not require ductwork airtightness measurement when the default-value is used in the regulatory EP-calculation. Thus, measurements are only mandated when a specific airtightness level is used in EP-calculations or required by a voluntary certification scheme. In such case, measurements have to be performed according to a national scheme regarding ductwork airtightness measurement. This scheme requires testers to be qualified and qualified testers have to annually declare their measurement results in standard record files. In 2017, we created a national database from those records. The database includes about 1,000 measurements that were performed, mainly in new highly efficient buildings.

This paper presents the national ductwork airtightness measurement scheme and database and gives some figures regarding main characteristics of the buildings and ventilation systems. Then, the paper analyzes the measurement results regarding ductwork airtightness classes depending on several factors, in particular building's use, type of ventilation system and targeted class.

Although earlier ductwork airtightness measurements were only performed in non-residential buildings, we observe that the number of measurements performed in single-family houses and multi-family dwellings has significantly increased the last 2 years. They represented 76% of the measurements performed in 2016. Regarding ductwork airtightness performance, Class A is the most frequent result for residential buildings, which are mainly equipped with single-exhaust ventilation system. Class B is the most frequent result for non-residential buildings (office buildings, schools, and hospitals) which are mainly equipped with a balanced ventilation system. Those results only apply to the buildings of the database and cannot be generalized to all new buildings in France.

## KEYWORDS

Ductwork airtightness, building, measurements, database.

## 1 INTRODUCTION

Duct leakage is known to be detrimental to energy performance and indoor climate (Andersson, 2013) (Carrié, 1999). In order to limit the negative effects of leaky duct systems, French authorities developed an approach to improve ductwork airtightness which builds on the success and lessons learnt from the envelope airtightness approach, including mandatory justification of the airtightness level achieved with third-party testing, unless the default value is used (Charrier, 2017). These ductwork airtightness requirements are expected to boost the market similarly to what happened with the envelope airtightness market as described by Charrier (Charrier, 2015).

In the French EPB regulations, a default value for ductwork leakage class can be used. Based on leakage classes defined in EN standards 12237 and 1507, the default value corresponds to 2.5\*class A. Since the current EPB regulation (RT2012), if a better-than-default class is used, it must be justified. Furthermore, the Effinergie+ and BEPOS-Effinergie labels, firmly based on the current regulation, require justifying achieving ductwork leakage Class A as a minimum (Carrié, 2016). Figure 1 gives an overview of the evolution of the regulatory and voluntary requirements since 2000. Note that both residential and non-residential buildings are concerned. The Effinergie+ and BEPOS labels are meant to experiment requirements for future updates of the regulation, similarly to the past BBC-Effinergie label (tightening RT2005 regulatory levels) which has been very popular and useful to tune the requirements of the RT2012 regulation.

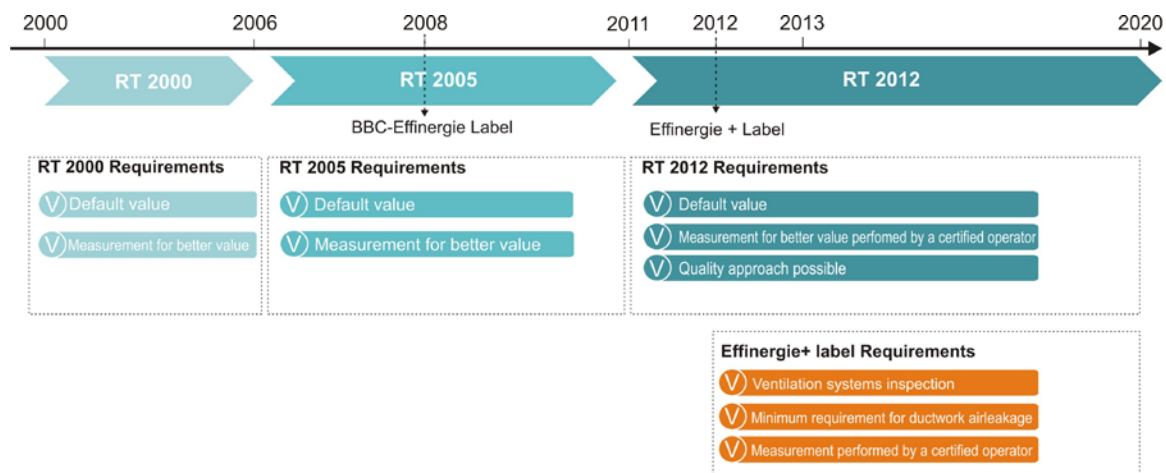


Figure 1: Evolution of French requirements on ductwork airtightness since 2000 for residential and non-residential buildings

The RT2012 regulation gives two options to justify using a ductwork airtightness class different from the default value as input in the EPB calculation. The class achieved can be justified:

- Either with a ductwork airtightness measurement, performed by a certified tester;
- Or by the application of a certified quality management approach (QMA) on ductwork airtightness that allows testing only a sample of buildings. Although a similar QMA option is popular for envelope airtightness (Charrier, 2014), it has never been used in practice for ductwork airtightness and is currently under revision. In both cases, ductwork airtightness tests must be performed by a third-party tester, qualified by the certification body Qualibat.

## 2 PRESENTATION OF THE FRENCH NATIONAL DUCTWORK AIRTIGHTNESS MEASUREMENT SCHEME AND ITS DATABASE

### 2.1 Qualification requirements

In 2012, Effinergie introduced a training scheme for testers within the creation of the Effinergie+ label. Then, the government created a qualification for ductwork airtightness testers. To be qualified, a tester has to:

- Undergo a qualifying State-approved training;
- Pass the training examination (the theoretical part, with a State-approved multiple choice questionnaire; and the practical part, with a test performed in situ with a certified tester),

- Justify sufficient testing experience.

Once qualified, every tester is subjected to yearly follow-up checks, organized by the certification body. The follow-up checks include an analysis of some reports to verify their compliance with applicable standards and guidelines. Checks are based on the documentation sent every year, but also on site, in particular, in case of complaints or doubts about the quality of their work. Those checks can lead to de-qualification. As of February 2017, 58 testers have been qualified by Qualibat.

Tests have to comply with the European standards EN 12237, EN 1507, EN 13403 and EN 12599, and with the French technical report FD E 51-767. For the Effinergie labels, testers have to additionally comply with the Effinergie measurement protocol, and soon with the recently issued Promevent protocol. Whenever a test is performed, either for a certified QMA or for a systematic test, it must be performed after any works that could impact the final ductwork airtightness. FD E 51-767 specifies the reporting format. In particular, the report indicates if the ductwork airtightness complies with the input class used in the EP calculation. A new version of FD E 51-767 should be published soon. It has been modified to ease the measurement and avoid damage to the ductwork when preparing the section under test.

## **2.2 Development of a ductwork measurements database**

Each qualified tester is required to fill in a register with all test results and communicate this register to the certification body every year for verification purposes. This register includes:

- Building general information: owner, location, use, year of the construction, year of the rehabilitation;
- Special requirements: label, certification, ductwork airtightness class target;
- Ventilation system main characteristics: number of stories, type of system, nature, geometry and insulation of ducts, type of terminal devices;
- Measurement protocol: tester's name, date of measurement, measurement device, time of measurement (building state);
- Measurement input data: ductwork surface area, test pressure;
- Measurement results: leakage airflow, leakage factor  $f$ , airtightness class.

All registers are consolidated in a common database. Currently, 983 measurements have been recorded in the database. Those measurements were performed by certified testers since the introduction of the training scheme in 2012 (last updating in January 2017). A similar scheme exists since 2007 regarding building airtightness. It has led to a growing database of more than 100,000 tests (Bailly et al., 2016).

## **3 RESULTS**

### **3.1 Main characteristics of buildings and ventilation systems in the database**

Measurements registered in the database were essentially performed in new buildings: 97% of measurements have been performed in buildings built after 2011 (see Figure 2). Although earlier ductwork airtightness measurements were only performed in non-residential buildings, we observe that the number of measurements performed in single-family houses and multi-family dwellings significantly increased the last 2 years. They represented 76% of the measurements performed in 2016.

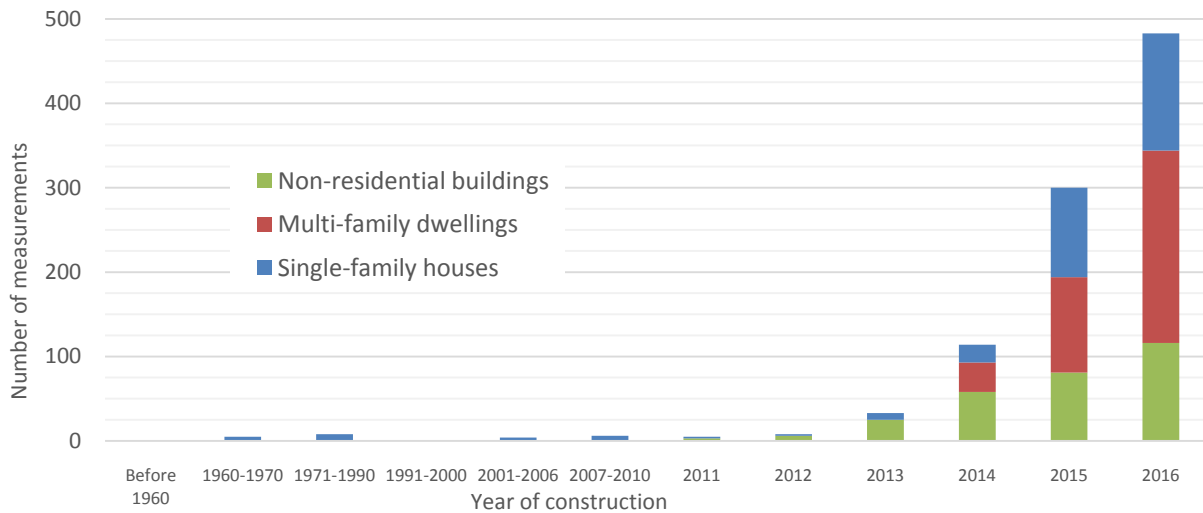


Figure 2: Number of ductworks airtightness measurements depending on the construction year and the use of the building

Figure 3 shows that for non-residential buildings, measurements were essentially performed in office buildings, schools, and hospitals.

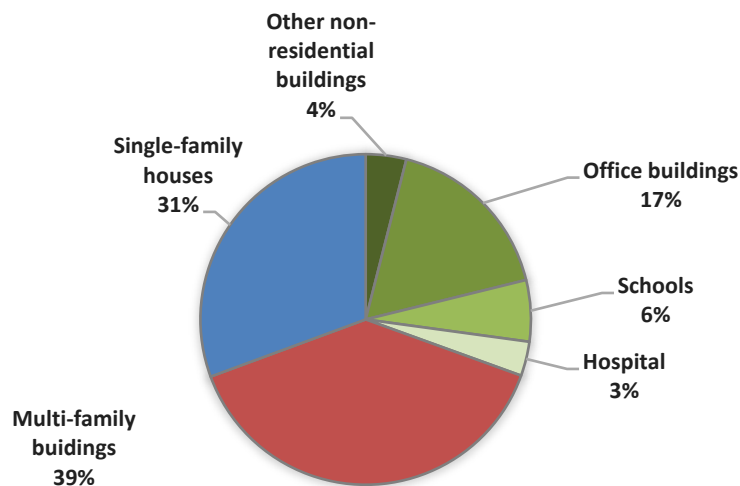


Figure 3: Distribution of buildings' use

In new French buildings, either balanced ventilation systems or single-exhaust ventilation systems are implemented. Figure 4 shows that residential buildings, both multi-family dwellings, and single-family houses, are mainly equipped with single-exhaust ventilation systems, and non-residential buildings are equipped with balanced ventilation systems.

Those figures cannot be generalized to all new French buildings. In fact, low-energy certified buildings represent 44% of the measurements recorded in the database but only 10% of the new building stock in France.

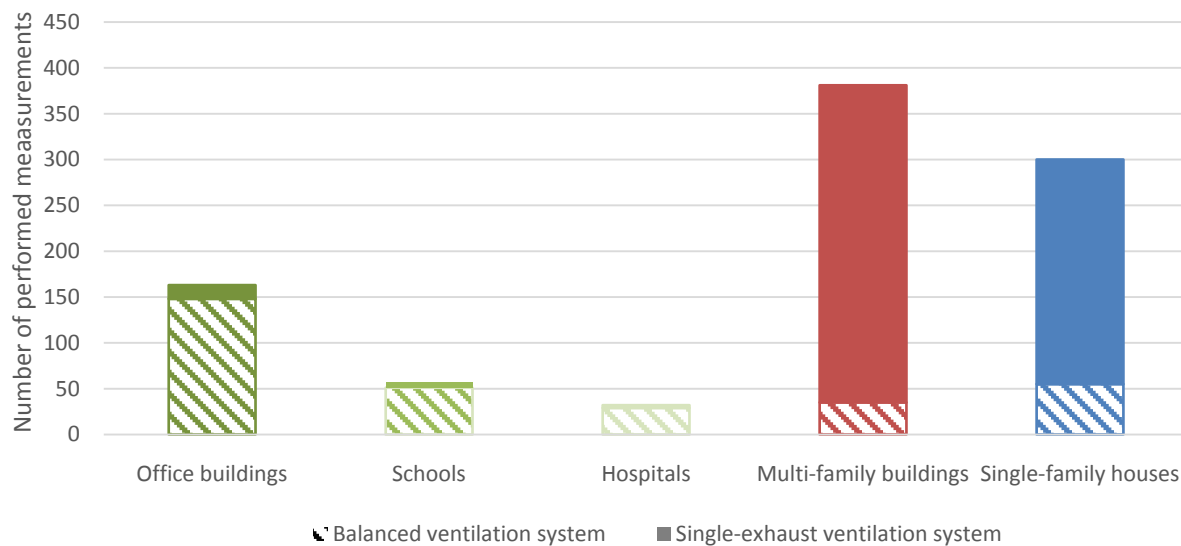


Figure 4: Type of ventilation system depending on buildings' use

Three different types of ducts are used: rigid ducts, semi-rigid ducts, and flexible ducts. Table 1 presents the distribution of the type of ductwork depending on the building's use and the type of ventilation system. Balanced ventilation systems are mainly connected to rigid ducts, especially in non-residential buildings. For single-exhaust ventilation system, it depends on the type of building. Rigid ducts are widely used both in non-residential buildings and multi-family buildings. On the contrary, flexible ducts are the main type of ductwork implemented in single-family houses equipped with single-exhaust ventilation systems. This practice is consistent with the type of ducts generally implemented in all buildings in France, as it corresponds to the French standards and professional recommendations.

Table 1: Type of implemented ducts depending on building's use and type of ventilation system

	Balanced ventilation system			Single-exhaust ventilation system		
	Rigid ducts	Semi-rigid ducts	Flexible ducts	Rigid ducts	Semi-rigid ducts	Flexible ducts
Office buildings	<b>85%</b>	0%	5%	<b>11%</b>	0%	0%
Schools	<b>79%</b>	0%	<b>11%</b>	<b>11%</b>	0%	0%
Hospitals	<b>89%</b>	0%	0%	<b>7%</b>	0%	4%
Multi-family buildings	4%	2%	3%	<b>78%</b>	1%	12%
Single-family houses	7%	5%	6%	4%	3%	<b>75%</b>

### 3.2 Measured ductwork airtightness classes

Ductwork airtightness measurements are performed in order to justify either the respect of a certification requirement, the respect of an EP-calculation declaration, or without specific requirement. The information regarding target classes is available for about half of the measurements (521), amongst which 23 measurements target class C, 91 target class B, 305 target class A and 153 declared as "notarget class". As shown in Figure 5, the distribution of the specific ductwork airtightness measured class depends on the chosen target class:

- when the most airtight class (class C) was targeted, less than half of the measured ductworks meets the target (almost only hospitals). For the others, the quality of the ductwork is significantly poorer as they only achieve class A;
- when class B or class A was targeted, most ductworks meet this target class or better. However, 16% (target class A) and 35% (target class B) of the measured ductworks achieve worse classes;
- when the measurement was performed with “no target class”, the results are quite good as 75% of the measured ductwork reach class A or better. Even though there was no target class, mandating a measurement suggests a special awareness regarding ductwork airtightness for those buildings, i.e. presumably better results than the average. Again, it should be noted that these results only apply to the buildings of the database and cannot be generalized to all new buildings in France.

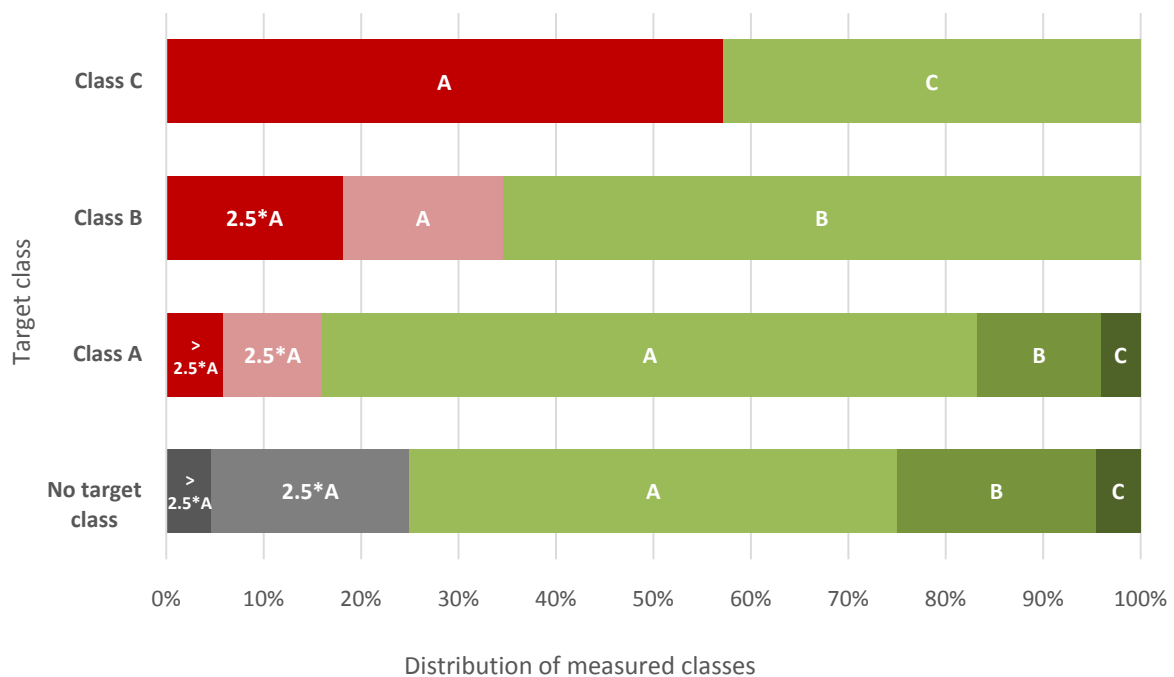


Figure 5: Specific ductwork airtightness measured class depending on target class

Figure 6 presents the results of ductwork airtightness measured class in residential buildings. For both single-family houses and multi-family buildings, most measured ductworks met leakage class A (respectively 64% and 54%). In multi-family buildings, 23% of measured ductworks achieved a better class (mainly B), whereas ductworks of higher classes are only 7% in single-family houses. The wide use of flexible ducts in single-family houses could explain these results (see Table 1).

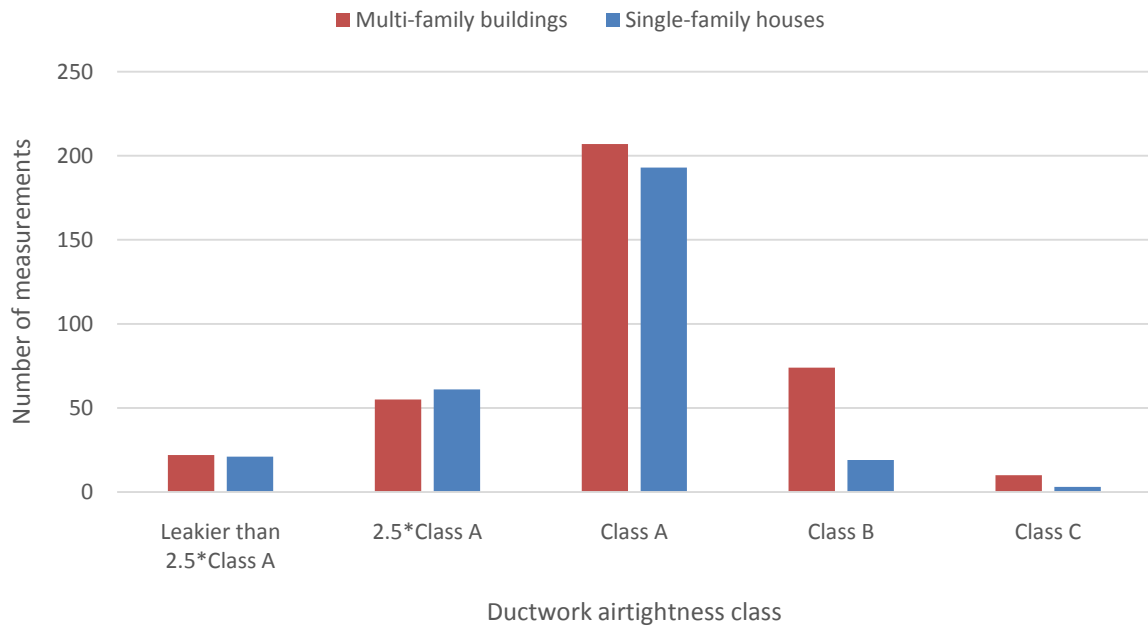


Figure 6: Specific ductwork airtightness measured class in residential buildings

Figure 7 presents the results of ductwork airtightness measured class in non-residential buildings. Ductworks in these buildings are overall tighter than in the residential sector: 48% of them meet class B. Even if our sample is too small to make statistics, we observe that class C is more frequently achieved in hospitals where rigid ducts are widely used.

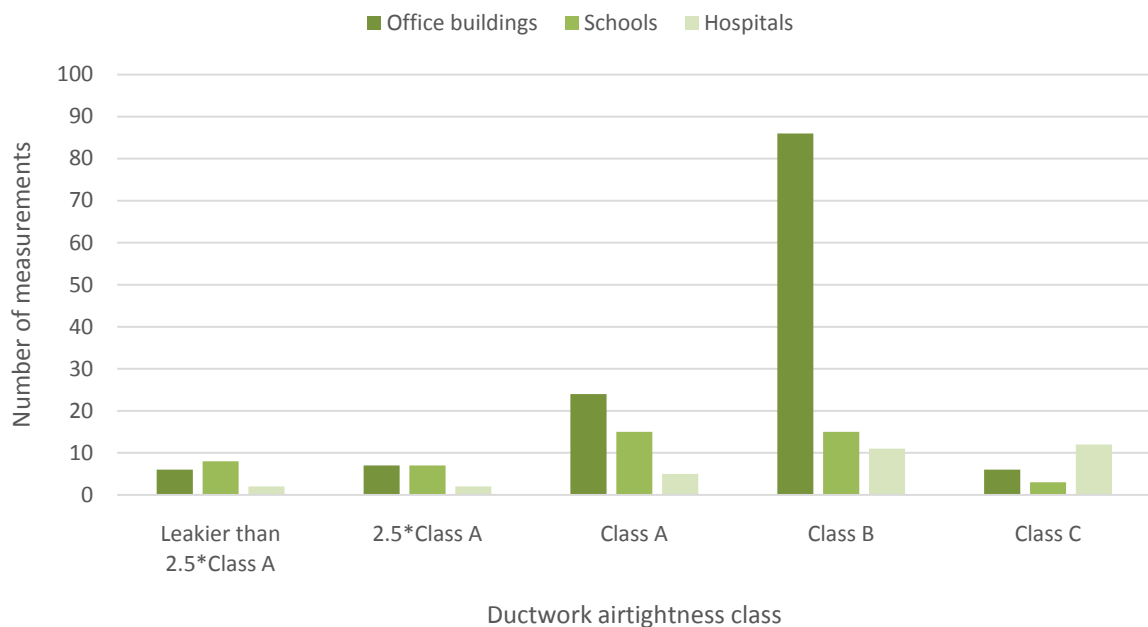


Figure 7: Specific ductwork airtightness measured class in non-residential buildings

## 4 CONCLUSIONS

The French Ministry in charge of construction created a qualification scheme for ductwork airtightness testers since 2012. Each qualified tester is thereby required to feed a database with building general information, targeted certification and/or class, ventilation system's main characteristics, data on the measurement protocol, measurement input data and measurement output results. So far 983 measurements have been logged in the database. The number of ductwork airtightness measurements that are performed by qualified testers is growing each year, with almost 500 measurements in 2016.

All measurements considered in the database were performed:

- on new residential building: both multi-family buildings and single-family houses, mainly equipped with single-exhaust mechanical ventilation systems;
- on new non-residential buildings: mostly office buildings, schools, and hospitals, mainly equipped with balanced mechanical ventilation systems.

In residential buildings, most measured ductworks met leakage class A. In non-residential buildings, ductworks are overall tighter: almost half of them met class B. Nevertheless, when a target class was defined, it was not widely achieved, especially for the tightest class, class C.

All measurements in the database were performed according to specific and not common demands. Thus, all results presented in this paper only apply to the buildings of the database and cannot be generalized to all new buildings in France.

## 5 ACKNOWLEDGEMENTS

The database is the property of the French Ministry in charge of the Construction. The analysis was performed by Cerema. The sole responsibility for the content of this publication lies with the authors.

## 6 REFERENCES

- Andersson, J. (2013). Quality of ventilation systems in residential buildings: status and perspectives in Sweden. In edited proceedings of the AIVC- TightVent international workshop, Brussels, 18-19 March 2013, ISBN 2-930471-43-3, INIVE, Belgium. pp. 159-166.
- Bailly, A., Guyot, G., Leprince, V., 2016. Analyses of about 90 000 Airtightness Measurements Performed in France on Residential and Non-Residential Buildings from 2008 to 2014, in Proceedings IAQ 2016 Defining Indoor Air Quality: Policy, Standards and Best Practices Co-Organized by ASHRAE and AIVC. Alexandria, VA, USA.
- Charrier, S., Mélois, A. and Carrié, F.R. (2017). Ductwork airtightness in France: regulatory context, control procedures, results. QUALICheck fact sheet # 54, available at <http://qualicheck-platform.eu/wp-content/uploads/2017/02/QUALICheck-Factsheet-54.pdf>
- Carrié, F. R., Andersson, J., Wouters, P. (1999). Improving ductwork—A time for tighter air distribution systems. Air Infiltration and Ventilation Centre, Coventry, UK. 126 p. ISBN 1 902177 10 4.

- Charrier, S., Ponthieux, J., Huet, A. (2014). The Airtightness Quality Management Approach in France – Assessment after more than Five Years of Operation. *International Journal of Ventilation*. ISSN 1473-3315. Vol. 13(2), pp. 125-140.
- Carrié, F.R., and Dervyn, Y. (2016). The Effinergie approach to ease transitions to new regulatory requirements. QUALICHeCK fact sheet # 45, available at <http://qualicheck-platform.eu/wp-content/uploads/2017/02/QUALICHeCK-Factsheet-45.pdf>
- Carrié, F.R. and Charrier, S. (2015). Building regulations can foster quality management — the French example on building airtightness. QUALICHeCK fact sheet # 01, available at <http://qualicheck-platform.eu/wp-content/uploads/2015/02/QUALICHeCK-Factsheet-01.pdf>

# Impact of ductwork airtightness on fan energy use: calculation model and test case

Valérie Leprince<sup>\*1</sup>, François Rémi Carrié<sup>2</sup>

*1 PLEIAQ  
84 C Avenue de la Libération  
69330 Meyzieu, France*

*2 ICEE  
93 rue Molière  
69003 Lyon, France*

*\*Corresponding author: valerie.leprince@pleiaq.net*

## ABSTRACT

This paper proposes a methodology to assess fan energy use savings when improving ductwork airtightness. This methodology is based on new standard FprEN 16798-5-1:2016. Unlike the classical "cube law", it considers pressure drops at air terminal devices separately from the pressure drops in the rest of the system. The calculation tool based on this methodology: a) gives the fan energy use before and after airtightness improvements with various inputs depending on the initial state; b) indicates whether or not the required airflow rates are met at the air terminal devices; c) gives a range of energy savings assuming on the one hand perfect fan adjustment, no errors in input data and constant fan efficiency, and on the other hand, safe-side estimates of deviations from these assumptions.

Using experimental data from an earlier study on a scale 1 ductwork built in a laboratory, the tool gives results in good agreement with measured energy savings. The deviation without pressure adjustment between experimental and theoretical savings lies in the region of 5 percentage points. With ideal pressure adjustment and when required airflow rates were met before tightening, the maximum fan energy savings by tightening the ductwork from 1.5 times Class A to Class C reaches 51% according to the tool versus 46% according to measurement data.

## KEYWORDS

Ductwork airtightness, fan energy use impact.

## 1 INTRODUCTION

There are a number of studies that demonstrate significant energy use impacts of ductwork leakage (Soenens & Pattijn, 2011), (Stroo, 2011), (Berthault, Boithias, & Leprince, 2014), (Dyer, 2011) and (Bailly, Duboscq, & Jobert, 2014).

Nevertheless, there remain fundamental issues regarding the methods used to evaluate the energy savings of better ductwork airtightness. Designers and consultants commonly use the cube-law (or slight variants) to obtain estimates of the fan energy savings due to reduced airflow rates resulting from lower leakage rates. This law simply states that the fan power demand scales with the cube of the airflow rate. It is based on similarity principles assuming the fan serves a ductwork system with a constant opening. In this case, the pressure drop through the system scales with the square of the airflow rate. In practice, leakages only have an impact on the ductwork pressure drop and not on air terminal devices pressure drop therefore, in calculation, it is necessary to consider separately pressure drop in ductwork and pressure drop at ATD.

Another common implicit assumption when using the cube-law for duct tightening applications is that the fan is adjusted to deliver the required airflow rate at the air terminal devices. This may not be true with the fan in place if it is not strong enough and/or properly adjusted to compensate for the leaks in the system.

To our knowledge, this can result in very optimistic estimates of energy savings, which can be problematic both for the customer with much longer Return On Investment and for the reputation of the service provider. To avoid these problems, this paper details a methodology to give realistic but conservative energy-savings estimates.

**2 OBJECTIVES**

The main objectives of this study are:

- a) to develop a methodology that gives realistic and conservative estimates of fan energy use impacts of duct airtightness improvements;
- b) to develop a tool implementing the methodology;
- c) to test the tool on real test case.

This methodology is consistent with standard FprEN 16798-5-1:2016.

**3 THEORETICAL APPROACH**

The methodology is structured around 4 methods outlined in Table 1. In short, while method 1 is firmly based on FprEN 16798-5-1:2016, method 2 considers some measured input data, rather than manufacturer data, which can be more accessible in a field study. Method 3 builds on method 2 but adjusts the fan to meet the required airflow rate and pressure needed at fan. Method 4 modifies the input data within confidence bounds defined by the user to give safe-side estimates. Table 5 helps the user choose between the methods depending on the access to input data and the objective of the calculation.

Table 1: Outline of the 4 methods

Method	Short description	Pre-requisites	Limits / issues
Method 1	Based on the new standard FprEN 16798-5-1 methodology. Re-calculates fan and ductwork pressure (not ATD pressure) to calculate leakage airflow rate.	Requires knowledge of the fan properties and pressure at ATD (measurement or design value).	Does not include an adjustment of the fan (either pressure or flowrate): depending on the system, flowrate may exceed required flowrate at ATDs after refurbishment.
Method 2	Builds on method 1 but uses measured instead of manufacturer's data for the fan.	Requires measurements of pressure, flowrate and power at fan (also pressure measurement at ATD).	Likely less accurate than method 1 (measurement uncertainty) but easier to gather information. Does not include adjustment of the fan.
Method 3	Builds on method 2 but includes an adjustment of the fan to adapt flowrate and pressure set-point. Considers separately pressure losses at ATDs and pressure losses in ductwork.	Requires measurements of pressure, flowrate and power at fan (also pressure measurement at ATD).	Calculated set-point may not be consistent with the installed fan.
Method 4	Builds on method 3 but includes uncertainty in input data and conservative estimates of fan efficiency variations between operating points.	Requires measurements of pressure, flowrate and power at fan and estimation of uncertainty (also pressure measurement at ATD).	Method 4 is likely not relevant with large uncertainty estimates.

Table 2: Choice of the method

	Method 1	Method 2	Method 3	Method 4
<b>Access to input data</b>				
You have manufacturers data on installed fan	X			
You can perform measurement on site of flowrate, pressure and power at fan		X	X	X
<b>Objective of the calculation</b>				
You want to perform a calculation that comply with the standard	X	X		
You want to take into account gain due to pressure and flowrate adjustment			X	X
You want to estimate the maximal gain with air tightening (this may include fan change hypothesis)			X	
You want to perform a safe-side calculation	X	X		X

### 3.1 System representation and variables

The approach is based on the system representation proposed in Figure 1

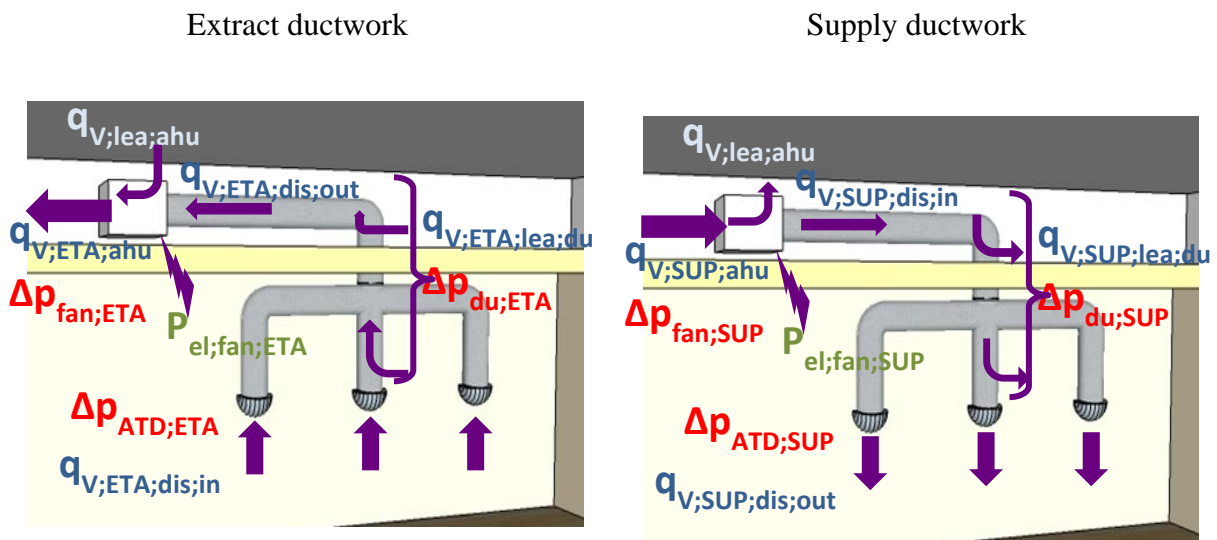


Figure 1: System representation

Table 3: Variables and subscripts used in the paper

Variable		Subscript	
Symbol	Meaning	Symbol	Meaning
A	Area	ATD	Air Terminal Device
c	leakage coefficient	ahu	Air handling unit
$P_{el}$	Electrical power	des	Design
$q_V$	Volume airflow rate	dis	Distribution system
u	uncertainty	du	Duct
$\eta$	fan efficiency	el	Electrical
$\Delta p$	Pressure difference	ETA	Extract air
$\Delta p_{fan;step}$	Pressure step between two fan setting	fan	at fan
		in	entering the system
		lea	leakage
		mes	measured
		new	after tightening
		old	before tightening
		out	leaving the system
		req	required
		SUP	Supply air

Identifiers for the control of the fan are given in Table 3, it shall not be mingled with the control of the volume airflow rate in the ventilation system (Table 4) which is not necessarily made at fan.

Table 4: Identifiers for FAN\_CTRL

SYS_TYPE	Identifier	Meaning
SINGLE_ZONE or MULTI_ZONE	NO_CTRL	No control: the fan reacts on the variable flowrate according to its characteristics
SINGLE_ZONE or MULTI_ZONE	CONST_PRES	The fan is controlled to achieve a constant pressure difference between a specific point in the distribution system and the surrounding
MULTI_ZONE	MIN_PRES	The fan is controlled to the minimum pressure difference necessary in the system
SINGLE_ZONE	DIRECT	The fan is controlled directly according to the variable flowrate

Table 5: Identifiers for AIR\_FLOW\_CTRL

Identifier	Meaning
NO_CTRL	No flow rate control, continuous operation
ON/OFF_CTRL	Time dependent flowrate control, continuous operation during occupancy time
MULTI_STAGE	Multi stage variable flowrate control
VARIABLE	Continuously variable flowrate control

### 3.2 Basic principles for all methods

All methods shown in this paper are firmly based on FprEN 16798-5-1:2016 whose aim is to evaluate the energy performance calculation of mechanical ventilation and air conditioning systems. The methods give estimates, before and after tightening the ductwork, of:

- the fan energy use;
- the overall airflow rates at the ATDs.

#### Yearly calculation

FprEN 16798-5-1 gives basic equations for one ventilation stage of operation. To assess the yearly performance of a system, the calculation has to be iterated for several stages of operation. Each of these stages is characterized by:

- A subset of input values common to all stages
- Another subset of input values specific to that stage (Table 2).

Annual cost estimates assume a fixed cost of electricity and without consideration for peak service subscription.

Table 6: Specific input values for each stage

Function of the dependence of the efficiency of the supply/extract fan on the volume flowrate derived from manufacturer's data, provided according ISO 5801	$f_{\eta}(q_v)$
Function for the dependence of the pressure difference over the supply/extract fan on the volume flowrate, derived from manufacturer's data, provided according ISO 5801	$f_{\Delta p}(q_v)$
Supply fan design pressure difference	$\Delta p_{fan; SUP; des}$
Extract fan design pressure difference	$\Delta p_{fan; ETA; des}$
Total required supply air volume flowrate (at air terminal devices) (sum for each ventilation zone)	$q_{V; sup; dis; req}$

Total flowrate to be extracted (at air terminal devices) (sum for each ventilation zone)	$q_{V;ETA;dis;re}$
Operationrequirement signal	$f_{OP;V}$

### Flowrate at air terminal devices

If there is either no control of the airflow rate or an on/off control (Table 4), the standard method does not adjust the fan according to duct leakages. Therefore, the power of the fan remains the same but the airflow rate at the air terminal devices may change. Note that in this case, the required flowrate may not be met. This requires both to compare energy use and to check actual airflow rate at ATDs before and after air tightening of the ductwork.

### Use of default values

The methods use default values consistently with FprEN 16798-5-1 regarding the airtightness of the heat exchanger and of the air handling unit.

### Pressure in the ductwork to calculate the leakage airflow rate

The leakage airflow rate is calculated with the ductwork airtightness class and pressure according to clause 6.3.2.2.2 of FprEN 16798-5-1. The duct pressure is:

$$\Delta p_{du;SUP/ETA} = \frac{\Delta p_{fan;SUP/ETA} + \Delta p_{ATD;SUP/ETA}}{2} \quad (1)$$

$\Delta p_{fan;SUP/ETA}$  Pa      Supply/Extract fan pressure difference  
 $\Delta p_{ATD;SUP/ETA}$  Pa      Pressure drop at air terminal device at maximum flowrate (the farthest from the fan in terms of resistance to flow passage), on the supply/extract ductwork.

$\Delta p_{fan;SUP/ETA}$  and  $\Delta p_{ATD;SUP/ETA}$  can be either a design value (method 1) or a measured value (methods 2, 3, 4).

### 3.3 Method 1

Apart from minor adjustments mentioned above, method 1 almost fully reproduces calculation performed in FprEN 16798-5-1:2016.

### 3.4 Use of measured values (methods 2, 3, 4)

Method 2, 3, 4 perform the same calculation as method 1 but with the measured input data described in Table 3 for each ventilation stage instead of detailed characteristics of air handling units.

Table 7: Measured values specific for Method 2, 3 and 4

Electrical fan power of the supply fan	$P_{el;fan;SUP;mes}$	Joule/h
Electrical fan power of the extract fan	$P_{el;fan;ETA;mes}$	Joule/h
Volume airflowrate supplied to the ventilation system (at ahu)	$q_{V;SUP;dis;in;mes}$	$m^3/h$
Volume airflow rate extracted from the ventilation system	$q_{V;ETA;dis;out;mes}$	$m^3/h$
Supply fan pressure difference	$\Delta p_{fan;SUP;mes}$	Pa
Extract fan pressure difference	$\Delta p_{fan;ETA;mes}$	Pa

### Calculations before airtightening

The fan airflow rate and fan energy use are directly inferred from the measured values. The difference between the measured fan airflow rate and the calculated leakage airflow rate gives the airflow rate at the ATDs, which is compared to the required airflow rate.

### Calculation of the airflowrate after airtightening

The volume airflow rate supplied/extracted to the distribution system ( $q_{V;SUP/ETA;dis;in}$ ) is calculated as follows:

If AIR\_FLOW\_CTRL = NO\_CTRL (the airflow rate remains set to the measured airflow rate)

$$q_{V;SUP;dis;in} = q_{V;SUP;dis;in;mes} \quad (2)$$

$$q_{V;ETA;dis;out} = q_{V;ETA;dis;out;mes} \quad (3)$$

If AIR\_FLOW\_CTRL = ON/OFF\_CTRL

$$q_{V;SUP;dis;in} = f_{op;V} * q_{V;SUP;dis;in;mes} \quad (4)$$

$$q_{V;ETA;dis;out} = f_{op;V} * q_{V;ETA;dis;out;mes} \quad (5)$$

If AIR\_FLOW\_CTRL = MULTI\_STAGE

The standard's algorithms remain the same

If AIR\_FLOW\_CTRL = VARIABLE (the airflow rate adapts to the required airflow rate within the bounds of the fan curve, measured values are not used)

$$q_{V;SUP;dis;in} = f_{op;V} * \min(\max(q_{V;SUP;ahu;min}; q_{V;SUP;dis;in;req}); q_{V;SUP;ahu;max}) \quad (6)$$

$$q_{V;ETA;dis;out} = f_{op;V} * \min(\max(q_{V;ETA;ahu;min}; q_{V;ETA;dis;out;req}); q_{V;ETA;ahu;max}) \quad (7)$$

where

$q_{V;SUP;ahu;min/max}$ handling unit	$m^3/h$	minimum/maximum flowrate to be supplied by air
$q_{V;ETA;ahu;min/max}$ handling unit	$m^3/h$	minimum/maximum flowrate to be extracted by air
$q_{V;SUP;dis;in;req}$	$m^3/h$	required airflowrate to be supplied at air handling unit
$q_{V;ETA;dis;out;req}$	$m^3/h$	required airflowrate to be extracted at air handling unit

### Efficiency of the supply /extract fan before and after air tightening (methods 2 and 3)

The efficiency of the fan is:

$$\eta_{fan;SUP} = \frac{q_{V;SUP;dis;in;mes}}{P_{el;fan;SUP;mes}} * \Delta p_{fan;SUP;mes} \quad (8)$$

$$\eta_{fan;ETA} = \frac{q_{V;ETA;dis;out;mes}}{P_{el;fan;ETA;mes}} * \Delta p_{fan;ETA;mes} \quad (9)$$

### 3.5 Additional specificities of method 2

#### Supply/extract fan pressure difference after air tightening

This method does not include setting of the fan (see method 3 to include pressure and flowrate setting)

If FAN\_CTRL=NO\_CTRL

$$\Delta p_{fan;SUP/ETA} = \Delta p_{fan;SUP/ETA;0} - \left( \frac{q_{V;SUP/ETA;dis;in/out}}{q_{V;SUP/ETA;dis;in/out;mes}} \right)^2 * (\Delta p_{fan;SUP/ETA;0} - \Delta p_{fan;SUP/ETA;mes}) \quad (10)$$

where:

$\Delta P_{fan;SUP/ETA;0}$  Pa Pressure difference over the supply /extract fan if the air volume flow is 0 (1st key parameter determining the fan characteristic curve). If it is unknown it can be determined with a two-point measurement using equation 10

$\Delta P_{fan;SUP/ETA;mes}$  Pa Measured pressure difference over the supply/extract fan before air tightening

Note that this formula is not in the standard, but is included in FprEN 16798-5-1 excel sheet.

If FAN\_CTRL= DIRECT (only for SINGLE\_ZONE)

$$\Delta p_{fan;SUP/ETA} = \left( \frac{q_{V;SUP/ETA;ahu}}{q_{V;SUP/ETA;dis;in/out;mes}} \right)^2 * \Delta p_{fan;SUP/ETA;mes} \quad (11)$$

If FAN\_CTRL= CONST\_PRES

$$\Delta p_{fan;SUP/ETA} = \left[ \left( 1 - f_{\Delta p;SUP/ETA;ctrl} \right) \left( \frac{q_{V;SUP/ETA;ahu}}{q_{V;SUP/ETA;dis;in/out;mes}} \right)^2 + f_{\Delta p;SUP/ETA;ctrl} \right] * \Delta p_{fan;SUP/ETA;mes} \quad (12)$$

If FAN\_CTRL=MIN\_PRES

$$\Delta p_{fan;SUP/ETA} = \left[ \left( 1 - f_{\Delta p;SUP/ETA;ctrl} \right) \left( \frac{q_{V;SUP/ETA;ahu}}{q_{V;SUP/ETA;dis;in/out;mes}} \right)^2 + f_{V;max;SUP/ETA}^2 * f_{\Delta p;SUP/ETA;ctrl} \right] * \Delta p_{fan;SUP/ETA;mes} \quad (13)$$

Where

$f_{\Delta p;SUP/ETA;ctrl}$  - Controlled portion of the total supply/extract design pressure difference

$f_{V;max;SUP/ETA}$  - Maximum part load factor of the zone air volume airflow rates

### 3.6 Additional specificities of method 3

Method 3 adjusts fan pressure and flowrate set-point after air tightening to provide the required pressure and flowrate at airterminal devices.

#### Air volume flow rate at air handling unit after air tightening

Assuming perfect adjustment of the airflowrate is equivalent to assume that the AIR\_FLOW\_CTRL is VARIABLE with no maximum limit. Therefore, in this method, for all values of AIR\_FLOW\_CTRL:

$$q_{V;SUP;dis;in} = f_{op;V} * \max(q_{V;SUP;ahu;min}; q_{V;SUP;dis;in;req}) \quad (14)$$

$$q_{V;ETA;dis;out} = f_{op;V} * \max(q_{V;ETA;ahu;min}; q_{V;ETA;dis;out;req}) \quad (15)$$

#### Supply/extract fan pressure difference

Air leakages increase the ductwork pressure drop. Therefore, after air tightening, the fan pressure can be reduced. The new setting for fan pressure is calculated for the maximum required flowrate at the ATDs for all stages of operation.

$$\Delta p_{fan;SUP/ETA;set} = \Delta p_{ATD;SUP/ETA;req} + \left( \frac{q_{V;SUP/ETA;dis;in/out;max}}{q_{V;SUP/ETA;dis;in/out;mes;max}} \right)^2 * (\Delta p_{fan;SUP/ETA;mes;max} - \Delta p_{ATD;SUP/ETA}) \quad (16)$$

Where:

$q_{V;SUP/ETA;dis;in/out;mes;max}$	$m^3/h$	maximum measured flowrate maximum in the variable inputs) for supply/extract
$\Delta p_{fan;SUP/ETA;mes;max}$	Pa	Corresponding measured pressure at fan
$q_{V;SUP/ETA;dis;in/out;max}$	$m^3/h$	Corresponding maximum flowrate at air handling unit after refurbishment
$\Delta p_{fan;SUP/ETA;req}$	Pa	Required pressure drop at ATD
$\Delta p_{fan;SUP/ETA}$	Pa	Measured pressure drop at ATD

Therefore,

If FAN\_CTRL=NO\_CTRL

$$\Delta p_{fan;SUP/ETA} = \Delta p_{fan;SUP/ETA;0} - \left( \frac{q_{V;SUP/ETA;dis;in/out}}{q_{V;SUP/ETA;dis;in/out;max}} \right)^2 * (\Delta p_{fan;SUP/ETA;0} - \Delta p_{fan;SUP/ETA;set}) \quad (17)$$

If FAN\_CTRL= DIRECT (only for SINGLE\_ZONE)

$$\Delta p_{fan;SUP/ETA} = \left( \frac{q_{V;SUP/ETA;dis;in/out}}{q_{V;SUP/ETA;dis;in/out;max}} \right)^2 * \Delta p_{fan;SUP/ETA;set} \quad (18)$$

If FAN\_CTRL= CONST\_PRES

$$\Delta p_{fan;SUP/ETA} = \left[ (1 - f_{\Delta p;SUP/ETA;ctrl}) \left( \frac{q_{V;SUP/ETA;dis;in/out}}{q_{V;SUP/ETA;dis;in/out;max}} \right)^2 + f_{\Delta p;SUP/ETA;ctrl} \right] * \Delta p_{fan;SUP/ETA;set} \quad (19)$$

If FAN\_CTRL=MIN\_PRES

$$\Delta p_{fan;SUP/ETA} = \left[ (1 - f_{\Delta p;SUP/ETA;ctrl}) \left( \frac{q_{V;SUP/ETA;dis;in/out}}{q_{V;SUP/ETA;dis;in/out;max}} \right)^2 + f_{V;max;SUP/ETA}^2 * f_{\Delta p;SUP/ETA;ctrl} \right] * \Delta p_{fan;SUP/ETA;set} \quad (20)$$

### 3.7 Additional specificities of method 4

Method 4 performs the same calculation of method 3 but modifies the following input parameters to obtain a conservative estimate of energy savings:

- Measured inputs
- Fan efficiency
- Fan pressure setting

The user give a range of uncertainty for these input values, which are re-calculated as follows:

$$A_{du;SUP;met 4} = A_{du;SUP} * (1 - u_{Adu}) \quad (21)$$

$$A_{du;ETA;met 4} = A_{du;ETA} * (1 - u_{Adu}) \quad (22)$$

$$c_{lea;du;SUP;old;met 4} = c_{lea;du;SUP;old} * (1 - u_{Cleaold}) \quad (23)$$

$$c_{lea;du;ETA;old;met 4} = c_{lea;du;ETA;old} * (1 - u_{Cleaold}) \quad (24)$$

$$c_{lea;du;SUP;new;met 4} = c_{lea;du;SUP;new} * (1 + u_{Cleaew}) \quad (25)$$

$$c_{lea;du;ETA;new;met 4} = c_{lea;du;ETA;new} * (1 + u_{Cleaew}) \quad (26)$$

$$\Delta p_{ATD;SUP;met 4} = \Delta p_{ATD;SUP} * (1 + u_{pATD}) \quad (27)$$

$$\Delta p_{ATD;ETA;met 4} = \Delta p_{ATD;ETA} * (1 + u_{pATD}) \quad (28)$$

$$q_{V;SUP;dis;req;met 4} = q_{V;SUP;dis;req} * (1 + u_{qV;dis;req}) \quad (29)$$

$$q_{V;ETA;dis;req;met 4} = q_{V;ETA;dis;req} * (1 + u_{qV;dis;req}) \quad (30)$$

$$P_{el;fan;SUP;mes;met 4} = P_{el;fan;SUP;mes} * (1 - u_{pelfan}) \quad (31)$$

$$P_{el;fan;ETA;mes;met 4} = P_{el;fan;ETA;mes} * (1 - u_{pelfan}) \quad (32)$$

$$q_{V;SUP;dis;in;mes;met 4} = q_{V;SUP;dis;in;mes} * (1 - u_{qV;mes}) \quad (33)$$

$$q_{V;ETA;dis;out;mes;met 4} = q_{V;ETA;dis;out;mes} * (1 - u_{qV;mes}) \quad (34)$$

$$\Delta p_{fan;SUP;mes;met 4} = \Delta p_{fan;SUP;mes} * (1 - u_{pfan;mes}) \quad (35)$$

$$\Delta p_{fan;ETA;mes;met 4} = \Delta p_{fan;ETA;mes} * (1 - u_{pfan;mes}) \quad (36)$$

$$37)$$

### Efficiency of the supply/extract fan

$$\eta_{fan;SUP} = \left( \frac{q_{V;SUP;dis;in;mes;met 4}}{P_{el;fan;SUP;mes;met 4}} * \Delta p_{fan;SUP;mes;met 4} \right) * (1 - u_{fan;eff}) \quad (38)$$

$$\eta_{fan;ETA} = \left( \frac{q_{V;ETA;dis;out;mes;met 4}}{P_{el;fan;ETA;mes;met 4}} * \Delta p_{fan;ETA;mes;met 4} \right) * (1 - u_{fan;eff}) \quad (39)$$

### Supply and extract fan pressure difference

$$\Delta p_{fan;SUP/ETA;set} = \Delta p_{ATD;SUP/ETA;req} + \left( \frac{q_{V;SUP/ETA;dis;in/out;max}}{q_{V;SUP/ETA;dis;in/out;mes;max} * (1 - u_{qV;mes})} \right)^2 * (\Delta p_{fan;SUP/ETA;mes;max} * (1 - u_{pfan;mes}) - \Delta p_{ATD;SUP/ETA;met 4}) + \Delta p_{fan;step} \quad (40)$$

## 4 LABORATORY EXPERIMENTS



Figure 2: Laboratory replication of real ductwork system in Autun (France). Source : (Berthault, Boithias, & Leprince, 2014)

Berthault et al. (Berthault, Boithias, & Leprince, 2014) built an extract air duct system similar in size and ventilation characteristics to ductwork systems commonly found in France in multi-family buildings to study, among other things, the impact of ductwork airtightness on fan energy use. The facility consists in an 18.7 m<sup>2</sup> ductwork connected to a constant pressure extract fan, eight self-adjusting Air Terminal Devices. Four of them can be manually set to a minimum and maximum airflow rate. The minimum and maximum airflow rates are 260 m<sup>3</sup>/h and 425 m<sup>3</sup>/h, respectively. The ductwork was initially class C but holes were intentionally drilled to reach 1.5 class A. Power, flowrate, and pressure measurement at fan were performed before and after drilling.

The fan is naEC motor, with an impeller with forward blades and direct drive. Fan power for pressure and airflow rates used in the study are given in Table 5

Table 8: Fan properties

Airflowrate	Pressure	Power
425 m <sup>3</sup> /h	120 Pa	63 W
260 m <sup>3</sup> /h	120 Pa	40 W

We have compared the results obtained by measurements with those obtained with our methodology. Note that in our calculation, consistently with the fan characteristics, the fan control is set to "constant pressure"; the airflow control is set to "variable" because the self-adjusting ATDs are maintaining the flowrate on a large scale of pressure.

## 5 RESULTS

Table 4 shows the annual operating energy cost savings. Absolute cost savings are low as it is a small ductwork, but method 3 shows that tightening the ductwork from 1.5· Class A to class C can reduce energy use up to 53% (with a suitable fan adjustment).

Table 9: Theoretical and experimental cost savings on test case, improving the airtightness from 1.5· Class A to Class C. Maximum and minimum airflow rates are used 2 and 22 hours per day, respectively

Results based on	Cost before retrofitting	Required airflow rate met before retrofitting	Cost after retrofitting	Required airflow rate met after retrofitting	Cost savings in €	Cost savings in %
Fan power measurements (no fan adjustment)	68€	Yes	61€	Yes	- 7€	-11%
Method 1	71 €	Yes	60 €	Yes	- 11 €	-15%
Method 2	68 €	Yes	57 €	Yes	- 11 €	-16%
Method 3	68 €	Yes	32 €	Yes	- 36 €	-53%
Method 4	61 €	Yes	47 €	Yes	- 14 €	-23%
Fan power measurements (with fan adjustment)	68€	Yes	47€	Yes	- 21€	- 31%
Cube-law	68€	Yes	40€	Yes	-28€	-59%

Figure 3 and Figure 4 compare the economy planned by the tool for minimum and maximum flow rate with measurement results with and without pressure adjustment. The darkest part of each bar represents the power difference between 1.5· Class A and Class C. The left bar represents measurement data with no pressure adjustment (pressure is maintained at 120 Pa, to be compared with methods 1 and 2), whereas the right bar gives measurement data with pressure adjustment: the pressure is at 120 Pa for 1,5· Class A and 90 Pa for Class C (to be compared with methods 3 and 4).

At the maximum airflow rate (Figure 3), the results of Method 1 and 2 are in good agreement with measurement data with no fan pressure adjustment (120 Pa). The measurement data with fan pressure adjustment (90 Pa) for the tightest system shows that the measured energy savings are very close to the energy savings estimated with method 3, which is likely close to the maximum savings achievable given its assumptions. Conversely, method 4 deviates more from the experimental results with a conservative estimate of 15%.

At the minimum airflow rate (Figure 4), the deviations are larger due to the very low differences in fan power demand induced by air tightening: an absolute difference of 1 W corresponds to a relative difference of 2 percentage points. Note also that the fan pressure could not be adjusted below 90 Pa although less pressure was needed. Therefore, method 3 overestimates the savings, but the measured data remains within the range given by method 4 and 3.

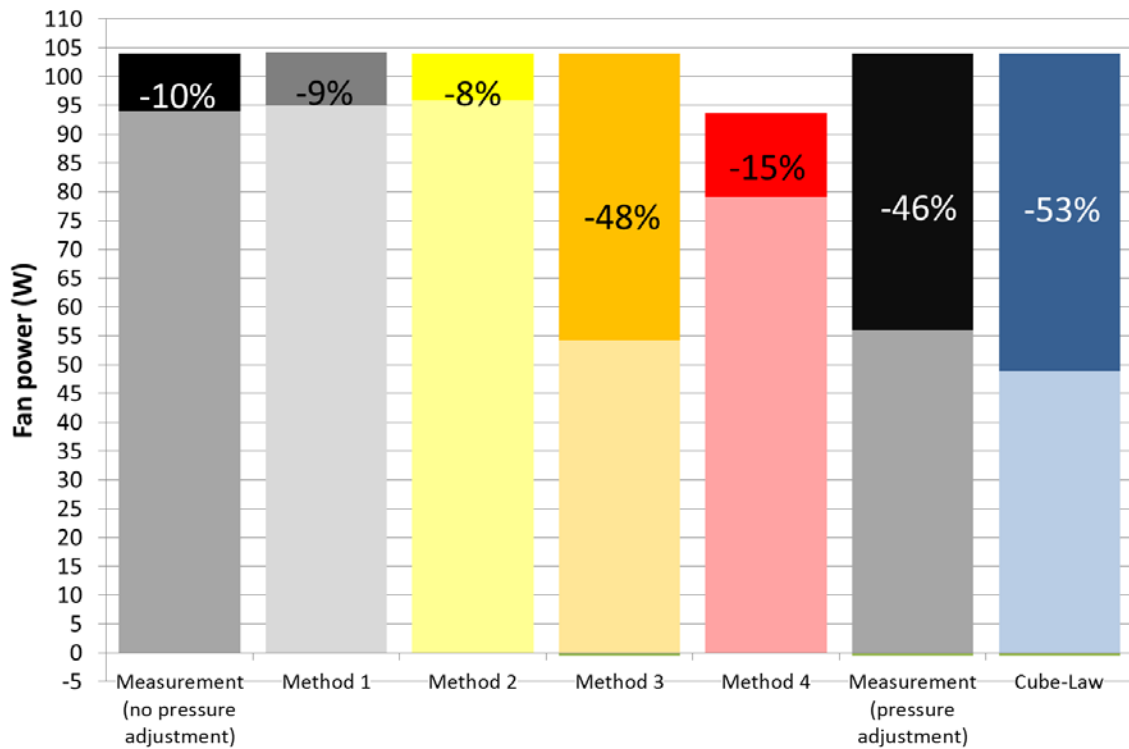


Figure 3: Theoretical and experimental cost savings on test case, improving the airtightness from 1.5 · Class A to Class C. Results for maximum airflow rate.

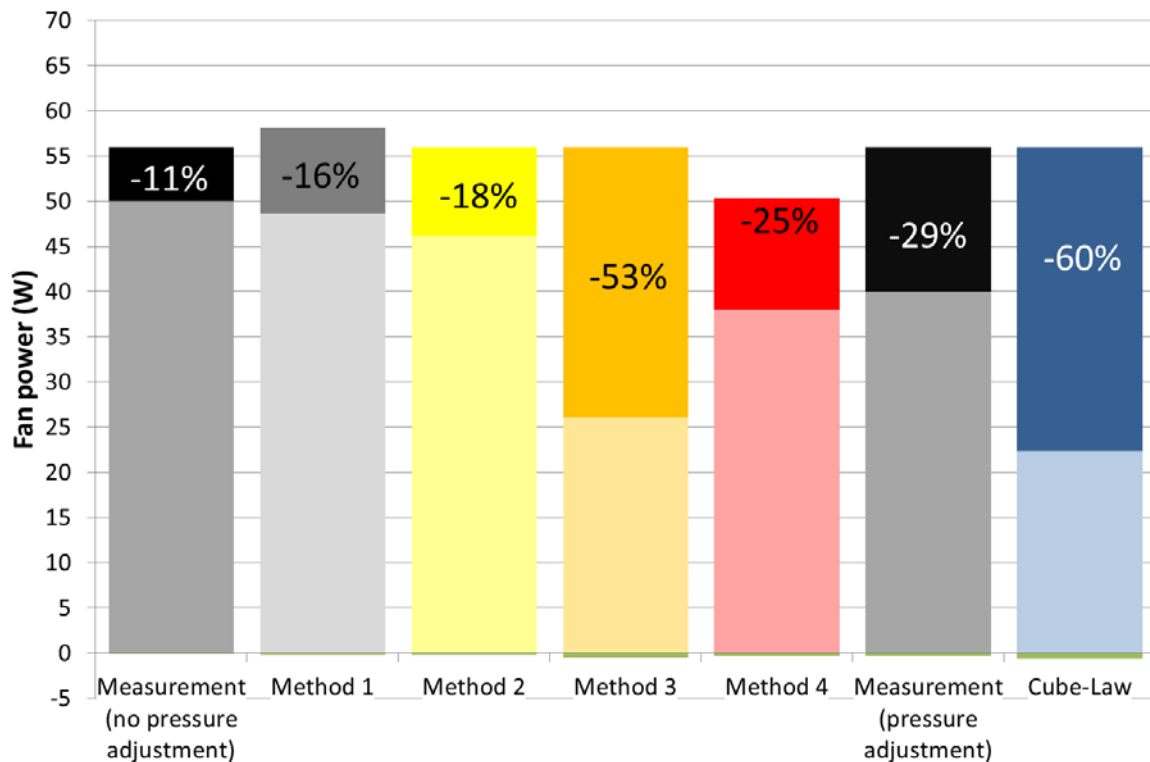


Figure 4: Theoretical and experimental cost savings on test case, improving the airtightness from 1.5 · Class A to Class C. Results for minimum airflow rate.

## 6 DISCUSSION

The methodology includes 4 methods that can be used depending in particular on the accessibility to the fan characteristics input data and the objective of the calculation.

Method 1 uses theoretical input data, however, when dealing with existing installations, it may be difficult to obtain accurate information on the air handling unit (nominal efficiency of the fan, function of the dependence of the pressure difference over the supply extract fan, etc.). Method 1 assumes that the fan has been tested according to ISO 5801, and that characteristics obtained with this standard are available. If not, the user could guess this input data to use method 1, but experience shows that this can be very challenging and inappropriate for the desired level of accuracy of the fan energy savings, in particular with old installations. In our experience, method 2 is more appropriate in such cases.

Method 1 includes airflow rate adjustment only with a variable or multistage airflow control. Therefore, when there is either no control or an on/off control of the airflow rate in the ductwork system, leakages reduce the airflow rate at the ATDs but have no impact on the fan energy use. This is not strictly true because the fan sees a slightly different pressure drop before and after sealing if the leaks are close to the fan; however, we expect this has a minor impact and only fan adjustment can give significant energy savings.

To overcome these limitations, methods 2-3-4 introduce a subset of measured input data substituting the theoretical input data. Method 2 has the same limitations as method 1 regarding the adjustment of the fan. Because fan adjustment after air tightening (new speed, new pressure set point, etc.) is desirable and may be suggested by a consultant to his client, method 3 assumes a "perfect" fan adjustment to meet the required airflow rates at the ATDs. To avoid unpleasant surprises in terms of actual energy savings, method 4 introduces factors on some of the input data to perform a "safe-side" calculation. For instance, it assumes that the fan efficiency decreases with decreasing airflow rates (unlike method 1, 2, 3 that assumes constant fan efficiency).

Note that, similarly to the cube-law, methods 3 and 4 adjust the fan set-point considering the impact of leakages both on airflow rate and pressure drop; however, the fundamental difference are that methods 3 and 4:

- take into account separately the pressure drop in the ductwork and the pressure drop at air-terminal devices. Only the post-tightening pressure drop in the ductwork is assumed to be proportional to square of the airflow rate (whereas the cube law assumes the pressure at the fan is proportional to the square of the airflow rate). The pressure at the ATD is set after tightening independently of the leakages;
- the energy use is calculated to ensure required airflow rates and pressures are met after refurbishment. If the measured initial airflow rates are insufficient, the tool adjusts these boundary conditions. In such cases, air tightening and fan adjustment may result in no or even increased energy use to obtain the required airflow rates at the air terminal devices.

Because method 3 calculates energy use assuming the fan is set at the optimum calculated set-point, it gives the maximum savings achievable with ductwork airtightening with the fan in place. Note, however, that the optimum set-point is calculated based on the equations provided in EN 16798-5-1. As a result, this set-point may not be reachable with the existing fan, for instance, because it is outside its range of operation or because of the fan behaviour deviates from the assumed behaviour in the standard.

Method 4 calculates the minimum economy assuming that "everything that can go wrong will go wrong", i.e., using the worst possible value of each input within a range defined by the user. Therefore, it is overly pessimistic in terms of achievable energy savings, in particular, if

the user cannot define reasonable deviation ranges for the input values. It would be interesting to refine this analysis with error propagation or a stochastic approach to give more realistic results, although the selection of proper ranges of deviations would remain an issue.

Nevertheless, on the test case, theoretical and field results are in good agreement both with and without fan adjustment. Also, method 1 (based on manufacturer's data) and method 2 (based on measurement) give consistent results. The energy savings in our test case reach 53%. These significant energy savings are possible because the required flowrate were met before retrofitting.

As expected, the cube-law overestimates the energy savings with 53% at maximum flowrate (versus 46% measured) and 60% at minimum flowrate (versus 29% measured). In this specific experiment, because we had the required airflow rates at the ATDs, the deviations between the cube law and method 3 are rather small. Otherwise, they would be much larger because the airflow rate would be first transferred from the leakages to the ATDs before any reduction of the fan airflow rate can occur.

One limitation of this study is that the methodology does not account for the impact of ductwork leakages on heating, cooling and humidity losses. Energy losses due to over-ventilation can be estimated based on:

- The leakages located in the conditioned zone;
- The increased ventilation airflow rates due to leakages, using equations in FprEN 16798-5-1. If the required airflow rates at ATD are not met pre-tightening, the leakage airflow rate needs to be first transferred from the leakages to the ATDs before any reduction of the ventilation airflow rate can occur in the conditioned zone;
- The indoor temperature during the heating period.

Nevertheless, when air is preconditioned, the impact of leakage is difficult to calculate as it depends in particular on:

- whether the heat losses through the leaks are completely, partly or not recoverable;
- the part of the energy demand for space conditioning the building that has to be provided by the ventilation system.

## 7 CONCLUSIONS

The methodology developed in this paper allows one to assess fan energy savings resulting from ductwork airtightness improvement scenarios, because of the decrease of the airflow rate and pressure drops as the ductwork system gets tighter. The methodology does not require inputs related to the building energy performance, except for those characterizing the ventilation system energy use. Although consistent with FprEN 16798-5-1:2016, the methodology includes a number of new equations to substitute fan manufacturer's input data with field data and to take into account pressure drops at air terminal devices separately from the pressure drops in the rest of the system. The methods developed assess energy savings with various sub-sets of input data depending on the initial state, including whether or not the required airflow rates were met. The methodology provides a range of energy savings resulting from different scenarios (e.g., no or perfect fan adjustment) including the accessibility and reliability of the input data (e.g., uncertainties in measured pressures, airflow rates, and fan power demand) to have safe-side estimates.

Measurement data on an experimental ductwork with an airtightness class of 1.5 · Class A and Class C is in the range of values given by our methodology. The deviation without pressure adjustment between experimental and theoretical savings lies in the region of 5 percentage points. With ideal pressure adjustment and when required airflow rates were met before

tightening, the maximum fan energy savings by tightening the ductwork from 1.5 · Class A to Class C reaches 53% according to the tool versus 46% according to measurement data.

The results obtained are promising and thereby support using this methodology for assessing fan energy use impacts of ductwork leakage. This could be useful either to designers or consultants willing to explore different ductwork airtightness scenarios in new systems or the relevance of duct-sealing measures in existing systems. Ductwork leakages have also a significant impact on heating, cooling and humidity losses; however, a more global approach to the building-system interaction seems necessary to address this issue. It would be worth investigating how this could be done without a complex energy performance of building simulation.

## **8 ACKNOWLEDGEMENTS**

This work was supported by Mez-Technik. The views and opinions of the authors do not necessarily reflect those of MezTechnik. The published material is being distributed without warranty of any kind, either expressed or implied. The responsibility for the interpretation and use of the material lies with the reader. In no event shall ICEE, PLEIAQ or Mez-Technik be liable for damages arising from its use. Any responsibility arising from the use of this report lies with the user.

## **9 REFERENCES**

- Bailly, A., Duboscq, F., & Jobert, R. (2014). Impact of a poor quality of ventilation systems on the energy efficiency for energy-efficient houses. *35th AIVC Conference " Ventilation and airtightness in transforming the building stock to high performance"*. Poznań, Poland.
- Berthault, S., Boithias, F., & Leprince, V. (2014). DUCTWORK AIRTIGHTNESS: RELIABILITY OF MEASUREMENTS AND IMPACT ON VENTILATION FLOWRATE AND FAN ENERGY CONSUMPTION. *35 TH AIVC-4 TH TIGHTVENT & 2 ND VENTICOOL conference*. Poznan.
- Dyer, D. F. (2011). Case study: Effect of excessive duct leakage in a large pharmaceutical plant. *32nd AIVC Conference " Towards Optimal Airtightness Performance"*. Brussels, Belgium.
- Soenens, J., & Pattijn, P. (2011). Feasibility study of ventilation system air-tightness. *32nd AIVC Conference " Towards Optimal Airtightness Performance"*. Brussels, Belgium.
- Stroo, P. (2011). Class C air-tightness: Proven roi in black and white. *32nd AIVC Conference " Towards Optimal Airtightness Performance"*. Brussels, Belgium.

# Utilization of heat recovery ventilation: problem statement based on steady-state two-zone energy use analysis and field studies

Arnold Janssens

*Research group Building Physics, Construction and Services  
Faculty of Engineering and Architecture - Ghent University  
SintPietersnieuwstraat 41 B4  
9000 Gent, Belgium*

*\*Corresponding author: [arnold.janssens@ugent.be](mailto:arnold.janssens@ugent.be)*

## EXTENDED SUMMARY

This presentation gives an introduction to the topical session on the utilization of heat recovery in residential ventilation systems.

The European market for residential ventilation is highly driven by energy performance regulations. In new buildings the share of balanced ventilation with heat recovery is increasing as a result of more severe energy performance requirements (NZEB). The energy labeling for residential ventilation units and the ecodesign requirements for ventilation units may be drivers for a more wide-spread application of heat recovery ventilation in new buildings.

The methods used to assess the influence of heat recovery ventilation on the energy use of buildings in energy labelling and certification are typically based on single zone energy balance equations. Multi-zoning is often not considered although heating behaviour and set-points differ in different rooms of a dwelling. As a result of this the energy savings of heat recovery ventilation as assessed with single zone methods may be larger than when the spatial variations in dwellings are taken into account. This is related to the fact that the recovered heat supplied to the dwelling through the ventilation system is not ‘useful’ to reduce space heating and cooling demand at all time and in every room (eg in unheated rooms like bedrooms).

This presentation shows the results of a field study where the metered energy use for heating in 114 low-energy houses was compared to the design targets extracted from EPC-declaration files for the individual houses. Half of the houses had individual balanced mechanical ventilation systems with rotary heat recovery, while the other half had individual demand-controlled ventilation system with natural supply and mechanical exhaust. Apart from the differences in ventilation systems, the houses were largely identical. The field study was part of the European demonstration Project ECO-Life (2010-2016), <http://www.ecolife-project.eu/TheConcertoInitiative.html>. The monitoring results indicated that although the designed heating energy use in the houses with heat recovery was lower than in the houses without, there were no significant differences between the heating energy use in both types of dwellings.

To explore the reasons for this result, a two-zone steady-state energy use analysis was conducted to investigate the relation between spatial variations in the dwellings and the utilization of heat recovery. One zone represents the rooms in a house which are regularly

heated and are typically equipped with heat emitters and local controls, such as living room and kitchen. The other zone represents the rooms which are rarely heated or have no individual heat emitters or controls, eg bed rooms, bath rooms and hallway.

The results show the differences between a single zone and two-zone approach in terms of the effects of heat recovery ventilation on heating energy use, and define the main influencing parameters for the utilization of heat recovery in residential ventilation systems.

## **ACKNOWLEDGEMENTS**

This work was supported by the EU Concerto initiative, ‘Sustainable Zero Carbon ECO-Town Developments Improving Quality of Life across EU’ (ECO-Life) (TREN/FP7EN/239497/"ECO-Life"), <http://www.ecolife-project.eu/index.html>, project leader COWI. The support is gratefully acknowledged, as is the input received from the ECO-Life partners.

# **Influence of the zoning, the climate, and the airtightness on the energy needs of a building with mechanical ventilation system with heat recovery.**

José Manuel SalmerónLissén

*GrupoTermotecnia - AICIA -Universidad de Sevilla  
EscuelaTécnica Superior de Ingenieros  
Camino de los Descubrimientos s/n, 41092 SEVILLA - España  
\*Corresponding author: jms@us.es*

## **EXTENDED SUMMARY**

In new buildings, the number of balanced ventilation systems with heat recovery is increasing as a result of more severe energy performance requirements. This is a common frame in the whole Europe, for example in Spain the global primary energy needs for single family dwellings built after 2014 varies from 10 to 68.5 kWh/m<sup>2</sup>, and for multi-family dwellings between 10 and 36.3 kWh/m<sup>2</sup>, in France the equivalent figure goes from 40 to 65 kWh/m<sup>2</sup>, while in Portugal the figure is around 32.5 kWh/m<sup>2</sup> independently of the climate.

The methods used to assess the influence of heat recovery ventilation on the energy use of buildings are typically based on single zone energy balance equations to obtain the building energy needs. Even when the energy balance is carried out using a multi-zone approach, ventilation and infiltration flow and their temperatures are commonly evaluated using single zone calculation methods, which definitively affects the calculation of the energy needs. This is due to the fact that single zone methods for ventilation and infiltrations are easier to use, faster to obtain the results and additionally enough accurate to evaluate parameters regarding the indoor air quality. Thus, many single-zone software tools have been used widely, although some papers (Salmerón et al. 2015) put the emphasis on high errors in the estimation of airflows under these assumptions.

On the other hand, the energy balance software resolves a multizonal equation, the problem here is related to the reduction in the energy consumption obtained with the heat recovery in the ventilation system, because frequently this is assessed in steady-state, with single-zone assumptions, constant infiltrations independently of wind velocity and other parameters. And finally the energy consumption of additional devices that are required are not considered in the calculations, for example this is the case when the energy consumption of the supply fan is neglected or when the increase in the energy consumption of the exhaust fan due to the increased pressure drop in the heat exchanger is not considered.

In order to compare the situations, this paper quantifies:

1. The variation on the energy consumption of a building according to the unizone or multizonal approach used for the assessment of the ventilation plus infiltration airflows.
2. The variation on the energy consumption when the heat recovery is assessed in steady-state, with single-zone assumptions, and constant infiltrations or in the actual situation (transient, multi-zone, variable infiltrations).
3. The variation on the energy consumption when the consumption of additional fans or the increase in the consumption of the existing exhaust fan is considered.

These variations will be shown depending on the airtightness of the building envelope using computer simulations. This is particularly interesting because in the Mediterranean region of Europe heat recovery is beginning to be implemented without taking into account properly the airtightness, for example taking default values that are not realistic for this region but for northern regions where the level of awareness regarding the relative weight of airtightness of builders and householders in general is higher. In Spain for example, the mean level of airtightness of the building envelope for new buildings is around the higher level of the standard EN ISO 15242 (CEN 2007), while in northern countries this value is nearer the lowest value.

Finally, the results will be graphically shown as a function of the climate using the global climate severity index that has been proposed by the authors (Salmerón et al. 2014) , and that has been proved to be useful for showing in the same scale the energy consumption of different locations.

In the conclusions, we found significant differences in some cases that reveal:

- The specifications that software tools for assessing airflows must have for the correct evaluation of the ventilation systems with heat recovery.
- The specifications for the software tools used for the assessment of the global energy consumption when a heat recovery system is implemented.

In addition, we anticipate that our simulation analysis will be the starting point for more sophisticated in situ experimental case studies. For example, we can envisage that the effect of user behaviour is crucial for the final energy consumption. This means that the consumption based on simulation can be very different for the actual consumption even when this has been carried out with the correct assumptions and level of modelization. Thus, a solution for the ventilation system that theoretically will lead to an interesting energy saving together with an adequate level of indoor air quality, can be a bad solution in practice in the case that the system is not operated as it is prescribed. This use or operation includes, not only the airflow rates in each moment, but also the conditioning profile –understood as the period when the air conditioning system is on or off- of the different rooms of the dwelling.

## REFERENCES

- Salmerón J.M., J.G. Ramos, S.Á. Domínguez, J. L. Molina Félix, F.J. Sánchez de la Flor. (2015) Influence of air quality performance requirements on the demand of energy, 36th AIVC conference 2015.
- CEN. (2007) EN ISO 15242 Ventilation for buildings. Calculation methods for determination of air flow rates including infiltration, CEN, Bruxelles.
- Salmerón, J.M., Álvarez, S., Molina, J.L., Ruiz, A., Sánchez, F.J. (2014) Tightening the energy consumptions of buildings depending on their typology and on Climate Severity Indexes, Energy and buildings 2014. DOI: 10.1016/j.enbuild.2012.09.039.

# A ‘use factor’ for HRV in intermittently heated dwellings

Willem Faes<sup>1</sup>, Hugo Monteyne<sup>1</sup>, Michel Depaepe<sup>1</sup>, and Jelle Laverge<sup>2,\*</sup>

*1 ATHT research group  
Ghent University  
SintPietersnieuwstraat 41 B4  
Ghent, Belgium*

*2 Building Physics, Construction and Services  
research group  
Ghent University  
SintPietersnieuwstraat 41 B4  
Ghent, Belgium*

*\*Corresponding author: [jelle.laverge@ugent.be](mailto:jelle.laverge@ugent.be)*

## ABSTRACT

When considering the performance of HRV systems, the discussion is generally focusing on the reported effectiveness of the air-to-air heat exchanger. Although some excellent presentations at the AIVC conference in the past have dealt with uncertainties related to the test of that effectiveness, the fact that the heat recovered by the HRV unit might not be useful in an intermittently heated dwelling without room-by-room based demand control is usually not considered. Therefore, the ‘use-factor’ for the recovered heat is quantified in this paper.

The goal of this project was to investigate the performance of heat recovery units in low energy buildings by simulating different buildings under varying conditions. The influence of several parameters on this performance is studied: the type of building, the insulation and airtightness, the ventilation flow rates, the ventilation strategy, the heat exchanger effectiveness, the occupancy pattern and the demanded comfort level.

The results suggest that, although a heat exchanger can have an effectiveness of e.g. 75%, only approximately 40% of the heat in the extracted air is recovered and supplied usefully to the rooms.

## KEYWORDS

MHRV, air-to-air heat exchanger, use factor, effectiveness

## 1 INTRODUCTION

A balanced ventilation system is usually equipped with two duct systems and two electrical fans, displacing the same amount of air. Polluted indoor air is extracted from the wet rooms (i.e. kitchen, bathroom and hall) and fresh outdoor air is supplied to the dry rooms (i.e. bedrooms, living room and study). When an air-to-air heat exchanger (AAHX) is installed between the two air streams, the cold supply air is preheated by the warm extracted air. The use of a mechanical heat recovery ventilation (MHRV) system thereby reduces the heat demand of the building.

MHRV systems can be compared on several levels. Producers of heat exchangers provide an effectiveness of the device, depending on the flow rates. These values can be high, more than 90% (EUROVENT, 2017). This is however a value representing the effectiveness on component level. There can be leakages in the duct system or short circuits between the supplied and extracted air. These unintentional air flows will reduce the efficiency on unit level (Manz, 2001). Also the airtightness of the building will have an influence on the efficiency of the system. It was found in the studies by Binamu and Lindberg (2001), Roulet

(2001) and Dodo (2011) that the efficiency of the heat recovery drops when the building has a bad airtightness, because no energy can be recovered from air leakages. This observation lead to the inclusion of minimum airtightness recommendations for dwellings equipped with MHRV, e.g. a maximum leakage of 1 ACH50 is recommended in the Belgian residential ventilation standard NBN D 50-001.

Different results were obtained by Juodis(2006), who studied the influence of the building's thermal properties on the effectiveness of the heat recovery. The author defined a balance temperature of a building at which the heat gains compensate the losses. The closer the external temperature is to this balance temperature, the smaller the effectiveness of the heat recovery, because the losses are already compensated by the gains. According to the author, the average annual effectiveness of the heat recovery decreases when a building has more insulation and better airtightness since this reduces the balance temperature of the building.

However, there is more. The approach proposed by Juodis is inherently steady state, while (especially) residential buildings are usually heated according to a dynamic heating pattern and only partially heated. In a building where all rooms have a heat demand, the percentage of the heat in the extracted air that is usefully recovered is equal to the effectiveness of the AAHX. The occupants of a house do not always heat the entire building, but e.g. heat only the occupied rooms. The non-occupied dry rooms will in this case still receive preheated supply air. The heat in this air is recovered by the AAHX, but will not completely contribute to the reduction of the heat demand of the building. It will instead unnecessarily elevate the temperature in the empty rooms and increase the transmission and exfiltration losses to the exterior.

In this paper, we propose the adoption of a 'use factor' that accounts for this effect when the implementation of MHRV is considered. We first propose a definition of this use factor and then show it's effect through the dynamic heat load simulation of an archetypical Belgian detached dwelling.

## **2 USE FACTOR DEFINITION**

For a given case, the total amount of heat that is extracted by the ventilation system,  $Q_e$ , and the amount of heat recovered from the extracted air by the heat exchanger,  $Q_r$  can be determined as well as the total yearly heat demand,  $Q$ . Additionally, the heat demand of the building can also be calculated/measured/simulated when no heat exchanger is installed between the two air streams (or a heat exchanger with an effectiveness of 0%). This heat demand is called  $Q_0$ . Likewise, the heat demand  $Q_1$ , with a perfect heat exchanger (100% efficiency) between the two airstreams can be defined. Finally, a situation where all ventilation flow rates are reduced to  $0\text{m}^3/\text{h}$  can be considered, resulting in the heat demand  $Q_{nv}$ .

With these concepts, assuming flow rate and effectiveness are constants, the ratio of  $Q_r$  and  $Q_e$  are equal to the test effectiveness  $\eta_1$ .

$$\eta_1 = \frac{Q_r}{Q_e} \quad (1)$$

A second effectiveness,  $\eta_2$ , is defined as the ratio of the useful recovered heat ( $Q_0 - Q$ ) to the heat recovered by the heat exchanger ( $Q_r$ ) or the fraction of the recovered heat that has been usefully supplied to the rooms. This is nothing other than the use factor described above. The heat that was not usefully supplied (e.g. supplied to a non-heated room), is then represented by  $1 - \eta_2$ .

$$\eta_2 = \frac{Q_0 - Q}{Q_r} \quad (2)$$

Alternatively, a third effectiveness,  $\eta_3$ , is defined as the ratio of the useful recovered heat ( $Q_0 - Q$ ) to the extra heat loss incurred by adding ventilation without heat recovery ( $Q_0 - Q_{nv}$ ).

$$\eta_3 = \frac{Q_0 - Q}{Q_0 - Q_{nv}} \quad (3)$$

The use factor for the MHRV is then defined as the ratio of  $\eta_3$  en  $\eta_1$ .

### 3 USE FACTOR VALUES FOR AN ARCHETYPICAL DWELLING

The effect of the use factor defined above is illustrated on an archetypical Belgian detached dwelling, of which the floor plan is shown in figure 1. The total volume of the dwelling is 379 m<sup>3</sup> and the gross floor area is 137 m<sup>2</sup>. TRNSYS was used to simulate the building and calculate all room temperatures and heat demands. The study was limited to the Belgian climate, and only the heating period was taken into account.

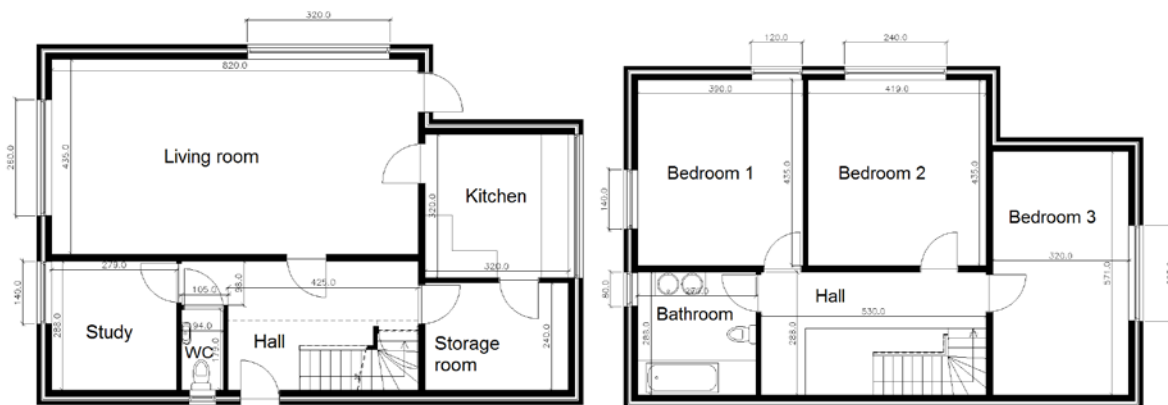


Figure 1:Figure caption

Table one lists the results for  $\eta_1$ ,  $\eta_2$ ,  $\eta_3$  and the alternative use factor based on  $\eta_3$  for this case study dwelling under different general energy performance levels of the building envelope (including insulation and airtightness), expressed as the total annual heat load per square meter of floor area.

Table 1: Table Caption

EP level	$\eta_1$	$\eta_2$	$\eta_3$	UF ( $\eta_3$ )
60 kWh/m <sup>2</sup> a	0,75	0,50	0,56	0,75
30 kWh/m <sup>2</sup> a	0,75	0,52	0,64	0,86
15 kWh/m <sup>2</sup> a	0,75	0,49	0,74	0,99

There is a large difference in values obtained for the two alternative definitions of the use factor. The use factor based on the amount of usefully supplied heat to the room,  $\eta_2$  can be as low as 50%. This means that less than 40% of the heat extracted by the ventilation system is actually supplied usefully to the rooms of the dwelling. The use factor based on the saved heating demand at the building level is much higher and more dependent on the overall energy performance of the envelope.

Both approaches are valid but should be used in different contexts. From the perspective of the operational assessment of the MHRV unit, the first approach is a good measure of the cost-benefit balance, operational cost and return on investment that is to be expected. The second approach relates to the expected impact on the annual heat load calculation.

$\eta_2$ , in contrast to  $\eta_3$ , is correlated to the occupancy rate of the dwelling (assuming that heating patterns and occupancy are correlated). This is due to the fact that  $\eta_2$  is a ratio of heat fluxes at the unit level ( $Q_r$ ) and at the room level ( $Q_0 - Q$ ), while  $\eta_3$  is only a function of room/building related parameters.

The improvement of the energy performance of the building envelope causes the temperature throughout the dwelling to be more constant over time and uniform with respect to the different spaces, therefore reducing the effect of intermittent dynamic heating. Similarly, the second use factor increases substantially with decreasing flow rate, since the denominator (the increase in annual heat load due to ventilation) decreases more rapidly than the nominator because the temperature redistribution that is cause by the circulation of air is smaller.

Both use factor definitions are independent of the test effectiveness of the AAHX ( $\eta_1$ ).

#### 4 CONCLUSIONS

This paper proposed two alternative definitions for a use factor for the performance assessment of MHRV ventilation. It shows that, based on a simulated case study for an archetypical Belgian detached dwelling, although a heat exchanger can have an effectiveness of e.g. 75%, only as little as 40% of the heat in the extracted air is recovered and supplied usefully to the rooms.

#### 5 REFERENCES

Binamu, A. and Lindberg, R. (2001). The impact of air tightness of the building envelope on the efficiency of ventilation systems with heat recovery.

Dodoo, A., Gustavsson, L., and Sathre, R. (2011). Primary energy implications of ventilation heat recovery in residential buildings. *Energy and Buildings*, 43(7), 1566-1572.

Eurovent. Eurovent Certification. <http://www.eurovent-certification.com/>. Accessed: 10-04-2017.

Juodis, E. (2006). Extracted ventilation air heat recovery efficiency as a function of a building's thermal properties. *Energy and Buildings*, 38(6), 568-573.

Manz, H., Huber, H., & Helfenfinger, D. (2001). Impact of air leakages and short circuits in ventilation units with heat recovery on ventilation efficiency and energy requirements for heating. *Energy and buildings*, 33(2), 133-139.

Roulet, C. A., Heidt, F. D., Foradini, F., and Pibiri, M. C. (2001). Real heat recovery with air handling units. *Energy and Buildings*, 33(5), 495-502.

# Methodology for the characterization of the envelope airtightness of the existing housing stock in Spain

Irene Poza-Casado<sup>\*1</sup>, Alberto Meiss<sup>1</sup>, Miguel Ángel Padilla-Marcos<sup>1</sup>, and Jesús Feijó-Muñoz<sup>1</sup>

*1 GIR Arquitectura & Energía  
Universidad de Valladolid  
Avda/ Salamanca, 18 - 47014  
Valladolid, Spain*

*\* Corresponding author: irene.poza@uva.es*

## ABSTRACT

It has already been proved that air leakage causes a great impact in the energy performance of buildings in cold climates. In recent years, many studies have been carried out in northern Europe, US and Canada. Regulations in these countries establish maximum air leakage rates for the construction of new dwellings and the refurbishment of the existing ones. However, there is a lack of knowledge relating to the housing stock in Spain.

In temperate climate countries, air leakage has traditionally been part of natural ventilation. On the one hand, current Spanish building regulations (CTE) establish controlled ventilation in dwellings to ensure indoor air quality (IAQ). On the other hand, air leakage is only considered concerning windows characteristics. Ventilation rates are calculated based on ideal airtight envelopes. Therefore, problems of over-ventilation, uncontrolled air flows, poor indoor air quality and energy consumption are caused.

A national research is being accomplished within INFILES project (2016-2018), where nine Universities on different locations are participating with coordinated field measurement campaigns.

The dwellings to be tested were chosen by establishing a nonprobability statistical sampling method. With the aim of representing the major characteristics of the Spanish housing stock in the most reliable way, a proportional quota sampling scheme was designed: as a consequence, 411 tests are being carried out in order to characterize the airtightness of the construction system of the envelope and to determine typical air leakage paths in dwellings. Stratification was performed with real data by taking into account different variables which have been proved to be relevant concerning airtightness: climate zone, year of construction and typology (single-family houses or multi-family buildings).

The air leakage rate is being determined using a standardized building pressurization technique, in accordance with UNE-EN 13829 and ISO 9972:2006 regulations. Typical air leakage paths are determined using infrared image technique. A specific software has been developed to retain dwellings characterization data: location, year of construction, typology, size, height, construction technology, property developer, retrofitting state, window area, energy systems, and others, up to a total of 140 parameters.

The aim of the project is to develop a wide database with representative samples of residential buildings in Spain. In this way, it will be possible to relate the main factors that have an impact on airtightness. The main objective is to know ventilation rates due to air leakage and its energy impact in order to design guidelines with real data, which is obtained from the tests. A subsequent control regulation proposal for the envelope airtightness will be developed. Consequently, Spanish regulations will be consistent with European directives.

## KEYWORDS

Air leakage; residential buildings; fan pressurization test; Blower Door

## 1 INTRODUCTION

In recent years, the interest on airtightness in buildings has significantly grown. European Directives [1] set the need to enhance the energy performance of buildings, which is affected by uncontrolled air leakage through the building envelope. The lack of airtightness can also cause problems of over-ventilation, thermal comfort, noise, uncontrolled air flows, poor indoor air quality (IAQ) and affect the health of its occupants.

Most European countries have already adapted their regulations [2], establishing maximum values of air leakage rates. However, there has not been a development of regulations in southern Europe. Still, some studies on airtightness have been carried out in recent years in Italy [3], Greece [4], Portugal [5],[6] and Spain [7],[8], [9] .

D'Ambrosio Alfano et al. [3] conducted an experimental study on 20 residential buildings in southern Italy focusing on metrological aspects, energy consumption and indoor comfort. Sfakianaki et al. [4] also performed 20 tests in dwellings in Greece, which were classified according to their airtightness level. They also performed a statistical test between regression coefficients of the measurements.

In Portugal, Ramos et al. [5] studied 49 apartments from two social housing neighbourhoods to investigate the impact of user behaviour on airtightness levels. Pinto et al. [6] carried out airtightness tests on 5 flats in Portugal with identical construction characteristics in the same building, with the aim of characterizing the air permeability of building and components.

In Spain, Tiberio and Branchi [7] tested more than 120 apartments of 25 recent buildings in northern Spain to determine the most important reasons for the increase of air leakage rates. Fernández-Agüera et al. [8] conducted Blower Door tests in 45 units in seven early twenty-first-century buildings in southern Spain. Results were reported and compared to the data of other buildings in southern Europe and a statistical analysis was performed.

Meiss and Feijó-Muñoz [9] established an evaluation procedure for the energetic effects of air leakage through an experimental study carried out in 13 dwellings in residential blocks, located in the north and central part of Spain. It has been estimated that air leakage in Spain represents between 10.5 and 25.4% of winter energy demand in buildings built under the current Spanish Technical Building Code (CTE) [10], between 21.9 and 27% in buildings subject to CT-79 Regulations [11] and between 11.3 and 13.0% in old buildings without energy regulation (but retrofitted by their owners) [9].

In order to provide a response to the lack of knowledge in this field in Spain, a national research is being accomplished within *INFILES* project BIA2015-64321-R (2016-2018): *Energy impact of airtightness level in residential buildings in Spain: analysis and characterization of the air leakage*.

A wide database with representative samples of residential buildings in Spain is being developed. The aim of the research project is to understand the airtightness behaviour of the architectural envelope in the Spanish residential building stock by means of an experimental and numerical study, which is being carried out throughout the Spanish geography. Air leakage rates of typical construction system solutions are being characterized and quantified. Guidelines for Spanish regulations, which currently do not consider airtightness, will be proposed in order to be consistent with European directives.

## 2 REGULATIONS IN SPAIN

In Spain and Mediterranean countries, ventilation has traditionally been done in a natural way. Thus, air leakage supplied the lack of mandatory ventilation systems [8]. Regulations have tended to an increasing thermal insulation of that envelope, which led to a better energy performance of buildings. However, it also affected IAQ as a consequence of the lack of ventilation. To solve this, in 2006, Spanish regulations [12] implemented specific ventilation systems to assure an adequate IAQ. Nevertheless, ventilation rates are calculated based on ideal airtight envelopes and air leakage is not considered, resulting in oversized ventilation systems.

Currently, air leakage is only taken into account concerning windows characteristics (Table 1), as part of the *DB-HE* “*Limitation of the energy demand*” [13].

Table 1: Maximum airtightness values for the elements of the envelope concerning climate zones in winter [ $\text{m}^3/\text{h}\cdot\text{m}^2$ ] at a pressure difference of 100Pa

Parameter	Zone $\alpha$	Zone A	Zone B	Zone C	Zone D	Zone E
Windows airtightness	$\leq 50$	$\leq 50$	$\leq 50$	$\leq 27$	$\leq 27$	$\leq 27$

Zone  $\alpha$  refers the Canary Islands climate, zones A and B mild-climate areas and zones C, D and E to cold climates.

## 3 METHODOLOGY

### 3.1 Sampling

A sampling has been carried out with the aim of reproducing the Spanish building stock to extrapolate the results to other cases in similar conditions defined by its parameters.

As Price et al. [14] mentions, the best way to estimate the relevant statistical distribution of leakage parameters would be to perform measurements in a simple random sample of dwellings. However, such a sampling strategy would be impractical, since it would require significant resources. Taking into account the objectives and characteristics of the present research, a quota sampling scheme has been considered, even though uncertainty is always larger with a non-probability sampling than with a simple random sample. The Spanish housing-stock is partitioned into non-overlapping groups called strata.

A proportional allocation is established. That is, the number of samples per stratum is determined proportional to its size (Equation 1):

$$N_i = n \cdot \frac{N_i}{N} \quad (1)$$

where:

$N_i$  = sample size of stratum  $i$ .

$n$  = sample size.

$N_i$  = population size of stratum  $i$ .

$N$  = population size.

#### 3.1.1 Parameters considered

Previous studies, which have established predictive models in residential buildings based on factors directly related to airtightness, have been assessed (Table 2).

Table 2: Parameters considered in previous characterization studies.

Parameter	Sfakianaki et al. (2008)	Price et al. (2006)	Orme et al. (1994)	McWilliams et al. (2006)	Sherman (2006)	Chan et al. (2012)	Erinjeri et al. (2009)	Zou (2010)	Montoya et al. (2010)	Pan (2010)	Kirstic et al. (2015)
Age of the building	x		x	x	x	x	x	x	x		x
Type of construction/ construction building system	x	x	x					x	x	x	x
Floor area		x		x	x	x	x		x	x	
Climate zone	x			x	x	x	x				x
Height/number of storeys		x			x	x		x	x		
Type of foundation/floor structure			x	x		x		x			
Energy-Efficiency Programs				x	x	x		x			
Significant penetrations											x
Economic status				x	x	x					
Surface area								x		x	x
Ducted air system through unconditioned space			x			x					
Ventilation type/presence of ducts				x				x			
Joinery/sealing			x								x
Retrofitting work/renovation						x		x			
Insulation position/thickness									x		x
Window frame length	x							x			
Complex floor plan			x		x						
Air barrier			x								x
Design target											x
Management context											x
% transparent part of the envelope											x
Windows/glazing											x
Installation layer								x			
Heating system									x		

The majority of the studies agree that the most relevant parameters are the age of the building, type of construction/materials, floor area and climate zone. It is assumed that if the sample reproduces the building stock with respect to important characteristics, it will reproduce it in the same way with respect to minor characteristics.

The age of the building has an impact on airtightness in several ways. Firstly, materials and their joints become deteriorated overtime [15]. An increase of 10-15% on air leakage every 10 years has been estimated [16], [17]. Secondly, construction systems are developed and improved. However, in milder-climate countries, where there is no airtightness standard for new buildings, recent dwellings are not necessarily more airtight than older ones [18]. Thirdly, the age of the building is associated with regulations, which establish requirements and conditions the building construction systems.

It has been considered advisable to eliminate floor area as a parameter. The representativeness of the sample would be ensured, since a parallelism between the year of construction and the floor area has been found. Greater surfaces are registered in houses before 1900, 1980s and 1990s, whereas in the 1950s and 1960's the houses were designed with markedly inferior floor areas [19].

Construction building system is not initially used as a sampling parameter because statistical sources do not contemplate its actual distribution in the housing stock in Spain. Regarding type of construction, most studies focus on the characterization of single-family housing.

However, in Spain multi-family buildings represent more than 70% of real estate [20], so the study must inexorably reflect both typologies, with particular focus on multi-family dwellings.

Climate zone has also an important influence on airtightness of dwellings. Buildings in cold climates tend to be tighter due to comfort and energy behaviour, whereas in milder climates dwellings are leakier [16]. Climate zones not only determine weather conditions, but also building systems and regulations [21].

All things considered, the sampling method takes into account objective parameters whose distribution is known. Age of the building involves 10 periods of time, according to data sources [19]; typology is considered within two categories (single-family and multi-family buildings) [19]; a wide variety of climate zones is covered, divided into 4 areas: Oceanic, Continental (cold climates), Mediterranean (mild climate) and Hot desert area (Canary Islands) (Figure 1).

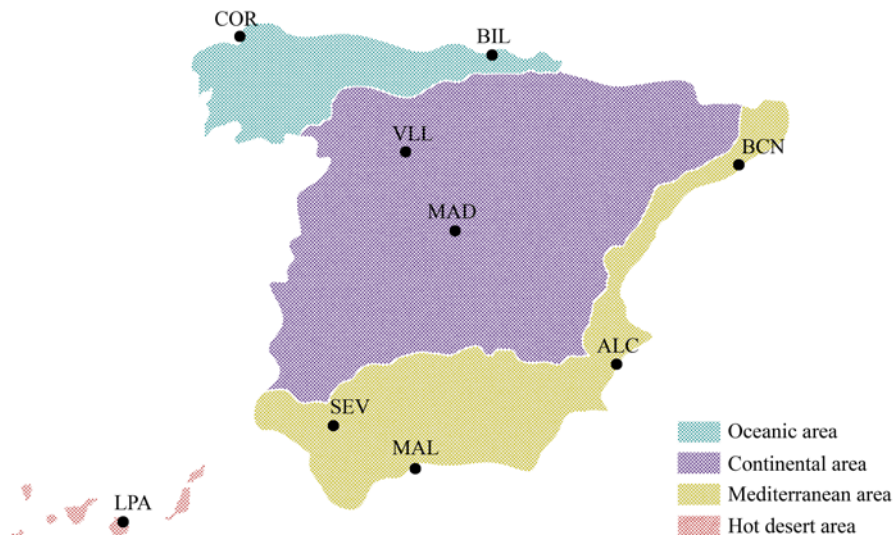
Figure 1: Location of the participant universities and climate zones in Spain.

where:

COR: La Coruña. Universidad de la Coruña

BIL: Bilbao. Universidad del País Vasco

VLL: Valladolid. Universidad de Valladolid



MAD: Madrid. Universidad San Pablo CEU

BCN: Barcelona. Universidad Politécnica de Cataluña

ALC Alicante. Universidad de Alicante

MAL: Málaga. Universidad de Málaga

SEV: Sevilla. Universidad de Sevilla

LPA: Las Palmas. Universidad de las Palmas de Gran Canaria

### 3.1.2 Size and distribution of the sample

The number of tests is conditioned by the purpose of the study, the accepted accuracy, the availability of the resources and the duration of the research project. Since the kind of sampling used has a probabilistic structure, the formulation used to obtain the sample size in random processes for large populations is used (Equation 2).

$$n = \frac{Z^2 \sigma^2}{E^2} \quad (2)$$

where:

Z is the critical value, depending on the confidence level.

$\sigma$  is the population standard deviation (unknown value in Spain)

E is the margin of error

n is the sample size

$\sigma$  value has been calculated from an experimental study carried out in Italy [3], due to the similarity of both contexts and related climate conditions. Considering  $Z = 1.96$  for a confidence level of 95%,  $\sigma = 17.584$  and  $E = \pm 0.4$ , a sample size of 423 tests is obtained. Due to the numerical rounding made in the stratification, the total sum of tests is slightly reduced (411). The specific sample distribution is detailed in Table 3.

Table 3: Sample distribution

Age of the building	Type	Oceanic		Continental		Mediterranean				Hot desert
		COR	BIL	VLL	MAD	BCN	ALC	MAL	SEV	LPA
<1900	S	1	-	-	-	1	1	-	-	-
	M	-	1	-	2	3	-	-	-	-
1900-1920	S	1	-	-	-	1	-	-	-	-
	M	-	1	-	2	3	-	-	-	-
1921-1940	S	1	-	-	-	1	-	-	-	-
	M	-	1	-	3	4	-	-	-	-
1941-1950	S	1	-	-	-	1	1	-	1	-
	M	-	1	-	3	3	1	-	1	-
1951-1960	S	1	-	-	1	1	1	1	1	-
	M	1	3	-	8	7	1	1	1	1
1961-1970	S	1	-	-	1	2	1	1	2	1
	M	3	7	2	19	19	5	3	4	2
1971-1980	S	1	-	-	3	3	2	2	2	1
	M	5	5	2	23	22	8	6	5	2
1981-1990	S	1	-	-	3	3	3	2	2	1
	M	2	1	1	9	6	5	5	2	2
1991-2001	S	1	-	1	4	3	2	2	3	1
	M	3	2	1	13	10	3	4	3	2
2002-2011	S	2	-	1	3	2	3	1	3	1
	M	6	3	1	13	9	12	6	3	2
TOTAL		31	25	9	110	104	49	34	33	16

where:

S: single-family houses

M: multi-family dwellings

### 3.2 Testing method.

Measuring campaigns are organized between late 2016 and 2017, taking into account the number of tests to be carried out on each location and the typical climatic conditions, since regulations [22] restrict wind velocity during the test.

All the tests are being performed following a determined common protocol which includes the preparation of the dwellings and the cases classification proceeding.

Tests are conducted according to EN-13829 [22] and ISO 9972:2015 [23] with a Fan pressurization method, commonly called Blower Door Test using an automated performance test. Depressurization and pressurization tests are carried out within the deliberately conditioned space. During the test, all openings of the envelope are closed or sealed [22]. Measurements of air flow rate and indoor-outdoor pressure difference are taken over a range of applied pressure differences in increments of 6 Pa. The minimum pressure difference is 11 Pa and the highest-pressure difference is 65 Pa.

The building leakage curve is calculated as:

$$q = C \cdot \Delta p^n \quad (3)$$

where:

$q$  is the air flow rate through the building envelope [ $\text{m}^3/\text{h}$ ]

$C$  is the air leakage coefficient [ $\text{m}^3/(\text{h} \cdot \text{Pa}^n)$ ]

$\Delta p$  is the induced pressure difference [Pa]

$n$  is the air flow exponent (0.5-1 for fully developed turbulent and laminar flow respectively).

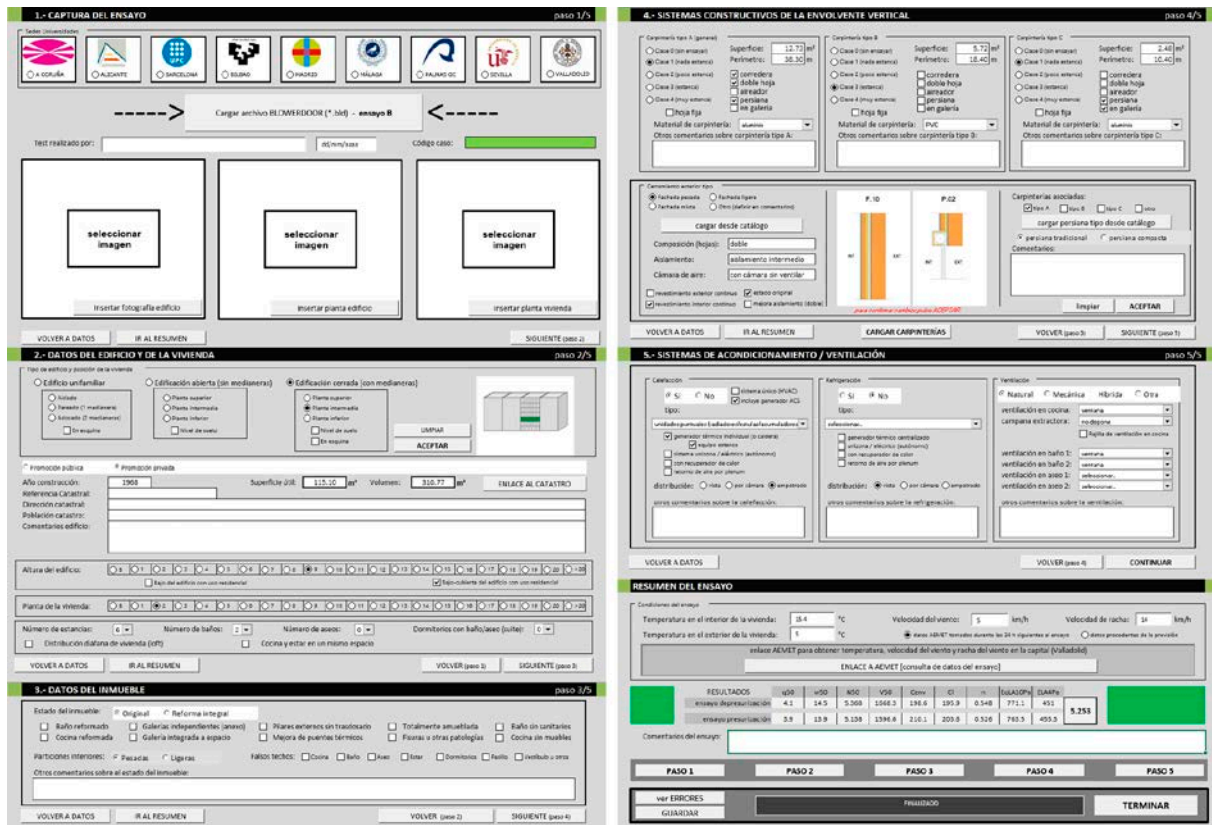
Methods A (test of the building in use) and B (test of the building envelope) are performed as describe in EN-13829 [22]. The fan is mounted on the main door. During the depressurization stage, leakage paths are identified using infrared image technique with a thermographic camera.

### 3.3 Parameters under study

A specific tool, *infil-APP* (Figure 2), has been developed to retain dwellings characterization data in a dataset format. The objective is the fulfilment of a wide database for a subsequent analysis of the parameters that have a major influence on airtightness.

The tool has been conceived for easy, fast and intuitive use. It retains: graphic information, test results, climatic conditions during the test and a wide characterization of parameters; and stores them tabulately. Year of construction, location, detailed dimensions (net floor areas, envelope surface areas and internal volumes), heat loss form factor, typology of the building and its position with respect to adjacent houses or apartments, property developer, height, number of rooms, retrofitting state, furnishing, presence of false ceilings, construction technology, area and perimeter of window frames and blinds, energy and ventilation systems, among others, are also saved. Once each case study is completed, a full report and a data sheet are obtained.

Figure 2: Screenshots of infil-APP.



Airtightness values of the buildings will be compared taking into account 50 Pa as a reference pressure. Air change rate ( $n_{50}$  value) and air permeability ( $q_{50}$  value) is analysed, considering the inner volume of the measured building and the envelope area respectively.

## 4 CONCLUSIONS

A rigorous and simple methodology has been established in order to carry out coordinated field measurement campaigns. The aim of INFILES project (ref. BIA2015-64321-R) is to know the behaviour of the envelope of the housing stock in Spain regarding airtightness. A quota sampling scheme has been designed to create a wide database, taking into account different parameters related to air leakage: climate zone, year of construction and typology (single-family houses or multi-family buildings).

With *infil-APP*, characterization data and results are being retained in a homogeneous dataset. In this sense, a subsequent analysis of the results can be performed, guaranteeing the same proceedings and criteria.

## 5 ACKNOWLEDGEMENTS

This publication presented the methodology under the research project *INFILES: Repercusión energética de la permeabilidad al aire de los edificios residenciales en España: estudio y caracterización de sus infiltraciones*, funded by the Spanish Ministry of Economy and Competitiveness (ref. BIA2015-64321-R).

## 6 REFERENCES

*European Directive on Energy Performance of Buildings (EPBD e 2002/91/CE)*. .

F. Ossio, A. De Herde, and L. Veas, “Exigencias europeas para infiltraciones de aire: Lecciones para Chile,” *Rev. la Constr.*, vol. 11, no. 1, pp. 54–63, 2012.

F. R. D’Ambrosio Alfano, M. Dell’Isola, G. Ficco, and F. Tassini, “Experimental analysis of air tightness in Mediterranean buildings using the fan pressurization method,” *Build. Environ.*, vol. 53, pp. 16–25, 2012.

A. Sfakianaki *et al.*, “Air tightness measurements of residential houses in Athens, Greece,” *Build. Environ.*, vol. 43, no. 4, pp. 398–405, 2008.

N. M. M. Ramos, R. M. S. F. Almeida, A. Curado, P. F. Pereira, S. Manuel, and J. Maia, “Airtightness and ventilation in a mild climate country rehabilitated social housing buildings - What users want and what they get,” *Build. Environ.*, vol. 92, pp. 97–110, 2015.

M. Pinto, J. Viegas, and V. P. de Freitas, “Air permeability measurements of dwellings and building components in Portugal,” *Build. Environ.*, vol. 46, no. 12, pp. 2480–2489, 2011.

A. Jiménez Tiberio and P. Branchi, “A study of air leakage in residential buildings,” in *2013 International Conference on New Concepts in Smart Cities: Fostering Public and Private Alliances (SmartMILE)*, 2013, pp. 1–4.

J. Fernández-Agüera, S. Domínguez-Amarillo, J. J. Sendra, and R. Suárez, “An approach to modelling envelope airtightness in multi-family social housing in Mediterranean Europe based on the situation in Spain,” *Energy Build.*, vol. 128, pp. 236–253, 2016.

A. Meiss and J. Feijó-Muñoz, “The energy impact of infiltration: a study on buildings located in north central Spain,” *Energy Effic.*, vol. 8, no. 1, pp. 51–64, 2014.

*Spanish Technical Building Code. Código técnico de la Edificación (CTE)*. 2013.

*Norma Básica de Edificación NBE-CT-79. Condiciones térmicas en los edificios*. 1979.

*Spanish Technical Building Code. Código técnico de la Edificación (CTE). Documento básico HS Salubridad*. 2009.

*Spanish Technical Building Code. Código técnico de la Edificación (CTE). Documento básico HE Ahorro de energía.* 2013.

P. N. Price, A. Shehabi, and R. Chan, “Indoor-outdoor Air Leakage of Apartments and Commercial Buildings,” 2006.

P. Ylmén, M. Hansén, and J. Romild, “Durability of airtightness solutions for buildings,” in *35th AIVC Conference “Ventilation and airtightness in transforming the building stock to high performance,”* 2014.

J. McWilliams and M. Jung, “Development of a Mathematical Air-Leakage Model from Measured Data,” 2006.

W. R. Chan, I. S. Walker, and M. H. Sherman, “Durable Airtightness in Single- Family Dwellings : Field Measurements and Analysis,” 2015.

M. H. Sherman and R. Chan, “Building Airtightness : Research and Practice,” 2004.

Instituto Nacional de Estadística, “INEbase,” 2016. [Online]. Available: <http://www.ine.es/>. [Accessed: 19-May-2016].

Dirección General de Arquitectura Vivienda y Suelo; Ministerio de Fomento, “Boletín Especial Censo 2011. Parque edificatorio,” 2011.

W. R. Chan, J. Joh, and M. H. Sherman, “Analysis of air leakage measurements of US houses,” *Energy Build.*, vol. 66, pp. 616–625, 2013.

*EN 13829:2002: Thermal performance of buildings - Determination of air permeability of buildings - Fan pressurization method. (ISO 9972:1996, modified).* 2002.

*International Standard ISO 9972. Thermal performance of buildings - Determination of air permeability of buildings - Fan pressurization method.* 2015.

# On the design and testing of Airtightness Modifier dedicated to the TIPEE IEQ House

Maxime Paquet<sup>1</sup>, Martin Marcelli<sup>1</sup>, Aline Bachelet<sup>1</sup>, Ekaterina Obukhova<sup>1</sup>,  
Emma Calamote<sup>1</sup>, Florian Lae<sup>1</sup>, Jérôme Nicolle<sup>2</sup> and Marc Abadie<sup>\*1</sup>

*1 University of La Rochelle  
23 avenue Albert Einstein  
La Rochelle, France*

*2 TIPEE platform  
8 Rue Isabelle Autissiers  
Lagord, France*

*\*Corresponding author: mabadie@univ-lr.fr*

## ABSTRACT

This paper aims to present the elaboration of a device able to modify the airtightness of a test House. This project has been conducted with three Master student groups in the framework of their research projects from 2015 to 2017. The TIPEE IEQ test House, comprising of two floors and eight rooms, is dedicated to the study of Indoor Air Quality (IAQ), thermal comfort and energy consumption. Its envelope has been designed to reach an airtightness target slightly lower than the French Energy Efficiency Standard RT2012 requirement for dwellings i.e.  $Q_{4 Pa}$  value equals to  $0.5 \text{ m}^3/\text{h}\cdot\text{m}^2$  ( $n_{50} = 1.2 \text{ ACH}$ ). The role of the new device, called Building Airtightness Modifier (BAM) in this paper, is to allow the experimental researchers to adapt the envelope airtightness of the test house (or part of it) in a gradually fashion from the lower value of 0.5 to about  $2 \text{ m}^3/\text{h}\cdot\text{m}^2$ . The main objective here is to evaluate the influence of envelope airtightness on IAQ and heating/cooling/ventilation system efficiency. In this paper, the description of the TIPEE IEQ test House is given in a first part. Then, the design process of the BAM is presented. Tests performed by the students on both experimental bench and in situ show a good agreement with the initial design objectives.

## KEYWORDS

Building Airtightness Modifier, airflow rate, test house, measurement

## 1 INTRODUCTION

The Building Airtightness Modifier (BAM) were designed to modify the test house airtightness within a range representative of the French residential building stock in order to simulate any type of building envelope. Two main objectives have been considered:

1. To vary the airflow rate across the building envelope at standard pressure indoor to outdoor pressure difference from its initial low value  $Q_{4 Pa}=0.5 \text{ m}^3/\text{h}\cdot\text{m}^2$  ( $n_{50} = 1.2 \text{ ACH}$ ) to a upper value encountered in France.
2. To keep the nature of the airflow through the building envelope representative of the reality i.e. the value of the airflow exponent  $n$ .

The first objective helps determining the maximum airflow through one single BAM. Figure 1 presents the evolution of  $Q_{4 Pa}$  in France with time. The airtightness range corresponds to 0.5 to  $2.0 \text{ m}^3/\text{h}\cdot\text{m}^2$ . The BAM have then to provide  $1.5 \text{ m}^3/\text{h}\cdot\text{m}^2$  i.e. **a total airflow of  $23.4 \text{ m}^3/(\text{h}\cdot\text{BAM})$  under 4 Pa-pressure gradient** (considering a total of 16 BAM).

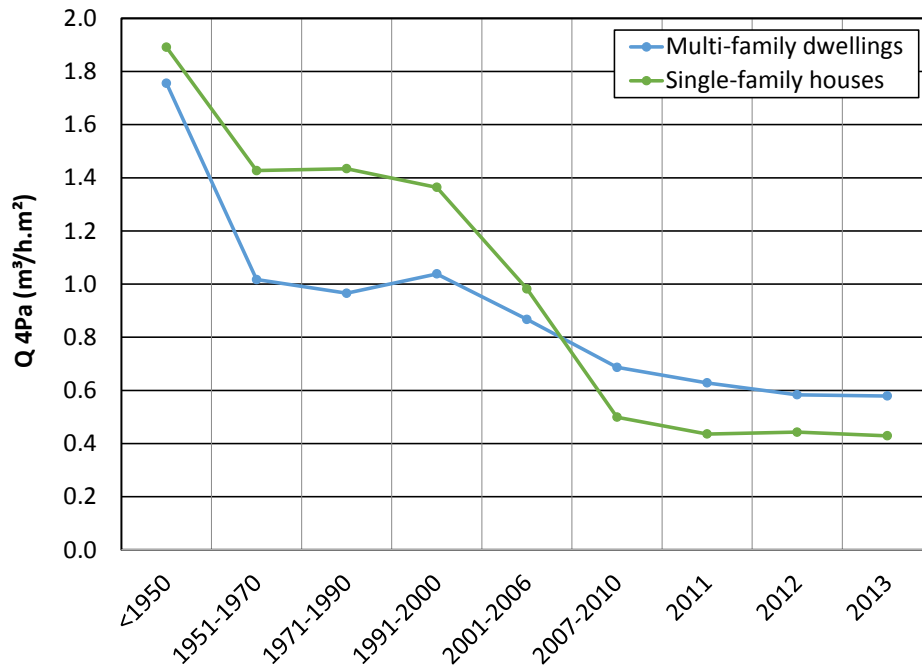


Figure 1: Evolution of the airtightness envelope measurements and their results for residential buildings in France (from Bailly et al., 2015).

To fulfil the second objective, the airflow exponent  $n$  has to be defined. The airflow rate across the building envelope,  $Q_{env}$  (m³/h), is calculated from the difference between the indoor and outdoor pressure,  $\Delta p$  (Pa) using the following power law equation:

$$Q_{env} = C_{env} \times \Delta p^n \quad (1)$$

where  $C_{env}$  is the airflow coefficient (m³/(h.Pa<sup>n</sup>)) and  $n$ , the airflow exponent (-) that characterises the flow regime, with values ranging from 0.5 for turbulent flow to 1 for laminar flow (EN ISO 9972:2015).

The study of airflow exponent  $n$  identifies the type of air pathway, which helps characterise the usual infiltration pathways. The majority of airflow exponent for leakage openings at joints or material interfaces are found to be between 0.5-0.7. On the other hand, the exponent for porous surfaces varies between 0.5 and 1 (Orme et al., 1998). A value of 0.66 is the reference adopted in countries where airtightness standards are traditionally high because air leakage pathways in residential units are dominated by developing flows in cracks such that  $n = 0.67$  (Walther and Rosenthal, 2009). More recently, Walker et al. (2013) have studied the link between the measurement uncertainty and the power-law, and especially the flow exponent  $n$ . Using the Residential Diagnostics Database (about 7000 measurements), they calculated a mean value of 0.646 (standard deviation,  $sd=0.057$ ). The values measured in countries such as Italy, 0.55–0.69 with a mean on the order of 0.60 (D’Ambrosio Alfano et al., 2012), or Spain, 0.54 to 0.64 with a median of 0.58 (Fernández-Agüera et al., 2016), are lower because  $n$  tends to be higher in leakage openings with larger flow resistance than those found in the Mediterranean area. In 2016, Bailly et al. studied the airtightness measurements of about 90,000 residential and non-residential buildings in France (2008 to 2014) and evaluated the flow exponent to 0.667 ( $sd = 0.05$ ). The BAM have to produce an airflow nature characterized by an **exponent  $n$  of about 0.667**.

## 2 METHODOLOGY

### 2.1 Description of the TIPEE IEQ test House

This research test House has been built up in order to work on Indoor Air Quality, comfort and energy consumption in real conditions. With a surface area of 150 m<sup>2</sup>, it consists of 2 levels with a kitchen/living-room, an office room and a WC located in the first level and 3 bedrooms and a bathroom in the second floor. An additional technical room is dedicated to the measurement and control systems and is completely independent from the rest of the house. The main characteristics of the test house are: low-emission internal surfaces, adaptable ventilation systems (extract or supply/extract, with or without heat recovery system), automatic control of windows opening and sunscreens and centralized energy meters. A particular effort has been made to improve the performance of the building envelope to ensure airtightness (design  $Q_{4 Pa} = 0.5 \text{ m}^3/\text{h}\cdot\text{m}^2$ ,  $n_{50} = 1.2 \text{ ACH}$ ). In order to artificially vary the permeability of the envelope to mimic the behaviour of older buildings (more porous building envelopes and/or natural ventilation), cylindrical holes (23 cm in diameter) have been uniformly distributed over the house envelope (Figure 2). These holes are reservations for the BAM studied in this paper and described in the next section.



Figure 2: BAM locations in the test house (left: outside view; right: inside view).

### 2.2 Design of the BAM

The technical constraints for the design of the BAM were initially:

1. Total airflow rate of 23.4 m<sup>3</sup>/h under 4 Pa-pressure gradient for each BAM,
2. External dimensions: diameter  $D = 20\text{cm}$  and length  $L = 35\text{cm}$ .

Two different approaches have been considered: multiple circular ducts and rectangular cracks (Figure 3). Pressure drop across the BAM have been calculated with classic approach (friction + local losses) for the first configuration. The correlation of Baker et al. (1987) has been used for the rectangular cracks. Figure 4 presents the characteristic curves of these two BAM designs (called “initial” in Figure 4). In addition to the airflow rate at 4 Pa (Target), the BAM should also produce airflow of the same nature of real envelope i.e. with an exponent  $n$  of about 0.67. As a consequence, the circular configuration with  $n = 0.52$  has been rejected. Note that the rejection of this configuration has also been motivated for technical building complexity and maintenance for cleaning. The rectangular cracks configuration has been adopted. The initial design suffers some modifications because of changes in allowable spaces for the cracks so that their widths had to be shortened. The final design includes 8 slots instead of 4; its characteristic curve and its dimensions are presented in Figure 4 and 5, respectively.

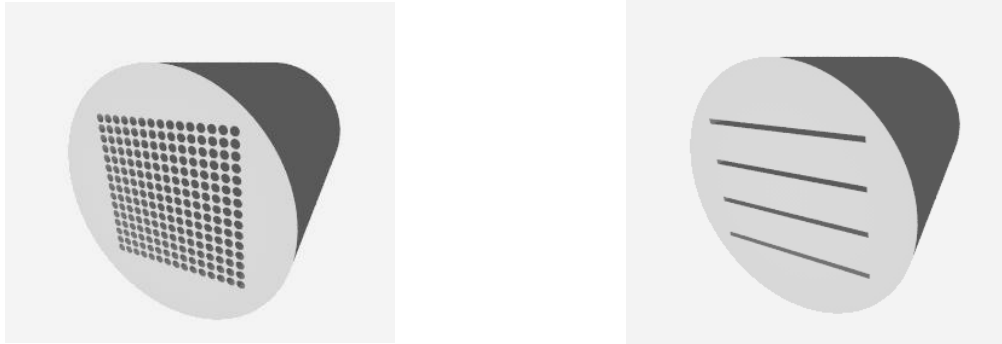


Figure 3:Initial design (left: circular ducts; right: rectangle cracks).

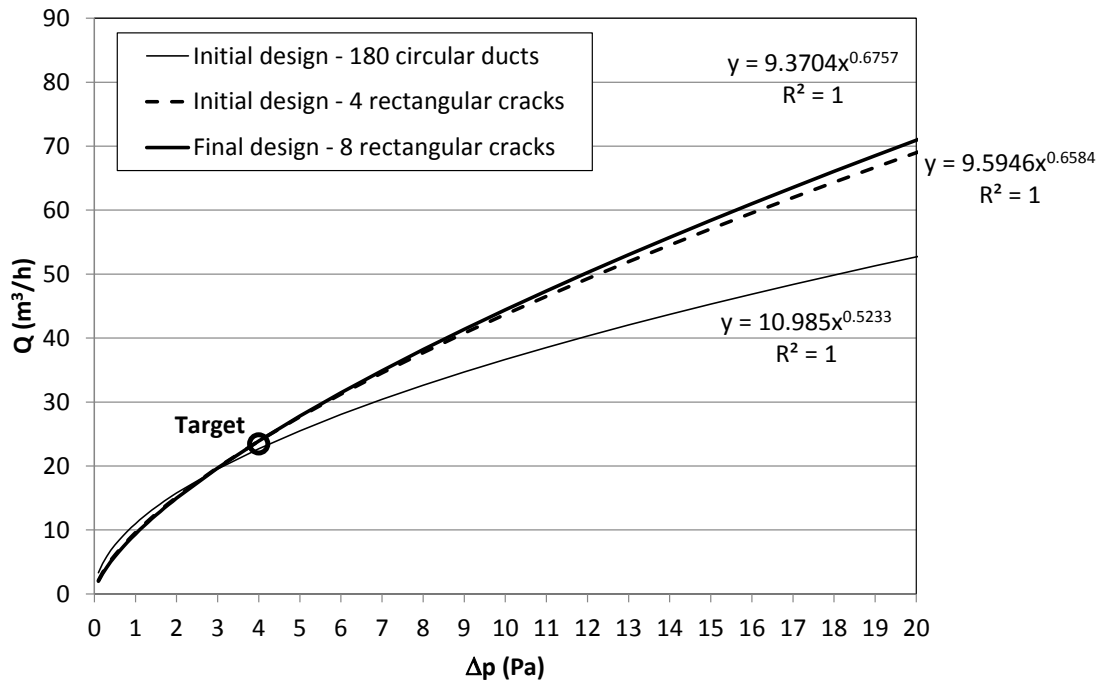


Figure 4:Characteristic curves of different BAM designs.

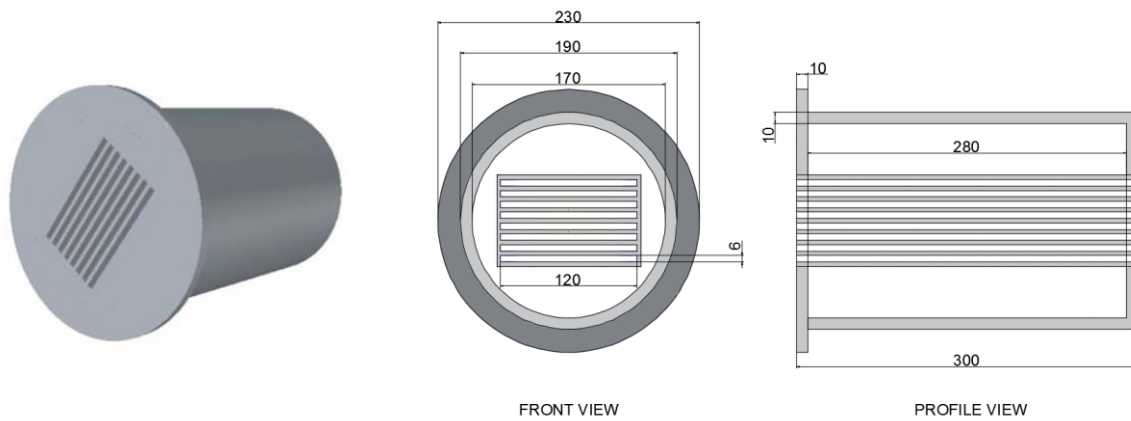


Figure 5:Final design (dimensions are in mm).

### 3 RESULTS AND DISCUSSION

#### 3.1 Testing on the experimental bench

The prototype has been first tested in the laboratory. The main parts of the experimental bench are: a variable speed fan equipped with an iris diaphragm to measure the airflow rate, a circular duct (D = 20 cm, L = 3 m), a static pressure point at 1 m from the duct end and the BAM prototype (Figure 6).

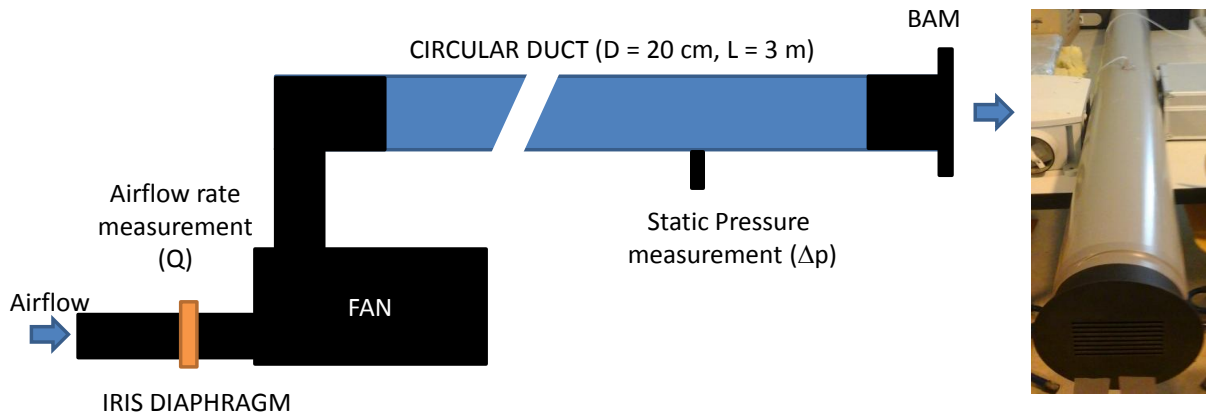


Figure 6: Experimental set-up.

The test consisted in measuring the airflow rate according to the pressure gradient around the BAM from 10 to 70 Pa with 10 Pa increment. The results of 3 validated tests are presented in Figure 7. The repeatability of the tests is positive with differences lower than 3 m<sup>3</sup>/h. On the whole, the airflow rates are lower than expected. However, the airflow rate target at 4 Pa is only 10% lower than the design one; this will only affect the highest envelope permeability that can be adjusted in the test House (1.4 instead of 1.5 m<sup>3</sup>/h.m<sup>2</sup>). Also, the nature of the airflow through the envelope will be slightly more turbulent than the expected one (0.59 instead 0.667).

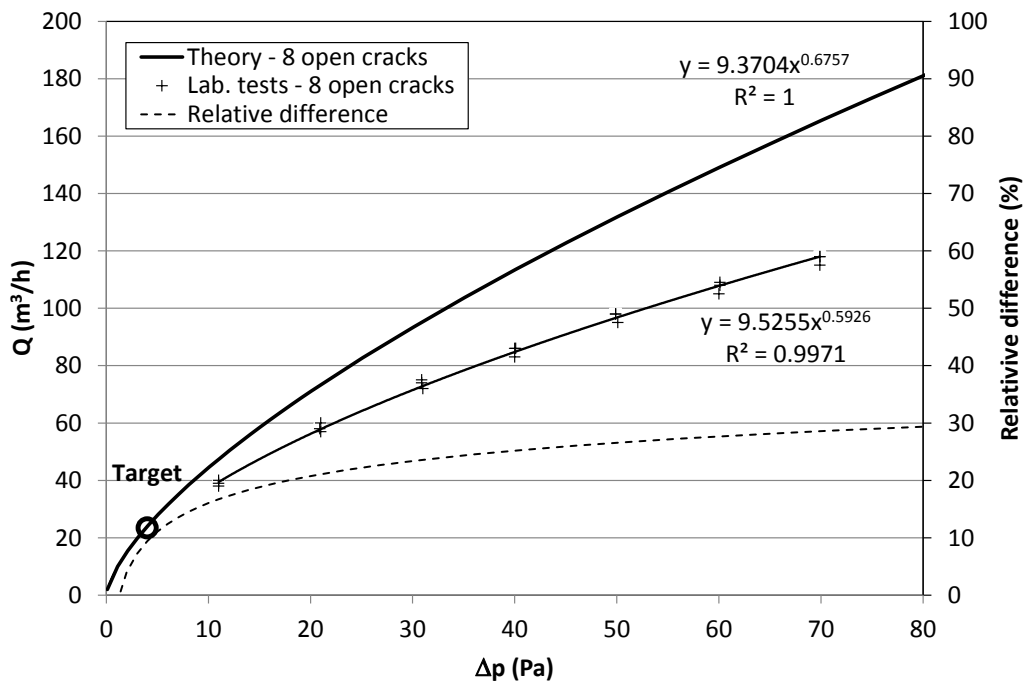


Figure 7: BAM characteristic curves obtained by measurement in the laboratory.

### 3.2 Testing in the test House

In a second step, the prototype has been tested in the test House by placing it in one reservation of a bedroom located in the second floor (Figure 8a). The test has been performed according to the International Standard EN ISO 9972 (2015) using a Minneapolis blower door (Figure 8b). The BAM characteristic curve has been obtained by making the difference between the measurements when the BAM was fully open (airflow through BAM + room infiltration) and test with a completely sealed BAM (room infiltration only), Figure 8c and 8d respectively.

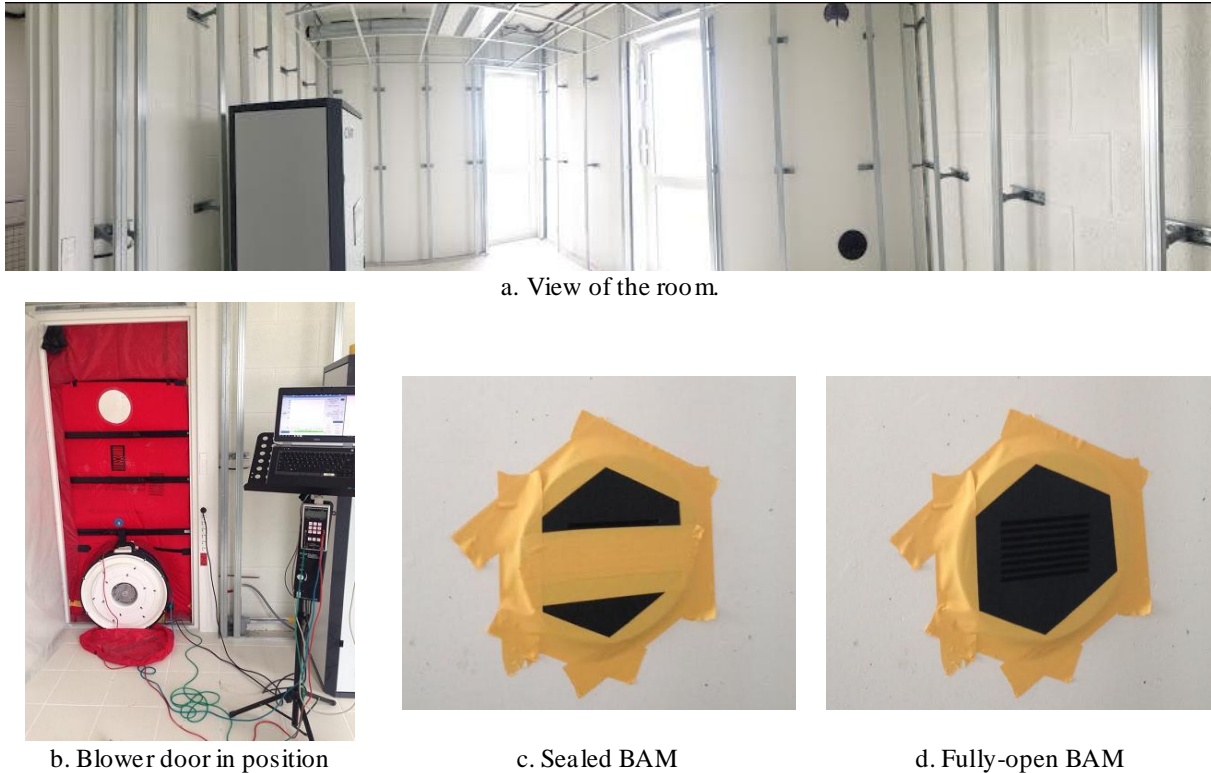


Figure 8: Experimental set-up in the test House.

Figure 9 presents the BAM characteristic curve obtained in this in-situ test. Similar deviation from the theory is observed with the same relative difference for high pressure gradient. This difference is slightly higher at 4 Pa in this case. Figure 10 presents a comparison between the curves from the lab. and in-situ tests for pressure gradient that can be encountered in real buildings (0 to 30 Pa). The difference between the two tests is essentially lower than 10% showing a good repeatability of the tests with two measurement equipment.

The difference between the theory used in the design process and the experimental results can come from limitation of the theoretical calculations. The correlation of Baker et al. (1987) has been developed for crack's length smaller than 15.2cm (the actual length of BAM is 30cm) and smooth surface (the surface presents a non-negligible roughness). In this way, pressure losses may have been underestimated by the theory. Another factor is the possible interaction among the airflows exiting from the cracks that may increase the pressure drop in relation to the theory that supposes that the cracks' airflows are independent.

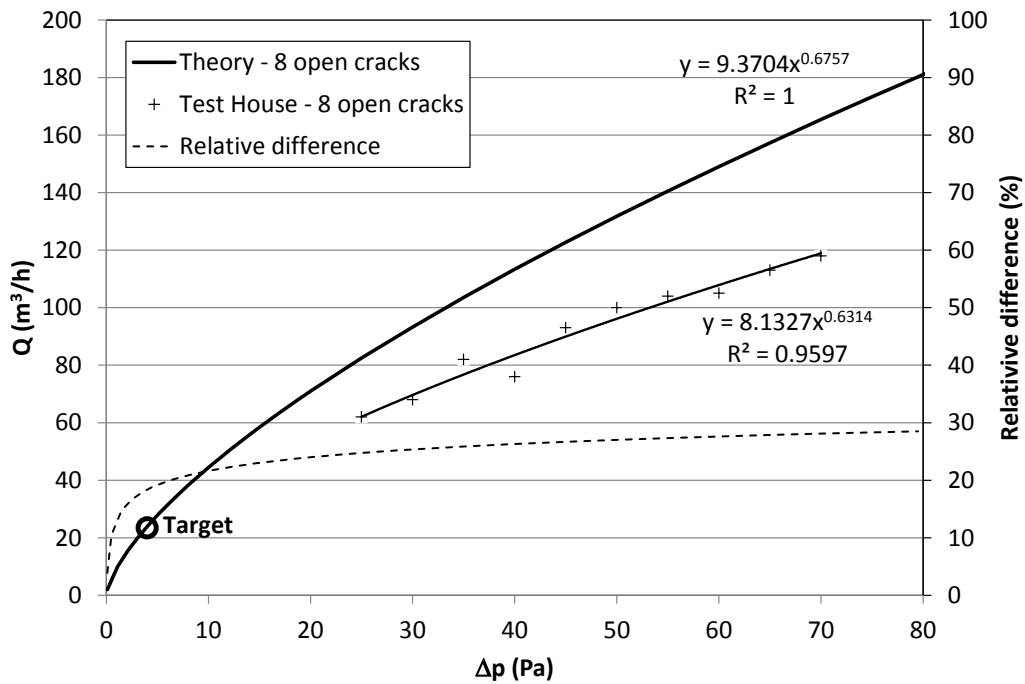


Figure 9: BAM characteristic curves obtained by in-situ measurement.

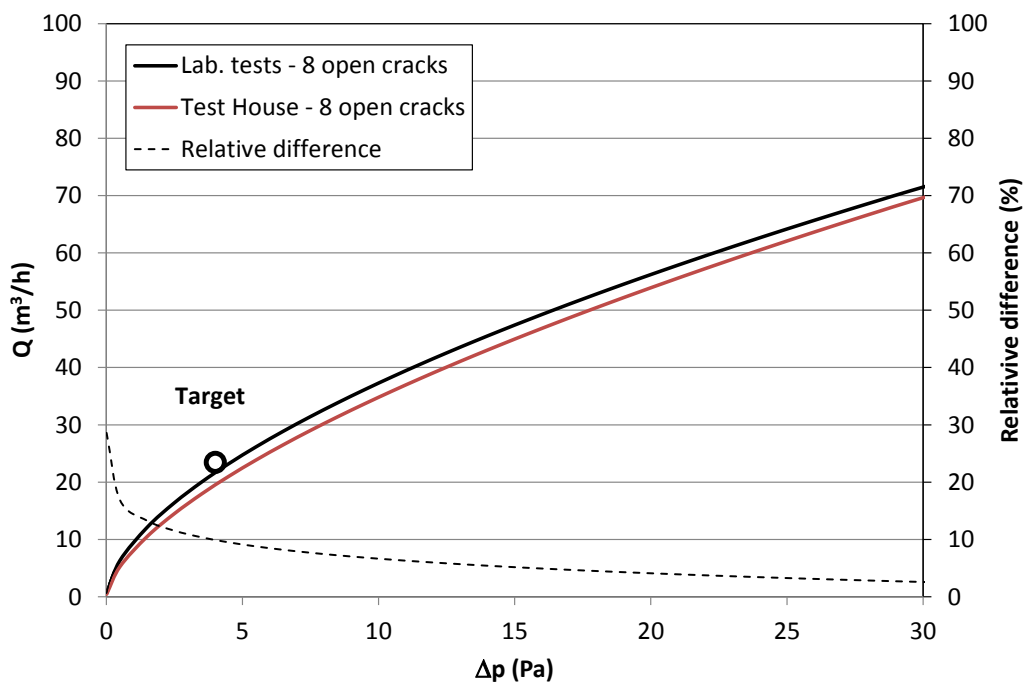


Figure 10: BAM characteristic curves obtained by lab. and in-situ measurements.

### 3.3 Perspectives

Perspective of this work is to allow the determination of the infiltration rate (airflow through the BAM) in the test house by simple measurement of pressure gradient at each module. In parallel of this work, pressure coefficients on the test house envelope have been measured according to wind direction in a small scale house in the wind tunnel of the Research Laboratory in Hydrodynamics, Energy and Atmospheric Environment (LHEEA). These

results with the BAM characteristic curve have been implemented into CONTAM to allow the modelling of the airflow through the envelope and in the house (Figure 11).



Figure 11: Scale model (left) and CONTAM simulation of natural ventilation through the BAM (right).

## 4 CONCLUSIONS

The motivations, designs and experimental testing regarding the development of the BAM for the Típee test House have been presented in this paper. A good agreement has been found between the characteristic curves obtained experimentally in a lab bench and in-situ. On the whole, the actual airflows through the BAM are slightly lower than initially expected considering same pressure gradient. However, the BAM will still be able to represent the whole range of envelope permeability encountered in the French buildings. Moreover, those measured correlations will be used to model the airflows through the building envelope for projects related to energy consumption and IAQ.

## 5 ACKNOWLEDGEMENTS

Marc Abadie, associate Professor at University of La Rochelle, wants to thank all students from the Civil Engineering Department that took part of this development in the frame of their research projects during the last 3 years.

## 6 REFERENCES

- Bailly, A., Guyot, G., Leprince, V. (2015). 6 years of envelope airtightness measurements performed by French certified operators: analyses of about 65,000 tests. *Proceedings of the 36<sup>th</sup> AIVC – 5<sup>th</sup> TightVent – 3<sup>rd</sup> Venticool Conference*, 23-24 September, Madrid, Spain.
- Bailly, A., Guyot, G., Leprince, V. (2016). Analyses of About 90,000 Airtightness Measurements Performed in France on Residential and Non-Residential Buildings from 2008 to 2014. *Proceedings of the ASHRAE and AIVC IAQ 2016—Defining Indoor Air Quality: Policy, Standards and Best Practices*, Alexandria, Virginia, USA, September 12–14, 2016.
- Baker, P.H., Sharples, S., Ward, I.C. (1987). Airflow Through Cracks, *Building and Environment*, 22, 293–304.
- D'Ambrosio Alfano, F.R., Dell Isola, M., Ficco, G., Tassini, F. (2012). Experimental analysis of airtightness in Mediterranean buildings using the fan pressurization method. *Building and Environment*, 53, 16–25.

EN ISO 9972:2015. *Thermal performance of buildings – Determination of air permeability of buildings – Fan pressurization method*. (ISO 9972:1996, modified).

Fernández-Agüera, J., Domínguez-Amarillo, S., José Sendra, J., Suárez, R. (2016). An approach to modelling envelope airtightness in multi-family social housing in Mediterranean Europe based on the situation in Spain. *Energy and Buildings*, 128, 236-253,

Orme, M., Liddament, M., Wilson, A. (1998). Numerical data for Air Infiltration and Natural Ventilation Calculations. *AIVC Technical Note 44*, 108p.

Walker, I.S., Sherman, M.H., Joh, J. and Chan, W. R. (2013). Applying Large Datasets to Developing a Better Understanding of Air Leakage Measurement in Homes. *Journal of Ventilation*. March.

Walther, W., Rosenthal, B. (2009). Airtightness Testing of Large and Multi-family Buildings in an Energy Performance Regulation Context. *Information Paper no P165*, EPBD buildings platform.

# Component leakage: potential improvement graphs and classification of airpaths

Martin Prignon<sup>\*1</sup>, Felipe Ossio<sup>2</sup>, Manon Brancart<sup>3</sup>, Arnaud Dawans<sup>3</sup> and Geoffrey van Moeseke<sup>1</sup>

*1 Université catholique de Louvain  
Place de l'Université, 1,  
B-1348 Louvain-la-Neuve, Belgium  
[\\*martin.prignon@uclouvain.be](mailto:martin.prignon@uclouvain.be)*

*2 Pontificia Universidad Católica de Chile  
Avda. Libertador Bernardo O'Higgins, 340  
Santiago, Chile*

*3 Entreprises Jacques Delens S.A.,  
Av du Col vert, 1,  
1170 Brussels, Belgium*

## ABSTRACT

Last years, interest in airtightness increases among all construction fields and airtightness becomes a major issue in the reduction of energy consumption in buildings. Nevertheless, there is a lack of understanding of air displacements through weak spots in buildings (airpaths). Firstly we develop first the concept of **Potential Improvement Graph** (PIG chart). These graphs represent the “improvement curves” of a given airpath (airflow indicator against airpath parameter). As an airpath can have multiple significant parameters, PIG charts can be n-dimension graphs. Such curves could be used by the contractor to anticipate the impact of a corrective measure on the airflow. Secondly we define three types of airpaths: opening, junction and residual. We suggest that a discontinuity in the air barrier can always be defined as a function of these three types of airpaths. This paper concludes on opportunities given by this work. (1) It could be used as a basis for other projects on air leakage at airpath scale. Such projects would force the researcher, and help the reader, to understand issues of air displacements. (2) This work can also be used as a basis for the development of tools to help field actors to deal with airtightness. Such tools would encourage their users to think in terms of air displacement.

## KEYWORDS

Airtightness ; Air leakage path ; Air displacement ; Classification ; Component leakage

## 1 INTRODUCTION

Projects and research aiming to reduce energy consumption in buildings are encouraged for several years now. First years, air leakage issue was hardly tackled in these projects, even if it could be responsible for up to 30% of the heating demand in winter (Kalamees, 2007) (Meiss & Muñoz, 2015). However, recently requirements about airtightness increasingly appear in regulations or in specifications for buildings. Airtightness becomes a big issue for many actors in the construction field, which are often powerless to deal with this little known concept.

The complexity of creating new airtightness predictive models and using existing ones has already been highlighted (Prignon & van Moeseke, 2017). The same paper highlighted the capabilities of single component models to be used as suitable tools for practical use. To develop these models, there is a need to focus on the understanding of air displacements around “airpaths”. We define here an airpath as a spot in the building where air can leak (e.g. porous surfaces or flaws in building components among others).

Single component models study individually different airpaths of the building and consider the total building leakage as a sum of all these airpaths. Interesting point in these models is that they focus on the understanding of air displacements. Such understanding could help to interpret some observations made as the difference between results of tests in pressurization or in depressurization (d'Ambrosio Alfano, Dell'Isola, Ficco, & Tassini, 2012). Unfortunately, existing single component models are often outdated (Orme, Liddament, & Wilson, 1998) or currently not enough developed (Hassan, 2013).

This paper is part of the “AirPath50” project which aims to develop the understanding of air displacements at airpath scale. In this paper we present first the concept of PIG charts (airflow against a chosen parameter). Secondly, we suggest the classification of airpaths in 3 main types covering all different situations of air barrier discontinuity encountered in practice.

## 2 PIG CHARTS

We stress the importance of understanding air displacements at weak spots of the building. Graphs develop in this context represent the airflow (or an airflow indicator) against a main airpath parameter. These graphs give a powerful visualization of the airpath both in a theoretical and a practical point of view. In a fundamental way, these graphs describe different phenomena (equations, models) governing the displacement of air and they develop the limits between different phenomena. In a practical way, a contractor can extract from these graphs the potential impact of one or another airpath on the building air leakage. Thus he can prioritize its actions as function of their impact, this is why we called these graphs “**Potential Improvement Graphs**” (PIG charts).

We develop the case of a circular opening in a plate to give a better understanding of these graphs. In this example, the PIG chart represents the airflow against the radius of the opening (Figure 1). For the creation of this PIG chart we consider a theoretical case of a plate of 1m x 1m, of 0.5 m width, with a medium porosity of  $10^{-12}$  m<sup>2</sup> and a discharge coefficient of 0.6. Air density and air velocity are taken at 275K. A pressure difference of 50 Pascal is applied between both sides of the plate and the air can flow only through the surface and the opening. Four different behaviors are considered and explained hereafter (I, II, III and IV on the figure).

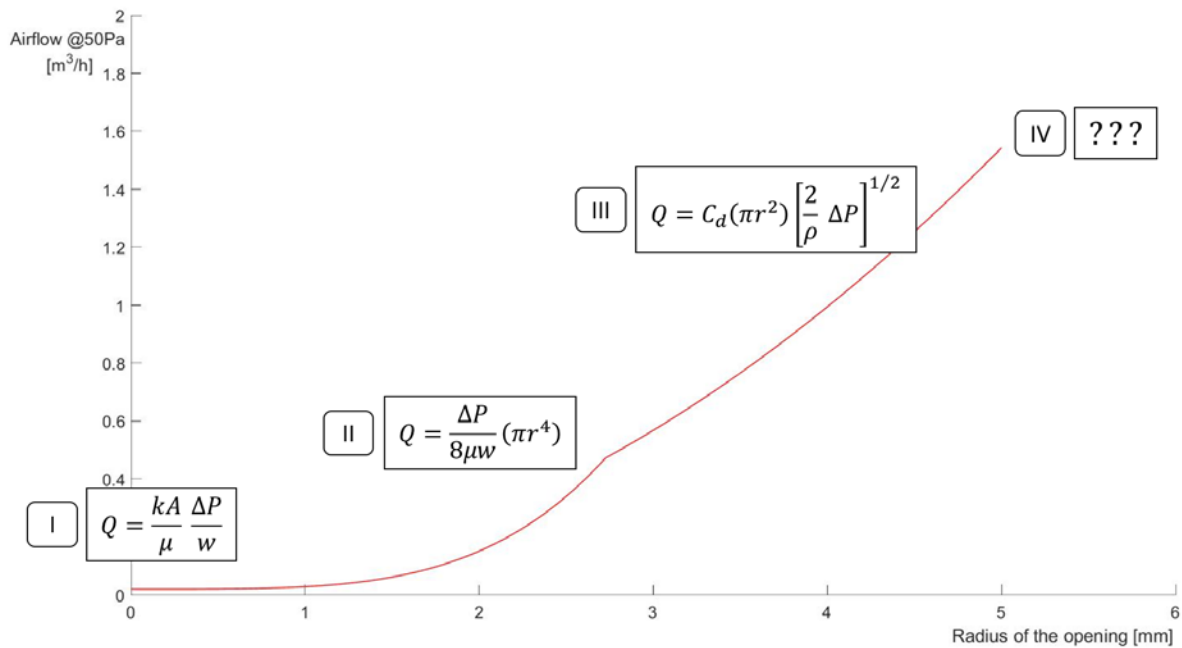


Figure 1: PIG chart for the case of a circular opening in an infinite plate

- When the radius is zero, air flows only through the surface and is computed with Darcy's law (equation 1). It depends then on the permeability of the porous medium ( $k$ ), the area of the surface ( $A$ ), the dynamic viscosity of the fluid ( $\mu$ ), the pressure difference ( $\Delta P$ ) and the width of the plate ( $w$ ). We consider the air flow through only one square meter of plate.

$$Q = \frac{kA \Delta P}{\mu w} \quad (1)$$

- Once the radius increases, air looks for the path of least resistance and flows through the hole. When the radius is very small, the flow can be modeled by equation 2 (flow through a cylinder). In this case airflow is highly depending on the radius ( $r^4$ ) of the opening.

$$Q = \frac{\Delta P}{8\mu w} (\pi r^4) \quad (2)$$

- At some point, flow is governed by the orifice equation (equation 3). The airflow depends less on the radius ( $r^2$ ) but depends on the air density ( $\rho$ ) and discharge coefficient ( $C_d$ ). The discharge coefficient takes into account the fact that the opening is not an ideal nozzle. It takes positive values lower than 1 (1 is for the perfect nozzle).

$$Q = C_d(\pi r^2) \left[ \frac{2}{\rho} \Delta P \right]^{1/2} \quad (3)$$

- When the radius is very large, two issues can be encountered and the model becomes much more complex. First, the airflow becomes too important for the hypothesis. Until here, airflow models consider the pressure difference between both sides as constant. But if ratio between volume and airflow is too small, the problem is not

static anymore and the pressure difference can vary in time. This is never the case if both volumes are considered as infinite, but it can still be encountered in practice and must be mentioned. Second, often in multilayers surfaces only the layer responsible for airtightness (air barrier) is considered since its resistance is much higher than other layers. But when the resistance of this layer becomes too small, other layers have to be taken into account as new airpaths hidden behind the air barrier.

In the example, a clear break between behaviors II (flow through a cylinder) and III (flow through an orifice) can be seen (Figure 1). In real cases, the transition would be much smoother and the PIG charts would be more like Figure 2.

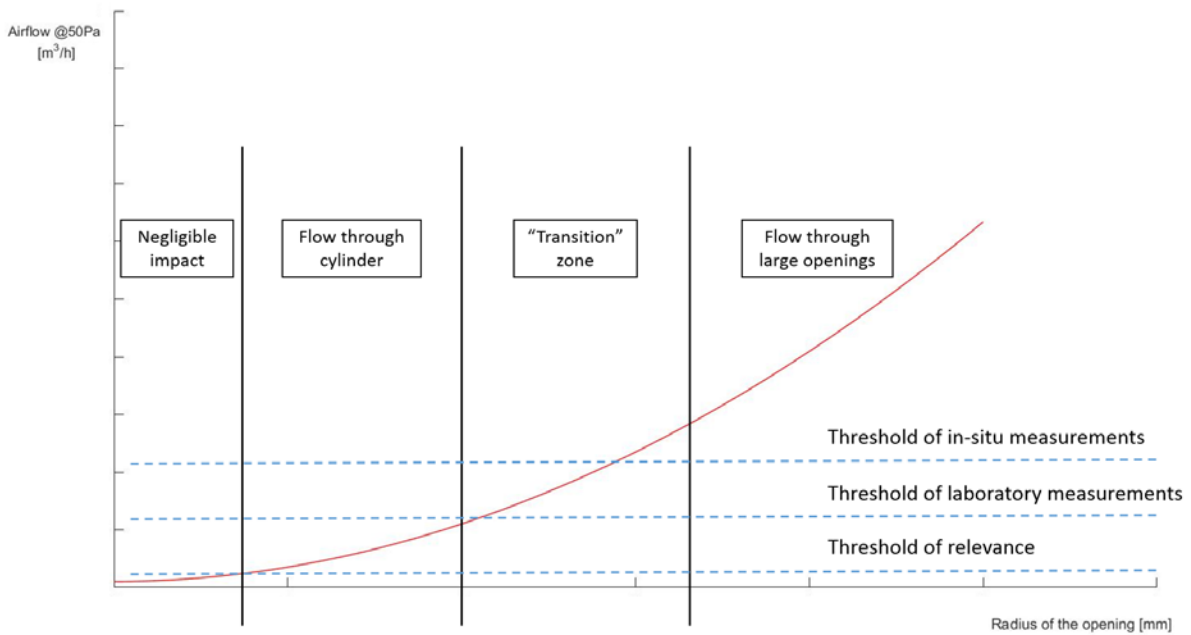


Figure 2: Smooth PIG chart with transition zone

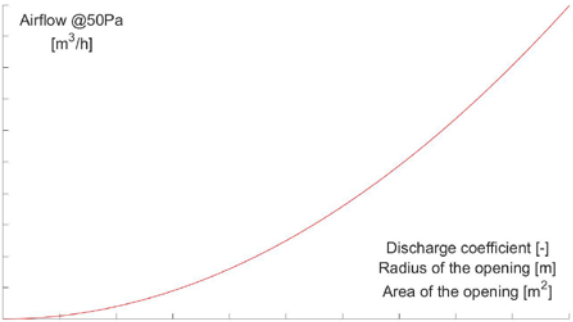
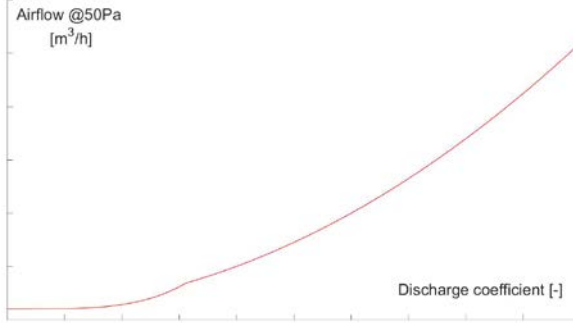
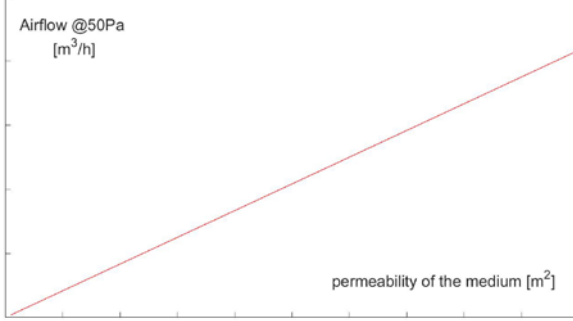
Some point of the PIG chart are not relevant since their values are too low to have a significant impact on total building airtightness (threshold of relevance). There are also two thresholds related to measurement equipment and measurement conditions (thresholds of in-situ and laboratory measurements). These three threshold are represented with dot lines on the graph Figure 2.

The “AirPath50” project aims to establish PIG charts through numerical simulations, in-situ tests and laboratory tests. We have to tackle many scientific issues related to these graphs. First, the issue of uncertainties in the case of in-situ and laboratory measurements (necessary to establish two thresholds). Second, the issue of the definition of a minimum “relevant value” in practice (necessary to establish the third threshold). Third, the issue of limits between behaviors and of “transition zones”. Fourth, the issue of variability of parameters (as discharge coefficient in the above example) with main parameter variation (radius of the opening in the same example). Fifth the issue of parameter identification. Indeed, in the example of circular opening in infinite plate, we show the study of only one parameter (radius of the opening). Other graphs could be obtained for the same airpaths with other parameters (e.g. the width of the plate ( $w$ )). PIG charts should be n-dimensions graphs (with n parameters).

### 3 CLASSIFICATION OF AIRPATHS

In a perfect world, each airpath of each site should have its own PIG Chart. We try to make an exhaustive list of airpaths based on in-situ observations (tracer gas during fan pressurization testing), discussions with relevant professionals (one architect and three contractors) and reading of reports (Relander & Holøs, 2010) (Carrié, Jobert, & Leprince, 2012) and guides (Jaggs & Scivyer, 2009) (Mees & Loncourt, 2015). This list brings out many different situations, but all discontinuities in the air barrier can be simplified in a function of three main types of “theoretical airpaths” (Table 1).

Table 1: three types of airpath, example of real cases and suggested PIG charts

Description and example of theoretical airpaths	Expected PIG chart
<p><b>Opening</b>            In this airpath, the air flows through the element responsible for the discontinuity. Abscissa from PIG charts can depend on the component. This value can in some cases be obtained by the manufacturer.  <u>Ex:</u> electrical outlet, window, door, ventilation ducts.</p>	
<p><b>Junction</b>            In this airpath, the air flows through the junction between the air barrier and the element responsible for the discontinuity. This element can be another air barrier.  <u>Ex:</u> junction between two air barriers, junction between an air barrier and a window or a door</p>	
<p><b>Residual</b>            In this airpath, the air flows through the remaining surface behind the discontinuity. It depends on the permeability of the medium.  <u>Ex:</u> remaining layers behind an electrical outlet</p>	

We suggest in this work that airflow passing through a discontinuity in the air barrier can always be described as a function of the three airpaths presented above. Three real cases are hereafter described in terms of airpaths:

- An electrical outlet appears in three categories: air flows through the openings of the electrical outlet itself (opening), through the junction between the box and the wall (junction) and through the remaining layers of the wall behind the electrical outlet (residual).
- A window appears only in two categories: air flows through the junction between window and wall (junction) and through the window flaws (opening). Airflow in the window depends on its class and on its surface.
- A ventilation duct appears in two categories: air flows through the tightening around the duct where air barrier is cut (junction) and through the flaws in the ducts (opening). Airflow through the ventilation duct depends on its class, on its perimeter and on its total length in the airtight envelope. Indeed, for the part of the duct inside the envelope, the duct itself becomes the air barrier.

Most of these cases are already known by contractors. For example, outlet are often encased in plaster to reduce the permeability of the medium of the “residual airpath”. Plaster also increases the quality of the junctions between the outlet and the wall. Nevertheless the plaster is sometimes not perfectly set (bottom of the box, Figure 6) and leaks can be observed at these points. PIG charts could be helpful for contractors to understand and quantify the impact of a poor execution.



Figure 6: electrical outlet encased in a wall<sup>1</sup>

A component can have many different airpaths, thus many different parameters. This is why study of local air leakage is complex and time consuming.

#### 4 CONCLUSION AND FURTHER WORK

In this paper, we present first the concept of PIG charts. These graphs represent airflow indicator against a chosen parameter. An airpath often depends on more than one parameter thus complete PIG charts can have n-dimensions. “n” is the number of parameters having a significant impact on airflows. Such graphs fit well in the “Airpath50” project since it helps to visualize air behavior at airpath scale. We define then three types of airpaths. We suggest that a discontinuity in an air barrier can always be defined as a function of these three types of airpaths.

---

<sup>1</sup> Picture from <http://www.selfmatic.be>

We highlight many issues in chapter 2 which have to be tackled early in the project:

- Calculation of uncertainties in the case of in-situ and laboratory measurements (necessary to establish two thresholds).
- Definition of a minimum “relevant value” in practice (necessary to establish the third threshold).
- Establishment of limits between behaviors and of “transition zones”.
- Study of variability of parameters (as discharge coefficient in the above example) with main parameter variation (radius of the opening in the same example).
- Identification of “n” parameters.

Further research could use this work as a basis to develop works on air leakage at building component scale. Such works would force researchers to understand issues of air displacements which are sometimes missing in current research. This work can also be used as a basis for the development of tools to help the contractor or the designer dealing with airtightness. Such tools would encourage their users to think in terms of air displacement.

## 5 ACKNOWLEDGEMENTS

We would thank the company *Jacques Delens* for its mobilization in this work and the availability of their construction sites. This work is part of the “AirPath50” project funded by INNOVIRIS.

## 6 REFERENCES

- Carrié, F. R., Jobert, R., & Leprince, V. (2012). Methods and techniques for airtight buildings. AIVC, Contributed Report 14.
- d'Ambrosio Alfano, F. R., Dell'Isola, M., Ficco, G., & Tassini, F. (2012). Experimental analysis of air tightness in Mediterranean buildings using the fan pressurization method. *Building and Environment*, 53, 16-25.
- Hassan, O. A. (2013). An alternative method for evaluating the air tightness of building components. *Building and environment*, 67, 82-86.
- Jaggs, M., & Scivyer, C. (2009). A practical guide to building airtight dwellings. NHBC foundation.
- Kalamees, T. (2007). Air tightness and air leakages of new lightweight single-family detached houses in Estonia. *Building and Environment*, 42(6), 2369-2377.
- Mees, C., & Loncourt, X. (2015). L'étanchéité à l'air des bâtiments. *Technical Information Note*. Belgian Building Research Institute.
- Meiss, A., & Muñoz, F. J. (2015). The energy impact of infiltration: a study on buildings located in north central Spain. *Energy Efficiency*, 8(1).
- Orme, M., Liddament, M. W., & Wilson, A. (1998). Numerical Data for Air Infiltration & Natural Ventilation Calculations. *Technical Note AIVC 44*. International Energy Agency.

Prignon, M., & van Moeseke, G. (2017). Factors influencing airtightness and airtightness predictive models: A literature review. *Energy and Buildings*, 146, 87-97.

Relander, T.-O., & Holøs, S. B. (2010). Testing a component method to estimate the airtightness of windtightened wood-frame houses. *Project Report 66*. Sintef.

# The effect of refurbishment and trickle vents on airtightness: the case of a 1930s semi-detached house.

Ben Roberts<sup>\*1</sup>, David Allinson<sup>1</sup>, Kevin Lomas<sup>1</sup>, and Stephen Porritt<sup>1</sup>

*1 School of Civil and Building Engineering  
Loughborough University  
Loughborough, UK  
Presenting author*

*\*Corresponding author: b.m.roberts@lboro.ac.uk*

## ABSTRACT

As UK homes are insulated and draught proofed in an attempt to reduce wintertime heating demand they become more airtight. Any reduction in infiltration could have a detrimental effect on indoor air quality. Controllable background ventilation provided by trickle vents is one method of maintaining indoor air quality.

A 1930s semi-detached 3-bedroom house was refurbished with double-glazed windows, trickle vents, doors and loft insulation. 167 blower door tests were carried out pre- and post-refurbishment between January and March 2017 to understand the repeatability of the test and quantify how trickle vents affect airtightness.

The refurbishment reduced air leakage by 29% from 20.8 to 14.7 m<sup>3</sup>/h/m<sup>2</sup> at 50Pa (with all windows and trickle vents closed), but still in excess of the current UK regulations for new builds (10 m<sup>3</sup>/h/m<sup>2</sup> at 50Pa). Opening trickle vents provided limited additional ventilation, only increasing air change rate by 1.8 m<sup>3</sup>/h/m<sup>2</sup> with all vents open. The test was found to be repeatable with a standard error of 0.07 m<sup>3</sup>/h/m<sup>2</sup> at 50Pa with no relationship between the test result and wind speed or direction.

The results lead to two important conclusions. Firstly, after refurbishing older homes of this type, infiltration rates are still well above recommendations for adequate indoor air quality. Secondly, the omission of trickle vents in older homes may not unduly diminish indoor air quality.

## KEYWORDS

Houses; refurbishment; airtightness; measurement; trickle vents.

## 1 INTRODUCTION

Houses are refurbished to improve energy efficiency and airtightness to reduce heating energy demand and improve thermal comfort. This can reduce unintended infiltration, potentially allowing indoor pollutants to build up (Sullivan, et al., 2013). Poor indoor air quality (IAQ) occurs when the presence of airborne pollutants impairs the health or comfort of building occupants. To ensure good IAQ, ventilation must be at a sufficient level to provide outdoor air for breathing, dilution and removal of pollutants and odours, control of humidity and provision of air for fuel-burning appliances (HM Government, 2010). Such ventilation may be provided by operable windows but in modern houses trickle vents are installed to ensure the provision of a steady, draught free, background airflow. Trickle vents are integrated into windows frames and can be manually opened or closed.

Hong (2004) measured airtightness using fan pressurisation in 191 English dwellings pre- or post-refurbishment. Refurbishments included loft insulation, cavity wall insulation, draught proofing and new central heating systems. Only a small improvement in airtightness (0.7 m<sup>3</sup>/h/m<sup>2</sup> at 50Pa) was found between pre- and post-refurbishment dwellings, owing to the improvement in airtightness from measures like cavity wall insulation and draught proofing being offset by new envelope penetrations. The same study states that whilst loft insulation

can contribute to a  $4\text{m}^3/\text{h}/\text{m}^2$  at 50Pa increase in airtightness, poor installation such as leaving large gaps at the eaves can render this measure ineffective (Hong, et al., 2004).

Oreszczyn, et al.(2005)conducted blower door tests on 10 houses that had replacement windows and found a mean reduction in air change rate of 0.2 ACH. They suggest that the installation of new windows could have a significant effect on the airtightness of homes and that 65% of UK homes installed with new windows could have air change rates below 0.5ACH. The authors suggest that the installation of trickle vents might be beneficial to improve IAQ, but did not directly test this.

Gillott, et al. (2016) measured the airtightness of a recently built test house constructed in the style of a 1930s semi-detached house during a phased retrofit programme. Replacement of single-glazing with double-glazing, and loft and cavity wall insulation reduced infiltration by 12%. Draught-proofing yielded a 41% reduction. Sealing envelope pipe penetrations reduced infiltration by 11%. Floorsealing at the skirting boards reduced infiltration by 33%.

Purpose-provided openings like trickle vents are specified for installation in new build homes to ensure ventilation rates are sufficient to ensure good IAQ(HM Government, 2010). However, monitoring of exhaled  $\text{CO}_2$  in newly-built dwellings shows that trickle vents may be ineffective in providing sufficient fresh air with Sharpe et al. (2015) reporting  $\text{CO}_2$  concentrations up to 1571ppm in bedrooms with trickle vents open, compared to 972ppm with windows open. In an energy-efficient dwelling, bedroom  $\text{CO}_2$  concentrations of 3500ppm were measured, despite trickle vents being open (McGill, et al., 2015).

The current UK building regulations do not require the installation of trickle vents in refurbished windows where they did not already exist (HM Government, 2010). However the building regulations do state that if the room is not otherwise adequately ventilated it would be good practice to fit trickle vents. In existing dwellings, habitable rooms should have trickle vents sized to a minimum of  $5000\text{mm}^2$  equivalent area<sup>1</sup> (EA) and in wet rooms  $2500\text{mm}^2$  EA (HM Government, 2010).

This paper aims to quantify the effects of refurbishment on airtightness in a UK house and assess whether trickle vents installed to building regulation standards are capable of providing sufficient fresh outdoor air for satisfactory indoor air quality. Data are presented from 167 blower door tests pre- and post-refurbishment of a 1930s semi-detached house, including various trickle vent opening areas. Comment is made on the repeatability of the blower door test method.

---

<sup>1</sup>A measure of the aerodynamic performance of a ventilator. It is the area of a sharp-edged circular orifice which air would pass through at the same volume flow rate, under an identical applied pressure difference as the opening under consideration(HM Government, 2010).

## 2 METHODS

### 2.1 Test house description



Figure 1 – Ashby Road Test Houses pre-refurbishment, only the left house was used



Figure 2 – Ashby Road Test Houses post-refurbishment, only the left house was used

The test facility comprises a matched pair of two adjoining unoccupied semi-detached two-storey houses. In this study, the left hand house (Figure 1 and Figure 2) was used. The house is located in a residential area of Loughborough, UK ( $52.7721^{\circ}$  N,  $1.2062^{\circ}$  W). The front of the house faces south towards a front garden and a road, the rear of the property faces north to a large back garden and adjoins the other house to the east. There are neighbouring houses of similar roof heights to the east and west.

The house has a total floor area of  $90\text{m}^2$  including both floors and a total volume of  $216\text{m}^3$  (Figure 5). The house was built in the 1930s in a manner typical of the era with uninsulated brick cavity walls and suspended timber floors ventilated below by air bricks. Until 2016 the houses had been largely unrefurbished since their construction (Figure 1) apart from open fireplaces in the living and dining rooms which were removed, bricked up and plastered. During the summer of 2016 the single-glazed wooden-framed windows were replaced with uPVC double glazing throughout which included replacement of 3 existing wooden doors with uPVC doors. The roof was re-tiled at the same time and the loft insulated with the loft hatch insulated but not draught-stripped. Prior to this in 2015, existing wooden fascia and soffits at the eaves were replaced with uPVC (Figure 2). Refurbishment works and associated U-values are listed in Table 2. Prior to commencement of testing all wall and fireplace vents were internally sealed with aluminium tape. Air bricks ventilating the subfloor were left unblocked (see Figure 5 for locations).

The new double glazing was installed with trickle vents to the building regulation specification for existing dwellings (HM Government, 2010). To comply, habitable rooms must have a minimum  $5000\text{mm}^2\text{EA}$  and wet rooms (kitchen and bathroom)  $2500\text{mm}^2\text{EA}$ . Trickle vents could be manually opened or closed using a flap shutter (Figure 3 and Figure 4).

Table 1 - Trickle vent locations (by room) and sizes

Room	Number of vents	Trickle vent equivalent area ( $\text{mm}^2$ )	Trickle vent geometric free area ( $\text{mm}^2$ )
Living room	4	5000	6400
Dining room	3	5000	6400
Kitchen	2	2500	3200
Bathroom	2	2500	3200
Rear bedroom	4	5000	6400
Front bedroom	4	5000	6400
TOTAL	19	25000	32000



Figure 3 – Trickle vent closed



Figure 4 – Trickle vent open

Indoor temperature data were collected in the houses via Grant U-type thermistors<sup>2</sup> connected to a DT85 Datalogger in order to provide inputs to blower door fan control software and for comparison with measured airtightness. A thermistor was placed in the volumetric centre of every room and shielded from incoming solar radiation. Outdoor temperature data were collected using the same thermistor as used indoors and connected to the same data logger. The outdoor sensor was shielded in a naturally aspirated EML SS1 sensor shield (EML, 2017) and placed to the north of the houses to further reduce interference from solar radiation. Indoor and outdoor temperatures were logged at one minute intervals during testing. All thermistors were calibrated prior to placement using a temperature-controlled water bath and calibrated thermometer.

Wind data was sourced from the University weather station approximately 1km from the test house and measured at one minute intervals.

Table 2 – Pre- and post-retrofit U-values of construction elements. U-values from SAP(BRE, 2014).

Building element	Pre-retrofit	Estimated U-value (W/m <sup>2</sup> K)	Post-retrofit	Estimated U-value (W/m <sup>2</sup> K)	Area (m <sup>2</sup> )
Roof	No loft insulation, pitched with clay tiles.	2.3	300mm fibreglass, pitched with clay tiles over vapour-permeable membrane	0.16	45.6 <sup>a</sup>
External walls	Brick internal/external uninsulated cavity	1.6	No change	1.6	81.6
Internal partition walls	Brick covered with gypsum plaster, wallpaper and paint	2.1	Re-painted	2.1	53.9
Party wall	As internal partition walls	0.5	Re-painted	0.5	42.2
Floors (except kitchen)	Suspended timber boards with carpet tile (linoleum in bathroom)	0.8	No change	0.8	40.2
Floors (kitchen)	Solid concrete and linoleum cover	0.7	No change	0.7	5
Windows	Single-glazed, wooden framed	4.8	New uPVC double glazing	1.4	20.3 <sup>b</sup>
External doors	Wooden, single-glazed sections	3	New uPVC with double glazing	1.4	5.5

<sup>a</sup> Horizontal area (not pitched).

<sup>b</sup> Total area including frames.

<sup>2</sup> Accuracy ±0.2°C (Grant Instruments (Cambridge) Ltd., 2017)

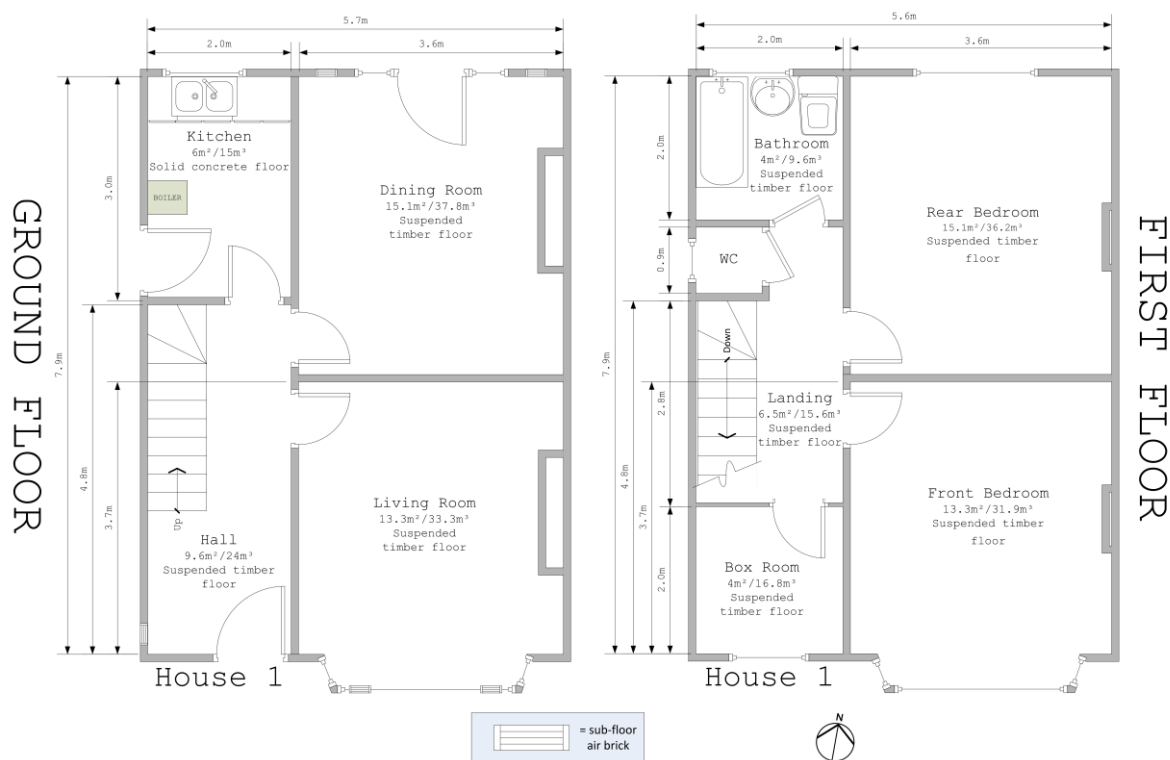


Figure 5 - Floor plan of house 1 (right side wall is a party wall).

## 2.2 Air tightness measurement

The airtightness of the house was measured with a Model 3 Minneapolis Blower Door via depressurisation. This method was selected due to its speed and simplicity compared to other methods for determining air change rates such as tracer gas techniques. The blower door test method uses the relationship between flow through the envelope and the pressure difference across it to quantify airtightness (Sherman, 1987).

In accordance with a standard testing protocol (ATTMA, 2016), all external doors and windows were closed and internal doors propped open. Water traps in sinks and baths were filled with water and wall vents and fireplace vents were sealed with aluminium tape. Gas central heating was turned off during testing. Trickle vents were opened or closed depending on the testing phase. The same operator conducted all tests, apart from the pre-retrofit test. At points during testing, direction of fan airflow was reversed to pressurise the building and smoke sticks used to qualitatively examine air leakage of particular building elements.

The air tightness measurements were conducted in three phases: pre-retrofit; post-retrofit with all vents closed; and post-retrofit with various amount of trickle vent opening. To determine which envelope opening to place the blower door into, six tests were carried out: two with the blower door in the front door, two in the side (kitchen door), and two in the rear door (dining room) on the same day. This examined which door was most suitable to use because sealing the blower door in a particular opening removes what could be a substantial leakage area from the results. The front door has a semi-circular upper portion and despite filling the arched portion with a wooden panel, a perfect seal could not be achieved (Figure 6). The kitchen door entered into a very small room and the internal door partially blocked the air-flow to the fan (Figure 5 (floorplan) and Figure 7). Therefore the rear dining room was selected as the door to use for all tests (Figure 8).



Figure 6 – Front door with a semi-circular wooden panel to fill the gap in the upper arch.



Figure 7 - Kitchen (side) door has potential interference from internal doors.



Figure 8 – Blower door apparatus set up in the rear door (dining room). All main tests were conducted from this opening.

The air infiltration data which forms this research was gathered from 167 separate blower door tests. One pre-retrofit (no trickle vents installed)(Beizaee, et al., 2015) and 166 post-retrofit.

Pre-retrofit airtightness data was collected on 3 July 2013 (Beizaee, et al., 2015) via a single test. Post-retrofit airtightness testing was conducted on 13 days between 4 January 2017 and 15 March 2017. 34 blower door tests were carried out with trickle vents closed, but not sealed (excluding the extra four tests on the front and side doors). This phase of testing provided comparison to pre-retrofit measurements, a baseline measurement for comparison with trickle vent opening and allowed comment on the repeatability of the testing under various internal/external environmental conditions. Ten additional tests were conducted with the trickle vents fully sealed with masking tape to test the airtightness of the brand new trickle vents in their closed position. Trickle vents were sealed and blower door tests performed on 3 February and 13 February to provide a variety of indoor/outdoor conditions. Trickle vent testing comprised 118 tests with at least one trickle vents open.

### 2.3 Data analysis

Data were analysed to compare pre- and post-refurbishment airtightness, the impact of trickle vent opening, and the repeatability of the fan pressurisation test. The results of a blower door test quantify the envelope leakage at an elevated pressure of 50Pa (Sherman, 1987). To derive a value for an estimate of the infiltration rate at normal pressure the K-P model was used by dividing  $ACH_{50}$  by 20 (Persily, 1982).

Air temperature data and wind data were averaged for the duration of each individual test to enable comparison between tests.

## 3 RESULTS

### 3.1 Pre- and post-refurbishment air tightness

The refurbishment reduced mean air leakage ( $q_{50}$ ) by  $6.1 \text{ m}^3/\text{h}/\text{m}^2$  (29%) with all windows and trickle vents closed (see Table 3 for summary of results). However, the post-refurbishment  $q_{50}$  value is still in excess of the current regulations for new builds ( $10 \text{ m}^3/\text{h}/\text{m}^2$ ).

Table 3 - Summary of blower door test results

q50 (m <sup>3</sup> /h/m <sup>2</sup> )	Pre-refurbishment		q50 (m <sup>3</sup> /h/m <sup>2</sup> )	Post-refurbishment	
	n50 (ACH <sub>50</sub> ) (1/h)	ACH (1/h)		n50 (ACH <sub>50</sub> ) (1/h)	ACH (1/h)
20.8	21.5	1.1	14.7	15.3	0.8

Using smoke sticks it was found that the new windows were well sealed, as were the trickle vents with flaps in the closed position. Air leakage identified by the smoke sticks was higher around plumbing and electrical penetrations, the insulated loft hatch, and the interface between the wall and the ground floor above the suspended, ventilated timber floor.

### 3.2 Impact of trickle vent opening

There was a linear relationship between the measured air tightness and the open geometric free area of trickle vents ( $r^2=0.86$ ) (Figure 9). Comparing sealed trickle vents with closed trickle vents, the mean q50 values were similar, 14.4m<sup>3</sup>/h/m<sup>2</sup> (n = 10) and 14.7m<sup>3</sup>/h/m<sup>2</sup> (n = 34), respectively. Compared to having no trickle vents open, when half the trickle vents required by the building regulations in new build properties was used, q50 increased by 6.7% (to 15.7m<sup>3</sup>/h/m<sup>2</sup>). Doubling the number of trickle vents to building regulation standard increased q50 by 12.2% to 16.5m<sup>3</sup>/h/m<sup>2</sup> (n50 = 17.24 ACH<sub>50</sub>), an increase of 1.8m<sup>3</sup>/h/m<sup>2</sup> at 50Pa or 0.1 ACH at atmospheric pressure.

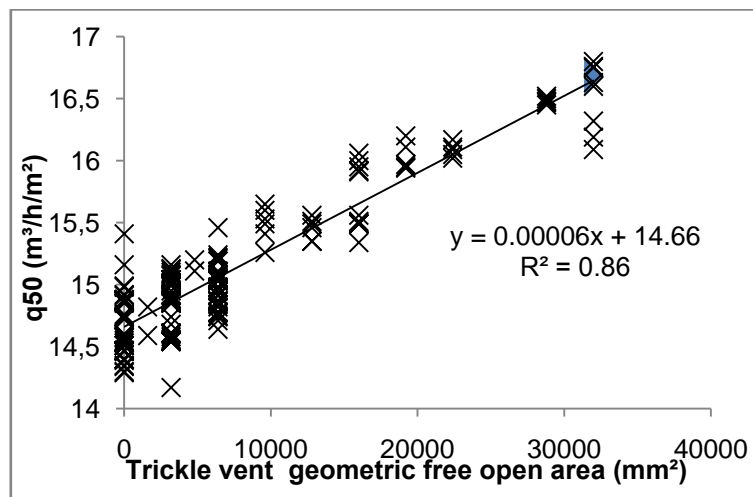


Figure 9 – Comparison of measured q50 to the geometric free area of trickle vent opening.

### 3.3 Repeatability of blower door test under various conditions

To test the repeatability of the blower door test method under a variety of internal and external conditions, 34 samples of measured airtightness with trickle vents closed collected over 13 days were used for analysis. The mean q50 value was 14.7m<sup>3</sup>/h/m<sup>2</sup> with a standard deviation of 0.2m<sup>3</sup>/h/m<sup>2</sup> and a standard error of 0.07m<sup>3</sup>/h/m<sup>2</sup>.

ATTMA (2016) notes that where wind speeds are higher than 6m/s the test results could be invalid. The maximum wind speed recorded during testing was 6.8m/s. Figure 10 shows no discernible relationship between q50 and wind speed. Therefore at this test site, under the wind regime experience the fan pressurisation test method can be applied under a variety of wind speeds without influencing the results. Similarly, measured q50 remains close to the mean value regardless of wind direction (Figure 11).

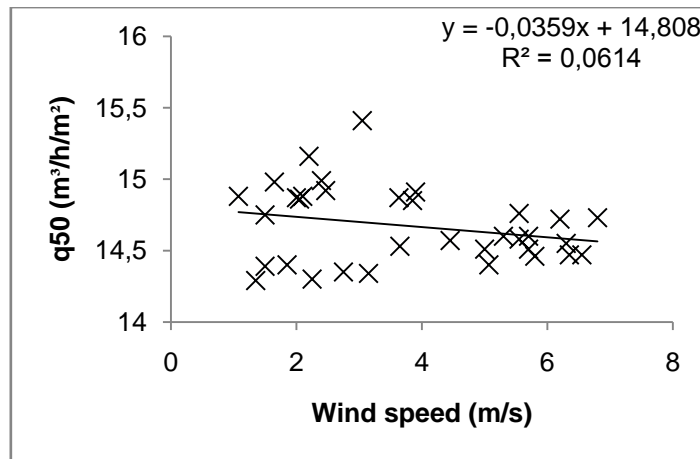


Figure 10–Comparison of measured wind speed to measured q50.

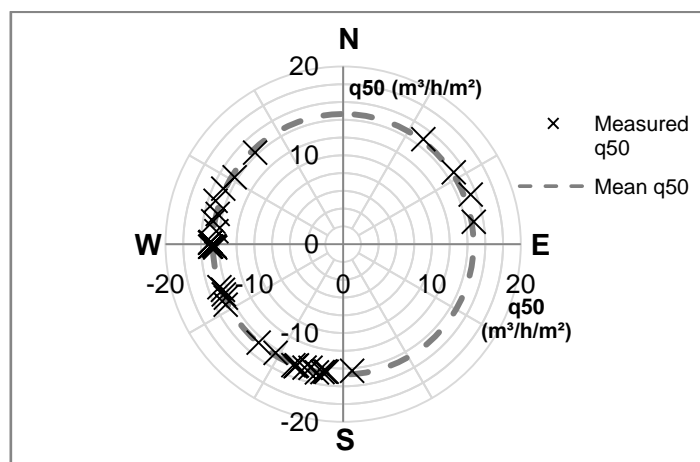


Figure 11 - Comparison of measured wind direction to measured and mean q50. North is top.

Indoor temperatures ranged from a maximum of 20.8°C to a minimum of 14.5°C. Outdoor temperatures ranged 15.3°C to 5°C. The maximum and minimum difference between indoor and outdoor temperature was 13°C and 0.9°C respectively. No clear relationship between  $\Delta T$  and q50 values was found (Figure 12).

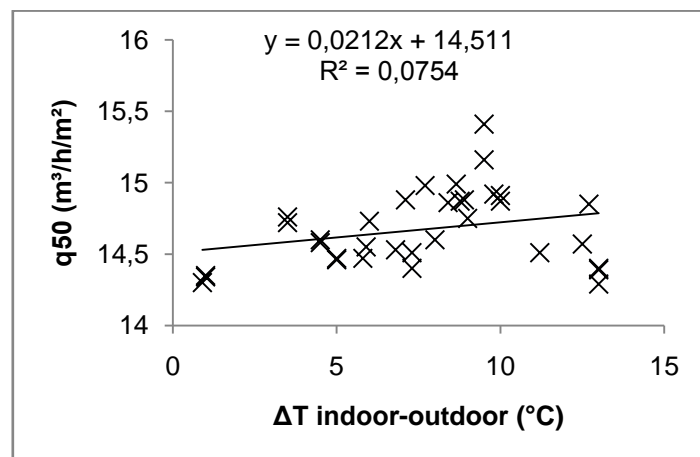


Figure 12 – Comparison of measured indoor-outdoor temperature against measured q50.

## 4 DISCUSSION

### Effect of refurbishment on airtightness

The air change rate of the dwelling, post-retrofit with trickle vents closed was 0.8 ACH. Studies have shown that health risks to humans rarely occur until air change rates fall below 0.5 ACH (Oie, et al., 1999; Emenius, et al., 2004; Emenius, et al., 2004). Therefore there is minimal risk to human health because of poor IAQ, even after retrofit, in a house of this type.

Even after significant refurbishment, the house was not particularly airtight in comparison to a new build property in the UK, where building regulations specify a maximum of  $10 \text{ m}^3/\text{h}/\text{m}^2$  (HM Government, 2014) or compared to the UK average of  $11.5 \text{ m}^3/\text{h}/\text{m}^2$  at 50 Pa (Stephen, 1998). Recent studies which have found air quality issues in refurbished and newly built homes are generally concerned with deep refurbishments or those built to Passivhaus standard or similar (Less & Walker, 2014; Langer, et al., 2015; Derbez, et al., 2014). It is unlikely that existing homes, such as the one studied will suffer air quality issues unless a deep refurbishment is undertaken, with a particular focus on airtightness.

Oreszczyn et al. (2005) measured a mean reduction in air change rate of 0.23 ACH after new double-glazing was installed in 10 dwellings. This study found a very similar reduction, 0.3 ACH, but unlike the aforementioned study included loft insulation and door replacement.

This study found that replacement glazing (in combination with loft insulation) was considerably more effective in increasing airtightness than the findings of Gillott, et al. (2016) which was for a house of similar construction and layout. However, this study used a real original 1930s house, which prior to refurbishment had wooden-framed single-glazing. Gillott, et al. (2016) upgraded wooden-framed single-glazing to double-glazing, but the house was built in 2007 to a 1930s construction style. Therefore the single-glazing was likely to be in better condition than in the 1930s house in this study. Gillott, et al. (2016) mention this issue in their paper, which leads to the conclusion that draught proofing and floor sealing is the most effective measure in improving airtightness. However, the findings of this study indicate that in a real house, with poorly fitting single-glazing in decaying wooden frames, replacing windows could improve airtightness.

### Effect of trickle vent opening on airtightness

Opening all trickle vents to UK building regulation standards provided only a small increase in air change rate of 12.2% (from 14.7 to  $16.5 \text{ m}^3/\text{h}/\text{m}^2$  at 50 Pa, all closed to all open respectively).

A study in Scottish dwellings found that once trickle vents are set in position, open or closed, they are very rarely changed again (Sharpe, et al., 2015). However in older, less airtight homes, such as the one studied, air quality issues are not likely to arise regardless of what position the trickle vents are left in.

### Limitations and further work

A limitation of this study is that indoor air quality is not measured directly, because indoor pollutants like humidity,  $\text{CO}_2$  and VOCs are not generated due to the houses being unoccupied and largely unfurnished. Therefore all assumptions on provision of indoor air quality are based solely on measured airtightness. This is problematic because the relationship

between ventilation rates and IAQ is complex due to transient effects, the characteristics of specific sources, and other factors (Persily, 2016).

Further limitations include wind data being sourced from the University weather station 1km away from the test house. Due to the nature of local topography and sheltering or canyoning effects of surrounding buildings and trees the onsite wind speed and direction may have differed somewhat from the data used.

Further work could explore how further refurbishment, such as insulation of the brick cavity, draught proofing and addressing the gaps around the ventilated suspended timber floor affects the airtightness of the house. The use of tracer gas to directly measure ventilation rate, rather than air leakage at elevated pressure could provide a true measure of infiltration rather than airtightness at elevated pressure.

## **5 CONCLUSIONS**

The results lead to two main conclusions. Firstly, refurbishing older homes of this type is unlikely to have a negative impact on indoor air quality because measured airtightness exceeds standards for new build dwellings. Therefore, the omission of trickle vents, which are not stipulated in building regulations for existing dwellings may not unduly diminish indoor air quality in older, less airtight homes.

Refurbishing a 1930s semi-detached house with loft insulation and new double-glazing reduced air leakage of the dwelling by 29% ( $6.1\text{m}^3/\text{h}/\text{m}^2$ ) from 20.8 to  $14.7\text{m}^3/\text{h}/\text{m}^2$  at 50Pa in what was, and remains, a leaky house in comparison to current UK standards for new builds. Trickle vents provided limited additional ventilation of  $1.8\text{m}^3/\text{h}/\text{m}^2$  at 50Pa (from  $14.7$  to  $16.5\text{m}^3/\text{h}/\text{m}^2$  at 50Pa, all closed to all open respectively), an increase of 12.2% when opened to UK building regulation stipulated levels. Whilst not a concern for a leaky home such as the one studied, this could have negative implications for air quality in a more airtight home which relies on trickle vents to provide sufficient background ventilation.

The blower door test was found to be repeatable with a standard error of  $0.07\text{m}^3/\text{h}/\text{m}^2$  at 50Pa based on 34 tests with trickle vents closed. There was no relationship between air tightness and wind speed or direction, or the indoor/outdoor temperature difference.

## **6 ACKNOWLEDGEMENTS**

This research was made possible by Engineering and Physical Sciences Research Council (EPSRC) support for the London-Loughborough Centre for Doctoral Research in Energy Demand (grant EP/L01517X/1). The authors acknowledge the assistance of Noamson Pillai with some of the tests. Loughborough University is acknowledged for funding the majority of the refurbishments outlined in this paper and for continued maintenance of the test houses and security provision.

## 7 REFERENCES

- ATTMA, 2016. *Technical Standard L1: measuring air permeability in the envelopes of dwellings*. Buckinghamshire: The Air Tightness Testing & Measurement Association.
- Beizaee, A. et al., 2015. Measuring the potential of zonal space heating controls to reduce energy use in UK homes: the case of un-furnished 1930s dwellings. *Energy and Buildings*, Volume 92, pp. 29-44.
- BRE, 2014. *The Government's Standard Assessment Procedure for Energy Rating of Dwellings*, Garston, Watford: Building Research Establishment.
- Derbez, M. et al., 2014. Indoor air quality and comfort in seven newly built, energy-efficient houses in France. *Building and Environment*, Volume 72, pp. 173-187.
- Emenius, G. et al., 2004. Building characteristics, indoor air quality and recurrent wheezing in very young children (BAMSE). *Indoor Air*, 1(14), pp. 34-42.
- Emenius, G. et al., 2004. Indoor exposures and recurrent wheezing in infants: a study in the BAMSE cohort. *Acta Paediatrica*, 7(93), pp. 899-905.
- EML, 2017. *SS Range of Naturally Aspirated Sensor Shields*, North Shields, UK: Environmental Measurements Limited.
- Gillott, M. et al., 2016. Improving the airtightness in an existing dwelling: the challenges, the measures and their effectiveness. *Building and Environment*, Volume 95, pp. 227-239.
- Grant Instruments (Cambridge) Ltd., 2017. *Temperature and humidity probes*. s.l.:Grant Instruments (Cambridge) Ltd..
- HM Government, 2010. *The Building Regulations Approved Document F: ventilation (2010 edition incorporating 2010 and 2013 amendments)*, London: HM Government.
- HM Government, 2014. *The Building Regulations 2010 Approved Document L1A: conservation of fuel and power in new dwellings, 2013 edition with 2016 amendments*, London: HM Government.
- Hong, S., Ridley, I. & Oreszczyn, T., 2004. *The impact of efficient refurbishment on the airtightness in English dwellings..* Prague, Czech Republic, 25th AIVC (Air Infiltration and Ventilation Centre) Conference. 15-17 September, 2004.
- Langer, S. et al., 2015. Indoor air quality in passive and conventional new houses in Sweden. *Building and Environment*, Volume 93, pp. 92-100.
- Langer, S. et al., 2016. Indoor environmental quality in French dwellings and building characteristics. *Atmospheric Environment*, Volume 128, pp. 82-91.
- Less, B. & Walker, I., 2014. *Indoor Air Quality and Ventilation in Residential Deep Energy Retrofits*, Berkeley, CA (US): Ernest Orlando Lawrence Berkeley National Laboratory.

- McGill, G., Oyedele, L. O. & McAllister, K., 2015. Case study investigation of indoor air quality in mechanically ventilated and naturally ventilated UK social housing. *International Journal of Sustainable Built Environment*, 4(1), pp. 58-77.
- Oie, L. et al., 1999. Ventilation in homes and bronchial obstruction in young children. *Epidemiology*, 10(3), pp. 294-299.
- Oreszczyn, T., Mumovic, D., Ridley, I. & Davies, M., 2005. The reduction in air infiltration due to window replacement in UK dwellings: Results of a field study and telephone survey. *International Journal of Ventilation*, 4(1), pp. 71-78.
- Persily, A., 1982. *Understanding air infiltration in homes*, NJ, USA: Princeton University (PhD Thesis).
- Persily, A., 2016. Field measurement of ventilation rates. *Indoor Air*, 26(1), pp. 97-111.
- Sharpe, T. et al., 2015. Occupant interactions and effectiveness of natural ventilation strategies in contemporary new housing in Scotland, UK. *International Journal of Environmental Research and Public Health*, 12(7), pp. 8480-8497.
- Sherman, M. H., 1987. Estimation of infiltration from leakage and climate indicators. *Energy and Building*, Volume 10, pp. 81-86.
- Stephen, R., 1998. *Air tightness in UK dwellings: BRE's test results and their significance*, Garston, Watford, UK: Building Research Establishment.
- Sullivan, L. et al., 2013. *Mechanical ventilation with heat recovery in new homes*, Milton Keynes: Zero Carbon Hub and NHBC,.
- Sundell, J., 2004. On the history of indoor air quality and health. *Indoor Air*, 14(7), pp. 51-58.

# Impact of airtightness on the heat demand of passive houses in central European climate

Aleš Vlček<sup>1</sup>, Jiří Novák<sup>\*2</sup>

*1 Czech Technical University  
Faculty of Civil Engineering  
Thákurova 7  
166 29 Prague, Czech Republic*

*2 Czech Technical University  
Faculty of Civil Engineering  
Thákurova 7  
166 29 Prague, Czech Republic*

*\*Corresponding author: jiri.novak.4@fsv.cvut.cz*

## ABSTRACT

Excessive air leakage through the building envelope increases the infiltration heat loss and therefore lowers the energy efficiency. Therefore, very good airtightness is required in case of well insulated buildings equipped with a mechanical ventilation system with heat recovery (e.g.  $n_{50} < 0.6 \text{ h}^{-1}$  for passive houses). Although the building industry has progressively adopted strategies to comply with such strict limits, it is still important to study how and how much the airtightness influences the energy efficiency of different types of buildings in different climatic conditions.

This study investigates the impact of building envelope airtightness on the heat demand of a single-family house and a multi-family residential building in the central European climate (Prague). Both model buildings are passive houses, equipped with a balanced mechanical ventilation system with heat recovery. Their heat demand was calculated in function of the envelope airtightness ( $n_{50}$  varying from 0 to  $1 \text{ h}^{-1}$ ). Several combinations of leakage distribution over the building envelope and wind shielding conditions were considered. The single-family house was modelled as a single zone building. In the multi-family building, each flat and the staircase were considered as separate pressure zones. The heat demand was calculated considering the following alternatives of internal air leakage between the zones:

- no internal air leakage between zones
- each flat connected with the staircase (air leakage between flats not allowed)
- each flat connected with the staircase and neighbouring flats (air leakage between flats allowed)

The air leakage distribution over the residential building envelope and the characteristics of the internal leakage paths were estimated from results of airtightness tests of a real building. For the purpose of this study, transient thermal and air infiltration models were developed using Matlab – Simulink. Iterative approaches were adopted for a reliable coupling of the thermal and air infiltration models (differently in the single and multi-zone models).

The heat demand increases noticeably with the building envelope air permeability. The increase is more pronounced in case of the residential building (eg.  $3 \text{ kWh}/(\text{m}^2 \cdot \text{a})$  per unit of  $n_{50}$  against  $4 \text{ kWh}/(\text{m}^2 \cdot \text{a})$  for the single-family house under the same conditions). The wind shielding and the leakage distribution influence significantly the results. The highest heat demand was identified in cases with the air leakage paths distributed half and half at the bottom and on the top of the building. The internal air leakage does not affect significantly the heat demand of the residential building, which depends mostly on the envelope air leakage and its distribution. However, significant air flow rates were detected between the zones (up to  $24 \text{ m}^3/\text{h}$  between flats). The internal leakage may therefore cause an issue for IAQ, ventilation system function and fire safety.

## KEYWORDS

Airtightness, air leakage, heat demand, thermal simulation, airflow simulation

## 1 INTRODUCTION

Excessive air leakage through the building envelope may substantially increase the infiltration heat loss. Consequently, the heat demand increases, which results into a lower energy efficiency of the building. This impact is particularly significant in case of well insulated buildings equipped with a mechanical ventilation system with heat recovery, where the transmission and ventilation heat losses were minimized. This is the reason why strict airtightness requirements were set for this category of buildings (e.g.  $n_{50} < 0.6 \text{ h}^{-1}$  for passive houses).

Compliance with such a low limit value of  $n_{50}$  requires special design approaches during the planning phase, a particular care, systematic control and use of special products during the construction works. Although the building industry has progressively adopted suitable strategies to achieve very good airtightness, the building practitioners and investors still ask whether the strict requirements are justified and which effect would produce a deviation from them (both upwards and downwards) in terms of energy consumption. Therefore, it is still important to study, how and how much the airtightness influences the energy efficiency of different types of buildings in different climates.

Numerous studies were published during the last years which investigate the impact of airtightness on energy efficiency of buildings in different European countries. No similar study has been carried out in the Czech Republic until now. In pursuit of filling this gap, the authors present here a numerical investigation of the impact of building envelope airtightness on the heat demand of a single-family house and a multi-family residential building in the central European climate (Prague). Several combinations of leakage distribution over the building envelope and wind shielding conditions are considered. In case of the multi-family residential building, the impact of internal air leakage is studied as well. With regard to increasingly tighter energy efficiency policies, this work is focused on buildings with low energy consumption (passive houses) and very low airtightness levels.

## 2 CALCULATION METHODS

In order to calculate the heat demand, a simplified transient model was developed in Matlab – Simulink. This model consists of two parts coupled to each other: thermal model and infiltration model. The calculation time step is one hour and the model uses hourly weather data. The model was first developed as single-zone and then adapted in order to allow for multi-zone simulations.

### 2.1 Thermal model

Fig. 1 shows the thermal model network (single-zone case). The model requires only limited amount of input data and its simplicity allows the coupling with the infiltration model to be handled easily. Based on the results of its validation, it is supposed to provide a reasonable accuracy for the purpose of this study (Kopecký 2016).

The thermal model calculates the internal air temperature, corresponding heat loss and heat demand. The heat capacity is calculated considering an effective thickness of 100 mm for all building components in contact with the internal air. The effect of heat recovery from the exhaust air is obtained by reducing the supply air flow rate by the factor  $(1-\eta)$ , where  $\eta$  is the efficiency of heat recovery. The supply air flow rate (as well as the internal heat gains)

follows an occupancy schedule. The infiltration air flow rate is taken from the infiltration model.

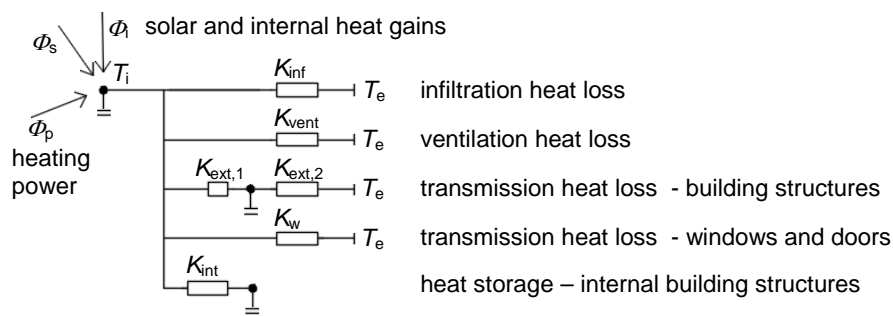


Figure 1: The thermal model network.

## 2.2 Infiltration model

The infiltration model calculates the infiltration air flow rate as a sum of air flow rates through the individual leakage paths. The air flow rate through the leakage paths is calculated using the power law equation in function of pressure difference, taking the air flow coefficient  $C$  and the air flow exponent  $n$  as leakage paths characteristics. The pressure differences are calculated with regard to wind pressure and stack effect. The pressure difference induced by the balanced ventilation system was supposed to be low in comparison with the wind and stack effect and therefore neglected in the calculation.

The pressure difference due to the stack effect is calculated from the leakage path position on the building envelope (height above the 1<sup>st</sup> floor) and the internal air temperature. Since the infiltration air flow rate and the internal temperature influence each other, the internal temperature is corrected by means of an iterative approach as explained in the next section.

The wind pressure is calculated in function of the wind speed at the building height and the wind direction. The wind speed taken from the weather data is corrected in order to account for the building height and the surrounding obstacles (wind shielding effect) according to (ASHRAE 2001). Wind pressure coefficients  $C_p$  for façades and roof in function of wind incidence angle are taken from (Orme 1998).

The infiltration model was validated with the computer program CONTAM. A single-zone model (the single-family house of this study) was modelled in CONTAM with the same settings. The difference between the results did not exceed 1.4 % for the air flow rate through the individual leakage paths and 0.3 % for the total air flow rate.

## 2.3 Coupling of the thermal and infiltration model

For each calculation time step, the infiltration model calculates the infiltration air flow rate based on an initial internal air temperature. The resulting infiltration air flow rate is transferred to the thermal model, which calculates the internal air temperature. Since the calculated internal air temperature may differ from the initial one, the calculated temperature is sent back to the infiltration model in order to adjust the stack effect pressure differences and recalculate the infiltration air flow rates. For each calculation time step, this iterative process is repeated until the difference between the internal air temperatures and infiltration air flow rates from two successive iterations is less than a pre-set limit.

### 3 CASE 1 – A SINGLE-FAMILY HOUSE

#### 3.1 Building description

The size, thermal performance and building services of the studied building (fig. 2) are representative for a typical single-family passive house built recently in the Czech Republic. The building has two storeys and it is intended for a four member's family. The floor area is 132 m<sup>2</sup> and internal air volume is 352 m<sup>3</sup>. The mean thermal transmittance of the building envelope is  $U_{em} = 0.21 \text{ W}/(\text{m}^2 \cdot \text{K})$  and the heat demand calculated by means of monthly method according to (EN ISO 13790) is 16.1 kWh/(m<sup>2</sup>·a). The building is equipped with a balanced mechanical ventilation system with heat recovery. The efficiency of the heat recovery is  $\eta = 75 \%$ .

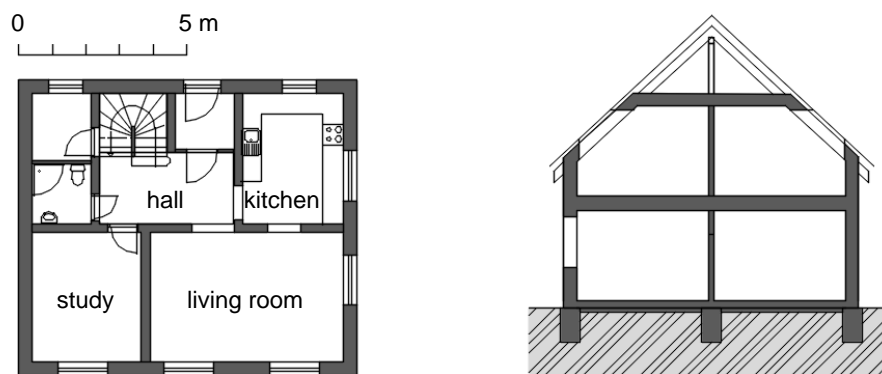


Figure 2: The studied single-family house. Left - first floor plan. Right - cross section.

#### 3.2 Simulated alternatives

The objective of this work is evaluation of the building airtightness on the heat demand. In this study, the building airtightness is expressed in terms of the air change rate at 50 Pa,  $n_{50}[\text{h}^{-1}]$ . The heat demand of the building was calculated several times with the  $n_{50}$  varying stepwise from 0 to 1.0 h<sup>-1</sup> with an increment of 0.1 h<sup>-1</sup>. This range was supposed as typical for the energy efficient buildings equipped with the ventilation system in question. For example, the Czech technical standard (CSN 73 0540-2: 2011) recommends to fulfil the limit value of  $n_{50} = 1.0 \text{ h}^{-1}$  in case of buildings equipped with mechanical ventilation system with heat recovery and  $n_{50} = 0.6 \text{ h}^{-1}$  in case of buildings with very low heat demand equipped with the same ventilation system (typically passive houses).

Since the wind can significantly influence the infiltration, the study of the airtightness impact on the heat demand as described above was repeated three times, considering the following wind shielding conditions:

- no wind (hypothetical case, the infiltration is driven by the stack effect only)
- heavy shielding (buildings in city centres)
- moderate shielding (buildings in suburban or wooded areas)
- no shielding (buildings in open terrain)

The single-family houses are usually built in suburban areas of larger towns or in smaller villages surrounded by the buildings and trees of similar height. The villages are rarely situated in completely open country exposed to undisturbed wind. Therefore, the moderate shielding can be considered as typical for this category of buildings.

For the case of moderate shielding, the impact of leakage distribution over the building envelope was studied. On each of the building faces, the air leakage was concentrated into leakage paths(spots) located at different heights (fig. 3):

- lower leakage path 0.5 m above the 1<sup>st</sup> floor – representing the leakage through the external wall/slab on the ground interface and other leakages in the lower part of the external wall (e.g. electrical boxes)
- middle leakage path 4.05 m above the 1<sup>st</sup> floor – representing the leakage through the external wall/pitched roof interface and other leakages in the upper part of the external wall (e.g. electrical boxes in the 2<sup>nd</sup> floor, penetrations of structural elements – joists etc.)
- upper leakage path 5.82 m above the 1<sup>st</sup> floor – representing the leakage through the pitched roof /ceiling interface and other leakages in the upper part of the external wall (e.g. electrical boxes in the 2<sup>nd</sup> floor, penetrations of structural elements of the roof truss)
- leakage paths in the middle-height of the building openings (windows, doors) - representing the leakage through the window or door/external wall interface and the leakage of the element itself

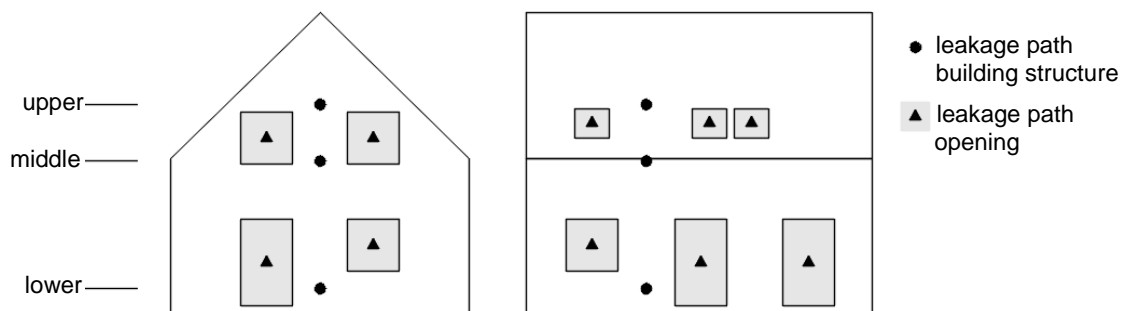


Figure 3: The position of the leakage paths.

Note that the horizontal position of the leakage paths has no significance for infiltration calculations, since average wind pressure coefficients  $C_p$  apply for whole area of each building face. Tab. 1 shows the five studied alternatives of the overall building envelope leakage distribution.

Table 1: Overview of the studied alternatives of the leakage distribution over the building envelope

leakage path	share of the leakage path on the overall envelope air leakage				
	alt. 1	alt. 2	alt. 3	alt. 4	alt. 5
lower leakage paths	30 %	70 %	10 %	40 %	50 %
middle leakage paths	30 %	10 %	10 %	10 %	0 %
upper leakage paths	30 %	10 %	70 %	40 %	50 %
openings leakage paths	10 %	10 %	10 %	10 %	0 %

In all the studied alternatives, the building was modelled as a single zone. The reasons are that the internal doors remain commonly open in a single-family house and the ventilation system considered in this study requires interconnections allowing for air flow between the rooms. The same time schedules (tab. 2) and the same weather data (test reference year for Prague) were used in all simulations.

Table 2: Time schedules for single-family house simulations

		0:00 ÷ 8:00	8:00 ÷ 16:00	16:00 ÷ 0:00
number of persons	[ - ]	4	0	4
ventilation air flow rate	[ m <sup>3</sup> /h ]	100	35 ( $n = 0.1 \text{ h}^{-1}$ )	100
internal heat gains	[ W ]	500	100	500

### 3.3 Results

In all the studied alternatives, the heat demand increases linearly with the air change rate at 50 Pa,  $n_{50}$  (fig. 4). The increase of the heat demand may range from approx. 2 to 4 kWh/(m<sup>2</sup>·a) per unit of  $n_{50}$ , depending on the wind shielding and the leakage distribution. For the likely most common case, i.e. almost uniform distribution of the air leakage (alt.1 in tab. 1) and moderate wind shielding, the heat demand corresponding to the building with  $n_{50} = 0.6 \text{ h}^{-1}$  is about 8% higher than the heat demand of an ideally airtight building. In case of a building with  $n_{50} = 1 \text{ h}^{-1}$ , the increase of the heat demand reaches 14 %.

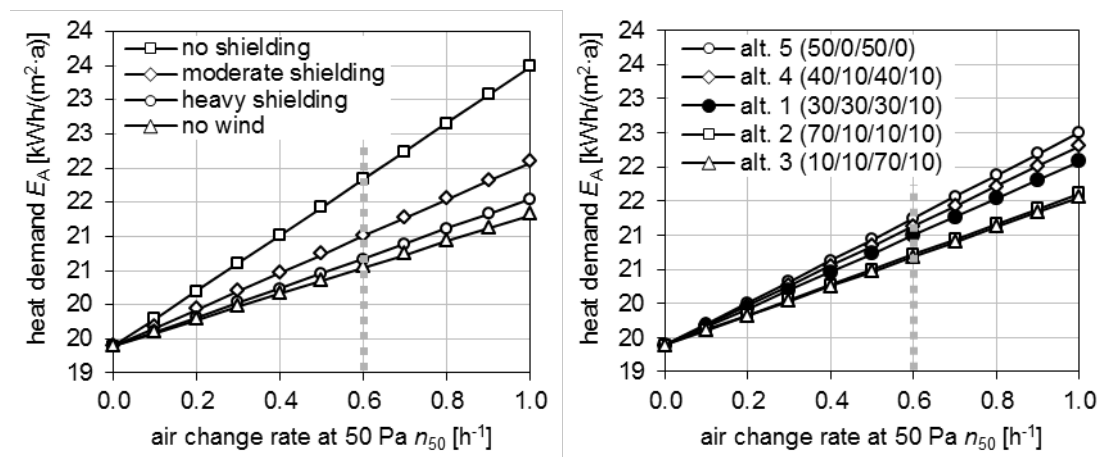


Figure 4: Simulation results for single-family house. Left – influence of wind shielding, the leakage distribution corresponds to alt. 1 in table 1. Right – influence of leakage distribution, moderate shielding

Unfavourable shielding conditions can significantly strengthen the impact of airtightness on heat demand. Considering the same level of airtightness, the increase of the heat demand of the studied house would be approx. 50 % higher in case of “no shielding” compared to the case of “moderate shielding”. On the other hand, the difference of the heat demand between the cases “moderate shielding” and “heavy shielding” is rather small. Under moderate and heavy shielding (usual conditions) the stack effect is the dominant driving force of air infiltration.

The influence of the leakage distribution is noticeable, but seems not to be really significant in comparison with the impact of the wind shielding. The lowest heat demand is obtained if the air leakage is concentrated either on the top or on the bottom of the building envelope (alt. 2 and 3 in tab. 1). Splitting the air leakage half on the top and half on the bottom of the building leads to the highest heat demand (alt. 4 and 5). The uniform leakage distribution leads to heat demand rather closer to the unfavourable cases.

## 4 CASE 2 – A MULTI-FAMILY RESIDENTIAL BUILDING

### 4.1 Building description

The studied building (fig. 5) represents an example of a real multi-family residential passive house. The building was built in a suburb of Prague in 2012. Its airtightness was tested and studied in detail (Novák 2013). Therefore, data concerning the envelope airtightness, the leakage distribution and data concerning airtightness of internal partitions are available.

The building has 4 residential floors above the ground level and a parking in the underground. In the residential part, 14 flats are spread around the central staircase including an elevator shaft. The flats are of different sizes, the expected number of inhabitants is 40. The buildings height above the ground is 12.3 m. The floor area of the heated residential part is 1173 m<sup>2</sup> and its internal volume 3933 m<sup>3</sup>. The mean thermal transmittance of the building envelope (heated zone) is  $U_{em} = 0.3 \text{ W}/(\text{m}^2 \cdot \text{K})$  and the heat demand calculated by means of monthly method according to (EN ISO 13790) is 14.1 kWh/(m<sup>2</sup>·a). The building is equipped with a decentralised balanced mechanical ventilation system with heat recovery (the efficiency is  $\eta = 75 \%$ ). Each flat has its own air handling unit. The air change rate at 50 Pa, resulting from an overall airtightness test carried out at commissioning of the building is  $n_{50} = 0.48 \text{ h}^{-1}$ .



Figure 5: The studied multi-family residential building. Left – 3<sup>rd</sup> floor plan. Right – completed building

## 4.2 Simulated alternatives

The heat demand of the multi-family residential building was calculated in function of the  $n_{50}$  value ranging from 0 to 1 h<sup>-1</sup> with an increment of 0.2 h<sup>-1</sup>. In such a markedly compartmented building, the use of the single-zone model is not suitable. Therefore, the original thermal and infiltration models were adapted, including their coupling, in order to allow for multi-zone simulations.

In the thermal model, the heated space consists of two zones: one zone representing all the flats and a second zone representing the staircase. The infiltration model consists of five pressure zones. The flats of each floor are grouped into one zone (four zones, referred to as flats hereafter). The staircase is considered as a separate zone. Following alternatives of connection between the pressure zones were considered (fig. 6):

- alt. 1 no internal air leakage between zones (airtight internal partitions)
- alt. 2 each flat connected with the staircase (air leakage between flats not allowed)
- alt. 3 each flat connected with the staircase and neighbouring flats (air leakage between flats allowed)

The characteristics of the internal leakage paths were estimated from the results of the airtightness tests (Novák 2013). These characteristics were kept constant in all simulations, regardless the airtightness level of the building envelope.

In case of the residential building, a more detailed distribution of the wind pressure coefficients  $C_p$  over the envelope was considered. Each face of the building was divided into several regions with characteristic  $C_p$  values for high-rise buildings (Orme 1998).

Identical air leakage distribution was considered in all simulations (i.e. unlike in the single-family house study, the effect of leakage distribution over the building envelope was not studied here). The total air leakage through the building envelope was distributed between the envelope area enclosing the flats (61 % of the total air leakage) and the envelope area enclosing the staircase (39%). This proportion reflects real leakage distribution deduced from the results of airtightness testing. The air leakage proper to each of these two areas was equally divided among the four floors (25 % each). In case of flats, this “floor leakage” was equally divided between two leakage paths: one at the top and one at the bottom of the zone height, as shown on fig. 6. In case of staircase, the “floor leakage” was concentrated into one leakage path in the mid-height of the floor (fig. 6).

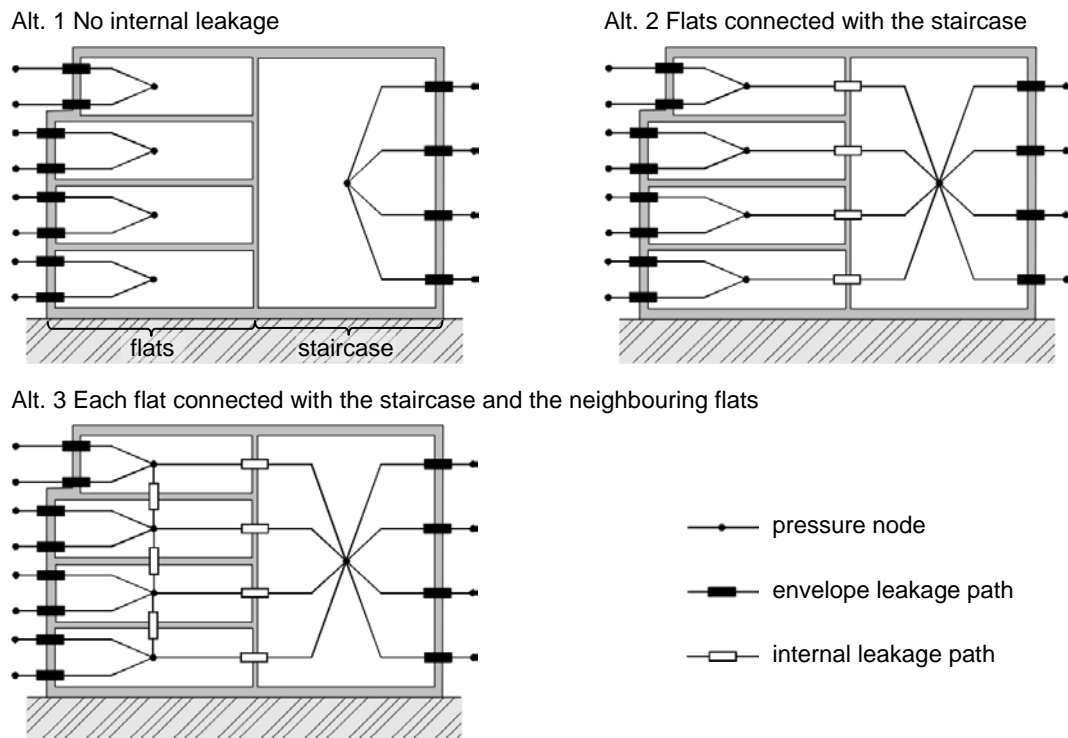


Figure 6: Infiltration model networks for the multi-family residential building. Schematic cross section.

The same time schedules (tab. 3) and the same weather data (test reference year for Prague) were used in all simulations.

Table 3: Time schedules for multi-family residential building simulations

			0:00 ÷ 8:00	8:00 ÷ 16:00	16:00 ÷ 0:00
flats (total figures)	number of persons	[ - ]	40	0	40
	ventilation air flow rate	[ m <sup>3</sup> /h ]	1000	230 ( $n = 0.1 \text{ h}^{-1}$ )	1000
	internal heat gains	[ W ]	5400	1400	5400
staircase	number of persons	[ - ]	0	0	0
	ventilation air flow rate	[ m <sup>3</sup> /h ]	34	34	34
	internal heat gains	[ W ]	0	0	0

### 4.3 Results

The increase of the heat demand ranges from approx. 3 to 5kWh/(m<sup>2</sup>·a) per unit of  $n_{50}$ , depending on the wind shielding. Under moderate wind shielding, the heat demand corresponding to the building with  $n_{50} = 0.6 \text{ h}^{-1}$  is about 13 % higher than the heat demand of an ideally airtight building. These figures are markedly higher than in case of the single-family house showing a more significant impact of airtightness on the heat demand in case of

residential buildings (compare fig. 4 and fig. 7). Since the residential buildings are higher, they suffer from stronger wind pressure than low-rise single-family houses (higher  $C_p$  values).

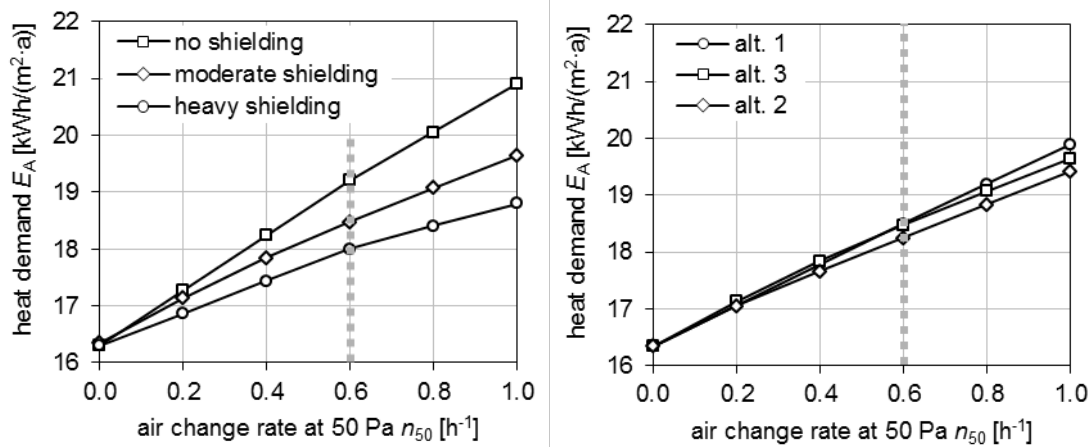


Figure 7: Simulation results for multi-family residential building. Left – influence of wind shielding, no internal leakage (airtight internal partitions). Right – influence of the internal leakage, moderate shielding.

Different alternatives of connections between the pressure zones led to very similar results in terms of heat demand (fig. 7, right). However, the airtightness of internal partitions strongly affects the distribution and magnitude of the internal air leakage. Significant air flow rates were identified from the staircase to adjacent flats and between neighbouring flats (fig. 8).

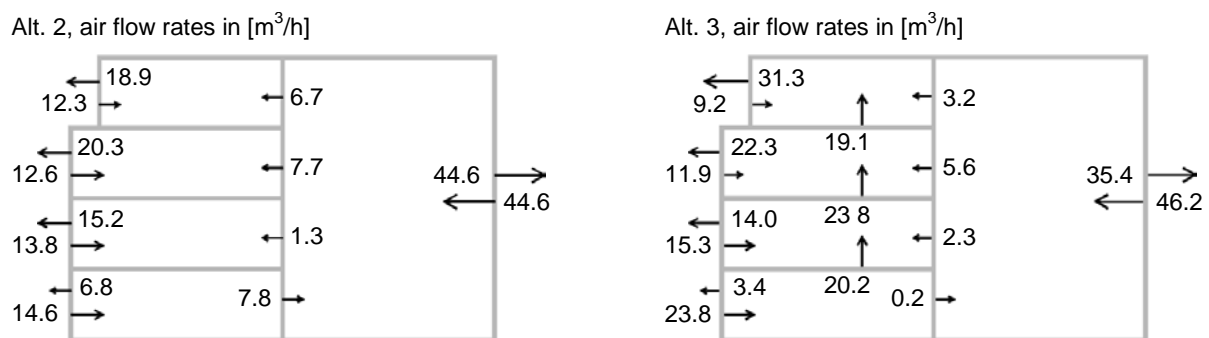


Figure 8: Average air flow rates between the pressure zones for January (schematic cross section). Left – alt. 2, flats connected with the staircase. Right – alt. 3, each flat connected with the staircase and neighbouring flats.

## 5 DISCUSSION AND CONCLUSIONS

This study confirms a significant impact of air leakage through the building envelope on the heat demand of passive houses in Central European climate. This impact is more pronounced in case of higher residential building. Exposure to the wind considerably amplifies the impact of air leakage. Even under typical wind exposure (moderate shielding), the air leakage corresponding to  $n_{50} = 1 \text{ h}^{-1}$  can increase the heat demand of about 14 % (single-family house) or 20 % (residential building), with reference to an ideally airtight building. Hence, seeking for even better airtightness remains a meaningful challenge.

Despite simplifications and limited extent of this study, one can try, based on its results, to estimate approximately an appropriate level of airtightness requirements for passive houses in Central European climate. Generally, a factor causing an increase of heat demand higher than 10 % can be perceived as a critical threat for energy efficiency targets. On the other hand, a factor causing an increase lower than 5 % would obviously be of minor significance (e.g. due to uncertainties in determination of the factor itself and in the calculation method). Therefore,

let us set lower and upper limits of acceptable increase of heat demand due to the air leakage to 5 and 10 % respectively with reference to an ideally airtight building. Then, we can find a corresponding range of  $n_{50}$  being about  $0.4 \div 0.7 \text{ h}^{-1}$  for single-family houses and  $0.2 \div 0.5 \text{ h}^{-1}$  for residential buildings. From this point of view, the commonly accepted limit value of  $n_{50} = 0.6 \text{ h}^{-1}$  seems to be appropriate for single-family houses, but could be further reduced for residential buildings. Achievement of  $n_{50}$  values ranging from 0.2 to  $0.5 \text{ h}^{-1}$  should not represent an issue in case of residential buildings due to usually favourable envelope area to volume ratio (A/V). Moreover, field experience proves that such values can be achieved in practice, in particular if systematic control is required (mandatory airtightness testing).

An unfavourable distribution of the air leakage over the building envelope can strengthen the increase of the heat demand. The worst case occurs if the air leakage paths are concentrated at the bottom and at the top of the height of a pressure zone. Therefore, the design and construction of connections between the building elements in these locations merit a particular attention.

The influence of internal air leakage on the heat demand was found negligible. However, leaky internal partitions result into significant air exchange between adjacent pressure zones causing potential interference with the ventilation system. Transport of contaminants (or fumes in case of fire) due to the internal air leakage represents a potential IAQ issue and fire safety risk. Further investigation is needed in order to decide whether and to what degree the airtightness of internal partitions should be required.

## 6 ACKNOWLEDGEMENTS

This work has been supported by the Ministry of Education, Youth and Sports within National Sustainability Programme I, project No. LO1605.

## 7 REFERENCES

Kopecký, P. (2016). Comparative testing of simplified lumped parameter building thermal models. *Proceedings of conference CESB 16 - Central Europe towards sustainable building 2016, 22<sup>nd</sup> – 24<sup>th</sup> June 2016, 789 – 796*. Grada Publishing a.s. ISBN 978-80-271-0248-8

ASHRAE (2001). *2001 ASHRAE Handbook - Fundamentals*, American Society of Heating, Refrigeration and Air-Conditioning Engineers, Inc. Atlanta. ISBN 1-883413-88-5

Orme, M., Liddament, M., Wilson, A. (1998). *Numerical Data for Air Infiltration and Ventilation Calculations*. Coventry: AIVC. ISBN 1 946075 97 2.

ČSN 730540-2: 2011. *Thermal performance of buildings – Part 2: Requirements*. Czech office for standards, metrology and testing.

Novák, J. (2013). Airtightness of a multi-family passive residential building in the Czech Republic. *Proceedings of 8th International BUILDAIR-symposium 2013, Hannover*

EN ISO 13790:2008. Energy performance of buildings – Calculation of energy use for space heating and cooling. European Committee for Standardization

# **Demand controlled ventilation in school and office buildings: lessons learnt from case studies**

Bart Merema<sup>1\*</sup>, Muhannad Delwati<sup>2</sup>, Maarten Sourbron<sup>2</sup>, Hilde Breesch<sup>1</sup>

<sup>1</sup>*KU Leuven, Department of Civil Engineering,  
Construction Technology Cluster  
Technology Campus Ghent  
Gebroeders DeSmetstraat 1  
9000 Gent, Belgium  
\*bart.merema@kuleuven.be*

<sup>2</sup>*KU Leuven, Department of Mechanical Engineering  
Applied Mechanics and Energy Conversion Section  
Celestijnenlaan 300A  
3001 Leuven, Belgium*

## **ABSTRACT**

Demand controlled ventilation (DCV) refers to a ventilation system with air flow rates that are controlled based on a measurement of an indoor air quality (IAQ) and/or thermal comfort parameter. DCV operates at reduced air flow rates during a large amount of the operation time. Due to this decrease, less energy is needed for fan operation and heating/cooling the supply air. However, uncertainty still exists about the IAQ performance and ventilation efficiency in the room, especially at lower air flow rates. Aim of this paper is to evaluate the IAQ performance, ventilation efficiency, operation and energy efficiency of DCV in school and office buildings based on measurement results. This research was done in cooperation with Flemish manufacturers of ventilation components, engineering offices designing HVAC and industrial federations.

Four case studies with large and varying occupancy and with different use and ventilation systems are selected. First case study is a school building with natural air supply and mechanical extraction controlled by measured indoor CO<sub>2</sub> concentration. Second study consist of an educational building with lecture rooms. In this building balanced mechanical ventilation is controlled by CO<sub>2</sub> and temperature measured at the extract air grill. Finally, in two different office buildings, three landscaped offices are evaluated. Here the balanced mechanical ventilation is controlled by CO<sub>2</sub> concentration and temperature.

To evaluate IAQ, ventilation efficiency and the energy savings of the system, the following parameters are monitored: CO<sub>2</sub> concentrations and air? temperatures at different positions in the room and at the extract air grill, position of the variable air volume (VAV) boxes, supply and extract air flow rates and the occupancy of the room. Measurements lasted for at least two typical weeks in autumn and winter 2015-2016.

The results show that a DCV system is able to guarantee a good IAQ in all the studied cases even at reduced air flow rates. The VAV boxes react well to predefined set points for CO<sub>2</sub> concentration. The effect of the reduced air flow on the ventilation efficiency is negligible. Moreover, during the measurement period, the reduction of the fan energy ranges from 25-55% compared to a constant air volume system (CAV). For the heat losses, the reduction was 25-32% compared to a CAV during the measurement period. Energy reductions of both the fan and heat losses are calculated according to a design airflow rate of 29 m<sup>3</sup>/h.pers, i.e., IDA3 in EN 13779. However, commissioning of the DCV is necessary to maintain these high energy reductions and good IAQ and ventilation efficiency. To conclude, DCV is an interesting ventilation system in rooms with a large and varying occupancy such as lecture rooms and landscaped offices.

## **KEYWORDS**

Demand controlled ventilation, energy savings, IAQ, ventilation efficiency, office and school buildings

## 1 INTRODUCTION

Demand controlled ventilation (DCV) can reduce the energy use significantly compared to a constant air volume (CAV) system. DCV operates at reduced air flow rates during a large amount of the operation time. Due to this decrease, less energy is needed for fan operation and heating/cooling the supply air. Mysen et al. (2005) showed that the energy demand in school buildings was reduced by 38% for a CO<sub>2</sub>-DCV compared to a CAV. In addition, Wachenfeldt et al. (2007) showed with measurements and simulations of a school building that the energy demand for respectively heating and fan use was reduced by 21% and 87% compared to a CAV. Maripuu (2009) showed that by implementing a DCV system in a university building the energy use for the fans was decreased by 50%. Ahmed (2015) showed for the implementation of DCV a decrease of 33-41% for the energy needed for heating, cooling and fans in an office building. In addition, measurements of the CO<sub>2</sub> concentration inside the office indicated a good indoor air quality (IAQ) with values below 900 ppm.

The air flow pattern is affected due to the lower air flow rates and velocities and might not cover the whole occupied zone. Fisk et al. (2012) measured the spatial variability of CO<sub>2</sub> concentration in occupied meeting rooms. In a crowded conference room the CO<sub>2</sub> concentration varied among different measurement positions up to approximately 300 ppm and fluctuated substantially with time for the measurement positions. Measurements for ventilation efficiency in a landscaped office by (Martínez et al., 2015) showed values between 0,55 and 0,66. The efficiency was affected by supply air that was mixed with extract air resulting in a higher CO<sub>2</sub> concentration at the supply.

However, there is still uncertainty about the indoor air quality (IAQ) and the ventilation efficiency of the room. The aim of this paper is to assess the IAQ, ventilation efficiency and energy efficiency of real DCV systems. Five rooms with large and varying occupancy in four school and office buildings in Belgium are selected. Overall lessons from these case studies are discussed. This measurement campaign is part of an applied research project about DCV in school and office buildings in cooperation with Flemish manufacturers of ventilation components, engineering offices HVAC and industrial federations.

## 2 METHOD

First, a description of the case study buildings and the systems is presented. All the case studies analysed are located in Belgium. Afterwards, the measurement setup for the evaluation of IAQ, ventilation efficiency and energy efficiency is shown.

### 2.1 Case studies

Table 1 summarizes the building, use, ventilation system and control properties of the case studies. Four different case studies are analysed with 3 different types of rooms:

- a classroom
- a lecture room
- three landscaped offices.

In all the case studies the DCV system is controlled by measured CO<sub>2</sub> concentrations in the zone. With exception of the kindergarten the ventilation system is also temperature controlled. For all the case studies a brief description is given with the important details.

Table 1; building, use, system and control properties for all case studies

Case study	Measurement period	Room type (floor area)	Ventilation system	DCV	Air flow (m <sup>3</sup> /h)	Design occupancy (person/m <sup>2</sup> )	Setpoint system
Kindergarten De Boomhut	16-27 November 2015	Classroom (66m <sup>2</sup> )	Natural air supply and mechanical extraction	CO <sub>2</sub>	200-600	20 (3,3)	1100 ppm?
Infracx	14 February – 2 March 2016	Landscaped office (200m <sup>2</sup> )	Balanced mechanical ventilation	CO <sub>2</sub> +T	550-1400	20 (10)	700 ppm
Test lecture room	8-19 February 2016	Lecture room (140m <sup>2</sup> )	Balanced mechanical ventilation (displacement)	CO <sub>2</sub> +T	400-2200	80 (1,75)	1000 ppm (21°C)
KU Leuven office	25 November - 8 December 2016	2 Landscaped offices (70m <sup>2</sup> and 72m <sup>2</sup> )	Balanced mechanical ventilation	CO <sub>2</sub> +T	70-420 70-500	12 12 (6)	800 ppm (23,8°C)

### Kindergarten De Boomhut

This kindergarten includes four rectangular classrooms of each 66 m<sup>2</sup> and is used for pupils from the age of 3-6. An impression of this building is shown in Figure 1. The classroom is used by approximately 15 pupils during the measurement period.



Figure 1. left) View of south-east façade of the kindergarten “De Boomhut”,right) interior of the classroom measured

The classrooms used for measurements are located at the north-west side. Fresh air is supplied in each classroom through self-regulating grills integrated in the windows with a maximum supply of 550 m<sup>3</sup>/h. The air is mechanically extracted by one centrifugal duct fan per two neighbouring classrooms with a capacity of 400-1200 m<sup>3</sup>/h. The extract air grill in the classroom is located at the mezzanine, just below the ceiling. The extraction air flow rate is controlled by the highest indoor CO<sub>2</sub> concentration of the two classrooms, with the setpoint at 1100 ppm?. In each classroom a CO<sub>2</sub> sensor is placed near the extraction air grill. A more detailed description of this case study is given in the study of (Merema et al., 2016).

### Test lecture rooms KU Leuven

Figure 2 shows the plan and cross section of the test lecture rooms at the Technology Campus Ghent of KU Leuven (Belgium). This case study building contains 2 large lecture rooms with 140 m<sup>2</sup> floor area and a maximum occupancy of 80 students each. The building is built according to the Passive House standard. Balanced mechanical ventilation is provided with a total supply airflow of 4400 m<sup>3</sup>/h. The AHU regulates the VAV boxes by sending a request signal to control the airflow based on CO<sub>2</sub> concentrations and operative temperature in the

classrooms. Each classroom is a single zone with a supply and return VAV. Setpoint for CO<sub>2</sub> and indoor temperature (heating) are set at respectively 1000 ppm and 21°C. A more detailed description of this case study can be found in (Merema et al., 2015).

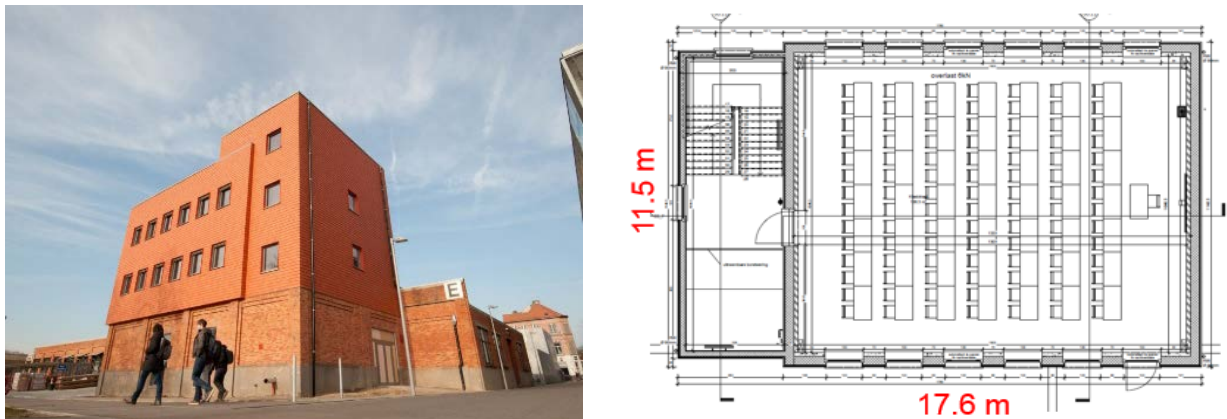


Figure 2; Plan and outside view of the test building

### Office building Infrac

The office building, shown in Figure 3, includes 2 landscaped offices per floor. In one large landscaped office of 200 m<sup>2</sup> measurements have been carried out. Balanced mechanical ventilation is provided in which air is supplied by grills in the floor. Each landscaped office is a single zone with a supply VAV. The supply VAV controls the Air flow rate varies between 550 and 1400 m<sup>3</sup>/h based on the measurement of the CO<sub>2</sub> concentration and the operative temperature at the extract air grill. Setpoint for the DCV system is set at 700 ppm and 21°C.



Figure 3; Impression of the Infrac office building and landscaped office

### Office building KU Leuven

The office building for the administration and logistics, shown in Figure 4, consists of two upper floors with open landscaped offices and, two floors for the servers and a supercomputer. Two landscaped offices with a design occupancy of 12 persons (both approximately 70 m<sup>2</sup>), each with a different orientation (north and southeast), are studied in detail. Balanced mechanical ventilation is provided, fresh air is supplied through air grills in the ceiling. Each landscaped office is a single zone with a supply VAV. The supply VAV controls the air flow rate (70-420 in office 1 and 75-500 m<sup>3</sup>/h in office 2) based on the CO<sub>2</sub> concentration and the temperature measured inside the extract air grill. Setpoints for the DCV system are set at 800 ppm and 23.8°C. A more detailed description of this case study is given in the study of (De Klerck and Massagé, 2017).



Figure 4; Impression of the KU Leuven office building and landscaped office 2

## 2.2 Measurement setup

Measurements are carried out during occupied hours for a period of at least two consecutive weeks for each case study during autumn/winter between November 2015 and December 2016. In all the case studies a minimum of 2 CO<sub>2</sub> sensors are installed in the occupied zone and 1 at the extract air grill for measurements of the IAQ and ventilation efficiency. The ventilation efficiency is defined by (1) according to EN 13779 (2010).

$$\varepsilon_v = \frac{C_{ETA} - C_{SUP}}{C_{IDA} - C_{SUP}} \quad (1)$$

In which  $\varepsilon_v$  is the ventilation efficiency,  $C_{ETA}$  CO<sub>2</sub> concentration of the extraction air,  $C_{IDA}$  CO<sub>2</sub> concentration in the occupancy area and  $C_{SUP}$  CO<sub>2</sub> concentration of the supply air. For a good operating and well-designed ventilation system the efficiency is between 0,70 and 1,10.

Properties of the sensors used for these measurements are listed in Table 2. Time interval used for the IAQ and ventilation efficiency measurements in all case studies is 1 minute. The measurement height used for the CO<sub>2</sub> sensors inside the occupied zone is 1m high. Occupancy of the rooms is measured during the measurement period by counting the number of people or with use of counting cameras (Test lecture room).

Table 2; Properties of the sensors used for measurements

Parameter	Type sensor	Accuracy
Air temperature	Omega PT100	±0,10°C
CO <sub>2</sub> concentration	VAISALA GMW 94	±30 ppm + 2% of reading
	Telaire 700LI	±50 ppm + 5% of reading

## 3 RESULTS

### 3.1 IAQ

Figure 5 presents the results of the CO<sub>2</sub> measurements during operating hours for the both the sensor installed in the occupied zone (sensor with highest values) and the sensor located at the extraction air.

In all the case studies measured the 75% quartile value both in the zone and at the extraction is below the CO<sub>2</sub> setpoint of the ventilation system. This indicates that the ventilation system is able to maintain the CO<sub>2</sub> concentrations below the predefined CO<sub>2</sub> setpoint. Only the results for the kindergarten “De Boomhut” shows that values inside the occupied zone are

above the predefined setpoint. Here the data is used of the sensor which was installed beneath the mezzanine, which is a semi-enclosed space.

In the office buildings the IAQ is equal to IDA class 1 (EN 13779, 2010), which indicates that the IAQ is the highest possible that can be achieved. This shows that the DCV system is able to deliver a good IAQ. The IAQ in the school buildings is comparable to IDA class 3 which is the basis level for an acceptable IAQ. In all the case studies for the outdoor CO<sub>2</sub> concentration a default value of 430 ppm is assumed for the calculations of the IDA class.

The highest CO<sub>2</sub> concentrations are found for the kindergarten “De Boomhut”. Here the median value in the occupied zone is 950 ppm. Lowest values are found in the KU Leuven building (zone 10) with a median value of just 500 ppm in the occupied zone. A remark is that in this zone the occupancy density was low, most of the time the occupancy rate was below 50%. Furthermore, it is noticed that in most (3 out of 5) case studies the CO<sub>2</sub> concentration in the occupied zone is at least 100 ppm lower than at the extraction air grill, which indicates a good operation of the ventilation system. In all the cases measured the 75% quartile is below the set point of the ventilation system. This has an impact on the ventilation efficiency (see next paragraph). CO<sub>2</sub> concentration in the landscaped offices is approximately 200 ppm lower, Because the controlling Set points are lower (800 ppm vs 1000 ppm) and the occupancy density is lower compared to classrooms (lecture rooms), as shown in table 1.

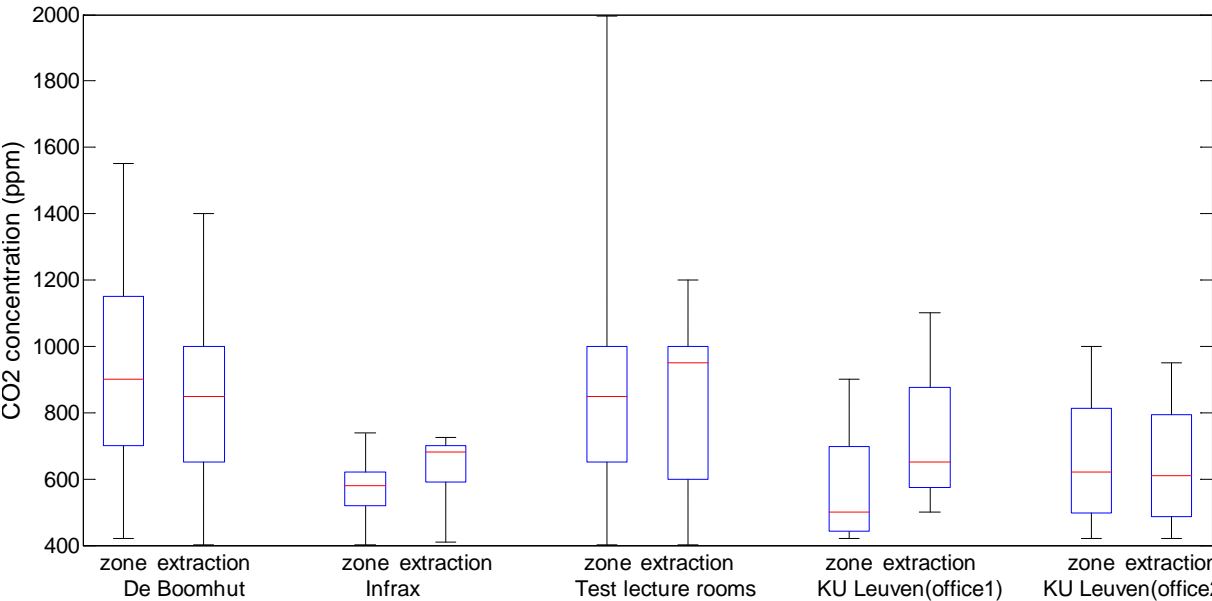


Figure 5; CO<sub>2</sub> concentrations during operating hours for all case studies

**3.1 Ventilation efficiency**

Additionally, the ventilation efficiency of the system is determined based on the CO<sub>2</sub> data of the sensor installed in the occupied zone and the sensor at the extract air by using equation 1. Table 3, shows the results for ventilation efficiency for all the case studies during operating hours and how the fresh air is supplied. A ventilation effectiveness of 1 means that there is a complete mixture of air and pollutants (EN 13779, 2010) between the occupied zone and the extraction air. A good operating and well-designed ventilation system should show values of 0,70-1,10 for the ventilation efficiency. For systems with displacement ventilation values between 1-2 are more typical.

It can be seen in Table 3 that for all the case studies analysed the ventilation efficiency is between 0,89 and 1,50. This indicates that in all cases measured the DCV system is working efficiently as designed. The value presented is an average value for the complete measurement period, the standard deviation is also indicated. Both the Test lecture rooms and the Infrac case show an efficiency of around 1,50. This can be explained by the fact that the test lecture rooms uses displacement ventilation while in Infrac air is supplied via the floor at low air speed. For the KU Leuven offices it can be seen that there is a difference 0,35 in ventilation efficiency. This can be explained by the fact that in office 2 the occupancy rate was higher compared to office 1 which resulted in higher CO<sub>2</sub> concentrations inside the occupied zone.

Table 3; Ventilation efficiency

Case study	Ventilation efficiency (std. dev.)	Air Supply
De Boomhut	0,89 (0,32)	Grill above windows
Infrac	1,50 (0,27)	Air supply in floor
Test lecture rooms	1,49 (0,55)	In each corner of the room an air grill (displacement ventilation)
KU Leuven office	1,27 (office 1) 0,92 (office 2)	Air supply in ceiling

### 3.2 Energy efficiency

The total fan energy demand and ventilation heat losses for the complete measurement period are calculated and shown in Table 4. Energy reductions for both fan and heat losses are compared to the design occupancy with an air flow rate of 29 m<sup>3</sup>/h.pers. Heat losses, due to ventilation, are calculated based on the air flow rate and the temperature difference between zone and supply air temperature after heat exchanger (or in case of natural ventilation outdoor temperature). For the energy reduction both on the fan and heat losses the results are compared to a design air flow rate of 29 m<sup>3</sup>/h.pers (EN 13779, 2010). Furthermore, the heating degree days are indicated for the complete month during the measurement period.

In all the cases it is shown that significant energy reductions can be achieved by implementing a DCV system. In all case studies reductions on the fans are at least 50% and on heat losses 34%. Highest reductions are found for the fans with a maximum of 55% for the test lecture rooms case. The lowest was found for the office building of KU Leuven with 50%, which still is a significant energy reduction. For heat losses the reductions are minimal 34% (KU Leuven office) and maximal 47% (test lecture rooms).

The test lecture rooms showed the largest reductions for both fan and heat losses. This was mainly attributed by the varying occupancy rate both in time and group size (20-80 persons). The heat losses in the KU Leuven office are the lowest with 34%. Here the heating demand was high since the setpoint used for heating was 23.8°C. This resulted in the fact that the system operated at a high air flow rate to heat up the space for a long time during cold periods.

Table 4; Reduction in fan energy and heat losses for DCV compared to CAV

Case study	Fan energy (%)	Ventilation heat losses(%)	Heating degree days
De Boomhut	50	36	Nov 2015: 192
Infrac *	-	-	-
Test lecture rooms	55	47	Feb 2016: 346
KU Leuven office	50	34	Dec 2016: 365

\*Energy consumption and heat losses were not measured in this case study. However, the ventilation system operated 67% of the time during operating hours on a minimum airflow which indicates an energy saving potential.

## 4 CONCLUSIONS

The measurement results shows that in all the case studies the DCV system was able to deliver and maintain a good IAQ, even at reduced air flow rates. The VAV boxes or extract fans respond well to predefined setpoints regarding the CO<sub>2</sub> concentration and temperature. Even at low air flow rates it was noticed that the ventilation efficiency was not affected. This shows that demand controlled ventilation is effective in distributing the air at reduced air flow rates. The measurements for ventilation efficiency showed that during the design air flow rate there was a difference of 100 ppm in CO<sub>2</sub> concentration between the occupied zone and the extraction air grill. This shows that the position of the CO<sub>2</sub> sensor is of importance for the performance of the DCV.

Results of the case studies shows that significant reductions in energy consumption are achieved for both the fans and heating system. This means that DCV has a high energy saving potential for rooms with a varying occupancy profile, both in size and time, such as landscaped offices and classrooms.

However, commissioning is necessary for a good energy and IAQ performance of a DCV system. The measurement campaign revealed some problems with the ventilation system. The ventilation system in the Infrac office building was noticed to operate during 67% of the time at the minimum airflow rate. This could indicate that the minimal airflow rate is too high compared to the actual occupancy. Furthermore, the position of the CO<sub>2</sub> sensor has a large impact on the operation of the system. In the Test lecture rooms this position was changed because first results of ventilation efficiency indicated a large difference between CO<sub>2</sub> measured at the extract air grill and the occupied zone.

## 5 ACKNOWLEDGEMENTS

This research is funded by Flanders Innovation and Entrepreneurship (VLAIO). This support is gratefully acknowledged. TETRA 140345: "Optimisation of demand controlled ventilation in nZEB commercial buildings"

## 6 REFERENCES

Ahmed, K., Kurnitski, J., Sormunen, P., (2015). *Demand controlled ventilation indoor climate and energy performance in a high performance building with air flow rate controlled chilled beams*, Energy and Buildings 109, 115-126

De Klerck, L., Massagé, G. (2017). *Evaluation of the indoor climate and the operation of a demand controlled ventilation system in an office building*, MSc Thesis, KU Leuven Technologiecampus Gent

EN 13779. (2010). *Ventilation for non-residential buildings – Performance for ventilation and room-conditioning systems*. CEN, Brussels.

Fisk W.J., Mendell M.J., Davies M, Eliseeva E., Faulkner D., Hong T., Sullivan D.P., (2012).

*Demand controlled ventilation and classroom ventilation.* LBNL 6563E. Lawrence Berkeley National Laboratory

Maripuu, M. L. (2009). *Demand controlled Ventilation (DCV) systems in commercial buildings: functional requirements on systems and components.* PhD Göteborg: School of Electrical and Computer Engineering, Chalmers tekniska högskola.

Merema B., Breesch H., Sourbron M. (2016). *Impact of demand controlled ventilation on indoor air quality, ventilation effectiveness and energy efficiency in a school building.* Indoor Air 2016. Gent, Belgium, 3-8 July 2016

Merema B., Breesch H., Sourbron M., Verplaetsen J., Van den Bossche P. (2015). *Demand controlled ventilation in practice: Case study.* Effective ventilation in high performance buildings. AIVC conference. Madrid, 22-23 September 2015

Mysen M., Berntsen S., Nafstad P., Schild P.G. (2005). *Occupancy density and benefits of demand-controlled ventilation in Norwegian primary schools,* Energy and Buildings 37, 1234–1240.

Wachenfeldt B.J., Mysen M., Schild P.G. (2007). *Air flow rates and energy saving potential in schools with demand-controlled displacement ventilation,* Energy and Buildings 39, 1073-1079.

# Experimental and Numerical Investigation of Air Distribution in a Large Space

Ali Alzaid<sup>\*1</sup>, Maria Kolokotroni<sup>\*1</sup>, Hazim Awbi<sup>2</sup>

*1 Mechanical Engineering, School of Engineering  
and Design, Brunel University  
Uxbridge, Middlesex UB8 3PH, UK  
lg15aaa4@brunel.ac.uk  
Maria.kolokotroni@brunel.ac.uk*

*2 School of construction Management & Engineering,  
University of Reading  
Reading RG6 6UA, UK*

## ABSTRACT

A literature review has revealed that there is a very limited number of numerical or experimental studies of the air flow for mechanically ventilated large occupied rooms. Existing literature suggests that a room with more than 5 meters floor-to-ceiling height can be considered as a large space. The aim of this paper is to present a set of detailed air temperature and velocity measurements in a large open plan office located in south England. External weather conditions were monitored with a meteorological station located on the roof of the building to include air temperature, relative humidity, solar radiation and wind speed/direction. The monitored office has dimensions of 15.5m x 14m x 6m ceiling height with brick external walls and metal roof which includes two large skylights. The open plan office is used by 12 people with positioned desks and computers while lighting is provided by Theroux. The total internal gain heat load in the office is 27 W/m<sup>2</sup>. This large occupied open plan office is supplied by a mechanical cooling using overhead mixing ventilation system which operates during the summer months.

Measurements were carried out in the summer of 2016 which included some periods with external temperatures up to 28.9°C and solar radiation up to 740 W/m<sup>2</sup>. The measurements were used to validate a Computational Fluid Dynamic (CFD) model of the office building executed using ANSYS Fluent. A comparison between numerical results and experimental results show good agreement. The validated CFD model was used to study in more detail the existing ventilation system and proposed improvements for its performance including further commissioning.

## KEYWORDS

Large space, Air distribution, Experimental measurements, CFD model, Model validation

## 1 INTRODUCTION

Ventilation of large spaces differs from spaces with small volume, especially when the ceiling height is more than in typical spaces usually around 3m. This is because convection currents and thermal stratification have a powerful influence on the flow pattern in a large enclosure. When warm air under the effect of buoyancy escalates in a large open space, a positive temperature gradient between the floor and the ceiling will be formed which is known as stratification (Calay et al. 2000). According to Li et al. (2009), an enclosure which has more than 5 meters floor-to-ceiling height can often be considered as a large space. The air flow pattern in large enclosures should be arranged and controlled to ensure an acceptable indoor air quality in the occupied zone without the need for too much air flow rates (Heiselberg et al. 1998). Mateus & Carrilho da Graça (2017) made an extensive literature survey of existing studies of HVAC systems performance in large rooms, and they found that only three types of room air distribution strategies are used in large rooms. These are displacement ventilation, mixing ventilation and underfloor air distribution systems. Furthermore, their review divulged that there are rareness of researches which make a comparison between ventilation model simulations and measured air temperature in large spaces. These measurements are needed for commissioning, diagnostic and assessment

purposes. Unluckily, the considerable volume and envelope area associated with large enclosures adds to the difficulty of making measurements (International Energy Agency (IEA) 1998). A mixing ventilation system is a type of system where the fresh air is mixed with impure enclosure air to provide a fresh supply of air and reduce the impurity concentrations (Awbi 2011). The air jet is usually supplied in the top parts of the enclosure with velocity  $> 2.0$  m/s to provide air circulation within the enclosure. The temperature and contaminant concentration in the room should be uniform. Whereas a displacement ventilation system is based on the fundamental of displacing the impure enclosure air with fresh outside air. The cool air usually supplied at near the floor with low velocity (normally  $< 0.5$  m/s) to make an upward air motion (thermal plumes) as it gets warmed by heating sources in the enclosure. Therefore, vertical gradients of air velocity, temperature and contaminant concentrations will usually be created. Displacement ventilation system is usually more energy efficient compared to the mixing ventilation system because it needs lower fan power and has higher ventilation performance.

Due to the expensive and lengthy nature of experimental measurements, Computational Fluid Dynamic (CFD) is a helpful tool to conduct parametric studies. Several models can be used for simulation of turbulent flow. Reynolds-averaged Navier-Stokes (RANS) equation simulation using one and two-equation turbulence models such as RNG  $k-\epsilon$  models, SST  $k-\omega$  model and Reynolds Stress model (RSM) are often used. Furthermore, large-Eddy simulation (LES) and direct numerical simulation (DNS) are time-resolved methods which can be used for simulations. To estimate the quality of the numerical predictions a comparison between experimental results and the numerical predictions is a common procedure (Svensson et al. 2012).

The objective of this paper is to present a set of detailed air temperature and velocity measurements in a large occupied open plan office located in southern England. This large office is supplied by a mechanical overhead mixing ventilation system which operates during the summer months. The experimental data were used to validate two turbulence models: RNG  $k-\epsilon$  model and SST  $k-\omega$  model. The validated model was used to study in more detail this ventilation system and proposed improvements for its performance.

## **2 DESCRIPTION OF THE CASE-STUDY AND VENTILATION SYSTEM**

The large open plan office used by research staff and students was chosen as the case-study of large space because its floor-to-ceiling height is 6m. The enclosure has dimensions of 15.5m x 14m x 6m and a floor area of 201  $m^2$  with brick external walls and metal roof which includes two large skylights. Two big rectangle windows are located on the south side wall of the building with dimensions 3.5m x 1.1m and 4.2m x 1.1m. There is one door on each end wall of the building. The researchers' large open plan office includes 12 personal computers, peak occupancy of 12 occupants and artificial lighting comprising of 23 luminaires each equipped with two 49 W lamps. The total internal heat gain in the office is 27  $W/m^2$ . The office is supplied by a mechanical cooling overhead mixing ventilation system which operates during the summer months. The external air is delivered into the building interior through a 13m long cylindrical supply duct with 0.7m diameter. This duct has eight air diffusers located at a height of 3.7 m above the floor with dimension of 0.8m x 0.15m and divided into seven segments. Air exhaust is via two return grills located at a height of 3.7m with dimensions 1.0m x 0.5m each, see Figure 1.

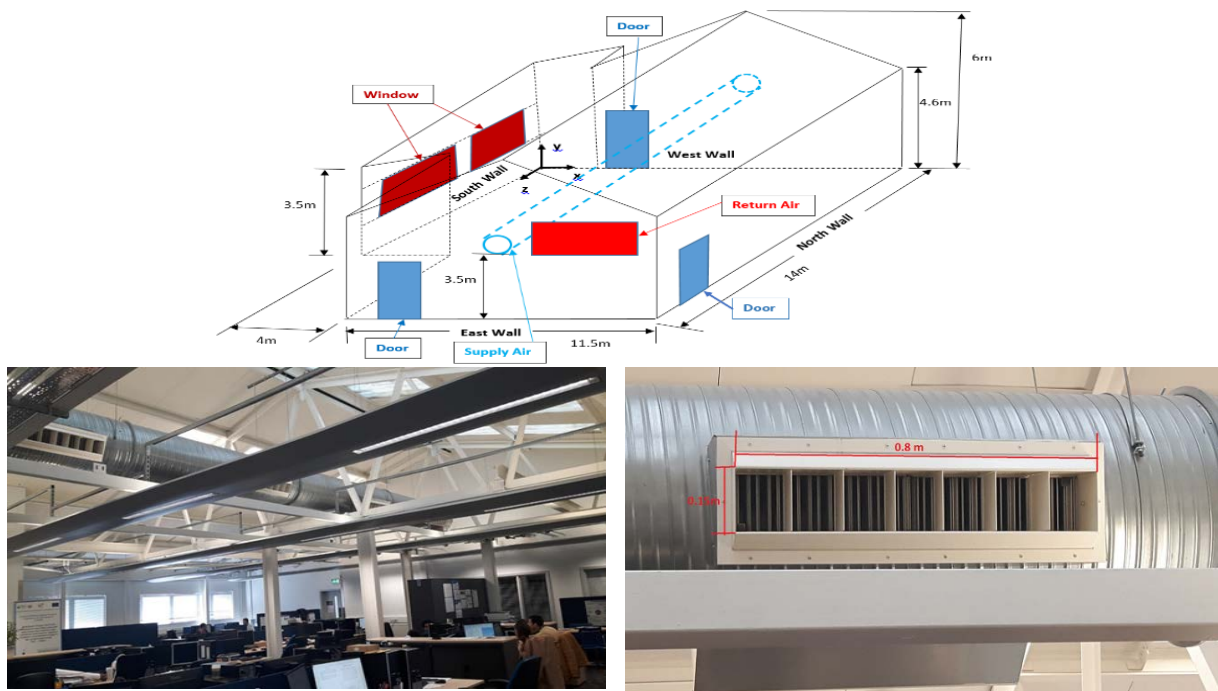


Figure 1: Sketch and photos of the researchers' office and an air diffuser at (CSEF) building

The measurements were carried out over a period of 28 days from 24/8/2016 to 21/9/2016 which can be considered late summer season in London. During this period and according to the on-site weather station the external average temperature was  $18.5^{\circ}\text{C}$ , the maximum was  $28.9^{\circ}\text{C}$ , the minimum temperature was  $11.3^{\circ}\text{C}$  while solar radiation was up to  $740 \text{ W/m}^2$ . On the other hand, the external average relative humidity for the same periods was 80%, the maximum was 100% and the minimum was 39.4%. In general this period of the year can be considered to be almost the hottest days in London.

### 3 EXPERIMENTAL SET-UP

Air temperature and relative humidity were measured using nine HOBO Temp/RH data loggers attached to three columns which are (C1, C5 and C8) at three different heights of 0.1, 1.2 and 1.8m, measuring temperature and relative humidity distributions between the floor and ceiling, see Figure 2. In addition, six HOBO, Temp/RH data logger, were used to measure air temperatures at the six diffusers and three more loggers were mounted at the height of 4m at three different points to measure the air temperature and relative humidity in the area above the occupied zone from 24/8/2016 to 21/9/2016. The accuracy of the air temperature measurement is  $\pm 0.21^{\circ}\text{C}$  and  $\pm 3.5\%$  for the relative humidity measurements (HOBO n.d.).

Measurements of mean air velocity and temperature were conducted using a TA465 AirFlow instrument over five days from 5/9/2016 to 9/9/2016 at three different times of a day which were (11:00, 13:00 and 15:00). Seven different spots throughout the enclosure area have been assigned to capture vertical gradients of velocity and air temperature. These locations were chosen to describe the indoor environment in the occupied zone. The velocities were measured over two minutes with a sampling interval of ten seconds at heights of 0.1, 1.2, 1.8m at each spot. These measurements were repeated over five days three times a day. The accuracy of the velocity measurement is estimated to be  $\pm 0.015 \text{ m/s}$  or  $\pm 3\%$  while the error of measured temperature is estimated to be  $\pm 0.3^{\circ}\text{C}$ .

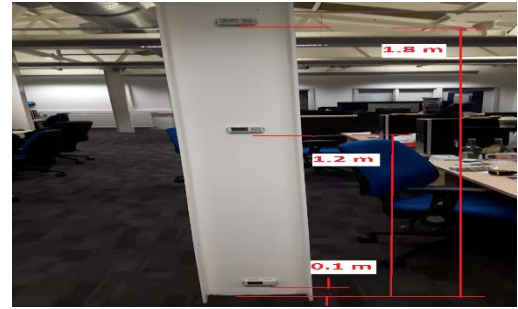
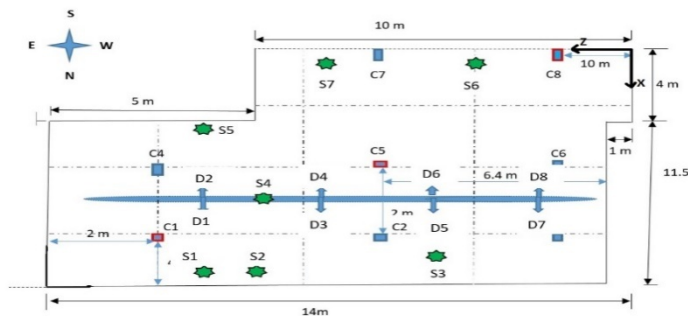


Figure 2: Schematic layout of the researchers' office at (CSEF) building and HOBO Temp/RH data logger location attached to the column at three different heights of 0.1, 1.2 and 1.8m

## 4 MEASUREMENT DATA

### 4.1 Temperature and Relative Humidity Data

Figure 3 shows the air temperatures for C1 at four heights and at the supply diffuser D1 over nine days. It compares expected results for the temperatures at column C1 for different heights 0.1, 1.2, 1.8, 4.0m as well as the temperatures at diffuser D1 plus the external temperatures. There were sharp drops in temperature in each day at 06:00 for interior temperature lines which are temperature lines at 0.1, 1.2, 1.8, 4.0m and at D<sub>1</sub> due to turning on time for the cooling system. On 03-04/09/2016, the air temperature readings were nearly the lowest compared with the other days as they were weekend days. The air temperature reached a peak on 7/9/2016 where both the diffuser and external temperature were higher than 28 °C.

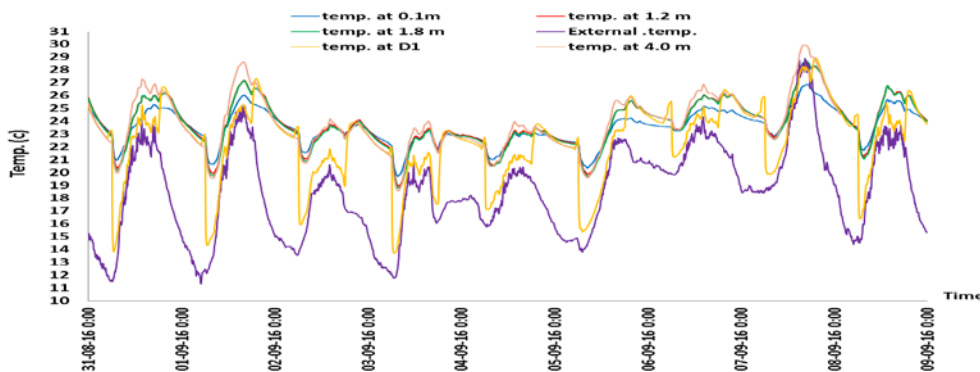


Figure 3: Air temperatures for C1 at four levels external and diffuser D1 over nine days.

There was nearly a 5 °C difference between the diffuser and outside air temperature when the cooling system was off. Whereas, the difference has been reduced to be approximately 1 °C when the cooling system was turned on. Also, the air temperature at the diffuser has risen sharply by 3 °C when the system was turned off due to hot air rising by buoyancy force. Then there was a moderate decrease in the temperature to match the temperatures at 1.2m, 1.8m and 4.0m, see Figure 4. In addition, temperatures at 1.2m were precisely the same as the temperatures at 1.8m during the ON period of the ventilation system which was from 06:00 to 18:00. However, the temperatures at 4.0m were higher than those at 0.1, 1.2m and 1.8m from 06:00 to 18:00. There was a steady state situation for all the temperatures from 15:00 to 17:00.

Figure 5 shows the temperature trends for three different locations in the enclosure which were C<sub>1</sub>, C<sub>5</sub> and C<sub>8</sub> at 1.2m over 9 days as well as the external temperature. The temperature

at point C<sub>8</sub> was much higher than the temperatures at C<sub>1</sub> and C<sub>5</sub> because it was very close to the external wall facing the south and this can be seen clearly at the mid-day of 7/9/2016.

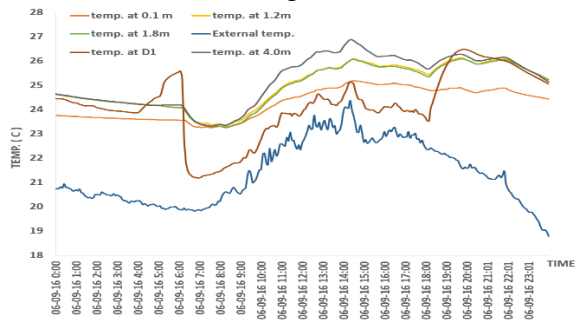


Figure 4: Air temperatures for C1 at four levels, external and diffuser D1 for one day

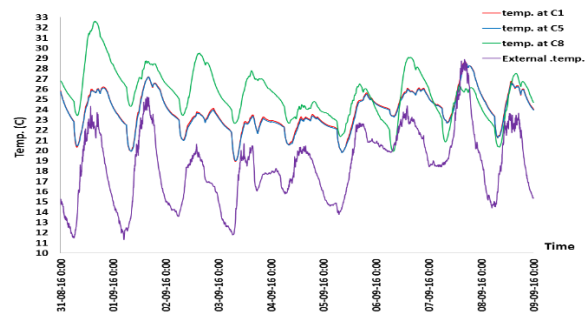


Figure 5: Temperature for C1, C5, C8 and external over nine days at height 1.2m

## 4.2 Velocity and Temperature Data

The measured velocities are presented in Figure 6 for six different spots in the enclosure. Air velocity at spots 1 and 3 show similar trend compared to the other spots because they have similar air flow direction and were located at the same distance from the diffusers. Spot 5 has the maximum velocity for both heights 0.1m and 1.2m compared to the others. Both spots 5 and 2 have similar air velocity tendency while it was different for spot 6. The velocity at spot 4 was close to 0 m/s for the three levels due to its location as it was under the main duct.

Figure 7 shows the air velocity for seven spots (see Figure 2) as measured at 1.2m height and at 15:00 over five days. The velocity at spots 1, 6 and 7 was within the acceptable range, while it was just above that range at spots 2 and 3. At spot 5, the velocities were twice the recommended velocity in the occupied zone which is 0.25 m/s.

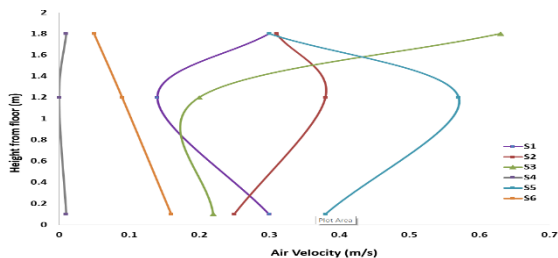


Figure 6: Air velocity in six spots at different heights

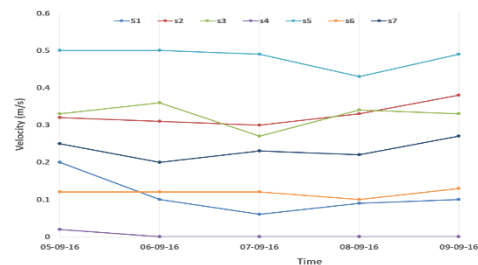


Figure 7: Air velocity in six spots at 1.2 heights over five days

Figure 8 illustrates the air temperatures for the seven spots that were mentioned above at 1.2m over five days. All the seven spots had approximately 28 °C as maximum temperatures on 07/09/2016 compared to the other days due to the high ambient temperature on that specific day. The air temperatures were almost the same at all the spots during the five days.

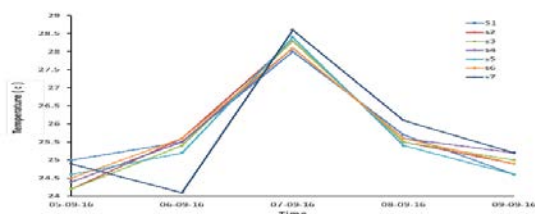


Figure 8: Air temperatures in seven spots over five days

## 5 CFD MODELLING RESULTS AND DISCUSSION

ANSYS Workbench 17.1 with Fluent 17.1 (ANSYS Fluent 2016) was used to simulate the case study numerically. The fundamentals of modelling room air flow are turbulence modelling, treatment of airflow and heat convection near the wall, boundary condition, discretization of the domain and the solution method. The CFD simulation model was assumed to be steady-state and the simulation time was 15:00 h on September 6th, 2016 with four selected room locations used for further analysis as shown see Figure 2. These four spots are S1 which is in the north-east quarter of the office room and facing the airflow of diffuser one, S4 which is located in the middle of the office underneath the supply duct, S5 which is located in south-east quarter of the office and facing the air supply from diffuser two and S6 which is in the south-west quarter of the office and close to the windows.

Thai et al. (2007) made an evaluation of various turbulence models in predicting the airflow and turbulence in enclosed environments using CFD, and they recommended RNG  $k-\epsilon$  model to be used in forced convection flow which is often performed in enclosures with mechanical ventilation systems. However, they recommended SST  $k-\omega$  model for high buoyancy flow in predicting air velocity, temperature and turbulence quantities. For that reason, both of RNG  $k-\epsilon$  model and SST  $k-\omega$  model were used to validate the CFD model and compare their performance by utilising the temperature and air velocity measurements. Awbi (1998) pointed out that the convective heat transfer coefficient forecasted using a wall function is intensely critical to the distance of the point from the surface ( $y_p$ ) at which the wall function is applied, i.e. the value  $y^+$  at that point. He proposed in his study that an optimum position for a heated wall or heated floor is about 5 mm and about 30 mm for a heated ceiling.

### 5.1 Boundary Conditions and Physical model

The quality of the numerical solution is invariably dependent on the accuracy of the boundary conditions and how these are combined with the numerical model. In this investigation, the following boundary conditions were defined based on the measurements carried out.

1. The condition of the air supply is set in the CFD model at values of 23°C for all the eight air diffusers while the inlet velocities were not equal and modelled as seen. They were 2.72 m/s for diffuser one, 3.2 m/s for diffuser two, 2.97 m/s for diffuser three, 3.1 m/s for diffuser four, 1.0 m/s for both diffusers five and six and 0.95 for both diffusers seven and eight based on measured data. These values were chosen to correspond with the measured values.
2. The wall temperatures were measured at different points and were found to be between 28 and 29°C. Whereas the ceiling and window temperatures were 35 and 39 °C respectively.
3. The body of the occupant was presented as a cylinder of height 1.4m and diameter of 0.4 m giving a body surface area of approximately 1.85 m<sup>2</sup> according to (Pinkel 1958). The clothing temperature is set to a value of 33.7 °C as mentioned by Zolfaghari & Maerefat (2010).

The ANSYS code was used to construct the three-dimensional geometry and generate the mesh. Non-uniform grid strategy was utilised to cover the whole computational domain for the room. The finer grid was used close to inlet, outlet and walls, and also the area that were anticipated to have the steep velocity gradient. A grid independency study was performed using the RNG  $k-\epsilon$  model, and three grids densities, i.e. (15, 082, 503), (16, 045, 809) and (16, 791, 869) were tested. The results are discussed in the following section.

The finite-volume solver Fluent 17.1 was used to simulate the flow field of the ventilated enclosure. The governing equations were solved with a segregated scheme, and the SIMPLE algorithm solved the coupling between pressure and velocity. The discretization, the non-

linear and the viscous terms were calculated with second order upwind scheme while the BODY FORCE WEIGHTED scheme was used to reveal convergence when two consecutive iterations for the local variable was less than  $10^{-3}$  whereas for energy it was less than  $10^{-6}$ . Besides that, the net mass flow rate imbalance was less than 0.003% of the total flux through the system, and the net heat imbalance was less than 0.3% of the total energy flux through the system too.

## 5.2 Grid Independency Study

The mean air velocity and temperature profiles along the height of 0.1, 1.2, 1.8m of the spot (S2) for three mesh densities are shown in Figure 9 (a) and (b). It can be seen that the predicted mean temperature gradient for of the three meshes are incredibly fused with less than 0.4% difference between the two finer meshes, which indicates the coarse mesh is still fine enough at the three heights for temperature prediction. In addition, the predicted mean velocity along three heights at spot (S2) are compared for the three tested meshes, and finer two meshes show small difference which is about 3%. Thus, the medium grid has been chosen based on their two comparisons (Chen et al. 2013).

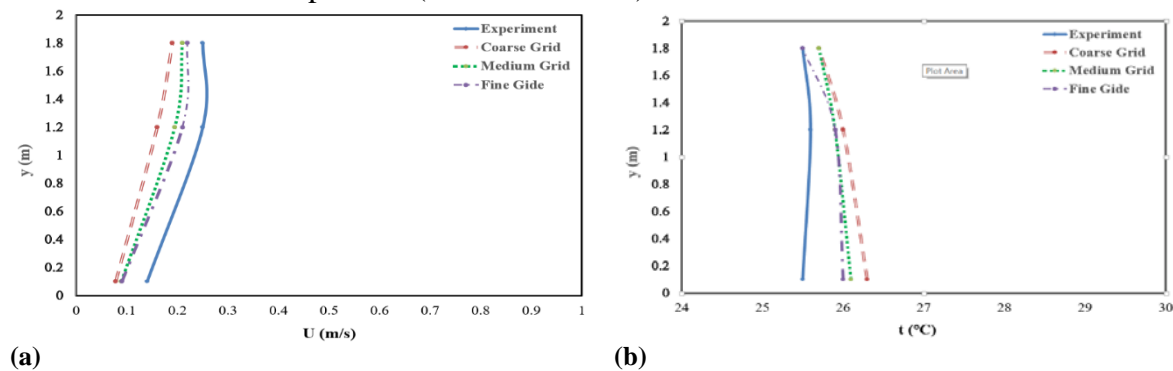


Figure 9: Comparisons between simulation results profiles along the height of 0.1, 1.2, 1.8m of the spot (S2) for three mesh densities (a) mean velocity and (b) mean temperature.

## 5.3 CFD Validation with Measurement

Figure 10(a) and (b) shows the comparisons of the mean air velocity and temperature profiles between simulation results using the two turbulent models and experimental data at four different spots. Figure 10(a) shows both turbulence models are able to predict the velocity distributing satisfactory when compared with the experimental results. Nonetheless, the less satisfactory agreement with measurement was observed in the spot (S5) at the height 1.2m. This is due to its location which is near to the one of the room doors. The predicted temperature profile is indicated in Figure 10(b) in which model SST k- $\omega$  shows slightly better agreement with measurement than the RNG k- $\epsilon$  model. The high-temperature discrepancy between the prediction and measurement was up to  $3.5^{\circ}\text{C}$  in the spot (S6) for RNG k- $\epsilon$  model probably due to its location near the sunny windows. Extra heat flux may be conveyed into the office and help to heat up the air around a spot (S6). To sum up, the prediction from SST k- $\omega$  show better agreement with measurements in comparison with RNG k- $\epsilon$  model. Hence, all results presented in the next section are based on SST k- $\omega$  turbulence model.

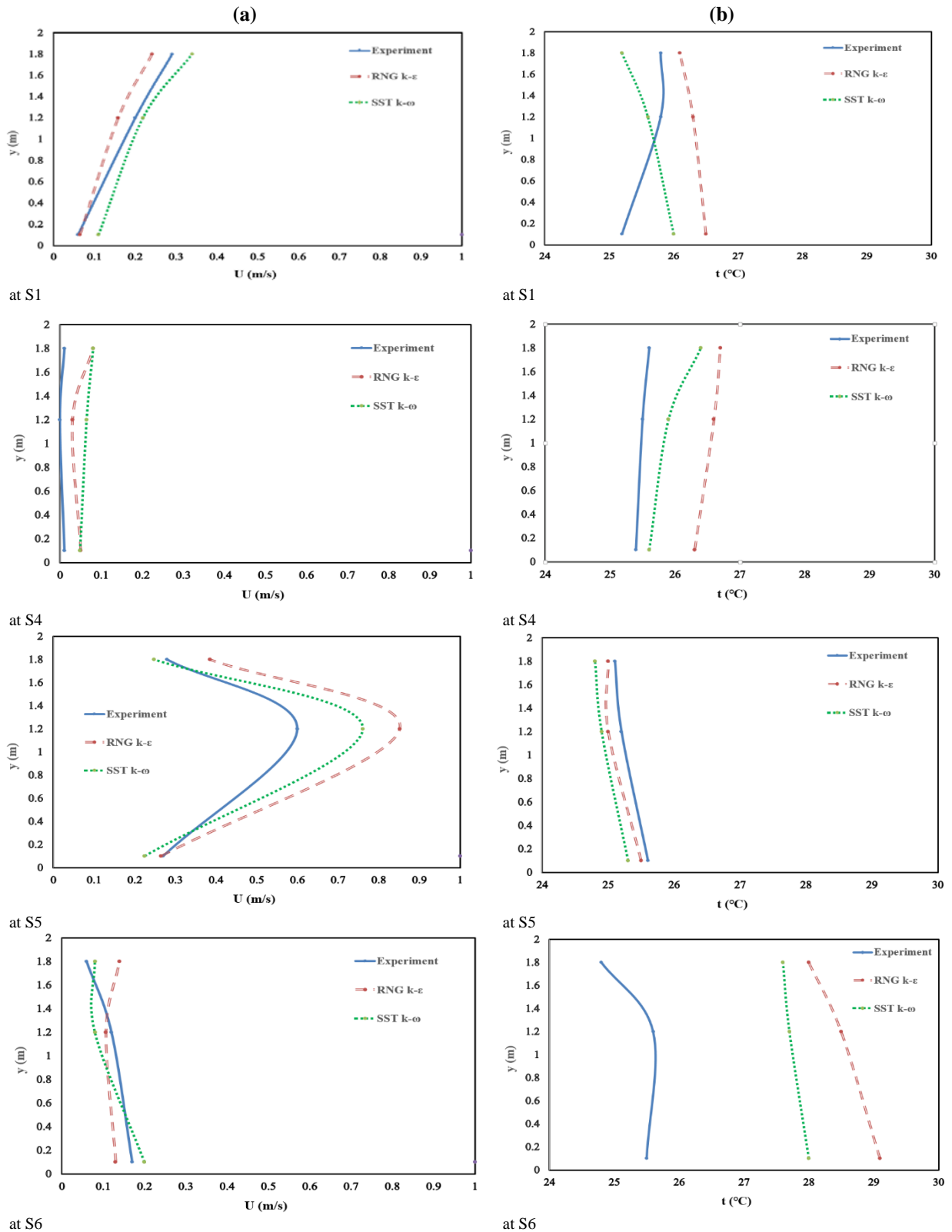


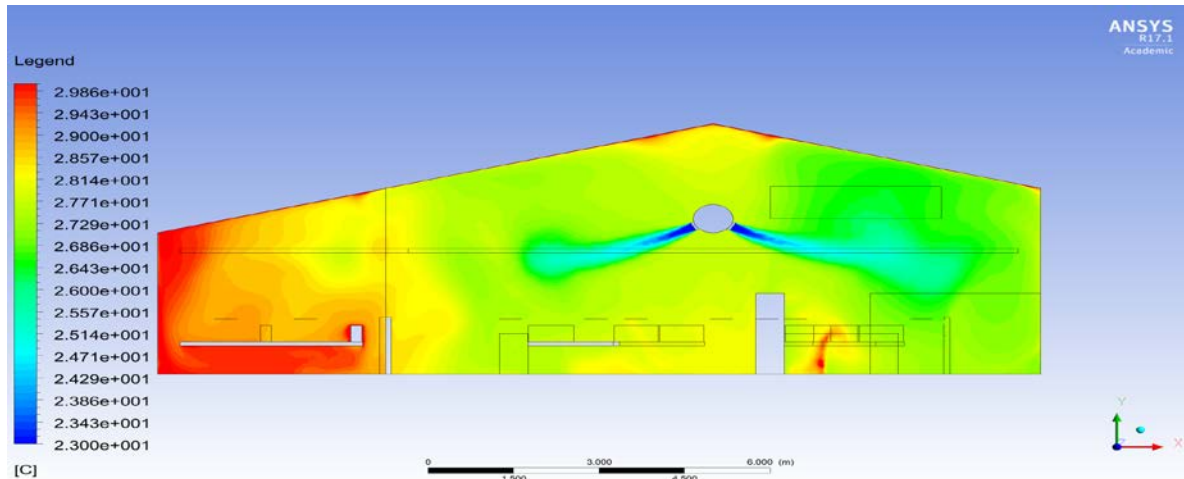
Figure 10: Comparisons between simulation results with measurements along three heights for aspect (S1, S4, S5 and S6) (see Figure 2): (a) mean velocity and (b) mean temperature.

#### 5.4 Results from Case Study

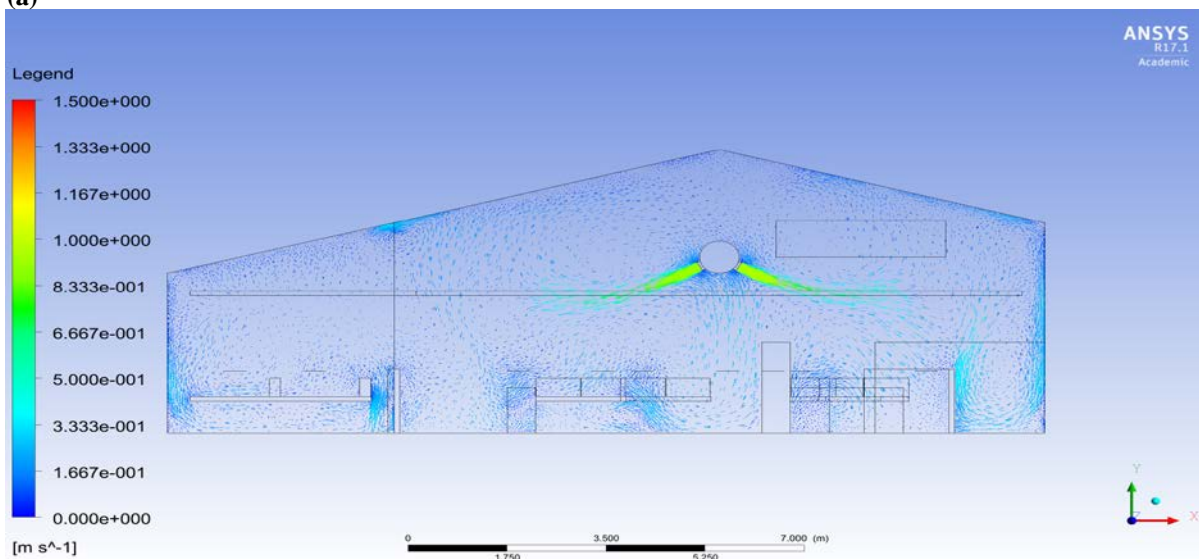
The qualitative numerical results indicating the temperature contour for a cross-section (at 4m) from the west wall in Figure 2 is shown in Figure 11(a), wherean apparent temperature stratification is observed. The cold air supply gets warmer while it spreads along the office. It

can be observed that the temperature tends to rise continuously along to the south wall. A convective plume is created when the air approaches the solar heated wall. It should be noted that the mean temperature at height 4m was nearly the same as the measured mean temperature (26°C).

Figure 11(b) displays the predicted velocity vector fields for the same cross-section. A cross-recirculation is created in different parts of the occupied zone of the office due to the partitions and furniture. The window thermal plume generates strong buoyancy force which moves the air up to the ceiling. On the other side of the room, the main flow is merged with the downward generated flows from the supply duct which increases the momentum of the air penetrating into the office.



(a)



(b)

Figure 11: Cross-section (4m) from the west wall in (Figure 2): (a) Temperature counter (b) Vector velocity.

## 6 CONCLUSION

In this paper, full-scale measurements of a mechanically ventilated large space have been carried out. First, the validation of two turbulence models RNG  $k-\epsilon$  and SST  $k-\omega$  was performed. According to the results, both models were capable of somewhat capturing the main flow features when results were compared the experimental findings. However, the predictions from SST  $k-\omega$  model were slightly better for the mean velocity values. The validated CFD model was therefore used to study the room ventilation system. In order to

modify the current system, it was found that the eight air diffusers should have the same air velocity to achieve optimum air distribution. On the whole, the current study is a step towards understanding and later improve currently used ventilation systems for large spaces by studying different types of ventilation systems such as the impinging jet system.

## 7 REFERENCES

ANSYS Fluent, 2016. Theory guide.

Awbi, H.B., 1998. Calculation of convective heat transfer coefficients of room surfaces for natural convection. *Energy and Buildings*, 28(2), pp.219–227.

Awbi, H.B., 2011. Energy Efficient Ventilation for Retrofit Buildings retrofit degli edifici. , pp.23–46.

Calay, R.K., Borresen, B.A. & Holdø, A.E., 2000. Selective ventilation in large enclosures. *Energy and Buildings*, pp.281–289.

Chen, H.J., Moshfegh, B. & Cehlin, M., 2013. Investigation on the flow and thermal behavior of impinging jet ventilation systems in an office with different heat loads. *Building and Environment*, 59, pp.127–144.

Heiselberg, P., Murakami, S. & Roulet, C., 1998. Ventilation of large spaces in buildings. *Final Report IEA Annex*.

HOBO, Onset HOBO and InTemp Data Loggers. Available at: <http://www.onsetcomp.com/> [Accessed May 16, 2017].

International Energy Agency (IEA), 1998. IEA Annex 26: Energy Efficient Ventilation of Large Enclosures - Technical Synthesis Report.

Li, Q. et al., 2009. CFD study of the thermal environment in an air-conditioned train station building. *Building and Environment*, 44(7), pp.1452–1465.

Mateus, N.M. & Carrilho da Graça, G., 2017. Simulated and measured performance of displacement ventilation systems in large rooms. *Building and Environment*, 114, pp.470–482. Available at: <http://dx.doi.org/10.1016/j.buildenv.2017.01.002>.

Pinkel, D., 1958. The use of body surface area as a criterion of drug dosage in cancer chemotherapy. *Cancer research*, 18(3), pp.853–856.

Svensson, K. et al., 2012. Numerical and Experimental Investigation of Flow Behavior in a Confluent Jet Ventilation System for Industrial Premises. *DiVA Portal*, pp.1–6.

Thai, Z.Q. et al., 2007. Evaluation of various turbulence models in predicting airflow and turbulence in enclosed environments by CFD: part 1 - Summary of prevalent turbulence models. *Hvac&R Research*, 13(6), pp.853–870.

Zolfaghari, A. & Maerefat, M., 2010. A new simplified thermoregulatory bioheat model for evaluating thermal response of the human body to transient environments. *Building and Environment*, 45(10), pp.2068–2076.

# Development of protocol for sub-metering for ventilation models and verification for shopping centres

Matthias Haase\*<sup>1</sup>,

*1 SINTEF Building and Infrastructure  
Høyskoleringen 7b  
Trondheim, Norway*

*\*Corresponding author: Matthias.haase@sintef.no*

## ABSTRACT

Shopping centres are complex buildings with specific needs. The use that different areas are put to affects energy consumption, whereas the different functional patterns and stakeholder groups influence energy use. They are also associated with specific requirements that make it relevant to consider different types of performance indicators.

The study investigates the energy conservation measures applicable for management, operation and use of shopping centres and aims to perform the measurements and verification of the energy savings of shopping centres. Its main focus was to track inefficient use and user implications in complex buildings (shopping centres) with focus on the ventilation. First, the main predictor variables and performance indicators associated with ventilation were identified.

A protocol for sub-metering of ventilation related energy consumption and flows (mainly electricity for fans, but also heating and cooling) was defined as necessary basis in order to be able to track inefficient use and user implications. User profiles were split into sub-categories, owners, tenants (shop owners, differentiating by size and type) and end-users (shopper, with appropriate differentiation) are three minimal differentiations.

Energy can be considered to follow function because energy in the end is used to meet requirements defined by the activities that take place in a shopping centre. In a SC, requirements are diversified by the type of tenants (shops, retail, restaurants, cafes, etc.), by the size of tenants rental space (stalls, retail units, independent anchor stores etc.), or by the type of spaces (common areas, offices, storage etc.). The different activities can be characterized by functional patterns for various groups; – opening hours for customers will differ from operational hours for technical services and lighting. Facility operation has to meet the requirements of staff before the shopping centre opens to the public. In shopping centres, many tasks are performed outside of opening hours which require maintaining health and safety for the workers. Examples are cleaning, sanitation, loading and re-stocking of goods. In relation to this, the ratio of full operation of HVAC and lighting vs. opening hours or service hours is one index that could be used as a performance indicator.

The proposed method provides a solid basis for validation and thus performance based economic models that were introduced in order to be able to quantify cost-effective refurbishment investments of ventilation systems and strategies. The results of key performance indicators provided valuable input in the decision making process for deep retrofitting plans. Different proposals for visualization of results (feedback to managers, tenants, customers) were investigated and are discussed.

## KEYWORDS

Ventilation in renovated buildings; Controls and user interaction; Innovative ventilation concepts and combined systems;

## 1 INTRODUCTION

In the re-cast of the Energy Performance of Buildings Directive (EPBD) adopted in May 2010, a benchmarking mechanism for national energy performance requirements was introduced. The EPBD recast required the Commission to establish a comparative

methodology by 30 June, 2011. Ecofys conducted a study in 2011 for European Council for an Energy Efficient Economy (ecee) to determine cost-optimal levels to be used by Member States for comparing and setting these requirements (Boermans et al. 2011). The report aimed to contribute to the ongoing discussion in Europe around the details of such a methodology by describing possible details on how to calculate cost optimal levels and pointing towards important factors and effects. This report gives suggestions regarding the implementation of the EU directive 2010/31/EU and disseminates the acquired information and knowledge. The revised Energy Performance in Buildings Directive (EPBD) 2010/31/EU calls for a calculation of the cost optimal energy standards and renovation standards. Cost optimal calculations can often be too short-sighted to deal with the urgent need for societal answers to the climate change challenges and can risk underestimating the potential for energy renovations in the building sector. The calculation should be informed by a long term cost effective figure of reaching a certain energy efficiency target which sufficiently contributes to mitigating climate change (EEB, 2010). Life-cycle costing based on net present value (NPV) provides a sound basis for the development of a common methodology for calculating cost-optimal levels of renovation.

Shopping centres are not interchangeable with other kinds of complex buildings, such as office blocks, hospitals or schools. The character of shopping centres, form, function, usage, and users has implications for energy use. To support the understanding of what causes the main inefficiencies in energy usage and how to develop the best solutions sets, a definition of shopping centres was developed, based on existing literature.

The definition chosen in this study describes a shopping centre as "*a formation of one or more retail buildings comprising units and 'communal' areas which are planned and managed as a single entity related in its location, size and type of shops to the trade area that it serves*" (Bointner et al. 2015).

The definition gives an indication of the main form and function in shopping centres. In addition, location, type of development, the size and the GLA, the type of anchor stores and the trip purpose are all aspects that have been used to indicate the needs that a shopping centre serves within social and physical context, these are presented in Table 1. Climate and regional differences have implications for retrofitting practice and the definition and supporting table present climatic and regional differences and are registered in the description of ten representative reference buildings (Bointner et al. 2015).

In general, the shopping centre industry is used to key performance indicators (KPIs).

Example of KPI for a Shopping centre real estate company are: Total property return, Occupancy, Like-for-like, NRI (net rental income) and Growth in EPS (earnings per share).

This work will identify the main predictor variables and performance indicators found in shopping centres in a context with user and occupant expectations and requirements. Form follows function to a large degree in shopping centres. However, the needs of retail activity and the requirements associated with the different stakeholders and their typical functional patterns actively influence shopping centre architecture and energy consumption (Haase et al. 2015; Woods et al. 2015).

## **2 METHOD**

The paper develops performance indicators based on the technical functionality of shopping centre architecture, for example flexibility and universal design, in short meeting user needs. Subsequently, predictor variables and performance indicators associated with several aspects were examined.

The IPMVP Volume III focuses on energy savings in new constructions where Volume I mainly refers to retrofit constructions. The fundamental difference between M&V in new and

retrofit construction is related to the baseline. The baseline in a retrofit project is usually the performance of the building or system prior to modification. This baseline physically exists and can therefore be measured and monitored before the changes are implemented. In new construction the baseline is usually strictly hypothetical; it does not physically exist, and therefore cannot be measured or monitored. A new construction baseline can be defined or characterized by code or regulations, common practice, or even the documented performance of similar constructed buildings.

Energy codes and standards can provide a convenient, clearly defined, and consistent baseline in order to ensure appropriateness. Whole building energy simulation tools in particular require high level of design detail for proper analytical rigor, requiring a fairly well-developed design of the building. M&V requires baselines that are consistent and repeatable, or that can at least be readily adjusted to allow performance comparisons on a broader scale.

An accurate determination of energy savings is a key condition for long term success of energy management projects. Energy savings are determined by comparing measured energy use before and after implementation of an energy saving measurements.

To perform these kinds of analysis, it is necessary to:

Identify the market segments and the segmentation of the current energy performance requirements (different requirements for different building types) where applicable; define and select a sufficient number of reference buildings that are characterised by their functionality, characteristics and regional conditions, including indoor and outdoor climate conditions; specify packages of energy saving- energy efficiency- and energy supply measures to be assessed; assess the corresponding energy-related investment costs, energy costs and other running costs of relevant packages applied to the selected reference buildings; use, when appropriate, the established reference buildings and relevant packages to identify, using the same methodology, cost-optimal energy performance requirements for building elements and technical building systems.

**3 RESULTS**

The results are divided into architectural, energy flows and protocol issues, discussed in the following sub-sections.

**3.1 Architecture, typology and layout of shopping centres**

Architecture encompasses technology, functionality and aesthetics. In this section, architectural form has been considered in context with user and occupant expectations and requirements to build a basis for energy performance indicators that relates to shopping centre form, layout, users requirements and cultural context. There are different types of shopping centres (see Table 1) and there is a typology associated with the usage that different areas in shopping centres are put to, functional patterns and stakeholder groups are associated with the areas. The different shopping centre types and typologies may vary according to for example size and use, for example it may be expected that speciality centres will have smaller circulation areas and less storage space than regional centres, and some centres do not have restaurants, staff rooms or atriums [2].

Table 1: Shopping Centre typology [2].

<b>Location</b>	<b>Type of development</b>	<b>Size</b>	<b>GLA [m<sup>2</sup>]</b>	<b>Anchor store</b>	<b>Trip purpose</b>
Town Centre	Neighbourhood centre/ community centre	Small shopping centres	5,000 – 19,999 m <sup>2</sup>	Supermarket or hypermarket	Convenience shopping
Shopping/ urban	Speciality centre (market halls, historical buildings,		Usually 5,000 m <sup>2</sup> and above	Traditional markets, tourist shops	Leisure, convenience shopping

Out-of-Town Shopping/suburban	other)				
	Retail Park and Factory Outlets		5,000 – 30,000 m <sup>2</sup>	None	Household shopping, Comparison shopping, leisure shopping
	Regional centre	Medium/large shopping centres	20,000 – 79,999 m <sup>2</sup>	One or more department stores	Comparison shopping
	Super-regional centre	Very large shopping centres	80,000 m <sup>2</sup> and above	Several department stores, entertainment centres	Comparison shopping, leisure

Table 2: Typical Areas in Shopping Centres [2].

Typology	Main usage				Location					
					Common areas	Shop/ retail areas	Behind the Scenes	Outdoors		
Common Areas	Circulation	Main horizontal circulation	Vertical circulation	Emergency exits	Atrium location	Main usage areas	Within retail units and stalls	None	Benches paths, play areas and other	
	Entrance	Main entrance	Side entrance	From car park						
	Sanitary	Toilets	Child care							
	Parking	Entrance	Circulation	Parking						
Restaurants/cafes/Food courts	Entrance	Seating	Service	Food preparation			Food serving in-store and restaurants		Kitchens, prep, storage	Pavement cafes
Shops/Retail/Other	Entrance	Sales	Service	Staff rooms / storage	Atrium, corridors	Main retail	Storage, staff rooms in some units	Storage, staff rooms	Temporary/permanent	
Behind the Scenes	Entrance	Trolleys Services	Trucks Waste	Sanitary	None	Storage, staff rooms and waste areas in some units	Main usage areas	Delivery waste storage	Temporary/permanent	
	Storage	Pathway	Shafts	Emergency exits						
Outdoors	Restaurants/cafes	Entrance	Seating	Service	Benches, paths, play areas and other	Temporary or permanent retail units, or stalls	Main usage areas	Delivery and waste storage	Main usage areas	
	Parking	Circulation	Parking lot	Service						
	Leisure	Resting/Recreation	Seating	Other						
	Delivery area	Containers								

However, there are certain areas that may be considered standard for all shopping centres.

Table 2 describes the five main areas in shopping centres, their usage and different locations within a centre and shows an overlap in usage, for example not all retail takes place in clearly defined retail units; some take place in common areas in temporary or permanent units.

Restaurants, food courts and cafes may be found within retail units and on occasion stores

may be found in restaurants and cafes. In addition, centres that offer leisure activities, or specialised functions like conference facilities, are typologies not covered in this overview. Typical examples which impose other usages include cinemas, bowling alleys, or swimming complexes. Hotels or apartments may also be located within shopping centres. For these typologies additional performance indicators apply which are not covered.

Table 2 offers insight in the broad range of activities which take place in shopping centres, giving customer satisfaction requires a broad range of services from shops, toilets and deliveries, to technical rooms, child minders, cafes and car parks. The range of activity requires a complex and flexible physical structure, one that allows for, amongst other things, changing retail, demographic and technical needs.

### **3.2 Energy use and flows in shopping centres**

Shopping centres are complex buildings with specific needs. The use that different areas are put to affects energy consumption, whereas the different functional patterns and stakeholder groups influence energy use. They are also associated with specific requirements that make it relevant to consider different types of performance indicators.

In the scope of this analysis both ventilation indicators and requirements with a direct or an indirect effect on energy consumption in shopping centres are identified. When defining the relevance of performance indicators; legal requirements (i.e. for work environment), ownership or authority over parts of the centre, and cultural context also come into play. As a result of the underlining complexity of performance requirements in SC, it may also be useful to distinguish between causes of energy use within a functional sub-division, meaning energy divided by the functions which it is used (by end use or supply system), and organizational sub-divisions of energy use distinguished by who pays for the energy and thus is related to billing practice, tenant agreements, and contracts with energy supply carrier companies.

The first three are mainly linked to the demand side and indicators that represent the requirements that can be found in norms, standards and the like. While different stakeholder groups, organisation and contextual aspects like climate and energy availability, also define the relevance of performance indicators, and suggest which priorities should be given when performance requirements are in conflict. The latter interest groups and contextual aspects also form billing practices, sub-metering and indicators for dividing the operational energy costs.

### **3.3 Protocol for sub-metering**

Figure 1 illustrates a functional sub division of energy end use within a shopping centre. Starting with the energy supply and the technical services in place, the energy use associated with heating, cooling and electricity are structured by end use. The diagram is easiest to comprehend for centralized HVAC systems, but in principle the structure is the same for all installations localized in tenants' retail space. In a typical shopping centre there will exist several heating, or cooling loops and many electrical subdivisions (distribution boards) on top of various end uses of energy.

The illustrated processes are usually in the control of facility managers and technical staff. A multitude of performance indicators can be related to this structure. Some performance indicators are important in the design and commissioning of the systems, other are of use in the day-to-day running of the centre. Reading the diagram from left to right, the potential of increasing energy efficiency lies both in production, distribution and end-use.

Energy can be considered to follow function because energy in the end is used to meet requirements defined by the activities that take place in a shopping centre. In a SC, requirements are diversified by the type of tenants (shops, retail, restaurants, cafes, etc.), by the size of tenants rental space (stalls, retail units, independent anchor stores etc.), or by the type of spaces (common areas, offices, storage etc.). The different activities can be characterized by functional patterns for various groups; – opening hours for customers will differ from operational hours for technical services and lighting. Facility operation has to meet the requirements of staff before the shopping centre opens to the public. In shopping centres many tasks are performed outside of opening hours which require maintaining health and safety for the workers. Examples are cleaning, sanitation, loading and re-stocking of goods. In relation to this, the ratio of full operation of HVAC and lighting vs. opening hours or service hours is one index that could be used as a performance indicator.

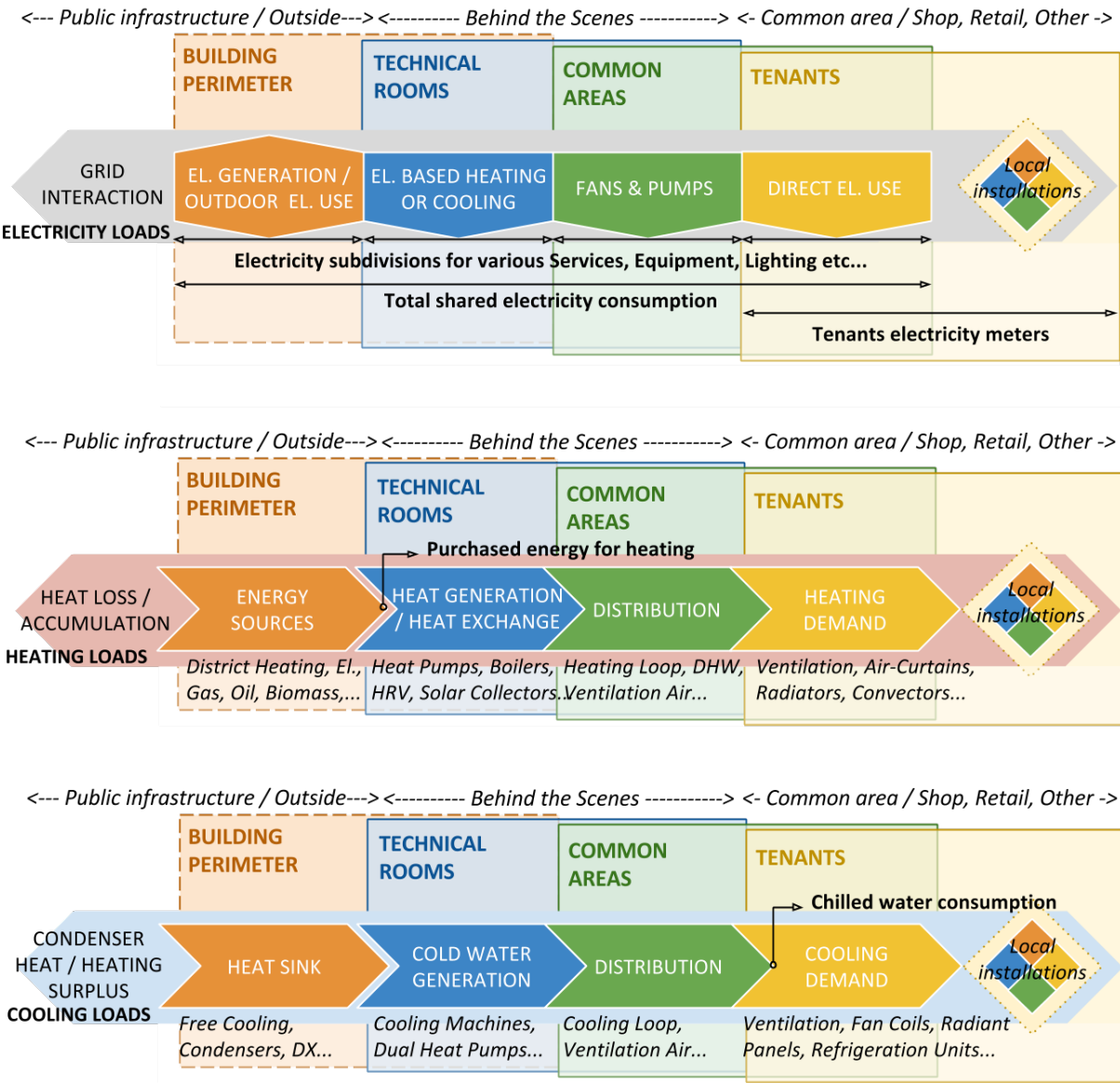


Figure 1 – Sub division of energy flows (electricity and thermal) associated with different end uses.

Therefore, six performance concepts are identified which form the structure of the next sections, all with contextual relevance to energy use and supply of energy in SC:

Concepts with functional element sub-division:

- Energy follows function
- Energy follows form
- Energy follows user needs

Concepts with organizational element sub-division:

- Energy follows stakeholders
- Energy follows organization
- Energy follows availability

The different concepts are explained in more detail in Haase and Skeie (2015).

### **3.4 The role of key performance indicators**

In typical shopping centres the retail units are often heated, cooled and ventilated separately from the common areas. The same retail units are often also connected to the central spaces by large open doorways through which air, odours, light, and noise exchanges occur, effectively linking the different spaces. This limits the accuracy of heating, cooling and ventilation assessments. Key performance indicators based on floor area can be used, but it is challenging to meet performance requirements, to keep within accepted limits of comfort and meet retailer needs in such an open indoor environment, where different spaces inside the shopping centre are effectively linked.

Comfort needs, however, are also socially constructed. In the design process, operation, meetings between tenant associations and management, labour meetings performance indicators can be important quantitative statements to meet user needs with regard to comfort and ensure high energy performance. Also building code requirements related to work space specifications can have an influence on the design choices. Access to daylight for shop workers e.g. is of importance for those shops that do not have direct access to daylight due to its location within the shopping centre.

Organisational forms can be observed in Real estate companies, property companies, management companies, facilities companies (outsourcing or within the same owner company) and tenant associations. Contracts between those organisations and the indicators used in those agreements are often based on KPIs which offers potential for introducing energy intensity related KPIs.

Nowadays, it is a challenge to transform the current energy system into modular power generation in order to improve the quality and the reliability of the electricity supply. The renewable energies and efficient solutions can overcome the oversizing problem of the electrical infrastructure for meeting the energy demand peaks as well as the energy transmission losses. It is important to operate with KPIs that can help to distribute energy production within the centre. However, the incorporation of renewable system in shopping centres must take into account that some problems in the supply can appear given its dependence of the climate conditions as well as the affections in the quality of the grid since they can generate frequency and voltage fluctuations and outages. Furthermore, any interaction in the grid must consider the grid capacity for admit new compounds.

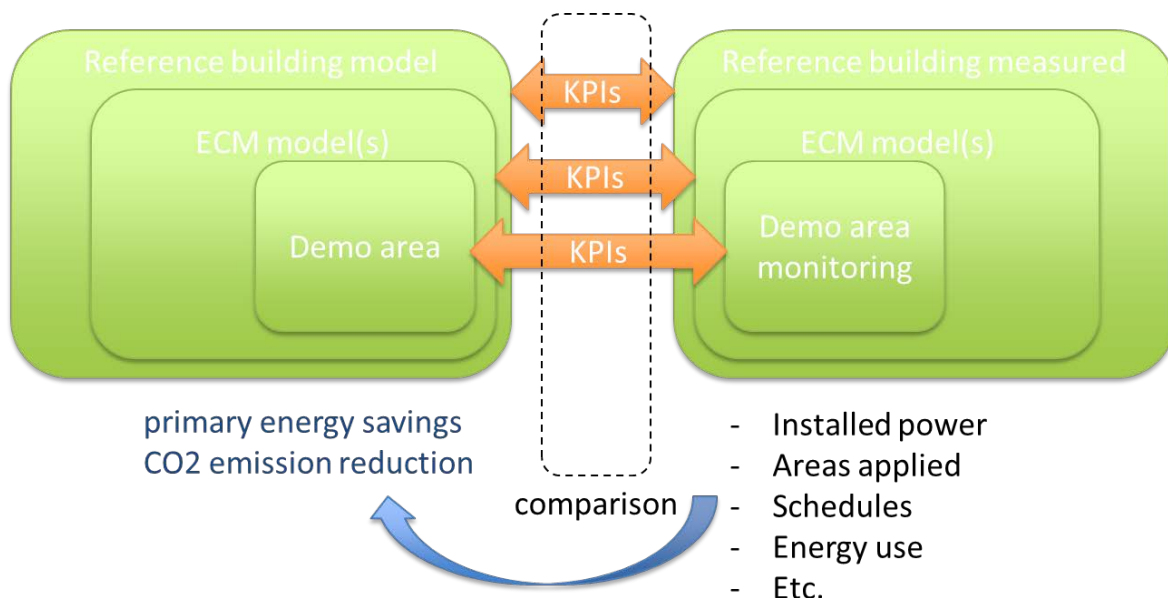


Figure 2 – Schematic description of procedure

The HVAC (heating, ventilating, and air conditioning) system is responsible for providing the thermal and hygienic needs of a shopping centre. An efficiently designed and operated building and HVAC system reduces the amount of energy needed to control hydrothermal conditions and air flow in a space. In addition to the passive solutions regarding thermal insulation, natural ventilation and solar gain controls there are specific solutions regarding the HVAC system, that promise to lead to energy savings. To reduce the consumption associated with HVAC the focus must be on:

- energy efficient equipment
- energy flux strategy
- equipment control and management.

#### Energy efficient equipment and components

The current equipment could be replaced with ones with greater efficiencies.

This is especially true when the existing systems are old, inefficient or malfunctioning. Some of the main predictor variables include:

- Efficiency of the heating system (boiler, Heat pumps, Combined heat and power (co- and tri-generation, Biomass boiler or District heating)
- Efficiency of air-conditioning systems (e.g., chillers);
- Efficiency of ventilation system
- Presence and efficiency of heat recovery systems;
- Performance parameters of economisers;
- Efficiency of auxiliary devices

The type of distribution system (radiant floor or ceiling, fan coils or primary air) should be also considered as a predictor variable with special attention to the efficiency of auxiliaries (e.g., fans, motors) and to the correct size of equipment and balance systems.

### Energy flux strategy and recovery

The recovery factor of the heat waste recovery system and the performance of free cooling should be considered. Thermal layout is important because it influences which thermal synergies (e.g., thermal cascade) can be exploited. For instance, the existence of interconnections and the supply and return temperatures of the refrigeration and heating/cooling duct are important predictor variables.

### Equipment control and management

Building system control and management strategies in shopping centres and retail buildings are crucial to ensure correct operation. The operation should therefore be regulated by a central unit (building management system – BMS) acquiring information from the field and deciding the best strategies to deliver the required conditions for each zone and tenant. Control strategies are very powerful predictor variables (on/off set points, temperature and rate set points etc.)

## **4 DISCUSSION**

The shopping centre market has changed from a fairly homogeneous, mass consumption market to one that is fragmented according to for example taste and lifestyles, reflecting a diverse and changing society. Shopping centre architecture therefore needs to meet needs of consumers who are more sophisticated and demanding. During the rehabilitation process it is important to keep in mind the four main stakeholders groups, namely customers, management, tenants and community. An integrated design process is needed that takes into account the goal to develop future markets where good architecture contributes to low-energy use, attractive trading jobs and meeting spaces, and thereby supporting the activities of all four groups. For Energy conservation measures (ECM) this implies a specific set of procedures in order to be able to implement these concepts in a measurement and verification of demonstration areas:

1. Comparison of key performance indicators (KPIs) in reference building model with measured data (e.g. electricity bill, district heating bill)
2. Definition of KPIs for reference model
3. Deduction of KPIs from reference model for ECM model
4. Deduction of KPIs from ECM model for demonstration area (e.g. installed power, schedules, areas, etc.)
5. Use of new KPIs for demo area
6. Comparison of monitoring KPIs with KPIs in demo area
7. Use of same KPIs in similar areas within the ECM model
8. Comparison of monitoring KPIs with KPIs in ECM model
9. Comparison of KPIs in ECM model with KPIs in reference model
10. Calculation of KPIs (e.g. energy consumption divided into electricity, energy need for heating and cooling, ventilation) for whole shopping centre
11. Calculation of KPIs for whole shopping centre (e.g. primary energy savings, CO<sub>2</sub> emission reduction, based on comparison with base case)

## 5 CONCLUSION

In the scope of this analysis both indicators and requirements with a direct or an indirect effect on energy consumption in shopping centres were identified. When defining the relevance of performance indicators; legal requirements (i.e. for work environment), ownership or authority over parts of the centre, and cultural context also come into play. Six performance concepts were identified which have contextual relevance to energy use and supply of energy in SC. As a result of the underlining complexity of performance requirements in SC, it may also be useful to distinguish between causes of energy use within a functional sub-division, meaning energy divided by the functions which it is used (by end use or supply system), and organizational sub-divisions of energy use distinguished by who pays for the energy and thus is related to billing practice, tenant agreements, and contracts with energy supply carrier companies.

A possible task for the future could be to identify if and how relevant energy performance indicators can be incorporated in contracts, or other forms of agreements between the stakeholders.

## 6 ACKNOWLEDGEMENTS

The research leading to these results has received funding from the European Community Seventh Framework Programme (FP7/2007-2013) under grant agreement n. 608678.

## 7 REFERENCES

Boermans, T., Bettgenhäuser, K., Hermelink, A. and Schimschar, S. Cost optimal building performance requirements, May 2011 © European Council for an Energy Efficient Economy, Commissioned by ecee with financial support from Eurima and the European Climate Foundation (ECF), access: [http://www.ecofys.com/files/files/cost\\_optimality-eceereport.pdf](http://www.ecofys.com/files/files/cost_optimality-eceereport.pdf); access date: 24.06.2014

Bointner, R., Toleikyte, A., Woods, R., Atanasiu, B., De Ferrari, A., Farinea, C. and Noris, F. (2014), Deliverable 2.1 report - Shopping malls features in EU-28 + Norway, EU FP7 project CommONEnergy – Reconceptualizing Shopping Malls, EPBD. 2010. Energy Performance in Buildings Directive 2008/0223, European Commission, Brussels, revised 2010. <http://eur-lex.europa.eu/LexUriServ/LexUriServ.do?uri=OJ:L:2010:153:0013:0035:EN:PDF>, access date: April 2015

Haase, M., Skeie, K.S., Woods, R., Mellegård, S., Schlanbusch, R.D., Homolka, S., Gantner, J., Schneider, S., Lam-Nang, F., (2015) Deliverable 2.3 report - Typical functional patterns and socio-cultural context, EU FP7 project CommONEnergy – Reconceptualizing Shopping Malls, ,access date: April 2015

Haase, M., Antolin, J., Belleri, A., Interactions of retrofitted shopping centres with local energy grids, proceedings IEECB&SD conference (IEECB&SD2016), Frankfurt, Germany, 16-18 March 2016

IPMVP, International Performance Measurement & Verification Protocol - Concepts and Options for Determining Energy and Water Savings, Revised March 2002. DOE/GO-102002-1554, <http://www.nrel.gov/docs/fy02osti/31505.pdf>, access date: Feb 2017

Woods, R., Mellegård, S., Schlanbusch, R.D., Haase, M., Skeie, K.S., Deferrari, A.,  
Cambronerovazquez, M.V., Ampenberger, A., Bointner, R. (2015), Deliverable 2.2 report –  
Shopping mallinefficiencies, EU FP7 projectCommONEnergy – Reconceptualizing Shopping  
Malls, ,access date: April 2015

# Heat Recovery Hybrid Ventilation System With a Thermal Storage

Akira Fukushima<sup>1</sup>, Sayaka Murata<sup>\*2</sup>, Masahiro Uozumi<sup>3</sup>

*1 Hokkaido University of Science  
Maeda 7-15-4-1 Teine-ku  
Sapporo006-8585, JAPAN  
fukushima-a@hus.ac.jp*

*\*2 Hokkaido Research Organization  
Kita19 Nishi 11, Kita-ku  
Sapporo 060-0814, JAPAN  
s.murata@hro.or.jp*

*3 Hokkaido University of Science  
Maeda 7-15-4-1 Teine-ku  
Sapporo006-8585, JAPAN*

## ABSTRACT

A “heat recovery hybrid ventilation system” is the combination of passive stack ventilation and mechanical push-pull ventilation. Two heat storage boxes are connected to the natural EA stack and the underfloor natural OA duct. The alternation is done periodically in a way of that the outdoor air is drawn through one of 2 boxes contains earth tiles and the indoor air is exhausted through the other box. After the heat in the exhaust air is stored in the box connected to the stack in time of the natural ventilation, the stored heat is recovered by the supply air in time of the mechanical backward ventilation. The system functions reversed in the box connected to the natural OA duct. Fan operation is controlled by the air temperature in in-outside chambers of the box.

The purpose of this study is the development of the heat storage box and the appropriate control system. First of all, the prototype box was made considering space to install and the sizes of parts as follows.

Box: Readymade Expanded Polystyrene box size of 600mm long, 350mm wide, and 200mm deep inside.

Earth tile: Interior finishing tile made from diatomaceous earth size of 6.5mm thick, 300x150mm.

Backward fan: 12V DC propeller fan with 120mm in diameter

In this paper, we proposed the numerical simulation model to simulate heat transfer in the heat storage box and evaluated the adequacy of the model by comparing the measurement and the numerical simulation results on the prototype box. The measurement has been done in 2 constant temperature rooms, and the exhaust fan was installed to simulate natural stack ventilation.

As a result, assuming that the amount of heat storage material is about three times as high as that of the prototype box and the EA / OA is switched when the outside and inside temperature of the box becomes the intermediate temperature between the room and the outdoor, it is estimated that the heat recovery efficiency is about 70% and switching time is 16 - 17 minutes.

## KEYWORDS

Hybrid Ventilation, Heat Recovery, Thermal Storage, Numerical Simulation Model, Control System

## 1 INTRODUCTION

Due to the high thermal insulation of houses, the ratio of ventilation load to the space heating energy consumption is increasing, and the reduction of ventilation load is required to achieve further energy saving. However, the adoption of a mechanical push-pull ventilation system with heat exchanger, which is a typical ventilation load reduction method, has a problem of increasing energy consumption for fan power. On the other hand, the passive ventilation system can reduce the energy consumption for fan power (Akira Fukushima, 1997)

and the maintenance load, but cannot reduce the heating load. Although there is a heat recovery type passive ventilation system using water circulation for buildings (C.A. Hviid, S. Svendsen, 2015), there is no simple system for detached houses yet. In this study, we proposed a hybrid heat recovery ventilation system that combines passive ventilation with respiratory heat recovery technology. The system collects heat of the EA by alternately passing the supply and the exhaust air to the heat storage material. The purpose of this study is the development of the heat storage box and the appropriate control system.

## 2 THE CONCEPT OF THE SYSTEM

Fig. 1 shows the concept of the system. Two heat storage boxes are connected to the natural EA stack and the underfloor natural OA duct. The alternation is done periodically that the outdoor air is drawn through one of 2 boxes contains heat storage material and the indoor air is exhausted through the other box. After the heat in the exhaust air is stored in the box connected to the stack in time of the natural ventilation, the stored heat is recovered by the supply air in time of the mechanical backward ventilation. The system functions reversed in the box connected to the natural OA duct. Fan operation is controlled by the air temperature in in-outside chambers of the box.

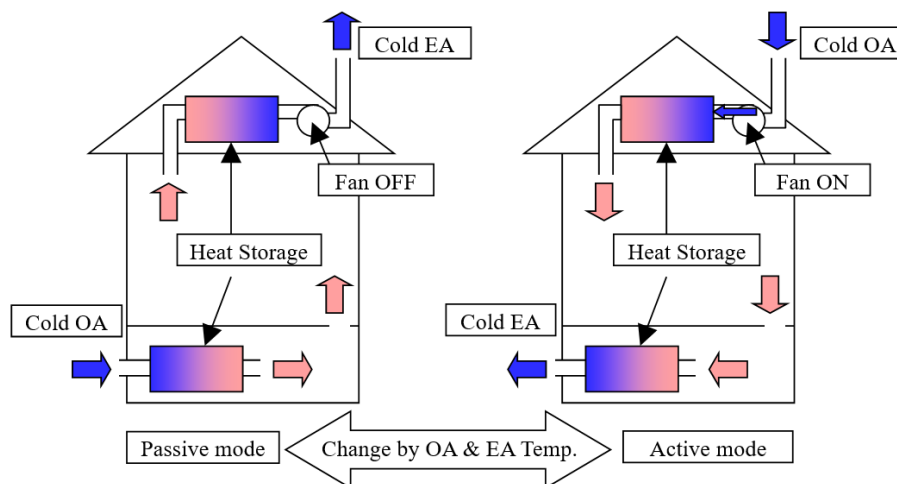


Figure 1: The concept of the system

## 3 TEMPERATURE SIMULATION OF THE HEAT STORAGE BOX

The simulation of the temperature of the heat storage box is carried out to examine the amount of heat storage material and control method, to keep the supply air temperature above a certain level and the heat recovery rate at 70%. This is a basic performance for a conventional push-pull mechanical ventilation system for general cold regions in Japan. The control method is investigated by the setting of the temperature at which switching between supply and exhaust is performed.

### 3.1 Simulation Method

First, the temperature simulation method of the heat storage box is developed, and the temperature of actual measurement is compared with simulated one. Next, several simulations are carried out by changing the amount of heat storage material and control method. Then, the proper control method for achieving the target of heat recovery rate is obtained.

Fig. 2 shows the simulation model.

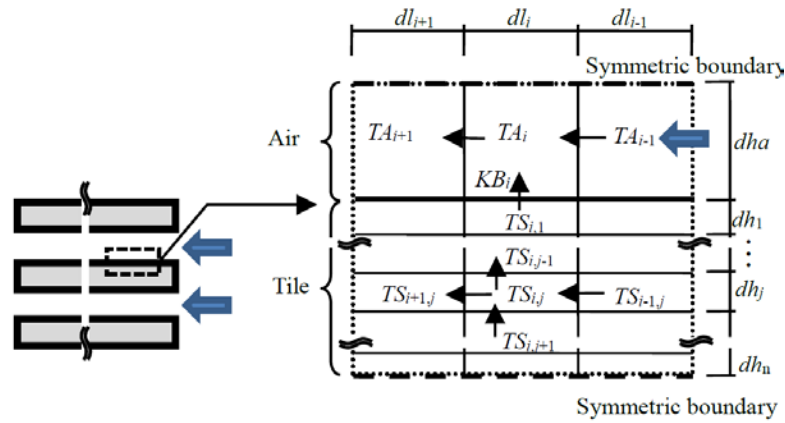


Figure 2: Thermal simulation model in the heat storage

The heat balance per unit width of one cell of air between the heat storage materials, is as follows

$$c \cdot \rho \cdot VA_i \frac{dT_{A_i}}{dt} = c \cdot \rho \cdot Q \cdot (T_{A_{i-1}} - T_{A_i}) + KB_i \cdot (TS_{i,1} - T_{A_i}) \cdot dl_i \quad (1)$$

Where:

$$VA_i = dl_i \cdot dha \quad (2)$$

$$KB_i = \frac{1}{\frac{1}{\alpha} + \frac{dh_1}{2} / KS} \quad (3)$$

- $c$ : specific heat of air [W/kg·K]
- $\rho$ : density of air [kg/m<sup>3</sup>]
- $\alpha$ : surface heat transfer coefficient [W/m<sup>2</sup>·K]
- $KS$ : thermal conductivity of heat storage material [W/m·K]
- $TA_i$ : temperature of air cell  $i$  [°C]
- $TS_{i,j}$ : temperature of heat storage material, cell  $(i, j)$  [°C]
- $dl_i$ : length of cell  $i$  [m]
- $dha$ : air cell thickness [m]
- $dh_j$ : heat storage material  $(i, j)$  thickness [m]
- $dh_j$ : calculation time interval [h]

Heat conduction between the air is ignored since it is considered to be extremely small as compared with advection (the amount of heat transferred by the air flow). The surface heat transfer varies with wind speed and temperature, but the radiation heat transfer coefficient is constant. So, the convective heat transfer coefficient is proportional to the wind speed. The numerical value is adjusted to match the actual measurement results.

The heat balance per unit width of one cell of the heat storage material is as follows

$$CS \cdot VS_{i,j} \frac{dTS_{i,j}}{dt} = HTL_{i,j} \cdot dl_i + KS \cdot \left[ \frac{TS_{i-1,j} - TS_{i,j}}{(dl_{i-1} + dl_i)/2} - \frac{TS_{i,j} - TS_{i+1,j}}{(dl_i + dl_{i+1})/2} \right] \cdot dh_j \quad (4)$$

Where:

$$\left[ \begin{array}{l} \text{When } j = 1 \\ \text{When } j = n \\ \text{Other} \end{array} \right. \quad \left. \begin{array}{l} HTL_i = KS \cdot \frac{TS_{i,j+1} - TS_{i,j}}{(dh_{j+1} + dh_j)/2} - KB_i \cdot (TS_{i,1} - TA_i) \\ HTL_i = KS \cdot \frac{TS_{i,j} - TS_{i,j-1}}{(dh_j + dh_{j-1})/2} \\ HTL_i = KS \cdot \left[ \frac{TS_{i,j+1} - TS_{i,j}}{(dh_{j+1} + dh_j)/2} - \frac{TS_{i,j} - TS_{i,j-1}}{(dh_j + dh_{j-1})/2} \right] \end{array} \right. \quad (5)$$

$$VA_i = dl_i \cdot dh_j \quad (6)$$

CS: heat capacity of heat storage material [W/m<sup>3</sup>]

n: number of divisions in the thickness direction of the heat storage material

The time interval of calculation was set to 0.0001s.

### 3.2 Analysis of the results

From the results of the temperature simulation, the heat storage rate(*S*) and the heat recovery rate(*E*) are obtained as follows.

$$\text{Heat storage rate}(S) \quad S = \frac{T_R - \overline{T_{EA}}}{T_R - T_O} \quad (7)$$

$$\text{Heat recovery rate}(E) \quad E = \frac{Q_S \cdot (\overline{T_{SA}} - T_O)}{Q_E \cdot (T_R - T_O)} \quad (8)$$

Where:

$T_O$ : outdoor temperature [°C]

$\overline{T_{SA}}$ : average OA temperature inside the box at the time of supply [°C]

$T_R$ : room temperature [°C]

$\overline{T_{EA}}$ : average EA temperature outside the box at the time of exhaust [°C]

$Q_S$ : supply air volume [°C]

## 4 COMPARISON BETWEEN SIMULATION AND MEASUREMENT

### 4.1 Heat storage box

Fig. 3 shows the prototype heat storage box and the measuring device.

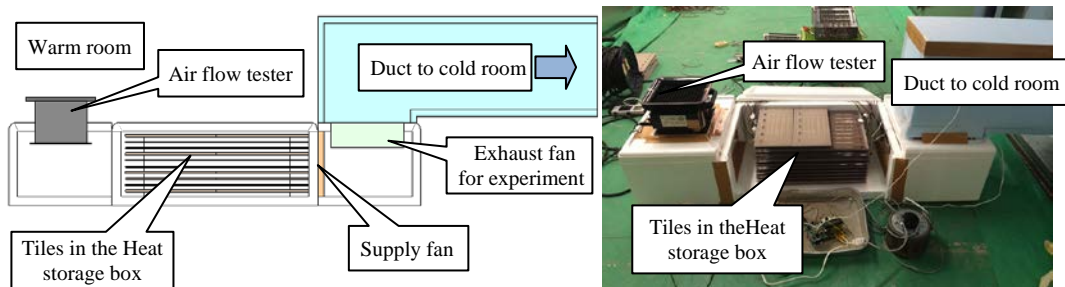


Figure 3: The prototype heat storage box and the measuring device.

Three ceramic tiles having a length of 303 mm, a width of 151 mm, and an average thickness of 6.75 mm were stacked in ten layers of a corrugated plate made of plastic having a height of 15 mm interposed therebetween.

The box was installed in the normal temperature room of two thermostatic chambers. It was connected to low-temperature room by the duct made of XPS. An exhaust fan was installed in the outside chamber to simulate natural ventilation. The air flow rate was measured by a hot wire type air flow meter at the indoor side of the heat storage box.

Thermocouples were used to measure the surface temperature of each layer of the ceramic tile, air temperature between layers and air temperature in the chambers both side of the heat storage box. The air temperatures in the in-outside chambers of the heat storage box were compared with the simulation results.

## 4.2 The conditions of measurement and simulation

We compare the simulation with the actual measurement results under the following two different control conditions.

- Switching on a steady state: Switch the supply and the exhaust every 5 hours.
- Temperature control: Switch to the supply at outside exhaust air temperature of 17°C, and switch to the exhaust at inside supply air temperature of 5°C.

Table 1 shows the conditions of measurement and simulation.

Table 1: The conditions of measurement and simulation

			Steady state	Temperature control
Tile for Heat Storage	Thermal conductivity	W/mK	0.3	
	Heat capacity	kJ/m <sup>3</sup> K	1620	
	Thickness	mm	6.75	
	width	mm	303	
	length	mm	453	
	Stacked Number		10	
	Stage spacing	mm	15	
Air flow rate	exhaust	m <sup>3</sup> /h	80	80
	air supply	m <sup>3</sup> /h	50	100
Temperature	Warm Room	°C	20	20
	Cold room	°C	-3	0

## 4.3 Actual measurement

Fig. 4 shows the actual measurement results when it is steady state switching, and Figure 5 shows the simulation result under the same condition.

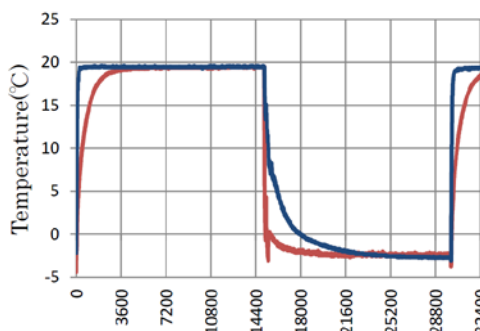


Figure 4: The test result (steady switching)

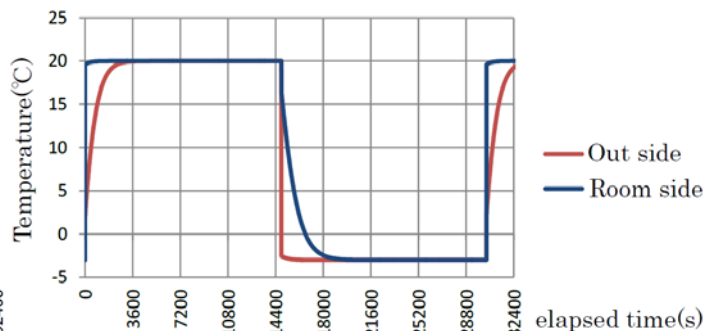


Figure 5: The simulation result (steady switching)

The figures show the temperature variation of one cycle of supply and exhaust. As you can see from the figures, both temperature of the actual measurement and the simulation reach a steady state in about 1 hour after switching to the exhaust, and the temperature change is similar. After switching to the supply, the temperature reaches a steady state for about 2 hours in the actual measurement and about 1.5 hours in the simulation. The reason why the simulation resulted in a shorter time may be the characteristics of the measuring device. Fig. 6 and Fig. 7 show the actual measured and simulated temperature variation respectively when switching was done with temperature control. As you can see from the figures, the time for the exhaust is almost the same between the actual measurement and the simulation, but the time for supply seems to be somewhat shorter in case of simulation. This is probably because the actual air supply volume may be less than 100 m<sup>3</sup>/h set as before. In spite of this results mentioned above, it is possible to grasp the temperature fluctuation generally, and also to predict the efficiency and switching temperature by the simulation for designing the performance.

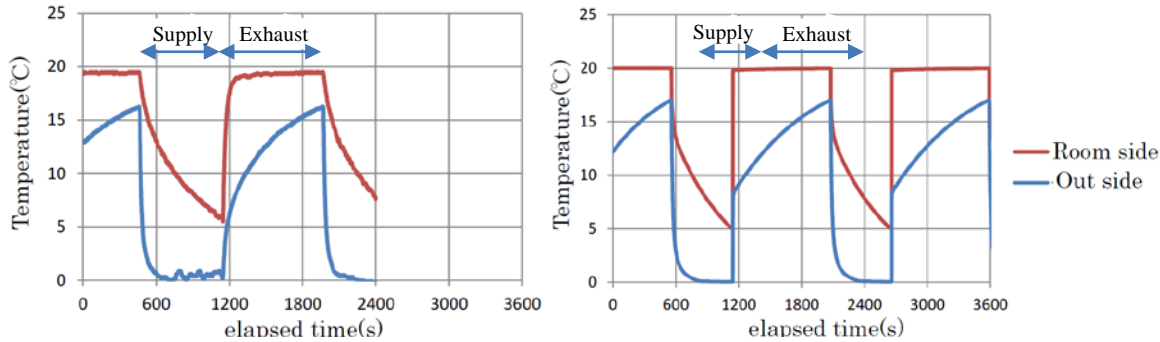


Figure 6: The test result (temp. control) Figure 7: The simulation result (temp. control)

**5 PERFORMANCE DESIGN BY SIMULATION**

**5.1 Thermal storage material**

The heat recovery rate in Fig. 7 calculated by the equation (8) is about 44%. If the switching temperature is lowered, the efficiency increases, but if the blowing temperature to the room is low, it becomes uncomfortable. Therefore, it is necessary to increase the amount of heat storage material in order to obtain higher recovery rate and to avoid frequent switching. The simulation was conducted under the condition shown in Table 2 (prototype, 2 to 4 times). The air flow rate was 80 m<sup>3</sup>/h for both supply and exhaust, and the outdoor temperature was 0°C, and the room temperature was 20°C.

Table 2: Conditions for Heat Capacity Simulation

Tiles		Prototype	2 times	3 times	4 times
length	mm	453	453	453	<b>604</b>
Stacking Number		10	<b>20</b>	<b>30</b>	30
Stacking Space	mm	15	7.5	5	5

Fig. 8 shows the heat storage rate, the heat recovery rate, the time of exhaust and supply at 10°C both at the switching temperature between supply and exhaust. Increasing the heat storage amount increases the heat storage rate and the heat recovery rate, and the switching time also becomes longer. Generally speaking, if the heat storage amount is tripled, the heat recovery rate exceeds 60% and the switching time also exceeds 10 minutes, so it is estimated that the amount of heat storage material is necessary about 3 times of prototype.

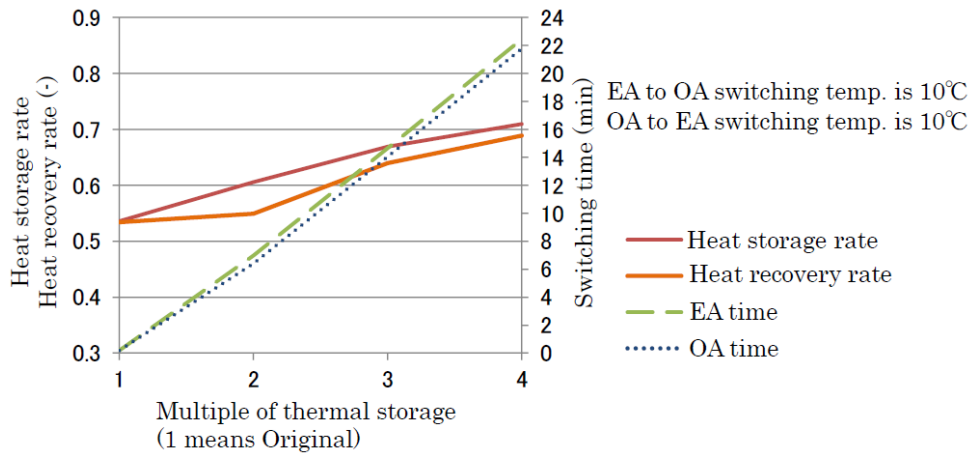


Figure 8: Simulated thermal performance of the box with the amount of heat storage material

## 5.2 Control method

Up to 24 ceramic tiles (the thermal storage material) can be stacked to be accommodated in the box, 604 mm for the length of 4 sheets of tiles, and the size of air space was set to 5 mm, which was tripled of the prototype heat storage material amount. Table 3 shows the conditions of air flow rate and switching temperature.

Table 3: Conditions for Control Method simulation

	OA	EA
Air flow rate[m <sup>3</sup> /h]	80 (partly 100)	
Switching temperature [ °C]	5,7,5,10	5,10,15
Outdoor temperature [ °C]	0, -10	
Room temperature [ °C]	20	

Fig. 9 shows the heat storage rate, the heat recovery rate, and the switching time when the outdoor temperatures are 0 and -10°C.

When the outside air temperature is 0°C and the switching temperature is 10°C, the heat recovery rate is around 70%. The lower the switching temperature from the exhaust to the supply, the shorter the switching time interval. When the switching temperature is 10°C, the times of supply and exhaust are equal.

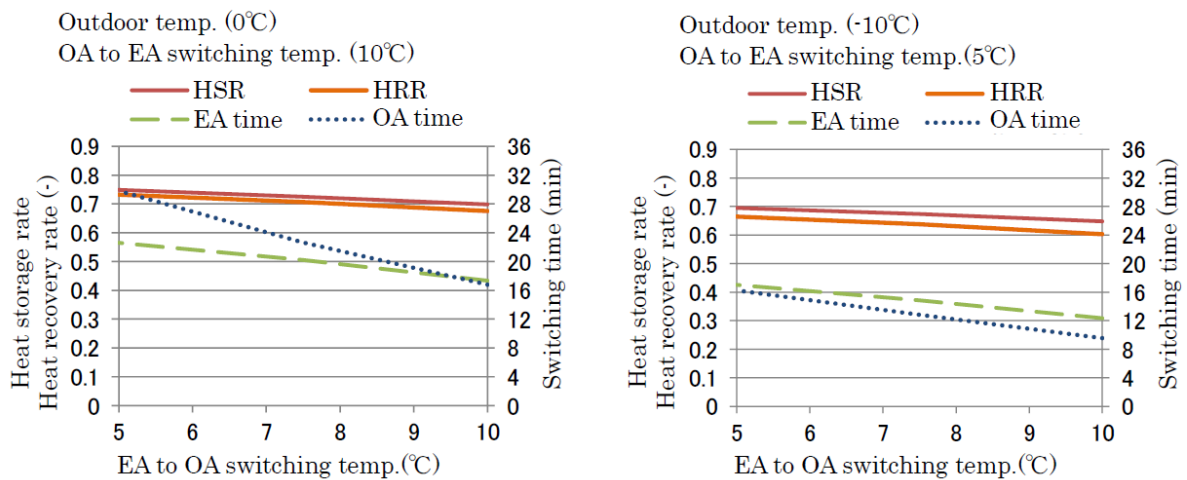


Figure 9: Simulated performance of the box with the switching time

When the outdoor temperature is  $-10^{\circ}\text{C}$  and the switching temperature is  $5^{\circ}\text{C}$ , the heat recovery rate is about 68%. In addition, the switching time between supply and exhaust becomes almost equal when the switching temperatures are  $5^{\circ}\text{C}$  both of supply and exhaust. From the above, when the switching temperature is set to an intermediate temperature between the rooms ( $20^{\circ}\text{C}$ ) and the outdoor, the heat recovery efficiency is about 70% and the switching time is 16 to 17 minutes.

## 6 CONCLUSION

The target of this study is the breathable hybrid heat recovery ventilation system using the heat storage material. We investigated the amount of heat storage material of the heat storage box and the proper switching temperature by the numerical simulation of the temperature in the heat storage box. As a result, assuming that the amount of heat storage material is about three times as high as that of the prototype model and the switching temperature is the intermediate temperature between the room and the outdoor, the heat recovery efficiency of 70% can be expected. The switching time can be 16 - 17 minutes.

## 7 ACKNOWLEDGMENT

This research is conducted by the Japan Society for the Promotion of Science Grant-in-Aid for Scientific Research / Basic Research (C) "Study on Respiratory Hybrid Heat Recovery Ventilation System Using Heat Storage".

This research cooperates with NPO Corporation Passive System Study Group.

## 8 REFERENCES

Akira Fukushima, Mutsuaki Miyaura, Masayoshi Inoue, Akira Doi (1997. 8). Passive Ventilation Strategy and Systems in Cold Region Part 1. *Journal of Environmental Engineering (Transaction of AIJ)*, 498, 51-56.

C.A. Hviid, S. Svendsen (2015. 6). Passive ventilation systems with heat recovery and night cooling: Building Physics for a Sustainable Built Environment, 6<sup>th</sup> IBPC, 99-104.

# A study of panel ridges effect on heat transfer and pressure drop in a ventilation duct

Thiago Santos<sup>\*1,2</sup>, Maria Kolokotroni<sup>1</sup>, Nick Hopper<sup>3</sup>, Kevin Yearley<sup>3</sup>

<sup>1</sup> Institute of Energy Futures, Brunel University  
London, Kingston Lane, Uxbridge, UB8 3PH, UK

<sup>2</sup> Federal Institute of Pernambuco, Av. Prof Luiz  
Freire, 500, Recife/PE –Brazil

\*Corresponding author:  
thiagosantos@ipojuca.ifpe.edu.br

<sup>3</sup> Monodraught Ltd.  
Halifax house, Halifax Road, High Wycombe, UK

## ABSTRACT

CFD simulations were conducted to assess turbulent forced convection heat transfer and pressure drop through a ventilation channel using a stack of panels with different ridge configurations containing Phase Change Material (PCM). First, an experimental rig using an existing commercial panel provided by a PCM manufacturer validates the model simulated in Ansys FLUENT. After that, 3D simulations with different designs were tested until the optimum configuration in terms of heat transfer and pressure drop was achieved. The optimum design by geometry and performance was drawn in 2D and a parametric analysis was performed by varying the spacing between ridges, height and ridge radius to identify difference in heat transfer performance. For both experiment and simulation, the flow rate in terms of Reynolds number based on the inlet hydraulic diameter of the channel ranged from 7200 to 21600. When compared with a flat and existing commercial panel, results show that the inclusion of ridges increase the Nusselt Number by 68 and 93% respectively at a Reynolds number of 21600. At a Reynolds number of 18736, the Nusselt number of the optimum panel is enhanced by 64 and 111% when compared to the flat and existing commercial panel, respectively. This panel was then taken forward to allow further refinements which include changes in panel thickness and number of panels per module. After more than 200 different panel designs and airflows simulations, a new design is proposed which reduces the number of panels per module from 9 to 6, thus reducing production costs but keeping nearly the same heat flux and pressure drop as the existing commercial panel. When 7 panels are used, it is possible to hold 13.68% more material with an increased pressure drop 3.36 times higher than the existing commercial panel (176.80 against 52.69 Pa) at a Reynolds number of 18736.

**KEYWORDS:** PCM-Air heat exchanger, Numerical simulation, Rib shape, Heat transfer enhancement/augmentation, Ventilative Cooling

## 1 INTRODUCTION

PCM-air heat exchangers are one of many thermal storage systems (TES) applications in constant study and development (Alizadeh & Sadrameli, 2016). The equipment uses the principle of thermal storage through latent heat in climates where night temperatures are cold enough to charge (solidify) the PCM and use it to cool the environment during the day. The concept has been studied extensively (Arzamendia Lopez *et al.*, 2013; Zalba *et al.*, 2004; Dolado *et al.*, 2011; Lazaro *et al.*, 2009) and performance in practice evaluated (Santos, Hopper & Kolokotroni, 2016; Kolokotroni, Santos & Hopper, 2016). The Phase Change Material in heat exchangers is commonly encapsulated in envelopes with small heat transfer efficiency. Thus, the increase of heat transfer between air and panel will increase the overall performance of the exchanger and lead to a fast thermal response, fast charging period and reduce energy consumption.

The introduction of ridges, fins, dimples and grooves are techniques commonly used to increase the heat transfer over a channel. These turbulators are widely applied and studied in engine turbine blades to protect them from exceeding the maximum allowable temperature.

In PCM-air heat exchangers, turbulators are used to increase cooling performance. However, turbulence also enhances pressure drop and consequently, an oversized fan is needed which will increase energy demand. Alternatively, a design with higher thermal efficiency and small pressure drop is desired and a motivation for researchers.

## Nomenclature

### Symbols

$\Delta T$	temperature difference (K)	$C_{p(air)}$	Specific heat of air (J/kg·K)
$T$	temperature (°C)	$Nu$	Nusselt number
$e$	Ridge height (m)	$Nu_o$	Nusselt number over a smooth surface
$h$	Channel gap (m)	$h$	Heat convection coefficient (W/m <sup>2</sup> )
$s$	Ridge spacing (m)	$D_h$	Hydraulic diameter (m)
$l$	total surface length (m)	$k$	Thermal conductivity (W/m <sup>2</sup> K)
$r$	Ridge radius (m)	$A$	Area (m <sup>2</sup> )
$E$	Sum of gaps (m)	$L$	Length (m)
$H$	Total height (m)	$W$	Width (m)
$p$	Pitch (m)	$\Delta p$	Pressure difference (Pa)
$T_t$	Sum of panel thickness (m)	$\Delta p_o$	Pressure difference of a smooth surface (Pa)
$\dot{m}$	Mass flow (kg/s)	$\dot{Q}$	Heat Flux (W)
$Re$	Reynolds number	$\eta$	Efficiency

### Subscripts

<i>air</i>	
<i>i</i>	Inlet
<i>o</i>	Outlet
<i>m</i>	Fluid
<i>s</i>	Surface

### Abbreviations

LMDT	Logarithmic Mean Difference Temperature
PCM	Phase Change Material
TES	Thermal Storage System
CFD	Computational Fluid Dynamics

Moon (Moon, Park & Kim, 2014) analysed sixteen ridge shapes (with different geometries) by varying pitch ratio. Results show that boot shaped ridge present the best results in terms of heat transfer with a pressure drop similar to a square ridge for a Reynolds number between 5000 and 50,000. The inclusion of dimples, protrusions or both dimples and protrusions also shows good results in heat transfer augmentation. Liu et al (Liu *et al.*, 2015) found that secondary protrusions cause downward flow, reducing recirculation in the adjacent primary dimple and improving the reattachment. In all cases studied, the area-averaged ratio between Nusselt and Nusselt over a smooth surface ( $Nu/Nu_o$ ) enhanced in 1.8 and 1.5 times for Reynolds ranging from 5000 to 27,500. Yang et al. (Yang *et al.*, 2017) introduced symmetric and staggered squared high ridges in channels with results showing that a larger blockage ratio corresponds to a larger heat transfer coefficient and also a higher friction factor with symmetric arrangement and higher blockage increasing  $Nu/Nu_o$  in the range of 6-7 and 3.5 for a staggered arrangement and higher blockage

Promvong and Thianpong (Promvong & Thianpong, 2008) experimented with four different shaped ridges (wedge pointing upstream, wedge pointing downstream, triangular and rectangular ridge) staggered and in-line over a turbulent channel ( $Re = 4000 - 16,000$ ). The result shows improvements in heat transfer when compared to a smooth channel where the wedge downstream in-line with the best performance in terms of Nusselt number ratio ( $Nu/Nu_o \cong 4.4$ ) and the rectangular ( $Nu/Nu_o \cong 3.7$ ), the worst. When pressure drop is taken into account, the triangular staggered has the best thermal performance ( $\eta = \frac{Nu}{Nu_o} / \left(\frac{\Delta p}{\Delta p_o}\right)^{1/3} \cong 1 - 1.1$ ) followed by triangular in line and staggered upstream wedge. After that, Thianpong et al. (Thianpong *et al.*, 2009) experimentally studied different heights of triangular ridges staggered and in-line through a constant heat-fluxed channel for Reynolds number of 5,000 to 22,000. The result shows an increase of approximately 1.8 – 4 in terms of

Nusselt number when compared to a smooth channel and a variation of thermal performance up to 1.3.

The present study focusses on the design of a panel surface able to enhance the heat transfer efficiency of PCM-air heat exchangers where pressure loss is an important parameter for systems requiring low power demand and noise levels.

## 2 METHODOLOGY

The designing process of the panel started by using existing literature as a basis where rounded ridges were selected for the PCM panel due to the reduced pressure drop, relative ease in manufacture and lower cost of production.



Figure 1: Existing panel in use for the PCM-Air heat exchanger (Rubitherm)

First, ten 3D designs were evaluated in terms of heat transfer and pressure drop through CFD simulations over a section of one panel channel and compared with the existing panel (Figure 1) in use and a dimpled panel. Each design was drawn with different rounded losange, protrusion and groove radius and also height and pitch. Surface temperature is fixed at 20 °C because is a melting point of a PCM used for this application and an inlet channel temperature of 26 °C is a common return air through recirculation or an outside air during cooling periods. The mesh was generated as coarse and adapted through Ansys FLUENT until no changes on the fourth decimal case of inlet pressure and outlet temperature were found, the turbulence model used was realizable  $R - \epsilon$  with scalable near wall treatment function and under-relaxation factors were adjusted to allow convergence and simulation stops when residuals achieved  $10^{-5}$ . The flow rate in terms of Reynolds number were based on the inlet hydraulic diameter of the channel and ranged from 7,200 to 21,600. The results were compared and one design uniform along its width was selected due to easy in manufacture for a more detailed analysis. Moreover, an experiment using the existing panel with 1, 2 and 3 modules measured and analysed the pressure drop through the channel and validated the CFD model. Results show that even if the existing panel is not uniform along its width, simulations in 2D present sensible results compared to the experiment measurements with a maximum difference of 16.05 Pa (or -23.85%) for 3 modules at  $Re = 21,600$  and 0.77 Pa (or -6.96%) for  $Re = 10,089$  and 2 modules. This higher pressure drop compared to the experimental values was expected because the PCM panel has an undulated surface on the existing panel and simulations considered the plane on top of the undulation. To validate the heat transfer simulation, temperature data of one unit installed in a seminar room was used. The temperature before and after the PCM was stable for a couple of hours and the average of that was assumed to be the panel surface temperature.

Furthermore and based on the optimum design by geometry and performance of the first set of simulations, 13 surface geometries were generated in 2D to perform a parametric analysis varying ridge height (ridge height/channel gap) [ $0.0625 < e/h < 0.3125$ ], ridge pitch (ridge spacing / total surface length) [ $0.0223 < s/l < 0.0558$ ] and ridge radius [ $2.5 < r < 7.5$ ]

evaluate pressure drop and heat transfer efficiency. These dimensions are represented in Figure 2.

The optimum design was again selected for further refinements by generating 9 surfaces to evaluate the gap between panels (sum of gaps/total height) [ $0.254 < E/H < 0.397$ ], panel thickness (sum of panel thickness/total height) [ $0.6032 < T_t/H < 0.7460$ ] and number of panels [ $4 < p < 9$ ] with the final design being used to fabricate the panel.

## 2.1 Heat transfer:

The heat transfer between panels and air was calculated by the energy balance through the air crossing the volume control and is given by:

$$\dot{Q}_{air} = \dot{m}_{air} C_{p(air)}(T_o - T_i) \quad (W) \quad (2.1)$$

Where:  $\dot{m}_{air}$  is the air mass flow rate in  $\frac{kg}{s}$ ;  $C_{p(air)} = 1006.43 \left[ \frac{J}{kgK} \right]$ ;  $T_i = 26^\circ C$ ;  $T_o$  is the air outlet temperature calculated by CFD,  $\dot{Q}_{air}$  is in Watts and is assumed that there are no losses through the walls.

### 2.1.1 Nusselt number and convective heat transfer coefficient:

Nusselt number is a dimensionless term equal to the temperature gradient on the surface and provides the ratio between convective and conductive heat transfer (Incropera, 2007) given by:

$$Nu = \frac{hD_h}{k_{air}} \quad (2.2)$$

Where  $D_h$  is the hydraulic diameter,  $k_{air}$  is the thermal air conductivity and  $h$  is the convective heat transfer coefficient.

To evaluate  $h$ , a control volume is applied (Figure 2) and all energy released by the air ( $\dot{Q}_{air}$ ) is absorbed through convection ( $\dot{Q}_c$ ) by the panel (Eq. (2.3)).

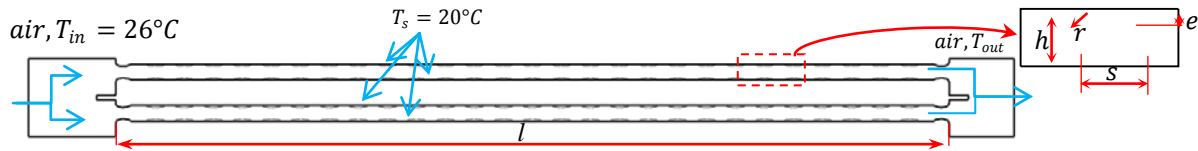


Figure 2: PCM panel control volume

$$\dot{Q}_{air} = \dot{Q}_c$$

$$\dot{m}_{air} C_{p(air)}(T_{out} - T_{in}) = hA_{panel} \Delta T \quad (2.3)$$

Where  $A_{panel} = L_{panel} \cdot W_{panel}$ . For cases using constant surface temperature, the difference between hot and cold is given by a logarithmic mean temperature difference  $\Delta T_{LMDT}$  (Incropera, 2007):

$$\Delta T_{LMDT} = \frac{(\Delta T_o - \Delta T_i)}{\ln\left(\frac{\Delta T_o}{\Delta T_i}\right)} = \frac{(T_s - T_{m,o}) - (T_s - T_{m,i})}{\ln\left[\frac{(T_s - T_{m,o})}{(T_s - T_{m,i})}\right]} \quad (2.4)$$

Where  $T_{m,o}$  is the outlet fluid temperature;  $T_{m,i}$  is the inlet fluid temperature and  $T_s$  is the surface temperature. Adding Eq. (2.4) in Eq. (2.3):

$$h = \frac{\dot{m}_{air} C_{p(air)}(T_o - T_i)}{(L_{panel} \cdot W_{panel}) \left( \frac{(T_s - T_{m,o}) - (T_s - T_{m,i})}{\ln\left[\frac{T_s - T_{m,o}}{T_s - T_{m,i}}\right]} \right)} \quad \left[ \frac{W}{m^2K} \right] \quad (2.5)$$

### 2.1.2 Efficiency

The introduction of ridges requires more pumping power from the system. The thermal enhancement factor (Tyagi *et al.*, 2015),  $\eta$ , analyse the ratio of the convective heat transfer of the augment surface over a smooth surface at a constant pumping and is given by:

$$\eta = \frac{\left(\frac{Nu}{Nu_o}\right)}{\left(\frac{\Delta p}{\Delta p_o}\right)^{1/3}} \quad (2.6)$$

Where  $Nu_o$  and  $\Delta p_o$  are the Nusselt number and the pressure drop in a smooth panel. Values higher than 1 suggest an increase in heat transfer or reduction on pressure drop when compared to a smooth panel and values lower than 1 suggest the opposite.

## 3 SIMULATION RESULTS AND DISCUSSION

### 3.1 3D simulations

The first set of simulations started by generating a batch of ten 3D panels with different configurations at  $Re = 18736$  plus the existing panel and dimpled panel as the two examples presented in Figure 3. The control volume is the channel where the air crosses and exchange heat with the panel with Figure 4 showing an example of the section modelled for simulation in Ansys FLUENT.

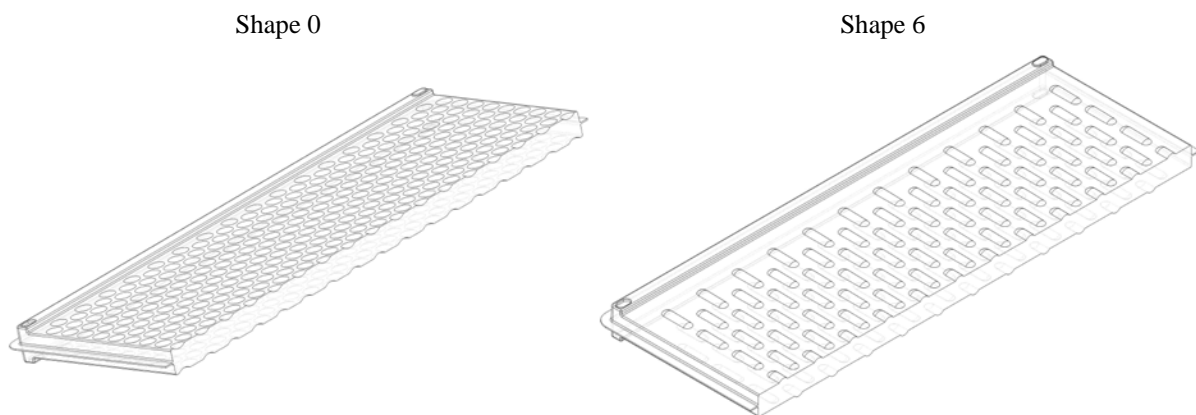


Figure 3: Examples of 2 designs used for 3D simulation.



Figure 4: Existing panel sectioned and the section used for 3D simulation.

The results of pressure drop, outlet temperature and heat flux from the 3D simulation are presented on Table 1 sorted by heat flux; shapes 6 and 3 revealed a high heat flux at a cost of a high pressure drop. Alternatively, shapes 2, 1 and 9 show promises in terms of heat transfer in comparison to other shapes with approximately double heat transfer compared to the existing panel with a reasonable increase in pressure drop. Based on these results and due to the simplicity of its design in manufacture, shape 9 was chosen for additional refinements.

Table 1: Pressure drop, outlet temperature and Heat Flux of one 3D panel sectioned at  $Re = 18736$

Shape	Pressure drop (Pa)	Outlet temperature (°C)	Heat Flux (W)
6	105.54	21.28	-757.29
3	93.12	21.59	-706.33
2	60.62	21.71	-687.09

<b>1</b>	44.23	21.78	-676.52
<b>9</b>	55.58	21.88	-660.97
<b>8</b>	17.00	22.00	-641.10
<b>0</b>	30.82	22.52	-558.39
<b>5</b>	24.47	22.69	-531.15
<b>10</b>	50.37	23.21	-447.00
<b>4</b>	31.13	23.84	-346.19
<b>Existing</b>	10.58	23.91	-335.61
<b>7</b>	40.49	24.03	-316.54

### 3.2 2D simulations

In first instance, 13 variations (Shapes 11 to 23) based on Shape 9 were drawn and sectioned along their length for 2D simulation. In each case, 7 panels per module were used to perform a parametric analysis of the spacing between ridges, ridge height and radius. The most effective in terms of heat transfer and pressure drop (Shape 11, Figure 5) was used to generate 9 more cases (Shapes 24 to 32) by varying panel thickness, spacing between panels and total of panels per module.

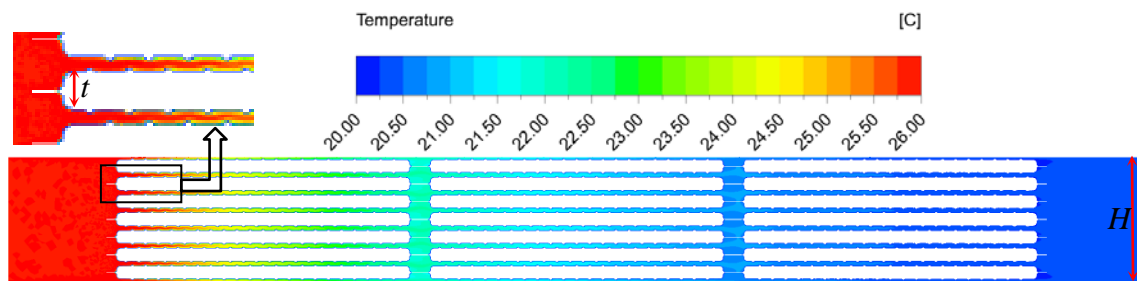


Figure 5: Temperature distribution of Shape 11 at  $Re = 18736$

The results presented in Table 3 show that Shapes 11, 24 and 25 have higher Heat Flux compared to the existing panel, with Shape 11 able to transfer approximately 14% more energy at  $Re = 18736$  and hold 13.68% more PCM. These shapes have a pressure drop higher than the existing panel. However, fan Head curve (Figure 6) shows that the AHU can provide sufficient pressure at the required airflow to overcome this drop. Furthermore due to the increased energy transfer, less airflow is required over the panels and consequently less electric energy demanded.

Table 3 also shows that Shape 27 displays similar levels of performance to the existing panel in terms of heat transfer and pressure drop. Therefore this arrangement could be integrated with little change to the systems operation. This design would also be seen to reduce costs as only six panels are required per module and the quantity of PCM would be reduced by 2.56% as can be seen on Table 2. This table also shows that shapes 27, 28, 29 and 30 reduce PCM volume even if different amount of panels per module are used due to the increase in panel thickness. Shape 26 has the highest increase in volume and but the higher pressure drop (323.34 Pa at  $Re = 18,736$ ) which makes shape 11 the most reasonable in terms of increase in volume change, pressure drop and heat transfer.

Table 2: Volume change in comparison with existing panel

	<b>11</b>	<b>24</b>	<b>25</b>	<b>26</b>	<b>27</b>	<b>28</b>	<b>29</b>	<b>30</b>	<b>31</b>	<b>32</b>
	13.68%	0.08%	2.63%	20.51%	-2.56%	-2.56%	-2.56%	-2.56%	3.93%	2.31%
<b>Panels per module</b>	7	9	8	6	6	6	5	4	8	9

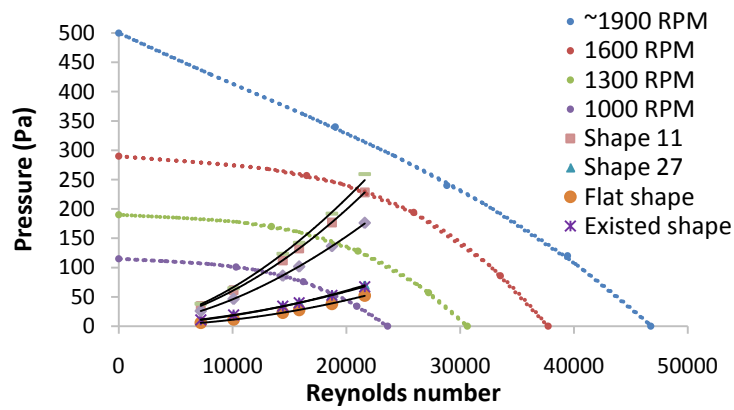


Figure 6: Head curve of panels 11, 24, 25, 27 as well as the Flat and the existing shape with fan curves at different rotation speeds.

The Nusselt number indicates how much energy is exchanged by convection or conduction. When  $Nu = 1$ , it means the heat transfer is purely by conduction and a higher Nusselt number shows more efficient heat transfer. This makes Shape 29 and the existing panel having the worst performance when compared to other shapes. On the other hand, shape 26, 11 and 24 (Figure 7, right) have the best performance at any Reynolds number evaluated by showing an average increase of 2.2 times for shape 26, 2.02 for shape 11 and 2.03 for shape 24 for Reynolds between 7,200 and 22,000. This increase allows a fast response by the PCM-Air heat exchanger when the heat load increases suddenly. Furthermore, when no air is crossing the thermal batteries, shapes 26 and 11 lose less energy through free convection due to a lower surface area when compared to the existing panel.

When Nusselt number is compared with a smooth surface ( $Nu/Nu_o$ ), shapes 24, 26 and 11 present the best results, showing an average increase of 2, 1.8 and 1.75. As it can be seen in Figure 7 (left) where the ratio for all cases are presented, the inclusion of ridges favoured heat transfer by the increase of turbulence at lower Reynolds number allowing a reduction in PCM-Air heat exchanger air flow, saving energy and reducing noise. The result also shows that the existing panel perform better than a smooth surface only at low Reynolds numbers (1.27 and 1.09 for 7,200 and 10,089 respectively). For Reynolds numbers above 10,089 the existing panel have a performance similar to a smooth panel.

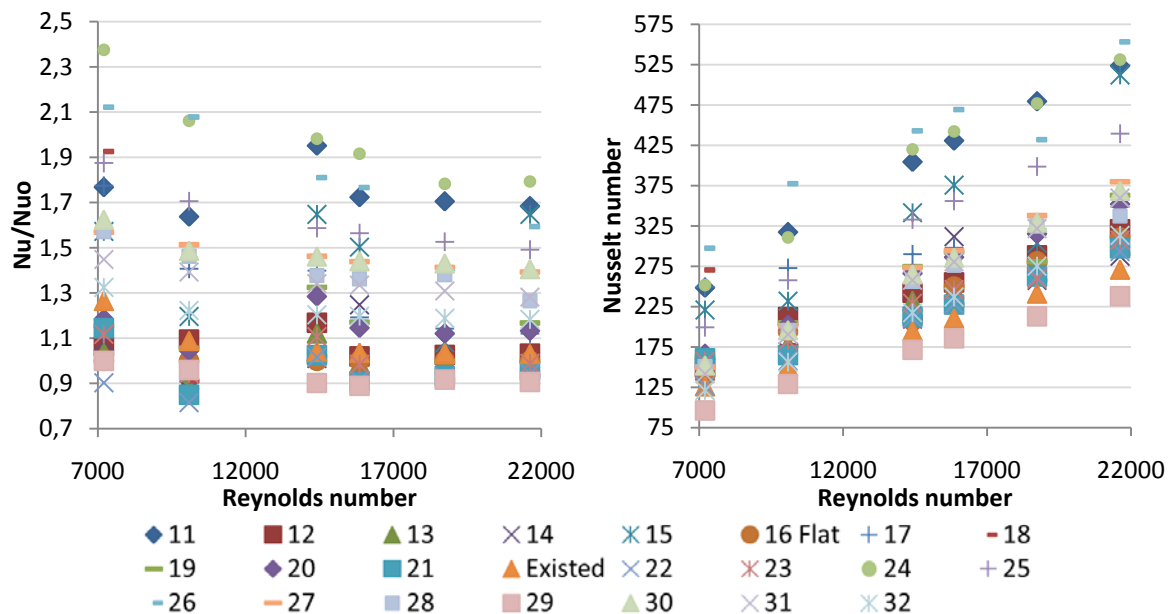


Figure 7: Ratio between Nusselt number and a smooth panel and Nusselt number

Comparing the ratio between Nusselt and pressure drop shows how efficient the panel performs. Figure 8 shows that shapes 11, 24, 25, 27, 28 and 30 have values above 1, which means that the inclusion of ridges enhance the heat transfer at a lower cost in terms of pressure drop when compared to a smooth surface. Values below 1 means that the pressure drop increases in a proportion higher than Nusselt number, leading to an increase of noise and energy cost with a small benefit on heat transfer. Shape 26 has the best performance in terms of Nusselt number but the higher pressure drop lowers its efficiency (0.86 in average).

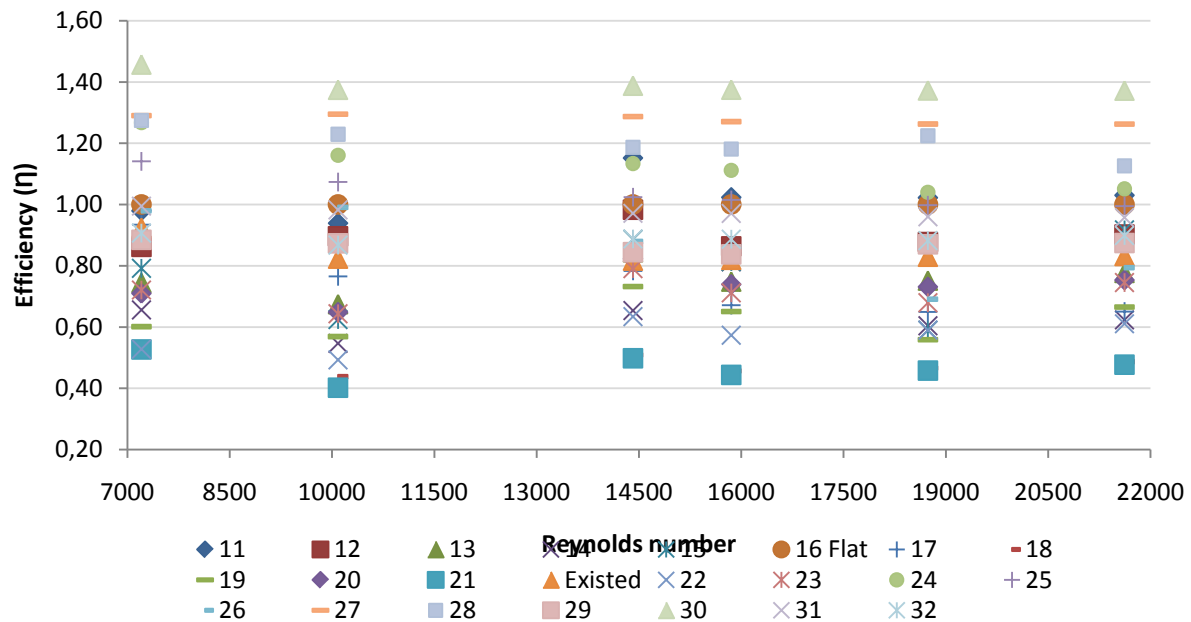


Figure 8: Efficiency

#### 4 CONCLUSIONS

More than 200 simulations were performed with different surface designs and air flows until the optimum design in terms of heat transfer, pressure drop and low production cost was achieved. Shape 11 doubled the heat transfer and holds 13.68% more material than the existing commercial panel. The pressure drop increased by 3 but the fan is capable to provide the required air flow. More power from the fan is demanded but due to the increase of heat transfer a lower air flow will be requested by the PCM-air heat exchanger unit. At present, the developed design is being fabricated and future experimental tests will validate its performance.

#### 5 ACKNOWLEDGEMENTS

The first author would like to thank Science Without Borders program of Cnpq - Brazil, for doctoral funding (PDE: 200815/2014-8).

Table 3: Outlet temperature, Pressure drop and Heat transfer (W) for each shape at  $Re = 10,089$  and  $18,736$ .

	Outlet Temperature (°C)		Pressure drop (Pa)		Pressure drop in comparison with existed plate (%)		Heat Flux (W)		Heat Flux in comparison with existing panel (%)		Number of panels per module	
	Reynolds	10089	18736	10089	18736	10089	18736	10089	18736	10089		18736
	Shapes	Existing	293.89	294.14	19.17	52.69	-	-	-453.77	-802.97		-
11		293.29	293.44	61.28	176.80	320	336	-505.47	-915.65	11.39	14.03	7
27		293.95	294.14	18.45	53.43	96	101	-449.03	-802.33	-1.04	-0.08	6
24		293.43	293.28	46.94	191.98	245	364	-493.64	-941.45	8.79	17.25	9
25		293.34	293.49	46.35	136.48	375	393	-501.24	-907.63	9.60	4.33	8
17		293.39	293.92	71.87	207.32	252	261	-497.35	-837.75	3.27	3.13	7
20		293.72	293.98	48.36	137.64	423	445	-468.62	-828.14	7.00	2.85	7
15		293.52	294.00	81.14	234.30	556	614	-485.53	-825.89	11.60	2.85	7
26		293.28	294.00	106.59	323.34	386	412	-506.42	-825.89	3.92	-0.38	6
19		293.69	294.16	73.99	217.10	152	163	-471.55	-799.93	-0.32	-1.34	7
28		293.98	294.17	19.46	54.72	86	181	-446.35	-798.81	2.38	-1.34	6
31		293.66	294.19	32.91	84.17	110	116	-473.54	-795.44	3.27	-1.58	8
13		293.91	294.21	29.1	86.13	272	284	-452.31	-792.23	-2.78	-2.04	7
23		293.77	294.21	16.50	95.27	570	612	-464.56	-792.23	-1.56	-2.08	7
12		293.72	294.22	21.02	60.91	544	550	-468.62	-790.31	1.01	-2.14	7
22		294.04	294.24	52.22	149.41	60	72	-441.17	-786.62	0.65	-2.79	7
21		293.97	294.24	109.37	322.44	245	252	-446.70	-786.30	-1.96	-4.21	7
18		293.84	294.25	104.34	289.60	80	85	-458.35	-785.82	-8.65	-9.62	7
16		293.86	294.28	11.55	38.09	76	82	-456.71	-780.53	-	-17.92	7
14		293.99	294.35	46.96	132.91	169	50	-444.88	-769.15	2.72	-24.33	7
29	294.35	294.62	15.33	44.70	245	364	-414.51	-725.72	8.79	17.25	5	
30	294.91	295.04	14.62	43.21	100	100	-365.66	-659.05	0.00	0.00	4	
32	293.75	295.360	32.41	26.42	320	336	-466.11	-607.60	11.39	14.03	9	

## 6 REFERENCES

- Alizadeh, M. & Sadrameli, S.M. (2016) Development of free cooling based ventilation technology for buildings : Thermal energy storage ( TES ) unit , performance enhancement techniques and design considerations – A review. *Renewable and Sustainable Energy Reviews*. [Online] 58, 619–645. Available from: doi:10.1016/j.rser.2015.12.168.
- Arzamendia Lopez, J.P., Kuznik, F., Baillis, D. & Virgone, J. (2013) Numerical modeling and experimental validation of a PCM to air heat exchanger. *Energy and Buildings*. [Online] 64, 415–422. Available from: doi:10.1016/j.enbuild.2013.04.017.
- Dolado, P., Lazaro, A., Marin, J.M. & Zalba, B. (2011) Characterization of melting and solidification in a real-scale PCM-air heat exchanger: Experimental results and empirical model. *Renewable Energy*. [Online] 36 (11), 2906–2917. Available from: doi:10.1016/j.renene.2011.04.008.
- Incropera, F.P. (2007) *Fundamentals of heat and mass transfer*. John Wiley.
- Kolokotroni, M., Santos, T. & Hopper, N. (2016) Ventilative cooling of a seminar room using active PCM thermal storage. *REHVA*. 53 (1), 36–40.
- Lazaro, A., Dolado, P., Marín, J.M. & Zalba, B. (2009) PCM–air heat exchangers for free-cooling applications in buildings: Experimental results of two real-scale prototypes. *Energy Conversion and Management*. [Online] 50 (3), 439–443. Available from: doi:10.1016/j.enconman.2008.11.002.
- Liu, J., Song, Y., Xie, G. & Sunden, B. (2015) Numerical modeling flow and heat transfer in dimpled cooling channels with secondary hemispherical protrusions. *Energy*. [Online] 79 (C), 1–19. Available from: doi:10.1016/j.energy.2014.05.075.
- Moon, M.A., Park, M.J. & Kim, K.Y. (2014) Evaluation of heat transfer performances of various rib shapes. *International Journal of Heat and Mass Transfer*. [Online] 71, 275–284. Available from: doi:10.1016/j.ijheatmasstransfer.2013.12.026.
- Promvong, P. & Thianpong, C. (2008) Thermal performance assessment of turbulent channel flows over different shaped ribs. *International Communications in Heat and Mass Transfer*. [Online] 35 (10), 1327–1334. Available from: doi:10.1016/j.icheatmasstransfer.2008.07.016.
- Rubitherm (n.d.) *Rubitherm*. [Online]. Available from: <https://www.rubitherm.eu/en/index.php/productcategory/makroverkaspelung-csm> [Accessed: 2 May 2017].
- Santos, T., Hopper, N. & Kolokotroni, M. (2016) Performance in practice of a ventilation system with thermal storage in a computer seminar room. In: Per Kvols Heiselberg (ed.). *12th CLIMA REHVA World Congress*. 2016 Aalborg. p. 11.
- Thianpong, C., Chompookham, T., Skullong, S. & Promvong, P. (2009) Thermal characterization of turbulent flow in a channel with isosceles triangular ribs. *International Communications in Heat and Mass Transfer*. [Online] 36 (7), 712–717. Available from: doi:10.1016/j.icheatmasstransfer.2009.03.027.
- Tyagi, K., Singh, P., Pandit, J., Ramesh, S., et al. (2015) Experimental study of heat transfer augmentation in high aspect-ratio channels featuring different dimple configurations. In: *ASME Turbo Expo 2015: Turbine Technical Conference and Exposition*. 2015 ASME. pp. 1–11.
- Yang, W., Xue, S., He, Y. & Li, W. (2017) Experimental study on the heat transfer characteristics of high blockage ribs channel. *Experimental Thermal and Fluid Science*. [Online] 83, 248–259. Available from: doi:10.1016/j.expthermflusci.2017.01.016.
- Zalba, B., Marín, J.M., Cabeza, L.F. & Mehling, H. (2004) Free-cooling of buildings with phase change materials. *International Journal of Refrigeration*. [Online] 27 (8), 839–849. Available from: doi:10.1016/j.ijrefrig.2004.03.015.

# Development and measurement results of a compact Counterflow Heat Recovery Fan for single/double room ventilation

Christoph Speer<sup>\*1</sup>, Rainer Pfluger<sup>1</sup>

*1 University Innsbruck  
Institute for Structural Engineering and Material Sciences  
Unit for Energy Efficient Buildings  
Technikerstrasse 13, 6020 Innsbruck, Austria  
\*Corresponding author: christoph.speer@uibk.ac.at*

## ABSTRACT

With the combination of two fans and a heat exchanger in one single component there is the possibility to design a compact and highly efficient ventilation system especially for use in building modernization. One crossflow fan generates both airflows (outdoor/supply and extract/exhaust air) and simultaneously acts as counterflow heat exchanger. The space between the fan blades is filled with elements which operate as regenerative heat exchanger. The modified laboratory prototype of the so called Counterflow Heat Recovery Fan was optimized for the use as single/double room unit. The modelling and operation modes of the modified concept as well as simulation results of the fluid mechanical behaviour are presented. Based on the numerical optimization the first laboratory prototype of the single/double room unit was manufactured. The measurement results are compared with the simulation and the further research focus is discussed.

## KEYWORDS

heat recovery fan  
compact ventilation system  
facade integrated  
night ventilation

## 1 INTRODUCTION

To ensure adequate air quality, ventilation is necessary in new buildings as well as in the modernization of existing buildings. Through the installation of a mechanical ventilation system with heat recovery it is possible to provide a controlled air exchange and to reduce the energy loss at the same time. Especially in the refurbishment of buildings space-saving solutions are beneficial. With the goal to construct a compact and cost-saving decentralized ventilation system the CHRF (Counterflow Heat Recovery Fan) was developed. The key component of the CHRF is a rotating crossflow fan, which generates both airflows (outdoor/supply and extract/exhaust) and simultaneously acts as a counterflow heat exchanger. The flow conduction and the manufactured laboratory prototype are shown in figure 1. The system is divided into two levels. Supply and extract air are placed in the first level, outdoor and exhaust air in the second level. Through the stationary inner part of the fan the airflows perform a level change so that the crossflow fan acts as a counterflow heat exchanger at both levels. The developed concept of the CHRF, simulation results as well as

the measurement results of the laboratory prototype are described collectively in (Speer, 2015a).



Figure 1. Concept of the Counterflow Heat Recovery Fan. Cross section of the flow conduction (left) (Zgaga et al., 2014) and manufactured laboratory prototype (right) (Speer et al., 2015).

The used crossflow fan has to fulfil two functions, generating both airflows as efficient as possible and acting as a highly efficient counterflow heat exchanger. Different possible concepts of this component are presented in (Speer, 2015b), two promising variants are shown in figure 2. Both variants consist of a cross flow fan with 30 blades which mainly generates the air flows and intermediate elements which are responsible for the regenerative heat recovery. These elements can for example be built out of foam material (figure 2a), or horizontal thin layers (figure 2b).

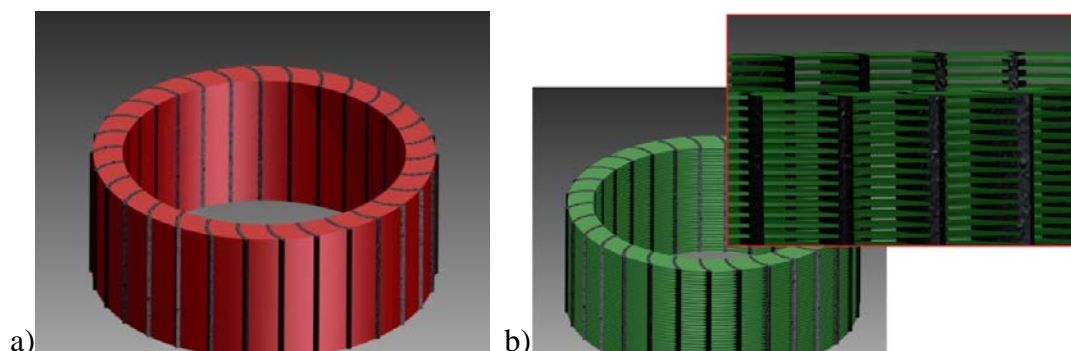


Figure 2. Fan model with 30 blades (black) for the ventilation and a) porous foam (red) b) horizontal thin layers (green) for the heat recovery. (Speer, 2015b)

Within the framework of the development of a CHRF for the use as single/double room unit, the flow conduction concept was modified to improve the ventilation efficiency as well as the heat recovery rate by increasing the cross sectional area used for in- and outlets of the fan. The air flows use a much larger surface area by entering the fan radially, perform a level change along a helix curve and exit the fan again radially. With this flow conduction concept almost the entire available surface is used to reduce the pressure drop and to increase the heat recovery. The modified concept is shown in figure 3. The cooling mode, described below, is a promising operating mode for night ventilation. Conventional ventilation systems are normally not designed for heat recovery mode in winter and night ventilation in summer because of the wide range of flow range necessary for that concept. The large diameter of the CHRF however provides the option for high flow rates without much additional effort for cost and space. If the unit is integrated in the external wall, the external pressure drop can be reduced to a minimum, which is necessary for high efficient night ventilation at large flow

rates. As shown below, the flow rate can be increased by a factor of almost 10 from heat recovery mode to cooling mode.

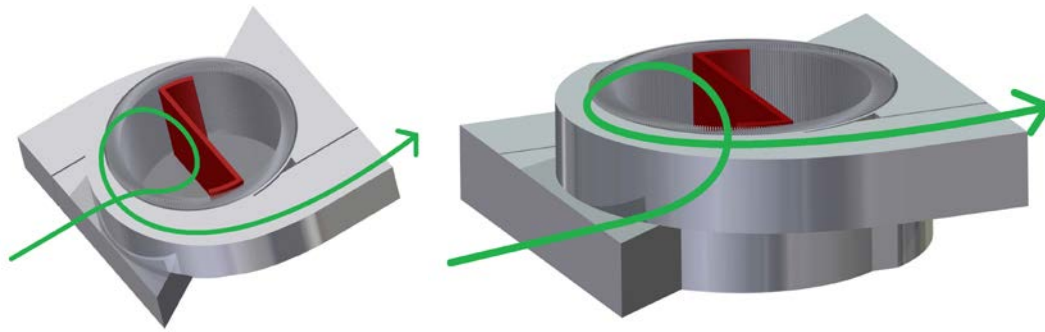


Figure 3. Design and flow conduction of the modified CHRf concept. (Speer et al., 2016)

## 2 MODELLING AND OPERATING MODES OF THE MODIFIED CONCEPT

In addition to the fluid mechanical and thermal demands we designed the modified concept to meet further requirements. Outdoor air and extract air intake are constructed with large openings to enable the implementation of filters inside the system with low pressure drops. Furthermore acoustic elements can be installed along the spiral casing to reduce the sound pressure level as close as possible to the point of origin. The acoustic elements can be adjusted to the rotational speed of the main operating modes. The occurring characteristic frequencies of a CHRf and possible solutions to reduce the noise level are discussed in (Speer et al., 2016). The construction model consists of layers which are responsible for the flow conduction, the stationary inner part, adapters for in- and outlets, a crossflow fan and a metallic plate to connect motor and fan.

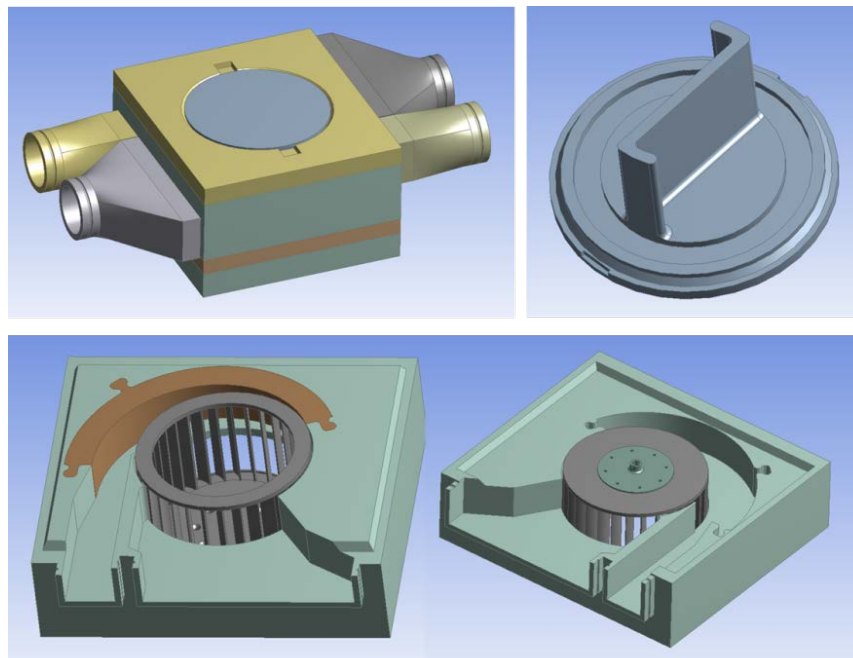


Figure 4. Construction model of the CHRf for the use as single/double room unit.

The flow conduction of the system in the normal heat recovery mode is shown in figure 5. Air intake and exit is guided radially through the cross flow fan. Furthermore, there is the possibility to operate the system in the cooling mode, shown in figure 6. In this mode the air intake is guided axially to the centre of the crossflow fan and the air flow is blown out radially through all open flow paths.

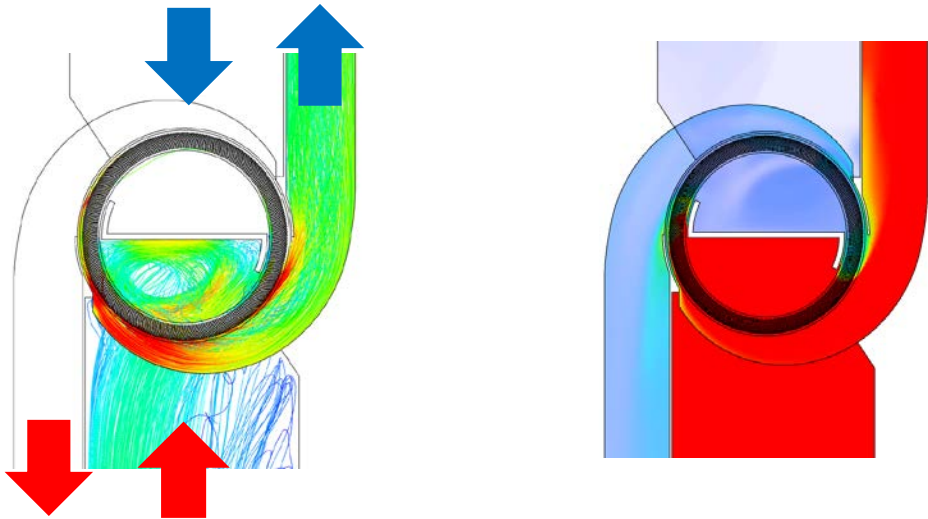


Figure 5. Numerical calculation results (CFD) of the heat recovery mode. Flow conduction of one airflow (left) and tracer gas concentration to visualize leakage (right). (Speer et al., 2016)

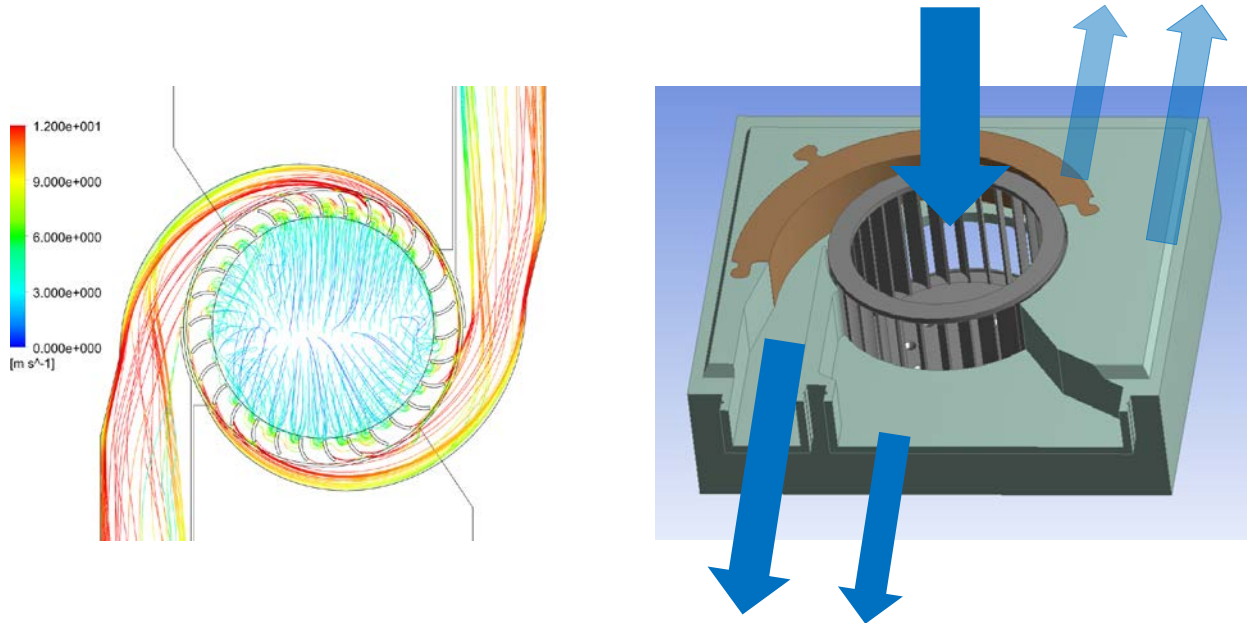


Figure 6. Numerical calculation results (CFD) (left) and schematic flow conduction (right) of the cooling mode.

The working principle of the CHRf allows generating high flow rates in for night ventilation in the so called “cooling mode” because the already installed fan can be used as a large radial fan and no longer as cross flow fan. There are still questions to work on so that this property can be used in an efficient way and without high installation effort. The definition of flow paths to be used and the implementation of the conduction for the axial outdoor air intake will be part of further research. The dimensions of the single/double room unit, shown in figure 4, are about 350x400x200 mm with a fan diameter of 190 mm and small enough to integrate it in the external wall insulation.

### 3 SIMULATION RESULTS OF THE MODIFIED CONCEPT

The fluid mechanical simulation model is based on the construction model in chapter 2 and the intermediate elements of the crossflow fan are realized as porous media, described in figure 2a). The achieved flow rates without external pressure and with an external pressure of 50 Pa (at 50 m<sup>3</sup>/h) at each in- and outlet are shown in figure 7. The flow resistance loss coefficient of the intermediate porous elements is varied between 0 and 300 m<sup>-1</sup> and the rotational speed of the crossflow fan is set to 15 Hz. Higher rotational speeds up to about 30Hz are considered, but to ensure the comparison with measurement results of the laboratory prototype we perform the parametric study with a lower speed. The correlation of the rotational speed with the generated flow rate is in this range nearly linear. The variant with external pressure drop and a flow resistance loss coefficient of 300 m<sup>-1</sup> for the porous elements still leads to flow rates of 28 m<sup>3</sup>/h at a low rotational speed of 15 Hz. The resulting flow rates for the cooling mode are shown in figure 8. The same variant with external pressure drop and high flow resistance loss coefficient leads to flow rates of 165 m<sup>3</sup>/h for the cooling mode. If the external pressure drop is reduced and the intermediate porous elements are removed, the flow rate is increased up to 260 m<sup>3</sup>/h at a low rotational speed of 15 Hz. In order to compare the simulation results with the laboratory measurements which are performed without external pressure drop and porous elements, we get simulated flow rates for these boundary conditions of 53 m<sup>3</sup>/h for the heat recovery mode and 265 m<sup>3</sup>/h for the cooling mode.

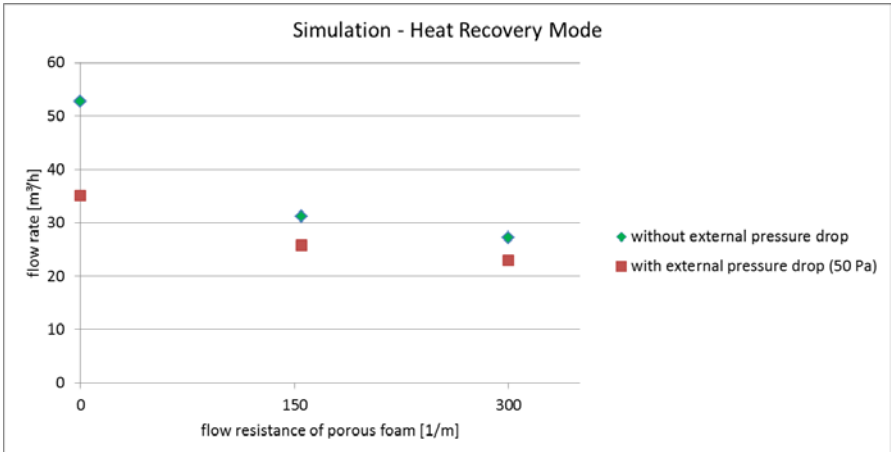


Figure 7. Flow rates of the heat recovery mode at different flow resistance loss coefficients for the porous elements without external pressure (green) and with an external pressure of 50 Pa (red) at each in-/outlet.

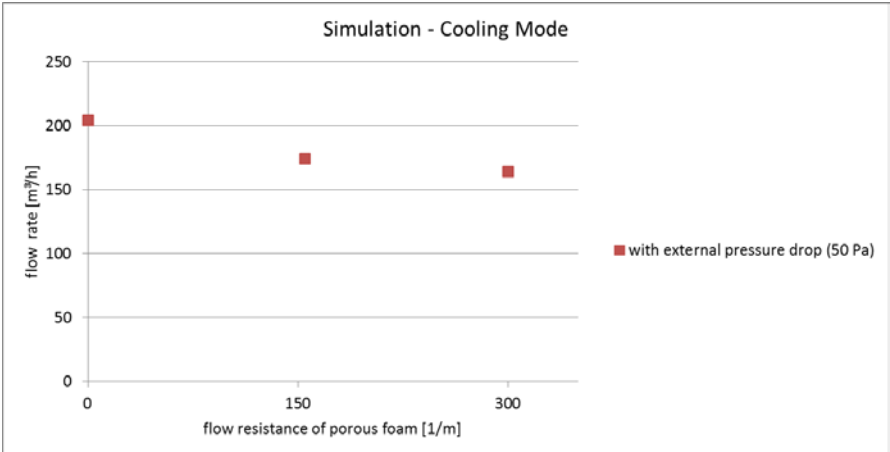


Figure 8. Flow rates of the cooling mode at different flow resistance loss coefficients for the porous elements without external pressure (green) and with an external pressure of 50 Pa (red) at each in-/outlet.

#### 4 MEASUREMENT RESULTS OF THE LABORATORY PROTOTYPE

The manufacturing of the laboratory prototype is based on the construction model in figure 4. All parts of the casing are frazedout of polypropylene andthe cross flow fan with 30 blades was built by rapid prototyping (3d-plotting). The assembled laboratory prototype is shown in figure 9.



Figure 9. Photo of the manufactured laboratory prototype of the CHRF for the use as single/double room unit.

The following measurements are performed without external pressure drop and intermediate porous elements. The rotational speed of the fan is varied between 10 and 20 Hz and the averaged flow rates of the heat recovery mode and the cooling mode are measured. The results are shown in figure 10. For the heat recovery mode the flow rates are nearly linear in the range of 40-80 m<sup>3</sup>/h, for the cooling mode in the range of 150-400 m<sup>3</sup>/h.

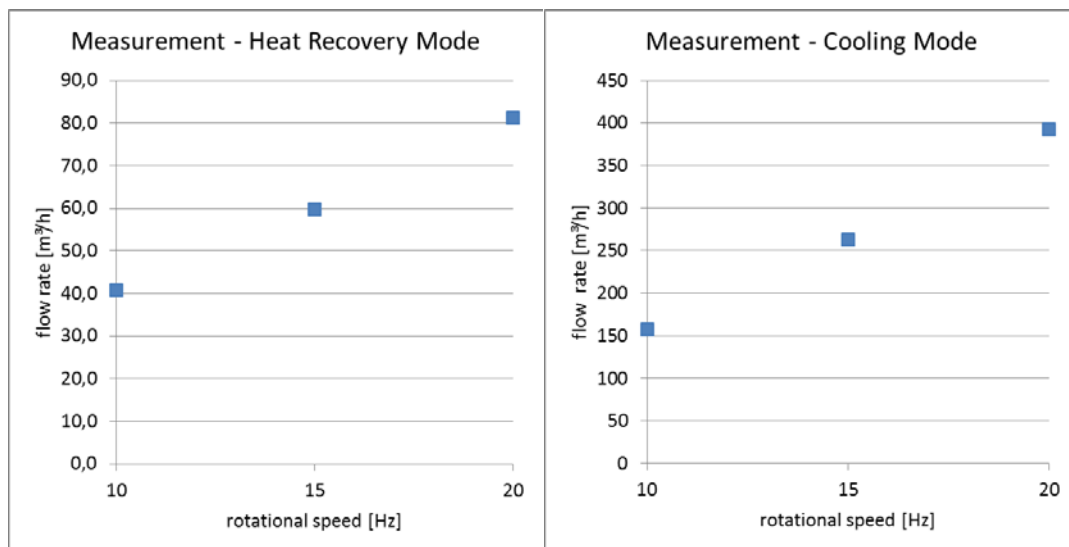


Figure 10. Measured flor rates of the laboratory prototype at different rotational speeds without external pressure and porous elements for heat recovery mode (left) and cooling mode (right).

In figure 11 the comparison of the measured flow rate values at a velocity speed of 15 Hz with the simulation results are shown for heat recovery and cooling mode. The measured flow rate of the heat recovery mode is slightly above, the flow rate of the cooling mode is slightly below the simulated value but agrees with good accuracy.

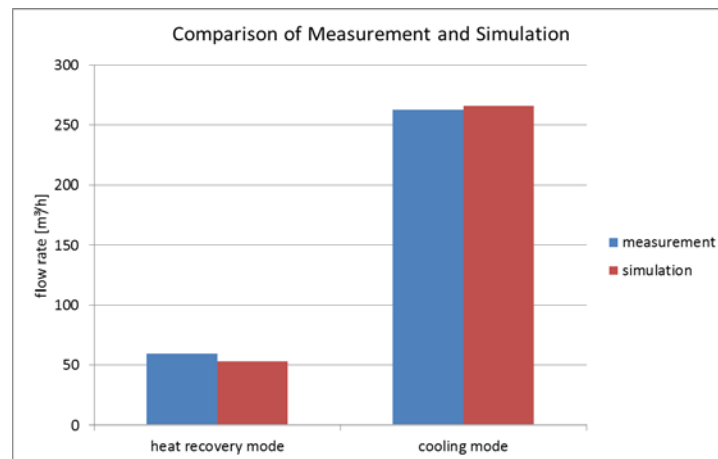


Figure 11. Comparison of measurement and simulation of the flow rates for heat recovery and cooling mode without external pressure and porous elements.

## 5 CONCLUSION

The development of the CHRF for the use as single/double room unit delivers successful simulation as well as measurement results in terms of flow rates which agree with good accuracy. Due to the high flow rates additional rooms could also be supplied. Further laboratory measurement with implemented porous elements are required to ensure adequate heat recovery rates and low internal leakage. Furthermore the systemic power consumption of the modified concept must be measured to ensure high ventilation efficiency. The promising development of the modified CHRF concept can be scaled up for higher flow rates in order to open up further fields of application. The systemic advantage to generate high flow rates for the cooling mode should be used, hence a simple installation concept, e.g. for wall-integrated operation, should be developed to enable the axial outdoor air intake.

## 6 ACKNOWLEDGEMENTS

This work was carried out as part of the research project HeatXFan within the framework of the funding program “Energieforschung” of the Austrian Research Promotion Agency (FFG).

## 7 REFERENCES

Zgaga, J., Lanthaler, D., Speer, C. and Pfluger, R. (2014). Development of a decentralized and compact comfort ventilation system with highly efficient heat recovery for the minimal invasive refurbishment of buildings. Proceedings of the 35<sup>th</sup> Air Infiltration and Ventilation Centre Conference – AIVC 2014. 648-654

Speer, C. (2015a). Simulation und Entwicklung eines hocheffizienten Wärmerückgewinnungsventilators. Dissertation. University Innsbruck.

- Speer, C., Pfluger, R., Zgaga, J., Lanthaler, D., Recla, F. and Feist, W. (2015). Entwicklung und messtechnische Untersuchungen eines dezentralen und kompakten Wärmerückgewinnungsventilators. BAUPHYSIK 37. 179-185
- Speer, C. (2015b). Rotor Concepts For The Counterflow Heat Recovery Fan. Conference Proceedings: 17<sup>th</sup> International Conference on Sustainable Building – ICSB. 1795-1798
- Speer, C., Pfluger, R. and Speer, A. (2016). Development of a modified concept and acoustic measurements of the Counterflow Heat Recovery Fan. Indoor Air 2016 Proceedings (The 14<sup>th</sup> international conference of indoor air quality and climate).

# Full-scale experimental study of ceiling turbulent air jets in mechanically ventilated rooms

Chi-Kien Nguyen<sup>\*1</sup>, Damien David<sup>1</sup>, Frédéric Kuznik<sup>1</sup>, Gilles Rusaouën<sup>1</sup>

*1 Université de Lyon, CNRS, INSA de Lyon, UCBL  
CETHIL UMR5008, F-69621, France*

*\*Corresponding author: [chi.nguyen@insa-lyon.fr](mailto:chi.nguyen@insa-lyon.fr)*

## ABSTRACT

Experimental investigation of ceiling circular grille air jets was conducted in a full-scale entirely controlled test room (6.2 x 3.1 x 2.5 m). Our case study is based on a realistic ventilation system configuration: it introduces a plenum box, two air exhausts, as well as a vertical wall near the air inlet. Analyses were initially concentrated at the air inlet region since it is the zone having strong gradients.

Deviations concerning the trajectory of the actual jet were observed with respect to the theoretical jet. These results are particularly interesting because, based on the academic configuration of the circular turbulent air jet, which is very well documented in the literature; our configuration introduces architecture elements which will necessarily have an impact on the jet. Therefore, it is this deviation from the theoretical model which will become discriminating as to the capacity of a CFD numerical model to simulate airflows in buildings. These results obtained allow for further cases studies under non-isothermal and moisture conditions and also in the presence of condensation in order to provide new useful data concerning airflow and hygrothermal fields in mechanically ventilated rooms.

## KEYWORDS

HVAC, mixing ventilation, turbulent jet, room interaction, full-scale experimentation

## 1 INTRODUCTION

Understanding room air distribution is essential to the buildings ventilation systems design and occupants' thermal comfort and indoor air quality controls. Indoor thermal comfort prediction requires the determination of the airflow and hygrothermal fields within ventilated rooms. In addition, it is clear that air distribution in occupied zones is one of the determining factors that directly affect indoor air quality. For instance, too low air change rate trap all pollutants, contaminants harming the occupants' health while a very high airflow can cause a feeling of discomfort.

Indoor air distribution investigation involves two common methods: numerical simulation and full-scale measurements. By using Computational Fluid Dynamics (CFD) model, numerical simulation is most convenient and efficient for predicting airflow and hygrothermal transfer in ventilated rooms (Chen, 2009). However, this method is limited by the lack of relevant experimental data, especially from full-scale measurements. In fact, experiments in full-scale rooms can provide valuable data concerning room airflows characteristics, including the turbulent flow characteristics.

Numerous theoretical studies based on full-scale experiments have been conducted since the 1940s on the behavior and characteristics of circular turbulent air jets (Corrsin, 1946), (Abramovich, 1963), (Rajaratnam, 1976), (Chen and Rodi, 1980). In HVAC applications, several studies were conducted in order to improve the knowledge of vertical jet development and room air distribution (Tuve, 1953), (Koestel, 1954), (Shepelev, 1961) and (Grimityn,

1970). A summary and review of research mentioned above can be found in the study of Li (*Li and al., 1993*). They confirmed that it is possible to predict indoor air velocity and temperature based on the characteristics of diffuser air jets. They also suggested further research to examine the effects of room geometry on the jet development. Indeed, while turbulent free air jet theory has been widely studied by many researchers, few studied a realistic vertical air jet having interaction with the room.

Consequently, the main objective of the present experimental research is to get improved knowledge of the mean and turbulent characteristics of a nearly-free circular vertical air jet. This configuration is particularly interesting since it is based on an academic configuration of the circular turbulent air jet, which is very well documented in the literature; our configuration introduces architecture elements which will necessarily have an impact on the jet. Therefore, it is this deviation from the theoretical model which will become discriminating when evaluating the capacity of a CFD numerical model to predict airflows and coupled transfers in buildings.

The article will be organized as follows: firstly, the experimental set-up will be described. Then, the second part provides a description of the theoretical model of a turbulent free vertical jet from the literature. The last part is devoted to presenting the tested configuration as well as the experimental results of the studied jet.

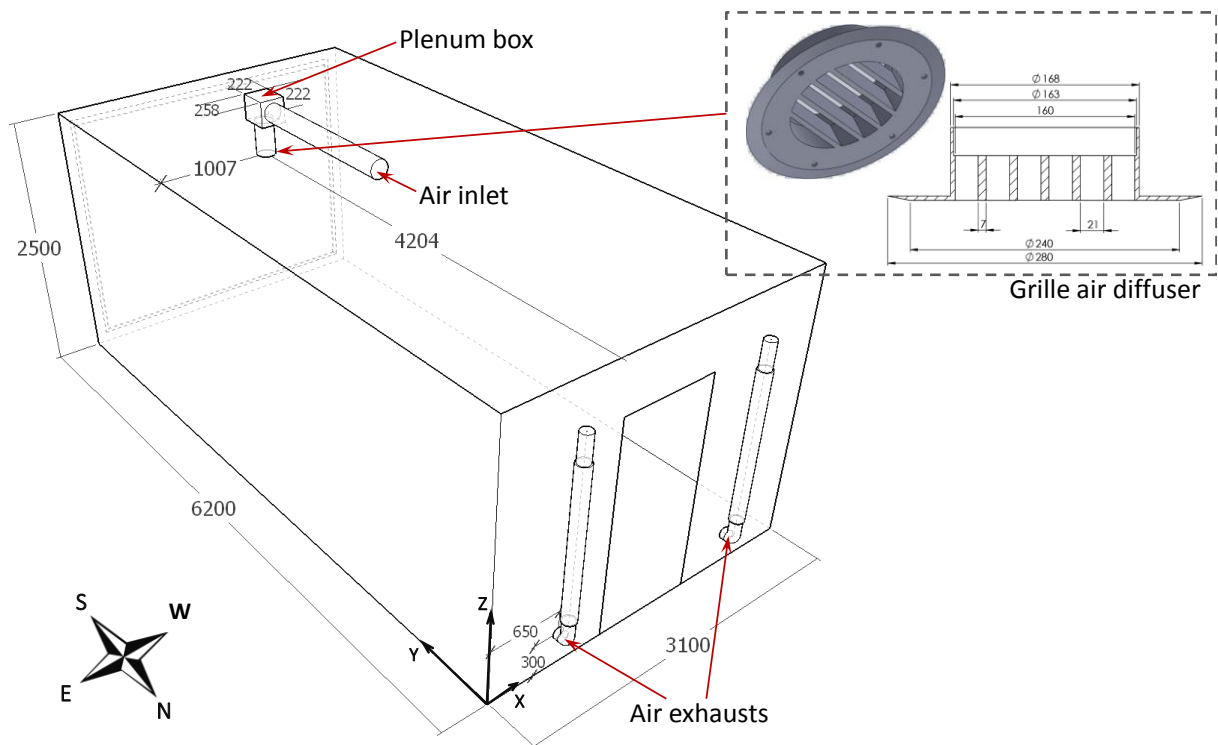


Figure 1: Scheme of MINIBAT test room with flow configuration

## 2 EXPERIMENTAL FACILITY AND MEASUREMENT APPARATUS

### 2.1 MINIBAT test room

Experimental investigation was conducted in a full-scale entirely controlled test cell entitled "MINIBAT". It is located at the CETHIL laboratory – INSA de Lyon, France. It consists of three distinct parts: a test room, a thermal buffer zone and a climatic chamber.

The test room, with dimensions  $L \times W \times H = 6.20 \times 3.10 \times 2.50$  m, is the place where the experimentation is carried out (c.f. Figure 1). Five of its façade are surrounded by the thermal

buffer zone that allows maintaining a stable temperature. The South façade is in contact with the climatic chamber through a glazing wall. The climatic chamber acts like a weather generator which is capable of simulating outdoor temperature and solar conditions.

Air temperature inside thermal buffer zone is entirely regulated thanks to controlled mechanical ventilation operating in closed loop. Air distribution inside the thermal buffer zone is ensured by means of air ducts network, which allows a regular and homogeneous air mixing.

The climate chamber is also temperature controlled. The temperature range allowed by the system goes from -10 °C to 40 °C. There is also an artificial sunlight system in the climatic chamber. This system was not used for this study; therefore they will not be described in the present paper.

## 2.2 Cell envelope

The envelope of the thermal buffer zone consists of 20 cm thick cellular concrete, covered by 10 cm of extruded polystyrene. The insulating layer has been added in order to reduce the air temperature fluctuation observed in previous studies carried out at MINIBAT ( $\pm 1.5$  °C according to (Hohota, 2003), (Kuznik, 2005),  $\pm 1.3$  °C according to (Gavan, 2009)). Thus, a fluctuation of  $\pm 0.6$  °C around the setpoint temperature has been recorded.

The opaque vertical walls separating the test room and the thermal buffer zone are made of 5 cm thick agglomerated wood panels covered on their internal faces by 13 mm thick plasterboard. The floor is made of 20 cm thick cellular concrete. The ceiling consists of 2.5 cm thick plywood plate, covered with 4.5 cm thick of glass wool. The South façade comprises a 1.2 cm thick high-resistance laminated glazing.

## 2.3 Measurement apparatus – Boundary conditions and indoor air measurements

There are sensors which are devoted to the measurement of the boundary conditions around the test cell (wall temperatures and ventilation characteristics). Other sensors are devoted to the measurement of the indoor temperature and velocity fields.

In order to precisely check the boundary conditions of wall temperature on the different test cases, a network of 180 Pt100 probes was implemented on both external and internal sides of 6 walls of the test room. Each wall surface has 36 measurement points, except the North wall and the South (glazing) wall which have 18 measurement points.

Air supply parameters are regulated in temperature and humidity by using Pt100 probes and SHT75 probes. The measurements are recorded at 5 locations: 3 points inside the air handling unit (AHU): air inlet, cooling coil and air supply; 2 other points are located inside Minibat test room which are air inlet and air exhausts. Besides, airflow rate are regulated thanks to a propeller flow meter with an accuracy of  $\pm 0.5$  m<sup>3</sup>/h.

We have designed and programmed a mobile robot (c.f. Figure 2) equipped with various sensors, in order to determine indoor air velocity, temperature and humidity fields.

The robot chassis is made of aluminium alloy whose dimensions are 0.4 x 0.3 x 0.12 m (L x W x H). The main masts (1) and (3) are made of carbon fiber. The robot is equipped with 4 Mecanum wheels; each of these wheels has its own geared motor and its own rotary encoder. This configuration makes it possible to independently control the movement of each wheel.

The four motors are driven by a microcontroller, which is controlled by a mini PC (2). The exact position of the robot inside the room can be determined thanks to a Lidar (laser detection and ranging) system (4).

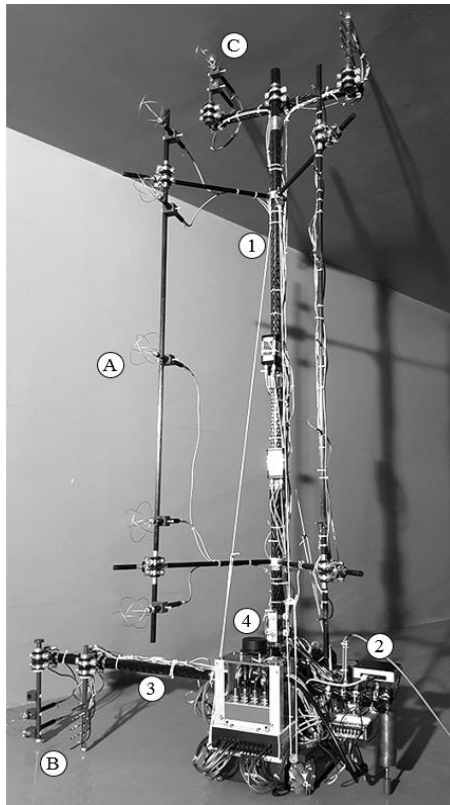


Figure 2: Mobile robot with sensors equipped

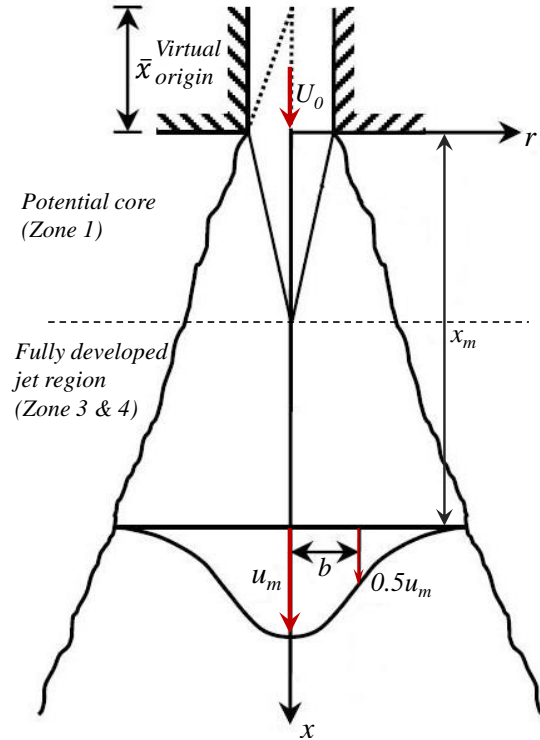


Figure 3: Scheme of theoretical free air jet

Air temperature measurements on the robot is achieved using thermocouples with a diameter of  $25\ \mu\text{m}$ , which allows a very fast-response and a high accuracy ( $\pm 0.06\ ^\circ\text{C}$  in mean value). Air relative humidity measurements are done using SHT75 probes with an absolute accuracy of  $\pm 1.8\ \%\text{RH}$ . Air velocity measurements are carried out using thermoelectric anemometers with an accuracy of  $\pm 1.5\%$  of the measured value.

The sensors are implemented along three vertical profiles. There are two profiles located near the ground (B) and near the ceiling (C). Each of these profiles contains 5 temperature and humidity probes, and 2 anemometers. They capture high gradients, which make it possible to distinguish the different types of boundary conditions at the walls. There is a central profile with vertical amplitude of 1.5 m (A). The main purpose of this profile is to measure air jet characteristics. It includes 7 measurements of air temperature and humidity, and 5 measurements of air velocity.

Compared to the mobile arm on rail system used previously by (Hohota, 2003) and (Kuznik, 2005), there are two main advantages of using the mobile robot system: air flow disturbances reduction and free access to the entire volume of the test room. In addition, it is important to mention that the total heat gain (due to the microcontroller, mini PC, Lidar and data acquisition center) is of order of 10 W, thus air flow characteristics disturbance is minimal.

## 2.4 Experimental protocol

For each measurement campaign, three days are required in order to obtain steady state within the test room. During this stage, air change rate, air temperature and humidity setpoints are fixed depending on the configuration tested. Once the steady state reached, the mobile robot is used to examine the area of interest (1 x 1 m around the air inlet with a mesh of 10 cm).

For each robot position, air velocity and temperature are measured with an acquisition frequency of 10 Hz (100 ms between each measure). Recorded values are averaged over 2000 samples, i.e. 200 s in order to reduce fluctuations.

### 3 THEORETICAL FREE JET MODEL

#### 3.1 Air jet theory

According to ASHRAE Handbook Fundamentals (ASHRAE, 2013), an air jet that is not affected and obstructed by neighbouring elements such as ceiling, walls, other surfaces, is considered a free jet. The theory is based on a jet with a homogeneous velocity equal to  $U_0$  across the duct outlet. The development of an air jet can be divided into four zones (c.f. Figure 3):

- Zone 1: the potential core zone where centerline velocity  $u_m$  is equal to outlet velocity  $U_0$ ;
- Zone 2: the transition zone, which have a negligible length for a circular jet, according to (Kuznik, 2005);
- Zone 3: the zone of fully developed jet, characterized by heat and mass transfers and by turbulence as well as the similarity of the velocity profiles;
- Zone 4: the terminal zone where residual velocity decreases rapidly, often assume to subside below 0.25 m/s.

#### 3.2 Centreline velocity decay in zone 3

From a technical point of view, zone 3 is the most important area since, in most cases, it is the part of the jet that enters the occupied region. Therefore, it influences occupants' thermal comfort and indoor air quality. We are mainly interested in this area which allows describing heat and mass transfers with the room ambience.

Proposed by (Li et al., 1993) and (Goodfellow, 2001), the centreline velocity decay is given by the following equation:

$$\frac{u_m}{U_0} = \frac{K_1 \sqrt{A_0}}{x + \bar{x}} \quad (1)$$

In this equation,  $U_0$  is the averaged initial velocity at the diffuser outlet of effective area  $A_0$ .  $u_m$  is the centreline velocity at distance  $x_m$  (c.f. Figure 3). This formula includes two empirical constants:  $\bar{x}$  is the virtual origin of the jet and  $K_1$  represents the centreline velocity decay coefficient. These two parameters, which are interdependent according to (Zou, 2002), depend mainly upon the type of jets, the type of outlets and the jet initial velocity.

According to Tuve's experimental study (Tuve, 1953),  $K_1$  varies between 5.7 and 7 for a horizontal circular jet. Recently, Malmström's study (Malmström, 1992) concluded that  $K_1$  depends on the jet initial velocity rather than Reynolds numbers  $Re_0$ : it varies between 3 and 6 for  $U_0 < 5$  m/s and remains equal to 6 for  $U_0 > 5$  m/s. For an ascending vertical circular jet, (ASHRAE, 2013) suggests a value of 4.7.

As for the virtual origin, some researchers ((Rajaratnam, 1976), (Goodfellow, 2001)) set  $\bar{x} = 0$  since the length of the fully developed jet zone is usually preponderant. According to Zou's study (Zou, 2001), for  $U_0 < 5$  m/s, the virtual origin varies between 0 and 4 times the diffuser outlet diameter. In our present study, since the length of the jet is limited by the height of the cell (2.5 m), taking into account the virtual origin allows a correction of the jet behaviour.

#### 3.3 Jet boundaries

According to (Rajaratnam, 1976), the boundary (or expansion) of the jet can be obtained using this equation:

$$b = K_2 (x + \bar{x}) \quad (2)$$

where  $b$  is the radial distance at which  $u(r=b) = 0.5u_m$ ;  $K_2$  represents jet expansion coefficient.

$K_2$  also depends on the type and initial velocity of the jet. It has been evaluated by various researchers in the literature: 0.097 according to (Abramovich, 1963), 0.151 according to (Tollmien, 1926), 0.1 according to (Rajaratnam, 1976).

### 3.4 Velocity profiles in the cross-section of a jet

(Rajaratnam, 1976) and (Goodfellow, 2001) demonstrated that, in the fully developed jet region, transverse velocity distribution at different heights of the jet were found to have a similar shape. These profiles could be approximated by the following Gauss error-function:

$$\frac{u}{u_m} = \exp\left(-\ln 2 \cdot \left(\frac{r}{b}\right)^2\right) \quad (3)$$

where  $u$  is the jet velocity corresponding to the radial distance  $r$ .

## 4 EXPERIMENTAL RESULTS

### 4.1 Flow configuration

The air in the test room is ventilated using a closed-loop air handling unit. As illustrated in Figure 1, the ceiling supply air diffuser is located 1.0 m from the East wall and 4.2 m from the North wall. Its diameter is 16 cm and it is equipped with grilles with an effective area/total area ratio of 76% (c.f. Figure 1).

The two air exhausts, which are circular with a diameter of 10 cm, are located in the North wall. They are distanced by 0.3 m from the floor and 0.65 m from the adjacent vertical walls (East and West). This disposition allows us to promote homogeneous air distribution within the test room.

Based on theoretical configuration of a totally free circular vertical jet, which is very well documented in the literature (Goodfellow, 2001), our configuration approaches realistic cases in buildings. Indeed, due to limited dimensions of a room, supply air inlet should be located near a vertical wall. Considering the available space above suspended ceiling, a plenum box must be used before the air inlet. These architecture elements will necessarily have an impact on the jet behaviour and performance, as will be described in next sections.

Table 2: Test cell walls temperature (°C)

	Ceiling	Floor	S	N	E	W
Mean value	28.0	27.8	28.3	27.7	27.8	27.8
SDEV	0.2	0.3	0.2	0.1	0.3	0.3

Table 1: Air supply parameters

	Flow rate (m <sup>3</sup> /h)	U <sub>0</sub> (m/s)	Re <sub>0</sub> (-)	T <sub>0</sub> (°C)
Value	150.1	2.1	21538	28.0
SDEV	2.3	-	-	0.1

### 4.2 Jet behaviour and characteristics

In the present paper, the case of an isothermal jet is analyzed. The boundary conditions and air supply parameters are summarized in Tables 1 and 2. Investigations were carried out following 11 measurement planes around the air inlet with a mesh size of 10 cm, thus a total of 121 measurement positions.

$K_1$  and  $\bar{x}$  are based on the linear regression of the function  $U_0/u_m = f(x/\sqrt{A_0})$ .  $K_2$  is determined using equation (2) for 5 height positions of the jet. In our jet configuration ( $U_0 = 2.1$  m/s ;  $Re_0 = 21538$ ),  $K_1$ -value is equal to 4.4; quite similar to the value recommended by ASHRAE (ASHRAE, 2013). The length of virtual origin can be neglected ( $\bar{x} = -0.004$  m).  $K_2$ -value is found to be equal to 0.15.

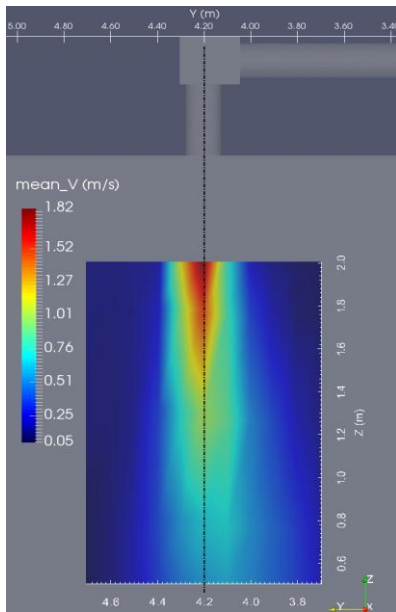


Figure 4: Jet behaviour following plane  $x = 1.0$  m

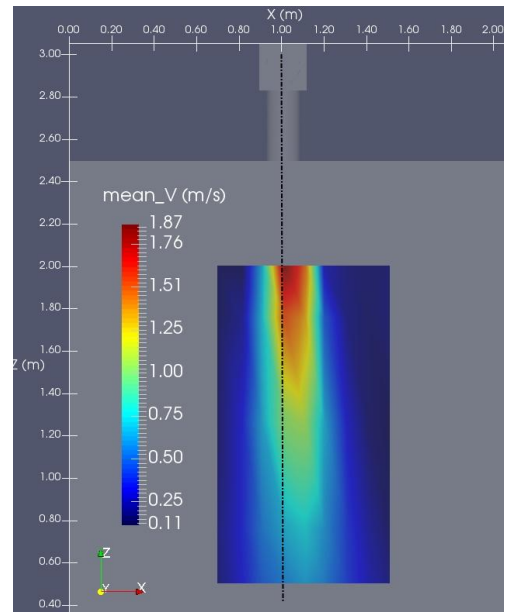


Figure 5: Jet behaviour following plane  $y = 4.2$  m

Figure 4 and Figure 5 show an airflow visualization following 2 section planes  $x = 1.0$  m and  $y = 4.2$  m. As a reminder, the point  $(x = 1.0; y = 4.2$  m) corresponds to the centre of the diffuser in MINIBAT coordination (c.f. Figure 1). As can be seen in 2 figures, the jet trajectory was deviated in both direction  $x$  and  $y$ . In  $y$ -direction, the jet is deviated to the air exhaust side; we can confirm that the plenum box presence air exhausts aspiration could be the origin of this jet deviation. In  $x$ -direction, the jet is deviated to the West wall side (i.e. the opposite direction of the near wall (East wall)). Thus, a near wall situated 1 meter from an air inlet could have a significantly impact on the jet behaviour.

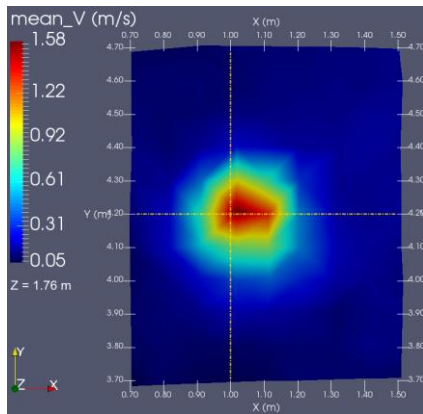


Figure 6: Jet behaviour following plane  $z = 1.76$  m

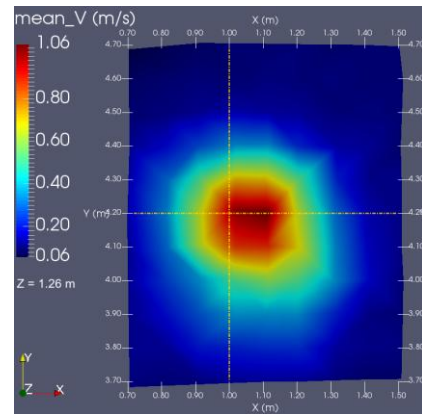


Figure 7: Jet behaviour following plane  $z = 1.26$  m

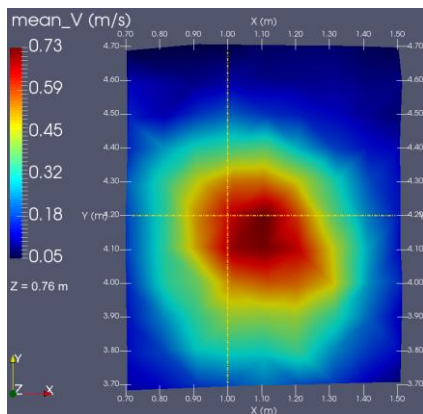


Figure 8: Jet behaviour following plane  $z = 0.76$  m

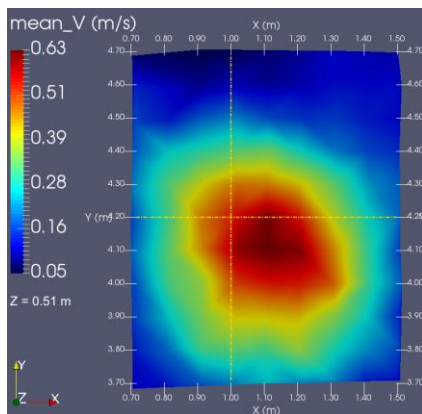


Figure 9: Jet behaviour following plane  $z = 0.51$  m

Figure 6 to Figure 9 show air jet velocity isocontours followings 4 section planes  $z = 1.76$  m,  $z = 1.26$  m,  $z = 0.76$  m and  $z = 0.51$  m. As can be seen clearly, the studied jet is no longer axisymmetric; instead, it spreads with a deviation to the opposite side of the near wall. Indeed, from the theoretical axe ( $x = 1.0$  m), the jet spreads about 10 cm to the left (near wall) and about 30 cm to the right. Besides, a further refine of the examine mesh is necessary in order to obtain more precise isocontours.

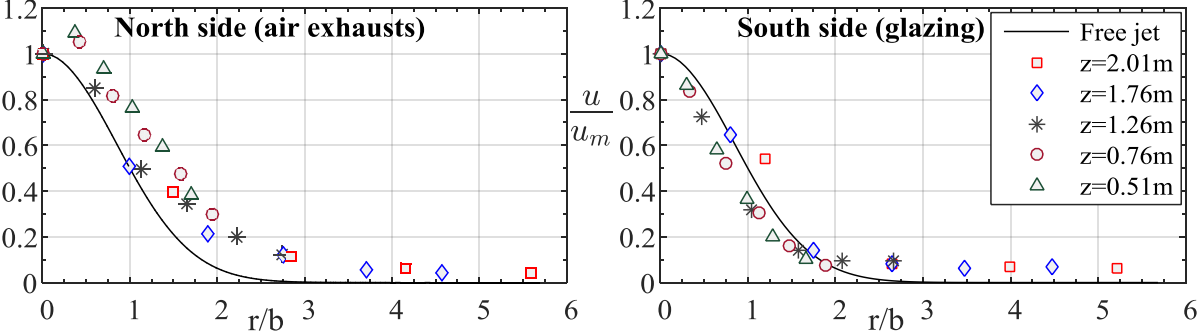


Figure 10: Velocity profiles in the cross-section of the jet following y-direction

Jet velocity profiles in y-direction and on both side of the jet axe are shown on Figure 10. As expected, all velocity profiles according to 5 height positions are similar to each other and to the theoretical profile. Otherwise,  $u/u_m$  values of the air exhaust side are all greater than the theoretical curve. Some values of  $u/u_m$  is greater than 1 (i.e.  $z = 0.76$  m and  $0.51$  m); it means that centreline velocity of the studied jet is not necessary the maximum velocity, as can be seen in figure below.

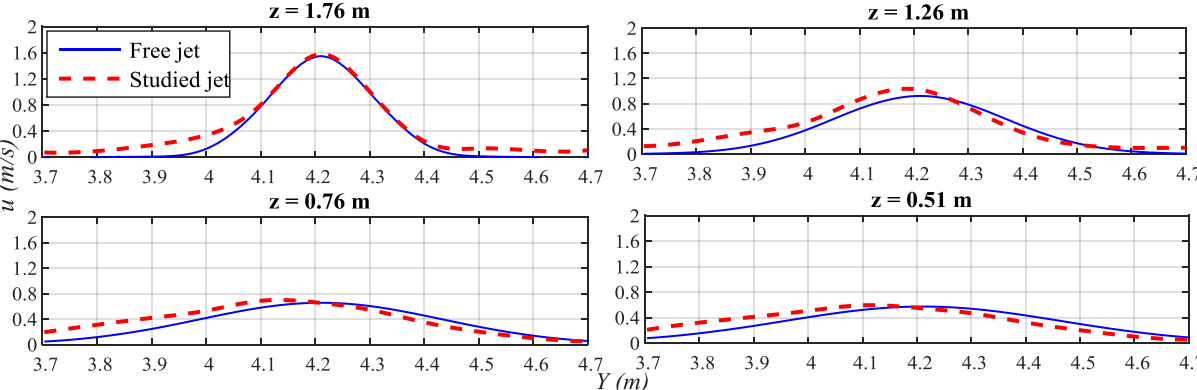


Figure 11: Velocity distribution for 4 height positions of the jet

The velocity distribution according to 4 height positions of the jet is presented in Figure 11. For  $z = 1.76$  m, the maximum velocity of the studied jet stay on the free jet theoretical axe. For  $z = 1.26$  m, it lightly shifts to the left side (air exhausts side). Moving farther away from the air diffuser, maximum velocity position is completely deviated to the left side, at the order of 10 cm for  $z = 0.51$  m.

### 5 CONCLUSION

The main objective of this research is to get improved knowledge of the mean and turbulent characteristics of a nearly-free circular vertical air jet in a mechanically ventilated room with the presence of a near wall, a plenum box and air exhausts. As expected, experimental results show a deviation with respect to theoretical values. Indeed, the presence of architecture

elements have a significantly impact on the jet behaviour and thus, its real trajectory is deviated compared to a totally free air jet.

Following the present study, it is necessary to refine the experimental measurements by adding additional examine planes with a finer mesh around the air diffuser in order to obtain a higher precision, particularly in the jet region. On the other hand, the results obtained allow for more thorough research under non-isothermal conditions, with the presence of moisture, as well as in condensation condition.

## 6 REFERENCES

- Abramovich, G.N. (1963). The theory of turbulent jets. *The Massachusetts Institute of Technology Press, Cambridge*.
- ASHRAE. (2013). Chapter 20 Space Air Diffusion. *ASHRAE Handbook Fundamentals, Atlanta : SI Edition, 20.1-20.9*.
- Chen, C.J., Rodi, W. (1980). Vertical turbulent buoyant jets: a review of experimental data. *NASA STI/Recon Technical Report A*, vol. 80.
- Chen, Q. (2009). Ventilation performance prediction for buildings: A method overview and recent applications. *Building and environment, vol. 44, no 4, 848-858*.
- Corrsin, S. (1946). Investigation of flow in an axially symmetrical heated air jet of air. Technical report. Wartime report W-94, NACA.
- Gavan, V. (2009). Full-scale experimental evaluation and modelling of a double-skin facade. Optimal control of thermal and visual comfort. *PhD thesis, INSA de Lyon, 220 p*.
- Goodfellow, H.D. (2001). Industrial ventilation design guidebook. *Academic press, Chapter 7.4 Air jets*.
- Grimityn, M. (1970). Zuluftverteilung in Räumen. *Luft-und Kältetechnik*, vol. 5, 246-256.
- Hohota, R. (2003). Moisture modeling in a CFD code (low velocity in large cavity) – comparison with the experimental (in French). *PhD thesis, INSA de Lyon, 246 p*.
- Koestel, A. (1954). Computing temperatures and velocities in vertical jets of hot or cold air. *ASHVE Transactions 60*.
- Kuznik, F. (2005). Experimental study of horizontal anisothermal axisymmetric jets developing near a wall: Application to numerical modeling of ventilated cavities (in French). *PhD thesis, INSA de Lyon, 190 p*.
- Li, Z.H., Zhang, J.S., Zhivov, A.M. and al. (1993). Characteristics of diffuser air jets and airflow in the occupied regions of mechanically ventilated rooms - a literature review. *ASHRAE Transactions, n°99, 1119–1127*.
- Malmström, T.G., Kirkpatrick, A.T., Christensen, B., and al. (1997). Centreline velocity decay measurements in low-velocity axisymmetric jets. *Journal of Fluid mechanics*, vol. 346, 363-377.

- Rajaratnam, N. (1976). Turbulent jets. *Elsevier, Chapter 2. The circular turbulent jet.*
- Shepelev, I. (1961). Supply ventilation jets and air fountains. Proceedings of the academy of construction and architecture of the USSR, no. 4.
- Tollmien, W. (1926). Sonderabdruck aus zeitschrift fur angewandte. *Mathematik und Mechank*, vol. 6, 468-478.
- Tuve, G.L. (1953). Air velocities in ventilating jets. *Heating, Piping and Air Conditioning*, 181-191.
- Zou, Y. (2001). Air jet in ventilation applications. *Bulletin n°55. Building Services Engineering, Royal Institute of Technology, KTH*, 63 p.
- Zou, Y. (2002). An experimental investigation of turbulent wall jets. *ASHRAE Transactions*, n°108, 203-206.

# Technologies to overcome effects of condensation in exchangers of ventilation units - analysis of monitored field studies

Bart Cremers<sup>\*1</sup>, Tristan Bakker<sup>1</sup>

<sup>1</sup>*Zehnder Group Zwolle  
Lingenstraat 2  
8028 PM Zwolle, The Netherlands  
\*bart.cremers@zehndergroup.com*

## ABSTRACT

Balanced ventilation with heat recovery is an efficient way to maintain low heating demand for ventilation in residential buildings. Laboratory measurements of today's heat recovery ventilation units show high temperature recovery efficiency during standard conditions. In practice, however, the recovery efficiency may decrease due to circumstances that deviate from the standard laboratory conditions.

The present study shows detailed measurements of twofield tests with similar balanced ventilation systems installed in houses. One of the houses is in The Netherlands and has a heat exchanger installed (for heat recovery). The other house is in Austria and has an enthalpy exchanger installed (for heat and moisture recovery). During the same period in October and November 2016, various parameters were monitored among which temperatures and humidities of the air streams, extract and supply fan speeds and their corresponding flow rates. Outdoor temperatures vary in the range of 22 °C at the start of the observed period until -2 °C at the end of the observed period. Data is monitored on a 5-minute interval time, and later analysed using the hourly averaged values of the parameters.

From the monitored data, it is shown how the thermal recovery efficiency correlates with other parameters as outdoor temperature, and the combination with the dew point of the extract air. The effects of condensation on fan behaviour is shown for a mass flow balance correcting algorithm, and compared to measurements without correction of mass flow balance. Moreover, the thermal recovery efficiency is shown for the ventilation systems with enthalpy exchanger to compare them with the systems with heat exchanger.

Conclusion of the present study is that a mass flow balance correcting algorithm maintains a high thermal recovery efficiency for a balanced ventilation system, even when condensation occurs in the extract channels of the heat exchanger. Because of moisture transfer, enthalpy exchangers experience no condensation, and therefore show no change in thermal recovery efficiency than heat recovery systems, even when outdoor temperature drops below the dew point of the indoor climate. For the enthalpy recovery units, the thermal recovery efficiency is only a function of ventilation air flow rate.

## KEYWORDS

Residential ventilation, heat recovery efficiency, condensation, mass flow balance, enthalpy exchanger

## 1 INTRODUCTION

Balanced ventilation with heat recovery is an efficient way to maintain low heating demand for ventilation in residential buildings (Cremers, 2012). Laboratory measurements of today's heat recovery ventilation units show high temperature recovery efficiency during standard conditions. In practice, however, the recovery efficiency may decrease due to circumstances that deviate from the standard laboratory conditions.

Maintaining a high thermal recovery efficiency not only safeguards a comfortable supply temperature of fresh air during cold outdoor periods, it also reduces the heating demand for the building further. Using an enthalpy exchanger, the supply of fresh air is maintained not only on a high temperature level, but also on a high humidity level, leading to higher indoor

humidity levels, and therefore increasing the level of comfort in the cold season (Cremers, 2014).

## 2 MONITORING SET-UP

The present study shows monitored data from two field studies with similar balanced ventilation systems installed in houses. One of the houses is in The Netherlands and has a heat exchanger (for heat recovery) installed (see fig. 1). The other house is in Austria and has an enthalpy exchanger installed (for heat and moisture recovery). The monitoring results presented in this work are part of a larger monitoring project of six ventilation installations in The Netherlands, Germany and Austria.



Figure 1: Photograph of the ventilation unit with a heat exchanger in the house in The Netherlands.

During the same period in October and November 2016, various parameters are monitored on a 5-minute interval time, and later analysed using the hourly averaged values of the parameters. The temperatures and humidities are measured with built-in sensors. They are located in the ventilation unit in the outdoor air (ODA), the supply air (SUP), the extract air (ETA) and the exhaust air (EHA). More specifically, outdoor and extract air temperature are measured when they enter the ventilation unit. The supply and exhaust air temperature are measured in the outlet of the fans. Also monitored are the fan speeds of the extract and supply fan, and their corresponding flow rates.

Outdoor temperatures vary in the range of approximately 22 °C at the start of the observed period until -2 °C at the end of the observed period.

## 3 RESULTS AND ANALYSIS

The results are presented mainly in the thermal recovery efficiency as a function of the outdoor temperature. The thermal recovery efficiency based on the supply side is calculated as the temperature change in the supply channel relative to the maximum possible temperature change  $(T_{\text{SUP}} - T_{\text{ODA}}) / (T_{\text{ETA}} - T_{\text{ODA}})$ . The thermal recovery based on the extract side is calculated as the temperature change in the extract channel relative to the maximum possible temperature change  $(T_{\text{ETA}} - T_{\text{EHA}}) / (T_{\text{ETA}} - T_{\text{ODA}})$ . Unlike for standardized laboratory measurements, both recovery efficiencies are deliberately not corrected with mass flows to see the effect of any imbalance due to possible condensation.

### 3.1 Heat recovery without mass flow balance correcting algorithm

Heat recovery ventilation units without mass flow balance correcting algorithm are used in many dwellings nowadays. The two fans in these units run in constant fan speed. This means that for a specific flow pre-set as decided by the user (low, medium, high) the fan speed is independent of any change in the air resistance of the system, including ducts and the unit itself.

In fig. 2 the thermal recovery efficiency based on the supply side for a unit without mass flow balance correcting algorithm is shown as a reference. This has been monitored in 2014 with a unit that had a commissioned air flow unbalance of 7% (with less extract than supply air) with an average extract air flow of 210 m<sup>3</sup>/h. This had the effect, as shown in fig. 2, that for a heat exchanger without any condensation, the thermal efficiency was monitored to be between 85% and 95%.

When outdoor temperature drops below approximately 7 °C, there is a chance that condensation may be formed. Without mass flow balance correcting algorithm, the condensation in the extract channels of the heat exchanger increases the resistance, and therefore the extract flow decreases. This makes the unbalance in condensing cases even larger, which is showed in fig. 1 by a decreasing thermal recovery efficiency, even down to 60%.

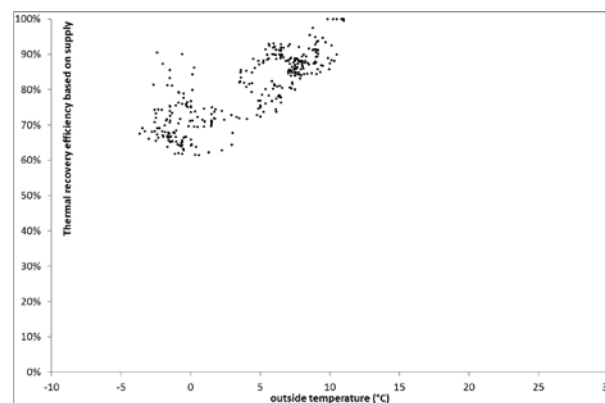


Figure 2: Thermal recovery efficiency based on supply for a heat recovery unit without mass flow balance correcting algorithm.

### 3.2 Heat recovery with mass flow balance correcting algorithm

Heat recovery units with mass flow balance correcting algorithm preserve the mass flow balance when the air resistance changes in the system because of condensation or even filters accumulating with dust. However, because the occupant changes the flow rate according to his presence and behaviour in the house, the fan percentages itself do not give a clear picture. The ratio between the supply fan percentage and the extract fan percentage gives a clearer picture. Fig. 3a shows fairly constant ratio of 1.15 for outdoor temperature above approximately 10 °C. Apparently in this installation the resistance of the supply side is larger than the extract side, so the supply fan must work harder for the same air flow rate. For outdoor temperature below 10 °C, there is a decreasing trend in the ratio, which - after closer observation of the parameters - comes from the effect that the extract fan percentage increases for colder outdoor temperatures.

Although the fan percentages change relative to each other, fig. 3b shows that the mass balance is preserved, noticed by the ratio between supply mass flow and extract mass flow which stays at a value of  $1 \pm 0.04$ .

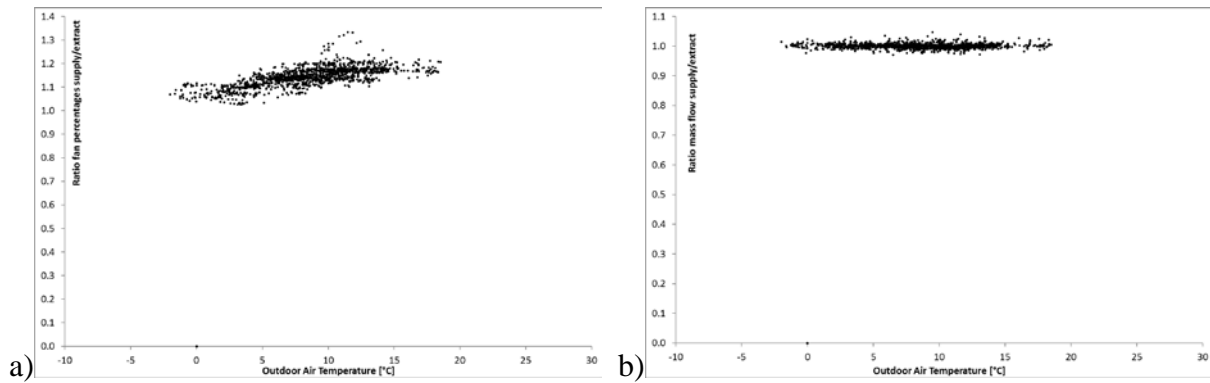


Figure 3: Ratio in fan percentage (a) and ratio in mass flow (b) between supply air and extract air.

The resulting thermal recovery efficiency based on the supply is shown in fig. 4a as a function of outdoor temperature. With the mass flow balance correcting algorithm, there is no effect from any unbalance in the mass flows. Fig. 4a indeed shows that high recovery efficiency can be maintained (above 88% for the temperature range between -2 and 19 °C) for an average flow rate of 180 m<sup>3</sup>/h.

It seems however that there is still a trend for the recovery efficiency to decrease when outdoor temperatures get lower. This trend is also observed in two similar ventilation systems during the same monitoring period. However, the decreasing trend is much less than for heat recovery units without mass flow balance correcting algorithm.

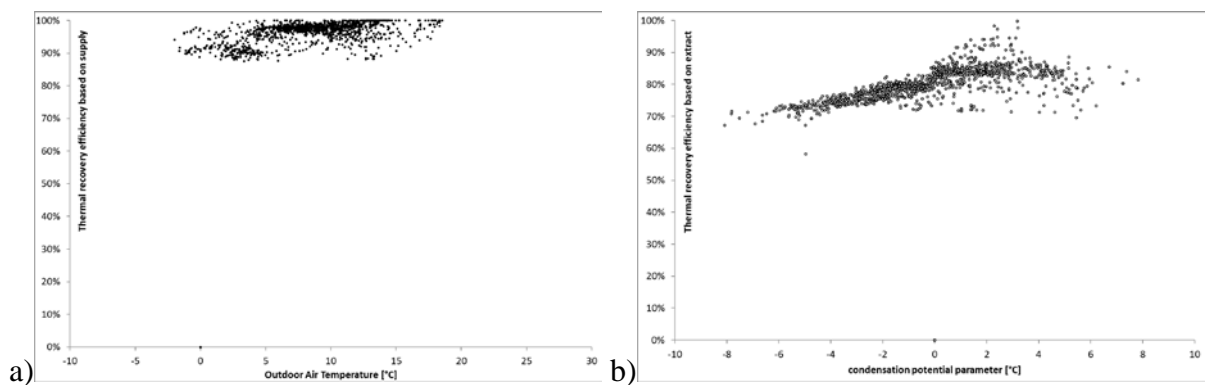


Figure 4: a) Thermal recovery efficiency based on supply as function of outdoor temperature; b) Thermal recovery efficiency based on extract as a function the condensation potential parameter. Both are for a unit with heat exchanger and a mass flow balance correcting algorithm.

Further analysis of condensation effects has been focused on the thermal recovery efficiency based on the extract. In fig. 4b it has been expressed as a function of the condensation potential parameter (outdoor temperature minus dew point of extract air). It is likely that condensation will take place when this condensation potential parameter is below zero, and the more negative it is, the more condensation can be formed.

Fig. 4b shows that for negative values of the condensation potential parameter, the thermal recovery efficiency based on the exhaust deviates from the positive values, and shows a decreasing trend for more negative values. This is a clear indication that condensation in the heat exchanger is hindering the thermal transfer between the two air streams in the heat exchanger, and therefore the recovery efficiency is going down. The water in the exchanger decreases the area for an efficient heat transfer. Because mass balance is still preserved (see fig. 3b), the decrease in recovery efficiency is much less than for units without mass flow balance correcting algorithm.

### 3.3 Enthalpy recovery

Enthalpy recovery units have an exchanger which not only transfers heat, but also moisture. The moisture is transferred in vapor form through microscopic channels in the foils of the enthalpy exchanger. Because of the moisture transfer, condensation is not likely to be formed in these exchangers.

Fig. 5 shows the thermal recovery efficiency based on the supply as a function of outdoor temperature. The hourly averaged values appear as two distinct, nearly horizontal lines, and a lower line made up of occasional dots.

The two distinct lines show that the recovery efficiency for a unit with enthalpy exchanger is not a function of the appearance of condensation anymore (in fact, there is no condensation). The recovery efficiency remains only a function of the flow rate as set by the end user. The highest line (approximately 95%) corresponds to a set flow rate of 100 m<sup>3</sup>/h and the other horizontal line (approximately 90%) corresponds to a set flow rate of 160 m<sup>3</sup>/h.

The other dots in the graph - below 70% - belong to circumstances where heat recovery is not needed (e.g. when a comfortable indoor temperature has been reached, outside the heating season), and therefore the recovery efficiency is automatically gradually decreased by activating a bypass mechanism.

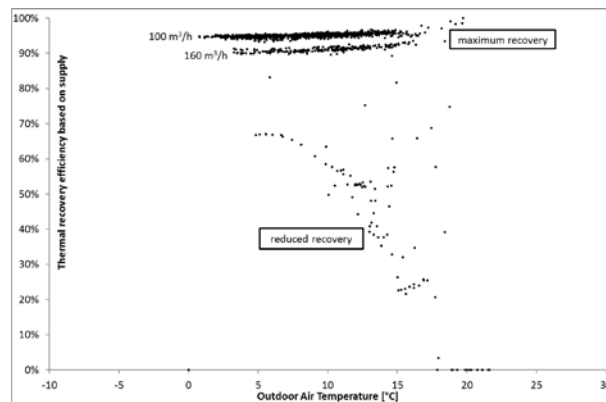


Figure 5: Thermal recovery efficiency (supply) against outdoor temperature for a unit with enthalpy exchanger.

## 4 CONCLUSIONS

Conclusion of this study is that a mass flow balance correcting algorithm maintains a high thermal recovery efficiency for a balanced ventilation system, even when condensation occurs in the extract channels of the heat exchanger. Although the condensation hinders the efficient area for transfer of heat through the foils, it has no effect on the balance between extract and supply air stream anymore. Therefore, thermal recovery efficiency stays above 88% (compared to monitored values down to 60% for units without mass flow balance correcting algorithm).

Because of moisture transfer, enthalpy exchangers experience no condensation, and therefore show no change in thermal recovery efficiency, when outdoor temperature drops below the dew point of the indoor climate. For the enthalpy recovery units, the thermal recovery efficiency is only a function of ventilation air flow rate.

## 5 REFERENCES

- Cremers, B.E. (2012). Long term monitoring of residential heat recovery ventilation with ground heat exchange. *REHVA Journal*, August 2012, p. 41–46.
- Cremers, B.E. (2014). The effect of enthalpy recovery ventilation on the residential indoor climate. *Proceedings of 35<sup>th</sup> AIVC conference*, Poznan, Poland, p. 78.

# A Method to Measure Emission Rates of PM<sub>2.5</sub>s from Cooking

Catherine O’Leary<sup>1</sup> and Benjamin Jones<sup>\*1</sup>

*1 University of Nottingham  
B12 Paton House,  
Department of Architecture and Built Environment,  
University of Nottingham, NG7 2RD, UK*

*\*Corresponding author:  
Benjamin.Jones@nottingham.ac.uk*

## ABSTRACT

Exposures to airborne fine particulate matter with a diameter of <2.5µm (PM<sub>2.5</sub>) are linked to multiple negative health effects, including cardiovascular and respiratory disease. Existing investigations of PM<sub>2.5</sub> primarily focus on external sources and exposures, because outdoor air is easier to observe, and therefore, more widely monitored. However, as people spend up to 70% of their time in their own homes, exposures to indoor pollutants could have a greater impact on health. One method of investigating indoor exposures in a stock of houses is by modelling them. However, this process requires an understanding in the uncertainty of emission rates from internal sources.

Cooking has been identified as key source of PM<sub>2.5</sub> in non-smoking households. Existing studies of emission rates use a range of techniques from small scale test chambers, which give control over all parameters in unrealistic conditions, to personal monitoring studies in real conditions where there is no control over influencing parameters. Reported emissions rates for single sources vary significantly indicating poor repeatability, and are generally presented without an indication of the uncertainty in them; for example, as a probability density function (PDF). Therefore, existing emission rates have limited use for stochastic indoor air quality modelling.

This paper seeks to develop a methodology to measure emissions rates of PM<sub>2.5</sub>s from the cooking of foods. A two-phase investigation measured the variation in emission rates when toasting bread in an electric toaster, a process that is simple and repeatable with fewer variables than many other cooking processes.

Phase one was conducted in a domestic kitchen. A TSI SidePak™ AM510 optical monitor measured temporal concentrations during and after toasting (n=40). A number of problems with the procedure were identified: (i) the recording time-step was too long, which lead to insufficient data points during the emission period; (ii) the ventilation rate and mixing conditions were unknown, although steps were taken to control them, which increased measurement uncertainty; (iii) the relative humidity was not monitored, which can affect the performance of the SidePak™ at high levels, and (iv) when the toaster and bread were not isolated at the end of the toasting period, increasing uncertainty in the total emission period.

The second phase used a test chamber, which offered greater control over the indoor conditions. An experimental procedure was followed which was similar to that use during the first phase, but with a one-second time-step, the toaster and toasted bread were sealed after the emission period, and the chamber was flushed with outside air between tests. Relative humidity and temperature were monitored during tests. Emission rates are estimated using an established model and reported as a histogram.

## KEYWORDS

Food, Toast, Emission Rates, Fine Particulate Matter, Indoor Air Quality

## 1 INTRODUCTION

Fine particulate matter (PM<sub>2.5</sub>) is composed of airborne solid or liquid particles of diameter less than 2.5µm (Pope and Dockery, 2006). Due to their small size, when breathed in, these particles can bypass the body’s defences (Pope and Dockery, 2006) and exposure to elevated concentrations has been associated with chronic and acute, respiratory and cardiovascular diseases (Lewtas, 2007), as well as other possible health implications (Rückerlet *al.*, 2011).

The health impacts of exposure to air pollutants, including PM<sub>2.5</sub>s, can affect people at all stages of life, from before birth to death (RCP, 2016).

In the UK, energy use in residential buildings is estimated to account for around 26% of the country's total carbon dioxide (CO<sub>2</sub>) emissions (Wilkinson *et al.*, 2009), which has influenced the move to reduce the energy demand of the existing building stock (Wilkinson *et al.*, 2009). Retrofit and intervention strategies can involve reducing infiltration (Wilkinson *et al.*, 2009) but do not necessarily include any additional purpose-provided ventilation, potentially lowering overall airflow rates. Furthermore, whilst all new dwellings are required to have localised mechanical extract ventilation in the kitchen, when refurbishing existing dwellings, they are not required where they are not already present (HM Government, 2010).

People spend 70% of their time in their houses (Laderet *et al.*, 2005) and so a reduction in the supply of fresh air could offer protection from outdoor pollutants, but could also trap pollutants emitted indoors (Shrubsole *et al.*, 2012). Key indoor sources of PM<sub>2.5</sub> include cooking, smoking, spray aerosols, and various forms of combustion, including burning candles and incense (Afshari *et al.*, 2005). Cooking is interesting because it is a common activity where total source removal is not possible.

One method to investigate indoor exposure to PM<sub>2.5</sub> at stock level is to use models. However, their predictions are highly sensitive to the emission rates used (Das *et al.*, 2014). When representing cooking sources, a constant value of 1.6 mg/min is used by Shrubsole *et al.* (2012), despite emission rates having been shown to vary with fuel type (Olson and Burke, 2006), food type and cooking method (Fortmannet *et al.*, 2001), and oil type (Torkmahallehet *et al.*, 2012). Additionally, reported emission rates are highly varied, from 0.025 mg/min for pork roast (Fortmannet *et al.*, 2001) to 1496 mg/min (Olson and Burke, 2006). They are also frequently based on a small number of measurements from which it is difficult to determine uncertainty and the probability density functions (PDFs) required by stochastic stock modelling. This paper evaluates existing measurements of PM<sub>2.5</sub> emission rates from the cooking of food in Section 2. It then applies these to develop methods for deriving PDFs of PM<sub>2.5</sub> emission rates in Sections 3 and 4.

## 2 EXISTING MEASUREMENT METHODOLOGIES

Existing measurement methodologies of emission rates from foods cooked in houses can be divided into five categories, each of which has its own benefits and frequency in the literature. The first method is personal monitoring, which is generally rare. Olson and Burke (2006) used it to determine emission rates using measurements of PM<sub>2.5</sub> concentration made during four, seven-day monitoring periods by 37 participants. Concentration peaks from cooking were identified using diaries, and the emission rate calculated using a mass balance approach that considered a house to be a single well-mixed space. A total of 411 cooking events found that emission rates ranged between 0.6 to 1496 mg/min ( $\mu=36$  mg/min). However, the approach was found to overestimate the true emission rates because of the combined effect of the close proximity of the sensor to the source, and the assumption of the whole house being considered well-mixed. The cooking methods were recorded but details of the food were not.

The second approach uses monitors located in a place of interest, most frequently in dwellings. He *et al.* (2004) measured PM<sub>2.5</sub> mass concentrations for 48 hours in 15 houses in Brisbane, Australia. Elevated concentrations were linked to events using occupant diary entries and catalogued into 21 activity types. In each house an air exchange rate (AER) test and controlled cooking test were conducted. The latter consisted of frying half an onion in vegetable oil on "high" heat under both minimum and normal ventilation conditions. This provided an opportunity for direct comparison between houses. Emission rates were determined using a mass balance relationship for a total of 106 cooking events where emission rates ranged from 0.03 to 2.78 mg/min ( $\mu=0.11$  mg/min). The lack of control over

ventilation rates and emission periods led to large errors. A monitoring study is a simple way of monitoring typical concentrations found in dwellings and the emission rates associated with them. But, the lack of information on the food prepared and the cooking methods limits the ability of its findings to be extrapolated to the wider population.

The third method uses managed tests conducted in semi-controlled conditions in the field, typically in a residential setting; see Dacunto *et al.* (2013) and Fortmann *et al.* (2001). Both studies investigate emission rates from varying sources and in a residential setting, for some of the tests, using gas and electric stoves. They use different mass balance relationships to estimate emission rates. The AERs were measured using tracer gas decay, and the test environments flushed with outside air between tests. Dacunto *et al.* (2013) conducted 66 measurements in 3 locations, including both cooking and non-cooking sources, with duplicates of most, but not all, tests. The lowest emission rate of 0.1 mg/min was from oven cooking frozen pizza. The highest cooking emission rate of 15.2 mg/min was from fried chicken breast. Fortmann *et al.* (2001) conducted 32 cooking tests using a variety of foods and cooking methods based on the US diet, under multiple ventilation conditions, in a single location. 7 tests were repeated but comparing changes using gas and electric heat sources. However, only 4 tests were duplicated exactly to investigate variability, suggesting high variability that exceeds 100% and a need for more repetitions. Estimated emission rates ranged from 0.025 mg/min, for pork roast with exhaust ventilation, to 10.3 mg/min, for frying tortillas on an electric range. The range of emission rates from both of these tests highlights the need to understand the population diet when choosing sources for investigation, whilst the low repeatability – indicated in the repeatability tests (Fortmann *et al.*, 2001) and large standard deviations (Dacunto *et al.*, 2013) – calls for more repetitions.

The fourth method uses large scale chambers to obtain a further level of control over ventilation rates and mixing conditions, pollutant concentrations in the supply air, and internal materials to minimise sink effects. By creating a test chamber within a building, the effect of outside air and natural ventilation processes is reduced, and over-pressurising the test chamber controls the direction of background ventilation (Afshari *et al.*, 2005). Afshari *et al.* (2005) investigated concentrations of fine and ultrafine particles from 10 cooking and non-cooking sources, under identical conditions, in a full-scale test chamber. Lee and Wang (2006) found PM<sub>2.5</sub> emission rates of 0.72–1.83 mg/min, for 5 mosquito coils tested in a large environmental chamber. Temperature, relative humidity, AER, mixing conditions, and leakage were all controlled during these tests, which reduces error in the estimated emission rates. Finally, Pagels *et al.* (2009) investigated chemical composition and mass emission of candle smoke particles. Although these are not cooking sources and the emission rates are not useful for direct comparison, they also used a positively pressurized stainless-steel chamber, with controlled relative humidity, temperature, ventilation rates and mixing conditions, and filtered supply air.

The fifth and final method uses small-scale chambers. Géhin *et al.* (2008) utilised a hexagonal test chamber, volume  $2.36 \pm 0.05 \text{ m}^3$ , first designed for vacuum cleaner efficiency characterisation, to investigate fine and ultrafine particle emission rates for cooking and non-cooking sources. The control measures used in large chamber tests are also used, and the internal surfaces were treated with an antistatic coating, and an upward current of filtered air were employed to reduce sink effects. Torkmahalleh *et al.* (2012), measured emissions from heating cooking oils in a laboratory fume hood operating at  $65 \text{ m}^3/\text{h}$  ( $80 \text{ h}^{-1}$ ), with 5 repetitions of each test. Mixing conditions were tested using SF<sub>6</sub> and a grid equivalent to the full size of the hood with grid points located 10 cm apart. The small size of the chamber means the air is very well mixed, but the method of heating the cooking oils in a beaker on a hot plate is far abstracted from real cooking methods, and so the resulting emissions may not reflect those found in a domestic kitchen. This may also be true for the emissions from Géhin *et al.* (2008) because the airflow conditions may have impacted the emissions from the combustion source.

### 3 EXPERIMENT PHASE 1

#### 3.1 Method

The first phase of tests follows the third method described in Section 2. They were conducted in a residential kitchen, volume 35.4 m<sup>3</sup>, in Nottingham, UK, in July 2015. Although it was not possible to control the ventilation conditions precisely, all windows, and internal and external doors were closed during tests, and a wall mounted kitchen extractor fan was used to stabilise the ventilation rate. Mixing conditions were not tested, and no mixing fan used, additionally, the ventilation rate was not measured.

One SidePak™ AM510 Personal Aerosol Monitor (TSI Inc., Shoreview, MN, USA) was used to monitor PM<sub>2.5</sub> concentrations, at height 1.1 m, 1 m from the source; see Figure 1. Concentrations are time-averaged and reported at 1 minute intervals following Ott *et al.* (2006), with the calibration factor – required for the conversion of optical readings to mass concentrations – set to the default 1.0, as no concurrent gravimetric sampling was available.

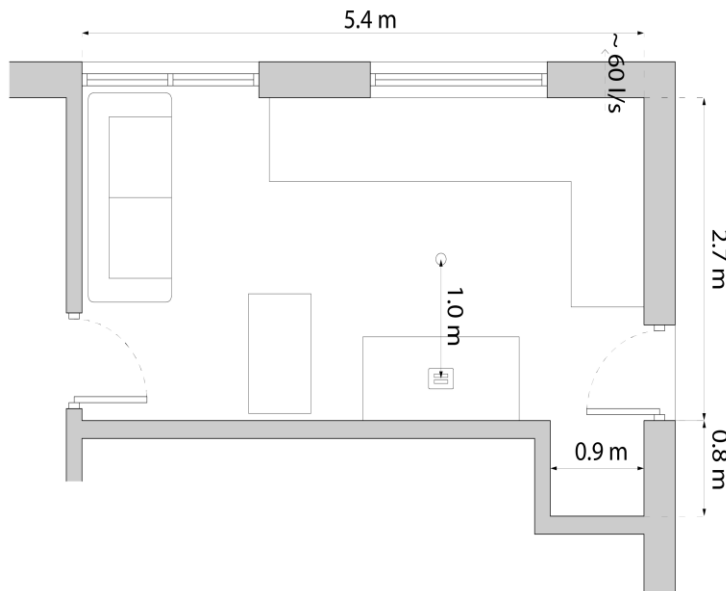


Figure 1 - Kitchen Plan

The test consisted of toasting 2 slices of bread (medium sliced white or wholemeal Hovis 800g loaf) in a supermarket branded toaster on setting 6, the highest setting. The test is simple and repeatable, with a predefined cooking time, and slices of bread with consistent weight and geometry. The start and end of the toasting time were recorded, and concentrations were allowed to return to background levels between tests, or left for a minimum 25 minutes. The test was repeated a total 40 times with 50% wholemeal. The toaster was new at the start of testing, and was not cleaned between tests.

In addition, 6 plume tests were conducted in the kitchen in October 2015, to observe the concentration profile during the emission period. A tube attached to the SidePak™ inlet was positioned in the plume, 20 cm above the toaster, with concentrations logged at 1 second intervals. The decay was not monitored and the room was flushed with outside air between tests.

#### 3.2 Emission Rate Calculation

The method used to determine emission rates is based on the widely used mass balance model; see Dacunto *et al.* (2013), Olson and Burke (2006) and Ott *et al.* (2006).

$$C(t) = C_b + \frac{G}{(\lambda + k)V} + \left( C(0) + C_b + \frac{G}{(\lambda + k)V} \right) e^{-(\lambda+k)t} \quad (1)$$

Here,  $C(t)$  is the concentration at time  $t$ ,  $C_b$  the background concentration,  $C(0)$  the initial concentration,  $G$  the emission rate,  $V$  the mixing volume, and  $(\lambda+k)$  the total decay rate due to ventilation, deposition, and coagulation.

Ott established three phases in during emissions: an  $\alpha$ - or emission period when air is not well-mixed, a subsequent  $\beta$ -period when emissions cease and mixing is incomplete, and a  $\gamma$ -period of well mixed decay (Ott *et al.*, 2006). During the  $\beta$ - and  $\gamma$ -periods, equation (1) is simplified to give

$$C(t) = C_b + (C_p - C_b)e^{-(\lambda+k)(t-t_p)} \quad (2)$$

$C_p$  is the peak concentration at time  $t_p$ , and  $(\lambda+k)$  is determined by log-linear regression. For a rectangular source function, the peak concentration should occur at the end of the  $\alpha$ -period, but it is often observed later indicating that full-mixing is not instantaneous. Ott *et al.* (2006) proposes the *theoretical peak estimation* method where the decay rate is determined from the  $\gamma$ -period and extrapolated back to the start of the  $\beta$ -period. This theoretical peak,  $C_p$ , is then used to estimate the emission rate over an emission period of time  $T$ , where

$$G = (\lambda + k)V \left[ \frac{(C_p - C_b) - (C(0) - C_b)e^{-(\lambda+k)T}}{1 - e^{-(\lambda+k)T}} \right] \quad (3)$$

### 3.3 Calibration Factors

Concurrent gravimetric sampling to determine custom calibration factors (CFs) was unavailable. TSI calibrate SidePak™s using Arizona Test Dust, and so if the aerosol has a different density, size distribution, shape, or refractive index, the CF is expected to vary (Jiang *et al.*, 2011). Two CFs are available for toasting bread; Dacunto *et al.* (2013) found CF=0.47 for burned toast, whereas Jiang *et al.* (2011) found CF=0.79. Dacunto attributes the difference to levels of charring. In absence of further information, the data are processed twice, applying each CF.

### 3.4 Results

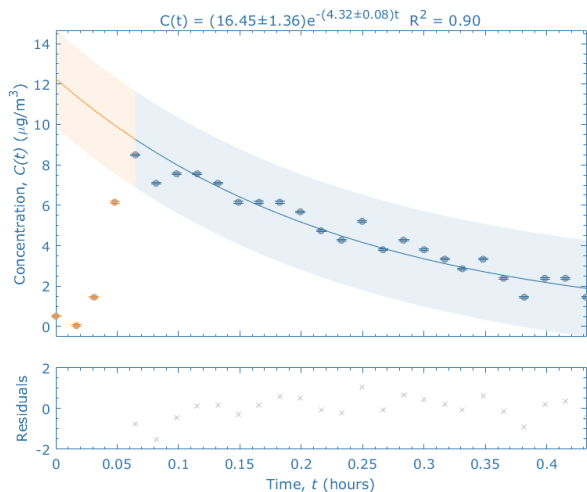


Figure 2 - Example Decay and Emission, CF = 0.47

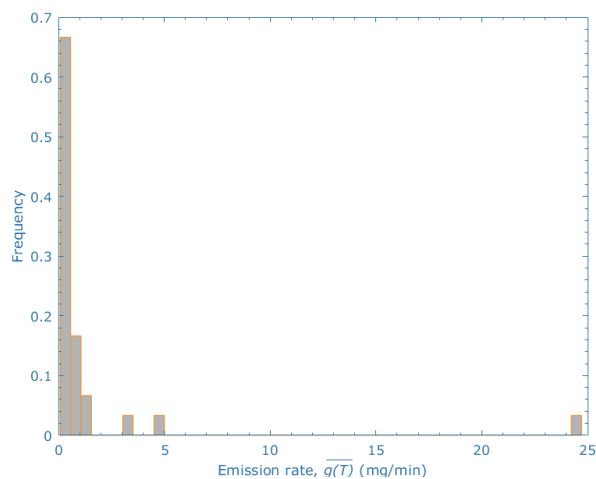


Figure 3 – Phase 1 Emission Rates Histogram, CF = 0.47

Figure 2 shows the concentrations recorded in a sample test, highlighting the  $\alpha$ - and  $\beta$ - periods (orange), the  $\gamma$ -period (blue), and the fit of the curve predicted using the log-linear regression during the  $\gamma$ -period. All tests were processed using the same method and were eliminated from further analyses if the  $R^2$  value for the log-linear regression of the decay was  $<0.7$ , and when emission rates were calculated to be negative (indicating a problem with the test) or could not be estimated. One further outlier was eliminated using *Chauvenet's Criteria*, leaving 29 of 40 tests to determine an average emission rate.

Figure 3 shows the distribution of emission rates calculated for CF=0.47, although the shape of the distribution is identical for both CFs. The data is significantly positively skewed and the median is much less than the mean. This is attributed to a few tests having a high emission rate. Table 1 presents summary the statistics for both CFs, and shows that its value has a significant impact.

Table 1: Phase 1 Emission Rates (mg/min)

CF	N	Mean	SD	Percentiles				
				2 <sup>nd</sup>	25 <sup>th</sup>	50 <sup>th</sup> (Median)	75 <sup>th</sup>	98 <sup>th</sup>
0.47	29	0.662	1.009	0.097	0.179	0.309	0.626	0.097
0.79	29	1.113	1.697	0.163	0.301	0.519	1.052	0.163

The peak concentration occurred after the end of the toasting period. The reasons are unclear and investigations are hampered by the poor resolution of the 1 minute logging interval. The calculation method assumes the delay is due to the time taken for the air to become well-mixed, but emissions may have continued after the toasting period (the toast and toaster were unsealed), or the composition and chemistry of the particles may have evolved. The plume tests in Figure 4 show that the PM<sub>2.5</sub>s are emitted during toasting, but their emission rate is variable, so toasting is a non-rectangular source function.

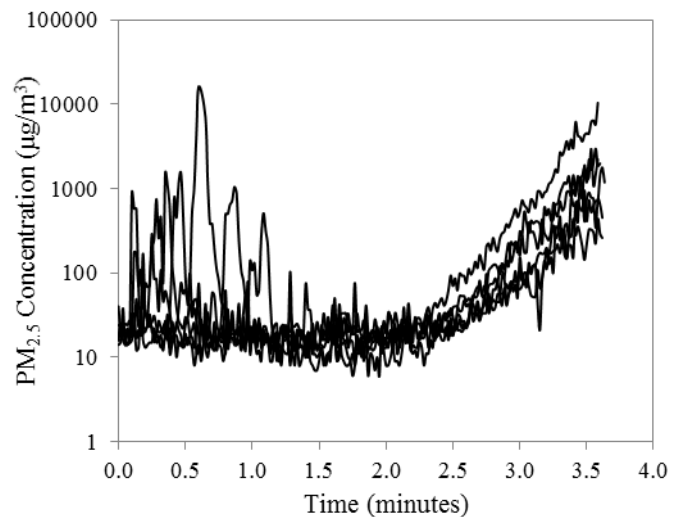


Figure 4 - Plume Test Concentrations during the  $\alpha$ -period

## 4 EXPERIMENT PHASE 2

The second test phase was developed in response to the problems encountered in phase 1. It combines conditions similar to field tests (method 3 in Section 2) by following Dacunto *et al.* (2013), and large scale chamber tests (method 4 in Section 2), following Afshari *et al.* (2005).

### 4.1 Method

Tests were conducted in a chamber with dimensions 2.62×3.49×2.35m, in Nottingham, UK, during May 2017; see Figure 5. The test chamber was repurposed for air quality measurements using plastic sheeting on its floors and by removing unnecessary furniture and fixings. Custom boards were installed into the open window and door to control the ventilation conditions. A low level 0.1×0.1m opening is located in the doorway, and an extractor fan fitted into the window, designed to provide an exhaust flow rate of 85m<sup>3</sup>/h (AER=3.96h<sup>-1</sup>) (Screwfix, 2017). A desk fan was used to aid mixing.

Two SidePak™ AM510 personal aerosol monitors logged PM<sub>2.5</sub> mass concentrations at 1 second intervals, to improve resolution. Both SidePak™s were

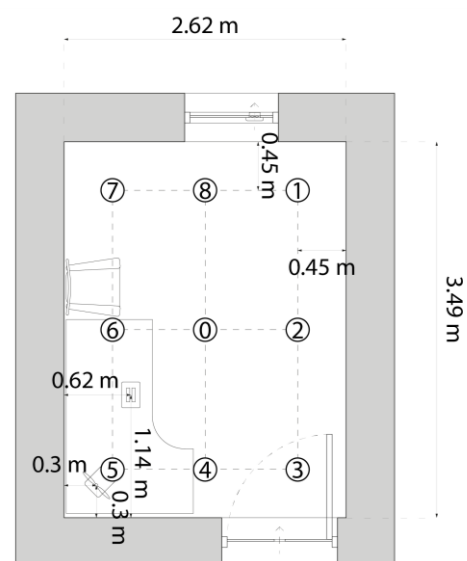


Figure 5 - Test Chamber Plan

mounted on tripods at height 1.1 m. The first was centrally located (see position 0 in Figure 5) whereas the second was moved through all 9 positions between tests to evaluate the room mixing conditions, the results of which are not discussed here. Gravimetric sampling was conducted, and so a default CF=1.0 was used.

In addition, 2 IAQ-Calc Indoor Air Quality Meters (Model 7545, TSI Inc., Shoreview, MN, USA) monitored indoor and outdoor temperatures, CO<sub>2</sub> concentration, and relative humidity. Chamber relative humidity was maintained below 70% for all tests, to minimise its influence on SidePak™ performance. When required, an electric oil-filled radiator was used to maintain the relative humidity.

At the start of each test day, PM<sub>2.5</sub> background concentrations were monitored for 5 minutes periods. The phase 1 toasting tests were repeated exactly using wholemeal bread, as there was no noticeable difference in emissions from white and wholemeal bread in Phase 1. The toaster was located on a table; see Figure 5. The start and finish of the  $\alpha$ -period were recorded when the toaster was switched on, and when the toasting ended, respectively. Thereafter, the toast and toaster were sealed in a box and the  $\beta$  and  $\gamma$ -periods were observed for 20 minutes. The room was then flushed with outside air to restore concentrations to background levels.

## 4.2 Results

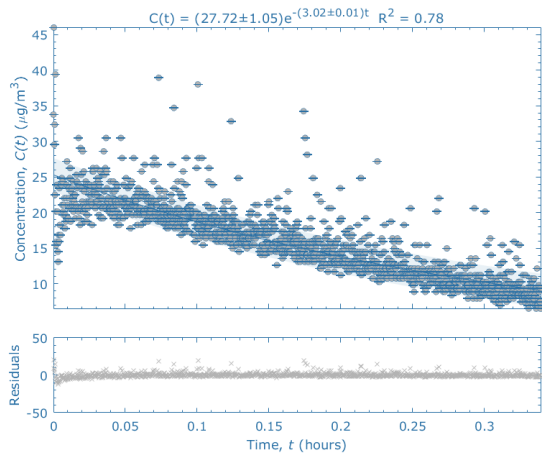


Figure 6 - Example Decay, CF = 0.47

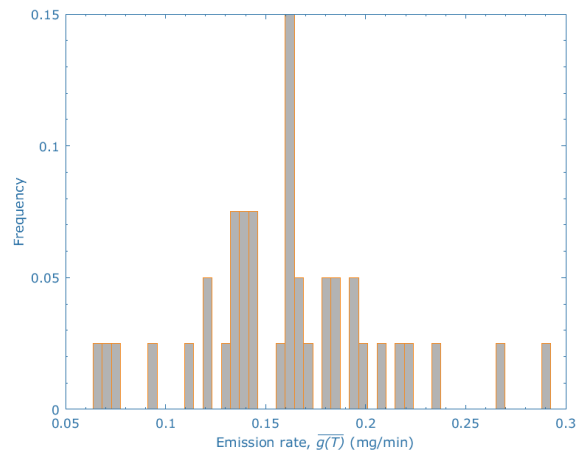


Figure 7 - Phase 2 Emission Rates Histogram, CF = 0.47

The data were processed using the method described in Sections 3.2 and 3.3, except that the decay was determined using the  $\beta$ - and  $\gamma$ -periods together, due to the difficulty in identifying the peak concentration over the background noise attributable to the 1-second logging interval (see Figure 6). Tests were not eliminated according to a minimum threshold R<sup>2</sup>-value, because visual inspections indicate a good fit even when R<sup>2</sup><0.7. Here, noisy data from the 1-second time-step makes the R<sup>2</sup> a poor indicator of goodness-of-fit. A single outlier test was eliminated according to *Chauvenet's Criteria*.

Mean and median decay rates were 3.97 h<sup>-1</sup> and 3.33 h<sup>-1</sup>, respectively, compared to an expected air change rate 3.96 h<sup>-1</sup> from the fan. This suggests minimal decay due to other factors, such as deposition. It is also possible that the extract fan operated at a lower rate than specified, although this was confirmed independently. Figure 6 shows that the  $\beta$ -period is short, indicating good mixing.

Table 2: Phase 2 Emission Rates (mg/min)

CF	N	Mean	SD	2 <sup>nd</sup>	25 <sup>th</sup>	Percentiles		
						50 <sup>th</sup> (Median)	75 <sup>th</sup>	98 <sup>th</sup>
0.47	39	0.157	0.043	0.071	0.135	0.161	0.182	0.071
0.79	39	0.265	0.073	0.119	0.226	0.270	0.306	0.119

The resulting mean and median emission rates are approximately 25% and 50% of the values measured during phase 1. It is possible the different conditions and variations in the bread used may have modified the emissions. Additionally, as the  $\beta$ -periods were included when determining the decay rates, both they and the theoretical peaks may have been underestimated leading to lower emission rates. Further developments of the post-processing method are required to identify the peak concentration for high frequency data to help reduce this source of error.

The distribution of emission rates is given in Figure 7, and is smaller than the distribution obtained during phase 1 (see Figure 3). It has no outliers that increase the mean and the distribution is less skewed, but still appears to be non-Gaussian. The median is slightly greater than the mean (see Table 2) so there may be a slight negative skew, but this difference is small.

## 5 DISCUSSION

The mean emission rates from both phases, calculated using both CFs, are an order of magnitude lower than those reported by Dacunto and Jiang (see Table 3). There are two main unknowns which could have caused this difference: firstly the lack of gravimetric sampling, so the true calibration factor required may be very different, and secondly, the degree of charring. Whilst Dacunto and Jiang use a standard char-index to report the degree of charring in their tests, the authors have been unable to obtain this index for comparison. The estimated mean emission rates from Phase 2, for both CFs, are similar to the median 0.11 mg/min reported by He (see Table 3).

Table 3: Emission Rates Comparison

Source	N	Mean Emission Rate (mg/min)	SD	RSD
Phase 1 – CF 0.47	29	0.66	1.01	1.53
Phase 1 – CF 0.79	29	1.11	1.70	1.53
Phase 2 – CF 0.47	26	0.16	0.04	0.24
Phase 2 – CF 0.79	26	0.27	0.07	0.24
Toast, 90-95% char (Dacunto <i>et al.</i> , 2013)	3	9.5	10.8	1.14
Toast, 70-80% char (Jiang <i>et al.</i> , 2011)		4.2		
Toasting (He <i>et al.</i> , 2004)	18	0.11*	0.37	3.36

\*median; RSD, relative standard deviation.

Despite the larger number of repetitions in Phase 1, the variance of the emission rates remains large, indicated by the large relative standard deviation (RSD). Therefore, the test methodology from this phase is not highly repeatable, although it is significantly more consistent than the methodology from He. The improved method of Phase 2 used a smaller room volume with improved mixing to give a better defined  $\alpha$ -period and a more reproducible test. This is indicated by its RSD, which is smaller than the Phase 1 RSD by an order of magnitude.

The calibration factor is the largest source of uncertainty, because gravimetric sampling was not used. This problem is not unique to the SidePak™, but is also applicable to other optical monitors, which are commonly used to measure temporal concentrations of particulate matter. It is recommended to simultaneously conduct gravimetric sampling to determine custom calibration factors, although this may not always be possible.

The *peak estimation* calculation method may also be flawed because it assumes a constant emission rate over the emission period, which is not observed for this source, and may not be the case for other cooking sources. Pagels *et al.* (2009) used an iterative process to calculate emission rates by fitting a curve to the observed data and adjust the emission rate to obtain the best possible fit. There are two potential problems with this method. It shares the first with the *peak estimation* method, because they both assume a constant emission rate during the  $\alpha$ -

period, which was not observed here; see Figure 6. Therefore, the predicted curve would never be a good fit. Secondly, the curve predicted using the mass balance equation assumes instantaneous mixing, which is not observed in reality (Ott *et al.*, 2006). Ott suggests an alternative calculation method, known as the *area-under-the-curve* method. It uses the total mass emitted to estimate the average emission rate (Ott *et al.*, 2006). This method is not well established in literature, where preference is usually given to the *peak estimation* approach. The *area-under-the-curve* method is theoretically exact, but it assumes instantaneous full-mixing, which is not observed in practice.

Indoor environment modelling at stock level often use stochastic methods to explore uncertainties in indoor pollutant concentrations (Das *et al.*, 2014). These require probability density functions (PDFs) of emission rates, which could be obtained from the Phase 2 data by methods such as fitting a curve to Figure 9, or using bootstrapping techniques to account for uncertainty in all of the measurements. Future work will investigate this further.

## 6 CONCLUSIONS

There is growing evidence linking outdoor PM<sub>2.5</sub> exposure to a range of health effects, yet the impacts of exposure indoors is relatively unknown. Indoor environment modelling at stock level can be used to investigate these impacts, but they are highly sensitive to the emission rates used. Therefore, a better understanding of the emissions rates and their uncertainties from key indoor sources, such as cooking, is required. They should be presented as probability density functions so that probabilistic sampling methods can be employed to estimate uncertainty in indoor concentrations.

Five common methodologies are used to measure temporal variations in PM<sub>2.5</sub> concentrations during the cooking of foods. Most use the *peak estimation method*, derived from a mass-balance equation, to calculate emission rates from these measurements. Controlled field tests and large scale chamber tests are preferential methods because they offer a high level environmental control without abstracting conditions so far from reality that they render the calculated emission rates implausible. Most studies typically have a low number of repetitions, which is insufficient to produce PDFs or demonstrate emission rate distributions.

Two phases of tests were undertaken in different indoor environments to develop a methodology appropriate for measuring PM<sub>2.5</sub> emission rates from the cooking of foods. The toasting of bread is used as a simple and repeatable source. The first phase identified key flaws in the *field test* method and was used to inform a second phase. These proved to be better, but still problematic. Key problems identified are the need for calibration factors used by the optical measurement devices frequently used to measure temporal PM<sub>2.5</sub> concentrations, the need for full-mixing and a means of identify mixing conditions, and the need for a method to identify the  $\alpha$ -,  $\beta$ - and  $\gamma$ -periods used to determine emission and decay rates. The method does not require a known ventilation rate, though the model does depend on a constant decay rate, and so it must be steady. Additionally, further investigations into the measuring and modelling of non-constant emission rates is needed, as the *peak estimation method* used here may under- or over-estimate the total mass emitted depending on the emission profile.

## 7 REFERENCES

Afshari, A. *et al* (2005). "Characterization of indoor sources of fine and ultrafine particles: a study conducted in a full-scale chamber." *Indoor Air* 15(2): 141-150.

- Dacunto, P. *et al* (2013). "Real-time particle monitor calibration factors and PM<sub>2.5</sub> emission factors for multiple indoor sources." *Environmental Science: Processes & Impacts* 15(8): 1511-1519.
- Das, P., C. *et al* (2014). "Using probabilistic sampling-based sensitivity analyses for indoor air quality modelling." *Building and Environment* 78: 171-182.
- Fortmann, R., *et al*(2001). *Indoor air quality: residential cooking exposures*, State of California Air Resources Board.
- Géhin, E., *et al* (2008). "Size distribution and emission rate measurement of fine and ultrafine particle from indoor human activities." *Atmospheric Environment* 42(35): 8341-8352.
- HM Government. (2010). *The Building Regulations 2010. Approved Document F, Ventilation*. Norwich, Norwich : TSO.
- He, C., *et al* (2004). "Contribution from indoor sources to particle number and mass concentrations in residential houses." *Atmospheric Environment* 38(21): 3405-3415.
- Jiang, R.-T., *et al* (2011). "Determination of response of real-time SidePak AM510 monitor to secondhand smoke, other common indoor aerosols, and outdoor aerosol." *Journal of Environmental Monitoring* 13(6): 1695-1702.
- Lader, D., *et al* (2006). *The time use survey, 2005: how we spend our time*. London, UK, Office for National Statistics.
- Lee, S. C. and B. Wang (2006). "Characteristics of emissions of air pollutants from mosquito coils and candles burning in a large environmental chamber." *Atmospheric Environment* 40(12): 2128-2138.
- Lewtas, J. (2007). "Air pollution combustion emissions: Characterization of causative agents and mechanisms associated with cancer, reproductive, and cardiovascular effects." *Mutation Research/Reviews in Mutation Research* 636(1–3): 95-133.
- Olson, D. A. and J. M. Burke (2006). "Distributions of PM<sub>2.5</sub> Source Strengths for Cooking from the Research Triangle Park Particulate Matter Panel Study." *Environmental Science & Technology* 40(1): 163-169.
- Ott, W. R., *et al* (2006). *Exposure Analysis: Mathematical Modeling of Indoor Air Quality*, CRC Press: 533.
- Pagels, J., *et al* (2009). "Chemical composition and mass emission factors of candle smoke particles." *Journal of Aerosol Science* 40(3): 193-208.
- RCP (2016). *Every breath we take: the lifelong impact of air pollution*, The Royal College of Physicians.
- Pope, C. A. and D. W. Dockery (2006). "Health Effects of Fine Particulate Air Pollution: Lines that Connect." *Journal of the Air & Waste Management Association* 56(6): 709-742.

- Rückerl, R., *et al* (2011). "*Health effects of particulate air pollution: A review of epidemiological evidence.*" *Inhalation Toxicology* 23(10): 555-592.
- Screwfix. (2017) "*Manrose XF100S 20W Axial Bathroom Fan.*" Retrieved November, 2016, from <http://www.screwfix.com/p/manrose-xf100s-20w-axial-bathroom-fan/11097>.
- Shrubsole, C., *et al* (2012). "*Indoor PM2.5 exposure in London's domestic stock: Modelling current and future exposures following energy efficient refurbishment.*" *Atmospheric Environment* 62(0): 336-343.
- Torkmahalleh, M. A., *et al* (2012). "*PM2.5 and ultrafine particles emitted during heating of commercial cooking oils.*" *Indoor Air* 22(6): 483-491.
- Wilkinson, P., *et al* (2009). "*Public health benefits of strategies to reduce greenhouse-gas emissions: household energy.*" *The Lancet* 374(9705): 1917-1929.
- Zartarian, V.G., *et al* (1998). *Experiments to Measure the Effect of Cooking Activities on Indoor Air Quality in Homes*. 8th Annual Conference of the International Society of Exposure Analysis. Boston, M.A.

# An Experimental Validation of an Indoor Radon Model that examines Energy Retrofit Buildings

James A. McGrath<sup>1\*</sup>, Miriam A. Byrne<sup>1</sup>,

<sup>1</sup>*School of Physics and Centre for Climate and Air Pollution Studies,  
Ryan Institute,  
National University of Ireland, Galway,  
University Road,  
Galway  
Ireland*

\*Corresponding author: [james.a.mcgrath@nuigalway.ie](mailto:james.a.mcgrath@nuigalway.ie)

## ABSTRACT

The modelling framework IAPPEM was redeveloped to predict indoor radon concentrations in dwellings that have undergone an energy retrofit, and have experienced a consequent air tightness change. The framework is flexible, and allows for simulations to be carried out under various pre-retrofit radon concentration levels, multi-zone building geometries, ventilation configurations and retrofit types. However, detailed real-time radon concentration and ventilation data is necessary for model validation, and such data is non-existent in the Irish context. The generation of these data, which allows for full model validation and testing, is the focus of the current study. The objectives of the current study are to (i) fully characterise the ventilation status of selected Irish dwellings, through measurement, and determine the real-time radon concentrations therein (ii) parameterise the model for these selected dwellings, and make comparative predictions of radon concentrations. The current study focused on measuring hourly radon concentrations, using real-time radon monitors, in dwellings that are representative of the buildings stock undergoing energy retrofit. Each dwelling was monitored for a week-long period to establish time-varying fluctuations in indoor radon concentrations and obtain data on the minimum and maximum range. In addition, air exchange was measured using the tracer gas decay method with CO<sub>2</sub> as the tracer. Air exchange comprised of eight selected hourly measurements per dwelling over each measurement week to ensure that the effect of meteorological variations was captured. The model will predict indoor radon concentrations based on local meteorological conditions, building characteristics and in-situ characterisation of radon entry rates derived from experimental measurements. The model's output will be compared with the hourly radon concentrations collected during the sampling period. Time series analysis will be carried out, comparing experimental and predicted indoor radon concentrations.

## KEYWORDS

Field data  
Indoor radon concentrations  
Dynamic radon entry rates  
Ventilation in renovated buildings

## 1 INTRODUCTION

The negative impact on human health due to exposure to ionising radiation is well documented (WHO, 2009). In Ireland, radon gas is considered the greatest source of radiation exposure to the general population accounting for just over 55% of the average radiation dose (Connor et al., 2014). Radon gas (<sup>222</sup>Rn) is a naturally occurring odourless, colourless and tasteless gas; it arises as a product of Uranium (<sup>238</sup>U) decay, which is a radioactive material found in varying quantities in soil and rocks. Radon decays by emitting an  $\alpha$  particle into a series of short-lived radioactive progeny, two of which are polonium (<sup>218</sup>Po and <sup>214</sup>Po). If inhaled, the vast majority of radon is exhaled almost immediately. However, the short-lived decay products of radon can deposit on the bronchial epithelium and be exposed to alpha radiation (IARC, 2001).

Radon is the second highest leading cause of lung cancer, after smoking, in many countries. In an OECD survey of 30 countries, Ireland was found to have the eighth highest average indoor radon concentration, accounting for up to 250 cases of lung cancer each year (WHO, 2009, Colgan et al., 2008). Darby et al. (2005) examined radon levels from 13 European case-control studies and the associated risk of lung cancer; the study found that for every 100 Bq m<sup>-3</sup> increase in measured radon, there was an 8.4% (95% CI [3.0%, 15.8%]) increase in the risk of lung cancer.

The European Energy Efficiency Directive (2012) sets the policy roadmap for the period until 2020, and each Member State is required to reduce their energy consumption by 20% to meet the EU's greenhouse gas emission reduction commitments. In 2014, Irish buildings accounted for 35% of the total national energy consumption and approximately 59% of electricity consumption (SEAI, 2016). Retrofitting of the building fabric has been identified as one of the most cost-effective energy efficiency improvements to achieve energy savings in the economy (Johnston et al., 2005).

In the Irish context, the scope for energy efficiency gains to be made through retrofitting of the existing building stock has been continuously identified within the National Energy Efficiency Action Plans (DCENR, 2014b, DCENR, 2009, DCENR, 2011a). To this end, the Irish National Energy Retrofit Programme aims to upgrade 1.2 million residential, public and commercial buildings by 2020 (DCENR, 2011b, DCENR, 2014a). However, recent research has shown that energy retrofitting of dwellings may lead to greater airtightness, and there is a possibility that radon concentrations may accordingly increase (Pressyanov et al., 2015, Fojtikova and Rovenska, 2014, Jiránek and Kačmaříková, 2014, Fojtiková and Navrátilová Rovenská, 2015).

Studies have reported that indoor radon concentrations are strongly associated with the geogenic radon potential, building material, construction type, foundation and the year of construction (Demoury et al., 2013, Drolet and Martel, 2016, Borgoni et al., 2014, Collignan et al., 2016). However, even dwellings located in the same area, with assumed relatively homogeneous radon potential, have reported localised heterogeneities exert a strong influence on indoor radon concentrations (Drolet and Martel, 2016).

Small pressure differences between the indoor and outdoor environments gives rise to the convective transport of radon gas into dwellings; various factors including the stack effect, wind interaction with the building fabric, heating and mechanical ventilation all contribute to the pressure differences (Nazaroff, 1992).

Previous studies have modelled indoor radon concentrations in the residential microenvironment (Revzan and Fisk, 1992, Sherman, 1992, Man and Yeung, 1999, Fang and Persily, 1995, Kesikuru et al., 2001, Milner et al., 2014, Riley et al., 1999, Diallo et al., 2013). However the majority of these studies focussed either simulating the sub-slab gravel layer had on radon entry rates into buildings. Milner et al. (2014) investigated the impacts of indoor radon concentrations as a consequence of increasing the airtightness of the English housing stock; however, this study only assumed a steady state radon entry rate and did not account for dynamic radon entry rates into dwellings.

Collignan et al. (2012) reported dynamic radon entry rates that results in a high temporal variability of radon concentrations in residential buildings; factors that influence radon entry rate include wind speed, moisture content, pressure differences and radon concentration in the soil (Kesikuru et al., 2001, Riley et al., 1999, Andersen, 2001).

In response to the National Radon Control Strategy (NRCS, 2014), the modelling framework IAPPEM (McGrath et al., 2014a, McGrath et al., 2014b) was redeveloped during the EPA project UNVEIL: UNderstanding VEntilation and radon in energy efficient buildings in Ireland (2015-HW-DS-4). The model predicts radon concentrations in dwellings that have undergone an energy retrofit, and have experienced a consequent air tightness change. The framework is flexible, and allows for simulations to be carried out under various pre-retrofit

radon concentration levels, multi-zone building geometries, ventilation configurations (i.e. vent size/type) and retrofit types (e.g. cavity filling and external insulation). However, detailed real-time radon concentration and ventilation data is necessary for model validation, and such data is non-existent in the Irish context. The generation of these data, which would allow full model validation and testing, is the focus of the current study.

## **2 METHODOLOGY**

### **Site Selection**

Irish dwellings were recruited through existing local authority contacts, that are representative of those referred to in NSAI S.R. 54:2014 Code of Practice: Methodology for the energy efficient retrofit of existing dwellings (i.e. bungalow, semi-detached, terraced dwellings)(NSAI, 2014). Dwellings were selected where radon levels are both above and below the 200 Bq m<sup>-3</sup> Irish reference level, as pre-determined from passive radon monitoring carried out by the EPA.

Outdoor temperature and pressure data for the measurement dates were obtained from the Informatics Research Unit for Sustainable Engineering (IRUSE) at the National University of Ireland Galway, which maintains a full record of weather conditions in Galway, Ireland (53.280148, -9.059237).

All residential dwellings were located within approximately 3 km of National University of Ireland Galway.

### **Airflow and Air Tightness measurements**

Air exchange rate measurements were carried out for each dwelling using the CO<sub>2</sub> tracer gas decay technique. Air exchange comprised of eight selected hourly measurements per dwelling over each measurement week to ensure that the effect of meteorological variation was captured. The CO<sub>2</sub> tracer gas decay measurements involved releasing CO<sub>2</sub>, from a sealed cylinder, into the room, until concentrations exceeded 3500 ppm. A GrayWolf probe (GrayWolf Sensing Solutions; Shelton, CT, USA) was used for gas detection at one-minute intervals.

Air tightness testing was conducted in accordance NSAI Certification I.S. EN ISO 9972:2015 - Thermal Performance of Buildings – Determination of Air Permeability of Domestic Buildings – (Single or Single & Multi) Fan Pressurisation Method. A single measurement per dwelling was carried out, as weather variations over the course of the experimental period will induce pressure differentials of far less than 50 Pa, which is the design pressure for air-tightness testing.

### **Field Measurements and Data Collection**

In order to obtain representative values for radon entry rates into Irish dwellings, the methodology developed by (Collignan and Powaga, 2014) to characterise radon potential in existing dwellings will be employed. The methodology involves a blower door test to maintain the dwelling at successively different depressurization levels that heighten the convective radon flux into the dwelling. In steady state conditions, the radon flow leaving the building through the blower door corresponds to the radon entry rate.

Hourly radon concentrations were measured with a continuous radon monitor, a Rstone Continuous radon gas sensor (Radiansa Consulting S.L., Girona, Spain), for a week-long period to establish time-vary fluctuations in indoor radon concentrations and obtain data on the minimum and maximum range.

### Data analysis, model validation and simulation

The model will predict indoor radon concentrations based on local meteorological conditions, building characteristics and in-situ characterisation of radon entry rates derived from experiments. The model's output will be compared with the hourly radon concentrations collected during the experimental campaign. Time-series analysis was carried out, comparing experimental and predicted indoor radon concentrations.

## 3 RESULTS

As the experimental monitoring campaign is still ongoing only initial results are available to present within in paper. The initial results focus on data collected from 26 days monitoring within a single dwelling. The data was designed to capture the variability in radon concentration over an extended period.

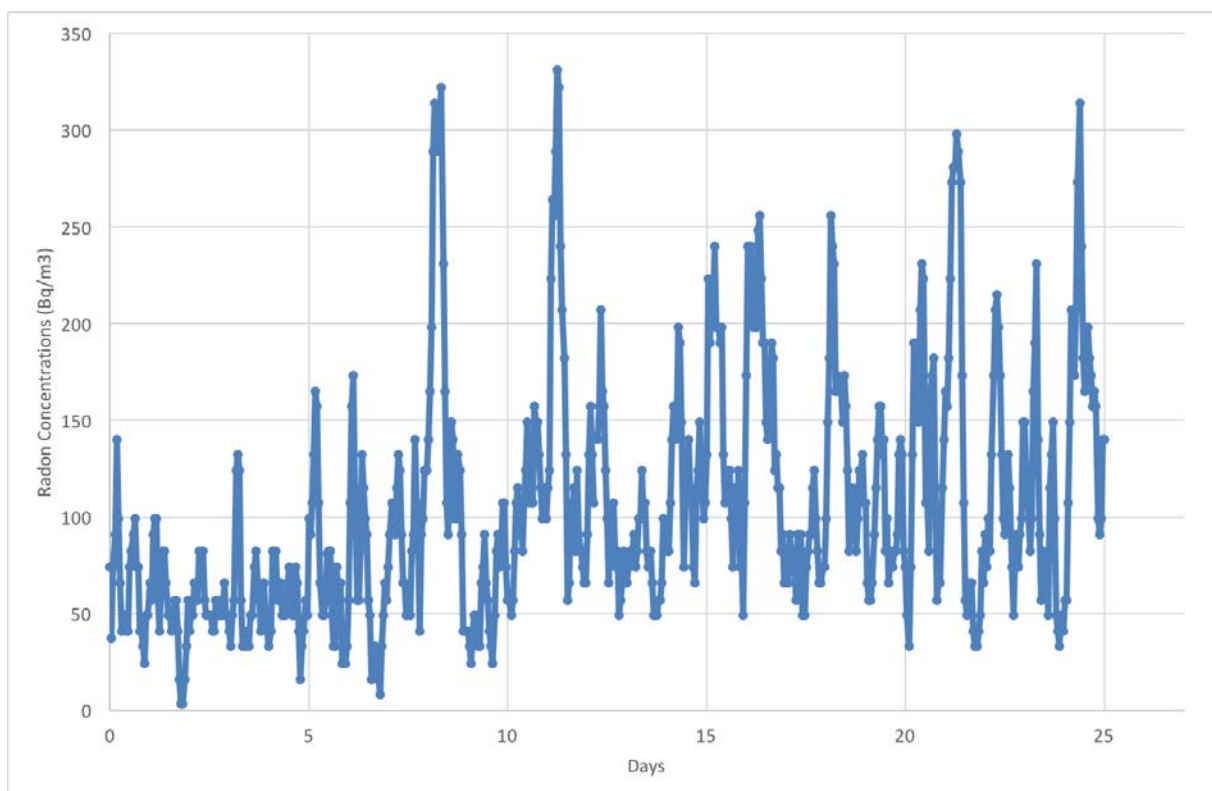


Figure 1. Time-series data from 26 days from hourly measurements.

Figure 1 illustrates the high temporal variability of the indoor radon concentrations in an unoccupied room. Table 1 summarises the mean, minimum and maximum for temperature, radon concentrations, pressure values and humidity over the 26 days. The results demonstrate that variations occur for the indoor pressure and radon concentration, while the indoor temperature remains relatively consistent over the sampling period.

Table 1. Summaries the data obtained from 26-day sampling in one residential dwelling.

Radon Concentration	Min	Max	Mean
Radon Concentration (Bq/m <sup>3</sup> )	3	331	105
Relative Humidity (%RH)	44	60	55
Pressure (mbar)	973	1017	1002
Temperature (Celsius)	21	27	23

#### 4 CONCLUSIONS

The current study focuses on measuring hourly radon concentrations, using real time radon monitors, in dwellings that are representative of the buildings to be undergoing energy retrofit. Each dwelling was monitored for a week long period to establish time varying fluctuations in indoor radon concentrations and obtain data on the minimum and maximum range. In addition, air exchange was measured using the tracer gas decay method with CO<sub>2</sub> as the tracer. Air exchange comprised of eight selected hourly measurements per dwelling over each measurement week to ensure that the effect of meteorological variations was captured.

The remaining work focuses on the model predicting indoor radon concentrations based on local meteorological conditions, building characteristics and in situ characterisation of radon entry rates derived from experimental measurements. The model's output will be compared with the hourly radon concentrations collected during the sampling period. Time series analysis will be carried out, comparing experimental and predicted indoor radon concentrations.

#### 5 ACKNOWLEDGEMENTS

This work represents research funded by Sustainable Energy Authority of Ireland (SEAI) Renewable RD&D Programme 2017 under the (RDD00128) 'The Relationship between Radon and Ventilation in Retrofit Buildings: Experimental Validation of Model Predictions' project.

#### 6 REFERENCES

- ANDERSEN, C. E. 2001. Numerical modelling of radon-222 entry into houses: an outline of techniques and results. *Science of the total environment*, 272, 33-42.
- BORGONI, R., DE FRANCESCO, D., DE BARTOLO, D. & TZAVIDIS, N. 2014. Hierarchical modeling of indoor radon concentration: How much do geology and building factors matter? *Journal of Environmental Radioactivity*, 138, 227-237.
- COLGAN, P., ORGANO, C., HONE, C. & FENTON, D. 2008. Radiation doses received by the Irish population. Radiological Protection Institute of Ireland (Ireland).
- COLLIGNAN, B., LE PONNER, E. & MANDIN, C. 2016. Relationships between indoor radon concentrations, thermal retrofit and dwelling characteristics. *Journal of Environmental Radioactivity*, 165, 124-130.
- COLLIGNAN, B., LORKOWSKI, C. & AMÉON, R. 2012. Development of a methodology to characterize radon entry in dwellings. *Building and Environment*, 57, 176-183.
- COLLIGNAN, B. & POWAGA, E. 2014. Procedure for the characterization of radon potential in existing dwellings and to assess the annual average indoor radon concentration. *Journal of Environmental Radioactivity*, 137, 64-70.
- CONNOR, C., CURRIVAN, L., CUNNINGHAM, N., KELLEHER, K., LEWIS, M., LONG, S., MCGINNITY, P., SMITH, V. & MCMAHON, C. 2014. Radiation Doses Received by the Irish Population 2014. Radiological Protection Institute of Ireland (Ireland).

- DARBY, S., HILL, D., AUVINEN, A., BARROS-DIOS, J., BAYSSON, H., BOCHICCHIO, F., DEO, H., FALK, R., FORASTIERE, F. & HAKAMA, M. 2005. Radon in homes and risk of lung cancer: collaborative analysis of individual data from 13 European case-control studies. *Bmj*, 330, 223.
- DCENR 2009. Maximising Ireland's Energy Efficiency. The National Energy Efficiency Action Plan 2009 – 2020. Dublin: The Department of Communications Energy and Natural Resources.
- DCENR 2011a. Ireland's second National Energy Efficiency Action Plan to 2020. Dublin: The Department of Communications Energy and Natural Resources.
- DCENR 2011b. National Energy Retrofit Programme. *In: THE DEPARTMENT OF COMMUNICATIONS ENERGY AND NATURAL RESOURCES* (ed.). Dublin.
- DCENR 2014a. Better Buildings. A National Renovation Strategy for Ireland. *In: THE DEPARTMENT OF COMMUNICATIONS ENERGY AND NATURAL RESOURCES* (ed.). Dublin.
- DCENR 2014b. National Energy Efficiency Action Plan 2014. Dublin: The Department of Communications Energy and Natural Resources.
- DEMOURY, C., IELSCH, G., HEMON, D., LAURENT, O., LAURIER, D., CLAVEL, J. & GUILLEVIC, J. 2013. A statistical evaluation of the influence of housing characteristics and geogenic radon potential on indoor radon concentrations in France. *Journal of Environmental Radioactivity*, 126, 216-225.
- DIALLO, T. M. O., COLLIGNAN, B. & ALLARD, F. 2013. Analytical quantification of airflows from soil through building substructures. *Building Simulation*, 6, 81-94.
- DROLET, J. P. & MARTEL, R. 2016. Distance to faults as a proxy for radon gas concentration in dwellings. *Journal of Environmental Radioactivity*, 152, 8-15.
- FANG, J. B. & PERSILY, A. K. 1995. Airflow and radon transport modeling in four large buildings. *TRANSACTIONS-AMERICAN SOCIETY OF HEATING REFRIGERATING AND AIR CONDITIONING ENGINEERS*, 101, 1100-1100.
- FOJTÍKOVÁ, I. & NAVRÁTILOVÁ ROVENSKÁ, K. 2015. Methodology for measurement in schools and kindergartens: experiences. *Radiation Protection Dosimetry*, 164, 612-617.
- FOJTIKOVA, I. & ROVENSKA, K. N. 2014. Influence of energy-saving measures on the radon concentration in some kindergartens in the Czech Republic. *Radiation protection dosimetry*, 160, 149-153.
- IARC 2001. Some Internally Deposited Radionuclides. 43:1–300. Iarc Monographs on the Evaluation of Carcinogenic Risks to Humans.
- JIRÁNEK, M. & KAČMAŘÍKOVÁ, V. 2014. Dealing with the increased radon concentration in thermally retrofitted buildings. *Radiation Protection Dosimetry*, 160, 43-47.

- JOHNSTON, D., LOWE, R. & BELL, M. 2005. An exploration of the technical feasibility of achieving CO<sub>2</sub> emission reductions in excess of 60% within the UK housing stock by the year 2050. *Energy Policy*, 33, 1643-1659.
- KESKIKURU, T., KOKOTTI, H., LAMMI, S. & KALLIOKOSKI, P. 2001. Effect of various factors on the rate of radon entry into two different types of houses. *Building and Environment*, 36, 1091-1098.
- MAN, C. K. & YEUNG, H. S. 1999. Modeling and measuring the indoor radon concentrations in high-rise buildings in Hong Kong. *Applied Radiation and Isotopes*, 50, 1131-1135.
- MCGRATH, J., BYRNE, M., ASHMORE, M., TERRY, A. & DIMITROULOPOULOU, C. 2014a. Development of a probabilistic multi-zone multi-source computational model and demonstration of its applications in predicting PM concentrations indoors. *Science of The Total Environment*, 490, 798-806.
- MCGRATH, J. A., BYRNE, M. A., ASHMORE, M. R., TERRY, A. C. & DIMITROULOPOULOU, C. 2014b. A simulation study of the changes in PM<sub>2.5</sub> concentrations due to interzonal airflow variations caused by internal door opening patterns. *Atmospheric Environment*, 87, 183-188.
- MILNER, J., SHRUBSOLE, C., DAS, P., JONES, B., RIDLEY, I., CHALABI, Z., HAMILTON, I., ARMSTRONG, B., DAVIES, M. & WILKINSON, P. 2014. Home energy efficiency and radon related risk of lung cancer: modelling study.
- NAZAROFF, W. W. 1992. Radon transport from soil to air. *Reviews of Geophysics*, 30, 137-160.
- NRCS 2014. The National Radon Control Strategy.  
<http://www.environ.ie/sites/default/files/migrated-files/en/Publications/Environment/EnvironmentalRadiation/FileDownload%2C35484%2Cen.pdf>.
- NSAI 2014. S.R. 54:2014 Code of Practice for the energy efficient retrofit of dwellings. In: NATIONAL STANDARDS AUTHORITY OF IRELAND (ed.).  
<http://www.ili.co.uk/en/S.R.54-2014.pdf>.
- PRESSYANOV, D., DIMITROV, D. & DIMITROVA, I. 2015. Energy-efficient reconstructions and indoor radon: the impact assessed by CDs/DVDs. *Journal of environmental radioactivity*, 143, 76-79.
- REVZAN, K. L. & FISK, W. J. 1992. Modeling Radon Entry into Houses with Basements: The Influence of Structural Factors. *Indoor Air*, 2, 40-48.
- RILEY, W. J., ROBINSON, A., GADGIL, A. J. & NAZAROFF, W. W. 1999. Effects of variable wind speed and direction on radon transport from soil into buildings: model development and exploratory results. *Atmospheric Environment*, 33, 2157-2168.
- SEAI 2016. Energy Efficiency in Ireland. In: IRELAND, S. E. A. O. (ed.).

SHERMAN, M. Simplified modeling for infiltration and radon entry. Proceedings, Thermal Performance of the Exterior Envelopes of Buildings Conference V, 1992.

WHO 2009. *WHO handbook on indoor radon: a public health perspective*, World Health Organization.

# Evaluating natural ventilation cooling potentials during early building designs

Jun Cheng<sup>1</sup>, Dahai Qi<sup>1</sup>, Ali Katal<sup>1</sup>, and Liangzhu (Leon) Wang<sup>\*2</sup>

*1Centre for Zero Energy Building Studies,  
Department of Building, Civil and Environmental  
Engineering, Concordia University, 1455 de  
Maisonnette Blvd. West, Montreal, Quebec, H3G  
1M8, Canada*

*2Centre for Zero Energy Building Studies,  
Department of Building, Civil and Environmental  
Engineering, Concordia University, 1455 de  
Maisonnette Blvd. West, Montreal, Quebec, H3G  
1M8, Canada*

*\*Corresponding author: leon.wang@concordia.ca,  
lzwang@gmail.com*

## ABSTRACT

Natural ventilation (NV) is an efficient way of cooling buildings, and its energy saving potentials however depend on many parameters including local hourly weather and climate conditions, types of ventilations, indoor cooling loads (or heat gains), operating schedules, window types, and opening-wallratios etc. Determination of the NV flow rate is thus challenging, although there are many empirical equations for different NV strategies, e.g. single-sided and cross-ventilation, considering different driving forces, e.g. wind, buoyancy and a mix of both. The main objectives of this study are to select coefficients for naturally ventilated buildings with a typical shape based on the existing empirical formulas, use the selected coefficients to develop a quick and relatively accurate method of evaluating NV potential for energy-saving analysis during early building design stages. By utilizing computational fluid dynamics (CFD), a series of computational simulations were conducted to calculate ventilation flow rate with different ventilation variables such as the wind incidence angle and the height of the building. Using the method developed, GIS maps for NV potentials of North America were created in a similar way as the well-known solar potential maps. These maps provide key graphical information of energy saving potentials of NV in terms of total hours, and associated energy savings suitable for NV for over 50 cities in the US and 10 cities in Canada.

## KEYWORDS

Natural ventilation potentials, building energy savings, GIS maps, evaluation,

## 1 INTRODUCTION

Driven by pressure difference due to wind and/or stack effects across building envelopes, natural ventilation (NV) is an effective and natural way of cooling building and reducing building energy usage while improving indoor air quality (when outdoor air is fresher than indoors). Therefore, it has been widely applied in the buildings.

According to opening locations, there exist two main types of NV: single-sided ventilation and cross-ventilation. In single-sided ventilation, only one façade is designed to have openings. In contrast, cross-ventilation has two or more openings on adjacent or opposite façades. The prediction of NV is challenging since it is closely related to the wind aerodynamics regime and the building's location, orientation, shape, window-to-wall ratio etc. Therefore, the decision whether to apply NV or not often needs to be made during early stages of building design, e.g. at the conceptual design stage, which is based on the analysis of the NV energy-saving potential. Since many details of the building are unknown at this stage and an in-depth engineering analytics (e.g. detailed whole-building computer simulations) is thus impossible and also unnecessary considering the time and cost, such an early analysis demands a quick and relatively accurate method to determine NV air flow rates and compare different

ventilation strategies based on a relatively simple strategy, such as a set of empirical equations.

Previous studies show quite a few empirical equations regarding airflow rate estimation for both single-sided ventilation and cross-ventilation under wind driven NV (Allard and Santamouris, 1998; Cockroft and Robertson, 1976; Crommelin and Vrins, 1988; H. Wang and Chen, 2012; Warren and Parkins, 1985). Although each of the empirical equations may apply to its specific case, they have more than one unknown parameters or coefficients that have not been identified for typical building shapes and types. As a result, it is hard to apply them to generic buildings for the early NV designs. Therefore, it is necessary to develop a simple and accurate method which can be directly used for the selection of coefficients for typical and generic buildings during the early design stage.

The objectives of this study are to select coefficients for naturally ventilated buildings with a common and typical shape based on the existing empirical formulas, using the selected coefficients to develop a quick and relatively accurate method of evaluating NV potential for energy-saving analysis during early building design stages. A series of CFD simulations were conducted to determine ventilation flow rate with different ventilation variables such as the wind incidence angle and the height of the building, which are compared with wind tunnel data. Using the method developed, GIS maps for NV potentials of North America were created following a similar way as the well-known solar potential maps.

## 2 METHODOLOGY

### 2.1 Empirical formulas

Based on our communications with NV consulting firms, a typical modern NV building may be assumed to be flat-roofed, symmetrical, less than six floors and the effect of internal partitions is neglected. Equations (1) and (2) were selected from the previous studies (Allard & Santamouris, 1998; Cockroft & Robertson, 1976), to calculate wind-driven single-sided ventilation and cross-ventilation flow rates, respectively. The selected equations are simple and applicable due to less unknown parameters compared to other equations available in the literature. For purposes of generalization, only the wind-driven NV is considered at this stage of the study, as the effective use of the force of buoyancy depends more greatly on the building's interior layout.

Single-sided ventilation:

$$Q = \frac{dv}{dt} = \pm \frac{1}{2} f C_D A \sqrt{\left| U_r^2 - \left( \frac{2\gamma P_a}{\rho V} \right) v \right|} \quad (1)$$

Cross ventilation:

$$Q = \sqrt{\frac{C_{p1} - C_{p2}}{\frac{1}{A_1^2 C_{D1}^2} + \frac{1}{A_2^2 C_{D2}^2}}} U_r = \sqrt{\frac{\Delta C_p}{\frac{1}{A_1^2 C_{D1}^2} + \frac{1}{A_2^2 C_{D2}^2}}} U_r \quad (2)$$

where  $dv$  is the decrease in volume of the original mass of air inside the building ( $m^3$ ),  $V$  is total volume of the building ( $m^3$ ),  $t$  is the time (s),  $\gamma$  is the specific heat ratio of air which equals to 1.4 for adiabatic flows and 1.0 for isothermal flows (Haghighat, Brohus, & Rao, 2000),  $\rho$  is the density of air ( $kg/m^3$ ) and  $P_a$  is the atmospheric pressure (Pa). Besides the

opening area  $A$  ( $m^2$ ) and reference wind velocity  $U_r$  (m/s), there are two key undetermined coefficients  $f$  and  $\Delta C_p$  for the evaluation of airflow rates under single-sided and cross ventilation respectively. According to Anderson et al. (Andersen, Heiselberg, & Aggerholm, 2002) and Wang et al. (L. Wang, Pan, & Huang, 2012), other critical coefficients related to airflow rates, such as wind velocity coefficients  $K$  and  $\alpha$  for wind profile correction and discharge coefficients  $C_D$  for window type selection, are simplified as constants.

The airflow rates through the openings under different scenarios, e.g. different wind incidence angles, can be determined by CFD simulations. Then the two key coefficients  $f$  and  $\Delta C_p$  can be calculated by Eqs. (1) and (2).  $f$  and  $\Delta C_p$  are correlated as the function of wind direction, and have little relation with the number of floors for low-rise residential buildings. The CFD simulation model is introduced in section 2.4.

For a given cooling load defined by the internal total cooling load (or heat gain),  $Q_{in}$ , the resultant indoor air temperature  $T_i$  could be obtained by:

$$T_i = \frac{Q_{in}}{mC} + T_o \quad (3)$$

where  $m$  is the mass flow rate of air from the NV,  $C$  is the specific heat of air and  $T_o$  is the outdoor air temperature.

The annual NV potential is quantified by the total number of hours in a year when the resultant indoor air temperature  $T_i$  falls within the defined acceptable comfort range for the occupants of the building. Section 2.2 list the evaluation approach using the empirical equations.

## 2.2 Evaluation approach

The methodology for the development of coefficient selection guidance and evaluation method is summarized as the procedure *a-f*:

- a. Choose building location, window facing, and weather data. Determine  $f$  and  $\Delta C_p$ .
- b. Choose type of terrain: open area, sub-urban, or urban, and determine  $K$  and  $\alpha$ .
- c. Choose the type of the window: casement, tilt, sliding window, and the value of  $C_D$  could be determined.
- d. Enter other parameters, such as building size, window area etc.
- e. Calculate airflow rates,  $T_i$ , by Eq. (3).
- f. Count annual NV hours based on the thermal comfort temperature range and calculated  $T_i$ . Then calculate energy savings can be determined.

## 2.3 GIS maps

To guide the NV early design, a NV potential map was created using geographic information system (GIS), which is a system designed to capture, store, manipulate, analyze, manage, and present spatial or geographic data. GIS maps have been widely applied for solar potential application (Šúri, Huld, & Dunlop, 2005; Šúri, Huld, Dunlop, & Ossenbrink, 2007). Follow the approach described in section 2.2, NV hours and for buildings in different locations were calculated. In this study, annual NV applicable hours of the North America were calculated,

which provide key graphical information of energy saving potentials of NV buildings in terms of total hours suitable for NV for over 50 cities in the US and 10 cities in Canada. The weather condition data use TMY weather files.

## 2.4 CFD simulation

To calculate the airflow rate, a CFD model was developed. The building is  $80\text{ m} \times 25\text{ m} \times 14.4\text{ m}$  ( $L \times W \times H$ ) and is placed within a larger computational domain which has an upstream length of  $4W$ , a lateral length of  $4L$  on both sides and a vertical length of  $4H$  above the building height as Jiang et al. (Jiang, Alexander, Jenkins, Arthur, & Chen, 2003), except instead of  $8W$ , there is a slightly shorter downstream length of  $6W$  in this study to reduce computational time. The building has four floors and uniformly distributed thirty-two windows on each long side (depends on ventilation strategy). With the consideration of the balance between energy-saving and daylighting requirements, the window-to-wall ratio (WWR) is set to be 30% in the model. The CFD model was developed in ANSYS 16.2. “CutCell” was selected as the meshing assembly method. Approximately 500,000 meshes were generated with a minimum size of 0.3 m. A steady state Reynolds-Averaged Navier-Stokes (RANS) standard  $k - \varepsilon$  turbulence model was selected. To investigate the grid independency, two incidence angles  $\theta$  of  $45^\circ$  and  $90^\circ$  with almost three times the number of meshes were used in the same model to compare the airflow rates for both single-sided and cross-ventilation. The results indicate that the difference in airflow rates for the different grid numbers varies from 0.07% to 15%, which is acceptable considering the difference in time consumption between the two scenarios.

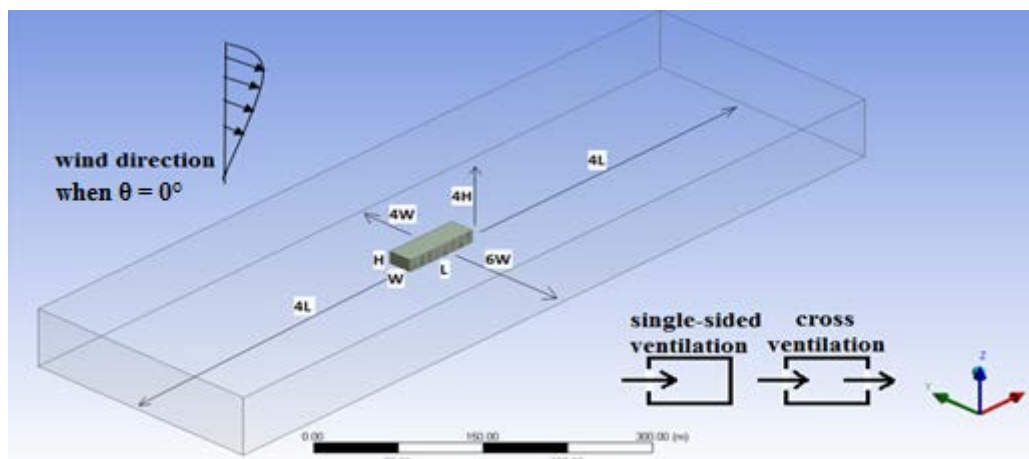


Figure 1: Schematic view of the model with outer domain ( $W$ =width,  $L$ =length and  $H$ =height).

## 3 RESULTS

### 3.1 Validation of CFD modelling method

Reynolds-averaged Navier-Stokes (RANS) and Large Eddy Simulation (LES) are the most common turbulence models for the CFD simulations of NV. To determine which model is more efficient and eliminate potential errors, validation study was undertaken using experiments from the literature (Jiang et al., 2003).

Jiang et al. (Jiang et al., 2003) conducted a series of boundary layer wind tunnel experiments in Cardiff University to simulate an urban atmospheric environment by using blockages, fences and Lego Duplo blocks. The model is cubic ( $250 \text{ mm} \times 250 \text{ mm} \times 250 \text{ mm}$ ) – see Figure 2. Three cases, including two single-sided ventilation and cross ventilation, were measured. For both windward and leeward single-sided NV cases, there is only one  $84 \text{ mm} \times 125 \text{ mm}$  opening in one facade. In case of cross ventilation, two openings with the same size are designed in opposite facades. The thickness of the walls was neglected since heat transfer is not considered in this validation study. After acquiring the simulation results, the mean velocity distributions at five locations around and inside model were compared with the Jiang’s wind tunnel test results. Both RANS (two-equation standard  $k - \epsilon$  models, precisely) and LES were used and the comparisons are demonstrated in Figure 3:

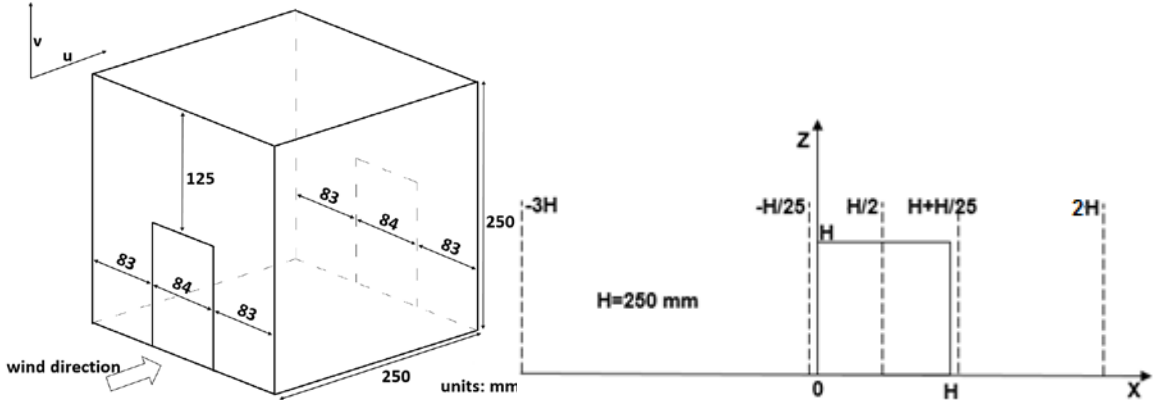


Figure 1: Schematic view of single-opening model and air velocity measurement locations.

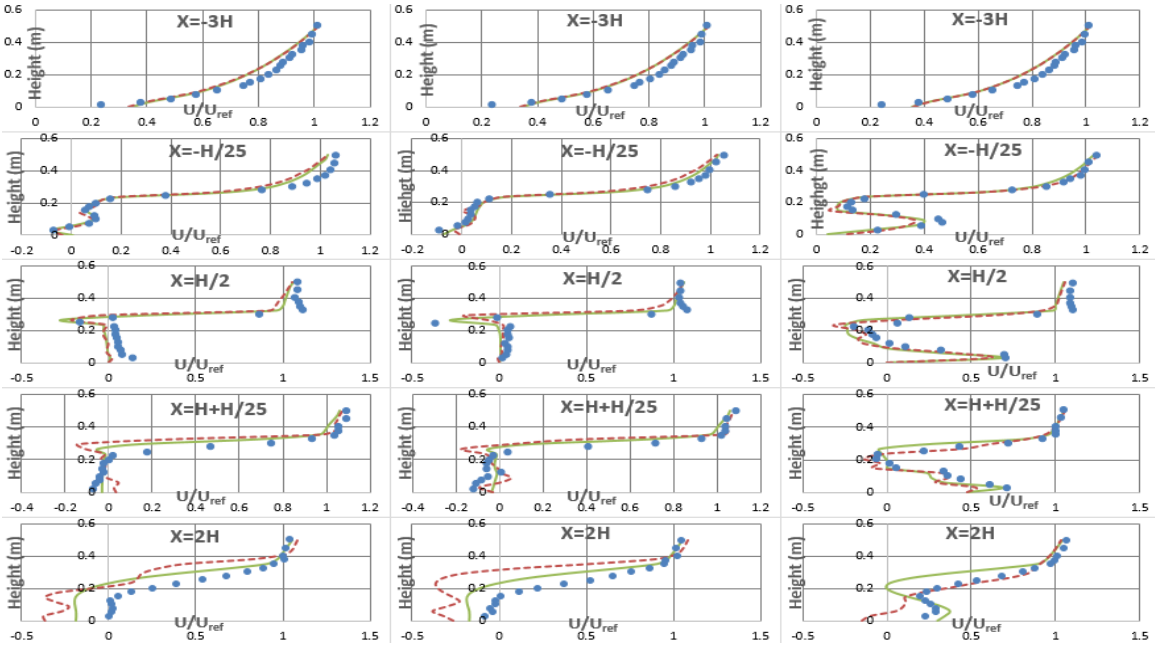


Figure 3: Mean velocity distributions for windward, single-sided ventilation (left column); leeward, single-sided ventilation (middle column) and cross-ventilation (right column). Dots: Experimental values, Jiang et al (Jiang et al., 2003); Solid line: RANS model; Dashed line: LES model.

The overall arrangement between the CFD predictions (RANS and LES) and experimental results is fairly similar along the streamline direction, which is close to the results from Jiang

et al. (Jiang et al., 2003). The difference of results between the two models are fairly small at most of the locations. Thus, the RANS standard  $k - \epsilon$  model was selected to conduct the rest of simulations considering it is acceptably accurate and time-efficient comparing to the LES model (Toja-Silva, Peralta, Lopez-Garcia, Navarro, & Cruz, 2015; Tominaga, 2015).

### 3.2 GIS maps for natural ventilation potentials

As an application of this study, the evaluation method based on empirical equations can provide a fast and relatively accurate energy saving potential analysis of NV for engineers and architects during the building early design stage. A typical building is a four-story rectangular building with same dimension as the base model located in open space of Toronto. Specifically, the indoor design temperature range,  $T_i = 21.5 \text{ }^\circ\text{C} \sim 27.8 \text{ }^\circ\text{C}$ , is set to achieve 80% thermal comfort acceptability based on the Adaptive Model for naturally ventilated buildings (Brager & De Dear, 2000). This building is set to be an office building with a combined internal heat gain of  $70 \text{ W/m}^2$  (AUTODESK; Chartered Institution of Building Services Engineers (CIBSE), 2015). The figure shown below illustrates the annual NV available hours under both single-sided (SS) and cross NV (CV) scenarios for all different window facing layouts.

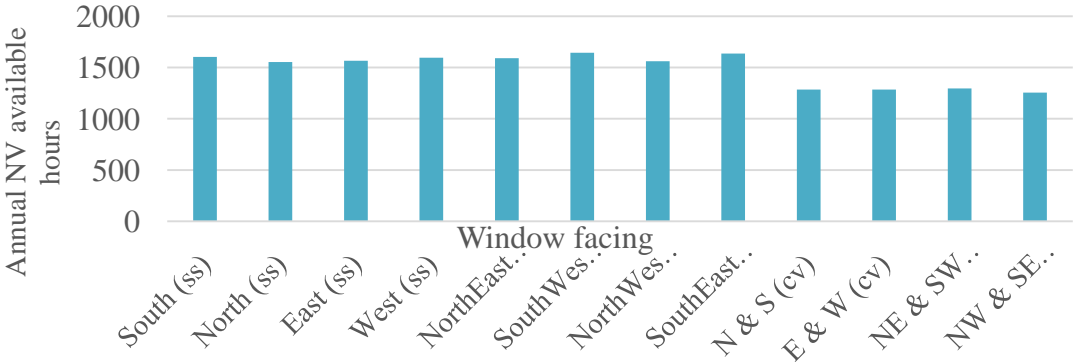


Figure 4: Annual NV available hours in Toronto for an internal cooling load of  $70 \text{ W/m}^2$ .

In detailed calculations, the wind incidence angle  $\theta$  for each hour is determined as the angle between hourly meteorological wind direction and the building orientation (i.e. window facing). Then, the value of  $f$  and  $\Delta C_p$  would be obtained correspondingly for the calculation of hourly airflow rate  $Q$  for both ventilation strategies. In combination with the internal heat gain  $Q_{in}$ , once the indoor air temperature  $T_i$  is calculated within the indoor design temperature range, that hour would be counted as an NV applicable hour. Specifically, for the case in Fig. 4, the building in Toronto achieves the maximum energy saving potential of 1,644 hours with the southeast facing single-sided NV.

Repeat the previous steps for the southeast facing single-sided NV buildings in the other major cities in US and Canada, we are able to plot the annual NV applicable hours using the GIS map visualizations in Figs. 5 and 6. It indicates that the maximum NV hours could be more than 2,500 hours and 80,000 kW in the US and 1,600 hours and 50,000 kW in Canada. The numbers could be used to determine the energy saving potentials of using NV and identify the optimum initial building designs for achieving energy savings during the conceptual design stage.

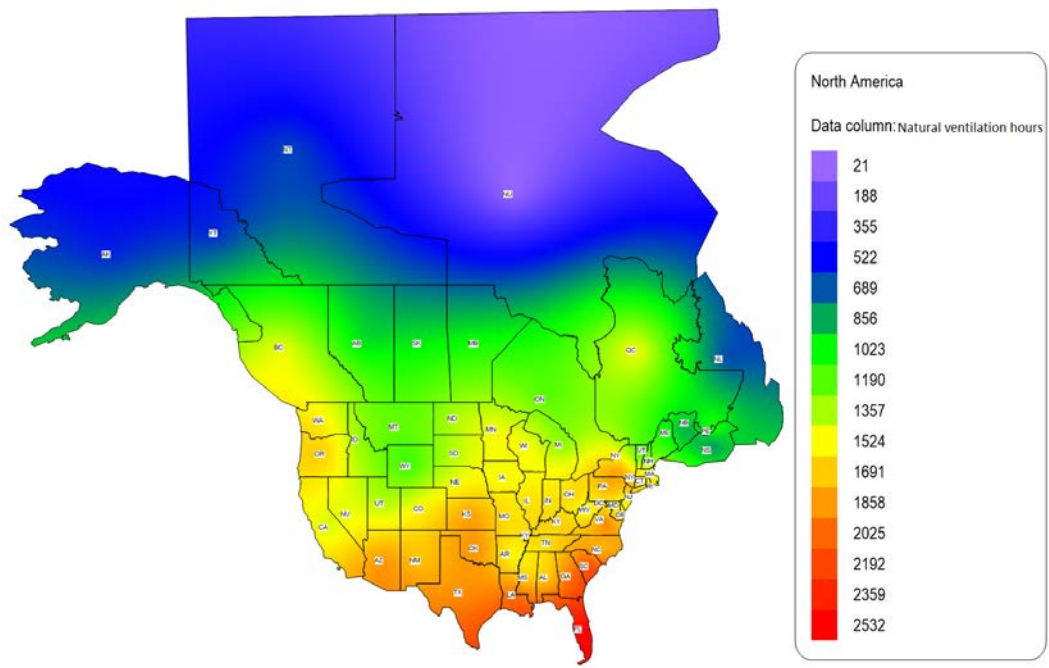


Figure 5: GIS map of NV potential hours (single-sided, building orientation: southeast) for the cooling load of 70 W/m<sup>2</sup>.

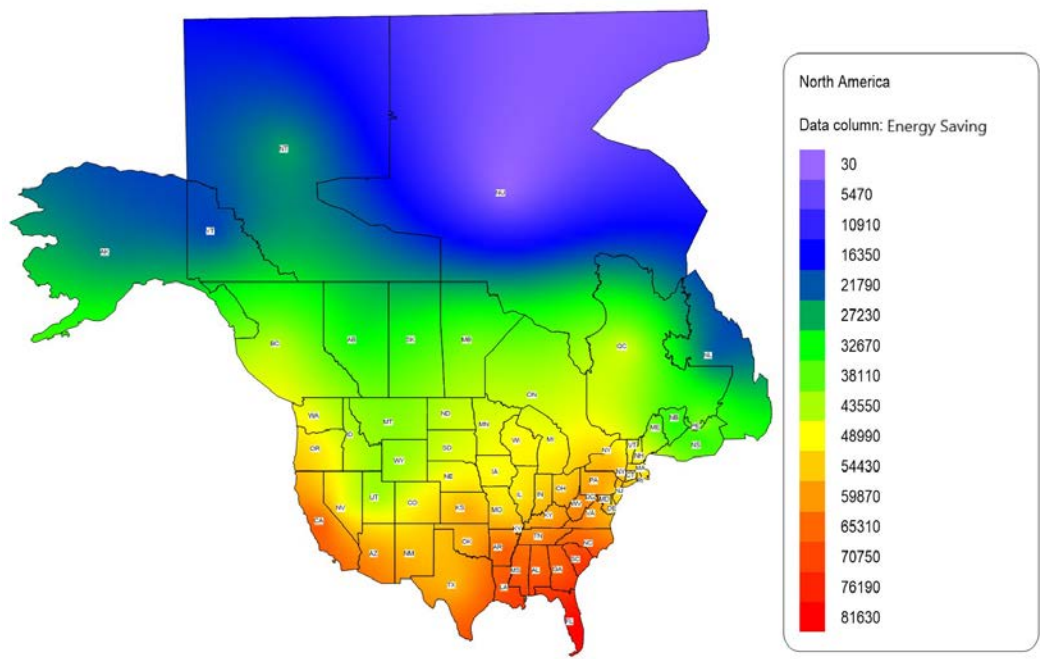


Figure 6: GIS map of NV potential energy savings, kW (single-sided, building orientation: southeast) for the cooling load of 70 W/m<sup>2</sup>.

#### 4 CONCLUSIONS

Natural ventilation has been widely used in buildings as an efficient way of reducing building energy usages and improving indoor air quality. However, determination of the NV energy saving potential is challenging because the naturally-driven airflow rates depend on many parameters including local hourly weather and climate conditions, types of NVs, amount of heat gains, operating schedules, window types, and opening areas percentages etc. This study aims to select coefficients for naturally ventilated buildings with a common shape based on

the existing empirical formulas, and use the selected coefficients to develop a quick and relatively accurate method of evaluating NV potential for energy-saving analysis during early building design stages. Using the method developed, GIS maps for NV potentials of the North America were created in a similar way as the well-known solar potential maps. The maps provide key graphical information of energy saving potentials of NV in terms of total annual NV applicable hours and energy savings for over 50 cities in the US and 10 cities in Canada. It was found that for the building defined in this paper, the maximum NV hours could be more than 2,500 hours and 80,000 kW in the US and 1,600 hours and 50,000 kW in Canada for single-sided ventilation with southeast building orientation. The proposed method and the GIS maps can be used to determine the viability of using NV and make initial building design decisions for energy savings during the conceptual design stage.

## 5 REFERENCES

- Allard, F., & Santamouris, M. (1998). Natural ventilation in buildings: a design handbook. In *London James James* (p. 378).
- Andersen, K. , Heiselberg, P., & Aggerholm, S. (2002). Naturlig ventilation i erhvervsbygninger (in Danish). *Statens Byggeforskningsinstitut*.
- AUTODESK. Example Internal Loads for Different Space Types. <https://doi.org/https://sustainabilityworkshop.autodesk.com/buildings/equipment-and-lighting-loads>
- Brager, G. S., & De Dear, R. (2000). A standard for natural ventilation. *ASHRAE Journal*, 42(10), 21–28. <https://doi.org/10.1017/CBO9781107415324.004>
- Chartered Institution of Building Services Engineers (CIBSE). (2015). *Guide A: Environmental design* (8th ed.). Norwich: Page Bros. (Norwich) Ltd.
- Cockroft, J. P., & Robertson, P. (1976). Ventilation of an enclosure through a single opening. *Building and Environment*, 11(1), 29–35. [https://doi.org/10.1016/0360-1323\(76\)90016-0](https://doi.org/10.1016/0360-1323(76)90016-0)
- Crommelin, R. D., & Vrins, E. M. H. (1988). Ventilation through a single opening in a scale model. *Air Infiltration Review*, 9(3), 11–15.
- Haghighat, F., Brohus, H., & Rao, J. (2000). Modelling air infiltration due to wind fluctuations—a review. *Building and Environment*, 35(5), 377–385. [https://doi.org/10.1016/S0360-1323\(99\)00028-1](https://doi.org/10.1016/S0360-1323(99)00028-1)
- Jiang, Y., Alexander, D., Jenkins, H., Arthur, R., & Chen, Q. (2003). Natural ventilation in buildings: Measurement in a wind tunnel and numerical simulation with large-eddy simulation. *Journal of Wind Engineering and Industrial Aerodynamics*, 91(3), 331–353. [https://doi.org/10.1016/S0167-6105\(02\)00380-X](https://doi.org/10.1016/S0167-6105(02)00380-X)
- Šúri, M., Huld, T. A., & Dunlop, E. D. (2005). PV-GIS: a web-based solar radiation database for the calculation of PV potential in Europe. *International Journal of Sustainable Energy*, 24(2), 55–67. <https://doi.org/10.1080/14786450512331329556>
- Šúri, M., Huld, T. A., Dunlop, E. D., & Ossenbrink, H. A. (2007). Potential of solar electricity generation in the European Union member states and candidate countries. *Solar Energy*, 81(10), 1295–1305. <https://doi.org/10.1016/j.solener.2006.12.007>
- Toja-Silva, F., Peralta, C., Lopez-Garcia, O., Navarro, J., & Cruz, I. (2015). Roof region

dependent wind potential assessment with different RANS turbulence models. *Jnl. of Wind Engineering and Industrial Aerodynamics*, 142, 258–271. <https://doi.org/10.1016/j.jweia.2015.04.012>

Tominaga, Y. (2015). Flow around a high-rise building using steady and unsteady RANS CFD: Effect of large-scale fluctuations on the velocity statistics. *Journal of Wind Engineering and Industrial Aerodynamics*, 142, 93–103. <https://doi.org/10.1016/j.jweia.2015.03.013>

Wang, H., & Chen, Q. (2012). A new empirical model for predicting single-sided, wind-driven natural ventilation in buildings. *Energy and Buildings*, 54, 386–394. <https://doi.org/10.1016/j.enbuild.2012.07.028>

Wang, L., Pan, Y., & Huang, Z. (2012). Factors Affecting Discharge Coefficient of Building Ventilation Windows (in Chinese). *Building Energy Efficiency*, 40(6).

Warren, P. R., & Parkins, L. M. (1985). Single-sided ventilation through open windows. In *Conf. proc. Thermal Performance of the Exterior Envelopes of Buildings, ASHRAE, Florida* (Vol. 49, p. 20).

# Challenges of using passive ventilation to control the overheating of dwellings in noisy environments

Nick Conlan<sup>\*1</sup> and Jack Harvie-Clark<sup>1</sup>

*1 -Apex Acoustics Ltd  
Design Works,  
William Street, Gateshead, UK  
\*nick.conlan@apexacoustics.co.uk*

## ABSTRACT

Where residential developments rely on opening windows to control overheating, there can be a compromise between allowing excessive noise ingress with windows open, or excessive temperatures with windows closed. This problem is exacerbated by the move towards better insulated, more airtight buildings and the need, particularly in urban areas, to consider development on noisier sites. A working group has been formed by the Association of Noise Consultants to provide guidance on acoustic conditions and design when considering both the provision of ventilation and prevention of overheating. The guidance produced by the group aims to clarify the relevant definitions of ventilation and overheating, give quantitative guidance as to how to assess internal noise levels and provide examples of acoustic design solutions. This paper discusses the development and contents of the guide and presents practical methods available to provide ventilation which controls overheating and noise levels without the need to introduce mechanical cooling systems. Case studies of projects include passive ventilation systems using attenuated façade vents and methods of using balconies to reduce noise levels incident on open windows.

## KEYWORDS

Noise, Overheating, Passive, Ventilation

## 1 INTRODUCTION

This paper has been produced partly in conjunction with the work undertaken by the Acoustic Ventilation and Overheating group (AVOG), as formed by the Association of Noise Consultants, which is producing the ANC Guide to Acoustics, Ventilation and Overheating in dwellings to support the “ProPG: Professional Practice Guidance on Planning & Noise” (ProPG) (IOA,ANC & CIEH,2017).

Although problems with overheating are becoming apparent throughout the UK, the highest proportion of residences where overheating is likely are within London, which experiences higher ambient temperatures. The London Plan (GLA,2016), Policy 5.9, sets out the cooling hierarchy within the sustainability agenda. The London Plan prioritises the requirement to reduce overheating through good building design, before considering passive and mechanical ventilation solutions. This prioritisation mirrors in many ways a good acoustic design approach described in the ProPG where the location, orientation and layout of properties should be considered first to reduce the necessity for façade sound insulation to mitigate any adverse effects. The priority described in the ProPG is for people to be able to freely open their windows without any adverse effects from external noise ingress.

The practical examples discussed in this paper follow this hierarchy by looking at options for reducing the internal noise impact by considering building location, orientation, internal

layouts, façade design, followed by passive ventilation options. Mechanical ventilation and mechanical cooling options are not considered within this paper.

## **2 ACOUSTIC, VENTILATION AND OVERHEATING GUIDANCE DOCUMENT**

The main aim of the Acoustic, Ventilation and Overheating Guidance (AVOG) document is to assist with the façade sound insulation design and assessment of indoor ambient noise levels for dwellings concurrently with the provision of ventilation and consideration of the overheating mitigation strategy.

Traditionally, the provision of façade sound insulation to protect against outdoor sound has been considered separately from the ventilation strategy and any strategy for mitigating overheating. These aspects have all-to-often been considered by different designers making different assumptions; this guide aims to assist designers to adopt an integrated approach to the acoustic design within the context of the ventilation and thermal comfort requirements.

The document aims to provide:

- an explanation of current definitions of ventilation and overheating;
- an indication of potential forms of criteria that could be chosen during the acoustic design; and
- examples of design solutions and case studies.

The guide is intended for the consideration of new residential development that will be exposed predominantly to airborne sound from transport sources, and to sound from mechanical services that are serving the dwelling. The guide seeks to encourage an assessment of noise that recognises the interdependence with the design for ventilation and overheating.

This guide is intended to be used by acousticians in order to:

- provide a means of assessment to satisfy the need to consider acoustics, ventilation and overheating at the planning stage
- provide a framework to inform the design of a residential development
- assist in educating clients, environmental health officers and other stakeholders of the interdependence of design for acoustics, ventilation and overheating

The guide is currently being finalised for review and is expected to be published towards the end of 2017.

## **3 GOOD ACOUSTIC DESIGN**

The priority of ‘good acoustic design’ aims to reduce the need for acoustic façade treatment by considering the building locations and orientation, internal layouts and mitigation for controlling noise at source. An example of ‘good acoustic design’ is a housing development in Swanley, Kent UK.

The proposed residential development site is affected by noise from an adjacent paper mill, as well as road and rail traffic noise. The guiding principles of ‘good acoustic design’ were prioritised by the design team; this inspired the massing of site layout, the internal dwelling layouts, and the holistic approach to achieving good internal environmental quality, which were essential to achieving planning permission.

The design team then developed a series of measures which were incorporated into the site proposals including:

- Apartment blocks adjacent to the paper mill, forming a noise barrier to shield the rest of the development and achieve reasonable external amenity area noise levels to proposed houses.
- Layout of apartments arranged so that no windows of habitable rooms face towards the paper mill.
- All apartment block balconies located on the opposite side from the paper mill.
- Building envelope and ventilation strategy developed to achieve paper mill noise levels within apartments to be significantly below guideline values from Table 4 of BS 8233.
- Noise barriers at the boundary of the site to control propagation of rail noise.
- Holistic approach to noise, ventilation provision and controlling overheating across the site.

The site layout can be seen in Figure 1 and the internal building layout and window locations can be seen in Figure 2. The resultant scheme was granted planning permission with no objections regarding noise from the paper mill, their acoustic consultant, or the local planning authority. It demonstrates how the design of the buildings can enable passive ventilation, and maximise the use of openable windows, on sites which have previously been considered as being too noisy.

For some developments, 'good acoustic design' may not suitably control noise levels across a site and other mitigation options must be provided to enable passive ventilation strategies for controlling overheating.



Figure 1: Site layout

Windows facing paper mill into communal circulation

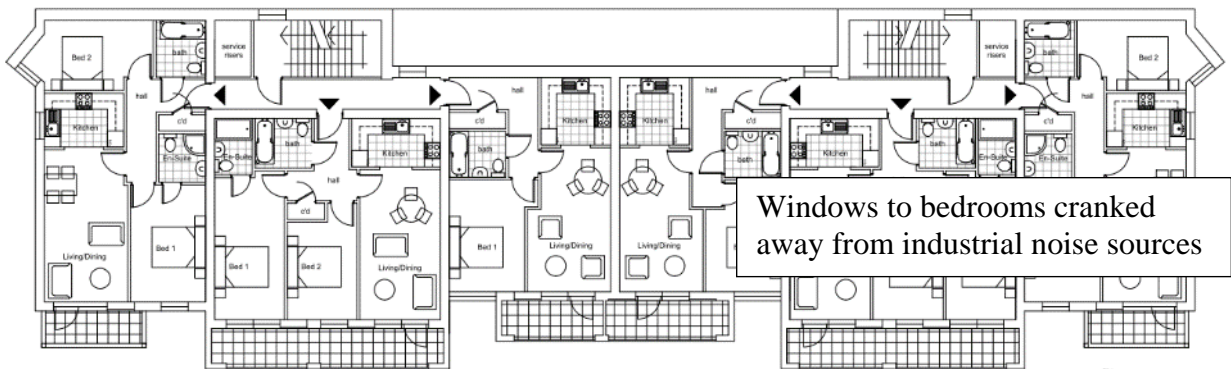


Figure 2: Internal layout and window locations

## 4 BALCONIES

Balconies can be used to reduce the noise levels at passive ventilation openings and this is supported in the draft ProPG which includes the statement:

“Where balconies are required, solid balustrades with sound absorption material added to the underside of balconies above is a good means of reducing noise entering the building.”

BS EN 12354-3 (BSI, 2000) provides a method for predicting the internal noise levels of buildings with various external façade shapes. It gives different façade shape level differences  $\Delta L_{fs}$ ; which is defined such that  $\Delta L_{fs}$  is 0 for a plane façade; and these values range from -1 for a shallow balcony with no parapet or absorption, up to 4 dB for a balcony with a solid parapet and absorptive soffit.

Naish & Tan (Naish & Tan, 2007) concisely summarised the research up to 2007 in their ICSV14 paper ‘A review of residential balconies with road traffic noise’ which describes different studies based on in-situ measurements, the use of scale models and numerical modelling techniques. They found that several studies (Gustafsson, 1973) (May, 1979) (Tzekakis, 1983), measured reductions in internal noise levels of 4 to 5 dB for balconies which had solid parapets and absorptive soffits, consistent with the values indicated in EN12354. Further studies (Hammad, 1983) (Lee, 2007) looked in more detail at increasing the absorption within the balcony and reducing the open area. These included scenarios which could provide up to 10 dB reduction compared to a plane façade.

More recently at Internoise2016, Yeung presented (Yeung,2016) in-situ measurements for balconies which varied from 5 dB reductions for modifications to the parapet and absorption to the balcony, up to a 17 dB reduction which was provided by a window arrangement which had the opening below the top of the parapet, and included absorptive linings to the parapet inner face.

At the same conference, Leung presented (Leung, 2016) findings from in-situ tests of a complete mock up. These included a scenario shown in Figure 3 where the balcony had an outer screen, and the inner façade had a door opening, with the purpose of providing natural ventilation. The balcony included absorptive finishes and the measurements found that a 10 dB improvement could be achieved, compared to a plane façade with the same opening size.

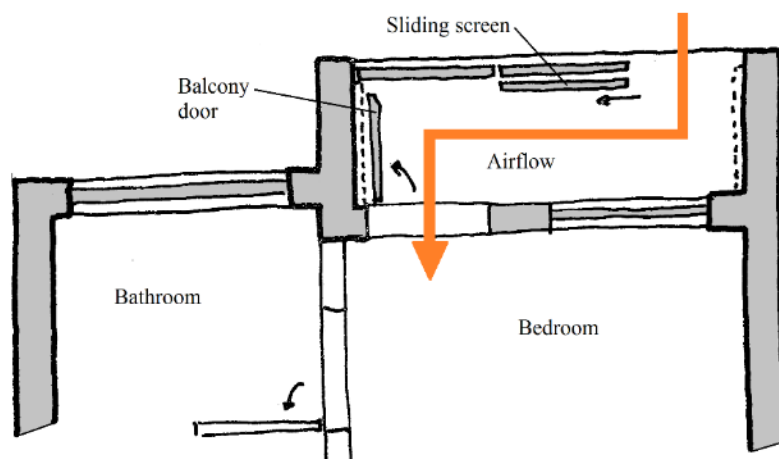


Figure 3: Section showing balcony arrangement

Although absorption to the underside of balconies is not a common solution in the UK there are examples of its approach within planning applications (AECOM, 2015) and there are some commercially available products as shown in Figure 4.



Figure 4: Absorptive lining to the underside of a balcony

## 5 PASSIVE VENTILATION OPTIONS

### 5.1 Ventilation rates to control overheating

The ventilation rates to control overheating are generally much greater than the ventilation rates required to meet the whole house indoor air quality requirements, and they can reach the rates associated with purge ventilation.

We find that typically 2 air changes per hour are required for controlling overheating which can require a façade equivalent open area of at least  $1/40^{\text{th}}$  of the floor area of the room, so for example a bedroom with a floor area of  $8\text{m}^2$  would require a facade opening of  $0.2\text{m}^2$ , which is approximately 4% of the façade area for that room.

### 5.2 Standard Windows

Opening windows are typically claimed to achieve a level difference of “10 – 15 dB” (WHO, 1999) between outside and inside. For the example bedroom described above, a  $0.2\text{m}^2$  open area would provide a predicted reduction of 11dB from external free field levels to the internal levels.

In practice, the attenuation achieved will depend on a variety of factors, and the extensive testing carried out at Napier University (Napier, 2007) illustrates the variation in level and frequency that may be found for different window types open to different extents. The size of and absorption in the room will also influence the in-situ level differences achieved by opening windows.

The Napier study suggests improvement of 2-3dB may be achievable if the type of window hinging and opening arrangements are optimised, however, in many situations opening windows do not provide sufficient attenuation of external noise ingress and further attenuation is required.

**5.3 Attenuated Windows**

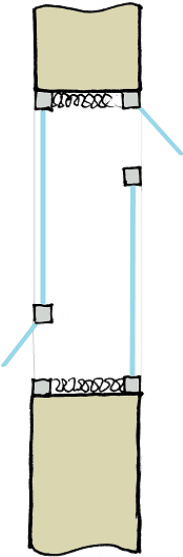
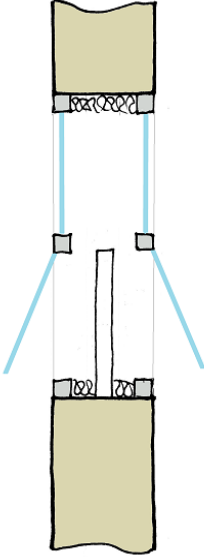
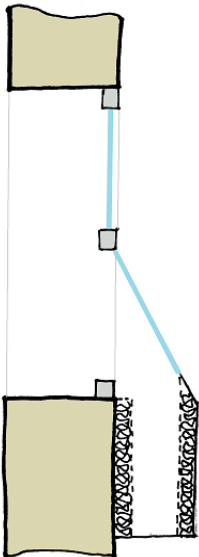
The authors are not aware of any project where enhanced acoustic performance from modified openable windows have been used for residential projects in the UK. Some performance data and options are included within a Danish study (Søndergaard, 2016) which was undertaken because of the need to provide openable windows in dwellings (0.35 m<sup>2</sup> open area), and the understanding that this limited land suitability for housing where the noise levels were too high.

The study includes three sets of measurements and is based on three different approaches:

- Dual glazing with top and bottom hung openings, not aligned, and absorptive linings between the glazing.
- Dual glazing with side hung windows which include a sliding barrier to remove the direct path from outside to inside.
- An externally mounted attenuator connected to the openable window.

The arrangement of the windows and summary of the test results are shown in Table 1. The paper includes a very comprehensive arrangement of tests, although it isn't clear what the measurement area is for establishing the sound reduction index, R<sub>w</sub> values. For vents, including open windows, D<sub>n,e,w</sub> (C; C<sub>tr</sub>) values would be more appropriate for undertaking noise ingress calculations.

Table 1: Glazing arrangement and test results

		
<p>The measured R<sub>w</sub> values ranged from 16 dB without absorption up to 30 dB with absorption to the reveals and cavity side of the window openings</p>	<p>The measured R<sub>w</sub> values ranged from 7 dB with no central barrier up to 23 dB for a barrier the same width as the window opening and absorption to the reveals</p>	<p>The external attenuator provided an R<sub>w</sub> of up to 21dB and in practice the length of the unit could be adjusted to provide higher values if required.</p>

Based on the measured performance, it would seem possible to use attenuated window systems where a reduction of 20dB was required for external to internal levels, while providing ventilation rates which could help control overheating.

## **5.4 Attenuated vents**

The following case studies for attenuated vents include large façade openings, with attenuation, to allow passive ventilation with reduced noise ingress compared to open windows.

### **5.4.1 Case Study 1 - North West Cambridge, Lots 3 and 5**

The North West Cambridge Development includes up to 1,500 affordable homes for University and College staff, 1,500 private homes and accommodation for 2,000 postgraduates. The scheme is separated in several different 'Lots' each with a different architect and a range of main contractors.

The site is exposed to motorway noise from the M11 and noise from the local traffic within the development. A sustainability statement for the development expressed a desire for natural ventilation for the University accommodation which meant that bespoke designs had to be developed to meet the acoustic and thermal insulation performance requirements for the façades, while allowing overheating to be controlled without a mechanical system.

The external façade levels were predicted based on traffic data and baseline measurements of the motorway noise levels. Maximum levels were not assessed for this project as the dominant source was steady noise from the motorway. A planning condition from the outline planning approval required good indoor ambient noise levels in living rooms and bedrooms when the spaces were being rapidly ventilated.

The building physics modelling established the ventilation rates required to control overheating and these were up to two air changes per hour which is considerably higher than the rates normally achieved with domestic MVHR units. To achieve two air changes per hour through a façade ventilator the open area for typical bedrooms was 0.2 m<sup>2</sup>.

For night-time periods a limit of 35 dB  $L_{Aeq,8hr}$  in bedrooms was required. Noise ingress calculations were undertaken for a 0.2 m<sup>2</sup> façade opening and an external upper level of 48 dB  $L_{Aeq,8hr}$  was used to establish the bedrooms which could be ventilated with openable windows to control overheating. For the façades which were predicted to be exposed to noise levels greater than these attenuated vents were used to provide sufficient air changes to control overheating. Further details of the project can be found in the planning documents submitted with the reserved matters applications (URS, 2013)

The external noise level at the site were up to 67dB  $L_{Aeq,16hr}$  during the daytime and 62dB  $L_{Aeq,8hr}$  during the night-time. These therefore required attenuation which could reduce the free field external levels by more than 27dB.

A section through the façade of Lot 3 can be seen in Figure 5, and the external facades can be seen in Figure 6 and Figure 7. An internal view of the rooms in Figure 8 shows the attenuated vent opening adjacent to the windows.

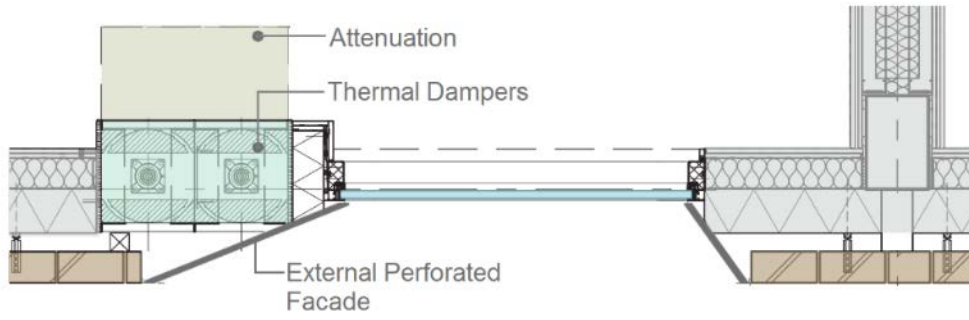


Figure 5: Lot 3 Section through the facade



Figure 6: Lot 3 façade showing perforated panels to window reveals

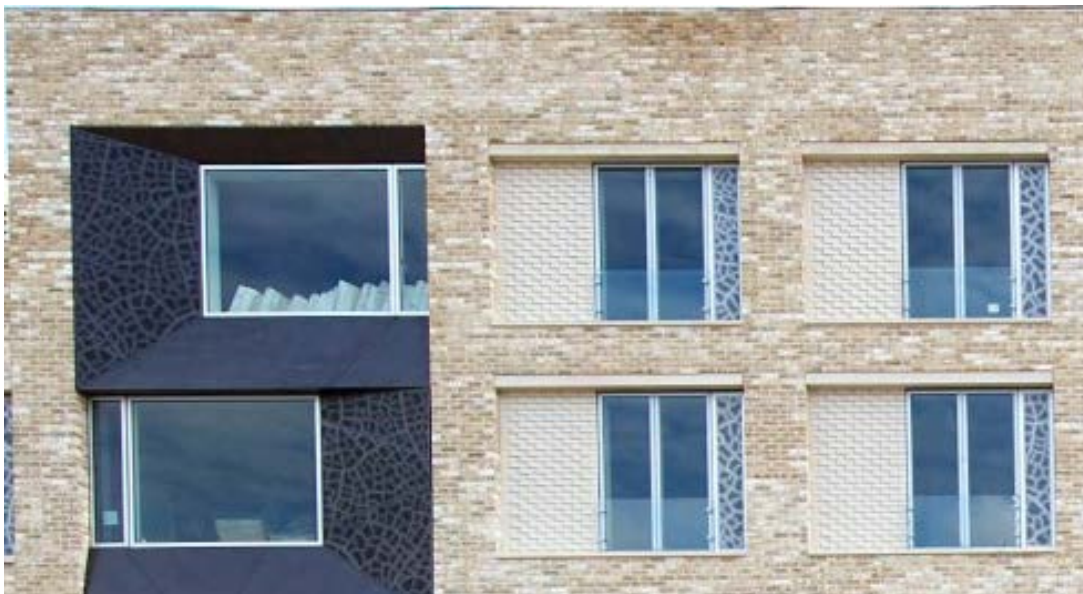


Figure 7: Lot 5 façade showing perforated panels adjacent to windows



Figure 8: Internal view of attenuated vent opening adjacent to the windows

#### 5.4.2 Case Study 2 - Clapham, London

The scheme is a large residential development alongside a busy railway line in London. The site is also affected by road traffic noise. This case study considers a typical bedroom located on the façade facing the railway at 1st floor level (i.e. that which is most affected by railway noise).

There were potential significant adverse effects due to noise ingress if open windows were used to control overheating, so criteria were developed to enable attenuated vents to be specified for the bedrooms overlooking the railway. The development overheating was assessed with the CIBSE Guide A (CIBSE,2006). The façade to the bedroom being assessed faces W/NW. Solar control glass was used to limit solar gains and relief of overheating is achieved by using a passive façade ventilator, referred to as the ‘louvered acoustic vent’.

The external noise levels at the façade of the bedroom being assessed have been determined from on-site measurements as 66dB  $L_{Aeq,8hr}$  and the internal noise level requirements during ventilation to control overheating were 40dB  $L_{Aeq,8hr}$ . Therefore, a sound reduction of more than 26dB was required through the attenuated vents.

The louvered acoustic vent was designed to provide a face area of around 1 m<sup>2</sup> and a ventilation free area of around 0.4 m<sup>2</sup>. It was anticipated that, in order to achieve comfortable internal temperatures, the louvered acoustic vent will need to be open for around 10-15% of the time (over the course of a year) depending on the occupants’ behaviour. The arrangement of the vents within the room and external and internal images of the attenuated vents are shown in Figure 9 and Figure 10.

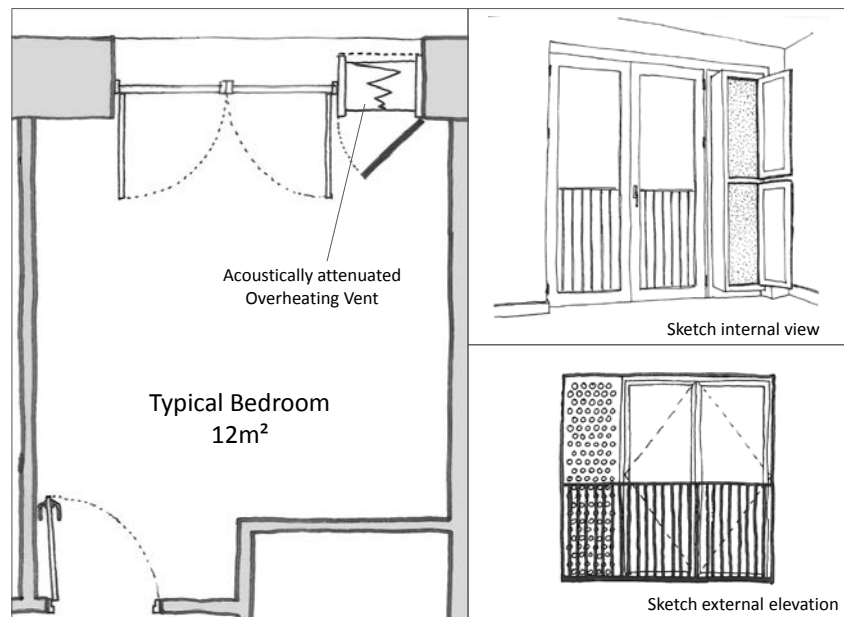


Figure 9: Clapham case study room arrangement

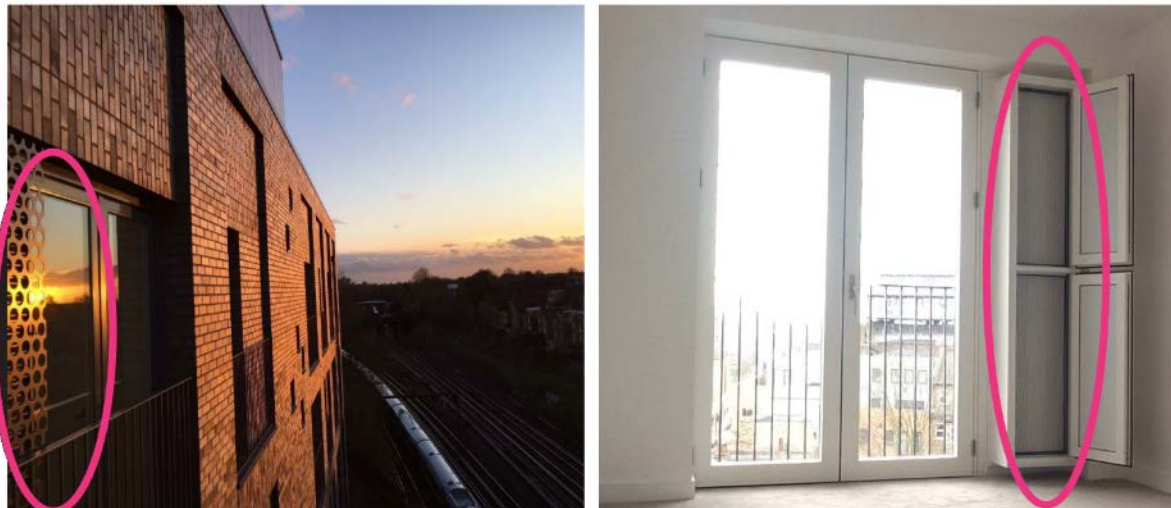


Figure 10: Clapham case study external and internal views

## 6 CONCLUSIONS

Following the principles of ‘good acoustic design’ can increase the number of habitable residential rooms which can be ventilated with openable windows. This considers the locations, orientation and layout of buildings to reduce the noise levels incident on the façades of habitable rooms.

The use of balconies can reduce noise levels incident at ventilation openings, and these can provide an additional 5dB improvement compared to designs without balconies. If the balconies are partially enclosed this can increase to 10dB improvement, with suitable treatments to the balconies.

Attenuated windows are not common in UK designs, but they have the potential to provide 10 dB improvement compared to a simple opening window. Consideration of the window hinging and opening arrangements can provide 2-3dB improvement for some noise sources.

Attenuated openings to provide ventilation rates to control overheating have been used on two separate case study projects in the UK. These are providing attenuation upto 27dB from external free-field to internal levels, while providing the ventilative cooling rates required to control overheating.

## 7 ACKNOWLEDGEMENTS

The authors would like to thank the members of the ANC Working group on Noise, Ventilation and Overheating, particularly the chair of the group, Anthony Chilton of Max Fordham.

## 8 REFERENCES

- AECOM (2015) *North West Cambridge LotM1/M2 Reserved Matters Noise Insulation Scheme*, Online reserved matters application, Cambridge City Council reference 15/1663/REM
- Institute of Acoustics, Association of Noise Consultants and Chartered Institute of Environmental Health, (2017) *ProPG: Professional Practice Guidance on Planning & Noise*, Draft
- The Greater London Authority(2016), *The London Plan - The spatial development strategy for London consolidated*.
- Chartered Institution of Building Services Engineers (2006), *Environmental Design: CIBSE Guide A*, 6<sup>th</sup> Edition.
- British Standards Institute (2000), EN 12354-3:2000 Building acoustics. Estimation of acoustic performance in buildings from the performance of elements. Airborne sound insulation against outdoor sound, *British Standards Institute*, London.
- Naish, D. and Tan, A. (2007), A review of residential balconies with road traffic noise, *Proceedings of 14th International Congress on Sound and Vibration, ICSV14*, Cairns, Australia, 9-12 July
- Gustafsson, J.-I. and Einarsson, S. (1973), Gallery houses with respect to traffic noise, *Proceedings of Inter-noise 73*.
- May, D.N. (1979), Freeway noise and high-rise balcony, *Journal of Acoustical Society of America* 65, 699-704
- Tzekakis, E.G. (1983), On the noise reducing properties of balconies, *Acustica* 52, 117-21
- Hammad, R.N.S. and Gibbs, B.M. (1983), The acoustic performance of building facades in hot climates: Part 2--Closed balconies, *Applied Acoustics* 16, 441-454
- Lee, P.J., Kim, Y.H, Jeon, J.Y. and Song K.D. (2007), Effects of apartment building façade and balcony design on the reduction of exterior noise, *Building and Environment* 42 (10, 3517-3528)

- Yeung, M. (2016), Adopting specially designed balconies to achieve substantial noise reduction for residential buildings”, *Proceedings of Inter Noise*, 1185-1190
- Leung, J. and Chu, M.W.(2016), Research and development of noise mitigation measures for public housing development in Hong Kong – A case study of Acoustic Balcony, *Proceedings of InterNoise*, 1199-1207
- Napier University (2007), NANR116: Open /Closed window research - Sound Insulation through ventilated domestic windows. *School of the Built Environment*, Technical report, Napier University.
- URS (2013) *North West Cambridge – Lot 5 Reserved Matters Application Noise Insulation Scheme*, Cambridge City Council, Planning application Ref: 13/1827/REM
- URS (2013) *North West Cambridge – Lot 3 Reserved Matters Application Noise Insulation Scheme*, Cambridge City Council, Planning Application Ref 13/1400/REM
- Søndergaard, L.S. and R Egedal, R. (2016), Open windows with better sound insulation, *Proceedings of Inter-Noise*, Hamburg, 1173-1184
- World Health Organisation, (1999), *Guidelines for community noise*, World Health Organisation, Geneva.

# Natural ventilation systems in Mediterranean schools. A prototype experience in Andalusia as an alternative to mechanical ventilation

Maite Gil-Báez<sup>\*1</sup>, Ángela Barrios-Padura<sup>2</sup>, Carmen Roldán-Vendrell<sup>3</sup>, and Marta Molina-Huelva<sup>4</sup>

*1 Andalusian Public Education Agency  
Government of Andalusia  
C/Judería 1, Edificio Vega del Rey, 1  
41900 Camas, Seville, Spain  
University of Seville, Department of Building  
Construction I*

*2 University of Seville, Department of Building  
Construction I  
Avda. Reina Mercedes, 2  
41012 Seville, Spain*

*\*Corresponding author:*

[gmaitegil@gmail.com/maite.gil@juntadeandalucia.es](mailto:gmaitegil@gmail.com/maite.gil@juntadeandalucia.es)

*Presenting author: underline First & Last name*

*3 Andalusian Public Education Agency  
Government of Andalusia  
C/Judería 1, Edificio Vega del Rey, 1  
41900 Camas, Seville, Spain*

*4 University of Seville, Department of Building  
Construction I  
Avda. Reina Mercedes, 2  
41012 Seville, Spain*

## ABSTRACT

In high density occupation rooms, it is necessary to control indoor air quality (IAQ) combined with other comfort parameters. An adequate IAQ in classrooms enhances children learning and academic results are improved.

In the last decade, international technical regulations have increased air-tightness requirement in buildings in order to reduce heat losses. Following this trend, current Spanish regulations are based on mechanical ventilation systems to guarantee IAQ in no residential buildings. However, its use in schools presents several problems due to operational costs and maintenance needs. To solve these issues, Andalusian government is developing a research work to design alternative systems. In this way, natural ventilation systems already in use in UK school buildings, are tested in Andalusian schools, under the conditions of the Mediterranean mild climate and regional scholar schedule, with different operating conditions from those already tested in northern regions.

In this paper is presented an experimental Natural Ventilation System to guarantee IAQ conditions. It is designed combining cross ventilation and stack effect strategies in each classroom, calculated with computational simulations and compared with a mechanical ventilation system under current Spanish regulations. Main conclusion derived from simulations is the feasibility of using natural ventilation systems to guarantee Indoor Air Quality in classrooms and enhance the energy efficiency of the buildings of Andalusian schools. Based on this, a standard Natural Ventilation System model is proposed to be used for design criteria in new buildings to be constructed in coming years in Andalusia.

Previous simulations show that these natural ventilation systems are an alternative to comply with Spanish technical regulations. In addition, using these systems is possible to reduce investment costs between 8-10% and to avoid running problems during the use of the buildings, in addition to savings due to energy consumptions and CO<sub>2</sub> emissions. Thus, this kind of systems could be used as passive actions to design Zero Energy Buildings.

This study will be extended with an experimental campaign in a new building located in the province of Seville, designed with both Natural and Mechanical Ventilation Systems and now under construction, is going to be used as a Test Building. It will be in use from September 2017 and a measure campaign is going to be developed during the whole scholar year, to analyse both natural and mechanical ventilation systems, comparing their operation, consumptions and users perception.

## KEYWORDS

Natural Ventilation Systems, Mediterranean climate, schools, prototype, technical regulations

## 1 INTRODUCTION

Directive 2002/91/EU about efficiency energy in buildings, (Europeo, Consejo, and Uni 2003) imposes energy savings in buildings by reducing consumptions. This requirement was developed in further Directives as 2010/31/UE (Comisión Europea 2010) defining nearly zero energy buildings (NZEBs). This subject has a high research activity as it is shown in (Deng, Wang, and Dai 2018), (Desideri et al. 2014), (Zhu 2014), (Pikas et al. 2015) (Attia and Carlucci 2015). Associated to climate, Krawczyk (Krawczyk 2014) shows the high dependence of demand with location. Regarding HVAC (heating, ventilation and air conditioning) systems Chenari et al. evaluated their greater effect on energy usage in buildings (Chenari, Dias Carrilho, and Gameiro da Silva 2016). In addition these HVAC systems accounts for 60–70% of total energy use in non-industrial buildings where infiltration and ventilation suppose between 30–50% of this energy consumption (Khan, Su, and Riffat 2008). Attia and Carlucci (Attia and Carlucci 2015), put the focus on space cooling, heating and ventilation operation to reduce energy demand.

Most of the strategies developed for energy savings in buildings operation use to combined different strategies as: increase buildings air-tightness (Inive / International Network for Information on Ventilation and Energy Performance n.d.), improve HVAC systems as its size (Sun et al. 2014) or HVAC loads and control based on real occupancy (Yang, Ghahramani, and Becerik-Gerber 2016). Besides, in high airtight buildings, heat gains are only dissipated by ventilation (Flourentzou, Pantet, and Ritz 2017), and additional systems or strategies are required in order to guarantee IAQ and reduce condensation problems and moistures. In addition, in classrooms, as high density occupation spaces, it is necessary to control indoor air quality (IAQ) in combination with other comfort parameters to enhance children learning and improve academic results. IAQ in schools has been studied recently in several locations: Greece (Barrett et al. 2015), (Kalimeri et al. 2016), Serbia (Jovanovi et al. 2014), USA (Air et al. 2007), The Netherlands (Classroom ventilation and indoor air quality — results from the FRESH intervention study 2016), (Toftum et al. 2015), Denmark (Assessment of ventilation and indoor air pollutants in nursery and elementary schools in France 2016), France (Indoor air quality in Portuguese schools : levels and sources of pollutants 2016; Pegas et al. 2011; Severo et al. 2016), Portugal (Almeida and De Freitas 2014). In some recent studies is analysed the Southern European climate, exposing the evidence of inadequate IAQ in schools and its negative effects on health (Rufo et al. 2016), (Chatzidiakou, Mumovic, and Summerfield 2017). So, in new high air-tight school buildings with high density occupation spaces, ventilation is an especially relevant design key for both end users health and energy consumption.

The use of Mechanical Ventilation Systems has been widely extended to achieve IAQ in last two decades, integrating sometimes heat recovery solutions to reduce energy consumptions (Wang et al. 2014). Following this trend “Standard Passivhaus” (Passivhaus Institut n.d.) is having an intense development in Europe, as a model of Zero Energy Building design. Being an appropriate solution for cold climate regions, however in mild climate zones, the primary energy savings linked to heat recovery can be smaller than the electricity required for running the required mechanical ventilation system depending on the building application and occupation pattern. In addition, as showed by Oropeza and Østergaard (Oropeza-Perez and Østergaard 2014), a dwelling considered as a passive house focused on heating savings presented overheating problems during warmer session. Furthermore, mechanical systems operation in schools presents several problems due to operational costs and maintenance needs which leads to the fact that they are not being used regularly. This is described for Almeida et al in Portugal (Almeida and De Freitas 2014), and the situation is similar to most

of the mild climate region of Spain. It makes necessary to search for alternative solutions for the specific conditions of mild climate schools.

At local level, in Spain, the current HVAC regulations (Ministerio de Industria 2013) develop a detailed technical framework for MVS design and implementation to ensure IAQ in non-residential buildings. Although regulation is open to alternative systems to the mechanical ones, the real situation is that the technical framework is not developed yet, indirectly favouring MVS system installation. This situation is similar in other countries as Swiss, as it is exposed in (Flourentzou and Pantet 2014).

Due to the problems derived from the inclusion of these MVS in school buildings built up in the last decade in Andalusia, regional government is developing a research work to design ventilation systems alternative to the mechanical ones. On this purpose, NVS which are already in use in UK school buildings, have been tested in Andalusian schools, under the conditions of the Mediterranean mild climate and the regional scholar schedule. The goal is to verify their adequateness to provide high indoor air quality and comfort conditions.

In this way, a design program for new buildings, has been developed in 2017. Within this program, NVS is under installation in a set of new school buildings in order to prove and validate its operation. Its main objective is to assess the NVS performance, previously modelled and tested at local scale, to a wider range. It will generate the required new knowledge about its application to schools under these conditions and it should give support to the future development of regional technical regulations. In addition, under the ClimAct project, in development since June of 2016 to December of 2019 in the framework of the program Interreg-Sudoe Program of European Union, Natural Ventilation Systems in Andalusian school buildings are going to be analysed, among other strategies, as a way to accomplish to a transition to a low carbon economy in schools in Mediterranean zone.

Within this framework, this paper presents the Natural Ventilation System model designed to guarantee IAQ conditions in classrooms, comparing results with the Mechanical Ventilation System operation. The model is designed to be included in each classroom and it is based on a cross ventilation strategy in combination with stack effect, in order to improve the air movement even in days with reduced indoor/ outdoor temperature difference and without wind conditions. Its performance was evaluated with computational simulations and compared with the Mechanical Ventilation System installed under current Spanish regulations in terms of final and primary energy and CO<sub>2</sub> emissions savings. Considering the results obtained, a standard model was proposed to be used in the classrooms of new buildings which will be constructed in Andalusia in coming years.

Main conclusion of simulations is the possibility of using natural ventilation systems in Andalusian schools to guarantee Indoor Air Quality and comfort conditions in classrooms. These systems are shown as an alternative to comply with Spanish technical regulations. At the same time with these systems is possible to reduce investment costs between 8-10% and to avoid running problems during the use of the buildings, in addition to savings due to energy consumptions and CO<sub>2</sub> emissions. Thus, the use of this kind of systems could be used as passive actions to design Zero Energy Buildings.

A new building located in the province of Seville, designed with both Natural and Mechanical Ventilation Systems and now under construction, is going to be used as a Test Building. It will start its operation on September 2017 and it will be used along the next year for tests campaigns. Consumptions and Indoor Environment Quality (IEQ) using both natural and mechanical systems will be compared. Expected results are the improvement of the IEQ, with less energy consumption, as well as the enhancement of the indoor thermal conditions in spring and autumn by reducing indoor overheating using the Ventilative Cooling effect. This experimental action is included in the "Energy Strategy of Andalucía 2020" (Agencia Andaluza de la energía 2016) of the Andalusian Energy Agency.

This paper is structured in 4 sections. Following this introduction in the second section the Mediterranean school buildings framework is exposed. In the third one the design methodology is presented and in the fourth the main conclusions are summarized.

## 2 MEDITERRANEAN SCHOOL BUILDINGS FRAMEWORK

### 2.1 Mediterranean climate. Temperatures during year

The results presented in this paper are focused on a building located in Seville, sub-climatic zone B4 in Andalusia (where there are five sub-climatic zones). This mild climate zone, presents soft thermal conditions. Hourly mean temperature evolution for the months within the scholar schedule is presented in Figure 1:

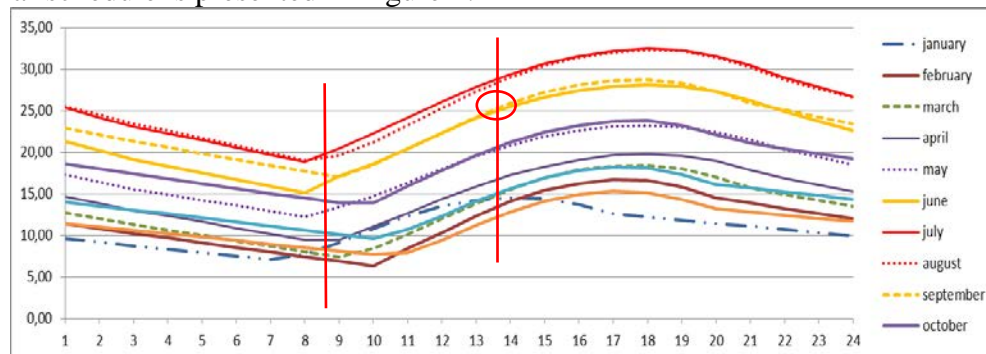


Figure 1. Hourly mean temperature evolution for the months within the scholar schedule for B4 zone in Andalusia. Data obtained from Spanish Ministry published data \*.met

In Figure 1, mild climate conditions are shown with the distribution of outdoor temperatures along the scholar session in a representative day of each month. Maximum temperatures from September to June into the school time, are below 30 °C and around 26°C in the last hour of the daily sessions, at 14:00. Furthermore, in winter season there are no days with temperatures under 5°C (mean temperatures of each month).

### 2.2 School buildings characteristics

There are more than 80,000 schools in the Mediterranean region (Promoting renovation of schools in a Mediterranean climate up to nearly Zero-energy buildings | ZEMedS n.d.). Being a big energy consumers, this sector consumes 4% of the energy in the commercial sector in Spain (Krawczyk 2014). Only in Andalusia there are more than 4500 public schools. There are relevant international R&D projects. (Home n.d.), (DOWNLOAD AREA | RENEW SCHOOL n.d.), (Erhorn-kluttig and Erhorn 2014), (Check and improve the energy performance of schools and disseminate best practices - Intelligent Energy Europe - European Commission n.d.), (Promoting renovation of schools in a Mediterranean climate up to nearly Zero-energy buildings | ZEMedS n.d.), (Teenergy Schools | High energy efficiency schools in Mediterranean Area n.d.) and an intense R&D activity in school buildings. Among other publications is relevant interesting CIBSE's School Design Group (CIBSE - School Design Group n.d.) publication TM57:2015 Integrated School Design (CIBSETM57 2015), with specific recommendations for school buildings. The school building segment is unique in the building domain since it has specific typologies, users and usage patterns, energy infrastructures, energy uses and functions, Veryschool Project (VERYSCHOOL.EU - Valuable Energy for a smart school n.d.). Main characteristics can be resumed in the next:

- a) Schools usually operate around 175 days in the year (half of days in a year). In Mediterranean zone there are the summer school holidays which last 2 months and a half as well as Christmas and Easter holidays. The number of school days is similar in other countries too, even being shorter the summer break.

- b) School buildings design is mainly based in a rational space organization. Classrooms have wide dimensioned windows in order to allow natural illumination of the space, are usually grouped and there is a corridor to access them, as well as there are top-hung windows to corridor to be used for both cross ventilation and illumination.



Fig. 2. Typical school building windows. a) left façade windows, b) right corridor windows

- c) School operation is usually organized with a break between lessons and a main break to go out to the courtyard and take a snack. In addition, there are several internal displacements and changes of class into the school building, so that classrooms are spaces with non-permanent occupation.
- d) Mediterranean schools present reduced heating requirements, due to the mild weather and internal gains. However, ventilation is necessary along the whole school year. Heating vs ventilation requirements are represented in the next Figure 3

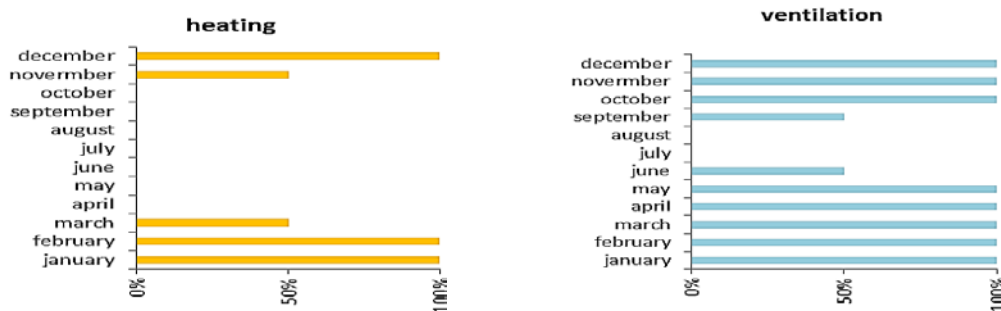


Fig. 3. Mild climate school heating and ventilation patterns.. a) Left. Heating profile estimation in terms of heating days percentage by month. b) right. Ventilation profile estimation in terms of percentage of ventilation days per month

### 2.3 Andalusian schools

With a high number of schools in Andalusia, built along long periods there are clear differences among them regarding their construction period. In older schools, the absence of regulations and construction standards resulted in less airtightness in buildings constructed in twentieth century. Ventilation was controlled opening doors and windows (Almeida, Ramos, and Freitas 2016), (Romana, Ianniello, and Igor 2013) as way to control contaminant levels and comfort conditions in classrooms (Stabile et al. 2016).

However in 21<sup>st</sup> century new schools construction criteria changed. In next figure a Mechanical Ventilation System installed in an Andalusian school under actual technical regulation (Ministerio de Industria 2013) is shown. It supposes a relevant capital cost, ducts integration in buildings, need of additional oversized electricity facilities which includes transformers, and maintenance of the whole set of direct and indirect installations.



Fig. 4. Mechanical Ventilation system in an Andalusian school. Roof tops

Nevertheless, these Mechanical Systems don't offer the indoor quality expected and estimated under calculations due to different usage patterns and maintenance issues associated both to operational and maintenance costs to be paid by end user. In addition, due to the high internal heat gains in classrooms, due to metabolic activity, the heating period is shorter than other spaces like residential buildings. Therefore, some valuable solutions in other applications, as could be heat recovery, would be cost efficient only in very cold regions (Erhorn-kluttig and Erhorn 2014). Besides, from the point of view of health, additional problems can appear with MVS as the Sick Building Syndrome (SBS), being a risk for airborne infectious diseases as presented by Pereira et al (Luiz et al. 2015).

Accordingly, regarding to the issues derived from the design of MVS as equipment, the associated capital, operational and maintenance costs and the low benefit derived from them under the real operation of the schools, more sustainable and environmental friendly solutions are required. In this framework is developed this work of analysis and promotion of Natural Ventilation Systems in Andalusian schools.

### 3 METHODOLOGY

The methodology followed in this study presents the next steps:

- 1) Study of International experiences in natural ventilation systems: with specific focus on the well established BB101 (Bb101 2006) in UK. The study was focused on the adaptation requirements of proven natural ventilation strategies for school buildings in northern countries to Andalusian schools.
- 2) Analysis of the forgotten Natural Ventilation examples in Andalusian schools of the early 20<sup>th</sup> century: Although similar devices based on these principles were used in Andalusian schools 30-40 years ago, the evolution of technical design and regulatory framework in buildings as well as end user changes of habits among other things have displaced them. In Figure 5 are shown an example taken from an old school.



Fig.5(left) Cross ventilation in an Andalusian school. Right) Natural Ventilation system in an Andalusian school built in 1985

- 3) A hypothesis is stated in Andalusia, proposing a system based in stack effect and cross ventilation, which is based in ancient examples and following BB101 recommendations.
- 4) Model building thermal simulation and CFD calculation: Using Designbuilder (DesignBuilder Software Ltd - Home n.d.), 10 options were calculated for the same theoretical building model (5 with NVS and 5 with MVS comparing pairs of options in each sub-climatic Andalusian zone) in order to calculate the energy savings that could be obtained using NVS instead of mechanical ones. CFD option was used to prove the effectiveness in the air flow through the classrooms. Ten options were calculated in the same building model (5 with NVS and 5 with MVS comparing pairs of options in each sub-climatic Andalusian zone) in order to obtain energy savings using a natural system for ventilation instead of a mechanical one. CFD option was used to prove the effectiveness in the air flow through the classrooms.
- 5) Standard Natural Ventilation System: Analysing results obtained, a standard solution was defined, in order to be used in new buildings design, simplifying the design process with no additional calculations.

### 3.1 Natural Ventilation System standard model

In Figure 6 the ventilation standard model proposed is shown. From left to right plants and roof are represented. This simple system is applicable for each classroom and it is composed by automatic intake windows in the facade and two stacks in the opposite wall connected with the roof for extraction.

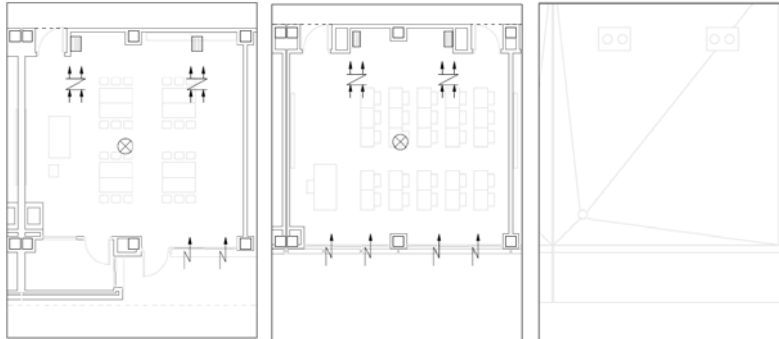


Figure 6. Standard classroom NVS model plants. Left) ground floor, middle) first floor plant and right) roof  
The automatic windows operation is controlled by a CO<sub>2</sub> level sensor disposed in the middle of the classroom roof, in order to avoid be damaged by the pupils. System outlets are connected from the classroom with the building roof using a dynamic aerator. In Figure 7 a section and an axonometric view are represented:

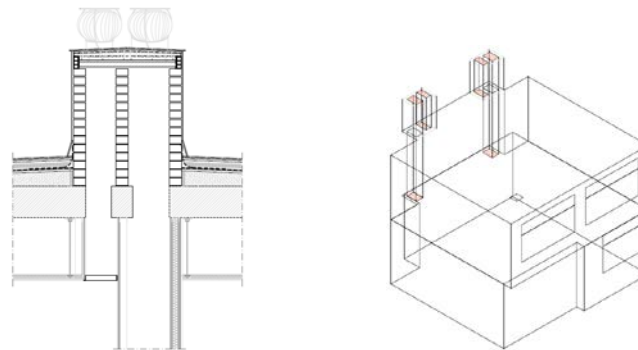


Figure 7. Standard classroom NVS details: left) section and right) axonometric view

### 3.2 Test Building description

The theoretical solution previously calculated is implemented in the design of a new school building, which is now under construction and it is being used as a prototype model, in order to test this standard solution. The school is located in “MairenadelAljarafe”, in a suburban area 8 km from the city center of Seville with an adequate and no contaminated outdoor air quality.



Figure 8 Location. Google maps image

The building is a pre-school and primary school level (from 3.-12 years old). There are 27 classrooms for 25 pupils and the teacher (675 children). Lessons are developed from 9:00 to 14:00 hours. The canteen operates from 14:00 to 16:00. In the afternoon there are extra-scholar activities for some children (not all of them), which are mainly sports and only from October to May. Building characteristics are shown in the next Figures and Tables.

Main characteristics of construction and materials are presented in Table 1:

Table 1: Characteristics and materials

Element	Material
Structure	Concrete
Roof	Slab concrete with insulation
Walls	Insulated cavity wall
Windows	Aluminium with thermal break / double glass 4/10/6. Brise-soleil sun blinds
Lighting	Fluorescent with electronic ballast T-5
Heating	Water radiators with natural gas boiler
Cooling	No cooling system
Ventilation	Natural Ventilation System Mechanical ventilation System

The building is developed in ground floor and first floor with a surface around 4,300 m<sup>2</sup>.

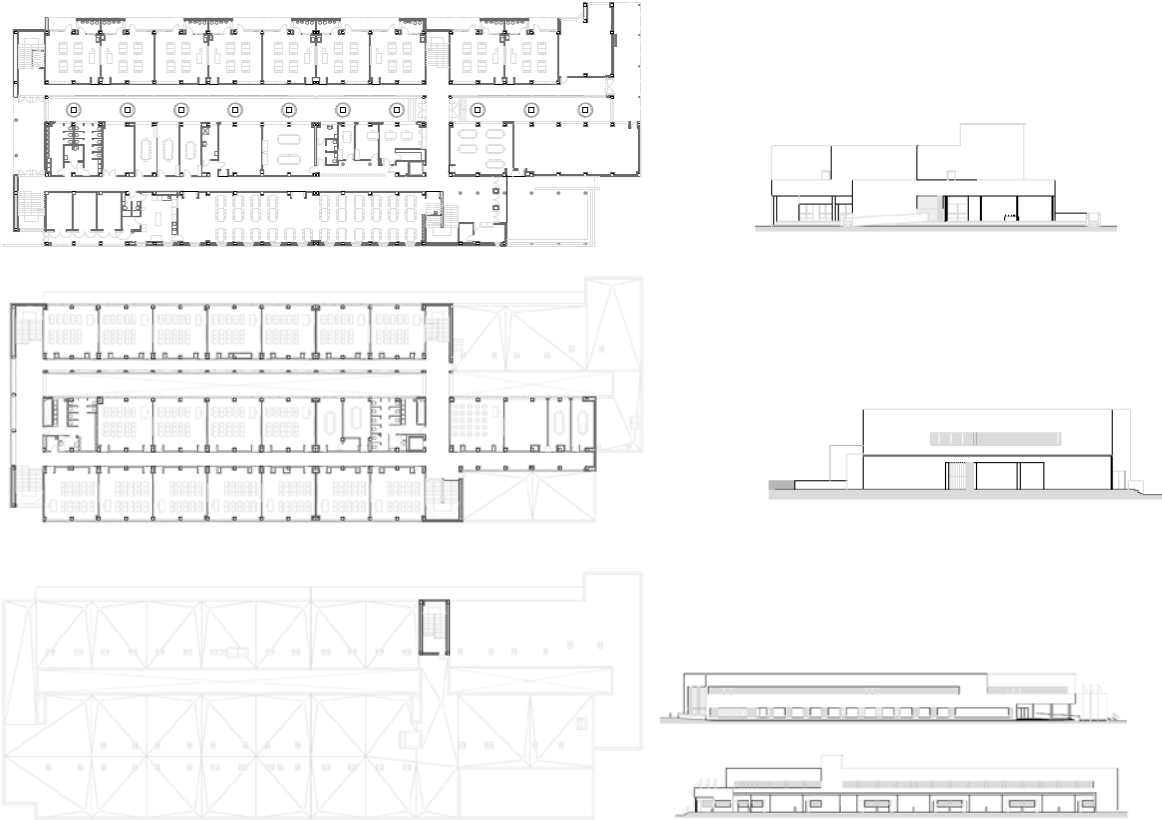


Figure 8Project plants and fronts (APAE\*)

The building is under construction and it is expected to be finished to the next scholar year and in operation since mid-September of 2017. Next images show the current construction works.



Figure Construction works images (APAE\*)

Considering project data, installed thermal power is 250.2 kW and installed electric power 294.5 kW, mainly due to the requirements of the mechanical ventilation system operation. Project data investment costs are 230,105 € for the MVS considering the electric transformer needed for the operation of this facility and 59,000 € for the NVS with a total investment cost of 4,464,839.49 €. NVS supposes in this case a 5.54% of the new building total cost.

### 3.3 Expected results

Project data presents a MVS with 6 machines (500 W; 2x1500 W and 3x11000 W). Considering 178 school days and the MVS operating an average of 4 hours per day, electric savings expected in terms of final energy is around 25.988 kWh per year. Even considering the energy use increase for heating, savings expected in terms of primary energy and CO<sub>2</sub> emissions could be around 52,770 kWh per year and 35.3 tons of CO<sub>2</sub> per year. Besides, maintenance costs and indoor comfort will be improved in addition to these.

## 4 CONCLUSIONS

The increase of the air-tightness in the buildings, thought to reduce energy savings is resulting in more ventilation requirements. Consequently, in 21th century's near zero energy buildings defined by European Directives, ventilation will be an essential design key.

Besides, in high density occupation rooms, as classrooms in schools, ventilation requirements are much more important than in other kind of buildings, so that if systems which use energy in their operation are designed to ventilate schools, these will have a high energy impact. In addition, in Mediterranean climate schools, ventilation is needed much more time than heating due to mild climate and internal gains.

Ventilation systems based in natural strategies offer the opportunity of ventilate with no energy consumption as well as to reduce the indoor overheating in autumn and spring seasons in mild climate locations. In addition more than 5.4% of initial investment cost can be saved, as well as electric power and maintenance costs due the operation of a mechanical system. Besides, these systems offer a healthier indoor environment in locations with an adequate outdoor air quality, thanks to they don't need filters and ducts which can suppose a source of contaminants if an adequate maintenance program is not followed.

A standard system model in classrooms has been included in a test building in which a measure program will be developed. This building is under construction and it will be operating next scholar year. With regard to project data, energy and CO<sub>2</sub> savings around 52,770 kWh and 35.3 tons of CO<sub>2</sub> in terms of final energy consumption and CO<sub>2</sub> emissions should be possible per year.

## 5 ACKNOWLEDGEMENTS

This study was performed as part of the ClimACT project (SOE1/P3/P0429EU) within the InterregSudoe Programme, funded by European Regional Development Funds.

We acknowledge APAE and everyone involved in the test building project their collaboration.

## 6 REFERENCES

- Agencia Andaluza de la energía. 2016. “ESTRATEGIA ENERGÉTICA DE ANDALUCÍA 2020.” : <https://www.agenciaandaluzadelaenergia.es/es/estra>.
- Air, Indoor, The Authors Journal, Blackwell Munksgaard, and Indoor Air. 2007. “Indoor Air Quality in Michigan Schools.” : 109–21.
- Almeida, Ricardo M S F, and Vasco Peixoto De Freitas. 2014. “Indoor Environmental Quality of Classrooms in Southern European Climate.” *Energy and Buildings* 81: 127–40.
- Almeida, Ricardo M S F, Nuno M M Ramos, and Vasco P De Freitas. 2016. “Thermal Comfort Models and Pupils’ Perception in Free-Running School Buildings of a Mild Climate Country.” *Energy & Buildings* 111: 64–75.
- “Assessment of Ventilation and Indoor Air Pollutants in Nursery and Elementary Schools in France.” 2016. : 350–65.
- Attia, Shady, and Salvatore Carlucci. 2015. “Impact of Different Thermal Comfort Models on Zero Energy Residential Buildings in Hot Climate.” *Energy and Buildings* 102: 117–28.
- Barrett, Peter, Fay Davies, Yufan Zhang, and Lucinda Barrett. 2015. “The Impact of Classroom Design on Pupils’ Learning: Final Results Ofaholistic, Multi-Level Analysis.” *Building and Environment* 89: 118–33.
- Bb101. 2006. Department for Education *Building Bulletin 101 Ventilation of School Buildings*.
- Chatzidiakou, Lia, Dejan Mumovic, and Alex James Summerfield. 2017. “What Do We Know about Indoor Air Quality in School Classrooms? A Critical Review of the Literature.” 8975(February).
- “Check and Improve the Energy Performance of Schools and Disseminate Best Practices - Intelligent Energy Europe - European Commission.” <https://ec.europa.eu/energy/intelligent/projects/en/projects/check-it-out> (March 23, 2017).
- Chenari, Behrang, João Dias Carrilho, and Manuel Gameiro da Silva. 2016. “Towards Sustainable, Energy-Efficient and Healthy Ventilation Strategies in Buildings: A Review.” *Renewable and Sustainable Energy Reviews* 59: 1426–47.
- “CIBSE - School Design Group.” <http://www.cibse.org/networks/groups/school-design> (March 22, 2017).
- CIBSETM57. 2015. *Integrated School Design*.
- “Classroom Ventilation and Indoor Air Quality — Results from the FRESH Intervention Study.” 2016. : 538–45.
- Comisión Europea. 2010. “Directiva 2010/31/UE Relativa a La Eficiencia Energética de Los

Edificios.” *Boletín Oficial* L135: 13–35.

Deng, S, R Z Wang, and Y J Dai. 2018. “How to Evaluate Performance of Net Zero Energy Building E A Literature Research.” *Energy* 71(2014): 1–16.

Desideri, Umberto et al. 2014. “Design of a Multipurpose ‘ Zero Energy Consumption ’ Building according to European Directive 2010 / 31 / EU : Life Cycle Assessment.” *Energy & Buildings* 80: 585–97.

“DesignBuilder Software Ltd - Home.” <https://www.designbuilder.co.uk/> (April 16, 2017).

“DOWNLOAD AREA | RENEW SCHOOL.” <https://www.renew-school.eu/en/links/download-area/> (March 23, 2017).

Erhorn-kluttig, Heike, and Hans Erhorn. 2014. “School of the Future – Towards Zero Emission with High Performance Indoor Environment.” *Energy Procedia* 48: 1468–73.

Europeo, E L Parlamento, E L Consejo, and D E L a Uni. 2003. “DIRECTIVA 2002/91/CE Relativa a La Eficiencia Energética de Los Edificios (DEEE).” *Directiva* 2002: 65–71.

Flourentzou, Flourentzos, and Samuel Pantet. 2014. “THEORETICAL AND REAL VENTILATION HEAT LOSSES AND ENERGY PERFORMANCE IN LOW ENERGY BUILDINGS.” (Mopec).

Flourentzou, Flourentzos, Samuel Pantet, and Katia Ritz. 2017. “Design and Performance of Controlled Natural Ventilation in School Gymnasiums.” *International Journal of Ventilation* 0(0): 1–12.

“Home.” <http://www.school-of-the-future.eu/> (March 23, 2017).

“Indoor Air Quality in Portuguese Schools : Levels and Sources of Pollutants.” 2016. : 526–37.

“Inive / International Network for Information on Ventilation and Energy Performance.” <http://www.inive.org>.

Jovanovi, Marina, Biljana Vu, Valentina Turanjanin, and Marija Zivkovi. 2014. “Investigation of Indoor and Outdoor Air Quality of the Classrooms at a School in Serbia.” 77: 42–48.

Kalimeri, Krystallia K et al. 2016. “Indoor Air Quality Investigation of the School Environment and Estimated Health Risks : Two-Season Measurements in Primary Schools in Kozani , Greece.” *Atmospheric Pollution Research* 7(6): 1128–42.

Khan, Naghman, Yuehong Su, and Saffa B Riffat. 2008. “A Review on Wind Driven Ventilation Techniques.” 40: 1586–1604.

Krawczyk, Dorota Anna. 2014. “Theoretical and Real Effect of the School’s Thermal Modernization - A Case Study.” *Energy and Buildings* 81: 30–37.

Luiz, Marcelo et al. 2015. “RISK ASSESSMENT FOR AIRBORNE INFECTIOUS

DISEASES BETWEEN NATURAL VENTILATION AND A SPLIT-SYSTEM AIR CONDITIONER IN A UNIVERSITY CLASSROOM.” : 1–5.

Ministerio de Industria, Energía Y Turismo. 2013. “Reglamento de Instalaciones Térmicas En Los Edificios.” : 137.

Oropeza-Perez, Ivan, and Poul Alberg Østergaard. 2014. “Potential of Natural Ventilation in Temperate Countries - A Case Study of Denmark.” *Applied Energy*.

“Passivhaus Institut.” [http://www.passiv.de/en/02\\_informations/02\\_passive-house-requirements/02\\_passive-house-requirements.htm](http://www.passiv.de/en/02_informations/02_passive-house-requirements/02_passive-house-requirements.htm) (March 23, 2017).

Pegas, P N et al. 2011. “Indoor Air Quality in Elementary Schools of Lisbon in Spring.” : 455–68.

Pikas, Ergo, Martin Thalfeldt, Jarek Kurnitski, and Roode Liias. 2015. “Extra Cost Analyses of Two Apartment Buildings for Achieving Nearly Zero and Low Energy Buildings.” *Energy* 84: 623–33.

“Promoting Renovation of Schools in a Mediterranean Climate up to Nearly Zero-Energy Buildings | ZEMedS.” <http://www.zemedes.eu/> (May 2, 2016a).

———. <http://www.zemedes.eu/> (March 23, 2017b).

Romana, Francesca, Elvira Ianniello, and Boris Igor. 2013. “PMV E PPD and Acceptability in Naturally Ventilated Schools.” *Building and Environment* 67: 129–37.

Rufo, João Cavaleiro et al. 2016. “Indoor Air Quality and Atopic Sensitization in Primary Schools: A Follow-up Study.” *Porto Biomedical Journal* 1(4): 142–46.

Severo, Milton et al. 2016. “Source Apportionment of CO<sub>2</sub>, PM<sub>10</sub> and VOCs Levels and Health Risk Assessment in Naturally Ventilated Primary Schools in Porto, Portugal ^ S Paci E.” 96: 198–205.

Stabile, Luca et al. 2016. “Effect of Natural Ventilation and Manual Airing on Indoor Air Quality in Naturally Ventilated Italian Classrooms.” *Building and Environment* 98: 180–89.

Sun, Yuming, Li Gu, C F Jeff Wu, and Godfried Augenbroe. 2014. “Exploring HVAC System Sizing under Uncertainty.” 81: 243–52.

“Teenergy Schools | High Energy Efficiency Schools in Mediterranean Area.” <http://teenergy.commpla.com/> (March 23, 2017).

Toftum, Jørn et al. 2015. “Association between Classroom Ventilation Mode and Learning Outcome in Danish Schools.” *Building and Environment* 92: 494–503.

“VERYSCHOOL.EU - Valuable Energy for a Smart School.” <http://www.veryschool.eu/> (May 2, 2016).

Wang, Yang et al. 2014. “Indoor Air Environment and Night Cooling Energy Efficiency of a Southern German Passive Public School Building Operated by the Heat Recovery Air

Conditioning Unit.” *Energy and Buildings* 81: 9–17.

Yang, Zheng, Ali Ghahramani, and Burcin Becerik-Gerber. 2016. “Building Occupancy Diversity and HVAC (Heating, Ventilation, and Air Conditioning) System Energy Efficiency.” *Energy* 109: 641–49.

Zhu, Zishang. 2014. “Assessment of the Technical Potential for Multifunction Building Zero-Carbon Renovation with EnergyPlus.” (November 2012): 178–88.

# Impact assessment of natural ventilation on thermal comfort levels in sustainable residential buildings

Elli Tsirintoulaki<sup>\*</sup>, Dionysia Kolokotsa, Konstantinos Gompakis and Nikolaos Kampelis

*Technical University of Crete, Environmental Engineering Department, GR 73100, Crete, Greece*

*\*Corresponding author: [etsirintoulaki@gmail.com](mailto:etsirintoulaki@gmail.com), [etsirintoulaki@isc.tuc.gr](mailto:etsirintoulaki@isc.tuc.gr)*

## ABSTRACT

In the present paper the impact of natural cross-ventilation on thermal comfort levels in sustainable residential buildings is evaluated. A sustainable dwelling is designed in Crete and various scenarios of different combinations of open windows and doors in the ground floor, the first floor and between the floors are tested to determine the final scenarios with the best possible airflow movement. Three scenarios with open windows and doors in the ground floor and six (6) between the floors (9 total scenarios) are chosen to be the final scenarios where the impact assessment of natural ventilation on thermal comfort levels is performed. Computational Fluid Dynamics (CFD) simulations with the 3D steady Reynolds-averaged Navier-Stokes (RANS) approach and the Shear Stress Transport (SST)  $k-\omega$  turbulence model are used for the study of thermal comfort levels, along with the Predicted Mean Vote (PMV) index. The Scenarios are tested for a typical summer day for four different hours and environmental conditions. The designed building is treated as a stand alone in all the simulations and it is not an existing construction. From the analysis of the results we observe that natural ventilation, in many cases, is an effective way to achieve indoor thermal comfort. In many Scenarios the high values of PMV from the Base Scenario (no windows or doors open) are decreased and in a few cases the values fall into the cold zone of comfort. The layout of the floors also affects the airflow movement in addition with the openings and the environmental conditions and can be used accordingly. According to the author's knowledge in the field of investigating natural ventilation via numerical approach simulation the present study is an original attempt to examine a more elaborate building architectural design and analyse performance in a dynamic way according to variable weather conditions.

## KEYWORDS

Natural ventilation, Thermal comfort, Computational Fluid Dynamics (CFD), Building simulation, Complex building geometry

## 1 INTRODUCTION

Natural ventilation is an alternative way to achieve indoor thermal comfort and healthy environmental conditions. It is linked to Indoor Air Quality (IAQ) and the comfort of the occupants as well as to the potential of reducing building energy consumption. Natural ventilation can be effectively used during the day for the improvement of thermal comfort levels and during the night for cooling the thermal mass of the building [1]–[5].

Over the years a lot of works study the impact of natural ventilation inside the buildings. For their study, some works [4]–[12] used field/experimental measurements or examined the natural ventilation in an existing building. In other works they preferred to use various software packages to model the study case and simulate the airflow pattern inside a space. Some used Flow Networks for their simulations [2], [13]–[15] while others used CFD analysis [1], [4], [5], [8], [11], [16]–[27].

According to the author's knowledge in the field of investigating natural ventilation via numerical approach simulation the present study is an original attempt to examine a more elaborate building architectural design. In most of the research works, the examined space, where the simulations were performed, had a simple geometry, except from three works [21],

[24], [27] where the effects of natural ventilation were examined in simple low-rise house geometry. In the work of Nikas et al [11] a simple cell is used but the impact of indoor layout on the indoor flow patterns from natural ventilation is examined.

The most common method for the evaluation of thermal comfort is the Predicted Mean Vote (PMV) with the Predicted Percentage Dissatisfied (PPD). PMV (Predicted Mean Vote) is a thermal comfort index. It was developed for the prediction of the human mean vote of thermal sensation from a large sample of people that was exposed to a given indoor environment. PMV has a 7 scale range from -3 to +3 (-3=cold, -2=cool, -1=slightly cool, 0=neutral, 1=slightly warm, 2=warm, 3=hot). The ideal value of PMV is 0, with a comfortable range from -0.5 to +0.5, but even in the comfortable zone some people will not be satisfied with the indoor temperature [28], [29].

Few works [2], [18], [30] address the results of their research to the architects and the necessity of taking into account natural ventilation systems from the early stage of architectural design. Bastile et al [18] studied the reduction of the energy consumption by natural ventilation and better bioclimatic design of the building and noted that the followed method is useful for an architect. Schulze et al [2] concluded that the method used, for their work, for the study of indoor airflow by natural ventilation can be used in the architectural design phase. Papamanolis [30] highlighted the importance of natural ventilation strategies, especially in Greece, as a design factor which is often ignored by the designers.

From literature we find that natural ventilation in buildings is still a concern and is studied with various software packages and field measurements. A numerical approach, mostly CFD, is used but there is no specific method in which provides best results, more accuracy and meets the computational demands. So far, the majority of the simulations are performed in a simple geometry and only one factor is investigated each time.

The objective of the present study is to assess the impact of natural cross-ventilation on thermal comfort levels in sustainable residential buildings. Alternative strategies were explored for the study of natural ventilation and the effect of a complex two story building geometry, with its inner layout, on indoor airflow patterns and thermal comfort levels for four different environmental conditions. Moreover, the thermal comfort is studied on seven human figures (Avatars) located in various spaces of the residence, and not just on some points in a specific height or plane of the building volume. In all the simulations the building is isolated modelled and various software packages are included in this research for the required simulations.

## 2 ARCHITECTURAL DESIGN

The building has openings in the North, East and South directions, avoiding completely the West. The floor plan of the house is elongated with the long sides facing the north-south direction. In the ground floor an open space of the Living room-Kitchen-Dining room is created and on the first floor the two bedrooms and the office are placed. The living room has N and S orientation, the kitchen E and N and the dining room S, but the open space layout of the ground floor allows the diffusion of light in the various areas. In the living room there is a two-story open space which allows communication with the hallway on the first floor and a two-story northern opening that creates a sense of unity. The office has N and E openings and the two bedrooms have E and S openings. The laundry and the 3 bathrooms are located in the western area of the residence with N and S windows. The floor plans of the residence are presented in **Figure 2.1** below.

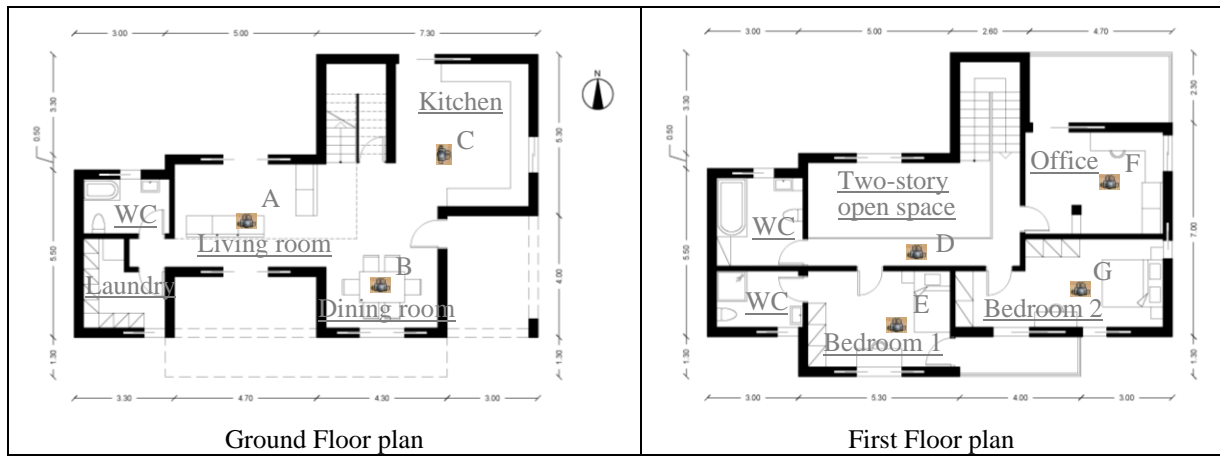


Figure 2.1 Floor plans and position of the Avatars inside the building

### 3 NATURAL VENTILATION MODELLING

For the study of natural ventilation and thermal comfort levels, the climate data of four hours of a typical summer day are chosen. The examined environmental conditions, as they were recorded from the meteorological station, are presented in the **Table 3.1** below.

Table 3.1 The examined outdoor conditions for the selected hours

Time	Temperature (°C)	Relative Humidity (%)	Wind speed (m/s)
2:00	25	65	2
8:00	25	65	1
14:00	30	40	7
20:00	27	50	5.5

#### 3.1 CFD simulation: computational settings and parameters

Regarding the creation of the model in Autodesk CFD [31] for the simulation of natural ventilation inside a building and its impact on thermal comfort levels, there are no specific instructions. From research, tutorials and documentation of the Autodesk Knowledge Network the following methodology is created. In this work, the building is treated as stand alone case for the CFD analysis. The steps for the model creation are:

- Creation of the building geometry in Revit
- Set of the orientation of the building, so that the domain in Autodesk CFD is on the x&y axes and the wind direction (NW) is on the y axis (it was observed that the software responded a little better if the domain was aligned to the axis)
- Hide, in the 3D view, the selected windows/doors that will be open in the simulation
- Launch in Autodesk CFD
- Use the Geometry Tools to:
  - Merge edges
  - Fill Void, to create the air volume inside the building since there are some windows/doors open
  - Create the Domain, the air volume of the environment around the building (150 × 150 × 30m)
- Assign the Materials in the imported geometry

- Assign the Boundary Conditions, velocity and temperature for inlet and pressure=0 for outlet for the domain and 70W heat generation for the human figures
- Set initial conditions, 26°C for the inside air volumes
- Create the Mesh of the model
- From the Solve dialog:
  - Set the Thermal Comfort Factors, Metabolic rate 60W/m<sup>2</sup>, Clothing 0.36clo and Relative Humidity (different values)
  - The location of the building, the study time and day and the orientation
  - For the turbulence the SST k- $\omega$  model is chosen
  - The PMV index is used for the thermal comfort assessment
- Run the Scenario

### 3.2 Presentation of the examined Scenarios

For the airflow movement inside the dwelling various scenarios were simulated in Blender software with the basic CFD plug-in and in Autodesk CFD. The examined Scenarios are presented in the **Figure 3.1** below.

Scenario	NE Perspective view	SE Perspective view	Openings
1			<u>Inlet:</u> N glass door of the living room <u>Outlet:</u> S window of the dining room
2			<u>Inlet:</u> N glass door of the living room <u>Outlet:</u> E kitchen window
3			<u>Inlet:</u> N glass door of the kitchen <u>Outlet:</u> S glass door of the living room
4			<u>Inlet:</u> N glass door of the living room <u>Outlet:</u> S window of the bedroom 1

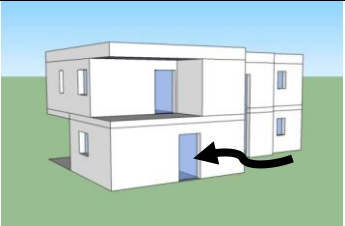
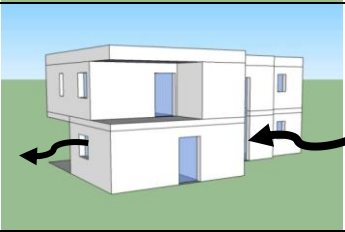
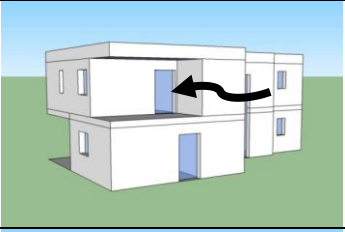
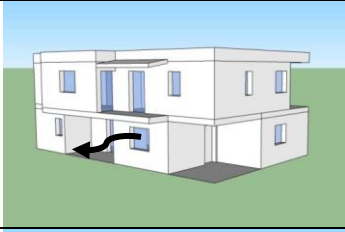
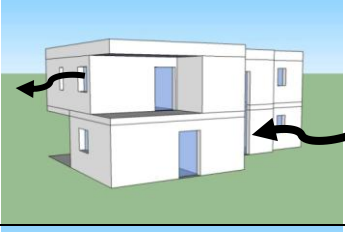
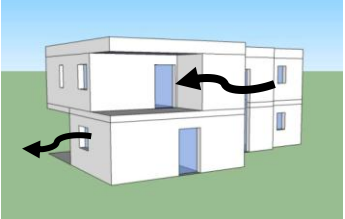
5			<u>Inlet:</u> N glass door of the kitchen <u>Outlet:</u> S window of the bedroom 1
6			<u>Inlet:</u> N glass door of the living room <u>Outlet:</u> S window of the bedroom 1 and E kitchen window
7			<u>Inlet:</u> N glass door of the office <u>Outlet:</u> S glass door of the living room
8			<u>Inlet:</u> N glass door of the living room <u>Outlet:</u> E window of the office
9			<u>Inlet:</u> N glass door of the office <u>Outlet:</u> S glass door of the living room and E kitchen window

Figure 3.1 Examined Scenarios

For the evaluation of the thermal comfort levels, seven (7) human figures (Avatars) are placed in the examined spaces of the building as they are depicted in **Figure 2.1**. One Avatar is placed in a room that is not examined to see if the changed conditions in the other spaces will affect it.

#### 4 RESULTS ANALYSIS AND DISCUSSION

In this section the results and analysis of Scenario 5 are presented. The airflow pattern inside the building, in 3D view, from the first set of simulations in Blender, and the airflow movement and PMV values of the Avatars, from the second set of simulations in Autodesk CFD, are depicted and discussed. From the thermal comfort results, PMV values appear on the body of the Avatars. In this study the PMV value on the heads of the Avatars is measured but not without leaving uncommented the thermal comfort levels on the rest of the body.

### 4.1 Scenario 5: openings in the kitchen and bedroom

In Scenario 5 the northern glass door of the kitchen (inlet) and the northern window of bedroom 1 (outlet) are open (**Figure 4.1**). The air is moving fast through the kitchen and the bedroom but stays in the dining and living room exploiting the height of the open space.

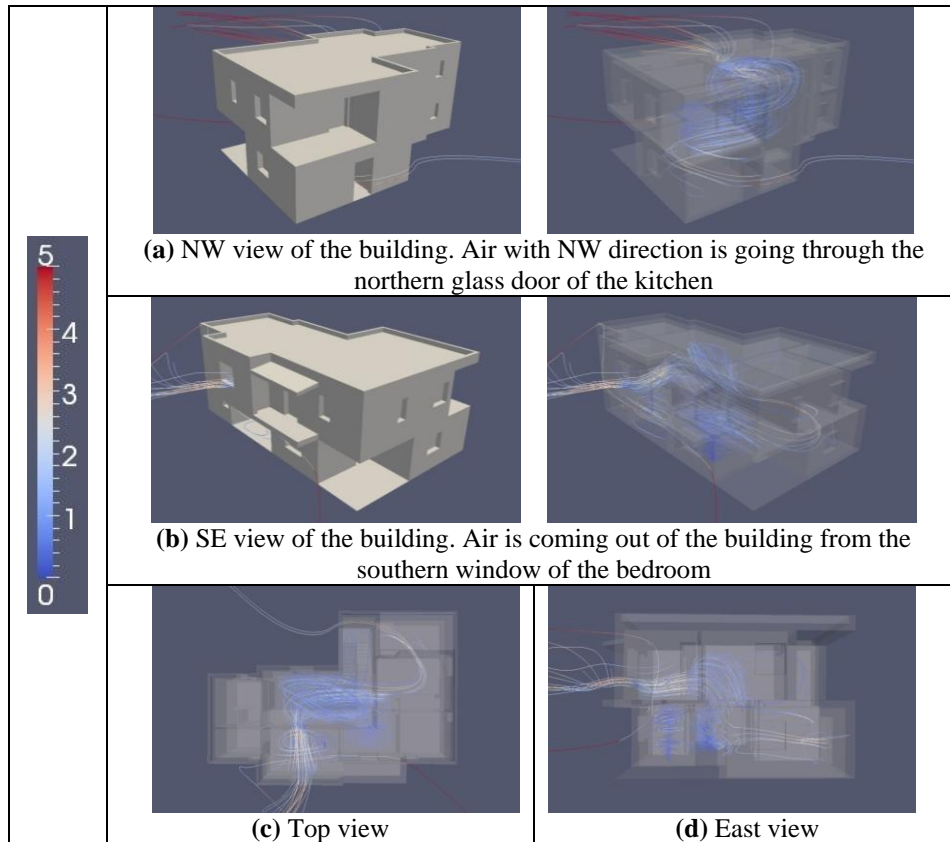
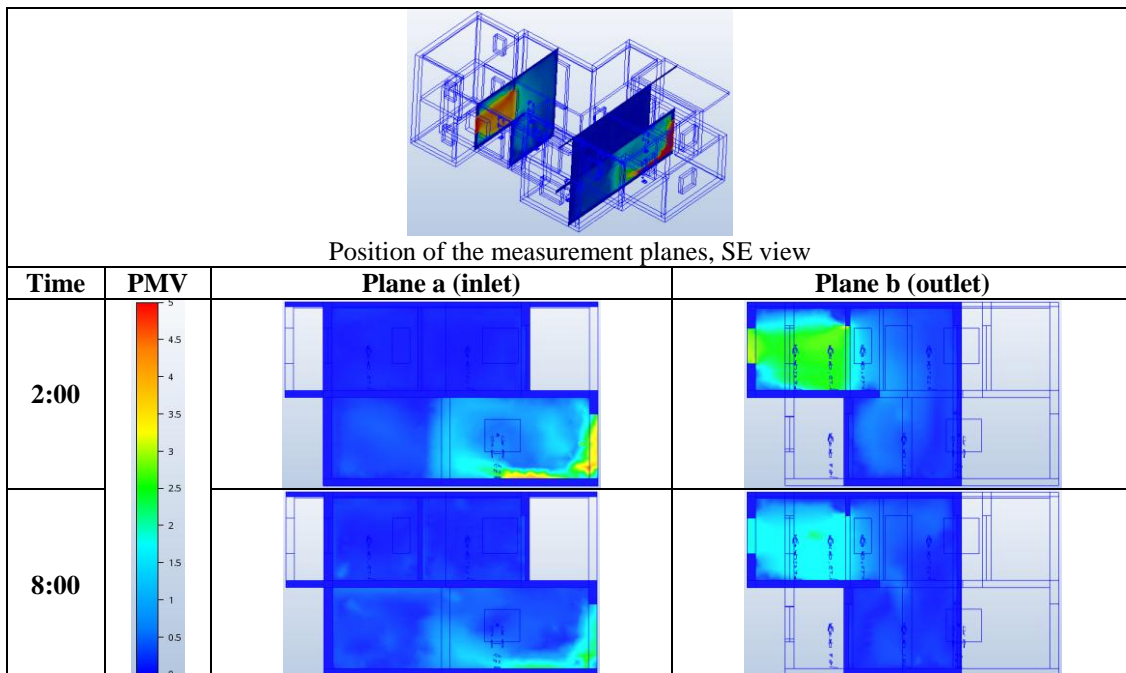


Figure 4.1 Airflow movement inside the building



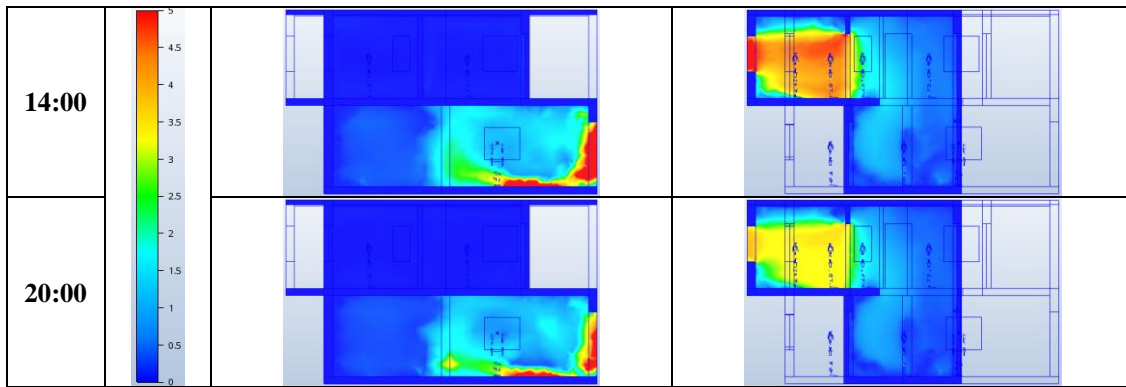


Figure 4.2 Velocity results for the four examined hours of the day

In the **Figure 4.2** below the measurement planes a (inlet) and b (outlet) are presented. The highest velocity is recorded close to the inlet kitchen opening and in the bedroom space. The air that is moving in the two story open space reaches 2m/s velocity at 14:00 and 20:00 o'clock. For the cases of 2:00 and 8:00 o'clock the maximum air speed is around 2m/s and for the 14:00 and 20:00 o'clock around 5m/s.

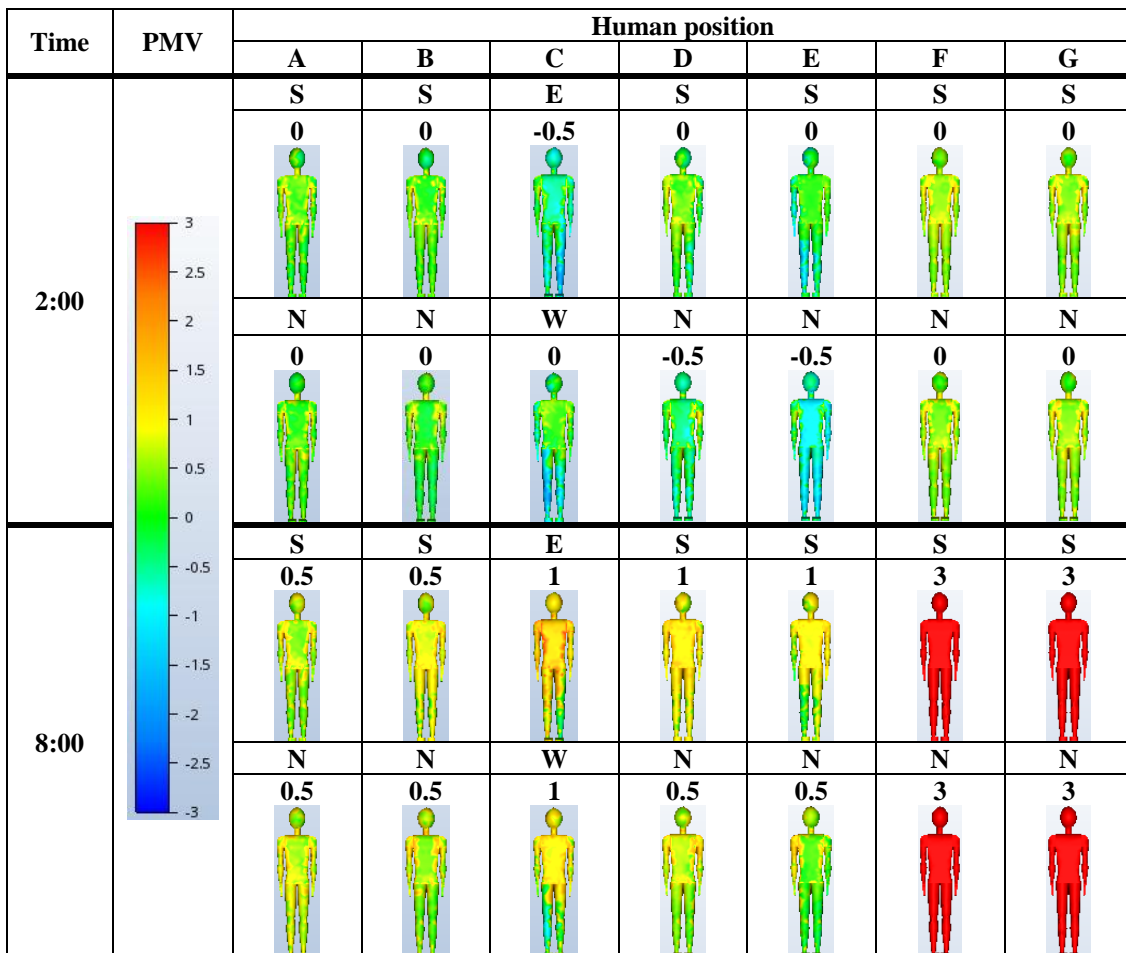


Figure 4.3 Detailed PMV results of the Avatars inside the building (A-G: position, S-E-N-W: orientation)

In the **Figure 4.3** above at 2:00 o'clock, Avatars C, D and E present a decrease of their PMV values but they remain in the comfort zone. Avatar C records high negative values on the legs, where the air is moving with high speed, and Avatar E on the northern side of the body where the air is coming from. In the case of 8:00 o'clock (**Figure 4.3**) the PMV of the Avatars A and

B is in the comfort zone, while the values of the Avatars C, D and E are moving around the high end of the comfort zone.

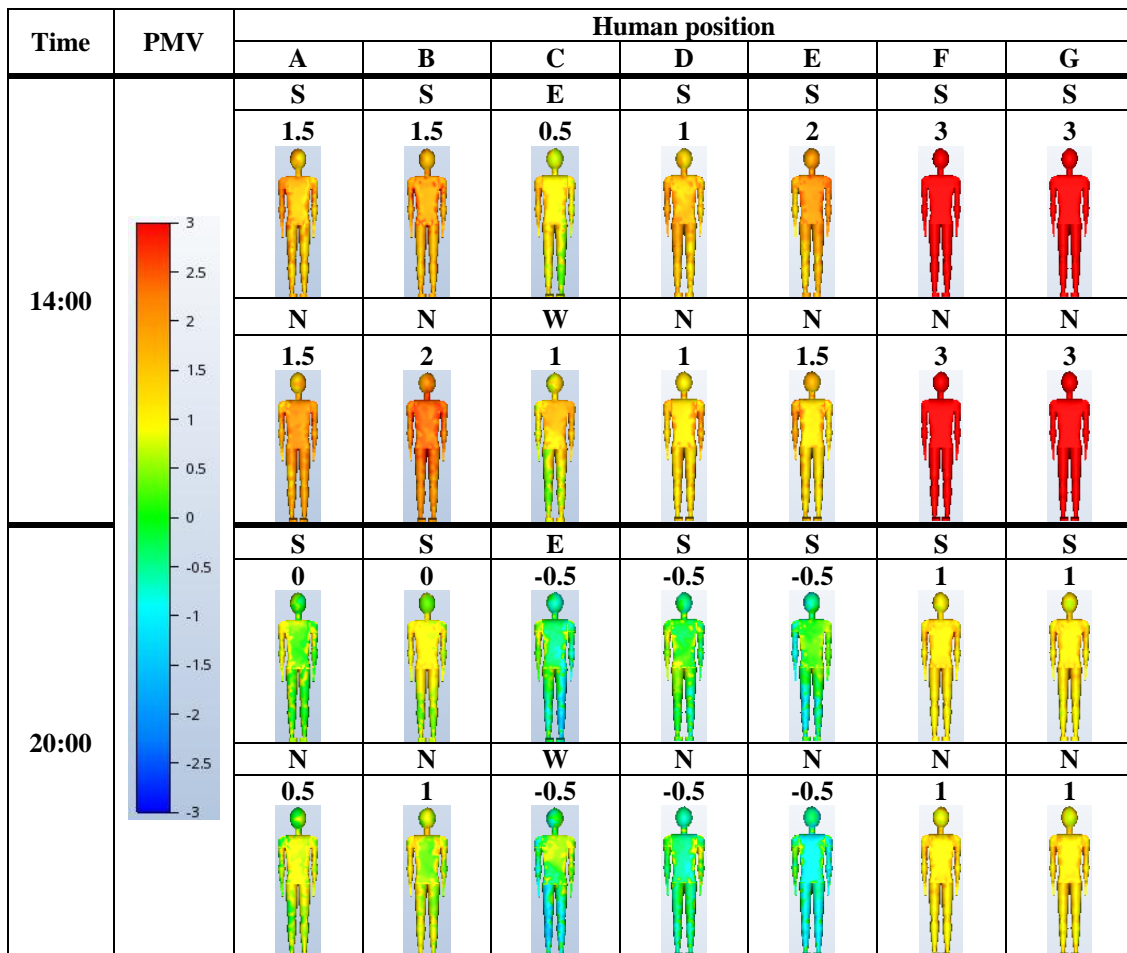


Figure 4.4 Detailed PMV results of the Avatars inside the building (A-G: position, S-E-N-W: orientation)

In the 14:00 o'clock case (**Figure 4.4**) none of the Avatars present PMV values in the comfort zone but Avatar C is close with a value of 0.75. At 20:00 o'clock (**Figure 4.4**) the PMV of the Avatars C, D and E is located in the low end of the comfort zone but higher negative values are observed on their legs.

Avatars F and G are in spaces that the air cannot reach, therefore they do not record any difference in the PMV values in any case of this Scenario.

## 5 CONCLUSIONS

In the presented paper the impact of natural cross-ventilation of sustainable residential buildings on thermal comfort levels is evaluated. A residence with bioclimatic parameters is designed in Chania, Crete, and is modelled for the study of the indoor airflow pattern, created by natural wind-driven cross-ventilation, from the different selection of the openings. Nine Scenarios of the previous study are chosen for the assessment of indoor thermal comfort. In all the simulations the building is isolated modelled.

A two story open space between the floors seems to be significant for the air movement and cooling of all the possible areas of the building, even if there are no open windows on the upper floor. The impact of the floors' layout on the indoor airflow needs to be studied and taken into account from the early stages of the architectural design. The geometry of the building, as well as the position of the selected openings affect the conditions of the incoming air. The position and orientation of the outlet opening regarding the inlet opening must be

cautiously selected so the architectural design and environmental conditions can be best exploited. The asymmetric position of the selected openings is suggested for a better movement of the air inside the building.

Naturally wind-driven ventilation appears to be an effective way of cooling the building in many cases during the day. In the majority of the cases the thermal comfort levels drop 1 thermal zone and in many cases two thermal zones. Night ventilation is able to provide comfortable indoor conditions, but in a few cases it can drop the thermal comfort levels in the cool zone of comfort and thus creating uncomfortable conditions. The selected openings must be chosen regarding the environmental conditions, indoor conditions and the spaces that need cooling.

From this research it is also concluded that for the study of natural indoor ventilation and thermal comfort levels on a complex building geometry, the followed methodology can be applied. Natural ventilation has a significant impact on the quality of living standards and energy consumption and needs to be acknowledged both from the architects and the occupants. CFD simulations can be effectively used for the study of natural ventilation and the provided information can be used in the early stage of architectural design. Software packages prove to be a useful tool for the architects and other professionals and are frequently used for similar studies for the purpose of understanding and designing of appropriate actions.

## 6 REFERENCES

- [1] T. Ayata and O. Yıldız, "Investigating the potential use of natural ventilation in new building designs in Turkey," vol. 38, pp. 959–963, 2006.
- [2] T. Schulze and U. Eicker, "Controlled natural ventilation for energy efficient buildings," *Energy Build.*, vol. 56, pp. 221–232, 2013.
- [3] M. Santamouris and D. Kolokotsa, "Passive cooling dissipation techniques for buildings and other structures : The state of the art," *Energy Build.*, vol. 57, pp. 74–94, 2013.
- [4] G. M. Stavrakakis, M. K. Koukou, M. G. Vrachopoulos, and N. C. Markatos, "Natural cross-ventilation in buildings : Building-scale experiments , numerical simulation and thermal comfort evaluation," vol. 40, pp. 1666–1681, 2008.
- [5] G. Evola and V. Popov, "Computational analysis of wind driven natural ventilation in buildings," vol. 38, pp. 491–501, 2006.
- [6] X. Su, X. Zhang, and J. Gao, "Evaluation method of natural ventilation system based on thermal comfort in China," vol. 41, pp. 67–70, 2009.
- [7] N. H. Wong, H. Feriadi, P. Y. Lim, K. W. Tham, C. Sekhar, and K. W. Cheong, "Thermal comfort evaluation of naturally ventilated public housing in Singapore," vol. 37, pp. 1267–1277, 2002.
- [8] S. Cui, P. Stabat, and D. Marchio, "Numerical simulation of wind-driven natural ventilation : Effects of loggia and facade porosity on air change rate," *Build. Environ.*, vol. 106, pp. 131–142, 2016.
- [9] C. Chu, Y. Chiu, Y. Tsai, and S. Wu, "Wind-driven natural ventilation for buildings with two openings on the same external wall," *Energy Build.*, vol. 108, pp. 365–372, 2015.
- [10] P. Karava, T. Stathopoulos, and A. K. Athienitis, "Airflow assessment in cross-ventilated buildings with operable façade elements," vol. 46, pp. 266–279, 2011.
- [11] K. Nikas, N. Nikolopoulos, and A. Nikolopoulos, "Numerical study of a naturally cross-ventilated building," *Energy Build.*, vol. 42, no. 4, pp. 422–434, 2010.
- [12] D. Kolokotsa, G. Saridakis, A. Pouliezos, and G. S. Stavrakakis, "Design and installation of an advanced EIB ( TM ) fuzzy indoor comfort controller using Matlab ( TM )," no. October 2015, 2006.

- [13] A. L. Pisello, V. L. Castaldo, J. E. Taylor, and F. Cotana, "The impact of natural ventilation on building energy requirement at inter-building scale," *Energy Build.*, vol. 127, pp. 870–883, 2016.
- [14] J. Good, A. Frisque, and D. Phillips, "The role of wind in natural ventilation simulations using airflow network models," 2008.
- [15] O. Kinnane, D. Sinnott, and W. J. N. Turner, "Evaluation of passive ventilation provision in domestic housing retrofit," *Build. Environ.*, vol. 106, pp. 205–218, 2016.
- [16] J. A. Castillo and G. Huelsz, "A methodology to evaluate the indoor natural ventilation in hot climates: Heat Balance Index," *Build. Environ.*, vol. 114, pp. 366–373, 2016.
- [17] M. A. Menchaca-Brandan, F. A. Dominguez Espinosa, and L. R. Glicksman, "The influence of radiation heat transfer on the prediction of air flows in rooms under natural ventilation," *Energy Build.*, vol. 138, pp. 530–538, 2017.
- [18] A. Bastide, P. Lauret, and H. Boyer, "Building energy efficiency and thermal comfort in tropical climates Presentation of a numerical approach for predicting the percentage of well-ventilated living spaces in buildings using natural ventilation," vol. 38, pp. 1093–1103, 2006.
- [19] E. Prianto and P. Depecker, "Characteristic of airflow as the effect of balcony , opening design and internal division on indoor velocity A case study of traditional dwelling in urban living quarter in tropical humid region," vol. 34, pp. 401–409, 2002.
- [20] W. Liping and W. N. Hien, "The impacts of ventilation strategies and facade on indoor thermal environment for naturally ventilated residential buildings in Singapore," vol. 42, pp. 4006–4015, 2007.
- [21] O. A. R. Mohamad Mohd Faizal, Hagishima Aya, Tanimoto Jun, Ikegaya Naoki, "Wind-induced natural ventilation in typical single storey terraced houses in Malaysia," pp. 587–593, 2013.
- [22] S. Gilani, H. Montazeri, and B. Blocken, "CFD simulation of stratified indoor environment in displacement ventilation : Validation and sensitivity analysis," *Build. Environ.*, vol. 95, pp. 299–313, 2016.
- [23] T. Van Hooff, B. C. C. Leite, and B. Blocken, "CFD analysis of cross-ventilation of a generic isolated building with asymmetric opening positions : Impact of roof angle and opening location," vol. 85, 2015.
- [24] A. Baghaei Daemei, A. Khalatbari Limaki, and H. Safari, "Opening Performance Simulation in Natural Ventilation using Design Builder (Case Study: A Residential Home in Rasht)," vol. 100, pp. 412–422, 2016.
- [25] T. Van Hooff, B. C. C. Leite, and B. Blocken, "CFD simulation of wind-driven upward cross ventilation and its enhancement in long buildings : Impact of single-span versus double-span leeward sawtooth roof and opening ratio," vol. 96, pp. 142–156, 2016.
- [26] T. Van Hooff, B. Blocken, and Y. Tominaga, "On the accuracy of CFD simulations of cross-ventilation flows for a generic isolated building : Comparison of RANS , LES and experiments," *Build. Environ.*, vol. 114, pp. 148–165, 2017.
- [27] S. Hawendi and S. Gao, "Impact of an external boundary wall on indoor flow field and natural cross-ventilation in an isolated family house using numerical simulations," *J. Build. Eng.*, vol. 10, no. December 2016, pp. 109–123, 2017.
- [28] P. O. Fanger, *Thermal Analysis and Applications in Environmental Engineering*. New York: McGraw-Hill, 1970.
- [29] B. W. Olesen and K. C. Parsons, "Introduction to thermal comfort standards and to the proposed new version of EN ISO 7730," vol. 34, 2002.
- [30] N. Papamanolis, "Natural ventilation as a design factor in buildings in Greece," *Archit. Sci. Rev.*, vol. 43, no. 4, pp. 175–182, 2000.
- [31] "Autodesk Knowledge Network." [Online]. Available: <https://knowledge.autodesk.com/>. [Accessed: 28-Apr-2017].

# Inter-model comparison of indoor overheating risk prediction for English dwellings

Giorgos Petrou<sup>\*1</sup>, Anna Mavrogianni<sup>2</sup>, Anastasia Mylona<sup>3</sup>, Rokia Raslan<sup>2</sup>, Gurdane Virk<sup>4</sup> and Michael Davies<sup>2</sup>

*1 UCL Energy Institute,  
University College London,  
Central House, 14 Upper Woburn Place  
London WC1H 0NN, United Kingdom  
Email: giorgos.petrou.16@ucl.ac.uk*

*2 UCL Institute for Environmental Design  
and Engineering  
University College London,  
Central House, 14 Upper Woburn Place  
London WC1H 0NN, United Kingdom*

*3 CIBSE  
222 Balham High Road  
London SW12 9BS, United Kingdom*

*4 Atkins  
Euston Tower, 286 Euston Rd, Kings Cross,  
London NW1 3AT, United Kingdom*

## ABSTRACT

According to the 2016 Household Projections report, England's housing stock could reach 28 million households by 2039 with approximately one fifth being new constructions. A significant proportion of these newly built dwellings may face a high risk of overheating as a result of the combined effects of climate change and more stringent building thermal efficiency standards, if not appropriately designed. Reliable methods for predicting indoor overheating risk are required to avoid potentially negative impacts of excess indoor temperature exposure on occupant thermal comfort and wellbeing while simultaneously minimising the use of mechanical ventilation and cooling. Building Energy Simulation (BES) software are widely used in the building construction industry to estimate the overheating risk of new developments. CIBSE's recently released methodology for predicting overheating in new dwellings aims to achieve consistency between existing prediction methods currently applied by building designers and engineers. BES tools are abstract representations of reality and large differences in model outputs are often observed between tools. The level of overheating risk predicted through the CIBSE method may hence depend on the choice of software and its underlying assumptions. Such an effect could directly impact CIBSE's efforts in creating a standardised procedure across the industry. This research project utilised inter-model comparison along with sensitivity analysis to investigate the differences in overheating risk prediction between two commonly used software packages, *EnergyPlus* and *IES VE*. The sensitivity analysis resulted in a total of nine variations of the single-aspect, high-rise flat, simulated in each software. Looking at individual models, there was a general agreement between neither software's predictions and the literature's suggestions on the factors that may be driving overheating. Measures such as increased thermal mass, external shading, north-facing direction and cross-ventilation lowered the predicted risk. However, discrepancies between software were observed with only two *EnergyPlus* models successfully meeting both overheating criteria, compared to all the *IES VE* models. This work therefore concludes that the choice of BES tool could greatly impact the predicted risk of overheating.

## KEYWORDS

Overheating, Simulations, Inter-model Comparison, Sensitivity Analysis, Thermal Comfort

## 1 INTRODUCTION

Overheating qualitatively describes the condition under which occupants of a dwelling feel uncomfortably hot due to the indoor environment (CIBSE, 2013). Indoor comfort and wellbeing is crucial for human health since people spend most of their time inside buildings (WHO, 2009). Concerns regarding overheating have intensified recently. Along with the projected rise in ambient temperature, climate change is expected to cause an increase in

the frequency and severity of extreme heat episodes (Murphy et al., 2009). Such events have been catastrophic in the past, with the 2003 European heatwave leading to an increase in mortality of more than 2,000 in England and Wales (Johnson et al., 2005), and nearly 15,000 in France (Fouillet et al., 2006). An increase in overheating risk may also be an unintended consequence of current building regulations due to the increased levels of thermal insulation and airtightness required (HMG, 2016; Shrubsole et al., 2014).

An important step in mitigating overheating is its accurate and systematic prediction (ZCH, 2015). To encourage the design of thermally comfortable homes, the Chartered Institution of Building Services Engineers (CIBSE) has recently released the Technical Memorandum 59 (TM59), a new methodology for the application of Building Energy Simulation (BES) software to predict the overheating risk in new homes (CIBSE, 2017). Although such software have powerful dynamic modelling capabilities, they are still limited by their core assumptions. Given the exact same inputs, two BES tools may generate different predictions of building energy and thermal performance due to their algorithmic differences (R. Judkoff & Neymark, 1995; Crawley et al., 2008; Raslan, 2010).

EnergyPlus and IESVE are two commonly used BES tools in academic research and the construction industry (EnergyPlus, 2017a; IES VE, 2017a). They have both been validated and verified in the past (EnergyPlus, 2017b; IES VE, 2017b). One of the most commonly used testing procedures is the Building Energy Simulation Test (BESTEST) (R. Judkoff & Neymark, 1995). This is a structured method of comparison between software on progressively more complex models. A set number of models with predefined inputs are simulated in BES tools and a comparison of the results indicates the differences in the simulation engines. This method is now the basis of the ANSI/ASHRAE 140 standard (Ron Judkoff & Neymark, 2006). Although this assessment has aided in the identification and subsequent resolution of many internal errors, no such comparative procedure has focused on overheating. However, an important finding with regards to overheating emerges from the most recently published BESTEST results for IES VE and EnergyPlus: for many of the models tested, the maximum and average temperature predicted by EnergyPlus was greater than for IES VE by more than 1 °C (EnergyPlus, 2017b; IES VE, 2017b).

This has motivated the work presented in this paper, which aims to establish how the choice of BES tool may impact the overheating assessment. In particular, it aims to quantify and analyse potential discrepancies between EnergyPlus and IES VE for a typical English dwelling archetype. This is achieved by evaluating the overheating risk for both software under different input variations. Through this process, useful conclusions on the implementation of CIBSE's new methodology are drawn, which may also inform and motivate further research in the prediction of overheating risk.

## 2 LITERATURE REVIEW

CIBSE TM52 suggested three methods for predicting overheating risk (CIBSE, 2013): (i) Building Energy Simulations (BES), (ii) monitoring, (iii) questionnaire surveys. All three methods may be used for existing buildings but only the BES method can be employed to predict the overheating risk in new dwellings. For predominantly naturally ventilated homes, compliance is based on successfully meeting the following two criteria (CIBSE, 2017):

1. The number of hours for which  $\Delta T = T_{op} - T_{max}$  is greater or equal to one degree Celsius during the period May to September, inclusive, should not exceed 3% of the occupied hours (hours of exceedance).
2. The bedroom's operative temperature ( $T_{op}$ ) should not exceed 26°C for more than 1% of the annual occupied hours (22:00-07:00). This is equivalent to 32 hours in a year.

Operative temperature ( $T_{op}$ ) is the weighted mean of the room's air and radiant temperature (CIBSE, 2015).  $T_{max}$  is the maximum acceptable comfort temperature based on the thermal comfort model presented in (CIBSE, 2013). In the case of vulnerable occupants or predominantly mechanically ventilated dwellings, the criteria are slightly modified (CIBSE, 2013, 2017).

## 2.1 Overheating

Previous modelling studies are generally in agreement with respect to the determinant factors of building overheating. Hacker et al. (Hacker et al., 2008) established that an increase in thermal mass leads to more stable temperatures and a lower risk of overheating. Mavrogianni et al. (Mavrogianni et al., 2009) identified the dwelling's floor level to be a key factor, with an increase of 50% in the likelihood of heat-related death for the tallest buildings compared to the average in height buildings in London. Taylor et al. (Taylor et al., 2014) demonstrated that the building's orientation is greatly influential on overheating. In a more recent study, Mavrogianni et al. (Mavrogianni et al., 2017) identified internally positioned wall and floor insulation to be positively correlated with high indoor temperatures, while occupant behaviour was recognised as another highly influential factor for overheating. This was also recognised in an empirical validation study of an overheating model by Symonds et al. (Symonds et al., 2017). The importance of natural ventilation as a preventive measure of overheating was discussed by Porritt et al. (Porritt et al., 2012), who identified controlled natural ventilation, especially night-cooling, to be particularly important.

## 2.2 Sensitivity Analysis and Inter-model comparison

Sensitivity analysis is a valuable method of establishing the effect of inputs on key outputs (Tian, 2013). This method has been employed in the past in the field of overheating to determine some key factors of overheating homes (Mavrogianni et al., 2014; Mavrogianni et al., 2017) or to calibrate BES models (Pereira, Bögl, & Natschläger, 2014). In its simplest form, Local Sensitivity Analysis (LSA) is performed by varying one factor at a time and observing its impact on the output of interest (Tian, 2013). Statistical analysis may then be used to quantify its importance.

Inter-model comparison is a structured way of establishing disagreements between software (Raslan, 2010). The same input is compiled for both software and used to create the closest possible models. Following the simulation, the output is compared and analysed to determine the level of agreement.

## 3 METHODS & METHODOLOGY

An inter-model comparison was performed in parallel to an LSA to determine differences in predictions for nine variations of the base case (BC), as described in Table 1. For each model, the statistical significance of the difference in the mean operative bedroom temperatures between the two software was assessed using a two-tailed t-test, with the null hypothesis being that temperatures should be similar within a 95% confidence interval.

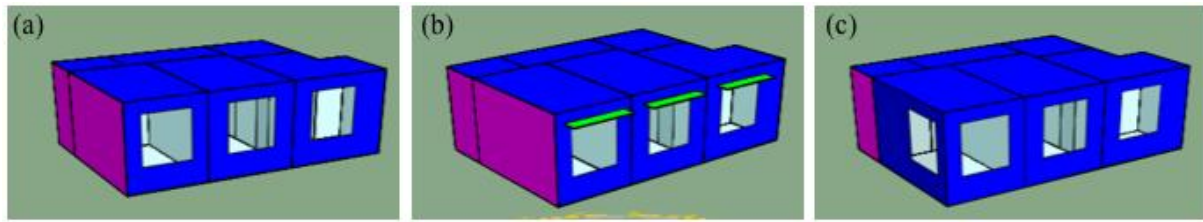


Figure 1: Visualisations of the base case (a), case with external shading (b) and the dual aspect case (c) using the IES VE Model Viewer II.

The base case (Figure 1) dwelling is a naturally ventilated, free-running, single aspect, top-floor flat originally created by Oikonomou et al. (Fig. 2, Model VII Oikonomou et al., 2012). The thermal properties of the building's fabric and windows complied with the most recent building regulations for new builds (HMG, 2016). Infiltration rate was kept constant for all models, based on an air permeability of  $5.0 \text{ m}^3/(\text{h}\cdot\text{m}^2)$ , with an added air exchange of  $13 \text{ l}\cdot\text{s}^{-1}$  for the kitchen and  $8 \text{ l}\cdot\text{s}^{-1}$  for the bathroom (HMG, 2013, 2016). The Design Summer Year 1 CIBSE Weather File was used, with the specified location being the London Weather Centre (CIBSE, 2017). The internal gains for a double bedroom flat with separate living room and kitchen were modelled as instructed in TM59 (CIBSE, 2017). Throughout the day, TM59 requires the opening of windows when the internal temperature of an occupied room exceeds  $22 \text{ }^\circ\text{C}$ . Although EnergyPlus will model the opening of windows when a threshold is exceeded, it will only do so if the internal temperature is higher than the external. As ventilation was expected to be a critical factor, IES VE was set to operate windows in a similar manner as EnergyPlus. Internal doors were modelled to be open only during the waking hours (08:00-23:00). The bedroom was occupied at all times, while the kitchen and living room were modelled as occupied between 09:00-22:00.

Table 1: A summary of the different variations of the basic model simulated.

Code	Description
BC	Floor level: 11.2 m, orientation: south facing, single aspect, top level flat, Lightweight construction: Timber frame, external brick layer and internal plasterboard U-values: Wall – $0.17 \text{ W/m}^2\text{K}$ , window – $1.28 \text{ W/m}^2\text{K}$ , floor – $0.18 \text{ W/m}^2\text{K}$ , roof – $0.13 \text{ W/m}^2\text{K}$
G	Ground-Level Flat, floor Level: 0 m, flat of similar temperature above
M	Mid-level flat, floor level: 5.6 m, flats of similar temperature above and below
W	West-facing flat
N	North-facing flat
E	East-facing flat
HW	Heavyweight construction: Concrete blocks, external brick layer, internal dense plaster and carpet
SH	Shading: Overhang external shading, length of 2.2 m and width of 0.5 m over windows
DA	Dual aspect model with a second window included in the bedroom

## 4 RESULTS

Following the methods described in section 3, the overheating risk was evaluated for all models and is presented in Figure 2. A simple inspection reveals the discrepancy in predictions between the two software, with only two out of the nine models passing both TM59 criteria for EnergyPlus, contrary to the success of every model simulated in IES VE. In general, overheating risk does appear to increase with floor level for both software. Orientation also appears to be a driving factor of overheating in both software, as suggested

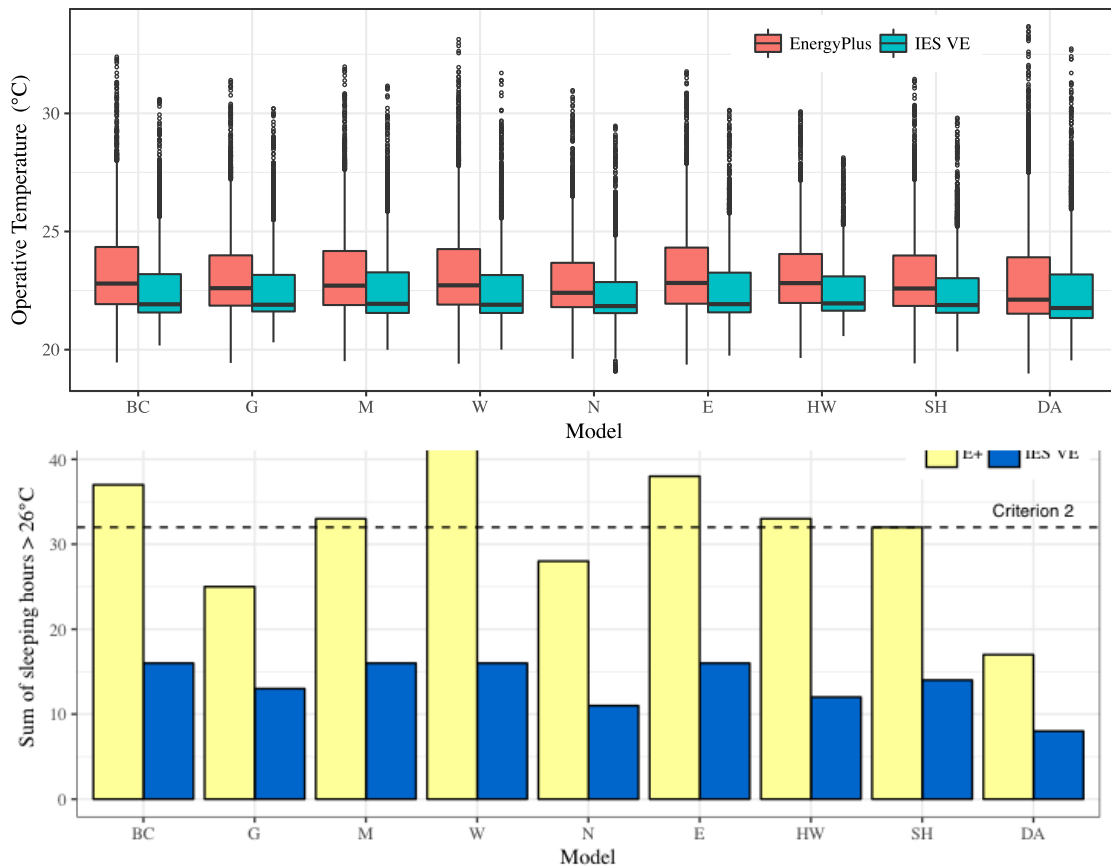


Figure 2: Parts (a) and (b) display the results of criterion 1 and 2 for all models, respectively. A high overheating risk is suggested for any model that surpasses either criterion line.

by the literature. North-facing flats succeed in meeting both criteria, with this model having the lowest risk of overheating for EnergyPlus. On the contrary, the west-facing flats appear to be the most prone to overheating between all other choices modelled. The increase of thermal mass resulted in the decrease of overheating risk for both software, with EnergyPlus passing the first criterion but failing the second. The equivalent model in IES VE recorded no hours above the  $T_{max}$  and successfully reduced the hours recorded for criterion 2. External shading played an important role in overheating for both software, especially for criterion 1. Its inclusion has led to the approximate halving of all hours of exceedance for either software, with the bedroom in IES VE recording no temperatures above  $T_{max}$ . As could be expected, its effectiveness diminishes for criterion 2. The increased solar gains in the dual-aspect flat increased the hours of exceedance in the bedroom by more than two times in EnergyPlus and more than three times in IES VE. However, the hours of exceedance in all other rooms and the hours recorded for criterion 2 have decreased. This may be attributed to the increased ventilation and cooling rate associated with cross-ventilation.

Figure 3 illustrates the distribution of operative temperatures for each model iteration in both softwares. The median temperatures predicted by EnergyPlus are in all cases greater than those in IES VE. Similar changes in the distributions of either software can be noticed for every model iteration. Another important observation is that overall and for individual cases, there is a greater spread in indoor temperatures for EnergyPlus models, suggesting greater fluctuations in temperature. The mean Interquartile Range (IQR) is  $2.23 \pm 0.06^{\circ}\text{C}$  for EnergyPlus and  $1.58 \pm 0.05^{\circ}\text{C}$  for IES VE. For both software, the North-facing model iteration shows the smallest IQR with the heavyweight iteration following closely. In EnergyPlus, the greatest IQR is seen in the basic case while for IES-VE it is the dual aspect flat. Statistically significant differences in the mean bedroom temperature between the two software were found at the 5% significance level for all nine model iterations.

Figure 3: Box Plot of hourly averaged bedroom operative temperatures for the whole period of interest. The points above the upper whisker suggest a significant degree of positive skewness.

Operative temperature time series graphs allow the better understanding of the behaviour of certain model iterations during the warmest 15 days of the weather file (Figure 4). The rate of change of indoor temperatures appear similar between software. For the base case, the mean temperature difference between the two software is  $1.16 \pm 0.02^\circ\text{C}$ . Contrasting the base case with the dual aspect models demonstrates a clear increase in the peak bedrooms temperature of the dual aspect flats on most days. Similarly, there is a decrease in the minimum temperatures reached. Both software predicted temperatures above  $32^\circ\text{C}$ , with EnergyPlus predicting a maximum temperature of  $33.7^\circ\text{C}$ . This was more than  $4^\circ\text{C}$  above the day's estimated  $T_{max}$ . On the same day, temperatures above  $33^\circ\text{C}$  persisted for five consecutive hours in EnergyPlus. The maximum temperature predicted by IES VE was  $32.7^\circ\text{C}$ . Furthermore, it may also be noted that the software are now in closer agreement, with a mean temperature difference of  $0.79 \pm 0.02^\circ\text{C}$ . This may possibly be attributed to similar effects of cross-ventilation on the indoor temperatures of either software. Looking at the heavyweight construction, the increase in thermal mass parameter has resulted in smaller temperature fluctuations for both software. Comparing the base case with the heavyweight iteration for each software shows that the increase in thermal mass had a more significant effect in IES VE than EnergyPlus, with the mean temperature difference increasing to  $1.25 \pm 0.02^\circ\text{C}$ .

## 5 DISCUSSION

The findings presented above suggest that the choice of BES tool is critical to the estimation of overheating risk, with the software disagreeing on the predicted risk of overheating in seven out of the nine cases. Due to the non-linear interaction of the many factors influencing the internal environment of the modelled flats, it is currently unclear why this level of disagreement exists. However, a few generic suggestions could be made with the way natural ventilation is modelled in each software being possibly crucial. EnergyPlus calculates the wind pressure coefficients depending on the building's geometry and location while IES VE has stored coefficients which depend on the opening's height and exposure (EnergyPlus, 2015; IES VE, 2015). The levels of agreement for this factor seem to depend on the existence of single-sided or cross ventilation, as seen in **Σφάλμα! Το αρχείο προέλευσης της αναφοράς δεν βρέθηκε.** From the same figure, it can be suggested that the modelling of thermal mass could also be an important factor for the observed differences. Other possible causes may include the simulation of solar and conductive gains.

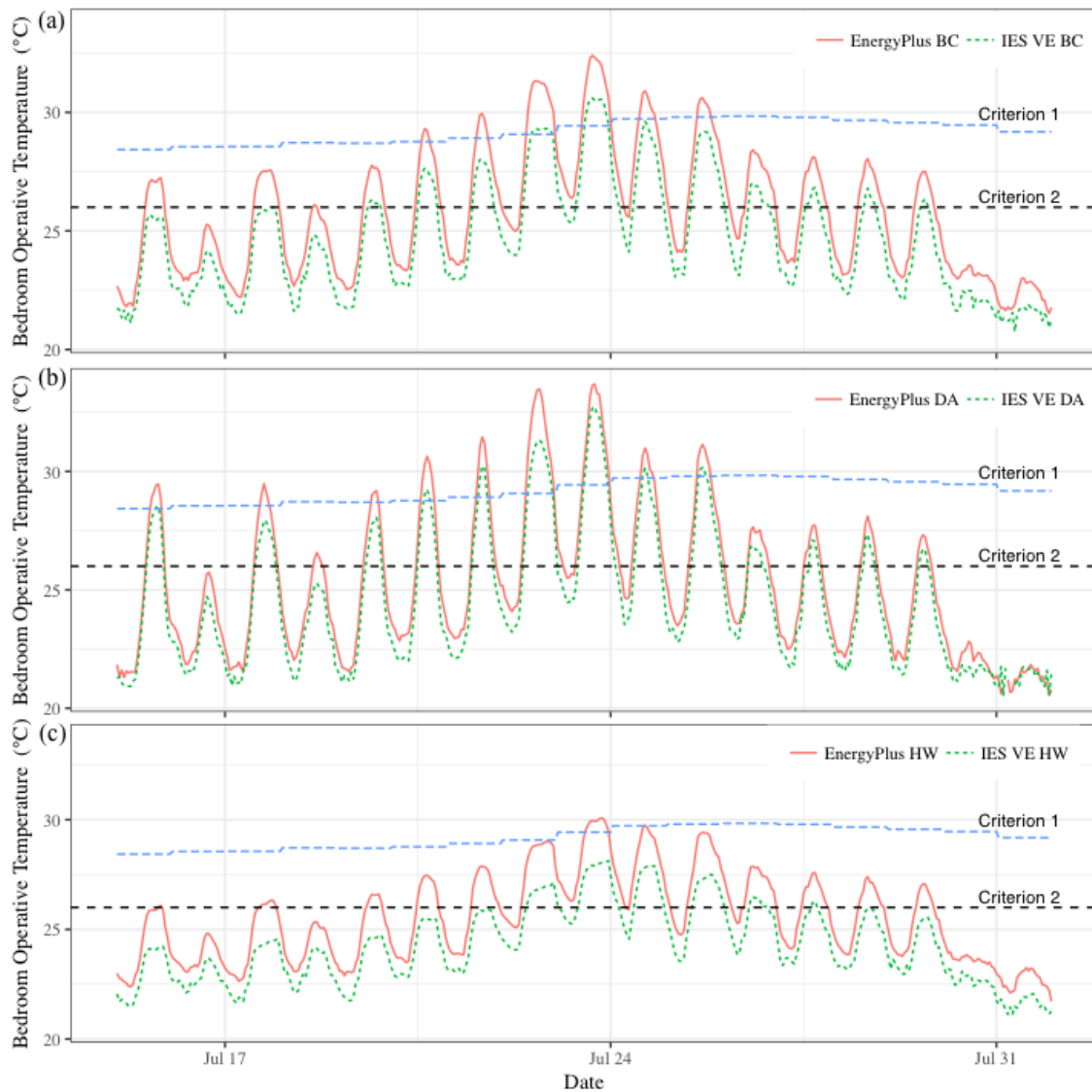


Figure 4: A comparison between the hourly estimated bedroom operative temperatures of the base case (a), the dual aspect flat (b) and the heavyweight construction flat (c). The bedroom operative temperature range was set to be equal for all three parts.

The sensitivity analysis results are in agreement with the findings of existing literature with regards to the inputs identified to be important for overheating. Features such as high thermal mass, north-facing orientation, external shading and secondary window in a single zone may all significantly help reduce the overheating risk. However, care should be taken when applying such measures and evaluating risks based only on the two suggested criteria. Dual-aspect flats with a S-W orientation have resulted in a significant increase in indoor temperatures of bedrooms during the day and decrease during the night. This is due to the additional solar gains dominating the increased cooling from cross-ventilation during the day. However, the model benefits from the addition of the secondary window overnight. Although single-aspect flats are expected to be at a higher risk of overheating due to the reduced ventilation cooling (ZCH, 2015), this research recommends that S-E or S-W facing dual aspect flats should also be tested if present in the building being investigated. Another possible concern that arises involves heavyweight constructions that may not be sufficiently ventilated, as shown by the predicted high overnight indoor temperatures.

This work has also demonstrated the levels of uncertainty that are involved in the prediction of overheating risk. Overall, the choice of BES tool appears to be a determinant factor in the overall prediction of overheating risk, which may depend on software default

hardcoded assumptions that are not always transparent. In addition, a modeller may choose from a number of options the way certain physical processes will be simulated within the software, directly influencing the end prediction. Finally, the parameters which describe the dwelling along with its occupation pattern should be known and inputted accurately in order to minimise external errors (Imam, Coley, & Walker, 2017). As the prediction of overheating risk involves absolute limits, it may be the case that a combination of all these errors could lead to the passing or failing of the criteria. This indicates that modellers should not consider the criteria as simply a binary indicator where every successful result is of equal merit. Taking into account the uncertainties involved in building overheating modelling, a more nuanced approach towards the interpretation of overheating risk predictions and mitigation actions may need to be adopted by building modellers and designers.

## 5.1 Limitations and Future Work

This work identified appreciable differences in the prediction of overheating between IES VE and EnergyPlus and offered preliminary interpretations of their causes. As part of ongoing work, a more thorough investigation of algorithmic differences between the software examined will identify the source of these discrepancies. However, empirical validation is needed in order to determine which software's predictions are closer to reality. In addition, although the local sensitivity analysis performed in this paper allowed for the direct comparison of the software, this work was limited by not investigating the interaction of inputs. For this purpose, future work will involve global sensitivity analysis techniques.

It should be highlighted that this work did not aim to establish the effectiveness of the suggested criteria in predicting thermally uncomfortable environments in dwellings. Such endeavour would be of great interest and importance but was out of the scope of this research.

## 6 CONCLUSIONS

This work aimed to quantify the differences in the prediction of overheating risk between two commonly used software, IES VE and EnergyPlus. Modelling inputs identified in the literature as being key overheating factors were varied. An inter-model comparison procedure was run in parallel with local sensitivity analysis, generating nine models within each software. When analysed using the CIBSE TM59 criteria, the results suggested a significant discrepancy between the two software for all models. EnergyPlus predicted a failure in one or both of the criteria in seven model iterations out of nine, while IES VE predicted passing the criteria for all models. Within each software, the factors expected to increase the risk of overheating agreed to a satisfactory level with the literature. Further work is required to determine the exact causes for the observed differences and to establish a truth standard by empirically validating either software's prediction.

## 7 ACKNOWLEDGEMENTS

This research was made possible by support from the EPSRC Centre for Doctoral Training in Energy Demand (LoLo), grant numbers EP/L01517X/1 and EP/H009612/1 and the Chartered Institution of Building Services Engineers. We would also like to thank Ms Eleni Oikonomou for providing the characteristics for a base case model.

## 8 REFERENCES

CIBSE. (2013). *The limits of thermal comfort: avoiding overheating in European buildings, TM52: 2013*. London: Chartered Institution of Building Services Engineers.

- CIBSE. (2015). *Guide A, Environmental Design*. London: Chartered Institute of Building Services Engineers.
- CIBSE. (2017). *Design methodology for the assessment of overheating risk in homes, TM59: 2017*. London: Chartered Institution of Building Services Engineers.
- Crawley, D. B., Hand, J. W., Kummert, M., & Griffith, B. T. (2008). Contrasting the capabilities of building energy performance simulation programs. *Building and Environment*, 43(4), 661–673.
- EnergyPlus. (2015). *EnergyPlus Engineering Reference Guide*.
- EnergyPlus. (2017a). EnergyPlus. Retrieved 22 May 2017, from <https://energyplus.net>
- EnergyPlus. (2017b). Testing and Validation. Retrieved 22 May 2017, from <https://energyplus.net/testing>
- Fouillet, A., Rey, G., Laurent, F., Pavillon, G., Bellec, S., Guihenneuc-Jouyaux, C., ... Hémon, D. (2006). Excess mortality related to the August 2003 heat wave in France. *International Archives of Occupational and Environmental Health*, 80(1), 16–24.
- Hacker, J. N., Saulles, T. P. D., Minson, A. J., & Holmes, M. J. (2008). Embodied and operational carbon dioxide emissions from housing: A case study on the effects of thermal mass and climate change. *Energy and Buildings*, 40(3), 375–384.
- HMG. (2013). *The Building Regulations 2010 incorporating 2010 and 2013 amendments - Approved Document F1 Means of Ventilation*. London: NBS.
- HMG. (2016). *Conservation of fuel and power in new dwellings. Building Regulations Approved Document L1A*. London: NBS.
- IES VE. (2015). MacroFlo Calculation Methods. Retrieved 22 May 2017, from <http://www.iesve.com/downloads/help/Thermal/Reference/MacroFloCalculationMethods.pdf>
- IES VE. (2017a). IES VE. Retrieved 22 May 2017, from <https://www.iesve.com>
- IES VE. (2017b). Software Validation. Retrieved 22 May 2017, from <https://www.iesve.com/software/software-validation>
- Imam, S., Coley, D. A., & Walker, I. (2017). The building performance gap: Are modellers literate? *Building Services Engineering Research and Technology*, 38(3), 351–375.
- Johnson, H., Kovats, R. S., McGregor, G., Stedman, J., Gibbs, M., & Walton, H. (2005). The impact of the 2003 heat wave on daily mortality in England and Wales and the use of rapid weekly mortality estimates. *Euro Surveill*, 10(7), 168–171.
- Judkoff, R., & Neymark, J. (1995). *International Energy Agency building energy simulation test (BESTEST) and diagnostic method*.
- Judkoff, R., & Neymark, J. (2006). Model validation and testing: The methodological foundation of ASHRAE Standard 140. In *Transactions-American Society of Heating Refrigerating and Air Conditioning Engineers* (Vol. 112, p. 367). ASHRAE; 1999.

- Mavrogianni, A., Davies, M., Chalabi, Z., Wilkinson, P., Kolokotroni, M., & Milner, J. (2009). Space heating demand and heatwave vulnerability: London domestic stock. *Building Research & Information*, 37(5–6), 583–597.
- Mavrogianni, A., Davies, M., Taylor, J., Chalabi, Z., Biddulph, P., Oikonomou, E., ... Jones, B. (2014). The impact of occupancy patterns, occupant-controlled ventilation and shading on indoor overheating risk in domestic environments. *Building and Environment*, 78, 183–198.
- Mavrogianni, A., Pathan, A., Oikonomou, E., Biddulph, P., Symonds, P., & Davies, M. (2017). Inhabitant actions and summer overheating risk in London dwellings. *Building Research & Information*, 45(1–2), 119–142.
- Murphy, J., Sexton, D., Jenkins, G., Boorman, P., Booth, B., Brown, K., ... Kendon, E. (2009). *UKCP09 Climate change projections*. Exeter: Met Office Hadley Centre.
- Oikonomou, E., Davies, M., Mavrogianni, A., Biddulph, P., Wilkinson, P., & Kolokotroni, M. (2012). Modelling the relative importance of the urban heat island and the thermal quality of dwellings for overheating in London. *Building and Environment*, 57, 223–238.
- Pereira, W., Bögl, A., & Natschläger, T. (2014). Sensitivity Analysis and Validation of an EnergyPlus Model of a House in Upper Austria. *Energy Procedia*, 62, 472–481.
- Porritt, S. M., Cropper, P. C., Shao, L., & Goodier, C. I. (2012). Ranking of interventions to reduce dwelling overheating during heat waves. *Energy and Buildings*, 55, 16–27.
- Raslan, R. (2010). *Performance Based Regulations: The Viability of the Modelling Approach as a Methodology for Building Energy Compliance Demonstration*. University College London.
- Shrubsole, C., Macmillan, A., Davies, M., & May, N. (2014). 100 Unintended consequences of policies to improve the energy efficiency of the UK housing stock. *Indoor and Built Environment*, 23(3), 340–352.
- Symonds, P., Taylor, J., Mavrogianni, A., Davies, M., Shrubsole, C., Hamilton, I., & Chalabi, Z. (2017). Overheating in English dwellings: comparing modelled and monitored large-scale datasets. *Building Research & Information*, 45(1–2), 195–208.
- Taylor, J., Davies, M., Mavrogianni, A., Chalabi, Z., Biddulph, P., Oikonomou, E., ... Jones, B. (2014). The relative importance of input weather data for indoor overheating risk assessment in dwellings. *Building and Environment*, 76, 81–91.
- Tian, W. (2013). A review of sensitivity analysis methods in building energy analysis. *Renewable and Sustainable Energy Reviews*, 20, 411–419.
- WHO. (2009). *Improving public health responses to extreme weather/heat-waves - EuroHEAT*. World Health Organisation (WHO).
- ZCH. (2015). *Overheating in homes, The big picture, Full Report*. Zero Carbon Housing.

# Towards Real-Time Model-Based Monitoring and Adoptive Controlling of Indoor Thermal Comfort

Ali Youssef<sup>\*1</sup>, Pieter Truyen<sup>1</sup>, Peter Bröde<sup>2</sup>, Dusan Fiala<sup>3</sup>, and Jean-Marie Aerts<sup>1</sup>

<sup>1</sup>*KU Leuven, M3-BIORES  
Kasteelpark Arenberg 30 bus 2456  
3001 Heverlee, Belgium*

<sup>2</sup>*Leibniz Research Centre for Working Environment  
and Human (ifADo)  
Ardeystraße 67  
44139 Dortmund, Germany*

<sup>3</sup>*Institute for Building Materials, Building Physics,  
Building Technology and Design (IBBTE)  
Keplerstraße 11  
D-70174 Stuttgart, Germany*

## ABSTRACT

Thermal comfort is an important aspect of the building design and indoor climate control as modern man spends most of the day indoors. Conventional indoor climate design and control approaches are based on static thermal comfort models that views the building occupants as passive recipients of their thermal environment. Assuming that people have relatively constant range of biological comfort requirements, and that the indoor environmental variables should be controlled to conform to that constant range. The (r)evolution in modern sensing and computing technologies (price, compact size, flexibility and stretchability) is making it possible to continuously measure signals in real-time from human body using wearable technologies and smart clothing. Many advanced and accurate mechanistic thermoregulation models, such as the ‘Fiala thermal Physiology and Comfort’ model, are developed to assess the thermal strains and comfort status of humans. However, the most reliable mechanistic models are too complex to be implemented in real-time for monitoring and control applications. Additionally, such models are using not-easily or invasively measured variables (e.g., core temperatures), which are often not practical and undesirable measurements for monitoring during varied activities over prolonged periods. The purpose of this work is to develop a databased mechanistic (grey box) model, with minimum number of parameters and non-invasive input variables, for real-time monitoring and controlling of individual occupant’s thermal comfort. Eight healthy males (mean  $\pm$  standard deviation: age  $22.8 \pm 1.3$  years, height  $1.81 \pm 0.06$ m, body surface area  $1.94 \pm 0.11$  m<sup>2</sup>) are used as test subjects to perform the designed experiments. The experimental protocol involved step-changes of exercise on treadmill inside to simulate step-changes in activity level. Metabolic heat production was calculated based on the continuously measured O<sub>2</sub> consumption and CO<sub>2</sub> production. Rectal temperature are continuously measured. Mean clothing layer and mean skin temperatures were calculated based on measured temperatures from eight body locations. The experiments were performed with the subjects wearing dry and wet underwear layer and constant ventilation rate. First-order multi-inputs-single-output discrete time transfer function, with only mean skin temperature and metabolic heat production or mean underwear temperature as inputs, was found to be the best to describe the dynamic responses of the rectal temperature. That with average coefficient of determination  $R^2 = 0.96 \pm 0.2$  and average Young Identification Criterion  $YIC = -9.20 \pm 4.2$ ).to The resulted models were compact enough (two inputs) to be implemented in real-time. Hence, the resulted model structure can be implemented in closed-loop algorithm for online identification of the model and parameters estimation is foreseen to be employed for occupant-based climate control applications and smart clothing.

## KEYWORDS

thermal comfort, indoor climate control, dynamic modelling, model-based control

# 1 INTRODUCTION

Thermal comfort is an important aspect of the building design and indoor climate control as modern man spends most of the day indoors. Conventional indoor climate design and control approaches are based on static thermal comfort models that views the building occupants as passive recipients of their thermal environment. the primary purpose of HVAC was to maintain constant thermal environmental conditions throughout the interior aiming for an optimum ‘steady-state’ temperature setting based on Fanger’s Predicted Mean Vote and Predicted Percentage Dissatisfied (PMV-PPD) model (Fanger, 1970; Parsons, 2014). Many advanced and accurate mechanistic thermoregulation models, such as the ‘Fiala thermal Physiology and Comfort’ model, are developed to assess the thermal strains and comfort status of humans (Havenith and Fiala, 2015). Most accurate and reliable models however, are too complex to enable real-time monitoring and control of the environmental conditions. Therefore, new models need to be found that are both simple and accurate. Early detection of core body temperature gain is key to the implementation of suitable strategies (i.e. cooling) to avoid exertional heat stroke (Niedermann et al., 2014). However, on the one hand, existing methods are invasive (inserting rectal or oesophageal temperature probes, etc.) and not convenient for long-term monitoring due to subject discomfort. On the other hand, the application of noninvasive measurement methods (tympanic membrane, oral, axillary) have demonstrated only limited accuracy for use in working environments. Most of the current methods to measure and predict the core body temperature in comparison to the rectal temperature method, neither meet the requirement of an accurate measurement of the core body temperature ( $\pm 0.1$  °C) nor do they enable the continuous measurement of the core body temperature in changing working conditions (Niedermann et al., 2014). Therefore, the purpose of this work was to develop an adaptive dynamic model with minimum number of parameters and non-invasive input variables, to predict the core body temperature for real-time monitoring and controlling of individual occupant’s thermal comfort.

## 2 MATERIALS AND METHODS

### 2.1 Experiments and test subjects

The data used in this paper was obtained from conducted human experiments at Leibniz Research Centre for Working Environment and Human Factors at the University of Dortmund (IfADo) (Bröde et al., 2008; Niedermann et al., 2014). During these experiments, measurements from eight healthy male students (mean  $\pm$  standard deviation: age  $22.8 \pm 1.3$  years, body height  $1.81 \pm 0.06$  m, body mass  $75.1 \pm 6.6$  kg and body surface area  $1.94 \pm 0.11$  m<sup>2</sup>) were collected. In order to reduce the evaporation to the environment, the experiments were carried out under a high humidity condition with air temperature ( $T_a$ ) of 20 °C, relative humidity (RH) of 80%, yielding ambient water vapour pressure ( $P_a$ ) of 1.87 kPa, and air velocity of 0.5 ms<sup>-1</sup>. Globe temperature was equal to  $T_a$ . The subjects wore their own briefs, socks and sport shoes, and a four layer clothing ensemble consisting of polypropylene underwear (HHS, Helly Hansen Super Bodywear 140 g.m<sup>-2</sup>), a hooded TYCHEM ® C Standard coverall as intermediate layer preventing both wicking and evaporation, additional cotton (CO, type ‘‘Gnägi’’, Switzerland) mid layer and an impermeable PVC outer layer. Trials were performed with the CO mid layer either dry (dry condition) or wetted using  $618 \pm 16$  g of water (wet condition). The sequence of those conditions was balanced across subjects who visited the laboratory at the same time of day (for more information about the experiments see Bröde et al. 2008; Niedermann et al. 2014).

The experimental protocol itself contained of a 30-minute resting phase followed by three phases inside a climatic chamber, each lasting 30 minutes and separated by a 3-minute period

where the fully clothed person's weight was determined. The first exercising phase comprised of 2 minutes of treadmill walking at 4.5 km.h<sup>-1</sup> followed by 28 minutes of standing in the room. Treadmill work was performed during the second and third phase.

## 2.2 Measurements

Metabolic heat production rate ( $Q_{met}$ , W.m<sup>-2</sup>) was calculated according to ISO 8996 (ISO, 2004) from the analysis of O<sub>2</sub> consumption (Servomex Series 1100, Servomex Ltd., UK) and CO<sub>2</sub> production (UNOR Infrarot-Gasanalysator, maihak AG, Germany) of expired air collected with Douglas bags during the last 10 minutes of phases 1 and 3, respectively. Mean skin temperature ( $T_{skm}$ , °C) was calculated as the average of thermistor recordings (YSI 427, Yellow Springs, USA) at eight body sites (forehead, left chest, right frontal thigh, left dorsal thigh, right scapula, right upper arm, left lower arm and left hand) according to a variant of the ISO 9886 scheme (ISO, 1992). The rectal temperatures ( $T_{re}$ , °C) were continuously recorded with a flexible thermistor probe at a depth of 10 cm from the anal sphincter (YSI 401, Yellow Springs, USA). Water vapour pressure ( $uwP_{air}$ , kPa) and air temperature ( $uwT_{air}$ , °C) in the clothing's microclimate were measured by data loggers (HandyLog DK502, Driesen + Kern GmbH, Germany) positioned at the right chest and left scapula between the underwear HHS layer and TYCHEM® layer and, correspondingly, at the contra lateral sites between the CO mid and PVC outer layer. An example of the different measured variables during the conducted experiments is shown in Figure 1 for subject #1 under dry conditions.

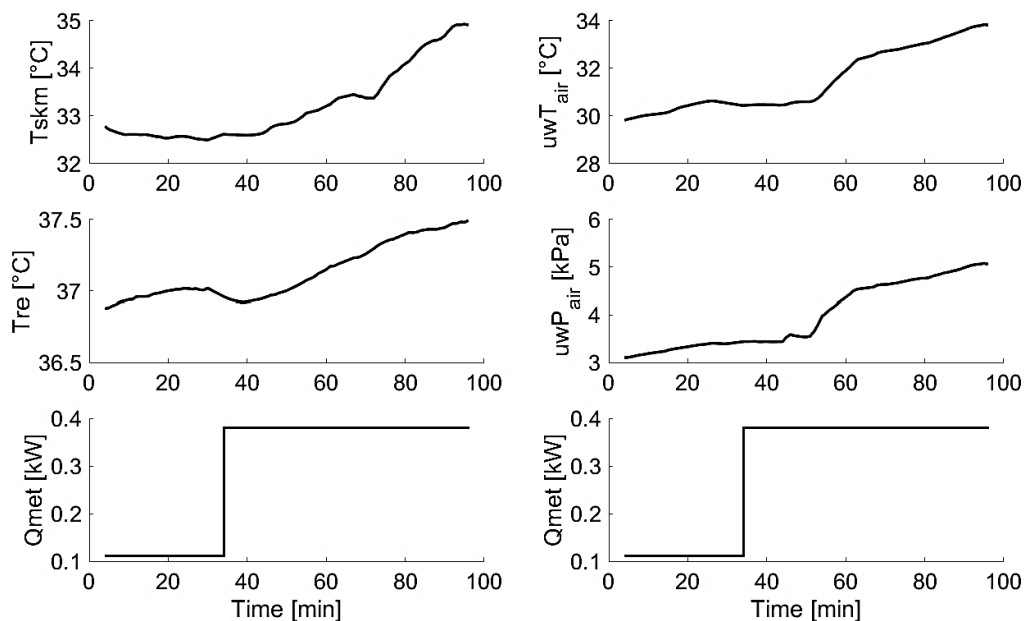


Figure 1. The dynamic response of mean skin temperature ( $T_{skm}$ , °C), rectal temperature ( $T_{re}$ , °C), mean underwear air temperature ( $uwT_{air}$ , °C) and mean underwear water vapour pressure ( $uwP_{air}$ , kPa) to step increase in the metabolic heat production rate ( $Q_{met}$ , kW) for test subject #1 at dry conditions.

## 2.3 System identification and online modelling

The human system is considered as Complex, Individually different, Time varying and Dynamic (CITD) systems (Quanten et al., 2006; Youssef et al., 2014). Although the system

(body thermoregulation) under study is inherently a non-linear system, the essential perturbation behaviour can often be approximated well by simple linearized transfer function (TF) models (Young et al., 1991; Youssef, 2014). The dynamic responses of the core body temperature, represented by the measured rectal temperature  $T_{re}$ , is modelled using different input variables using both single-input-single-output (SISO) and multiple-input-single-output (MISO) discrete-time transfer function (DTF). Mean skin temperature  $T_{skm}$ , mean underwear temperature  $uwT_{air}$ , underwear water vapour pressure  $uwP_{air}$  and metabolic heat production  $Q_{met}$  are considered separately and combined as input variables to model the rectal temperature  $T_{re}$ . For the purposes of the present paper, therefore, the following linear, discrete-time-system was considered,

$$T_{re}(k) = \sum_{i=1}^{nu} \frac{B_i(z^{-1})}{A(z^{-1})} u_i(k - \delta_i) + \xi(k)$$

(1)

where,

$$A(z^{-1}) = 1 + a_1 z^{-1} + a_2 z^{-2} + \dots + a_n z^{-n}$$

$$B_i(z^{-1}) = b_{0,i} + b_{1,i} z^{-1} + b_{2,i} z^{-2} + \dots + b_{m,i} z^{-m}$$

(2)

where  $T_{re}(k)$  is the model output and  $u_i(k)$  is the  $i^{\text{th}}$  model input, while  $A(z^{-1})$  and  $B_i(z^{-1})$  are appropriately defined polynomials in the backshift operator  $z^{-1}$ , i.e.,  $z^{-i}y(k) = y(k - i)$ . While,  $nu$  is number of model inputs (i.e.,  $nu = 1$  for SISO and  $nu > 1$  for MISO systems) and  $\xi(k)$  is additive noise, a serially uncorrelated sequence of random variables with variance  $\sigma^2$  that accounts for measurement noise, modelling errors and effects of unmeasured inputs to the process (assumed to be a zero mean). The simplified refined instrumental variable (SRIV) algorithm was utilised in the identification and estimation of the models (model parameters and model structure) (Young et al., 2000; Young and Jakeman, 1980). The appropriate model structure was identified, i.e., the most appropriate values for the triad  $[n, m, \delta]$  (see equations 1 and 2). Two main statistical measures were employed to determine the most appropriate values of this triad. Namely, the coefficient of determination  $R_2^T$ , based on the response error; and  $YIC$  (Young's Information Criterion), which provides a combined measure of model fit and parametric efficiency, with large negative values indicating a model which explains the output data well and yet avoids over-parameterisation (Young, 2011). The modelling procedures were applied on the data from both dry and wet conditions.

### 3 RESULTS AND DISCUSSIONS

#### 3.1 Model identification

##### - Dry condition

The SRIV algorithm combined with the root mean square error (RMSE),  $YIC$  and  $R_2^T$  suggested, in general, that a first order (number of poles,  $n = 1$ ) MISO DTF models, including the metabolic heat production  $Q_{met}$  and mean skin temperature  $T_{skm}$  as model inputs (i.e.,  $nu = 2$ ), described the dynamic responses of the rectal temperature  $T_{re}$  most accurately (i.e.,  $R_2^T = 0.98 \pm 0.17$  and  $YIC = -7.63 \pm 2.40$ ). More specifically, the SRIV algorithm identified the following general discrete-time TF model structure represented by the triad  $[1 \ 1 \ 1 \ \delta_1 \ \delta_2]$ ,

$$T_{re}(k) = \left[ \frac{B_1(z^{-1})}{A(z^{-1})} \frac{B_2(z^{-1})}{A(z^{-1})} \right] \cdot \begin{bmatrix} Q_{met}(k - \delta_1) \\ T_{skm}(k - \delta_2) \end{bmatrix} + \xi(k)$$

(3)

where the time delays  $\delta_1$  and  $\delta_2$  were different from test subject to another (Table 1).

Table 1. The resulted MISO model structures  $[nm_1m_2\delta_1\delta_2]$  and the mean estimated polynomials  $A(z^{-1}), B_1(z^{-1})$  and  $B_2(z^{-1})$  with metabolic heat production  $Q_{met}$  and mean skin temperature  $T_{skm}$  as model inputs, showing the mean model identification criteria  $R_2^T$ , YIC and RMSE for all the test subjects under dry condition.

	$n$	$m$	$m$	$\delta_1$	$\delta_2$	$A(z^{-1})$	$B_1(z^{-1})$	$B_2(z^{-1})$	$R_T^2$	YIC	RMSE
<b>Mean</b>	<b>1</b>	<b>1</b>	<b>1</b>	<b>5</b>	<b>4</b>	<b>0.05</b>	<b>0.0012</b>	<b>0.0026</b>	<b>0.98</b>	<b>-7.63</b>	<b>0.007</b>
± Standard deviation	1	1	1	± 4	± 3	± 0.076	± 3.50×10 <sup>-4</sup>	± 0.010	± 0.17	± 2.40	± 2.70×10 <sup>-4</sup>

Additionally, the results have shown that a first MISO DTF models, with the mean skin temperature  $T_{skm}$  and the mean underwear temperature  $uwT_{air}$  as model inputs, were able to describe the dynamic responses of the rectal temperature  $T_{re}$  sufficiently (i.e.,  $R_2^T = 0.95 \pm 0.05$  and  $YIC = -9.66 \pm 3.22$ ). More specifically, the SRIV algorithm identified the following general discrete-time TF model structure represented by the triad  $[1 \ 1 \ 1 \ \delta_1 \ \delta_2]$ ,

$$T_{re}(k) = \left[ \frac{B_1(z^{-1})}{A(z^{-1})} \frac{B_2(z^{-1})}{A(z^{-1})} \right] \cdot \left[ \begin{matrix} T_{skm}(k-\delta_1) \\ uwT_{air}(k-\delta_2) \end{matrix} \right] + \xi(k) \quad (4)$$

The mean estimated model polynomials,  $A(z^{-1}), B_1(z^{-1})$  and  $B_2(z^{-1})$ , resulted from the data from all the eight test subjects are presented in Table 2.

Table 2. The resulted MISO model structures  $[nm_1m_2\delta_1\delta_2]$  and the mean estimated polynomials  $A(z^{-1}), B_1(z^{-1})$  and  $B_2(z^{-1})$  with mean skin temperature  $T_{skm}$  and mean underwear temperature  $uwT_{air}$  as model inputs, showing the mean model identification criteria  $R_2^T$ , YIC and RMSE for all the test subjects under dry condition.

	$n$	$m$	$m$	$\delta_1$	$\delta_2$	$A(z^{-1})$	$B_1(z^{-1})$	$B_2(z^{-1})$	$R_T^2$	YIC	RMSE
<b>Mean</b>	<b>1</b>	<b>1</b>	<b>1</b>	<b>3</b>	<b>4</b>	<b>0.25</b>	<b>0.052</b>	<b>0.0030</b>	<b>0.95</b>	<b>-5.63</b>	<b>0.022</b>
± Standard deviation	1	1	1	± 2	± 3	± 0.22	± 4.2×10 <sup>-3</sup>	± 0.023	± 0.05	± 3.25	± 1.85×10 <sup>-3</sup>

#### - Wet condition

The same MISO model structure, as resulted for the dry condition (i.e.,  $[1 \ 1 \ 1 \ \delta_1 \ \delta_2]$ ), was best to describe the dynamic responses of the rectal temperature of all the test subjects under wet condition (see Tables 3 and 4).

Table 3. The resulted MISO model structures  $[nm_1m_2\delta_1\delta_2]$  and the mean estimated polynomials  $A(z^{-1}), B_1(z^{-1})$  and  $B_2(z^{-1})$  with metabolic heat production  $Q_{met}$  and mean skin temperature  $T_{skm}$  as model inputs, showing the mean model identification criteria  $R_2^T$ , YIC and RMSE for all the test subjects under wet condition.

	$n$	$m$	$m$	$\delta_1$	$\delta_2$	$A(z^{-1})$	$B_1(z^{-1})$	$B_2(z^{-1})$	$R_T^2$	YIC	RMSE
<b>Mean</b>	<b>1</b>	<b>1</b>	<b>1</b>	<b>4</b>	<b>7</b>	<b>0.03</b>	<b>0.00017</b>	<b>-0.015</b>	<b>0.98</b>	<b>-8.88</b>	<b>0.03</b>
± Standard deviation	1	1	1	± 3	± 3	± 0.010	± 5.42×10 <sup>-5</sup>	± 0.007	± 0.15	± 1.63	± 4.42×10 <sup>-3</sup>

Table 4. The resulted MISO model structures  $[nm_1m_2\delta_1\delta_2]$  and the mean estimated polynomials  $A(z^{-1}), B_1(z^{-1})$  and  $B_2(z^{-1})$  with mean skin temperature  $T_{skm}$  and mean underwear temperature  $uwT_{air}$  as

model inputs, showing the mean model identification criteria  $R_2^T$ , YIC and RMSE for all the test subjects under wet condition.

	$n$	$m$	$m$	$\delta_1$	$\delta_2$	$A(z^{-1})$	$B_1(z^{-1})$	$B_2(z^{-1})$	$R_T^2$	YIC	RMSE
<b>Mean</b>	<b>1</b>	<b>1</b>	<b>1</b>	<b>4</b>	<b>6</b>	<b>0.21</b>	<b>0.052</b>	<b>0.0030</b>	<b>0.95</b>	<b>-5.63</b>	<b>0.022</b>
$\pm$ Standard deviation	<b>1</b>	<b>1</b>	<b>1</b>	$\pm 2$	$\pm 3$	$\pm 0.32$	$\pm 4.2 \times 10^{-3}$	$\pm 0.023$	$\pm 0.05$	$\pm 3.25$	$\pm 1.85 \times 10^{-3}$

The results showed that a higher time delays ( $\delta_1 \delta_2$ ) in case of wet condition in comparison to dry conditions. The used SRIV algorithm is suitable to be run in closed-loop for online model estimation. One of the main advantages of the above mentioned approach is that it is automatically accommodating with the multiple-time delays that were observed with the various identified TF models for different test subjects.

#### 4 CONCLUSIONS

Eight healthy males (mean  $\pm$  standard deviation: age  $22.8 \pm 1.3$  years, height  $1.81 \pm 0.06$ m, body surface area  $1.94 \pm 0.11$  m<sup>2</sup>) are used as test subjects to perform the designed experiments. The experimental protocol involved step-changes of exercise on treadmill inside to simulate step-changes in activity level. Metabolic heat production was calculated based on the continuously measured O<sub>2</sub> consumption and CO<sub>2</sub> production. Rectal temperature are continuously measured. Mean clothing layer and mean skin temperatures were calculated based on measured temperatures from eight body locations. The experiments were performed with the subjects wearing dry and wet underwear layer and constant ventilation rate. First order MISO DTF models were found to be the most suitable (i.e.,  $R_2^T = 0.96 \pm 0.2$  and  $YIC = -9.20 \pm 4.2$ ) to describe the dynamic response of the rectal temperature of the tested subjects under both dry and wet conditions. Paring the mean skin temperature  $T_{skm}$ , with the mean underwear temperature  $uwT_{air}$  once and with the metabolic heat production  $Q_{met}$  another, was found the most suitable model inputs to the MISO DTF. It is suggested to use the mean skin temperature  $T_{skm}$  with the mean underwear temperature  $uwT_{air}$  for online prediction of the rectal temperature and further model-based controlling of the body thermal comfort.

#### 5 REFERENCES

- Bröde, P., Havenith, G., Wang, X., Candas, V., den Hartog, E.A., Griefahn, B., Holmér, I., et al. (2008), “Non-evaporative effects of a wet mid layer on heat transfer through protective clothing”, *European Journal of Applied Physiology*, Vol. 104 No. 2, pp. 341–349.
- Fanger, P.O. (1970), *Thermal Comfort : Analysis and Applications in Environmental Engineering*, 1st ed., Danish Technical Press, Lyngby.
- Havenith, G. and Fiala, D. (2015), “Thermal Indices and Thermophysiological Modeling for Heat Stress”, *Comprehensive Physiology*, Vol. 6, John Wiley & Sons, Inc., Hoboken, NJ, USA, pp. 255–302.
- Niedermann, R., Wyss, E., Annaheim, S., Psikuta, A., Davey, S. and Rossi, R.M. (2014), “Prediction of human core body temperature using non-invasive measurement methods”, *International Journal of Biometeorology*, Springer Berlin Heidelberg, Vol. 58 No. 1, pp. 7–15.

- Parsons, K.C. (Kenneth C.. (2014), *Human Thermal Environments : The Effects of Hot, Moderate, and Cold Environments on Human Health, Comfort, and Performance*, 3rd ed., CRC Press.
- Quanten, S., de Valck, E., Cluydts, R., Aerts, J.-M. and Berckmans, D. (2006), “Individualized and time-variant model for the functional link between thermoregulation and sleep onset.”, *Journal of Sleep Research*, Vol. 15 No. 2, pp. 183–98.
- Young, P., Price, L., Berckmans, D. and Janssens, K. (2000), “Recent developments in the modelling of imperfectly mixed airspaces”, *Computers and Electronics in Agriculture*, ELSEVIER SCIENCE BV, Vol. 26 No. 3, pp. 239–254.
- Young, P.C. (2011), *Recursive Estimation and Time-Series Analysis: An Introduction for the Student and Practitioner*, Springer.
- Young, P.C., Chotai, A. and Tych, W. (1991), “Identification, estimation and control of continuous-time systems described by delta operator models.”, Kluwer Academic Publishers, 28 April.
- Young, P.C. and Jakeman, A. (1980), “Refined instrumental variable methods of recursive time-series analysis Part III. Extensions”, *International Journal of Control*, Taylor & Francis, Vol. 31 No. 4, pp. 741–764.
- Youssef, A. (2014), *Model-Based Control of Micro-Environment with Real-Time Feedback of Bioresponses*, KU Leuven.
- Youssef, A., Exadaktylos, V. and Berckmans, D. (2014), “Modelling and quantification of the thermoregulatory responses of the developing avian embryo: Electrical analogies of a physiological system”, *Journal of Thermal Biology*, Vol. 44, pp. 14–19.

# Application of open-source CFD software to the indoor airflow simulation

CongWang<sup>\*1</sup>, Sasan Sadrizadeh<sup>1,2</sup>, and Sture Holmberg<sup>1</sup>

*1 Royal Institute of Technology  
KTH, Brinellvägen 23  
Stockholm 10044, Sweden*

*2 Lawrence Berkeley National Laboratory  
1 Cyclotron Road, Berkeley  
California 94720, USA*

*\*Corresponding author: congwang@kth.se*

## ABSTRACT

The use of open-source CFD has been growing in both industry and academia. Open-source CFD saves users a considerable license cost and provides users with full transparency of implementation and maximum freedom of customization. However, it is often necessary to assess the performance of an open-source code before applying it to the practical use. This study applies one of the most popular open-source CFD codes – OpenFOAM to the indoor airflow and heat transfer prediction. The performance of OpenFOAM is evaluated and validated against a well-documented benchmark test. Various OpenFOAM built-in turbulent viscosity models are attempted within the framework of Reynolds Averaged Navier-Stokes Simulation (RANS) approach and the simulation results are compared to the experimental data. Among all models, the  $k - \omega SST$  model has shown the best overall performance, whereas the standard  $k - \epsilon$  model is the most robust one despite its deficiencies. The results of this study demonstrate the capability of OpenFOAM in the field of indoor air simulation and promote users' confidence in using OpenFOAM in their research work.

## KEYWORDS

Computational Fluid Dynamics, OpenFOAM, indoor air flow, thermal manikin, turbulence models

## 1 INTRODUCTION

Accurate prediction of air movement, temperature and contaminant distribution as well as many other parameters of air flow in an enclosed environment is of paramount importance in assessing occupants' comfort and health. Due to the prohibitive cost of laboratory experiment, Computational Fluid Dynamics (CFD) has nowadays been increasingly utilized to simulate the indoor climate. Chen & Srebric (Chen & Srebric, 2000) summarized indoor and outdoor environment studies conducted by using CFD and concluded that CFD was a powerful tool to predict airflows in the built environment. Gao & Niu (Gao & Niu, 2004) summarized various issues regarding CFD studies of the thermal environment around a human body. Norton et al. (Norton et al. 2007) reviewed the applications of CFD in the ventilation design for the agricultural industry. Sadrizadeh et al. (Sadrizadeh et al. 2014) employed CFD to investigate the transport and dispersion of airborne bacteria in an operating theatre.

The majority of these research studies reply on closed-source and commercial CFD tools, such as ANSYS FLUENT, ANSYS CFX, STAR-CCM+, etc. Users benefit from using commercial CFD codes in many aspects. Commercial CFD codes are verified extensively by different user groups and validated against various benchmark tests. In addition, users can easily get support from the commercial CFD vendors when they are faced with code-related problems, an important advantage especially for inexperienced users. Therefore, users tend to gain confidence and feel proficient in using commercial CFD codes. Despite these merits, however, one major disadvantage of proprietary CFD packages is that they provide limited insight and serve as a black-box, that is, the implementation details are not transparent to users and users have limited or even no access to the code. Moreover, the use of commercial

CFD packages usually involves a considerable license cost and license fees increase with increasing use. As an alternative to commercial CFD packages, various open-source CFD codes have been developed and become available to the public. Most open-source CFD packages are free-licensed, which allows anyone to use the software and source code for free. Most importantly, open-source CFD tools offer users full transparency of technology and maximum freedom of customization, With Open-source CFD, users can easily implement a new technology and adapt the code to their own need. Among all, OpenFOAM is one of the most popular general-purpose open-source CFD codes, which is an object-oriented C++ tool box originally developed for the Finite Volume (FV) method (Jasak 1996; Weller et al. 1998). OpenFOAM has been reported to be adequate for a broad range of fluid dynamics applications (Jasak et al. 2007) and have good parallel scalability for both simple test cases (Axtmann&Rist 2016) and complex industrial cases (Lui 2015). OpenFOAM is also supplied with pre- and post-processing utilities, which permits a complete analysis and solution of problems within a consistent software package.

OpenFOAM has found its way into the automotive and railway industry to resolve aerodynamics (Blacha et al. 2016), aeroacoustics (Zörner et al. 2010; Wang 2013) and combustion (Migliaccio et al. 2009). Despite its established role in these fields, few applications of OpenFOAM to the indoor environment simulation have been found until recently. Ramechecandane et al. (2010) utilized OpenFOAM to investigate the particle dispersion with the presence of an inhomogeneous electric field. Konstantinov et al. applied OpenFOAM to the numerical simulation of the airflow and thermal comfort in a passenger car cabin (Konstantinov&Wagner 2016), a train cabin (Konstantinov&Wagner 2014), and an aircraft cabin (Konstantinov et al. 2014). Some researchers have developed innovative models and technologies of their own within the OpenFOAM framework. For instance, Liu et al. (2016) implemented a fast fluid dynamics (FFD) model based on OpenFOAM to simulate the indoor airflow. Similarly, Xue et al. (2016) proposed a new semi-Lagrangian-based PISO method implemented in OpenFOAM for fast and accurate indoor environment modelling.

One major disadvantage with open-source CFD is that their performance may not be well validated. Bugs or inappropriate implementation may exist in open-source CFD codes. As regards OpenFOAM, due to the limited number of applications in indoor airflow simulation, it is of value to assess the accuracy and robustness of OpenFOAM before applying it to practical use. Ito et al. (Ito et al. 2015a) validated several commercial CFD packages as well as OpenFOAM against a benchmark test that were performed on a non-isothermal flow in a 3D room, in which OpenFOAM achieved the closest match with the experimental data. Ito et al. (Ito et al. 2015b) further conducted a comprehensive analysis of cross-ventilation and floor-heating-induced natural convection using OpenFOAM and compared the simulation with measurements. Despite these existing studies, more extensive benchmark tests are still desirable to validate OpenFOAM as a useful tool in indoor environment simulation. This study aims to provide more validation evidence for OpenFOAM by performing a CFD simulation of airflow and heat transfer around a thermal manikin.

Thermal manikins have been broadly used in the indoor environment research in both laboratory experiment and numerical simulation. This study attempts to simulate a well-documented benchmark test of a thermal manikin (Nilsson et al. 2007) using OpenFOAM. Similar studies exist in the literature. Martinho et al. (Martinho et al. 2012) analyse the influence of various factors on the accuracy of CFD by comparing simulation results obtained from ANSYS CFX to the experimental data. Sadrizadeh & Holmberg (Sadrizadeh & Holmberg, 2016) used the same benchmark test to evaluate the performance of nine

turbulence models in ANSYS FLUENT. Ito et al. (Ito et al. 2015c) validated the simulation results obtained from Star-CD against the same benchmark test.

The complex state of indoor airflow and heat transfer requires appropriate turbulence treatment. Due to the low computational cost and moderate accuracy, RANS remains to be the dominant approach. Therefore, this study tests a number of OpenFOAM built-in turbulent viscosity models within the RANS framework against the experimental data.

## 2 METHODOLOGY

### 2.1 Experimental Setup

The experimental benchmark test on a thermal manikin was performed through cooperation between the Aalborg University in Denmark and Gävle University in Sweden (Nilsson et al. 2007). The experimental apparatus is a box-shape chamber with a dimension of 2.44 m × 2.46 m × 1.2 m. The chamber is made of 12-mm wood with a thermal conductivity of 0.15 W/(m·K) and the coefficient of convective heat transfer between the chamber wall and the outdoor air is 10 W/(m<sup>2</sup>·K) (Ito et al. 2015c). A sitting-posture manikin was placed along the centre line of the chamber, facing the inlet at a distance of 0.7 m away from the toe. The manikin was kept at a constant temperature of 34 °C without clothing or hair to facilitate the heat transfer. The incoming air was supplied over the full cross-section at a mean velocity of 0.27 m/s and mean temperature of 20.4 °C. Two circular exhaust outlets of a diameter 0.25 m were positioned on the rear wall with one 0.6 m away from the ceiling and the other 0.6 m away from the floor. Figure 1 shows the experiment rig and geometry of the simulation.

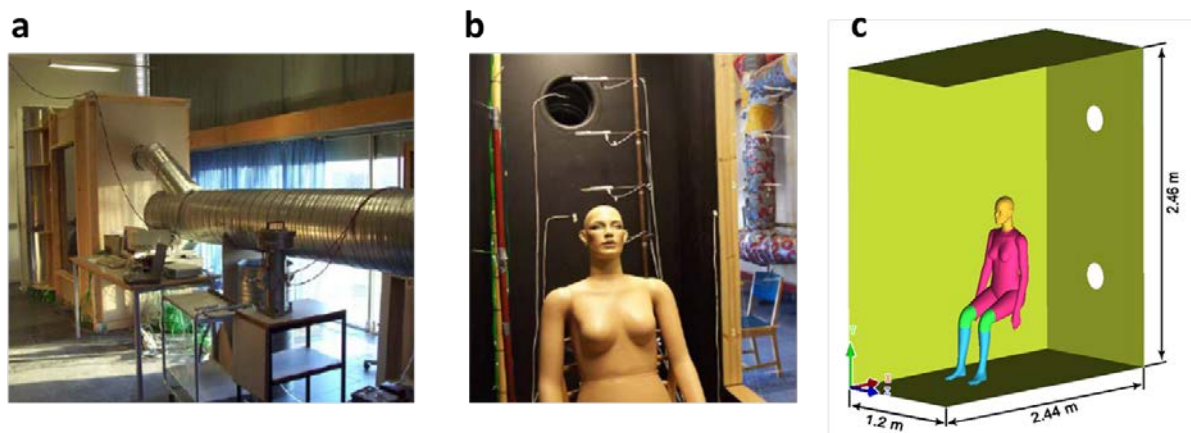


Figure 1: a) Experimental setup; b) Thermal manikin; c) CAD geometry for simulation.

The temperature and velocity distribution were measured at different locations along several vertical lines L1 – L4, as shown in Figure 2 a). In particular, the temperature is measured at L2 and L4, whereas the velocity is measured at L1 and L3. The vertical distribution of the temperature of the air is also measured 1.08 m ahead of the inlet, which has been used as inlet boundary condition for temperature in CFD simulation, as presented in Figure 2 b). The heat loss from the manikin to the ambient is also measured and documented.

### 2.2 Numerical Simulation

The numerical simulation is performed using OpenFOAM 2.3.1, which attempts to replicate the conditions in the experiment. The setup of the simulation is described in the section.

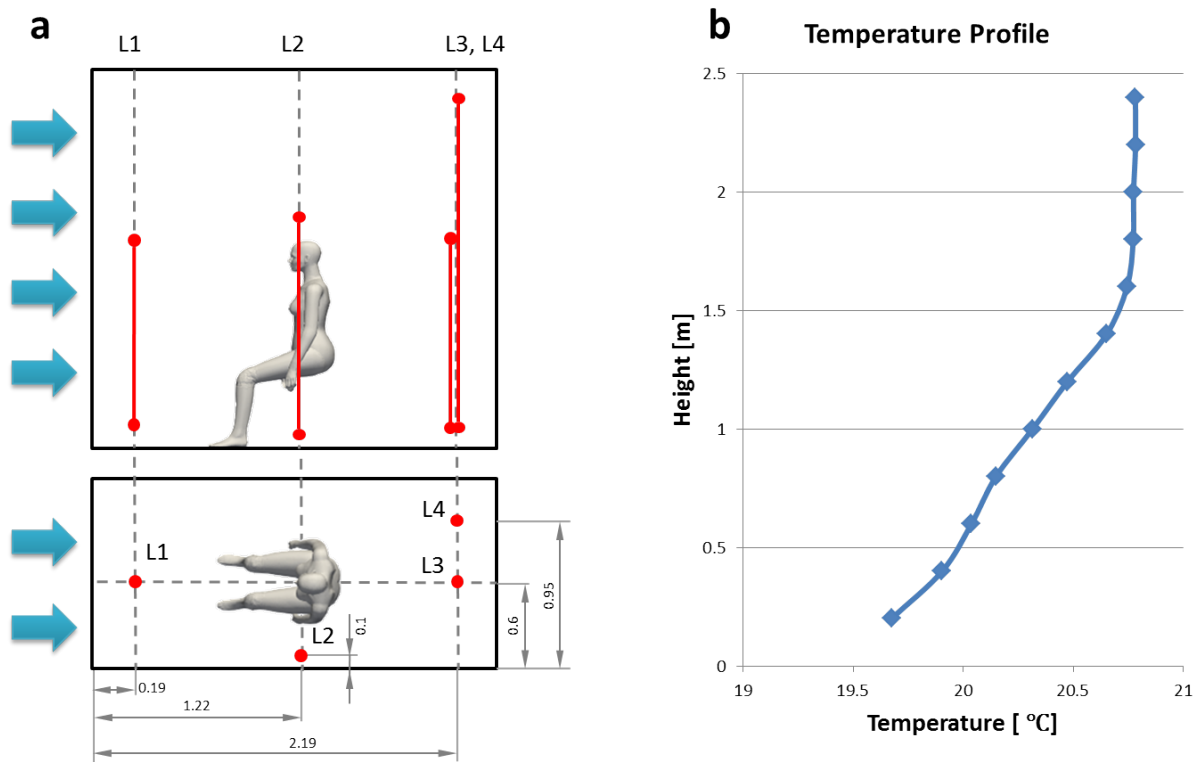


Figure 2: a) Locations of measurement lines; b) Temperature profile measured ahead of the inlet.

### 2.2.1 Mesh

The mesh is created using OpenFOAM native mesher – *snappyHexMesh*, which generates 3-dimensional hexahedra dominant meshes from triangulated geometries. The *snappyHexMesh* meshing utility adopts the cut-cell method, which is a top-down approach in contrast to the well-known bottom-up approaches such as the Delaunay or Advancing Front. A Cartesian mesh is firstly created as the base mesh and the hexahedra cells are then split and snapped to the geometry surfaces. Such an approach shows relative robustness in handling dirty geometries and favourable parallel scalability, and more importantly facilitates the automation of the meshing process. However, the cut-cell approach suffers from lack of control over surface meshes and limited robustness in boundary layer inflation. The limited capability of generating perfect boundary conformal meshes and failure in boundary layer addition are continually reported in the community of *snappyHexMesh* users.

The created mesh contains a total number of 1.4 million cells. The size of the cells of the base mesh is approximately 6.7 cm and the cells are continuously refined approaching the manikin and walls. To ensure the grid independence, the simulation is also performed on a coarser mesh and a finer mesh respectively.

### 2.2.2 Boundary Conditions

While a temperature profile presented in Figure 2 b) is used as the inflow boundary condition for temperature, the velocity is assumed to be 0.27 m/s uniform over the whole cross-section. The turbulence intensity and mixing length are specified at the inlet. Following Ito et al. (Ito et al. 2015c), the turbulence intensity is assumed to be 5% and the mixing length 0.16 m. The boundary condition for temperature at the surface of manikin is constant 34 °C and at walls makes the walls transfer heat with outdoor air at a temperature of 20.4 °C. For the calculation of radiation, the emissivity is set as 0.9 for all solid surfaces and 1.0 for inlet and outlet.

### 2.2.3 Turbulence Models

As pointed out in the previous section, RANS is the dominant approach in indoor air flow and heat transfer simulation. The RANS approach relies on the appropriate selection of turbulent viscosity models. Therefore, various turbulent viscosity models available in OpenFOAM are used in this study. Specifically, this study considers five two-equation models – the standard  $k - \varepsilon$  model, the RNG  $k - \varepsilon$  model, the realizable  $k - \varepsilon$  model, the Launder-Sharma low-Re  $k - \varepsilon$  model and the  $k - \omega$  SST model; one four-equation model – the  $\overline{v^2} - f$  model. The applications of these models are commonly found in the literature.

The standard  $k - \omega$  SST model, which solves two semi-empirical transport equations for the turbulence kinetic energy ( $k$ ) and the turbulence dissipation rate ( $\varepsilon$ ), has a broad range of applications and has been reported to provide acceptable accuracy for simple flows. Derived using the renormalization group (RNG) method purely from the instantaneous Navier-Stokes equations, the RNG  $k - \varepsilon$  model solves a slightly different equation for  $\varepsilon$  and has been found to exhibit better performance in indoor air flow simulations than the standard one (Chen 1995). Different from the standard and RNG  $k - \varepsilon$  models, the realizable  $k - \varepsilon$  model is ‘realizable’ in terms of the consistency with the physics of turbulent flow, which satisfies certain mathematical constraints on turbulence quantities. The Launder-Sharma model is the most widely used low-Re  $k - \varepsilon$  model, which solves the transport equation for a modified dissipation rate and is supposed to account for the damping effect in the near-wall region. The  $k - \omega$  SST model solves for the specific dissipation rate  $\omega$  (also referred to as turbulent frequency) and combines the best behaviour of the  $k - \varepsilon$  model in the freestream and the standard  $k - \omega$  model in the near-wall region. The  $\overline{v^2} - f$  model solves two additional equations for a velocity scale  $\overline{v^2}$  and a relaxation function  $f$ , which takes into account the near-wall anisotropy and non-local pressure-strain effects. The model has been successfully applied in the literature to the indoor ventilation design (e.g. Chen et al. 2013).

### 2.2.4 Solvers

There are a number of solvers available in OpenFOAM that are designed for heat transfer problems. As the buoyant effect is significant in this benchmark test and the temperature difference is not very small, the *buoyantSimpleFoam* solver is used to solve the fluid flow. *buoyantSimpleFoam* is a steady-state solver that directly solves compressible turbulent flows to account for buoyancy without imposing the Boussinesq approximation on the fluid.

To solve the radiative heat transfer, the finite volume discrete ordinate method (fvDOM) is employed, which solves the radiative transfer equation for a discrete number of finite solid angles using the finite volume method. In this study, the angular space  $4\pi$  is discretized into 20 azimuthal angles and 7 polar angles, leading to a total number of 140 equations to be solved. The *buoyantSimpleFoam* solver together with appropriate boundary conditions automatically handles the coupling between the convective and radiative heat transfer.

## 3 RESULTS AND DISCUSSION

The velocity distribution at two vertical lines – L1 and L3, is presented for both the simulation and experiment in Figure 3. As a uniform velocity profile of 0.27 m/s is specified at the inlet in the simulation, the predicted velocity at L1 deviates very little from the inlet, as shown in Figure 3 a). However, small discrepancies can be observed between simulated and measured values, which may imply that a more precise boundary condition for the velocity should be applied to the inlet. Figure 3 b) shows that the velocity values at L3 predicted by different turbulence models are nearly identical, but slightly deviate from the experimental

results. All models tend to over-predict the velocity at lower height but under-predict the velocity at larger height and close to the floor.

Figure 4 presents the predicted and measured temperature profiles at L2 and L4. As with the velocity profiles, different turbulence models give rather similar temperature profiles. At L2, the temperature is underestimated for all locations except for the one close to the floor. At L4, all simulations overestimate the temperature at large height and underestimate the temperature at medium and low height. Similar to L2, the temperature at the floor level is significantly overestimated. This remarkable discrepancy can be ascribed to the deficiency of the inlet boundary condition for temperature. As can be seen from Figure 2 b), temperature measurement at the floor level is not available.

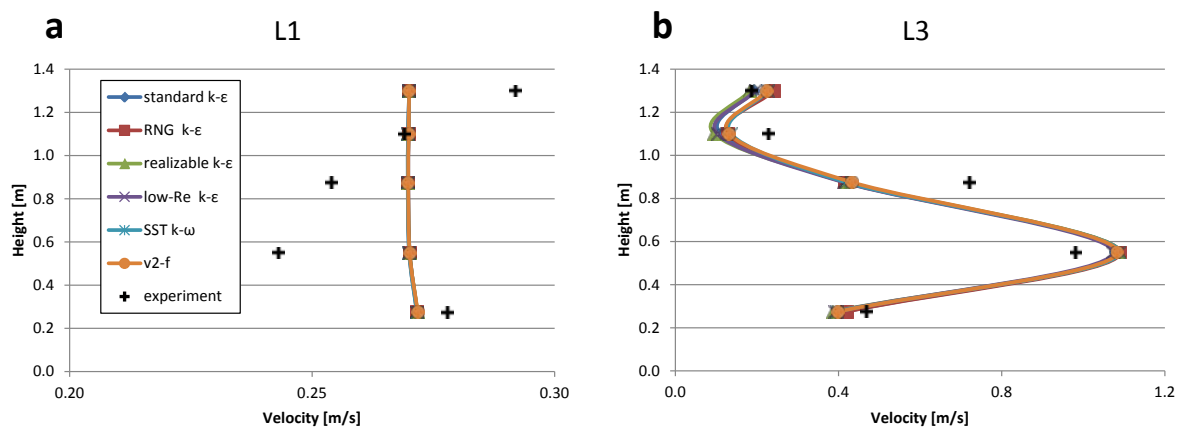


Figure 3: Velocity profiles at a) L1 and b) L3.

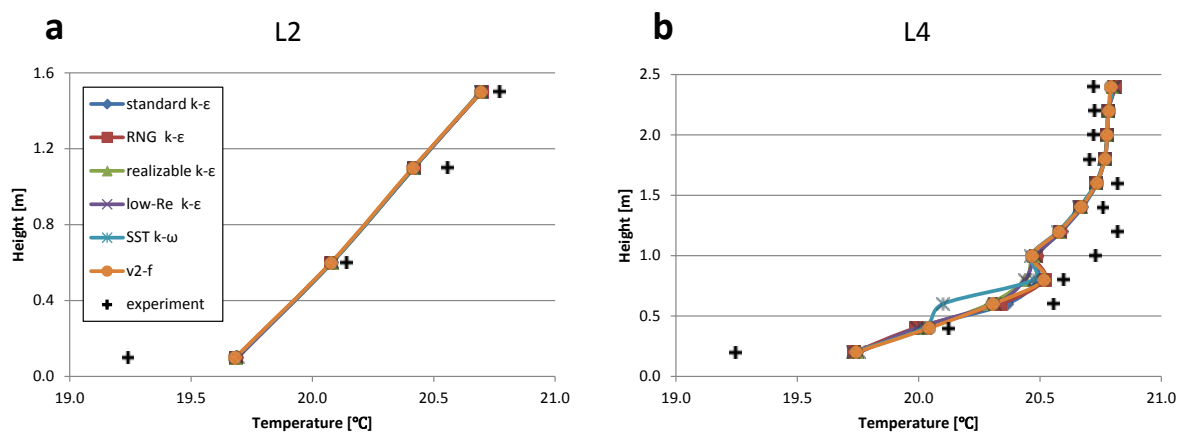


Figure 4: Temperature profiles at a) L2 and b) L4.

Figure 5 compares the predicted heat flux that the manikin releases to the surroundings with the experimental data. All turbulence models overestimate the total heat flux from the manikin. Not surprisingly, the most remarkable deviation occurs to the standard  $k - \epsilon$  model, which over-predicts the heat flux by as high as  $40 \text{ W/m}^2$ . The best match to the measurement belongs to the  $k - \omega$  SST model, followed by the  $\overline{v^2} - f$  model. The RNG  $k - \epsilon$  model and realizable  $k - \epsilon$  model perform fairly well and, as expected, exhibit superiority over the standard one. Although the performance of the Launder-Sharma low-Re  $k - \epsilon$  model is better than the standard  $k - \epsilon$  model, it is not as good as that of other models. It is noteworthy that the values of radiative heat flux predicted by different simulations are nearly identical,

ranging from 36% (standard  $k - \epsilon$  model) to 43% ( $k - \omega$  SST model) of the total heat flux, which is consistent with Martinho et al. (Martinho et al. 2012) who finds out that the radiative heat flux accounts for approximately 40% of the total heat flux. The different total heat fluxes result mainly from the different values of predicted convective heat flux. As the measurement does not distinguish the radiative heat flux from the convective one, however, it is hardly possible to evaluate the accuracy of convective and radiative heat flux prediction individually.

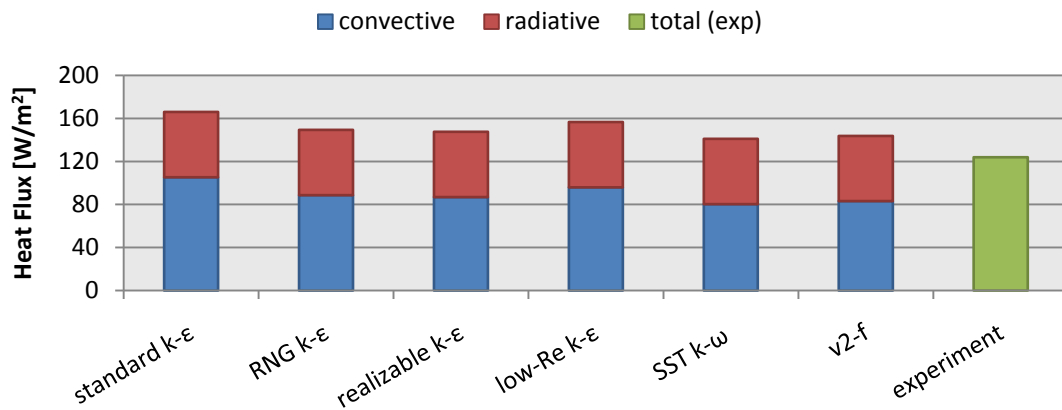


Figure 5: Predicted and measured heat fluxes from the thermal manikin.

Figure 6 presents the distribution of the convective, radiative and total heat flux over the manikin surface predicted by the  $k - \omega$  SST model. As can be seen from Figure 6 b), the radiative heat flux is higher where the manikin ‘sees’ the surroundings than where the manikin ‘sees’ itself. The radiative heat transfer between different parts of the manikin is much lower than that between the manikin and the surroundings. Thus, the distribution of the radiative heat flux over the manikin surface justifies the utilization of fvDOM that takes into consideration the real human geometry and posture.

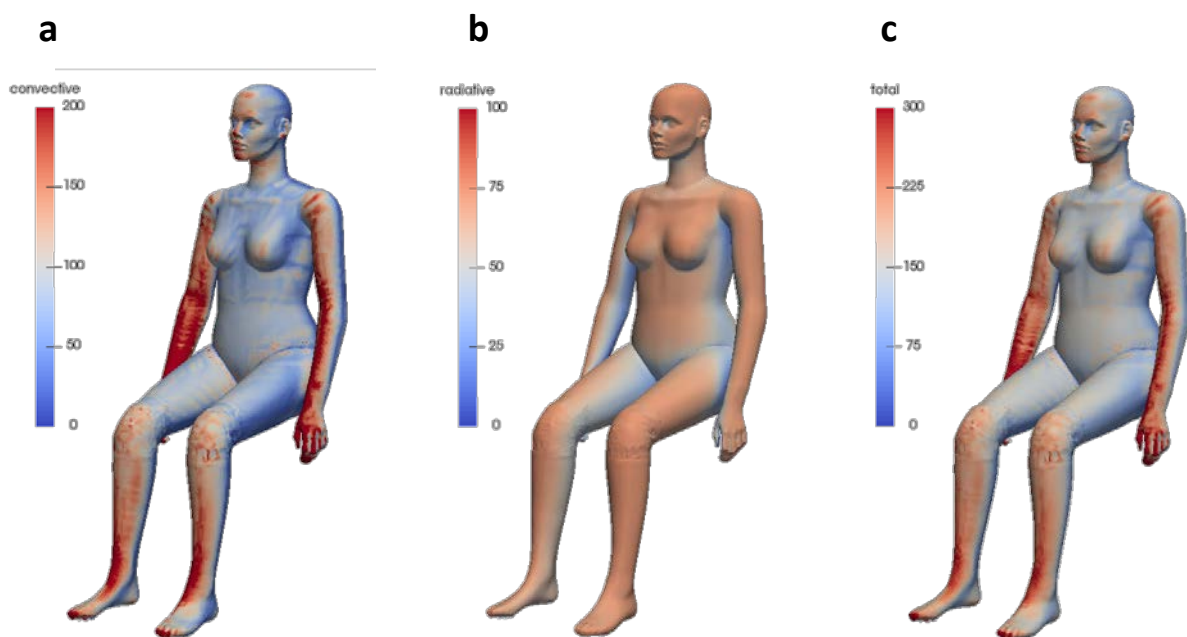


Figure 6: a) convective heat flux, b) radiative heat flux, and c) total heat flux over the manikin surface [ $\text{W}/\text{m}^2$ ].

Despite deviations from the experimental data, the simulation results obtained by OpenFOAM are comparable to the results obtained by commercial codes in the previous studies (Sadri-zadeh & Holmberg 2016; Ito et al. 2015c). In the simulation, the standard  $k - \varepsilon$  model has shown the best robustness and easiest convergence among all models used in the simulation. The  $\overline{v^2} - f$  model has demonstrated significant convergence difficulties and has also been found to be sensitive to the initial conditions and the types of near-wall treatment. As it resolves two additional equations, the  $\overline{v^2} - f$  model is also more computationally expensive than any other model. Despite the better accuracy of the RNG and realizable  $k - \varepsilon$  models, their convergence is not as good as the standard one. Therefore, it is beneficial to start the simulation of the RNG  $k - \varepsilon$ , realizable  $k - \varepsilon$ , or  $\overline{v^2} - f$  model from an established simulation of the standard  $k - \varepsilon$  model. The  $k - \omega$  SST model has shown the best trade-off between robustness and accuracy, which provides good accuracy without incurring significant computational or convergence difficulties.

## 4 CONCLUSIONS

In this study, we investigate the prediction capability of an open-source CFD code – OpenFOAM, in the applications of indoor airflow and heat transfer simulations. For the ease of validation, the simulation is performed on a well-documented benchmark experimental test, conducted collaboratively by the Aalborg University in Denmark and Gävle University in Sweden. Six OpenFOAM built-in turbulent viscosity models have been attempted and their performances are compared and evaluated against the experimental data. The velocity and temperature distribution predicted by different models are rather closed to each other, but noticeable discrepancies with experimental data are observed. As regards the heat flux from the manikin to the surroundings, the  $k - \omega$  SST model shows the best match with the measurement, followed by the  $\overline{v^2} - f$  model. Despite the relatively good accuracy, the  $\overline{v^2} - f$  model is more computationally expensive and less robust than any other model used in the simulation. The RNG  $k - \varepsilon$  model and the realizable  $k - \varepsilon$  model overcome some of the shortcomings of the standard  $k - \varepsilon$  model and offer acceptable accuracy.

Despite the discrepancies that exist between the simulation and experiment, the performance of OpenFOAM is comparable to that of commercial codes used in previous studies in the literature. This study enhances our confidence in applying OpenFOAM to more involved studies in the future. It should, however, be emphasized that OpenFOAM has a steep learning curve due to its limited documentation. Proficient use of OpenFOAM and, in general, open-source CFD, requires more demanding competence of users than do commercial codes.

## 5 REFERENCES

- Axtmann, G., & Rist, U. (2016). Scalability of OpenFOAM with Large Eddy Simulations and DNS on High-Performance Systems. In *High Performance Computing in Science and Engineering '16* (pp. 413-424). Springer, Cham.
- Blacha, T., Gregersen, M. M., Islam, M., & Bensler, H. (2016). *Application of the Adjoint Method for Vehicle Aerodynamic Optimization* (No. 2016-01-1615). SAE Technical Paper.
- Chen, H. J., Moshfegh, B., & Cehlin, M. (2013). Investigation on the flow and thermal behavior of impinging jet ventilation systems in an office with different heat loads. *Building and Environment*, 59, 127-144.

- Chen, Q. (1995). Comparison of different k- $\epsilon$  models for indoor air flow computations. *Numerical Heat Transfer, Part B Fundamentals*, 28(3), 353-369.
- Chen, Q., & Srebric, J. (2000). Application of CFD tools for indoor and outdoor environment design. *International Journal on Architectural Science*, 1(1), 14-29.
- Gao, N. P., & Niu, J. L. (2005). CFD study of the thermal environment around a human body: a review. *Indoor and built environment*, 14(1), 5-16.
- Ito, K., Inthavong, K., Kurabuchi, T., Ueda, T., Endo, T., Omori, T., ...& Matsumoto, H. (2015a). CFD Benchmark Tests for Indoor Environmental Problems: Part 1 Isothermal/non-isothermal flow in 2D and 3D room model. *International Journal of Architectural Engineering Technology*, 2(1), 1-22.
- Ito, K., Inthavong, K., Kurabuchi, T., Ueda, T., Endo, T., Omori, T., ...& Matsumoto, H. (2015b). CFD benchmark tests for indoor environmental problems: Part 2 cross-ventilation airflows and floor heating systems. *International Journal of Architectural Engineering Technology*, 2(1), 23-49.
- Ito, K., Inthavong, K., Kurabuchi, T., Ueda, T., Endo, T., Omori, T., ...& Matsumoto, H. (2015c). CFD benchmark tests for indoor environmental problems: Part 3 numerical thermal manikins. *International Journal of Architectural Engineering Technology*, 2(1), 50-75.
- Jasak, H. (1996). Error analysis and estimation for finite volume method with applications to fluid flow.
- Jasak, H., Jemcov, A., & Tukovic, Z. (2007). OpenFOAM: A C++ library for complex physics simulations. In *International workshop on coupled methods in numerical dynamics* (Vol. 1000, pp. 1-20). IUC Dubrovnik, Croatia.
- Konstantinov, M., Lautenschlager, W., Shishkin, A., & Wagner, C. (2014). Numerical simulation of the air flow and thermal comfort in aircraft cabins. In *New Results in Numerical and Experimental Fluid Mechanics IX* (pp. 293-301). Springer International Publishing.
- Konstantinov, M., & Wagner, C. (2014). Numerical simulation of the air flow and thermal comfort in a train cabin. In *Proceedings of the second international conference on railway technology: research, development and maintenance*. Pombo, J., (Editor) Civil-Comp Press, Stirlingshire, United Kingdom, paper (Vol. 328).
- Konstantinov, M., & Wagner, C. (2016). Numerical simulation of the thermal comfort in a model of a passenger car cabin. In *New Results in Numerical and Experimental Fluid Mechanics X* (pp. 383-393). Springer International Publishing.
- Liu, P. (2015). Scalability Performance Analysis of OpenFOAM on Modern HPC Clustering Technologies. In *The 3rd OpenFOAM User Conference 2015, Stuttgart, Germany*.
- Liu, W., Jin, M., Chen, C., You, R., & Chen, Q. (2016). Implementation of a fast fluid dynamics model in OpenFOAM for simulating indoor airflow. *Numerical Heat Transfer, Part A: Applications*, 69(7), 748-762.
- Martinho, N., Lopes, A., & da Silva, M. G. (2012). Evaluation of errors on the CFD computation of air flow and heat transfer around the human body. *Building and Environment*, 58, 58-69.
- Migliaccio, M., Beatrice, C., Briani, M., & Fraioli, V. (2009). *Numerical simulations of diesel engine combustion by means of OpenFOAM CFD ToolBox* (No. 2009-24-0002). SAE Technical Paper.

- Nilsson, H.O., Brohus, H., Jensen, M.K. & Nielsen, P.V. (2007). *Benchmark Tests for a Computer Simulated Person - Manikin Heat Loss for Thermal Comfort Evaluation*. [www.cfd-benchmarks.com](http://www.cfd-benchmarks.com) [1 May 2017].
- Norton, T., Sun, D. W., Grant, J., Fallon, R., & Dodd, V. (2007). Applications of computational fluid dynamics (CFD) in the modelling and design of ventilation systems in the agricultural industry: A review. *Bioresource technology*, 98(12), 2386-2414.
- Ramechecandane, S., Beghein, C., & Allard, F. (2010). Modeling fine particle dispersion in an inhomogeneous electric field with a modified drift flux model. *Building and Environment*, 45(6), 1536-1549.
- Sadrizadeh, S., Tammelin, A., Ekolind, P., & Holmberg, S. (2014). Influence of staff number and internal constellation on surgical site infection in an operating room. *Particuology*, 13, 42-51.
- Wang, C. (2013). Numerical Investigation of Flow Induced Noise in a Simplified HVAC Duct with OpenFOAM. Master Thesis. Royal Institute of Technology, Sweden
- Weller, H. G., Tabor, G., Jasak, H., & Fureby, C. (1998). A tensorial approach to computational continuum mechanics using object-oriented techniques. *Computers in physics*, 12(6), 620-631.
- Xue, Y., Liu, W., & Zhai, Z. J. (2016). New semi-Lagrangian-based PISO method for fast and accurate indoor environment modeling. *Building and Environment*, 105, 236-244.
- Zörner, C., Islam, M., & Lindener, N. (2010). The aerodynamics and aeroacoustics of the new Audi A8. *ATZ worldwide*, 112(6), 22-29.

# Experimental study on the in-situ performance of a natural ventilation system with heat recovery

Paraskevi Vivian Dorizas<sup>\*1</sup>, Tom Lipinski<sup>2</sup>, Dimitrios Makris-Makridis<sup>2</sup>, Samuel Stamp<sup>1</sup>, and Dejan Mumovic<sup>1</sup>

*1 UCL Institute for Environmental Design and Engineering, The Bartlett, Faculty of the Built Environment, University College, WC1H 0NN, London, UK*

*2 Ventive Ltd, Swan Street, Old Isleworth, TW7 6RS, London, UK*

*\*Corresponding author: p.dorizas@ucl.ac.uk*

## ABSTRACT

Combining heat recovery with natural ventilation is a relatively new topic of significant academic and commercial interest. The present study shows the performance of a recently developed Passive Ventilation system with Heat Recovery (PVHR) installed in a primary school building. The study includes (i) long term (12-month period) monitoring of the thermal environment and CO<sub>2</sub> concentrations and (ii) intense short term monitoring (2-week period during the heating season) of the environmental conditions in two classrooms, including detailed monitoring of the temperatures and bi-directional air speeds within the system itself. Airtightness measurements using the Blower Door test method were performed, while time-varying ventilation rates within each classroom were estimated by using a form of continuity equation taking into account CO<sub>2</sub> generation rates by occupants. Preliminary results show that average ventilation rates in the two classrooms ranged between 4.20 l/s/p and 5.93 l/s/p, above the recommended minimum set by BB101 (3 l/s/p). Furthermore, CO<sub>2</sub> concentrations for the majority of the monitoring period were below 1500 ppm, while future research steps are also suggested.

## KEYWORDS

Natural ventilation, Infiltration, PVHR, Air tightness, Indoor Air Quality (IAQ), Schools

## 1 INTRODUCTION

Natural ventilation strategies consume negligible amount of energy by utilizing natural driving forces of wind and buoyancy and provide a viable alternative to energy consumption by mechanical ventilation and air-conditioning systems, and a fundamental method towards energy efficient design of buildings (Calautit and Hughes 2014).

Several studies have been published on the evaluation of the performance of wind driven ventilation techniques such as the wind towers. These studies are mainly based on numerical methods (Montazeri 2011) such as CFD models (Ghadiri et al., 2013) and analytical methods (Hedeyat et al., 2015) using alternative semi-empirical approaches (Jones and Kirby 2009) or envelope flow models. The measurement of the performance of such systems has been restricted to laboratory conditions (wind tunnel tests) and only a few of them are examined *in situ* (Kirk and Kolokotroni 2004), making this a critical approach which needs further research.

According to Shao et al, 1998 passive stack systems that are designed without heat recovery may lead to wasteful heat loss. Natural ventilation systems combined with the application of

heat recovery techniques which utilize internal dissipated heat, can lead to significant reductions in the overall energy consumption. Currently, passive ventilation systems with heat recovery (PVHR) constitute an area of research which is expanding however little has been published so far on systems' *in-situ* performance (Lipinski et al., 2017).

This study reports on the preliminary results and the main objectives are: 1. to evaluate aspects of the indoor environmental quality of the classrooms that have a natural ventilation system combined with heat recovery installed; 2. to examine to which extent the required ventilation rates are being achieved in context of the air tightness levels of the classrooms; 3. to give a preliminary indication of the heat recovery performance and the parameters that are affecting the air flows within the system.

## 2 METHODOLOGY

### 2.1 Sampling site description and monitoring period

The study took place in 2 classrooms (#1 & #2) of a primary school building built in 1971 and located at Forest Hill, in South East London within the London Borough of Lewisham. The school is located in a suburban residential area and has low to moderate traffic on its adjoining streets.

The monitoring period involved both the short and the long term monitoring in order to cover a broader source of information. Long-term measurements were carried out in one classroom (#1) from February until November 2016 while short-term monitoring took place in two classrooms (#1 and #2) for two consecutive weeks from the 19<sup>th</sup> of January until the 2<sup>nd</sup> of February 2017. Monitoring is still ongoing but for the purpose of the paper a specific period was chosen to present the preliminary findings. Both classrooms had natural ventilation systems with heat recovery installed and were selected in order to meet the requirements set by Mumovic et al., 2009 having "reasonable occupancy patterns, typical teaching activities and microclimatic conditions which would not reduce the potential for natural ventilation". The classrooms also had central heating systems (with multiple radiators positioned around the classroom) and windows on a single façade (North-West). Table 1 summarizes some of the main characteristics of the two classrooms.

Table 1: Main characteristics of the classrooms

	Floor area (m <sup>2</sup> )	Volume (m <sup>3</sup> )	Window area/ openable area (m <sup>2</sup> )	Orientation	Window opening types & glazing	Number of students/ teachers	Age of children
Classroom #1	60	180	12.6/ 1.1	North-West	Top-hung/ double glazing/ aluminium frame	29/1	8-9
Classroom #2	60	180	12.6/ 0.5			30/1	10-11

### 2.2 Passive Ventilation with Heat Recovery: description

The PVHR system consists of three key components: the roof cowl, the coaxial heat exchanger and the flow splitter as shown in Figure 1. The coaxial heat exchanger is designed to be directly connected to the cowl assembly and the flow splitter/ceiling diffuser below. Its structure is designed to channel two air flows to pass through Heat Exchanger fins without contamination caused by air mixing. The fins enable the transfer of heat from the warmer outgoing airflow to the cooler incoming airflow, principally by means of convection and conduction. Further details on the system's description can be found on Lipinski et al., 2017.



Figure 1: Key components of the PVHR system

### 2.3 Parameters measured and instrumentation

Indoor temperature, relative humidity and CO<sub>2</sub> concentrations were measured throughout both the long term and short term monitoring periods. CO<sub>2</sub> concentrations were monitored at 3 different locations within each of the two classrooms in order to examine the horizontal and vertical distribution of CO<sub>2</sub> concentrations. Two of the sensors were located at seated breathing level (1.10m) according to the ISO 7726: 2001, with one at the centre of the classroom and one next to the window. The third CO<sub>2</sub> sensor was placed at high level (2.70m) near the system's extract. All monitoring equipment was calibrated before installation and correction factors between the monitoring instruments were estimated during preliminary measurements in a lab under constant conditions.

Outdoor weather conditions including temperature, relative humidity, wind speed and wind direction were simultaneously monitored throughout the short term monitoring period. Moreover, temperatures and air velocities were measured in both the supply and extract air channels before and after the heat exchanger of each of the systems in the two classrooms (Figure 2). It should be noted that the air velocity sensors were bi-directional in order to examine in detail the characteristics of air flows inside the system. The technical specification of the monitoring equipment used is summarized in Table 2. The logging interval for all of the aforementioned parameters was 90s.

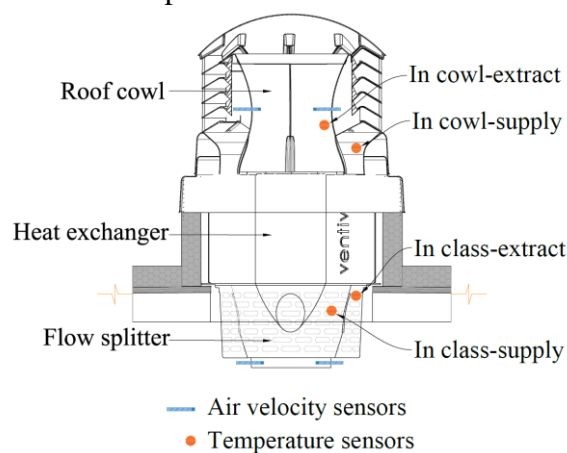


Figure 2: PVHR section and location of air velocity (blue bars) and temperature sensors (orange dots)

Table 2: Technical specification of monitoring equipment

Parameter Measured	Sensor Type/ Supplier/ Principle of operation	Range/ Resolution	Accuracy
1xbuilt-in RH	GD47/ Eltek Ltd/ NDIR infrared sensors  Compliant to: EN300-220-1 EN16000-26	0-100%/ 0.1%	±2%
1x built in T		-20-60°C/0.1°C	±0.4°C
1xbuilt-in CO <sub>2</sub>		0-5000ppm/ 3% of measured value at 20°C	±50ppm
External RH	GD13Ecf/ Eltek	0-100%/ 0.1%	±2%
External T		-40 to +85°C/ 0.1°C	±0.4°C
Wind Speed / Wind direction	Davis Anemometer connected to GD18Wcf /Eltek/ Wind vane cup anemometer	0-58m/s / 0.45m/s & 1°	±5%/ 7°
Air velocity (inside the system) connected to an Eltek GS 44 voltage transmitter	AVS Series 1000-bidirection/ Degree Controls Inc. Thermistor based sensor	-2.5 to +2.5m/s / 256 steps	From 15-35°C, 5% of full scale, 3% of full scale at 21°C
Temperature (inside the system) connected to a GS34 transmitter	Thermistor/ ELCM-U-VS-02-0	-50°C to +150°C	±0.1°C

## 2.4 Data processing and analysis

### *Ventilation rates*

Time varying ventilation rates in each of the two classrooms were estimated using the mass balance equation. The rate of change in the concentration of the monitored gas is a function of the concentration of the incoming air to the concentration of the outgoing air plus the internal generation rate of the gas under investigation. In this case the gas was CO<sub>2</sub>. The time derivative of the monitored concentration is given by the following formula (Coley and Beisteiner 2002):

$$V \frac{dC(t)}{dt} = G + QC_{ex} - QC(t) \quad (\text{Eq.1})$$

The integrative solution of the above equation gives:

$$C(t) = C_{ex} + \frac{G}{Q} + \left( C_{in} - C_{ex} - \frac{G}{Q} \right) e^{-\left(\frac{Q}{V}\right)t} \quad (\text{Eq.2})$$

Where C(t) is the internal concentration of CO<sub>2</sub> in ppm (time dependant), C<sub>ex</sub> is the external concentration of CO<sub>2</sub> in ppm, C<sub>in</sub> is the initial concentration of CO<sub>2</sub> in ppm, G is the generation rate of CO<sub>2</sub> within the classroom (cm<sup>3</sup>/s, depending on the activity performed by the students), Q is the internal-external exchange rate (m<sup>3</sup>/s), V is the volume of the room and t is the time (s).

The methodology used by Coley and Beisteiner 2002 was adopted in which 20min averaged blocks of data were considered (to reduce noise). Student's presence along with their level of physical activity, sex and age were logged in detail on daily basis throughout the short term monitoring period from which a generation rate of CO<sub>2</sub> was estimated. The averaged generation rate of CO<sub>2</sub> for students was equal to 0.0043 l/s per person and for teachers was equal to 0.0052 l/s/p, which are in agreement with Persily, 1997. Eq. 2 was solved using MATLAB R2012b. The assessment of uncertainties of this methodology will be presented in detail in a future study.

### *Air permeability*

Air permeability measurements took place in the two classrooms using aRetrotec DM2 gauge and a 3000 fan. In the present study both pressurization and depressurization tests were

performed in general following to the ISO EN 9972 (EN ISO 13829), according to the method of a building in use, fulfilling the following measurement conditions: 1. The results from the indoor to outdoor temperature difference (in Kelvin) multiplied by the height (in m) should be less than 250mK, 2. The wind speed should be less than 6m/s. However, some critical differentiations were considered. Due to the size of the building and for matters of simplification the airtightness test was performed in each of the two classrooms. In this way the expected result would measure all barriers of a single zone and would include the air leakage related both to the indoor and outdoor environment. For this reason the envelope area that was taken into account in the calculations of the air permeability was equal to the entire envelope area of each of the classrooms including floor, ceiling, external and internal walls. Two different modes of air tightness were measured in each of the two classrooms, with the natural ventilation system being sealed (baseline airtightness) and unsealed. In this study the Blower Door device was supplemented with smoke tests for a qualitative examination of the air flows.

### 3 RESULTS AND DISCUSSION

#### 3.1 Indoor Environmental conditions and CO<sub>2</sub> concentrations

The daily average concentrations of CO<sub>2</sub> throughout the long term monitoring period (Feb-Nov 2016) of classroom #1 are shown in Figure 3. The daily average concentrations for the entire period were below 1500ppm for the majority of the cases. Also, there is a decreasing trend on the average concentrations moving from winter to summer months possibly related to the additional ventilation rates through openable windows during summer months. According to the BB101 for teaching spaces that natural ventilation is used, the maximum concentrations should not exceed 2000ppm for more than 20 consecutive minutes each day. For this case for 15 days out of 110 days (13.6%) of monitoring in total during the long term measurements, the CO<sub>2</sub> concentrations at breathing level exceeded 2000ppm for durations that ranged between 30min and 180min. However, the percentage of time that the CO<sub>2</sub> exceeded 2000 ppm throughout the long term monitoring period was equal to 3%. In this particular installation purge ventilation was to be manually provided by the user with exceedance of 2000ppm communicated by red ‘traffic light’ on the classroom sensor (as stipulated in the BB101). It appears that in the cases where CO<sub>2</sub> concentrations remained above 2000ppm the windows have not been opened. Following the study the guidance has been issued to include automatic purge ventilation in all future PVHR projects to address this user dependent variability.

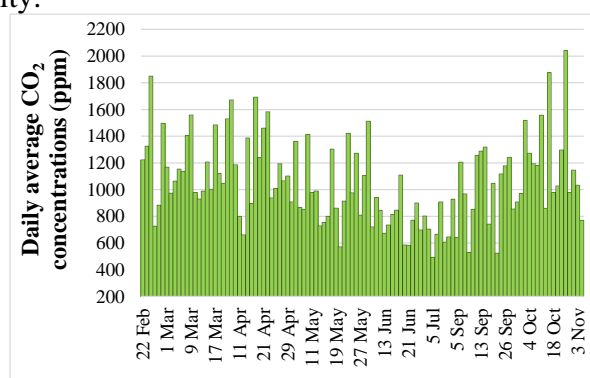


Figure 3: Daily average of CO<sub>2</sub> concentrations during the reaching hours at the long term monitoring period

The monthly ranges for temperature and relative humidity are shown in Figure 4. Monthly average temperatures ranged from 19 to 24°C while relative humidity ranged from 40 to 59% indicating a satisfactory thermal environment throughout the year.

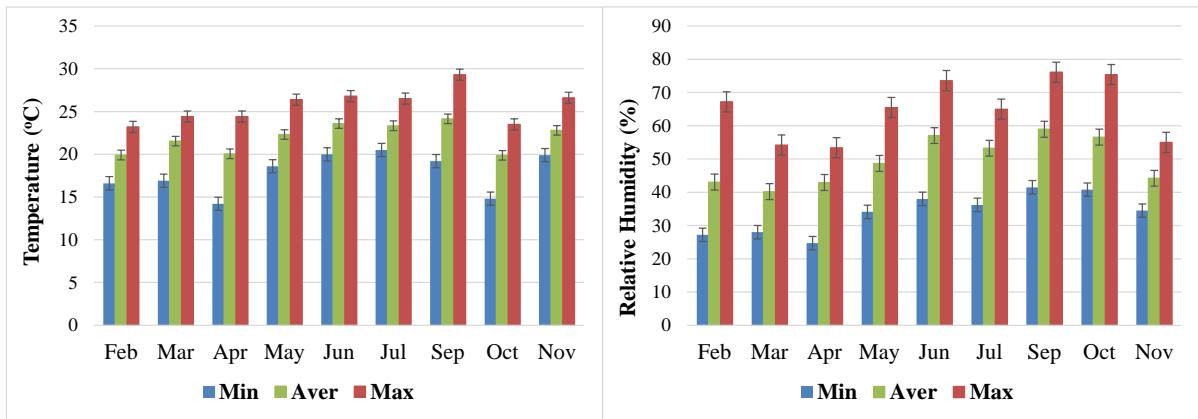


Figure 4: Monthly ranges of temperature (left) and relative humidity (right) during the long term monitoring period

Descriptive statistics of temperature, relative humidity and CO<sub>2</sub> concentrations during the teaching hours (8:50AM -15:30PM) for the short term monitoring period (19/1-1/2/17) are summarised in

Table 3. Average temperatures in both of the classrooms are slightly above the recommended winter comfort temperatures set in CIBSE guide A (19-21°C) by 0.9°C in Classroom #1 and 2.9°C in classroom #2. Relative humidity levels remained low in both classrooms. Mean CO<sub>2</sub> concentrations for both classrooms were below 1500ppm.

Table 3: Descriptive statistics of indoor environmental parameters during the teaching hours

		Mean	Median	Min	Max	St Dev
Classroom #1	Temperature (°C)	21.9	21.9	19.2	24.1	1
	Relative Humidity (%)	39	37	25	56	7
	CO <sub>2</sub>	995	950	546	1914	263

Figure 5 presents the cumulative frequency distribution of CO<sub>2</sub> concentrations in the two classrooms (classroom #1 depicted in the left chart, classroom #2 on the right) for the short term monitoring period. As can be seen, for 5% of the cases at the middle point (representative of the classroom's mean concentration) of classroom #1 and approximately 20% of the cases in classroom #2 CO<sub>2</sub> levels exceeded 1500ppm. Also, the CO<sub>2</sub> concentrations near the window of classroom #2 weresignificantly lower compared to the corresponding readings at the extract level and middle point (difference of about 460ppm), likely indicating fresh air supply from the window at that point (or higher levels of infiltration). CO<sub>2</sub>concentrations at the extract level and middle point (mean concentration of the room) were very similar in classroom # 2 which according to thedefinition of the contaminant removal effectiveness (CRE), of REHVA can be considered as a fully mixed situation.

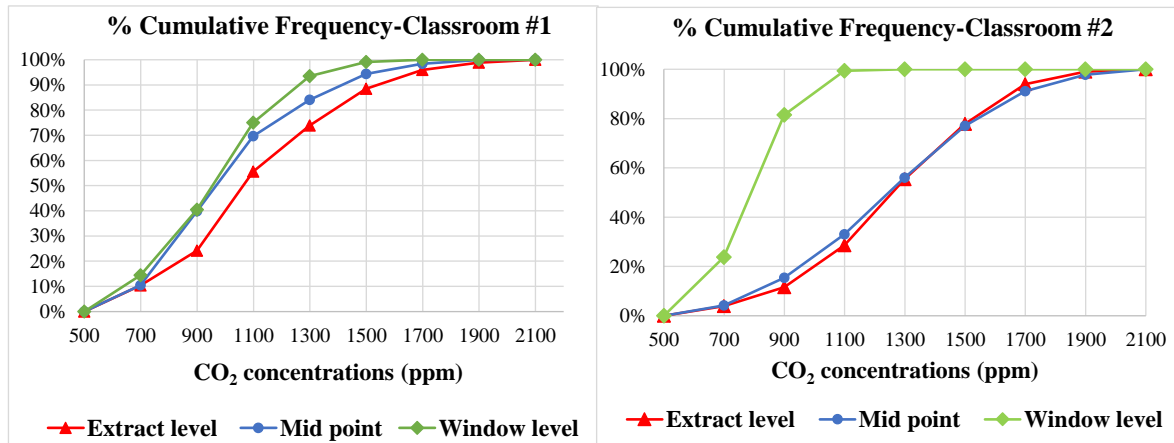


Figure 5: Cumulative frequency distributions of CO<sub>2</sub> at extract level, middle point and window level

### 3.2 Ventilation rates

As aforementioned, time varying ventilation rates were estimated using the mass balance equation for 20min blocks of data (using time-averaged values of CO<sub>2</sub> and G). Table 4 presents the descriptive statistics of ventilation rates in l/s/p, the corresponding indoor to outdoor temperature difference and wind speed in each of the two classrooms during the short term monitoring period. It can be seen averaged ventilation rates in both of the classrooms are above the minimum ventilation rates of 3 l/s/p required by BB101.

Table 4: Descriptive statistics of Ventilation rates, corresponding Indoor/outdoor temperature differences and wind speed

	Classroom #1		Classroom #2		Wind speed (m/s)
	Ventilation rates (l/s/p)	$\Delta T (T_{\text{indoor}} - T_{\text{outdoor}})$	Ventilation rates (l/s/p)	$\Delta T (T_{\text{indoor}} - T_{\text{outdoor}})$	
Average	5.93	16.5	4.2	17.62	0.9
Median	5.50	16.5	3.35	17.23	0.9
Min	0	10.7	0	10.72	0
Max	17.74	23.4	13.57	25.01	2.2
Stdev.	3.97	3.3	3.57	3.13	0.5

The diurnal variation of CO<sub>2</sub> concentrations, the number of people and corresponding estimated ventilation rates for one indicative day in each of the classrooms are shown in Figure 6. The trend of the CO<sub>2</sub> concentrations follows the number of students inside the classrooms while the ventilation rates are inversely correlated to the CO<sub>2</sub> concentrations with some time lag being evident. In classroom #1 (Figure 6, left) half of the windows opened at 11:03AM and remained open until the rest of the day. As for classroom #2, half of the windows opened from 11:24AM until the end of the day.

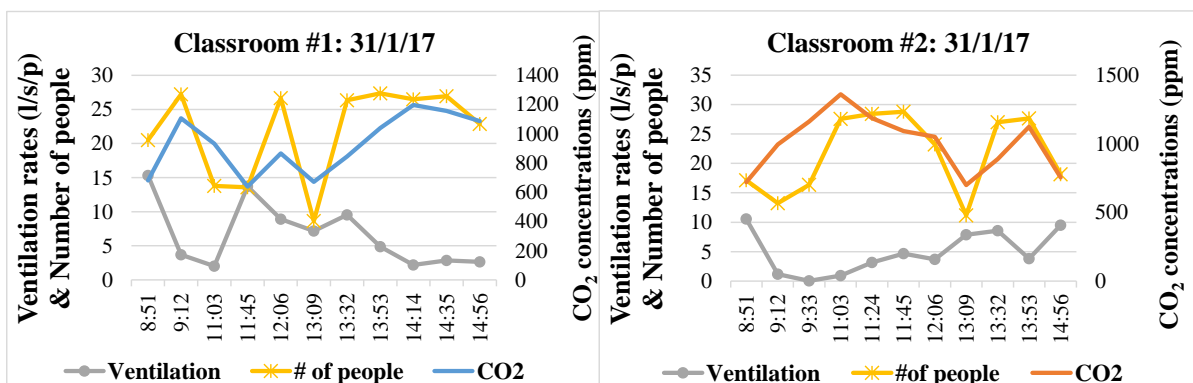


Figure 6: Diurnal variation of CO<sub>2</sub>, number of people and ventilation rates

### 3.3 Air permeability

Air permeability values are summarized in Table 5. According to the approved document L2A classification, the worst allowable air permeability for new buildings is  $10\text{m}^3/\text{m}^2\text{h}$  at 50Pa. Baseline air permeability in both classrooms (with ventilation systems sealed) was greater than this value. To this end, considering that the PVHR system is designed for airtight buildings (recommended airtightness  $\leq 5\text{m}^3/\text{m}^2$  at 50Pa) it can be assumed that the system's heat recovery performance is undermined in this particular case.

Table 5: Air permeability rates in the two classrooms

	System sealed (baseline)		System fully open	
	Mean air permeability $q_{50}$ at 50 Pa ( $\text{m}^3/\text{h}/\text{m}^2$ )	Mean air leakage $n_{50}$ at 50 Pa (ACH)	Mean air permeability $q_{50}$ at 50 Pa ( $\text{m}^3/\text{h}/\text{m}^2$ )	Mean air leakage $n_{50}$ at 50 Pa (ACH)
Classroom #1	13.4	15.83	26.68	31.42
Classroom #2	10.23	12.19	23.81	28.25

### 3.4 System

Since PVHR is a natural ventilation system, driven exclusively by wind and buoyancy, the surrounding conditions (e.g. window opening) will influence its operation and the balance of supply and extract. Using the output of the bi-directional air velocity sensor located in the air flow terminal of the system (within the classroom, ceiling level), the air flows were categorized in “positive supply” and “negative supply”. The system in classroom #1 supplied fresh air (“positive supply”) in the classroom for 19% of the occupied hours during the short term monitoring period, while the system in classroom #2 supplied fresh air in the classroom for 9% of that time. At this point it is worth mentioning that the installation of the system in classroom #2 was found to be defective (due to fitting inaccuracies) therefore its performance could have been affected. In addition for the above, considering amount of time that the systems “positively supplied” fresh air in the two classrooms, the windows were closed for 81% of that time in classroom #1 and for 96% of that time in classroom #2. Negative supply is a design feature of Purge ventilation mode and is enabled by opening windows. When PVHR system is installed in particularly ‘leaky’ buildings it can occur also at times when windows are closed due to high levels of infiltration.

Figure 7 (left for classroom #1 and right for classroom #2) presents the relative frequencies of the systems’ supplying fresh air (“positive supply”) and extracting stale air (“negative supply”) to and from the classrooms. In green striped bars are the relative frequencies of the air flows that the terminal of the system supplied fresh air in the classroom (“positive supply”, 19% of the time for classroom #1 and 9% of the time for classroom #2) for five wind speed bins. The blue and orange bars are the corresponding relative frequencies of air flows for classrooms #1 and #2 respectively that the system extracted fresh air from the classroom to the outdoor environment (“negative supply”, 81% of the time for classroom #1 and 91% of the time for classroom #2). It can be seen that in both classrooms, the distributions of air flows for the case of the “positive supply” are extending towards higher wind speeds (2-3m/s) whereas in the case of the “negative supply” (extract air flows) the distributions are peaking closer to lower wind speeds (1-2m/s).

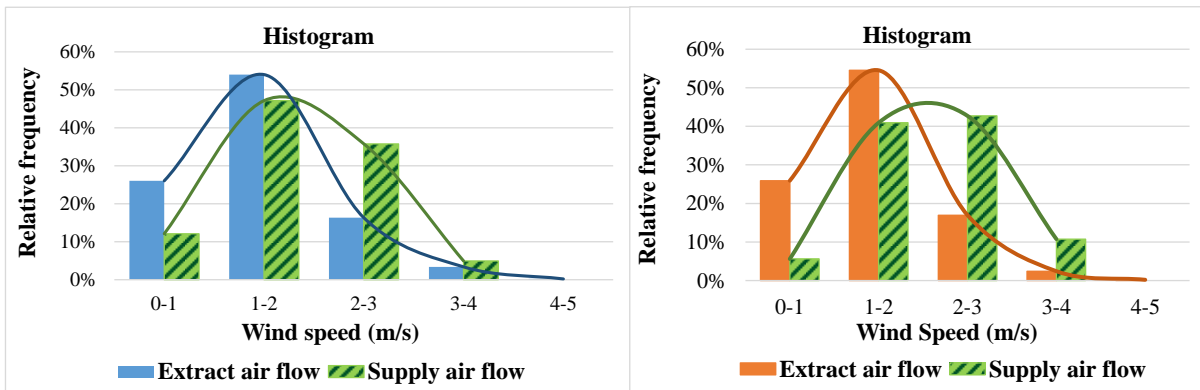


Figure 7: Histogram of extract and supply air flows in the “supply ductwork” of the system for several wind speed bins in classroom #1 (left) and classroom #2 (right)

Figure 8 presents average temperatures developed inside the PVHR system, the classroom and the external environment across the short term monitoring period for the cases that the system was supplying fresh air (“positive supply”) to the classrooms (left: classroom #1, right: classroom #2). The exact location of the temperature sensors is shown in orange dots in Figure 2. As it can be seen, the temperature increased by approximately 10°C and 16°C in classrooms 1 and 2 respectively from the point right before the air entered the heat exchanger (in cowl-supply) and the point the air was supplied in the classrooms (in class-supply). It can further be seen that the supplied air temperature of the system to the classroom (in class-supply) is very similar to the indoor temperature of the classroom. Considering the following formula the heat recovery efficiency was calculated.

$$E_{\text{Heat Recovery}} = \frac{T_{\text{in class supply}} - T_{\text{in cowl supply}}}{T_{\text{in class extract}} - T_{\text{in cowl supply}}} \times 100\% \quad (\text{Eq.3})$$

Preliminary findings show that for the percentage of time that the system was supplying fresh air in the classrooms, the heat recovery efficiency was equal to 82% in classroom #1 and equal to 88% in classroom #2. These heat recovery efficiencies are unexpectedly high. A further CFD study is being conducted to establish whether higher than expected supply temperatures are influenced by the classroom air temperature or due to specific airflow balance within the system itself.

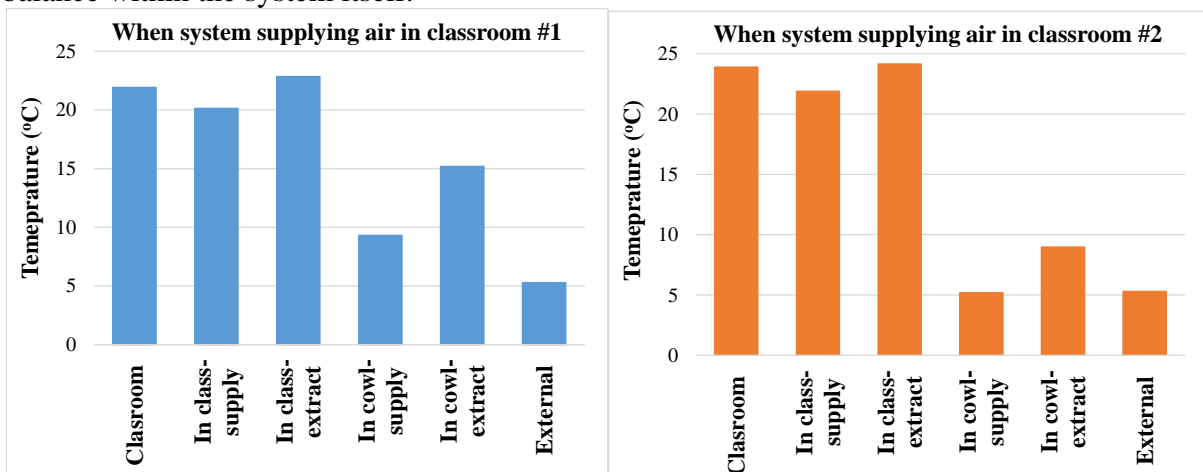


Figure 8: Average temperatures within the systems’ ductworks when the system is supplying air in the classrooms

#### 4 CONCLUSIONS

This paper presented preliminary findings of a study in progress of the performance of a passive ventilation system with heat recovery (PVHR) installed in two classrooms of a refurbished school.

The thermal environment of the classrooms with the ventilation system was satisfactory overall, being within the recommended thermal guidelines of CIBSE guide A and IAQ guidelines of BB101. As for the CO<sub>2</sub> concentrations, they were below 1500ppm for 95% and 80% of the cases in the two classrooms. Regarding the ventilation performance based on occupant generated CO<sub>2</sub> concentrations, the average estimated ventilation rates were equal to 5.93 and 4.2 l/s/p in the two classrooms, both above minimum requirements of 3 l/s/p set in the BB101. The air permeability measurements indicated relatively leaky building's fabric, a fact that directly impacts the ventilation balance within the system and the system's heat recovery performance. As for the preliminary results of impact of environmental conditions, it was found that for higher wind speeds (between 2 and 3 m/s) the system was mainly supplying fresh air in the classrooms while for lower wind speeds (between 1 and 2 m/s) the system was mainly extracting stale air from the classroom to the outdoor environment. The heat recovery efficiency of both systems in the two classrooms was higher than designed. A further CFD study is being conducted to establish parameters that are affecting the supply air temperature and are contributing to the air flow balance of the system and the surrounding environment. Further research will also involve the estimation of uncertainties on the calculation of ventilation rates using the occupant generated CO<sub>2</sub> concentrations.

## 5 ACKNOWLEDGEMENTS

This project was funded by the Innovate UK and Ventive Ltd under the KTP scheme. The authors would like to acknowledge Ventive Ltd for their support and for providing Ventive 900 PVHR systems to be examined for this particular study. We are also greatly indebted to the school directors and pupils, without whose consent this study would have not been possible.

## 6 REFERENCES

- BB101 (2016). Building Bulletin 101. *Guidelines on ventilation, thermal comfort and indoor air quality in schools*.
- Calautit, J.K., Hughes, B.R. (2014). *Wind tunnel and CFD study of the natural ventilation performance of a commercial multi-directional wind tower*. Building and Environment. 80, 71-83.
- CIBSE guide A (2006). Environmental Design. The Chartered Institution of Building Services Engineers London
- Coley, D.A., Beisteiner, A. (2002). *Carbon Dioxide Levels and ventilation rates in schools*. International Journal of Ventilation, 1:1, 45-52, DOI: 10.1080/14733315.2002.11683621
- Jones, B.M., Kirby, R. (2009). *Quantifying the performance of a top-down natural ventilation Windcatcher*. Building and Environment. 44, 1925-1934.
- Kirk, S. and Kolokotroni, M. (2004). *Windcatchers in modern UK buildings: Experimental study*. International Journal of Ventilation. 3 (1), 67-78, 10.1080/14733315.2004.11683904
- Lipinski, T., Dorizas, P.V., Makris-Makridis, D., Mumovic, D. (2017). *Passive ventilation system with heat recovery in an urban school: Performance in use*. CIBSE Technical

Symposium. Delivering resilient high performance buildings, 5-7 April 2017,  
Loughborough University, UK

Persily, A. K., (1997). *Evaluating building IAQ and ventilation with carbon dioxide*.  
ASHRAE Trans 103 (2). 193-204

REHVA guidebook 2004. *Ventilation effectiveness*. Federation of European Heating and Air-  
conditioning Associations. Guidebook No2

Shao, L., Riffat, S.B., Gan, G. (1998). *Heat recovery with low pressure loss for natural  
ventilation*. Energy and Buildings. 28(2), 179-184

# An interface of night ventilation and mass structure for passive cooling design strategy in Ghadames traditional dwellings

<sup>1</sup>*Dr. Jamal Alabid, Leicester School of Architecture,  
De Montfort University LE1 9BH*

<sup>2</sup>*Dr. Ahmad Taki Leicester School of Architecture,  
De Montfort University LE1 9BH*

## ABSTRACT

The effectiveness of night ventilation strategy for residential buildings in the old town of Ghadames has been investigated in this study. Methods of field surveys including observations, temperature measurements and interviews were conducted to determine the characteristic building parameters and strategies including window patterns and space organisation that mostly contributed to achieve an efficient indoor comfort conditions especially at night summer time. Results showed that skylight openings can be a good window pattern for enhancing night ventilation in hot arid climate. Further findings indicated that majority of occupants tend to feel thermally satisfied with indoor air conditions particularly during daytime. Due to high thermal mass structure in traditional dwellings indoor air gets warmer at night and small roof aperture would be not sufficient to readily extract warm air, so that a fixed roof fan is used to enhance air buoyancy. It is also observed that double ceiling height in the central hall plays an important role in balancing air change during day and night keeping interior at acceptable thermal conditions. The lower surface temperature due to standing wall to wall with surrounding buildings apparently has an impact on indoor thermal comfort conditions. However, the study suggested that new courtyard design in residential buildings should be considered taking into account all these passive design strategies in such a way to promote indoor climate conditions. Finally, and based on field surveys and measurements a preliminary design priorities and recommendations for passively ventilated dwellings in hot arid context are suggested.

**Keywords:** Traditional dwellings, night purge ventilation, thermal mass and hot climate.

## BACKGROUND

All vernacular dwellings have perfect building physics especially under extreme weather conditions (Nguyen et al., 2011). It can be so often difficult to maintain thermally comfortable conditions relying on thoroughly passive design strategies. Although it does not contradict the fact that vernacular housing generally does well adapt to local climatic conditions, meanwhile uses low energy design principles to achieve acceptable indoor thermal and health conditions. In hot regions cooling loads can be efficiently improved applying mass structure especially if combined with night ventilation strategy (Ben Cheikh & Bouchair 2004). Stack ventilation occurs in presence of greater pressure differences as the fact that warm air is more buoyant than cool air due to the less density causing air thermal buoyancy (Kleiven, 2003). This type of stack pressure would be applicable for single-sided openings or in the case of placing higher windows. However, IEE (2013) pointed out that placing roof vents along sides would enhance ventilation and relieve any problems of single-sided ventilation whilst a reverse air flow potentially will occur when outside temperature is lower than inside. Not only inside and outside thermal discrepancy and air density affect natural ventilation driven by stack effect but also wind velocity and direction is of importance (Gładyszewska-Fiedoruk & Gajewski 2012). This study investigates the advantage of having sky-windows in enhancing natural ventilation at night through stack effect and different thermal pressure.

## THE METHODOLOGY OF THE RESEARCH

This study has employed methods of field surveys to investigate the efficiency of applying passive cooling techniques in vernacular architecture of Ghadames. Observation of dwellers' behaviour and indoor climate conditions was the first method to carry out this work coupled with temperature measurements and assessment of residents' thermal satisfaction in naturally ventilated houses. The research also documented the work through drawings, sketches and photos to help understanding the way these houses were built to achieve acceptable indoor environment in such hot climate.

## GHADAMES LOCATION AND CLIMATE

Ghadames is a town located in the Sahara Desert built over 400 years ago on an Oasis that lies approximately 630 km to the south-west of Tripoli close to the junction between Libya, Tunisia and Algeria with an altitude of 340 to 370m above sea-level (Chojnacki, 2003).Ghadames falls in the most extreme zones within the Libyan climates as located in the Sahara Desert region with almost eight months of hot and dry period and four moderate and partly cold winter period as can be seen in Figure 1.

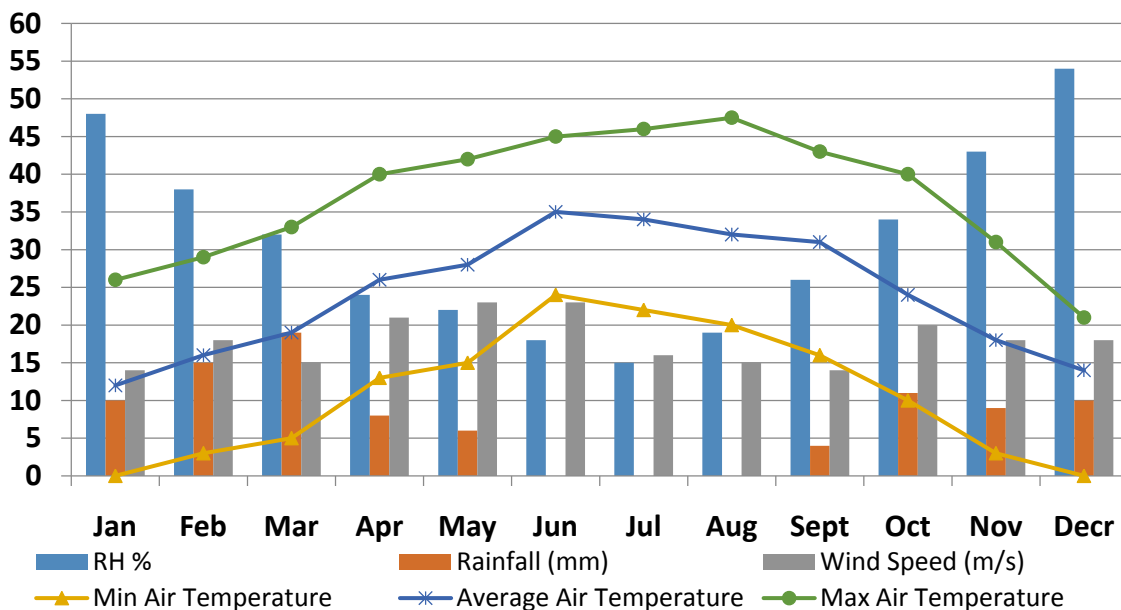


Figure 1. Ghadames climate conditions of the year 2013

## THE URBAN STRUCTURE OF THE OLD TOWN

The Oasis is inhabited thousands of years ago as excavation found in the area goes back to 4,000 years but existing buildings are dated back no more than 400 years and majority within 200 years' time. It can be noted that climate simply is the main deriving and dominant force in the solutions used to build old settlements in this Oasis. The building form is highly compact and tightly interwoven built up on an inclined land centralized to the southwest of the Oasis forming a large complex of townhouses.

## THE TRADITIONAL HOUSE (FORM AND LAYOUT)

The form of the house combines high degree of compactness with minimum exposure to outdoor and relatively small plot area ranges from 25 to 50 m<sup>2</sup>. The space organisation of rooms varies according to the privacy level and functionality though. It therefore constructed in three storey design to accommodate fully-sheltered ground floor consists of usually main entrance with stairs, guest room, storage and cesspit room. The first floor is a semi-private family area centralised by living-room which is surrounded by number of rooms. The central hall is constructed in double-volume height with steps leading to mezzanine level which also consists of other private

bedrooms. Stairs lead up to the roof level where kitchen is found as well as summer shed space used so often at summer nights.

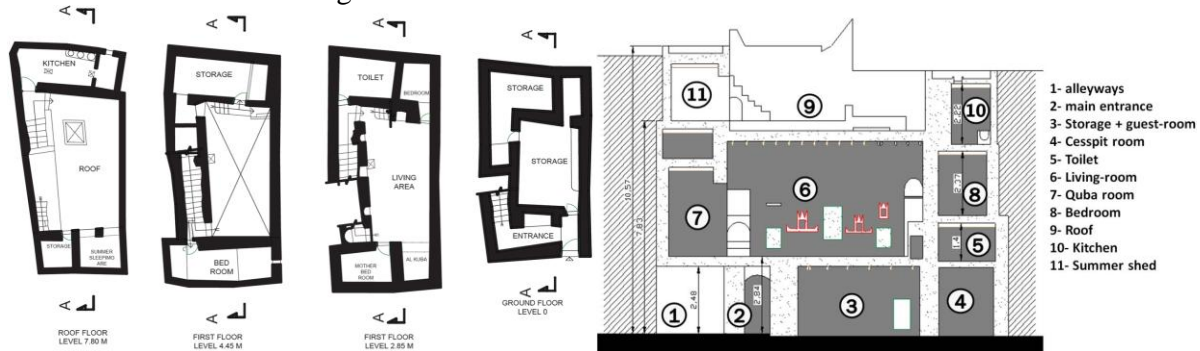


Figure 2. Typical traditional Ghadamesian house  
Source © (Gabril 2014, p.49)

## CONSTRUCTION MATERIALS

Building material is one of the key aspects characterises the desert architecture which so often called adobe architecture in some literature. The selection of specific material and method of construction was not a choice of people rather influenced by many factors predominantly the ecological land cover especially the abiotic elements such as soil, climate and other geological conditions. Equally importantly, the economic structure of society and inherited experience and knowledge of construction methods and techniques have an impact on the way local dwellings were built. In the case of Ghadames old town it is barely distinguishing individual buildings because of houses stand wall to wall having same constructional materials, façade finishing and similar heights. Al-Zubaidi (2002) stated that rocks and mud are the most common building materials in the old town of Ghadames due to the nature of the desert land.

However, traditional houses constructed not only with sun-dried mud and stone which is mainly used in the bearing walls but also gypsum, limestone and wood are commonly used particularly in roof construction and finishing as Figure 3 shows. The roof is given more attention and care as constructed with many layers to ensure it stands heavy loads and be thermally insulated. In general, all envelope components of the house are heavy in mass and thick walls and roofs which by experience proved to maintain good indoor thermal conditions. Rocks are used in foundations and on ground floor for only the first 1.5m height.

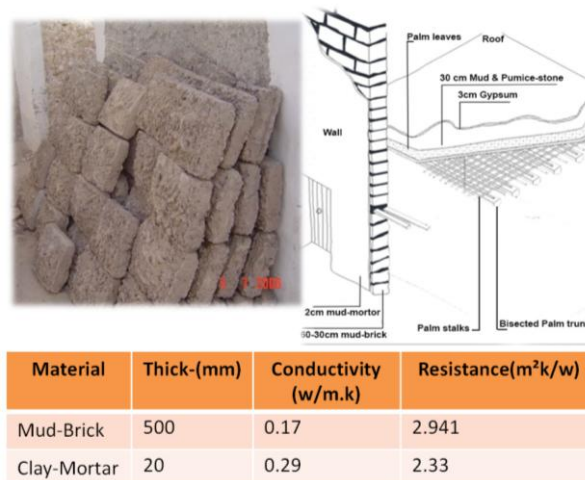


Figure 3. Construction materials in traditional house of Ghadames

The external surface reflectance is a significant issue in hot climates and hence light colours (often white) with increasingly brighter tonalities helps to reflect solar light falling incidentally from the sky. Brighter colours not only reflect light but also absorb less solar heat so it contributes to increase daylight whilst reduces heat gains through building fabric (Ealiwa, 2000 and Elaiab, 2014). Cheng et al. (2005) found that an increase in indoor temperatures about two degrees higher

than outdoor temperature when black test cell was used whereas it was three degrees below in the case of using white test cell. This result and others convey the message that local architecture in hot regions used white finishing materials for the same reason. However, studies showed that envelope optimisation in design could save energy up to 47% at peak cooling demands and around 35% of total energy use (Sadineni et al., 2011).

### COMBINING THERMAL MASS STRATEGY WITH NIGHT VENTILATION

Heavyweight structure has the ability to soak up a great amount of heat and store it for up to 12 hours with only small increase in internal surface temperature and hence it helps to maintain surface temperature below the ambient air temperature for most of the hot day time (Andjelkovic et al., 2012). The effectiveness of applying thermal mass especially in extreme conditions such as in cold and hot climates has been acknowledged by many research group suggesting to integrated with night purge strategy (Shaviv et al., 2001) and (Krüger et al., 2010). It is also found that the greater the daily and seasonal temperature variations in the region the more effective the thermal mass to reduce cooling loads (Yang and Li, 2008). This aspect is discussed in more details in chapter (2) for further information.

However, traditional wall in old settlements of Ghadames is made out of sun-dried mud bricks with thickness of up to 750mm and in most cases not exposed to sun. Although the roof is the most exposed component in the house envelope but it is also well-insulated with approximately 400mm thickness of five layers. On 03<sup>rd</sup> of October 2014 temperature measurements were recorded in traditional and modern houses of Ghadames during the day and at night for five days to assess the thermal fabric performance of both dwellings.

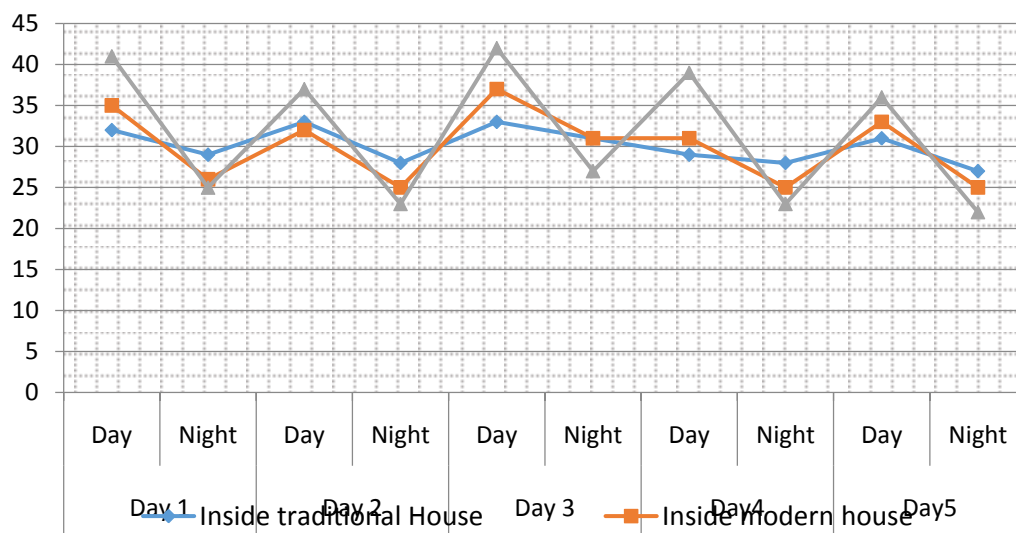


Figure 4. Thermal mass effect on indoor thermal conditions  
Source © (Author, 2014)

indicates that the house fabric of old settlements shows more stability in indoor thermal conditions than modern houses despite the fact that temperature variation in October is inconsiderable at daily cycle. Both traditional and modern houses were unoccupied during temperature records and windows were opened day and night in both dwellings including the roof aperture in traditional house. From **Σφάλμα! Το αρχείο προέλευσης της αναφοράς δεν βρέθηκε.** one can also notice that the temperature trend for both dwellings almost following outdoor air temperature and being within its amplitude throughout. In fact, a previous study by Chojnacki (2003) showed better results indicating that traditional house of Ghadames provided almost a constant indoor air temperature about 28°C in summer throughout the monitored weeks.

By the current study it is found that there is slight difference between outside air temperature in old and new towns of Ghadames which may refer to the difference in microclimate surrounding the two areas. Summer nights in Sahara Desert is well-known as winter of the summer where temperature sometimes drops down to less than 10°C. It therefore very important to strip away indoor warm air stored in by the fabric during the day.



Figure 5. Night time ventilation in traditional house of Ghadames  
Source © Author

Figure 5 demonstrates the night purge ventilation and the use of fan to enhance the air circulation. At night when the indoor air gets warmer it becomes lighter in density as less molecules in the air contents and the opposite is true for cold air making it weighs more so it sinks from lower temperature through the roof aperture into the house driving the warm air up with the assistance of the fixed fan.

### INDOOR THERMAL ENVIRONMENT AND OCCUPANTS' PERCEPTION

During the visit to the three case studies in the old town interviews were conducted with a number of professionals and meanwhile temperature was recorded and participants' thermal sensation also was assessed. The temperature measurements shown in Table 1 were all taken at the same day (27/09/2014) with different times inside the central hall (living room) during the interviews for every 15 minutes for almost an hour each. All records are an average of five interviews. The table indicated that inhabitants in old town settlements feel happy with such indoor physical environment. It may also confirm the validity of the adaptive model (AMV) for naturally ventilated dwellings. Meanwhile, predicted mean vote (PMV) model shown overestimation values

Table 1. Indoor temperature measurements inside traditional houses

Location	(°C) T air	T surface (°C)	air velocity	RH (%)	Activity <sup>a</sup> (Met)	<sup>a</sup> (clo)	AMV	PMV
Living room	32.2	31.7	0.04	40	1.0	0.55	0.71	2.12
Basement	29.2	28.1	0.02	58	1.2	0.55	0.42	1.30
alleyway	30.7	28.3	0.5	49	1.45	0.55	0.285	1.51
Upper- roof	38.6	39.1	0.65	26	1.4	0.55	2.30	4.13

The householders were asked to make a preference according to the scale given in Figure 6. The Figure revealed that 43% wanted no change, whereas 45% prefer to be cooler. However, despite the fact that none of the respondents were using AC there was some preferred to be warmer which indicates that comfort temperature is highly subjective.

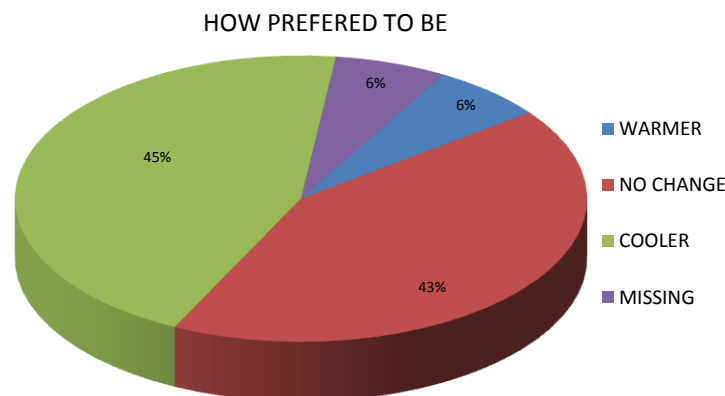


Figure 6. Householders preference of thermal change

## CONCLUSION

This study has investigated the impact of applying night ventilation strategy coupled with thermal mass construction on indoor thermal performance of traditional dwellings of Ghadames. Observing daily cycles of climate conditions and building users' behaviour was a powerful research technique to analyse and understand how our buildings behave and be conditioned with less energy demand. Thermal mass structure in the traditional architecture of Ghadames has great impact on passively cooling indoor environment. In addition, the house structure kept cool during the day due to minimum exposure to solar radiation where internal surface temperature so often less than ambient temperature. Heat stored during the day through mainly roof construction is controlled by a number of ways such as creating double ceiling height, thick roof structure with a number of layers and also placement of skylight aperture that helps warm air to be extracted at night via stack effect. It is also observed that occupants uses fixed fan installed beneath the skylight in order to fasten the extraction process of warm air at night time. It can be concluded that simple passive design strategies like all mentioned in this paper successfully controlled thermal indoor conditions in traditional houses which can bring a number of benefits to our today's housing including cutting down energy bills. Finally, this study showed that thermal comfort zone can vary depends on outdoor conditions and personal perception and may be AMV comfort model works better for naturally ventilated buildings. This study suggests that roof openings can replace wall windows especially when solar shadings are provided and thick walls should be considered in hot climate architecture. It can be said that site conditions and microclimate of traditional settlements highly contributed to mitigate extreme outdoor conditions.

## REFERENCES

- Al-Zubaidi, M.S., 2002. The Efficiency of Thermal Performance of the Desert Buildings—The Traditional House of Ghadames/Libya. In *Annual Conference of the Canadian Society for Civil Engineering*. Montreal: Quebec, Canada, pp. 1–8.
- Andjelkovic, B. et al., 2012. Thermal mass impact on energy performance of a low, medium and heavy mass building in Belgrade. *Thermal Science*, 16(suppl. 2), pp.447–459.
- Ben Cheikh, H. & Bouchair, A., 2004. Passive cooling by evapo-reflective roof for hot dry

- climates. *Renewable Energy*, 29(11), pp.1877–1886.
- Cheng, V., Ng, E. & Givoni, B., 2005. Effect of envelope colour and thermal mass on indoor temperatures in hot humid climate. *Solar Energy*, 78(4), pp.528–534.
- Chojnacki, M., 2003. Traditional and Modern Housing Architecture and Their Effect on The Built Environment in North Africa. In *'Methodology of Housing Research'*. Stockholm: Royal Institute of Technology (KTH), pp. 1–22.
- Ealiwa, A., 2000. *Designing for Thermal Comfort in Naturally Ventilated and Air Conditioned Buildings in Summer Season of Ghadames, Libya*. De Montfort University, Leicester.
- Elaiab, F.M., 2014. *Thermal comfort Investigation of multi-storey residential buildings in Mediterranean climate With reference to Darnah , Libya*. The University of Nottingham.
- Gabril, N.M.S., 2014. *Thermal Comfort and Building Design Strategies for Low Energy Houses in Libya: Lessons from the vernacular architecture*. University of Westminster.
- Gładyszewska-Fiedoruk, K. & Gajewski, A., 2012. Effect of wind on stack ventilation performance. *Energy and Buildings*, 51, pp.242–247.
- Kleiven, T., 2003. Natural Ventilation in Buildings. *Buildings*, (7242), pp.1–11. Available at: <http://doi.wiley.com/10.1002/9781119951773>.
- Krüger, E., González Cruz, E. & Givoni, B., 2010. Effectiveness of indirect evaporative cooling and thermal mass in a hot arid climate. *Building and Environment*, 45(6), pp.1422–1433.
- Nguyen, A.-T. et al., 2011. An investigation on climate responsive design strategies of vernacular housing in Vietnam. *Building and Environment*, 46(10), pp.2088–2106.
- Sadineni, S.B., Madala, S. & Boehm, R.F., 2011. Passive building energy savings: A review of building envelope components. *Renewable and Sustainable Energy Reviews*, 15(8), pp.3617–3631.
- Shaviv, E., Yezioro, A. & Capeluto, I.G., 2001. Thermal mass and night ventilation as passive cooling design strategy. *Renewable Energy*, 24(3-4), pp.445–452.
- Yang, L. & Li, Y., 2008. Cooling load reduction by using thermal mass and night ventilation. *Energy and Buildings*, 40(11), pp.2052–2058.

# Indoor Air Quality and Thermal Comfort, in Irish Retrofitted Energy Efficient Homes

Áine Broderick<sup>1\*</sup>, Miriam Byrne<sup>1</sup>, James McGrath<sup>1</sup> and Marie Coggins<sup>1</sup>

*School of Physics,  
National University of Ireland, Galway,  
University Road,  
Galway, Ireland.*

*\*Corresponding author:  
a.broderick13@nuigalway.ie*

## ABSTRACT

Indoor air quality and thermal comfort was measured in 14 three-bedroom, semi-detached, cavity wall naturally-ventilated homes during the winter following an energy efficient retrofit. As part of the energy retrofit, homes received new windows and doors, an upgraded heating system, attic insulation, and wall vents, as well as pumped beaded wall insulation into three external walls. Temperature and relative humidity (RH), as well as concentrations of total volatile organic compounds (TVOCs), PM<sub>2.5</sub>, CO<sub>2</sub>, and CO were measured over a 24-hour period in the main living area and main bedroom of each home. Concentrations of NO<sub>2</sub> and formaldehyde were measured in the living room only. Benzene, toluene, ethylbenzene, xylene, and NO<sub>2</sub> were measured over a three week period and radon was monitored over three months. The average winter air change rate was 0.59 h<sup>-1</sup>. The average PM<sub>2.5</sub> concentrations during the winter period were 18.5 µg/m<sup>3</sup>. The 24 hour average formaldehyde and TVOC concentrations were 19.4 ppb and 379.7 ppb respectively. The average 24 hour temperatures and humidity levels found in the living room and bedrooms in the retrofitted dwellings were 20.0 °C and 19.1 °C and 46.8 %RH and 50.4 %RH, respectively.

## KEYWORDS

Indoor air quality, retrofit, occupant behaviour, thermal comfort

## 1 INTRODUCTION

In most developed countries, people are known to spend more than 90% of their time indoors (Vardoulakis, 2009) and a substantial percentage of this time is in the dwelling; as a result exposure to pollutants in the dwelling is likely to significantly influence human health. Over the last number of years, more dwellings are being retrofitted to reduce energy usage to meet energy efficiency targets and as a method for reducing fuel poverty. There is still limited knowledge on the unintended consequences of retrofitting such as the impact of reducing ventilation rates in indoor air quality. While there have been studies that have assessed the impact of retrofitting on indoor air quality across one season (Broderick et al., 2017), there are few studies which have monitored indoor air pollutants over six to twelve months after an energy efficient upgrade (Földváry et al., 2015, Coombs et al., 2016, Wells et al.,

2015). Studies such as Wells et al. (2015) have reported short term increases in PM<sub>2.5</sub> and formaldehyde concentrations immediately following a retrofit, but a long term decrease one year after the retrofit.

Pollutants such as BTEX, VOCs, and carbon monoxide have been known to vary seasonally, with winter having the highest concentrations (Elbayoumi et al., 2014). Concentrations of VOCs during the winter period can be three to four times than concentrations during the summer period (Schlink et al., 2004). Parameters such as CO<sub>2</sub>, temperature and humidity can vary seasonally, studies such as Derbez et al. (2014) and Földváry et al. (2015). Földváry et al. (2015) have reported differences in CO<sub>2</sub>, temperature, and humidity between winter and summer in energy efficient homes. Elements such as weather conditions, occupant behaviour, and outdoor concentrations can influence the concentrations of indoor air quality parameters (Schlink et al., 2010).

## Methodology

The dwellings were monitored during the winter period following the retrofit. The dwellings recruited were constructed in accordance with the Irish Building Regulations (Building Control Act, 1990). The dwellings were of cavity wall construction and were built in 2000. The dwellings had a volume between 100 – 126 m<sup>3</sup> and had a D1 or D2 building energy rating. Indoor air pollutants and thermal parameters were monitored in the main living room and bedroom in each dwelling. A basic layout of the dwellings is shown below (Figure 1).

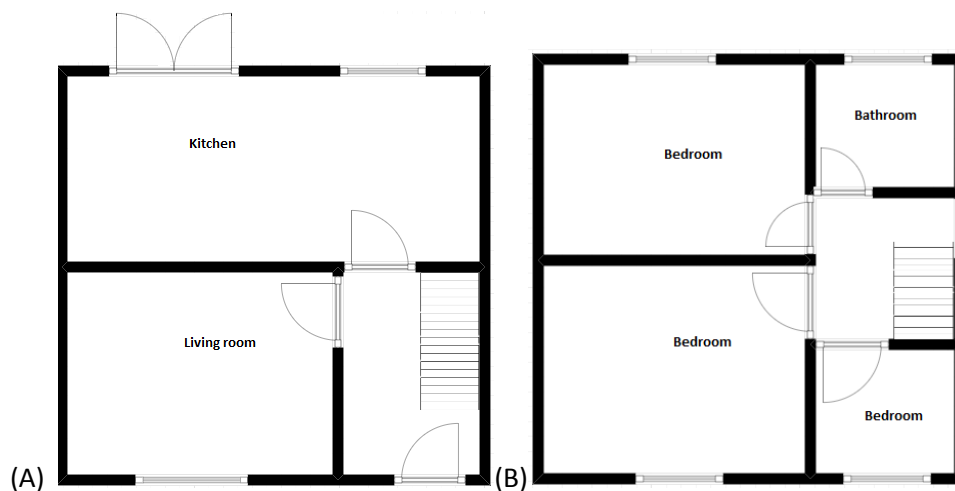


**Figure 1:** Schematic showing typical layout of the 3 bed roomed semi detached dwellings.  
(A) Downstairs (B) Upstairs (Broderick et al., 2017)

A TSI SidePak AM510 Personal Aerosol Monitor fitted with a PM<sub>2.5</sub> impactor was used to collect and log real-time data on airborne PM<sub>2.5</sub>. The monitor was set to log at 1 minute intervals to allow assessment of peaks and daily variability in exposure to be determined. Carbon monoxide levels were measured using EL-USB-CO carbon monoxide loggers. A Graywolf IQ 610 was used to monitor CO, CO<sub>2</sub>, total volatile organic compounds (TVOCs), temperature (Wet bulb and Dry bulb), and relative humidity (%RH). Carbon Dioxide levels were monitored using Telaire 7001. A Graywolf TG 502 was used to monitor total volatile organic compounds (TVOCs), temperature (Wet bulb and Dry bulb), and relative humidity (%RH). Average indoor nitrogen dioxide levels were measured using NO<sub>2</sub> passive diffusion

tubes supplied by Gradko Environmental. NO<sub>2</sub> was monitored in the main living room only. Total Volatile Organic Compounds (TVOCs) concentrations were collected using a GrayWolf IQ-610 photoionisation detector. Average BTEX levels were measured using BTEX Passive Diffusion Tubes supplied by Gradko Environmental. BTEX levels were monitored in the main living room and bedroom. Formaldehyde measurements were made using a GrayWolf FM-801 formaldehyde meter. Formaldehyde was monitored only in the main living room. Air exchange rates were determined in the living room of each house by using CO<sub>2</sub> as a tracer gas and measuring the rate of decay over a one hour period (Cui et al., 2015). Air change rates were expressed as h<sup>-1</sup>.

The comfort vote was measured at two times during the 24 hour monitoring period; in the morning and in the evening. The comfort vote is a subjective occupant thermal scale going from “-3” (cold) to “+3” (hot), with “0” as “neutral”. The occupants completed a short comfort survey, which also incorporated the level of activity, location in the dwelling, and what the occupants were wearing at the time.

### **Retrofit specifications**

The dwellings were upgraded over the summer periods of 2015 and 2016. Each of the dwellings received pumped insulation (using extruded polystyrene beads) (Figure 2), 300 mm thick attic insulation (mineral rock wool). The dwellings had the windows and doors replaced with more energy efficient models. Each of the dwellings had the boiler upgraded to a 90% efficient boiler with heating controls (modulating condensing balanced boiler). Background vents with covers were installed in the dwellings and extract fans with humidity control were installed in the kitchen and bathroom.

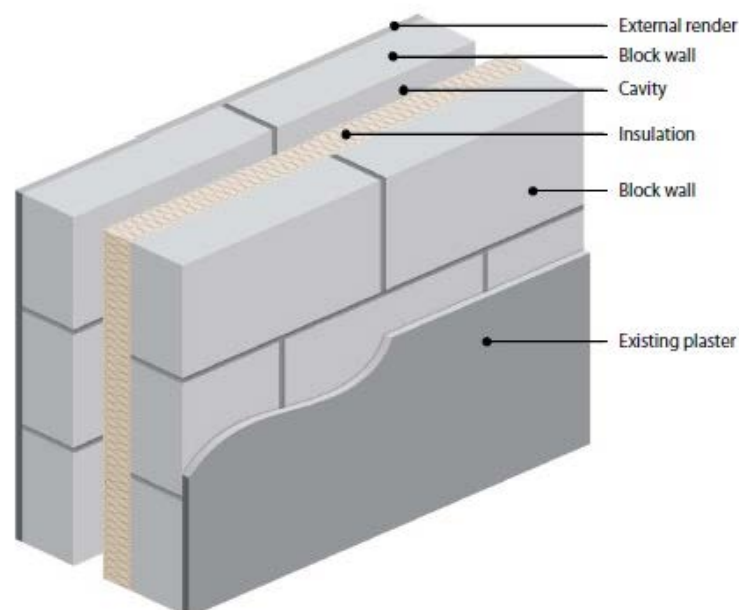


**Figure 2:** Schematic showing cavity wall (NSAI, 2014)

### **Data Analysis**

The statistical package SPSS (version 23) was used to calculate 24 hour means, standard deviations and ranges for each variable.

### **Indoor air quality guidelines**

Each of the dwellings indoor air quality and thermal parameters were compared to international guidelines.

## Results

Table 1 and Table 2 summarise a sample of the IAP measurement data collected during the winter period following a retrofit. The majority of the post retrofit winter IAP concentrations were found to be within WHO guidelines. The average winter air change rate was  $0.59 \text{ h}^{-1}$ . Data for radon,  $\text{NO}_2$ , and BTEX are pending. The  $\text{PM}_{2.5}$  concentrations of  $18.5 \mu\text{g}/\text{m}^3$  were similar to those found in French dwellings during the winter period ( $16.9 \mu\text{g}/\text{m}^3$ ) (Derbez et al., 2014). Formaldehyde concentrations ( $19.4 \text{ ppb}$ ) were similar to those found in Swedish homes during the heating season ( $17.0 \text{ ppb}$ ) (Langer and Bekö, 2013). Concentrations of TVOCs were found to be higher in the current study compared to French dwellings (Derbez et al., 2014). The temperatures found in the living room and bedrooms in the retrofitted dwellings were similar to those found in renovated UK homes by Hong et al. (2009) ( $20.02^\circ\text{C}$  in the living room,  $19.1^\circ\text{C}$  in the bedroom and  $19.7^\circ\text{C}$  in the living room and  $18.2^\circ\text{C}$  in the bedroom, respectively).

Table 1: Post retrofit winter 24 hour mean temperature and relative humidity

Winter	(N=14)		
	Mean	SD	Range
Temperature (living room)	20.2	2.0	18.0 – 23.5
Temperature (bedroom)	19.1	1.9	16.2-23.2
RH (living room)	46.8	9.5	30.2 – 55.6
RH (bedroom)	50.4	3.6	33.8 – 55.3

Table 2: Post retrofit 24 hour winter IAP concentrations

Pollutant	(N=14)		
	Mean	SD	Range
PM <sub>2.5</sub> ( $\mu\text{g}/\text{m}^3$ ) 1	18.5	3.6	11.8 – 23.4
CO <sub>2</sub> (ppm) 1	726.5	93.5	557.0 – 842.5
CO (ppm) 1	0.7	0.4	0.1 – 1.4
Formaldehyde (ppb) 1	19.4	5.8	10.8 – 29.7
TVOC (ppb) 1	379.7	108.4	206.2 – 547.5
	124 hour averages		

## Thermal comfort

Post retrofit, the majority the occupants ( $n=13$ ) were satisfied overall with the comfort during the winter period in their dwellings. 21 % ( $n=3$ ) occupants reported that their dwellings were draughty during the winter period after the retrofit due to issues with the vents located in the living room. The comfort vote during the winter monitoring was between “neutral” and “warm” in the cavity wall dwellings.

## Discussion

Previous studies have shown that air change rates decreased in the dwellings that had their three walls filled with insulation and windows and doors changed (Shrubsole et al., 2012). The increase in temperature in the dwellings may have been due to the increased insulation and the upgraded more efficient boiler. Heat loss in the dwellings can be decreased through increased cavity wall insulation. Byrne et al. (2016) reported a heat loss reduction in dwellings

of between 21 to 66 % in cavity wall homes and a 37% to 77% reduction in externally insulated wall dwellings. Due to the lower outdoor temperatures during the winter period, dwelling occupants in this study tended to limit the amount of time for which windows and doors were open during the monitoring period. The occupants reported cleaning and using aerosols products such as cleaning sprays and odour masking sprays, which, when combined with lower ventilation rates during the winter period, can lead to increases in pollutant concentrations.

## 5 CONCLUSIONS

This study aimed to assess the impact of retrofitting dwellings on indoor air quality, thermal comfort, and ventilation. The results indicate that the concentrations of pollutants and thermal parameters were in line with previous studies, however the findings of this study cannot be generalised to other homes due to the limited sample number. As the data presented is only a sample of the IAP monitored, and studies have shown that pollutant levels can vary following the retrofit, these dwellings are currently being monitored during the summer period. Future studies on energy efficient dwellings should investigate indoor air quality in dwellings over the different seasons so as to ensure that energy retrofit programmes do not have a negative impact of health. This study provides valuable data which can be used in health impact assessments to assess the impact retrofitting has on health and can also aid in the progress of indoor air quality metrics.

## 2 ACKNOWLEDGEMENTS

This project is sponsored by the Irish Environmental Protection Agency under the Strive 2007- 2013 Research Programme. The authors thank the study participants for volunteering to be part of the study.

## 3 REFERENCES

- BRODERICK, Á., BYRNE, M., ARMSTRONG, S., SHEAHAN, J. & COGGINS, A. M. 2017. A pre and post evaluation of indoor air quality, ventilation, and thermal comfort in retrofitted co-operative social housing. *Building and Environment*.
- BUILDING CONTROL ACT 1990. Building Control Act. In: ENVIRONMENT, D. O. (ed.). Dublin.
- BYRNE, A., BYRNE, G., O'DONNELL, G. & ROBINSON, A. 2016. Case studies of cavity and external wall insulation retrofitted under the Irish Home Energy Saving Scheme: Technical analysis and occupant perspectives. *Energy and Buildings*, 130, 420-433.
- COOMBS, K. C., CHEW, G. L., SCHAFFER, C., RYAN, P. H., BROKAMP, C., GRINSHPUN, S. A., ADAMKIEWICZ, G., CHILLRUD, S., HEDMAN, C., COLTON, M., ROSS, J. & REPONEN, T. 2016. Indoor air quality in green-renovated vs. non-green low-income homes of children living in a temperate region of US (Ohio). *Science of The Total Environment*, 554–555, 178-185.
- CUI, S., COHEN, M., STABAT, P. & MARCHIO, D. 2015. CO<sub>2</sub> tracer gas concentration decay method for measuring air change rate. *Building and Environment*, 84, 162-169.

- DERBEZ, M., BERTHINEAU, B., COCHET, V., LETHROSNE, M., PIGNON, C., RIBERON, J. & KIRCHNER, S. 2014. Indoor air quality and comfort in seven newly built, energy-efficient houses in France. *Building and Environment*, 72, 173-187.
- ELBAYOUMI, M., RAMLI, N. A., YUSOF, N. F. F. M. & AL MADHOUN, W. 2014. The effect of seasonal variation on indoor and outdoor carbon monoxide concentrations in Eastern Mediterranean climate. *Atmospheric Pollution Research*, 5, 315-324.
- FÖLDVÁRY, V., BEKÖ, G. & PETRÁŠ, D. 2015. Seasonal variation in indoor environmental quality in non-renovated and renovated multifamily dwellings in Slovakia. *Healthy Buildings Europe*.
- HONG, S. H., GILBERTSON, J., ORESZCZYN, T., GREEN, G. & RIDLEY, I. 2009. A field study of thermal comfort in low-income dwellings in England before and after energy efficient refurbishment. *Building and Environment*, 44, 1228-1236.
- LANGER, S. & BEKÖ, G. 2013. Indoor air quality in the Swedish housing stock and its dependence on building characteristics. *Building and Environment*, 69, 44-54.
- NSAI. 2014. *CODE OF PRACTICE S.R. 54:2014 Code of practice for the energy efficient retrofit of dwellings* [Online]. Available: <http://www.ili.co.uk/en/S.R.54-2014.pdf> [Accessed 08/02/2016].
- SCHLINK, U., REHWAGEN, M., DAMM, M., RICHTER, M., BORTE, M. & HERBARTH, O. 2004. Seasonal cycle of indoor-VOCs: comparison of apartments and cities. *Atmospheric Environment*, 38, 1181-1190.
- SCHLINK, U., THIEM, A., KOHAJDA, T., RICHTER, M. & STREBEL, K. 2010. Quantile regression of indoor air concentrations of volatile organic compounds (VOC). *Science of the Total Environment*, 408, 3840-3851.
- SHRUBSOLE, C., RIDLEY, I., BIDDULPH, P., MILNER, J., VARDOULAKIS, S., UCCI, M., WILKINSON, P., CHALABI, Z. & DAVIES, M. 2012. Indoor PM 2.5 exposure in London's domestic stock: Modelling current and future exposures following energy efficient refurbishment. *Atmospheric Environment*, 62, 336-343.
- VARDOULAKIS, S. 2009. Human exposure: indoor and outdoor. *Issues in Environmental Science and Technology*, 28, 85.
- WELLS, E. M., BERGES, M., METCALF, M., KINSELLA, A., FOREMAN, K., DEARBORN, D. G. & GREENBERG, S. 2015. Indoor air quality and occupant comfort in homes with deep versus conventional energy efficiency renovations. *Building and Environment*, 93, 331-338.

# Evaluation of thermal comfort in an office building served by a liquid desiccant-assisted evaporative cooling air conditioning system

Hye-Jin Cho<sup>1</sup>, Jang-Hoon Shin<sup>1</sup>, Joon-Young Park<sup>1</sup>,  
Won-Jun Kim<sup>1</sup>, and Jae-Weon Jeong<sup>\*1</sup>

*1 Department of Architecture Engineering, College of Engineering, Hanyang University,  
222 Wangsimni-Ro, Seungdong-Gu, Seoul, 04763, Republic of Korea*

*\*Corresponding author: [jjwarc@hanyang.ac.kr](mailto:jjwarc@hanyang.ac.kr)*

## ABSTRACT

Recent studies examined a liquid desiccant indirect and direct evaporative cooling assisted 100% outdoor air system (LD-IDECOAS) as an energy conserving alternative to conventional air conditioning systems. An IDECOAS was introduced as an environmental-friendly air conditioning system that uses latent heat of water evaporation to cool the process air. Recently, studies suggested the integration of a liquid desiccant (LD) system with an IDECOAS to overcome a cooling reduction in evaporative cooling performance in a hot and humid climate. The supply air (SA) temperature and humidity ratio of the proposed system depends on SA flow rate and removal moisture content. However, a supplying air flow method in a conventional variable air volume (VAV) system and a relatively unstable air conditioning performance of an indirect evaporative cooler (IEC) and direct evaporative cooler (DEC) in cooling seasons could cause SA temperature to fluctuate above and below the set point temperature, and this could result in occupants feeling uncomfortable in a conditioned zone. Therefore, the purpose of the present study involves estimating thermal comfort in an office building that is served by a liquid desiccant indirect and direct evaporative cooling assisted 100% outdoor air system (LD-IDECOAS). Predicted Mean Vote (PMV) method is selected to evaluate as to whether an indoor thermal environment complies with recommended comfort zone conditions as proposed by the ASHRAE Standard 55. The seasonal mode of operation of LD-IDECOAS is suggested and used to estimate thermal properties of supply air (SA) while serving the proposed system. Energy performance and thermal environment of a building model are predicted via a series of energy simulations by using a TRNSYS 17 program integrated with an engineering equation solver program. The simulation results indicate that LD-IDECOAS did not completely cool the conditioned zone occasionally in a cooling season. However, the results also suggested that the thermal environment in a conditioned zone is generally in compliance with the ASHRAE Standard 55. Accordingly, it is concluded that using the LD-IDECOAS in an office building can produce energy savings with an acceptable level of thermal comfort.

## KEYWORDS

Liquid desiccant and evaporative cooling-assisted 100% outdoor air system (LD-IDECOAS); thermal comfort; PMV; energy simulation

## 1 INTRODUCTION

The emergence of environmental issues, such as global climate change, has led to numerous studies that focus on a liquid desiccant system and evaporative cooling-assisted air conditioning system as an alternative to a vapor compression refrigerant system [1-3]. A recent study by Kim et al [4-7] suggested the use of a liquid desiccant and indirect and direct evaporative cooling-assisted 100% outdoor air system (LD-IDECOAS) as an environmental-friendly and energy saving air conditioning system. IDECOAS is an evaporative cooling-assisted air conditioning system that uses the latent heat of water evaporation to cool incoming air. However, the cooling performance of IDECOAS significantly decreases in a hot and humid climate due to an increase in the latent load of outdoor air [8]. Therefore, integration of a liquid desiccant system with an evaporative cooling system, such as liquid

desiccant and dew point evaporative cooling assisted 100% outdoor air system (LDEOS), desiccant-enhanced evaporative (DEVap) cooling system and liquid desiccant and evaporative cooling-assisted 100% outdoor air system (LD-IDECOAS), is suggested to overcome a reduction in evaporative cooling performance in a hot and humid climate. A liquid desiccant system is a cooling system that handles a latent load of outdoor air (OA) by absorbing water vapor of OA through a liquid desiccant dehumidifier that plays a significant role in improving the evaporative cooling performance of an evaporative cooling-assisted air conditioning system in a hot and humid region. Furthermore, the system significantly impacts energy consumption. Recent studies [6,7] indicated that LD-IDECOAS provides annual operating energy savings of 68% and 23% when compared with those of a conventional VAV system and IDECOAS, respectively, thereby proving that it possesses significant energy saving potential when compared with a VAV and IDECOAS. However, simulation operations and operation results have resulted in various considerations. The temperature and humidity ratio of supply air (SA) depend on SA flow rate and dehumidification mass rate of incoming air when LD-IDECOAS is operated. A sharp increase in the latent load in a conditioned zone results in the failure of the indoor humidity control and a decrease in the cooling performance of the proposed system. Thus, if the operation performance of both liquid desiccant system and evaporative cooling system is less than the expected performance, there is a limit to stably controlling the indoor air condition, and this could cause occupants to feel uncomfortable in a conditioned zone.

Accordingly, the aim of the present study involves using energy simulations to evaluate the influence of fluctuations in supply air temperature on the thermal environment of occupants that is served by LD-IDECOAS. In this study, a thermal comfort evaluation is conducted based on the ASHRAE Standard 55. Additionally, energy performance and indoor thermal environment of the building model are predicted via a series of energy simulations by using a TRNSYS 17 program that is integrated with an engineering equation solver program.

## **2 SYSTEM OVERVIEW**

### **2.1 LD-IDECOAS**

LD-IDECOAS consists of a LD system, an indirect evaporative cooler (IEC), and a direct evaporative cooler (DEC) (Figure 1). A LD system dehumidifies the outdoor air to control the latent heat of the OA prior to the entry of the OA into the evaporative cooling system. After the exit of process air from the LD system, the IEC and DEC provide sensible and adiabatic cooling of the entering air to satisfy the required temperature of the SA. The heating coil (HC) and sensible heat exchanger (SHE) that are located at the EA side are operated to maintain a set point temperature of the neutral deck by using the remaining heat in the EA. The SA flow rate is modulated based on the air conditioning load in a conditioned zone in a manner similar to the conventional VAV system.

In the summer, process air is initially dehumidified by the LD unit. The dehumidified air is sensibly cooled by the IEC, and subsequently the set point of SA is achieved by entering the DEC. In intermediate seasons when outdoor air is relatively dry and cool, the LD unit is not operated and the target SA point is satisfied with the IEC and DEC. Conversely, in the winter, the LD unit and DEC are turned off, and only IEC is used as the SHE to reduce the heating load of OA by regenerating the remaining heat from EA. The HC is operated if auxiliary heating is required to satisfy the target SA point.

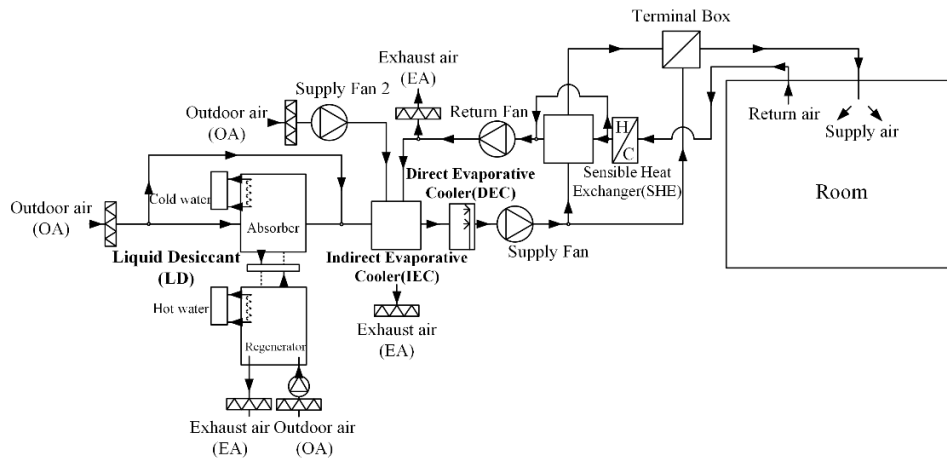


Figure 1: A schematic diagram of the LD-IDECOAS

## 2.2 The LD-IDECOAS operation mode

Previous study indicates that the operation mode of the LD-IDECOAS is determined by OA conditions [6]. The operation mode is classified into three modes based on OA conditions, namely, Regions A, B, C, and D (Figure 2).

### Operation mode for Region A

Region A presents outdoor air conditions above line “a” and “b” that indicate the humidity ratio (HR) of SA and enthalpy or wet-bulb temperature of SA at the set point (i.e. 15°C, saturated condition), respectively (Figure 2). In Region A, hot and humid outdoor air is initially dehumidified through the LD unit until the conditions of OA satisfy the condition of line “a” by using a by-pass damper to control the air flow rate. The dehumidified air is sensibly cooled by the IEC until the wet-bulb temperature of the exiting air reaches the wet-bulb temperature on line “b,” and subsequently the isentropic cooling of the process air in the DEC satisfies the target cold deck SA temperature.

### Operation mode for Region B and C

In Regions B and C, the LD system is deactivated due to dry OA. The induced OA bypasses the LD and is sensibly cooled by the IEC to reach the target SA temperature (i.e. 15°C). Additionally, the DEC is operated to satisfy the set point SA temperature.

### Operation mode for Region D

Region D presents outdoor air conditions when the dry-bulb temperature of OA is lower than the set point value. In Region D, dry and cold OA bypasses the LD unit and DEC, while IEC preheats incoming air as a sensible heat exchanger to regenerate waste heat from exhaust air such that the dry-bulb temperature of OA satisfies the SA set point. An auxiliary HC located at the exhaust air is required to recover the required heat if the heat reclaimed from IEC is not sufficient to enable a cold deck to reach the SA target temperature (i.e., 15°C).

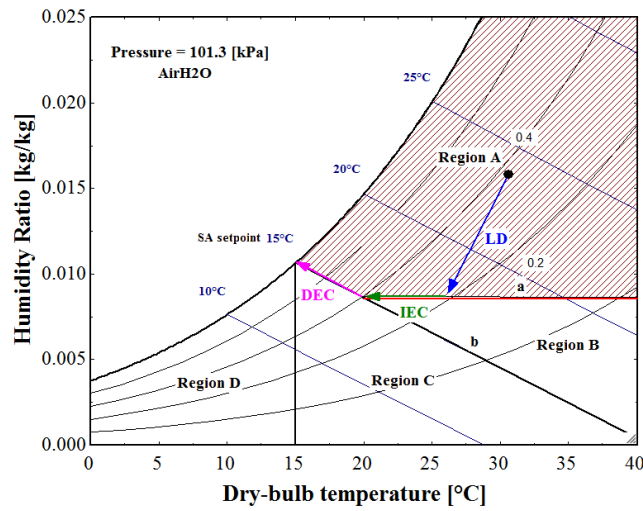


Figure 2: Psychrometric chart in Region A

### 3 SIMULATION OVERVIEW

In this study, the simulation procedure to predict the PMV is presented to evaluate the influence of fluctuations in the supply air temperature on thermal comfort in an office building served by LD-IDECOAS. Thermal loads and PMV values are estimated by using TRNSYS 17 [10], and an engineering equation solver (EES) [11] is applied to calculate annual thermal loads and supply air conditions based on the operation mode of LD-IDECOAS. The simulation is conducted using IWEK weather data from Seoul, South Korea.

#### 3.1 Simulation model overview

A building located in Seoul, Republic of Korea that consists of a single-story office building with a floor area corresponding to  $100\text{m}^2$  and 5 persons. All individuals possess their own computer and are engaged in light work. Based on ISO-7730 [12], each occupant generates 75W sensible heat and 75W latent heat. Each computer adds 230W sensible heat to the space, and the heat generation density of the light corresponds to  $13\text{W}/\text{m}^2$ . Table 1 provides a summary of detailed physical information with respect to the building model.

Table 1: Simulation information related to the building model used in the study

<i>Location</i>	Seoul, Republic of Korea	
<i>Building</i>	$10 \times 10 \times 3 \text{ m}^3$	
<i>Schedule</i>	7:00AM–10:00 PM (weekdays)	
<i>Heat gain</i>	Occupants	5 persons/ $100 \text{ m}^2$
	Lights	$13 \text{ W}/\text{m}^2$
<i>U-value</i>	Exterior wall	$0.468 \text{ W}/\text{m}^2\text{K}$
	Roof	$0.360 \text{ W}/\text{m}^2\text{K}$

### 3.2 Calculations for the thermal load and target supply airflow rate

LD-IDECOAS varies the supply air (SA) flow rates in response to changes in the thermal load in a conditioned zone. An increase in the indoor air temperature modulates the damper to satisfy the maximum SA flow rate to remove the cooling load. Conversely, the damper is controlled to deliver the proper amount of SA flow rate in response to the reduced cooling load. Accordingly, it is necessary to estimate the design SA flow rate to ensure a proper SA flow rate.

#### Thermal load in the building model

In this study, the peak cooling load of the model space is estimated by using a TRNSYS 17 program. The obtained peak sensible and latent cooling loads of the model space correspond to 16.14 kW and 2.40 kW, respectively.

#### Target supply air flow rate

All systems are simulated based on the seasonal operation schedule. The cooling set point of the model building corresponds to 24°C/55% during the summer (i.e., June, July, and August), and the heating set point corresponds to 20°C during the winter (i.e., November, December, January, February, and March). The design SA flow rate is calculated by using Eq. (1) if the peak sensible cooling load and the design indoor and supply air temperature are known, and the design supply air humidity ratio is obtained by using Eq. (2). The design supply air humidity ratio and air flow rate calculated by the two equations correspond to 9.70 g/kg and 1.428 m<sup>3</sup>/s, respectively. The expressions are as follows:

$$Q_{sen} = \dot{m}_{sa} \cdot c_p \cdot (DBT_{ra} - DBT_{sa}) \quad (1)$$

$$Q_{lat} = h_{fg} \cdot \dot{m}_{sa} \cdot (w_{ra} - w_{sa}) \quad (2)$$

### 3.3 Simulation overview of LD-IDECOAS

It is necessary to satisfy the SA condition set point by using the LD unit, IEC and the DEC to provide a thermally comfortable environment. The inlet and outlet air conditions of each component of LD-IDECOAS are calculated by using Eq. (3) - (6). With respect to the LD unit, the incoming air temperature leaving the LD unit is determined by using Eq. (3) if the following three parameters: DBT of OA ( $DBT_{LD,out}$ ); solution inlet temperature ( $T_{sol,inlet}$ ), and effectiveness of LD unit ( $\epsilon_{LD,T}$ ) are known. After calculating the temperature of the incoming air leaving the LD unit, the outlet air temperature of IEC ( $DBT_{IEC,pri,out}$ ) is determined by using Eq. (4) with respect to the effectiveness of IEC ( $\epsilon_{IEC}$ ). Subsequently, the temperature of the air leaving the DEC ( $DBT_{DEC,out}$ ) is determined by Eq. (5) with respect to the known effectiveness of DEC ( $\epsilon_{DEC}$ ). Additionally, the humidity of air leaving the LD unit ( $w_{LD,out}$ ) is determined by using Eq. (6) assuming that the value of the dehumidification effectiveness of the LD unit is the same as the value of the  $\epsilon_{LD,T}$  as shown in previous studies by Katejanekaren and Kumar (2008) and Katejanekaren et al (2009) [13,14]. The dehumidification effectiveness of the LD unit is obtained by using an existing model proposed by Chung and Luo (1999) [15]. Additionally, the effectiveness of IEC and DEC are assumed as 80% and 90%, respectively, based on manufactured cut-sheets. The expressions are as follows:

$$\varepsilon_{LD,T} = \frac{(DBT_{OA} - DBT_{LD,out})}{DBT_{OA} - T_{sol,inlet}} \quad (3)$$

$$\varepsilon_{IEC} = \frac{(DBT_{LD,out} - DBT_{IEC,pri,out})}{DBT_{LD,out} - WB T_{IEC,sec,inlet}} \quad (4)$$

$$\varepsilon_{DEC} = \frac{(DBT_{IEC,pri,out} - DBT_{DEC,out})}{DBT_{IEC,pri,out} - WB T_{IEC,pri,out}} \quad (5)$$

$$\varepsilon_{LD,w} = \frac{(W_{OA} - W_{LD,out})}{W_{OA} - W_e} \quad (6)$$

The operation modes of the three components are determined based on the outdoor air conditions. After calculating the SA temperature and humidity ratio through Eq. (3) - (6), the indoor air properties are obtained by substituting the SA properties into the building model that is implemented by TRNSYS 17.

### 3.4 The simulation approach to calculate PMV

This study uses the predicted mean vote (PMV) method, which is the most extensively and widely accepted index to evaluate thermal comfort [16]. The value of the PMV index is within a seven-point thermal sensation scale as shown in Table 2 to ensure thermal comfort. The ASHRAE Standard 55-2004 recommends maintaining the PMV index at level 0 with a tolerance of  $\pm 0.5$ .

The index is based on the energy balance of the human body with its environment and guarantees thermal comfort by predicting the average thermal sensation response of large groups of individuals who are exposed to different thermal conditions over long periods [17].

#### Indoor thermal environment condition

Thermal environment evaluation in an office building served by LD-IDECOAS is performed to examine the influence of variations in the SA temperature on building occupants in terms of thermal comfort. The thermal comfort evaluation is conducted during summer (i.e., June, July, and August) and winter (i.e., November, December, January, February, and March). The PMV index is influenced by the following six variables: metabolic rate ( $M$ ), clothing insulation ( $I_{cl}$ ), air temperature ( $T_a$ ), mean radiant temperature ( $T_{mr}$ ), air velocity ( $V_a$ ), and air relative humidity (Rh) [17]. With respect to the PMV prediction model, the PMV index is set as an output parameter, and the air temperature, mean radiant temperature, and air velocity are set as input parameters. The remaining variables (i.e., metabolic rate, clothing insulation, air velocity) are considered as constant values and are summarized in Table 3. The metabolic rate and clothing insulation in an office building are determined based on ISO-7730. Additionally, the maximum velocity of static airflow is set at 0.1 m/s given that low values of wind velocity are measured inside due to the prevalence of closed windows in an office building.

Table 2: Input values of the metabolic rate, clothing insulation, and air velocity

Parameter	Contents
Metabolic rate [met]	Seated, light work, typing: 1.2 (70W/m <sup>2</sup> )
Clothing Insulation [clo]	Underwear, pants, short shirts, socks, shoes: 0.5 (summer)
	Underwear, pants, shirts, jacket, socks, shoes: 1.0 (winter)
air velocity [m/s]	Static air flow rate: maximum 0.1 m/s

Finally, the hourly PMV values are calculated by inputting the indoor air temperature, relative humidity, and mean radiant temperature values.

### Calculation of PMV index

The PMV index is calculated based on Eq. (7) as follows:

$$PMV = (0.303e^{(-0.036M)} + 0.028) \cdot L \quad (7)$$

where L denotes the thermal load in the human body and is defined as the difference between the internal heat from the human body and the heat loss from the environment. The thermal load L is calculated from Eq. (8) as follows:

$$\begin{aligned} L = & (M - W) - 0.0014 \cdot M \cdot (34 - T_{a,in}) \\ & - 3.05 \cdot 10^{-3} \cdot [5733 - 6.99 \cdot (M - W) - p_{a,in}] \\ & - 0.42 \cdot (M - W - 58.15) \\ & - 1.72 \cdot 10^{-5} \cdot M \cdot (5867 - p_{a,in}) \quad (8) \\ & - 39.6 \cdot 10^{-9} \cdot F_{cl} \cdot [(T_{cl} + 273)^4 - (T_{mr} + 273)^4] \\ & - F_{cl} \cdot h_c \cdot (T_{cl} - T_{a,in}) \end{aligned}$$

The other factors required in Eq. (4) are obtained from Eq. (9) – (12) as follows:

$$\begin{aligned} T_{cl} = & 35.7 - 0.0275 \cdot (M - W) \\ & - I_{cl} \cdot [(3.96 \cdot 10^{-8} \cdot F_{cl} \cdot [(T_{cl} + 273)^4 \\ & - (T_{mr} + 273)^4] + F_{cl} \cdot h_c \cdot (T_{cl} - T_{a,in})] \quad (9) \\ h_c = & \begin{cases} 2.38 \cdot (T_{cl} - T_{a,in})^{0.25}, & A > 12.1 \cdot \sqrt{v_{a,in}} \\ 12.1 \cdot \sqrt{v_{a,in}}, & A \leq 12.1 \cdot \sqrt{v_{a,in}} \end{cases} \quad (10) \\ A = & 2.38 \cdot (T_{cl} - T_{a,in})^{0.25} \quad (11) \end{aligned}$$

$$F_{cl} = \begin{cases} 1.0 + 0.2 \cdot I_{cl}, & I_{cl} \leq 0.5 \text{ clo} \\ 1.05 + 0.1 \cdot I_{cl}, & I_{cl} > 0.5 \text{ clo} \end{cases} \quad (12)$$

## 4 SIMULATION RESULTS

### 4.1 PMV value in the summer season

Fig. 3-a shows the PMV values for the building model served by LD-IDEAS during summer (i.e. June, July, and August) when the cooling set point corresponds to 24°C, 55%. The results indicate that the PMV values fluctuate based on the supply air conditions. A few values exceed +1.0 indicating that individuals experience a hot feeling with respect to human thermal sensations. This is mainly because the LD-IDEAS is not completely performed in extremely humid climates. Nevertheless, the PMV values mainly vary from -0.5 to +1.0 which is an ideal statement for human thermal environment, thereby indicating that the indoor air control mostly progresses properly by handling the latent load with the LD unit with the exception of certain extremely humid periods.

## 4.2 PMV value in the winter season

Fig. 3-2 shows the PMV values for the building model served by LD-IDECAOS during winter (i.e., November, December, January, February, and March) when the heating set point corresponds to 20°C. The PMV values in winter mostly fluctuate from -0.6 to +0.6, thereby indicating that LD-IDECAOS offers a proper heating performance for building occupants although the measurement range slightly exceeds the recommended thermal environment range as suggested by the ASHRAE Standard.

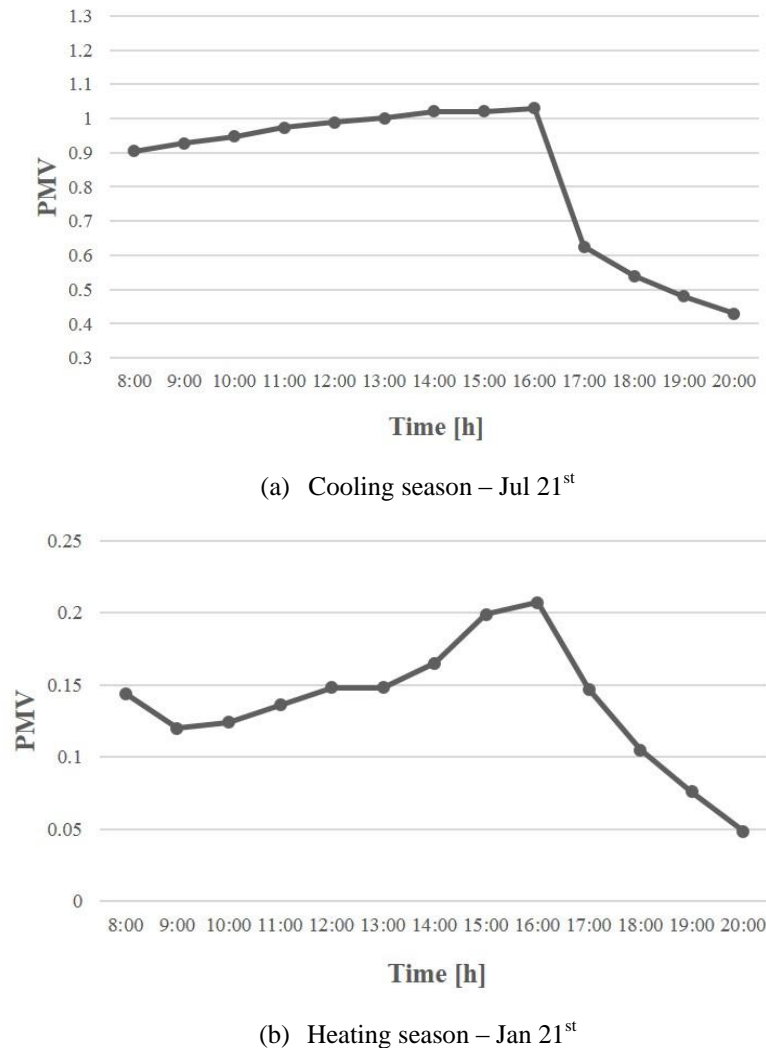


Figure 3: PMV value of LD-IDECAOS: (a) cooling season – Jul 21 and (b) heating season - Jan 21<sup>st</sup>

## 5 CONCLUSION

In this study, a PMV predicting model was developed to use energy simulationsto evaluate the influence of the supply air temperature on the thermal environment of occupants that is served by LD-IDECAOS. First, the PMV index that constitutes the most representative index to evaluate thermal comfort was used. An office building model served by a LD-IDECAOS was developed through TRNSYS 17 corresponding to the physical information of the building. Based on the operation mode of LD-IDECAOS as suggested by extant studies, PMV values during summer (i.e. June, July, and August) and winter (i.e. November, December, January, February, and March) were calculated.

During summer, the PMV values mostly vary from -0.5 to +1.0, and this indicates that the LD-IDECOAS properly cooled the conditioned zone by generally handling the latent load of incoming air with the LD unit. Similarly, the PMV values in winter are maintained within a tolerance of  $\pm 0.6$ , and thus imply that LD-IDECOAS offers proper heating performance to building occupants although the measurement range slightly exceeds the recommended thermal environment range as suggested by the ASHRAE Standard. Accordingly, it is concluded that the use of the LD-IDECOAS in an office building produces energy saving with an acceptable thermal comfort level.

## 6 ACKNOWLEDGEMENTS

This work was supported by the National Research Foundation (NRF) of Korea (No. 2015R1A2A1A05001726), the Korea Agency for Infrastructure Technology Advancement (KAIA) grant (16CTAP-C116268-01), and the Korea Institute of Energy Technology Evaluation and Planning (KETEP) (No. 20164010200860).

## 7 REFERENCES

- [1] W. Goetzler, R. Zogg, J. Young, C. Johnson, Alternatives to Vapor-Compression HVAC Technology, *ASHRAE Journal* 56(10) (2014) 12-23.
- [2] UNEP, 2010 Report of the Refrigeration, Air Conditioning and Heat Pumps Technical Options Committee, United Nations Environment Programme. Montreal Protocol on Substances that Deplete the Ozone Layer. 2011.
- [3] J. Woods, E. Kozubal, Combining liquid desiccant dehumidification with a dew-point evaporative cooler: A design analysis, *HVAC&R Research* 19(6) (2013) 663-675.
- [4] M.H. Kim, J.H. Kim, O.H. Kwon, A.S. Choi, J.W. Jeong, Energy conservation potential of an indirect and direct evaporative cooling assisted 100% outdoor air system, *Building Services Engineering Research and Technology* 32 (4) (2011) 345-360.
- [5] M.H. Kim, J.W. Jeong, Cooling performance of a 100% outdoor air system integrated with indirect and direct evaporative coolers, *Energy* 52 (1) (2013) 245-257.
- [6] M.H. Kim, J.Y. Park, M.K. Sung, A.S. Choi, J.W. Jeong, Annual operating energy savings of liquid desiccant and evaporative-cooling-assisted 100% outdoor air system, *Energy and Buildings* 76 (2014) 538-550.
- [7] M.H. Kim, J.S. Park, J.W. Jeong, Energy saving potential of liquid desiccant in evaporative cooling-assisted 100% outdoor air system, *Energy* 59 (2013) 726-736.
- [8] M.H. Kim, A.S. Choi, J.W. Jeong, Energy performance of an evaporative cooler assisted 100% outdoor air system in the heating season operation, *Energy and Buildings* 46 (2012) 402-409.
- [9] TRANE (2011), Applications Engineering Manual Chilled-Water VAV Systems.
- [10] S.A. Klein, W. A. Beckman, J. W. Mitchell, and J.A. Duffie, TRNSYS 17 transient system simulation program, user manual. Solar Energy Laboratory; 2010.
- [11] S.A. Klein, W.A. Beckman, J.W. Mitchell, and J.A. Duffie. EES-Engineering Equation Solver for Microsoft Windows Operating Systems, F-Chart Software, 2008.
- [12] ISO 7730, 2010, Ergonomics of the thermal environment-Analytical determination and interpretation of thermal comfort using calculation of the PMV and PPD indices and local thermal comfort criteria.
- [13] T. Katejanekarn, S. Chirattananon, S. Kumar, An experimental study of a solar-regenerated liquid desiccant ventilation pre-conditioning system, *Solar Energy* 83 (6) (2009) 920-933.

- [14] T. Katejanekarn, S. Kumar, Performance of a solar-regenerated liquid desiccant ventilation pre-conditioning system, *Energy and Buildings* 40 (7) (2008) 1252–1267.
- [15] T.W. Chung, C.M. Luo, Vapor pressure of the aqueous desiccants, *Journal of Chemical and Engineering Data* 44 (5) (1999) 1024–1027.
- [16] ASHRAE Standard55, 2005, Thermal Environmental Conditions for Human Occupancy, chapter 5.2.1.2
- [17] P.O. Fanger, 1967, Calculation of Thermal Comfort: Introduction of a Basic Comfort Equation, *ASHRAE Transactions.*, vol.73, Pt2

# Energy Efficiency in a Thermal Comfort Field Work in Spain

Elena Barbadilla-Martín<sup>\*1</sup>, José Guadix Martín<sup>2</sup>, José Manuel Salmerón Lissén<sup>3</sup> and Pablo Aparicio-Ruiz<sup>4</sup>

*1 Grupo de Ingeniería de Organización. Universidad de Sevilla  
Camino de los Descubrimientos S/N  
41092 Sevilla, España  
Corresponding author: ebarbadilla@us.es*

*2 Grupo de Ingeniería de Organización. Universidad de Sevilla  
Camino de los Descubrimientos S/N  
41092 Sevilla, España*

*3 Grupo de Termotecnia. Universidad de Sevilla  
Camino de los Descubrimientos S/N  
41092 Sevilla, España*

*4 Grupo de Ingeniería de Organización. Universidad de Sevilla  
Camino de los Descubrimientos S/N  
41092 Sevilla, España*

## ABSTRACT

It is estimated that HVAC systems represent the highest energy consumption (approximately half of the total energy consumed) and one of the highest cost, especially in non-residential buildings. Therefore, that energy consumption is related to the cost of the building, the energy consumption and the thermal comfort. Although the comfort of the users should be a factor to be aware of, it may not be the only one. It is advisable to have a balance between this variable and energy consumption, because of its impact on the environment and climate change.

## KEYWORDS

Adaptive thermal comfort, energy efficiency, HVAC system

## 1 INTRODUCTION

Global energy dependence has grown exponentially. According to the International Energy Agency from 1971 to 2014 global energy consumption increased by 92% and continues increasing (Martinez-Molina, Tort-Ausina, Cho, & Vivancos, 2016).

This, together with the existing debate on climate change and the depletion of fossil fuels, highlights the need for a more sustainable environment in order to reduce energy consumption and greenhouse gases emissions to the environment.

Achieving these goals is a challenge that requires innovative research to improve the use of energy sources and new technologies and methodologies. However, reducing the associated energy and environmental impact is a difficult task (Soares et al., 2017).

The construction sector is one of the largest energy consumers, representing a higher percentage than industry and transportation together. In 2004 the construction sector accounted for 40%, 39% and 37% of the total energy demand in the EE.UU., UK and EU respectively (Yang, Yan, & Lam, 2014). Globally, buildings contribute to more than 30% of CO<sub>2</sub> emissions and account for around 40% of the total energy demand and this ratio is expected to soon reach 60% (Shaikh, Nor, Nallagownden, Elamvazuthi, & Ibrahim, 2014), accounting the HVAC systems for approximately half of the total energy consumed.

Moreover, it is estimated that people spend 60-90% of their time inside buildings, so the assurance of comfort has become increasingly important in recent years.

The concept of comfort has undergone an important transformation, all due to the exponential growth of the results of the investigations that in that field have taken place in the last years. Initially, the key magnitude in comfort was simply an acceptable air quality inside the buildings. At present, however, users have certain expectations about comfort and a greater degree of exigency. The term comfort has become a complex concept determined by three basic factors: thermal comfort, visual quality and air quality and other acoustic and ergonomic conditioners (Dounis & Caraiscos, 2009).

Among all of them, thermal comfort is a decisive factor in health, productivity in working environments and comfort in general and from which significant economic and social costs can be derived (Soares et al., 2017).

Although the comfort of the users should be a factor to be aware of, it may not be the only one. It is advisable to have a balance between this variable and energy consumption, because of its impact on the environment and climate change.

## **2 COMFORT AND ENERGY EFFICIENCY**

The thermal comfort-energy efficiency balance represents a major challenge in the operation and management of buildings.

In the field of thermal comfort many studies have been carried out in buildings of different nature and in areas with different climatology (Pellegrino, Simonetti, & Chiesa, 2016).

The conventional thermal comfort model based on PMV and PPD was derived from climate chamber experiments where in most cases users wore standardized clothing and carried out sedentary activities. Numerous subsequent studies demonstrated that this stationary approximation fails. Most criticisms of the PMV and the PPD are based on the fact that they do not take into account the adaptation that takes place in changing thermal environments due to the thermal perception, also changing, of the users of such buildings.

People are able to adapt to the changing conditions of the thermal environment, which forms the basis of the adaptive theory of thermal comfort. Likewise, the adaptive principle also states that if there is a change that leads to discomfort, people react in such a way that they tend to restore their sense of comfort (Bhaskoro, Gilani, & Aris, 2013).

The inside temperature where most people are comfortable is known as neutral temperature or comfort temperature. Nicol and Humphreys proposed that such temperature was closely correlated with the outside temperature.

They also suggested that an algorithm could be constructed to determine the optimum indoor temperature as a linear function of the mean outdoor temperature and to use that reference for both the FR buildings and the HVAC system of conditioned buildings (McCartney & Nicol, 2002).

In many countries researches has been carried out to develop comfort temperature models. The results agree that an indoor comfort temperature could reduce the energy consumption of HVAC systems without sacrificing the comfort of the users (Bhaskoro, Gilani, & Aris, 2013) and that the use of temperatures based on the adaptive approach instead of fixed temperatures lead to energy savings without increasing the thermal discomfort of the occupants (Yang, Zheng, Mao, Lam, & Zhai, 2015).

Until recently, problems related with thermal comfort had been approached separately from the problems related to energy efficiency, so that in the literature studies can be found in the two fields separately, but there is a smaller number of investigations integrating both concepts simultaneously.

### 3 METHODOLOGY

In the present work we intend to investigate the relationship between thermal comfort based on adaptive theory and energy efficiency, all based on a real field study.

Figure 1 represents the research methodology. The objective of the first phase is to analyse the comfort range of the users, the second phase is the implementation of the adaptive law and in the third phase it is intended to carry out the verification of energy saving.

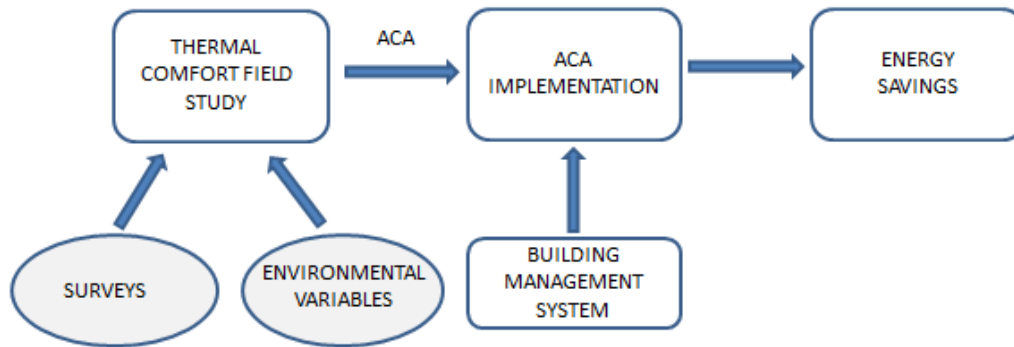


Figure 1 :Research methodology

#### 3.1 Field study

The study design, the methods used in the field study and the data analysis were based on the methodology of the ASHRAE model and the SCATs project (McCartney & Nicol, 2002), (de Dear & Brager, 1998).

The field study was carried out in three buildings of the tertiary sector, non-residential and dedicated to university teaching (11 office spaces) in the South area of Spain.

The field study was carried out for a year collecting about 4,000 thermal sensation data.

In relation to the indoor environment, the variables of air temperature, relative humidity, globe temperature, air velocity, surface temperature, CO<sub>2</sub> concentration and luminosity were monitored by sensors that were installed in the rooms.

To evaluate the thermal comfort of the occupants, a longitudinal questionnaire and two additional questionnaires on clothing and satisfaction with other environmental factors were elaborated. A thermal sensation scale based on the ASHRAE scale was used for the thermal sensation vote.

For the analysis of the data, the interaction between the thermal sensation and the indoor environment was first analysed, and secondly the relation between the comfort temperature and the external temperature, based on the adaptive principles (equation 1 and equation 2).

$$T_{\text{comfort}} = T_{\text{globe}} - TSV/G \quad (1)$$

$$T_{\text{comfort}} = a + b * T_{\text{rm}} \quad (2)$$

Where  $T_{\text{comfort}}$  is the inside comfort temperature,  $T_{\text{globe}}$  is the globe temperature,  $TSV$  is the thermal sensation vote,  $G$  is the Griffith constant and  $T_{\text{rm}}$  the running mean temperature. As a result of the field study, an adaptive comfort algorithm (ACA) was obtained. A clear dependence between the temperature of comfort and the outside temperature was identified.

### 3.2 ACA implementation

The validation of the adaptive law and the quantification of the energy saving will be carried out in the monitored spaces of one of the three buildings in the field study.

The building has a centralized HVAC system. Each room in the building has a ventilation grille and one or two fans-coils for heating and air-conditioning. The fan-coils are controlled by the users of the room through a thermostat located in the same that also has a sensor to control the ambient temperature.

The implementation of the ACA obtained from the field study was carried out using a control module available in the application of the system.

The implementation of the new control law took place both during a winter period and during a summer period. During this implementation, the environmental variables of the rooms and the thermal perception of the users continued to be monitored.

### 3.3 Verification of energy saving

In order to evaluate the energy savings derived from the implementation of the adaptive comfort algorithm it is necessary to develop a model since it is not possible to evaluate simultaneously the same situation: with the ACA and without it.

For this purpose, a simplified characterization model (SCM) based on transfer functions(Stephenson & Mitalas, 1971)and (Ponsoda, Blanes, & Bader, 2011)will be used. Models based on transfer functions are used in all scientific fields to evaluate dynamic responses.

Figure 2represents the methodology used, in which the developed model will provide the energy consumption that would have been if the building had not been improved, that is to say, if the building continued in the initial situation.

Obtaining the model requires a period of monitoring on the starting situation of the building, so it requires the monitoring of a base period that represents the energy performance of the building.

Finally, having the SCM identified, it could be excited with the measured data of the improved situation, that is to say, with the real interior conditions. These excitations will result in the consumptions that would have been obtained if the improvement would not have taken place (Figure 3).

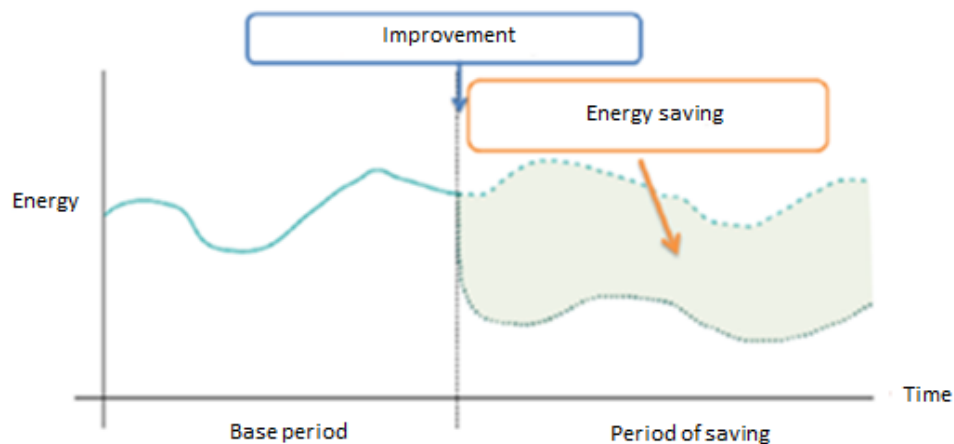


Figure 2 : Verification of energy saving-I

The saving is obtained by comparing the actual measured value and the value estimated by the SCM with the actual excitations of the improved situation measured.

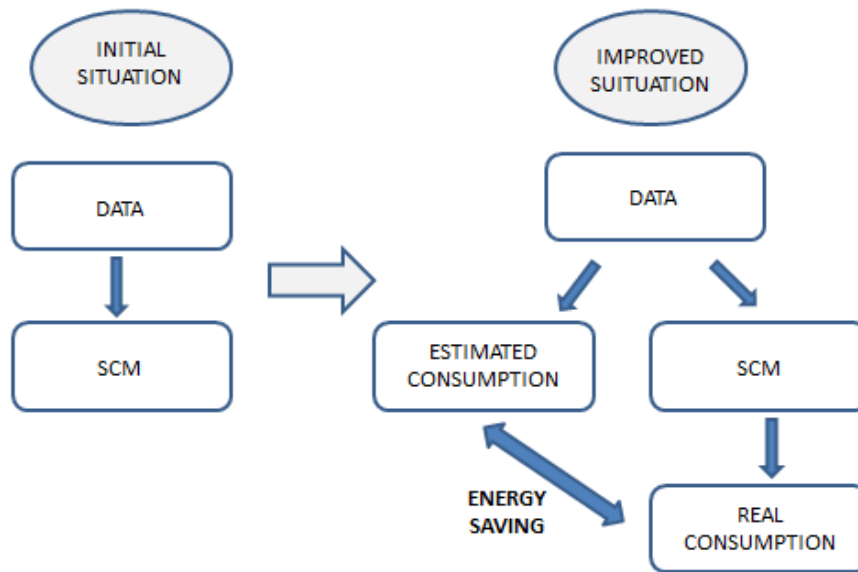


Figure 3 : Verification of energy saving-II

#### 4 CONCLUSIONS AND FUTURE DEVELOPMENTS

A field study was carried out in three buildings in order to investigate the comfort of the users. A relation between indoor comfort temperature and outdoor temperature was identified (ACA), based on the adaptive thermal comfort theory. Actually the ACA has been implemented in the building management system of the building and we are developing a model based on transfer functions in order to evaluate the expected energy saving.

#### 5 REFERENCES

- Bhaskoro, P. T., Gilani, S. I. U. H., & Aris, M. S. (2013). Simulation of energy saving potential of a centralized HVAC system in an academic building using adaptive cooling technique. *Energy Conversion and Management*, 75, 617–628. <http://doi.org/10.1016/j.enconman.2013.06.054>.
- de Dear, R., & Brager, G. (1998). Developing an adaptive model of thermal comfort and preference. *ASHRAE Transactions*, 104(1), 145–167.
- Dounis, A. I., & Caraiscos, C. (2009). Advanced control systems engineering for energy and comfort management in a building environment-A review. *Renewable and Sustainable Energy Reviews*, 13(6–7), 1246–1261. <http://doi.org/10.1016/j.rser.2008.09.015>.
- Martinez-Molina, A., Tort-Ausina, I., Cho, S., & Vivancos, J. L. (2016). Energy efficiency and thermal comfort in historic buildings: A review. *Renewable and Sustainable Energy Reviews*, 61, 70–85. <http://doi.org/10.1016/j.rser.2016.03.018>.
- McCartney, K. J., & Nicol, F. J. (2002). Developing an adaptive control algorithm for Europe. *Energy and Buildings*, 34(6), 623–635. [http://doi.org/10.1016/S0378-7788\(02\)00013-0](http://doi.org/10.1016/S0378-7788(02)00013-0).

- Pellegrino, M., Simonetti, M., & Chiesa, G. (2016). Reducing thermal discomfort and energy consumption of Indian residential buildings: Model validation by in-field measurements and simulation of low-cost interventions. *Energy and Buildings*, *113*, 145–158. <http://doi.org/10.1016/j.enbuild.2015.12.015>.
- Ponsoda, E., Blanes, S., & Bader, P. (2011). New efficient numerical methods to describe the heat transfer in a solid medium. *Mathematical and Computer Modelling*, *54*(7–8), 1858–1862. <http://doi.org/10.1016/j.mcm.2010.11.067>.
- Shaikh, P. H., Nor, N. B. M., Nallagownden, P., Elamvazuthi, I., & Ibrahim, T. (2014). A review on optimized control systems for building energy and comfort management of smart sustainable buildings. *Renewable and Sustainable Energy Reviews*, *34*, 409–429. <http://doi.org/10.1016/j.rser.2014.03.027>.
- Soares, N., Bastos, J., Pereira, L. D., Soares, A., Amaral, A. R., Asadi, E., Gaspar, A. R. (2017). A review on current advances in the energy and environmental performance of buildings towards a more sustainable built environment. *Renewable and Sustainable Energy Reviews*, *77*(February), 845–860. <http://doi.org/10.1016/j.rser.2017.04.027>.
- Stephenson, D. G., & Mitalas, G. P. (1971). Calculation of heat conduction transfer functions for multi-layer SLABS.” *ASHRAE Trans.*, vol. 77, no. Pt2, pp. 117–126, 1971.
- Yang, L., Yan, H., & Lam, J. C. (2014). Thermal comfort and building energy consumption implications - A review. *Applied Energy*, *115*, 164–173. <http://doi.org/10.1016/j.apenergy.2013.10.062>.
- Yang, L., Zheng, W., Mao, Y., Lam, J. C., & Zhai, Y. (2015). Thermal Adaptive Models in Built Environment and Its Energy Implications in Eastern China. *Energy Procedia*, *75*, 1413–1418. <http://doi.org/10.1016/j.egypro.2015.07.237>

# The influence of occupancy behaviour on the performance of mechanical ventilation systems regarding energy consumption and IAQ

Nicolás Carbonare\*, Fabien Coydon, Arnulf Dinkel, Constanze Bongs

*Fraunhofer Institute for Solar Energy Systems ISE  
Heidenhofstrasse 2  
79110 Freiburg, Germany  
nicolas.carbonare@ise.fraunhofer.de*

## ABSTRACT

It has already been proven that a large portion of the energy consumption gap between simulations and reality is due to the occupant behaviour in buildings. The improving airtightness of buildings makes that Indoor Air Quality (IAQ) can no longer rely on air renewal through infiltrations, bringing the need of ventilation systems. Within this frame, an ongoing dissertation focuses on the relationship between occupancy behaviour and ventilation systems in low energy buildings. In this paper, focus is made on a high rise residential multifamily building in south Germany, which has been retrofitted and then measured for two years to obtain post-refurbishment information. The occupant's behaviour nature was captured in 27 dwellings by measurements of inside temperatures and window openings and applied to the dynamic simulation environment WUFI+. In addition, a presence estimation model was developed in order to represent user behaviour as close as possible to reality. Different behaviours' scenarios (concerning window opening, temperature set point, presence, activities) were combined with different control strategies for mechanical ventilation systems, with the aim of analysing the impact of these variables on the energy consumption, thermal comfort and IAQ. The results show that there is a significant energy savings potential that can be achieved regarding to the occupant behaviour, and that the most challenging issue is the trade-off between these energy savings and maintaining healthy environments with higher IAQ. The challenges of the next generation of control strategies for ventilation systems will be to provide high flexibility to make the systems compatible with different user behaviours.

## KEYWORDS

Ventilation systems, Occupant behaviour, Indoor Air Quality, Energy-efficient buildings, Simulation

## 1 INTRODUCTION

The world's increasing energy demand has led in the last twenty years to an increasing interest on energy efficiency. The efforts towards the energy consumption reduction in the residential sector have brought up the retrofit of buildings as a solution in European countries. The high air tightness is a characteristic of these retrofits, as it contributes to reduce the heating energy consumption. Within this frame, mechanical ventilation systems acquired relevance to keep a desirable indoor air quality (IAQ) in retrofitted buildings.

On the other hand, the evaluation of these aforementioned technologies reveals that the performance is lower than expected in practical applications. It is already clear that the diversity of the occupant plays a key role on this underperformance (Hong et al., 2016).

This paper aims therefore at studying the relationship between mechanical ventilation technologies and the role of the occupant in low-energy buildings through building simulation. It will contribute to set the ground for further research about the interaction between ventilation systems and OB, with the overall objective of reducing the gap between predicted and observed energy performance, while aiming at guaranteeing an acceptable IAQ and thermal comfort.

## **2 METHODOLOGY**

The modelling of the OB represents a key step on this study, as it is the source of diversity, which influence on ventilation systems will be studied. Thus, it results of utmost importance to describe it as precisely as possible, through a combination between measurements and estimation methods. To carry out the study, measurements from a 16-storey multifamily building in South Germany (retrofitted to passive house standard in 2011) were taken, observing the behaviour of the occupants particularly in 27 dwellings (Kagerer et al., 2013). The aim is to capture the diversity of the occupant's behaviour in this building, and to apply it to simulations on a low-energy dwelling to analyse its effects on the performance of the ventilation system.

### **2.1 Occupancy Behaviour modelling**

Initially the goal was to determine how the OB can be represented regarding the inputs of the simulation. The variables that will be taken into account are window opening behaviour, temperature set point and internal gains (heat, moisture and CO<sub>2</sub>). Window opening and internal temperature were measured in the dwellings every six minutes, and the internal gains were estimated taking the measurements of heating power, domestic hot water and electricity consumption. The dependency of window opening profiles on ambient temperature is neglected by utilizing the measured outdoor conditions as input for weather data.

Due to the wide range of OB, the first step was to perform a statistical analysis of the measurements regarding window opening and indoor temperature. The aim was to obtain typical patterns of behaviour of both variables, grouping the similar ones into clusters. A hierarchical clustering method was selected and applied, taking into account the optimal number of clusters for each variable. The analysis is performed as if both variables (indoor temperature – IT – and window opening – WO) were independent.

The window opening behaviour is then clustered and grouped into six main behaviours, whereas in the case of indoor temperature three clusters were modelled. To illustrate this procedure, the figure 2-1 shows the yearly-averaged hourly profile for each dwelling, grouped into their cluster category. It can be clearly observed that each window opening profile has strong similarities with others of the same cluster and differences with those from the other clusters. The table 1 summarizes the evaluated alternatives in the simulations.

Six different random profiles were selected, considering one case per WO cluster and two from each IT cluster, which will be used as inputs of the simulation software. In the case of the indoor temperature, the set-point for heating devices was defined taking into account these differences among the OB. The simulation procedure will be described in the next chapters.

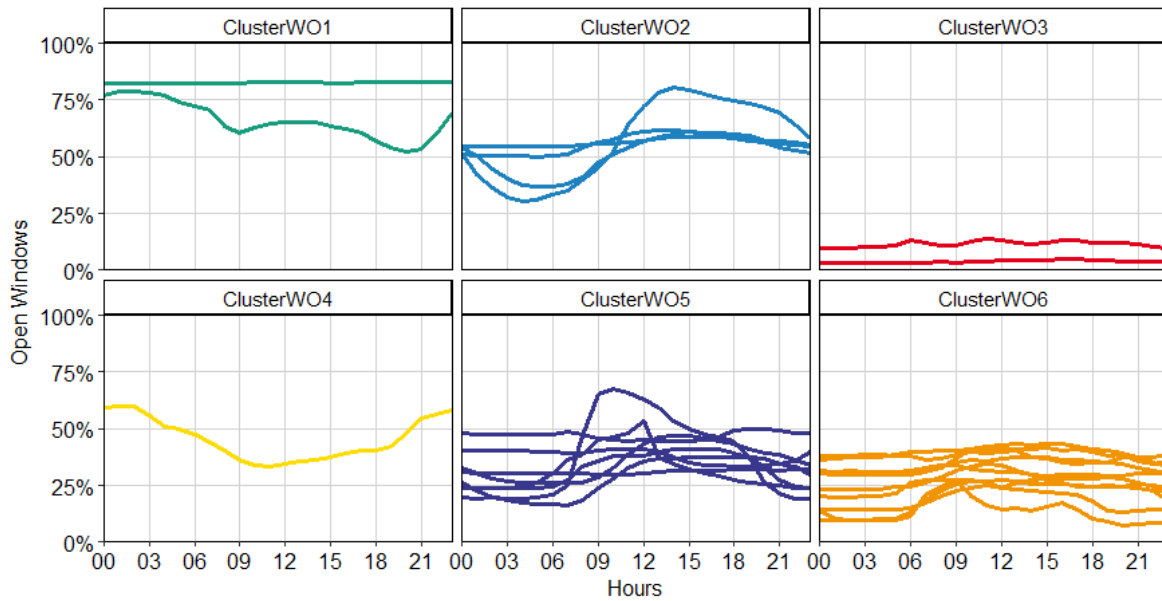


Figure 2-1: Window opening clusters

Table 1: Clusters characteristics

Simulation name	Window Opening	Indoor Temperature	Number of occupants
C1-1	Cluster WO1	Cluster IT1	1
C2-2	Cluster WO2	Cluster IT2	1
C3-3	Cluster WO3	Cluster IT3	1
C4-3	Cluster WO4	Cluster IT3	2
C5-1	Cluster WO5	Cluster IT1	2
C6-2	Cluster WO6	Cluster IT2	2

## 2.2 Presence and internal gains estimation

The variation of the internal loads can have an effect equal to the variation of the outdoor temperature in low-energy buildings (Johansson et al., 2011). In addition, according to Firlag (Firlag and Zawada, 2013) the internal loads are much lower than stated in norms. This produces an underestimation from the heating energy consumption, since the contribution of the internal heat sources is lower than expected. Andersen (Andersen et al., 2016) highlighted the importance of proper modelling of CO<sub>2</sub> and moisture sources in residential environment. Thus, it results of importance to estimate the internal loads dynamically. Some of them are related to the presence of the occupants, like the heat emissions of human metabolism; others, like the moisture gains from plants, are constant. As the presence was not measured, an estimation model was suggested to be developed, based on the measurements of window openings and instantaneous electrical power.

A literature review was carried out before defining the rules, in order to assess the current advances in the matter of presence estimation. These models attempt to build the other way round of the estimation: through the number of occupants and highly detailed stochastic models they estimate first if the dwelling is occupied or not, and then the activity the occupant performs, obtaining a 100% simulated electrical and heating load profile for a house. The main different amongst them is the number of states: while (Aerts et al., 2015) proposed a three state model (Present active, present passive or absent), others proposed a two-state model (active or passive in (Fischer et al., 2015), present or absent in (Kleiminger et al.,

2013). In this case, the presence estimation model will be a three-state model, as the internal heat gains are affected by passive or active status of the occupants.

Therefore, a set of assumptions and rules were set in order to obtain the estimation model. Given that the measurements are taken every six minutes, four periods are considered at every time step (24 minutes). That means, for each calculation at, for example, 11:00 AM, the results of the activity between  $\pm 2$  periods are observed (10:48 AM – 11:12 AM). Since the windows are seen as a change of state, the standard deviation within these four periods is calculated. The instantaneous electrical power is relevant when it overcomes the stand-by operation value for a relevant period. In that sense, the mean is calculated in the observed range and then contrasted to the stand-by pre-calculated value. The result of an estimation model on a typical day for a random dwelling can be seen in the figure 2-2 (left side). Worth to say, a value of 1 means “active” state, 0.5 is “passive” (sleeping) and 0 is “absent”.

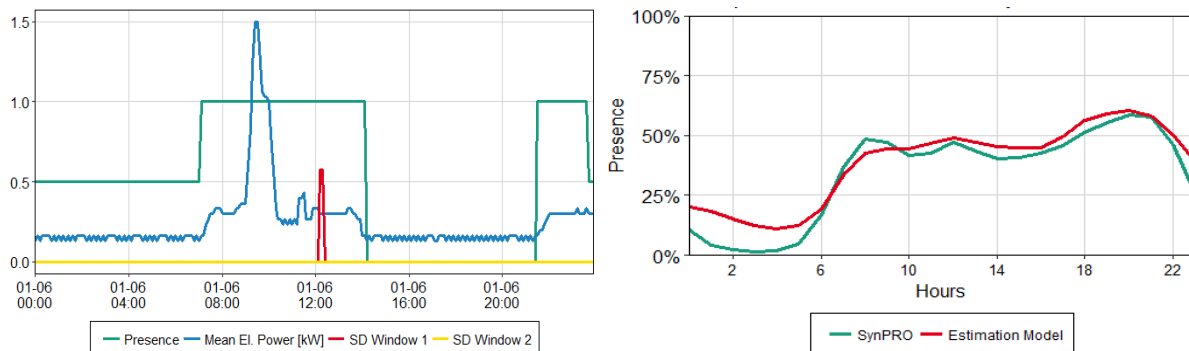


Figure 2-2: Presence estimation model (left) and validation (right)

To allow a crossvalidation of the proposed presence model, three separate multifamily buildings with six dwellings each were simulated with the tool SynPRO (Fischer et al., 2016), in which individual heating, DHW and electricity load profiles are generated stochastically. As inputs for the profile generation, similar social background and building envelope characteristics to the monitored building were selected, in order to obtain a representative occupant profile. The figure 2-2 (right side) compares the monthly-averaged hourly presence profiles for both simulations and estimation models.

The SynPRO profile fits the proposed model. It is worth mentioning that the drawn simulated profile is divided through the average number of occupants, in order to obtain a percentage value of the occupancy state. It is also relevant that the absent and passive state in the developed model were merged into only one (not active) to make it comparable with SynPRO simulation. Further cross validations of the model in comparison with other publications (Aerts et al., 2015; Kleiminger et al., 2013) were successfully carried out.

Besides the internal gains associated with the different activities, it is unneglectable that the room, in which these take place, plays also a role. The application of Agent-based Models to residential environments is still in development and has not yet reached enough interest from researchers (Zhang and Jia, 2016), as multi-occupant models with multi-space possibilities are still found to be weak in reproduction and prediction. Thus, an approximation was proposed here by defining rules and making assumptions about the occupants' movement. The last step refers to the determination of the internal loads. The general structure was built following these publications (Firląg and Zawada, 2013; de Gids W.F. and Wouters P., 2010). These were defined basically considering heat, moisture and CO<sub>2</sub> loads. There were no internal loads assigned to storage room and corridor. The table 2 presents a summary of the assumptions

taken to build the whole internal gains map. The category “others” is associated namely with heat absorption by evaporation (wet towels, for example) and heat losses on heating and DHW distribution systems.

Table 2: Internal loads summary

Category	Convection heat [W]	Radiation heat [W]	Humidity [g/h]	CO <sub>2</sub> [g/h]	Observations
1 Adult - Active	80	40	45	40	
1 Adult - Passive	60	30	25	20	
Appliances	95% consumption		0	0	Surface distributed
Washing machine	25% consumption		200	0	Bathroom
Dishwasher	25% consumption		200	0	Kitchen/Living room
Cooking	600	200	500	0	12-12:30 & 18-18:30
Shower	0	0	1% consumption	0	
Plants	0	0	75	Neglected	Surface distributed
Others	50	25	15	0	

### 2.3 Simulation

The simulation is based on the floor plan of one dwelling of the refurbished building (Figure 2-3) and it is assumed to be 10 m above ground level. The selected dynamic simulation environment is WUFI+ (Pazold and Antretter, 2012).

Regarding the initial simulation assumptions, the floor, ceiling and internal walls will be modeled as adiabatic surfaces, as it is assumed that the neighbor dwellings contain similar room temperatures. The external wall consists of 16 cm EPS isolation, resulting in a total thickness of 37.5 cm and a U-value of 0.19 W/m<sup>2</sup>K. The windows are modelled with a U-value of 1.2 W/m<sup>2</sup>K and a frame factor of 0.71. Table 3 summarizes the thermal characteristics of the dwelling.

Table 3: Building characteristics of the simulations

Building characteristics	Unit	Value
Outer wall U-value	[W/m <sup>2</sup> K]	0.19
Inner wall U-value	[W/m <sup>2</sup> K]	0.92
Windows U-value	[W/m <sup>2</sup> K]	1.20
Frame factor	[-]	0.71
Windows g-value	[-]	0.51
Infiltration rate n50	[1/h]	0.21
Leakage exponent	[-]	0.61
Leakage coefficient	[m <sup>3</sup> /h Pa]	1.03

The inputs of window opening and temperature set point are independent from the outdoor ambient conditions and will be taken directly from the measured data. It is assumed that the driving forces associated with external ambient conditions are coherent, since the weather data used for the simulation is also measured from Freiburg in the year 2013.

Regarding the heating and ventilation systems (HVAC), they are modelled as ideal, meaning that the software responds immediately to meet the heating demands, representing therefore the heating energy demand and not the performance of a specific facility. On the other hand, ventilation systems are also ideally modelled, and so are the different control strategies approached on this study. The assumed heat recovery efficiency is 80 % in all

cases. Regarding shading devices, there is no shading accounted on the living room, whereas on the bedroom is set to 0.1 (10 % sun exposure) when sleeping ( $R$ -value =  $0.2 \text{ W/m}^2\text{K}$ ). Taking into account the internal doors (relevant for multizone airflow model), the living-sleeping room door was set to 0.2 (opening rate) except while sleeping, when it is set to 0. This is also valid for the corridor-bathroom door (while presence in bathroom). The corridor-storage room door is neglected and set permanent to closed state.

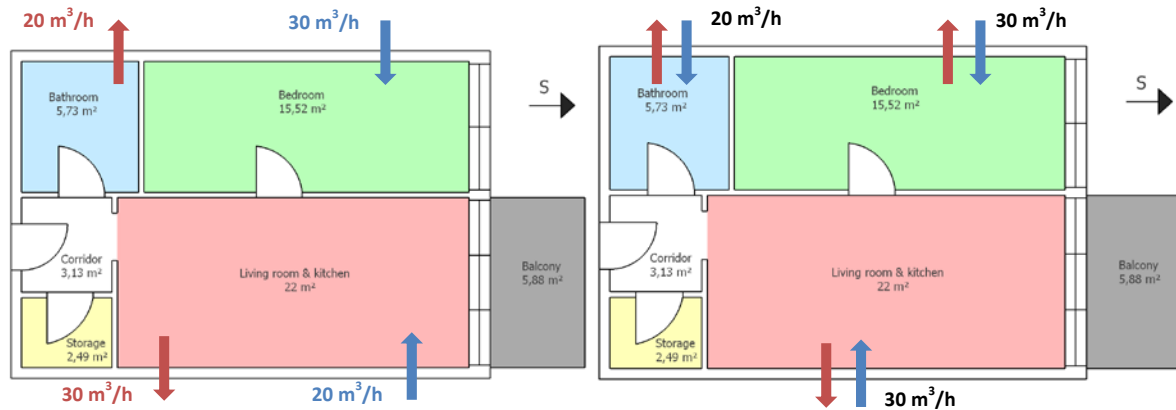


Figure 2-3: Simulated floor plan. Centralized system (left) and decentralized system (right)

In total, 48 simulations were carried out, selected according to the six clusters defined on table 1, and taking into account the following ventilation systems concepts (evaluated with and without heat recovery systems – HRC):

- Cen\_CAF: Centralized ventilation with constant volume flow ( $v = 50 \text{ m}^3/\text{h}$ )
- Dec\_CAF: Decentralized ventilation with constant volume flow ( $v = 80 \text{ m}^3/\text{h}$ )
- Dec\_RHu: Decentralized ventilation with relative humidity control
- Dec\_CO2: Decentralized ventilation with  $\text{CO}_2$  control

In the case of centralized ventilation systems, the airflows were taken from the reference building. The control strategies are defined with the following ventilation rates into four steps, and then illustrated in the figure 2-4:

- 10-20-30-40  $\text{m}^3/\text{h}$  in kitchen/living room and bedroom
- 5-10-15-20  $\text{m}^3/\text{h}$  in bathroom

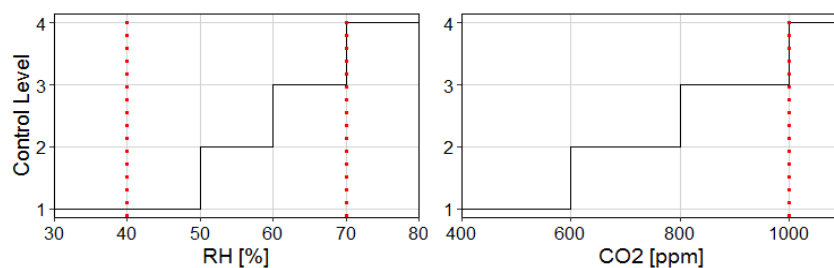


Figure 2-4: Ventilation control systems

## 2.4 Performance indicators

The performance indicators are defined following the work of Coydon (Coydon, 2015):

Energy performance:

- Heating demand due to ventilation, natural and mechanical [ $\text{kWh/m}^2\text{a}$ ]
- Electricity demand of the fans [ $\text{kWh/m}^2\text{a}$ ]

Hygrothermal comfort:

- Average temperature difference between indoor and supply air (1)
- Average relative humidity under 40% (2)

Indoor air quality:

- Average exposure to CO<sub>2</sub> concentrations above 1000 ppm (3)

$$\Delta T_{\text{comf}} = \frac{\sum \max(0; T_{\text{in}} - T_{\text{sup}})}{\text{presence}} \quad (1)$$

$$\Delta RH_{\text{comf}} = \frac{\sum \max(0; 40 - RH_{\text{in}})}{\text{presence}} \quad (2)$$

$$\Delta CO_{2\text{-IAQ}} = \frac{\sum \max(0; C_{CO_2} - 1000 \text{ ppm})}{\text{presence}} \quad (3)$$

Given that the simulation does not allow introducing specific fan power (SFP), it will be calculated separately following typical industrial standards, adopting the values of 0.4 Wh/m<sup>3</sup> for the systems with HRC, and 0.15 Wh/m<sup>3</sup> for the cases without HRC.

### 3 DISCUSSION OF RESULTS

#### 3.1 Energy consumption

The figure 3-1 illustrates the way heat recovery influences the energy consumption related to mechanical ventilation systems. Not only there is a reduction on energy consumption, but also a lower variation among the different control strategies (summarized in one box) can be observed. Heat recovery provides an average energy saving of 74% on mechanical ventilation systems and 37.3% considering also heat losses on natural ventilation.

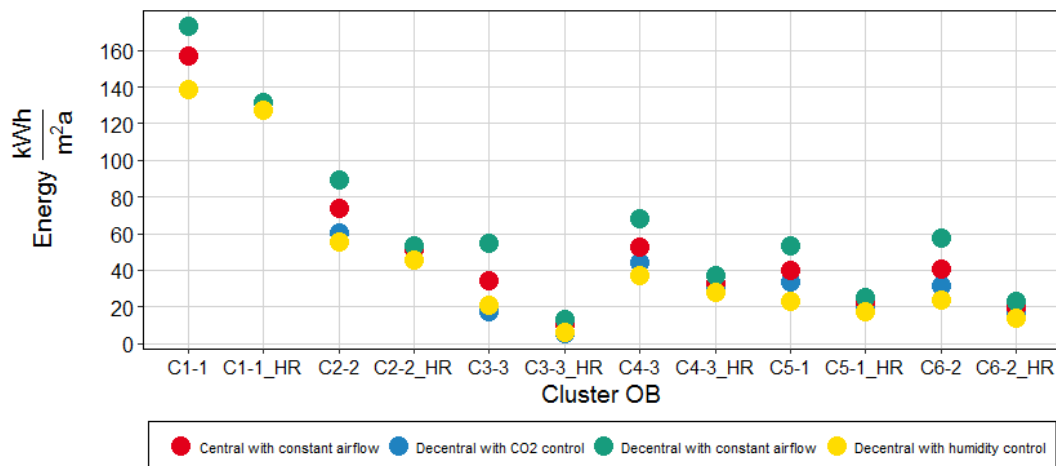


Figure 3-1: Final energy consumption with and without heat recovery

The analysis will focus therefore only on simulations with heat recovery. Figures 3-2 and 3-3 illustrate the total energy demand regarding control strategies, different occupancies and natural ventilation. Even though there is energy optimization potential, the overall energy consumption that predominates is led by natural ventilation, dependent on the WO behaviour of the occupant. This is correspondent with the clustered profiles presented on the figure 2-1. The cluster WO3 (lowest WO) consumes in every case at least seven times less energy due to

ventilation than clusterWO1 (highest WO). This pictures the influence of the OB on the performance of ventilation systems and highlights the importance of studying it and developing techniques of inducing an “energy saving” behaviour.

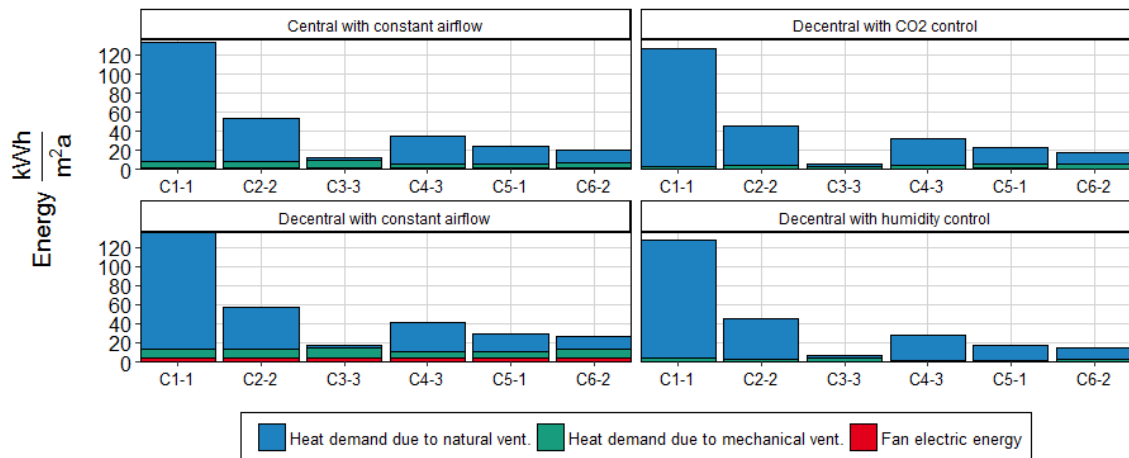


Figure 3-2: Final energy consumption due to ventilation

Moreover, focusing on mere mechanical ventilation, the optimization potential can be easily identified. The figure 3-3 shows that the energy consumption of the controlled systems is always lower than for the constant airflow cases. The simulations with only one occupant (clusters WO1-3) present their lowest consumption with CO<sub>2</sub> control (2% lower than RH), whereas the ones with two occupants (WO 4-6) have lower consumption with RH control (45% lower than CO<sub>2</sub>). It results also that the energy savings provided by a proper control system (70.1 % for mechanical ventilation, 22.7 % for final energy demand) is on a similar range as the savings obtained by the implementation of heat recovery (74 % and 37.3 %).

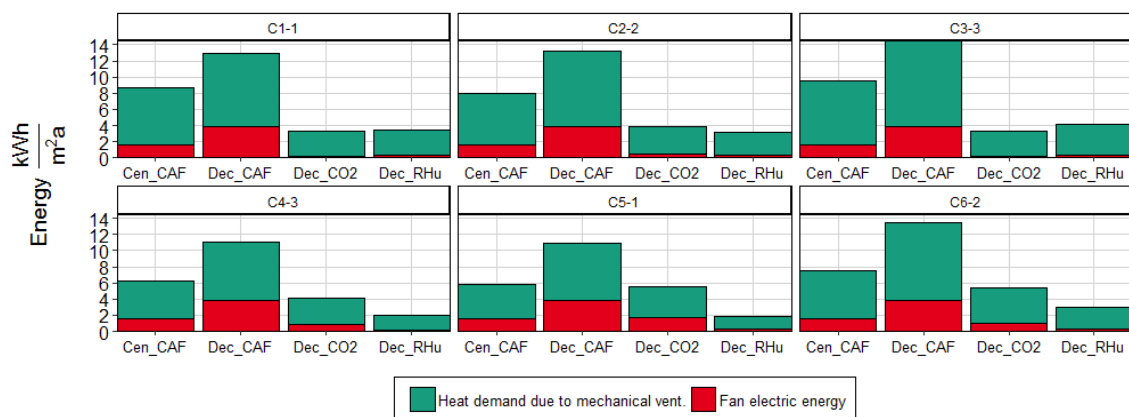


Figure 3-3: Final energy consumption due to mechanical ventilation

### 3.2 Comfort and IAQ

Relative humidity and CO<sub>2</sub> indicators do not vary with heat recovery. Analysis is then carried out only with heat recovery. The figure 3-4 summarizes the performance indicators, while showing the final energy consumption due to mechanical ventilation. Observing the comfort temperature difference, the value is directly related to the WO behaviour, as natural ventilation also contributes to this difference.

Considering relative humidity, it is noticeable that the constant airflow systems provide higher air flows, causing draught in the dwellings. The general WO behaviour combined with the ventilation strategies resulted in no case where RH stayed always above 40%. The

cluster 1-1 is the evidence that a higher WO leads to a lower hygrothermal comfort and undermines the influence of the ventilation control systems on RH comfort. The cases with two occupants lead to better comfort results, as the humidity internal loads are higher, providing an average value closer to 40%.

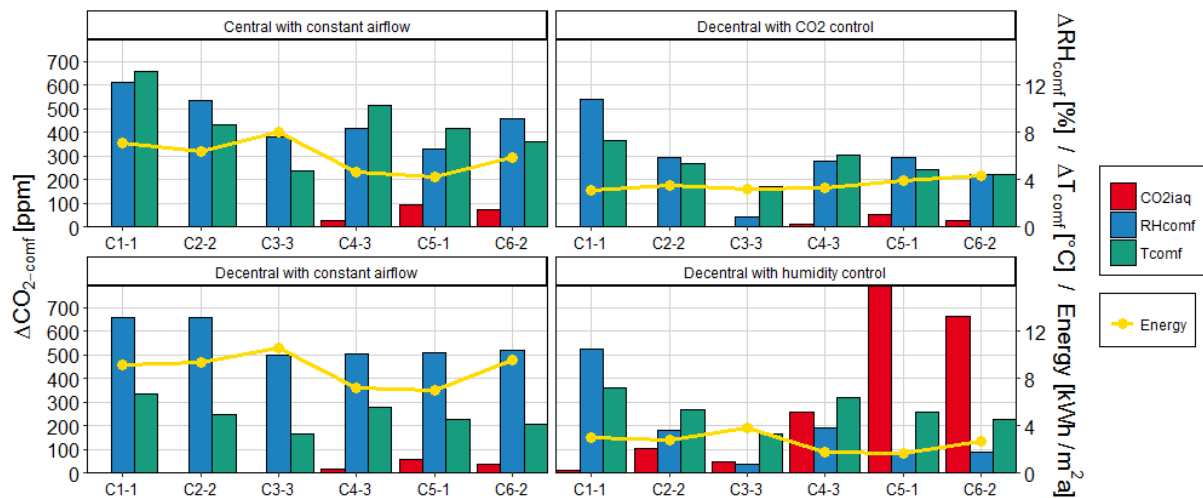


Figure 3-4: Performance indicators and energy consumption

Regarding CO<sub>2</sub>, it is almost not an issue in dwellings with only one occupant (only with RH control system). In dwellings with two occupants, no control system was able to keep always the CO<sub>2</sub> level under the set maximum value, and the CO<sub>2</sub> control system reaches the same comfort and IAQ performances as the constant airflow cases, but lowering the energy consumption. The cases with two occupants lead to worse IAQ results, as the CO<sub>2</sub> internal loads are much higher, resulting then in higher energy consumptions and average CO<sub>2</sub>.

The trade-off between the energy consumption, thermal comfort and OB is clear, in particular for the dwellings with two occupants. There is almost no case where the three variables present their most acceptable values at the same time. It is remarkable though, that the Cluster 3-3 presented the best results of the study, with rather high comfort standards and low energy consumption. Needless to say, it is the occupant with lowest WO. The fact that only one occupant lives there plays also a role in the acceptable IAQ performance, as the internal gains are considerably lower as in an apartment with two occupants.

#### 4 CONCLUSIONS

This work presents the results of a simulation of a low energy building, focusing on the occupancy behaviour and ventilation systems. Different OB variables were captured through measurements on a low-energy multifamily building in South Germany; others were estimated through model development. The application of these models into a dynamic simulation environment contributed to a results analysis, where a trade-off between energy consumption, hygrothermal comfort and IAQ could be identified. Results are highly dependent on the OB, having a stronger influence on the energy consumption than the ventilation control system, which also shows optimization potential.

As for future research, it would be interesting to compare cases of low WO frequency and higher number of occupants, to see to what extent the optimal case of the cluster C3-3 and CO<sub>2</sub> control system is an “optimization”, rather than a result of low internal heat gains. In addition, although several estimations were found on the literature, the issue regarding the different internal loads should be further addressed and become a subject of research due to its

importance on the building simulation and its lack of precise knowledge among the available models in the area. Centralized ventilation concepts with different control systems should be also studied. Furthermore, the next efforts will focus on the development of new simulation models of ventilation and control systems, in order to optimize the latter.

Last but not least, not only is capturing better the diversity of OBand its influencea challenge, but also trying through technology to provide the users a better understanding to generate a culture of “energetic behaviour”, to reduce their impact on the current energy consumption models.

## **5 ACKNOWLEDGEMENTS**

The study presented in this paper is funded by the German Ministry of Economics and Labour BMWi under the reference FKZ03ET1401A.

## **6 REFERENCES**

- Aerts, D., J. Minnen, I. Glorieux, I. Wouters and F. Descamps (2015). “A probabilistic activity model to include realistic occupant behaviour in building simulations” 2014, 1–12.
- Andersen, R. K., V. Fabi and S. P. Corgnati (2016). “Predicted and actual indoor environmental quality. Verification of occupants’ behaviour models in residential buildings” *Energy and Buildings* 127, 105–115.
- Coydon, F. (2015). *Holistic evaluation of ventilation systems*: Fraunhofer-Verlag.
- de Gids W.F. and Wouters P. (2010). “CO2 as indicator for the indoor air quality - General principles” AIVC Information Paper 33, 1–4.
- Firląg, S. and B. Zawada (2013). “Impacts of airflows, internal heat and moisture gains on accuracy of modeling energy consumption and indoor parameters in passive building” *Energy and Buildings* 64, 372–383.
- Fischer, D., A. Härtl and B. Wille-Hausmann (2015). “Model for electric load profiles with high time resolution for German households” *Energy and Buildings* 92, 170–179.
- Fischer, D., T. Wolf, J. Scherer and B. Wille-Hausmann (2016). “A stochastic bottom-up model for space heating and domestic hot water load profiles for German households” *Energy and Buildings* 124, 120–128.
- Hong, T., S. C. Taylor-Lange, S. D’Oca, D. Yan and S. P. Corgnati (2016). “Advances in research and applications of energy-related occupant behavior in buildings” *Energy and Buildings* 116, 694–702.
- Johansson, D., H. Bagge and L. Lindstrij (2011). “Measurements of occupancy levels in multi-family dwellings—Application to demand controlled ventilation” *Energy and Buildings* 43 (9), 2449–2455.
- Kagerer, F., S. Herkeland R. Bräu (2013). *Sanierung eines Hochhauses auf Passivhausstandard – ein Jahr Betriebserfahrungen*. Frankfurt am Main.
- Kleiminger, W., C. Beckel, T. Staake and S. Santini (2013). “Occupancy Detection from Electricity Consumption Data” 2013, 1–8.
- Pazold, M. and F. Antretter (2012). “Hygrothermische Gebäudesimulation mit multizonen Gebäudedurchströmungsmodell”.
- Zhang, C. and Q.-S. Jia (2016). “A review of occupant behavior models in residential building: Sensing, modeling, and prediction” 28th Chinese Control and Decision Conference (CCDC), 2032–2037.

# Thermal performance of ventilated solar collector with energy storage containing phase change material

Yue Hu<sup>\*1</sup>, Per Kvols Heiselberg<sup>2</sup>

*1 Aalborg University*

*Department of Civil Engineering, Thomas Mannsvej  
23*

*9220 Aalborg, Denmark*

*\*Corresponding author: hy@civil.aau.dk*

*2 Aalborg University*

*Department of Civil Engineering, Thomas Mannsvej  
23*

*9220 Aalborg, Denmark*

## ABSTRACT

This paper presents a ventilated solar collector with energy storage of fins containing Phase Change Material (PCM) in the air cavity and investigates its thermal performance. The idea is to use PCM in combination with ventilation as a thermal controller of indoor environment and to consequently decrease the building energy consumption both in summer and winter time. The main parts of the solar collector are plate fins with small thickness containing PCM fitted into the ventilation cavity, which is a good way to compensate the low thermal conductivity of PCM. The solar collector can absorb large amount of solar energy because of the high latent capacity of PCM. The energy is supplied into the indoor environment by means of ventilation. The system can be integrated into the building envelopes such as windows for low-energy building.

This study starts with examining the discharge process of PCM fins by numerically investigating 9 cases of PCM fins in different fin thickness and air gap thickness in a transient 2D model. Then the charge process of PCM fins in consideration of solar radiation is studied in a time-dependent 3D model. The results show that for discharge process, a larger fin thickness and a smaller air gap thickness are good for the increase of total heat exchange amount of PCM fins during discharge process. However, when continuing to increase the fin thickness and keeping the air gap thickness fixed at 5 mm, the total heat exchange amount does not continue the increase trend. The fin thickness of 20 mm has the largest heat exchange amount and the largest utilization percentage. Mechanical ventilation is needed only in cases with air gap thickness as 5mm. The system has the potential to completely or partly substitute the air-conditioning and heating system and a big energy saving potential.

## KEYWORDS

Low-energy building, ventilated solar collector, Phase Change Material, heating and cooling unit

## 1 INTRODUCTION

Building energy use is approximately 40% of the total energy use in Europe (Soares, Costa, Gaspar, & Santos, 2013). The main part of it is to cover the heating and cooling demand. In order to decrease this energy use and obtain higher energy efficiency, Thermal Energy Storage (TES) technics have been used in buildings. A novel idea of TES is to add Phase Change Materials (PCMs) to building elements and air conditioning systems, and this idea is gaining increasing interests in research as well as in the building market (Iten, Liu, & Shukla, 2016).

PCMs can store not only sensible heat energy but also latent heat energy, although the amount of sensible heat energy is much smaller in comparison with latent heat capacity (Akeiber et al., 2016). The heat been stored is much higher than the normal thermal mass applied in buildings. In addition, the temperature of PCMs will stay almost constant in the phase change period, which means the surface temperature of building envelope will not be too high, thus avoiding a high heat transfer (Osterman, Tyagi, Butala, Rahim, & Strith, 2012), which is good for maintain indoor thermal comfort.

PCMs are well known of their advantages that can be perfectly applied in lightweight building façades (Fang, Tang, & Cao, 2014). Various kinds of PCMs can be used for thermal storage

and thermal control for such building components. There are many studies about the PCMs integrated in opaque constructions, but limited research on integration in transparent materials and shading components. Michal et al. (Pomianowski, Heiselberg, & Lund Jensen, 2012) implemented PCMs in concrete and tested the performance of the hollow core deck made of this new material. The results show that there is a potential to apply PCMs in concrete elements. Hicham et al. (Karlsen, Heiselberg, Bryn, & Johra, 2016)(Heiselberg et al., 2013) put PCM shading device into a double layer ventilated window and tested its efficiency. The results show that both shading and ventilation could improve the energy efficiency in comparison with the original non-ventilated ones. Diarce et al. (Diarce et al., 2013) put a PCM sheet into a ventilated façade, the thermal performance of such device was investigated in comparison with different traditional ventilation systems by means of simulation in Design Builder software. The results indicated that the implement of PCM sheet is advantage for prevent overheating problems. Alvaro et al. (De Gracia et al., 2013) put macro-encapsulated PCM into the ventilated façade and investigated its effect through different control strategies. The experimental results shows that free cooling during night is the most effective control strategy to decrease the indoor cooling load.

The basic principle of the ventilated solar collector with PCMs is to combine the advantages of solar energy capture and latent heat storage of PCMs. In the winter condition, the PCMs are charged by the solar energy in the daytime and discharged in the night (and during some of the daytime) by means of ventilation air. The building energy use is then diminished by this principle. The energy efficiency will be further improved if solar control strategies are taken into consideration in summer daytime.

In this paper, fins containing PCM are chosen to fit in the ventilation cavity as a compensation to its low thermal conductivity and to increase heat transfer surface. Firstly, this paper presents the concept of ventilated solar collector in combination with PCM. Then the COMSOL Multiphysics program is used for the thermal performance of the ventilation cavity. The PCM fins are considered fully charged as initial condition and the discharge procedure is investigated.

## 2 MODELS AND METHODS

### 2.1 Concept of ventilated solar collector in combination with PCM

In this study, the development and design of the ventilated solar collector with PCM fins fitted in the air cavity is based on commercial product produced by the company Climawin, which produces a series of active ventilated solar collectors, but without PCM. Figure 1 shows the concept of ventilated solar collector with PCM.

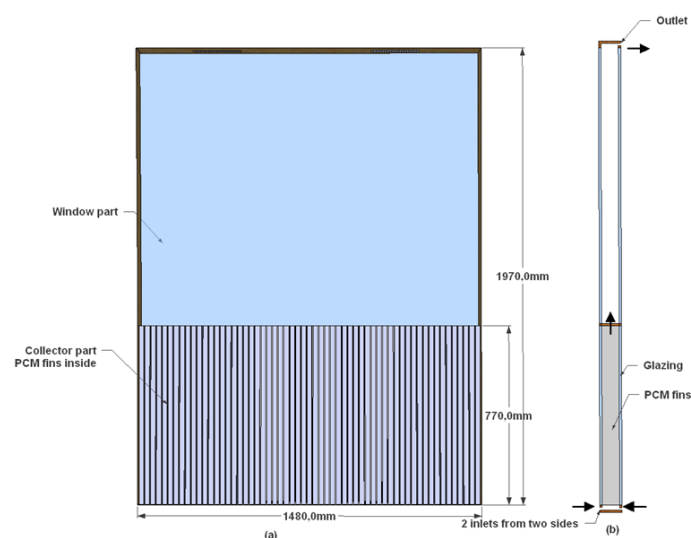


Figure 1: Ventiladed façade with solar collector consist of PCM fins (a) Front view; (b) Side view

## 2.2 Thermal properties of PCM

The Paraffin wax with a phase transition at approximately 21.7 is chosen for this model. The main thermal properties of the PCM shown in Table 1 are provided by Energain DuPont(DuPont<sup>TM</sup>. (2007). *Data Sheet - Measured Properties.*, n.d.).

Table 1: Thermal properties of paraffin wax (DSC method: 0.2 K/min; range of temperature: 5-30 °C)

Thermal property	Density(kg/m <sup>3</sup> )	Thermal conductivity(W/(m·K))	Total heat storage capacity(kJ/kg)	Total latent heat(kJ/kg)
Paraffin wax	1001.5	0.14	140	70

The specific heat has been measured experimentally at Artois University(Dû, Zalewski, Lassue, Dutil, & Rousse, 2012). The results are compared to the information provided by the manufacturer Energain including the total heat capacity and latent heat and they turned out to be in great consistency. The peak melting temperature is 20.0 °C and the peak freezing temperature is 15.4°C according to the record. Figure 2 shows the experimental fictive heat capacity.

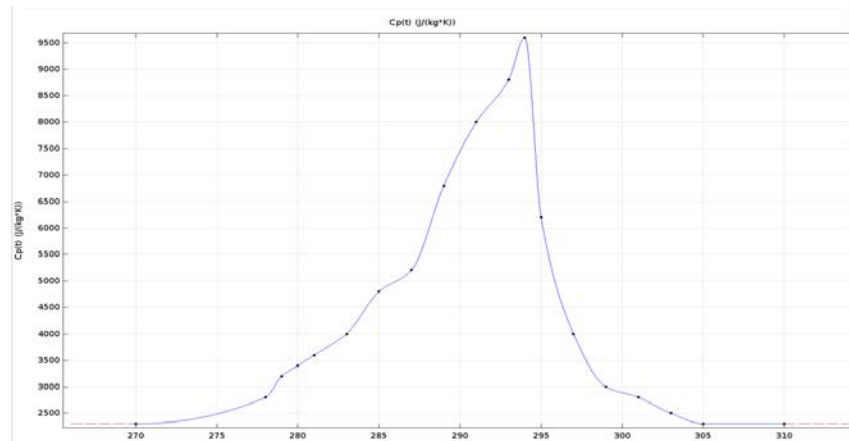


Figure 2: The fictive specific heat of PCM [20]

## 2.3 Model description

The air cavity of ventilated solar collector is of 1.31 m in height, 1.06m in width and 0.075 mm in depth. The PCM fins are fixed in the air cavity vertically. The inlet is in the bottom of the air cavity while the outlet is in the top. The optimizations of the thickness of PCM fins as well as the distance between fins are based on the simulation conducted in the COMSOL Multiphysics program. The ventilation cavity is simplified to a 2D model and only a section of the fin with air path. The PCM fins are supposed to fill the whole ventilation cavity so a length of 1.31m is chosen for all the fins in this program.

## 3 DISCHARGE PROCESS OF PCM FINS

### 3.1 Boundary conditions and equations

Some assumptions are made to investigate the discharge process of the PCM fins.

- The airflow rate is chosen as 106 m<sup>3</sup> /hat which condition the air states in the air path are all laminar flow.
- The inlet air temperature is defined as 273.15K to simplify the simulation.
- The physics condition of the model is defined as conjugate heat transfer, with conjugation of heat transfer and laminar flow.
- The PCM fins are considered as fully charged with an initial temperature of 300.15K.
- The vertical boundaries are defined as symmetric as they almost face the same sections.
- The simulations are from 0s to 18000 s with a time step of 10 s.

The boundary conditions are the same for all simulation models in order to insure the comparable results. Symmetry boundary condition is considered for simplification of the calculation as seen in Figure 3.

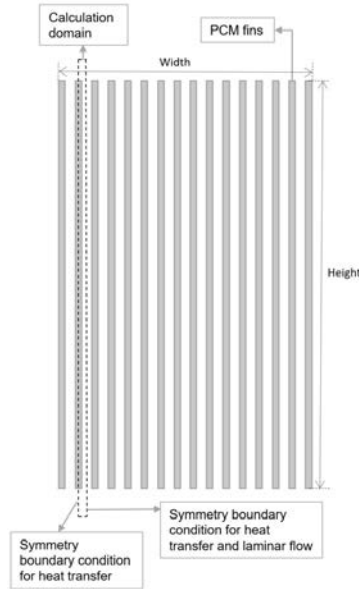


Figure 3: Calculation domain in COMSOL model

The Non-Isothermal Flow and Conjugate Heat Transfer interfaces contain the fully compressible formulation of the continuity equation and momentum equations:

$$\frac{\partial \rho}{\partial t} + \nabla \cdot (\rho \mathbf{u}) = 0 \quad (1)$$

$$\rho \frac{\partial \mathbf{u}}{\partial t} + \rho \mathbf{u} \cdot \nabla \mathbf{u} = -\nabla p + \nabla \cdot (\mu (\nabla \mathbf{u} + (\nabla \mathbf{u})^T)) - \frac{2}{3} \mu (\nabla \cdot \mathbf{u}) \mathbf{I} + \mathbf{F} \quad (2)$$

Where

$\rho$  is the density (kg/m<sup>3</sup>)

$\mathbf{u}$  is the velocity vector (m/s)

$p$  is pressure (Pa)

$\mu$  is the dynamic viscosity (Pa·s)

$\mathbf{F}$  is the body force vector (N/m<sup>3</sup>)

For heat equation,

$$\rho C_p \left( \frac{\partial T}{\partial t} + (\mathbf{u} \cdot \nabla) T \right) = -(\nabla \cdot \mathbf{q}) + \tau : S - \frac{T}{\rho} \frac{\partial \rho}{\partial T} \left( \frac{\partial p}{\partial t} + (\mathbf{u} \cdot \nabla) p \right) + Q \quad (3)$$

Where

$C_p$  is the specific heat capacity at constant pressure (J/(kgK))

$T$  is absolute temperature (K)

$\mathbf{q}$  is the heat flux by conduction (W/m<sup>2</sup>)

$\tau$  is the viscous stress tensor (Pa)

$S$  is the strain-rate tensor (1/s)

$Q$  contains heat sources other than viscous heating (W/m<sup>3</sup>)

For heat transfer in PCM:

$$\rho C_p \frac{\partial T}{\partial t} = -(\nabla \cdot q) - T \frac{\partial E}{\partial t} + Q \quad (4)$$

where  $E$  is the elastic contribution to entropy ( $J/(m^3 \cdot K)$ )

### 3.2 Results

When cold air goes through the gaps between the fins from below, the PCM in the lower part of the fins melt first and faster than in the upper part. The cold air is heated and temperature increases along the vertical length. Heat transfers from the hot PCM fins to the inlet air, in which progress the PCM is discharged.

At first fin depth as 0.075 m is chosen. There are 9 cases to be investigated as listed in Table 2. The airflow rate is chosen as constant for all the cases, which means the air velocity in the gaps between fins would be different. The total fin surface area and total PCM volume for different cases are also different. Those factors have an interaction influence to the performance of the ventilated solar collector.

Table 2: Analysis conditions for discharge process of PCM fins

Case	Fin thickness (mm)	Air gap thickness (mm)	Fin number	Fin depth (mm)	Air flow rate ( $m^3/h$ )	Air velocity in gap (m/s)	Total fin surface area ( $m^2$ )	Total PCM volume ( $m^3$ )
1	5	5	106			0.75	22.30	0.052
2	5	10	70			0.56	14.73	0.034
3	5	15	53			0.50	11.15	0.026
4	10	5	70			1.11	15.69	0.069
5	10	10	53	75	106	0.75	11.88	0.052
6	10	15	42			0.62	9.42	0.041
7	15	5	53			1.50	12.62	0.078
8	15	10	42			0.93	10.00	0.062
9	15	15	35			0.76	7.86	0.052

Figure 4 and Figure 5 show the average air temperature of outlet for different cases. As shown in Figure 4, for the same air gap thickness, outlet air temperature of fin thickness of 5 mm reaches the inlet air temperature faster than in the other cases. Nevertheless, the larger the fin thickness, the more stable the outlet air temperature due to the larger total PCM volume, which contributes to more heat being stored. As seen in Figure 5, for the same fin thickness, air gap thickness of 5 mm has the higher heat exchange rate and air gap thickness of 15 mm has the lower air change rate compared to other cases. Meanwhile, air gap thickness of 5 mm has the highest outlet average temperature compared to other cases.

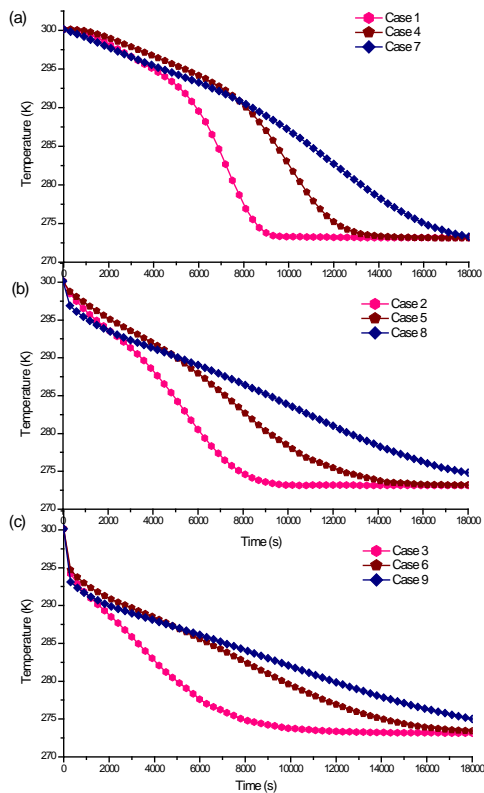


Figure4:Outlet air temperature of fins with same air gap thickness (a) air gap thickness=5 mm; (b) air gap thickness=10 mm; (c) air gap thickness=15 mm.

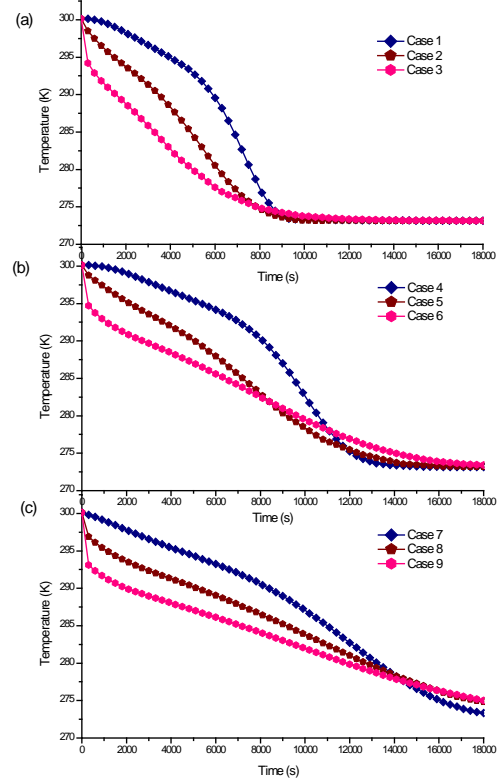


Figure5:Outlet air temperature of fins with same fin thickness (a) fin thickness=5 mm; (b) fin thickness=10 mm; (c) fin thickness=15 mm.

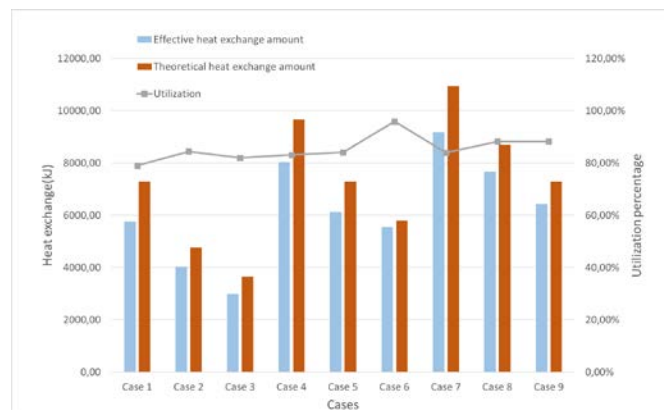


Figure6:Total heat exchange amount between inlet air and PCM fins for 9 cases

Figure 6 presents the total heat exchange amount for different cases. There is a similar pattern shown as the average outlet air temperature, which is in connection with total PCM volume. The comparison of effective heat exchange amount and theoretical heat exchange amount shows that case 6 has the largest PCM utilization percentage. Cases 1, 5, 9 have the same theoretical heat exchange amount but PCM utilization percentage is increasing. Table 3 shows the correlations of fin thickness and air gap thickness to other factors.

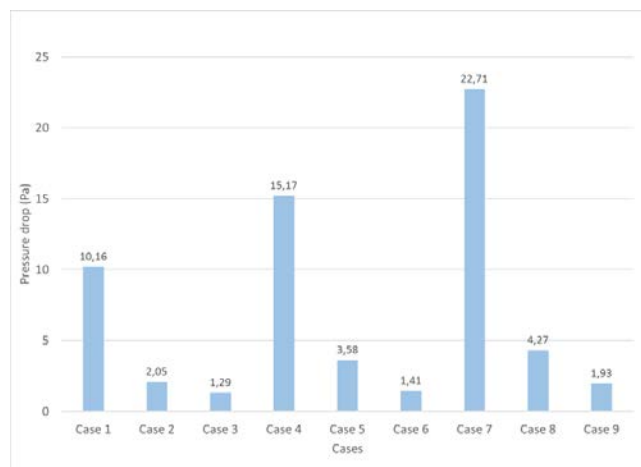
Table 3: The correlations of fin thickness and air gap thickness to other factors

	Number of fins	Air velocity	Surface area	Total PCM amount	Heat exchange rate	Discharge time	Total heat exchange amount
Fin thickness	-	+	-	+	-	+	+
Air gap thickness	-	-	-	-	+	-	-

As shown in table 3, when the fin thickness increases, the heat exchange rate decreases and the discharge time increases consequently. Nevertheless, the total heat exchange rate increases, and the outlet air temperatures are more stable as seen in Figure 4. The total heat exchange amount is more directly in connection with the total PCM volume, which means a larger fin thickness and a smaller air gap thickness. So it can be concluded that a larger fin thickness and a smaller air gap thickness are good for discharge process of PCM fins. However, cases 5-9 could not be fully discharged in 5 hours. Case 4 has the second total heat exchange amount and a relatively short discharge time, which means 10 mm fin thickness and 5 mm air gap thickness is the optimized size of the PCM ventilation unit.

Figure 7 (a) shows the pressure loss of ventilation cavity is shown in, and Figure 7 (b) shows the fan energy consumption for the 18000 s considering the fan efficiency as 0.7. Cases 1, 4, 7 are used for mechanical ventilation and other cases are suited for nature ventilation.

(a)



(b)

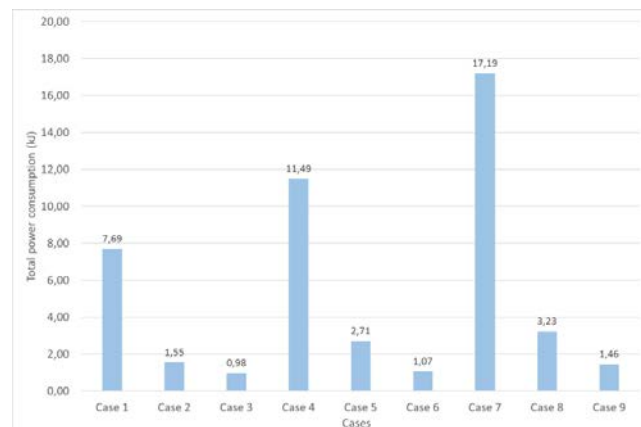


Figure 7: Pressure loss and total fan energy consumption of ventilation cavity (a) Results for different groups; (b) Total fan energy consumption for 5 hrs.

Two more cases are investigated to further evaluate the influence of fin thickness to the total heat exchange amount. As shown in Table 4, the air gap thickness is fixed at 5 mm and fin thickness increased from 15 mm to 25 mm. Figure8 shows the outlet air temperature, and the heat exchange rate of the discharge process tends to be in two stages. In the first stage, the heat exchange rate is mainly influenced by total surface area of fins. Case 7 has the largest fin surface area and heat exchange rate. In the second stage, the heat exchange rate is mainly influenced by the total PCM volume. Case 11 has the largest total PCM storage volume and heat exchange rate. The discharge time of the two cases are more than 5 hours. Figure9 shows the total heat exchange amount, and the fin thickness of 20 mm has the largest heat exchange amount. The effective value of heat exchange amount is compared with the theoretical value. It turns out that the largest utilization percentage of PCM is a fin thickness of 20 mm.

Table 4: Analysis conditions for discharge process of PCM fins

Case	Fin thickness (mm)	Air gap thickness (mm)	Fin depth (mm)	Air flow rate(m <sup>3</sup> /h)	Air velocity in gap (m/s)	Total fin surface area (m <sup>2</sup> )	Total PCM volume(m <sup>3</sup> )
7	15	5			1.50	12.62	0.078
10	20	5	75	106	1.78	10.58	0.083
11	25	5			2.12	9.30	0.086

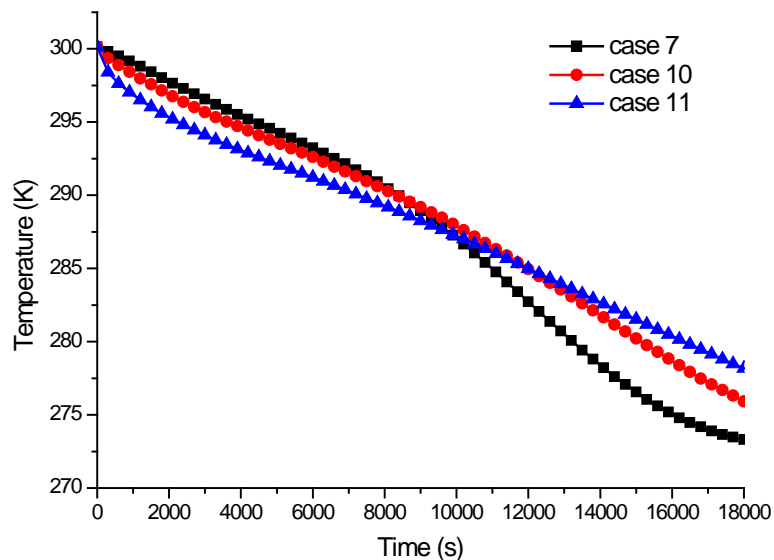


Figure8: Outlet air temperature with air gap thickness as 5 mm

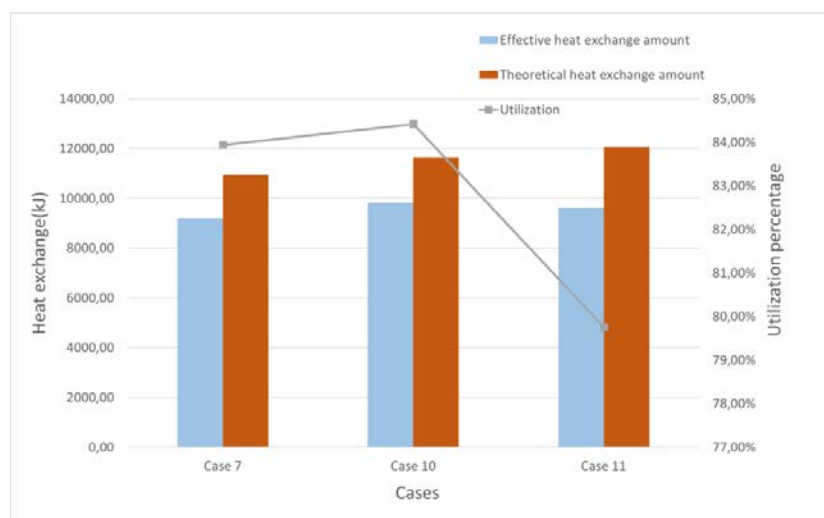


Figure9: Total heat exchange amount between inlet air and PCM fins

#### 4 CONCLUSION AND DISCUSSION

This paper propositions a ventilated solar collector with fins containing Phase Change Material (PCM) in the air cavity. The discharge and charge process of PCM fins are analysed and the thermal performance of the PCM fins in the air cavity are investigated. The main conclusions are as listed below.

1. For the discharge process, the heat exchange rate is in proportion to the total fin surface area while total heat storage amount is in proportion to the total PCM volume. The larger the fin thickness, the more stable the outlet air temperature.
2. The heat exchange rate of discharge process tends to be in two stages. In the first stage, the heat exchange rate is mainly influenced by total surface area of fins. In the second stage, the heat exchange rate is mainly influenced by the total PCM volume. A greater fin thickness and a smaller air gap thickness are good for the increase of total heat exchange amount of PCM fins during the discharge process.
3. Considering the discharge time, cases 5-9 cannot be fully discharged in 5 hours while case 4 has a high total heat exchange amount and a relatively short discharge time, which makes 10 mm fin thickness and 5 mm air gap thickness the optimized size of a PCM fin device.
4. However, when increasing the fin thickness and air gap thickness fixed at 5 mm, the total heat exchange amount does not continue the increase trend. The fin thickness of 20 mm has the largest heat exchange amount and the largest utilization percentage.
5. Pressure drop and energy consumption results show that mechanical ventilation should be considered when the air gap thickness is 5 mm. For other cases nature ventilation would be sufficient.

There is more work to be done for the system. Firstly, the inlet air temperature should be taken directly from outdoor environment. Thus the real outdoor environment should be taken into account for the further simulation work. What is more, the charge and discharge process should be investigated consecutively to get an overall evaluation of the thermal behaviour of the device. Last but not least, the system should be installed into a building site to further study the effect of the thermal behaviour of indoor environment and control strategies during different seasons.

#### 5 REFERENCES

- Akeiber, H., Nejat, P., Majid, M. Z. A., Wahid, M. A., Jomehzadeh, F., Zeynali Famileh, I., ... Zaki, S. A. (2016). A review on phase change material (PCM) for sustainable passive cooling in building envelopes. *Renewable and Sustainable Energy Reviews*, 60, 1470–1497. <https://doi.org/10.1016/j.rser.2016.03.036>
- De Gracia, A., Navarro, L., Castell, A., Ruiz-Pardo, Á., Álvarez, S., & Cabeza, L. F. (2013). Thermal analysis of a ventilated facade with PCM for cooling applications. *Energy and Buildings*, 65, 508–515. <https://doi.org/10.1016/j.enbuild.2013.06.032>
- Diarce, G., Urresti, A., García-Romero, A., Delgado, A., Erkoreka, A., Escudero, C., & Campos-Celador, Á. (2013). Ventilated active façades with PCM. *Applied Energy*, 109, 530–537. <https://doi.org/10.1016/j.apenergy.2013.01.032>
- Dû, M. Le, Zalewski, L., Lassue, S., Dutil, Y., & Rouse, D. (2012). Thermophysical characterization of a composite phase change material : the specific case of Energain ®, 1–10.

DuPont<sup>TM</sup>. (2007). *Data Sheet - Measured Properties*.(n.d.).

Fang, G., Tang, F., & Cao, L. (2014). Preparation, thermal properties and applications of shape-stabilized thermal energy storage materials. *Renewable and Sustainable Energy Reviews*, 40, 237–259. <https://doi.org/10.1016/j.rser.2014.07.179>

Heiselberg, P., Larsen, O. K., Liu, M., Zhang, C., Johra, H., Herold, L., ... Heusler, I. (2013). CLIMAWIN. Department of Civil Engineering, Aalborg University.

Iten, M., Liu, S., & Shukla, A. (2016). A review on the air-PCM-TES application for free cooling and heating in the buildings. *Renewable and Sustainable Energy Reviews*. <https://doi.org/10.1016/j.rser.2016.03.007>

Karlsen, L., Heiselberg, P., Bryn, I., & Johra, H. (2016). Solar shading control strategy for office buildings in cold climate. *Energy and Buildings*, 118(130), 316–328. <https://doi.org/10.1016/j.enbuild.2016.03.014>

Osterman, E., Tyagi, V. V. V., Butala, V., Rahim, N. A. A., & Stritih, U. (2012). Review of PCM based cooling technologies for buildings. *Energy and Buildings*, 49, 37–49. <https://doi.org/10.1016/j.enbuild.2012.03.022>

Pomianowski, M., Heiselberg, P., & Lund Jensen, R. (2012). Dynamic heat storage and cooling capacity of a concrete deck with PCM and thermally activated building system. *Energy and Buildings*, 53, 96–107. <https://doi.org/10.1016/j.enbuild.2012.07.007>

Soares, N., Costa, J. J., Gaspar, A. R., & Santos, P. (2013). Review of passive PCM latent heat thermal energy storage systems towards buildings' energy efficiency. *Energy and Buildings*. <https://doi.org/10.1016/j.enbuild.2012.12.042>

# Energy performance prediction of thermoelectric ceiling radiant panels with a dedicated outdoor air system

Hansol Lim<sup>1</sup>, Janghoon Shin<sup>1</sup>, Shiyong Li<sup>1</sup>, Hye-Jin Cho<sup>1</sup> and Jae-Weon Jeong<sup>\*,1</sup>

*1 Department of Architecture Engineering, College of Engineering, Hanyang University,  
222 Wangsimni-Ro, Seungdong-Gu, Seoul, 04763, Republic of Korea  
\*Corresponding author: jjwarc@hanyang.ac.kr*

## ABSTRACT

This paper proposes a dedicated outdoor air system (DOAS) with thermoelectric module radiant cooling panels (TEM-RCP). The DOAS involves the concept of a decoupled system with a parallel sensible cooling unit. This concept implies decoupling of ventilation and air-conditioning functions. The DOAS treats latent loads from outside air intake as a 100 % OA ventilation system. Additionally, a parallel sensible cooling unit, such as ceiling radiant cooling panel (CRCP), generally removes sensible loads. In the study, the variable air volume system and DOAS CRCP using chilled water were also considered as a conventional HVAC system and traditional parallel cooling unit of DOAS, respectively. The two cases were compared to investigate the possibility of applying TEM-RCP on DOAS. Mathematical simulation models were developed, and the operating and annual energy consumptions for all three cases were estimated. The results indicated that the thermal performance was satisfied in all cases including the proposed systems. The proposed system resulted in annual energy consumption savings of 44.5 % when compared with the variable air volume system. On the other hand, the energy consumption of TEM-RCP exceeded that of the CRCP by 33 % due to its low coefficient of performance (COP) and additional energy from heat rejection. The proposed system did not exhibit benefits in terms of energy consumption when compared with that of the DOAS CRCP. However, it could be easily controlled by using input current without refrigerants and still continue to display energy saving potential when compared with the VAV system.

## KEYWORDS

Dedicated outdoor air system; radiant cooling; cooled ceiling; thermoelectric modules

## 1 INTRODUCTION

A decoupled system concept of a dedicated outdoor air system (DOAS) with parallel sensible cooling is used due to benefits including energy conservation and indoor air quality. The DOAS effectively accommodates latent loads and part of sensible loads. The system uses 100 % outside air with a minimum air flow rate for ventilation integrated with a parallel cooling unit, such as ceiling radiant cooling panel (CRCP), to remove sensible loads. A CRCP is an efficient way to achieve occupant thermal comfort and is generally used with metallic ceiling water panels. The coolant of this system involves water chilled by a vapor compression system that uses refrigerants. This system exhibits good efficiency. However, a concern involving the depletion of the ozone layer by refrigerants such as CFCs persists (Kim et al., 2016).

Hence, a thermoelectric module (TEM) is studied as a non-vapor compression technique without a refrigerant. Previous studies developed an air-cooled type TEM radiant cooling panel (TEM-RCP) and investigated its performance (Tan and Zhao, 2015). Nevertheless, there is a paucity of investigations examining the use of a TEM-RCP combined with a HVAC system. Additionally, previous studies did not focus on the use of a water-cooled type TEM-RCP given considerations to reduce system size. However, a water-cooled type exhibits better efficiency when compared to an air-cooled type with respect to aspects involving heat rejection (Lee, 2017). Therefore, the present study proposed a water-cooled type TEM-RCP for parallel sensible cooling in DOAS. The study developed mathematical simulation models

for DOAS TEM-RCP and CRCP systems. Furthermore, a variable air volume (VAV) system was simulated as a case for conventional HVAC system for comparison purposes. Finally, annual energy consumptions of both systems were compared to evaluate the possibility of applying TEM-RCP on a DOAS system.

## 2 SYSTEM DESCRIPTION

### 2.1 Variable air volume system

As shown in figure 1, a conventional VAV system was selected to compare operating energy consumption in a cooling season with a decoupled system involving a DOAS with a parallel cooling unit. In the VAV, the air flow rate is determined based on a sensible and latent load. Therefore, fan energy also varies with loads. In a cooling season, a dehumidification process occurs at the cooling coil and reheats air by using a heating coil to satisfy supply air temperature. Additionally, an enthalpy based economizer is used in the intermediate season.

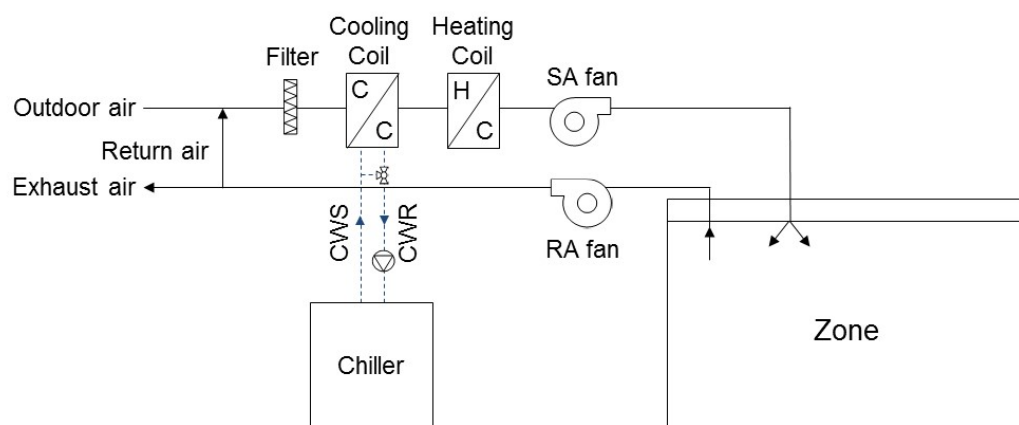


Figure 1: Schematic of a conventional VAV system

### 2.2 Dedicated outdoor air system with a chilled water ceiling radiant panel

The conventional DOAS considered in this study is shown in Figures 2 and 3. The DOAS consists of an enthalpy wheel, a sensible wheel, and a cooling coil. In the DOAS, a minimum ventilation air flow rate is supplied irrespective of the load. The enthalpy wheel reduces the work of the cooling coil by exchanging water and heat with exhaust air without mixing. The remaining latent load is removed at the cooling coil, and the sensible wheel reheats the supply air. Additionally, the CRCP that uses chilled water is used to accommodate the sensible load that remains after the DOAS satisfies the whole latent load and a part of the sensible load as shown in Figure 2. In this study, a single electric chiller was simulated to supply chilled water for the cooling coil and CRCP. A detailed operation mode of the DOAS is described in a previous study (Kim et al., 2016).

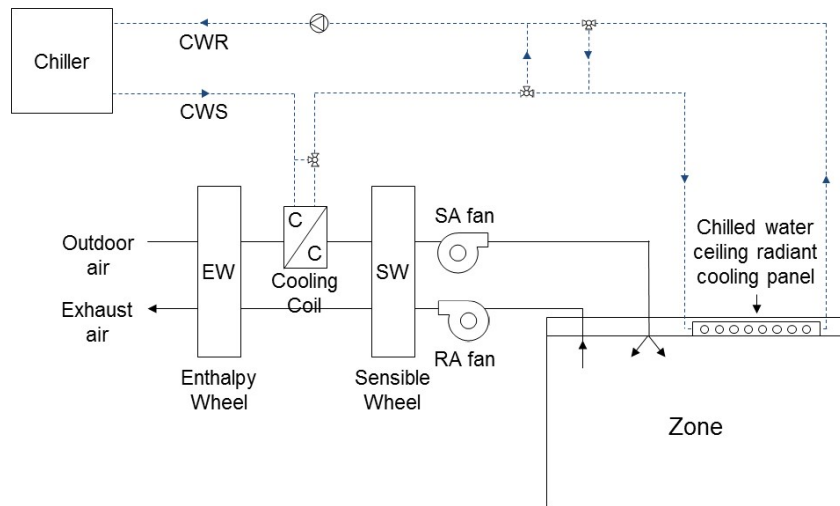


Figure 2: Schematic of DOAS with a chilled water ceiling radiant cooling panel

### 2.3 Dedicated outdoor air system with a thermoelectric module ceiling radiant panel

The configuration of the third case was similar to that of case in chapter 2.2 with the exception of the parallel cooling unit. The TEM RCP was used to investigate the energy potential of the TEM as a parallel cooling unit. The water-cooled type was selected to cool the hot side of TEM, and chilled water was supplied by using a cooling tower. Therefore, this system includes a chiller and cooling tower (Figure 3). A detailed configuration of the water-cooled TEM RCP is shown in figure 4. The cold side of TEMs was bonded to a thin aluminum panel with insulation to prevent heat conduction from the hot side to the cold side of the TEMs. The hollow metallic blocks were termed as water blocks, and they possess fins inside with high thermal conductivity that were bonded for heat removal on the hot side of the TEMs.

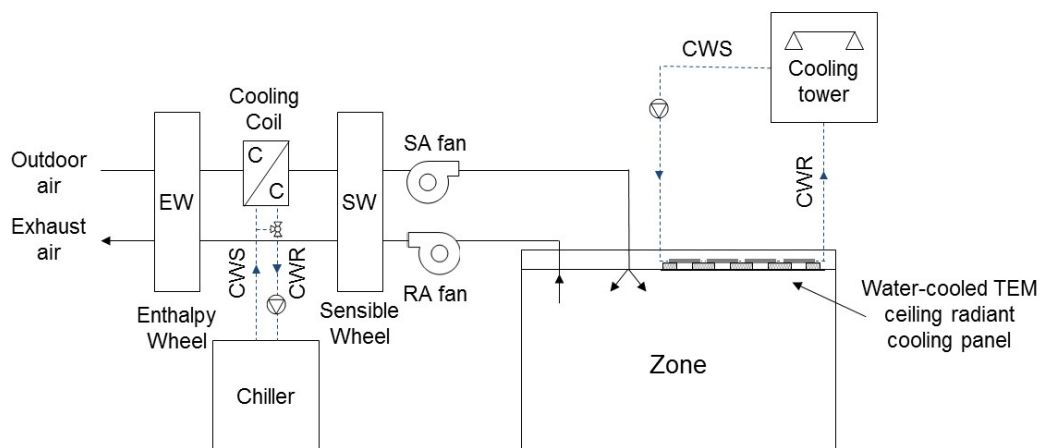


Figure 3: Schematic of DOAS with a water-cooled TEM radiant cooling panel

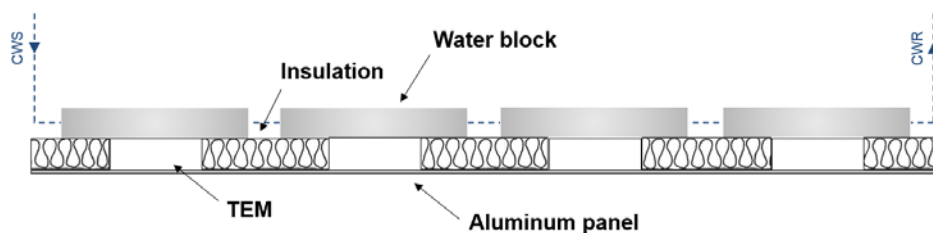


Figure 4: The configuration of the water-cooled TEM radiant cooling panel

### 3 SIMULATION OVERVIEW

#### 3.1 Model space

The sensible and latent loads of the design space were derived by using TRNSYS 17. The design space involved a floor area of 100 m<sup>2</sup> with a height of 3 m. Two windows with an area corresponding to 10 m<sup>2</sup> were located on the south and west exterior walls. The selected window-to-wall ratio corresponded to 0.17. The sensible and latent heat generation rates of an occupant were set as 75 W and 45 W, respectively, based on ASHRAE Standard 90.1. Typical occupancy and system schedules for an office building were applied to derive the typical loads for the model space. The set points of indoor temperature and relative humidity corresponded to 25 °C and 50 %, respectively for the cooling mode and 20 °C for heating mode, respectively. All U-values for the roof, ceiling, wall, and windows were selected based on local criteria.

#### 3.2 DOAS components

In the DOAS simulation, a polynomial empirical model for an enthalpy wheel was used to predict the efficiency of wheel as shown in Eq. (1) and (2) based on previous studies (Jeong et al., 2003; Jeong and Mumma, 2005). The temperature ( $T_{SA,in}$ ) and relative humidity ( $RH_{SA,in}$ ) of supply air, the face velocity of incoming supply air ( $V_{SA,in}$ ), and the ratio of exhaust air to outdoor air flow rate ( $Q_R$ ) were used to predict sensible effectiveness. Additionally, two factors, namely temperature ( $T_{EA,in}$ ) and relative humidity ( $RH_{EA,in}$ ) of exhaust air, were added to estimate the latent effectiveness as follows:

$$\varepsilon_{sen,max} = f(V_{SA,in}, T_{SA,in}, RH_{SA,in}, Q_R) \quad (1)$$

$$\varepsilon_{lat,max} = f(T_{SA,in}, T_{EA,in}, RH_{SA,in}, RH_{EA,in}, Q_R, V_{SA,in}) \quad (2)$$

The maximum values of sensible and latent effectiveness were assumed as 80% to prevent the occurrence of impractical results. A speed control was necessary to adjust the humidity ratio of supply air ( $W_{SA,set}$ ) when the humidity ratio of outdoor air ( $W_{OA}$ ) was lower than that of supply air (i.e., set point). The varying speed ( $Spd$ ) of the enthalpy wheel is simulated by using Eqs. (3) to (6) (Jeong et al., 2003) as follows:

$$DFR = 2430.6 \times \frac{(W_{RA} - W_{OA}) / (T_{RA} - T_{OA})}{RH_{OA}^2} \quad (3)$$

$$Spd = f(DFR, \varepsilon_{lat}) \quad (4)$$

$$\varepsilon_{lat} = \frac{W_{SA,set} - W_{OA}}{W_{RA} - W_{OA}} \times 100 \quad (5)$$

$$\varepsilon_{sen} = 13.844 \times \ln(Spd) + 38.469 \quad (6)$$

The sensible wheel effectiveness ( $\varepsilon_{SW}$ ) was derived by using Eq. (7). The required amount of heat with respect to the supply air was reclaimed from the exhaust air to satisfy the set point. The sensible wheel effectiveness was also controlled based on the rotation speed of the wheel as described in Eq. (6). In the study, the maximum effectiveness was assumed as 85 % at full-speed operation (Rabbia and Dowse, 2000). The expression for sensible wheel effectiveness is as follows:

$$\varepsilon_{SW} = \frac{T_{SA,set} - T_{SW,in}}{T_{RA} - T_{SW,in}} \times 100 \quad (7)$$

### 3.3 Radiant cooling panel

#### 3.3.1 Ceiling radiant cooling panel

The radiant cooling panel accommodated the additional sensible load of a zone to maintain the room temperature setpoint. In case of the CRCP, chilled water from the chiller was used to accommodate the remaining sensible load of the zone. A single chiller provides a constant flow rate of chilled water that enters the cooling coil in the DOAS and CRCP. The inlet temperature was maintained at 16 °C by mixing the water leaving the cooling coil and CRCP by using a 3-way valve. The constant water flow rate of the chilled water was determined based on the maximum remain heat of the zone during a year in which it was assumed that the maximum leaving water temperature corresponded to 21 °C at CRCP (Uponor, 2013). The energy consumption of the CRCP occurred at the chiller and is described in chapter 3.5.

#### 3.3.2 Thermoelectric module radiant cooling panel

In the TEM RCP case, the TEM was modeled by using a previous developed model (Chen et al., 2013) in Eqs. (8) to (13). The thermophysical properties of a compact TEM ( $\alpha$ : Seebeck coefficient,  $\rho$ : electrical resistivity,  $\kappa$ : thermal conductivity) were calculated by using Eqs. (8) to (10) that involve using maximum heat capacity ( $Q_{max}$ ), temperature of the hot side ( $T_h$ ), maximum temperature difference between the cold and hot sides of the TEM ( $\Delta T_{max}$ ), maximum input current of the TEM ( $I_{max}$ ), uniform cross-sectional area of the entire TEM ( $A$ ) and height of the thermoelement ( $l$ ). With respect to the TEM that was used in the study, the packing fraction of the total TEM area was covered by a thermoelement ( $f$ ) corresponding to 0.5, and the number of thermocouples in a TEM ( $N$ ) corresponded to 127. The expressions are as follows:

$$\alpha = \frac{Q_{max} (T_h - \Delta T_{max})}{N T_h^2 I_{max}} \quad (8)$$

$$\rho = \frac{A f (T_h - \Delta T_{max})^2 Q_{max}}{2 T_h^2 l N^2 I_{max}^2} \quad (9)$$

$$\kappa = \frac{l (T_h - \Delta T_{max})^2 Q_{max}}{A f T_h^2 \Delta T_{max}} \quad (10)$$

The cold surface temperature of the radiant panel ( $T_c$ ) also corresponded to 16 °C and is the same as that of the CRCP considering the dew point temperature of indoor air. On the hot side, the water from the cooling tower dissipated the rejected heat from the TEM. Therefore, the temperature of the hot side of the TEM ( $T_h$ ) corresponds to the summation of wet-bulb temperature of outdoor air ( $T_{wb, OA}$ ) and the approach of the cooling tower that is assumed two. The lumped thermophysical properties ( $S$ : Seebeck coefficient,  $R$ : Electrical resistivity,  $K$ : Thermal conductivity) of TEM are also estimated by using Eqs. (11) to (13) as follows:

$$S = 2N\alpha \quad (11)$$

$$R = \frac{4N^2l}{Af\rho} \quad (12)$$

$$K = \kappa \frac{Af}{l} \quad (13)$$

The estimated thermophysical properties were used to determine the required input current by using Eq. (14)(Lim and Jeong, submitted). In the equation, it is necessary to define the number of TEMs on the radiant panel (n) based on the maximum remain sensible load of the zone. In the study, it was assumed that twenty TEMs could accommodate the entire sensible load. The cooling load ( $Q_c$ ) corresponded to the remaining sensible load that should be removed by the TEM radiant cooling panel. The input voltage (V) and the amount of heat rejection ( $Q_h$ ) are calculated by using Eqs. (15) and (16) as follows:

$$I = \left\{ \frac{(nAf\alpha^2T_c^2) - \sqrt{(nAf_p\alpha^2T_c^2)^2 - 2\rho(nAf\alpha^2T_c^2)(\kappa\Delta Tnaf + lQ_c)}}{nAf\alpha^2T_c^2} \right\} \times I_{max} \quad (14)$$

$$V = IR + S\Delta T \quad (15)$$

$$P = V \times I = Q_h - Q_c \quad (16)$$

### 3.4 Cooling tower

The cooling tower was simulated with constant water and air flow rates. The water flow rate of the cooling tower ( $\dot{m}_w$ ) was derived based on the maximum heating load of TEM during a year ( $Q_{max, h, TEM}$ ) by using Eq. (17). It was assumed that the range of the cooling tower and heat exchange efficiency of the water block ( $eff_{wb}$ ) corresponded to 10 and 0.8, respectively. Additionally, the liquid to gas ratio (LG ratio) of the cooling tower was determined as 0.1 based on manufacturer data. The air flow rate of cooling tower is calculated from the LG ratio as follows:

$$\dot{m}_w = Q_{max, h, TEM} / (C_{p,w} \cdot Range \cdot eff_{wb}) \quad (16)$$

### 3.5 Electrical chiller

An air-cooled electric chiller model was used in the DOE-2.1 building energy simulation program to simulate the energy consumption of the chiller. This model required a cooling capacity factor (CAPFT), an energy input to cooling output factor in temperature (EIRFT), and an in part load ratio (EIRFPLR) that were derived by using Eqs. (17) to (19). It was assumed that the temperature of the supplied cooling water ( $T_{CWS}$ ) corresponded to 8°C. The temperature of outdoor air ( $T_{OA}$ ) was varied with respect to weather data from the international weather for energy calculations 2 (IWEC 2). The part load ratio (PLR) is defined in Eq. (20), and the required power of the chiller (P) is derived by using Eq. (21) as follows:

$$CAPFT = f(T_{CWS}, T_{OA}) \quad (17)$$

$$EIRFT = f(T_{CWS}, T_{OA}) \quad (18)$$

$$EIRFPLR = f(PLR) \quad (19)$$

$$PLR = \frac{\text{Required cooling load}}{\text{Capacity of chiller} \cdot CAPFT} \quad (20)$$

$$P = P_{ref} \cdot CAPFT \cdot EIRFT \cdot EIRFPLR \quad (21)$$

## 4 RESULTS

### 4.1 Performance of thermoelectric module radiant cooling panel

As shown in figure 5, the annual performance of TEM-RCP was analyzed in terms of input current and coefficient of performance (COP). The mean input current corresponded to  $2.9 \pm 1.9$ , and the minimum and maximum value corresponded to 0.5 and 11.3, respectively. During the cooling season, the input current increased based on the increase in the remaining sensible load of the zone and wet-bulb temperature of OA. Thus, there was an increase in the temperature difference between the hot and cold sides of the TEM. The COP was calculated by using Eq. (22). The mean value for the COP for cooling (denoted as  $COP_c$ ) corresponds to  $5.6 \pm 3.1$  with minimum and maximum values corresponding to 0.6 and 12.3, respectively. The aforementioned values are considerably high and indicate the possibility of applying the TEM on a radiant cooling panel. However, the COP of the TEM significantly decreased when the temperature difference increased in the cooling season such that it is necessary to define a proper temperature difference with a cooling load in order to use the TEM-RCP. The expression for the COP for cooling is as follows:

$$COP_{cooling} = \frac{Q_c}{P_{TEM}} \quad (22)$$

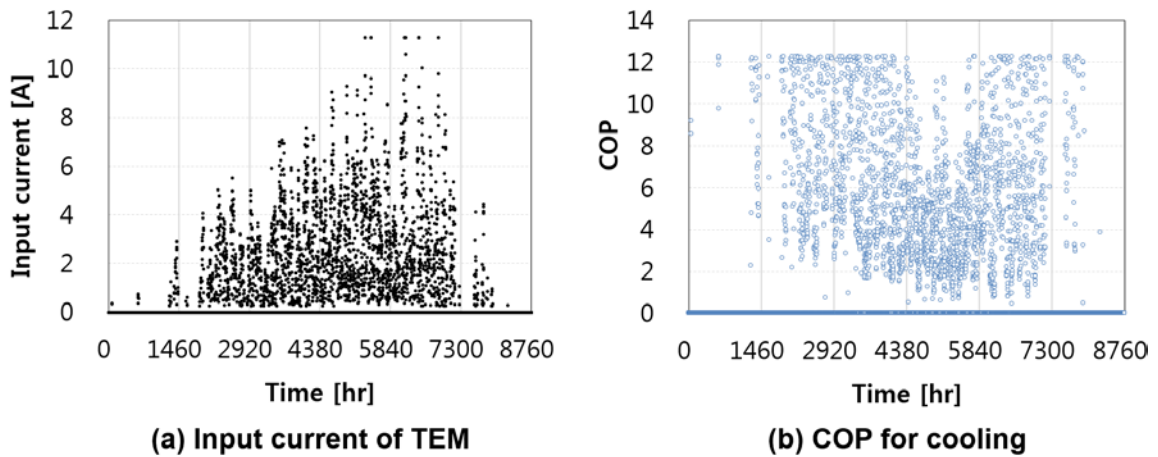


Figure 5: Annual performance of the TEM-RCP in DOAS

### 4.2 Annual energy consumption of systems

The annual electrical energy consumption was compared based on the system and its components (i.e., the chiller, TEM, electrical heating coil, parallel heating unit, pump, and

fan) as shown in Figure 6. The maximum chiller and fan energy among the systems was consumed by the VAV. It is because the DOAS reduced the chiller energy by accommodating the sensible load by using a parallel cooling unit (i.e., radiant cooling panel) and supplying a minimum ventilation air flow rate.

In case of the DOAS CRCP system, a single chiller supplied the entire cooling capacity of the cooling coil and CRCP such that the energy savings of the chiller did not considerably exceed that of the DOAS TEM-RCP system. Conversely, the energy consumption from the TEM occurred in the DOAS TEM-RCP system. With respect to the VAV system, the heating coil also consumed additional energy to reheat the supply air. The heating coil contributed to reducing energy consumption from the parallel heating unit. However, the energy saving was relatively small when compared with energy consumption from the heating coil.

The DOAS TEM-RCP exhibits the maximum pump energy among the systems due to the large water flow rate of the cooling tower. The reason as to why the DOAS TEM-RCP exhibits a water flow rate that exceeds that of the CRCP is because the TEM exhibits heat rejection that exceeds the remaining sensible heat load of the zone. The minimum pump energy was exhibited by the pump in the VAV system because it consists of a single pump with a chiller. Additionally, the fan energy of the DOAS TEM-RCP exceeds that of the DOAS CRCP due to the fan of the cooling tower.

On an overall basis, the total energy consumption of DOAS is lower than that of the VAV system. Furthermore, the DOAS CRCP exhibited the smallest energy consumption among the systems. The findings indicated that the DOAS TEM-RCP displayed energy savings of 44.5 % when compared with that of the VAV system. However, the DOAS TEM-RCP has not replaced the CRCP to date due because it is associated with a low COP and a high amount of heat rejection.

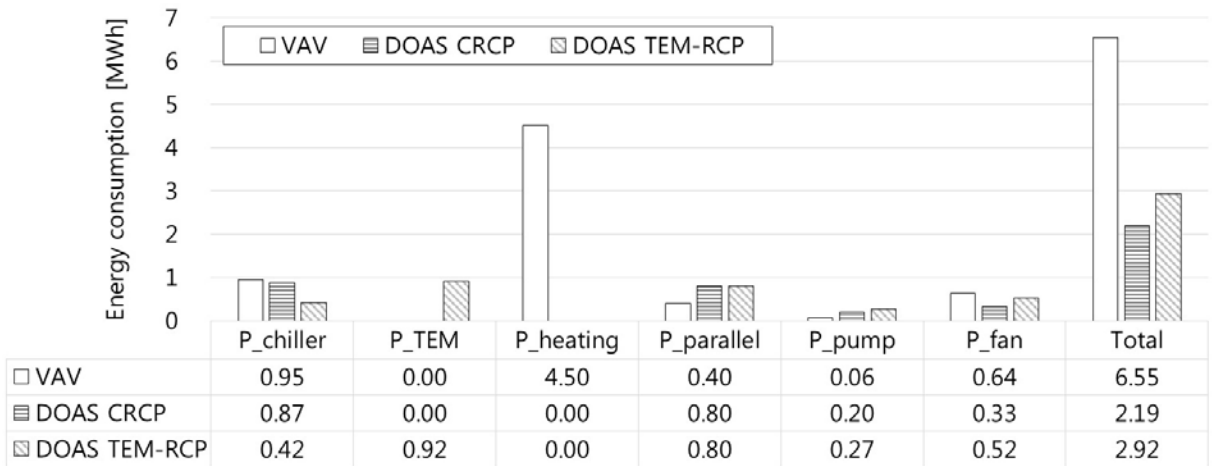


Figure 6: A comparison of the annual energy consumption of systems

### 5 CONCLUSIONS

In this study, DOAS TEM-RCP was suggested and compared with a VAV system and DOAS CRCP with respect to the annual energy simulation. The results indicated that the proposed system reduced annual energy consumption by 44.5 % when compared with that of the VAV system. Additionally, the energy consumption of the TEM-RCP increased by 33 % when compared with that of the DOAS CRCP. This is because the TEM does not display an optimal COP value given high wet-bulb temperatures that prevail in summer. Thus, the proposed system could be limited such that it exhibits a relatively high energy consumption when

compared with that of the DOAS CRCP. However, the DOAS TEM-RCP can easily control the surface temperature of RCP without refrigerants and exhibits an energy saving potential when compared with the VAV system. A future study will include a simulation for an air-cooled TEM-RCP to investigate improved applications of TEM-RCP with DOAS.

## **6 ACKNOWLEDGEMENTS**

This work was supported by a National Research Foundation (NRF) grant (No. 2015R1A2A1A05001726) of Korea and a Korean Agency for Infrastructure Technology Advancement (KAIA) grant (16CTAP-C116268-01).

## **7 REFERENCES**

- Kim, M., Yoon, D.S., Kim, H.J., Jeong, J.W. (2016). Retrofit of a liquid desiccant and evaporative cooling-assisted 100% outdoor air system for enhancing energy saving potential. *Appl. Therm. Eng.* 96, 441–453.
- Tan, G., Zhao, D. (2015). Study of a thermoelectric space cooling system integrated with phase change material. *Appl. Therm. Eng.* 86, 187–198.
- Lee, H.S. (2017). *Thermoelectrics: Design and Materials*. John Wiley & Sons, Inc..
- Jeong, J. W., Mumma, S. A., Bahnfleth, W.P. (2003). Energy conservation benefits of a dedicated outdoor air system. *ASHRAE Trans*, 109(2), 627-636.
- Jeong, J. W., Mumma, S. A. (2005). Practical thermal performance correlations for molecular sieve and silica gel loaded enthalpy wheels. *Appl. Therm. Eng.* 25, 719-740.
- Rabbia, M., Dowse, G. (2000). *Energy recovery ventilation-understanding energy wheels and energy recovery ventilation technology*. Carrier Corporation.
- Uponor. (2013). *Radiant cooling design manual: embedded systems for commercial applications*. Uponor, Inc.
- Chen, M., Snyder, G. J. (2013). Analytical and numerical parameter extraction for compact modelling of thermoelectric coolers. *Int. J. Heat Mass Transf.* 60, 689-699.
- Lim, H., Jeong, J. W. (Submitted). Energy-saving potential of thermoelectric modules integrated into liquid desiccant system for solution heating and cooling. *Energy Convers.*

# Microorganism contaminants removal in a liquid desiccant dehumidification system

Joon-Young Park<sup>1</sup>, Eun-Ji Choi<sup>1</sup>, Seong-Yong Cheon<sup>1</sup>,  
Hye-Won Dong<sup>1</sup>, and Jae-Weon Jeong<sup>\*1</sup>

*1 Department of Architectural Engineering, College of Engineering, Hanyang University,  
222 Wangsimni-Ro, Seungdong-Gu, Seoul, 04763, Republic of Korea*

## ABSTRACT

The main focus of this research is to estimate the ability of a liquid desiccant (LD) system operation to remove microorganism particles. The dehumidification performance of the LD systems generated by using a lithium chloride (LiCl) solution as the liquid desiccant material. To verify the removal performance of microorganism particles, the experimental method was divided into cases where the process air passed or bypassed the LD unit. Two types of microorganism particles, bacteria and mold, were considered for the measurement of the microorganism particles, with a minimum fan flow rate (800 m<sup>3</sup>/h). To verify the accuracy of the experiment, a duct system and an LD system were sealed with duct tape to prevent air leakage. Experimental results were obtained with a bio-contaminant sampler using a tryptic soy agar (TSA) and a potato dextrose agar (PDA). The measuring points were situated at a same distance from the liquid desiccant system inlet and outlet duct. The results show that the LD system has the ability to remove microorganism contaminants. The bacteria removal efficiencies were 77.5% and 81.3% for the sampling process air of 200 and 500 L, respectively, while the fungi removal efficiencies were 38.8% and 44.4% for 200 and 500 L, respectively, of sampling process air. In addition, experiment results show that the LD system significantly affected the removal of microorganism contaminants. When the process air passed through the LD unit, microorganism contaminants contained in the process air were inactivated by the sanitizing effect of the desiccant solution or by filtering of the LD unit.

## KEYWORDS

Liquid desiccant, Indoor air quality, Microorganism contaminants, Removal efficiency

## 1 INTRODUCTION

For the last couple of decades, modern building designs have become technically advanced in order to ensure airtightness and energy saving. To inhibit heat losses from air leakage and infiltration, buildings are constructed with airtight materials and advanced technologies. However, if sufficient ventilation (i.e., fresh outdoor air) is not supplied, it could possibly cause health problems for the occupants (e.g., sick building syndrome (SBS)). To overcome this problem, a minimum required outdoor air (OA) flow rate has been recommended by ASHRAE (ASHRAE, 2013). In spite of the recommended minimum ventilation rate, the required ventilation rate is insufficient. Owing to the absence of an adequate ventilation rate, the indoor air quality (IAQ) does not meet the occupants' satisfaction level.

Several existing studies have indicated that the ventilation rate has a significant effect on the IAQ. In addition, based on the relationship between the ventilation rate and IAQ, researchers have proposed a new type of ventilator to meet the required ventilation and IAQ by using 100% OA as the supply air (SA) (Jeong et al. 2003, Kim et al. 2013). If the 100% OA system is operated without a filter, contamination of the IAQ can occur owing to pollutants in the room and secondary contamination in the polluted SA. In urban environments, there is an increased need for an appropriate response against contaminated SA when polluted OA is supplied (Baek et al. 1997).

Several studies addressed the potential of a liquid desiccant (LD) application to improve air quality of the process air (Rafique et al. 2016). In conventional heating, ventilation, and air

conditioning(HVAC) systems, condensation occurs on the cooling coil surface to perform the dehumidification of process air. This causes the growth of microorganism compounds, such as bacteria and fungi, on the coil surface, which threatens indoor air quality. However, the LD system can dehumidify the process air without cooling coils causing such problems (Liu et al. 2006).

In addition, the desiccant solutions have a sanitizing effect on biological contaminants such as fungi, bacteria, and viruses. Wang (Wang et al. 2011) conducted an empirical analysis on the microorganism removal effect in an LD system using LiCl and triethylene glycol (TEG) solutions. They showed that the TEG solution provided higher microorganism removal performance than the LiCl solution. Kovak (Kovak et al. 1997) also indicated the sanitizing effect of liquid desiccant in the desiccant-based air conditioning system. The LD system prevents the growth of microorganisms inside the conditioned space indirectly through the humidity control of the indoor air (Harriman 1989).

The main purpose of this study is to empirically analyze the microorganism contaminant removal performance of the LD unit. To evaluate the microorganism removal impact of the LD unit, the existing pilot LD unit was operated and then the variation of microorganisms contained in OA was measured while the OA was passing through the LD unit. Tryptic soy agar (TSA) and potato dextrose agar (PDA) samplers were used to quantitatively estimate biological contaminant removal from the process air in an LD unit operation (BUCK Co. 2016).

To verify the direct removal efficiency of the LD unit, the experimental method was divided into a natural removal method and a forced removal method. The natural removal method is defined to be the removal effect caused by natural air flow, and the forced removal method is caused by the removal effect of the LD unit operation. The microorganism removal efficiency of the LD unit is evaluated by comparing the natural and forced removal methods.

## **2 SYSTEM OVERVIEW**

The LD system can effectively remove latent heat loads by removing the moisture included in OA. Moisture removal performance is generated by a partial pressure difference between the process air and the desiccant solution. Any change in this partial pressure difference caused by the temperature and concentration of the desiccant solution affect the dehumidification performance (ASHRAE. 2009, ASHRAE. 2012). During the dehumidification process, the LD system may remove air contaminants by injecting the desiccant solution into the dehumidifier and passing it through the packed-bed packing material. An LD pilot system was used in this study to evaluate the air contaminants removal performance. The LD pilot system considered in this study used a LiCl solution for generating the dehumidification effect on the process air designed by 2000 m<sup>3</sup>/h. The pilot system consisted of a packed-bed tower absorber and regenerator with solution cooling and heating sources. The dehumidification process of the process air was carried out in the absorber tower, which was packed with a honeycomb medium made of porous wood fiber material (Figure 1).

As shown in Figure 1, two dry-bulb temperature and humidity sensors (T/R1 and T/R2) and one air flow sensors (F1) are installed at the inlet and outlet of the LD unit. In addition, water temperature sensors (T1) is also installed at the cooling water supply paths. The solution concentration supplied to the absorber is also measured by using a specific gravity hydrometer.

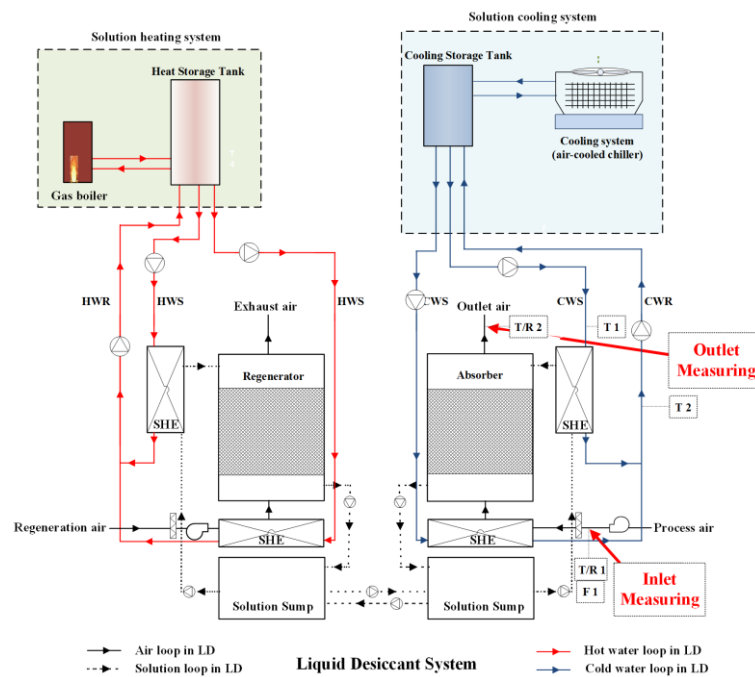


Figure 1: Schematic diagram of the LD unit

### 3 EXPERIMENTAL SETUP

In order to confirm microorganism removal efficiency of the LD unit with the LiCl solution, a removal efficiency of the microorganism contaminants was estimated on August 4, 2016. Bacteria and fungi were conducted as sample microorganism contaminants to measure the number of colony forming units (CFU) at the inlet and outlet of the LD system. To detect the microorganism contaminants, a bio-contaminant sampler was used to collect both bacteria and fungi by using a TSA and PDA, respectively. While detecting the microorganism contaminants, the sampler was sampled at a flow rate of 100 L/min at the inlet and outlet of the LD system. According to the characteristics of the sampler, the microorganism sampling collected was 200 L and 500 L of induced OA, four times each sampling. In addition, to verify the accuracy of the experimental data, the base condition of OA was collected by the TSA and PDA without the sampler, before the data were measured.

The experiment condition was also controlled by system bypassed/passed methods. The experimental data were measured four times for each experimental method (bypassed and passed), and were considered with the minimum system fan flow rate (800 m<sup>3</sup>/h), in accordance with ASHRAE standard 52.2 (ASHRAE. 2012). The average dry-bulb temperature of the OA at the time of the experiments was 30–32 °C, and the average relative humidity was 52–58% (e.g., a humidity ratio between 0.0152 and 0.0174 kg/kg). In addition, the LiCl solution was maintained in a 25 °C and 36% condition and 0.63 kg/s of inlet mass flow rate while injecting into the absorber tower. Figure 2 shows the experimental conditions on the microorganism contaminants.

The microorganism contaminants were collected by a bio-contaminant sampler (BUCK BioCulture Model B30120), which can detect the microorganism contaminants by using the agar, depending on the contaminants type (BUCK Co. 2016). According to the agar type, the bacteria and fungi were collected, and then, each type of contaminant was counted in the CFU after incubating in the incubator (Vision Scientific Co. 2010). The bacteria were cultivated for 1–2 days at 32 °C and the fungi were incubated for 3–4 days at 25 °C. Table 1 shows the specification of the bio-contaminants sampler.

Table 1: Specification of the bio-contaminant sampler (BUCK Co. 2016).

Device	Type	Characteristics	
Bio-contaminants sampler	Impactor type	Detection flow	30–120 L/min
		Detecting accuracy	±5% of set point
		Holes	380 (1 mm diameter)
		Compatibility	90 mm agar plate



Figure 2: Experimental conditions of the microorganism contaminants

After cultivation, the experimental data were counted with the CFU value under conducted experiment conditions. However, in order to convert to CFU per unit volume (CFU/m<sup>3</sup>), a calibration was carried out by means of following equations.

$$l_{ave} = \frac{l_{beg} - l_{end}}{2} \quad (1)$$

$$V = \frac{l_{ave} \times T}{10^3} \quad (2)$$

$$V_{25^{\circ}C, 1atm} = V_{air} \times \frac{K}{T^2} \times \frac{P}{P_{1atm}} \quad (3)$$

$$F = \frac{CFU}{V_{25^{\circ}C, 1atm}} \quad (4)$$

$$\varepsilon_{mic} = \frac{(F_{in} - F_{out})}{F_{in}} \times 100 \quad (5)$$

A sampling flow rate of the bio-contaminants sampler can be estimated as the average flow rate during the experiment period, which can be calculated by means of Equation 1. According to the calculated average sampling flow rate, a total volume of the collected sampling air was calculated by means of Equation 2. The total volume of the collected air is estimated under experiment conditions, but in order to calibrate the total volume in standard state air (25 °C, 1atm), Equation 3 was used. Based on the calculated standard state air volume, a concentration of the total airborne microorganism contaminants was calculated using Equation 4. In this study, the concentration of the total airborne microorganisms was considered as experimental data to evaluate the microorganism contaminants removal

efficiency of the LD system. The microorganism contaminants removal efficiency of the LD unit is presented by means of Equation 5.

## 4 EXPERIMENTAL RESULTS

### 4.1 Microorganism removal efficiency

In order to verify the microorganism removal efficiency of the LD unit, a variation of bacteria and fungi concentrations were sampled by using the bio-contaminant sampler with a TSA and PDA, respectively.

Figure 3 shows the bacteria and fungi removal efficiency of the LD unit measured in this research. One can see that bacteria removal efficiency was 77.5% and 81.3% for the sampling process air of 200 and 500 L, respectively. On the contrary, when the LD unit was bypassed, the number of bacteria colonies increased approximately 37.5% and 13.7% for 200 and 500 L of sampling air, respectively, because of resuspended bacteria from the duct surface (Figure 4).

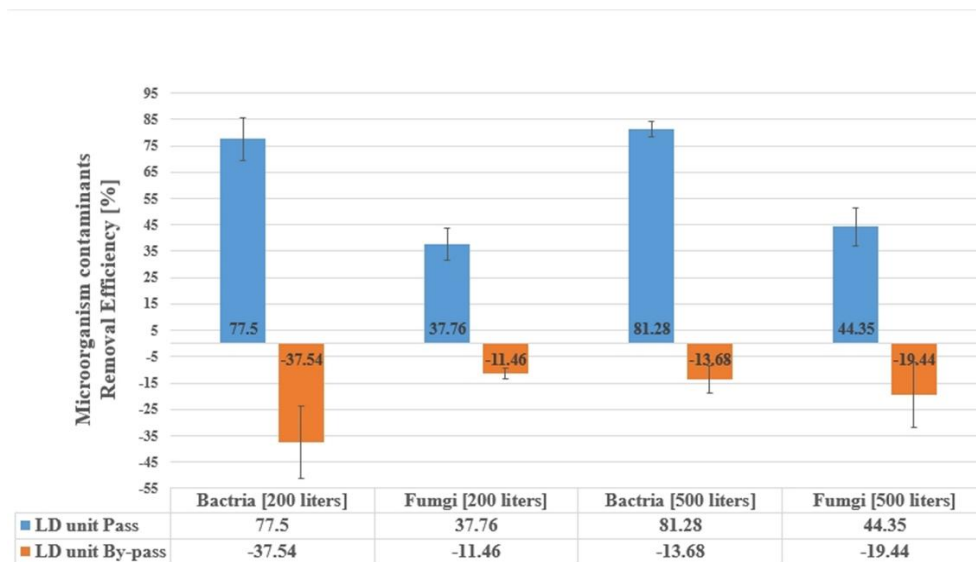


Figure 3: Microorganism removal efficiency

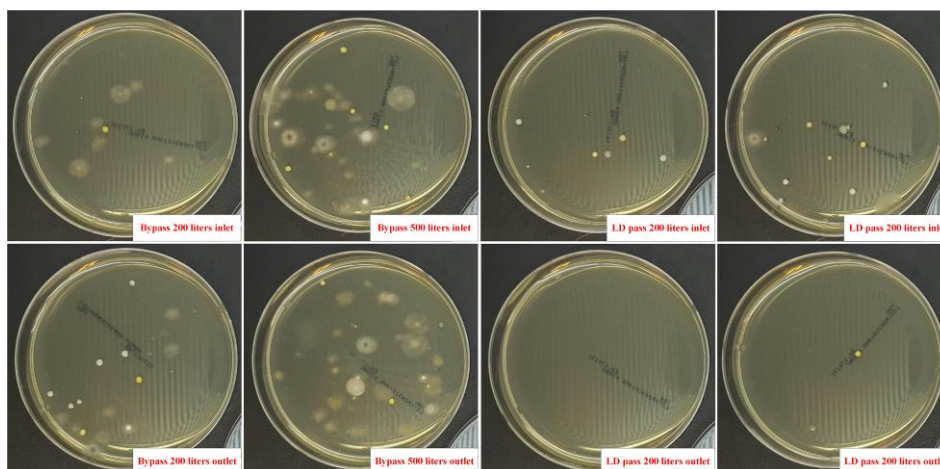


Figure 4: Representative experimental results of the bacteria

Similarly, one can also see that the fungi removal efficiency of the LD unit was 38.8% and 44.4% for 200 and 500 L of sampling process air, respectively. However, when the process air bypassed the LD unit, the results show that the number of fungi colonies was increased 11.5% and 19.4% for 200 and 500 L of sampling air, respectively, because of resuspended fungi from the duct surface (Figure 5).

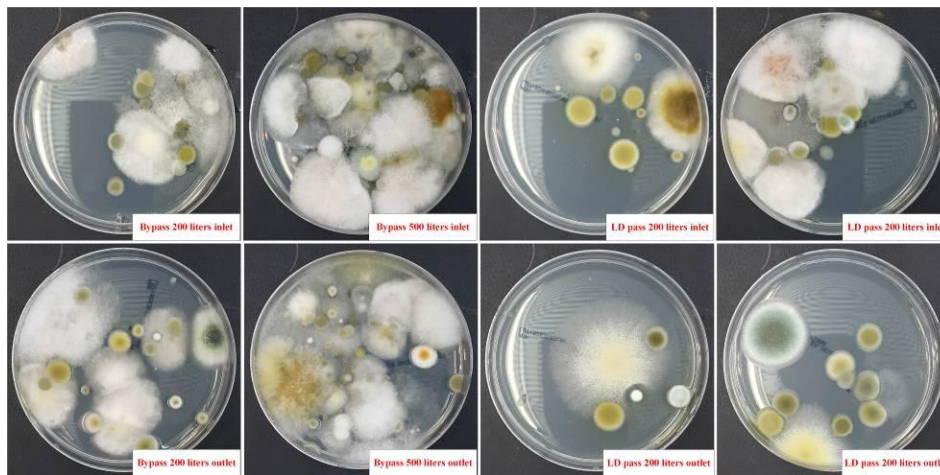


Figure 5: Representative experimental results of the fungi

## 4.2 Discussions

Based on the literature review of the air quality improvement potential of the LD unit, this study focused on conducting an empirical analysis on the removal ability of the LD unit. The sanitizing effect of the liquid desiccant solution observed in the study had a significant impact on microorganism removal. When the process air passed through the LD unit, the concentration of both bacteria and fungi was decreased at the outlet of the LD unit. However, these results have shown that the differences in removal efficiency between bacteria and fungi were due to the high resistance of fungi on the sanitizing materials.

## 5 CONCLUSIONS

In this study, the microorganism contaminant removal efficiency of an LD unit was evaluated by empirical analysis based on a pilot system operation. The literature review on the air quality improvement potential of LD units showed that the LD unit has the ability to remove microorganism contaminants. Similar to previous research, the experimental results of this study showed that the LD unit can remove microorganism contaminants.

The experimental results showed microorganism removal efficiencies of 77.5% and 81.3% for bacteria with the process air of 200 and 500 L. However, while bypassing the LD unit, the number of bacteria increased approximately 37.5% and 13.7% for the 200 and 500 L of sampled OA, respectively. Similarly, the results on fungi removal shows 38.8% and 44.4% for 200 and 500 L of collected OA. In addition, when the process air bypassed the LD unit, the removal efficiency results increased by 11.5% and 19.4% for 200 and 500 L of OA, respectively.

These results indicate that the LD unit can promptly remove microorganism pollutants that have negative effects on the human health. Considering that the outdoor air has pollutants, the

advantages of the LD unit in terms of microorganism removal performance would be helpful in improving the indoor air quality.

## 6 ACKNOWLEDGEMENTS

This work was supported by a National Research Foundation (NRF) of Korea (No. 2015R1A2A1A05001726) and a Korea Agency for Infrastructure Technology Advancement (KAIA) grant (16CTAP-C116268-01).

## 7 REFERENCES

ASHRAE. (2013). *ANSI/ASHRAE Standard 62.1-2013*, Ventilation for Acceptable Indoor Air Quality. Atlanta: American Society of Heating, Refrigerating, and Air-Conditioning Engineers, Inc.

Jeong, J. W., Mumma, S.A., and Bahnfleth, W.P. (2003). Energy Conservation Benefits of a Dedicated Outdoor Air System with Parallel Sensible Cooling by Ceiling Radiant Panels. *ASHRAE Transactions*, 109(2), 627–636.

Kim, M.H., Park, J.S., and Jeong, J. W. (2013). Energy saving potential of liquid desiccant in evaporative-cooling-assisted 100% outdoor air system. *Energy*, Vol. 59, pp. 726–36.

Baek, S. O., Kim, Y. S., and Perry, R. (1997). Indoor air quality in homes, offices and restaurants in Korean urban areas - Indoor/outdoor relationships. *Atmospheric Environment*, Vol. 31(4), pp. 529–544.

Rafique, M.M., Gandhidasan, P., and Bahaidarah, H.M. (2016). Liquid desiccant materials and dehumidifiers—A review. *Renewable and Sustainable Energy Reviews*, Vol. 56, pp. 179–195.

Liu, X., Li, Z., Jiang, Y., and Lin, B. (2006). Annual performance of liquid desiccant based independent humidity control HVAC system. *Applied Thermal Engineering*, Vol. 26, pp. 1198–1207.

Wang, Y.F., Chung, T.W., and Jian, W.M. (2011). Airborne fungi inactivation using an absorption dehumidification system. *Indoor and Built Environment*, Vol. 20(3), pp. 333–339.

Kovak, B., Heimann, P.R., and Hammel, J. (1997). The sanitizing effects of desiccant-based cooling. *ASHRAE Journal*, Vol. 39 (4), pp. 60–64.

Harriman III, L. G. (1989). *The Dehumidification Handbook*.

BUCK Company. (2016) Bio-contaminants sampler Model B30120 Technical brief, *BioCulture*.

ASHRAE. (2009). *ASHRAE Handbook: Fundamentals, Chapter 32 SI*, Sorbents and Desiccants. Atlanta: American Society of Heating, Refrigerating and Air-Conditioning Engineers, Inc.

ASHRAE. (2012). *ASHRAE Handbook: HVAC systems and equipment, Chapter 24 SI*, Desiccant dehumidification and pressure – Drying equipment. Atlanta: American Society of Heating, Refrigerating and Air-Conditioning Engineers, Inc.

ASHRAE. (2012). *ASHRAE Standard, 52.2-2012*, Method of testing general ventilation air-cleaning devices for removal efficiency by particle size. Atlanta: American Society of Heating, Refrigerating and Air-Conditioning Engineers, Inc.

Vision Scientific Company. (2010). Twin-room-incubator Model VS-1203P4S.

# The Development of Archetypes to Represent the Chilean Housing Stock

Constanza Molina<sup>1</sup>, Benjamin Jones<sup>\*1</sup>, Michael Kent<sup>1</sup> and Ian P Hall<sup>2</sup>

*1 Department of Architecture and Built Environment,  
University of Nottingham  
Nottingham, NG7 2UH, UK.*

*\*Corresponding author:  
benjamin.jones@nottingham.ac.uk*

*2 Division of Respiratory Medicine, School of  
Medicine,  
University of Nottingham  
Nottingham, NG7 2UH, UK.*

## ABSTRACT

There are three common methods used to analyse Indoor Air Quality in buildings: in-site measurements, laboratory measurements, or the simulation of indoor spaces using a validated computational model. Each have their advantages, but computational models are generally used to predict air quality in a wide range of indoor environments because they are quick, cheap, and non-invasive. A wide range of inputs are required to accurately simulate airflow and pollutant transport. However, this information may not exist or may only exist in abstract forms. Furthermore, the collation and processing of data can be time consuming and can introduce systematic error when it is undocumented. A documented database containing a range of building archetypes with statistically representative values of related parameters can facilitate the simulation process. The archetypes might then be used to predict and evaluate the impacts of new policies on the indoor air quality of a stock of houses.

This paper describes a method to identify sets of archetypes that are statistically representative of the Chilean housing stock. The Santiago housing stock comprises 41% of the Chilean housing stock and is well documented (55% of all dwellings are surveyed), and so it used to represent the Chilean stock. All available data on the Santiago housing stock, including CENSUS data and annual building statistics reports, are utilised. The archetypes account for elements of building design that affect indoor pollutant concentrations, which can be used for indoor environment modelling. Some similarities are found between houses belonging to Santiago and the rest of country, and although a database that encompassed both Santiago and the remaining stock is desirable, the houses outside Santiago are more difficult to categorise and so an independent analysis is required. Dwellings were categorised according to relevant factors, such as geometry and total floor area, and allocated to weighted groups by dwelling type to form a series of archetypes. Notable architectural elements and values of relevant parameters are used to identify each archetype. These can be used to model the air quality found across the entire Chilean housing stock using validated tools, such as CONTAM or EnergyPlus.

The representative archetypes provide a better understanding of the current Chilean housing stock and will enable the testing of a range of interventions designed to improve indoor air quality in Chilean houses. Existing databases are non-exhaustive and contain errors and so knowledge gaps are highlighted. This information can be used to inform future surveys of the Chilean housing stock.

## KEYWORDS

**Statistical Methods; Indoor Air Quality; Dwellings; Modelling**

## HIGHLIGHTS

- A list of archetypes is selected to statistically represent the Chilean housing stock.
- 3 sets of archetypes are proposed that are suitable for different studies using 13, 35 or 88 houses to represent 35%, 63% or 91% of the housing stock, respectively.
- Show areas where there is poor quality or a lack of data on the characteristics of Chilean houses, occupants, and their behaviour.

## 1 INTRODUCTION

Air Quality assessments are either conducted for outdoor ambient air or for indoor air. Air quality in indoor environments depends on a range of factors such as the building's design, use, and environment. Indoor exposures are then affected by three systems, which makes indoor air quality (IAQ) analysis a complex task because they involve: i) a heterogeneous, and sometimes peculiar, building stock; ii) a population with varied characteristics, composition and behaviours; and iii) the presence of mixtures of pollutants that may be difficult to identify and quantify. These three systems are constantly interacting with each other, and their parameters and characteristics need to be considered in order to analyse their relationship in a building stock. When considering different building types, dwellings are a focus of attention because people spend most of their lives in them (McCurdy & Graham, 2003). Also, concentrations of some pollutants indoors are found to be higher than those outdoors (Chen & Zhao, 2011; Cometto-Muñiz & Abraham, 2015), and so there is likely to be a higher degree of exposure to them indoors (e.g. de Bruin *et al.*, 2008; Guo *et al.*, 2004). Therefore, housing and public health interventions that aim to improve indoor air should account for the heterogeneity of houses and the air within them.

Modelling a housing stock is a quicker and more economic method of assessment when compared to *in-situ* measurements. Modelling approaches commonly use a set of reference buildings, known as *archetypes*, which represent classes of houses found in the residential sector. Generally, the larger the numbers of archetypes used to represent the whole stock, the more widespread are the conclusions derived from the results.

The aim of this study is threefold. Firstly, to increase the knowledge of the Chilean housing stock, its composition and characteristics, from an air quality viewpoint; see Section 2.1. Secondly, to consider the variables that should be taken into account by both modelling and field studies so that they can be developed into a useful database; see Section 2.2. Finally, to use the housing classifications to choose a suitable number of archetypes that can be used for further analysis of the housing stock; see Section 2.3. These archetypes can then be used to represent the Santiago housing stock for IAQ and exposure analyses. Although the study is confined to the capital region of Santiago de Chile, it is possible to extend it to cover other locations in Chile.

## 2 MATERIALS AND METHODS

There are two approaches to modelling building stock energy demand: the bottom-up and the top-down approaches (Kavgic *et al.*, 2010). This study selects a series of archetypes to model the air quality in the Santiago building stock using a bottom-up approach. This allows the modeller to work with disaggregated data, which provides a better understanding of how individual components (e.g., house typology, an architectural element), or changes to them, impact predictions.

This study follows 4 steps defined by Ghiassi and Mahdavi (Ghiassi & Mahdavi, 2017): i) Choose variables that most affect model predictions and their categories, ii) classify dwellings into groups, iii) decide on an appropriate number of dwelling archetypes, and iv) determine the stochastic representation of other properties and components that affect pollutant concentrations and that will allow the re-diversification of the stock. It also considers the development and application of archetypes in other countries for both energy consumption (e.g. Ballarini *et al.*, 2014; Swan & Ugursal, 2009) and air quality-related studies (e.g. Persily *et al.*, 2006; Shiet *et al.*, 2015).

## **2.1 Characteristics of dwellings in Chile and Santiago**

Chile is divided into 15 regions located in 7 different climate zones. Its housing stock comprises 6m houses whose characteristics vary according to the local weather conditions and the availability and the affordability of building materials. Chile is over 4,300km long, yet 41% of the population live in the metropolitan and capital region of Santiago de Chile whose stock is estimated to comprise 2.4m houses.

## **2.2 Sources of information on the building stock**

Three databases containing information on the buildings' characteristics are used: CENSUS 2002 (INE, 2003), CENSUS 2012 (INE, 2013), and the Annual Building Permit Reports (INE, 2016). CENSUS surveys are conducted every 10 years, and they collect basic self-reported information on each house and its occupants, hereon termed *cases*. The Annual Reports data is compiled and updated monthly, and contains information about building projects at the design stage.

CENSUS 2002 data provides information on basic geometry (i.e. apartment or house), the number and use of rooms, and information on occupants. It does not include information about the year of construction, the type of house (whether it is detached, semidetached or terraced), the size of the building, or the number of floors. For the purpose of this study, the cases are selected by occupancy (i.e. occupied houses), number of homes (equal to 1), and location (Santiago). By recoding the variables they are easier to control and missing data can be removed, including houses with absent occupants, empty houses (6.6%) and cases with more than 1 home per building (5.8%). The maximum number of occupants and enclosed areas are arbitrarily set to 6 and 7, respectively. The total remaining cases in Metropolitan Santiago is 1,369,314, representing a 68% of the Santiago stock.

Similar information is available from the last CENSUS 2012. However, this database is rejected due to inconsistencies in the data collection methods and to changes in the categories collected (structural differences). A new CENSUS 2017 is ongoing and the data may be available for future updates.

The last and most detailed database is the Annual Building Permit Reports, which contains statistical information of more than 103,146 construction projects or 1,337,639 houses built between 1990 and 2016, and corresponds to 55% of the Santiago stock. This information is reported by the owner and the architect of the project when applying for a construction permit and part of the information is compiled and registered by the National Institute of Statistics. The figures are published in an Annual Report. The data includes the total constructed area, number of floors, building type (detached, semidetached, terraced or apartment), and building materials. Although this database gives more detailed information on the buildings, it contains significant and obvious deficiencies that appear to be transcription errors. Therefore, this database is excluded from the classification process but is instead used to provide other peripheral values, such as building type and year of construction. The remaining cases have been collated and can be used to statistically determine parameters of interest for each archetype, such as floor area, or the number of storeys.

Consequently, the CENSUS 2002 database is used to classify the building stock according to key parameters and to select archetypes, and the Building Annual Reports aggregated databases are used to provide additional information on the archetypes.

## **2.3 Selection of relevant variables and categorization process**

The building design variables used during the categorization process were selected by their relevance to the final indoor pollutant concentration, based on information collected from the

literature. Two types of study are considered: those using field measurements and those modelling indoor pollutants. The former uses indoor measurements of concentrations of selected pollutants in order to identify common air quality issues and to relate them to a building's characteristics (Gilbert *et al.*, 2008; Langer & Bekö, 2013; Langer *et al.*, 2016). Some focus on sensitive groups of the population, showing the relationships between health outcomes and indoor variables (Chin *et al.*, 2014; Singleton *et al.*, 2017). The latter model one or more residences that represent the housing stock (A. Persily *et al.*, 2010; Shi *et al.*, 2015). Studies that use housing stock models to predict energy demand are also included in the literature review due to the similarity of their methods used to analyse data, although there are some differences between the key variables that are considered. Studies of IAQ using measurements of indoor pollutant concentrations relate their results to air change rates and the type of ventilation system, the location of the dwelling, the year of construction (correlated with emission rates), pollutant sources and their locations, occupancy levels and behaviour, and environmental parameters (i.e. temperature and relative humidity). Other modelling studies, especially those investigating air infiltration rates, generally require similar variables: building type, geometry and size, permeability of the envelope, year of construction, number of floors, building orientation (Jones *et al.*, 2015; A. Persily *et al.*, 2010; Shi *et al.*, 2015). CONTAM is a multi-zone airflow and transport pollutant modelling tool (Dols & Polidoro, 2015) widely used to model indoor pollutant concentrations found in different building types (Nget *et al.*, 2013), the analyses of strategies that might affect IAQ, and the parameters that most affect occupant exposures. It requires the definition of indoor zones and the interactions between them, and outdoor environmental parameters, such as wind speed and direction. These parameters are used to inform inputs to the database. The resulting data is then used to select key variables for a categorization process based on house geometry or type, building size, and construction period. Ventilation and infiltration in Chilean houses is largely natural via windows and doors opening, and through the envelope. Therefore, mechanical ventilation systems are not expected to be influential and so the type of ventilation is not included as a variable. Following categorization of the dwellings into groups, average values of each group were related to each archetype, such as floor area, number of storeys, and number of occupants (see Table 2).

### 2.3.1 Geometry

The CENSUS 2002 shows that 95.44% of the dwellings located within the urban area of the capital city are classified as a house or an apartment. Therefore, the housing stock can be divided approximately into those two categories. Other categories, such as the *conventillo* or *ruca* vernacular building types, correspond to building types that were built before 1935 and do not comply with the current building codes. By classifying in this way, the same dataset is then aggregated according to the building size.

### 2.3.2 Building Size

Dwelling floor area is not included in the CENSUS surveys and so the number of rooms and bedrooms are used to approximate it. The maximum number of zones is arbitrarily set up to a threshold of 7 and the number of bedrooms ranges from 0 (i.e. in cases such as studio rooms) to 6 or 7 in apartments and houses, respectively. This gives 105 separate groups, hereon termed *cells*, where each dwelling is assigned to only one. The buildings are categorised according to their size within each cell, and distributed into smaller sub-cells based on the type of house and construction period.

### 2.3.3 Type of House

The dwelling type is given by the Building Permit datasets. Three categories can be considered according to the number of attachments or shared walls: i) detached, ii) semi-detached and end-terrace, and iii) mid-terrace. None of the databases include information on the position of a dwelling within a terraced block of houses (e.g. end or mid-terrace) or the number of houses in a block. Therefore, the proportions of end- and mid-terrace buildings are estimated according to the probability of obtaining a given housing type. For example, the maximum number of houses in a block is arbitrarily limited to 20, and when a terrace contains 3 houses, 1 is classed as terraced whereas the other 2 houses are classed as semi-detached.

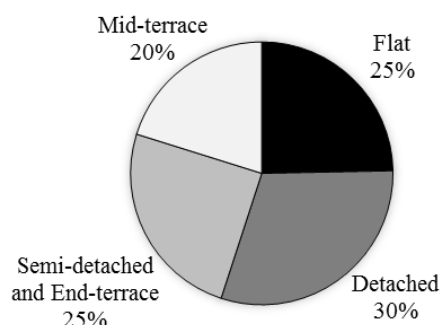


Figure 1: Proportion of apartments and houses in Santiago considered in the classification process.

### 2.3.4 Construction Period

Table 1: Proportion of dwellings by construction period. Sources: Annual Reports (INE, 2017).

Construction period	Number of Dwellings	Percentage
1990 - 2007	890,889	66.6%
From 2008	446,750	33.4%
<b>Total</b>	<b>1,337,639</b>	<b>100%</b>

Table 2: Variables considered in the categorization process.

Variables	Categories: Percentage	Source of information	Cumulative Number of cells
<b>Geometry:</b>	Apartments: 22.6% Houses: 77.4%	CENSUS 2002	2
<b>Building size:</b> Number of zones: from 1 to 7 and Number of bedrooms: from 0 (studio) to 6 (apartments) or 7 (houses)	-	CENSUS 2002	105
<b>Type of house:</b>	Detached: 40.92% Semi-detached/ end-terraced: 32.58% Mid-terrace: 26.50%	Building permits	217
<b>Construction period:</b>	1990 - 2007: 66.6% > 2007: 33.4%	Building permits	434
<b>Total cells:</b>			<b>434</b>

The envelope structure and design of a house affects its thermal performance and airtightness. In Chile, dwellings built before 2000 had no thermal requirements and are generally considered as non-insulated, although some may have been. Dwellings designed between

2000 and 2007 are required to meet a maximum thermal transmittance for the roof, but not for the walls and windows. After 2007, building codes were upgraded and all new dwellings must meet a maximum thermal transmittance for all envelope components in contact with the ambient air. The requirement varies along the length of the country depending on the number of heating degree days. New changes to the building codes are about to be adopted, and so the database will need to be updated in the near future and new archetypes may be required. In this study, the housing stock is divided into two age-related groups: those constructed before 2008 when little or no insulation was required by law, and those built thereafter with high levels of insulation; see Table 1. Houses constructed before 2008 that have been weatherised are not included. The Annual Reports are used to obtain the proportion of the stock belonging to each group because they contain the total number of dwellings registered per year (INE, 2017).

**2.3.5 Floor Area, Number of Storeys, and Number of Occupants**

These values are given by the Building Permits aggregated database. The number of zones reported in the database can be associated with those of each archetype, and the mean calculated from each subset. The number of storeys and the number of occupants can be determined by the mode value in each cell. The relevant factors considered for the grouping process are given in Table 2.

**3 RESULTS AND DISCUSSION**

**3.1 Selection of Archetypes**

Each house is classified into one of 434 archetypes and the most representative can be selected using a range of statistical tests. A frequency plot can be used to rank the number of times each archetype appears in the database from highest to lowest; see Figure 2.

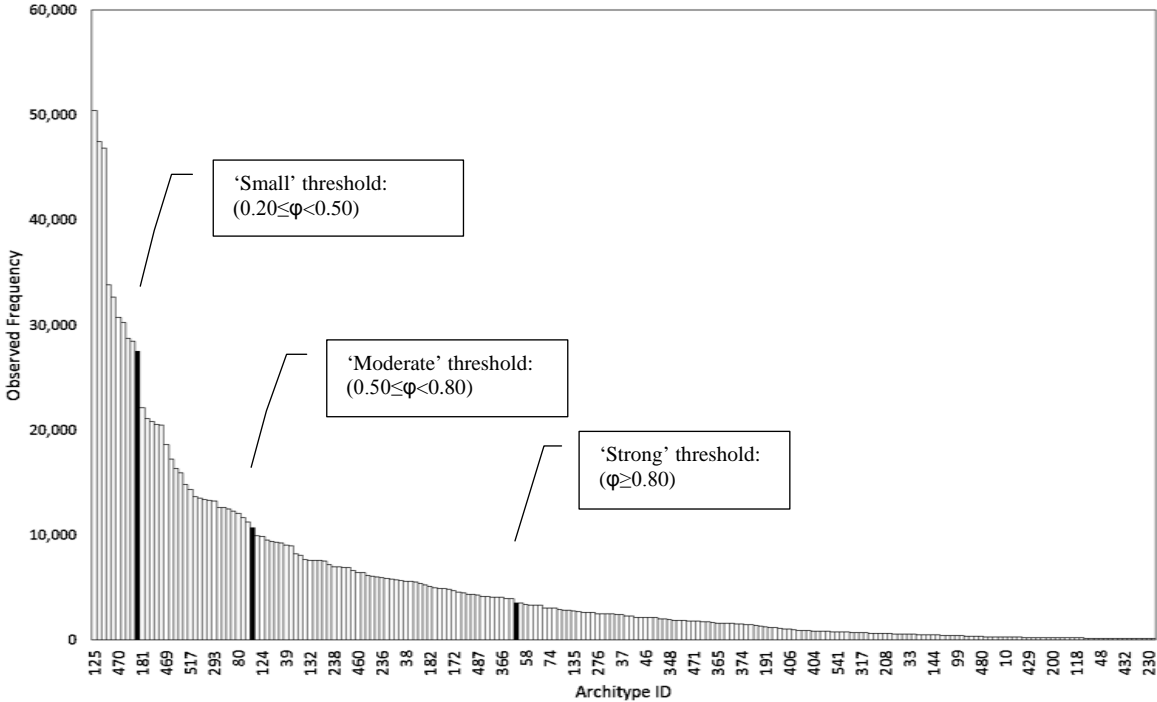


Figure 2: Frequency distribution of the archetypes.

Figure 2 shows that the archetype with the highest frequency has an ID of 125. Chi-squared ( $\chi^2$ ) tests of statistical significance can be performed to compare the difference in frequency of each archetype to a lower ranked archetype (Field, 2013). For each comparison, effect sizes ( $\phi$ ) are used to obtain a standardised measure of the difference that is independent from the sample size (Cohen, 1990, 1992). Estimations of effect sizes across the whole stock can be quantified using the tables of Ferguson (2009) to show those considered be *small* ( $0.20 \leq \phi < 0.50$ ), *moderate* ( $0.50 \leq \phi < 0.80$ ) and *strong* ( $\phi \geq 0.8$ ) in magnitude, and are given in Table 3. Therefore, this approach accounts for both descriptive (percentages) and inferential (effect size) statistics. By comparing each archetype against the highest ranked archetype, those that have an effect sizes smaller than a particular threshold can be considered representative and those with larger differences can be excluded. Figure 3 shows the number of archetypes required to represent each centile of the building stock for each effect size threshold.

Table 3: Effect size of the archetypes classification. Effect size moderate or greater than 0.5 was considered relevant to this study.

Ferguson’s benchmark for Effect Sizes	Number of archetypes (retained)	Percentage of the stock represented
<b>Small: <math>\phi = 0.2</math></b>	13	35.3%
<b>Moderate: <math>\phi = 0.5</math></b>	35	62.8%
<b>Strong: <math>\phi = 0.8</math></b>	88	90.5%

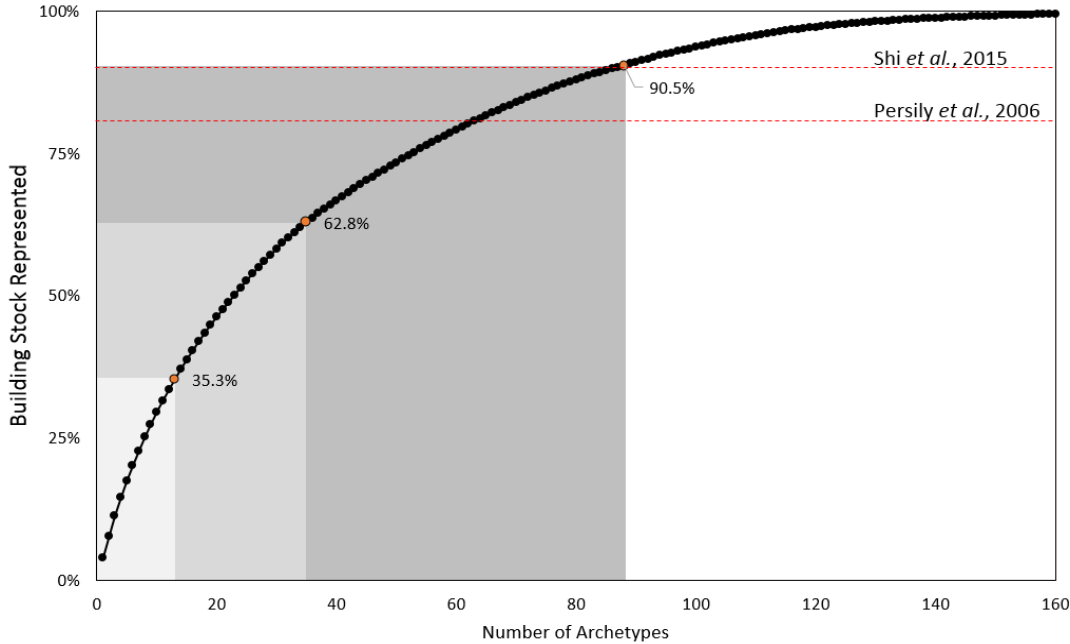


Figure 3: Cumulative distribution of the archetypes according to the percentage of the housing stock represented by the effect size thresholds and two thresholds obtained from the review of the literature (dashed lines).

Figure 3 shows that 99.5% of the Santiago de Chile housing stock can be represented by 160 archetypes. However, limiting factors, such as time and effort, may require a more expedient number of archetypes. The gradient of the line in Figure 3 decreases as the number of archetypes increases, and so there is a law of diminishing returns where adding more archetypes to a set does not significantly increase the proportion of the building stock represented. Therefore, Figure 3 can be used to choose an appropriate number of archetypes for any given modelling task. Table 3 and Figure 3 show that an effect size of *moderate*

magnitude ( $0.50 \leq \varphi < 0.80$ ) requires the first 35 archetypes given in Figure 2 to represent 63% of the stock. Table 4 shows the characteristics of these 35 archetypes. Similarly, an effect size of *small* magnitude ( $0.20 \leq \varphi < 0.50$ ) requires the first 13 archetypes.

**Table 4:** Characteristics of the selected 35 archetypes.

Variable	Category, Value	Frequency
Type of building	Apartment	10
	Detached	10
	Semidetached / End-terrace	8
	Mid-terrace	7
Number of Zones	3-6	
Number of Bedrooms	1-3	
Age period	Before 2008	24
	From 2008	11

### 3.2 Examples of Archetype Parameters

Table 5 presents the first 13 ranked archetypes identified in Figure 2, which represent 35.3% of the housing stock of Santiago de Chile. The ID Number indicates the initial position of each archetype among all 434. No statistical data on individual room heights are available to compute volumes, and so they are obtained from building codes, which specify a minimum of 2.4m.

**Table 5:** Architectural elements and values of relevant parameters to be used when modelling the archetypes values obtained either from the databases or assumed from other sources.

ID Number	Weighting factor	Construction Period	Type of dwelling	Number of Zones	Number of Bedrooms	Mean floor area [m <sup>2</sup> ]	Number of storeys
125	48338	1	D	4	2	66.58	1
134	45455	1	D	5	3	150.56	1
24	44917	1	A	4	2	70.32	4-storey building
237	38490	1	S+E	4	2	55.05	1
246	36195	1	S+E	5	3	103.53	2
32	32387	1	A	5	3	104.33	4-storey building
349	31312	1	M	4	2	50.64	1
358	29444	1	M	5	3	146.79	1
133	27545	1	D	5	2	150.56	1
31	26356	1	A	5	2	104.41	4-storey building
181	24242	2	D	4	2	70.37	1
190	22796	2	D	5	3	157.59	1
73	22526	2	A	4	2	73.08	4-storey building

**D:** Detached; **A:** Apartment; **S+E:** Semidetached and End-terrace; **M:** Mid-terrace.

**1:** built between 1990-2007 period; **2:** Built during or after 2008.

## 4 CONCLUSIONS

This paper uses available data contained within national censuses and building reports to identify sets of archetypes that are statistically representative of the housing stock of the metropolitan and capital region of Santiago de Chile. This is considered a proxy of the entire Chilean housing stock because 41% of the population is located there. The proportion of the stock represented increases with the number of archetypes, but there is a law of diminishing returns. Therefore, the number of archetypes can be chosen based on the research question and available resources.

The descriptive parameters of each archetype are informed by the elements of building design recorded by IAQ field studies and required as inputs to energy, ventilation, and pollutant transport modelling tools. Therefore, they can be used to model indoor environments and to test a range of interventions designed to improve IAQ in Chilean houses.

The archetypes increase our understanding of the Chilean housing stock, highlight its heterogeneity, and show all available data on their characteristics. Existing databases are non-exhaustive and contain errors and so areas are highlighted where there is poor quality, or a lack of data, on the characteristics of houses, and occupants and their behaviour. This information can be used to inform future surveys of the Chilean housing stock.

Both the database and the archetypes will be shared in a public domain in the future.

## 5 REFERENCES

- Ballarini, I., Corgnati, S. P., & Corrado, V. (2014). Use of reference buildings to assess the energy saving potentials of the residential building stock: The experience of TABULA project. *Energy Policy*, 68, 273-284.
- Chen, C. & Zhao, B. (2011). Review of relationship between indoor and outdoor particles: I/O ratio, infiltration factor and penetration factor. *Atmospheric Environment*, 45(2), 275-288.
- Chin, J. Y. *et al.* (2014). Levels and sources of volatile organic compounds in homes of children with asthma. *Indoor Air*, 24(4), 403-415.
- Cohen, J. (1990). Things I have learned (so far). *American psychologist*, 45(12), 1304-1312.
- Cohen, J. (1992). A power primer. *Psychological bulletin*, 112(1), 115-159.
- Cometto-Muñiz, J. E., & Abraham, M. H. (2015). Compilation and analysis of types and concentrations of airborne chemicals measured in various indoor and outdoor human environments. *Chemosphere*, 127, 70-86.
- de Bruin, Y. B. *et al.* (2008). Characterisation of urban inhalation exposures to benzene, formaldehyde and acetaldehyde in the European Union. *Environmental Science and Pollution Research*, 15(5), 417-430.
- Dols, W. S., & Polidoro, B. (2015). *CONTAM User Guide and Program Documentation*.
- Ferguson, C. J. (2009). An effect size primer: A guide for clinicians and researchers. *Professional Psychology: Research and Practice*, 40(5), 532.

- Field, A. (2013). *Discovering statistics using IBM SPSS statistics* (4th ed.). London: Sage.
- Ghiassi, N., & Mahdavi, A. (2017). Reductive bottom-up urban energy computing supported by Multivariate Cluster Analysis. *Energy and Buildings*, *144*(5), 372-386.
- Gilbert, N. L., Guay, M., Gauvin, D., Dietz, R. N., Chan, C. C., & Lévesque, B. (2008). Air change rate and concentration of formaldehyde in residential indoor air. *Atmospheric Environment*, *42*(10), 2424-2428.
- Guo, H., Lee, *et al.* (2004). Risk assessment of exposure to volatile organic compounds in different indoor environments. *Environmental Research*, *94*(1) 57-66.
- INE. (2003). Censo de Población y Vivienda 2002. Santiago de Chile: Instituto Nacional de Estadísticas.
- INE. (2013). Censo de Población y Vivienda 2012. Santiago de Chile: Instituto Nacional de Estadísticas.
- INE. (2016). Bases Edificación. Santiago de Chile: Instituto Nacional de Estadísticas.
- INE. (2017). Número de viviendas autorizadas total país y región metropolitana (Jan 2017 ed.). Santiago de Chile: Instituto Nacional de Estadísticas.
- Jones, B. *et al.* (2015). Assessing uncertainty in housing stock infiltration rates and associated heat loss: English and UK case studies. *Building and Environment*, *92*, 644-656.
- Kavgic, M. *et al.* (2010). A review of bottom-up building stock models for energy consumption in the residential sector. *Building and Environment*, *45*(7), 1683-1697.
- Langer, S., & Bekö, G. (2013). Indoor air quality in the Swedish housing stock and its dependence on building characteristics. *Building and Environment*, *69*, 44-54.
- Langer, S., Ramalho, O., Derbez, M., Ribéron, J., Kirchner, S., & Mandin, C. (2016). Indoor environmental quality in French dwellings and building characteristics. *Atmospheric Environment*, *128*, 82-91.
- McCurdy, T., & Graham, S. E. (2003). Using human activity data in exposure models: Analysis of discriminating factors. *J Expo Anal Environ Epidemiol*, *13*(4), 294-317.
- Ng, L. C., Musser, A., Persily, A. K., & Emmerich, S. J. (2013). Multizone airflow models for calculating infiltration rates in commercial reference buildings. *Energy and Buildings*, *58*, 11-18.
- Persily, A., Musser, A., & Emmerich, S. (2010). Modeled infiltration rate distributions for US housing. *Indoor Air*, *20*(6), 473-485.
- Persily, A. K., Musser, A., & Leber, D. D. (2006). *A collection of homes to represent the US housing stock*: US Department of Commerce, Technology Administration, National Institute of Standards and Technology.

- Shi, S., Chen, C., & Zhao, B. (2015). Air infiltration rate distributions of residences in Beijing. *Building and Environment*, 92, 528-537.
- Singleton, R., Salkoski, A. J., Bulkow, L., Fish, C., Dobson, J., Albertson, L., . . . Ritter, T. (2017). Housing characteristics and indoor air quality in households of Alaska Native children with chronic lung conditions. *Indoor Air*, 27(2), 478-486.
- Swan, L. G., & Ugursal, V. I. (2009). Modeling of end-use energy consumption in the residential sector: A review of modeling techniques. *Renewable and Sustainable Energy Reviews*, 13(8), 1819-1835.

# The Cleanliness Classification of Air-handling Components- A success Story in Finland

Laura Sariola<sup>1</sup>, Pertti Pasanen<sup>\*2</sup>

*1 The Building Information Foundation RTS sr,  
Malminkatu 16 A,  
00100 Helsinki,  
Finland*

*2 University of Eastern Finland,  
Department of Environmental and Biological  
Sciences,  
P.O. Box 1627,  
70211 Kuopio, Finland*

*\*Corresponding author: pertti.pasanen@uef.fi*

## ABSTRACT

**INTRODUCTION:** The Finnish Society of Indoor Air Quality and Climate (FiSIAQ) introduced over twenty years ago in 1995 a Classification of Indoor Climate, Construction Cleanliness, and Finishing Materials and the third edition will be published autumn in the year 2017. Based on the criteria set in the classifications, The Building Information Foundation RTS sr started the M1-labelling of air handling components in 1999. Name of the classification is Cleanliness Classification of Air Handling Components.

**METHODS:** The criterion of the M1-classification of air handling components has not been revised during the years. The committee of Indoor Air PT17 has an authorization to accepted new criteria and test criterion groups for the class M1. Classified ducts and joints and other parts has been classified almost twenty years. The test scheme has to be accepted according to specified criteria in the classification working group before the tests. The classification criteria concern also dust-free warehousing and use on site. The new Indoor Air Classification 2017 and especially the changes made to the Cleanliness Classification of Air handling Component criteria and product groups will be presented.

**RESULTS:** The Finnish classification system has established a solid position in air -handling markets in Finland. Most of the factories producing duct-work components are located in Finland and some of them are located also in Sweden and Estonia. In February 2017 there were almost 330 M1-labelled air handling products from 13 companies representing 70% of the Finnish markets. The cleanliness classification of air handling components follows the changes, developments and needs of the market. According to development of the products and their features, new group of products will be gathered to keep the system practical.

**CONCLUSIONS:** The Indoor Air Classification 2017 includes the Cleanliness Classification of Air Handling Components. A result of implementation the system is that manufactures have developed HVAC components, products and production processes continuously in order to fulfil cleanliness criteria with low dust, low oil contamination and low odour emissions. The adopted system improves high quality of supply air in the ventilated offices, homes and other conventional buildings.

## KEYWORDS

HVAC, emissions, oil, dust, cleanliness, classification

## 1 INTRODUCTION

High indoor air quality is recognized as an important issue for both national health and economy in Finland. The Finnish Society of Indoor Air Quality and Climate (FiSIAQ) introduced over twenty years ago in 1995 a Classification of Indoor Climate, Construction Cleanliness, and Finishing Materials and the third edition will be published in 2017. Based on the criteria set in the classifications, The Building Information Foundation RTS sr started the M1-labelling of air handling components in 1999. Name of the classification is Cleanliness Classification of Air Handling Components.

The Cleanliness Classification of Air Handling Components is a part of the Classification of Indoor Air updated later on the year 2017. The whole classification system is part of the new environmental classification system called RTS Green Leadership Tool (RTS GLT) published on the spring 2017.

The RTS environmental classification (RTS GLT) is based on European standards (CEN TC 350 standards) and it brings together the common best practices in the sector in Finland, such as the Finnish Classification of Indoor Environment representing Indoor Air Class S1 and S2, M1-classification for building products and air-handling components, Cleanlinessclassification of construction work P1. The connections between classifications and their components are introduced on the following figure (Figure 1).

## Classifications and certifications at RTS

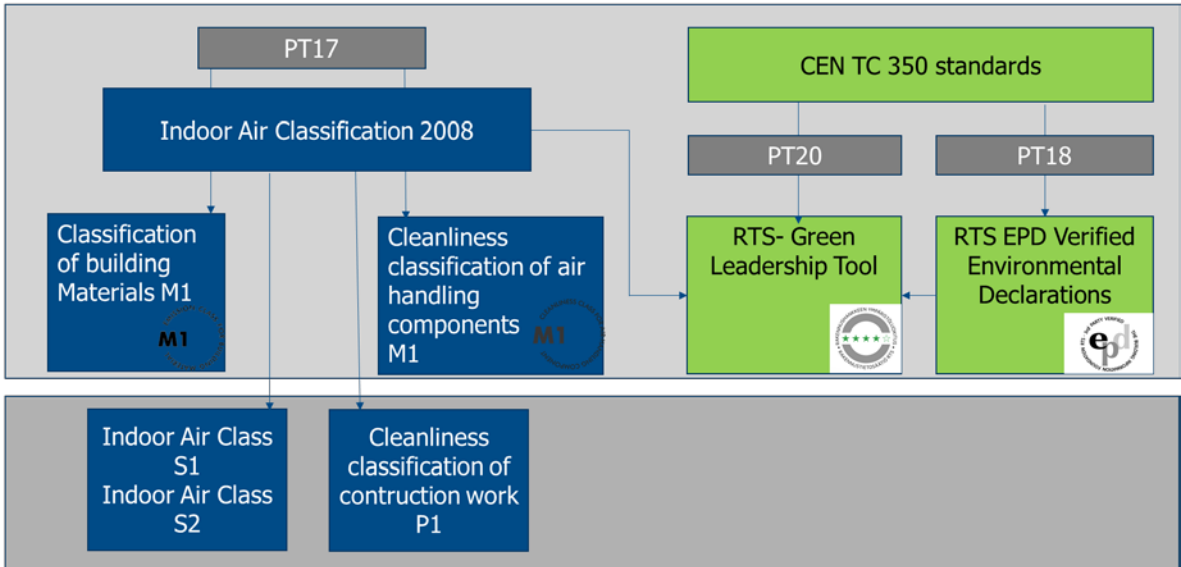


Figure 1 Classification connections in the Building Information Foundation RTS sr

### 1.1 Confidentiality and impartial operator

The Building Information Foundation RTS sr is a private, non-profitmaking Foundation whose task is to foster both good planning and building methods and good property management practices. The Foundation and its activities are directed by a Board and an Assembly that represents the entire building and construction industry through 54 associations and organisations. One of the main activities are organization and finance of the extensive committee work.

The Committee PT 17 Indoor Air is responsible for development and update of the Indoor Air Classification. The classification work is developed and supervised by the committee appointed by the Director General of the Building Information Foundation RTS sr. Other mission for the committee is to promote building methods aimed at good indoor climate in other ways as by active participation and discussion to regulatory preparation work.

Classification applications and matters relating to classification decisions are examined by a separate classification working group nominated by the Committee PT17. The working group consists of a representative of the Finnish Society of Indoor Air Quality (FISIAQ), technical expert and the secretary of the classification working group. There are high demands

for ethics, trust and confidentiality and therefore The Building Information Foundation RTS process all documents and information submitted by applicants in support of their application in high confidence. None of the background information leaks outside the foundation. However, the product fulfilling the criteria and permitted to label with M1-classification status are published.

The classification system is voluntary for the manufacturers, importers and exporters of air-handling components and systems outside the Finland as well. Cleanliness Classification of Air-handling Components is based on general and component-group-specific requirements. The general requirements for a classified component are:

- a) a classified component shall not increase the concentration of contaminants that are detrimental to health or comfort in the air handling system or supply air
- b) a classified component shall not produce odours, or gaseous or particulate contaminants that decrease the quality of supply air
- c) a classified component shall be easy to clean

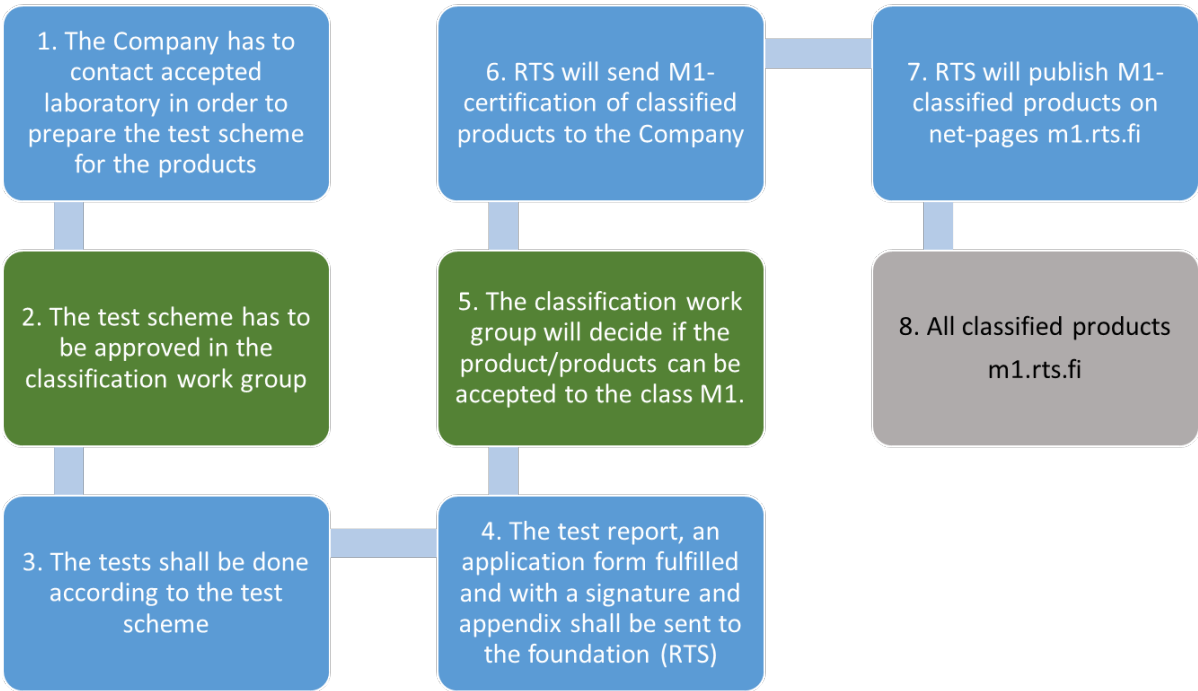


Figure 2 Classification procedure

**2 METHODS**

The criterion of the M1-classification of air handling components has not been revised during the years. The committee of Indoor Air PT17 has an authorization to accepted new criteria and test criterion groups for the class M1. Classified ducts and joints and other parts has been available almost twenty years. The test scheme has to be accepted according to specified criteria in the classification working group before the tests. The classification criteria concern also dust-free warehousing and use on site. Principles for classifying air-handling components are product specific. Similar principle for all air-handling components is that the products shall be protected to get dirty inside during factory storage, transportation and on construction

site. The protection has to be effective enough. For example both duct ends have to be capped and joint and other parts have to be protected e.g. by covering them by plastic film.

## 2.1 Tests and product grouping before classification

There are multiple steps to be fulfilled before M1-classification status. First the company has to contact approved testing laboratory in order to prepare test scheme. The applicant is responsible for documentation. After that the test scheme has to be approved in the classification work group. After acceptance the tests shall be done according to the test scheme. After the tests, the test report, an application form fulfilled and with appendix as product information shall be sent to the foundation. The classification work group will decide if the product/products can be accepted to the class M1.

- a) Product testing before classification: Classification requires the product to be tested by an approved testing laboratory in accordance with the required methods.
- b) Selection of testing laboratory: The products shall be tested by a competent and impartial laboratory approved by the classification working group. A list of approved laboratories can be found on the Internet. The applicant is responsible for documentation.
- c) Testing methods: The products must be tested according to the cleanliness testing instructions for air-handling products (dated 2 November 2001) or according to later updated or new product specific instructions. The research report must contain the details listed in the model test report.

Criteria for air-handling components: Group specific requirements for metal ducts and accessories.

<i>Pollutant</i>	<i>Criterion</i>
Surface density of oil in ducts	0.05 g/m <sup>2</sup>
Surface density of oil in accessories, terminal units, and air and fire dampers	
Parts manufactured by cutting, bending or jointing	0.05 g/m <sup>2</sup>
Parts manufactured from deep-drawn sheet metal, processes requiring oil	0.3 g/m <sup>2</sup>
Mineral fibres released into air flow	0.1 fibres/m <sup>3</sup>
Amount of surface dust (after manufacture)	<0.5 g/m <sup>2</sup>

## 2.2 Principles for air-handling components

### 2.2.1 Sheet metal ducts and parts, valves, dampers, and fire dampers

- a) The product shall be tested in accepted laboratory
- b) The ducts, ducts parts, regulators and fire dampers, as well as the cleaning openings and hatches, can be cleaned in accordance with Finnish construction regulations or type approval instructions and the SFS-EN 12097 (Ventilation for Buildings. Ductwork. Requirements for ductwork components to facilitate maintenance of ductwork systems) standard.
- c) The ducts and duct parts can withstand at least 10 cleaning cycles using the cleaning procedures intended for them without their structure being subject to harmful changes. Ducts and duct parts must not allow fibres to become detached into air intakes during or after cleaning by more than 0.01 piece/cm<sup>3</sup> (Cleanliness testing instructions for ventilation products 2000).
- d) Any insulation materials that are used inside the ductwork fulfil the requirements set for fireproof building materials and requirements in accordance with combustibility Sh1 and fire spread class PII 1 (B-s1,d0) (RakMK E1).

- e) The regulators, valves and fire dampers do not prevent ducts from being cleaned. It is possible to restore regulators to their original position after cleaning. It is possible to check the position of dampers without opening the channel.
- f) The internal surface of the products is of a type that does not promote the accumulation of dirt within the products. The roughness of the channel material is less than 1 mm. The seams of channels of diameter 200 mm or less and their related connecting parts are not more than 2 mm high inside the channel. The seams of ducts of diameter 315 mm or more and related connecting parts are not more than 3 mm high inside the channel. The products do not contain burrs that could complicate cleaning or break cleaning equipment.
- g) The seals of the products fulfil the requirements of class C of the SFS-EN 12599:en (Ventilation for buildings. Test procedures and measurement methods to hand over air conditioning and ventilation systems) standard.
- h) The sealants do not discharge harmful materials into the air flow or any agents that may cause poor air quality
- i) Classified products are marked in such a way that they can be easily distinguished from unclassified supplies. The marking can withstand normal transportation, storage and handling on construction sites.
- j) The products are protected from becoming dirty on the inside during factory storage and transportation by means of closing off the ends of the ducts or packing the parts in closed boxes and protecting the load by covering it or using similar methods. The techniques used for protection (such as plugs) and the storage boxes are of a type that can withstand the prevailing conditions during transportation and on construction sites, as well as being opened and closed several times. If the ducts are transported inside each other, the cleanliness of their external surfaces is the same as that of their internal surfaces. Product-specific transportation, storage, installation and servicing instructions are issued and the instructions cover essential matters related to cleanliness.

### **2.2.2 Fire and noise dampers**

- a) The product shall be tested in accepted laboratory
- b) The products fulfil the requirements set out in RakMK (Finnish regulation) (fire, noise-dampening)
- c) The noise-reduction properties of the product are known.
- d) No labels or similar items are affixed to the surfaces of products
- e) The perforated metal sheet or other material used in the noise-dampener fulfils the requirements that are presented in the classification instructions in relation to processes that require oil 0.3 g/m<sup>2</sup> (300mg). The certificate is to be attached to the application.
- f) The technical noise-related features, usage and cleaning instructions of the noise-dampeners, along with the nominal air flow and any applicable usage restrictions are available with the product as well as separately.
- g) The products fulfil the requirements of Section 3.2.2.1 of the Classification of Indoor Climate. The noise-dampener does not produce odour that reduces the quality of incoming air or that introduces impurities in the form of gas or particles.
- h) Classified products are marked in such a way that they can be easily distinguished from unclassified supplies. The marking can withstand normal transportation, storage and handling on construction sites
- i) The products are protected from becoming dirty on the inside during factory storage and transportation by packing the parts in closed boxes and protecting the load by

covering it or using similar methods. The techniques used for protection and the storage boxes are of a type that can withstand the prevailing conditions during transportation and on construction sites, as well as being opened and closed several times. Product-specific transportation, storage, installation and servicing instructions are issued and the instructions cover essential matters related to cleanliness.

### 2.2.3 Terminal devices

- a) The product has to be tested in accepted laboratory: Textile terminal devices shall be tested according to the testing protocol for building materials.
- b) The technical noise and flow properties are known. The certificate is to be attached to the application.
- c) No labels or similar items are affixed to the surfaces of products
- d) The perforated metal sheet, nozzle duct material or other material used in the terminal device fulfils the requirements that are presented in the classification instructions in relation to processes that require oil  $0.3 \text{ g/m}^2$ . The certificate is to be attached to the application.
- e) Usage and cleaning instructions for terminal devices, along with the nominal air flow and any applicable usage restrictions, are available with the product as well as separately.
- f) The terminal device does not product odour that reduces the quality of incoming air or that introduces impurities in the form of gas or particles.

### 2.3 Requirements for announcement of changes in the product product and production method changes

The classification is for both the company and the product. If the product will remain the same the classification is valid for 3 years, the retests is obligatory after 6 years. The company holding the right of use the M1-label is responsible and obligated to give the foundation prior notice of changes relating to the product and its methods of manufacturing. The foundation is not responsible for the requirements guaranteed to the product or the properties. It is the responsibility of the holder of the classification to ensure that the product has an approved quality control system.

The classification is valid for three years. Right of use of a classification label provides the company which has been granted classification the right to label the classified product with the label and to use the label for marketing purposes. The company must use the valid classification symbol, which is a registered trade mark.



Figure 3

### 3 RESULTS

The Finnish classification system has established a solid position in air-handling markets in Finland. Most of the factories producing duct-work components are located in Finland and some of them are located also in Sweden and Estonia. In May 2017 there were almost 330 M1-labelled air handling products from 13 companies representing 70% of the Finnish markets. The cleanliness classification of air handling components follows the changes, developments and needs of the market. According to development of the products and their features, new group of products will be gathered to keep the system practical.

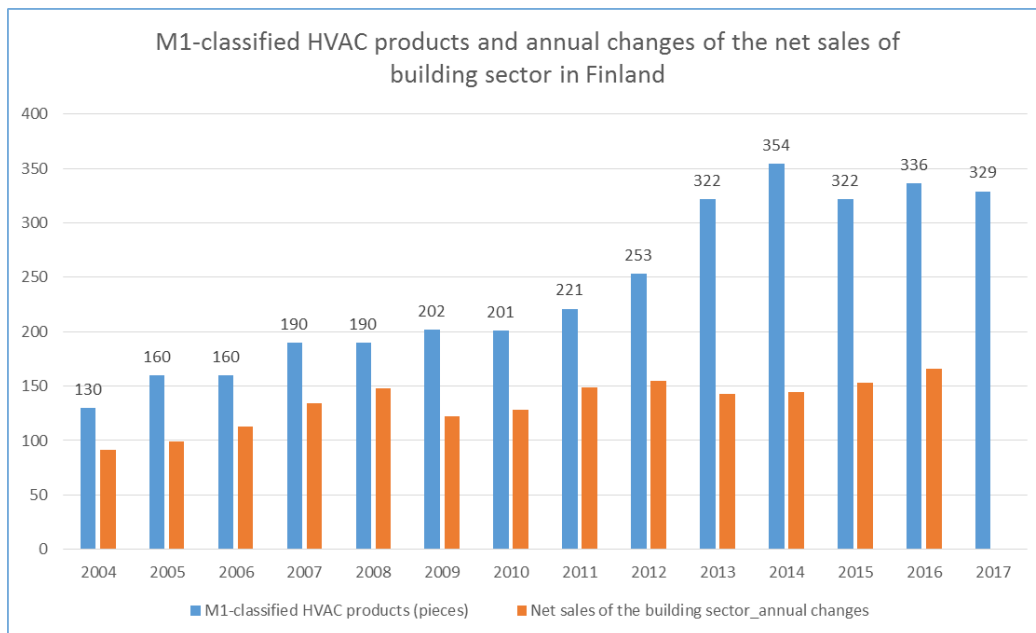


Figure 3 Development of the cleanliness classified HVAC products

### 4 CONCLUSIONS

Air-handling components and devices contribute to the indoor air quality in all kinds of buildings. This paper concluded that with impartial certification system and with commitment of manufacturers it is possible to improve indoor air quality. Besides the criteria for oil and dust, there are remarkable advantages of the criteria concerning dust-free warehousing and use on site for indoor air quality and for the cleanliness class P1 for construction work.

### ACKNOWLEDGEMENT

The authors wish to thank Mrs. Vuokko Lappalainen (University of Eastern Finland) for information gathered to the paper.

### 7 REFERENCES

- FISIAQ( 2008). Classification of indoor climate 2008, Target values, design guidance and product requirements.
- FISIAQ( 2017, draft). Classification of indoor climate 2017, Target values, design guidance and product requirements.
- The Building Information Foundation RTS. 2017. <http://m1.rts.fi>
- SFS-EN 12599:enVentilation for buildings. Test procedures and measurement methods to hand over air conditioning and ventilation systems
- SFS-EN 12097:enVentilation for Buildings. Ductwork. Requirements for ductwork components to facilitate maintenance of ductwork systems.

# **Circadian House: a vision for homes designed to be healthy and human-centric**

Peter Foldbjerg<sup>1\*</sup>, Per Arnold Andersen<sup>1</sup>, Nicolas Roy<sup>1</sup>, Jens Christoffersen<sup>1</sup>

*1 VELUX A/S,*

*Daylight, Energy and Indoor Climate,*

*Ådalsvej 99, Hørsholm, Denmark*

*\*Corresponding author: e-mail address*

*Presenting author: underline First & Last name*

## **ABSTRACT**

Based on a series of workshops, a Circadian House is defined as a house that is designed to support a healthy life for its occupants through a human-centric design. The workshops were held in 2012-2013 and defined 3 key principles and ten key factors to consider in the design of homes.

## **KEYWORDS**

Residential buildings, health, indoor climate, circadian rhythm

## **1 INTRODUCTION**

Much focus on sustainable buildings has been on energy aspects. However, health is the most precious resource we have, and energy is only one aspect of sustainability. A primary goal for sustainability should be to sustain good health and a healthy living environment. This was the starting point for a series of workshops with international experts initiated by the VELUX Group, based on a wish to start a discussion on how to create healthier homes.

The result is a vision to realize healthy homes that support the different biological needs of their occupants, in particular including their circadian rhythms, sleep-wake cycles and preferences for temperature and fresh air, as well as the relation to the outdoor environment.

Three key principles were identified: Live in balance with nature, Adaptability and Sensibility. Ten key factors further go a step further: Variation, Stimulation/absence of stimulation, Outdoor/indoor relation, Light/darkness, Electrical lighting, Cool/warm, Silence/sounds, Rest/activity, Control and Flexibility related to seasons.

The principles and guidelines presented here can be used to guide and improve the design of residential buildings of all types, including apartment buildings, and are applicable to both new and existing dwellings (Circadian House, 2013).

## **2 METHODS**

In the context of this paper, a Circadian House is understood as a dwelling that promotes health by synchronising the circadian rhythms of its occupants to the 24h day-night cycle and the seasonal changes of day length.

This paper is based on discussions and findings of 5 workshops; “Light and circadian rhythms”, “Indoor climate”, “The historical perspective”, “What to monitor and how” and “Condensation of the specifications”(WS 5). The workshops were carried out by scientists and consultants specialized in healthy buildings, indoor environment, architecture and planning from November 2012 to August 2013. See the Acknowledgements section.

### **3 RESULTS**

It is not possible to include all results in this short paper. In the following we will highlight selected key results organised around a selection among the ten key factors.

#### **3.1 Contact to nature**

Dwellings should have at least one outdoor or semi-outdoor space (e.g. a garden, terrace or balcony) that provides direct contact to nature. Research studies show that improved mood and reduced stress are consistent benefits of living in close contact with nature (Veitch and Galasiu, 2012).

Outdoor spaces must be treated as an extension of the house and designed to inspire the occupants to spend as much time as possible outside, offering a close contact to nature in all seasons of the year. Outdoor spaces should be designed for a variety of activities such as dining, playing, working, relaxing etc. People affected by the seasonal changes in day length will benefit from extra exposure to high levels of daylight in outdoor and semi-outdoor spaces. Also, exposure to daylight and sunlight outside allows our body to produce vitamin D, which people in modern societies often lack due to the large amount of time spent indoors. Balconies and terraces should be shielded from wind and have good connections to relevant rooms of the house in order to maximise their use.

#### **3.2 View to outside**

Views to the outdoor surroundings are crucial in order to maintain contact with nature and satisfy our needs for orientation in time and place while indoors. There is clear evidence of the benefits of window views, particularly views offering contact to life and nature. A good view can have restorative benefits (leading to e.g. stress relief) and sometimes even result in quicker recovery time after illness and less post-surgery pain medication.

It is important to analyse view content on-site and make sure that all main living and activity rooms in the house have generous views to the sky and ground, and to natural and/or urban landscapes around the house. Shading systems should be designed so that adequate views to the outside can be maintained in the rooms even at moments when it is necessary to block direct sun penetration. To this effect, it is important to consider proper control of sunlight in summer (Kaplan, 2001; Kellert, 2008).

#### **3.3 Healthy Light**

Light is used by individuals for image forming light detection (vision) under a range of varied lighting levels and for a variety of non-image forming light detection (non-vision) tasks including as a daily time cue for sleep timing and as a modulator of levels of alertness. In addition, there is increasing evidence that human biology can be affected by changing light levels across the seasons. Seasonal depression has been linked to reduced light exposure in winter, whilst vitamin D synthesis requires light exposure around 300nm in the UV range and attenuated levels of vitamin D have been linked to increased vulnerability to both developmental and somatic diseases in adults (Wirtz-Justice et al 1996). It should also be noted that UV light also has strong germicidal actions that can prevent the spread of some diseases in buildings. The principles and guidelines for Healthy Light should incorporate all

of these divergent biological roles of light. How our biology responds to light intensity, spectrum, timing, duration and its spatial distribution is highly complex and varies greatly between image- and non-image forming light detection tasks (Boyce et al., 2003; Brainard & Veitch, 2007).

Healthy lighting should consider the following factors:

- The total daily light dose, which varies between individuals and as we age;
- Healthy light is linked to healthy darkness at night;
- Light sources with a broad daylight spectrum;
- Light received at eye level;
- Levels of UV-rich light reaching the skin;
- Timing, variation and duration of light exposure over the day and across the seasons

The dynamic variation of light is a critical factor in setting and maintaining our 24h daily rhythms – our circadian rhythms, which in-turn play a key role in the regulation of the sleep/wake cycle. Sleep disruption has been linked to poor cognitive function, stress, depression, poor social interaction, metabolic and cardiovascular disease, and an increased susceptibility to infection and even cancer. As a result an appropriate light signal during the day and darkness at night are critical in maintaining key aspects of our overall health. Outdoor daily light exposure allows us to regulate our sleep/wake timing, levels of alertness and the synthesis of vitamin D. The reality is, however, that we spend most of our time indoors where we are exposed to relatively low light levels of a limited spectral range, and where the patterns of light and darkness occur at irregular intervals. Until recently in the history of our species, the dwelling space was used primarily as a space for sleep with most activities taking place outside. Today, work, entertainment, socializing, eating and sleep all take place in the same or similar physical spaces. Collectively, the consequences of poor light exposure and the subsequent impact upon health are placing a substantial burden on the individual, society and the broader economy.

In order to align our body clock, morning light is the most important signal for entrainment. Light in the morning also increases our levels of alertness, allowing increased performance at the beginning of the day. Whereas reduced light levels in the evening promote sleep at night. For those times when seasonal daylight is not available in the morning, electric lighting can be used to support our non-visual light needs; mimicking the morning, daytime and evening periods in spectrum, intensity and dynamics. Although much is still unknown about the specifics of how light interacts with our non-visual light systems, the data we have already can be used to suggest some important approaches to the nature of daily light exposure:

- The intensity of light should provide opportunities for exposure to high daylight levels at the level of the eye, within the range of more than 1,000 lux up to around 5,000 lux, and should be designed to minimize visual discomfort.
- The light dose per day exposed to >1,000 lux should on average be more than 200 minutes with high intensity boosts, especially, in the morning.
- Good spatial distribution of daylight and sunlight is achieved by distributing windows in multiple external walls and the roof rather than placing them with only one orientation.
- Daylight with minimal spectral filtering should be delivered at those times of day when it is most needed for circadian regulation.

- A dwelling should follow the natural cycle of light and dark exposure - allowing high exposure to daylight in rooms used in the morning and in the main activity rooms used throughout the day, and complete darkness in the bedrooms at night.
- It is important to carefully consider exposure to darkness during the sleeping periods – as circadian and alertness regulation requires both light and dark periods over the day.

### **3.4 Healthy Indoor Air**

Opening windows brings in fresh outdoor air and provides contact to the outside and rapid changes of indoor air quality. It allows you to sense changes in weather during the day and over the year. Contact to the outside is important for the well-being of occupants in residential buildings.

Airings should be a part of the daily cycle. It is executed by many families and associated with wellbeing, comfort and health. Operable windows ideally should be combined with a general system for basic fresh air supply using ventilation grilles in the facades or mechanical ventilation.

Opening windows provides the occupants with an immediate change in the indoor environment, i.e. with a direct effect on air temperature, air velocity and air change rates. Efficient airings can be achieved by having more than one operable window and by locating these windows towards different orientations or at different heights in each main room. There should also be good options for cross and stack ventilation between rooms through the building.

Ventilation devices should be designed in such a way that occupants can prioritize privacy and silent operation when they prefer minimum sensory stimulation, e.g. during night time, but without compromising the basic requirements for ventilation. Control of the systems (and the momentary fresh air supply) is important. For more information about control of ventilation, see also under ‘building controls’.

Many indoor air pollutants often present in dwellings cannot be sensed by humans and the house should, therefore, offer protection from these ‘stealth pollutants’. To minimize adverse health effects from indoor air pollution, the primary strategy should be source control.

The kitchen can be the most affected room due to the pollutants (particles, NO<sub>x</sub>, etc.) emitted from the stove and oven when cooking. The negative health effect is increased if the kitchen is in open connection with the dining area, as exposure to cooking-related particles are not limited to the kitchen area in that case. The most effective means of reducing pollutant exposure from cooking is by using an efficient cooking hood and ensuring that it will be turned on and in use whenever the kitchen is used for cooking. The cooking hood should be sufficiently quiet so that it does not annoy the occupants, but should be audible so that it is not forgotten.

In kitchens and bathrooms, exposure to (excess peak levels of) moisture is also an issue. Well-functioning ventilation systems and adequate cooking hoods also take care of that.

Note that periodical exposure to pollutants in small and non-harmful doses, particularly as a child, will decrease the risk of developing allergies at a later stage in life. The effect is referred to as the hygiene hypothesis and is related to the functioning of the immune system.

### **3.5 Healthy Thermal Environment**

Preferably indoor temperature varies over the course of the day, in parallel with the outdoor temperature, which typically increases during the day and drops during the night. The indoor temperature should also follow the seasons (with limitations, of course), with minimum levels during the winter and maximum levels in summer (Brager and de Dear, 1998).

Solar gains through windows have a large impact on the indoor temperature and should primarily be controlled with shading. Solar gains provide spatial variation of temperature in the rooms with local warm and cool spots. During winter with little solar gains, a local 'hot spot' should be provided for in e.g. the living room, typically with a high temperature (vertical) radiant heat source. This 'hot spot' allows the occupants to seek a warm or cool position in the room that suits them and may thermally differ from the position of others in the same room. This 'hot spot' can look like a fireplace or gas stove in older houses, but then in a modern form without the air pollution side effects, e.g. hot water based local heating systems.

Architectural spaces should ideally promote people to have an active and healthy lifestyle, as opposed to being more passive. A thermally comfortable environment is not necessarily one that favours physical health. An example is a study (Lichtenbelt&Kingma, 2013), which showed that for persons exposed to an indoor temperature at the low end or even just below the comfort range, non-shivering thermogenesis is activated which leads to increased metabolism. It is thus a quality of the indoor environment if there is some temperature variation and temperatures in winter are a bit on the cold side (and in summer on the warm side).

In summer the main issue is to keep the dwelling cool and avoid too high temperatures from excess solar gains. Overheating can normally be avoided by the use of solar shading and natural ventilation through window openings. Additional summer ventilation can be achieved by cross ventilation or stack ventilation (e.g. with windows and/or skylights in adjacent walls/roofs). Bedrooms are particularly important and must be designed and located to minimise overheating, e.g. by choosing a north/east location.

### **3.6 Building controls**

It is important that the functioning of control systems is transparent and comprehensible for the occupants and they can easily adjust the interior daylight levels, electric lighting, temperature, fresh air supply etc. according to their personal needs. Automatic systems are often of advantage, but always see to it that easy-to-use options to override the systems are available. Feedback indicators on e.g. indoor air quality and temperatures (telling you that the systems have understood that you want some kind of change and giving you information about the current status of e.g. temperature, CO<sub>2</sub>-levels, etc.) are a plus as they help occupants to use the building service systems 'as intended'.

It is important that many indoor climate parameters can be controlled at the individual room level, not just at building level. Automated control strategies that work in one kind of room may not work in other room types.

Control strategies, where possible, should support the circadian rhythms of residents. For example, the control strategy for electric lighting could include light sources with varying spectrum and intensity enabling programming according to time of day and type of room. Also, e.g. heating systems could be programmed to anticipate daily temperature changes.

A building control system needs to be robust toward different kinds of occupant use, toward failures/problems of parts of the systems, toward incorrect design assumptions (e.g. number of persons per room) and against occupant misuse.

At least, the following systems require some central control in combination with manual override options and an interface:

- Mechanical ventilation systems;
- Heating systems;
- Window opening systems;
- Solar shading systems;
- Electric lighting systems.

## **4 DISCUSSION**

During the workshops, several fundamental questions were asked about the link between housing quality, indoor environment, circadian rhythms and health. Questions like: Can a house really support circadian rhythms? Not by just providing for the adequate amount of daylight given the time of day, but also, e.g. by allowing indoor temperatures to follow (to a certain extent) the variation in outside temperatures. Can a building's design really support a healthy and active lifestyle? And how can the indoor environment in our homes promote comfort and wellbeing, rather than just maintain acceptable indoor conditions? In the 1860s, Florence Nightingale identified five essential points in securing health in dwellings: pure air; pure water; efficient drainage; cleanliness; and light, especially sunlight. "Do not build good hospitals, build good homes" is her famous quote (still very true).

## **5 CONCLUSION**

Based on the discussions, the core elements of a Circadian House have been identified under 3 key principles and 10 key factors.

### **5.1 Key principles**

- Live in balance with nature - A house in balance with nature allows the occupants to live with and follow the daily and seasonal cycles of the outdoor environment.
- Adaptability - A house whose space and occupants can adapt to changing conditions (daily, seasonal) and needs.
- Sensibility - A house that provides protection against harmful substances, which humans cannot sense, and allows freedom to control parameters that can be sensed.

### **5.2 Key factors**

- Variation: the focus on nature's cycles implies that the indoor environment should vary in time and space rather than target uniformity or non-variability.
- Stimulation/absence of stimulation: The level of stimulation from environmental factors (light, sound, air, temperature) should be higher during day than night.

- Outdoor/indoor relation: Outdoor and semi-outdoor areas are designed to be inspiring and easily accessible; and occupants are able to follow (changes in) outdoor conditions in all main living areas of the house.
- Light/darkness: Exposure to high levels of daylight are needed in the main living areas of the house during daytime, with special attention to the rooms that are mainly used in the morning, whereas the bedrooms need to provide complete darkness at night time.
- Electrical lighting should follow, support and supplement change and variation in the light spectrum and intensity through the course of the day and distribution in space.
- Cool/warm: The house should provide temporal and spatial variation in the thermal environment that are logical (and e.g. follow – to a certain extent) outside temperature variations.
- Silence/sounds: The presence of sound and contact to sounds from outdoors are desired during daytime, whereas quiet spaces are needed at night time.
- Rest/activity: The house design should inspire the occupants to be active, but also have areas for rest and restitution.
- Flexibility related to the seasons: the use of outdoor and semi-outdoor spaces should be stimulated outside the heating season.
- The occupants should be able to control the systems that influence parameters that can be sensed, e.g. like lighting level, air quality and indoor temperature.

## 6 ACKNOWLEDGEMENTS

The work is based on workshop discussions and correspondence with the following, without whom there would have been no Circadian House specification. Anna Wirz-Justice, University of Basel, Switzerland; Anne Helene Garde, National Research Center for the Working Environment, Denmark; AtzeBoerstra, BBA Binnenmilieu, The Netherlands; Dean Hawkes, University of Cambridge, UK, Francis Allard, University of La Rochelle, France, Hal Levin, Building Ecology, US, JelleLaverge, University of Gent, Belgium, Koen Steemers, University of Cambridge, UK, Luc Schlangen, Phillips Lighting, The Netherlands, MariëlleAarts, Eindhoven University of Technology, The Netherlands, Nick Baker, University of Cambridge, UK; Ole Bouman, Biennale Shenzhen; Pawel Wargocki, Technical University of Denmark; Per Olaf Fjeld, University of Oslo, Norway; Richard Hobday, Independent researcher, UK; Russell Foster, University of Oxford, UK; StaffanHygge, University of Gävle, Sweden; Thomas Witterseh, Danish Technological Institute, Denmark; Truus de Bruin, Delft University of Technology, The Netherlands. The VELUX Group provided financial support for the workshops.

## 7 REFERENCES

Boyce, P. R., Hunter, C., &Howlett, O. 2003. The benefits of daylight through windows. Troy,NY: Lighting Research Center. (<http://www.lrc.rpi.edu/programs/daylightDividends/index.asp>).

- Brager GS and de Dear RJ, 1998. Thermal adaptation in the built environment: a literature review. *Energy and Buildings*, Volume 27, Issue 1, February 1998, Pages 83–96.
- Brainard GC and Veitch JA, 2007. *Lighting and Health workshop* – final report based on a workshop session at the Commission Internationale de l’Eclairage meeting in Beijing (2007). NRCC report 50464. NRC Institute for Research in Construction, Montreal, Canada. See:<http://archive.nrc-cnrc.gc.ca/obj/irc/doc/pubs/nrcc50464/nrcc50464.pdf>
- CIBSE. 2013. TM52: The limits of thermal comfort: avoiding overheating in European buildings. *Circadian House, Principles and Guidelines for Healthy Homes*. (2013).
- Commission Internationale de l'Eclairage (CIE). 2004/2009. *Ocular lighting effects on human physiology and behaviour*. (CIE 158:2004). Vienna, Austria: CIE.
- Heschong, Lisa. 1979. *Thermal Delight in Architecture*, MIT Press
- Hobday, R. 2010. *Designing Houses for Health - A Review* ([http://centrallobby.politicshome.com/fileadmin/epolitix/stakeholders/Designing\\_Houses\\_for\\_Health\\_JUNE\\_2010\\_final.pdf](http://centrallobby.politicshome.com/fileadmin/epolitix/stakeholders/Designing_Houses_for_Health_JUNE_2010_final.pdf))
- Hobday RA, Dancer SJ. *Roles of sunlight and natural ventilation for controlling infection: historical and current perspectives*. *J Hosp Infect* 2013;84:271-282.
- Kaplan, R. 2001. *The nature of the view from home: Psychological benefits*. *Environment & Behavior*, 33(4), 507-542.
- Kellert, S.R., Heerwagen, J. and Mador, M. 2008. *Biophilic Design: The Theory, Science, and Practice of Bringing Buildings to Life*. John Wiley and Sons
- Van Marken, Lichtenbelt WD and Kingma BR, 2013. *Building and occupant energetics: a physiological hypothesis*. *Architectural Science Review*, Vol. 56, Issue 1, 2013.
- Veitch, J.A., and Galasiu, A.D. *The physiological and psychological effects of windows, daylight, and view at home: Review and research agenda*. In. Ottawa, ON: NRC Institute for Research in Construction, 2012.
- Wirz-Justice, A., Graw, P., Krauchi, K., Sarrafzadeh, A., English, J., Arendt, J., et al. (1996). 'Natural' light treatment of seasonal affective disorder. *Journal of Affective Disorders*, 37(2-3), 109-120.

# Contaminant stratification in displacement ventilated spaces - a two zone model approach. Model prediction compared to experimental data.

Tor Helge Dokka<sup>1</sup>, Niels Lassen<sup>1</sup>, Maria Myrup<sup>1</sup>,

*1 Skanska Technology  
Lakkegt. 53  
0187 Oslo, Norway*

## ABSTRACT

Displacement ventilation (DV) is an alternative to conventional mixing ventilation in various types of rooms. DV is superior to mixing ventilation when it comes to removing contaminants and surplus heat in a room if designed and applied correctly. In the design process of a space with DV it is necessary to have design methods and simulation tools that can predict the vertical contaminant stratification that arise.

In this paper, both steady state and transient models for prediction of contaminant stratification are proposed. The models are based on a two-zone approach, where also a model for the entrainment of clean air in the human boundary layer is included. Sub-models for convective air flow rates and boundary layer air flow in the rooms are also included. The proposed models can be used for design of displacement ventilation and for evaluation of different ventilation efficiency indices.

Predictions from the model have been compared to measurements in fourteen empirical cases found in the literature. The evaluation of the two contaminant models (steady state and transient) is promising for most of the variables compared. However, experimental results for indices measuring air quality in the inhalation zone is better than the predicted values. This under-prediction is conservative if the models are to be used for design of DV and determining necessary ventilation air flow rates.

## KEYWORDS

Displacement ventilation, mathematical models, contaminants, inhalation zone, entrainment.

## 1 INTRODUCTION

The main objective of ventilation is to provide sufficiently clean air for the occupants, i.e. without any harmful or unpleasant contaminants. Secondary objectives can be the removal or supply of heat, or controlling the humidity level. With regard to air quality, this can be done by diluting contaminants and/or by supplying clean air to the inhalation or occupation zone. Conventional dilution ventilation is primarily based on the first principle (dilution/mixing) and so called displacement ventilation is mainly based on the second principle (supplying clean air and displacing polluted air). The fact that cool air is denser than warm air, leads to a buoyancy effect of warm air raising. Above monitors, lamps, people, radiators, etc. warm air will raise towards the ceiling. Such vertical currents of warm air are often called plumes. If there is no air supply near the ceiling, and no other “disturbing” air currents/movements, a layer of warm air will accumulate below the ceiling. The thickness of this layer is mainly dependent of the plume air flow rates and the ventilation air flow rates. This accumulation will lead to a vertical temperature gradient in the room, with low temperature at floor level and a higher temperature at ceiling level. If the pollution sources in the room are associated with the heat sources, and therefore the plumes, the pollution is also accumulated in a layer near the ceiling, causing a vertical contaminant gradient. This principle is used in displacement ventilation where clean and cool air is supplied to the lower part of the room while the polluted and warm air generated in the occupation zone is transported by the plumes to the upper zone. The height of the clean zone and the polluted zone are dependent of the

magnitude of the supplied ventilation air flow and the convective air flows in the room. Displacement ventilation should ideally, given the same air flow rates, give much cleaner and cooler air in the inhalation and occupation zone, compared to conventional mixing ventilation. Chemical and physical measurements in laboratories and in real rooms show that the air quality in the occupation zone and the inhalation zone is substantially better than standard mixing ventilation, see e.g. Mundt (Mundt, 1996), Mattson (Mattson, 1999), Brohus&Nielsen (Brohus, 1996a), Holmberg et.al. (Holmberg, 1990) and Hatton&Awbi (Hatton, 1998). In addition, laboratory and field experiments show that people perceive the air as more pleasant in displacement ventilated rooms compared to rooms with dilution ventilation, see e.g. Ørhede et.al. (Ørhede, 1996) and Brohus et.al. (Brohus, 1996b). Displacement ventilation has successfully been used in industrial premises, where large concentrated heat and pollution sources often are present at floor level. Displacement ventilation has also grown popular in comfort ventilation, especially in northern Europe.

In the design process of a building or room it is of interest to predict the thermal comfort, indoor air quality, the heating and cooling load and energy use during various seasons. Good simulation tools make it possible to design optimal ventilation solutions. Most existing models and simulation tools for IAQ and energy use are based on the assumption of full mixing, and are unable to predict the advantages of displacement ventilation. However, various alternative methods and models have been proposed to predict the effect of displacement ventilation. Skåret (Skåret, 2000) has proposed a transient two-zone model to predict vertical contaminant stratification in a room. Flow element models are used to calculate the air exchange between the two zones. Koganei et.al. (Koganei, 1993) has proposed a two-zone model for vertical contaminant distribution, assuming piston flow in the lower clean zone. The most advanced models for prediction of vertical contaminant and temperature stratification are CFD models (CFD: Computational Fluid Dynamics). CFD models are based on the governing equations for fluid flow and heat transfer, i.e. conservation of mass, energy and momentum, and different rate laws (e.g. Fourier's law and Fick's law), together with turbulence models, and can also be used to model displacement ventilation. However, the modelling of thermal plumes and boundary layer flow, which is important in displacement ventilated rooms, is difficult in CFD models, as shown by Jacobsen & Nielsen (Jacobsen, 1993).

The aim of this work has been to develop both simplified hand calculation methods and more refined models for implementation in building simulation tools. Models for vertical contaminant stratification in displacement ventilated rooms are proposed, covering both stationary and transient conditions. All models are based on a two-zone model approach, assuming a lower clean and cool zone and an upper polluted and warm zone.

## **2 THEORY AND MODELS**

### **2.1 The two zone approach**

The model is based on a two-zone model approach as illustrated in figure 1, with a lower clean zone (zone 1) and an upper polluted zone (zone 2). Air exchange between the two zones is calculated with sub-models for plumes and the boundary layer flow, see e.g. Dokka (Dokka, 2000) and Dokka & Tjelflaat (Dokka, 2001).

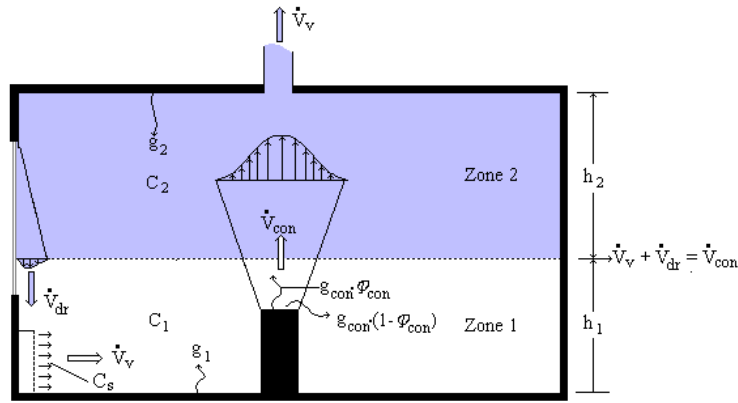


Figure 1: Principles and variables in the two-zone model.

Referring to figure 1, if we assume that the density of air is constant, an air mass balance of zone 1 (clean zone) can be written as (see figure 2):

$$\overbrace{\dot{V}_v + \dot{V}_{dr}}^{\text{Air flow to zone 1}}(h_1) = \overbrace{\dot{V}_{con}}^{\text{Air flow from zone 1}}(h_1) \quad (\text{m}^3/\text{h}) \quad (1)$$

The air mass balance for zone 2 gives the same result. In practice, only the ventilation air flow ( $\dot{V}_v$ ) is known, and the down draft air flow ( $\dot{V}_{dr}$ ) and the convective air flow ( $\dot{V}_{con}$ ) are dependent on the height of the clean zone ( $h_1$ ), i.e. the height of zone 1 has to be iterated until equation (1) is satisfied.

Referring to figure 1, the transient contaminant mass balances for the two zones become:

$$g_1 + (1 - \varphi_{con})g_{con} + \dot{V}_v C_s + \dot{V}_{dr} C_2 - \dot{V}_{con} C_1 = V_1 \frac{dC_1}{dt} \quad (\text{g/h}) \quad (2)$$

$$g_2 + \varphi_{con} g_{con} + \dot{V}_{con} C_1 - \dot{V}_{dr} C_2 - \dot{V}_v C_2 = V_2 \frac{dC_2}{dt} \quad (\text{g/h}) \quad (3)$$

where  $V_1$  and  $V_2$  are the air volumes of zones 1 and 2 respectively, and  $t$  is time.  $g_1$  and  $g_2$  are the “cold” contaminant generation in zone 1 and 2 respectively, while  $C_1$ ,  $C_2$  and  $C_s$  are the contaminant concentration in zone 1, zone 2 and the supply air.  $g_{con}$  is the “hot” contaminant generation associated with the heat sources, and  $\varphi_{con}$  are the part of the hot contaminants that follow the plume air flow to zone 2. Equations (2) and (3) are two coupled ordinary linear differential equations, which for example can be solved by the eigenvalue/eigenvector method (Dokka, 2000):

$$C_1(t) = d_1 \exp(\lambda_1 t) + d_2 \exp(\lambda_2 t) + C_{1\infty} \quad (\text{g/m}^3) \quad (4)$$

$$C_2(t) = d_1 k_1 \exp(\lambda_1 t) + d_2 k_2 \exp(\lambda_2 t) + C_{2\infty} \quad (\text{g/m}^3) \quad (5)$$

where the steady state concentrations are given by:

$$C_{1,\infty} = \frac{b_1 \cdot a_{22} - b_2 \cdot a_{12}}{\det(\vec{A})} \quad (\text{g/m}^3) \quad (6)$$

$$C_{2,\infty} = \frac{b_2 \cdot a_{11} - b_1 \cdot a_{21}}{\det(\vec{A})} \quad (\text{g/m}^3) \quad (7)$$

The entries in the coefficient matrix and the source vector is:

$$\begin{aligned} a_{11} &= -\frac{\dot{V}_{con}}{V_1} & ; & & a_{12} &= \frac{\dot{V}_{dr}}{V_1} \\ a_{21} &= \frac{\dot{V}_{con}}{V_2} & ; & & a_{22} &= -\frac{\dot{V}_{dr} + \dot{V}_v}{V_2} \end{aligned} \quad (1/\text{h}) \quad (8)$$

$$b_1 = \frac{g_1 + g_{con}(1 - \varphi_{con}) + \dot{V}_v C_s}{V_1} & ; & b_2 = \frac{g_2 + g_{con} \varphi_{con}}{V_2} \quad (\text{g/hm}^3) \quad (9)$$

The constants  $d_1$  and  $d_2$  can be calculated as:

$$d_1 = \frac{[C_1(0) - C_{1\infty}]k_2 - C_2(0) + C_{2\infty}}{k_2 - k_1} \quad (\text{g/m}^3) \quad (10)$$

$$d_2 = \frac{C_2(0) - C_{2\infty} - [C_1(0) - C_{1\infty}]k_1}{k_2 - k_1} \quad (\text{g/m}^3) \quad (11)$$

The eigenvalues ( $\lambda$ ) and the entries in the eigenvectors ( $k$ ) are given as:

$$\lambda_{1/2} = \frac{a_{11} + a_{22} \pm \sqrt{(a_{11} + a_{22})^2 - 4 \cdot (a_{11} \cdot a_{22} - a_{12} \cdot a_{21})}}{2} \quad (1/\text{h}) \quad (12)$$

$$k_1 = \frac{\lambda_1 - a_{11}}{a_{12}} & ; & k_2 = \frac{\lambda_2 - a_{11}}{a_{12}} \quad (-) \quad (13)$$

## 2.2 Contaminant removal efficiencies

From the derived expressions in the preceding section, the mean concentration in the complete room and in the occupation zone can be calculated as:

$$\langle C \rangle = \frac{C_{1\infty} h_1 + C_{2\infty} (h_{ceil} - h_1)}{h_{ceil}} \quad (\text{g/m}^3) \quad (14)$$

$$C_{occ} = \begin{cases} C_{1\infty} & ; \text{if } h_1 \geq h_{occ} \\ \frac{C_{1\infty} h_1 + C_{2\infty} (h_{occ} - h_1)}{h_{occ}} & ; \text{if } h_{occ} > h_1 \end{cases} \quad (\text{g/m}^3) \quad (15)$$

where  $h_{occ}$  is the height of the occupation zone. The contaminant removal efficiency in the complete room and in the occupation zone can now be calculated:

$$\varepsilon^C = \frac{C_{2\infty} - C_s}{\langle C \rangle - C_s} \quad (-) \quad (16)$$

$$\varepsilon_{occ}^C = \frac{C_{2\infty} - C_s}{C_{occ} - C_s} \quad (-) \quad (17)$$

If we assume that air in the human boundary layer is entrained evenly from floor level to the height of the inhalation zone ( $h_{exp}$ ), the mean concentration entrained in the human boundary layer is given by the expression:

$$C_{exp} = \begin{cases} C_{1\infty} & ; \text{if } h_1 \geq h_{exp} \\ \frac{C_{1\infty}h_1 + C_{2\infty}(h_{exp} - h_1)}{h_{exp}} & ; \text{if } h_{exp} > h_1 \end{cases} \quad (\text{g/m}^3) \quad (18)$$

where we have assumed that the entrained concentration is the same as the concentration in the inhalation zone, which has been experimental verified by Brohus&Nielsen (Brohus, 1996a).  $h_{exp}$  is the height to the inhalation zone (exposure). The contaminant removal efficiency in the inhalation zone can now be calculated as:

$$\varepsilon_{exp}^C = \frac{C_{2\infty} - C_s}{C_{exp} - C_s} \quad (-) \quad (19)$$

### 3 COMPARISON WITH EXPERIMENTAL DATA

#### 3.1 Experimental test cases

Data from 14 experimental cases (14) have been taken from the literature to evaluate the contaminant models. Data sets for evaluation of the contaminant model have been taken from Mattson (Mattson, 1999): three office cases and two classroom cases; Heiselberg& Sandberg (Heiselberg, 1990): five office cases; and from Brohus& Nielsen (Brohus, 1996a): four meeting room cases. The different cases are shortly described in table 1.

Table 1: Description of the test cases used in the evaluation of the contaminant model.

Case	First author	Type of room	Heat sources	Heat load	Flow rate	Floor area/ceil.height
1	Mattson	Office	Thermal manikin, PC, ceiling light	295 W	20,9 l/s	15,1 m <sup>2</sup> /2,5 m
2	Mattson	Office	Thermal manikin, PC, ceiling light	395 W	20,9 l/s	15,1 m <sup>2</sup> /2,5 m
3	Mattson	Office	Thermal manikin, PC, ceiling light	395 W	36,6 l/s	15,1 m <sup>2</sup> /2,5 m
4	Heiselberg	Office	Heated slender cylinder	600 W	10,6 l/s	15,1 m <sup>2</sup> /2,5 m
5	Heiselberg	Office	Heated slender cylinder	600 W	21,1 l/s	15,1 m <sup>2</sup> /2,5 m
6	Heiselberg	Office	Heated slender cylinder	600 W	31,4 l/s	15,1 m <sup>2</sup> /2,5 m
7	Heiselberg	Office	Heated slender cylinder	600 W	41,9 l/s	15,1 m <sup>2</sup> /2,5 m
8	Heiselberg	Office	Heated slender cylinder	600 W	52,5 l/s	15,1 m <sup>2</sup> /2,5 m
9	Brohus	Meet.room	Thermal manikins, point source	771 W	40,3 l/s	48 m <sup>2</sup> /4,0 m
10	Brohus	Meet.room	Thermal manikins, point source	771 W	40,3 l/s	48 m <sup>2</sup> /4,0 m
11	Brohus	Meet.room	Thermal manikins, point source	381 W	80,6 l/s	48 m <sup>2</sup> /4,0 m
12	Brohus	Meet.room	Thermal manikins, point source	381 W	80,6 l/s	48 m <sup>2</sup> /4,0 m
13	Mattson	Classroom	Person simulators, ceiling light	2900 W	191 l/s	60,5 m <sup>2</sup> /3,0 m
14	Mattson	Classroom	Person simulators, ceiling light	2900 W	117 l/s	60,5 m <sup>2</sup> /3,0 m

COMMENT: In the cases of Heiselberg& Sandberg (cases 4-8), the convective air flow rates around the heated cylinder are measured and not calculated values. For all other cases the convective air flow induced by heat sources are calculated.

### 3.2 Results and discussion

Fig. 2 shows the height of zone 1 (the clean zone), also called the stratification height or the height of the stationary front. The predicted height of zone 1 is calculated after equation (1). Higher ventilation air flow or down draught air flow raises the height of zone 1, while higher convective air flows induced by heat sources lower the height of zone 1. The measured height of zone 1 is defined as the height where the concentration is 50% of the concentration in the extract, as proposed by Heiselberg & Sandberg (Heiselberg, 1990). The predicted and measured heights of zone 1 seem to follow each other for the different cases quite well. Only in case 2 (the office case of Mattson) is there a significant under-prediction. But in this case the measured height of zone 1 is uncertain due to few measuring points for the concentration (based on a linear interpolation), and could in reality be much closer to the predicted value.

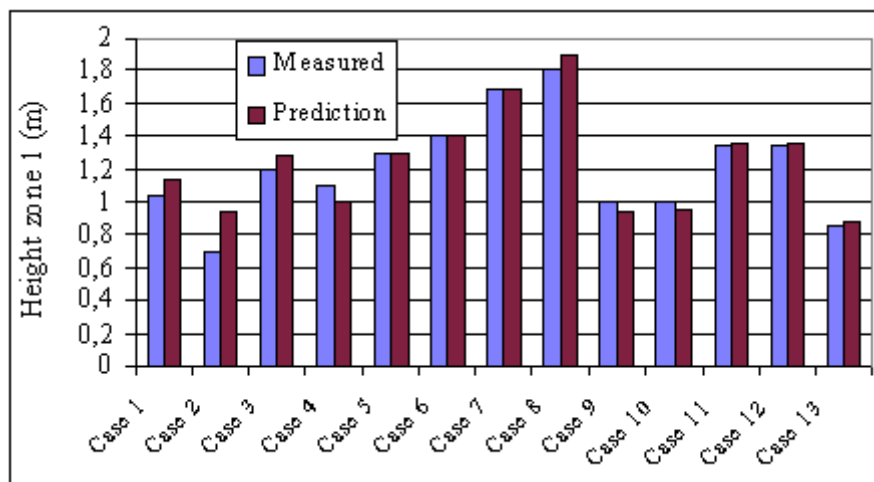


Figure 2: Comparison of predicted and measured height of zone 1.

Fig. 3 shows the contaminant removal efficiency for the complete room. The predicted values calculated after equation (16). This index shows the ability of the ventilation systems to remove contaminants from all points in the room under steady state conditions. The measurements and predictions are close for all the compared cases.

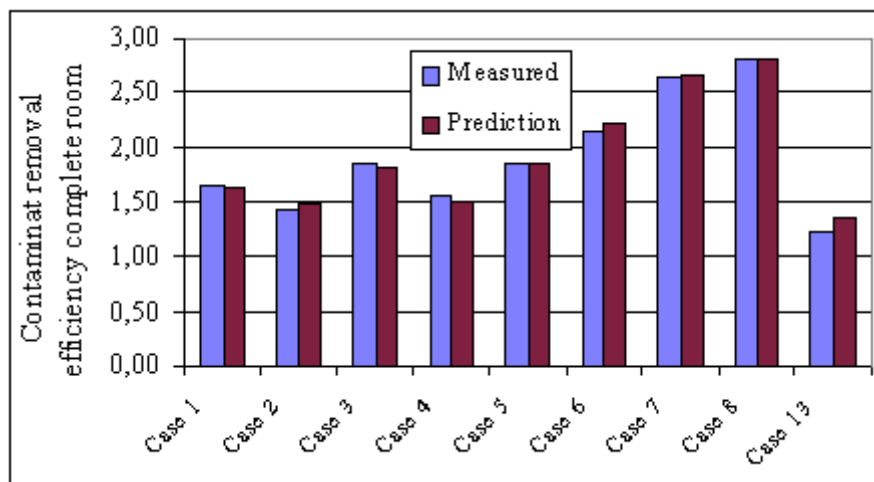


Figure 3: Comparison of predicted and measured contaminated removal efficiency for the complete room

Fig. 4 shows the contaminant removal efficiency for the occupation zone. The predicted values calculated after equation (17). This index shows the ability of the ventilation systems to remove contaminants from the occupation zone. The predicted efficiency is very close to the measured value in all cases.

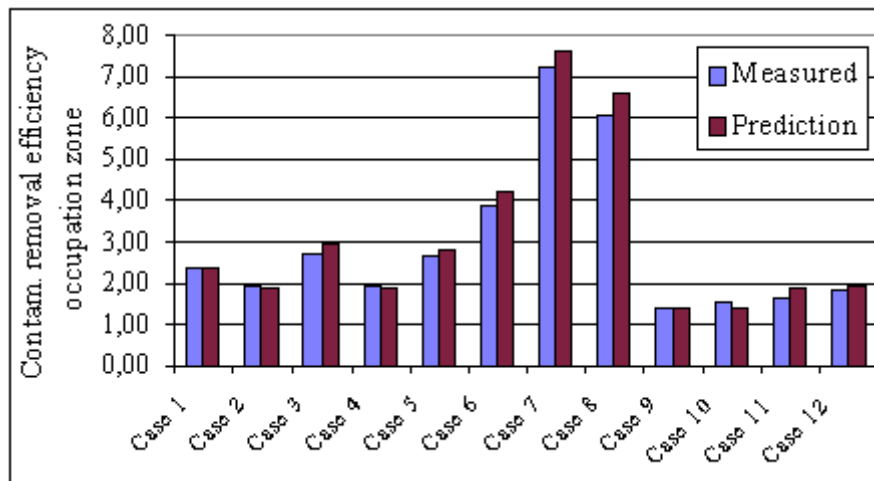


Figure 4: Comparison of predicted and measured contaminant removal efficiency in the occupation zone.

Fig. 5 shows the contaminant removal efficiency in the inhalation zone for the cases with seated persons (person simulators). This efficiency shows the ventilation systems ability to provide clean air to the occupants. A high efficiency value means that the concentration to which the occupant is exposed is low compared to the concentration in the extract. The comparison shows that the model under-predicts the measured efficiency, especially for case 3 (office case). In case 3 the air in the inhalation zone is almost as clean as the supply air, which implies that the air in the boundary layer around the person is entrained from the clean air layer at floor level. In our model (eq.18), which on this point is similar to the model proposed by Brohus & Nielsen (Brohus, 1996a), it is assumed that the air in the human boundary layer is entrained evenly from all heights up to the height of the inhalation zone. Cases 9, 11 and 13 in Fig. 5, seems to correspond well to this assumption, but also in case 2 (office case) the air in the inhalation zone is substantially better than predicted by the model. However, the model gives in all cases a conservative estimate of the air quality in the inhalation zone. If the contaminant removal efficiency in the inhalation zone is to be used for design of DV-systems and determining the necessary air flow rates it is preferable that the model under-predicts the efficiency to be on the safe side (conservative).

Fig. 6 shows the contaminant removal efficiency in the inhalation zone for standing persons. Compared to seated persons, the inhalation zone for standing persons is often located high into the polluted zone (zone 2), and one would expect that the efficiency was lower in these cases. This holds true for cases 2 and 3, where both the efficiency for seated and standing persons are measured. The efficiency for the seated persons are much higher than for the standing persons. The model under-predicts the efficiency substantially for cases 1 and 3, but predicts quite closely for the other cases (2, 10, 12). The reason for under-prediction in cases 1 and 3, could be due to the fact that zone 1 is relatively high in these cases, and that the human boundary layer is therefore entraining air to the inhalation zone mostly from the clean zone (zone 1).

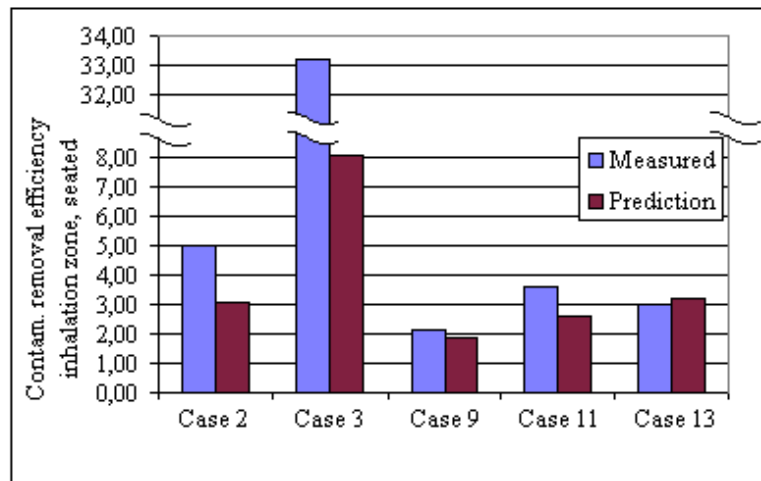


Figure 5: Comparison of predicted and measured contaminant removal efficiency in the inhalation zone, seated persons

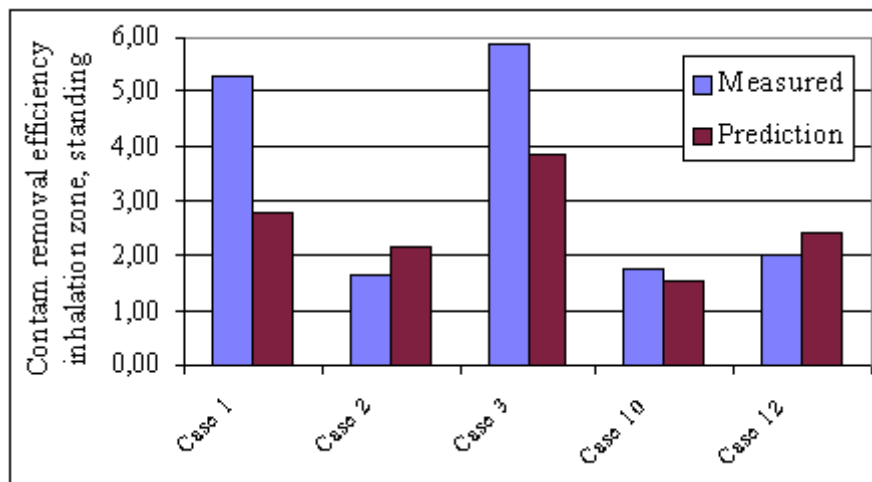


Figure 6: Comparison of predicted and measured contaminant removal efficiency in the inhalation zone, standing persons

#### 4 CONCLUSIONS AND FURTHER WORK

The evaluation of the proposed contaminant model is very promising for most of the variables compared, where model prediction is close to the measured values. However, experimental results for indices measuring air quality in the inhalation zone is better than the predicted values. This under-prediction is conservative if the models are to be used for design of DV and determining necessary ventilation air flow rates.

If the models is to be used for design, it should also be compared to results from more “real life” experiments with e.g. moving people and different “non-ideal” settings, like furniture placed in front of DV-supply vents. Such experiments has currently been undertaken and will be reported in the future.

## 5 ACKNOWLEDGEMENTS

This work has been supported by the Research Council of Norway and several partners through the Research and Development project “Naturligvis”, grant number 245435.

## 6 REFERENCES

- Elisabeth Mundt (Mundt, 1996), “The performance of displacement ventilation systems; Experimental and Theoretical studies”, Ph.D. thesis, Royal Institute of Technology, Stockholm 1996.
- Mattson M. (Mattson, 1999); “On the efficiency of displacement ventilation” Ph.D. thesis, Royal Institute of Technology, Gavle, Sverige 1999.
- Brohus H., Nielsen P.V. (Brohus, 1996a) “Personal Exposure in Displacement Ventilated Rooms”, *Indoor Air* 6/96, pp.157-167. Munksgaard 1996.
- Holmberg.R.B. et. al.(Holmberg, 1990), “Inhalation-zone air quality provided by displacement ventilation”. *Proceedings Roomvent '90*, Oslo Norway. 1990.
- Hatton A., Awbi H.B. (Hatton, 1998), “A study of the air quality in the breathing zone” *Proceedings ROOMVENT '98* Stockhom, Sweden, Vol.2, pp. 159 – 166.
- Ørhede E., Breum N.O., Skov T.,(Ørhede, 1996) “Percieved and Measured Indoor Climate with Dilutionversus Displacement Ventilation : an Intervention Study in a Sewing plant”, *Indoor Air* 6/96,pp. 151-156. Munksgaard 1996.
- Brohus H. et.al.,(Brohus, 1996)“Perceived air quality in a displacement ventilated room”, *Proc. Indoor Air'96* Nagoya, Japan, Vol.1, pp. 811-816. 1996
- Skåret E. (Skåret, 2000), “Ventilasjonsteknisk handbook” Håndbok 48, Byggforsk, 2000 (In Norwegian)
- Koganei M., Holbrook G.T., Olesen B., Woods J. (Koganei, 1993)“Modelling the thermal and indoor air quality performance of vertical displacement ventilation”. *Proceedings of Indoor Air '93*, Helsinki, Vol. 5, pp. 241-426.
- Jacobsen T.V.& Nielsen P.V.,(Jacobsen, 1993)“Numerical modelling of thermal environment in a displacement ventilated room”. *Proceedings Indoor Air '93* Helsinki Finland.
- Dokka TH, “Modelling of Indoor Air Quality inresidential and commercial buildings”, Doctoralthesis, Norwegian University of Science and Technology, Trondheim 2000
- Dokka T.H., Tjelflaat P.O. (Dokka, 2001) A simplified model for for human induced convective air flows – model prediction compared to experimental data”.*Proceedings of the 4th International Conference on IAQ, Ventilation & Energy Conservation in Buildings (IAQVEC 2001)*, Vol 2, Changsha, PRC, October 2001
- Heiselberg P., Sandberg M.,(Heiselberg, 1990) “Convection from a slender cylinder in a ventilated room”, *Proceedings Roomvent '90*, Oslo Norway. 1990.

# Study of variants to classical mechanical exhaust ventilation systems by using mechanical exhaust in habitable rooms

Ivan Pollet<sup>\*1,2</sup>, Anneleen Vens<sup>1</sup>, Frederik Losfeld<sup>1</sup> and Xavier Faure<sup>3</sup>

*1 Renson  
Maalbeekstraat 10  
Waregem, Belgium*

*\*Corresponding author: ivan.pollet@renson.be*

*2 Ghent University  
Department of Biosystems Engineering  
Coupure Links 653  
Ghent, Belgium*

*CEA tech  
5, rue de l'Halbrane  
Bouguenais, France*

## ABSTRACT

Nowadays, due to the higher energy performance of dwellings, ventilation plays an increasing role in maintaining a good indoor comfort. Therefore new ventilation strategies in combination with demand controlled ventilation are needed to accomplish high energy-efficient ventilation (limiting ventilation losses and auxiliary energy consumption) while providing good indoor air quality, thermal and acoustic comfort.

The classic ventilation approach of mechanical extract is based on air supply in the living rooms which is transferred towards the wet or functional rooms where the air is extracted. In this paper a modification on this principle is presented with natural air supply in the living rooms and mechanical extraction in bedrooms (night zone) or each room.

By means of different simulation studies the performance of these ventilation strategies combined with demand controlled is compared in terms of indoor air quality and average air flow rates according to different national methodologies (Belgium and France). The evaluation of the indoor air quality is based on the exposure to CO<sub>2</sub> and relative humidity in the rooms.

Besides simulations, results of an in-situ measurement campaign of a ventilation system according to the modification are presented.

It is found that by applying the modified ventilation strategies a remarkable better indoor air quality and even a more energy efficient ventilation -compared to the classic ventilation approach- can be achieved.

## KEYWORDS

Demand controlled ventilation, extraction from habitable rooms, simulation, in-situ measurement

## 1 INTRODUCTION

On continent Europe, demand controlled ventilation (DCV) as well as heat recovery (HR) are usually applied to realize energy efficient mechanical ventilation systems (MV). For the moderate climate zone of Western Europe, with about 2500–3000 heating degree days, the payback time for investments in heat recovery ventilation is long, especially in buildings with relatively low air change rates such as dwellings. Due to its competitive price setting, low electricity cost as well as due to reports in popular media and scientific literature about possible health risks associated with heat recovery systems, simple central MEV dominates the residential ventilation market in this region. The great variability of a dwelling occupancy

in time and place, enhances the potential of DCV. By applying DCV, heating energy related to ventilation is reduced by 20 to 50%, while electricity consumption is similarly reduced (Pollet, et al., 2013).

The critical zones with respect to IAQ within the dwelling are the bedrooms, due to its long occupancy period and limited volume, enforced by possible small air flow rates caused by noise complaints or low pressure levels. Adding a mechanical extraction to these habitable rooms equipped with natural air supply (in case of MEV systems) could improve IAQ. The aim of this paper is to assess theoretically as well as experimentally, the energy saving potential and the indoor air quality (IAQ) to which the occupants of the dwelling are exposed when applying a DCV system consisting of natural air supply and mechanical extract from each room, compared to normative demand controlled MEV systems which only extract in the wet rooms. The impact of mechanical extraction in the living room instead of natural supply was also analysed. The theoretical comparison is done in a Belgian and French context.

## 2 SYSTEM DESCRIPTION

The demand controlled systems considered were (see Figure 1):

- (REF) natural air supply in all habitable rooms and demand controlled mechanical extraction in wet rooms
- (1) natural air supply in all habitable rooms and demand controlled mechanical extraction in each room (both wet and habitable)
- (2) natural air supply only in the bedrooms (night zone) and demand controlled mechanical extraction in each room (both wet and habitable)

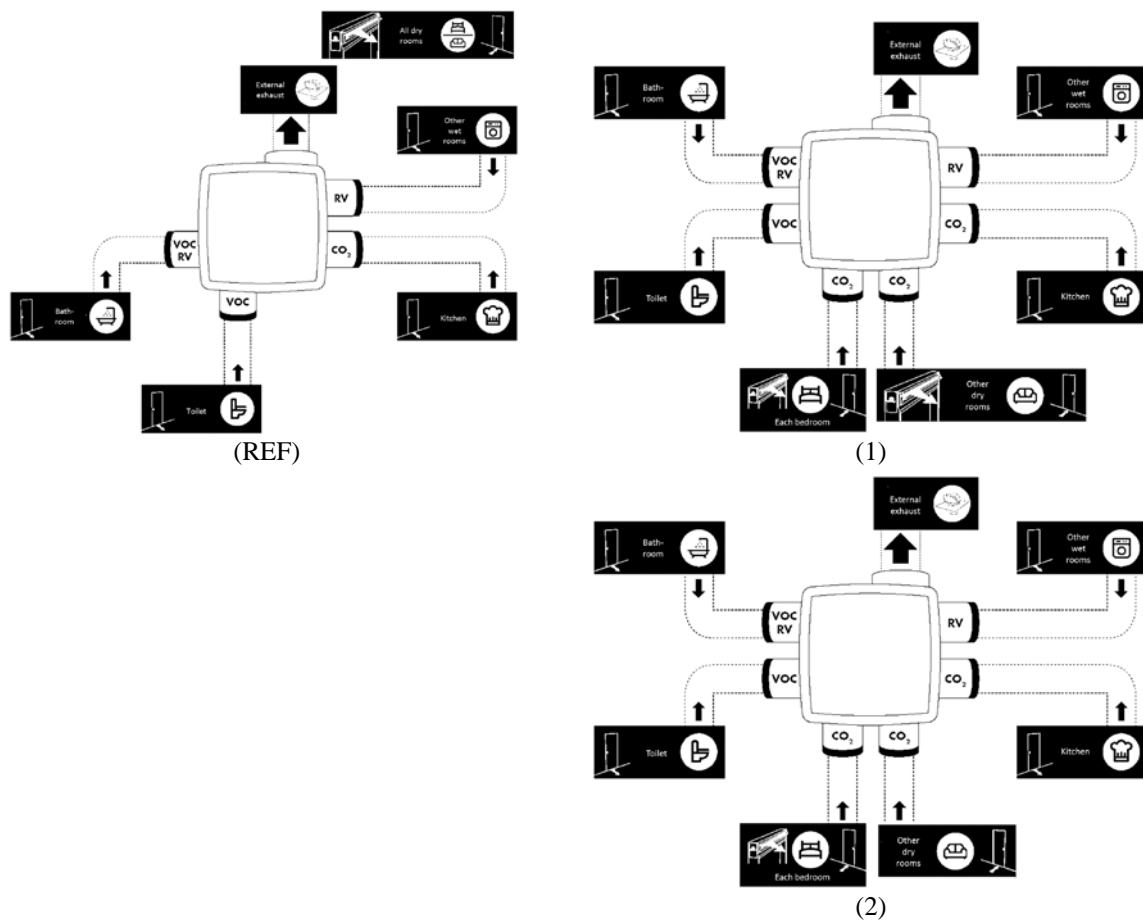


Figure 1: Considered ventilation systems (sensors for Belgium)

### 3 METHODS

#### 3.1 Simulations

The different ventilation systems were simulated in the national indicated softwares and the IAQ performance was checked according to the national criteria (see Table 1).

Table 1: Country specific parameters

	<b>Belgium</b>	<b>France</b>																				
Software	Contam	MATHIS or TRNSys-Contam																				
CO <sub>2</sub> criterion	[ppm.h cumulative] Base: Δ600 ppm Threshold: 100.10 <sup>3</sup> ppm.h per person	[ppm.h per room] Base: 2000 ppm Threshold: 400.10 <sup>3</sup> ppm.h per room																				
CO <sub>2</sub> control	Δ400 – 600 ppm for q <sub>min – max</sub> = 3 – 30 m <sup>3</sup> /h  3 bedroom detached single family house with a pressure controlled 2 Pa air inlet	1600 - 2000 ppm for q <sub>min – max</sub> = 1 – 30 m <sup>3</sup> /h  3 bedroom detached single family house (F3) with a humidity controlled 20 Pa air inlet (hygro B)																				
CO <sub>2</sub> control in case of inversion study		<table border="1"> <thead> <tr> <th></th> <th>&lt;1000</th> <th>&gt;1000</th> <th>&gt;1500</th> <th>&gt;2000 ppm</th> </tr> </thead> <tbody> <tr> <td>1</td> <td>0</td> <td>0</td> <td>0</td> <td>5 m<sup>3</sup>/h</td> </tr> <tr> <td>2</td> <td>0</td> <td>0</td> <td>5</td> <td>10 m<sup>3</sup>/h</td> </tr> <tr> <td>3</td> <td>0</td> <td>5</td> <td>10</td> <td>15 m<sup>3</sup>/h</td> </tr> </tbody> </table>		<1000	>1000	>1500	>2000 ppm	1	0	0	0	5 m <sup>3</sup> /h	2	0	0	5	10 m <sup>3</sup> /h	3	0	5	10	15 m <sup>3</sup> /h
	<1000	>1000	>1500	>2000 ppm																		
1	0	0	0	5 m <sup>3</sup> /h																		
2	0	0	5	10 m <sup>3</sup> /h																		
3	0	5	10	15 m <sup>3</sup> /h																		

Air flow rates were compared to reference ventilation systems. Furthermore, possible reserve flow of indoor air to the habitable rooms was investigated. Generally, and especially in France, regulation states that the air circulation must appear fundamentally from the habitable rooms to the wet rooms. Therefore, the reverse air flow rate through the doors and/or the origin of the air that flows to the wet rooms were investigated. This research was done by reproducing the MATHIS hypotheses in a TRNSys-CONTAM coupling. Three different CO<sub>2</sub> control strategies in the bedroom were analysed as listed in Table 1. The output was the frequency of inverted air flow through the bedroom doors.

#### 3.2 In-situ measurements

In a 4 bedroom detached single family house in Belgium equipped with a demand controlled MEV system, CO<sub>2</sub> measurements were carried out in the main bedroom (2 persons). Bedrooms were equipped with a CO<sub>2</sub> controlled mechanical extract in addition to the natural supply. During the first week the extract ventilation rate in the main bedroom was proportionally controlled on CO<sub>2</sub> between 800 and 1000 ppm for minimum and maximum air flow rates of 3 and 30 m<sup>3</sup>/h respectively. During the second week the extract ventilation in the bedrooms was switched off to compare with a reference MEV system.

## 4 RESULTS

### 4.1 Simulations

In any of the simulations performed, the relative humidity levels in the wet rooms complied with the national criteria set for those rooms. The results of the Belgian simulations are shown in Figure 2 where the IAQ is traded off against the ventilation losses for the three ventilation strategies considered. It is clear that

- Extracting from habitable rooms (1) and (2) has a positive impact on the IAQ compared to the reference system, since  $\text{CO}_2$  exceeds above  $\Delta 600$  ppm are negligible.
- When there is no natural air supply present in the living room (2) IAQ stays excellent due to the mechanical extract in the living room and the air transfer from the (unoccupied) bedrooms with natural air supply. Moreover, due to more air transfer rates in the dwelling, the ventilation losses are smaller compared to (1).

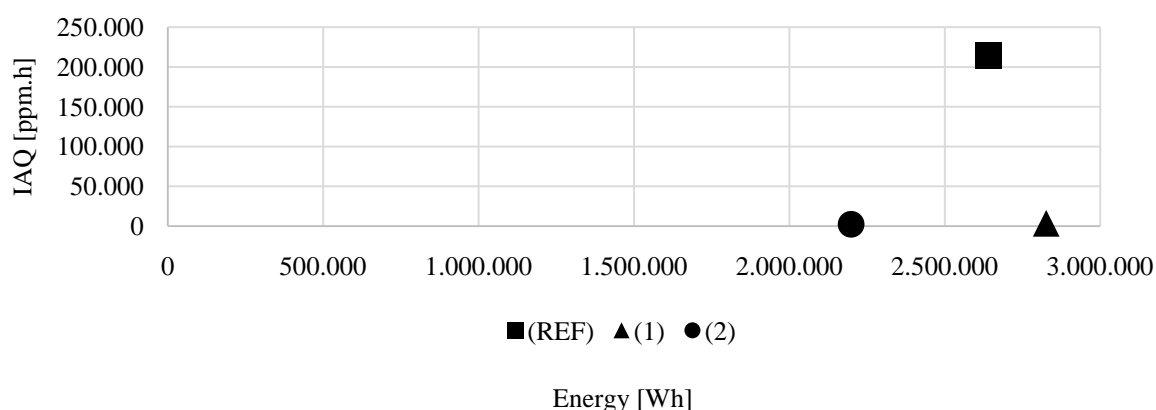


Figure 2: Belgium

The results of the French simulations are summarized in Table 2. Cumulative exposure to  $\text{CO}_2$  concentrations above 1200 and 2000 ppm are listed. Bearing in mind that the  $\text{CO}_2$  is controlled on a threshold of 2000 ppm, the exposures to levels above 1200 ppm are quite high. Due to the extraction directly from the bedrooms (and not from the living room), cumulative exceeds of 2000 ppm  $\text{CO}_2$  are not found in contrast to the reference system, similar to the effects found in the Belgian simulations. However, the cumulative exceeds of 1200 ppm are even higher with extraction from the bedrooms. This can be explained by a humidity controlled extraction from the wet rooms at lower mean air flow rates for configuration 1 compared to the reference (as simulated).

Table 2: France [kppm.h]

	<b>CO<sub>2</sub> threshold</b>	<b>Living room</b>	<b>Room 1</b>	<b>Room 2</b>	<b>Room 3</b>
(REF)	1200 ppm	1375	1752	1408	0
	2000 ppm	0	283	170	0
(1)	1200 ppm	1662	2168	3349	0
	2000 ppm	122	0	0	0

The average air flow rate in case of extraction from the habitable rooms was not necessarily higher than in the reference case, due to smart controlled ventilation according to the needs.

The results of the examination of the inverted air flow rate through the bedroom doors in France are summarized in Table 3 for different controlled strategies of the bedroom extraction

(no living room extraction). It shows the percentage of time inverted air flow rates are observed.

Table 3: Inverted air flow frequency

	Bedroom door 1		Bedroom door 2	
	All time	Occupied	All time	Occupied
(REF)	1.0	0.6	1.8	1.2
(1) 1 threshold	3.2	0.7	4.2	2.2
(1) 2 thresholds	3.9	2.0	4.5	2.3
(1) 3 thresholds	4.3	2.7	5.8	4.3

The augmented percentages in the case of (1) are also associated with higher cumulative flows due to extract from the bedrooms. In the reference case inversions also occur due to wind and thermal effects that are higher than the mechanical extract forces. Adding extract in the bedrooms implies an inversion part induced by the mechanical extract in the bedroom. However, the level of reversed flow is limited and can be restricted by adjusting the total extract rate from the wet rooms compared to the one from the bedrooms. In any case the instantaneous total extract from wet rooms should be higher than the extract rate from bedrooms to restrict backflow.

It's important to note that at the wet and functional rooms, there is no inversion at all. Pollution risk from toilets, bathroom or kitchen is not present. Moreover the inversions occur -as for the reference- only when the humidity and as a consequence the air flow rate in the wet rooms is low. It was also found that when a CO<sub>2</sub> controlled extraction is present in any habitable room, living rooms as well as bedrooms, negligible CO<sub>2</sub> loaded reversed air flow rate will occur.

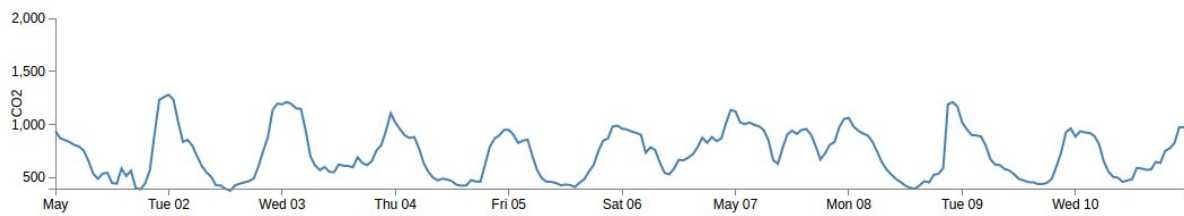
As a conclusion about the occurrence of reversed flow one can state:

- An increase in inversions, depending on the extraction in the wet rooms compared to the bedrooms, is observed.
- Frequency of occurrence remains low (below 6%) for this housing configuration, compared with 2% for the base case, or even less than 4.5% compared with just under 1% during occupation.
- The inversions are observed systematically for low relative humidity in the wet rooms.
- There is no evidence of inversion in the wet rooms.
- The inversions make more use of the air inlets of the living room and permeability of the common rooms (living room and hall).
- Extraction in any habitable and wet room, also prevents inversion at the transfer openings of doors.

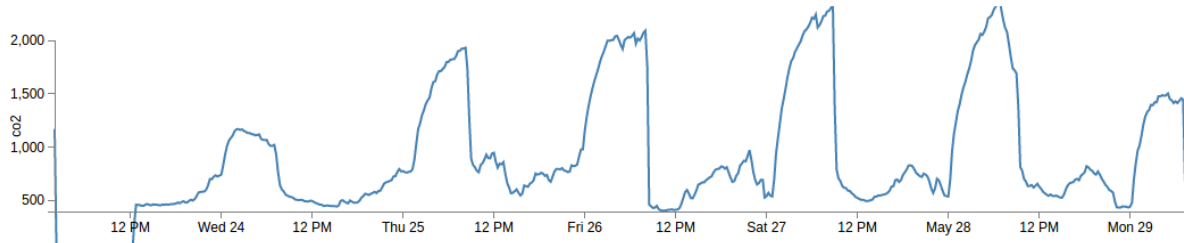
If mechanical extraction is present in the habitable room, the natural supply in this habitable room can be dimensioned smaller, with consequences on thermal as well as acoustic comfort. In that way, high performance MEV systems can be designed.

**4.2 In-situ measurements**

Measurement results in a 2 person bedroom equipped with CO<sub>2</sub> controlled extract are plotted on Figure 3. CO<sub>2</sub> concentrations never exceed 1200 ppm and decrease to outdoor concentration during inoccupancy. When the natural air supply is closed and the extract ventilation is turned off each night the CO<sub>2</sub> concentrations exceed 2000 to 2500 ppm (excepts for the first night when only one person was present in the bedroom).



(a) with natural air supply and mechanical extract ventilation



(b) without natural air supply and without mechanical extract ventilation

Figure 3: CO<sub>2</sub> concentration in 2 pers. bedroom

## 5 CONCLUSIONS

Based on 2 building simulation tools of Belgium and France, an improved mechanical extract ventilation system with extraction from bedrooms (or all habitable rooms) showed better performance concerning IAQ in the habitable rooms, while mean air flow rates are similar to the reference case due to smart ventilation. Simulation tools provide the evidence to recognize innovative concepts within energy performance regulations.

## 6 REFERENCES

Pollet, I. et al., 2013. Performance of demand controlled mechanical extract ventilation system for dwellings. *Journal of sustainable engineering design*, 1(3).

# The effectiveness of mechanical exhaust ventilation in dwellings

Romy Van Gaever\*<sup>1</sup>, Jelle Laverge<sup>2</sup> and Samuel Caillou<sup>1</sup>

*1 Belgian Building Research Institute (BBRI)  
Avenue P. Holoffe 21  
Limelette, Belgium*

*2 Ghent University (UGent)  
Sint Pietersnieuwstraat 41  
Ghent, Belgium*

*\*Corresponding author: romy.van.gaever@bbri.be*

## ABSTRACT

Ventilation systems play an important role in providing a good indoor air quality in dwellings. Mechanical exhaust ventilation systems implement natural vents to supply outdoor air to the dwelling. Natural driving forces, i.e. wind and thermal draught, influence the flow rates through these supply vents. Therefore, the flow rates depend on the weather conditions and vary in time. This study considers the influence of the wind and thermal draught on the operation of a mechanical exhaust ventilation system in a reference dwelling. Furthermore, the influence of the sizing of the natural vents and the airtightness of the dwelling envelope are taken into account. This paper covers a simulation study investigating the effects of wind, thermal draught, the sizing of the natural vents and the building airtightness on the flow rates in the dwelling by using multizone airflow and contaminant transport calculation software (Contam). Wind and thermal draught create a spread on the supply flow rates. Therefore, the flow rates through the vents are not always as designed. The airtightness also influences the flow rate through the vents. Both effects (wind/thermal draught and airtightness) depend largely on the sizing of the natural vents.

## KEYWORDS

Mechanical exhaust ventilation, flow rates, IAQ, Airtightness

## 1 INTRODUCTION

Mechanical exhaust ventilation systems (called systems C in this paper) supply outdoor air to the dwelling by using natural supply vents and extract the indoor air from the dwelling with a mechanical ventilator (AIVC, 1996). The natural supply vents are openings in the building envelope designed for a specific airflow rate at a specific pressure difference. Currently, the Belgian standard NBN D50-001 (1991) defines the flow rate of a fully opened natural supply vent at a pressure difference of 2 Pa. Supply vents can also be self-regulating to prevent overventilation at high wind pressures. Self-regulating vents respond to the wind pressure and reduce the airflow through the supply vents by closing a valve when the wind pressure exceeds a predefined pressure, e.g. the design pressure. In Belgium, these self-regulating vents are classified into 5 categories, i.e. P0 (non-self-regulating) to P4, each with specific characteristics for the pressure profile of the closing valve (NBN EN 13141-1: 2004).

The actual pressure differences over the supply vents fluctuate in time due to natural driving forces, i.e. wind and thermal draught. Therefore, the actual supply flow rates through the vents vary in time depending on the weather conditions.

However, the mechanical extraction ensures a specific extraction rate in the dwelling and as a result the same airflow rate must enter the dwelling. The air flow can enter the dwelling through the natural supply vents but also through the cracks in the building envelope. Due to

the natural forces and the airtightness of the dwelling, the flow rates through the vents and the flow paths through the dwelling are not always as designed, depending on the sizing of the vents.

This paper discusses the influence of the wind and thermal draught on the airflow rate through the natural vents by taking the sizing of the natural vents and the airtightness of the dwelling envelope into account. This influence is investigated based on multi-zone flow rate simulations in CONTAM

**2 METHODS**

The simulation study uses multi-zone airflow and contaminant transport calculation software CONTAM to determine the airflow through the natural vents in two reference dwellings.

The first reference dwelling used in this study represents a one-storey detached, three-bedroom house with a total living area of 117 m<sup>2</sup> (Figure 1).

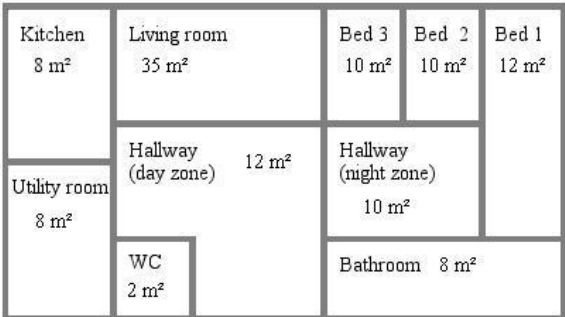


Figure 1: the one-storey dwelling is one of the two reference dwellings used in this study

The second dwelling is a two-storey detached, three-bedroom house with the same total living area as the one-storey reference dwelling. The day zone (living room, kitchen, utility room, WC, entranceway) is located downstairs and the night zone (bedrooms, bathroom, hallway) upstairs (Figure 2).

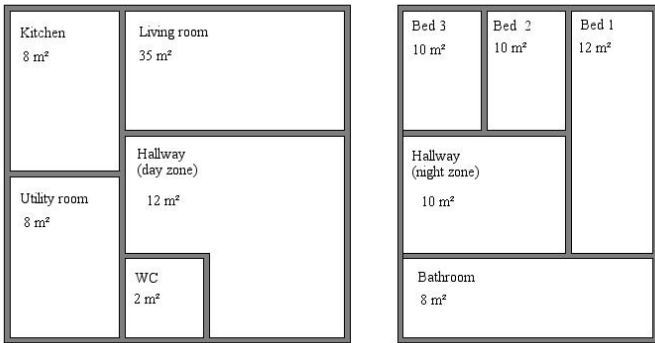


Figure 2: the two-storey dwelling, with the day zone downstairs and the night zone upstairs, is the second reference dwelling used in this study.

The design airflow rate for each room in these dwellings is calculated based on 7 l/s.person (Class II NBN EN 15251). The supply and extraction airflows are balanced.

Both dwellings are equipped with a system C. This systems implements natural supply vents in the living room and bedrooms. The sizing of these vents varies throughout the study:

	<b>Living room</b>	<b>Bedroom 1</b>	<b>Bedroom 2/3</b>
1	100 m <sup>3</sup> /h @ 2 Pa	50 m <sup>3</sup> /h @ 2 Pa	25 m <sup>3</sup> /h @ 2 Pa
2	100 m <sup>3</sup> /h @ 10 Pa	50 m <sup>3</sup> /h @ 10 Pa	25 m <sup>3</sup> /h @ 10 Pa
3	100 m <sup>3</sup> /h @ 20 Pa	50 m <sup>3</sup> /h @ 20 Pa	25 m <sup>3</sup> /h @ 20 Pa

The natural supply vents used in this study are both self-regulating (class P3), namely the supply vents @ 2 Pa and non-self-regulating (class P0), namely the supply vents @ 10 Pa and @ 20 Pa. The design flow rates of self-regulating vents of class P3 occur at 2Pa while by closing the valve the flow rate at 4.5 Pa is maximum 1.5 times the flow rate at 2 Pa. The non-self-regulating vents of class P0 don't include a closing valve.

The airtightness, defined as the airflow through the dwelling envelope per m<sup>2</sup> at a pressure difference of 50 Pa (air permeability q<sub>50</sub>), also varies throughout the study(Belgian Building Research Institute (BBRI), 2015):

Airtightness 1	+/- airtight
Airtightness 2	1 m <sup>3</sup> /h.m <sup>2</sup>
Airtightness 3	3 m <sup>3</sup> /h.m <sup>2</sup>
Airtightness 4	6 m <sup>3</sup> /h.m <sup>2</sup>

To transfer the air from one room to another, air flows through internal openings. Four different internal transferscenarios are implemented:

Internal transfer 1	Closed doors with transfer grilles and closed staircase
Internal transfer 2	Closed doors with transfer grilles and open staircase
Internal transfer 3	Open doors and closed staircase
Internal transfer4	Open doors and open staircase

The internal transfer openings are simulated as follows:

Transfer openings in closed doors with flow coefficients (C) accordingly to the design flow rate of the transfer opening, e.g.  $C = 0.00593037 \text{kg/s/Pa}^n$  for a transfer opening of 25 m<sup>3</sup>/h @ 2Pa and a flow exponent  $n = 0.5$ . Open doors with flow coefficients of  $C = 1 \text{ m}^3/\text{s/Pa}^n$  and a flow exponent  $n = 0.5$ .

The hourly Test Reference Year Uccle is used to determine the outdoor conditions. This file contains, among other parameters, the wind speed, the wind direction and the outdoor temperature of an entire 'reference' year in Uccle. The indoor temperature is 18°C. The simulation reporting time is set to each minute, corresponding to the simulation time step.

The airtightness is simulated by 2 cracks in the outer wall of each room. The first crack is located at ¼ of the height of the wall and the second at ¾. The in-/exfiltration rate through each crack is determined according to the surface area that each cracks represents (uniform airtightness/air permeability). The in/exfiltration rate through the roof is evenly divided over the cracks in the walls.

### 3 RESULTS AND DISCUSSION

The simulation results show the influence of wind, thermal draught, the building airtightness and the sizing of the natural supply vents on the airflow rate through the natural vents or in other words on the effectiveness of a system C.

Following three schemes are investigated:

1. No wind, no thermal draught in an airtight and a leaky building
2. Influence of wind and thermal draught in an airtight building
3. Influence of wind and thermal draught in a leaky building

To clearly show the simulation conditions of each scheme, a table summarizes these conditions for each presented result.

#### 3.1 No wind and no thermal draught in an airtight and a leaky building

The simulations investigate the influence of the sizing of the natural supply vents on the airflow rate in both an airtight and a leaky dwelling without the influence of the weather conditions, i.e. no wind and no thermal draught (Figure 3). Thereby, the flow rate through the vents only depends on the mechanical extraction rate of the ventilation system.

Simulation conditions	
Dwelling	Reference dwelling 1 (one-storey)
Airtightness	Airtight Leaky: 1 m <sup>3</sup> /h.m <sup>2</sup> , 3 m <sup>3</sup> /h.m <sup>2</sup> , 6 m <sup>3</sup> /h.m <sup>2</sup>
Outdoor conditions	Steady state: no wind, no thermal draught
Size natural supply vent	P3@ 2 Pa, P0@ 10 Pa, P0@ 20 Pa
Internal resistance	Closed doors

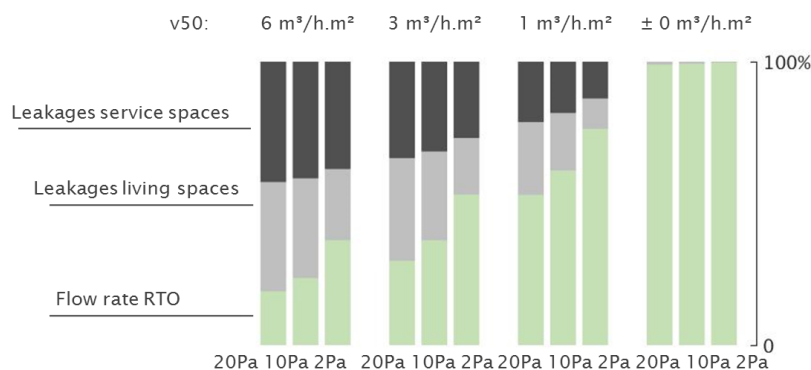


Figure 3: This figure represents the percentages of the total supply flow rate through the natural vents (RTO) (light green), through the leakages in the building envelope in the living spaces (light grey) and through the leakages in the service spaces (dark grey) for different levels of airtightness (increasing airtightness from left to right) and different sizes of natural vents (increasing sizes from left to right).

In an airtight dwelling and given no wind and no thermal draught, the sizing of the supply vents doesn't influence the flow rate of the building. Approximately 100% of the flow rates enters through the vents independent of the size. In a leaky dwelling, the sizing of the supply vents influences the flow rate through the supply vents. In a leaky dwelling, air will enter through the vents but also through the leakages in the building envelope. The lower the airtightness of the dwelling, the more air will enter through the leakages. Furthermore, a lower airtightness leads to a lower total supply flow rate (vents + leakages) in the living spaces but additional supply flow rate in the service spaces. Smaller vents (10 Pa and 20 Pa) enhance both these effects (Figure 3).

### 3.2 Influence of wind and thermal draught in airtight building

The simulations investigate the influence of wind and thermal draught, independently (results not shown), and simultaneously on the flow rate of an airtight dwelling (Figure 4). Furthermore, the influence of the internal transfer openings (Figure 4 and Figure 5) and the sizing of the supply vents is taken into consideration (Figure 6). The flow rate in the dwelling no longer depends solely on the mechanical extraction of ventilation system but also on the outdoor weather conditions.

Simulation conditions	
Dwelling	Reference dwelling 2 (two-storey)
Airtightness	Airtight
Outdoor conditions	Steady state: fixed values for wind speed and direction (results not shown) Steady state: fixed values for thermal draught (results not shown) Transient: TRY Uccle
Size natural supply vent	P3@ 2 Pa (Figure 4 and Figure 5) P0@ 10 Pa (Figure 6)
Internal resistance	Closed doors + closed staircase (Figure 4) Closed doors + open staircase (results not shown) Open doors + closed staircase (results not shown) Open doors + open staircase (Figure 5 and Figure 6)

In an airtight dwelling and due to wind only, the airflow rates through the vents are not as designed (results not shown). The flow rates through the vents in the living spaces at the windward side are higher, while the flow rates in through the vents in the living spaces at the leeward are lower. Leading in some cases, even to reverse airflow rates, i.e. extraction. Due to only thermal draught (results not shown), the flow rates through the vents in the living room on the ground floor are higher, while the flow rates in bedrooms on the first floor are lower for outdoor temperatures <the indoor temperature (18°C). The effect increases with decreasing outdoor temperature. Therefore, the wind and thermal draught are responsible for a flow rate variability.

The results of the simulations with the transient TRY Uccle conditions are presented in a frequency distribution graph, showing the percentage of time when a certain airflow rate occurs.

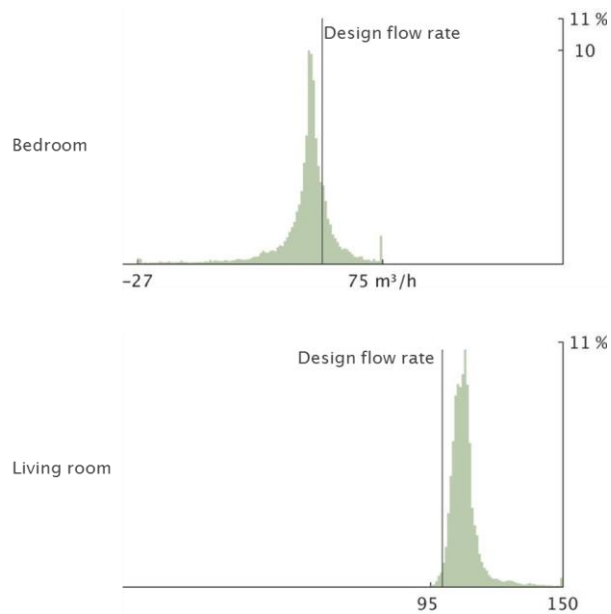


Figure 4: This figure represent the frequency distribution graph of the airflow rates ( $\text{m}^3/\text{h}$ ) through the natural self-regulating vents of 2 Pa in both the living room on the ground floor (bottom) and a bedroom at the first floor (top) of an airtight building with closed doors and a closed staircase (high internal resistance). The design flow rates for the living room ( $100 \text{ m}^3/\text{h}$ ) and bedroom ( $50 \text{ m}^3/\text{h}$ ) are indicated by the vertical line.

In the airtight dwelling, the airflow rates in the living room on the ground floor and in the bedroom at the first floor vary in time and are not as designed. The flow rate in the living room is mostly higher than designed (Figure 4: bottom) and in the bedroom lower than designed. In the bedroom even reversed flow, i.e extraction, occurs sometimes (Figure 4: top).

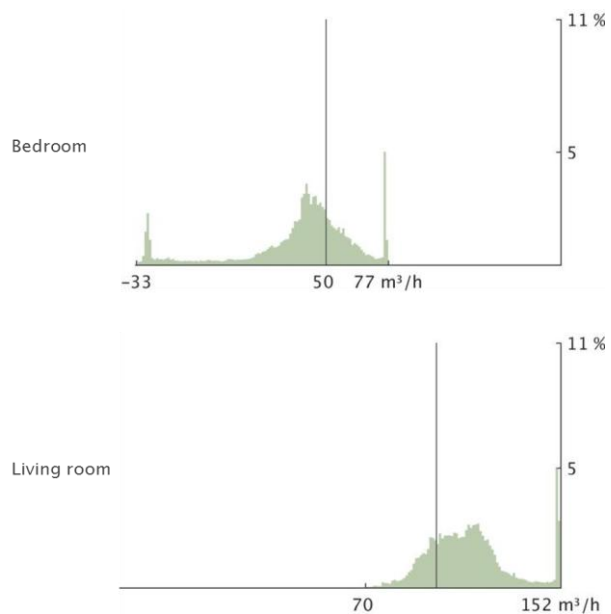


Figure 5: This figure represent the frequency distribution graph of the airflow rates ( $\text{m}^3/\text{h}$ ) through the natural self-regulating vents of 2 Pa in both the living room on the ground floor (bottom) and a bedroom at the first floor (top) of an airtight building with open doors and an open staircase (low internal resistance). The design flow rates for the living room ( $100 \text{ m}^3/\text{h}$ ) and bedroom ( $50 \text{ m}^3/\text{h}$ ) are indicated by the vertical line.

In an airtight building the negative effect of thermal draught is higher with lower internal resistance, i.e. bigger openings (Figure 4 and Figure 5). Therefore, the open doors and open staircase lead to the least controlled airflow rates, i.e. widest distribution and thus the least favourable scenario. The following simulations all implement this scenario as it is the most negative. A narrower distribution occurs at high internal resistance, meaning closed doors and a closed staircase with transfer openings (internal transfer scenario 1) lead to more controlled airflow rates closer to the design flow rate.

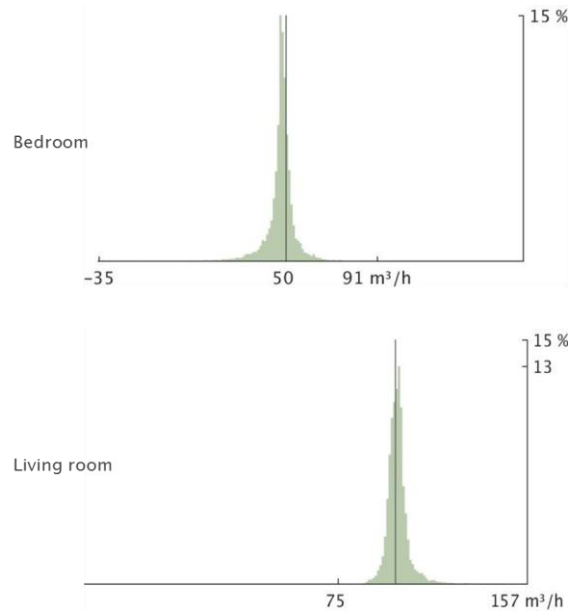


Figure 6: This figure represent the frequency distribution graph of the airflow rates ( $\text{m}^3/\text{h}$ ) through the natural vents of 10 Pa in both the living room on the ground floor (bottom) and a bedroom at the first floor (top) of an airtight building with open doors and an open staircase (low internal resistance). The design flow rates for the living room ( $100 \text{ m}^3/\text{h}$ ) and bedroom ( $50 \text{ m}^3/\text{h}$ ) are indicated by the vertical line.

In an airtight dwelling, the smaller supply vents, i.e. 10 Pa, lead to more controlled airflow rates compared to the larger self-regulating vents of 2 Pa (Figure 5 and Figure 6). The smaller vents reduce both the variable effect of the wind and the effect of thermal draught on the reduction of the flow rate in the bedrooms

### 3.3 Influence of wind and thermal draught in a leaky building

The simulations investigate the influence of wind and thermal draught (simultaneously) on the flow rate in a leaky dwelling. Airflow will enter the dwelling through the designated supply vents but also through the leakages in the building envelope. Furthermore, the influence of the sizing of the supply vents is taken into consideration. The airflow rates through the vents and the leakages not only depend on the mechanical ventilation and weather conditions, but also on the level of airtightness of the building envelope.

<b>Simulation conditions</b>	
Dwelling	Reference dwelling 2 (two-storey)
Airtightness	Leaky: $3 \text{ m}^3/\text{h}\cdot\text{m}^2$
Outdoor conditions	Transient: TRY Uccle
Size natural supply vent	P3@ 2 Pa (Figure 7) P0@ 10 Pa (Figure 8)
Internal resistance	Open doors + open staircase

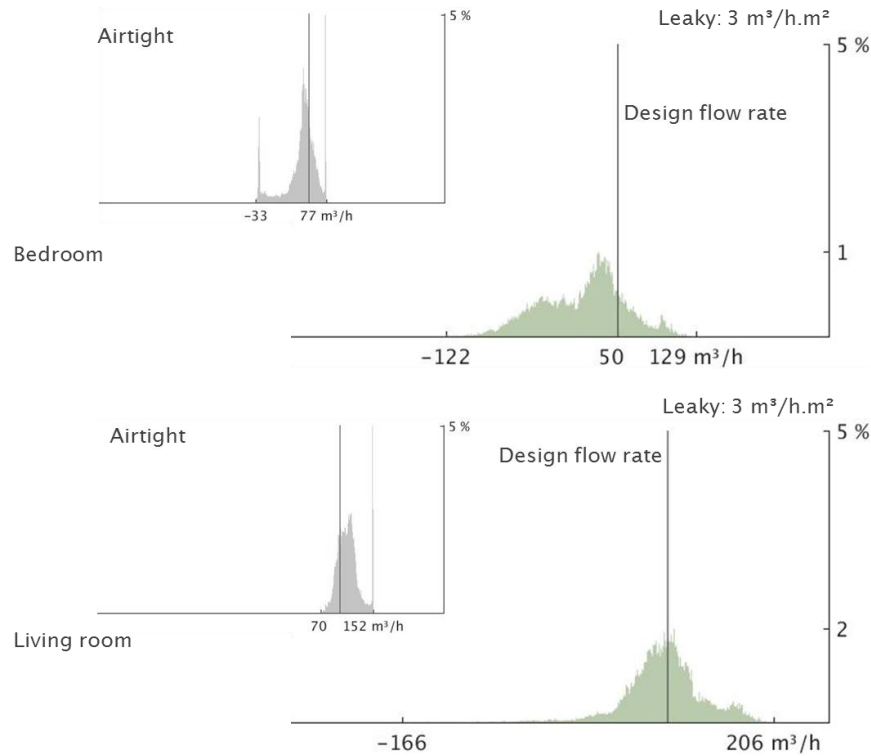


Figure 7: This figure represent the frequency distribution graph of the airflow rates ( $\text{m}^3/\text{h}$ ) through the natural vents of 2 Pa in both the living room on the ground floor (bottom) and a bedroom at the first floor (top) of a leaky building ( $q_{50} = 3 \text{ m}^3/\text{h.m}^2$ ) (right) with open doors and an open staircase. The design flow rates for the living room ( $100 \text{ m}^3/\text{h}$ ) and bedroom ( $50 \text{ m}^3/\text{h}$ ) are indicated by the vertical line. As a reference the results of the airtight building (i.e. results Figure 5) are repeated (smaller graphs on the left).

In the leaky dwelling, as in the airtight dwelling, the airflow rate through the natural supply vents in the living room (ground floor) and in the bedroom (first floor) varies in time and is not as designed (Figure 7). However, the influence of the wind and thermal draught is even bigger in the leaky building as the flow rates are even more variable. Reversed flow, i.e extraction, occurs sometimes both in the bedroom and living room.

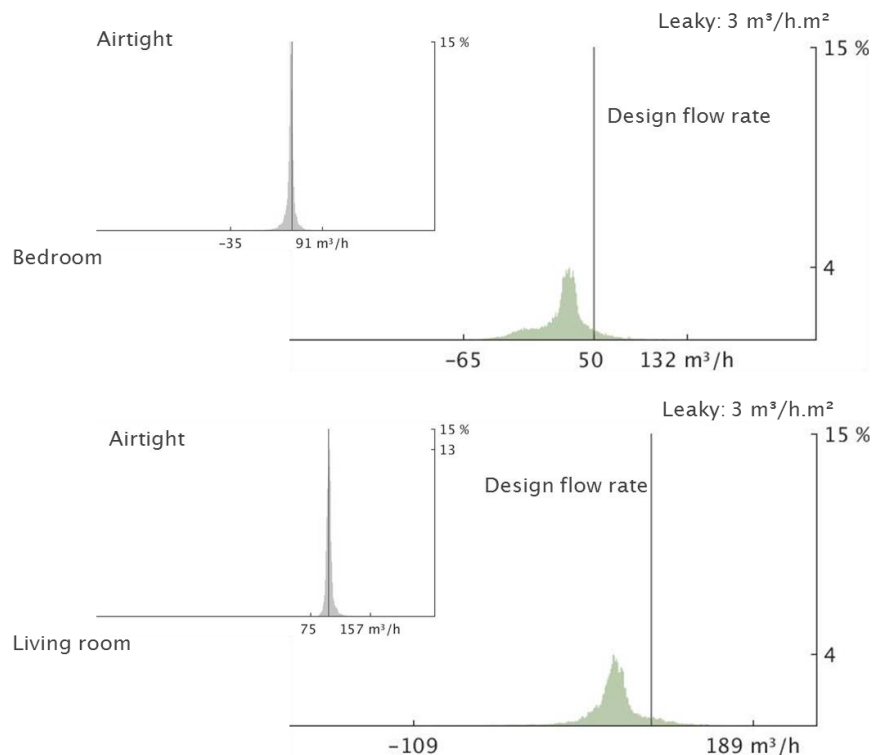


Figure 8: This figure represent the frequency distribution graph of the airflow rates ( $\text{m}^3/\text{h}$ ) through the natural vents of 10 Pa in both the living room on the ground floor (bottom) and a bedroom at the first floor (top) of a leaky building ( $q_{50} = 3 \text{ m}^3/\text{h.m}^2$ ) (right) with open doors and an open staircase. The design flow rates for the living room ( $100 \text{ m}^3/\text{h}$ ) and bedroom ( $50 \text{ m}^3/\text{h}$ ) are indicated by the vertical line. As a reference the results of the airtight building (i.e. results Figure 6) are repeated (smaller graphs on the left).

The smaller natural supply vents of 10 Pa aren't as favourable as in the airtight building. The airflow rates through the supply vents in the leaky building ( $q_{50} = 3 \text{ m}^3/\text{h.m}^2$ ) are lower and more variable (wider spread) compared to the vents in the airtight building (Figure 8). However, compared to the larger self-regulating supply vents of 2 Pa in the same leaky dwelling, the flow rate is less variable (narrower spread) but nearly always lower than the design flow rate (Figure 7 and Figure 8).

#### 4 CONCLUSIONS

Without the influence of the outdoor conditions, i.e. no wind and no thermal draught, the sizing of the natural supply vents doesn't influence the airflow rate through the supply vents in an airtight building. However, the sizing does influence the airflow rate through the supply vents in a leaky building. The flow rate through the vents reduces and the flow rate through the leakages increases with decreasing airtightness. This effect increases with smaller supply vents.

In an airtight dwelling, wind and thermal draught influence the flow rate through the natural supply vents. The flow rates are variable in time and not as designed. Wind is responsible for higher flow rates in the rooms at the windward side and lower or even negative flow rates at the leeward side. Thermal draught is responsible for higher supply flow rates downstairs (living room) and lower supply flow rates upstairs (bedrooms)

In an airtight building, the internal transfer and sizing of the natural supply openings influence the flow rate through the supply vents. Bigger transfer openings, e.g. open doors, enhance the

negative effect of thermal draught, while smaller natural supply openings, e.g. P0@10Pa, lead to less variable and more controlled flow rates, closer to the desired design flow rate.

In a leaky dwelling, wind and thermal draught also influence the flow rate through the natural supply vents with even bigger negative effects than in an airtight building. Smaller natural supply vents are not as favourable in leaky buildings as in airtight buildings. Lower flow rates occurs compared to the airtight dwelling. However, compared to the larger supply vents in the same leaky dwelling, the flow rate is less variable but nearly always lower (than the design flow rate).

## 5 ACKNOWLEDGEMENTS

This paper is based upon work supported by the Federal Public Service Economy (FPS Economy) in Belgium.

## 6 REFERENCES

AIVC. (1996). *A Guide to Energy Efficient Ventilation*.

Belgian Building Research Institute (BBRI). (2015). *TV: Luchtdichtheid van gebouwen*.

Belgisch Instituut voor Normalisatie (BIN). (2004). *NBN EN 13141-1: Luchtverversing van gebouwen - Prestatiebeproeving van onderdelen/producten voor luchtverversing in woningen - Deel 1: Binnen en buiten gemonteerde luchtroosters*.

Belgisch Instituut voor Normalisatie (BIN). (1991). *NBN D 50-001: Ventilatievoorzieningen in woongebouwen*. Brussel.

Belgisch Instituut voor Normalisatie (BIN). (2007). *NBN EN 15251: Binnenmilieu-gerelateerde inputparameters voor ontwerp en beoordeling van energieprestaties van gebouwen voor de kwaliteit van binnenlucht, het thermisch comfort, de verlichting en akoestiek*.

# Investigation of future ventilation flow rate requirements for dwellings in Belgium: from the application of FprEN16798-1:2016 to proposed robust rules

Samuel Caillou\*<sup>1</sup>, Romy Van Gaever<sup>1</sup> and Jelle Laverge<sup>2</sup>

*1 Belgian Building Research Institute (BBRI)  
Avenue P. Holoffe 21  
Limelette, Belgium*

*2 Ghent University (UGent)  
Sint Pietersnieuwstraat 41  
Ghent, Belgium*

*\*Corresponding author: romy.van.gaever@bbri.be*

## ABSTRACT

In the context of the PREVENT project, preparing a possible revision of the Belgian residential ventilation standard, the way of expressing ventilation requirements, among others in terms of ventilation flow rates, needs to be investigated. The aim of this paper is to propose and compare ways of expression of the ventilation requirements in terms of flow rates with respect to their robustness across dwellings.

The application of the different methods proposed in the recently developed new draft standard FprEN 16798-1:2016 has been compared for a series of Belgian dwelling configurations: method based on the perceived air quality, method using criteria for pollutant concentration and method based on pre-defined ventilation flow rates. The calculated flow rates varied significantly depending on the calculation method used.

Based on these results, some rules to express the ventilation requirements in dwellings in Belgium are proposed. One should first consider the ventilation flow rates for normal use during occupied periods. This flow rate could be based on those for occupancy per person proposed in FprEN 16798-1:2016 for non-adapted persons, provided it is higher than those for emissions from building. The determination of the number of persons could be based on a minimum of one person per bedroom, at least one bedroom for two persons, and a number of persons in the living rooms based on the total number of persons in the bedrooms. Second, a minimum flow rate for unoccupied periods and a minimum flow rate for rooms without any IAQ sensor (in case of demand controlled ventilation and manually controlled ventilation) could be set based on the flow rate for the emissions from building materials. Finally, the design flow rate of the system at the building level could depend on the control strategy of the ventilation system (i.e. sensor and actuator location) with a minimum corresponding to the highest value for the total flow rates for occupied periods in the night zone (bedrooms and similar) and those in the day zone (living room and similar).

The proposed rules could lead to more robust and efficient ventilation requirements for dwellings in the future in Belgium.

## KEYWORDS

Ventilation flow rates, residential ventilation, bioeffluents, building emissions, humidity

## 1 INTRODUCTION

The national ventilation standard for dwellings in Belgium (NBN D 50-001) is more than 25 years old. Since then the context of ventilation of dwelling has changed: building are more and more energy efficient and airtight, requesting on one hand robust ventilation requirements, but raising on the other hand the pressure on these requirements to be appropriate and efficient. However, since the publication of this Belgian standard in 1991, some questions remain the same: those about the definition of IAQ, the way of expression of ventilation requirements and the appropriate level of ventilation requirements. Among other issues with the Belgian standard, the minimum required ventilation flow rates are usually

higher compared to those required in other European countries (actually, they are similar to those in The Netherlands) (Brelh 2011) and they are, based on repeated statements by trade associations, considered too high by most of the ventilation professionals in Belgium.

In the context of the PREVENT project, preparing a possible future revision of the residential ventilation standard in Belgium, the way of expressing ventilation requirements, among others in terms of ventilation flow rates, needs to be assessed on its robustness.

The aim of this project was not to carry out research about the appropriate level of IAQ requirements and flow rates, but rather to use the most recent international research results and CEN standard framework on this topic. Nevertheless, there is no general scientific consensus on metrics and associated requirements, as shown for example during the spring 2016 AIVC workshop on this topic.

Recently, the new draft standard FprEN 16798-1:2016 (entitled “Energy performance of buildings – Part 1: Indoor environmental input parameters for design and assessment of energy performance of buildings addressing indoor air quality, thermal environment, lighting and acoustics”) has been developed. This standard should supersede EN 15251:2007 and is associated with the technical report FprCEN/TR 16798-2. This new standard has been recently rejected at the final vote of the CEN procedure. Nevertheless, since a slightly modified version of the standard is expected to be accepted in the near future, this document is however very important in order to investigate the way of expressing required ventilation flow rates for residential ventilation in Belgium.

The aim of this paper is to propose a way of expression of the ventilation requirements in terms of flow rates for a possible future ventilation standard for dwellings in Belgium. The different methods proposed in FprEN 16798-1:2016 to determine ventilation flow rates have been applied to 5 typical dwelling configurations to serve as basis for the discussion.

## 2 METHODS

Five typical dwelling configurations have been used for application of the FprEN 16798-1:2016 to determine ventilation flow rates.

These five dwelling configurations are a flat studio, an apartment with 1 bedroom, a medium house with 3 bedrooms and relatively small spaces, the same medium house but with relatively larger space surface areas, and finally a large house with 5 bedrooms. The composition of the dwellings and the surface area of the spaces are given in Table 1.

The following general methods described in the document FprEN 16798-1:2016 have also been applied on the 5 typical dwellings, using indoor air quality of category II as described in this document.

Method 1 is based on perceived air quality with the sum of the flow rate for bioeffluents (7 l/s.pers.) and the flow rate for building emissions (0.35, 0.7 and 1.4 l/s.m<sup>2</sup> respectively for very low polluting buildings LPB-1, low polluting buildings LPB-2 and non-low-polluting buildings LPB-3).

Method 2 is using limit values of substance concentration. Two substance concentrations have been considered with this method 2: 800 ppm of CO<sub>2</sub> (corresponding to a flow rate of 7 l/s.pers for emission rate of 20 l/h.pers.) and 100 µg/m<sup>3</sup> of formaldehyde (limit recommended by WHO) combined with material sources showing a maximum concentration of 100 µg/m<sup>3</sup> after 28 days of testing according to CEN/TS 16516 for the sum of all the materials (floor,

ceiling and walls) present in the space. This could correspond for example to emission of formaldehyde from only the floor material with a maximum concentration of 100  $\mu\text{g}/\text{m}^3$  after 28 days (as currently required for example for new building in Belgium); or to a combination of emissions of formaldehyde from all the floor, ceiling and wall materials (with the same loading factors as for the reference room in CEN/TS 16516: 1 for the walls and 0.4 for the floor and the ceiling) leading to a sum of concentration after 28 days not higher than 100  $\mu\text{g}/\text{m}^3$ . Given the size of the reference room (12  $\text{m}^2$  of floor area) and of the flow rate (15  $\text{m}^3/\text{h}$ ) in CEN/TS 16516, this correspond to an average flow rate of 0.35  $\text{l}/\text{s}\cdot\text{m}^2$  of floor area. Method 3 is based on predefined ventilation flow rates. The documents FprEN 16798-1:2016 and FprCEN/TR 16798-2:2016 propose different approaches using predefined flow rates for residential applications. The 2 following approaches have been used in this comparison: (1) supply air flow based on perceived IAQ for adapted persons (with 2.5  $\text{l}/\text{s}\cdot\text{pers}$  and 0.15  $\text{l}/\text{s}\cdot\text{m}^2$ ) and (2) design extract air flow rates as described in Table I.8 of FprEN 16798-1:2016 (20-40  $\text{l}/\text{s}$  for kitchen, 10-15  $\text{l}/\text{s}$  for bathroom, 10  $\text{l}/\text{s}$  for other wet room, 10-15  $\text{l}/\text{s}$  for toilets).

The ventilation flow rates required in the current Belgian standard NBN D 50-001 have also been applied on the 5 dwellings for the comparison.

Table 1: Composition of the 5 dwelling configurations, showing the surface area of the spaces (in  $\text{m}^2$ ), the total surface area (in  $\text{m}^2$ ) and the number of occupants in the dwellings.

	<b>Flat studio</b>	<b>Apartment</b>	<b>Medium house, small spaces</b>	<b>Medium house, large spaces</b>	<b>Large house</b>
Living room	25	30	30	45	55
Corridor 1		8	12	16	20
Kitchen	10	10	10	16	16
Toilet 1		2	2	2	2
Bedroom 1		16	12	18	18
Bedroom 2			8	12	12
Bedroom 3			8	12	12
Bedroom 4					10
Bedroom 5					10
Corridor 2			10	12	16
Bathroom 1	6	8	8	12	12
Bathroom 2					8
Toilet 2			2	2	2
Laundry					8
Total surface	41	74	102	147	201
Nb of persons	1	2	4	4	6

### 3 RESULTS AND DISCUSSION

Beside the general method (method 1 to method 3) to determine ventilation flow rates, the documents FprEN 16798-1:2016 and FprCEN/TR 16798-2:2016 propose different approaches using default design ventilation air flow rates for residential buildings:

- Total air change rate for the dwelling;
- Supply air flow rates based on air flow rates per person;
- Supply air flow rates based on perceived IAQ for adapted persons;
- Design extract air flow rates.

However, these approaches can lead to very different total flow rates for the dwelling, as demonstrated by the examples treated in FprCEN/TR 16798-2:2016, for example for a one-bedroom dwelling, with 67 m<sup>3</sup>/h, 50.4 m<sup>3</sup>/h and 34.96 m<sup>3</sup>/h respectively for the first 3 approaches listed here above. This is probably the result of a compromise, in these documents, between the very different approaches, standards and requirements currently in use in the different countries across Europe. However, this does not converge to an equivalent IAQ between the different methods described in the standard. Therefore this does not answer to the need of a robust and founded way to describe ventilation requirements for dwellings, as needed for the moment to develop a new standard in Belgium. Moreover, the need for IAQ should be the same for the occupants in residential or in commercial buildings, which seems to not be the case in these documents.

Therefore, in this study, we applied the general methods described in FprEN 16798-1:2016 to determine flow rates, to 5 typical dwelling configurations, representative for the Belgian market. The flow rates obtained with these methods have been compared to the flow rates required in the current standard for dwellings in Belgium. The total ventilation flow rate per dwelling is presented in Figure 1, for the 5 type of dwellings, in the following order: required flow rate for supply in the current Belgian standard, required flow rate for extraction in the current Belgian standard, method 1 for very low polluting building (LPB-1), method 1 for low polluting building (LPB-2), method 1 for non-low-polluting building (LPB-3), method 2, method 3 with predefined flow rates for adapted persons, and finally method 3 with design extract airflow rates.

These results of the comparison confirm very different flow rates according to the approach used. The proportion of the flow rate from one approach to each other was very similar for the different types of dwelling tested (except, to some extent, for the flat studio).

The highest flow rate was always obtained with the method 1 and non-low-polluting building and the lowest with the method 3 for adapted persons for residential applications, with a factor of around 7 between these extreme values. This difference is huge. Even if the building emission can largely vary from one building to another, the risk to have non-low-polluting building or high emission rates is probably as high in residential buildings as it is in commercial buildings. If anything, the floor area per person is usually higher in dwellings, so the weight of emissions in determining the flow rate should be higher. The predefined flow rate for dwellings for adapted persons could maybe be too low in case of high building emissions in dwellings. On the other hand, method 1 based on perceived IAQ for both bioeffluents and building emissions on a cumulative basis could be a bit too conservative for residential buildings. For example, even for the very low polluting building, the flow rates resulting from method 1 are close to or even (substantially) higher (except for the flat studio) the those prescribed in the current flow rates in the Belgian standard which are already considered to be very high. By the way, FprCEN/TR 16798-2:2016 recommends to consider that the persons are adapted in residential applications. Maybe we could at this stage distinguish between some criteria for the health and some for comfort. Method 2 from FprEN 16798-1:2016 is interesting for that point of view.

The flow rates resulting from the method 2 are quite intermediate between those for method 1 and those for adapted persons in residential buildings. Method 2 allows to calculate the design flow rate for the most critical or relevant pollutant (or group or pollutants). Method 2 allows then to consider different pollutants and to look at the most critical one. So in stead of the cumulative basis supposed in method 1, it considers the maximum of the flow rates required

for each type of pollution. This can be applied for the CO<sub>2</sub>, in order to achieve sufficient comfort against bioeffluents for example, and for the building emissions, in order to limit the health risk for the occupants. In this comparison, this has been done for a CO<sub>2</sub> concentration of 800 ppm above outdoor (corresponding to 7 l/s.pers) and for formaldehyde with a concentration limit value of 100 µg/m<sup>3</sup> in the spaces (as recommended by the WHO) and building materials with a total emission corresponding to 100 µg/m<sup>3</sup> after 28 days of testing according to the CEN/TS 16516. This corresponds to a ventilation flow rate for the building emission of 0.35 l/s.m<sup>2</sup>. Applying method 2 could also be done for different hypothesis about the building emissions, based for example on practical definitions of different types of building load, from very low polluting buildings to non-low-polluting building (as used for method 1). The advantage of this method 2 is to look at the most critical pollutant as explained above.

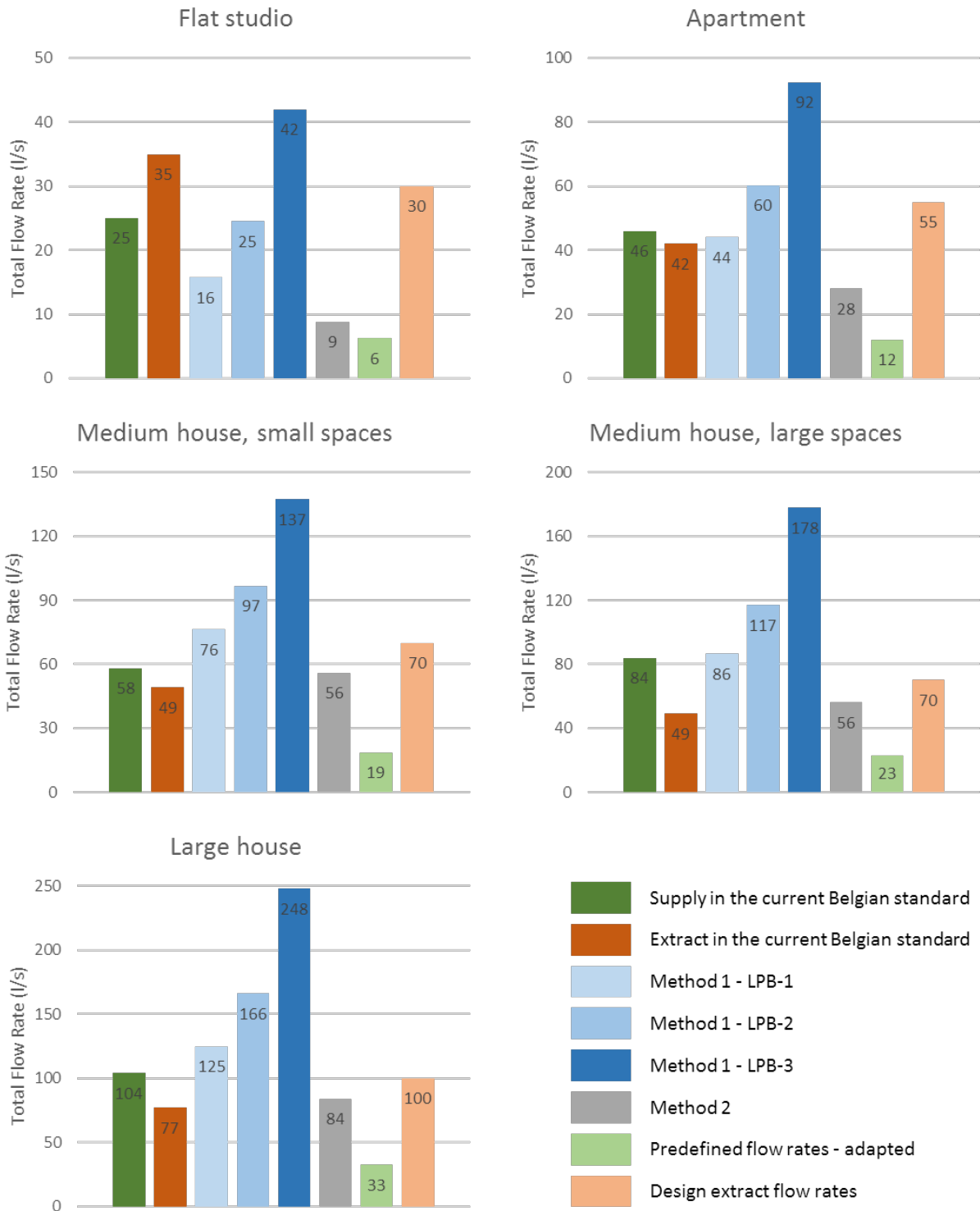


Figure 1: The total ventilation flow rate per dwelling, for the 5 type of dwellings as indicated, calculated according to the Belgian standard: required flow rate for supply in the current Belgian standard, required flow rate for extraction in the current Belgian standard; and according to FprEN 16798-1:2016 and FprCEN/TR 16798-2:2016: method 1 for very low polluting building (LPB-1), method 1 for low polluting building (LPB-2), method 1 for non-low-polluting building (LPB-3), method 2, method 3 with predefined flow rates for adapted persons, and finally method 3 with design extract airflow rates.

The flow rates based on design extract air flow rates from FprEN 16798-1:2016 are intermediate compared to the other calculated flow rates. But they are always higher compared to the required flow rates for extraction in the current ventilation standard in Belgium. The practice in Belgium has however shown that the required flow rates for extraction in Belgium (for example used for exhaust mechanical ventilation system, widely spread in the Belgian market) are largely sufficient to control the humidity from the wet spaces. To our knowledge, no problem of moisture or building damage has been reported since more than 25 years in buildings with extract flow rates corresponding to the current standard in Belgium.

These extract flow rates from FprEN 16798-1:2016 are also (slightly to substantially) higher than the supply flow rates obtained with the other methods, especially method 3 for adapted persons, method 2 and method 1 for very low polluting building. However previous research work in Belgium showed that the control of bioeffluents (with a flow rate of 7 l/s.pers corresponding to category II in the draft standard) is the limiting factor compared to the control of humidity in the wet spaces (Van Gaever et al. 2017). In other words, the average flow rate needed to control humidity in the wet spaces is significantly lower compared to the average supply flow rate needed for the occupants based on 7 l/s.pers.

## **4 PROPOSED APPROACH FOR THE BELGIAN STANDARD**

In the context of the development of new basis for a future ventilation standard for dwellings in Belgium (PREVENT project), different solutions have been investigated for the expression of the ventilation requirements for dwellings. These solutions are, at least partially, based on the currently available CEN documents FprEN 16798-1:2016 and FprCEN/TR 16798-2:2016 discussed in this paper.

The proposed approach for the requirements of ventilation of dwellings in the context of the PREVENT project is summarized hereafter.

### **4.1 Sources of pollutants in dwellings and rationales for ventilation requirements**

The main pollutant sources in dwellings are bioeffluents from the persons, humidity in the wet spaces and emissions from materials. Bioeffluents can be considered to mainly impact the comfort of and the perceived IAQ by the occupants. Humidity control is crucial to avoid moisture problems and mold developments (and to limit the associated health risks). Emissions from materials impact the comfort and the perceived IAQ, but presents above all a risk for the health of the occupants.

Among these sources, only the emissions from materials can partly be controlled at the source by choosing low emitting products and materials. Ideally, the ventilation flow rates in a standard for dwelling should then take into account the building load for the material emissions in order to encourage owners, builders and designers to choose for low emitting products.

According to the approach of the method 2 from FprEN 16798-1:2016, the flow rate of a space and of the whole building should be based on the most critical pollutant among the above mentioned sources, bioeffluents, humidity and building emissions.

### **4.2 Design flow rates per space depending on the space type**

Because the occupant can spend a lot of time in the same space in a dwelling (for example in the bedroom during night), the way of requiring flow rates in dwelling should be done at the level of each space.

For the living spaces such as the living room and the bedrooms, the flow rate should be determined for the most critical pollutant: the bioeffluents or the building emissions.

For the building emission, the idea is to fix different flowrates per surface area of the space (in l/s.m<sup>2</sup>) for different categories of building emission load, as described for method 1 in FprEN 16798-1:2016. More investigation is still needed to propose these flow rates and practical definitions of these building categories for the Belgian market.

For the bioeffluents, the proposed flow rate corresponds to category II of FprEN 16798-1:2016, with a flow rate of 7 l/s.pers. The way to determine the number of person per space has also to be sufficiently robust. The current proposition is as follows. Each living space has to be attributed to one of these twofollowing space types: livingroom (or equivalent, for example hobby room) or bedroom (or equivalent, for example study room). In a dwelling there are at least one living room and one bedroom for 2 persons (or a combination of both in a studio). The additional bedrooms are considered for 1 person. The number of persons for each living room is determined by the sum of the persons for the bedrooms (i.e. number of bedrooms + 1). In case of several living rooms and bedrooms, the attribution between both is free for the designer of the building but the impact on the total flow rate is limited, as shown in the Table 2.

Table 2: Illustration of the impact of the attribution of the type of space (living room or bedroom) on the total flow rate of the dwelling (in l/s), depending on the number of living rooms and bedroom respectively.

Number of living rooms	Number of bedrooms									
	1	2	3	4	5	6	7	8	9	10
1	28	42	56	70	84	98	112	126	140	154
2	42	63	84	105	126	147	168	189	210	231
3	56	84	112	140	168	196	224	252	280	308
4	70	105	140	175	210	245	280	315	350	385
5	84	126	168	210	252	294	336	378	420	462

For the wet spaces such as kitchen, bathroom, toilet, etc., the required flow rates in the current standard can be considered sufficient to control the humidity in these spaces, as discussed above (see § 3). These flow rates are as follows: 21 l/s for an open kitchen, 14 l/s for a bathroom and equivalent wet space, and 7 l/s for a toilet.

### 4.3 Control and flow rate in use

Beside the design flow rate, it should be still possible to control the flow rates depending on the real needs during use of the dwelling, thanks to automatic Demand Controlled Systems (DCV) or manually controlled systems. In this context, the minimum operational flow rate should be determined for periods of absence of needs in the different spaces.

For the wet spaces, the flow rates could be regulated based for example on relative humidity detection. Minimum flow rate for wet spaces are probably not critical because the limiting factor for ventilation of dwellings has been identified to be the flow rate to control the bioeffluents from the persons (see § 3).

For the living spaces, the flow rates could be regulated manually or based on the presence or on the CO<sub>2</sub> concentration in the spaces. However, because the living spaces are not only

ventilated for the bioeffluents but also to control the building emissions (see § 4.1), the minimum flow rates for periods with low need (manually controlled on lower position, no detection of presence or CO<sub>2</sub> concentration lower than threshold values for example) in living spaces should be at least the flow rate to control these building emissions, as described above (see § 4.2). The aim of this minimum flow rate is double: (1) ensure a minimum flow rate for material emissions in case a person is present (in case of manually control or CO<sub>2</sub> detection for example); and (2) ensure a minimum flow rate during absence to limit the concentration of pollutants when a person enters the room.

Moreover, it is sometimes possible to have only a limited number of sensors (presence of CO<sub>2</sub>) for example only in the main living room and/or the main bedroom. In this case, a minimum flow rate during use for the spaces not equipped with a sensor should also be foreseen. For this purpose, the minimum flow rate of 4 l/s.pers proposed in the HealthVent project and recommended in the FprEN 16798-1:2016 could be an interesting basis. This flow rate should also be the minimum flow rates in case of manually controlled regulation (local or central) because this is equivalent to the absence of sensors in the spaces.

During use, the total supply and total extract flow rates should be equilibrated at the level of the building, by adjusting them towards the highest of both values.

#### **4.4 Design of the system at building level**

Finally, the design total flow rates of centralised system have to be determined. This could depend on the type of regulation of the system.

In case of no regulation or only centrally regulated systems, the total design flow rate at building level should be the sum of the design flow rates per space (see § 4.2). And the total supply and total extract flow rates should be equilibrated at the level of the building, by adjusting them towards the highest of both values.

In case of regulation of the flow rates locally (for example flow rates regulated independently for each space) or by zones (for example night and day zones), the design total flow rate at the building level could be lower because the probability to have a need of ventilation in all the spaces at the same time is low. The design total flow rate should be at least equal to the total design flow rate of each zone, night zone and day zone.

## **5 CONCLUSIONS**

The application of the different methods proposed in the recently developed new draft standard FprEN 16798-1:2016 has been compared for a series of typical Belgian dwelling configurations.

The calculated flow rates varied significantly depending on the calculation method used. These results emphasize the need for more coherent and robust methods of determination of flow rate requirements for dwellings in the CEN standard framework.

Based on these results, rules to express the ventilation requirements in dwellings for a future ventilation standard in Belgium have been proposed. The proposed rules could lead to more robust and efficient ventilation requirements for dwellings in the future in Belgium.

## **6 ACKNOWLEDGEMENTS**

This paper is based upon work supported by the Federal Public Service Economy (FPS Economy) in Belgium.

## 7 REFERENCES

FprEN 16798-1:2016. *Energy performance of buildings – Part 1: Indoor environmental input parameters for design and assessment of energy performance of buildings addressing indoor air quality, thermal environment, lighting and acoustics – Module M1-6.*

FprCEN/TR 16798-2:2016. *Energy performance of buildings – Part 2: Indoor environmental input parameters for design and assessment of energy performance of buildings addressing indoor air quality, thermal environment, lighting and acoustics – Module M1-6 – Technical report – Interpretation of the requirements in EN 16798-1.*

Brelih Nejc, Seppänen Olli. 2011. *VENTILATION RATES AND IAQ IN EUROPEAN STANDARDS AND NATIONAL REGULATIONS*. In proceedings of the 32nd AIVC Conference, 12-13 October 2011, Brussels, Belgium.

Van Gaever Romy, Laverge Jelle, Caillou Samuel. 2017. *The influence of different ventilation strategies and airflow control on the indoor air quality in dwellings*. AIVC workshop, 14-15 March 2017, Brussels, Belgium.

<http://www.healthvent.byg.dtu.dk/> last visit on 31/05/2017.

# Advanced airflow distribution methods for reducing exposure of indoor pollution

Guangyu Cao<sup>\*1</sup>, Peter Nielsen<sup>2</sup>, Arsen Melikov<sup>3</sup>, and Risto Kosonen<sup>4</sup>

*1 Norwegian University of Science and Technology, KolbjørnHejesvei 1b, 7491, Trondheim, Norway*

*2 Aalborg University, Thomas Manns Vej 23, Aalborg, Denmark*

*\*Corresponding author: Guangyu.cao@ntnu.no*

*3 Technical University of Denmark, Nils KoppelsAllé Building 402, room 234 2800 Kgs. Lyngby, Denmark*

*4 Aalto University, PL 14400, K4, Espoo, Finland*

*Note: the contact addresses may be re-arranged*

## ABSTRACT

The adverse effect of various indoor pollutants on occupants' health have been recognized. In public spaces flu viruses may spread from person to person by airflow generated by various traditional ventilation methods, like natural ventilation and mixing ventilation (MV). Personalized ventilation (PV) supplies clean air close to the occupant and directly into the breathing zone. Studies show that it improves the inhaled air quality and reduces the risk of airborne cross-infection in comparison with total volume (TV) ventilation. However, it is still challenging for PV and other advanced air distribution methods to reduce the exposure to gaseous and particulate pollutants under disturbed conditions and to ensure thermal comfort at the same time. The objective of this study is to analyse the performance of different advanced airflow distribution methods for protection of occupants from exposure to indoor pollutants.

The study shows that due to complex boundary conditions of the indoor environment, the conventional ventilation methods, like mixing ventilation, may not be able to protect occupants from exposure to various indoor airborne pollutants. The latest developed advanced airflow distribution methods, like protected zone ventilation, downward ventilation, bed and chair incorporated personalized ventilation and localized chilled beam may be used to reduce the personal exposure to various indoor airborne pollutants and ensure thermal comfort. Regarding the exposure to exhaled airflow, the exposure risk can be as high as 20 times by using MV than PV method.

## KEYWORDS

Advanced airflow distribution, personal exposure, indoor pollution, ventilation, indoor air quality

## 1 INTRODUCTION

The adverse effect of various indoor pollutants on occupants' health have been recognized. The traditional ventilation (air distribution) methods may increase the risk of airborne transmission of flu viruses between room occupants. Personalized ventilation (PV) supplies clean air directly into the breathing zone and improves the inhaled air quality and to reduces the risk of airborne cross-infection in comparison with total volume (TV) ventilation ((Bolashikov, Melikov and Krenek, 2011)). Regarding the exposure to exhaled airflow, the exposure risk can be as high as 20 times by using mixing ventilation than advanced ventilation, such as personalised ventilation (Nielsen et al. 2007, Cao et al. 2015). However, it

is challenging for the advanced air distribution methods with both gaseous and particulate pollutants under disturbed conditions.

The objective of this study is to analyse different advanced room air distribution methods for protection of occupants from exposure to indoor pollutants.

## 2 PROTECTED ZONE VENTILATION

During the recent years, the protected occupied zone ventilation (POV) and the protected zone ventilation (PZV) were developed by using downward plane jet to separate indoor space into source and protected zones. This has proven to reduce the personal exposure to indoor pollutant. Figure 1 shows that the use of a downward plane jet will interact with the exhaled jet and will reduce the exposure to airborne pollution from another person who stands close.

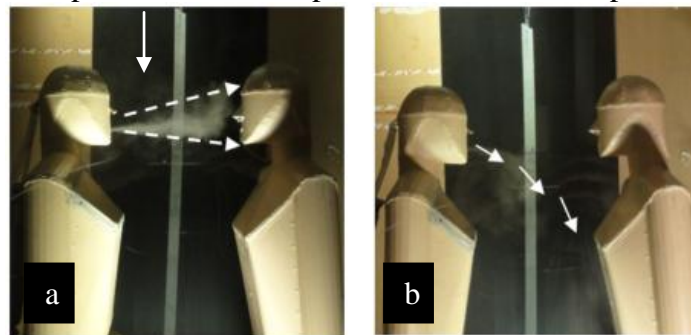
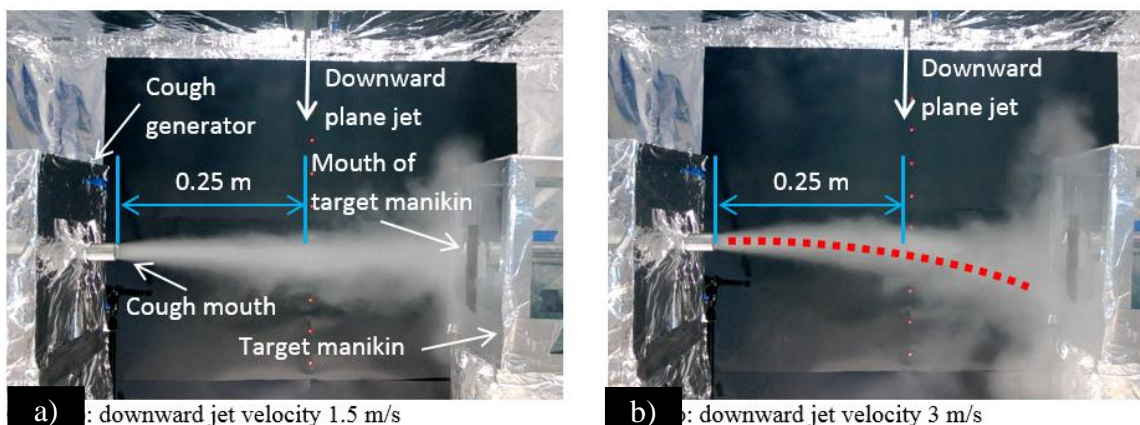


Figure 1: Smoke visualization of the performance of downward plane jet, a) without downward plane jet, b) with downward jet. (Cao et al. 2015)

Figures 2 show that the smoke visualization of the interaction of a cough jet and a downward plane jet. When the velocity of a cough is increased to 16 m/s, a downward jet with a velocity less than 6 m/s only marginally affects the travel of the cough jet. The cough jet may directly impinge the “mouth” area of the target thermal dummy (TTD). A downward jet with a velocity of 8.5 m/s may bend the cough jets downward, thus the cough jet cannot directly impinge the “mouth” area of the TTD. This may indicate the application of a downward plane jet for protected zone ventilation will depend on the moment of the pollutant source, like human respiratory activities.



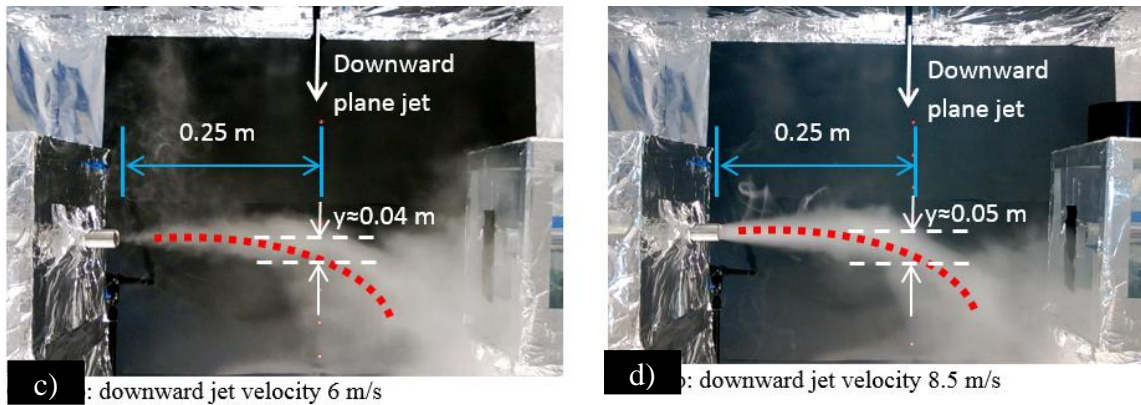


Figure 2: Smoke visualization of a cough of 16 m/s between two manikins with various downward plane jet velocities a) downward jet velocity 1.5 m/s, b) downward jet velocity 3 m/s, c) downward jet velocity 6 m/s, d): downward jet velocity 8.5 m/s (Cao et al. 2017)

### 3 DOWNWARD VENTILATION

The risk of airborne infection can be minimised in hospitalwards by using a high air change rate and high personal exposure index in a downward ventilation system where a ceiling-mounted low velocity diffuser are giving a downward supply flow outside the occupied zone. The supplied cool air reaches the floor and generates vertical displacement flow when the return openings are located near/on the ceiling. This type of flow (Fig. 2.) can provide cleaner air to inhalation compared to complete mixing air distribution. The system can handle a high flow rate without causing high velocity, and it is therefore appropriate for the ventilation of a hospital ward (Nielsen et al. 2010). Figure 3 shows the location of different exhaust outlet. A further improvement is to use a bed with personalized ventilation (Nielsen et al. 2007, Melikov et al. 2011).

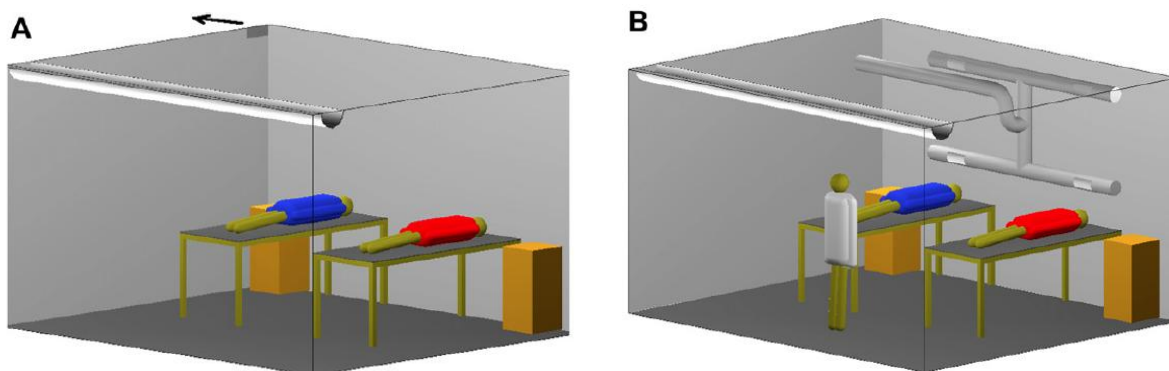


Figure 3: Personal exposure index with a ceiling installed low velocity diffuser

Figure 4 shows the personal exposure index which is concentration in return opening divided with inhaled concentration. Figure 4 a shows the personal exposure index for the target manikin when the source manikin is lying on the back, on the side, and sitting straight in the bed. The target manikin is standing simulating a healthcare person close to the downward flow below the ceiling mounted diffuser. Figure 4 b shows the personal exposure index for the target manikin when the source manikin is lying on the back, on the side, and sitting straight in the bed. The target manikin is standing and simulates a healthcare person close to the downward flow below the ceiling-mounted diffuser.

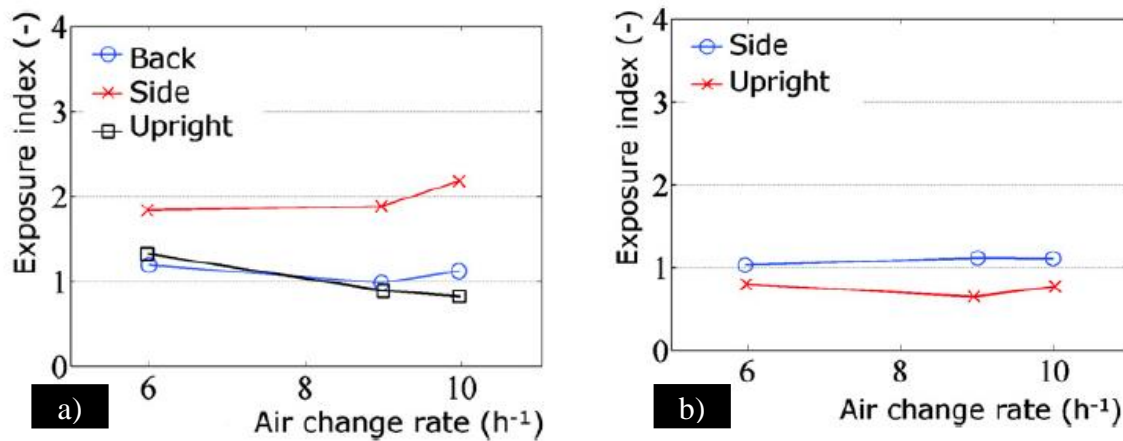


Figure 4: Personal exposure index with different ventilation systems: a) The room has one return opening. b) Four return openings at low level

#### 4 SEAT INCORPORATED PERSONALIZED VENTILATION

The seat-incorporated personalized ventilation (PV) method was developed for control of the free convective flow around the human body, with the aim of improving inhaled air quality. Two nozzles placed on the headrest sideways at the head level of a seated occupant supplied the clean air (Figure 5). The PV- methods have been proved to increase the amount of clean air into inhalation at reduced personalized flow rate and to reduce the risk of draft.

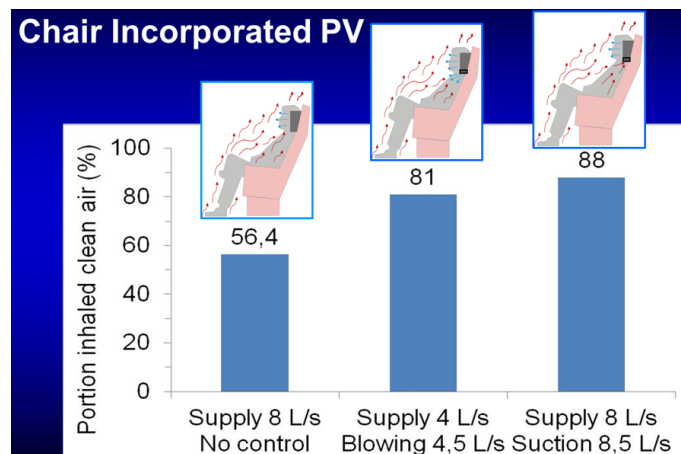


Figure 5: Supply airflow rate and portion of inhaled clean air (Bolashikov, Melikov and Krenek, 2011)

Two of the control strategies studied, namely weakening of the free convective flow by suction of part of its air at the breathing zone and weakening and diluting the free convective air by clean personalized air proved to be efficient. The comparison shown in Figure 6 documents that both strategies improved personal exposure effectiveness (PEE) dramatically: PEE increased from 22.8% without control to 79.5% when suction of 16 L/s was applied and to 92.4% when convective air was diluted by 4.5 L/s clean air. The improvement was higher when the suction and the dilution flows increased.

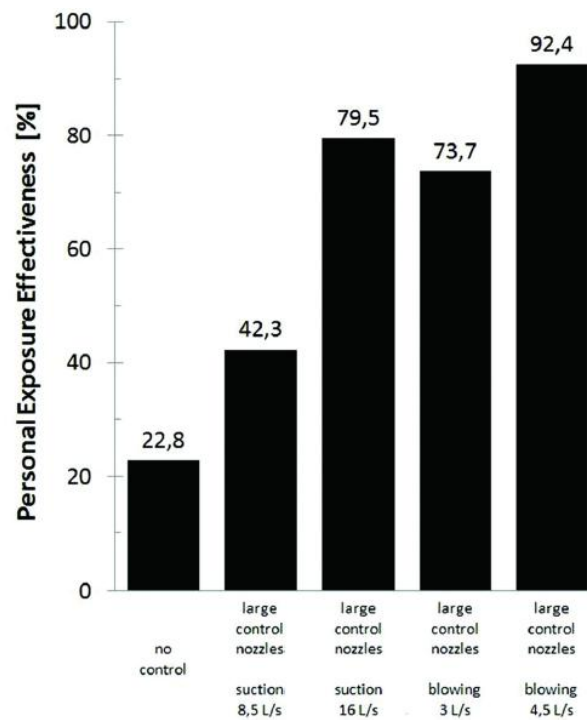


Figure 6: Impact of the control strategies on personal exposure effectiveness (PEE) at 6 L/s from “head rest” type PV nozzle by weakening of the free convective flow (suction) and use of its momentum to transport an additional amount of clean air (blowing), room temperature of 20°C. “Large ATDs”—personalized and control flows with large initial dimensions, i.e., low initial momentum. (Bolashikov, Melikov and Krenek, 2011)

## 5 LOCALIZED CHILLED BEAM

Microenvironment airflow may be affected by human subjective response. Recently, a new microenvironment control method was developed to create a comfort personal zone by using combined radiant and convective cooling by chilled ceiling combined with localized chilled beam (see Figure 7). This combination generated preferred thermal environment at the workstation and acceptable thermal environment in the rest of the occupied zone.

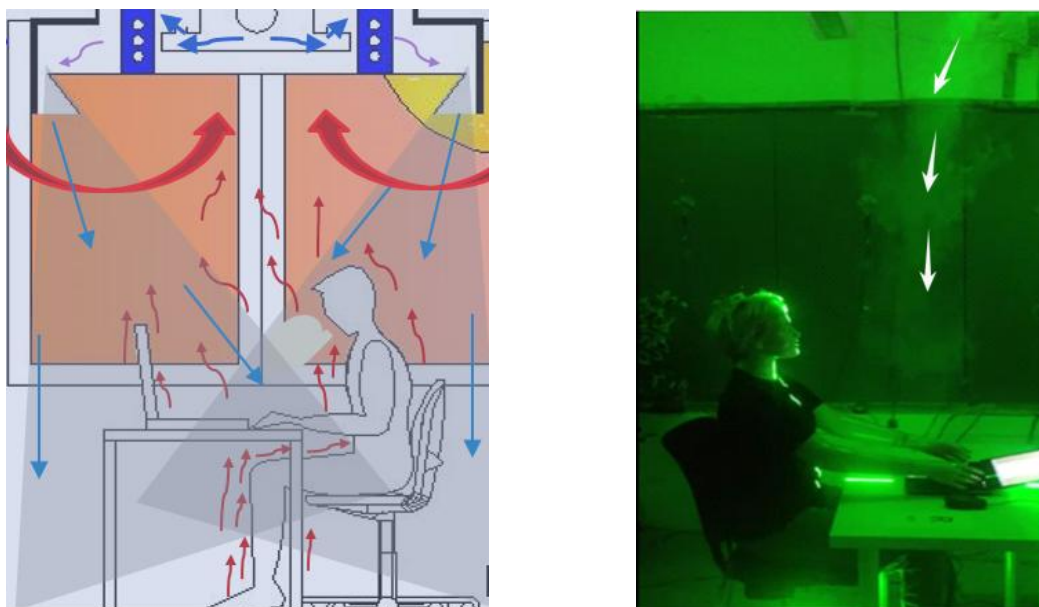


Figure 7: Microenvironment airflow distribution by a Localized chilled beam

## 6 CONCLUSIONS

Due to complex boundary conditions of the indoor environment, the conventional ventilation method, like mixing ventilation, may not be able to protect occupants from exposure to various indoor airborne pollutants. The latest developed advanced airflow distribution methods, like protected zone ventilation, downward ventilation, bed and chair incorporated personalized ventilation and localized chilled beam may be used to reduce the personal exposure to various indoor airborne pollutants and ensure thermal comfort.

## 7 REFERENCES

- Arghand, T., Bolashikov, Z., Kosonen, R., Aho, I., Melikov A. (2016). *Individually controlled localized chilled beam in conjunction with chilled ceiling: Part 1 – Physical environment*, Indoor Air 2016, Ghent, Belgium.
- Arghand, T., Pastuszka S, Bolashikov Z, Kaczmarczyk J., Kosonen R., Aho I., Melikov A. (2016)*Individually controlled localized chilled beam in conjunction with chilled ceiling: Part 2 – Human response*, Indoor Air 2016, Ghent, Belgium.
- Bolashikov, Z., Melikov, A. and Krenek, M. (2011)*Control of the Free Convective Flow around the Human Body for Enhanced Inhaled Air Quality: Application to a Seat-Incorporated Personalized Ventilation Unit*. HVAC&R: 22,161-188.
- Cao, G.Y., Nielsen, P.V., Jensen R.L., Heiselberg, P., Liu, L., Heikkinen, J. (2015)*Protected zone ventilation and reduced personal exposure to airborne cross-infection*. Indoor Air, 25 (3), 307-319.
- Cao, G.Y., Liu, SC., Boor, B., Novoselac, A. (2017) *Dynamic interaction of a downward plane jet and a cough jet with respect to particle transmission: An analytical and experimental study*. Journal of Occupational and Environmental Hygiene. Accepted March, 24, 2017. DOI: 10.1080/15459624.2017.1316383.
- Melikov, A., Bolashikov, Z., Georgiev, E. (2011)*Novel ventilation strategy for reducing the risk of airborne cross infection in hospital rooms*. In: Proceedings of Indoor Air 2011, University of Austin, paper 1037.
- Nielsen, P.V., Li, Y., Buus M., Winther F.V. (2010)*Risk of cross-infection in a hospital ward with downward ventilation*. Building and Environment, 45, 2008-2014.
- Nielsen, P.V., Jiang, H. and Polak, M. (2007)*Bed with Integrated Personalized Ventilation for Minimizing Cross Infection*. In Proceedings of Roomvent 2007: Helsinki 13-15 June 2007. FINVAC.

# Towards the definition of an indoor air quality index for residential buildings based on long- and short-term exposure limit values

Louis CONY RENAUD-SALIS<sup>\*1</sup>, Olivier RAMALHO<sup>2</sup> and Marc ABADIE<sup>1</sup>

*1 University of La Rochelle,  
Avenue Michel Crépeau  
17042 La Rochelle Cedex 1, France*

*2 Scientific and Technical Center for Building  
(CSTB), 84 Avenue Jean Jaurès, 77420 Champs-sur-  
Marne, France*

*\*Corresponding author: louis.cony-renaud-  
salis@univ-lr.fr*

## ABSTRACT

In the Framework of the IEA EBC Annex68 Subtask 1 working subject, we aimed at defining an indoor air quality index for residential buildings based on long- and short-term exposure limit values. This paper compares 8 indoor air quality indices (IEI, LHVP, CLIM2000, BILGA, GAPI, IEI Taiwan, QUAD-BBC and DALY) by using the French IAQ Observatory database that includes pollutant concentration measurements performed in 567 dwellings between 2003 and 2005. This comparison allows to make a relevant analysis of each index and determines their pros and cons i.e. the calculation method, selected pollutants, threshold concentrations, sub-indices and their aggregation. From this analysis, a new index is proposed in order to be as consistent as possible in regards of health impacts by taking both long- and short-term exposure limit values into account.

## KEYWORDS

IAQ, Indicator, Indices, Guideline value, Health assessment, Good IAQ, Bad IAQ

## 1 INTRODUCTION

Due to the huge number of various sources of emissions, pollutants, health impacts and toxicity levels, assessment of Indoor air Quality (IAQ) is a complex task (Hulin et Al., 2010, Wolkoff, 2013; Haverinen-Shaughnessy, 2015). One of the required tools to achieve that goal is a single Indoor Air Quality Index that would describe air quality in regards of health impacts. During the last decades, such indices were defined, yet, none was accepted as sufficiently relevant by the international scientist community. In this paper, we analyze 8 of them to evaluate their main pros and cons, expanding a first comparison study performed by Wei et al. (2016). Selected Indoor Air Quality Indices are IAPI (Sofuoglu and Moschandreas, 2003), LHVP (Castanet, 1998), CLIM 2000 (Castanet, 1998), BILGA (Castanet, 1998), GAPI (Cariou and Guillot, 2005), IEI Taiwan (Chiang and Lai, 2002), QUAD-BBC (Quad-BBC, 2012) and DALY (Logue et al., 2011). In a first part, the methodology used to compare the different indices is presented along with the description of the 8 IAQ indices, the pollutants of concern and their associated Exposure Limit Values (ELVs). Comparison and discussion are given in a second part which results in the definition of a new IAQ index.

## 2 METHOD

### 2.1 IAQ Indices

A total of 8 indices are studied in this paper: IEI, LHVP, CLIM 2000, BILGA, GAPI, IEI Taiwan, Quad-BBC, and DALY. Table 1 gathers all calculation equations of the different indices along with the reference studies that defined them.

Table 1: previously proposed approaches to define IAQ index

Index	Equation	Reference
<b>IAPI</b>	$I_{IAPI} = \frac{1}{I} \sum_{i=1}^I \frac{1}{J} \sum_{j=1}^J \frac{1}{K} \sum_{k=1}^K 10 \times \left[ 1 - \frac{C_{i,j,k}^{max} - C_{i,j,k}^{obs}}{C_{i,j,k}^{max} - C_{i,j,k}^{min}} \left( \frac{ELV_{i,j,k} - C_{i,j,k}^{obs}}{ELV_{i,j,k}} \right) \right] \quad (1)$ <p>where <math>I</math> is the number of level-3 groups, <math>J</math>, the number of level-2 groups in each level-3 group, <math>K</math>, the number of level-1 pollutant variables in each level-2 group and <math>max</math> and <math>min</math> are the measured maximum and minimum concentrations of the BASE study (Girman et al., 1995), respectively.</p>	Sofuoglu and Moschandreas (2003)
<b>LHVP</b>	$I_Q = \frac{[CO]}{5} + \frac{[CO_2]}{1000} + \frac{DTB}{1000} (2)$ <p>where <math>[CO]</math> and <math>[CO_2]</math> are carbon monoxide and dioxide concentration (ppm) respectively and <math>[DTB]</math> is the total airborne bacteria concentration (cfu/m<sup>3</sup>).</p>	Castanet (1998)
<b>CLIM 2000</b>	$I_{CLIM2000} = \frac{1}{4} \left( \frac{[CO]}{30} + \frac{[CO_2]}{4500} + \frac{[NO_2]}{0.4} + \frac{[HCHO]}{0.06} \right) (3)$ <p>where <math>[NO_2]</math> and <math>[HCHO]</math> represent the concentration of nitrogen dioxide and formaldehyde respectively; concentrations are expressed in mg/m<sup>3</sup>.</p>	
<b>BILGA</b>	$I_{BILGA} = \begin{cases} \max \left( \frac{E_{mean}^p - ELVc_T^p}{ELVa_T^p - ELVc_T^p} \right), & \text{if } E_{mean}^p < 0 \\ \max \left( \frac{E_{mean}^p - ELVc_T^p}{ELVc_T^p} \right), & \text{if } E_{mean}^p \geq 0 \end{cases} \quad (4)$ <p>where <math>E_{mean}^p</math> is the mean exposure to pollutant <math>p</math> over the period of time <math>T</math> and <math>ELVc_T^p</math> and <math>ELVa_T^p</math> are the Exposure Limit Values for chronic and acute effects.</p>	
<b>GAPI</b>	$GAPI = \sum_i W_i C_i \quad (5)$ <p>where <math>C_i</math> is the concentration of pollutant <math>i</math> and <math>W_i</math> is the impact weight coefficient of pollutant <math>i</math></p>	Cariou and Guillot (2005)
<b>IEI Taiwan</b>	$GAPI = \sum S_x W_x \quad (6)$ <p>where <math>S_x</math> is the score of category <math>x</math> and <math>W_x</math> is the impact weight coefficient of category <math>x</math></p>	Chiang and Lai (2002)
<b>Quad-BBC</b>	$I_{Quad-BBC} = \sum_{i=1}^p \frac{C_{obs}}{ELV} (7)$ <p>where <math>p</math> is the number of pollutants in the group and <math>obs</math> is the measured concentration.</p>	Quad-BBC (2012)
<b>DALY</b>	$DALY_{disease} = YLL_{disease} + YLD_{disease} (8)$ <p>where <math>YLL_{disease}</math> are Years of Life Lost due to premature death from the disease and <math>YLD_{disease}</math> are Years of Life Disability, weighted from 0 to 1 depending on disease severity.</p>	Logue et al. (2011)

Most indices from literature are based upon the same principle: an average indoor concentration is divided by an ELV, quite similar to hazard quotients used for health risk assessment. ELV are usually health-based but may be different to toxicological reference values and vary according to the index. Many indices use sub-indices dedicated to one pollutant that are aggregated to obtain a unique index. Nevertheless, the presence of sub-indices and its aggregation are important questions that induce debates. From Table 1, 4 main types of aggregation emerged:

- **Sum-average:** Most indices are based on a sum of pollutants' concentrations compared to a reference value. Sometimes the sum is divided by the number of studied pollutants. The aim is to quantify average level of quality in a room by considering each pollutant as equally important.
- **Maximum:** The BILGA index is calculated by taking the maximum value of all its sub-indices. The pollutant with highest toxicity exposure is the only one taken in account to assess IAQ.
- **Specific formula:** Some indices are not based on a concentration divided by an ELV but on a specific formula that returns a value per pollutant, which can be summed up to all pollutants to obtain a global health risk assessment level.
- **Score using breakpoint concentration:** the IEI Taiwan is based on the attribution of a score for each pollutant using 4 ranges of concentrations between breakpoints. Scores are summed in the category except if one score of the category is below 60, in which case the minimum score of the category is chosen. Scores of respective categories are then summed and weighted by a category coefficient.

Table 2 summarizes the main pros and cons of the published indices.

Table 2: Main pros and cons for IAQ indices and types of formula.

Type of aggregation	Corresponding indices	Main pros	Main cons
<b>Sum-average</b>	IEI, CLIM2000, LHVP, Quad-BBC	IEI values are limited between 0 and 10. Quad-BBC has an adaptive formula depending on the type of room.	Loss of information by ambiguity or eclipsing (Ministry of Environment, Forests and Climate Change, 2014): importance of a high value can be reduced in a mass of low values even if it exceeds hazardous threshold level.
<b>Maximum</b>	BILGA	Based on the most unfavourable pollutant level. Take into account both limited risks and important risks.	ELVs used are old and need to be updated
<b>Specific formula</b>	GAPI, DALY	GAPI has a flexible formula that can be readapted to any pollutants and many studies criteria. DALY is based exclusively on health impacts.	GAPI value has no real signification. DALY approach is very approximate and many pollutants lack of available data to be used efficiently.
<b>Score by breakpoint concentration</b>	IEI Taiwan	IEI Taiwan gathers both Sum-average and Maximum type advantages.	In practice, it is almost equal to Maximum type. Breakpoint concentrations and categories weights are defined subjectively without a related health correlation

## 2.2 Target pollutants

The pollutants used in the calculation of each index are listed in Table 3.

Table 3: Pollutants used in the calculation of each index.

Indices	Pollutants
<b>IAPI</b>	Formaldehyde, Benzene, Acrolein, Carbon monoxide, Carbon dioxide, PM <sub>10</sub> , PM <sub>2.5</sub>
<b>LHVP</b>	Carbon monoxide, Carbon dioxide
<b>CLIM 2000</b>	Carbon monoxide, Carbon dioxide, Formaldehyde
<b>BILGA</b>	Carbon monoxide (1h), Carbon monoxide(8h), Carbon dioxide, Formaldehyde, Radon
<b>GAPI</b>	Formaldehyde, Acetaldehyde, Acrolein, Hexaldehyde, Benzene, 1-Methoxy-2-propanol, Trichloroethylen, Toluene, Tetrachloroethylene, 1-Metoxy-2-Propyl, Acetate, Ethylbenzene, m,p-xylenes, styrene, o-xylene, 2-Butoxyethanol, 124-Trimethylbenzene, 1,4-dichlorobenzene, n-decane, 2-Butoxy ethyl acetate, n-undecane
<b>IEI Taiwan</b>	Carbon monoxide, Formaldehyde, Carbon dioxide, PM <sub>2.5</sub> and Total volatile organic compounds (TVOC)
<b>Quad-BBC</b>	Carbon monoxide, Formaldehyde, PM <sub>2.5</sub> , Radon, Toluene, o-xylene, Acetone, PM <sub>10</sub>
<b>DALY</b>	PM <sub>2.5</sub> , Carbon monoxide, Acrolein, Formaldehyde, Benzene

## 2.3 Exposure Limit Values (ELV)

Almost every index use Exposure Limit Value (ELV) to quantify the exposure level to a pollutant. Among the studied indices, 4 different types of ELV are used:

- Limited Risk Value (LRV): For exposure below LRV, health impacts are limited, null, or unknown.
- Important Risk Value (IRV): If exposure is above IRV, health impacts are proven, corresponding to irreversible lesions, chronic diseases, or even death.
- Toxicological Reference value (TRV): Based on animal toxicological studies by applying a conversion factor, or sometimes based on human epidemiologic studies.
- Indoor Air Guideline Values (IAGV): Threshold values defined by national or international organizations, e.g. the French Agency of Health and Environment Security (ANSES). According to the definition, there is no known health impact for the selected period below the threshold concentration.

Note that, among the 4 main ELV used, TRV are not accurate and may differ from one study to another; LRV and IRV are too old and too lax. IAGV seems to be the most relevant one, because it is current, accurate, and based on known health impacts.

## 2.4 Comparison procedure

In order to proceed with the comparison of IAQ indices, a common set of inputs is necessary. Most studied IAQ indices require both pollutants concentration levels and Exposure Limit Values (ELVs). Regarding the first kind of inputs, the French dwellings survey conducted from 2003 to 2005 by OQAI (French Indoor Air Quality Observatory) on 567 housings (Kirchner et al., 2007) was chosen as a reference for IAQ assessment in residential buildings. In this survey, only long-term effects were taken in account. NO<sub>2</sub>, SO<sub>2</sub>, O<sub>3</sub>, mold and bacteria were not measured. Whenever a pollutant concentration is not available but is needed in the calculation, the index formula was readapted so that it does not bias the results. As much as possible, all indices were calculated the same way as it was firstly described in the literature. Most indices need ELVs for considered pollutants. If the ELV was not clearly defined, the French Indoor Air Guideline Value (IAGV) was chosen (ANSES, 2011). If not available, international reference values were used instead e.g. WHO (WHO 2010), OEHHA (2016)...

The following procedure is applied to compare the indices. A first graph presents the distribution of the studied index according to its original scale considering the 567 dwellings (Figure 1, left). A second one is produced to transform the results using a common 3 level-scale with the following interpretation: good, intermediate or bad IAQ (Figure 1, right). All indices have an interpretation to determine if IAQ is good or bad in a dwelling in their original definition except for DALY and GAPI. The first approach quantifies DALY lost per year per 100,000 persons due to exposure to indoor air pollutants but there is no indication on how many DALYs should be lost per year to consider IAQ as good or bad. The GAPI index returns a value that relies on the weight of the selected criteria without any scientific signification.

A last graph (Figure 2) intends to detect eclipsing as defined by Sharma and Bhattacharya (2012) and inconsistencies. Most of IAQ indices employ aggregation (maximum, sum, weighted averages, root-mean-square formulation...) of sub-indices at some point so that information for a particular pollutant can be hidden by the weight of the other pollutants. In this analysis, the studied indices are plotted against the maximum value of the concentration of each pollutant to its ELV ratio (MAX) in order to identify whether the indices are not hiding critical cases or not. In Figure 2, some points are encircled in red, they are associated with dwellings that have a bad IAQ according to IAPI value whereas it has an excellent IAQ according to MAX index ( $<0.5$ ). On the contrary, points encircled in blue correspond to dwellings with an intermediate IAQ whereas MAX ( $>1$ ) characterizes a very bad IAQ (one pollutant at least is above short-term IAGV). In this example the dispersion is so high that IAPI is not able to distinguish the level of IAQ as shown by the green region of equal MAX and IAPI ranging from 4 to 10 and the orange region where IAPI predicts the same level of IAQ with a MAX ranging from 0.2 to 3.5. Short term IAGV was used as ELV to detect bad IAQ with certainty.

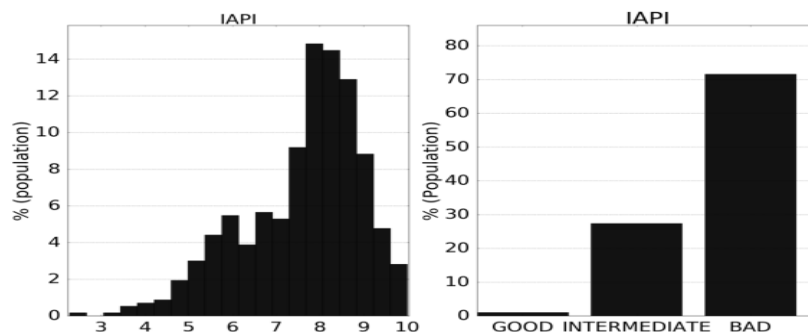


Figure 1: Representation of indices (left: original scale; right: common scale) – Example for IAPI.

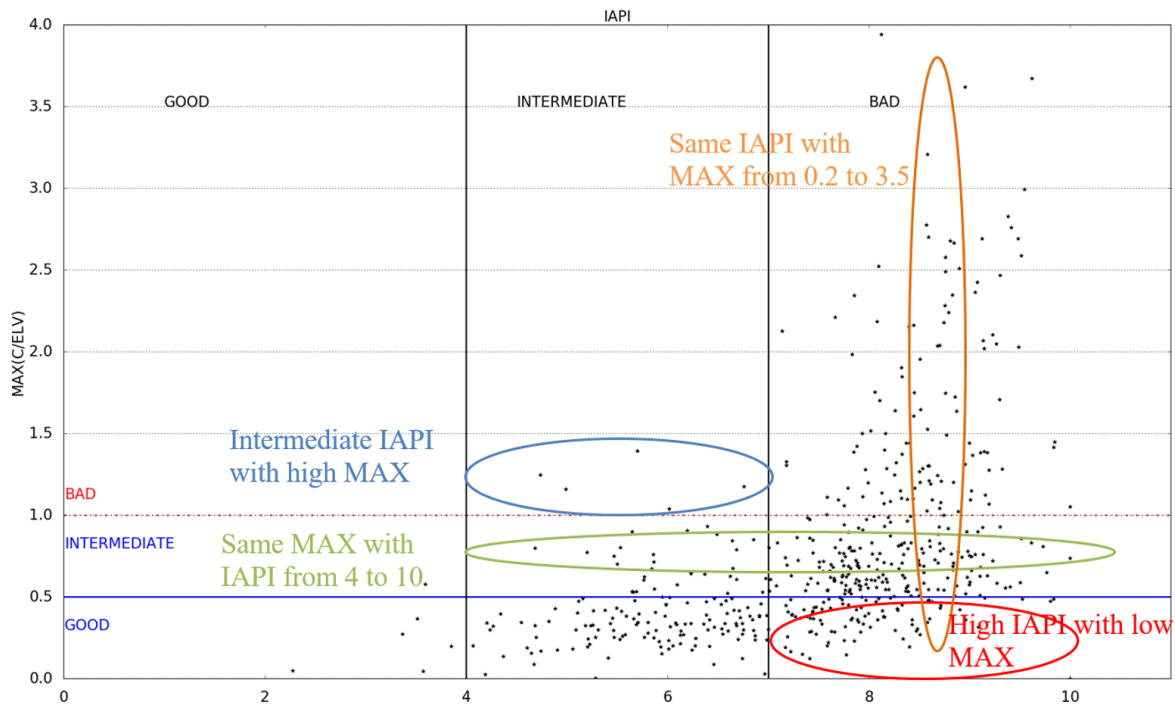


Figure 2: Detection of hidden information – Example for IAPI.

### 3 RESULTS AND DISCUSSION

#### 3.1 IAQ indices comparison

All results obtained by calculating the 8 IAQ indices are compiled in Figure 3 to 5. Since  $PM_{2.5}$  weights about 90% of DALYs lost and was not measured in every dwelling, we decided to consider only the dwellings where  $PM_{2.5}$  was measured (noted as “DALY (with  $PM_{2.5}$ )” hereafter). Figure 3 shows that some indices do not distinguish well the differences among the buildings (LHVP, GAPI, IEI Taiwan) whereas the others do. Figure 4 strengthens this observation. In particular, only two indices clearly classify the building population according to the interpretation scale: IAPI and DALY. However, they interpret the IAQ in opposite way with 70% and 20% of bad IAQ for IAPI and DALY, respectively. Figure 5 highlights the lack of correlation between the indices and the MAX except for DALY and, to a lower extent, BILGA and IAPI.

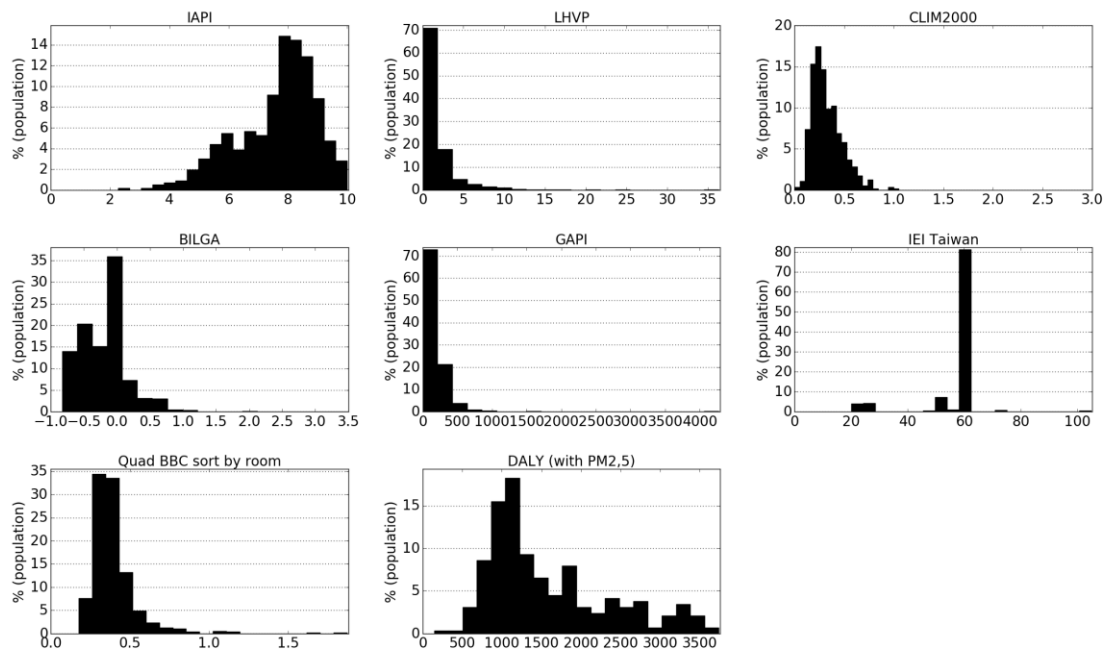


Figure 3: Representation of indices according to their original scale.

### 3.2 Proposal of a new index

Since there is no current consensus about the definition of good or bad IAQ, we propose a few statements that IAQ should reflect in our opinion:

- IAQ is good if there is no known health impact in a long-term perspective. Long-term (usually 1 year period) IAGV can be seen as the minimum threshold to be considered.
- IAQ is bad when the long-term (annual) average concentration is above short-term exposure maximum threshold. Short-term IAGV represents the maximal threshold for a long-term(annual) average concentration.
- Since the comparison is made with a critical threshold, if only one pollutant reaches this threshold, it is sufficient to affirm that IAQ is bad with certainty, no matter how low the concentration of the other pollutants are. The most unfavourable situation is relevant to define an IAQ index.
- There is no point in letting IAQ index values range from  $]-\infty; +\infty[$ . If the long-term (annual) average concentration of one pollutant is above critical threshold, no matter how high the concentration, IAQ remains bad; a maximum value for the index can be then defined. In the same way, concentration below the minimum ELV threshold refers to good IAQ so that an index minimum value can be proposed.

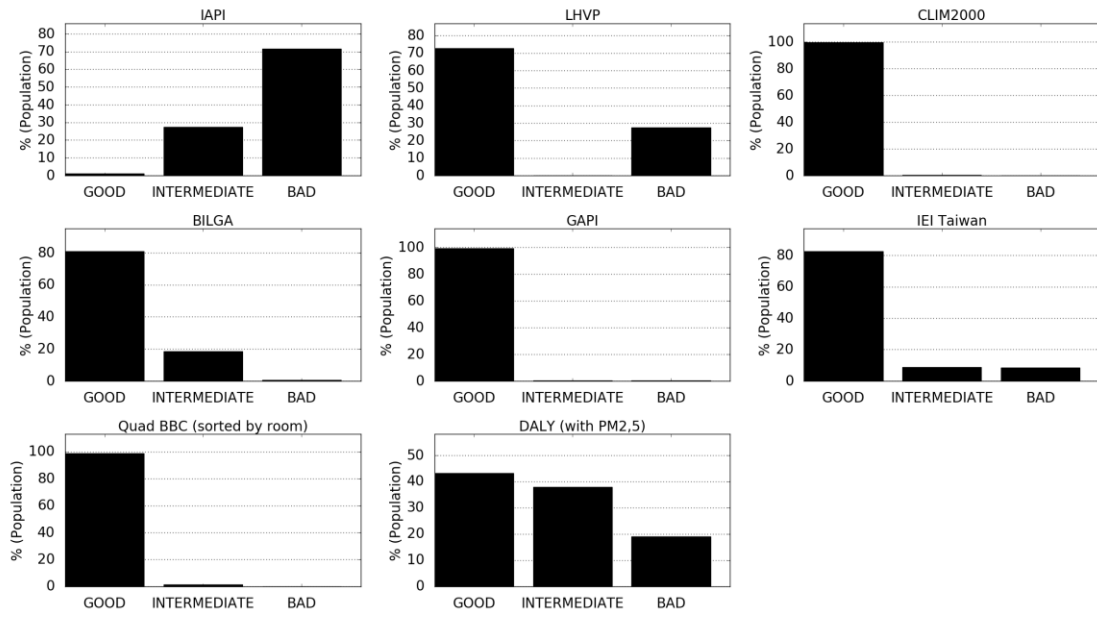


Figure 4: Representation of indices according to their interpretation scale.

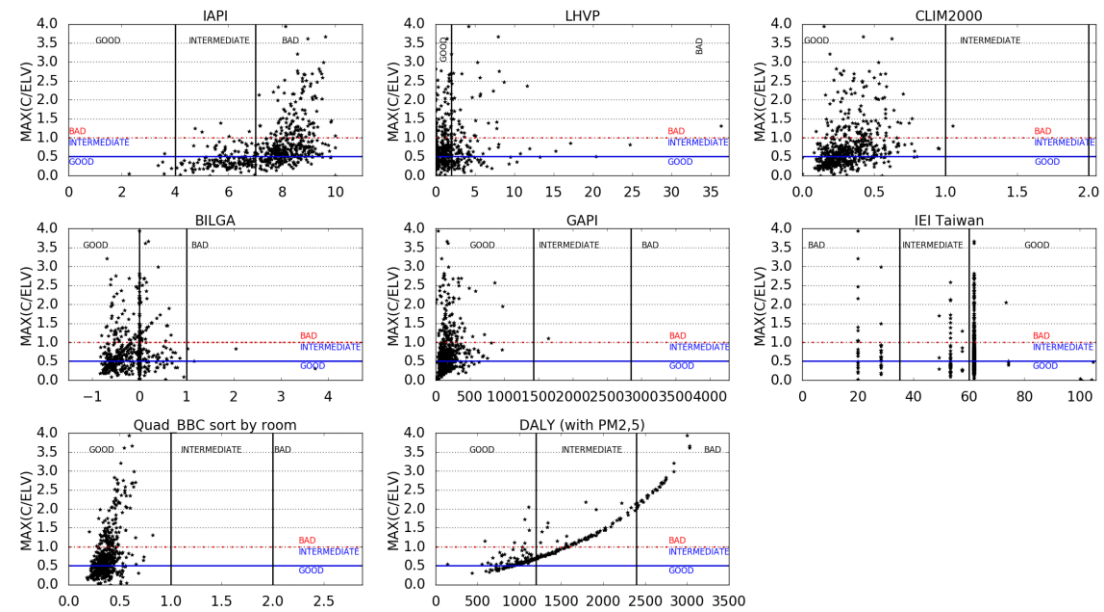


Figure 5: Comparison of indices with the MAX index.

Based on the previous points, the proposed formula for a new index, called ULR-IAQ, is the following:

$$I_{ULR-IAQ} = \max\left(\frac{10(C_{ind,i} - IAGV_{LT,i})}{IAGV_{ST,i} - IAGV_{LT,i}}\right)^{(9)}$$

$IAGV_{LT,i}$  is the indoor air guideline value for long-term exposure (usually 1 year) to apollutant,  $IAGV_{ST,i}$  is the indoor air guideline value for short-term exposure (shortest available) and  $C_{ind,i}$  is the indoor concentration of pollutant  $i$ . If  $C_{ind,i} > IAGV_{ST,i}$  then  $C_{ind,i} = IAGV_{ST,i}$  and if  $C_{ind,i} < IAGV_{LT,i}$  then  $C_{ind,i} = IAGV_{LT,i}$ .

This index varies from 0 to 10. A value of 0 means that IAQ is good; there is no known health impact due to the target indoor air pollutants. Index equals to 10 means a very bad IAQ; it is dangerous for human health even on short-term exposure and something must be done to improve IAQ. Between those two boundaries, a linear trend is used for sake of simplicity as we cannot currently define intermediate situations between good and bad IAQ.

The pollutants accounted for this new index have been selected according to the existence of a long- and short-term exposure IAGV and concentration level availability in the OQAI campaign (OQAI, 2007). They are<sup>1</sup>: formaldehyde [10; 50], acetaldehyde [160; 3000], acrolein [0.8; 6.9], benzene [2; 30], trichloroethylene [20; 800], toluene [70; 15000], tetrachloroethylene [250; 1380], styrene [250; 21000], o-xylene [200; 22000], PM<sub>10</sub> [20; 50], PM<sub>2.5</sub> [10; 25] and carbon monoxide [10; 100].

### 3.3 Evaluation of the proposed index

As for the previous indices, ULR-IAQ was calculated over the whole French dwellings measurement campaign of 567 housings. Results are presented in Figure 6. The new index shows another picture of the IAQ in French buildings: about 28% bad, 10% good and the remaining 62% with intermediate IAQ. This picture is close to the finding of Wei et al. (2016), using a more complex combination of index classification: 34% bad, 6% good and 60% intermediate IAQ. The third graph confirms the capability of detecting bad IAQ; this result is obvious as it is part of the definition of ULR-IAQ.

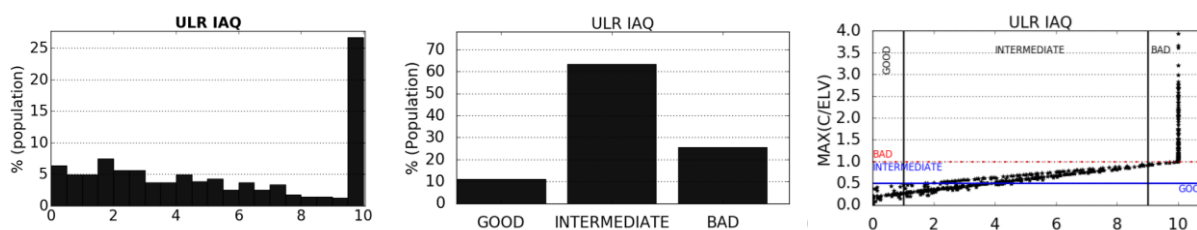


Figure 6: Results of ULR-IAQ, original scale (left), interpretation scale (middle) and comparison with max(right).

One key element to evaluate the IAQ is the list of target pollutants to be considered. A total of 12 pollutants have been used to evaluate the new index. However, not all pollutants have the same importance on the ULR-IAQ final value. Figure 7 reports how frequent each pollutant

<sup>1</sup> All pollutants are presented as follows: name [long-term ELV; short-term ELV]. All units are in  $\mu\text{g}\cdot\text{m}^{-3}$  except for carbon monoxide which is in  $\text{mg}\cdot\text{m}^{-3}$

has the first, second and third highest sub-index, respectively noted “pollutant 1, 2 and 3”. The result clearly points formaldehyde, acrolein, benzene, PM<sub>10</sub>, PM<sub>2.5</sub> and carbon monoxide as unavoidable when evaluating IAQ in dwellings. However, from literature, at least three more pollutants of interest should be added to the list i.e. radon, nitrogen dioxide and mould. Their harmful effects are known but there was no available data in the French survey to take them into account.

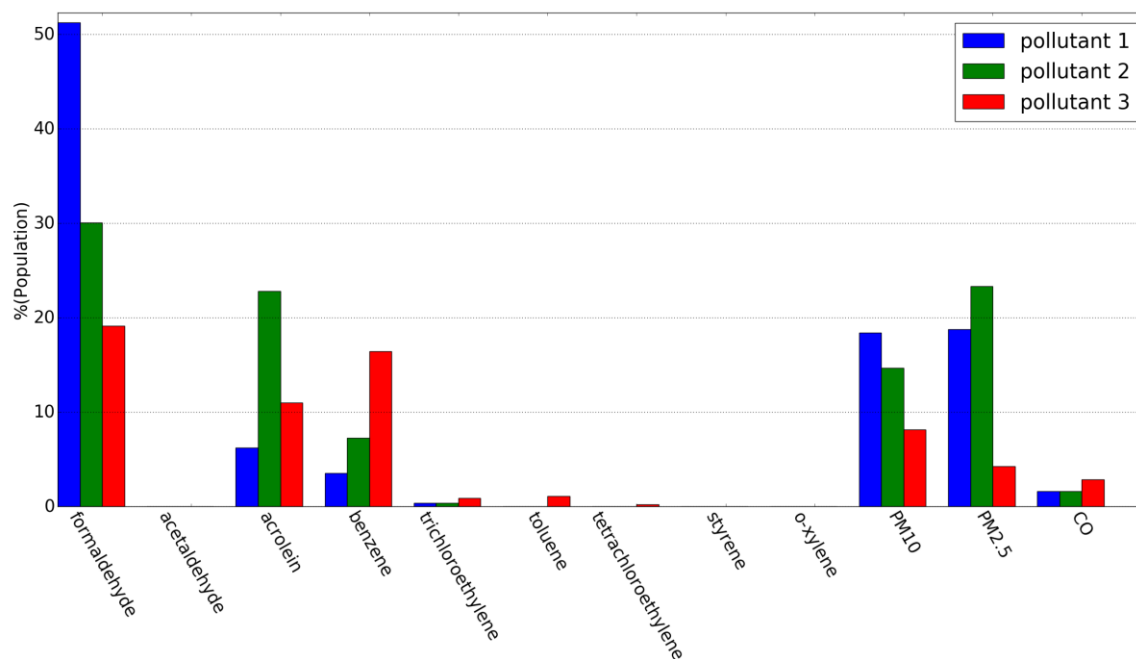


Figure 7: Frequency of pollutants corresponding to the 3 most unfavourable on the whole dwelling measurement campaign.

## 4 CONCLUSION

This work is based on the comparison of IAQ indices. Eight indices found in the literature were calculated and compared using the data of the French dwelling measurement campaign (567 housings) as inputs. By analysing the outputs and indices' original definitions, the advantages and drawbacks have been listed and the definition of a new index called ULR-IAQ has been proposed. The new index seems to give a better representation of the IAQ of the studied dwellings. In particular, the index allows the detection of bad IAQ caused by one (or more) pollutants, ability not included in the existing indices. The new index permits to limit the list of pollutants of interest to a minimum, a list in agreement with previous prioritization studies (INDEX, 2005; Kirchner et al., 2007).

## 5 AKNOWLEDGEMENTS

The authors want to thank the Nouvelle Aquitaine Region (CPER 2015-2020 “Bâtiment Durable”) and Health Agency (former ARS-Poitou-Charentes) for funding this research project.

## 6 REFERENCES

- ANSES (2011). *Proposition de valeurs guides de qualité d'air intérieur : évolution de la méthode d'élaboration des valeurs guides de qualité d'air intérieur*, collective expertise report, April, 89 pages.
- Cariou S. and Guillot J.M. (2005). Utilisation d'un indice global de la qualité de l'air intérieur pour suivre l'ensemble des COV présents et leur impact sur la santé humaine. *Air Pur*(69).
- Castanet S. (1998). *Contribution à l'étude de la ventilation et de la qualité de l'air intérieur des locaux*, PhD thesis, Institut National des Sciences Appliquées (INSA).
- Chiang C. M. and Lai C. M. (2002). A study on the comprehensive indicator of indoor environment assessment for occupants' health in Taiwan. *Building and Environment*, 37(4),387-392.
- Haverinen-Shaughnessy U, Shaughnessy R.J, Cole E.C, Toyinbo O, Moschandreas D.J.(2015). An assessment of indoor environmental quality in schools and its association with health and performance, *Building and Environment*. 93, 35-40.
- Hulin M., D. Caillaud, I. Annesi-Maesano (2010). Indoor air pollution and childhood asthma: variations between urban and rural areas, *Indoor Air* 20, 502-514.
- INDEX. (2005). *The INDEX project: Critical Appraisal of the Setting and Implementation of Indoor exposure Limits in the EU*. European Commission, Joint Research Centre, Institute for Health and Consumer Protection, Physical and Chemical Exposure Unit, Ispra, Italy (JRC/IHCP/PCE), Report, 338 pages.
- Kirchner S., Cochet C., Derbez M., Duboudin C., Elias P., Gregoire A., Jedor B., Lucas J.P., Pasquier N., Pigneret M. & Ramalho O. (2007), Etat de la qualité de l'air dans les logements français, *Environnement Risques & Santé*, 6(4), 259-269.
- Logue J.M., Price P.N., Sherman M.H., and Singer B. C. (2012). A Method to Estimate the Chronic Health Impact of Air Pollutants in U.S. Residences, *Environmental Health Perspective*, 120( 2).
- Ministry of Environment, Forests and Climate Change (2014). *National Air Quality Index*, Government of India.
- Moschandreas D. and Sofuoglu S. C. (1999). The Indoor Air Pollution Index. *Indoor Air* 9,2,261-266.
- Moschandreas D. J. and Sofuoglu S. C. (2004). The indoor environmental index and its relationship with symptoms of office building occupants. *Journal of the Air & Waste Management Association*, 54(11), 1440-1451.
- Office of Environmental Health Hazard Assessment (OEHHA) (2016). Acute, 8-hour and Chronic Reference Exposure Levels (chRELS), [www.oehha.ca.gov/air/allrels.html](http://www.oehha.ca.gov/air/allrels.html).
- OMS (2010). *WHO guidelines for indoor air quality: selected pollutants*, 484.

- Quad-BBC (2012). *QUAD – BBC Qualité d’air intérieur et systèmes de ventilation dans les bâtiments à basse consommation d’énergie*, final report.
- Sharma M., Bhattacharya A, (2012). *National Air Quality Index*. Control of Urban Series.
- Sofuoglu S. C. and Moschandreas D. J. (2003). The link between symptoms of office building occupants and in-office air pollution: the Indoor Air Pollution Index. *Indoor Air*, 13(4), 332-343.
- Wei W., Ramalho O., Derbez M., Riberon J., Kirchner S., Mandin C., (2016), Applicability and relevance of six indoor air quality indexes, *Building and Environment*, 109, 42-49.
- WolkoffP. (2013).Indoor air pollutants in office environments: assessment of comfort, health, and performance, *Int. J. Hyg. Environment and Health* 216,371-394.

# Pollutant exposure of the occupants of dwellings that complies with the Spanish indoor air quality regulations

Sonia Garcia Ortega<sup>\*1</sup>, Pilar Linares\_Alemparte<sup>2</sup>

*1 Eduardo Torroja Institute for  
construction sciences-CSIC  
4, Serrano Galvache St.  
Madrid, Spain  
soniag@ietcc.csic.es*

*2 Eduardo Torroja Institute for  
construction sciences-CSIC  
4, Serrano Galvache St.  
Madrid, Spain*

## ABSTRACT

The Spanish Technical Building Code establishes the criteria for indoor air quality fixing minimum and constant ventilation rates per local. Currently, there is a proposal to modify the regulations so that the IAQ criteria becomes more useful by setting it based on average concentrations of CO<sub>2</sub> and accumulated CO<sub>2</sub> in the habitable rooms. However, the indoor average concentration is not the average concentration at which the occupants are exposed. This paper analyses CO<sub>2</sub> concentrations, occupant exposures and occupants location inside dwellings according to the Spanish Technical Building Code change proposal. Legislation must continue advancing and adapting increasingly to the real needs of people and their protection.

## KEYWORDS

Indoor air quality, regulations, CO<sub>2</sub>, occupant exposure, occupant schedule

## 1 INTRODUCTION

In Spain, indoor air quality (IAQ) in dwellings is regulated in the DB HS3 of the Technical Building Code (CTE) (Ministry of Development, 2006), which was enforced in 2006. Since then, research has been developed to improve this regulation in order to make it more performance-based. As a consequence of this research a proposal for a modification of the Spanish regulations establishes two possibilities:

- the compliance with CO<sub>2</sub> concentration ratios: the yearly average of CO<sub>2</sub> must be lower than 900 ppm and the yearly accumulate over 1600 ppm must be less than 500 000 ppm/h; and
- the establishment of the constant flows of Table 1, as a simplified option.

Table 1: Minimum ventilation rates proposed for the Technical Building Code

Size of dwelling	Dry rooms			Wet rooms	
	Master Bedroom	Another bedrooms	Living and dining rooms	Whole minimum	Minimum per room
0 or 1 bedrooms	8	-	6	12	6
2 bedrooms	8	4	8	24	7
3 or more bedrooms	8	4	10	33	8

This paper compares the concentrations of CO<sub>2</sub> in the rooms and the exposure of occupants to CO<sub>2</sub> according to the criteria of the proposed modification of the Spanish regulation DB HS3 of the CTE.

## 2 CALCULATION PARAMETERS

The CO<sub>2</sub> generation and occupancy scenarios indicated in the proposed modification of DB HS3 were used (12 l/s sleeping periods and 19 l/s rest of time).

For occupant exposures, permanent occupation and occupant schedule were considered. The efficiency of ventilation was not taken into account, assuming well mixed air.

Six recently built real dwellings were chosen to perform the analysis. These apartments are representative of the current Spanish residential building stock and can be used as dwelling types.

- Type 1: Apartment: Living+Kitchen+ 2 Bedroom+1 Bathroom
- Type 2: Apartment: Living+Kitchen+2 Bedrooms+2 Bathrooms
- Types 3, 4 and 5: Apartment: Living+Kitchen+3 Bedrooms+2 Bathrooms
- Type 6: Apartment: Living+Kitchen+4 Bedrooms+2 Bathrooms

The case studies were reclassified taking into account their rooms and bathroom counts, also the number of occupants. The Spanish population and dwelling census (National Statistical Institute, 2011, 2016) was used in order to set the criteria to choose the most representative dwellings and occupancy (see some examples in Figure 1).

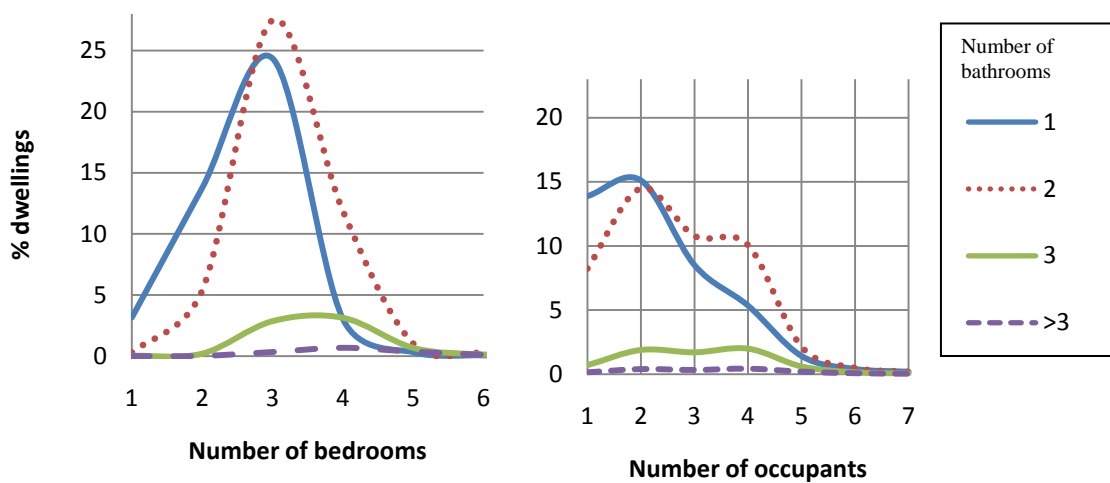


Figure 1: Number of bathrooms in Spanish dwellings according to the number of bedrooms and occupants

## 3 RESULTS

CO<sub>2</sub> concentrations in rooms, occupant exposures and their evolution over time according to the Spanish Technical Building Code change proposal have been studied. The results are described below.

### 3.1 Permanent occupation

When the occupants remain permanently in the dwelling in the same room, with the proposed constant ventilation flows, the steady state is reached achieving the equilibrium concentration results displayed in Table 2. Those equilibrium concentrations are the occupant exposures.

Table 2: Occupant exposures when the occupants remain permanently in the dwelling in the same room

	Ventilation flow(l/s)	Generation of CO <sub>2</sub> (l/h)	Occupant exposures(ppm)
Single bedroom (1 occ.)	4	12	1233
Double bedroom (2 occ.)	8	2 x 12	1233
Living room (4 occupants)	10	4 x 19	1983

At steady state, in order to not exceed an equilibrium concentration of 900 ppm CO<sub>2</sub> (considered as adequate air quality limit) or 1600 ppm CO<sub>2</sub> (considered as inadequate air quality), assuming an efficiency of 100% of the ventilation and an outdoor concentration of 400 ppm CO<sub>2</sub>, the flow rates displayed in Table 3 are needed.

Table 3: Needs of ventilation flow according with different concentrations objective

	Generation of CO <sub>2</sub> (l/h)	Goal equilibrium concentration (ppm)	Needs of ventilation flow (l/s)
Single bedroom	12	900	6.67
		1600	2.78
Double bedroom	2 x 12	900	13.33
		1600	5.56
Living room (4 occupants)	4 x 19	900	31.67
		1600	13.19

This approach is for 100% effective flow, so the actual flow rates should be higher, depending on the efficiency of the ventilation system.

However, steady state will not usually be achieved, depending -on our simplification model- of the size of the room.

### 3.2 Room size influence

When the occupants remain permanently in the same room, the concentration of CO<sub>2</sub> (constant generation) reaches the equilibrium in a time function of the room volume.

Accumulation = Generation - Elimination

$$VdC = Gdt - Q'Cdt \quad (1)$$

where:

V: volume of the room, m<sup>3</sup>

G: pollutant generation rate, mg / h

Q': effective ventilation flow, m<sup>3</sup> / h

C: concentration of the contaminant, mg / m<sup>3</sup>

t: time, h

Considering constant volume (of the room), constant CO<sub>2</sub> generation (human breath) and effective constant flow rate Q, after a space of time the equilibrium will be reached: constant concentration of CO<sub>2</sub> in the room. The time to reach this equilibrium, in the considered case

(proposed generation, pollutant concentration, constant ventilation flow according to the proposal) will therefore depend on the volume of the rooms. Because of this, when occupants go into and out of the room before the equilibrium time, the occupant exposures are lower than the occupant exposures with permanent occupation. In addition, the occupant exposures decrease as the room size increases.

For example, in the case of a bedroom -where the occupants spend more uninterrupted time-taking useful surfaces of 5, 10 and 15 m<sup>2</sup> and an average height of 2.5 m, the time to reach steady state varies from 4 to 12 hours. Mean concentrations during the first 8 hours range from 1132 to 955 ppm; reaching 900 ppm at 55', 1h 45' and 2h 35' respectively. Occupant exposures are showed in Table 4.

Table 4: Evolution of occupant exposures in function of bedroom size

Bedroom size (m <sup>2</sup> )	Ventilation flow per occupant (l/s)	Time to reach 900 ppm (hour - minutes)	Time to reach steady state (+/- 1%, hours)	Steady state concentration (ppm)	Occupant exposure after 8 hours (ppm)	Occupant exposure average (ppm)
5	4	0h - 55'	4	1233	1233	1132
10		1h - 45'	8		1222	1038
15		2h - 35'	12		1185	955

Representative Spanish single bedrooms are considered between 5 to 10 m<sup>2</sup>, and double bedrooms between 10 to 15 m<sup>2</sup>. Table 5 represented the results of both cases for the reason that ventilation flow is determinate according with the number of occupants.

In a real situation, in the most of the cases, occupants leave the rooms before the steady state - except small bedrooms. The occupant exposure average will be lower than the steady state concentration or the occupancy exposure of permanent occupation.

### 3.3 Occupant schedule

The CO<sub>2</sub> concentration per room and the occupant exposure for the six dwelling types are analyse using CONTAM. The used ventilation rates are the proposed for the Technical Building Code (see Table 1). Table 5 summarise it.

Occupation scenario or occupant schedule is according to the main following conditions:

- sleep periods for each occupant of 8 hours uninterrupted from 24:00 to 08:00 hours, in bedrooms;
- absences during the day:
  - from Monday to Friday an absence of 13 hours per day for 1 of the occupants and 8 hours per day for the rest;
  - Saturdays and Sundays 2 absences of 2 hours for each occupant;
- 2 occupants in the master bedroom and 1 occupant in each of the other bedrooms (until 4 occupants);
- simultaneous remain of all occupants in the living room for at least 2 continuous hours from Monday to Friday and at least 4 continuous hours on Saturdays and Sundays.

Table 5: Continuous ventilation rates values that fulfil the proposed IAQ requirements

Case study	Total whole dwelling continuous	Yearly average CO <sub>2</sub> concentration <sup>(1)</sup> (ppm)	Yearly CO <sub>2</sub> concentration accumulated over 1600 ppm <sup>(1)</sup> (ppm·h)
------------	---------------------------------	---	---

	ventilation rate (l/s)		
1	14	834	0
2	24	772	111 754
3, 4, 5	33	930	188 804
6	33	842	178 529

(1) The highest value per room in each dwelling or the highest of the group of dwellings

For each room, the average CO<sub>2</sub> concentration ranges between 600 ppm and 900 ppm, with a global average of 700 ppm (see Figure 3). The red dot represents the global average. The 400 ppm dot belongs to an empty bedroom in dwelling type 6 (400 ppm is the considered outdoor CO<sub>2</sub> concentration).

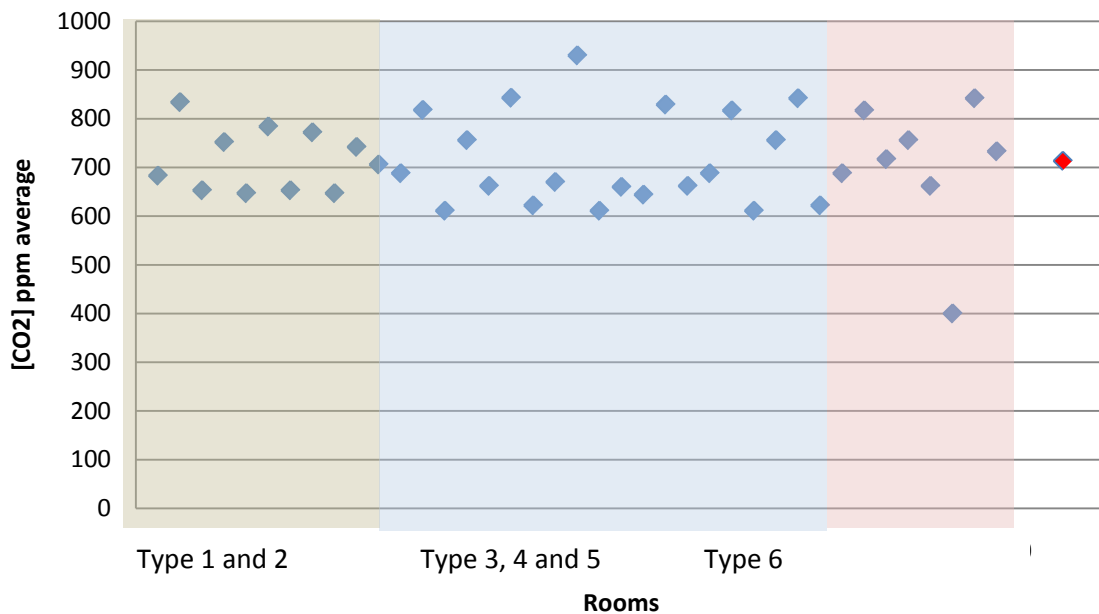


Figure 2: Average CO<sub>2</sub> concentration in the different rooms for the case studies. In red: global average

The average exposure to CO<sub>2</sub> during the period of occupation for the same case studies ranges from 969 ppm to 1238 ppm, with a global average of 1129 ppm (see Figure 4). The red dot is the global average.

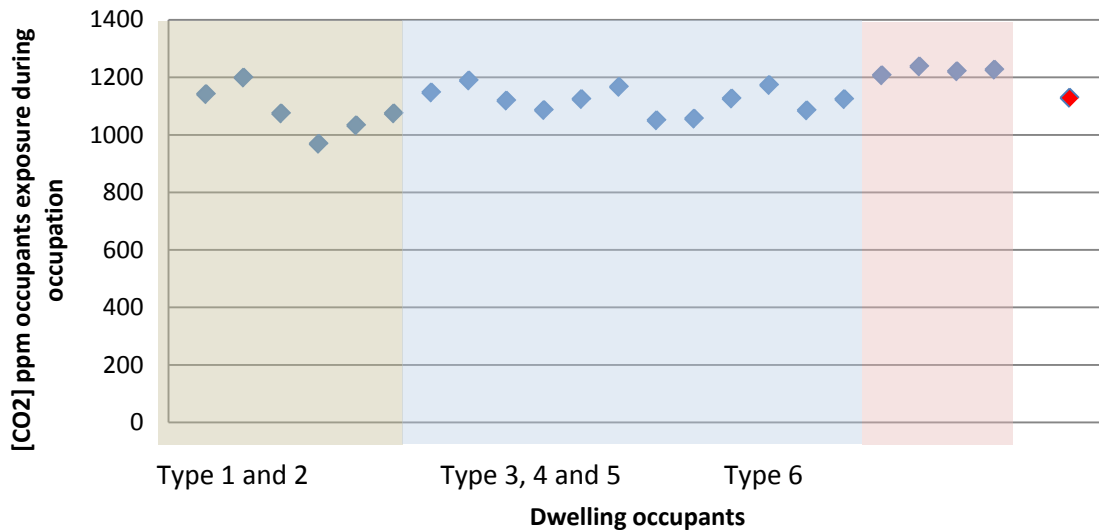


Figure 3: Occupant exposure to CO<sub>2</sub> in the case studies

In the case of the studied occupant's schedule and ventilation -based on constant flows-, the occupant exposures to CO<sub>2</sub> are higher than the average concentrations of CO<sub>2</sub> in rooms (see Figure 3 and Figure 4).

#### 4 CONCLUSIONS

About the proposal BuildingCode change in Spain we observe that:

- in dwelling with 4 or more bedrooms the ratio  $\frac{\text{total flow}}{\text{number of dry rooms}}$  decreases and the exposures increase because of the way of establishing the ventilations flows (a global minimum for wet zones);
- the general rules for establishing the occupants schedule allow the designers to modify it. Because the exposure is affected by the occupants' schedule, the occupants' protection will not be always the same.
- the exposure of occupants to CO<sub>2</sub> is higher than the average concentration of CO<sub>2</sub> in rooms. In order to protect the occupants, the regulations should focus on the occupant exposures, instead of focusing on the room average concentration.

This proposal represents a step forward because evaluates the compliance with air quality regulations according to a performance parameter such as the concentration of CO<sub>2</sub> in living spaces. However, the ultimate goal of the regulations is not to protect the rooms, but to protect the people.

In addition, considering an occupation higher than usual or expected could conduce to an excessive ventilation rate (more than necessary). The excessive ventilation rates increase cooling and heating demand and costs (Linares, 2015) so designers and users tend to reject them. The key would be to know how much ventilation is needed related to the real number of occupants and their schedule.

## 5 REFERENCES

Linares, P. (2015) *Energy saving as a consequence of the proposed change in Spanish Regulations relating to indoor air quality*. Madrid. 36th AIVC Conference " Effective ventilation in high performance buildings".

Ministry of Development (2006). *RD 314/2006, de 17 de marzo, por el que se aprueba el Código Técnico de la Edificación*. BOE-A-2006-5515

National Statistical Institute (2016). *Continuous household survey*. INE Instituto Nacional de Estadística. Spain.

National Statistical Institute (2011). *Censo de población y viviendas 2011* [Population and Housing Census 2011]. INE Instituto Nacional de Estadística. Spain.

# Method development for measuring volatile organic compound (VOC) emission rates from spray foam insulation (SPF) and their interrelationship with indoor air quality (IAQ), human health and ventilation strategies

Dzhordzhio Naldzhiev<sup>1,2</sup>, Dejan Mumovic<sup>1</sup> and Matija Strlič<sup>2</sup>

*1 Institute for Energy and Environmental Design  
University College London  
14 Woburn Place  
WC1H 0NN  
United Kingdom*

*2 Institute for Sustainable Heritage  
University College London  
14 Woburn Place  
WC1H 0NN  
United Kingdom*

## ABSTRACT

The polyurethane foam industry is projected to reach a worldwide value of up to \$74bn by 2022 and with airtightness of new and retrofitted properties continually increasing, an important question arises: what is the impact of these materials on the indoor air quality (IAQ), occupants' health and indoor environment?

As the foams are made in-situ through an exothermic reaction between two chemical mixtures (side A and side B), volatile organic compounds (VOCs) are emitted during their application and curing process. Current research, commercial practices and governmental advice suggests that emissions decrease over time and 8-24 h after application are usually sufficient for residents to return safely to their properties. However, there is still a lack of case studies and a fundamental absence of robust analysis on how ventilation strategies affect long term off-gassing rates and chemical emission quantities. The emission rates from SPF materials could have a direct impact on IAQ if they exceed the occupational exposure rates recommended by NIOSH, or other professional associations. But the difficulty in recording these emission rates is evident as there is still a lack of an international standard for their quantification.

To address this issue, we have developed an analytical methodology for measuring some of the composition materials of the foams and residual products associated with their application. The experiment consisted of two stages- active air sampling of spray foam emissions and spiking desorption tubes with a standard solution in order to develop calibration curves. The solution included SPF compounds, or by-products from their application, associated with possible acute impact on health: 1,4 dioxane, chlorobenzene, dibutyltin dilaurate, triethyl phosphate and bis(2-dimethylaminoethyl) ether. We managed to detect five of the chemicals of interest through air sampling and produce calibration curves for 1,4 dioxane, chlorobenzene and triethyl phosphate, which would allow us to quantify the emission rates at the next stage of research.

The results of the experiments successfully demonstrated proof of concept quantitative methodology for the compounds of interest. With further research and experiments, this technique has the capacity to be developed into an international standard for measuring VOCs from spray foam emissions and other buildings products. This would provide scientists and industry professionals with the tools to further develop retrofit and ventilation strategies in order to provide healthier buildings.

## KEYWORDS

Volatile organic compounds, spray polyurethane foam, indoor air quality, human health, ATD-GC-MS

## 1 INTRODUCTION

With people spending up to 90% of their time indoors, measuring the effect of building material emissions on human health and indoor air quality has quickly become a critical issue (Seddon, 2015)(Lai et al. 2004). Polyurethane spray foam (SPF) sales have topped £1bn in 2015, although the factors affecting their performance are widely unknown (Bomberg, 1998). Only in recent years, their impact on human health and indoor air quality (IAQ) has become an imminent topic for research with industrial and governmental bodies outpacing academic research (ASTM International 2017). The ASTM International consensus on standards for chemical emissions from spray foams (2017) represents 13 papers and signals the need for further understanding of the topic. According to a recent market study report (Markets and Markets, 2016)(Lucintel, 2017) the polyurethane foam industry will grow to \$60.5-74.24bn by 2022, therefore there is an urgent demand for scientific analysis of the impact of these materials on the indoor air quality, human health and effectiveness of different ventilation strategies.

Personal exposure levels to chemical compounds are affected by a mixture between indoor and outdoor pollutants rather than a single source. In order to determine more accurately the effect that building products have on human health, the emission rates of their compounds, or by-products associated with their application, must be recorded. Modern SPF insulating products are produced in-situ through a chemical exothermic reaction between the A-side component (usually MDI<sup>1</sup>, pMDI<sup>2</sup> or TDI<sup>3</sup>) and the B-side component (polyols, fire retardant, catalysts, blowing agents and surfactants). Exposure to the elements of the A-side during application (Crespo & Galan, 1999), its concentration (Lesage et al. 2007) and its impact on human health (Kupczewska-Dobecka et al. 2012) have been measured by using a variety of techniques and methodologies. These include impinger sampling with high-performance liquid chromatography and isocratic reverse phase analysis (HPLC/RP, isocratic) (Schlecht & Cassinelli 1998), impinge sampling with liquid chromatography coupled with ultraviolet detection (LC-UV) (Crespo & Galán 1999), glass fibre filter followed by liquid chromatography coupled with fluorescence detection (LC-FL). The B-side has been primarily analysed with automated thermal desorption-gas chromatography-mass spectrometry (ATD-GC-MS) for informing re-entry times after installation (Wood, 2017), measuring emissions of flame retardants and blowing agents (Poppendieck et al. 2016)(Sleasman, et al., 2017) and VOC emission testing under different application conditions (Won, et al., 2017).

Our experimental setup was designed to contribute to the development of international analytical standards and aimed to provide scientific evidence for the future establishment of voluntary and mandatory protocols for measuring emission rates from building products. The objectives of the experiment were:

- To determine robustness of ATD-GC-MS analytical method for qualitative and quantitative analysis of volatile organic compounds (VOCs), semi-volatile organic compounds (SVOCs) and very volatile organic compounds (VVOCs) from spray foam insulation products
- To examine which compounds and by-products associated with SPF could be detected by using Carbopack-B sorbent tubes and to establish calibration curves for some of the chemicals associated with acute impact on human health

---

<sup>1</sup>4,4' Methylene diphenyl diisocyanate, CAS #101-68-8

<sup>2</sup>Polymeric MDI, CAS # 9016-87-9

<sup>3</sup>Toluene diisocyanate, CAS #584-84-9

## 2 METHODS

The experiment was consisted of two stages: active air sampling of VOC emissions and spiking thermal desorption tubes with a solution consisting of SPF compounds and residual products from its application.

### 2.1 Spray foam active air sampling

A sample of a closed cell spray foam was provided by Q-Bot Ltd (London, United Kingdom). The sample was sprayed directly in a 568 mL expanded polystyrene cup by using remotely controlled robots. The conditions under which the foams were created were not recorded, but it was confirmed that standard procedures as per the manufacturer guidelines for the product application have been followed. The SPF was made on the 17<sup>th</sup> of January 2017 and stored in a sealed vacuum bag at room temperature (18-23°C) in the laboratory for a period of 129 days before being sampled thus providing sufficient time for the foam to cure.

The sample was then cut in a fume hood into ~3-5 cm pieces with a disposable steel knife in order to minimise airborne contamination and following best practice guides (ACC Spray Foam Coalition 2016). The pieces were placed in a 1-L glass bottle for a period of 1 h before sampling. The glass bottle was conditioned in an oven for 24h at 140°C prior to the experiment to ensure that there was no contamination. The weight of the sample was not recorded as the purpose of this stage of the experiment was to obtain qualitative results only.

The experimental setup for sampling can be seen in Figure 1. The glass bottle had an inlet and an outlet, to which Carbopack-B tubes were connected. The incoming air (blue in Figure 1) was filtered through the first tube and then travelled to the bottom of a plastic tube in order to ensure even airflow throughout the vessel. The second Carbopack-B tube was connected to a low flow air pump which was set to 40mL/min ( $\pm 5\%$ ) and air was extracted from the headspace for 44 min (red in Figure 1). For future experiments where quantitative results will be sought a second extraction tube will be coupled with the first one in a series. If any of the chemicals are found in the second tube, the results would not be used and either the extraction time would need to be adjusted or the model of sorbent within the tubes would need to be altered. Prior to sampling the tubes were conditioned at 50mL/min and heated to 350°C for 60 min. The equipment and process of analysis was fully automated with a central software and the experiment was undertaken with controlled flow and temperature.

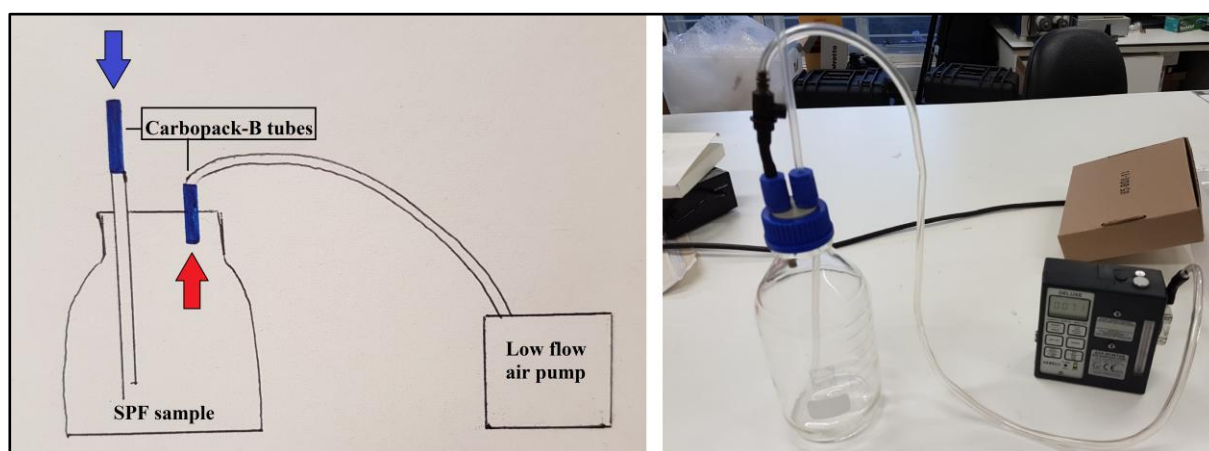


Figure 1. Experimental setup for VOC air sampling from SPF products

## 2.2 Desorption tube spiking

“Spiking” of a desorption tube consists of injecting a small quantity of a prepared chemical solution or standard directly onto the top mesh of the tube. We created a bespoke standard for the purpose of the analysis. Through previous work with solid-phase microextraction-gas chromatography-mass spectrometry (SPME-GC-MS) and literature review, it was determined that ATD-GC-MS would be more suitable for the analysis of the B-side and residual products of the foam (Schlecht & Cassinelli 1998; Creely et al. 2006; ASTM International 2017).

We selected chemicals that could possibly have a negative impact on health. The solution was made by using a micropipette and injecting individual chemicals into a 10-ml glass volumetric flask with quantities as per Table 1. The rest of the flask was filled with HPLC-grade 99.9% methanol.

Ten tubes were injected with 1 $\mu$ l, 5 $\mu$ l, 10 $\mu$ l, 15 $\mu$ l and 20 $\mu$ l of the solution respectively, to provide the calibration range as per Table 1, with an electronic pipette. Two tubes were used for each quantity in order to deliver average values and derive calibration curves. As per the air sampling method, the tubes were conditioned prior to the experiment with 50mL/min nitrogen at 350°C for 60 min. Once the tubes were spiked they were immediately placed within the ATD carousel and the analysis was started in order to ensure accurate results.

Table 1. Standard solution composition

Chemical	CAS Number	Individual weight in vial (mg)	ng/ $\mu$ l	Calibration range (ng)
1,4 dioxane	123-91-1	0.505	50.5	50.5-1010.0
Chloro-benzene	108-90-7	0.525	52.5	52.5-1050.0
Dibutyltin dilaurate	77-58-7	0.405	40.5	40.5-810.0
Triethyl phosphate	78-40-0	0.754	75.4	75.4-1508.0
N,N,N',N' – Tetramethyl-2,2'-oxybis(ethylamine)	3033-62-3	0.421	42.1	42.1-842.0

## 2.3 Instruments and analytical conditions

The samples were collected on Carboxen-100 desorption tubes, which have an analyte volatility range from n-C5 to n-C12 and are suitable for a wide range of VOCs. They are compatible for both active sampling and direct liquid injections. The tubes were placed in a carousel on a Perkins Elmer TurboMatrix 650 automated thermal desorption kit connected to a Perkins Elmer 500 gas chromatograph coupled with a Perkin Elmer Clarus 560D mass chromatograph. The column used was a 60m x 0.25mm x 1.5  $\mu$ m VOCOL fused silica capillary column with helium used as a carrier gas.

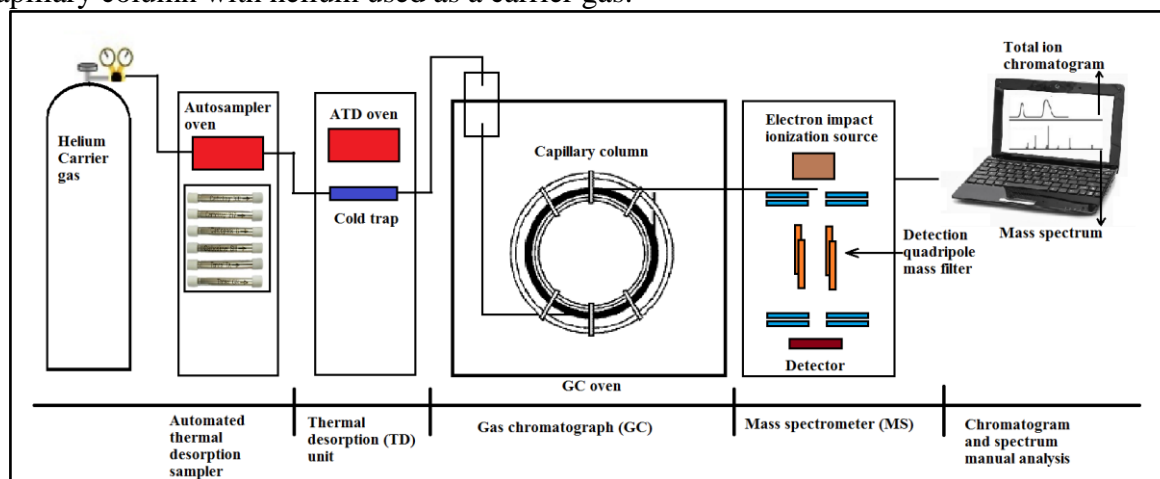


Figure 2. Experimental setup of analytical methodology

This technique allows for a non-destructive headspace analysis of the VOCs emitted by the insulation materials. Albeit in our case we cut the sample in order to exacerbate the emission rates and confirm the robustness and detection limits of the analytical methodology.

The method summary can be found in Table 2.

Table 2. ATD-GC-MS system settings

<b>ATD</b>	<b>Air sampling</b>	<b>Tube spiking</b>
<b>Purge</b>		
Prepurge time	1 min	1 min
Trap in line	No	No
Split	On	On
Flow rate	25 mL min <sup>-1</sup>	25 mL min <sup>-1</sup>
<b>Tube desorption</b>		
Time	8 min	8 min
Temperature	300 °C	300 °C
Split	Off	Off
<b>Trap desorption</b>		
Trap low temperature	-10 °C	-10 °C
Trap high temperature	330 °C	330 °C
Trap hold time	5 min	5 min
Split	On	On
Trap heating rate	40 °C sec <sup>-1</sup>	40 °C sec <sup>-1</sup>
Split flow rate	25 mL/min	35 mL/min
<b>Split ratios</b>		
Inlet	32.5:1	No split
Outlet	26.3:1	26.3:1
Total	58.8:1	26.3:1
<b>Other</b>		
Flow path temperature	250 °C	250 °C
GC cycle time	60 min	120 min
<b>GC</b>		
Helium Flow	1mL min <sup>-1</sup>	1mL min <sup>-1</sup>
<b>Temperature Profile</b>		
Initial Temperature	35 °C (hold 5 min)	50 °C (hold 5 min)
Ramp	10 °C min <sup>-1</sup>	10 °C min <sup>-1</sup>
Second Temperature	200 °C (hold 10 min)	100 °C (hold 0 min)
Ramp		7 °C min <sup>-1</sup>
Third Temperature		200 °C (hold 0 min)
Ramp		2 °C min <sup>-1</sup>
Final temperature		220 °C (hold 25.7 min)
Total run time	31.5 min	60 min
<b>MS</b>		
MS Ionization Mode	E+	E+
MS Inlet Temperature	200 °C	200 °C
MS Source Temperature	180 °C	180 °C
Mode	Scan	Scan
Mass Scan Range	45-300	45-550

### 3 RESULTS

The purpose of these experiments was to obtain qualitative results and establish calibration curves in order to deliver quantitative results in future research.

#### 3.1 Active air sampling chromatogram analysis

The experiment was successful and the chromatograms clearly showed that a number of VOCs were detected from the spray foam. The chromatograms were consistent and clearly resolved peaks could be analysed and identified. There were generally no unusual peak shapes, apart from peak tailing and background noise towards the end of the run. This could have been a sign that the detector temperature of the GC-MS was too low for the samples tested (Prichard, 2003).

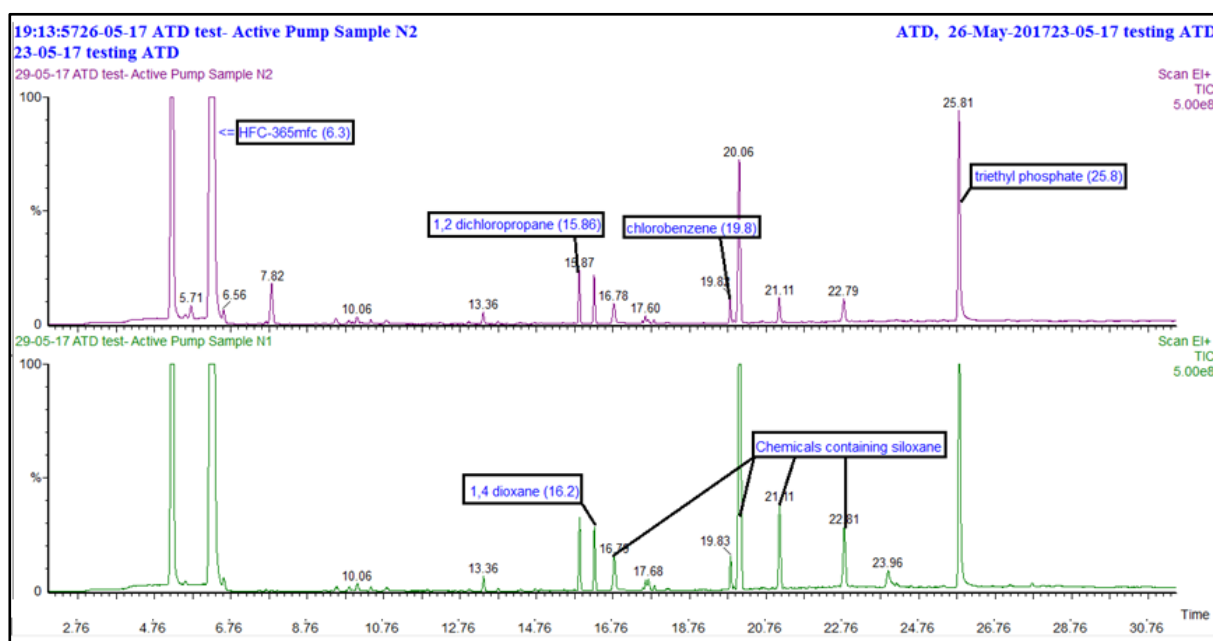


Figure 3. Air sampling chromatograms

The chromatograms displayed a good range of compounds, which was expected due to the complex structure of SPF products and the high sensitivity of the equipment. In order to detect the compounds, manual analysis of the peaks was undertaken through single ion monitoring.

Each of the peaks was cross-referenced to the NIST library database for qualitative assessment. The results were analysed by cross-checking what the peaks most likely are, based on NIST hits, and through searching for the composition chemicals of the foam and expected by-products found from previous analysis (Sleasman, et al., 2017) with the results summarised in Table 3. The ones in red could not be found in the NIST library. Those highlighted in yellow are compounds present in the NIST library, but could not be found during the analysis. The green ones are the detected compounds, which have been successfully matched to their mass spectra within the library.

Table 3: Table Caption

Composition	Target compound	CAS Number & Boiling Point	Product Function	Health impact labels <sup>4</sup>
Side A	Diphenylmethane-4,4'-diisocyanate (MDI)	101-68-8 ; 314 °C	Thermal Insulation (once blown)	
Side B	Dibutyltin dilaurate	77-58-7; 204°C	Catalyst	
	Triethyl Phosphate	78-40-0; 215°C	Flame retardant	
	1,1,1,1,3,3-pentafluorobutane (HFC-365mfc)	406-58-6; 40°C	Blowing agent	
	N,N,N',N'-Tetramethyl-2,2'-oxybis(ethylamine)	3033-62-3; 189 °C	Blowing catalyst	
	Tris(2-chloro-1-methylethyl)phosphate	13674-84-5; 235 °C	Flame retardant	
	N,N-bis[3-(dimethylamino)propyl]-N',N'-dimethylpropane-1,3-diamine	33329-35-0; 297.7 °C	Catalyst	
Residual products	1,4 dioxane	123-91-1; 101 °C	By-products	
	1,2-dichloropropane	78-87-5; 95.5 °C		
	Chlorobenzene	108-90-7; 132 °C		

With the Carbopack-B tubes, five of the chemicals were recorded by using this setup as per Table 2. The detected chemicals had boiling points between 40-215°C, which demonstrates the effectiveness of this method for a wide range of volatile compounds.

The most distinctive emission, associated with the highest peak, was the blowing agent HFC-365mfc. This is expected as the foam was cut, therefore releasing the blowing agent which was trapped within the closed cell structure of the foam. Future experiments would have to make bespoke vessels or emission chambers to ensure that only the surface emission are taken into account in testing. It must be pointed out that all of the residual elements were found even after the foam had cured for 129 days. This leads to the conclusion that the composition chemicals of the foam react with the indoor air (even filtered) and thus the residual compounds are released.

### 3.2 Spiked tubes analysis

The dibutyltin dilaurate and the N,N,N',N'-tetramethyl-2,2'-oxybis(ethylamine) could not be found on the chromatograms when using Carbopack-B tubes. The other three chemicals (1,4-dioxane, chlorobenzene and triethyl phosphate) registered clearly resolved peaks with a linear progression depending on the amount injected onto the tubes.

<sup>4</sup> All figures sourced from PubChem database and based on GHS classification

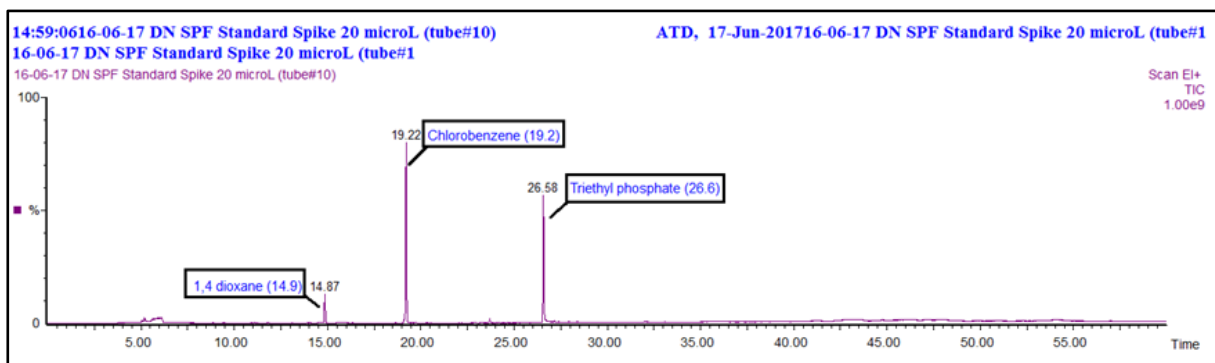


Figure 4. Spiked tubes chromatograms

Chromatographic peak areas were derived by integrating the peak area for each compound. The results were plotted against the known quantity of each material in order to form the calibration curves as per Figure 5. The calibration curves demonstrated a continuous linear increase when the average results for each point were calculated. The standard errors in slope and intercept have been calculated with the full data set. It should be noted that the linearity range has not been exceeded and further experiments will be conducted with higher amounts of the analytes to do so. Once the calibration curves are further established, we will be able to quantify the emission rates.

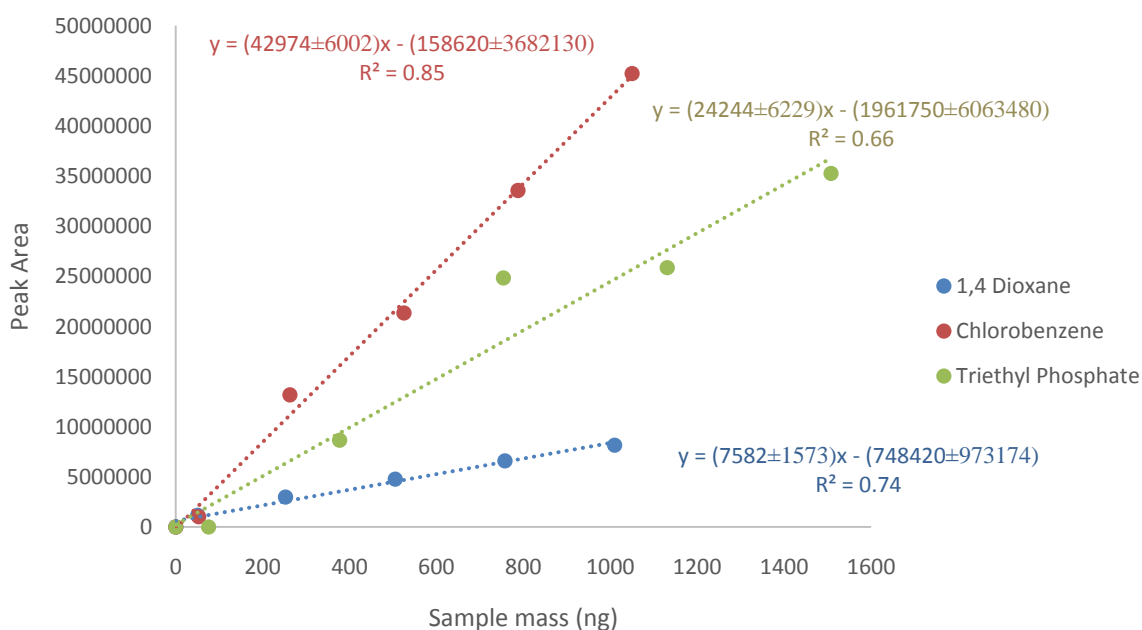


Figure 5. Calibration curves for 1,4-dioxane, chlorobenzene and triethyl phosphate

#### 4 DISCUSSION

The success of both experiments clearly demonstrates the potential of the technique and its repeatability in detecting the chemical compounds from SPF products and by-products released from them. As the isocyanates (MDI) are semi-volatile organic compounds, they demonstrate a high sink effect and due to their high boiling point, they could not be volatilised for analysis. They are highly unstable particles and adhere easily to surfaces therefore making them difficult to detect (Crespo & Galán 1999; Puscasu et al. 2015; Lesage et al. 2007; Kupczewska-Dobecka et al. 2012) and therefore for this reason ATD-GC-MS is not a suitable methodology for their analysis.

There were siloxane elements detected in all tests, which are most likely released from the column as they are also consistently present in the blank samples in very small quantities. It must be noted that some of the other compounds from SPF products have been successfully quantified through the use of Tenax-TA tubes, emission chambers and ATD-GC-MS such as tris(1-chloro-2-propyl)phosphate (TCPP) (Poppendieck et al. 2016), therefore reinforcing the case for the analytical methodology as proposed here.

1,4-Dioxane and chlorobenzene are known to cause headache, numbness and nausea (Agency for Toxic Substances and Disease Registry 1990), eye and nose irritation (Agency for Toxic Substances and Disease Registry 2012). These are one of the common health impact issues recorded after improper installation of SPF insulation products (Huang & Tsuang 2014). The results prove that the residual products from SPF can persist in the air if the foam is damaged and it is crucial that the emission rates are quantified in order to devise ventilation strategies to reduce their impact on IAQ and human health. Further investigation is needed in order to determine which chemicals exactly might be responsible for the negative side effects experienced under faulty applications. In addition, there is no internationally established “faulty application of spray foam insulation materials” definition, but only guidelines for environmental conditions during application and mechanical setup of the spraying equipment.

## **5 INTERRELATIONSHIP OF VOC, IAQ AND VENTILATION STRATEGIES**

Indoor air quality (IAQ) is directly linked with the health and comfort of the building occupants and is determined by the range of indoor and outdoor pollutants (Crump et al. 2009). The volatile organic compounds associated with the application of SPF materials, as per Table 3, could negatively impact IAQ unless robust ventilation strategies are in place to purge the emissions. Understanding how the risks of building product off-gassing can affect the IAQ parameters is crucial as air-permeability standards for new and retrofitted buildings is continually decreasing. For new build dwellings in the UK to comply with Building Regulations Part L1A, they usually need to achieve an air-permeability of  $5 \text{ m}^3/(\text{h}\cdot\text{m}^2)$  or lower. As air-tightness of buildings increases, the need to have robust ventilation strategies, natural or mechanical, in order to provide healthy IAQ and environment is becoming more apparent and necessary.

Higher ventilation rates are required immediately after application as the emission rates from SPF materials are usually the highest immediately after application (Duffy & Wood, 2017). But so far the focus of research has been on short term analysis such as re-entry times (Wood, 2017), VOC emissions under different applications (Won, et al., 2017) and negative impact associated with faulty SPF applications (Huang & Tsuang 2014). The potential long-term impact of these buildings materials and what ventilation strategies should be in place throughout the lifecycle of the building, in order to provide healthy IAQ, is still widely unknown. It is therefore crucial that an international standard for measuring emission rates from SPF materials is adopted in order for further long-term research on the topic to be undertaken.

## 6 CONCLUSIONS

The method of SPF VOC analysis by using ATD-GC-MS has proven to be appropriate with the potential to be developed into an international measurement standard. Carbopack-B tubes proved efficient in detecting five of the chemicals associated with SPF, which could be a cause for some of the common health impact issues. In addition, calibration curves were developed for 1,4-dioxane, chlorobenzene and triethyl phosphate, which could be used for quantification of the emission rates.

Unfortunately, the technique is unsuitable for measuring isocyanates due to their high boiling point, sink effect and instability (Streicher et al. 2000; Sebroski et al. 2012; Lesage et al. 2007).

The industrial development and growth of the SPF sector has steadily outgrown the research undertaken on its interrelationship with ventilation rates, IAQ and human health. It is therefore essential that this analytical methodology is further developed in order for an international standard to be established for measuring VOCs from these building products.

In our future research, we will further establish the methodology and develop the field through the following planned work:

- Other desorption tubes will be used in order to detect all chemicals associated with SPF application, apart from isocyanates, with ATD-GC-MS. This will allow for holistic studies to be undertaken with the same technique and enhance the speed with which an international standard is established.
- Long-term emission (>1-2 years) testing must be undertaken in order to determine how the chemicals might affect IAQ throughout the SPF lifecycle, rather than simply during and shortly after the installation process
- Real life case studies must be used to test various ventilation strategies and systems during and post-application of the foams. Through this data, the effectiveness of various natural or mechanical ventilation strategies will be tested in order to ensure that retrofitting measures, and new build applications, with SPF do not compromise the healthy IAQ.

## 7 ACKNOWLEDGEMENTS

The authors are grateful to Mark Underhill for technical support and to Q-Bot Ltd. for providing the samples.

The research has been funded through the EPSRC Centre for Doctoral Training in Science and Engineering in Arts, Heritage and Archaeology (SEAHA) and is partially funded by Q-Bot Ltd.

## 8 REFERENCES

- ACC Spray Foam Coalition, 2016. *Spray Polyurethane Foam : Guidance on Sampling Techniques for the Inspection of Installed SPF*, Available at: <https://polyurethane.americanchemistry.com/Spray-Foam-Coalition/Guidance-on-Sampling-Techniques-for-the-Inspection-of-Installed-Spray-Polyurethane-Foam.pdf>.
- Agency for Toxic Substances and Disease Registry, 2012. *PUBLIC HEALTH STATEMENT 1,4-Dioxane*,
- Agency for Toxic Substances and Disease Registry, 1990. *PUBLIC HEALTH STATEMENT CHLOROBENZENE*,
- ASTM International, 2017. *Developing Consensus Standards for Measuring Chemical Emissions from Spray Polyurethane Foam (SPF) Insulation*, West Conshohocken.
- Bomberg, M. L. J., 1998. Factors affecting the foam. In: *Polyurethane Foam in External Envelopes in Buildings*. s.l.:CRC Press, p. 339.
- Creely, K.S., Hughson, G.W. & Cocker, J., 2006. Assessing Isocyanate Exposures in Polyurethane Industry Sectors Using Biological and Air Monitoring Methods. , 50(6), pp.609–621.
- Crespo, J. & Galán, J., 1999. Exposure to MDI during the process of insulating buildings with sprayed polyurethane foam. *The Annals of occupational hygiene*, 43(6), pp.415–9. Available at: <http://www.ncbi.nlm.nih.gov/pubmed/10518467>.
- Crump, D., Dengel, A. & Swainson, M., 2009. *Indoor air quality in highly energy efficient homes – a review*, Available at: [http://www.zerocarbonhub.org/sites/default/files/resources/reports/Indoor\\_Air\\_Quality\\_in\\_Highly\\_Energy\\_Efficient\\_Homes\\_A\\_Review\\_NF18.pdf](http://www.zerocarbonhub.org/sites/default/files/resources/reports/Indoor_Air_Quality_in_Highly_Energy_Efficient_Homes_A_Review_NF18.pdf).
- Duffy, J. & Wood, R., 2017. VOC Analysis of Commercially Available Spray Foam Products. *Developing Consensus Standards for Measuring Chemical Emissions from Spray Polyurethane Foam (SPF)*, ASTM STP1589, pp. 43-56.
- Huang, Y.C.T. & Tsuang, W., 2014. Health effects associated with faulty application of spray polyurethane foam in residential homes. *Environmental Research*, 134, pp.295–300. Available at: <http://dx.doi.org/10.1016/j.envres.2014.07.015>.
- Kupczewska-Dobecka, M., Czerczak, S. & Brzézniński, S., 2012. Assessment of exposure to TDI and MDI during polyurethane foam production in Poland using integrated theoretical and experimental data. *Environmental Toxicology and Pharmacology*, 34(2), pp.512–518.
- Lai, H.K. et al., 2004. Personal exposures and microenvironment concentrations of PM 2.5, VOC , NO2 and CO in Oxford,UK. *Atmospheric Environment*, 38, pp.6399–6410.
- Lesage, J. et al., 2007. Airborne methylene diphenyl diisocyanate (MDI) concentrations associated with the application of polyurethane spray foam in residential construction. *Journal of occupational and environmental hygiene*, 4(2), pp.145–55. Available at: <http://www.ncbi.nlm.nih.gov/pubmed/17249149>.
- Lucintel, 2017. *Growth Opportunities in the Global Polyurethane Foam Market*, Irving: Lucintel.
- Markets and Markets, 2016. *Polyurethane Foam Market by Type (Flexible, Rigid, and Spray Foam), End-Use Industry (Bedding & Furniture, Building & Construction, Electronics, Automotive, Footwear, Packaging), and Region - Global Forecast to 2021*, Seattle: Markets and Markets .
- Poppendieck, D. et al., 2016. *Flame Retardant Emission from Spray Polyurethane Foam Insulation*, National Institute for Standards and Technology
- Prichard, E., 2003. *Practical Laboratory Skills Training Guides- Gas Chromatography*. London: Royal Society of Chemistry.
- Puscasu, S. et al., 2015. CIP10 optimization for 4,4-methylene diphenyl diisocyanate aerosol

- sampling and field comparison with impinger method. *Annals of Occupational Hygiene*, 59(3), pp.347–357.
- Schlecht, P.C. & Cassinelli, M.E., 1998. Determination of airborne isocyanate exposure. , pp.115–140.
- Sebroski, J.R. et al., 2012. Research Report for Measuring Emissions from Spray Polyurethane Foam (SPF) Insulation. In Pittsburgh: American Chemical Council Center for the Polyurethanes Industry, pp. 1–54. Available at: [https://pdfs.semanticscholar.org/739a/04fa6077aaf56a2b56dfc7234344fe5a4dd7.pdf?\\_ga=2.164247999.1837800315.1500438326-1432753515.1500438326](https://pdfs.semanticscholar.org/739a/04fa6077aaf56a2b56dfc7234344fe5a4dd7.pdf?_ga=2.164247999.1837800315.1500438326-1432753515.1500438326).
- Seddon, C., 2015. Measuring National Well-being- What we do, London: Office for National Statistics.
- Sleasman, K., Hetfield, C. & Biggs, M., 2017. Investigating Sampling and Analytical Techniques to Understand Emission Characteristics from Spray Polyurethane Foam Insulation and Data Needs. *Developing Consensus Standards for Measuring Chemical Emission from Spray Polyurethane Foam (SPF) Insulation*, pp. 228-277.
- Streicher, R. et al., 2000. Determination of Airborne Isocyanate Exposure : Considerations in Method Selection. *AIHAJ- American Industrial Hygiene Association*, 61, pp.544–556.
- Won, D., Wong, J., Nong, G. & Yang, W., 2017. VOC Emissions from Spray Foam Insulation Under Different Application Conditions. *Developing Consensus Standards for Measuring Chemical Emissions from Spray Polyurethane (SPF) Insulation, ASTM STP1589*, pp. 278-290.
- Wood, R., 2017. Estimating Re-Entry Times for Trade Workers Following the Application of Three Generic Spray Polyurethane Foam Formulations. *Developing Consensus Standards for Measuring Chemical Emissions from Spray Polyurethane Foam (SPF) Insulation*, pp. 148-166.

# The effect of enhanced stove design on 'real life' exposure to PM<sub>2.5</sub> and CO in rural dwellings in Salambu, Nepal

Binaya KC<sup>1,2</sup>, Ian P Hall<sup>\*2</sup>, Benjamin Jones<sup>3</sup>, Bim Prasad Shrestha<sup>1</sup>, Bijendra Shrestha<sup>1</sup> and Niroj Nepal<sup>4</sup>

*1Department of Mechanical Engineering, Kathmandu University, Dhulikhel, Kavre, Nepal*

*2Division of Respiratory Medicine, University of Nottingham, Nottingham NG72RD UK*

*\*Corresponding author: ian.hall@nottingham.ac.uk*

*3Department of Architecture and the Built Environment, University of Nottingham, Nottingham NG72RD UK*

*4Department of Community Programs, Dhulikhel Hospital, Dhulikhel, Kavre, Nepal*

## ABSTRACT

About 3 billion people worldwide, and more than 90% in developing countries, are at risk of developing respiratory and cardiovascular diseases and cancer, due to exposure to household air pollution attributable to the combustion of solid biomass fuels. In Nepal, various types of fuel are used, such as wood, animal dung, and agricultural residues, as a primary source of energy for domestic cooking and heating.

This study examined real-time exposures to particulate matter (PM<sub>2.5</sub>) and carbon monoxide (CO) attributable to cooking in households in a rural environment in the village of Salambu, Nepal, for two daily cooking sessions (morning and evening). The real-time cooking exposure was monitored in houses containing one of two different cook-stove designs. The stoves were either a traditional cook stove (TCS) or an improved cook stove (ICS). The TCS is a simple single pot three stone open fire stove without a chimney, whereas the ICS is designed for improved efficiency and reduced emissions having two pots and a chimney. Kitchen PM<sub>2.5</sub> and CO concentrations were recorded at 10 seconds interval for actual cooking periods and one-minute intervals for periods of around 24 hours under real life conditions.

The real-time mean averages,  $\mu$ , and standard deviations,  $\sigma$ , of PM<sub>2.5</sub> and CO concentrations during cooking periods were  $\mu=943.8\text{ug/m}^3$  ( $\sigma=426.5\text{ug/m}^3$ ) (13 households) and  $\mu=13.5\text{ppm}$  ( $\sigma=5.2\text{ppm}$ ) (13 households) respectively, in households using an TCS, and  $\mu=334.6\text{ug/m}^3$  ( $\sigma=228.6\text{ug/m}^3$ ) (13 households) and  $\mu=6.5\text{ppm}$  ( $\sigma=4.8\text{ppm}$ ) (13 households) respectively in the households using an ICS. We conclude that the real-time concentrations of both PM<sub>2.5</sub> and CO are comparatively lower in the households using an ICS than the households using a TCS. However, average PM<sub>2.5</sub> concentrations still exceed the WHO indoor air quality thresholds for PM<sub>2.5</sub> and national air quality guidelines. Furthermore, average 24-hour kitchen PM<sub>2.5</sub> and CO concentrations also exceed the WHO indoor air quality thresholds. Therefore, a significant proportion of the local population of this region remain likely to be at risk of developing diseases related to increased levels of air pollutants irrespective of their ownership of an ICS, although use of the ICS resulted in lower overall exposures and hence the absolute risk may be lower for those using an ICS. Additional measures to reduce exposures are required.

## KEYWORDS

Biomass fuel, household air pollution, real time emission exposure, traditional cook stove, improved cook stove

## 1 INTRODUCTION

Long term exposure to particulate matter (PM) is associated with increased risk of mortality and morbidity (WHO, 2005). Ambient particulate matter exposure has been estimated to be responsible for 4.2 million deaths and 103.1 million disability-adjusted life-years (DALYs), representing 7.6% of total global deaths and 4.2% of global DALYs in 2015 (Cohen, 2017). The major source of particle mass with aerodynamic diameter less than 2.5  $\mu\text{m}$  (PM<sub>2.5</sub>) exposures, particularly in low and middle income countries is the combustion of solid biomass fuels for domestic energy needs(IEA, 2016).

Traditional biomass fuels like fuel-wood, agricultural residue and animal waste have been a primary source of residential energy for cooking and heating in low and middle income countries for many years. In 2014 biomass energy shared 14% of total final energy consumption world-wide, out of which 10.4% had been used for household cooking and heating(REN21, 2016). Approximately half of the world's population, and more than 90% of households in rural parts of developing countries, primarily use solid biomass fuels for daily cooking and heating purposes(Bonjour, et al., 2013). In Nepal, according to WECS, energy from traditional biomass (mainly fuel wood, agricultural residue and dried animal dung) remains the predominant contributor of country's total energy consumption in last nine years supplying 86.9 % in 2000/01 and 87.1% in 2008/09(WECS, 2010).

Around the world for domestic cooking and household heating, traditional biomass fuels are often combusted indoors in a traditional stove or open fire(Smith, 2006) resulting in incomplete combustion. The incomplete combustion can generate higher concentrations of particulate matter, carbon monoxide (CO) and other health damaging pollutants (Naeher, et al., 2007). Two recent studies conducted in two different district of Nepal have found a daily indoor PM<sub>2.5</sub> concentration of 1376  $\mu\text{g}/\text{m}^3$ (Chen, et al., 2016) and a 48 hour average PM<sub>2.5</sub> concentration of 417.6  $\mu\text{g}/\text{m}^3$ (Barington, et al., 2017) in households using biomass fuel in Sarlahi and Janakpur respectively.

It is well understood that reduction in household air pollutants is likely to bring health benefits to all individuals who are dependent on biomass for cooking and heating. Replacement of traditional cook stoves with a more efficient improved cook stove has been found to be an effective solution to reduce indoor air pollution. The *planchamejorada* cook stove in Guatemala (Albalak, 2001), the *pastari* in Mexico (Cynthia, 2008) , the *justa* stove in Honduras(Clark, 2010) , *three pot metallic cook stove* and *2 pot mud cook stove*(Thapa & Shrestha, 2013) in Nepal are some of the developments made around the world in design and dissemination of improved cook stoves to try and reduce emissions. However, most of the work performed to date has measured mean exposures at a fixed point in a room, rather than measuring an individual's exposures using a personal monitoring system.

A number of efforts have been made by Nepali government, NGOs and academic institution to improve the indoor air environment by disseminating improve cook stoves in rural settings in Nepal. Kathmandu University in close collaboration with Dhulikhel hospital had designed

and successfully disseminated an improved cook stove (2 pot mud cook stove with chimney) in every household in the rural village of Salambu. The potential effect on real time personal exposure reduction after installation of improved stoves has yet to be monitored. In this paper we monitored personal real-time exposure to PM<sub>2.5</sub> and CO in households using traditional and improved cook stoves to quantify the effect of stove design on individual exposures and overall emissions.

## 2 METHODS

### 2.1 Study area and setting

The field work to monitor real time individual exposure to PM<sub>2.5</sub> and CO during cooking periods and 24 hour average PM<sub>2.5</sub> and CO concentrations was conducted in households in Salambu of MajhiFeda VDC, located in Kavrepalanchok district of central development region. MajhiFeda VDC has 624 households with a total population of 2669 (Central Bureau of Statistics, 2012). The emissions from two stove designs were monitored for morning and evening cooking period in 13 households in Salambu. About 99% of households in Salambu use biomass fuel for cooking and heating and most of the households have both traditional cook stoves (TCS) (figure 1 A) and improved cook stoves (ICS) (figure 1 B). Mixed fuel wood along with some agricultural residue, especially used to ignite the fire, is used with *Pinus roxburghii* (Salla) being the most common fuel wood in use.

### 2.2 Study Stoves

The real time personal exposure to PM<sub>2.5</sub> and CO during morning and evening cooking was compared between two stove designs, i) the TCS (figure 1 A) and ii) the ICS (figure 1 B). The TCS is simply an open fire where a cooking pot is normally adjusted in the centre of a triangular configuration of three stones. It has the advantage that fuel can be fed in from all directions which improves cooking speed but at the same time consumes more fuel wood.

The ICS on the other hand, is a fuel efficient two pot mud type stove which was disseminated by KU and installed by a trained local manufacturer. With the chimney attached to the stove design, most of the smoke coming from combustion is vented out of the kitchen area.



(A)(B)

Figure 1 Study stoves. (A) Traditional cook stove (TCS), locally made open fire stove adjusted with three stones. (B) Improved cook stove (ICS), two pot mud stove with chimney, manufactured by a trained local manufacturer.

## 2.3 Measurements and instruments

### 2.3.1 Indoor Air Pollution (IAP) meter

The real time personal exposures to PM<sub>2.5</sub> and CO and 24 hour average PM<sub>2.5</sub> and CO in the household were monitored using the IAP meter 5000 series (Aprovecho Research center, USA).

#### Testing Protocol

Real time pollutant concentrations were measured at 10 seconds interval over each cooking period from the moment the fire started till the fire extinguished. The IAP meter was turned on having set in 10 seconds mode and left in a clean environment for at least 10 minutes for background adjustment before it was worn by the subject (cook). Throughout the cooking period from the start of the fire, the wearer had the meter on her back with the adjustable tube attached to the meter box. The tube was adjusted over the left shoulder of the wearer with its inlet positioned on top of her shoulder (figure 2). The data stored in the SD card was downloaded to the computer after the completion of each test and processed through the software provided which was written for Microsoft excel.

A preliminary survey had shown that  $\geq 75\%$  households have both ICS and TCS. The study was therefore conducted in 13 randomly selected households where both ICS and TCS were present and in good working condition. The household owners were requested to cook their food using ICS in one day and using TCS on another day and real time pollutant exposures measured. The mean exposure level was calculated and compared for significant differences.

The 24 hour average concentrations were measured at 60 seconds interval over the 24 hour period in 6 randomly selected households from the 13 households, where 3 houses each were tested for ICS and for TCS. The same IAP meter was used and placed on the kitchen wall at approximately 1.5 m above the ground and 1 m from the stove (Fuyuen, 2017) for approximately 24 hours. The household owners were asked to use only ICS or TCS, depending on which stove design was selected for each particular house. It was found that in each household within 24 hours, the stove was used for two periods only, usually for morning cooking and for evening cooking. The mean emission concentration was calculated and compared for any significant difference.



Figure 2 Exposure monitoring by using IAP meter. (A) Exposure monitoring with ICS and (B) Exposure monitoring with TCS.

## 2.4 Data Analysis

Data were analysed using GraphPad Prism software (Version 6, GraphPad Software Inc.). The mean of the arithmetic means of indoor emissions of PM<sub>2.5</sub> and CO from ICS and TCS were obtained and compared for any significant difference using the t-test.

## 3 RESULTS

### 3.1 Time series Pollutant concentrations

Figure 3A and 3B shows an example of real time personalised PM<sub>2.5</sub> and CO concentrations monitored in the same house for morning cooking with ICS and TCS. The concentration of both PM<sub>2.5</sub> and CO increased markedly throughout the cooking period with the peak concentrations measured particularly at the start and at the end of cooking. The range of pollutant concentrations, peak concentration and average concentration was different for the two stove designs. The pattern of emissions for both morning and evening cooking for the respective stove designs were similar for all 13 cooking tests performed in different households. The peak PM<sub>2.5</sub> concentration with ICS in overall 13 tests was ranged from 1078 µg/m<sup>3</sup> to 9337 µg/m<sup>3</sup>, whereas with TCS, it ranged from 2115 µg/m<sup>3</sup> to 11399 µg/m<sup>3</sup>. Similarly the peak CO concentration ranged from 4.9 ppm to 40.3 ppm with ICS and 14.5 ppm to 88.8 ppm with TCS in overall 13 tests. The average concentration of PM<sub>2.5</sub> and CO emission with ICS ranged from 109 µg/m<sup>3</sup> to 869 µg/m<sup>3</sup> and 1.1 ppm to 10.8 ppm respectively whereas it ranged from 426 µg/m<sup>3</sup> to 1778 µg/m<sup>3</sup> and 8.1 ppm to 26.8 ppm respectively with TCS.

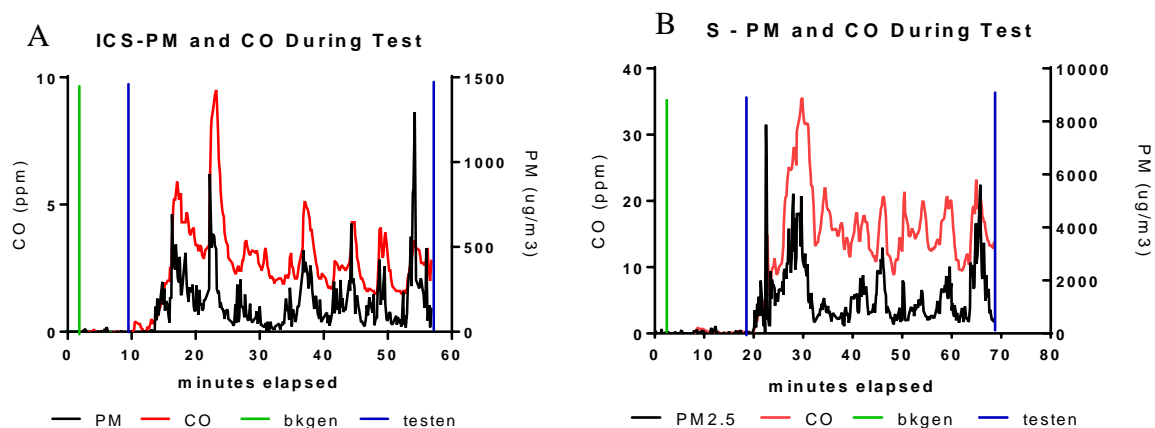


Figure 3 Real time PM<sub>2.5</sub> and CO measurement: The graph represents a time series emission exposure profile with the (A) ICS and (B) TCS conducted on a same house under identical conditions for morning cooking. Similar graphs were obtained for all other tests. bkgen indicates the start of the period for assessing background levels, and testen the cooking period.

### 3.2 PM<sub>2.5</sub> and CO concentrations

The real time exposures to PM<sub>2.5</sub> and CO were found to be reduced by 65% and 50% respectively in the households when the ICS was used compared with using the TCS. The real-time mean averages(SD)of PM<sub>2.5</sub> concentrations during cooking periods in the households using ICS and TCS were 334.6 µg/m<sup>3</sup> (228.6 µg/m<sup>3</sup>) and 943.8 µg/m<sup>3</sup> (426.5 µg/m<sup>3</sup>) respectively. Similarly, real time CO concentrations in the household using ICS and TCS were 6.5 ppm (4.8 ppm) and 13.5 ppm (5.2 ppm) respectively. The real time emission monitoring was carried out for the two stove designs in each house for 13 houses under the

same working condition and using same fuel and compared for significance level by paired t test. The reduction in exposure level was statistically significant ( $p < 0.001$ ).

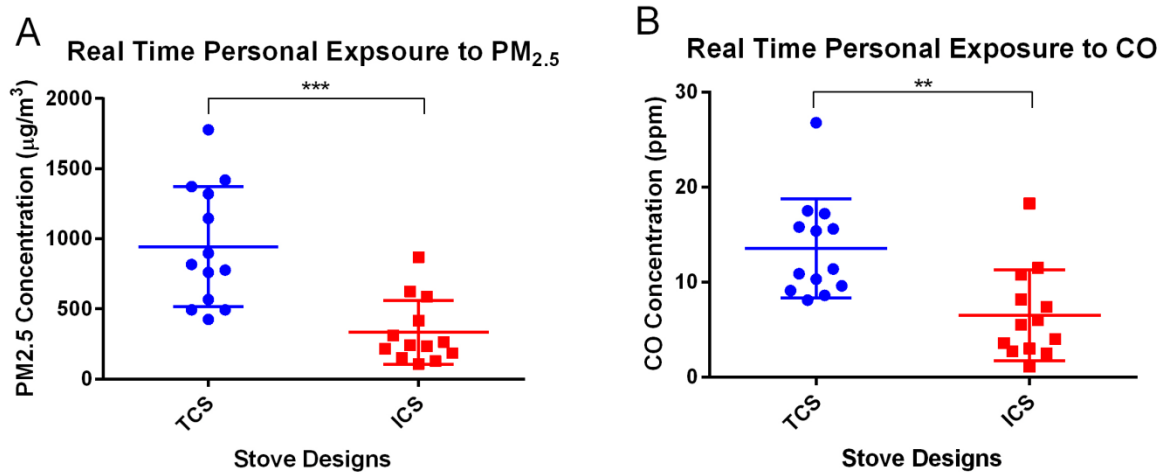


Figure 4 Comparison of real time pollutant exposure during cooking (A) PM<sub>2.5</sub> and (B) CO in a rural setting from two stove designs. The exposure to pollutants from two stove designs were measured in 13 households and the data represents the mean and standard deviation. \*\*\*= $p < 0.001$  and \*\*= $p < 0.01$ . TCS=Traditional Cook Stove, ICS = Improved Cook Stove.

24 hour average PM<sub>2.5</sub> and CO concentration in the household using ICS and TCS were also monitored. The mean 24 hour average PM<sub>2.5</sub> and CO concentrations were significantly lower in the households when using ICS compared to TCS (figure 5). The PM<sub>2.5</sub> and CO concentrations were found to be reduced from mean (SD) 2820 µg/m<sup>3</sup> (1657 µg/m<sup>3</sup>) to 375 µg/m<sup>3</sup> (173 µg/m<sup>3</sup>) and 16.3 ppm (4.65 ppm) to 9.4 ppm (3.37 ppm) respectively. The number of households tested for both stove designs was 3 and the reduction was statistically significant ( $p < 0.05$ ).

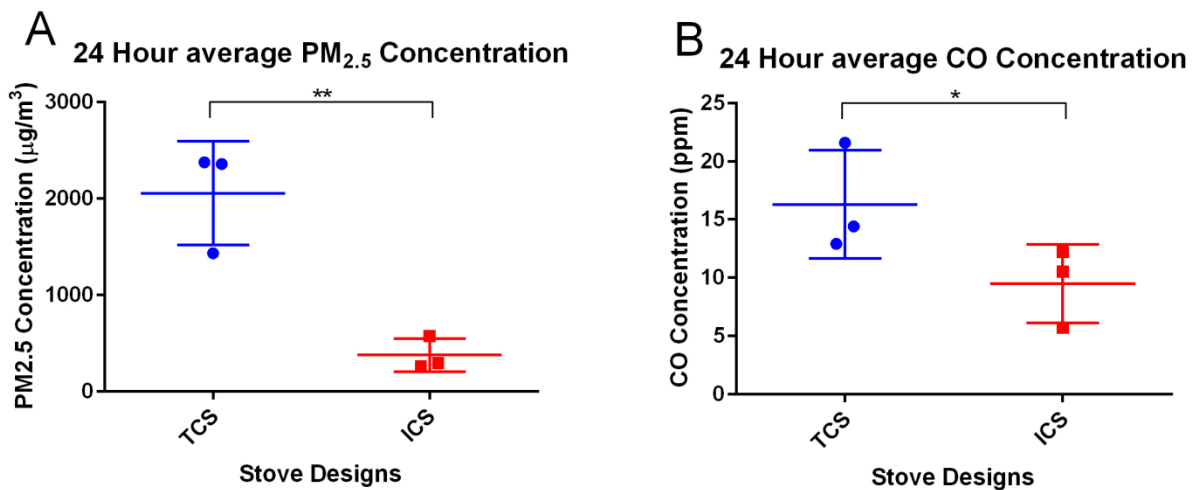


Figure 5 Mean 24-hour average concentration (A) PM<sub>2.5</sub> and (B) CO in the household using ICS and TCS. Mean average 24 hour concentration of PM<sub>2.5</sub> and CO in the household using ICS and TCS were measured (3 household for each stove designs). In each test the stove was used two times within 24 hour each for morning and evening cooking. \*\*= $p < 0.01$  and \*= $p < 0.05$ . TCS=Traditional cook stove, ICS= Improved cook stove.

Real time exposures to PM<sub>2.5</sub> and CO were measured in two cooking period, morning cooking and evening cooking in each household for both stove designs. No significant difference in

real time pollutant exposure was noted for both stove designs for morning and evening cooking (data not shown).

#### **4 DISCUSSION**

The findings from this study show that improved cook stove can significantly reduce the pollutant exposure levels in the household using biomass fuels, though the exposure level still exceed the WHO indoor air quality thresholds. Studies examining personal exposures to pollutants from biomass combustion in a real time cooking period are limited. However, several studies monitoring particulate matter emissions using traditional and improved cook stoves have identified significant reductions in mean PM concentrations of between 39% and 73% with use of improved cook stoves.

We found that daily average PM<sub>2.5</sub> concentration in homes using TCS is more than 20 times higher than the national indoor 24 hour standards set at 120 µg/m<sup>3</sup>(Nepal, 2009) and more than 100 fold higher than WHO ambient 24 hour average standards set at 25 µg/m<sup>3</sup>(WHO, 2005). Though only a few studies have been done in Nepal, the findings of this study are similar to comparative studies performed in other countries.

In this study, we also measured personal PM<sub>2.5</sub> and CO exposure for the actual cooking period with TCS and ICS in the same house in the same environment. The fuel used for all tests was the same and moisture content was in a range of 9 to 13%. We saw large reductions in personal exposure with ICS use. However, more studies need to be carried out to see the effects of housing size, position of stove in the kitchen, ventilation and other variables on emissions levels.

Although we found a significant reduction in emissions with ICS, the concentrations seen still exceed national and WHO indoor air quality thresholds, and hence a significant proportion of the local population of this region remain likely to be at risk of developing disease related to increased levels of air pollutants irrespective of their ownership of an ICS. More health impact studies on reduction of indoor air pollutant exposure after installation of ICS should be carried out, especially given that some of the previous studies have reported no significant health effects of controlling indoor pollutant exposure(Smith, et al., 2011; Guarnieri, et al., 2015; Heinzerling, et al., 2016).

#### **5 CONCLUSIONS**

In summary, we have demonstrated that efforts to reduce indoor air pollution through the installation of ICS have been successful. However, the reduced levels of air pollutants seen with ICS use still exceed national and WHO indoor air quality thresholds and hence additional work is required to identify ways to further reduce personal exposures to indoor air pollution.

#### **6 ACKNOWLEDGEMENTS**

We would like to thank all the house owners for kindly accepting us in their kitchen to conduct the test. We owe a very important debt to all the participants who took part in the study and happily agreed to take the bag-pack on their back throughout the cooking period. We are particularly grateful for the technical and equipment assistance provided by Central

for Rural Technology, Nepal. We appreciate the financial support of The University of Nottingham and International Centre for Integrated Mountain Development (ICIMOD).

## 7 REFERENCES

- Albalak, R. (2001). Indoor respirable particulate matter concentrations from an open fire, improved cook stove and LPG/open fire combination in a rural Guatemalan community. *Environ. Sci. Technology* , 2650-2655.
- Barington, S. E., Bakolis, et al. (2017). Patterns of domestic exposure to carbon monoxide and particulate matter in households using biomass fuel in Janakpur, Nepal. *Environmental pollution* , 220. 38-45.
- Bonjour, S., Adair-Rohani, H, et al. (2013). Solid fuel use for household cooking: country and regional estimates for 1980-2010. . *Environ. Health Perspect.* , 121, 784-790.
- CentralBureauofStatistics. (2012). *National Population and Housing Census 2011*. Retrieved April 20, 2017, from <http://unstats.un.org/unsd/demographic/sources/census/wphc/Nepal/Nepal-sensus-2011-Vol1.pdf>
- Chen, C., Zeger, S., et al. (2016). Estimating Indoor PM<sub>2.5</sub> and CO concentrations in Households in Southern Nepal: The Nepal Cookstove Intervention Trials. *PLoS ONE* , 11(7): e0157984. doi:10.1371/journal.pone.0157984.
- Clark, M. (2010). Indoor air pollution, cookstove quality, and housing characteristics in two Honduran communities. *Environ.Res.110* , 12-18.
- Cohen, A. J. (2017). Estimates and 25-year trends of the global burden of disease attributable to ambient air pollution: an analysis of data from the Global Burden of Disease Study 2015. *The Lancet* , 1907-1981.
- Cynthia, A. (2008). Reduction in personal exposures to particulate matter and carbon monoxide as a result of the installation of a Pastari improved cook stove in Micchoacan Mexico. *Indoor air,18* , 93-105.
- Fuyuen, Y. (2017). Assessment of traditional and improved stove use in household air pollution and personal exposures in rural western Kenya. *Environment Internations 99* , 185-191.

- Guarnieri, M., Diaz, E., et al. (2015). Lung Function in Rural Guatemalan Women Before and After a Chimney Stove Intervention to Reduce Wood Smoke Exposure. *Chest* , 148(5): 1184-1192.
- Heinzerling, A. P., Guarnieri, M. J., et al. (2016). Lung function in woodsmoke-exposed Guatemalan children following a chimney stove intervention. *Thorax* , 71: 421-428.
- IEA. (2016). *Energy and Air Pollution. World Energy Outlook Special Report*. France: International Energy Agency.
- Naeher, L. P., Brauer, M., et al. (2007). Woodsmoke health effects: a review. *Inhal. Toxicol* , 19 (1), 67-106.
- Nepal, (2009). *National Indoor Air Quality Standards and Implementation Guideline, 2009*. Kathmandu: Ministry of Environment, Science and Technology.
- REN21. (2016). *Renewables 2016 Global Status Report*. Paris: REN21 Secretariat.
- Smith, K. R. (2006). Health impacts of household fuelwood use in developing countries. *Unasylva* , 57, 41-44.
- Smith, K. R., McCracken, J. H., et al. (2011). Effect of reduction in household air pollution on childhood pneumonia in Guatemala (RESPIRE): a randomised controlled trial. *Lancet* , 378. 1717-26.
- Thapa, R. B., & Shrestha, R. M. (2013). Metallic improved cook stoves dissemination in Mountain Region Nepal; Experience, Financial Viability, opportunity and Challenges. *Rentec*.
- WECS. (2010). *Energy Sector Synopsis Report 2010*. . Kathmandu: Water and Energy Commission Secretariat.
- WHO. (2005). *WHO Air quality guidelines for particulate matter, ozone, nitrogen dioxide and sulfur dioxide*. Switzerland: WHO Press, World Health Organization.

# Field measurement of carbonyl compound and particles in South Korea residential spaces

KyungMo Kang<sup>1</sup>, Yun Gyu Lee<sup>\*2</sup>, Chulwoong Shin<sup>3</sup>

*1 Yonsei University  
50, Yonsei-ro, Seodaemun-gu,  
Seoul, South Korea*

*2 Korea Institute of Construction Technology  
283, Goyang-daero, Ilsanseo-gu, Goyang-si,  
Gyeonggi-do, South Korea  
\*Corresponding author: yglee@kict.re.kr*

*3 Korea Conformity Laboratories  
7, Jeongtong-ro, Duchon-ri, Deoksan-myeon,  
Jincheon-gun, Chungcheongbuk-do, South Korea*

## ABSTRACT

In Korea, a large amount of fine dust and carbonyl compounds is generated during cooking in the kitchen. The purpose of this study is to select 20 apartment houses and measure contaminants that are generated during cooking in apartment houses in Korea. The measurement result showed that 15 out of 20 apartment houses exceeded the guidelines for PM<sub>10</sub> based on its peak concentration. The concentration of carbonyl compounds was measured in the descending order of acrolein (270.0  $\mu\text{g}/\text{m}^3$ ), formaldehyde (239.5  $\mu\text{g}/\text{m}^3$ ) based on its average concentration. Acrolein and formaldehyde is harmful to the human body because time required for concentration to decrease by below guidelines is too long. The concentration of contaminants increased after cooking in most apartment houses even though there was a ventilation mechanism, and formaldehyde exceeded its standard concentration in 9 apartment houses. As a result of measuring various contaminants comprehensively, it can be determined that ventilation for cooking is insufficient to remove contaminants.

## KEYWORDS

Cooking emission, Range hood, Carbonyl compounds, Kitchen ventilation, Formaldehyde, Acrolein

## 1 INTRODUCTION

Awareness about indoor air quality and contaminants has increased in Korea based on previous experiences such as the so called sick building syndrome issue. For this reason, ventilation standards for detached houses and apartment houses have been established and the clean health housing construction standards of South Korea were put in place through the Indoor Air Quality Act (2003; 2009; 2013). The Ministry of the Environment of South Korea operates an 'eco label' for new apartment buildings as a part of source control measures in order to regulate contaminants such as particles, VOCs (Volatile Organic Compounds) and HCHO (Formaldehyde) emitted from building materials (Shim and Choi, 2017). Also, a study to solve the so called sick building syndrome by improving the indoor air quality of new apartment buildings in Korea was carried out in the past (Choi et al., 2009; Kim et al., 2008).

Although the indoor air quality problem is under control, the issue of contaminants generated indoors due to cooking in the kitchen has come to the fore in recent times. In general, contaminants generated during cooking in the kitchen are removed through the operation of a range hood. However, studies regarding the standards of range hoods such as their capture efficiency are still in progress internationally (AIVC, 2016).

In comparison to previous problems, the source control for cooking in the kitchen is practically difficult and large amounts of contaminants are generated during cooking (Cheng

et al., 2016; Huang et al., 2011; Seaman et al., 2009). Especially, carbonyl compounds are known to be major contaminants (sources in cooking fume emissions) that are generated during cooking in the kitchen based on studies over many years (Wang et al., 2017). The concentration of carbonyl compounds increases significantly during cooking, and carbonyl compounds including acrolein have a long half-life of over 10hr (Seaman et al., 2009). Therefore, if the indoor ventilation is low, indoor occupants may be exposed to a high concentration of carbonyl compounds for a long period of time, posing a significantly harmful influence to human health. For this reason, efforts are being made to clearly define HCHO as a representative substance and limit its standard concentration to  $210 \mu\text{g}/\text{m}^3$  in order to control the indoor concentration of carbonyl compounds in apartment houses in Korea. At present, the standard concentration of particles is  $100\sim 200 \mu\text{g}/\text{m}^3$ .

Therefore, the effects of cooking actions on the indoor air quality in apartment houses were evaluated in this study by measuring and analyzing contaminants generated during cooking in the kitchen inside apartment buildings in Korea.

Apartment buildings in Korea consist of mostly of reinforced concrete structures and the design entails that the living room and the kitchen are separated. Also, apartment buildings in Korea are concentrated mostly in downtown areas, so the outdoors concentration of contaminants has a significant effect on indoor space. In addition, when cooking is carried out in the kitchen, the concentration of indoor contaminants increases significantly. Therefore, the concentrations of indoors and outdoors contaminants as well as indoor contaminants before, during and after cooking were measured separately in this study.

## 2 SITE AND TEST CONDITIONS

### 2.1 Apartment buildings in Korea

Table 1: Summary of building information

Building no.	Floor areas, m <sup>2</sup>	Type of fuels	Type of ventilation	Type of cooking
B1	61	L	H+N.V	F
B2	59	L	H+N.V	F
B3	116	L	H	F
B4	74	L	H+N.V	F
B5	167	E	H	B
B6	48	L	N.V	B
B7	109	L	N.V	F
B8	72	L	N.V	F
B9	59	L	N.V	F
B10	72	L	H+N.V	F
B11	84	E	H	F
B12	72	L	N.V	F
B13	84	L	-	S
B14	68	L	H	F
B15	157	L	H+N.V	T
B16	74	L	H	B
B17	114	L	N.V	S
B18	106	L	H	B
B19	72	L	N.V	S
B20	108	L	N.V	F

\* L: LNG, E: Electricity

H: Hood, H+N.V: Hood + Natural ventilation, N.V: Natural ventilation

B: Broiling, F: Frying, S: Soup, T: Toast

The range hood is installed in most apartment buildings in order to remove contaminants generated during cooking, and LNG and electricity are used as the fuel for cooking. The number of target buildings for measurement was 20 apartment houses, and the measurement was carried out during summer (July) in Korea. The measurement was carried out with indoor temperatures ranging between 25 °C and 26 °C, and the indoor temperature increased by approximately 1~2 °C during cooking.

It was determined that the main cooking methods in Korea included boiling and frying, and these two methods were mainly used when the actual field measurement were carried out. No separate restriction was applied to the cooking method or time so that sampling was carried out and analyzed while indoor occupants carried out cooking as usual.

The indoor occupants removed indoor contaminants by operating the range hood or through natural ventilation during cooking except for one target apartment house, and the operation of all range hoods was stopped after cooking.

Among the 20 sampled apartment houses, there was no ventilation in one of the sampled apartment houses, the range hood was operated in 6 apartment houses, natural ventilation was carried out in 7 apartment houses and 6 apartment houses used both natural ventilation and a range hood.

## 2.2 Field measurement method

The measured contaminants and environmental conditions of the target buildings are shown in Table 2. The ventilation in a building was calculated using the CO<sub>2</sub> tracer gas method (ASTM, 2000), and the average ventilation of the target buildings and the standard deviation were 0.8±0.4 (1/h).

The contaminants were measured at 2 places including the kitchen and the living room at the same time. The background concentration of fine dust was measured for 1 hour before cooking. On the other hand, the carbonyl compounds were sampled (0.2~0.3L/min) at the site for 15 minutes before cooking, for 15 minutes during the cooking period and for 15 minutes after cooking equally using a mini pump, and the sampled carbonyl compounds were analyzed using the liquid chromatograph (LC) method. A total of 6 types of carbonyl compounds (formaldehyde, acetaldehyde, acrolein, Propionaldehyde, butyraldehyde, benzaldehyde) were analyzed using this method.

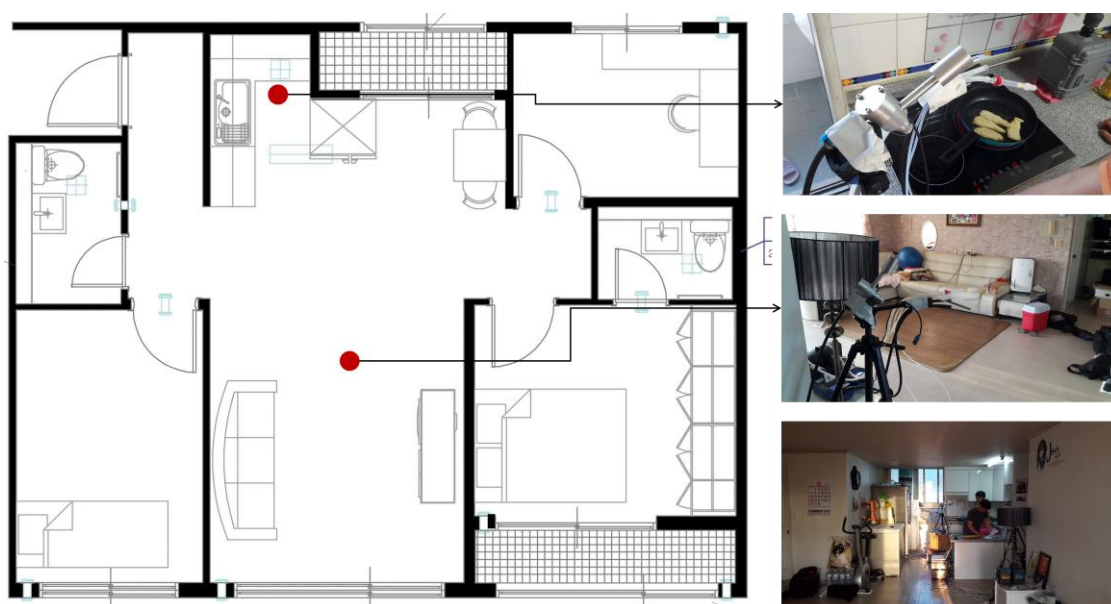


Figure 1: Example of plan & sampled compounds

Table 2: Measuring instrument

Measuring target	Measuring instrument
Air change rate	Photoacoustic multi-gas monitor (INNOVA 1412, Denmark)
Particle Matter	Aerosol monitor (TSI 8532, USA)
Indoor temperature, humidity	Data logger (SATO SK-L200, Japan )
Carbonyl compounds	HPLC-UV method with Mini pump (Walters Alliance HPLC, USA)

### 3 RESULT

#### 3.1 PM<sub>10</sub>, PM<sub>2.5</sub>

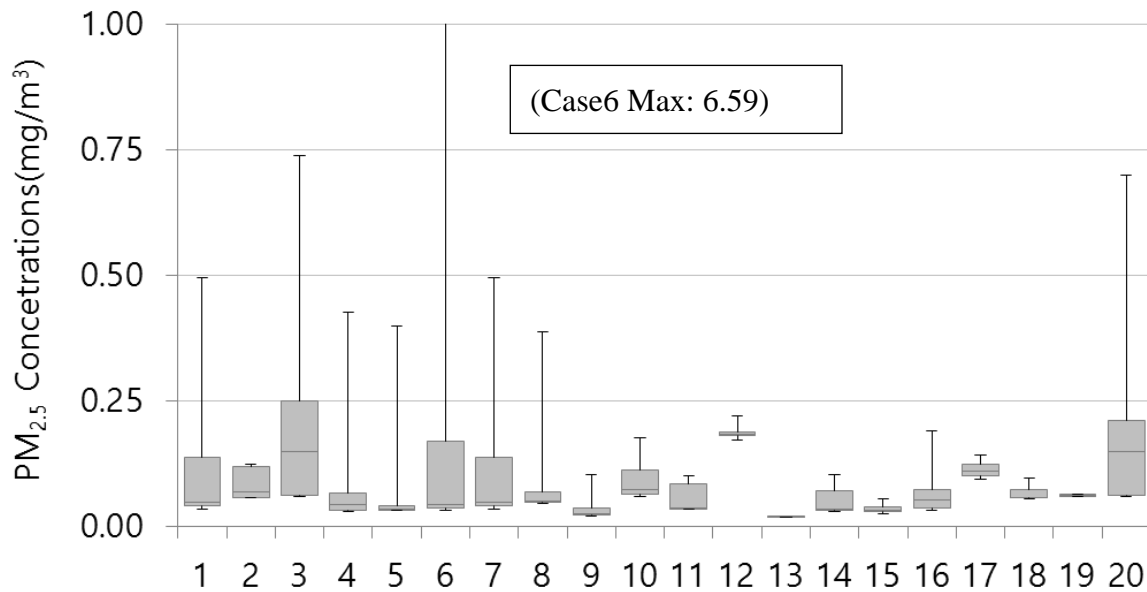


Figure 2: Result of PM<sub>2.5</sub>.in cooking period.

As a result of measuring fine dust in 20 apartment houses, it was confirmed that the concentration of fine dust (PM<sub>2.5</sub>) increased significantly during cooking as shown in Figure 2. While the background concentration in target buildings before cooking was 0.05mg/m<sup>3</sup>, the background concentration increased up to 6.59mg/m<sup>3</sup>during cooking. For PM<sub>2.5</sub>, the concentration of fine dust increased during cooking so that the maximum concentration measured was very high (maximum average concentration: 0.70 mg/m<sup>3</sup>).

The concentration of PM<sub>2.5</sub> during the cooking period was as high as 0.10 mg/m<sup>3</sup>. Some indoor occupants carried out natural ventilation activities or operated a range hood during cooking, but it was insufficient to remove all contaminants generated during cooking with regard to PM<sub>2.5</sub>.

Similar to PM<sub>2.5</sub>, the concentration of PM<sub>10</sub> also increased significantly. The average concentration in the 20 houses during cooking periods was 0.70 mg/m<sup>3</sup>, and 7 houses exceeded the standard concentration during cooking and 15 houses exceeded the maximum concentration. It was confirmed through this result that a large amount of fine dust was generated though cooking in the kitchen and that the operation of a range hood and natural ventilation methods that were occasionally utilized during cooking at home were insufficient to remove all of the fine dust.

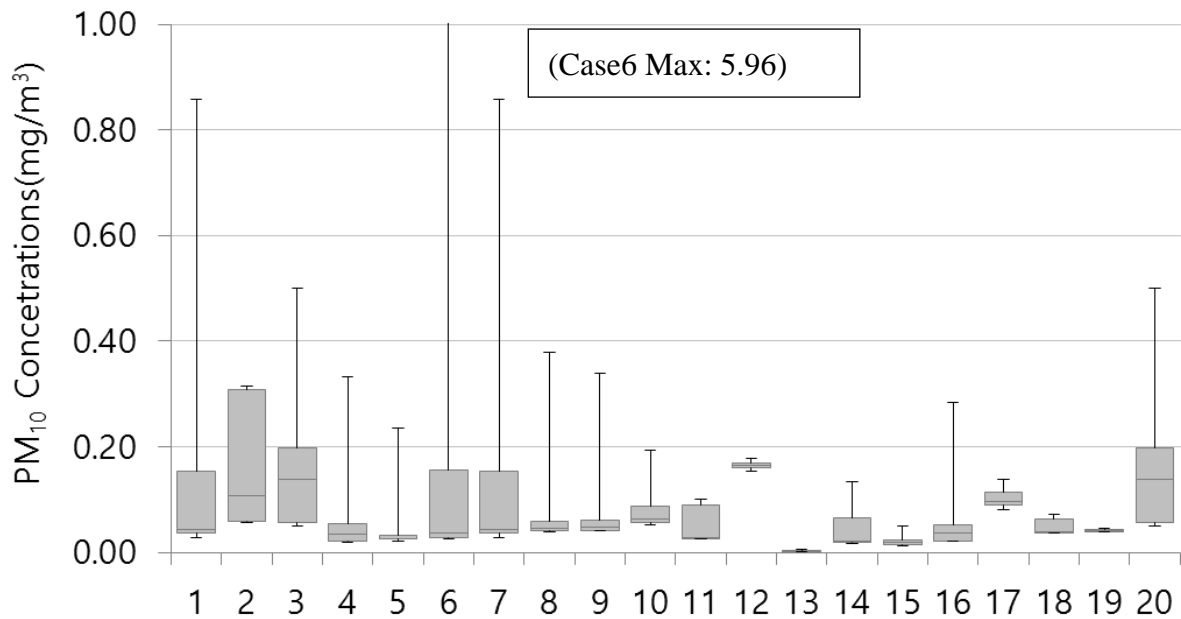


Figure 3: Result of PM<sub>10</sub>. In cooking and after cooking period.

### 3.2 Carbonyl compounds

Before measuring the concentration of carbonyl compounds according to cooking action, indoor contaminants were measured. The concentration of formaldehyde in the target buildings (n=20) was 194.4  $\mu\text{g}/\text{m}^3$  on average with its median value being 154.5  $\mu\text{g}/\text{m}^3$  and standard deviation being 121.8  $\mu\text{g}/\text{m}^3$ .

Table 3: Background concentration,  $C_{\text{background}}$  ( $\mu\text{g}/\text{m}^3$ , n=20)

	Mean	SD	Min	Max	Med
<b>Formaldehyde</b>	194.4	121.8	78.0	495.0	154.5
<b>Acetaldehyde</b>	85.1	41.1	36.0	210.0	79.5
<b>Acrolein</b>	253.7	112.6	96.0	501.0	210.0
<b>Propionaldehyde</b>	8.6	22.5	0.0	84.0	0.0
<b>Butyraldehyde</b>	120.8	63.9	30.0	234.0	103.5
<b>Benzaldehyde</b>	29.6	4.5	21.0	36.0	30.0

\*SD: Standard deviation, Min: Minimum, Max: Maximum, Med: Median, Max: Maximum

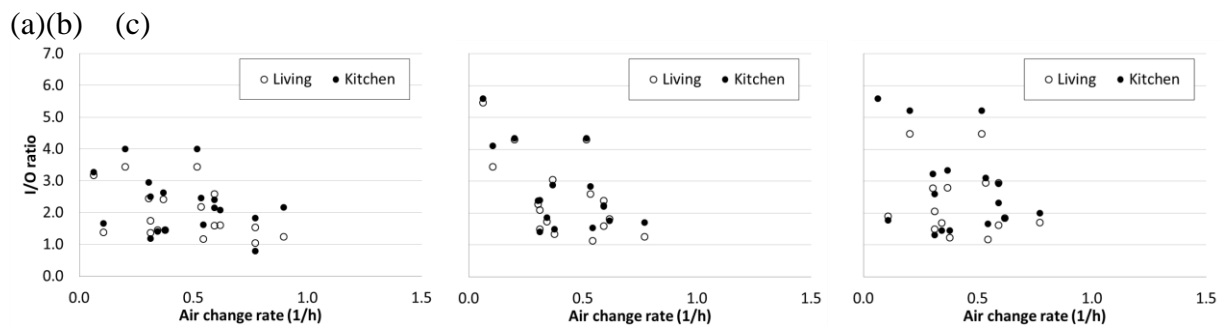


Figure 4: I/O ratios for formaldehyde concentration measured in residential with air change rate. (a) Data measured before cooking,(b) Data measured for cooking,(c) Data measured after cooking.

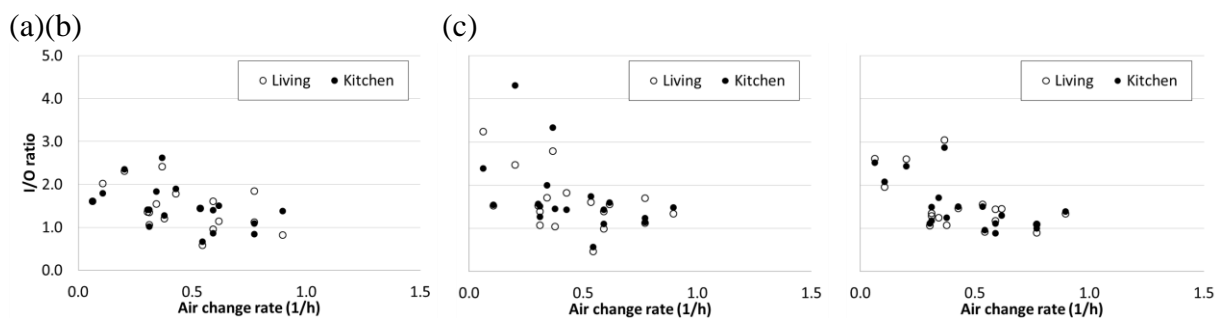


Figure 5: I/O ratios for acrolein concentration measured in residential with air change rate. (a) Data measured before cooking, (b) Data measured for cooking, (c) Data measured after cooking.

9 apartment houses exceeded  $210 \mu\text{g}/\text{m}^3$ , which is the formaldehyde standard concentration in apartment houses in Korea. The average concentration of contaminants in the target buildings was measured in the descending order of acrolein ( $254.0 \mu\text{g}/\text{m}^3$ ), formaldehyde ( $160.5 \mu\text{g}/\text{m}^3$ ), butyraldehyde ( $120.0 \mu\text{g}/\text{m}^3$ ), acetaldehyde ( $85.9 \mu\text{g}/\text{m}^3$ ), benzaldehyde ( $29.7 \mu\text{g}/\text{m}^3$ ) and propionaldehyde ( $7.8 \mu\text{g}/\text{m}^3$ ). The top two substances have a very long half-life and high concentrations of these substances shows that the necessary indoor ventilation is not being carried out properly.

Fig 4, 5 shows the correlation between I/O ratios for formaldehyde, acrolein concentrations and the air change rates. In spite of difference of quantities, similar to concentration of formaldehyde, acrolein also tended to be inversely proportional to ventilation.

The I/O ratios before cooking was 1.4, 2.0 although the ratio during, after cooking was higher than 1.4. This suggests that formaldehyde was significantly increased by cooking activities in Korea despite operating natural, mechanical ventilation. Formaldehyde concentrations in kitchen are more than living room for cooking and after cooking activities.

Table 4: Concentrations of carbonyl compounds entire period with mean and standard deviations ( $\mu\text{g}/\text{m}^3$ , n=20)

	Before Living	Before Kitchen	Cooking Living	Cooking Kitchen	After Living	After Kitchen	Outdoors condition
<b>Formaldehyde</b>	194.4±121.8	219.3±128.3	262.1±245.7	276.5±220.2	231.8±188.0	252.8±193.0	89.1±47.4
<b>Acetaldehyde</b>	85.1±41.1	84.8±35.4	125.1±78.9	154.8±101.7	115.8±79.1	116.3±665.9	61.1±22.6
<b>Acrolein</b>	253.7±112.6	252.0±123.7	280.8±178.4	301.8±173.0	270.2±152.1	261.8±134.6	184.8±92.2
<b>Propionaldehyde</b>	8.6±22.5	9.8±23.5	51.5±82.3	80.7±95.4	28.7±39.5	29.1±39.6	3.0±13.4
<b>Butyraldehyde</b>	120.8±63.9	120.5±60.6	113.6±59.0	117.6±63.92	100.4±58.3	105.0±50.2	157.4±118.9
<b>Benzaldehyde</b>	29.6±4.5	29.7±7.0	27.0±10.4	30.3±35.2	26.6±9.8	26.3±10.2	24.3±12.8

Judging from this result, the concentration of these two contaminants is determined by other factors including the cooking methods of indoor occupants and the cooking duration period in addition to ventilation. Table 4 indicates concentrations of carbonyl compounds entire period with mean and standard deviations. Every carbonyl compound concentrations in indoors were higher than outdoor concentration except butyraldehyde. Butyraldehyde, benzaldehyde is not relevant as to the cooking activities. Formaldehyde, acrolein was confirmed that the contaminants generated due to cooking still remained after cooking. Besides ventilation rates, the cause of increase concentrations is various conditions including various cooking types, different cooking behaviors, materials, time by indoor occupant and ventilation efficiency had significant effects.

#### **4 CONCLUSIONS**

A ventilator mechanism is installed mandatorily in Korea, and especially ERV (Energy recovery ventilator) is installed in many apartment houses, maintaining indoor air quality. However, the ventilator was not operated in most apartment houses in summer (and also winter) when the measurements were carried out. 15 apartment houses exceeded the Guidelines for PM<sub>10</sub> based on the maximum concentration and 7 apartment houses exceeded the Guidelines for PM<sub>2.5</sub> based on the average concentration. The average concentration of PM<sub>2.5</sub> during cooking period was 0.08 mg/m<sup>3</sup> and the average concentration of PM<sub>10</sub> was 0.1 mg/m<sup>3</sup>.

A very high concentration of most carbonyl compounds was measured during cooking period and the standard concentration of formaldehyde was exceeded in 9 apartment houses. A large amount of acrolein and formaldehyde was generated due to cooking actions, but ventilation in indoor spaces was not carried out properly during and after the cooking, so the high concentration status was maintained indoors for a long period of time after cooking.

The I/O ratio for formaldehyde before cooking was 2.0. The ratio during cooking was 2.7, 2.9. The I/O ratio for formaldehyde before cooking was 1.4. The ratio during cooking was 1.9, 1.7. This suggests that formaldehyde was significantly increased by cooking activities in Korea despite operating natural, mechanical ventilation. Formaldehyde concentrations in kitchen are more than living room for cooking and after cooking activities. Ventilation procedures are not being carried out properly for dilute contaminants and this is particularly so during cooking periods.

In this study, the contaminants generated due to cooking in the kitchen, a topic never studied before in Korea, were measured and the preliminary data regarding indoor air quality was presented. Ventilation is the most important means to prevent deterioration in the indoor air quality. Also, cooking styles and ventilation methods employed by indoor occupants may vary significantly, but generally speaking the ventilation methods employed in apartment houses in Korea are insufficient and so the level of indoor contaminants is high.

#### **5 ACKNOWLEDGEMENTS**

This study was carried out with research fund support as part of the residential environment research project of the Ministry of Land, Infrastructure and Transport. (Project No.: 17RERP-B082204-04)

## 6 REFERENCES

2003. Indoor Air Quality Control In Public Use Facilities, etc. Act, in: Korea, M.o.E.o.S. (Ed.)
2009. Standard for the Sick House Syndrome Improvement, Master Plan of Indoor Air Quality Control, in: Ministry of Environment(ME), K.M.o.K.E.M., Ministry of Land, and Transport and Maritime Affairs(MLTM) (Ed.).
2013. Clean Healthy Housing Construction Standards, in: Environment(ME), M.o. (Ed.). AIVC, 2016. Technical note AIVC 68. Air Infiltration and Ventilation Centre.
- ASTM, 2000. Standard Test Method for Determining Air Change in a Single Zone by Means of a Tracer Gas Dilution. American Society for Testing and Materials, West Conshohocken, PA.
- Cheng, J.-H., Lee, Y.-S., Chen, K.-S., 2016. Carbonyl compounds in dining areas, kitchens and exhaust streams in restaurants with varying cooking methods in Kaohsiung, Taiwan. *J Environ Sci-China* 41, 218-226.
- Choi, D.W., Moon, K.W., Byeon, S.H., Lee, E.I., Sul, D.G., Lee, J.H., Oh, E.H., Kim, Y.H., 2009. Indoor volatile organic compounds in atopy patients' houses in South Korea. *Indoor and Built Environment* 18, 144-154.
- Huang, Y., Ho, S.S.H., Ho, K.F., Lee, S.C., Yu, J.Z., Louie, P.K.K., 2011. Characteristics and health impacts of VOCs and carbonyls associated with residential cooking activities in Hong Kong. *J Hazard Mater* 186, 344-351.
- Kim, S.-S., Kang, D.-H., Choi, D.-H., Yeo, M.-S., Kim, K.-W., 2008. Comparison of strategies to improve indoor air quality at the pre-occupancy stage in new apartment buildings. *Build Environ* 43, 320-328.
- Seaman, V.Y., Bennett, D.H., Cahill, T.M., 2009. Indoor acrolein emission and decay rates resulting from domestic cooking events. *Atmospheric Environment* 43, 6199-6204.
- Shim, H., Choi, G., 2017. Study of construction convergence technology for performance improvement in functional building materials. *Journal of Building Engineering* 11, 108-114.
- Wang, L., Xiang, Z., Stevanovic, S., Ristovski, Z., Salimi, F., Gao, J., Wang, H., Li, L., 2017. Role of Chinese cooking emissions on ambient air quality and human health. *Sci Total Environ* 589, 173-181.

# Indoor air quality in mechanically ventilated residential dwellings/low-rise buildings: A review of existing information

Amar Aganovic\*<sup>1</sup>, Mathieu Hamon<sup>2</sup>, Jakub Kolarik<sup>3</sup>, and Guangyu Cao<sup>1</sup>

*1 Norwegian University of Science and Technology (NTNU), Department of Energy and Process*

*Kolbjørn Hejes vei 1*

*NO-7491 Trondheim, Norway*

*\*Corresponding author: amar.aganovic@ntnu.no*

*2 Technical University of Denmark (DTU), Department of Civil Engineering*

*Nils Koppels Alle*

*2800 Kgs. Lyngby, Denmark*

*3 INSA de Lyon, Energy and Environmental Engineering*

*20 Avenue Albert Einstein*

*69100 Villeurbanne, France*

## ABSTRACT

Mechanical ventilation has become a mandatory requirement in multiple European standards addressing indoor air quality (IAQ) and ventilation in residential dwellings (single family houses and low-rise apartment buildings). This article presents the state of the art study through a review of the existing literature, to establish a link between ventilation rate and key indoor air pollutants. Design characteristics of a mechanical ventilation system such as supply/exhaust airflow, system and design of supply and exhaust outlets were considered. The performance of various ventilation solutions was assessed by comparing reported ventilation rates, concentrations of CO<sub>2</sub> and total volatile organic compounds (TVOC) to minimum requirements defined by the latest version of the European Standard EN 15251:2007. Based on the literature review of these parameters, the authors noted that whenever the whole-house ventilation rate was reported below 0.5h<sup>-1</sup> or 14 l/s·person in bedrooms, the concentrations of the pollutants elevated above minimum threshold limits (CO<sub>2</sub>>1350 ppm; TVOC >3000 µg/m<sup>3</sup>) defined by the standard. Insufficient or non-existent supply of air was related to significantly higher pollutant concentrations. The authors additionally noted that the literature frequently reported the role of improper maintenance and use on deterioration of IAQ in residential dwellings. The summarized data and comments may provide useful information for future guidelines related to ventilation strategies designed for high IAQ in residential dwellings.

## KEYWORDS

Mechanical ventilation, residential dwellings ventilation rates, pollutants, indoor air quality

## 1. INTRODUCTION

Due to the tightly insulated building envelope, the provision of sufficient fresh air becomes more important than ever in residential dwellings for better indoor air quality (IAQ). In this case, natural ventilation is often unable to provide adequate ventilation for odour or contaminant removal, and mechanical ventilation (MV) is necessary to achieve minimum ventilation rates (Dimitroulopoulou, 2012). Still, nowadays only a few European national standards regarding IAQ in residential dwellings either recommend MV for ventilation system selection (Belgium and Germany) or stipulates that MV must be installed in dwellings as the only ventilation solution (Denmark and Poland). Other standards (France, Sweden and UK)

allow flexibility in the selection between natural and MV systems (Kunkel, 2015). Although all the standards provide guidance on whole-house ventilation rates, calculation tools for ventilation rates vary from standard to standard depending on whether the ventilation rate is regulated based on the number of persons, type of room or floor area. When mechanical ventilation is required, virtually every code specifies that a certain volume of air must be exhausted from wet-rooms (bathroom, kitchen and toilets), however few codes (Denmark, Poland and Belgium) have requirements for distributing fresh air throughout other, so called dryspaces where people spend most of their time. Several European national standards (France, UK, Germany and Sweden) do not include any requirements on ventilation rates for bedrooms, where people spend one-third of their life while sleeping: 12–14 h/day during infancy and 7–8 h/day during adulthood (Strøm-Tejsen et al., 2016). In addition, different requirements for building airtightness imposed by different national standards (Kunkel, 2015) make it even more difficult to harmonise the wide range of sizing rules for an adequate comparison across countries for assessing IAQ in mechanically ventilated dwellings. The first version of the standard addressing ventilation requirements for IAQ in residential buildings on a European level was published in 2007 as EN 15251:2007 and current representative of European standards for residential buildings. This standard is currently under revision and its last draft dates back to 2014. EN 15251:2007 offers three methods for defining the minimum ventilation rates (Table 1.).

Table 1. Ventilation rates defined by EN 15251:2007

Class	Expected percentage of dissatisfied	Supply Airflow							Exhaust Airflow		
		Total Ventilation Rate including Air Filtration(1)		Airflow per person	Air flow based on perceived IAQ for adapted persons		Airflow Bedroom level		Kitchen	Bathrooms	Toilets
	(%)	(l/s·m <sup>2</sup> )	ACH	(l/s·per)	q <sub>p</sub> (l/s·pers)	q <sub>b</sub> (l/s·m <sup>2</sup> )	Master Bedroom (l/s)	Other Bedrooms (l/s)	(l/s)		
I	15	0.49	0.7	10	3.5	0.25	20	10	28	20	14
II	20	0.42	0.6	7	2.5	0.15	14	8	20	15	10
III	30	0.35	0.5	4	1.5	0.1	8	4	14	10	7
IV	40	0.23	0.4	N/A	N/A	N/A	5	2.5	10	6	4

The supply ventilation rates is based on one of the three following criteria: total ventilation rate for the dwelling, supply airflow for bedrooms and supply airflow based on assumed number of occupants. EN 15251:2007 instructs to select the highest value from the three calculated methods for supply flow rate, compare it to the prescriptive total exhaust flow rate and select the higher of the latter two as the minimum design value for the total ventilation rate. Beside ventilation rates and air quality classes, pollutant limit values for two common air pollutants are also indicated in EN 15251:2007. Requirements for limiting carbon-dioxide (CO<sub>2</sub>) and total volatile organic compound (TVOC) levels in residential buildings as defined by different air quality classes (AQC) are presented in Table 2.

Table 2. Limit values of CO<sub>2</sub> and TVOC as given by EN 15251:2007

Air Quality Class	CO <sub>2</sub> (ppm)		TVOC (µg/m <sup>3</sup> )	Level
	Bedrooms	Other		

		rooms		
I	780	950	300	Very low polluting building
II	950	1200		
III	1350	1700	1000	Low polluting building

## 2. METHODOLOGY

The objective of this review is to:

1. Assemble, and summarize existing measurement data on ventilation rate, CO<sub>2</sub> and/or TVOC in mechanically ventilated European dwellings
2. By comparing assembled data to the existing standard for IAQ (EN 15251:2007) - identify and summarize direct and indirect relationships between characteristics of mechanical ventilation systems in residential dwellings/buildings and pollutant concentrations

Previous literature reviews on the relationship between a reduced risk of allergic manifestations among children in a Nordic climate and whole-house ventilation rates above 0.5 ACH (Wargocki 2002, Sundell 2011). To verify whether ventilation requirements stipulated by the current classes in prEN 15251:2007 are sufficient to reduce the pollutant concentrations, the results from previous research studies based on field experiments that reported CO<sub>2</sub> and TVOC concentrations in mechanically ventilated residential dwellings and low rise buildings are analysed and compared to limits indicated by EN 15251:2007.

Beside ventilation rate and airflow distribution through rooms in dwellings, the characteristics also include type of MV system (MEV- mechanically exhaust ventilation system, MES – mechanically supply ventilation system MVHR – mechanically ventilation system with heat recovery) and type of airflow control strategy (CAV – constant air volume systems, DCV) – demand control ventilation system). Since the main focus of the study was to analyse the relationship between the ventilation rate and CO<sub>2</sub> and TVOC concentrations, the keywords used for the search were: *mechanical ventilation, ventilation rate, residential dwellings/buildings, and indoor air quality*. Science direct and Google scholar engines were used to search the literature. The literature peer-reviewed publications: journals papers, conference proceedings. The classification process was based on whether the source article was *relevant and informative*– providing sufficient information on ventilation rates and pollutant levels of at least CO<sub>2</sub> or TVOC concentrations; or *relevant but non-informative*– containing incomplete information concerning ventilation rates or the indoor air pollutants.

## 3. RESULTS

In total, twenty articles were identified and those containing studies of residential dwellings including quantitative evaluations of ventilation rates and data of at least concentration levels of CO<sub>2</sub> or TVOC. Seven papers were excluded and judged as relevant but non-informative. The main reason for exclusion was that data on ventilation rates and IAQ pollutants in mechanically ventilated dwellings were lumped into the same ventilation category as natural ventilation systems. Thirteen papers were found to be informative and relevant for this study and the paper originated from eight European countries: Sweden (3), UK (3), France (2), Austria, Belgium, Finland, Netherlands and Norway. Three papers addressed both CO<sub>2</sub> and

TVOC concentrations, eight only CO<sub>2</sub> concentrations and two only TVOC concentrations along with ventilation rates. The articles were published from 2007 to 2016. Summarized information on the objective, number of dwellings, type of ventilation and control system, year of construction, airtightness, ventilation rates, CO<sub>2</sub> and TVOC concentrations are presented in Table 3.

### **3.1.CO<sub>2</sub> concentrations**

A Swedish study (Hesaraki, 2015) analyzed four different ventilation rates (Figure 1) in a recently renovated single house in Sweden equipped with mechanical exhaust ventilation. The mean CO<sub>2</sub> concentrations measured showed that increasing the whole house ventilation rate from 0.14 ACH to 0.3ACH (both < AQC IV EN 15251) decreased the CO<sub>2</sub> levels from over 1300 ppm (AQC II) to less than 1000 ppm (AQC I).

While the CO<sub>2</sub> concentrations were mostly kept within AQC III in ten new-built mechanically ventilated French dwellings (<0.6m<sup>3</sup>/h·m<sup>2</sup>), the limit levels were frequently exceeded in bedrooms due to low whole house ventilation rates <0.5 ACH (Figure 2). The same study (Guyot, 2015) also reported bad doors undercut as a reason for high CO<sub>2</sub> concentrations in main bedrooms.

A study from the UK (Mcgill, 2015) reported lower ventilation rates (< 4 l/s·person – below AQC III EN 15251) and average CO<sub>2</sub> concentrations exceeding 1000 ppm in bedrooms of two of four new built dwellings (airtightness level < 5m<sup>3</sup>/h·m<sup>2</sup>@50 Pa) with MVHR ventilation. Inadequate ventilation rates less than 11 l/s (< AQC II) were observed in all bedrooms during night. None of the cases complied with AQC I or II of EN15251 for minimum CO<sub>2</sub> concentrations in bedrooms (Figure 3).

Author(s)	Objective	Dwellings	Type of Mechanical Ventilation	Control system	Construction/Restoration year	Airtightness	Measurement Method	CO <sub>2</sub> concentrations (ppm)	TVOC (µg/m <sup>3</sup> )	Ventilation Rate
Berge et Mathiesen 2016	The indoor climate in a high-performance multifamily building was evaluated based on a user survey and measurements (Norway)	8(A)	MVHR (n=4)	CAV	2008 €	< 0.6 ACH @ 50 Pa	CO <sub>2</sub> concentrations were measured continuously in the period May 2013–April 2014 using Wisniewy WS42C sensors.	85% of the time < 750 2.2% of the time > 1200	N/A	24–52 m <sup>3</sup> /h (bedroom)
Derbez et al. 2014	Indoor air quality and comfort in seven newly built, energy-efficient houses (France)	7(D)	MVHR (n=7)	CAV	2008–2009 €	0.66–0.41 m <sup>3</sup> /h.m <sup>2</sup> @ 4 Pa 0.29–0.33 ACH @ 50 Pa	CO <sub>2</sub> concentrations were measured during three periods in summer and winter using a non-dispersive infrared probe. TVOC measurements were done using a photoionization detector	251–881 (median range for all houses)	6–278 (range winter) 128–569 (range summer)	0.10–1.30 ACH (whole house)
Fischer et al. 2014	Indoor air measurements were conducted in one unoccupied apartment of a NZE residential building with wooden construction (Sweden)	1(A)	MVHR (n=1)	N/A	2010 €	< 0.6 ACH @ 50 Pa	TVOCs were collected using the Field and Laboratory Emission Cell (FLEC) with a flow rate of 0.006 m <sup>3</sup> /h during 60 min.	N/A	150±20 (average + SD)	0.53 ACH (whole house)
Gayet et al. 2015	Ventilation performance and indoor air pollutants diagnosis in low energy houses (France)	19 (D)	MVHR (n=10)	CAV/DCV	N/A	6 m <sup>3</sup> /h.m <sup>2</sup> @ 50Pa	CO <sub>2</sub> concentrations were measured using a data logger with an infrared dispersive sensor for 7 days	661–1442 (mean - living room), 728–2351 (mean - bedroom)	N/A	0.11–0.79 ACH (whole house)
Hesarakis et al. 2015	To analyse the influence of different ventilation levels on indoor air quality and energy savings: a case study of a single-family house (Sweden)	1(B)	MEV (n=1)	CAV	1990s	N/A	CO <sub>2</sub> concentrations were measured using the "Exo 480 IAQ Probe" for three days per ventilation rate case	586–1337 (range)	N/A	0.14–1.0 ACH (whole house)
Hofstede et al. 2016	Monitoring IAQ in 62 dwellings for 12 months (Netherlands)	62(D)	MEV in wet rooms; MEV in all rooms; MVHR with various types of controls	CAV/DCV	N/A	10 ± 1.0 dm <sup>3</sup> /m <sup>2</sup>	The CO <sub>2</sub> concentrations were monitored for more than one year.	1399–1971 (mean)	N/A	37–52 m <sup>3</sup> /h (per person)
McGill et al. 2015	Bedroom environmental conditions in airtight mechanically ventilated dwellings (UK)	19 (D)	MVHR (n=17); MEV (n=2)	N/A	2010–2013	< 5 m <sup>3</sup> /h.m <sup>2</sup> @ 50Pa	CO <sub>2</sub> concentrations were measured continuously during July–August 2013 and November 2013–January 2014 using a Wobler data logger	610–1289 (mean - summer), 929–1291 (mean - winter)	N/A	3.53±16.84 l/s per person (summer); 3.74±5.58 l/s per person - (winter)
Järnström et al. 2006	Eight new residential buildings investigated for IAQ (Finland)	8(A)	MES (n=3); MEV (n=5)	N/A	1999–2002	< 4 ACH @ 50 Pa	TVOCs were collected on Tenax TA adsorbent at the air flow rate of ~100 ml min <sup>-1</sup> for 120 min	N/A	397 (mean) in MES 1098 (mean) in MEV	0.95 ACH (whole house)
Langer et al. 2015	20 new passive houses and 21 new conventionally built houses monitored for IAQ (Sweden)	5(D)	MVHR (n=5)	CAV	2010–2013	< 0.6 ACH @ 50 Pa	CO <sub>2</sub> was sampled in the bedroom using a Q-trak Indoor Air Quality Monitor for a one week period time. The TVOCs were sampled using radial diffusive tubes (Radello®) with an exposure time of 7 days	6% of the time > 1000	10 (median winter) 9.2 (median spring) 8.0 (median summer) 7.3 (median autumn)	0.68 ACH (whole house)
Laverge et al. 2015	Monitoring CO <sub>2</sub> in the exhaust spaces of 36 old, 39 standard and 39 low energy dwellings (Belgium)	78 (D)	MVHR (n=39); MEV (n=39)	CAV	2007–	0.5–3 ACH @ 50 Pa	CO <sub>2</sub> concentrations was monitored using a non-dispersive infrared logger for 9 days.	< 750 (living rooms), < 1250 (bedrooms)	N/A	0.26 ACH (whole house)
Billey et al. 2013	Monitoring the performance of the first new London dwelling certified to the Passive House standard (UK)	1 (D)	MVHR (n=1)	CAV	2010	0.44 ACH @ 50 Pa	The CO <sub>2</sub> concentrations were monitored for a one year period using Etek wireless data logging and monitoring system.	< 700 ppm (living room), 78% of time < 1000 (bedroom)	N/A	0.48 ACH (whole house)
Shaape et al. 2014	To assess indoor environmental quality in bedrooms of low energy houses (UK)	4(D)	MVHR (n=4)	N/A	N/A	2.45 m <sup>3</sup> /h.m <sup>2</sup> @ 50Pa	CO <sub>2</sub> was collected using a Wireless Sensor Technology (WST) during three different sample months in summer, spring and autumn	600–1100 (range) 858 (average winter)	N/A	9.76 l/s (bedroom)
Walker et al. 2015	To investigate IAQ in 123 mechanically ventilated buildings (Austria)	62 (70% H, 30% A)	MVHR (n=62)	CAV	2010–2012	N/A	The CO <sub>2</sub> concentrations were measured continuously for one week using method Wobler data logger. TVOCs were sampled by pumping air through charcoal tubes	1280–1360 (median)	120–300 (median)	20 to 25 m <sup>3</sup> /h per person (11%–21% of time (bedroom))

Table 3. Summary of papers providing background information about ventilation rates and indoor air pollutants

The graphical representation of indoor pollutant concentrations vs ventilation rates from articles presenting individual measurements in dwellings are based on the different metrics used for ventilation rates (Figure 1–3).

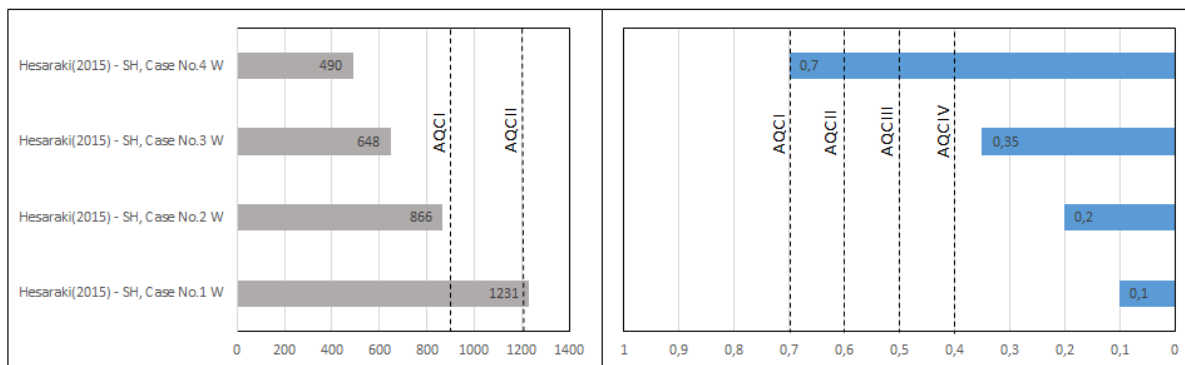


Figure 1. Average CO<sub>2</sub> concentrations (ppm) vs whole house-ventilations rates (ACH) compared to air quality classes defined by EN 15251 (Hesaraki, 2015)

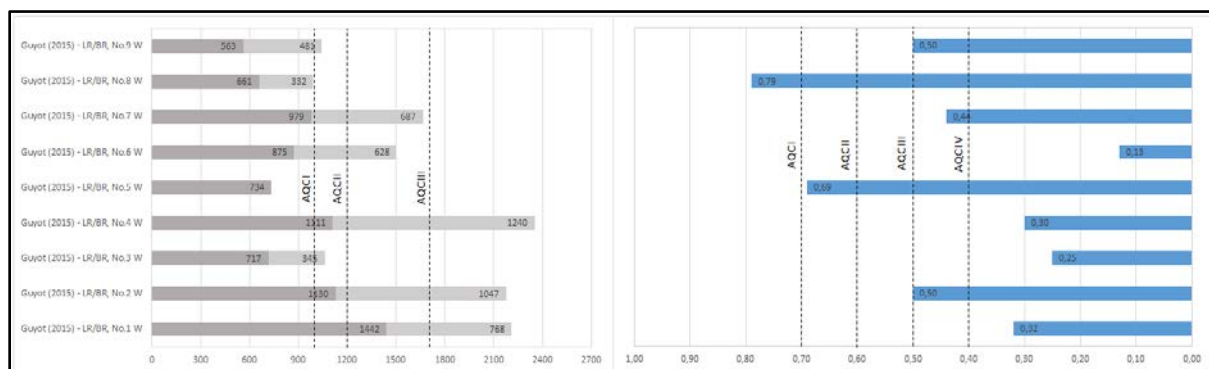


Figure 2. Average CO<sub>2</sub> concentrations in living rooms and bedrooms (ppm) vs whole house ventilation rates (ACH) compared to air quality classes defined by EN 15251 (Guyot, 2015)

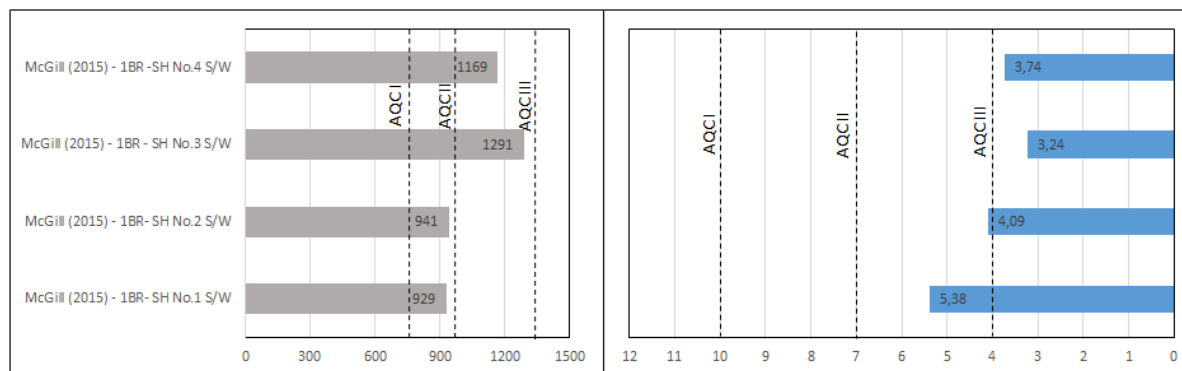


Figure 3. Average CO<sub>2</sub> concentrations (ppm) in bedrooms vs ventilation rates per person (l/s-person) compared to air quality classes defined by EN 15251 (McGill, 2015)

A French study (Derbez,2014) found that the median CO<sub>2</sub> concentrations measured using tracer gas method were lower than 1000 ppm in six highly airtight French houses (< 0.6m<sup>3</sup>/h·m<sup>2</sup>@4 Pa) equipped with MVHR ventilation systems. Concentrations ranged from 360 to 2030 ppm in winter conditions and from about 290 to 1950 ppm in summer conditions. The reasons for the maximum CO<sub>2</sub> concentrations exceeding the EN 15251 AQC III is that the MVHR systems were reported to be frequently switched off due to high noise levels. The maximum hourly average CO<sub>2</sub> concentrations reported in bedrooms of 62 Austrian homes (air tightness ≤0.6h<sup>-1</sup>) with MVHR systems built between 2010 and 2012 were above 1000 ppm (AQC I) in 52 of the houses about three months after the residents moved in and in 55 after about one year (Wallner, 2015). The same study reported that CO<sub>2</sub> concentrations in 39% of the bedrooms were exceeding 1400 ppm, indicating they were at least temporarily at a level of lower indoor air quality according to AQC III EN 15251. The high values of CO<sub>2</sub>

levellers were coincident with low ventilation rates: only 11% and 21 % of the bedrooms were supplied with airflow rates higher than 5.5 l/s-person (AQC III) in the first group and second group of measurements respectively.

Assessing the performance of a MVHR equipped highly insulated (airtightness  $\leq 0.44 \text{h}^{-1}$ ) London dwelling; (Ridley, 2012) reported peak  $\text{CO}_2$  concentrations in the living room of 815 ppm, while the bedroom  $\text{CO}_2$  concentrations exceeded 1000 ppm (AQC II) 22% of the time. As the internal doors were opened all time, the main reason reported for poorer indoor air quality in the bedroom was the lowest possible ventilation rate operated ( $0.43 \text{h}^{-1}$  – AQC IV).

The median  $\text{CO}_2$  concentration levels in bedrooms of 5 passive houses built between 2010 and 2013 (Langer, 2015) were 540 and 660 ppm respectively. The  $\text{CO}_2$  concentration exceeded 1000 ppm during 6% of the measured time. The median ventilation rates for the two types of houses were 0.60 and  $0.68 \text{h}^{-1}$  respectively (AQC II).

In five of the twenty-six houses monitored with MVHR systems (average airtightness  $3 \text{m}^3/\text{h}\cdot\text{m}^2 @ 50 \text{Pa}$ ), (Sharpe, 2014) reported average  $\text{CO}_2$  rates in bedrooms of 858 ppm while three of the bedrooms measured  $\text{CO}_2$  levels above 1000 ppm during 30 % of the time. The latter figure were attributed to family size as the houses where  $\text{CO}_2$  concentrations did not exceed 1000 ppm for more than 30 % of the time had 1-2 occupants compared to the other group with 4-5 occupants. The average ventilation rate was 6.61 l/s (AQC IV for main bedrooms and AQC III for other bedrooms).

In four apartments in newly built low-rise residential buildings ( $3 \text{m}^3/\text{h}\cdot\text{m}^2 @ 50$ ) equipped with MVHR system and delivering fresh air to every bedroom, it was reported  $\text{CO}_2$  levels below 750 ppm 85% of the time and levels 900-1200 ppm 5% of the time (Berge, 2016). Although none of the master or other bedrooms was supplied with enough volume of air to comply with minimum requirements set by EN 15251 AQC II,  $\text{CO}_2$  levels above 1200 ppm (AQC II) were measured only 2.2% of the time.

A very recent study on indoor air quality in Dutch residential buildings (Holsteijn, 2016) found that in apartments with only mechanical extraction in wet rooms had significantly higher  $\text{CO}_2$  levels exceeding 1200 ppm (7.62-12.42 h/day) compared to apartments with mechanical supply and/or exhaust systems in all rooms (2.65-4.40 h/day). The apartment equipped with mechanical extraction in all rooms and  $\text{CO}_2$  and humidity sensor but without heat recovery unit had lower  $\text{CO}_2$  values than in all other apartments with MVHR except for one room. The average ventilation rate in all apartments ranged from 10.3-14.4 l/s-person, satisfying the minimum requirements defined by AQC I EN 15251.

A Belgian study (Laverge, 2015) measured the  $\text{CO}_2$  and humidity levels for four groups of dwellings equipped with different ventilation systems: 36 with natural ventilation, 39 with exhaust-only ventilation and two types of MVHR: 23 for low energy houses and 16 extremely airtight passive houses. The average  $\text{CO}_2$  concentrations, measured in living rooms and bedrooms, was found to be in the same range for all groups. Although more stable concentrations over time were reported in dwellings with MVHR, the reason for relatively high  $\text{CO}_2$  levels is attributed to the fact that the ventilation system was operated with an average value of  $0.26 \text{h}^{-1}$  (AQC IV EN 15251).

### **3.2. TVOC concentrations**

Derbez, et al. 2014) reported highest concentrations of TVOCs were found in the house ( $1042 \mu\text{g}/\text{m}^3$ ) where painting activity generated air pollution and in house ( $3087 \mu\text{g}/\text{m}^3$ ) where besides painting, presence of occupants and ventilation system switched off. In other houses in pre-occupancy conditions, without painting and with ventilation system turned on, the measured TVOCs ranged from 130-525  $\mu\text{g}/\text{m}^3$ .

It's reported median TVOC concentrations of  $300 \mu\text{g}/\text{m}^3$  in the first group of measurements and an increase of 17% in the second group (Wallner, 2015). Only 3% of

the rooms with mechanical ventilation reported TVOC values exceeding  $3000 \mu\text{g}/\text{m}^3$  while in the follow-up measurements there were no houses exceeding  $3000 \mu\text{g}/\text{m}^3$ .

Langer, 2015 reported significantly higher median TVOC concentrations ( $272 \mu\text{g}/\text{m}^3$ ) in Swedish passive houses than in conventional houses ( $145 \mu\text{g}/\text{m}^3$ ), despite the former group having lower ventilation rates.

Fischer, 2014 evaluated the IAQ in an unoccupied apartment in a multi-story wooden passive building equipped with mechanical ventilation in Sweden. The average TVOC concentrations reported were  $150 \pm 20 \mu\text{g}/\text{m}^3$  while the reported AER was  $0.53\text{h}^{-1}$ .

Järnström, 2006 measured the TVOC concentration in apartments in Finnish buildings with mechanical supply and exhaust ventilation and showed the TVOC level was significantly lower than in buildings with mechanical exhaust ventilation. The mean TVOC concentration was  $780 \text{mg}/\text{m}^3$  in the newly finished buildings while the reported AER of 0.95 ACH was higher than AQC I as defined by EN 15251.

#### 4. DISCUSSION

Highly insulated houses rely upon controlled ventilation for good indoor air quality. In these dwellings mechanical ventilation systems are needed. This review aimed to characterize the relationship between indoor air pollutants and ventilation rates in mechanically ventilated dwellings. The majority of papers reporting  $\text{CO}_2$  and TVOC concentrations were built in mechanically ventilated dwellings with low levels of airtightness ( $<10\text{m}^3/\text{h}\cdot\text{m}^2@50$ ) or very low leakage levels required by passive house standard ( $\leq 0.6\text{h}^{-1}@50\text{Pa}$ ). It is difficult to adequately characterize indoor  $\text{CO}_2$  concentrations only as a function of ventilation rates as they also vary with time and occupancy. Another disadvantage for generalisation of existing data is a great variability in the methods used to characterize the  $\text{CO}_2$  concentrations in the papers identified. Short-term measurements may be inadequate to provide information on the long-term ventilation conditions in mechanically ventilated residential dwellings. Different metrics used for reporting average pollutant values (median vs. mean) and measurement time makes it more difficult to make absolute comparison between different studies. In most of the reports from field measurements the ventilation rate concentrations were above the minimum requirements for whole-house ventilation ( $>0.4$  ACH) defined by EN 15251:2007. Generally, papers reporting ventilation rates of at least air quality class III ( $>0.5$  ACH) as defined by EN 15251:2007 and that comply with class II for bedrooms ( $14 \text{l}/\text{s}\cdot\text{person}$ ) reported lowest average or median  $\text{CO}_2$  concentrations. Still, the  $\text{CO}_2$  concentrations exceeded frequently the EN 15251:2007 minimum levels ( $>1350$  ppm for bedrooms;  $>1700$  ppm for other rooms) for at least some of the measurement time. The main reason reported was poor use of the ventilation system by occupants. The most common behavior was changing the power settings of the MV system due to noise nuisance. Very few measurements of TVOCs are reported in the literature for mechanically ventilated dwellings. For Europe, only four papers were found which reported TVOC measurements and neither reported a prominent influence of the ventilation rate compared to other building characteristics.

#### 5. CONCLUSION

The available measurements of ventilation rates and  $\text{CO}_2$  concentrations in schools suggest that, based upon the current EN 15251:2007 ventilation standard, many new-built airtight residential dwellings are not adequately ventilated. Low ventilation rates were reported due to insufficient ventilation capacity, incorrect use of the control system and incorrect maintenance; the ventilation rates were frequently reported to be reduced or switched off by

users because of high noise levels or poor occupant understanding of how to use the ventilation system.

## 6. REFERENCES

- EN 15251:2007. Indoor environmental input parameters for design and assessment of energy performance of buildings. Brussels: European Committee for Standardization (CEN), 2007.
- Berge M., Mathisen H.M.(2016) Perceived and measured indoor climate conditions in high-performance residential buildings, *Energy Build.* 127:1057-1073.
- Derbez M., Berthineau B., Cochet V., Lethrosne M., Pignon C., Riberon J., et al., (2014). *Indoor air quality and comfort in seven newly built, energy-efficient houses in France.* *Build. Environ.*;72:173-187.
- Dimitroulopoulou, C. (2012). Ventilation in European dwellings: a review. *Building and Environment*, 47,109-125.
- Fischer A., Langer S., Evert Ljungstrom E., (2014) Chemistry and indoor air quality in a multi-storey wooden passive (low energy) building: formation of peroxyacetyl nitrate. *Indoor Built Environ*, 23,485-496.
- Guyot G., Bailly A., Bernard A.M., Perez G., Coeudevez C-S., et al. (2015). Ventilation performance and indoor air pollutants diagnosis in 21 French low energy homes. *36th AIVC Conference " Effective ventilation in high performance buildings", Madrid, Spain, 23-24 September 2015.*
- Hesaraki A., Myhren J.A.,Holmberg S.,(2015) Influence of different ventilation levels on indoor air quality and energy savings: a case study of a single-family house, *Sustain. Cities Soc.*, 19, 165–172.
- Holstejin van R.C.A, Li W., Harm J.J., Kornaat W., (2016) *Improving the energy and IAQ performance of Ventilation systems in Dutch dwellings.**Int.J.Vent.*,14(4), 363-370.
- Järnström, H., Saarela, K., Pasanen, A-L., Kalliokoski, P., (2006). Reference values for indoor air pollutant concentrations in new, residential buildings in Finland. *Atmospheric Environment*, 40, 7178–7191.
- Kunkel, S.; Kontonasiou, E.(2015). Indoor air quality, thermal comfort and daylight policies on the way to nZEB—Status of selected MS and future policy recommendations. *In Proceedings of the ECEEE Summer Study, First Fuel Now, Belambra Les Criques, Toulon, France.*
- Langer S., Ramalho O., Derbez M., Riberon J., Kirchner S., Mandin C., (2016)Indoor environmental quality in French dwellings and building characteristics, *Atmos. Environ*, 128, 82-91.
- Laverge J., Delghust M., Janssens A., (2015). Carbon Dioxide Concentrations and Humidity Levels Measured in Belgian Standard and Low Energy Dwellings with Common Ventilation Strategies. *International Journal of Ventilation*, 14 (2), 165-180.

- McGill, G., Oyedele, L.O., McAllister, K., (2015). Case study investigation of indoor air quality in mechanically ventilated and naturally ventilated UK social housing. (2015), *Int. J. Sustain. Built Environ.* 4, 58-77
- Ridley I., Clarke A., Berec J., Altamiranod H., Lewis S., Durdev M., Farr A., (2013). The monitored performance of the first new London dwelling certified to the Passive House standard, *Energy and Buildings*, 63, 67–78.
- Sharpe T.R., Porteous C.D.A., Foster J., Shearer D., An assessment of environmental conditions in bedrooms of contemporary low energy houses in Scotland, (2014). *Indoor Built Environ.* 23 (3), 393–416.
- Strøm-Tejsen P., Zukowska D., Wargocki P., Wyon D.P. (2016). The effects of bedroom air quality on sleep and next-day performance. *Indoor Air*.
- Sundell, J., Levin, H., Nazaroff, W.W., Cain, W.S., Fisk, W.J. et al. (2011). Ventilation rates and health: multidisciplinary review of the scientific literature. *Indoor Air*, 21, 191–204.
- Wallner P., Munoz U, Tappler P., et al. (2015). Indoor environmental quality in mechanically ventilated, energy-efficient buildings vs. conventional buildings. *International Journal of Environmental Research and Public Health*, 12, 14132-47.
- Wargocki, P., Sundell, J., Bischof, W., Brundrett, G., Fanger, O., et al. (2002). Ventilation and health in non-industrial indoor environments, Report from a European multidisciplinary scientific consensus meeting, *Indoor Air*, 12, 113–128.

# Reducing Uncertainty in Air Tightness Measurements

Iain Walker<sup>1</sup>

*1 Lawrence Berkeley National Laboratory  
1 Cyclotron Road  
Berkeley CA 94501, USA*

## SUMMARY

There are several methods for measuring air tightness that may result in different values and sometimes quite different uncertainties. The two main approaches trade off bias and precision errors and thus result in different outcomes for accuracy and repeatability. To interpret results from the two approaches, various questions need to be addressed, such as the need to measure the flow exponent, the need to make both pressurization and depressurization measurements and the role of wind in determining the accuracy and precision of the results. This article used a large dataset of blower door measurements to reach the following conclusions. For most tests the pressure exponent should be measured but for wind speeds greater than 6 m/s a fixed pressure exponent reduces experimental error. The variability in reported pressure exponents is mostly due to changes in envelope leakage characteristics. It is preferable to test in both pressurization and depressurization modes due to significant differences between the results in these two modes.

## KEYWORDS

Pressure testing, air tightness evaluation, air leakage, measurements, error analysis.

## 1 DATA SOURCES

We used a dataset from the Alberta Home Heating Research Facility (AHHRF) located south of Edmonton, Alberta, Canada. The facility consists of six test houses, each constructed in a different way in order to examine different heating and ventilating strategies. The houses were unoccupied and the fan pressurisation test system was automated, and in this study we used over 6000 of the resulting tests. Wind speed, wind direction, and ambient temperature data were taken from meteorological towers at the test site. The flow rates were measured using a laminar element flowmeter, and were corrected for pressure and temperature changes. Offset pressures due to stack and wind effects with the fan not in operation were measured between each data point. The houses were tested in a total of 97 configurations of open and closed flues, windows and passive vents, pressurization and depressurization, resulting in a wide range of total envelope air leakage, leakage distribution and air flow paths. Typically there were 30 to 100 tests in each configuration. The best test in each configuration was determined by first looking for low wind speed (less than 1.5 m/s) tests to reduce the uncertainty in the test results from fluctuating wind pressures. A total of 301 tests met this low wind speed criterion. For each configuration, these low wind speed tests were analyzed to find the test with the least wind-induced variability (a combination of minimal least squares fitting error and visual observation of the data) in the measured pressures and flows. This test was then used as the reference for all the other tests in a given configuration. The  $C$ ,  $n$ ,  $Q_{50}$ ,  $ELA_4$  and  $NL$  from the low wind speed test were the reference for other tests for comparison.

## 2 ANALYSIS AND DISCUSSION

The mean pressure exponent from the AHHRF data is 0.649 with a standard deviation (SD) of 0.073. The variability represented by the standard deviation includes both noise due to measurement uncertainty and differences between leakage configurations from home to home.

To estimate the fraction of this variability due to different home leakage configurations, we can examine the low wind speed tests only. For low wind speed tests the mean and standard deviation were 0.631 and 0.063, respectively. The standard deviation for the low wind speed tests is almost entirely due to the true variability in pressure exponent between different house configurations. These results indicate that the standard deviation in pressure exponent due to wind effects is 0.037 – or about one half of that due to true leakage variation. Examining differences between open/closed flue and pressurization/depressurization results showed that the variability in pressure exponent due to changes in building leakage configuration is significant (0.075) which implies that assuming a fixed pressure exponent can introduce significant errors. The extrapolation error from 50 Pa down to 4 Pa was estimated by adding or subtracting 0.075 from the fixed pressure exponent of 0.65 and extrapolating with these higher and lower pressure exponents. The resulting extrapolation errors in estimating ELA<sub>4</sub> for using the higher and lower exponents based on exponent variability 15% to 21%, with a typical value of 18%. Similarly, we can use the estimate of wind-induced exponent variability of 0.037 to estimate extrapolation errors for getting the wrong pressure exponent due to wind pressure fluctuations. The resulting errors are 9% and 10%.

There may also be a difference in the physical size of the holes in the envelope (ELA<sub>4</sub>) between pressurization and depressurization due to valving action. On average, there was a 24% RMS difference between the pressurization and depressurization ELA<sub>4</sub>. In general, the average ELA of pressurization and depressurization will be the quantity of interest since in normal operation the envelope will have areas of both pressurization and depressurization. Because the mean difference is small compared to the RMS difference a reasonable estimate of the uncertainty due to performing only pressurization or depressurization rather than averaging both together is half of the RMS difference, or 12%.

### **3 GUIDANCE FOR TEST METHOD SELECTION**

The fixed pressure exponent errors do not change much with wind speed but the fitted exponent results show lower errors at low wind speed and increasing error with wind speed. The fitted n results give lower RMS errors up to about 6 m/s, after which the fixed exponent gives less variability. This implies that an optimum would be to use fitted C and n for wind speeds below 6 m/s and a fixed exponent at higher wind speeds. Only 7% of the tests were above 6 m/s so if we had to choose one method we would choose the fitted C and n as they give lower errors for the majority of tests. If we want to estimate uncertainty for a typical test we can look at the uncertainties for the wind speeds that are most common: 2-4 m/s. In this range the wind-induced RMS errors for fitted C and n are about 10%, and for fixed exponent, about 17%.

### **4 ACKNOWLEDGEMENTS**

I would like to acknowledge the contributions of Jeffrey Joh and Max Sherman of LBNL and the staff of AHHRF, in particular Mark Ackerman of the University of Alberta.

# On the contribution of steady wind to uncertainties in building pressurisation tests

Valérie Leprince<sup>\*1</sup>, François Rémi Carrié<sup>\*2</sup>

*1 PLEIAQ  
84 C Avenue de la Libération  
69330 Meyzieu, France  
e-mail: valerie.leprince@pleiaq.net*

*2 ICEE  
93 rue Molière  
69003 Lyon, France*

## ABSTRACT

This paper analyses the contribution of a steady wind to the uncertainties in building pressurisation tests, using the approach developed in another paper (Carrié and Leprince, 2016). The uncertainty due to wind is compared to the uncertainties due to other sources of uncertainty (bias, precision and deviation of flow exponent).

The main results of this study are:

- The model error due to the wind on the estimated airflow rate is relatively small at the high pressure point (12% at 10m/s), but it can become very significant at the low pressure point (60% at 10m/s);
- At the high pressure point, the uncertainty due to wind remains smaller than that due to other sources of uncertainties up to 6m/s, whereas when a two-point pressurisation test is performed to calculate flowrate at 4Pa, the impact of wind may become dominant at 4m/s;
- Having a constraint either on the zero-flow pressure or on wind speed seems effective to control uncertainty (provided these quantities can be adequately measured);
- Averaging results between pressurisation and depressurisation is mostly beneficial at intermediate windspeed (around 4m/s) when a reference pressure of 4Pa is used;
- The uncertainty due to steady wind is mostly critical for single-sided dwellings or zones tested alone;
- For single-sided dwellings or zones, to estimate flowrate at 4Pa, it is better to perform:
  - o up to 5m/s, a 2-point test and extrapolate with a calculated flow exponent;
  - o above 5m/s, a test at 50 Pa and extrapolate with a default flow exponent.

## KEYWORDS

Airtightness; building; pressurisation test; infiltration; measurement; error; uncertainty

## INTRODUCTION

With the increasing pressure of energy performance of buildings regulations, building pressurisation tests become more and more common. Yet, there remain unanswered questions regarding the quantification of uncertainties in practice. The sources of uncertainties include model error due to wind, model error due to the deviation of the flow exponents, precision and bias error.

The objective of this study is to assess the impact of steady wind on airtightness testing uncertainty and compare it to other sources of uncertainty. This paper uses the modelling approach proposed by (Carrié, et al., 2016). The reader should refer to that paper for equations and demonstrations which are not repeated here.

## 1 APPROACH

This analysis assumes that:

- the building can be represented by a single zone separated from the outside by 2 types of walls: walls on the windward side of the building which are subject to the same upwind pressure; and walls on the leeward side which are subject to the same downwind pressure;
- the test is performed in isothermal conditions ; and

- the airflow rate through the leaks of the envelope is given by a power-law with the same flow exponent.

To estimate combined uncertainty, we use a similar approach to that proposed by (Sherman, et al., 1995), which includes:

- the standard uncertainty due to precision errors,  $u_{\text{precision}}$ ;
- the standard uncertainty due to bias errors,  $u_{\text{bias}}$ ;
- the standard uncertainty due to model errors,  $u_{\text{model}}$ , which is assumed to be due both to the wind effect on the pressure seen by the leaks and the guess or deviation of  $n$  over a range of pressure.

We have compared the model error due to wind with the combined expanded uncertainties due to other sources.

We have estimated the maximum error for a one-point measurement at 10 and 50 Pa and for a two-point measurement with determination of flowrate at reference pressure 4 and 50 Pa. Constraints were applied to perform a test valid according to ISO 9972:2015. However, we have also plotted results without the constraint on the zero-flow pressure (named "constraint D") to see its impact. We assessed the uncertainties when averaging results of pressurisation and depressurisation tests. We analysed separately the maximum error likely to happen when testing a building zone with facades exposed to wind:

- both upstream and downstream such as a detached house. In such cases, the leakage distribution, which is represented in our model by the ratio of the leakage coefficient upstream and downstream, is likely to have values contained in a "restricted range" between 2 and 8 ;
- either upstream only or downstream only, for instance, in single-sided dwellings. In such cases, there is no reason to assume that the leakage distribution would be restricted. Therefore, we should consider the "full range" of leakage distribution.

## 2 RESULTS

The results are summarised in Figure 1 to Figure 4 and Table 1.

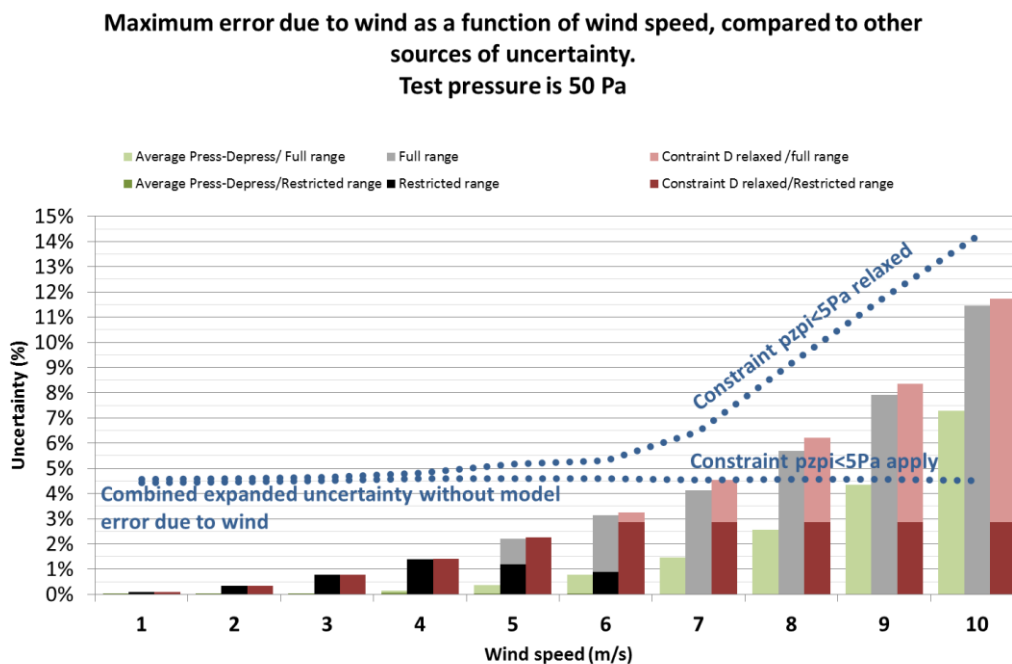


Figure 1: Model error due to wind at 50Pa, one point measurement

**2-points measurement, maximum error due to wind compared to other sources of uncertainty**  
**Reference pressure is 50 Pa**

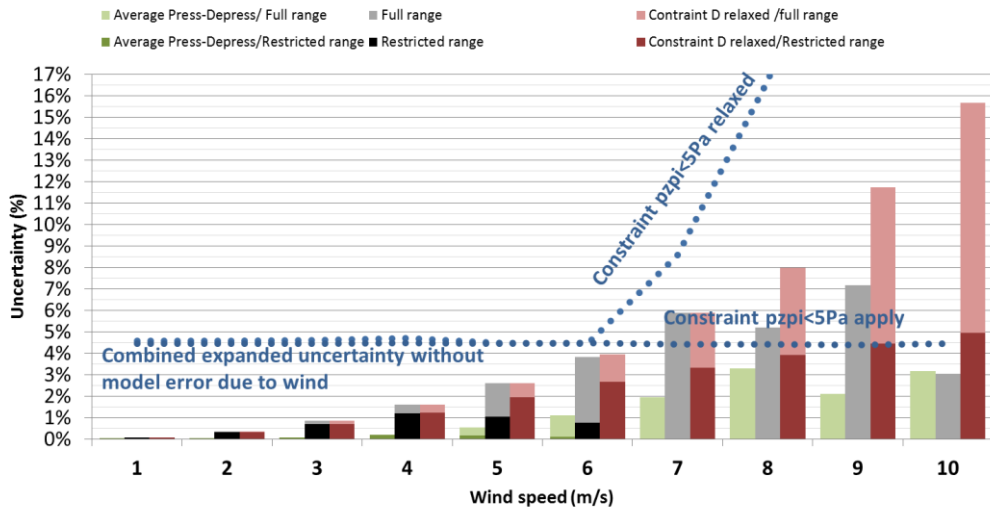


Figure 2: Model error due to wind at a reference pressure of 50 Pa with 2-points measurements

**Maximum error due to wind as a function of wind speed compared to other sources of uncertainty**  
**Test pressure is 10 Pa**

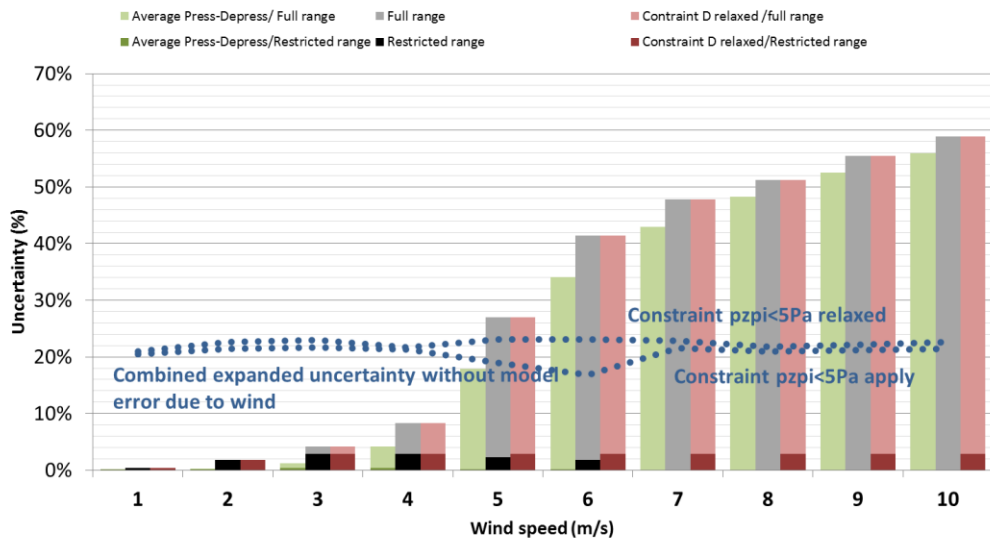


Figure 3: Model error due to wind at 10Pa, one-point measurement

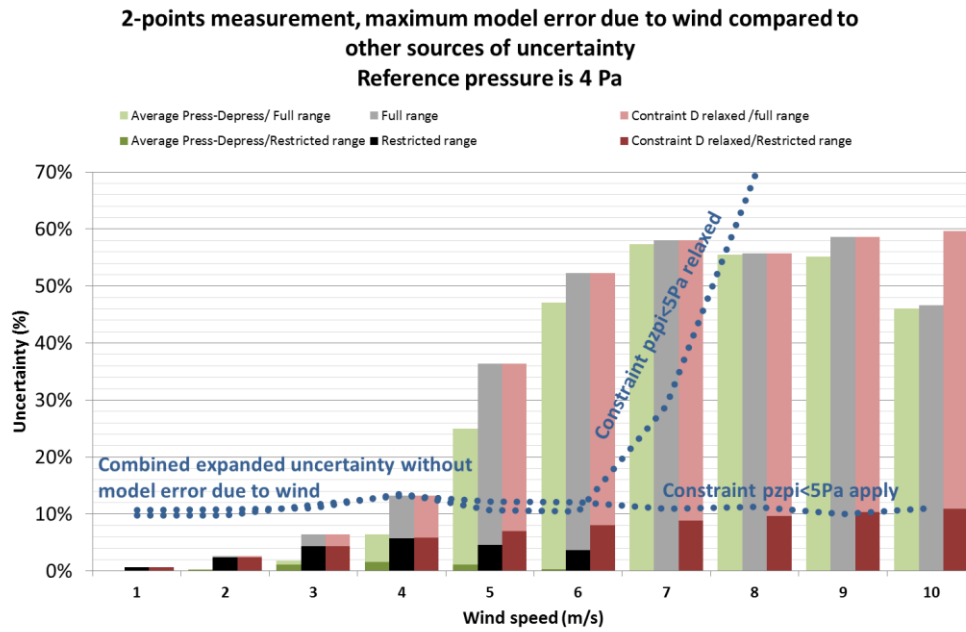


Figure 4: Model error due to wind at a reference pressure of 4 Pa with 2-point measurements

		At 4 Pa				At 50 Pa			
		Constraint D		No constraint D		Constraint D		No constraint D	
Range of z		Full	Restr.	Full	Restr.	Full	Restr.	Full	Restr.
1-point	6 m s <sup>-1</sup>	3%	1%	3%	3%	3%	1%	3%	3%
	10 m s <sup>-1</sup>	11%		12%	3%	11%		12%	3%
1-point combined	6 m s <sup>-1</sup>	32%	30%	33%	32%	6%	5%	6%	6%
	10 m s <sup>-1</sup>	34%		45%	44%	12%		15%	14%
2-point	6 m s <sup>-1</sup>	52%	4%	52%	8%	4%	1%	4%	3%
	10 m s <sup>-1</sup>	47%		60%	11%	3%		16%	5%
2-point combined	6 m s <sup>-1</sup>	53%	15%	53%	42%	6%	5%	6%	5%
	10 m s <sup>-1</sup>	48%		151%	139%	5%		44%	39%

Table 1: Summary of result: maximum error due to steady wind

### 3 DISCUSSION

One key result is that alone, the model error due to the wind on the estimated airflow rate is relatively small for the high pressure point, but it can become very significant with a low pressure point. While the error lies within 12% for wind speeds up to 10 m s<sup>-1</sup> at 50 Pa, it can reach 60% at the low pressure point (10 Pa).

However, there are other sources of uncertainty that are not taken into account in this study such as:

- wind fluctuations
- leaks that have different flow exponents
- the linear regression
- thermal draft
- uncertainty on building preparation.

### 3.1 What happens over 6m/s?

At 50Pa, up to 6m/s uncertainty due to wind remains below "other combined uncertainty". Therefore the uncertainty due to wind has almost no impact on the quadratic sum. It is seen on one- and two-point measurement graphs.

The uncertainty due to wind becomes dominant at 5 m/s for 10Pa (Figure 3) and at 4 m/s for 2-point test extrapolated at 4Pa (Figure 4).

Therefore, 6m/s is a relevant limit value for the high pressure station (50Pa), but is too high for low-pressure measurements.

### 3.2 Can we relax the zero-flow pressure constraint ("constraint D" on graphs) to allow testing in windy places?

The difference between with and without the zero-flow pressure constraint is the difference between the grey/black and the red bars on figures 1 to 4. Up to 6m/s there is not much difference between with and without applying this constraint. Constraint D limits the wind speeds for which the test can be performed to about  $6.2 \text{ m s}^{-1}$  with a restricted range of leakage distribution (see Figure 1, Figure 2, Figure 3, Figure 4) which is consistent with ISO 9972:2015 stating that constraint D is unlikely to be met above  $6 \text{ m s}^{-1}$ . Relaxing the constraint on the zero-flow pressure would allow one to perform a test above 6m/s in detached houses.

In detached houses (restricted range of leakage distribution), the uncertainty due to wind remains low even with wind speeds up to 10m/s and without constraint on zero-flow pressure. However, for 2-point tests above 6m/s, the combined uncertainty without wind increases rapidly without constraint D; it passes over 10% at 7m/s for a reference pressure at 50Pa.

These results suggest it is necessary:

- either to have a constraint on wind speed (maximum 6m/s); or
- to have a constraint on zero flow pressure (maximum 5Pa)

### 3.3 Does averaging pressurisation and depressurisation have a significant impact on results?

The difference between green and grey bars in figures 1 to 4 shows the effect of averaging pressurisation and depressurisation tests. This averaging can decrease the uncertainty due to wind up to 5 percentage points. At low wind speed, when averaging, the uncertainty due to wind is negligible; therefore other sources of uncertainties dominate.

At high wind speed, averaging is not enough to make uncertainty due to wind in the same range of other sources of uncertainties.

Averaging is mostly beneficial at intermediate wind speed (around 4m/s) when reference pressure is 4Pa. It keeps the error due to wind far below the "other" combined uncertainty.

### 3.4 Is the uncertainty different between tests in detached houses and single-sided dwellings?

The maximum uncertainty in detached houses (restricted range) is given by dark bars in the figures, and the maximum uncertainty without restriction on the leakage distribution is given by light bars. The uncertainty in detached houses remains below 12% even for wind speeds up to 10m/s with constraint D relaxed at 4Pa, whereas for a single-sided dwelling the uncertainty due to wind may reach 60% at high wind speed. Therefore, the uncertainty due to wind is mostly critical for single-sided buildings or zones.

### 3.5 To calculate the infiltration air flowrate is it better to have test results at 4Pa or to have test result at 50 Pa and estimate flowrate at 4Pa with a constant n of 2/3?

According to (Carrié, et al., 2016); figure 6), the uncertainty for a reference at 4 Pa (with  $n = 2/3$ ) when testing at a single pressure station of 50 Pa remains between 31 and 34% up to

10m/s when constraint D applies. When constraint D is relaxed, it increases from 5 m/s to reach 47% at 10m/s.

Comparing this result with Figure 4 suggests that up to 5m/s, it is better to perform a 2-point test and extrapolate with a calculated flow exponent and above 5m/s it is better to perform a test at 50 Pa and extrapolate with a default flow exponent.

For detached houses, Figure 4 suggests that a 2-point test is preferable up to 7 m/s (whether constraint D is relaxed or not).

### **3.6 What is the impact of steady wind on uncertainty compared to other sources of uncertainty?**

On figures 1-4, for detached houses (restricted range), the impact of steady wind is quite low compared to the other sources of uncertainty, but for a single-sided building (full range), it is important to check wind speed and/or pressure difference at zero flow to perform a reliable test.

### **3.7 Should tests be performed with one or several pressure stations?**

If the reference value is 50Pa, there is much less uncertainty due to wind if the test is performed at only one pressure point close to 50Pa. If the test reference is 4Pa, a 2-point test is better for low wind speeds and a one point test better for high wind speeds.

As expected, the low-pressure point is more sensitive to bias and precision errors. At a reference pressure of 50 Pa, these effects are not counterbalanced by better determining the flow exponent with the two-point analysis. Still, it may be useful to test envelopes at multiple pressure stations to identify suspicious results, e.g. due to moving valves.

## **4 CONCLUSION**

This study has shown that the impact of steady wind remains reasonable as long as the wind speed remains below 6 m/s. In detached houses, our results suggest that the impact of wind is always below the other sources of uncertainty considered in this paper; this is not true when testing single-sided zones. Testing at 50 Pa and using the same reference pressure (50 Pa) seems effective at limiting the uncertainty for wind speeds up to 9m/s (below 10%). These results apply only to tests performed according to ISO 9972:2015 protocols.

## **5 REFERENCES**

**Carrié, François Rémi and Leprince, Valérie. 2016.** Uncertainties in building pressurisation tests due to steady wind. *Energy and Buildings*, 2016, Vol. 116, 656-665.

**Sherman, M.H. and Palmiter, L. 1995.** *Uncertainty in Fan Pressurization Measurements*. Lawrence Berkeley National Laboratory : Report LBNL-32115., 1995.

# The impact of wind gusts on air infiltration in buildings

Dimitrios Kraniotis

*Oslo and Akershus University College of Applied Sciences  
Pilestredet 35, St. Olav plass 4  
0130 Oslo, Norway*

## SUMMARY

Air infiltration holds a central role in building energy consumption and is associated to several building physics phenomena. Air infiltration in buildings due to wind-induced pressure is a complex process, strongly influenced by the turbulent nature of wind. This extended summary highlights the findings of a series of studies with focus on unsteady wind and its impact on air exchanges in buildings. The focus is on wind gustiness and its relation to air infiltration under natural conditions. Wind spectrum analysis shows that high-frequency wind gusts provide important information, while only considering mean wind speed and direction are not adequate to predict air exchanges in buildings. The impact of gustiness becomes greater for evenly distributed leakages between windward (upstream) and leeward (downstream) façade. Infiltration measurements under unsteady wind can vary significantly from results estimated based on pressurization measurements. In addition, wind gustiness is responsible for large pressure differences across leakages, thus it can affect the results of leakage numbers and the uncertainty of such measurements especially when the measurement point is low.

## KEYWORDS

wind-driven air infiltration; unsteady wind; gustiness; spectrum analysis; air leakage

## 1 INTRODUCTION

Air infiltration is defined as the uncontrolled or unintentional flow of outside air to the internal space of a building through leakages in the envelope, typically cracks and/or large leakage areas (e.g. Chan *et al.*, 2013). Wind-induced pressure, stack effect and mechanical ventilation are the direct forces causing airflow in buildings. The unintentional nature of air infiltration and the complex aerodynamic phenomena that may occur around buildings or may govern the flows across small cracks (e.g. Walker *et al.*, 1998) has led to assumptions employment. In steady-state models, all the three driving forces as well as the resultant air flow through openings/cracks are taken into account by their mean values. For simplicity reasons, it is usual that the wind characteristics are expressed by a typical mean value at a reference height (Orme *et al.*, 1998), i.e. the height of the roof or the height of the meteorological instrumentation (10 m). In other words, the fluctuations of input parameter values, i.e. velocity, direction etc., are not considered. Air infiltration in buildings due to wind-induced pressure is a complex process, strongly influenced by the turbulent nature of wind (Haghighat *et al.*, 2000). Most of the models and studies exclude the dynamic nature of air infiltration, despite the fact that Hill and Kusuda (1975) have pointed it out decades ago.

This extended summary highlights the findings of a series of studies with focus on unsteady wind and its impact on actual air infiltration rates in buildings (Kraniotis, 2014a). Wind gustiness is under investigation and to this purpose both numerical (Computational Fluid Dynamics - CFD), experimental (tracer gas) and mathematical techniques (wind spectrum analysis) have been used. In particular, by employing the latter the aim to study the wind spectral density in different frequencies and moreover whether high-frequency wind gusts can relate to air infiltration rates.

## 2 RESULTS

The research conducted highlights the importance of dynamic characteristics of wind for a realistic estimation of air infiltration rates of buildings. Despite the value and the usefulness of artificial steady state techniques (pressurization methods) to evaluate the airtightness level of an envelope, the in-situ air exchanges can significantly vary under natural conditions.

A CFD study (Kraniotis *et al.*, 2014b) that simulates a periodic wind gustiness, shows that by holding mean wind speed and wind fluctuations amplitude same in different cases, wind gust frequency significantly affects the infiltration rates (Fig. 1a and 1b). The impact is greater for evenly distributed leakages between windward (upstream) and leeward (downstream) façade. The total area of leakages in the building envelope is 128 cm<sup>2</sup> and the airtightness level has been estimated as ACH<sub>50</sub> = 1.5 h<sup>-1</sup>. The results show that depending on the situation of the internal volume, wind gustiness can create high pressure differences of same magnitude as a pressurization test at 50 Pa. The latter implies that unsteady wind can strongly affect airtightness measurements when performed during a wind day, i.e.  $\bar{U} = 5$  m/s, which is characterized by high-frequent gusts, i.e.  $f = 0.5$  Hz (Fig. 1a). Fig.1b shows that even low-frequent gusts, i.e.  $f = 0.1$  Hz can result in approximately 15% of ACH that a pressurization test would result.

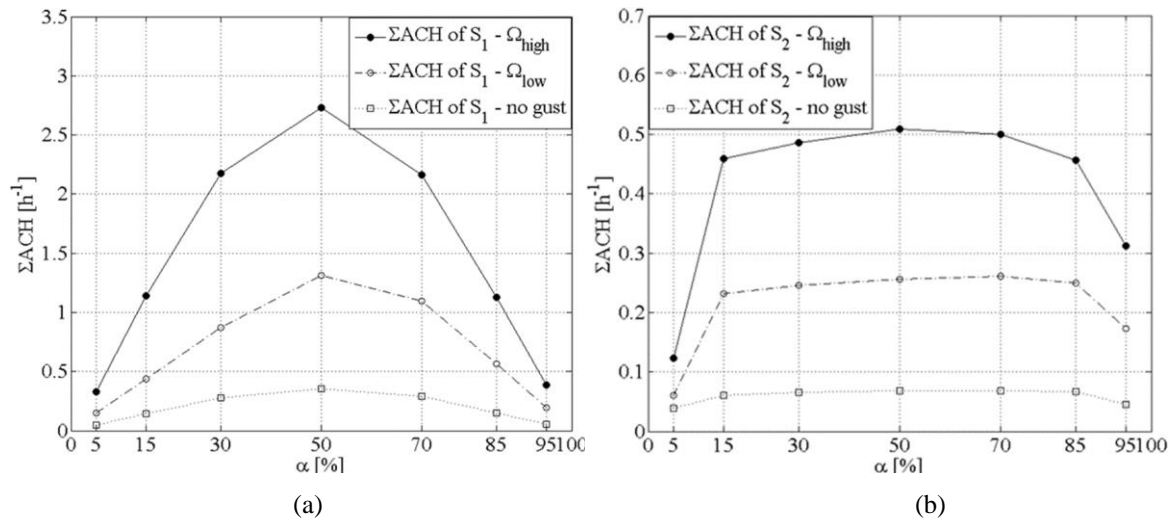


Figure 1: Air exchange variation with leakage distribution under three different wind-gustiness scenarios (Kraniotis *et al.*, 2014b). a) single-compartment building. b) double-compartment building of same volume as (a), while internal leakages of 8 cm<sup>2</sup> have been considered in the partition walls.

Carbon dioxide as a tracer gas has been used in these studies in order to quantify air infiltration rates. The results of two building-cases are shown in Fig. 2. It is clear that there is a significant variation among rates in each case. With the help of an ultrasonic anemometer, the turbulent wind and in particular wind gustiness has been analysed. In ventilation studies, Fast Fourier Transform (FFT) is often employed in order to derive a spectral analysis of the data and consequently to gain additional information about the wind energy distribution with respect to frequency (Newland, 1975):

$$S(f) = |v'(f)|^2 = \left| \int_{-\infty}^{\infty} v'(t) e^{-ift} dt \right|^2 \quad (1)$$

where, i.e. for the current project,  $S$  is the wind energy,  $f$  the frequency,  $v'$  the fluctuations of the wind orthogonal velocity  $v$ ,  $t$  the time and  $i$  the imaginary unit.

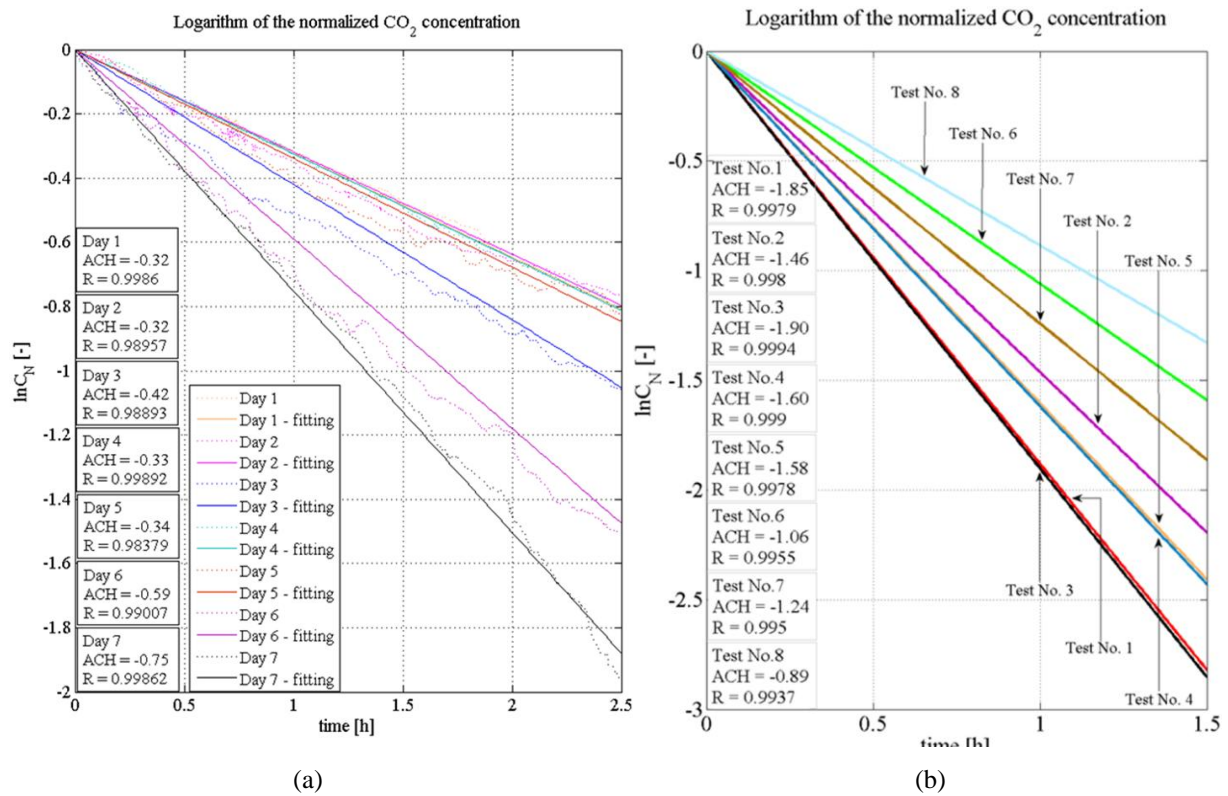


Figure 2: Decay of logarithm of the normalized carbon dioxide concentration  $C_N$  with time. a) tracer gas measurements in an office room of a building (Kraniotis *et al.*, 2014c), b) tracer gas measurements in a cubic test box (Kraniotis, 2014a).

Fig. 3 shows the filtered wind spectral density  $S_{yy}(f)$  for the case of the cubic test box. The results are linked to Fig. 2b. The findings of Fig.3 reveal that the wind spectral density in high-frequency region is important; wind events with high-frequency gusts have resulted in higher infiltration rates.

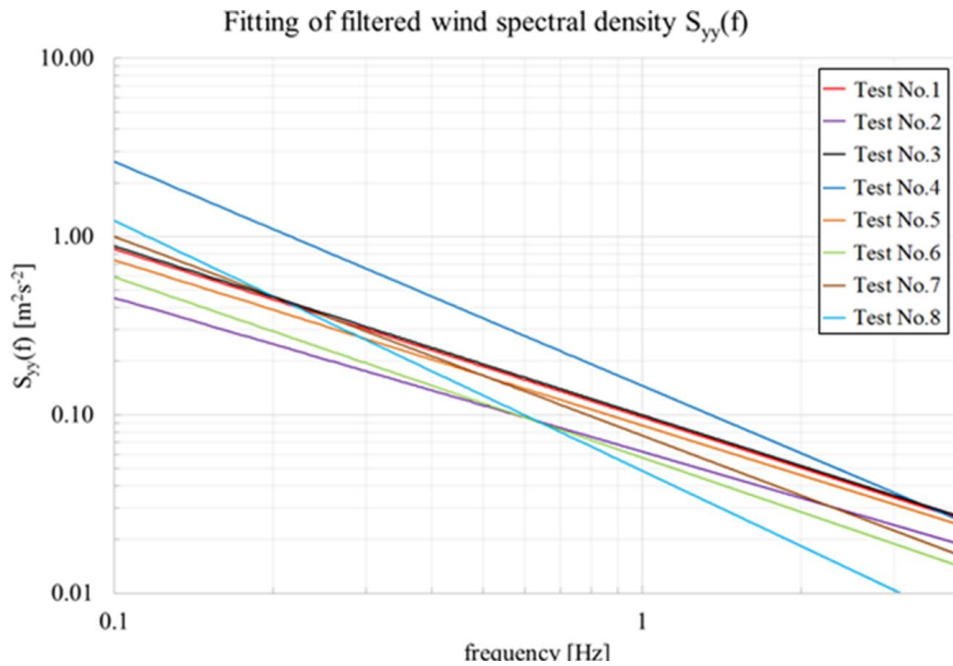


Figure 3: Filtered wind spectral density  $S_{yy}(f)$  for the case of the cubic test box (Kraniotis, 2014a).

Despite the few samples, a multiple linear regression (MLR) that takes into account both gust frequency (gustiness)  $G_c$  and gust strength  $S_g$ , along with wind direction  $\theta_w$  and mean wind speed  $\bar{U}$ , has been tested (Eq. 2).

$$ACH = a \cos \theta_w + \beta \bar{U} + \gamma G_c + \delta S_g + c \quad (2)$$

High value of  $G_c$  implies that high frequency fluctuations have occurred over a period of time. The second variable,  $S_g$ , gives the normalized cumulative strength of these events, providing a magnitude of the amplitude of the wind fluctuations that  $G_c$  refers to.

Fig. 4 shows the prediction of air exchanges is more accurate when high-frequency wind gusts are taken into consideration. When the gust analysis and the dynamic phenomena were studied on a 1s time interval basis the agreement between the regression analysis and the experimental results was very good. Analyzing the wind data on a 2s-basis, it results in good agreement as well. However, when using 1min or 10min as intervals the predicted values of ACH show moderate agreement with the MLR. In particular, for the tests No.1 and No.3 with the highest ACH and the highest wind gust frequencies (Fig. 2b) the 1min- and 10min-models shows their worst performance. It is remarkable that when the prevailing wind direction angle is oblique and not normal to the crack, these two models provides fairly good predictions, but still worse compared to the 1s- and 2s-models.

It very likely that increasing the time interval causes lack of the high frequency dynamic wind phenomena. Especially when the dominant wind is flowing normal or in small oblique angles to leakage paths, small-interval gusts should be considered. Otherwise, less dynamic data i.e. 1min or 10min intervals for the wind gusts could be enough.

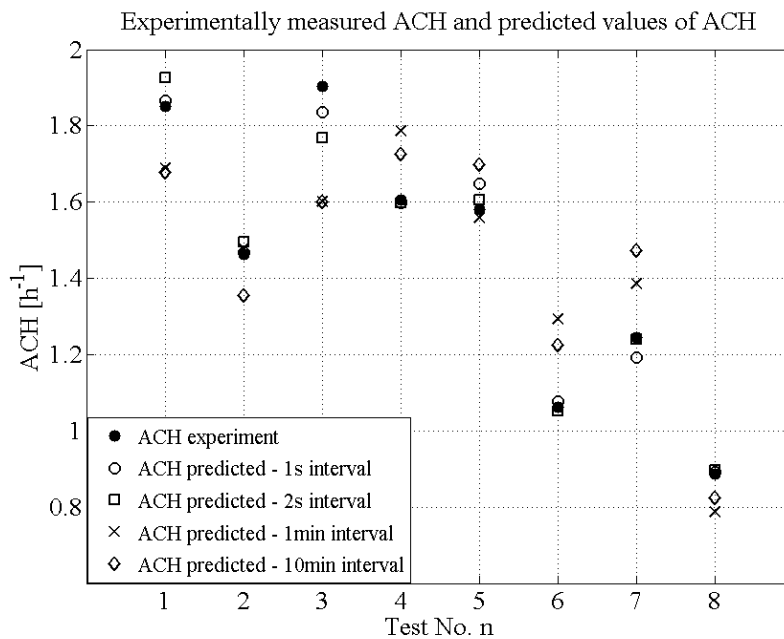


Figure 4: Experimentally measured infiltration rates and predicted values of ACH when 1s, 2s, 1min or 10min are used as time interval for depicting the wind gust phenomena (Kraniotis, 2014a).

### 3 REFERENCES

The author is grateful to Tormod Aurlien and Thomas Thiis, professors at the Norwegian University of Life Sciences, for their significant scientific contribution to the research conducted and the Department of Mathematical Sciences and Technology for financing this project.

### 4 REFERENCES

- Chan, W.R.;Joh, J.; Sherman, M.H. (2013) Analysis of air leakage measurements of US houses. *Energ Buildings*, 66, 616-625.
- Haghighat, F.; Brohus, H.; Rao, J. (2000) Modelling air infiltration due to wind fluctuations – A review. *Build. Environ*, 35, 377-385.
- Hill, J.E.; Kusuda, T. (1975) Dynamic characteristics of air infiltration. *ASHRAE Trans.*, 81, 168-185.
- Kraniotis, D. (2014) *Dynamic characteristics of wind-driven air infiltration in buildings. The impact of wind gusts under unsteady wind conditions*. Doctoral thesis, ISBN: 978-82-575-1260-6. Norwegian University of Life Sciences; Ås, Norway.
- Kraniotis, D.; Thiis, T.K.; Aurlien, T. (2014) A Numerical Study on the Impact of Wind Gust Frequency on Air Exchanges in Buildings with Variable External and Internal Leakages.*Buildings* 4, 27-42.
- Kraniotis, D.; Aurlien, T.; Thiis, T.K. (2014) Investigating instantaneous wind-driven infiltration rates using the CO2 concentration decay method. *Int. Journal of Ventilation*, 13, 111-124.

- Newland, D.E. (1975) *An introduction to random vibrations, spectral and wavelet analysis*. Longman Scientific & Technical.
- Orme, M.; Liddament, M.W.; Wilson, A. (1998) *Numerical Data for Air Infiltration and Natural Ventilation Calculations*. Air Infiltration and Ventilation Centre: Coventry, United Kingdom.
- Walker, I.S.; Wilson, D.J.; Sherman, M.H. (1998) A comparison of the power law to quadratic formulations for air infiltration techniques. *Energ Buildings*, 27, 293-299.

# Airtightness of Buildings – Considerations regarding the Zero-Flow Pressure and the Weighted Line of Organic Correlation

Christophe Delmotte

*Belgian Building Research Institute  
Avenue Poincaré, 79  
1060 Brussels, Belgium*

## ABSTRACT

This paper discusses two particular points of the buildings airtightness measurement method (ISO 9972) in relation with the calculation of the combined standard uncertainty: (1) the zero-flow pressure difference and (2) the weighted line of organic correlation.

The zero-flow pressure difference is measured at the start and the end of the test in order to calculate the change of pressure caused by the fan or blower door. Actually the zero-flow pressure difference fluctuates during the test in function of the wind and the temperature difference between inside and outside the building. One should therefore take this fluctuation into account in the uncertainty of the induced pressure difference. Theoretical developments are translated into a practical formula which could be applied in daily practice.

The air flow coefficient and air flow exponent are generally determined using an ordinary least squares regression technique (OLS). This is however not the most appropriate technique because there are uncertainties in both the measured air flow rates and the pressure differences. The paper shows how the weighted line of organic correlation (WLOC) could be used in order to take these uncertainties into account.

Applying both the uncertainty on the zero-flow pressure difference and the WLOC on a sample of measurements made under repeatability conditions has shown encouraging results regarding the reliability of combined standard uncertainties.

## KEYWORDS

Airtightness of buildings, zero-flow pressure, uncertainty, least-squares, line of organic correlation

## 1 INTRODUCTION

In European countries, increasing importance has been given to airtightness of buildings since the first publication of the directive on the energy performance of buildings in 2002. In some countries there even are requirements or financial incentives linked with the airtightness level. It is therefore more and more important to pay attention to the uncertainty of airtightness measurements.

The issue of uncertainty of airtightness measurements has already been dealt with in various publications (Persily 1985, Sherman 1994, Delmotte 2013, Walker 2013, Carrié 2014) but is still incompletely solved in practice. This was also a point of discussion during the last revision of ISO 9972.

This paper discusses two particular points of the buildings airtightness measurement method (ISO 9972) in relation with the calculation of the combined standard uncertainty: (1) the zero-flow pressure difference and (2) the weighted line of organic correlation.

The zero-flow pressure difference is measured at the start and the end of the test in order to calculate the change of pressure caused by the fan or blower door. Actually the zero-flow pressure difference fluctuates during the test in function of the wind and the temperature difference between inside and outside the building. One should therefore take this fluctuation into account in the uncertainty of the induced pressure difference. Theoretical developments are translated into a practical formula which could be applied in daily practice.

The air flow coefficient and air flow exponent are generally determined using an ordinary least squares regression technique (OLS). This is however not the most appropriate technique because there are uncertainties in both the measured air flow rates and the pressure differences. The paper shows how the weighted line of organic correlation (WLOC) could be used in order to take these uncertainties into account.

**2 ZERO-FLOW PRESSURE DIFFERENCE**

**2.1 Pressure difference induced by the fan**

In given climatic conditions (wind and temperature) and in the absence of fan, pressure differences  $\Delta p_{0,j}$  are naturally generated across the envelope of the building. The equilibrium internal pressure is such that the airflow that enters the building is equal to the flow that leaves. The sum of the airflows through the building envelope is therefore equal to zero (formally we should talk about mass flow). Accordingly, parts of the envelope must necessarily undergo underpressure while others are in overpressure.

In the absence of wind or temperature difference, the action of a fan located in the building envelope induces an identical pressure difference  $\Delta p$  across all points of the envelope. However, this is not quite true because the internal partitioning of the building may generate pressure losses. ISO 9972 requires opening all interior doors in order to minimize this effect.

When adding the effect of a fan to that of the wind and of the temperature difference, each point (j) of the envelope is subjected to a pressure difference  $\Delta p_{m,j}$  equal to the sum of those it would undergo for each of the two separate effects ( $\Delta p$  and  $\Delta p_{0,j}$ ) (Sherman 1990) (Figure 1 and Formula 1). Each point thus undergoes a similar change in pressure while keeping its relative difference compared to the other points. Note that this principle of addition is not true for air flow rates.

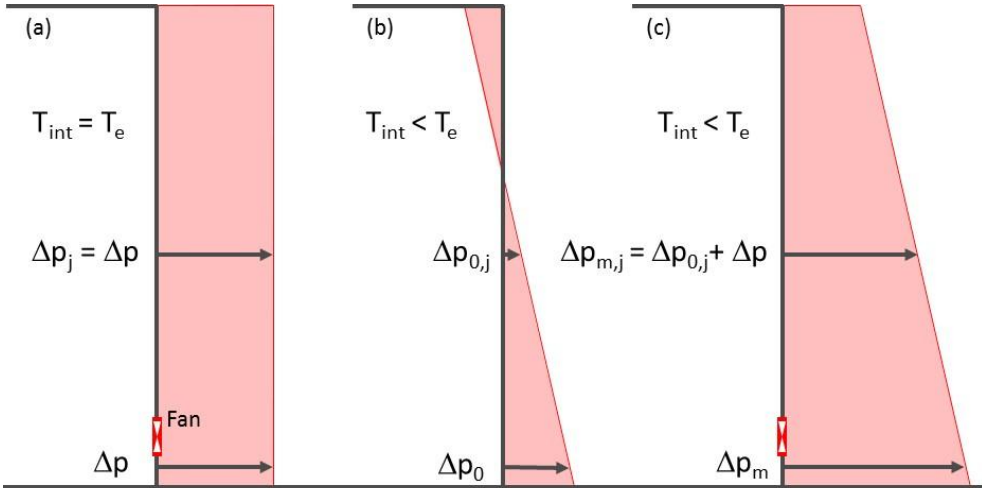


Figure 1: Example of pressure distribution over the height of a building (a) for a fan only, (b) for a temperature difference only and (c) for the combination of the fan and the temperature difference.

Additivity of pressure differences is used in ISO 9972 to indirectly measure the pressure difference induced by the fan:

1. Zero-flow pressure difference  $\Delta p_0$ : Pressure difference is measured at one point of the envelope when the building is subject to natural conditions only (fan off and covered)
2. Measured pressure difference  $\Delta p_m$ : Pressure difference is measured at the same point of the envelope when the fan is operating

3. Induced pressure difference  $\Delta p$  : Pressure difference induced by the fan is calculated by subtracting the first value from the second (Formula 2)

$$\Delta p_{m,j} = \Delta p_{0,j} + \Delta p \quad (1)$$

$$\Delta p = \Delta p_m - \Delta p_0 \quad (2)$$

## 2.2 Complete building pressurization

The calculation model adopted by ISO 9972 assumes the entire building envelope is either pressurized or depressurized. It is therefore necessary that the pressure difference induced by the fan overcomes the pressure differences generated by climatic conditions. In this way for example, a natural depression of -3 Pa could be overcome by an induced pressure of 8 Pa.

The fact that ISO 9972 requires the zero-flow pressure difference to be less than 5 Pa in absolute value and the lowest measured pressure difference ( $\Delta p_m$ ) to be at least 5 times the zero-flow pressure difference with a minimum of 10 Pa aims to respect the calculation model. Although it is not specified in ISO 9972, this implies that the zero-flow pressure difference is measured at a point where the pressure difference generated by the climatic conditions is a priori the largest. In practice, the measuring point is usually located close to the blower door (itself often installed on the ground floor of the building) and there is no guarantee that this is the best location.

## 2.3 Average pressure difference on the envelope

The calculation model adopted by ISO 9972 also assumes that the pressure difference between inside and outside the building is identical at all points of the envelope. This is only possible in the absence of wind and temperature difference and is therefore virtually impossible to satisfy in practice.

To overcome this problem, ISO 9972 requires the pressure difference induced by the fan to be much greater than the absolute value of the pressure differences generated by climatic conditions. In this way, variations in the pressure difference remain relatively low and it is assumed that the hypothesis of the model are fulfilled. Under these conditions ISO 9972 assumes the average value of the pressure difference which is applied to the envelope to be equal to the pressure induced by the fan. This is an approximation because the average value of the zero-flow pressure difference is not necessarily equal to zero (even if the total airflow is equal to zero).

When the fan puts the whole building envelope in positive or negative pressure, the airflow through the fan is equal to the air flow rate through the envelope. Following the model of ISO 9972, this flow is associated with the pressure induced by the fan and eventually allows to characterize the air permeability of the envelope.

## 2.4 Measurement uncertainty

When measuring the airtightness of a building, it is not possible to measure the zero-flow pressure during the test and the climatic conditions most generally don't remain constant (especially due to wind that can quickly change intensity and direction). So ISO 9972 requires the zero-flow pressure difference  $\Delta p_0$  to be measured for at least 30 seconds both at the start ( $\Delta p_{01}$ ) and the end ( $\Delta p_{02}$ ) of the test. However, nothing prevents climatic conditions being different during the test. In addition to the uncertainty of the measures themselves, some variability in climatic conditions should also be taken into consideration.

A typical example of evolution of the zero-flow pressure difference at the start (30 seconds), during (10 minutes) and at the end (30 seconds) of a fictitious test is shown in Figure 2. In

order to find the most probable value of this pressure during the test, ISO 9972 takes the mean of  $\Delta p_{01}$  and  $\Delta p_{02}$  (Formula 3).

The zero-flow pressure difference is no constant value. So one cannot calculate the Type A standard uncertainty (JCGM 2008) which would require to carry out several measurements of the same value. One should therefore calculate the Type B standard uncertainty (scientific judgement based on all of the available information on the possible variability). In order to take some variability in climatic conditions into account, one could consider a triangular distribution based on the average value of  $\Delta p_{0,1}$  and  $\Delta p_{0,2}$  and on the minimum and maximum values measured at the start and the end of the test. This should be added to the combined standard uncertainty of the induced pressure difference (Formula 4).

$$\Delta p = \Delta p_m - \frac{\Delta p_{0,1} + \Delta p_{0,2}}{2} \tag{3}$$

$$u_c(\Delta p) = \sqrt{u^2(\Delta p_m) + \frac{u^2(\Delta p_{0,1})}{4} + \frac{u^2(\Delta p_{0,2})}{4} + \left( \frac{\max(|\Delta p_{0,max} - \Delta p_{0,av}|; |\Delta p_{0,min} - \Delta p_{0,av}|)}{\sqrt{6}} \right)^2} \tag{4}$$

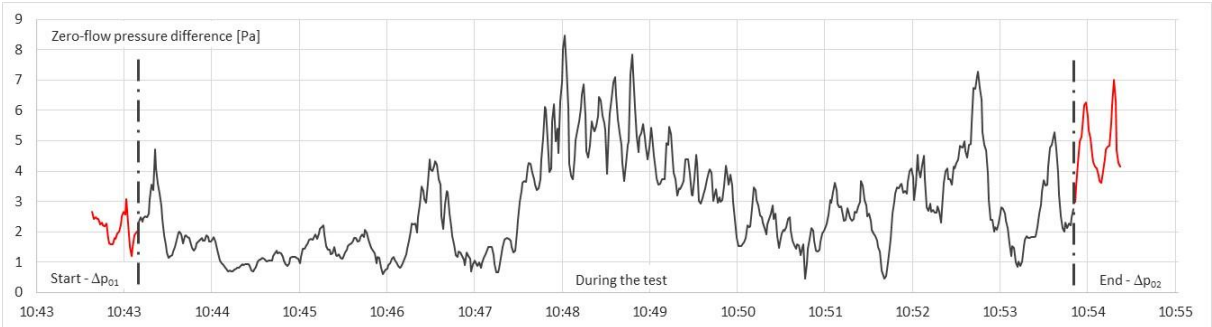


Figure 2: Example of evolution of the zero-flow pressure difference at the start (30seconds – max: 3,1 Pa – mean: 2,1 Pa – min: 1,2 Pa) , during (10 minutes – max: 8,5 Pa – mean: 2,7 Pa – min: 0,5 Pa) and at the end (30seconds – max: 7,0 Pa – mean: 4,8 Pa – min: 3,0 Pa) of a fictitious test.

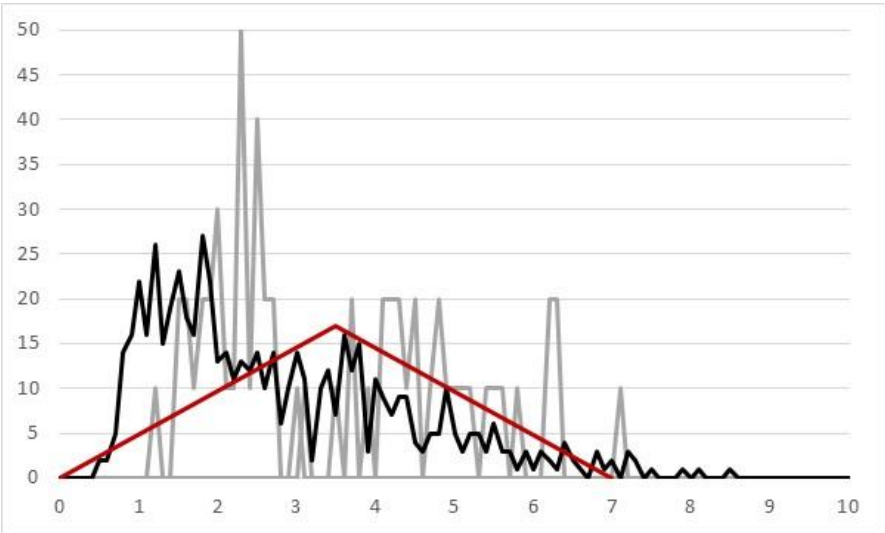


Figure 3: Example of triangular distribution for the estimation of the zero-flow pressure difference (red line) and its actual frequency distribution during a fictitious test (black curve). The grey curves are those of the zero-flow pressure difference at the start and at the end of the test.

In order to reduce the uncertainty related to the modelling, it could be worth measuring the pressure difference at several points of the envelope. This would give more chances to catch the greatest zero-flow pressure difference and determine the lowest measurement stage

accordingly. In this sense, looking for the location of the measurement point that provides the lowest zero-flow pressure difference in order to comply with the criteria of ISO 9972 is not recommended.

## 2.5 Impact of measurement uncertainty

In the framework of the buildings airtightness measurement, ISO 9972 assumes the relation between the airflow rate and the pressure difference has an exponential form (Formula 5).

$$q_{env} = C_{env} \cdot \Delta p^n \quad (5)$$

This exponential relation can be transformed into a linear relation as follows:

$$\ln q_{env} = \ln C_{env} + n \cdot \ln \Delta p \quad (6)$$

Introducing some estimation error E on the induced pressure difference in formula (6) leads to the following:

$$\ln q_{env} = \ln C_{env} + n \cdot \ln(\Delta p \pm E) \quad (7)$$

$$\ln q_{env} = \ln C_{env} + n \cdot \ln\left(\Delta p \left(1 \pm \frac{E}{\Delta p}\right)\right) \quad (8)$$

$$\ln q_{env} = \ln C_{env} + n \cdot \ln \Delta p + n \cdot \ln\left(1 \pm \frac{E}{\Delta p}\right) \quad (9)$$

The last formula shows that imperfect knowledge of the induced pressure difference can lead to shifting and rotating the linear relation (and thus modifying the  $C_{env}$  and  $n$  values). This is due to the fact that  $\ln(1 \pm E/\Delta p)$  strongly depends on  $E/\Delta p$  and that  $\Delta p$  typically varies from 10 Pa to 100 Pa. Lower pressure points are thus further shifted than higher pressure points (Figure 4).

In order to take this effect into account in the calculation of the combined standard uncertainty, it is important to select an appropriate least square regression method (see clause 3) (Delmotte 2103) (ISO/TS 28037).

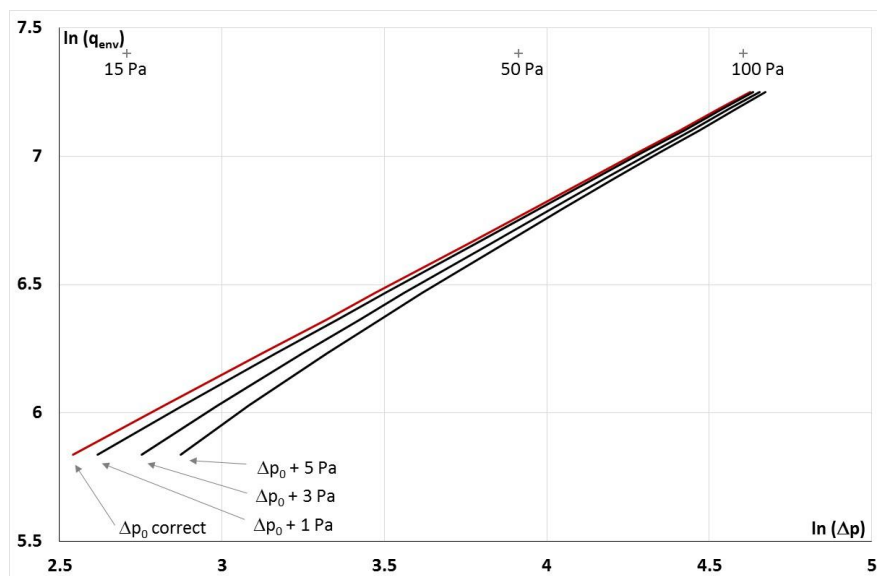


Figure 4: Imperfect knowledge of induced pressure difference leads to shifting and rotating the regression line

### 3 WEIGHTED LINE OF ORGANIC CORRELATION

#### 3.1 Applicability of least squares

ISO 9972 requires the use of a least squares technique for the calculation of the airflow coefficient  $C_{env}$  and the airflow exponent  $n$  based on a series of measurement points  $(\Delta p_i, q_{env,i})$  ( $i = 1 \dots N$ ). However it does not give further guidance.

The Ordinary method of Least Squares (OLS) is applicable when all  $y_i$  values ( $y_i = \ln q_{env,i}$ ) are equally uncertain ( $u_c(y_1) = u_c(y_2) = \dots = u_c(y_n)$ ) and the uncertainties on  $x_i$  values ( $x_i = \ln \Delta p_i$ ) are negligible (Delmotte 2013). When uncertainties of  $y_i$  values are not equal (and uncertainties of  $x_i$  values are negligible), it is advisable to use the Weighted method of Least Squares (WLS).

None of these two methods are theoretically applicable to the buildings airtightness measurement because both sets of  $x_i$  and  $y_i$  values have non negligible and unequal uncertainties. It is therefore proposed to examine the possibility of using the Weighted Line of Organic Correlation (WLOC) which takes both sets of uncertainties into account.

#### 3.2 Description of the method

The WLOC consists of finding the regression line  $y = a + b \cdot x$  that minimalizes the sum of the products of the weighted vertical and horizontal differences between the measurement points and the line (Figure 5); which comes to minimalizing the following sum:

$$\sum_{i=1}^N (v_i |x_i - x(y_i)| \cdot w_i |y_i - y(x_i)|) \quad (10)$$

$$\sum_{i=1}^N \left( v_i \left| x_i - \frac{y_i - a}{b} \right| \cdot w_i |y_i - (bx_i + a)| \right) \quad (11)$$

Weights  $v_i$  and  $w_i$  applied to each measurement point  $i$  are equal to the following, which means that points with higher uncertainty receive less importance than others:

$$v_i = \frac{1}{s(x_i)} = \frac{1}{u_c(x_i)} \quad (12)$$

$$w_i = \frac{1}{s(y_i)} = \frac{1}{u_c(y_i)} \quad (13)$$

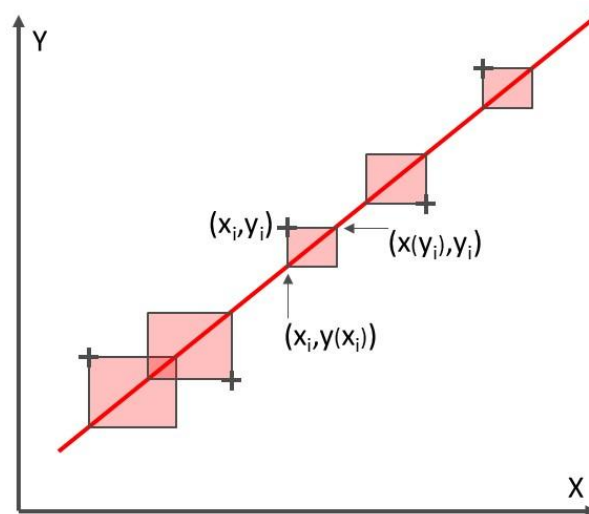


Figure 5: The (weighted)line of organic correlation minimalizes the sum of the products of the (weighted) vertical and horizontal differences between the measurement points and the line.

Constants a and b of this regression line are calculated as follows:

NOTE For the sake of simplification  $\sum x_i$  is used for  $\sum_{i=1}^N x_i$

$$a = \frac{\sum v_i w_i y_i - b \sum v_i w_i x_i}{\sum v_i w_i} = \bar{y} - \frac{S_y}{S_x} \bar{x} = \bar{y} - b \bar{x} \quad (14)$$

$$b = \frac{\sqrt{\sum v_i w_i \sum v_i w_i y_i^2 - (\sum v_i w_i y_i)^2}}{\sqrt{\sum v_i w_i \sum v_i w_i x_i^2 - (\sum v_i w_i x_i)^2}} = \sqrt{\frac{\Delta y}{\Delta x}} = \frac{S_y}{S_x} \quad (15)$$

a and b are eventually used for the calculation of n and  $C_{env}$  :

$$n = b \quad (16)$$

$$C_{env} = e^a \quad (17)$$

Other important characteristics of the weighted line of organic correlation are the following:

Weighted mean 
$$\bar{x} = \frac{\sum v_i w_i x_i}{\sum v_i w_i} \quad (18)$$

$$\bar{y} = \frac{\sum v_i w_i y_i}{\sum v_i w_i} \quad (19)$$

Variance 
$$S_x^2 = \frac{\sum v_i w_i (x_i - \bar{x})^2}{\sum v_i w_i} \quad (20)$$

$$S_y^2 = \frac{\sum v_i w_i (y_i - \bar{y})^2}{\sum v_i w_i} \quad (21)$$

Covariance 
$$S_{xy} = \frac{\sum v_i w_i (x_i - \bar{x})(y_i - \bar{y})}{\sum v_i w_i} \quad (22)$$

Coefficient of determination 
$$r^2 = \frac{S_{xy}^2}{S_x^2 S_y^2} \quad (23)$$

Advantages of WLOC is that it minimizes errors in both X and Y directions and that it provides a unique line identical regardless of which variable, X or Y, is used as the response variable (Helsel and Hirsch 2002) (Figure 4). Considering that the regression lines pass through the centroid of the data  $(\bar{x}, \bar{y})$ , this property becomes more important as one is interested in the estimate of the air leakage rate at low pressure difference (e.g. 4 or 10 Pa). Another advantage of WLOC is that it can be solved without iteration which is not the case of some other methods (e.g. ISO/TS 28037).

Experimental variances of a and b and their estimated correlation coefficient can be calculated as follows. These values are needed to calculate the combined standard uncertainty of the air leakage rate at reference pressure difference from the standard uncertainties of the input data (Delmotte 2013).

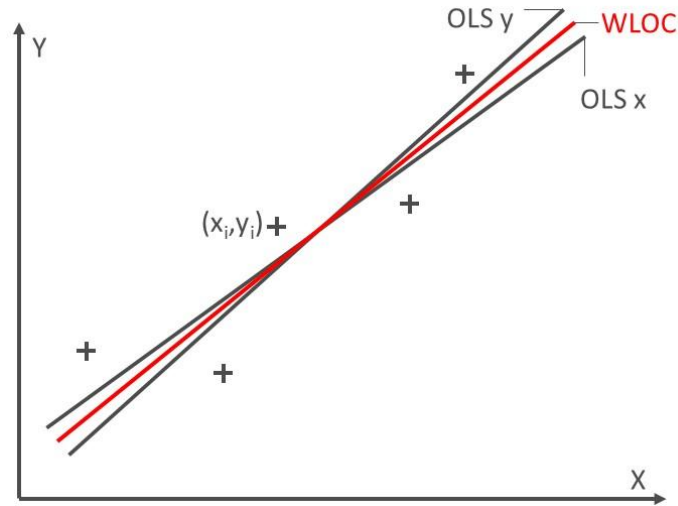


Figure 6: The weighted line of organic correlation provides a unique line identical regardless of which variable, X or Y, is used as the response variable.

### Experimental variance

$$s^2(a) = \sum \left( \frac{\partial a}{\partial x_i} \right)^2 \frac{1}{v_i^2} + \left( \frac{\partial a}{\partial y_i} \right)^2 \frac{1}{w_i^2} \quad (24)$$

$$s^2(b) = \sum \left( \frac{\partial b}{\partial x_i} \right)^2 \frac{1}{v_i^2} + \left( \frac{\partial b}{\partial y_i} \right)^2 \frac{1}{w_i^2} \quad (25)$$

### Estimated correlation coefficient

$$r(a, b) = \frac{s^2(a+b) - s^2(a) - s^2(b)}{2 s(a)s(b)} \quad (26)$$

with

$$\frac{\partial a}{\partial x_i} = \frac{\sqrt{\Delta y}}{\sqrt{\Delta x}} \left( \frac{-v_i w_i}{\sum v_j w_j} - \frac{(\sum v_j w_j x_j)^2 v_i w_i}{\Delta x \sum v_j w_j} + \frac{(\sum v_j w_j x_j) v_i w_i x_i}{\Delta x} \right) \quad (27)$$

$$\frac{\partial a}{\partial y_i} = \frac{v_i w_i}{\sum v_j w_j} - \frac{(\sum v_j w_j x_j) v_i w_i y_i}{\sqrt{\Delta x} \sqrt{\Delta y}} + \frac{(\sum v_j w_j x_j) (\sum v_j w_j y_j) v_i w_i}{\sum v_j w_j \sqrt{\Delta x} \sqrt{\Delta y}} \quad (28)$$

$$\frac{\partial b}{\partial x_i} = \frac{\sqrt{\Delta y}}{\sqrt{\Delta x}} \frac{((\sum v_j w_j x_j) v_i w_i - (\sum v_j w_j) v_i w_i x_i)}{\Delta x} \quad (29)$$

$$\frac{\partial b}{\partial y_i} = \frac{\sqrt{\Delta y}}{\sqrt{\Delta x}} \frac{((\sum v_j w_j) v_i w_i y_i - (\sum v_j w_j y_j) v_i w_i)}{\Delta y} \quad (30)$$

$$s^2(a + b) = \sum \left( \frac{\partial a}{\partial x_i} + \frac{\partial b}{\partial x_i} \right)^2 \frac{1}{v_i^2} + \left( \frac{\partial a}{\partial y_i} + \frac{\partial b}{\partial y_i} \right)^2 \frac{1}{w_i^2} \quad (31)$$

NOTE Since it is needed to make additions including sums of values, we use i and j (= 1 ... N) in order to make a distinction between both addition levels.

## 4 EXPERIMENTAL RESULTS

Applying both the uncertainty on the zero-flow pressure difference and the WLOC on a sample of 6 measurements made under repeatability conditions has shown encouraging results regarding the reliability of combined standard uncertainties. Compared to OLS, it has considerably reduced the repeatability standard deviation for low pressure stations (Figure 7). Moreover, combined standard uncertainties of the air leakage rate at reference pressure difference based on WLOC better fit to the variation of real data than OLS which strongly underestimates them (Figures 8 and 9).

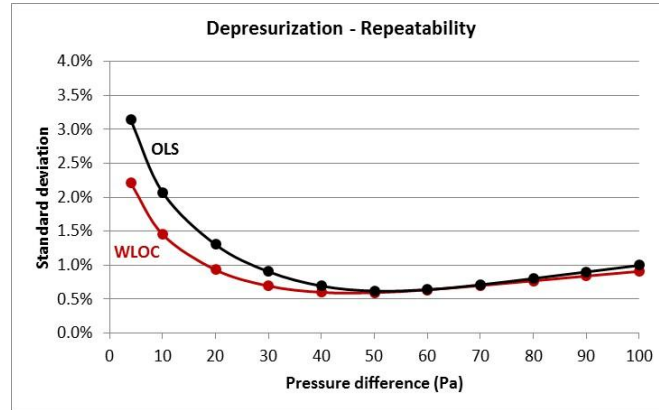


Figure 7: WLOC shows better repeatability than OLS (sample of 6 measurements under repeatability conditions)

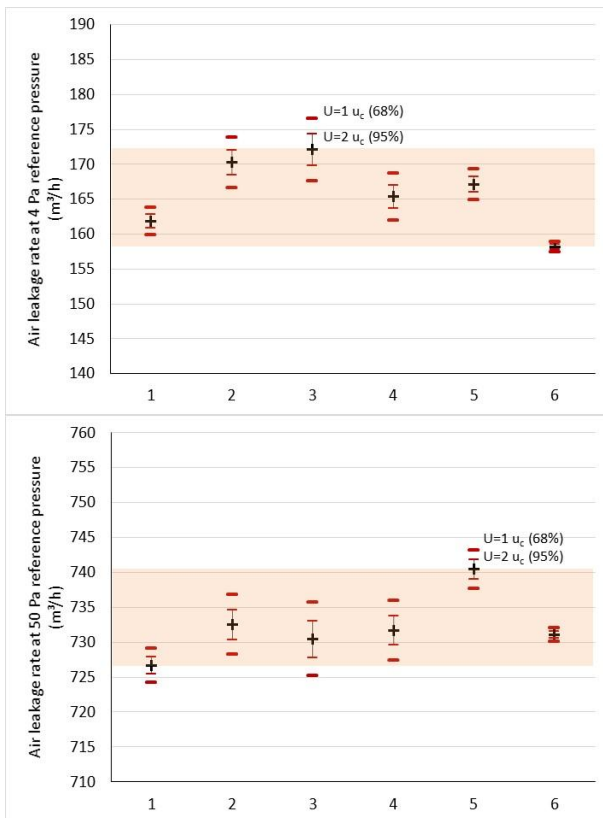


Figure 8: Combined standard uncertainties calculated with OLS strongly underestimate the variation of real data (sample of 6 measurements under repeatability conditions). Many results (+) are out of the 95% expanded uncertainty (U) of the other results.

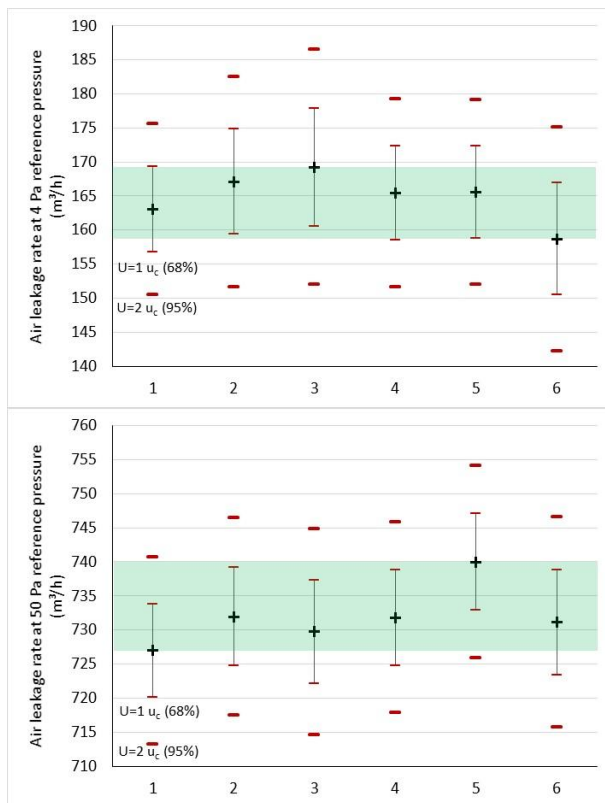


Figure 9: Combined standard uncertainties calculated with WLOC fit very well the variation of real data (sample of 6 measurements under repeatability conditions). All results (+) are within the 95% expanded uncertainty (U) of the other results.

## 5 NOMENCLATURE

- $C_{env}$  = Air flow coefficient
- $E$  = Estimation error on the induced pressure difference
- $i, j$  = element of a series
- $n$  = Air flow exponent (also referred to as “pressure exponent”)
- $N$  = Total number of measurement points
- $q_{env}$  = Air flow rate through the building envelope
- $s(x)$  = Experimental standard deviation of estimate  $x$
- $T_{int}$  = Internal air temperature
- $T_e$  = External air temperature
- $u_c(x)$  = Combined standard uncertainty of estimate  $x$
- $v_i$  = Weight attributed to estimate  $x_i$
- $w_i$  = Weight attributed to estimate  $y_i$
- $\Delta p$  = Induced pressure difference
- $\Delta p_0$  = Zero-flow pressure difference
- $\Delta p_{0,av}$  = Average value of  $\Delta p_{0,1}$  et  $\Delta p_{0,2}$
- $\Delta p_{0,max}$  = Maximum value of all  $\Delta p_0$  values measured at the start and at the end of the test
- $\Delta p_{0,min}$  = Minimum value of all  $\Delta p_0$  values measured at the start and at the end of the test
- $\Delta p_m$  = Measured pressure difference

## 6 REFERENCES

- Carrié, F.R., Leprince, V. (2014). *Model error due to steady wind in building pressurization tests*. 35<sup>th</sup> AIVC Conference, Poznań, Poland, 24-25 September 2014.
- Delmotte, C. (2013). *Airtightness of buildings - Calculation of combined standard uncertainty*. Athens, Greece, Proceedings of the 34<sup>th</sup> AIVC Conference, 26-26 September 2013.
- Helsel, D.R. and Hirsch, R. M. (2002). *Statistical Methods in Water Resources. Techniques of Water Resources Investigations*, Book 4, chapter A3. U.S. Geological Survey.
- ISO(2010). ISO/TS 28037. *Determination and use of straight-line calibration functions*. Geneva, Switzerland: International Standard Organization
- ISO(2015). ISO 9972, *Thermal performance of buildings — Determination of air permeability of buildings — Fan pressurization method*. Geneva, Switzerland: International Standard Organization
- JCGM(2008). JCGM 100, *Evaluation of measurement data — Guide to the expression of uncertainty in measurement*. Joint Committee for Guides in Metrology
- Persily A K., Grot R A.(1985). *Accuracy in pressurization data analysis*. ASHRAE Transactions, 1985, vol. 91, pt. 2B, Honolulu, HI
- Sherman, M.H. (1990). *Superposition in Infiltration Modeling*. Lawrence Berkeley Laboratory, University of California, LBL-29116
- Sherman, M.H., Palmiter, L. (1994). *Uncertainty in Fan Pressurization Measurements*. In *Airflow Performance of Envelopes, Components and Systems*, Philadelphia: American Society for Testing and Materials, LBL-32115.
- Walker I.S., Sherman M.H., Joh J., Chan W. R.(2013). *Applying Large Datasets to Developing a Better Understanding of Air Leakage Measurement in Homes*. International Journal of Ventilation, Volume 11 No 4 March 2013.

# Energy Performance Indicators for Ventilative Cooling

Flourentzos Flourentzou<sup>1\*</sup>, Jerome Bonvin<sup>1</sup>

<sup>1</sup>Estia SA  
EPFL Innovation Park  
1015 Lausanne, Switzerland  
www.estia.ch  
\*flourentzou@estia.ch

## ABSTRACT

The lack of indicators assessing ventilative cooling effectiveness in a way to compare it with active cooling technics, makes its acceptance more difficult. Practitioners, norms, standards and guidelines are used to design and evaluate cooling systems in terms of Cooling Power (CP) or Seasonal Energy Efficiency Ratio (SEER). What could be the CP of a passive technique based on a day to night offset of the cooling process? What could be the SEER of mechanical night ventilation for summer cooling?

IEA Annex 62 research collaboration for ventilative cooling developed energy performance indicators to characterise natural and mechanical ventilative cooling. The Cooling Requirement Reduction (CRR) expresses the cooling effectiveness of a ventilation strategy. It indicates to which extend an alternative strategy, like natural or mechanical night ventilation, meets the cooling needs, compared to those of a standard scenario without ventilative cooling. The ventilative cooling SEER (SEER<sub>vc</sub>) relates the additional electrical energy to run ventilation, with the Cooling Requirement Reduction. It can be compared to the SEER of conventional cooling systems.

In this paper we define in details these indicators and use them to assess different ventilative cooling systems, applied to a standard ventilative cooling test building, defined in IEA Annex 62 research works. We use them also to compare the effectiveness of ventilative cooling in specific climatic zones, with different thermal masses and different solar protection boundary conditions.

The results show that mechanical ventilative cooling with Specific Power Input > 0.4 W/(m<sup>3</sup>/h), running more than 800 hours per year for night cooling, might be even less efficient than conventional air conditioning systems of SEER > 3. They also show that the only real "free cooling" is natural ventilative cooling. A parametric analysis illustrates how with the use of these indicators we may quantify the risk of high-energy consumption due to bad design choices, such as very low thermal mass, bad ventilation control, bad solar control or a combination of them.

## KEYWORDS

ventilative cooling, performance indicators, passive cooling, IEA annex 62

## 1 INTRODUCTION

Modern high energy-performance buildings, with high-level envelope insulation and high airtightness have not a single dissipative element. Natural ventilative cooling is the only means of evacuating heat, without increasing energy consumption. Under these new conditions in building industry we observe increased overheating problems, even in Nordic climates. A recent survey of the court of auditors in Vaud Canton in Switzerland showed that in 9 out of 10 recent sustainable and high energy-performance state-buildings present overheating problems. It also showed that buildings with mechanical ventilative cooling present very high electrical consumption. (Court of Auditors - Vaud 2015). Summer overheating becomes a common problem all over Europe, from Mediterranean Sea to Baltic Sea. IEA Annex 62 revisits ventilative cooling technics in this new conditions and tries to assess simulation methods, define key performance indicators and recommend principles for standards and guidelines to integrate ventilative cooling (Kolokotroni, Heiselberg 2015).

This article is focused on energy performance indicators.

## **2 VENTILATIVE COOLING PERFORMANCE INDICATORS**

Annex 62 distinguishes 4 categories of indicators: system performance indicators, component performance indicators, boundary conditions and sensibility indicators.

### **2.1 System indicators for comfort and energy performance**

System indicators refer to the performance of the whole ventilative cooling system, generally of a room but it can also be of the entire building. There are system indicators concerning comfort and others concerning energy performance. This article uses 2 system indicators:

- The number of hours the internal temperature exceeds EN 15251 adaptive comfort zone 2. This indicator is used also in the Swiss standard SIA 180 (EN standards, Swiss standards).
- Cooling Requirements Reduction (CRR), which is defined in chapter 3.

### **2.2 Component indicators**

Component indicators refer to the performance of particular part of the ventilative cooling system. The ventilation effectiveness of a window or a set of windows is a component indicator. It can be expressed as the window airflow at 2°C and at 5°C temperature difference without wind presence.

Concerning energy performance indicators we define and test in this article 2 component indicators of a mechanical ventilation system:

- Ventilative Cooling Seasonal Energy Efficiency Ratio (SEER<sub>vc</sub>).
- Ventilative Cooling Advantage of a passive component compared to conventional cooling machine.

These component indicators are also defined in chapter 3.

### **2.3 Boundary conditions**

Almost all the ventilative cooling indicators need a dynamic simulation and this makes the control of simulation assumptions more difficult. The time-dependent variables, like heat gains, opening and closing the windows, which is sometimes conditional, solar gains, external climatic conditions need explicit and rigorous control of assumptions. This is the reason why we specify explicitly this category of indicators. Chapter 4 is especially dedicated to the boundary indicators with the main assumptions of the test case simulations.

### **2.4 Sensibility indicators**

This family of indicators test the result uncertainty due to input uncertain data but also due to risks of bad use of some components of the system. In this case, we use the sensibility indicator evaluating the risk of blind partial use.

## **3 DEFINITION OF 3 ENERGY PERFORMANCE INDICATORS**

Ventilative cooling provides comfort in place of an air conditioning system. Standard EN 15251 defines adaptive comfort (EN and ISO standards). ISO 7730 defines comfort according to Fanger's theory. Swiss norm SIA 180 accepted the two standards equivalent. However, the occupants can achieve adaptive comfort only in spaces where they may open the windows. For this reason, in closed spaces, or in spaces where the windows are not supposed to open during the hours of use, only ISO 7730 remains valid.

European standard EN 15255 defines a model to evaluate cooling requirements of a space. However, this standard does not define normalised boundary conditions. In the Swiss case, SIA 382/1 defined a set of normalised boundary conditions for the calculation of cooling requirements and SIA 180 defined boundary conditions for the calculation of internal temperature. For general-purpose spaces they consider acceptable adaptive comfort zone 2 and for closed spaces 10% PPD according to ISO 7730. Standard boundary conditions define

occupation schedules (internal gains, occupation density, airflow rates for indoor environment quality), standard meteorological files and set point temperature at 26°C (Swiss standards).

### 3.1 Cooling Requirements Reduction - CRR

This energy performance indicator expresses the ratio of cooling requirements saved of a scenario with respect to the one of the reference scenario (Equation 1).

$$CRR = \frac{Q_{t,c}^{ref} - Q_{t,c}^{scen}}{Q_{t,c}^{ref}} \quad \text{Equation 1}$$

Where  $Q_{t,c}^{ref}$  is the cooling requirements of the reference scenario and  $Q_{t,c}^{scen}$  is the cooling requirements of the ventilative cooling scenario.

CRR can range between a negative value and +1. If CRR is positive, it means that the ventilative cooling system reduces the cooling requirements of the building. If CRR is equal to 1, the ventilative cooling scenario has no cooling requirements. If CRR is zero, the ventilative cooling scenario does not reduce the cooling requirements of the building and if it is negative, ventilative cooling increases them (increased ventilation induces more heat than the one it extracts from the building).

CRR calculates cooling effectiveness of any ventilative cooling scenario, mechanical or natural.

### 3.2 Seasonal Energy Efficiency Ratio of the ventilative cooling system - SEER<sub>VC</sub>

When the driving force of ventilative cooling is mechanical system, cooling requirement reduction is not for free. It has an energy consumption. The ratio of the saved cooling requirements and the extra electricity consumed by the ventilation system for ventilative cooling, during the whole cooling season, gives SEER<sub>VC</sub>. It expresses the energy efficiency of the mechanical system (Equation 2).

$$SEER_{VC} = \frac{Q_{t,c}^{ref} - Q_{t,c}^{scen}}{E_{el,v}} \quad \text{Equation 2}$$

Where  $E_{el,v}$  is the extra electrical consumption of the ventilation system for ventilative cooling.

When the mechanical system is a ventilator or an air-handling unit providing ventilation for other purposes (hygienic ventilation), SEER<sub>VC</sub> accounts only the extra energy needed for ventilative cooling. This indicator is similar to the SEER of any conventional air conditioning unit and makes it possible to compare the ventilative cooling energy performance to the energy performance of conventional air conditioning systems.

### 3.3 Ventilative cooling advantage ADV<sub>VC</sub>

In buildings with the possibility to have conventional air conditioning, someone may need to decide if it is preferable to spend energy for ventilative cooling or for air conditioning. It is not always preferable to use mechanical ventilative cooling in the place of air conditioning when ventilative cooling cannot achieve the interior desired temperature conditions. The Specific Power Input (SPI) of the ventilation system, the extra number of hours it needs to run for ventilative cooling during the cooling season, the temperature difference between inside and outside, are factors that affect SEER<sub>VC</sub>. Ventilative cooling advantage (ADV<sub>VC</sub>) indicator defines the benefit of the ventilative cooling, i.e. the cooling energy difference divided by the energy for ventilation.

$$ADV_{VC} = \frac{E_{el,c}^{ref} - E_{el,c}^{scen}}{E_{el,v}} \quad \text{Equation 3}$$

Where  $E_{el,c}^{ref}$  is the electrical consumption of the cooling system in the reference case,  $E_{el,c}^{scen}$  is the electrical consumption of the cooling system in the ventilative cooling scenario and  $E_{el,v}$  is the extra electrical consumption of the ventilation system for ventilative cooling.

If  $ADV_{VC}$  is lower than one, electrical consumption of the ventilation system is lower than the one of the cooling system. If  $ADV_{VC}$  is equal to 1, the electrical consumption of ventilation system is equal to this of the cooling system.

CRR,  $SEER_{VC}$  and  $ADV_{VC}$  indicators refer to a baseline scenario, which needs to be standardized according to national conditions. For the purpose of this study, standard scenario uses the Swiss standard conditions of occupation according to SIA 2024, airflow rates for hygienic ventilation and internal heat gains according to the same standard, and windows closed with no extra ventilation for ventilative cooling.

#### 4 BOUNDARY CONDITIONS AND CALCULATION METHODS

We used as case study one of the meeting rooms of a primary school, located in Saviese (Switzerland). The meeting room is 5.12m wide, 7 m long and 2.8 m high. The Saviese primary school was built in 2014 and was designed to get a Minergie® label (Flourentzou, Ritz et Al 2015). Therefore, the building envelope is highly air tight and insulated.

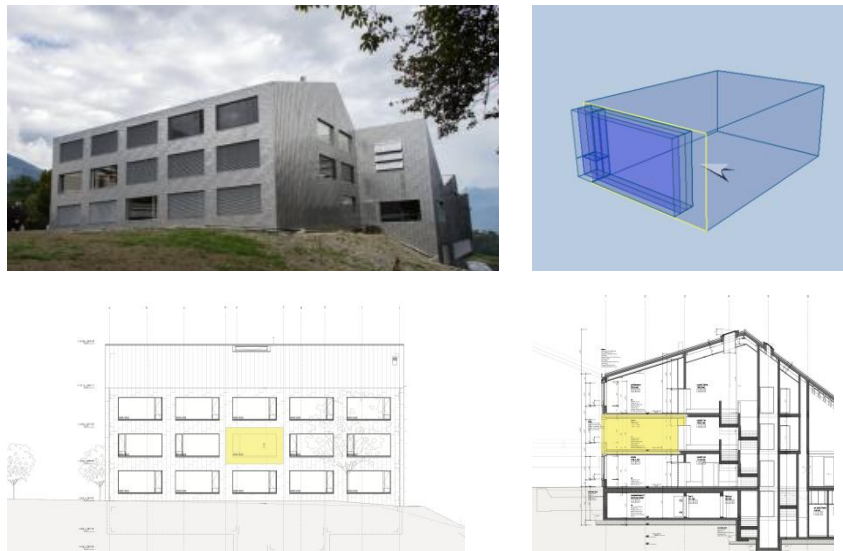


Figure 1: Saviese primary school. The modelled office-meeting room is the one highlighted.

The meeting room has only one window that is 4.00 m wide and 2.02 m high. The glazed area consists of a side-hung window of 1 m<sup>2</sup> (0.64 m wide per 1.56 m high) and fixed window of 7.9 m<sup>2</sup>. An exterior blind with adjustable slats shades both the side hung window and the fixed window. Blind g value is 0.1 and glazing g value 0.45 and the orientation is west.

The discharge coefficient of the blind has been measured in the meeting room in a single-sided ventilation experiment. The results are:

- Blind open:  $C_d = 0.62$
- Blind with slats at 45° or blind closed:  $C_d = 0.45-0.47$

Simulation boundary condition for the opening partially open 20 cm with the blinds closed assumes the discharge coefficient  $C_d = 0.25$ .

Simulation boundary condition for blind control with standard scenario assumes g glazing = 0.45 and g blind 0.1 when incident  $I > 200 \text{ MJ/m}^2$  and  $T_{ext} > 22^\circ\text{C}$  with blinds 100% rolled down.

Two additional sensibility indicators calculate performance indicators, one, R1, with blinds 50% closed and the other R2, with no blind use.

Occupation schedules follow the Swiss standard conditions SIA 2024 (Swiss Standards). If we summarize these conditions we have a variable occupation from 7:00 to 18:00 with maximum internal gains from occupants  $5 \text{ W/m}^2$ ,  $15 \text{ W/m}^2$  for lighting with natural light autonomy of 32%, and other internal gains of  $7 \text{ W/m}^2$ . Internal gains totalize  $150 \text{ Wh/m}^2$  per day.

The real thermal characteristics of the envelope (20 cm insulation -  $U_{wall} = 0.16 \text{ W/m}^2$ , triple glazing  $U_{win} = 0.9 \text{ W/m}^2$ ) respect the recommendations of a high performance energy passive standard (Minergie®). We transpose the level of envelope performance for southern climates to 10 cm -  $U_{wall} = 0.35 \text{ W/m}^2$  for insulation and double glazing  $U_{win} = 2.5\text{-}3.1 \text{ W/m}^2$  for windows

#### 4.1 Ventilative cooling strategies as simulation boundary conditions

Ventilative cooling strategies are rarely specified precisely. In Annex 62 simulation programs evaluation we found programs considering night ventilation as ventilation during specified night hours, as ventilation when internal temperature is higher than external temperature, sometimes with a limitation when internal temperature is lower than a certain threshold, sometimes not. We note that the results of system indicators are very sensitive on ventilation strategy assumptions and conditions on assumptions.

We define 3 ventilative cooling strategies in addition to the standard scenario. For each strategy we show the boundary conditions

Table 1: Ventilative cooling strategies

Strategy Name	When	T in Condition	T out Condition	Cooling extra Airflow*
A. Standard ventilation	7:00-18:00	-	-	0
B. Day ventilation	7:00-18:00	$T_i > 23^\circ\text{C}$	$T_i > T_o$	Window stack*
C. Night ventilation natural	24h	$T_i > 23^\circ\text{C}$	$T_i > T_o$	Window stack
D. Night ventilation mechanical	24h	$T_i > 23^\circ\text{C}$	$T_i - T_o > +2^\circ\text{C}$	$5.2 \text{ m}^3/\text{h.m}^2$

\* During occupation (7:00 - 18:00) there is a basic airflow rate of  $2.6 \text{ m}^3/\text{h.m}^2$  for hygienic ventilation and outside occupation hours there is a basic airflow rate of  $0.3 \text{ m}^3/\text{h.m}^2$

\* Stack ventilation is calculated dynamically according to Bernoulli's equation, using the window dimensions and discharge coefficients and in-out temperature difference without wind influence.

#### 4.2 Other boundary conditions

Air temperature set point for cooling requirement calculation during the hours of use:  $26^\circ\text{C}$ , according to Swiss norm SIA 2040

Air temperature set point for heating requirement calculation:  $21^\circ\text{C}$

#### 4.3 Calculation models and simulation tools

Annex 62 tested several dynamic simulation tools (EnergyPlus - US, BSim - DK, LESOSAI, - CH, SIA TEC-Tool - CH, TRNSYS - DE, DIAL+ - CH) to evaluate how do they take into account dynamically bulk airflow coupled with dynamic temperature evolution. Most of the simulation programs use EN 13790 or EN 13791 model to calculate interior temperature and Bernoulli's equation to calculate stack ventilation airflow rate. Some models may take into account wind influence, other not. In general it was observed good correlation between monitored and simulated temperatures and airflow rates.

For the purpose of this paper, DIAL+ calculates indoor temperature (EN 13791), cooling and heating requirements and maximum cooling and heating power (EN 15265, EN 15255), number of hours outside adaptive comfort zone EN 15251. The software uses Cocroft equations to consider multiple windows in different heights and Meteonorm meteorological files (Paule et Al, 2012).

## 5 SIMULATION RESULTS

### 5.1 Cooling Requirement Reduction

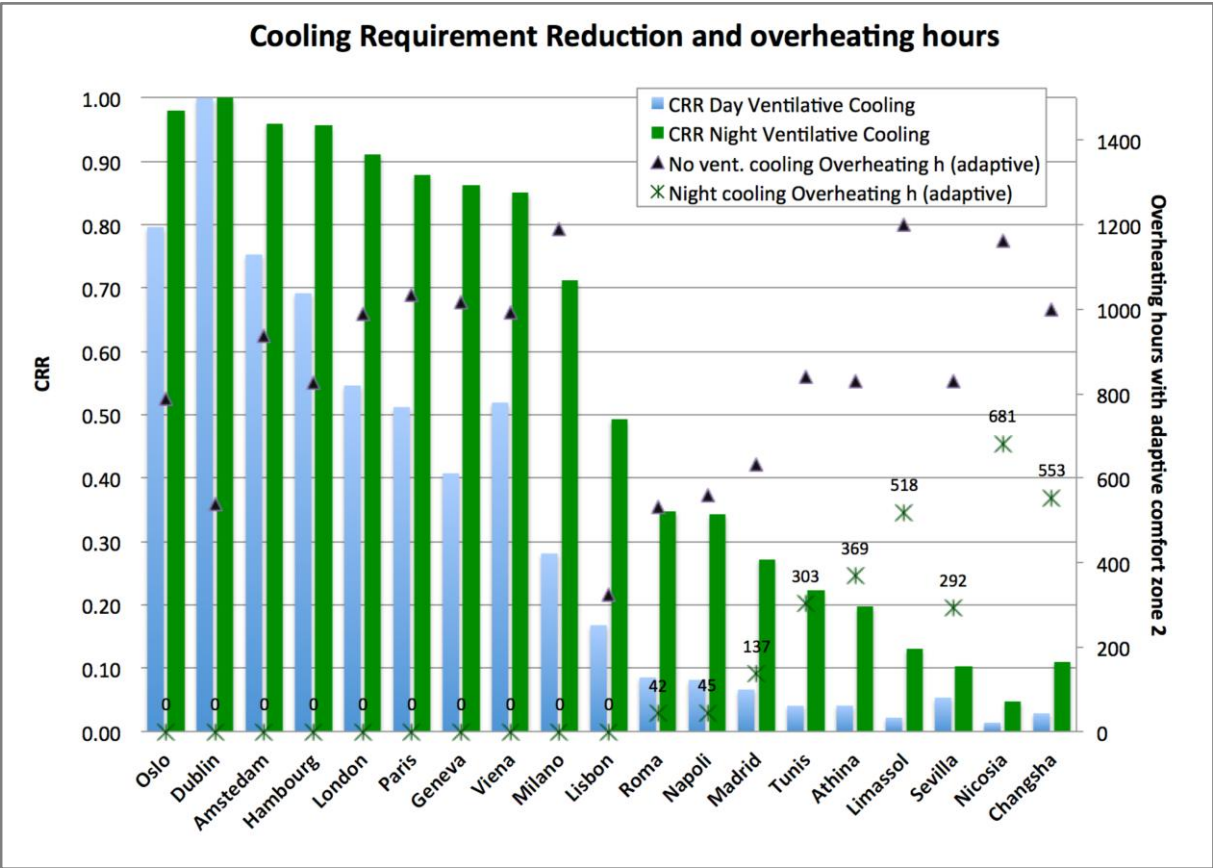


Figure 2: CRR for day and night ventilative cooling strategy and overheating hours according to class 2 adaptive comfort indicator for a standard scenario without ventilative cooling and a scenario with night cooling.

Table 2: Cooling requirements for a selection of sites [kWh]

	Dublin	London	Geneva	Vienna	Lisbon	Napoli	Athina	Nicosia
Heating demand [kWh/m <sup>2</sup> y]	15.5	10.9	19.9	18.6	14	26.6	20.8	14.8
A. Standard ventilation scenario	52	238	292	260	274	380	634	999
B. Day ventilation	0	108	173	125	228	349	608	985
C. Night ventilation natural	0	21	40	39	139	250	509	952
D. Night ventilation mechanical	0	14	30	23	131	223	449	710
R1 Blinds 50% without ventilative cooling	99	315	384	337	491	592	862	1270
R2 Blinds 0% without ventilative cooling	346	625	724	657	919	981	1280	1780

The results of figure 2 and table 2 show that near zero office buildings show results of the same order for heating demand (10-25 kWh/m<sup>2</sup>) and overheating hours without a ventilative cooling strategy (500-1200 hours outside adaptive comfort zone 2). Compared to the buildings before 2000, the results confirm that modern buildings reduced significantly heating

demand (10-30 kWh/m<sup>2</sup> instead of 100) but at the same time rise significantly cooling demand, especially for cold climates. This confirms Annex 62 initial hypothesis that summer comfort and cooling become a problem for all climates and necessity for a deep understanding of ventilative cooling strategy.

CRR graph and corresponding overheating hours for night ventilative cooling scenario show a very interesting result. This strategy may solve the problem for climates from Oslo to Milano. A ventilative cooling scenario with CRR up to 60% achieves adaptive comfort acceptable conditions. If we have a look on day ventilative cooling strategy, we may see on the graph that climates like Hambourg, Amsterdam, Oslo, Dublin may achieve CRR > 0.6. London, Paris, Geneva, Vienna, Milano may achieve adaptive comfort with night cooling but not with only day ventilative cooling. Lisbon is really on the limit. A southern Atlantic climate achieves CRR 0.5 but still 0 overheating hours with night cooling. For other Mediterranean and hot continental climates we may see that night ventilative cooling reduces cooling requirements by 10-35% but it cannot achieve complete adaptive comfort conditions. Overheating hours are reduced to 45-700 hours instead of 500-1200 hours without a ventilative cooling strategy. Although the effectiveness of this strategy is limited in hot summer days with hot nights, it is really effective in midseason. The added value of this strategy for hot climates is to reduce the cooling period. Cooling needs for climates like Athens are reduced to zero until mid may and after mid September.

The question is not only the quantitative value of CRR, which is a powerful indicator to evaluate energy performance of a ventilative cooling strategy and compare it with a conventional cooling system. Indicators with the quality of the achieved comfort and the deviation risk from the comfort objectives should complete decision aid information. In table 2 we may read the risks R1 and R2 in terms of cooling requirements and see 300% to 400% rise for cold climates and 50% to 200% rise for hot climates. A building with bad blind control in Geneva has the same cooling requirements with a building with good blind control in Athens. In cold climates, night ventilative cooling is not any more a sufficient strategy for a building with a bad blind control.

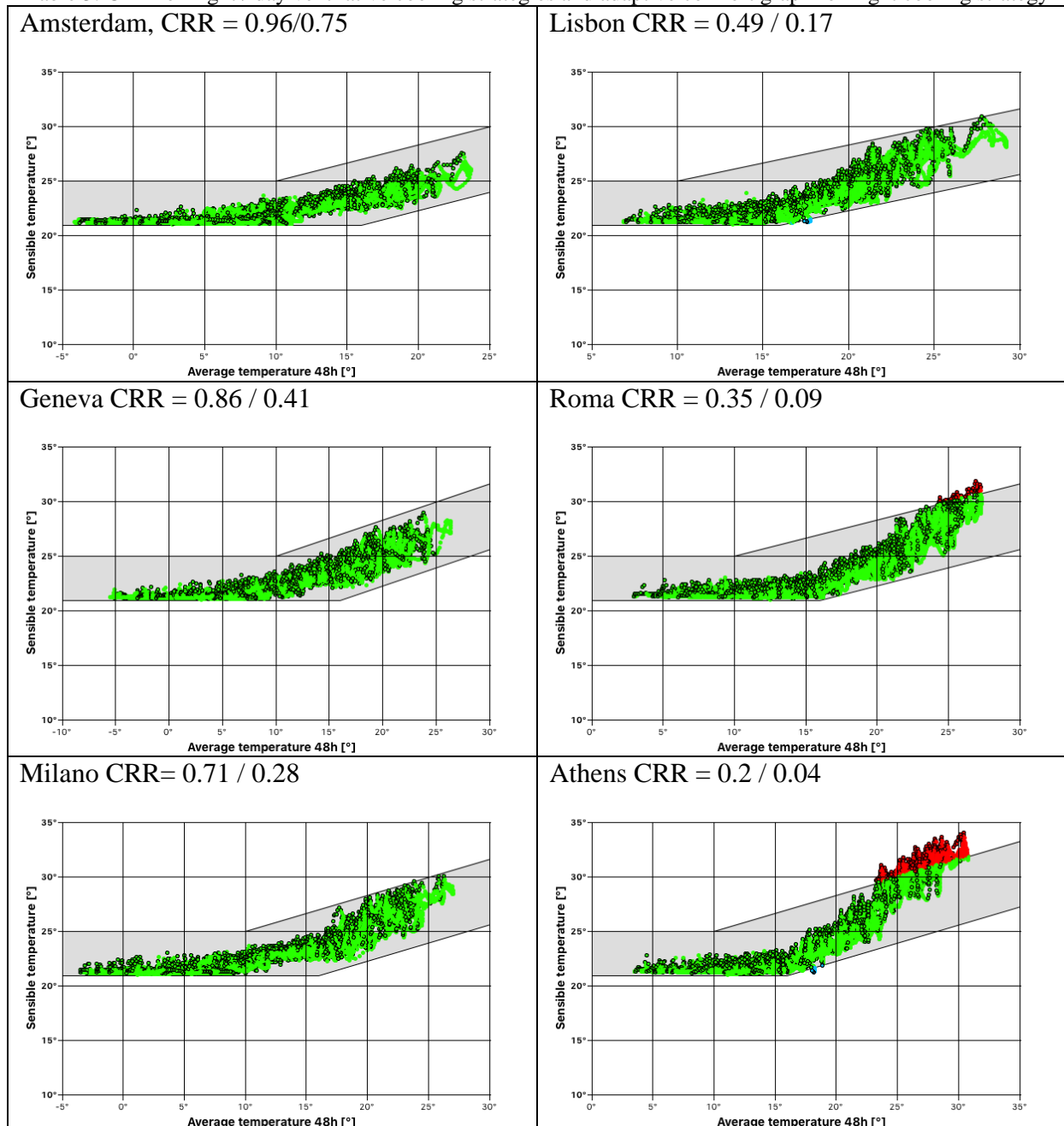
In table 3 we can see on the left column that although Amsterdam, Geneva and Milano have CRR > 0.6 for a night cooling strategy, they do not provide the same quality of comfort. In the same way we may see for hot climates the comparison of comfort conditions for Lisbon, Roma and Athens with CRR < 0.5. This table shows the necessity to use energy indicators in synergy with comfort indicators to drive decisions.

The analysis of these results rises a question: why do we calculate the cooling requirements reduction with cooling requirements calculated with a constant set point temperature (in our case 26°C) and not with an adaptive set point temperature like the adaptive comfort criterion? We have indeed calculated the cooling requirements for many climates with the two temperature set point criteria and found a perfect correlation line given as  $Q_{\text{adaptive}} = 0.61 Q_{26^{\circ}\text{C}}$ . The  $R^2$  of this correlation is 0.98. This explains why in almost all climates we have 0 overheating hours with CRR > 0.6 and justifies the use of a standard cooling requirement calculation with a fix set point temperature, available in most commonly used dynamic simulation programs of the market.

If we compare these results with climate oriented indicators, like for example Climatic Cooling Potential (Artman N et Al 2008) we observe the same general tendency, but with performance indicators depending on both climate and the building, we have more nuance in the answers concerning a particular building with a given use. CRR results are also in accordance with results for Passive Ventilative Cooling (PVC) potential and can be seen as complementary (Chiessa G et Al 2015). With CRR applied for example with day and night ventilative cooling strategies, we see on figure 2 that day ventilative cooling may provide sufficient comfort for some oceanic climates (CRR > 0.6) but not for continental climates where night cooling is necessary. And we may go further on; analyzing sensibility indicators

for insufficient blind control, and realize that night ventilative cooling is not sufficient for rooms with partial use of solar protection.

Table 3: CRR for night / day ventilative cooling strategies and adaptive comfort graph for night cooling strategy



## 5.2 Seasonal energy efficiency ratio $SEER_{VC}$ and ventilative cooling advantage $ADV_{VC}$

If we concentrate on two cities, Geneva and Roma, and we assume a cooling system  $SEER=3$  and a ventilation system  $SPI=0.45 \text{ W}/(\text{m}^3/\text{h})$  we have the results presented in table 4. In the reference scenario we produce the entire cooling requirements with a cooling machine of  $SEER=3$ . For scenario 2 and 3 we assume that natural ventilative cooling during day working hours and over 24h reduces cooling needs according to the simulations. For scenario 4 mechanical ventilative cooling is limited only from 01:00 to 07:00 and for scenario 5 mechanical ventilative cooling is switched on when  $\Delta T > 4^\circ\text{C}$  without time limitation.

Table 4: SEER<sub>VC</sub> and ADV<sub>VC</sub> for Geneva and Roma

	Geneva						Roma					
	Cool. R. kWh	Cool. Energy	Ventil. Energy	Total Energy	SEER <sub>VC</sub>	ADV <sub>VC</sub>	Cool. R. kWh	Cool. Energy	Ventil. Energy	Total Energy	SEER <sub>VC</sub>	ADV <sub>VC</sub>
1. Reference	292	97	0	97			351	117	0	117		
2. Day Nat VC	173	58	0	58			321	107	0	107		
3. 24h Nat VC	40	13	0	13			229	76	0	76		
4. Mech 6h VC	90	30	67	97	<b>3.01</b>	<b>1.0</b>	244	81	67	148	<b>1.60</b>	<b>0.53</b>
5. Mech ΔT> 4°	36	12	112	124	<b>2.29</b>	<b>0.8</b>	222	74	78	152	<b>1.65</b>	<b>0.55</b>

Scenario 5 runs ventilative cooling 1349 hours in Geneva and 940 hours in Roma. As we can see from the results that SEER<sub>VC</sub> are poor and in most cases ADV<sub>VC</sub> is lower than 1, compared to a conventional system of SEER=3. When there are no time limitations (scenario 5), ventilation energy is higher than scenario 4, with direct consequence even lower SEER<sub>VC</sub>. For Geneva ADV<sub>VC</sub> is very near to 1 for the optimum case, meaning that ventilative cooling with a dual ventilation system spends at least as many energy as an air-conditioning system of SEER = 3.

Sensitivity analysis showed that the optimum time for ventilative cooling when we need to reduce the hours of use, in all climatic conditions is at 04:00, the optimum mechanical ventilative cooling duration is around 810 hours per cooling season (6 hours per night) with ventilative cooling switched on when ΔT>4°C. Even with these optimum operating conditions, with hot climates it is difficult to have a positive ADV<sub>VC</sub> (i.e. a ventilative cooling SEER superior than the one of the cooling system). High performance dual ventilation systems have SPI>0.4 W/(m<sup>3</sup>/h) and single flow systems SFP>0.1 W/(m<sup>3</sup>/h).

The graphs of Figure 3 show the curve where ADV<sub>VC</sub> = 1. These curves are calculated for a particular site and a particular scenario for a given building. The curves of Figure 3 represent the optimum mechanical ventilative cooling scenario 1:00-7:00 with an airflow of 5.6 m<sup>3</sup>/hm<sup>2</sup>.

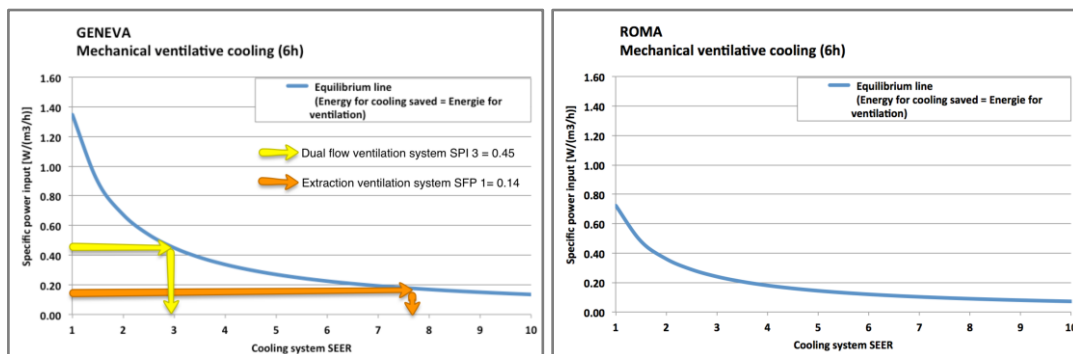


Figure 3: ADV<sub>VC</sub> = 1 curves for Geneva and Roma.

On the graph of Geneva we may see that for a ventilation system of SPI = 0.45 W/(m<sup>3</sup>/h) (category 3) the maximum conventional cooling system SEER that can be replaced without losing more energy is 3. For a single flow extraction system of SFP = 0.14 W/(m<sup>3</sup>/h) (category 1), ventilative cooling has the advantage over conventional cooling systems. The cooling system must have a SEER > 7.7 to be more advantageous than ventilative cooling.

### 5.3 Example of CRR and SEER<sub>VC</sub> of two ceiling fans

Simulations for this example follow the same protocol and boundary conditions. The reference scenario is a day ventilative cooling scenario. To account for the effect of a ceiling fan we simulate the cooling requirements at 29°C, assuming that a ceiling fan at a medium speed may reduce the perceived temperature by 3°C. It is a realistic scenario where occupants

open windows for fresh outside temperature and use ceiling fans when interior temperature is higher than 26°C. The interesting performance indicators of ceiling fans are found on table 5.

Table 5: Example of CRR and SEER<sub>vc</sub> of two ceiling fans 15W and 37W

	Cooling Requirements		Ceiling fan 15W		Ceiling fan 37W		
	at 26°C [kWh]	at 29°C [kWh]	<b>CRR</b>	El. Energy [kWh]	<b>SEER<sub>vc</sub></b>	El. Energy [kWh]	<b>SEER<sub>vc</sub></b>
Geneva	173	39	<b>0.77</b>	11.1	<b>12.0</b>	27.4	<b>4.9</b>
Rome	321	100	<b>0.69</b>	12.6	<b>17.5</b>	31.1	<b>7.1</b>

## 6 CONCLUSIONS

A set of ventilative cooling energy indicators is a powerful tool showing the potential of the passive strategies and offering the possibility to compare it with conventional cooling strategies. Natural ventilative cooling is a passive technique and can be called "free cooling". The only "cost" is the ability to leave the windows open in safety conditions during night. CRR analysis showed that this passive strategy is able to provide comfort for NZE buildings passively without extra energy consumption for continental European climates. It may reduce significantly cooling needs by reducing cooling season for hot Mediterranean climates. Ventilative cooling may replace cooling systems during mid season for these climates.

Mechanical ventilation is a more convenient strategy, running on independently of window use, but it costs energy. Energy performance indicators showed that even high energy-performance dual ventilation systems have a poor SEER<sub>vc</sub> < 3. It is necessary to optimise the ventilative cooling hours to the minimum in order to get the best SEER<sub>vc</sub> and get the advantage over conventional cooling systems. Optimal conditions for office buildings in almost all the climates is a temperature difference of  $\Delta T > 4^\circ\text{C}$  and a time limitation of 6 hours centred on the coldest moment of the night at 4:00 am. This limitation (6 hours per night 1:00-7:00) reduces ventilation time to ~800 hours and gives higher SEER<sub>vc</sub>.

## 7 REFERENCES

- Kolokotroni M, Heiselberg P. (2015). Ventilative cooling state of the art. *Department of civil engineering, Aalborg University, Aalborg*.
- Court of Auditors - Vaud (2015). Rapport 37, Audit du Développement Durable dans les bâtiments de l'Etat de Vaud, *Cour de Comptes du Canton de Vaud, Lausanne*.
- Flourentzou F, Ritz K, Pantet S, (2017), Design and performance of controlled natural ventilation in school gymnasiums, *International Journal of Ventilation*, Vol. 16 ,Iss. 2.
- Artmann N., Manz H., & Heiselberg P. (2008), Passive Cooling of buildings by night-time ventilation. Duebendorf: *Schlussbericht. Eidgenössisches Departement für Umwelt, Verkehr, Energie und Kommunikation, UVEK. Bundesamt für Energie BFE*.
- Chiesa G, Grosso M. (2015), "Geo-climatic applicability of natural ventilative cooling in the Mediterranean area", *Energy and Buildings 2015 107 pp376-391*
- Paule B., et al., DIAL+Suite (2012), A new suite of tools to optimize the global energy performance of room design, *Status Seminar, Zurich*.
- Swiss Standards: SIA 180 (Thermal protection and interior climate in buildings), SIA 382/1 (Ventilation and airconditioning - general basis and required performance), SIA 2024 (Data concerning use of rooms and technical installations for energy calculations),

EN Standards: EN 15251 (Indoor environmental input parameters...), EN 15265 (Sensible room cooling load...), EN 15265 (Calculation of Energy use for heating and cooling), ISO 13790 (Energy performance of buildings - Calculation of energy use for space heating and cooling), ISO 13791 (Thermal performance of buildings - Calculation of internal temperatures of a room in summer without mechanical cooling), EN ISO 7730 (Ergonomics of the thermal environment).

# Experimental evidence of effective single sided natural ventilation beyond 20ft or 2.5 floor to ceiling heights in open plan office spaces

Guilherme Carrilho da Graça<sup>\*1</sup>, Nuno Mateus<sup>1</sup>, Rafael Rebelo<sup>2</sup>

<sup>1</sup>Instituto Dom Luiz

Faculdade de Ciências, Universidade de Lisboa

1749-016 Lisboa, Portugal

<sup>2</sup>Faculdade de Ciências

Universidade de Lisboa

1749-016 Lisboa, Portugal

## KEYWORDS

Natural ventilation, Single-sided, Ventilation effectiveness

## SUMMARY

Most natural ventilation (NV) systems used in non-residential buildings are single sided (SS). These systems are easy to integrate in the building layout, since, unlike in cross-ventilation (CV), these systems do not require access to two facades or a central stack. Current knowledge about SS NV flow penetration away from the façade can be found in building regulations and design rules of thumb. Examples of these rules include California's Title 24 20ft rule [1], that limits the use of natural ventilation to office areas that are less than 20 ft (6 m) away from a façade with operable windows, and the CIBSE recommendations of maximum room depth of up to 2.5 room floor to ceiling heights [Σφάλμα! Δεν έχει οριστεί σελιδοδείκτης.] (2.5H) for SS NV systems. As expected, CV flows are subjected to similar limitations that set larger room depth limits (in fact the maximum distances between opposing room facades): 12m [1] or up to 5H [Σφάλμα! Δεν έχει οριστεί σελιδοδείκτης.].

In the case of SS systems these ad hoc rules can have a large negative impact in the adoption of NV. In a building design or refurbishment project, whenever the room depth exceeds these limits, designers must at least resort to mechanical ventilation and, in many cases, end up opting for a traditional HVAC system for the whole space. Apparently, the limits used in current design guidelines and building regulations have not been validated by research and may be overly conservative. Existing experimental [2,3] and numerical [4] investigations of fresh air penetration depth in SS systems indicates that these limits may be overly conservative. In all existing studies the average penetration depth, defined as the point beyond which the mean age of air exceeds the age of air at the exhaust, exceeds 3H. These studies are limited by the use of low internal gains and fully open rudimentary windows (or no windows at all).

The experimental study presented in this paper tries to fill the existing knowledge gap on the effectiveness of single sided natural ventilation beyond 20ft or 2.5 floor to ceiling heights in open plan office spaces. The study used three rooms shown in figures 1 and 2, with SS ventilation and different internal dimensions and depths that varied between 3.5 and 5.7H. In all of these spaces the internal CO<sub>2</sub> concentrations, air and surface temperatures were measured in 2-3 hour periods with standard occupation (7-12m<sup>2</sup> per occupant) and internal gains (25-30W/m<sup>2</sup>). The results confirm that the current regulation limitations are overly conservative. Adequate ventilation effectiveness can be achieved in room depths of 4H or even more in the case of displacement ventilation NV systems.

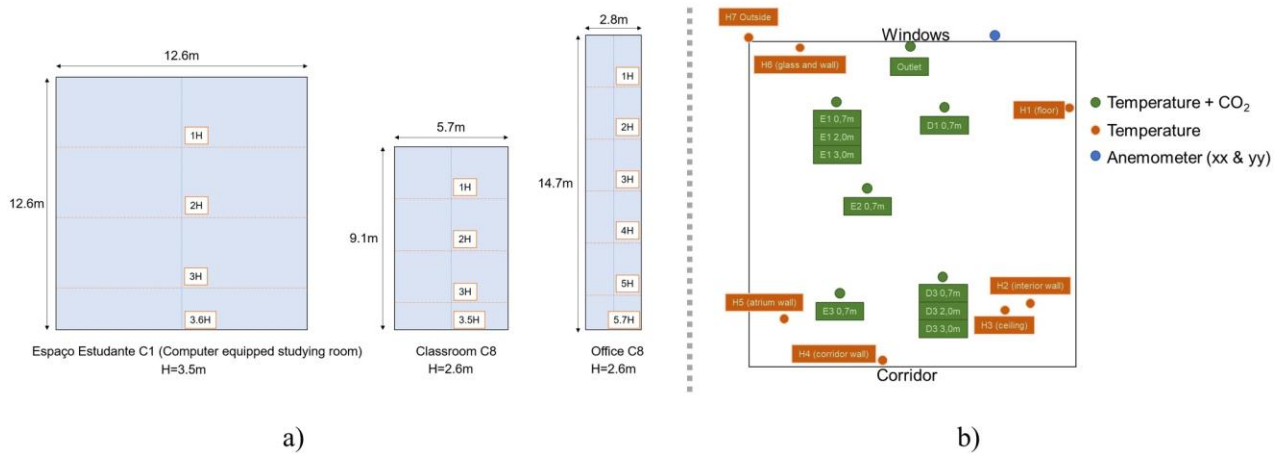


Figure 1: a) room floorplans with depth shown in floor to ceiling heights, b) schematics of the measurement setup used in room C1.

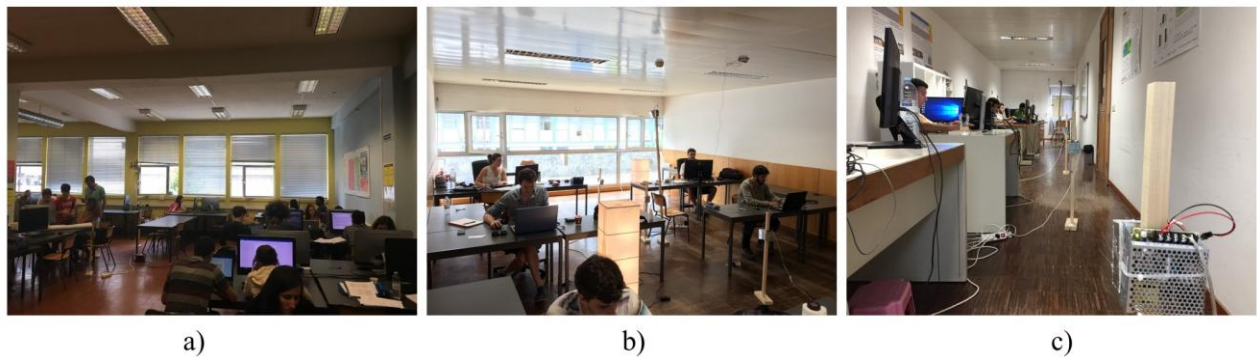


Figure 2: interior views of the three rooms during the measurements a) open space C8, b) open plan office C8, c) long office C8

## References

- [1] California Building Standards Commission (2013). California Building Standards Code, *California Code of Regulations*, Title 24.
- [2] White MK, Walker RR. The efficiency of single-sided and cross ventilation in office spaces. DOCUMENT-AIR INFILTRATION CENTRE AIC PROC 1996 (pp. 487-496).
- [3] Walker RR, White MK. Single-sided natural ventilation—How deep an office? *Building Services Engineering Research and Technology*. 1992 Nov 1;13(4):231-6.
- [4] Guohui Gan, Effective depth of fresh air distribution in rooms with single-sided natural ventilation, *Energy and Buildings*, Volume 31, Issue 1, January 2000, Pages 65-73, ISSN 0378-7788, [http://dx.doi.org/10.1016/S0378-7788\(99\)00006-7](http://dx.doi.org/10.1016/S0378-7788(99)00006-7).

# Automated window opening control system to address thermal discomfort risk in energy renovated dwellings. Summertime assessment.

Theofanis Psomas<sup>\*1</sup>, Per Heiselberg<sup>2</sup> and Thøger Lyne<sup>3</sup>

*1 Aalborg University  
Thomas Manns Vej 23  
Aalborg, 9220, Denmark  
\*th.psomas@gmail.com*

*2 Aalborg University  
Thomas Manns Vej 23  
Aalborg, 9220, Denmark*

*3 Visility ApS  
Universitetsparken 7  
Roskilde, 4000, Denmark*

## ABSTRACT

Major and deep energy renovations of single-family houses (more than 60% of the building stock) are expected in Europe over the next several years (Psomas et al., 2016a). A number of research projects have documented and verified overheating risk during the design and operation phase in nearly zero energy or existing renovated single-family houses without mechanical cooling systems in temperate climates. Post occupancy surveys and comfort studies have also monitored high indoor temperatures over 27°C and 28°C even in Northern countries (Psomas et al., 2016a). The main reasons of the thermal discomfort during the cooling period and transition months are the improvement of the airtightness, the increase of the outdoor temperatures (climate change and heat island effects) and the large south-oriented facades (Psomas et al., 2016a). For building occupants of these climates, overheating risk is a new challenge that they have never experienced before now. Users do not have the technical knowledge of how to efficiently decrease the risk, and their attitude and behaviour increase the problem (Psomas et al., 2016a). Health research shows that high indoor temperatures for extended periods significantly degrade the indoor environment and increase the morbidity and mortality.

Ventilative cooling through natural opening systems can be an energy-efficient, sustainable and inexpensive solution to avoid overheating occurrences in energy renovated dwellings in temperate climates (Psomas et al., 2016b). Ventilative cooling through manual control of the opening systems cannot ensure indoor environmental conditions inside the national regulations and comfort standards limits (major violations and poor air quality; Psomas et al., 2016b). Automated window opening control systems with rule based control (RBC) and integrated straightforward heuristic algorithms are already the industry standard for non-residential large-scale buildings.

Psomas et al. (2017) have developed and presented in detail a new automated window opening control system with integrated passive cooling methods and control strategies and real-time monitoring of the environmental parameters indoors and outdoors (temperature, carbon dioxide concentration and relative humidity) for residential buildings. The analysis directly compares the effectiveness of the manual control against the automated control of the window openings for an occupied representative deep renovated dwelling, from the 1930s, in temperate climatic conditions and for two complete summer periods (2015 and 2016): one without the automated system implemented (manual use of the windows and mechanical ventilation) and one with the system installed at the roof windows of the house (Psomas et al., 2017). Occupants of the house experienced identical weather conditions for both cooling periods (Psomas et al., 2017). Both dynamic and static thermal comfort and overheating methodologies, metrics and criteria in room, floor and house levels are used to carry out risk assessment. The performance indicators of the indoor air quality are the carbon dioxide concentration and the relative humidity (Psomas et al., 2017).

The indoor thermal and air quality assessments of the case study for both peak summer periods illustrate the fact that active and passive cooling components and systems, if manually controlled, cannot ensure high quality indoor environment (Figure 1). In contrast, the use of the new automated window opening control system may significantly decrease the indoor thermal discomfort assessed by static and dynamic criteria in all rooms without any significant compromise of the indoor air quality (Figure 1). For this case study, the automated system controls only a small part of the available air flow components of the house (roof windows). The low energy use

of the automated system and the total energy savings, more than 95%, from the deactivation of the mechanical ventilation system strengthen and enhance the possibility of use of these systems in the future. The description of the architecture of the components and control strategies and the identified limitations and suggestions after the monitoring campaign of the automated system may be used as a baseline for the development of automated systems applicable to other climatic conditions and building types.

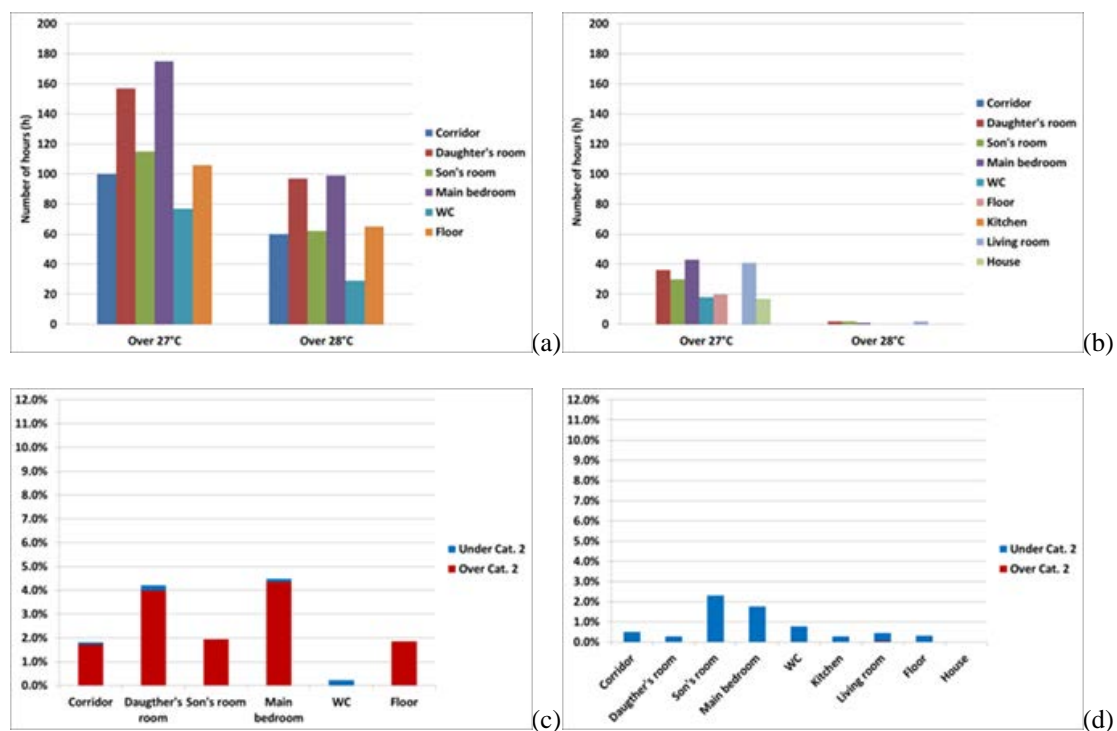


Figure 1: Overheating (a, b) and thermal discomfort (c, d; adaptive method, Category II) assessment in room, floor, and house level of the case study, for summer of 2015 (a, c) and 2016 (b, d).

## KEYWORDS

Overheating, residential building, passive cooling, adaptive comfort, indoor air quality.

## ACKNOWLEDGEMENTS

The research was developed within the framework of the project “Ventilative cooling in energy renovated residences” of Aalborg University, Denmark, and was supported by EUDP (Energy Technology Development and Demonstration Program) and VELUX A/S, DOVISTA A/S and VISILITY ApS (Grant number 64013-0544/2014-2017).

## REFERENCES

- Psomas, T, Heiselberg, P, Duer, K, Bjørn, E. (2016a). Overheating risk barriers to energy renovations of single family houses: Multicriteria analysis and assessment. *Energy and Buildings*, 117, 138-148.
- Psomas, T, Heiselberg, P, Duer, K, Bjørn, E. (2016b). Control strategies for ventilative cooling of overheated houses. Federation of European Heating, Ventilation and Air-Conditioning Associations: Proceedings of 12<sup>th</sup> REHVA World Congress, Aalborg, Denmark.
- Psomas, T, Heiselberg, P, Lyme, T, Duer, K. (2017). Automated roof window control system to address overheating on renovated houses: Summertime assessment and intercomparison. *Energy and Buildings*, 138, 35-46.

# Experiences regarding draught effects for ventilative cooling in cold climate

Maria Justo-Alonso<sup>1\*</sup>, Solveig Blandkjenn<sup>2</sup>, Hans Martin Mathisen<sup>2</sup>

*1 SINTEF Building and Infrastructure  
Høgskoleringen 7B  
7465 Trondheim, Norway  
\*Corresponding author:  
maria.justo.alonso@sintef.no*

*2 Norwegian University of Science and Technology,  
Kolbjørn Hejes vei 1b,  
7491 Trondheim - Norway*

## ABSTRACT

New buildings have to satisfy stricter standards regarding energy efficiency and consumption. This results in higher insulation levels and lower air leakages that reduce heating demands. However, together with the heating demands reductions, higher temperatures in summer and particularly shoulder season are more frequent even at moderate to cold climates. In order to ensure acceptable indoor environment quality, removal of excess heat becomes unavoidable. Using mechanical cooling in residential buildings is considered incompatible with achieving zero energy buildings (ZEB). Using ventilative cooling (VC) one can combine mechanical ventilation to supply minimum hygienic airflow rates and windows opening to supply cooling. The ZEB's ventilation systems gain larger importance as they can ensure minimum air quality, provide heating and in summer months remove excess heat.

The Living Lab in Trondheim (Norway) is built as zero emission building. In Norway, 100 % of the cooling needs can be covered by ventilative cooling, either by mechanical or natural ventilation. The ventilative cooling potential depends on many variables; the internal gains, solar gains, use of solar shading, windows g and Uvalues, heat loss coefficient of the building, ventilation flow rate, indoor and outdoor temperatures, etc. One additional consideration for cold climates is over cooling; this is an extra limitation on the use of window opening for cooling. Over cooling is related to thermal discomfort and extra energy use for heating.

The Living Lab has six motorized windows that enable for cross and buoyancy driven ventilation. In addition, three sliding doors can be used for cooling purposes with the restriction that their opening can only happen during occupied hours.

The goal of this paper is to develop a control system based on measurements. The control has to ensure sufficient cooling and hygienic airflow rates. This control ought to ensure thermal comfort without incurring increased energy use. The control is applied to the building in shoulder seasons and the measurements of the performance are presented.

## KEYWORDS

Ventilative cooling, energy saving, simulations IDA ICE, motorized window opening

## 1 INTRODUCTION

Super insulating buildings is the obvious solution to reduce energy use for space heating in cold climate countries. Modern super insulated buildings are constructed in materials with low U values and high airtightness. In airtight building's controlled ventilation has a major role to improve the indoor air quality (IAQ) and comfort (Sundell 2004). Accumulated "free heat gains" become negative when heating is not needed. Thermal discomfort due to high temperatures is experienced more often in super insulated buildings and to reach acceptable indoor climate, removal of excess heat is compulsory. The potential for ventilative cooling becomes larger (Finocchiaro, Wigenstad, and Hestnes 2010).

Windows in cold climates are often dimensioned with high g-factors, so that a larger share of the solar radiation is used for heating. In shoulder season and summer, this means that the gains due to solar radiation are a relevant heating source. Solar shading can be used to control this heat gain to a certain extent, but are seldom efficient enough to give full control of the solar radiation. Many occupants that have manually operated shadings often forget to close or intentionally leave the shading open when leaving home. For these reasons, cooling must be considered. With the goal of achieving the nZEB level, mechanical cooling is not considered as a satisfactory solution to limit over temperatures.

Mlecnik (Mlecnik et al. 2012) did some post occupancy questionnaires and concluded that 34% of his respondents experienced high indoor temperatures "sometimes" in the living room and 49% complained about bedroom over temperatures during summer. Samuelson's (Samuelsson 2009) research revealed that 50% of the residents were dissatisfied due to the high summer temperatures in passive houses in Sweden. In Norway, Georges (Georges, Wen, Justo Alonso, et al. 2016) (Georges, Wen, Alonso, et al. 2016; L. Georges, F. Håheim, and Alonso 2017) and Berge (Berge and Mathisen 2016; Berge, Thomsen, and Mathisen 2016) came to the same conclusion, users are dissatisfied due to too high temperatures in bedroom yielding the need to open windows, partly also during the winter.

VC should be perceived as a part of a total strategy that includes use of solar shadings, minimization of internal heat gains and intelligent use of thermal mass (Venticool 2013). Natural ventilative cooling is considered in this context a very good solution for removal of thermal loads. (Kolokotroni and Heiselberg 2015). In cold climates, the theoretical potential of heat removal by VC is 100%. However, in these locations the risk of over cooling has to be considered in detail (Justo Alonso, Kirkøen, and Mathisen 2015). Degree of window opening, window size, temperature differences between outdoor and indoor, etc., prove to have high relevance for the cooling potential (Kolokotroni and Heiselberg 2015).

The scope of this paper is the performance evaluation of the Living Lab natural VC control solution concerning thermal comfort and energy consumption. The resulting optimal control is compared in the same terms to improved window opening sizes, building cardinal orientation and building insulation levels

## 2 LIVING LAB

The Living Lab is a test facility installed in Trondheim, Norway (63°N) constructed to obtain the zero emission level (Finocchiaro et al. 2014). This residential single family house has a gross volume of approximately 500 m<sup>3</sup> and a heated surface (floor area) of approximately 100 m<sup>2</sup> (Finocchiaro et al. 2014).

Table 1 - Thermo-physical properties of building envelope components (Goia, Finocchiaro, and Gustavsen 2015)

Thermo physical properties	
U-value wall	0.11 W/m <sup>2</sup> K
U-value floor	0.10 W/m <sup>2</sup> K
U-value roof	0.10 W/m <sup>2</sup> K
U-value windows (south façade)	0.65 / 0.69 (when ventilated) W/m <sup>2</sup> K
U-value windows (north façade)	0.97 W/m <sup>2</sup> K
U-value windows (east-west façade)	0.80 W/m <sup>2</sup> K
U-value skylight	1.0 W/m <sup>2</sup> K
g-value for windows	0.5-
Air tightness, n <sub>50</sub>	0.5 ach

The building is equipped with a very comprehensive data acquisition system with access to 330 sensors that measure energy demand for heating, ventilation, lighting and appliances, and renewable energy produced by a roof-integrated PV system and façade-integrated solar thermal panels. The accumulation tanks and indoor environment are also fully monitored (Finocchiario et al. 2014).

The installed ventilation is a mixed-mode hybrid system with mechanical balanced ventilation and motor controlled windows. The mechanical ventilation is a balanced mechanical system with heat wheel recovery with 85 % rated efficiency and additional electric heating coils (Blandkjenn 2017). Supply units are placed in the living room and bedrooms and extracts are placed in the kitchen and bathroom. Table 2 shows the supplied and extracted airflow rates for each room in Living Lab (Blandkjenn 2017).

Table 2: Airflow rates in Living Lab during normal occupancy

Supply	Airflow rate [m <sup>3</sup> /h]	Extract	Airflow rate [m <sup>3</sup> /h]
Small bedroom	52	Bathroom	78
Master bedroom	52	Kitchen	52
Living room	26		
Total supply	130	Total extract	130

The dwelling has operable windows on every facade in order to profit from both stack and cross flow ventilation through mechanical opening of windows. On the north side, an elongated window is implemented. It is constructed with hinges at the top, and opens outwards to a maximum angle of 51°. On the west and east side there are glass sliding doors. Two sets of rooftop skylight triple glazed windows faces to the north. They open to a maximum angle of 32°. The south windows open to a maximum of 32°, it is a double skin window. See Figure 1 to see the location of the controllable windows.

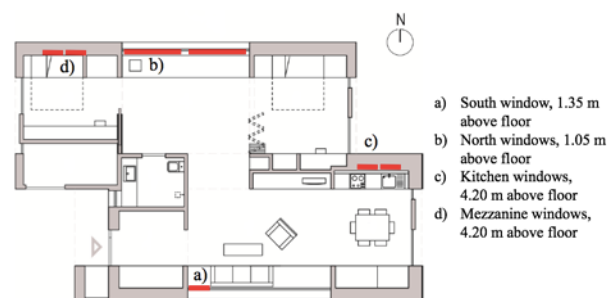


Figure 1. Position of automatically controlled windows in Living Lab (Blandkjenn 2017)

Table 3: Window areas and maximal openable areas (Finocchiario et al. 2014)

Window	Number of windows	Area per window [m <sup>2</sup> ]	Maximum openable area per window [m <sup>2</sup> ]
North	2	1.21	0.786
South	1	10.5	1.130
Skylights	4	0.484	0.338

### 3 OPTIMAL WINDOW CONTROL

In order to develop a reliable control strategy, measurements have been done in Living Lab and then these results have been used to develop a control strategy based on simulation with the program IDA ICE (EQUA 2016). The main results and graphs of this and next chapter are taken from the Master thesis of (Blandkjenn 2017).

### 3.1 Measurements results

Blandkjenn (Blandkjenn, 2017) carried out an extensive measurement campaign to reveal the most affecting parameters when creating a window control algorithm.

The southern window is a double skin window, where air might preheat before being supplied to the room. As this window is placed close to the sofa of the living room, the draught risk from this window needs to be assessed. Figure 2 shows the positioning of the measurement points for air velocity and temperature.

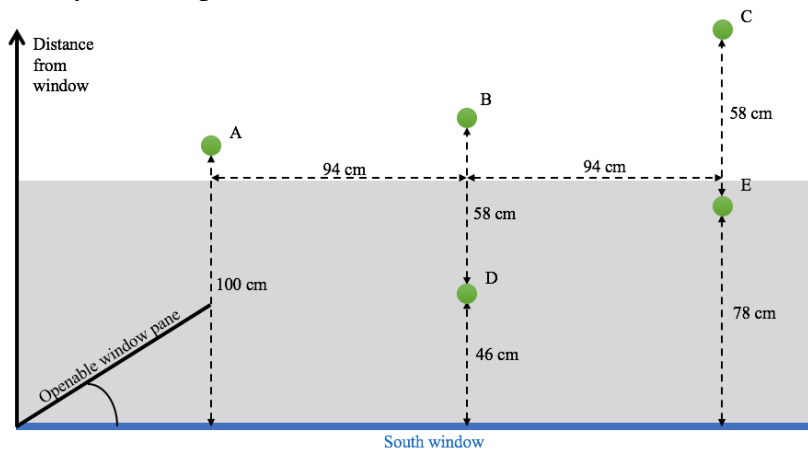


Figure 2. Measurement points near the south window

To determine the opened window's cooling effect the temperature difference between the air flowing from the window and the room air has been studied. Figure 3 shows the difference between the temperature measured one meter from the window and the room air. This graph distinguishes between the different levels of solar irradiance through the window (not specified). When the solar irradiance is above  $600 \text{ W/m}^2$ , the pre-heating of the air is so large that the air one meter from the window has the same temperature as the room.

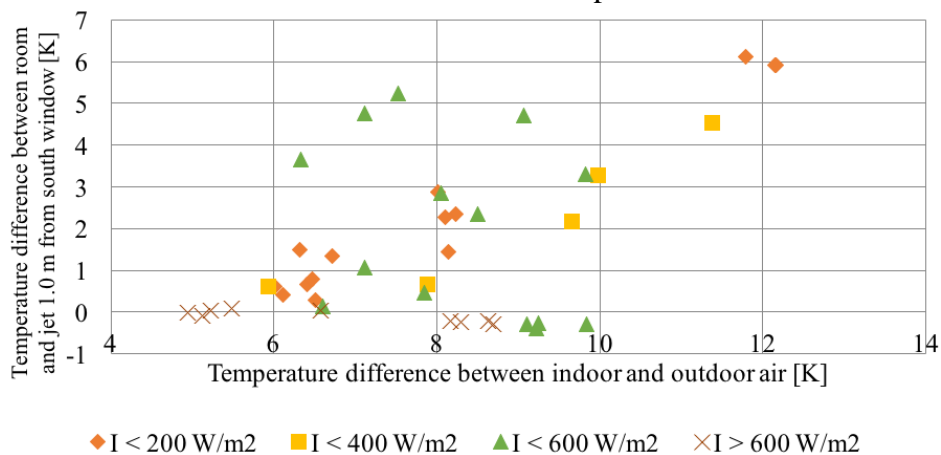


Figure 3. Temperature difference between air in the room and air in the jet 1 m from window, for different levels of solar irradiance. (Blandkjenn 2017)

When solar irradiance is lower than  $600 \text{ W/m}^2$ , the temperature difference increases with the temperature difference between indoor and outdoor air. It seems, Figure 4 left, that when the temperature difference between the indoor and outdoor air ( $\Delta T_{in-out}$ ) is below 6 K, the DR is very low. Even when the air in the jet is warmer than the average temperature of the room, air velocities above  $0.2 \text{ m/s}$  are still measured. This has a cooling effect on the people sitting in the room, even if the air temperature is not reduced. Jet temperatures were not measured  $0.4 \text{ K}$  over the room air. This means that the south window can be opened in most weather

conditions without risk of increasing the overheating, but the cooling capacity will be limited. In addition, the pre-heating of air through the south window reduces the risk of overcooling on cool days.

### Draught rates under different climatic conditions

Measurement proved that draught rates generally increased with  $\Delta T_{in-out}$ . However, there were many outlying measurements, especially when the temperature differences were low. The temperature difference is the main driving force for natural ventilation at higher temperature differences, but at lower temperature, differences in wind and solar conditions influence the airflows largely. The draught rates in front of the window were lower when the solar irradiance was higher. When the irradiance is larger, the  $\Delta T_{in-out}$  is lower because of the larger heating effect of the double skin window. A lower solar irradiance gave higher variance within the measuring points; this can be explained by sudden changes in cloudiness on warm days.

It is seen from Figure 4 right that there is no occurrence of draught rates lower than 20 % when the solar irradiance is below 70  $W/m^2$ . **This is therefore chosen as a lower limit for solar radiation to open the south window.**

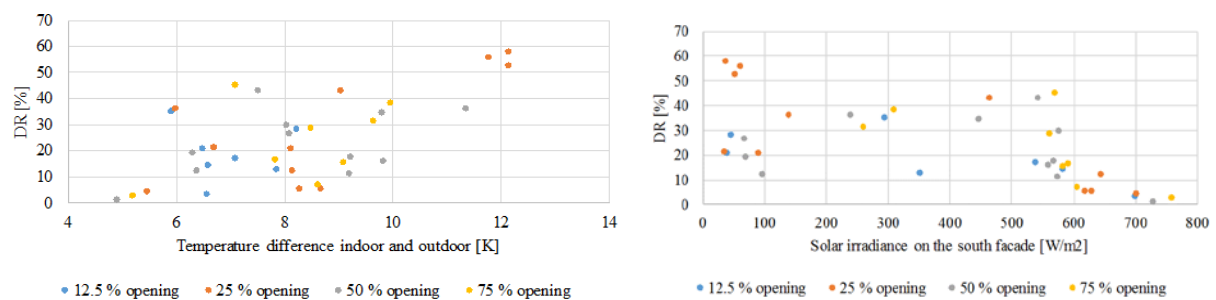


Figure 4 (left) Draught rates as a function of temperature difference, (right) Draught rates as a function of solar irradiance, for different window opening sizes measured in point D (Blandkjenn 2017)

The wind speed is studied, and it is measured to have a lower effect on draught rates than the temperature difference and the solar irradiance. **However, when the wind speed is above 2.0 m/s, the lowest measured draught rates are over 20 %. This is therefore chosen as an upper limit for the wind speed during openings of the south window.**

To establish rules for the use of the south window, the limits for  $\Delta T_{in-out}$ , wind speed and solar irradiance were chosen based on the measurements done 1.0 m from the window at 0.05 m height.

The maximum allowed  $\Delta T_{in-out}$  is defined as 10 K, the maximum wind speed is set to 2.0 m/s and the lower limit for solar irradiance is 70  $W/m^2$ . Figure 5 shows the measurements within these restrictions and for them, draught rates above 20 % only occur with window opening larger than 50 % and 75 %. When the window openings are restricted to 12.5 % and 25 % the thermal discomfort is reduced below 20 %. Due to limitations in data from the experiments, draught might still occur, but the hours of discomfort are assumed to be within the 3 % allowed deviation.

Because of the double skin construction, cooling will not always be achieved by opening the south window. It has been seen that the cooling effect of opening the south window has been near zero when the temperature difference between the indoor and outdoor air is below 6 K.

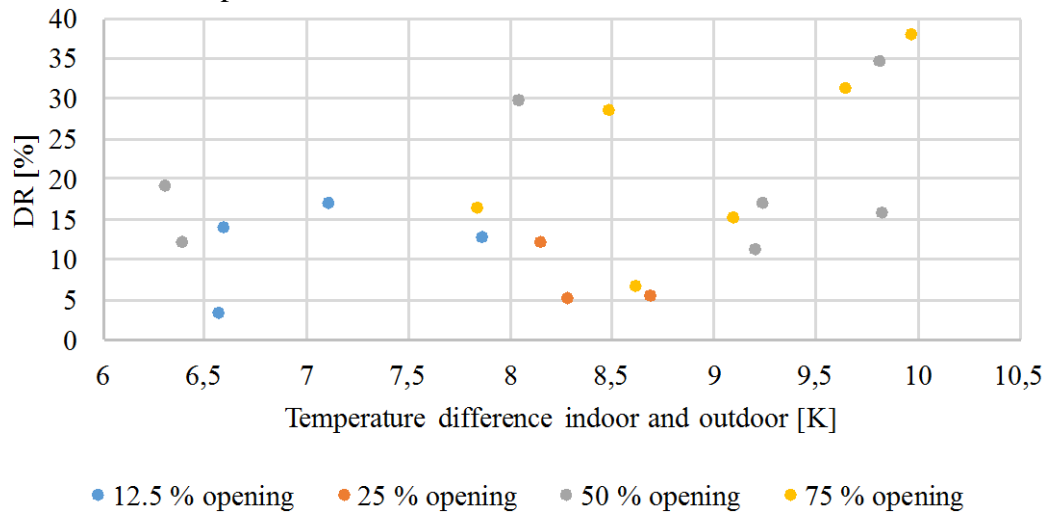


Figure 5. Measurements with  $dT < 10$  K,  $v < 2$  m/s and  $I > 70$  W/m<sup>2</sup> (Blandkjenn 2017)

A similar study was done for the north window concluding:

For  $\Delta T_{in-out}$  equal to 5.7 K, there was only unacceptable draught rates outside the occupied zone (less than 1m from the window). For  $\Delta T_{in-out}$  equal to 8.4 K and 9.5-9.9 K higher draught rates were measured. This indicates that the north window can be opened automatically if the outdoor temperatures are high enough. The draught rates increased as the opening was increased. The high risk of local thermal discomfort was expected for the north window as this window delivers unheated outdoor air at body height. Due to the limited number of measurements, it was possible to perform; it is hard to determine the exact temperature difference at which the north window can be opened without thermal discomfort. However, a limit of 6 K is proposed in this work. In addition, the cooling effect of the south window is very low for  $\Delta T_{in-out}$  below 6 K.

The wind speed was low during all experiments, and the prevailing wind direction was south-west. It is not possible to derive how variable wind conditions would influence the results. The same applies for the irradiance, and therefore these two parameters are not introduced in the control of the north window.

The purpose of the experiments was to investigate the local thermal discomfort caused by the window openings under different climatic conditions, and determine rules for when and how to use the windows for ventilative cooling. The rules established about the climatic conditions that allow for window ventilation in Living Lab are presented in Table 4

Table 4. Climatic rules for ventilative cooling through windows in Living Lab (Blandkjenn 2017)

Window combination	Temperature difference between indoor and outdoor	Wind speed	Solar irradiation
South window and one kitchen skylight	6 K – 10 K	< 2 m/s	> 70 W/m <sup>2</sup>
North window and one kitchen skylight	< 6 K	NA	NA

When these climatic requirements were satisfied, the draught rates 1.0 m from the north and south windows were deemed satisfactory when the north window was opened 25 % or 50 %, and when the south window was opened 12.5 % or 25 %. Therefore, these rules were chosen for the IDA ICE simulations to determine the thermal climate and energy consumption when applying the defined window control.

### 3.2 Simulated control

Simulations were realized using IDAICE. Based on the results from Justo Alonso(Justo Alonso, Kirkøen, and Mathisen 2015), using a PI-control does not improve the performance of the control and contrarily increases its difficulty.Improving the simulation form (Kirkøen 2015)a new model of the Living Lab was produced. The control was done following Table 4. In addition,from (Kirkøen 2015) and (Blandkjenn 2017), the windows opened when the average temperature is above 24 °C, and they close when the minimum temperature is below 22 °C.

Table 5. Thermal comfort and energy consumption with different window opening sizes(Blandkjenn 2017)

	Hours of thermal discomfort				Heating and cooling energy	
	Living room [h]	Building total [h]	Decrease living room	Decrease building total	Value [kWh]	Increase compared to closed windows
No openings	105	303			126.2	
Mech. Cooling	0	0	100 %	100 %	341.8	171.8 %
S12.5%, N25%	17	57	83.8 %	81.2 %	139.4	10.5 %
S12.5%, N50%	15	47	85.7 %	84.5 %	144.9	14.8 %
S25%, N25%	15	48	85.7 %	84.2 %	138.9	10.1 %
S25%, N50%	13	38	87.6 %	87.5 %	145.1	15.0 %

Table 5 shows that all the window opening sizes were efficient reducing the over temperatures significantly in the simulated period. However, only the largest opening yielded a number of hours of overheating within the 44 h limit. For the building as a whole, the hours of thermal discomfort decreased at least 81.2 %. Opening the north window 50 % decreased the hours of over temperature by 10 h compared to opening it 25 %. Opening the south window 25 % decreased the over temperature by 9 h compared to opening it 12.5 %. Therefore, it is concluded that larger opening size in both windows will give higher thermal comfort as long as windows are closed within the stated temperature limits. To maximize the thermal comfort without incurring in larger energy use, the north window should be opened 50 % and the south window opened 25 %.

The living room was the warmest zone in the building, with the lowest thermal comfort according to NS15251. Similarly, to the building as a whole, the thermal comfort in the living room increased with the window opening size. With the largest allowed window openings, only 13 hours of occupancy (against 105 without window opening) were outside the comfort requirements categories I and II in the standard. These simulations assume no solar shading, despite that previous studies(Kirkøen 2015; Risnes 2016) have shown the positive effects of solar shading in Living Lab. By using solar shading actively, the thermal climate can be improved further. The energy consumption for heating increased about 10 % in the scenarios

where the south window was opened 12.5 %, and ca 15 % in the scenarios where the south window was opened 25 %. Due to the low outdoor temperatures, high indoor temperature may happen during cold outdoor, and heating needs are triggered when opening windows. The size of opening in the south window was a bigger influence on the energy consumption than the opening in the north window. This is because the south window was used when the outdoor temperatures were lower and therefore the risk of undercooling is higher when the opening is larger. Given the double skin of south window, when the opening is smaller, the airflow is smaller, and will be heated more from the solar gains and heat loss through the inner pane than if we had a larger airflow. The lowest energy consumption is for opening the north window 50 % and the south window 12.5 %. This means that you have a small opening in the cooler periods and large openings when the heating demands are low. The conclusion drawn from the simulations with different window sizes is that a good thermal climate can be achieved with window ventilation without a high increase in energy consumption for heating. Generally, increased openings in the north window gave better thermal comfort - without increasing largely the energy consumption. According to the simulations, the operative temperatures can be kept within comfort categories I and II for 97 % of the time using the largest allowed window openings. Table 6 presents the results of a year energy simulation for this alternative.

Table 6. Full year simulation

Opening sizes	Hours of thermal discomfort [h]	Heating energy [kWh]
No openings	664	5361.0
N 50 %, S 25 %	134	5392.4

The allowed number of hours of thermal discomfort is 259 h, so the chosen solution gives thermal comfort within these limits. The energy for heating increases with 31.4 kWh per year, and ca.86 % of this difference occurs in April and May.

### 3.3 Levels of insulation

This chapter presents simulations done with increasing insulation levels to investigate the effect of natural VC in different types of buildings. The three simulated insulation levels; are the TEK10(Direktoratet for byggkvalitet 2011), the low-energy building(Norge 2013)and a passive house.(Norge 2013).Table 7shows the U-values of walls, roof and floor for the different simulations, and the average U-values of the building body including windows and doors.

Table 7.U-values for simulation scenarios

	U-value walls [W/m <sup>2</sup> ]	U-value floor [W/m <sup>2</sup> ]	U-value roof [W/m <sup>2</sup> ]	Average U- value [W/m <sup>2</sup> ]
TEK10	0.18	0.15	0.13	0.20
Low-energy building	0.15	0.10	0.10	0.18
Passive house	0.10	0.08	0.08	0.15

These simulations were done for May and June in Trondheim. Table 8presents the thermal comfort and energy consumption when applying ventilative cooling in buildings with the different insulation levels.

Table 8: Thermal comfort and energy consumption with and without window cooling

	Hours of thermal discomfort in building		Floor heating energy	
	Value [h]	Decrease	Value [kWh]	Increase
TEK10 closed	193		282.4	
TEK10 open	33	82.9 %	327.7	16.0 %
Low-energy closed	280		155.1	
Low-energy open	41	85.4 %	176.9	14.1 %
Passive house closed	452		57.5	
Passive hours open	44	90.3 %	72.3	25.7 %

Without window cooling the thermal comfort was worse for buildings with lower U-values, because more heat is trapped within the building. However, when applying window cooling the achieved thermal comfort is almost identical in the three simulated scenarios. Therefore, the higher is the insulation level, the larger is the ventilative cooling potential. This corresponds to the findings in literature that the potential of ventilative cooling is larger in well-insulated buildings (Finocchiaro, Wigenstad, and Hestnes 2010). The absolute increase in energy consumption is lowest when the U-value is lowest. Interestingly, the percentage increase in energy consumption when applying ventilative cooling is the smallest in a low-energy building. This can be explained by the very low energy consumption with passive house standard, where even the small amount of 14.8 kWh is a 25.7 % increase.

#### 4 CONCLUSIONS

This paper presents a control strategy for providing ventilative cooling by means of window use in a zero emission building located in a cold climate. The results from the simulations implied that there would be a severe risk of overheating in Living Lab if no active or passive cooling techniques are applied, mostly because shading is not considered. The results showed nonetheless that ventilative cooling could prevent overheating without significantly increasing the energy demand. This is proved achievable with a control grounded on on-off regulation and temperature difference limits, as they seem to be the most affecting parameters. The opening of the windows is very much based on the draught rate limitations; it proves that increasing window opening yields larger heating demands if the control is not accurate. The building insulation level also affects the energy consumption for both the heating and cooling, the lower the U-value, the lower demands for heating but higher demands for cooling and the larger the ventilative cooling potential.

#### 5 ACKNOWLEDGEMENTS

This work has been supported by the Research Council of Norway and several partners through the SINTEF/NTNU “The research centre of Zero Emissions Buildings” (ZEB). Grant number 193830. And the industrial project Ventilative Cooling with ENOVA.

## 6 REFERENCES

- Berge, M., and H.M. Mathisen. 2016. 'Perceived and measured indoor climate conditions in high-performance residential buildings', *Energy and Buildings*, 127: 1057-73.
- Berge, Magnar, Judith Thomsen, and Hans Martin Mathisen. 2016. 'The need for temperature zoning in high-performance residential buildings', *Journal of Housing and the Built Environment*: 1-20.
- Blandkjenn, S. 2017. 'Ventilative cooling of Zero Emission Buildings (ZEB)', NTNU.
- Direktoratet for byggkvalitet, Norway. 2011. 'Veiledning om tekniske krav til byggverk, TEK10.'
- EQUA. 2016. "IDA Indoor Climate and Energy." In. Stockholm: EQUA Simulation AB.
- Finocchiaro, L., F. Goia, S. Grynning, and A. Gustavsen. 2014. "The zeb living lab: a multi-purpose experimental facility." In *IEA EBC Annex 58 Expert Meeting*. Ghent.
- Finocchiaro, Luca, Tore Wigenstad, and Anne Grete Hestnes. 2010. "Potential of passive cooling, natural ventilation and solar control in cold climates office buildings." In *Renewable Energy Conference*. Trondheim.
- Georges, L., K. Wen, M. Justo Alonso, M. Berge, J. Thomsen, and R. Wang. 2016. 'Simplified space-heating distribution using radiators in super-insulated apartment buildings', *Energy Procedia*, 96: 455-66.
- Georges, Laurent, Kang Wen, Maria Justo Alonso, Magnar Berge, Judith Thomsen, and Ruzhu Wang. 2016. "Simplified space heating distribution using radiators in super insulated apartment buildings, ." In *SBE 16 Tallinn and Helsinki conference , Build green and renovate deep*. Tallinn and Helsinki.
- Goia, Francesco, Luca Finocchiaro, and Arild Gustavsen. 2015. "The ZEB Living Laboratory at the Norwegian University of Science and Technology: a zero emission house for engineering and social science experiments." In *7PHN Sustainable Cities and Buildings*. Copenhagen: The Research Centre on Zero Emission Buildings
- Justo Alonso, Maria , Cathrine Kirkøen, and Hans Martin Mathisen. 2015. 'Energy use consequences of ventilative cooling in a ZEB residential building.' in, *36th AIVC Conference 5th TightVent Conference 3rd venticool Conference. : Effective ventilation in high performance buildings, Madrid, Spain, 23-24 September 2015* (Air Infiltration and Ventilation Centre (AIVC)).
- Kirkøen, Cathrine. 2015. 'Ventilative cooling in Living Lab', Master's thesis, Norwegian University of Science and Technology.
- Kolokotroni, Maria, and Per Heiselberg. 2015. "Annex 62 Ventilative cooling state-of-the-art review." In. <http://venticool.eu/annex-62-publications/>: International Energy Agency.
- L. Georges, F. Håheim, and M. Justo Alonso. 2017. 'Simplified space-heating distribution using radiators in super insulated terraced houses', *Energy Procedia*.

- Mlecnik, E., T. Scutze, S. Jansen, G. de Vries, H. Visscher, and A. van Hal. 2012. 'End-user experiences in nearly zero-energy houses', *Energy and Buildings*.
- Norge, Standard. 2013. "NS 3700:2013, Kriterier for passivhus og lavenergibygninger. Boligbygninger. ." In *Criteria for passive houses and low energy buildings (Residential buildings.)*
- Risnes, Annelin. 2016. 'Indoor Environment in ZEB Living Lab', Master's thesis, Norwegian University of Science and Technology.
- Samuelsson, M. and Luddeckens, T. . 2009. 'Passive houses from a users perspective.'
- Sundell, J. 2004. 'On the history of indoor air quality and health', *Indoor Air*, 14, 51 – 58.
- Venticool. 2013. 'The international platform for ventilative cooling', Venticool.

# Coupling night ventilative and active cooling to reduce energy use in supermarkets with high refrigeration loads

Zoi Mylona<sup>\*1</sup>, Maria Kolokotroni<sup>1</sup> and Savvas Tassou<sup>1</sup>

*1 RCUK National Centre for Sustainable Energy Use  
in Food Chains (CSEF)  
Brunel University London  
Kingston Lane, Uxbridge, UB8 3PH, UK  
\*Corresponding author: zoi.mylona@brunel.ac.uk*

## ABSTRACT

Night ventilation is used extensively as a low energy strategy to cool buildings in climates where night temperatures are suitable. It can be used for spaces utilising natural or mechanical ventilation systems as well as active refrigerant cooling. Most published work focuses on domestic and relatively simple in operation commercial buildings such as offices. This paper presents a study of the cooling benefits of night ventilation for frozen food supermarkets with high cooling demand. Supermarkets present a unique space conditioning challenge because of the interaction between the HVAC system and the refrigerated display cabinets. HVAC systems are the largest consumer of energy after refrigeration in supermarkets depending on system design, geographical location and controls. The most common HVAC system used in supermarkets is the constant air volume (CAV) system integrating heating, cooling and ventilation in one system although different types of systems to decouple cooling and ventilation such as a combination of variable refrigerant flow (VRF) for heating and cooling and mechanical balanced or extract ventilation have been tried out to improve thermal comfort and reduce energy use.

This paper presents two case-studies (CS) which differ from typical supermarkets as they belong in a frozen food supermarket chain. CS1 is served by a typical CAV system for heating, cooling and ventilation (coupled HVAC), while CS2 provides conditioned air through a VRF system and ducted extract ventilation (decoupled HVAC). First, an analysis of their measured energy use and indoor environmental conditions is presented to highlight similarities and differences of the two systems. Then, a coupling approach for dynamic simulation of the air-conditioning with the refrigeration system by EnergyPlus is presented and the resulting models are validated against the monitored data from the two case-study supermarkets. Using the validated models, a parametric study of the coupled operation of night ventilation and active cooling for the climatic conditions of south east England is carried out and optimisation strategies are modelled. The parametric analysis indicates that the air flow rate of night ventilation and climatic conditions are significantly correlated with the impact of night ventilation on the total energy consumption of the supermarket. Simulations have revealed that night ventilation results to lower cooling energy use for both HVAC systems. Night ventilation is in use in CS1 but optimised control strategy with lower air flow rate reduced the total annual energy use of the store by 3% due to reduction in fan energy use and active cooling, although refrigeration energy use was remain stable. In CS2 active cooling during the night is replaced with night ventilative cooling which leads to a reduction of energy use by 3.3%. Such a percentage reduction equates to 35 kWh/m<sup>2</sup>/annum. The paper discusses the differences of the two systems (all air or decoupling of ventilation from heating/cooling) in terms of HVAC energy use, total energy use, impact on the refrigeration system and the importance of controls for the night ventilative cooling.

## KEYWORDS

Supermarket, Energy Use, HVAC, Night Ventilation, EnergyPlus, Frozen food, Environmental and Energy monitoring

## 1 INTRODUCTION

Retail stores are among the most energy-intensive commercial buildings, consuming two or three times as much energy per unit floor area as office buildings. In fact energy consumption in food supermarkets is around 3.5% of the total UK energy consumption (Tassou et al., 2011). Currently, there are over 1 million supermarkets in Europe (CREATIV, 2014). Thus,

just a small percentage reduction in energy use can result to substantial savings. Estimating 25% energy saving in Europe in supermarkets will result in 31 TWh of annual electricity savings which equates to carbon reductions of 16.2 million tons (CREATIV, 2014). Heating, Ventilation and Air-Conditioning (HVAC) systems contribute to a considerable amount of the total energy use and it is estimated that around 20%-35% of a supermarket's energy use consumed in HVAC. Food retail markets are complex environments designed to have high visibility display of goods with sufficient thermal comfort to encourage longer stay for the customers. The refrigeration requirements of the display goods and indoor environmental conditions are sometimes in conflict because of the significant heat exchanges between them. Thus, optimised control strategies for HVAC systems are required in order to achieve acceptable environmental conditions for customers and good operation of the refrigeration system.

Night Cooling (NC) has been receiving attention in recent years because of the energy saving potential mainly in buildings with reasonably high thermal mass. Most published work focuses on domestic buildings and offices. This paper is a study for the energy use and the potential for savings due to mechanical night ventilative cooling of the HVAC systems of frozen food supermarkets. Few studies to date have considered ventilative cooling strategies for supermarkets (Li-Xia Wu et al., 2006).

Many supermarkets use all air constant volume systems as the HVAC system. This system provides ventilation, heating and cooling by conditioning air in the central plant and providing it through overhead distribution ductwork to different parts of the stores, termed coupled HVAC. However, there are many supermarkets which use ceiling mounted cassette type air recirculating units for cooling and/or heating. In other words, the heating and cooling systems are decoupled from the ventilation which is provided through separate (usually exhaust only) ductwork, termed decoupled HVAC.

The two case study stores were selected according to the above categorisation. CS1 is a refurbished two storey building located in central west London using an all air constant air volume HVAC which represents the coupled HVAC case. CS2 is a new purpose built store located in a suburban commercial area in southern London. The heating and cooling requirements are fulfilled by a variable refrigerant flow (VRF) system with ceiling mounted cassettes in the sales area and represents the decoupled HVAC case as there is separate ductwork for extract mechanical ventilation. The refrigeration systems are stand-alone which cause remarkably high internal heat gains due to heat released to the sales area from the condensers. For that reason, the cooling demand is higher than heating (Mylona et al., 2017). Firstly, an analysis of the measured energy use and indoor environmental conditions of the stores is presented and the differences that observed are discussed. It continues to present the baseline models developed by EnergyPlus which enables the coupling approach of HVAC with the refrigeration system. The models are used for parametric analysis of the NC control strategy applied to stores as NC could reduce the high cooling requirements.

## **2 CASE STUDY STORES CONFIGURATION**

The two case study stores that were selected belong in the same supermarket chain with similar products and refrigeration system but different HVAC systems. CS1 is in a city location and surrounded by commercial buildings. It is a refurbished two storey heavy-weight (BS EN ISO 13790:2008) building with the sales area (469 m<sup>2</sup>) on the ground floor while the second floor is used as a storage area. The coupled HVAC system for the sales area is roof mounted AHU with a DX cooling coil (88kW) and an electric heating coil (24kW). The set point temperatures have been set to 19.5°C for heating and 20.5 °C for cooling. It is a Constant Air Volume (CAV) system which provides sales area with 6 m<sup>3</sup>/s in trading hours through 11 four way diffusers, 1 three-way and 3 two way blow fixed blade diffusers. There is also an electric door heater rated at 18kW. Ventilation rates for the exhaust system during

trading hours are set to 6 ach for sales and 1 ach for the storage area. There are also supplementary extract ducts only above the open front multi deck cabinets whose warm air is either exhausted directly to the atmosphere or used to heat the storage area on the ground floor when heating is required. The lighting system is typical T8 type fluorescent for the sales area. They consist of luminaires with 3 lamps; 21 in the tills area and 63 in the display area. LED strips are installed in the north-east and back sides of the sales area which operate 24hrs. CS2, a medium-weight building, is in a typical small out-of-town retail centre. It is single storey newly built with 315 m<sup>2</sup> sales area. The decoupled HVAC system of the sales area is a VRF system for both heating and cooling. Two equally sized outdoor condensing units provide total heating output of 113 kW and cooling output 101 kW delivered to sales area only through 7 ceiling cassettes and 1 door heater. The HVAC system is operated 24h with 20-21°C set point temperature for both cooling and heating; the heat pump works either as a compressor or evaporator controlled by the BEM system. Extraction of the air from sales and staff area is by an extract fan operated 24h hours. Ventilation rates for the exhaust system during trading hours have been set to 6 ach for staff areas and sales area, 10 ach for restrooms and cloaks and 1 ach for the storage area. During night time the exhaust fan is set to lower speed (3ach). The lighting luminaires are typical T8 type fluorescent for the sales area. They consist of luminaires with 3 lamps; 23 in the tills area and 30 in the display area. LED strips are installed in the north-east and back sides of the sales area which operate 24hrs. The refrigeration system consists of plugged-in cabinets and freezer and chiller coldrooms. The types of cabinets and the loads are presented in Table1.

Table 1: Refrigeration equipment and loads of CS1 & CS2

Case Study	Chilled food open front multi-deck cabinets	Lift up lid frozen food cabinets	Open top case frozen food cabinets	Freezer Coldroom	Chiller Coldroom
CS1	10	70	3	60m <sup>2</sup>	12 m <sup>2</sup>
<b>Refrigeration Load (kW)</b>	<b>20.3</b>		<b>30.7</b>	<b>30</b>	<b>5.2</b>
CS2	7	58	3	29m <sup>2</sup>	6m <sup>2</sup>
<b>Refrigeration Load (kW)</b>	<b>10.4</b>		<b>26.3</b>	<b>8</b>	<b>2.3</b>

### 3 MONITORING RESULTS ANALYSIS

#### 3.1 Energy Use

Figure 1 and 2 present an overview of hourly measured energy data using box whisker mean (BWM) plots. The mean hourly energy use of the months is presented based on hourly data. Figure 1 shows 5 years data for CS1. Winter 2013 was colder than the other winters (approximately 535 higher HDD); therefore energy use is higher during this winter. The store has a consistent energy demand during cold months with average trading hours energy use at around 0.14 kWh/m<sup>2</sup>sa with peaks on warm months 0.18kWh/m<sup>2</sup>sa before falling to the non-trading hours energy use (75<sup>th</sup> percentile). For CS2 (Figure 2) winter 2015 was colder than 2014 (average HDD for June 2013-May 2014 was 1760 and for June 2014-May 2015 was 1908) and this resulted in higher energy use. CS2 presented an average 0.14 kWh/m<sup>2</sup>sa (25<sup>th</sup> percentile) during trading time with peaks on warm months at around 0.17 kWh/m<sup>2</sup>sa.

As the HVAC of the CS1 is not operating during night (in comparison with CS2 where HVAC is on 24h) and only free night cooling is in operation, there is a difference between the non-trading time energy use between the two stores. CS2 energy use during non-trading times observed to be around 0.10 kWh/m<sup>2</sup>sa. On the other hand, energy use of CS1 during non-trading hours ranged from 0.09 to 0.12 kWh/m<sup>2</sup>sa.

Average annual energy use is 1103.3 kWh/m<sup>2</sup>sa for CS1 and 1117.3 kWh/m<sup>2</sup>sa for CS2 which are at the upper range of supermarkets and at the lower range of the convenience stores (Mylona et al., 2017) because of the higher refrigeration load.

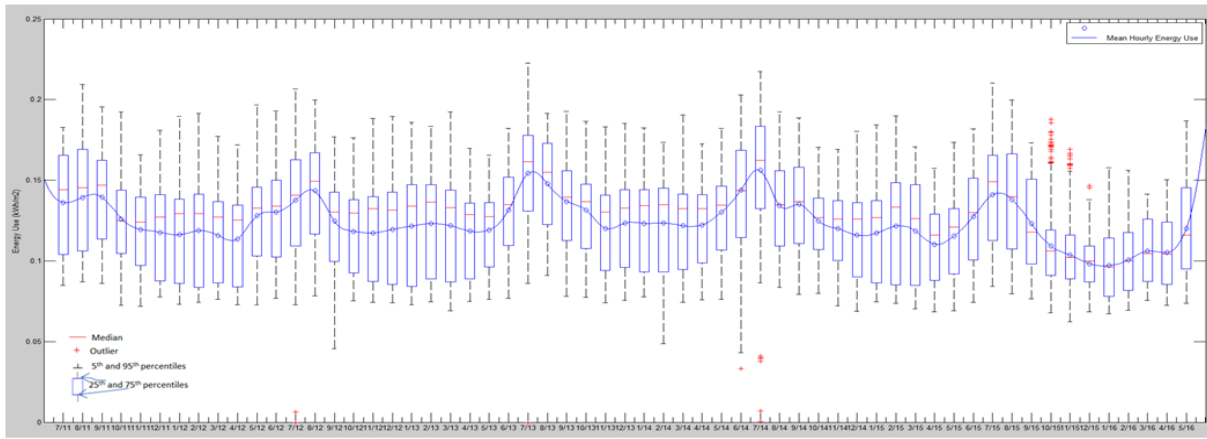


Figure 1: BWM plot of hourly measured energy use per sales area (July 11- June 16)

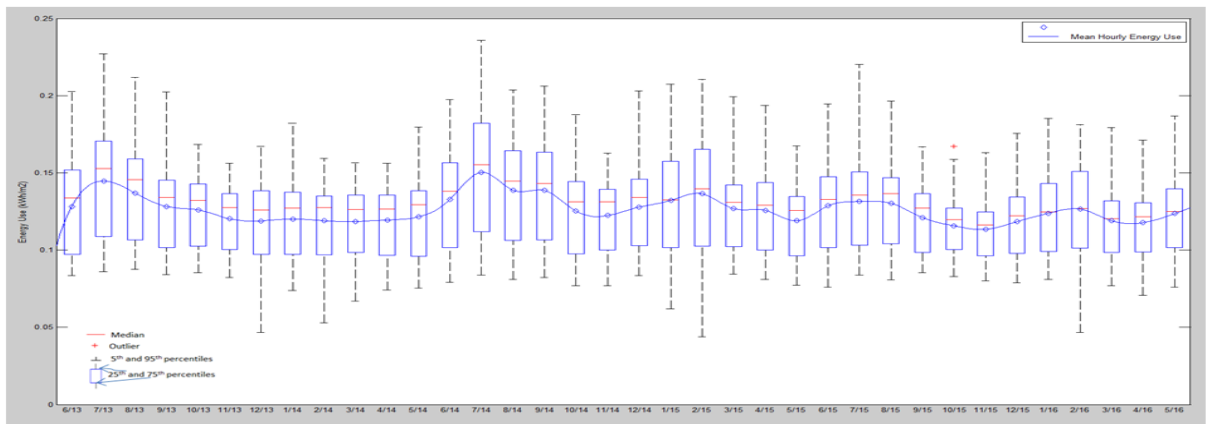


Figure 2: BWM plot of hourly measured energy use per sales area (June 13- June 16)

Figure 3 presents the correlation of their daily energy use with the outdoor air temperature. It is observed that for both stores there is an outdoor temperature where the daily energy use is at its lowest level. This is around 9°C for CS1 and between 8°C to 12°C for CS2. Above these temperatures the cooling requirements of the buildings increases and consequently the daily energy use; from 25%-50% for CS1 and from 19% to 42% for CS2. The maximum daily energy use monitored for warm days is almost the same for both stores but slightly higher for CS1.

However, a different pattern emerges for cold days and this is due to the different control strategy of the HVAC systems. CS1 with the free cooling during night and non 24h HVAC system, presented lower daily energy use during cold days. The 24h HVAC system in CS2 resulted in higher heating requirements and thus higher daily energy use during cold days.

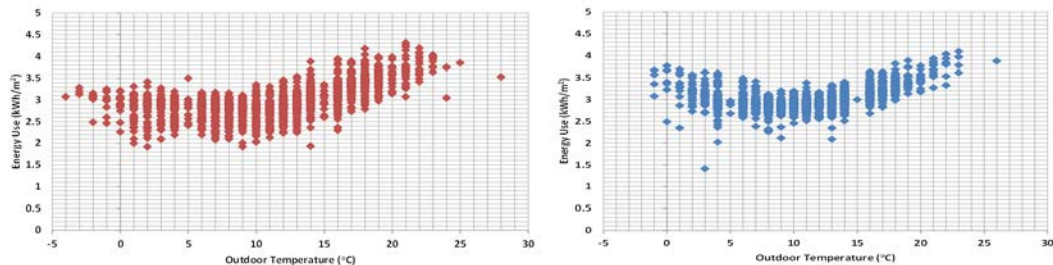


Figure 3: Daily Energy Use per sales area according to different outdoor temperatures (left: CS1, right: CS2)

### 3.2 Indoor environmental conditions

Figures 4 and 5 present the results in BWM plots for air temperatures for two months (July 2014 and December 2014), indicative for warm and cold periods respectively. In July and during trading hours, air temperature varied significantly between the days of the month and

ranged between 22°C to 24°C for the tills area and 21°C to 23°C for the display area. July 2014 was the warmest month of this summer and during the days of the highest outside temperature the temperature inside the store (both tills and display area) reached 28°C. For CS2, air temperature ranged between 22°C and 23.5°C in the tills area and between 19.5°C and 22°C in display area.

Internal patterns of temperature seems to follow external maximum air temperatures and the continuous opening of the door and heat gains of the single glassed windows in both case study stores affect significantly internal air temperature. This is the reason why the air temperature in the display area differs from the air temperature measured in the tills area. This is observed more remarkably in the CS2 where the temperature in the display area found to balance around the setpoint temperature (21°C) while the tills area presented temperature 1°C to 2°C higher or lower for warm months and cold months respectively. CS1 seemed to present insignificant fluctuations from the setpoint temperature (19.5°C) for December while a bigger difference was observed for the July (1.5°C to 2.5°C above the setpoint).

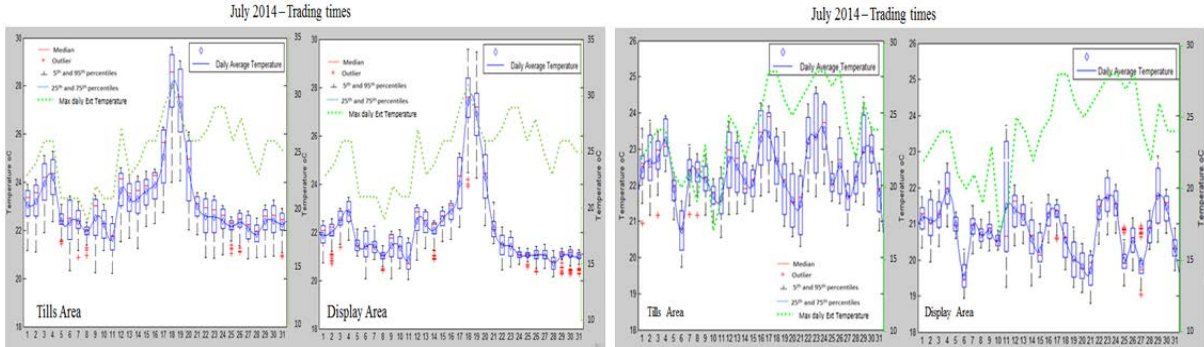


Figure 4: BWM plots of measured air temperature in sales area (tills and display) for June 2014 during trading times (left: CS1, right: CS2)

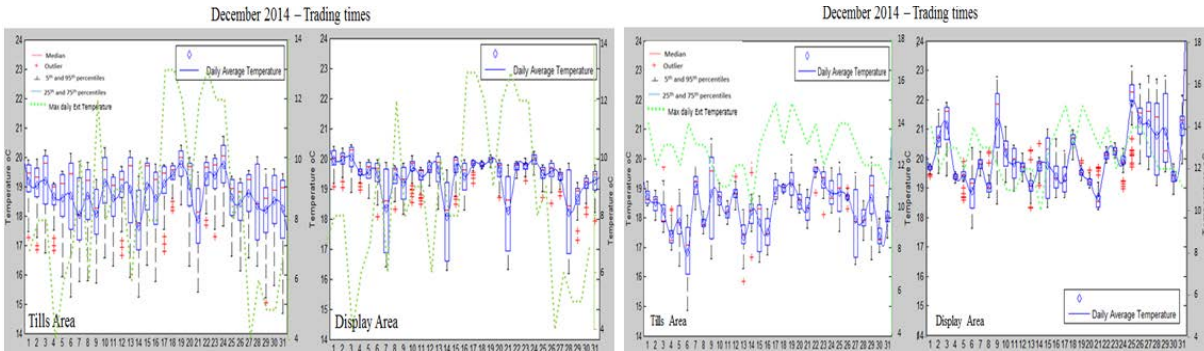


Figure 5: BWM plots of measured air temperature in sales area (tills and display) for December 2014 during trading times (left: CS1, right: CS2)

During non-trading times (Figures 6 and 7), different control strategy is used for the two case study stores as described in section 2. For CS1 where the ventilation is coupled with the heating and cooling system and the free cooling is in operation, the air temperature of the tills area ranged between 20°C and 22°C but reached up to 24°C during the warmest days of the month. The same applies for the display area. During December the effect of the free night cooling is significant due to outside conditions permitting and the air temperature of both tills and display area varied between 16°C (which is the minimum setpoint temperature that free night cooling is active) to 18°C.

For CS2, where the ventilation is decoupled from heating and cooling system and the HVAC is in operation 24h, during non-trading times of July, average air temperature in the tills area fluctuates between 21°C and 22°C, slightly higher than the setpoint temperature (20-21°C). In the display area the average air temperature is 1°C lower than the tills area. The opposite was

observed in December 2014; average air temperature in the tills area was 1°C lower than the temperature in the display area. In both cases, internal air temperature variations follow external daily minimum temperature pattern.

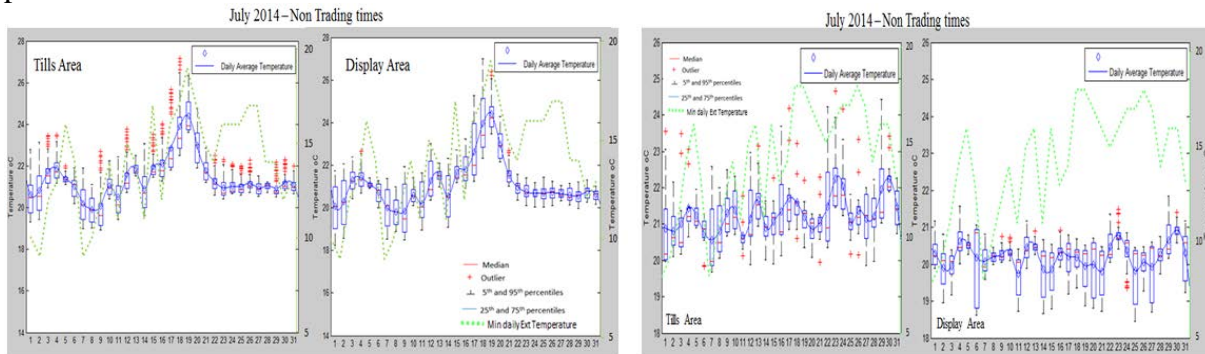


Figure 6: BWM plots of measured air temperature in sales area (tills and display) for July 2014 during non-trading times (left: CS1, right: CS2)

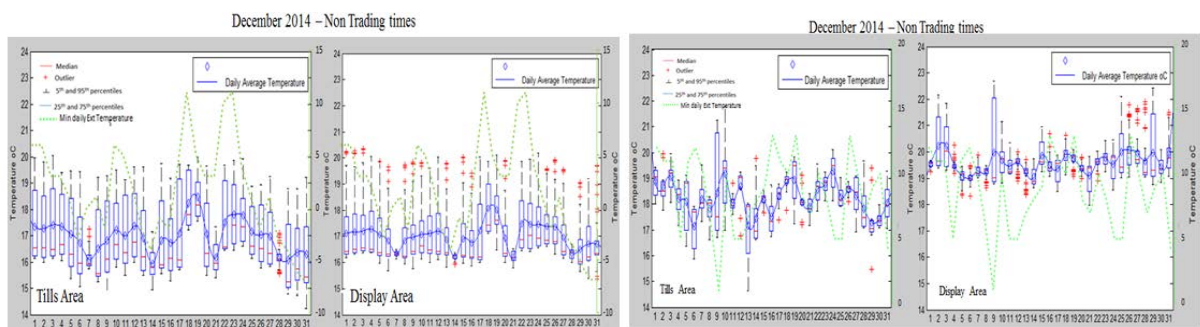


Figure 7: BWM plots of measured air temperature in sales area (tills and display) for December 2014 during non-trading times (left: CS1, right: CS2)

Relative Humidity (RH) does not present significant differences between tills and display areas; 40%-75% for CS1 and 40%-65% for CS2 for warm months and unremarkably lower in cold periods. Carbon dioxide concentration measurements ranged between 400 ppm during non-trading times and 650 ppm during trading times for both case study stores indicating good ventilation provision (CIBSE, 2015) (ASHRAE, 2013).

#### 4 ENERGYPLUS BASELINE MODEL DEVELOPMENT AND VERIFICATION

The model development of the baseline models and the verification methodology has been presented in (Mylona et al., 2017) where the CS2 model development is presented in detail. The same methodology and procedure was followed for CS1.

Following two levels of calibration; level 1 based on available design data to create the as-built model and level 2 that included the as-built and operating information, the final thermal model for CS1 with 14 thermal zones was validated against measured data for both energy use and temperature conditions for a year. The building's annual energy use from June 2014 to May 2015 is 1103.6 kWh/m<sup>2</sup> sales area. The final calibrated model prediction is 1098.5 kWh/m<sup>2</sup> sales area (a deviation of -0.5%). Regarding CS2, the thermal model that was developed has 9 thermal zones and the final calibrated model prediction is 1104.3 kWh/m<sup>2</sup> sales area while the measured energy use from June 2014 to May 2015 was 1143.4 kWh/m<sup>2</sup> (a deviation of 3.4 %).

ASHRAE Guideline 14-2002 defines the evaluation criteria to calibrate a simulation model. Monthly and hourly data, as well as spot and short term measurements can be used for calibration. Mean Bias Error (MBE) and Coefficient of Variation of the Root Mean Squared Error (CVRMSE) are used to evaluate the model uncertainties (ASHRAE, 2002).

According to the results, both case study stores EnergyPlus models presented MBE and CVRMSE values within acceptable limits for both energy use and indoor air temperature.

## 5 RESULTS AND DISCUSSION

A previous study for night ventilation implementation to a supermarket has concluded that longer night cooling activation results to fewer hours of AC system operation and higher energy savings (Li-Xia Wu et al., 2006). However, studies for offices and other non-domestic buildings have indicated that three control aspects should be taken into consideration (Kolokotroni, 1998); duration, system initiation and system continuation in order to maximise energy savings. In this case study, the following rules were implemented: i) initiation:  $T_{out} < T_{in}$ , ii) continuation:  $T_{out} < T_{in}$  and  $T_{out} - T_{in} < T_{offset}$  and iii) termination: continuation rule and  $T_{in} = T_{min}$ .

The continuation rule ensures that the outside air brought in is effective in cooling the building. When the temperature difference between inside and outside air ( $T_{offset}$ ) is low, the incoming air will have little effect on cooling while the ventilation fan energy use will increase the total energy use. However, if the outside air temperature is significantly lower than the inside air temperature,  $T_{min}$  will be achieved fast and the duration of night ventilation is decreased (Aria & Akbari, 2007).

Moreover, although NC could increase the total energy savings of the stores, attention should be paid in their conditions (temperature and RH) brought in store as it may affect the cold surfaces of the cabinets from condensation or it may be harmful to the operation of the refrigeration system or its controls. The stores' LT cabinets are glass lift up lid cabinets which during NC operation remain closed so the evaporator coils are not affected by the ambient air (if hot or humid) and thus crucial problems are not created in the evaporator coils operation. However, action might be taken to prevent condensation on the surface of the glass. Fogging and risk of condensation on the external side of the glass or the multi deck cabinets' curtains might occur in humid climatic conditions while reducing the ambient temperature.

### 5.1 Coupled HVAC: CS1

NC is already in operation in CS1 during non-trading times. The system is designed to provide free night cooling with  $6 \text{ m}^3/\text{s}$  when the return air and outside air temperature have  $1^\circ\text{C}$  difference and until the inside temperature reaches  $16^\circ\text{C}$ .

The parametric analysis was performed for different airflow rates according to fan speed ( $1-6 \text{ m}^3/\text{s}$ ),  $T_{offset}$  ( $1-20^\circ\text{C}$ ) and  $T_{min}$  ( $10-17^\circ\text{C}$ ). Minimum temperature inside the store was chosen not to fall below  $10^\circ\text{C}$  in order to avoid condensation on the glass cabinets. While setting the  $T_{min}$  to the lowest levels ( $10^\circ\text{C}$ ) and assuming that glass surface temperature does not drop below  $0^\circ\text{C}$ , RH less than 50% would ensure avoidance of condensation.

Figure 8 presents fan, heating and cooling energy use for different air flow rates,  $T_{offset}$  and  $T_{min}$ ; the combinations are integrated and are presented as a range of energy use in the graph. Figure 9 presents the cooling energy use for different  $T_{offset}$  and  $T_{min}$ . The air flow rate during night cooling plays an important role as the higher airflow increases the fans' energy use. However, low air flow rates could have similar effect on cooling demand with a reduction of heating requirements during the following day. In Figure 8, the fans' annual energy use range is indicated as a result of the different  $T_{offset}$ . Higher air flow rate has wider range because the reduction of the internal temperature to  $T_{min}$  is achieved fast and the duration of the NC is decreased.

For lower air flow rates there is a point where the maximum total energy use reduction occurred; energy use starts increasing until reaching the point where NC is not effective (total energy use equals the total energy use when NC is off) (Figure 10). This is due to the increase of the cooling energy which afterwards leads to an increase of the total energy use (Figure 9). This point is observed to range between  $5-7^\circ\text{C}$ . Refrigeration system energy use decreases

with lower  $T_{min}$  but after 5-7°C  $T_{offset}$  starts increasing again until the refrigeration energy use observed when NC is not in operation (Figure 11). The optimum combinations of parameters leads to up to 3 % of the total energy use from the baseline model – this equates to energy use reduction of 35.3 kWh/m<sup>2</sup>/year in the store.

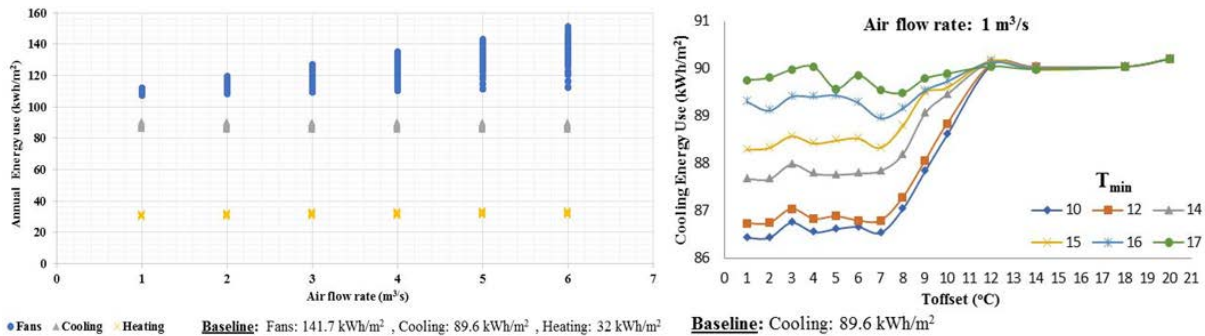


Figure 8: Heating, Cooling and Fans Energy Use for different air flow rates, Figure 9: Cooling Energy Use for different  $T_{offset}$  and  $T_{min}$ .

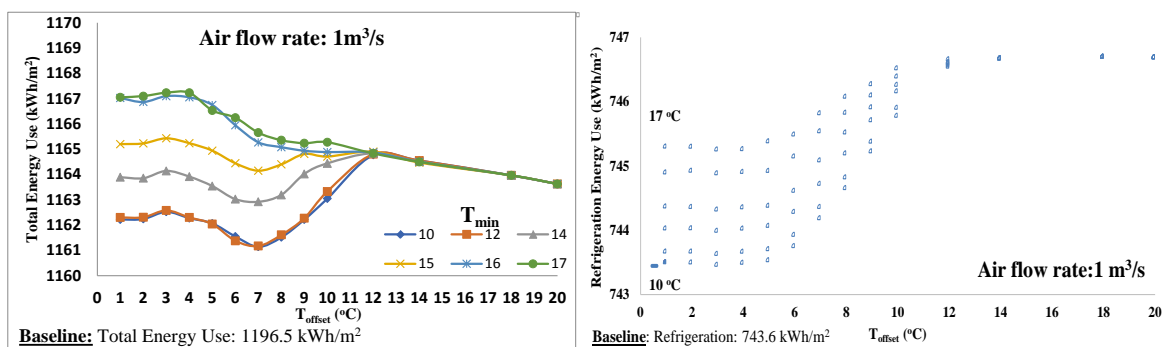


Figure 10: Total Energy Use for different  $T_{offset}$  and  $T_{min}$  Figure 11: Refrigeration Energy Use for different  $T_{offset}$  and  $T_{min}$

## 5.2 Decoupled heating/cooling from ventilation: CS2

For CS2 two different ways of providing night cooling were studied; exhaust and intake night ventilation. The same parameters as CS1 were used for the parametric analysis; different airflow rates according to fans speed (1-10 ach),  $T_{offset}$  (1-20 °C) and  $T_{min}$  (10- 17°C).

For both scenarios the HVAC control strategy of the store changed to facilitate night ventilation as follows: operation between 6:00 to 23:00 for weekdays and Saturdays and 9:00 to 18:00 for Sundays rather than 24h of the baseline model. This change alone would save 41 kWh/m<sup>2</sup> sales area per year without any effect on the refrigeration system operation and consumption but with significant decrease in the HVAC due to reduction in fans energy use and cooling requirements.

Without any change to the HVAC system of the CS2, control strategy for exhaust night ventilation resulted to the lowest air flow rates resulting to lower total energy use due to reduced fans energy consumption (Figure 12). Higher air flow rates presented to have strongest correlation with the  $T_{offset}$  as mentioned for CS1; while  $T_{offset}$  increases, a sharper reduction is occurred and this is because the cold air that is brought inside has bigger effect on the inside air temperature and  $T_{min}$  is achieved quickly and thus the duration of the NC is decreased.

It is also observed that for low air flow rates there is a specific  $T_{offset}$  where the total energy use starts slightly increasing ( $T_{offset} > 5^{\circ}C$ ). After that point, where the optimum total energy use reduction occurs, the cooling energy demand increases and with higher  $T_{offset}$  the cooling energy use increases more significantly as the NC is not more effective (Figure 13). For higher air flow rates this  $T_{offset}$  increases up to 7 °C. The optimum combinations of the parameters lead to 3.6% reduction in the total energy use which equals to 40.8 kWh/m<sup>2</sup> per

year. Refrigeration energy use was found to follow the same pattern with what was analysed for CS1; after a specific  $T_{offset}$  refrigeration energy use increases to the levels that NC is no more effective.

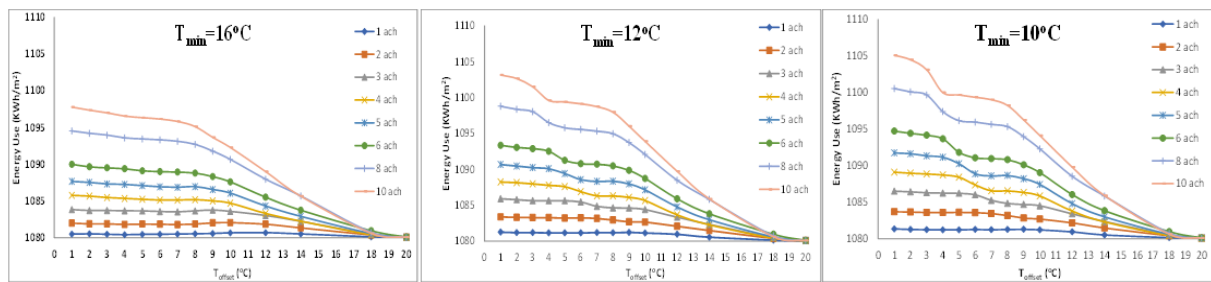


Figure 12: Total Energy Use with different air flow rates for different  $T_{offset}$  and specific  $T_{min}$ .

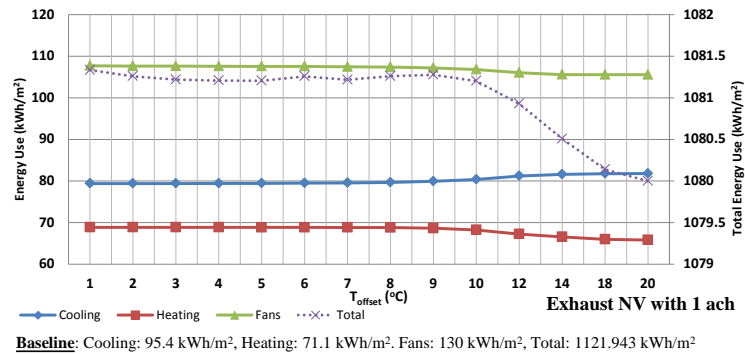


Figure 13: Cooling, Heating and Fans Energy Use for different  $T_{offset}$  for  $T_{min}=10^{\circ}\text{C}$  and with 1 ach air flow rate

For intake NC the results agreed with what has been discussed for exhaust NC control strategy but with results from CS1 as well. The air flow rate is a key parameter for the night cooling and the lower air flow rates lead to lower total energy use due to fans energy use decrease but with the same effect of night cooling due to the fact that the night cooling duration is bigger. However, as is proposed for CS1 for lower air flow rates there is point that the cooling requirements start increasing and NC is no more effective ( $T_{offset} > 7^{\circ}\text{C}$ ). With higher  $T_{offset}$  than  $2^{\circ}\text{C}$ , although the cooling energy demand increases, the fans energy usedrops more significantly and leads to lower total energy use. The highest total reduction observed for lower air flow rates. As the  $T_{min}$  increases the duration of the NC is decreasing and unremarkable reduction is observed on the total energy use. A reduction of around 3.2% on the total energy use (35 kWh/m<sup>2</sup>/annum) is calculated for this case study for intake night ventilation.

## 6 CONCLUSIONS

Two frozen food supermarkets were monitored (energy use and environmental conditions), EnergyPlus models were developed and validated against measurements and night ventilative cooling, taking into account interaction with HVAC and refrigeration systems, was explored as a strategy to reduce energy use. The two stores have the same refrigeration system but different HVAC; the bigger and the older (CS1) uses all air HVAC system with heating and cooling coupled with ventilation, the smaller and the newer (CS2) uses a different system providing heating and cooling (VRF) decoupled from ventilation.

- Energy use of both stores is similar and internal air temperature does not fluctuate significantly from setpoints. CS2 had more constant conditions than CS1.
- NC has good potential for the specific case studies as they include high refrigeration loads which are delivered with plugged-in cabinets. Cooling demand is significant higher than heating.

- Control strategy for NC plays an important role as proved in CS1 where NC is already in operation but with better controls bigger reductions are achieved.
- CS2 is cooled during the night to maintain the setpoint 24hrs. Implementing free exhaust or intake NC leads to a reduction in the total energy use.
- Simulations indicate that longer period of NC operation leads to higher energy savings enabled by lower air flow rates which have a small impact on fans energy use but cool effectively as longer period is needed to reach  $T_{min}$ .
- Inside-outside temperature is an important NC parameter. Parametric analysis indicated that optimum savings occurred if the air inside the stores has 5-7°C difference with the outside air. The higher the air flow rate, the higher this difference should be for better changes.
- With NC, cooling demand during the day is decreased in both stores.
- Refrigeration system energy use has an unremarkable reduction; with  $T_{offset}$  higher than 5-7 °C, refrigeration energy use starts increasing until it reaches energy use without NC.
- Although NC has good potential for total energy savings of the supermarkets, condensation problems might arise on the glass surface of the frozen food cabinets and care should be taken in the selection of the control parameters.

## 7 ACKNOWLEDGEMENTS

This work is carried out as part of the RCUK Centre for Sustainable Energy Use in Food Chains (EP/K011820/1) project. Thanks are due to Graham Ireland and Rick Jenkins for providing energy data and facilitating access to the case-study stores.

## 8 REFERENCES

- Aria & Akbari. (2007). A predictive Nighttime ventilation algorithm to reduce energy use and peak demand in an office building. *Energy and Power Engineering*, Volume 7, p 1821-1830.
- ASHRAE. (2002). *ASHRAE Guideline 14-2002, Measurement of Energy and Demand Savings*.
- ASHRAE. (2013). *Standard 62.1, Ventilation for Indoor Air Quality*.
- BS EN ISO 13790:2008. *Energy performance of buildings-Calculation of energy use for space heating and cooling*.
- CIBSE. (2015). *Guide A: Environmental Design, Chapter 1 Table 1.5*.
- CREATIV, I. E. (2014, February 14). *The future energy effective supermarket*. Retrieved from SINTEF: <http://www.sintef.no/projectweb/creativ/the-future-energy-effective-supermarket/>
- Kolokotroni, M. (1998, March 10). Night Ventilation for cooling: Field Tests and design Tools. *Low-Energy Cooling Technologies for Buildings: Challenges and Opportunities for the Environmental Control of Buildings*, Professional Engineering Publishing, London, UK, pp. 33-44.
- Wu L., J. Zhao, Z. Wang (2006). Night ventilation and active cooling coupled operation for large supermarkets in cold climates. *Energy and Buildings*, Volume 38 (12), p 1409-1416.
- Mylona Z., M. Kolokotroni, S. Tassou (2017). Frozen food retail: Measuring and modelling energy use and space environmental systems in an operational supermarket. *Energy and Buildings*, Volume 144, 129-143.
- Tassou S, Y. Ge, A. Hadaway, D. Marriot (2011). Energy consumption and conservation in food retailing. *Applied Thermal Engineering*, 31(2-3), pp. 147-156.

# Mixed-mode ventilative cooling opportunity for an existing shopping mall retrofit

Marta Avantaggiato<sup>\*1,2</sup>, Annamaria Belleri<sup>2</sup>, Michele De Carli<sup>2</sup> and Roberto Lollini<sup>1</sup>

*1 EURAC Research  
Viale Druso 1  
Bolzano, Italy*

*2 Department Industrial Engineering, University of  
Padua  
Street address  
Padova, Italy*

*\*Corresponding author:  
marta.avantaggiato@eruc.edu*

## ABSTRACT

Shopping centres currently design has included a small portion of automated windows sized for smoke ventilation. Their presence is mandatory for fire regulation and they are usually operated just in case of fire. Nevertheless, these buildings can potentially take advantage of those openable windows to exploit the potential of natural ventilation to guarantee the minimum air change rate required by IAQ standards and for ventilative cooling purpose reducing cooling and electrical consumption.

The work presented in this paper investigate the retrofit performance potential of a mixed-mode ventilative cooling strategy tailor-made for an existing shopping centre. At the present, natural ventilation in the case study common areas is provided just on the basis of the energy manager judgment, without taking into account a robust control strategy based on indoor-outdoor climatic condition, thermal comfort and building use. A building model was created within TRNSYS environment and calibrated based on the real monthly electrical energy consumption. Then, with the support of the TRNFLOW plug-in, that couple thermal and airflow simulations, we were able to simulate and test the effectiveness of the tailor-made mixed-mode strategy. The simulation results show that windows opening can be operated starting from March to November. Running common areas with mixed-mode strategy over a year can allow to save 265 MWh which means cutting the electrical consumption by 23%. The initial costs for control strategies implementation can be paid in the first year of operation.

The main contribution of this work is to demonstrate the feasibility of a mixed-mode ventilative cooling solution for an existing shopping mall common area retrofit highlighting how the exploitation of existing automated windows makes the solution cost-effective.

## KEYWORDS

mixed-mode strategy, electricity consumption reduction, shopping mall, common area retrofit, ventilative cooling

## 1 INTRODUCTION

At the present, few European shopping centres consider natural ventilation as a mean to meet air-change requirements or to exploit free cooling potential. These shopping centres are located in both mild climate (Carrilho da Graça G., 2012) and in more rigid climate as the Field's shopping centre (Tranholm G.T., 2012), proving how it is possible to take advantage of different climatic potentiality when proper design and control strategies are developed.

The common practice of mixed-mode ventilation in shopping malls is indeed to have a naturally ventilated large common space that is linked to individually air-conditioned retails lots (Hamlyn D., 2012). Most of the projects that exploit mixed-mode ventilation in shopping centres (Windowmaster, 2015) take advantage of the openable windows and skylights already designed for smoke ventilation. Openable windows located in big atria and galleries, the so-

called transitional spaces of a shopping centre, are required for smoke ventilation by fire regulation and are usually operated just in case of fire. The potential of these zones, such as the big volume involved and the range of more relaxed range of interior thermal conditions compared to the adjacent stores, as suggested by Hamlyn et al. (Hamlyn D., 2012), combined with the fact that no extra investment is necessary for windows automation, could allow for a very cost-effective retrofit solution in order to reduce electricity consumption for both ventilation and cooling.

A previous study (Avantaggiato M., 2015) showed how, when facing a retrofit, the ventilative cooling design have to consider the level of internal gains in order not to oversize the airflows. Overlooking this interdependency could lead to discomfort condition due to drafts and to extra investment costs for openings' actuators, which might not be necessary. Since employing mixed mode ventilative cooling can significantly reduce the cooling load, the impact of more efficient cooling systems could happen not to be relevant anymore. This suggests that when approaching both retrofit and a new design, ventilative cooling should therefore be considered before any HVAC improvements or before a new detailed design of any HVAC equipment.

The aim of this study is to explore the ventilative cooling opportunity of a mixed-mode ventilation strategy tailor-made for an existing shopping centre. At the present, in the case study, the Donauzentrum shopping centre, natural ventilation in common area is activated just on the basis of the energy manager judgment, without taking into account a robust control strategy based on indoor-outdoor climatic condition, thermal comfort and building use. The outcome of this work is to define and test the thermal and economic performance of a new control strategy for the automation of the windows based indoor-outdoor climatic condition, thermal comfort and users' occupancy of the common areas.

## 1.1 Case study

The case study presented in this paper is the "Donauzentrum" shopping centre, located in Wien, Austria. It opened in 1975 with 22'800 m<sup>2</sup> of retail space while today the total area occupied is around 130'000 m<sup>2</sup> including over 260 retail, dining and entertainment business. Since 1975, indeed, the mall has been several times extended and remodelled until reaching the present configuration into 2010.

Within the research activities of the CommONEnergy project, just part of the entire shopping centre has been considered which general characteristics are presented in Table 1 while Figure 1 on left shows the different block of the mall considered for the analysis. Blocks BT 4-5 and BT 1-3,9 are the oldest part and are also bridged by an above-ground tunnel used as shopping area. Block BT 7 is newest area of the mall, partly retrofitted in 2010.

Table 1 General info about Donauzentrum shopping centre

General info			
Building footprint [m <sup>2</sup> ]	58145	Common areas and galleries [m <sup>2</sup> ]	11257
Gross Leasable Area [m <sup>2</sup> ]	81364	Number of opening hours per day [h/d]	11
Food store vending area [m <sup>2</sup> ]	8131	Number of opening days per week [d/w]	9
Tenants vending area [m <sup>2</sup> ]	73233	Number of closing days per year [d/y]	10

## 1.2 Retrofit solution set

This shopping centre is one of the reference shopping centre within the EU FP7 CommONEnergy project (Bointer, R., 2014). One of the objective of the EU FP7 CommONEnergy (FP7-2013 grant agreement no 608678, 2014-2017) project is the development of architectural and energy systems retrofitting solution sets with the aim at reducing shopping centre energy needs, enhancing the overall energy efficiency to provide appropriate indoor environmental quality (IEQ) and exploiting renewable energy sources (RES).

A solution set is meant to be a combination of energy conservation (passive solutions) and energy efficiency measures (active solutions). The measures are integrated looking for and exploiting synergies among HVAC, lighting, refrigeration, energy use as well as for building correlated services (parking, RES harvesting and local energy production etc.).

The definition of the solution-set involves several steps. First step concerned the collection of data about the reference building features, operation modes and measured data to build an energy simulation model. Second step has been the creation of a building energy model enable to predict the energy consumption and loads on hourly basis, as well as indoor conditions and interactions among solutions. The model has been then calibrated against utility data in order to deliver results to be considered valuable to the building owners. The Integrated Modelling Environment (IME), a TRNSYS-based simulation environment, developed within the project (Dipasquale, 2016) is used to support all the shopping mall retrofitting phases. More info related to the methodology used for the calibration of the building energy model can be found in (Cambronero Vázquez, 2017). Once the baseline was finalized, the further step was the identification of inefficiencies and possibilities for the implementation of new solutions. The inefficiencies identification was supported by the analysis of the baseline outcomes model and by several interviews to the facility manager. These interviews were really fruitful to identify not only possibilities for the implementation of new solutions but also to understand the ideas of the management about future energy efficient actions. In the last steps we have the definition and implementation of the solution-set, the assessment of the potential energy saving and an economic analysis of the solution-set proposed. More information about the methodology followed for the solution-sets definition and the complete methodology can be found in the project report (Cambronero Vázquez, 2017).

Related to Donauzentrum case study, it comes out that one of the main interest of the management was the exploitation of ventilative cooling in common areas. Existing skylight windows were already used for natural ventilation purpose but without a specific strategy, just manually operated under the energy manager judgment. Taking into account this main demand, we carried out a feasibility study to define a mixed-mode ventilative cooling strategy. Particularly we define a control strategy in order to automatically operate and control the windows and the mechanical ventilation system on the bases of different conditions which are going to be presented in paragraph 2.2.

The most suitable natural ventilation strategy identified for the common areas is an enhanced stack ventilation, which use skylight and upper windows to flush out the warm air stacked in the upper part of the common areas because of thermal stratification. The fresh air enters at lower part from the entrance doors and is driven through the building by vertical pressure differences resulting from thermal buoyancy. Being the shopping centre locate in a dense urban contest and because of common areas features, the author believe that the main driving force is thermal buoyancy. For these reason the effect of wind pressure has been overlooked

The design of the ventilation strategy take advantage just of the existing openable windows, skylight and entrance doors, resulting in a very cost-effective solution since the investment costs are restrained to the connection of the window automation system to a building management system. A previous study about feasibility of ventilative cooling in shopping centres (Avantaggiato M., 2015) showed the evidence of dependence between the level of lighting power density and the percentage of hours of direct ventilative cooling use. The analysis of the actual electricity consumption of the shopping mall has showed how more than 50% of this consumption is due to lighting and electric equipment (Cambronero Vázquez, 2017). Being beneficial for both electricity consumption savings and for ventilative cooling purpose, we proposed as first step in the solution-set the reduction of internal gain due to lighting and appliances. Table 2 shows the value of lighting and appliance level considered before and after a potential retrofit of Donauzentrum. In the same table we can see the effect of these improvements on electricity consumption for lighting and appliances and the cooling

consumption. The impact of reduced internal gains is relevant especially for the electricity cooling consumption of the common area, resulting in a reduction of more than 50% of its consumption. This first improvement allowed to reduce the cooling demand of the common areas which results to be beneficial for the mixed-mode ventilative cooling effectiveness(Avantaggiato M., 2015).

Table 2 Comparison in term lighting, appliance level and electricity consumption before and after the application of the retrofit solution

	Lighting level W/m <sup>2</sup>	Appliance level W/m <sup>2</sup>	Electricity consumption for lighting and appliances MWh/year	Electricity consumption for cooling reduction %	Electricity consumption for cooling MWh/year	Electricity consumption for cooling reduction %
Before	35-22 <sup>1</sup>	10	1764	-11	1071	-57
After	4	5	1564		457	

More information related to the complete solution-set for the Donauzentrum shopping centre are reported in (Cambronerò Vázquez, 2017).

## 2 METHODOLOGY

In order to compare the effect of the mixed-mode ventilative cooling strategy two different yearly-based simulations have been run which represent two different scenario. A *reference scenario* where ventilation demand and cooling demand is fully covered by the HVAC system, which represent the situation after the improvement of the internal gain proposed in paragraph 1.2, and a *mixed mode scenario* in which depending on the outdoor and indoor conditions, the different MODEs which are going to be present in paragraph 2.3 can be operated.

For the baseline scenario, the heating and cooling set-points are the one reported in section 2.1. For the mixed-mode scenario a different cooling set-point has been used. From a real assessment of thermal comfort in shopping centre common areas, it comes out that operative temperature of 28 °C are judged as comfortable by costumers(Belleri, 2017). In order to make sure not to overcome this threshold because of the internal and solar gain affecting the mean radiant temperature, the cooling set point has been kept at 27 °C.

### 2.1 Building energy model

According to the methodology reported in paragraph1.1, based on the information collected related to the actual state of the mall, a building energy model was created within TRNSYS environment. Figure 1(right) shows a sketch-up of the building model used for the whole study. All details related to the building energy model used for the simulation ( e.g. internal gains, building thermal features, schedule,etc.)are collected in the project report(Cambronerò Vázquez, 2017) .For the content of this paper we are going to report just the information related to the simplified modelling of the HVAC system.

The model includes three different typologies of openings, the characteristics of which are collected in Table 3:

- entrance doors (WI\_E) ;
- skylights (WI\_SK);
- windows integrated in the lateral glazed facades (WI\_LW).

<sup>1</sup> These value refer to the average lighting level of two different common areas of the shopping centre.35 W/m<sup>2</sup> refer to BT1-3/9-4-5 while 22W/m<sup>2</sup> to BT7 ( see Figure 1-left).

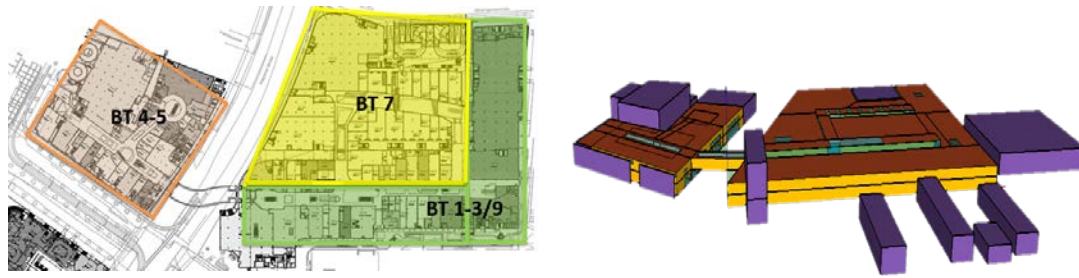


Figure 1 Different building block of Donauzentrum (left), Sketch-up of the building model used for the study (right)

Common areas and tenants are served by the same HVAC system. The system recovers 80% of the exhausted air and mix it with the outside fresh air. Air extractors balance the inlet mass flow. The system is a constant air volume system and the inlet air temperature is adjusted according to the outdoor temperature. If the outside temperature is lower than 13°C the inlet air temperature is the one resulting from the mixture between the temperatures of the recirculated air, assumed to be 80% of the total air flow, and the outside temperature. When the outside temperature is indeed greater than 13°C, the supplied air temperature is equal to the outside one. Heat recovery between recirculated and outside temperature is also taken into account (Table 3). This control has been set for all the days in which the shopping centre is opened. A CO<sub>2</sub>-based ventilation regulates the airflows based on the occupancy of the shopping mall. Since no information about the working airflows of the ventilation unit were provided, we assumed that the ventilation unit provides 37.8 m<sup>3</sup>/h per person as recommended by the European standard EN 15251, for retail buildings, referring to Category II (EN ISO 15251, 2008). Infiltration rates are set to 0.5 ach in each zone of the model but they change according to the wind pressure (Coblentz & Achenbach). The mall is connected to the local district heating system, which provides thermal energy for heating to the whole mall. A typical dry cooler provides cooling to the newest part BT7. In BT1-3/9 and BT4-5 block cooling is generated by a standard chiller coupled with an open cooling tower. The heating demand of the mall has been calculated by assuming a constant set point temperature of 18°C from 9 a.m. to 8 p.m. and a setback temperature of 13.5°C during night. The cooling demand has been calculated by imposing a set point temperature of 25°C from 9 a.m. to 8 p.m. The cooling system is turned off during the night. No additional air humidification is considered during the winter time. System efficiencies considered in the analysis are reported in Table 3.

Table 3 Efficiencies of the systems considered in the studies

Building Block	Ventilation specific power	EER	Heat Recovery	District Heating
BT 1-3-4-5-9	1.5 Wh/m <sup>3</sup>	3	60%	0.9
BT 7	0.9 Wh/m <sup>3</sup>	3.5	40%	0.9

## 2.2 Mixed-mode ventilative cooling modelling

Figure 1 (right) shows the common areas involved in the ventilation strategy. In order to assess energy savings in electricity consumption reduction and to evaluate the thermal condition inside common areas, we performed dynamic simulations using a specific Trnsys module for airflow and thermal models coupling, Trnflow.

Both skylights (WI\_SK) and façade windows (WI\_LW) are top-hung windows with a maximum opening angle equal to 45° which correspond to an opening factor of 0.5.

Figure 2 shows the common area involved in the strategy while Figure 3 shows some pictures of the existing openable windows typology in the same common areas. All the details of the opening considered in airflow network implemented in TRFLOW are showed in Table 4.

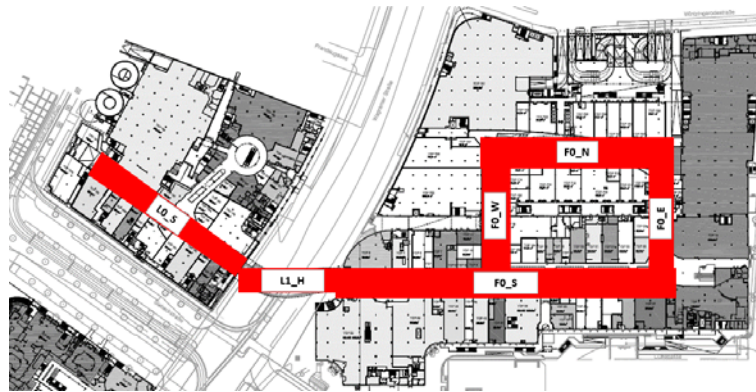


Figure 2 Common Areas involved in the ventilation strategy



Figure 3. Some of the openable windows considered in the ventilation strategy

Table 4 Details of the openings considered in the airflow network implemented in TRNFLOW

Zone	Reference link	Number openings	of	Height [m]	Width [m]	opening area [m <sup>2</sup> ]	Height from the ground [m]	max Opening factor
L1S	WI_SK_1	76		1	1	1	12	0.5
L1H	WI_SK_2	32		0.6	0.6	1.2	12	0.5
F0S	WI_SK_3	12		0.9	1.9	1.71	16	0.5
L0S	WI_E_1	1		10.1	4.6	46.5	0.10	0.2
L0S	WI_E_2	1		10.1	4.6	46.5	0.10	0.2
L1S	WI_E_3	1		12.8	5.8	74.2	0.10	0.2
F0S	WI_E_4	1		11.7	4.8	56.2	0.10	0.2
F0S	WI_LW_1	24		0.6	2	1.2	12.1	0.5
F0S	WI_LW_2	8		1.6	2	3.2	12.1	0.5

### 2.3 Control rules for mixed-mode ventilative cooling

The control rules for the mixed-mode operation have been developed taking into account both indoor and outdoor parameters. When the condition for the opening of the windows are reached the mechanical ventilation is switched off and vice versa, resulting in different working mode. The inputs needed for the control of mixed-mode ventilation and cooling are:

- Occupancy time schedule of the common areas which is from 9 a.m. to 8 p.m.;
- Outdoor air temperature,  $T_{ext}$ , [°C];
- Minimum outdoor temperature for windows opening,  $T_{ext\_min}$ , [°C] which in this case is equal to 14 °C;
- Heating temperature setpoint,  $T_{set\_H}$ , [°C];
- Cooling temperature setpoint,  $T_{set\_C}$ , [°C];

- Temperature threshold for night cooling activation  $T_{set\_NC}$ , [°C], which has been set equal to 22 °C;
- Air temperature inside the common areas,  $T_{zone}$ , [°C];
- Average air temperature inside the common area within the previous eight hours  $T_{zone\_avg\_8h}$ , [°C].

Based on input conditions different ventilation modes has been defined:

- ❑ MODE 0: during opening hours, when the outdoor temperature is below the  $T_{ext\_min}$ , minimum airflow rates are provided by mechanical ventilation and cooling demand is covered through mechanical cooling system;
- ❑ MODE 1: when the outdoor temperature is below the  $T_{ext\_min}$  and the  $T_{zone}$  falls into the three condition expressed in Figure 4, window WI\_SK and WI\_LW are open with a factor 0.5 with a windows opening factor equal to 0.5 while 0.3 for entrance doors (WI\_E). When windows are operated, the HVAC system is off;
- ❑ MODE 2: out of the opening hours and between 3 a.m. and 6 a.m., if the temperatures inside the zones in the previous eight ( $T_{zone\_avg\_8h}$ ) hours were higher than  $T_{set\_NC}$  °C, natural night cooling can be operated. In this mode, just WI\_SK and WI\_LW windows typology are used with maximum opening;
- ❑ MODE 3: during not occupied period and out of the interval between 3 a.m. and 6 a.m., just infiltration are considered, for all the year.

The control scheme is presented in Figure 4.

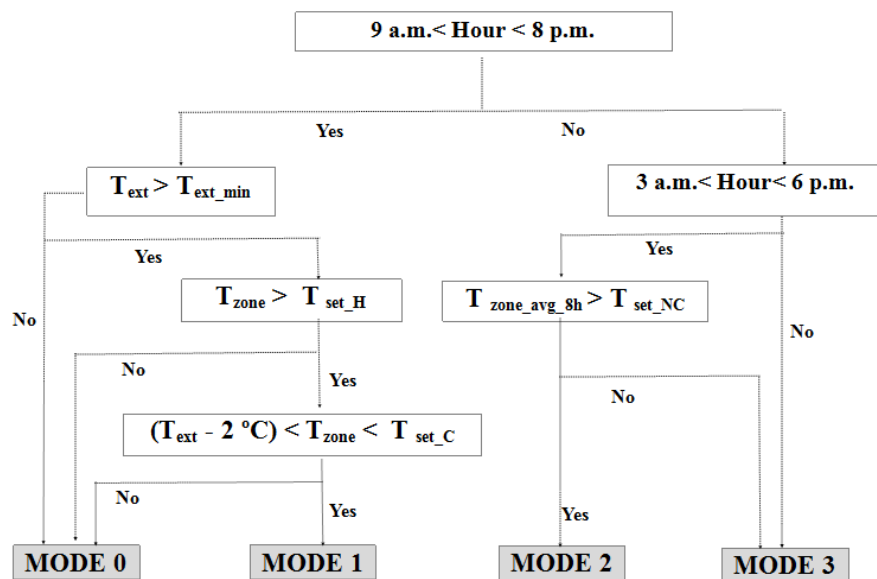


Figure 4 Control strategy scheme for mixed-mode ventilation in common areas in Donauzentrum

### 3 RESULTS

Based on the outdoor climate and indoor thermal conditions, daytime natural ventilation (MODE 1) can be activated from end of March up to early November while night cooling (MODE 2) is applied from early May to early September. According to simulation results, the building runs in MODE 1 for 25% of the shopping mall opening hours while MODE 2 runs for 9% of the closing hours. Running common area with mixed-mode strategy over a year can allow to save 265 MWh which means cutting the electrical consumption by 23%. The heating demand is not affected which proves how the mixed-mode control strategy prevents the opening of the windows when the outside conditions are too rigid and the recirculation of outside colder air may create a decrease of indoor temperature with consequent increase in the heating demand for compensation. Figure 5 shows the monthly electricity consumption for both reference and mixed-mode scenario. The cut of mechanical

ventilation electricity consumption in the mixed-mode scenario is highlighted during mid-season months when suitable outdoor temperature allow outdoor condition for recirculating fresher air from outside

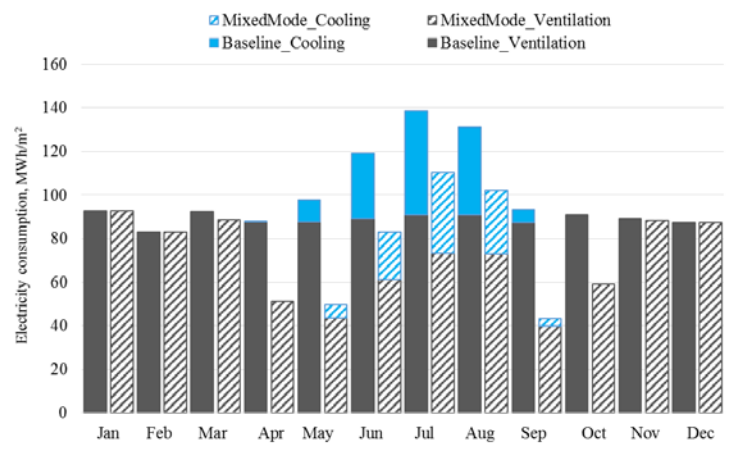


Figure 5 Monthly trend of electricity consumption for ventilation and cooling for Baseline scenario and Mixed-mode scenario

In Figure 6 and Figure 7 we report the mixed-mode operation respectively during a temperate and warm week of June. The grey column refers to the operation of the windows during day while the blue one to the operation at night. The main difference we might notice between the two graphs is that when the outdoor temperature is quite limited (below 24°C, Figure 6) the operation of the window is really often during the day. Once the outdoor temperature starts raising over suitable threshold for natural ventilation application (Figure 7) the operation during the day is limited with a preference for the active cooling system to maintain comfortable temperature inside common areas. Under mixed-mode operation comfortable condition can be provided during the day with operative temperature below 28 °C.

The effect of internal and solar gains is visible in the difference between the average air temperature and the operative temperature of the zones.

The operation costs that can be save by running the building in mixed-mode condition and the accepting new comfortable ranges in the common areas, are estimated to be around 26500 €/year<sup>2</sup>.

With an initial investment cost of 100€ per window module or entrance door which takes into account of the connection of windows automation to a building management system, installation and engineering and permitting costs, the solution turns to be very cost effective. Over an expected working period of 25 year, the estimated Pay Back Time is less than one year (with a discount factor lower than 8%) Further information about the economic analysis assumption can be found (Cambronero Vázquez, 2017).

The potential of mixed-mode operation especially on cooling side can be improved including a new portion of openable windows. The cooling effect can be boosted both during daytime and night-time because of the increased airflow that turn to be beneficial for air temperature offset and for indoor air quality issue

<sup>2</sup>The electricity price for Donauzentrum shopping centre is assumed to be 0.10 €/kWh

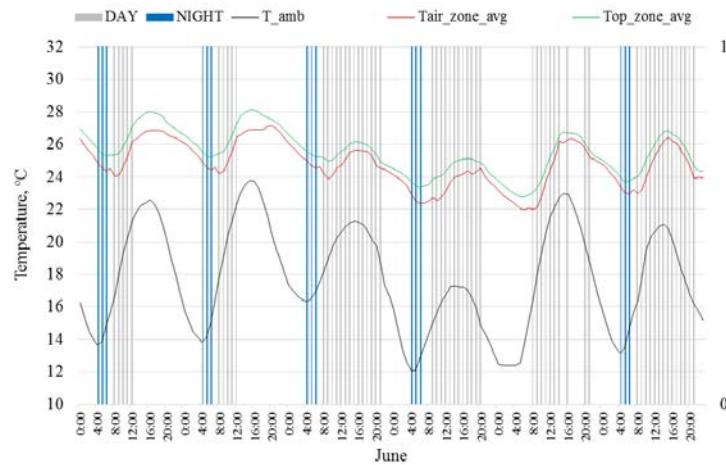


Figure 6 Temperature trends in correlation with windows operation during day (grey column) and night (blue column) during a temperate week of June (1<sup>st</sup>-6<sup>th</sup>)

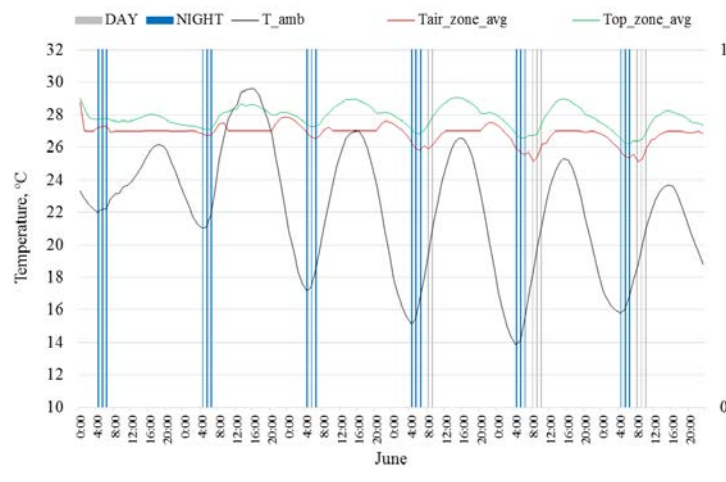


Figure 7 Temperature trends in correlation with windows operation during day (grey column) and night (blue column) during a warm week of June (1<sup>st</sup>-6<sup>th</sup>)

#### 4 CONCLUSIONS

The paper investigates a mixed-mode ventilative cooling retrofit opportunity for an existing shopping mall located in the city of Wien. The developed strategy interests the shopping mall common areas (shop galleries and atria) where openable windows were operated without a robust automated control but just on the energy manager judgement.

Considering an energy retrofit intervention on common areas, a first reduction of the internal gain for lighting and appliances is considered in order to reduce the cooling demand of these zones. Afterwards a control strategy for running the building in mixed-mode condition has been developed based on indoor-outdoor climatic condition, thermal comfort and users' occupancy:

Simulation results show how the daytime ventilative cooling can potentially work from end of March up to early November for a 25% of shopping mall opening hours. The exploitation at nighttime is limited to a 9% of unoccupied period and can run from early May to early September. Over a year running common area with mixed-mode strategy can allow to save 265 MWh which means cutting the electrical consumption by 23% which estimation in term of operational cost saved is about 26500 € per year. Under mixed-mode operation, comfortable condition can be provided during the day with operative temperature below 28 °C. With an estimated initial costs of 100 euro per module, the investments cost can be paid in the first year of operation.

The potential of mixed-mode operation especially on cooling side can be improved including a new portion of operable windows which allow for a booster of the cooling effect both during daytime and night-time because of the increased airflows.

For the real implementation of the mixed-mode operation a fine tuning of the control strategy should be operated taking into account a signals that override the opening of the windows in case of rain or in case of strong wind at windows level.

The study has demonstrated the feasibility of mixed-mode operation for shopping mall common area proving its effectiveness and cost effectiveness as retrofit solution when the synergy with the level of internal gain is taken into account. Overlooking this interdependency could lead to discomfort condition due to drafts and to extra investment costs for openings' actuators, which might not be necessary.

## 5 ACKNOWLEDGEMENTS

The research leading to these results has received funding from the European Community's Seventh Framework Programme (FP7/2007-2013) under grant agreement n° 608678. The authors would like to thank Drazen Ivanis and Sojka Ratislav, technical managers of the Donauzentrum shopping centre, for their help and collaboration.

## 6 REFERENCES

EN ISO 15251. (2008). *Indoor Environmental input parameters for design and assessment of energy performance of buildings addressing indoor air quality, thermal environment, lighting and acoustics*.

FP7-2013 grant agreement no 608678. (2014-2017). *CommONEnergy project*. Retrieved from <http://www.commonenergyproject.eu/>

Avantaggiato M. (2015). Ventilative cooling strategies to reduce cooling and ventilation needs in shopping centres. *36th AIVC Conference, 5th TightVent Conference, 3rd Venticool Conference*, (pp. 633-644). Madrid.

Belleri, A. (2017). *D3.3 -Ventilative Cooling; CommONEnergy project ( FP7-2013 grant agreement no 608678)*.

Bointer, R. (2014). *D21, Shopping mall features in EU-28 + Norway, CommONEnergy project ( FP7-2013 grant agreement no 608678)*. Retrieved from <http://www.commonenergyproject.eu/>

Cambronero Vázquez, M. V. (2017). *D5.1-Systemic solution-sets; CommONEnergy project ( FP7-2013 grant agreement no 608678)*.

Carrilho da Graça G., M. N. (2012). Thermal and Airflow simulation of a naturally ventilated shopping mall. *Energy and Buildings* 50, 177-188.

Coblentz, C., & Achenbach, P. (n.d.). *Field Measurements of air infiltration in ten electrically-heated houses*. 1963: ASHRAE Transaction 69 (1).

Dipasquale, C. (2016). *D4.1-Integrative Modeling Environment; CommONEnergy project ( FP7-2013 grant agreement no 608678)*.

Hamlyn D., C. D. (2012). Ventilation Approaches for Shopping Malls- An Examination of Natural and Hybrid Strategies. (pp. Volume 118, Part 1). ASHRAE Transactions.

Tranholm G.T., R. J. (2012). Reducing energy consumption in an existing shopping centre using natural ventilation. *33rd AIVC Conference " Optimising Ventilative Cooling and Airtightness for [Nearly] Zero-Energy Buildings, IAQ and Comfort"*, Copenhagen, Denmark, 10-11 October 2012.

Windowmaster. (2015). Retrieved from <http://www.windowmaster.com/building-types/shopping-centres>

# Defining the metrics to assess the Indoor Air Quality in low-energy residential buildings

Marc Abadie\*<sup>1</sup>, Pawel Wargocki<sup>2</sup>, Carsten Rode<sup>2</sup>

*1 Laboratoire des Sciences de l'Ingénieur pour  
l'Environnement (LaSIE) - University of La Rochelle  
Pôle Sciences et Technologie  
Avenue Michel Crépeau  
17042 La Rochelle Cedex 1, France  
marc.abadie@univ-lr.fr*

*2 Technical University of Denmark (DTU)  
Department of Civil Engineering  
Nils Koppels Allé  
2800 Kgs. Lyngby, Denmark*

## 1 EXTENDED ABSTRACT

### 1.1 About IEA EBC Annex 68

The overall objective of the IEA EBC Annex 68 is to provide scientific basis usable for optimal and practically applicable design and control strategies for high Indoor Air Quality (IAQ) in residential buildings. These strategies are intended to ensure minimal possible energy use. Consequently, Annex 68 is focused on low-energy residential buildings. The work of the Annex is organized into five subtasks (Figure 1): Subtask 1 is setting up the metrics to assess the performance of low-energy buildings as regards indoor air quality combining the aspirations to achieve very high energy performance without compromising indoor environmental quality. Subtask 2 is gathering the existing knowledge and providing new data about indoor air pollutants as well as combined heat, air and moisture transfer. Subtask 3 is identifying and developing modelling tools that can assist designers and managers of buildings in accounting for IAQ. Subtask 4 is developing design and control strategies for energy efficient ventilation in residential buildings that will not compromise indoor air quality. Subtask 5 is conducting field measurements to examine and optimize different control and design strategies.

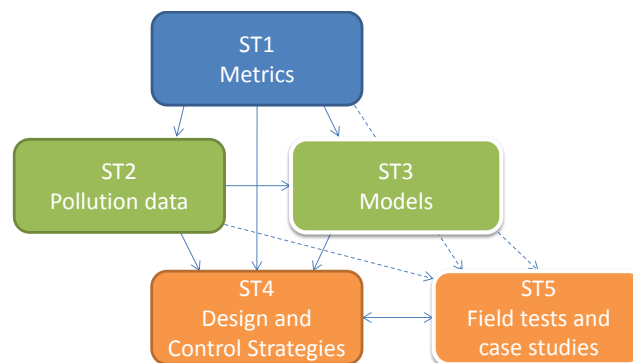


Figure 1: Schematic overview of the subtasks in Annex 68 and their interrelations.

### 1.2 Research Methodology

The working plan executed in Subtask 1 consists of the subsequent steps:

- Collection of data on indoor air pollution in residential buildings with a particular focus on low-energy buildings to provide an overview of the exposure of occupants to contaminants in residential buildings and to identify differences, if any, between low-energy buildings and the buildings that cannot be termed as low-energy (representative of the current building stock).
- Identification of target pollutants relative to indoor air.
- Compilation of pollutant Exposure Limit Values (ELV) relevant for the current project.
- Surveying IAQ indices developed previously.
- Defining the metric(s) that can be used to achieve the objectives of Annex 68 project considering the aspect of energy consumption.

### 1.3 Main Research Outcomes

From the pollutant concentrations collected and compiled in this study, lower pollutant concentration levels have been found in the newest low-energy buildings. However, some exceptions from this rule have been detected as for the case of France and Japan where new buildings presented higher levels for some pollutants coming from wood construction. By comparing collected concentration levels in this study with ELV, a list of target pollutants for long-term exposure has been defined: *acetaldehyde*, *acrolein*, *α-pinene*, *benzene*, *formaldehyde*, *naphthalene*, *nitrogen dioxide*, *PM10*, *PM2.5*, *radon*, *styrene*, *toluene* and *trichloroethylene*. Regarding the short-term exposure, this analysis led to the following shorter list: *acrolein*, *formaldehyde*, *nitrogen dioxide*, *PM10*, *PM2.5*, *radon* and *TVOC*. Two approaches to define metric for assessing the importance of measured concentrations of pollutants were selected from the literature survey on IAQ metrics. The first approach refers to the comparison of typical exposure concentrations to the existing exposure standards (ELV). Two indices are proposed i.e. IAQ-LTEL (Long-Term Exposure Limit) and IAQ-STEL (Short-Term Exposure Limit) to account for long and short-term exposures. In this approach the unbiased aggregation of indices for specific pollutants is achieved by selecting maximum index. The second approach is evaluating the direct health impacts of the pollution through the estimation of the Disability-Adjusted Life Years (DALYs) and is referenced as IAQ-DALY index. Finally, a graphical representation is proposed to facilitate the visual and quantitative comparison among a reference IAQ/Energy situation and possible air cleaning solutions. This representation provides an example of the possible approach for labelling indoor environments as regards IAQ and energy performance (Figure 2).

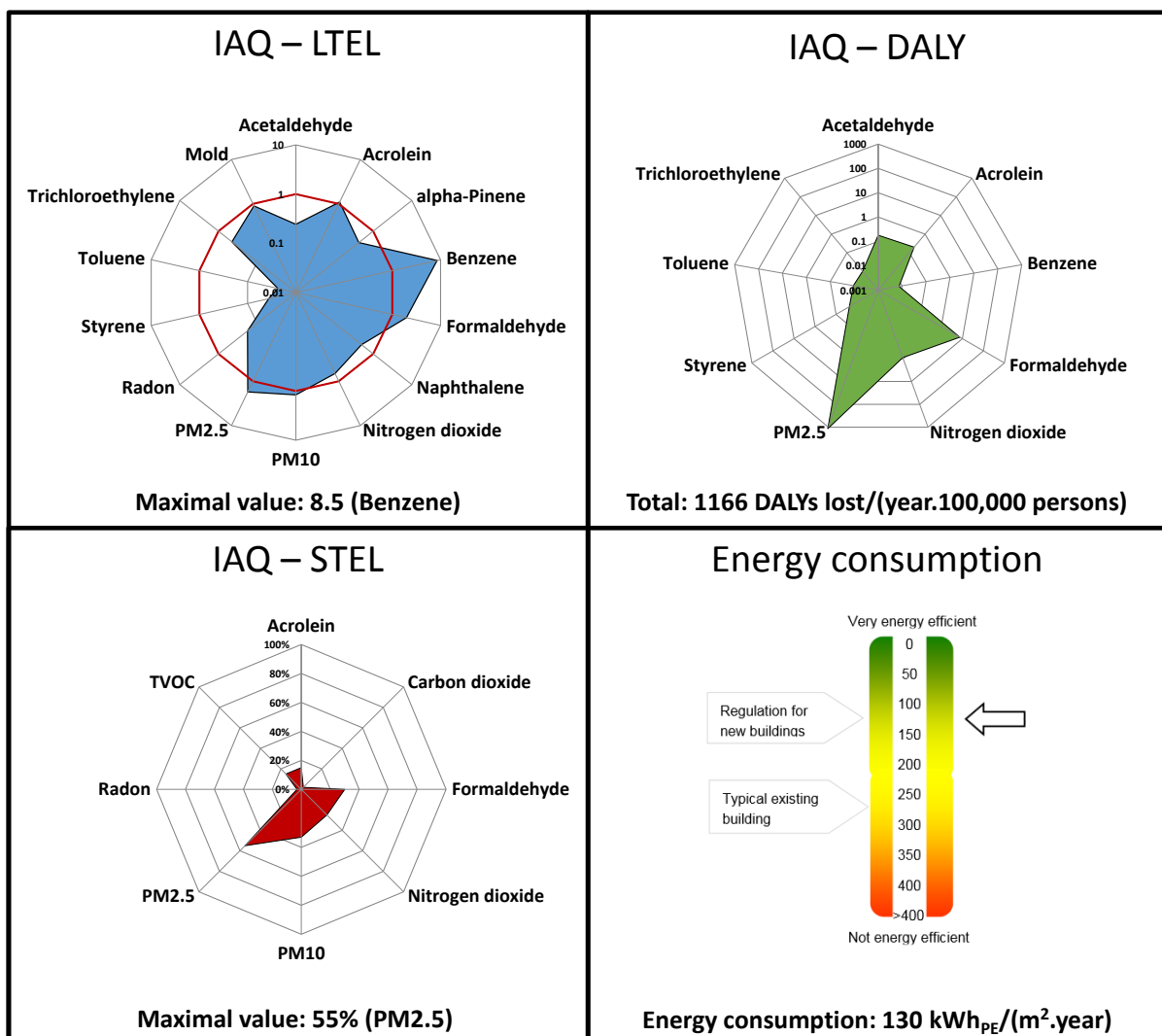


Figure 2: An example of IAQ/Energy dashboard for low-energy residential buildings (data represented here are just for display and do not represent actual situation).

### KEYWORDS

Indoor Air Quality, Residential Buildings, Metrics, Exposure Limit Values, DALYs

# On the use of co-simulating modelling tools to enhance our understanding and optimization of heat and mass flow effects in whole buildings

Carsten Rode, Denmark

## Extended Abstract for ST3 representation:

Since many simulation tools with very different features at different quality levels already exist, our focus in ST3 was NOT the development of a new model. Instead, the focus is on interoperability and quality assurance criteria.

1) **Interoperability** comprises technologies for Co-Simulation of emission, ventilation control and room models. The presentation sketches out the individual capabilities of the simulation models DELPHIN, THERAKLES and the ventilation system/equipment model in Modelica. Detailed VOC/pollutant emission from building structures and envelope systems under consideration of temperature and moisture effects can be simulated with DELPHIN.

THERAKLES can model hygrothermal behavior of rooms and construction and the influence of ambient climate and user behavior onto the room air conditions. A ventilation model that takes into account not just temperature and humidity conditions, but also pollutant concentrations within the room air is modeled and solved with Modelica.

The combination of the three distinct simulation software in a Co-Simulation can be achieved in different ways. First, the co-simulation technologies "FMI for Co-Simulation" and Waveform Relaxation method are introduced. An example for a coupled simulations is shown including the setup and execution of the simulation and the result of simulation tests are presented, including a discussion of overall simulation performance and Co-Simulation overhead.

2) **Strategies for ensuring quality** in building performance simulation include supporting actions as common exercises and a collaborative model development towards a fully coupled CHAMPS modeling platform. This platform will be an open-source repository for numerical solvers and data being able to capture the most important physical processes of coupled heat, air, moisture and pollutant transfer in buildings. This platform will be the basis for a seamless continuation of the modeling and software development activities of the IEA EBC Annexes – especially it will build upon the achievements of the Annex 60, an effort on “New generation computational tools for building and community energy systems based on the Modelica and Functional Mockup Interface standards”.

We complement the CHAMPS modeling platform by scientifically quality-checked reference solutions. The most important aspects are:

- Broad and hierarchically organized modeling scope
  - Most important CHAMPS aspects to be captured
  - Different modeling scopes (walls, rooms, buildings)
  - Different modeling depths (simplified, compact, expert levels)
  - Gradual buildup of model complexity
- Model-to-model comparison
  - Participation of most commonly used tools (e.g. IDA-ICE, TRNSYS, EnergyPlus)
  - Comparison with measured data not meaningful because of many uncertainties

- Focus on interoperability and performance
  - Test of different coupling technologies
  - Test of large problems on reasonable execution time
  - Test of numerical robustness
- Towards fully automated quality assurance checks
  - Automatic execution of test cases
  - Automated evaluation of results
  - Automatically generated reports and messaging system

In Annex 68, we are working towards these targets by definition of a common exercise based on the Passys Cells Project. We consider heat, air, moisture and VOC flows, coupled walls and rooms and a gradual buildup of model complexity by variants. CHAMPS-Multizone and CHAMPS-BES are used to provide initial solutions, IDA-ICE, EnergyPlus and NANDRAD serve for higher model complexity. Aspects as numerical performance and robustness are not yet addressed within Annex 68 ST3 CE, as well as process automatization.

# Design and operation of ventilation in low energy residences – A survey on code requirements and building reality from six European countries and China

Maria Bocanegra-Yanez<sup>1</sup>, Gabriel Rojas<sup>2</sup>, Daria Zukowska-Tejsen<sup>3</sup>, Esfand Burman<sup>4</sup>, Guangyu Cao<sup>5</sup>, Mathieu Pierre Yves Hamon<sup>5</sup> and Jakub Kolarik<sup>\*3</sup>

*1 University of Strathclyde  
16 Richmond Street  
G11XQ Glasgow, United Kingdom*

*2 Lawrence Berkeley National Laboratory  
1 Cyclotron Rd  
CA 94720, Berkeley, USA*

*3 Technical University of Denmark  
Brovej 118  
2800 Kgs. Lyngby, Denmark  
\*Corresponding author: jakol@byg.dtu.dk*

*4 UCL Institute for Environmental Design and  
Engineering  
Central House, 14 Upper Woburn Place  
London WC1H 0NN, United Kingdom*

*5 Norwegian University of Science and Technology  
Høgskoleringen 1, 7491  
Trondheim, Norway*

## ABSTRACT

One of the key objectives of the IEA Annex 68 research programme entitled “Indoor Air Quality Design and Control in Low Energy Residential Buildings” is to provide a generic guideline for the design and operation of ventilation in residential buildings. They need to have minimal energy consumption, and at the same time maintain a high level of Indoor Air Quality (IAQ). The paper reports on preliminary results of an interview survey conducted among different stakeholders involved in design, installation and operation of residential ventilation in countries involved in the Annex. There were two main objectives, firstly to describe and analyse a transition between actual requirements (national building codes, standards) and current practice. For the second to investigate current barriers and challenges regarding installation of mechanical ventilation in residences. In total, 37 interviews from six European countries and China have been analysed, certainly not enough for a representative sample. However, the results provide a valuable snapshot of current practices and insights into potential barriers. Results show that mechanical ventilation with heat recovery is becoming the dominating ventilation system installed in new residences in Europe. However, there are countries, where, due to tradition, national legislation and/or cost reasons, other types of ventilation like mechanical exhaust or manual window ventilation are applied. Demand Controlled Ventilation is often allowed or even recommended in standards, but rarely implemented in practice, except for humidity controlled trickle vents in France. The main barriers against mechanical ventilation with heat recovery seem to be high capital cost, space requirements and duct routing as well as problems resulting from poor construction, lack of commissioning and/or maintenance.

## KEYWORDS

Indoor air quality, residential ventilation, mechanical ventilation with heat recovery, low-energy housing

## 1 INTRODUCTION

To reduce building energy consumption and carbon emissions, Building regulations and standards require more insulated and airtight buildings, which may lead to a poor quality of

indoor environment if the ventilation provision is not sufficient. For instance, IAQ problems were found in all three investigated low energy dwellings in England due to operation and maintenance issues of the Mechanical Ventilation Heat Recovery (MVHR) system (McGill, Qin, and Oyedele 2014). Conversely, new built houses with good IAQ may also be found, like the houses investigated by Langer et al. (2015), where the mechanical ventilation ensured high ventilation rates.

One of the key objectives of IEA Annex 68 research project entitled “Indoor Air Quality Design and Control in Low Energy Residential Buildings” is to provide generic guideline for the design and operation of ventilation in residential buildings. In order to provide this guideline, investigation of the current situation of ventilation systems, regarding requirements and practice, in countries involved in the project is necessary. This is crucial since without a strong alignment between the two, no progress towards high IAQ in residences can be achieved. First, a review of the ventilation and IAQ requirements in six countries in Europe and China was conducted. Subsequently, interviews with relevant expert groups in these countries were carried out. Findings from the interviews were used to map the transition between today’s strict requirements (EU directives, national building codes, standards) on one side and the actual situation in practice, identifying key barriers, challenges and needs regarding design, commissioning, operation and maintenance of ventilation systems to ensure a healthy indoor environment in low energy domestic buildings.

## 2 METHODOLOGY

### 2.1 Literature review

A review of the national building regulations and standards in Austria, China, Denmark, Estonia, France, Norway and United Kingdom (UK) was conducted. This review focused on ventilation requirements highlighting key aspects such as recommended ventilation systems, background ventilation rates, supply and extract airflows from habitable rooms, wet rooms and kitchen, state-of-the-art system typology, and requirements for heat recovery.

### 2.2 Interviews

Gathering of the information about today’s practice in design, operation and commissioning of residential ventilation systems was based on semi-structured interviews. Five different interview templates were prepared dependent on the target group of stakeholders to be interviewed: *A. Ventilation designers / Consultants, B. Facility management companies/ Building administration, C. Public authorities, D. Housing developers, E. Producers of ventilation systems.* Each survey template consisted of two parts. The first part was focused on stakeholders’ opinion regarding state of the art for ventilation systems that are installed in modern dwellings. The second part focused on barriers and problems during design, commissioning, operation or maintenance as well as on key changes in legislation, technical measures, financial incentives, market requirements and outreach programmes that stakeholders believed were needed to provide high IAQ in energy efficient homes. Each of the two parts included 3 to 4 main (open) questions as well as several, more precisely defined sub-questions, which should help the interviewer to keep structure of the interview. A selection of the questions chosen for analysis in the present paper is shown in Table 1.

Table 1: Interview questions analysed in the present paper

State of the art	Barriers, problems and needs
a) What types of ventilation systems are installed in modern dwellings and what is the most prevailing system?	a) What are the main problems/barriers during the design process of a ventilation system?
b) Elaborate more on type, topology and setup of the system (centralised/decentralised, etc.).	b) What are the main problems during commissioning and operation (including maintenance)?

- 
- |   |   |
|---|---|
| <ul style="list-style-type: none"> <li>c) How integration of additional appliances that influence ventilation is handled (cooker hood, woodstove)?</li> <li>d) What type of a heat recovery system is typically installed?</li> <li>e) How efficient is the system in delivering the outdoor air to each location in the room?/ How is the air distributed in dwellings?</li> <li>f) What type of automatic control system to regulate the flow rate and flow balance is integrated with the ventilation system?</li> <li>g) What are requirements for minimum supply/exhaust airflows and IAQ in dwellings?</li> </ul> | <ul style="list-style-type: none"> <li>c) What are the main needs to ensure high IAQ and high energy efficiency in residential buildings?</li> <li>d) To what extent is MVHR accepted in your country/region? Please give a grade from 1 to 10 (1 = Not accepted, 10 = Fully accepted).</li> <li>e) How would you rank reasons why people do not use their mechanical ventilation system at homes?</li> </ul> |
|---|---|
- 

The results presented in the paper are based on 37 interviews: Austria (6), China (1), Denmark (5), Estonia (4), France (5), Norway (7) and United Kingdom (7).

### 3 RESULTS AND DISCUSSION

#### 3.1 Review of national requirements

Requirements to ventilation for residential buildings in the seven investigated countries are listed in Table 2. Mandatory mechanical ventilation has not been identified for any of the countries. For all cases, the recommendations prioritize neither mechanical ventilation (MV) nor natural ventilation including manual window ventilation (NV). All countries require minimum background ventilation rates (see Table 2), however, the requirements vary for the countries and are for some given as air change rate (ACH), while for other the airflows depend on the number of occupants, floor area, number of habitable rooms (i.e. living room, bedrooms, offices, etc.) or number of bedrooms only. The national building codes set also requirements to minimum exhaust rates from wet rooms in all investigated countries, e.g. in France the minimum extract rates depend on numbers of habitable rooms and in a 3-room dwelling there is required extraction of 45 m<sup>3</sup>/h for a kitchen and 30 m<sup>3</sup>/h for a bathroom and a toilet. According to the Danish building regulations, extraction of at least 20 l/s must be possible in a kitchen, and extraction of at least 15 l/s and 10 l/s in a bathroom and a toilet, respectively. For a comparison, the Chinese regulations state requirements in ACH, i.e. 3 h<sup>-1</sup> for a kitchen and 5 h<sup>-1</sup> for a bathroom/toilet. Dependent on the country either a kitchen hood integration in MV is required or it has to work as a separate system (exhaust outside or just recirculation). Requirements related to heat recovery in new mechanical systems, including minimum efficiency, apply only for some of the countries.

#### 3.2 State of the art for installed ventilation systems

Majority of the stakeholders provided information regarding multi-storey residential buildings (MFH), where the apartments range from 35 to 130 m<sup>2</sup>. Regarding single family houses (SFH), the only provided information was from France with range 90 - 110 m<sup>2</sup>. With respect to types of ventilation systems (questions a and b, see Table 1) interviews revealed that MVHR systems are dominant. However, there are variations in all countries. In Austria, natural ventilation as well as mechanical exhaust (MEV) systems are receiving comparable attention. For example, one HVAC planner in the province of Vorarlberg stated that they used to have a legal requirement to build all publicly built housing in Passive House (PH) standard, which required MVHR ventilation. After removing this requirement, implementation of MVHR dropped drastically and most new housing projects in that province installed a simple extract air system or solely rely on NV. That planner explained that “Non-public housing developers were put in a tight spot” having to argue why social housing had “higher standard”

than their buildings. He added that the situation was distorted due to the housing subsidies received by the social housing developers and that consequently, the private constructors were able to promote their views, that ventilation is a) questionable and b) the capital and operation costs are too high. At the same time, the designer referred to an Austrian research project (Ploß 2016) which showed that 70% of the 55 most economic building design variants (based on Lifecycle costs) were with MVHR, the rest with MEV. Since the cost differences between these 55 variants were negligible, his opinion was that the solution with the higher comfort should be prioritized. Another designer stated that in the projects, which do not aim for any public subsidy, manual window ventilation or MEV systems are applied. In France single extract, humidity based Demand Control Ventilation (DCV) systems applied in combination with humidity-sensitive trickle ventilators seem to be the state of the art. The dominance of MVHR systems is obvious in Scandinavian countries and in the UK. What is commonly mentioned by stakeholders from these countries is the maintenance issue. Centralized air handling systems are often used in social apartments, because inhabitants are not interested in maintaining a decentralized system and it is more expensive to service several individual units. On the contrary, they design decentralized systems for privately owned dwellings where inhabitants are responsible for maintaining the unit placed in their apartment. Generally, the stakeholders more often mentioned centralised ventilation systems. Decentralised system was never stated alone as an only solution provided.

Other appliances that influence ventilation (question c) are mostly taken into account. Kitchen hoods were, as expected, mostly mentioned. In the interviews from Estonia, the separate exhaust system for a kitchen hood is mentioned. None of the Austrian stakeholders mentioned integrated solution for a kitchen hood, but referred to the use of recirculating range hoods. In contrast to that, the Norwegian stakeholders mentioned that it is common to connect the kitchen hood to the system and in the case that the separated fan is used; the pressure-sensor is applied to ensure balanced ventilation. Danish designers also mentioned integration of a kitchen hood and consequent boost of a supply fan to provide balance. Another argument for integration of a kitchen hood was optimal functioning of a heat recovery. One of the Danish designers had an opposite opinion; noting that system could be polluted with fat from cooking.

Counter-flow plate heat exchanger is mostly used as heat recovery (question d), followed by cross-flow heat exchanger. Rotary heat exchangers were mentioned only in connection to decentralized ventilation units – it is not very clear from the answers, but it can be assumed that stakeholders refer to decentral (flat-wise) solutions. Either one unit per apartment in apartment buildings or installation in single-family houses. Rotors can potentially transfer condensable odorous substances (e.g. from cooking), so in centralized systems of apartment buildings there would be the risk of smelling a neighbour's lunch. Within one dwelling, a small potential odour transmission (e.g into a bedroom) is not considered a problem.

Efficiency in delivering air into particular rooms (question e) has been addressed in different detail by different stakeholders. Some described quite precisely their strategy for air distribution; others did not seem very interested or concerned about this issue and just mentioned mixing ventilation. When designing/implementing balanced systems in Austria, the so-called cascade systems seem to be preferred. A designer stated that if possible (due to a floorplan disposition) an extended cascade ventilation principle (with no supply air terminal in the living room) would be used. Otherwise, a standard air distribution (supply in bedrooms and living room, extract in kitchen/bath/toilet) would be adopted. Norwegian and Danish designers stated that in their systems fresh air is supplied into bedrooms and living room while it is extracted from bathrooms, toilets and kitchens. This principle is actually required by Danish building regulation. French designer pointed out important aspects regarding both MEV and MVHR system. In the case of single exhaust, a tight building is necessary to keep air distribution as designed. In the case of balanced systems, tight ductwork is necessary.

Table 2: Summary of requirements to residential ventilation; based on: OIB-Richtlinie 3 (2015), ÖNORM H 6038 (2014), GB/T 18883-2002 (2002), JGJ 134-2010 (2010), JGJ/T309-2013 (2013), BR15 (2017), Estonian legal acts 03.06.2015 nr 55 (2015), Estonian legal acts 05.06.2015 nr 58 (2015), Arrêté 24.03.82 (1983), DTU 68.32 (2017), TEK 10 (2010), The Building Regulations. Approved Document Part F (2010), The Scottish Building Regulations 2015 (2015); Legend: RH-relative humidity, E&W-England&Wales, S-Scotland

Country	Austria	China	Denmark	Estonia	France	Norway	UK
<b>Natural Ventilation (NV)</b>	Allowed	Not addressed	Allowed (same requirements to background vent. and energy req.)	Opening of windows only to improve thermal comfort in summer	Allowed (same requirements to background vent.)	Allowed (same requirements to background vent. and energy req.)	<u>E&amp;W</u> : Allowed (same req. to background vent.) <u>S</u> : not suitable if airtightness < 5 m <sup>3</sup> /hm <sup>2</sup> (50 Pa)
<b>Mechanical Ventilation (MV)</b>	Required if NV cannot ensure healthy IAQ	No addressed	Always MVHR	MVHR	MEV MEHV	Not specified	MEV MVHR
<b>Permission to switch off ventilation</b>	Not addressed, min. ACH=0.15 required during non-occupancy	No addressed	Not allowed	Not addressed	Never	Not addressed, but min. 0.7 m <sup>3</sup> /h m <sup>2</sup> during non-occupancy	Not addressed
<b>Heat Recovery</b>	None (local req. to receive subsidies)	Not addressed	decentralized ≥ 80% centralized ≥ 67%	N/A	Not addressed	≥ 70%	Not mandatory (recommended min. 66%)
<b>Kitchen hood integration</b>	Not integrated into MVHR	Not addressed The minimum exhaust ACH=3 h <sup>-1</sup>	Not addressed; recirculation not allowed	Not addressed	Not integrated	N/A	Not addressed The minimum exhaust is 30 l/s
<b>Background ventilation rate</b>	Min. ACH=0.15 required during non-occupancy	30 m <sup>3</sup> /h per person dwelling air; ACH=1h <sup>-1</sup>	0.3 l/s m <sup>2</sup> heated floor area	SFH: 0.42 l/s m <sup>2</sup> MFH: 0.5 l/s m <sup>2</sup>	Dependent on number of "main rooms" (3 rooms min. 75 m <sup>3</sup> /h)	1.2 m <sup>3</sup> /h m <sup>2</sup> (0.7 m <sup>3</sup> /h m <sup>2</sup> non-occupied space)	<u>E&amp;W</u> : min. 0.3 l/s m <sup>2</sup> net floor/n. of rooms (3 rooms - 76 m <sup>3</sup> /h) <u>S</u> : spec. by min. area of vent. opening
<b>Controls</b>	DCV recommended Min. 3 levels for fan speed required	Not addressed	DCV may be used; background vent. rate has to be ensured	DCV may be used (CO <sub>2</sub> < 1000 ppm)	Not addressed	Not addressed	DCV/ manual; RH contr. rec. in wet rooms; Trickle ventilators control by occupants

Considering the prevailing type of control (question f), application of DCV seems to be rare. As a designer from Austria noted, DCV for residential housing sector definitely does not prevail on the market. The higher costs came into effect. He also mentioned technical problems with positioning of sensors. According to his opinion, the only reasonable approach is to place a sensor in each room. This however increases both cost and complexity of the system. A special situation could be noted in France, where humidity based control is being used in combination with MEV systems. A French producer named different types of systems and mentioned that when balanced ventilation is used, airflows are fixed and occupants have possibility to boost a kitchen hood. Typical control consists of user-operated switch that allows changing amount of supplied air in relation to user activity in a dwelling: “away”, “normal occupation”, “party”, etc. Norwegian housing developer said that for decentralized systems occupants had possibility to adjust the airflow manually in three levels. In the case of centralized systems, occupants seldom can do any adjustments. Another Norwegian housing developer confirmed the previous statement, but added that there can be an “indirect control” in a bathroom, either a humidity-controlled valve or an on-off switch as well as in a kitchen there can be a switch on a kitchen hood. A centralized control was also mentioned by a producer from Estonia. Both developers and designers from the UK mentioned a manual (switch) or humidity based boost modes for bathroom and kitchen. They also mentioned that users can switch their system off, but they are encouraged by developers and installers not to do so. This topic seems to be also important for Danish designers who pointed out that even if a system has a simple “on/off” control, the off does not actually mean that there is no airflow through the system, because this is not allowed according to building code.

Answers to question regarding minimum required ventilation rates and IAQ in dwellings (question g in Table 1) indicated that stakeholders were mostly aware of the lower limits for ventilation flows imposed by particular building codes. The Austrian building code (OIB 3) has general statements on required ventilation for rooms where people reside and for sanitary rooms. No explicit values regarding air exchange rate, supply or exhaust airflows are given in the building code, but there is a reference to standard dealing in detail with ventilation plants (ÖNORM 2014). Several stakeholders from Austria mentioned a building certification program launched by the Austrian ministry (“klimaaktiv”) which includes measures to improve IAQ (system efficiency, filters, etc.). Extra points are given within the subsidy application if this “klimaaktiv” certification is done. In the case of Denmark, stakeholders mentioned that there is not a clear standard about indoor air requirements and that the documents available are old. This is rather interesting result, because IAQ is specifically mentioned both in the Danish building code (BR15 2015) as well as in related standards. Building regulation deals with general requirements for IAQ and in addition mentions specific pollution sources such as formaldehyde. In Estonia, stakeholders expressed clearly that supply and exhaust airflows need to follow Estonian requirements to the minimum airflows: 1 l/s m<sup>2</sup> supply in living room and bedrooms, 10 l/s exhaust from toilets, 15 l/s from bathrooms and kitchen 20 l/s. There is no regulation concerning air humidity. Recirculation is not allowed according to Estonian requirements. Ventilation designers in France mentioned that no IAQ classification schemes, guidelines or standards are applied, only exhaust airflow requirements and rules for air inlet sizing according to DTU 68.3 (2017). Minimum extract airflows are given for each type of a humid room depending on the total number of normal rooms. In Norway, the stakeholders reported that national standard (TEK 2010) determine minimum airflows regarding materials and number of persons. For non-occupied spaces, only minimal ventilation rate is required. In addition, a technical guideline developed by Norwegian Building Research Institute (Building series 2017), was used as well to show examples of ventilation requirements defined in TEK (2010). Approved Document Part F of the Building Regulations (HM Government 2010) and the Domestic Technical Handbook of the Scottish Building Regulations (The Scottish Government 2015), are the IAQ standards used for

ventilation in England and Wales, and Scotland, respectively. One of respondents mentioned that IAQ is not a design priority outside major cities i.e. they only provide a basic and cost-effective design to comply with the regulations. While more attention is paid to the other aspects of the design that are more pertinent in the given context.

### **3.3 Barriers, problems and needs**

Table 3 lists the barriers and problems identified in this survey. The number of times each item was raised in the interviews carried out in each country is provided in Table 3 as frequency of occurrence and the identified problems are listed in descending order of frequency.

The investment required to provide whole-house mechanical ventilation along with spatial and maintenance requirements of these systems are among key concerns during decision making and design phase. Several stakeholders pointed out that the capital cost required for MVHR systems is notably higher than conventional ventilation systems such as intermittent humidity-controlled extract ventilation (MEV). However, there is often no life-cycle consideration of operational savings achieved and the health benefits of better indoor air quality. Furthermore, these systems require more space and duct routing can be challenging. Maintenance is also a key consideration especially in decentralised installations in apartment blocks where the MVHR system is installed inside an apartment and access to the unit for regular maintenance might be difficult.

Most respondents also reported a dis-jointed approach to design, installation and commissioning of MVHR systems whereby designers are often not involved in system commissioning. This can lead to discrepancies between actual operation and design intent. Another issue that can exacerbate this problem is shortcomings in the skillset of installers who are often not up to date regarding the latest ventilation and energy efficiency requirements. Non-compliance with regulatory requirements due to poor system installation and lack of commissioning was raised as a common concern. Lack of clear instructions about system operation and maintenance requirements in user manuals and during building handover was another major issue.

System maintenance after building handover was a key problem raised in most countries. In addition to problems around access, respondents reported that unless there is a follow-up service contract in place, which is mostly applicable to apartment blocks with centralised systems, key maintenance requirements may not be met in practice as occupants are not well briefed about these requirements and the consequences of poor maintenance. Noise and the perceived cost of operation, which in extreme cases had led to occupants turning their systems off, were among other problems identified in the survey.

There was a stark contrast between feedback received from respondents in European countries and the feedback received from China. The 'blank-house' method used to procure most dwellings in China means designers and developers have very limited control on the indoor environment as air quality, to a large extent, is determined by the materials occupants use to decorate their homes. It should be noted that the feedback received from China in this survey is based on only one interview and therefore cannot be generalised. However, supportive evidence from the literature point to the significance of indoor sources of pollutions in new dwellings in China. Investigations carried out in China show rapid increase in pollutants emitted by indoor sources in new buildings and refurbishments (Du et al. 2014; Liu, Liu, and Zhang 2013; Zhang, Mo, and Weschler 2013).

#### **3.3.1 Potential measures to improve IAQ in energy efficient homes**

**Legislative requirements:** The key legislative requirements and improvement opportunities identified by the respondents can be summarized as follows: a) Calls for more flexibility in legislation, codes and building standards including a more holistic approach that allows for

trade-offs; b) The necessity of a coordinated approach to energy efficiency and indoor air quality; c) Control mechanisms required to ensure good implementation and operation.

As for post-handover phase, a respondent in France drew an analogy between the mandatory requirements for maintenance of heating systems in France and most European countries, where building owners are legally responsible for annual service and maintenance of these systems, and maintenance of MVHR systems. Currently, the responsibility for maintenance of mechanical ventilation systems in dwellings is not well-defined (e.g. MVHR filter replacement). **Technical measures:** in addition to legislative requirements, respondents suggested that training and accreditation of installers of ventilation systems would be necessary to improve the quality of installations and avoid problems such as excessive air leakage, unbalanced systems, draughts, noise and poor specific fan powers. Furthermore, it was stated that it is important to keep the design as simple as possible, and at the same time flexible for user control. A respondent in Denmark, however, pointed out that better IAQ performance in some circumstances may be achieved by refined zonal control and increasing the number of sensors. This shows that finding the right balance between system complexity and IAQ performance objectives seems challenging and may be very much country and even project dependent. It is also important to identify the risk factors and failure modes of a design strategy and specify appropriate mitigation measures throughout the building procurement process. **Financial incentives:** financial incentives in form of government subsidy or grants for specific systems or insurance incentives for system maintenance can be very effective. One respondent from Austria estimated that around 50% of the multi-family housing projects in Tirol, western Austria, utilise balanced ventilation system with heat recovery thanks to additional housing subsidies available for these systems. **Market requirements:** calls for quality labels for ventilation system, more building products with low emissions, and potential market interventions to balance energy effectiveness and cost of installation were among the key market requirements identified in the survey. A producer of ventilation systems in Estonia also suggested that there must be a level playing field in the market. This producer provides additional measures for heat recovery and frost protection in cold climate whereas their competitors do not necessarily consider these problems and the potential consequences. Stricter regulatory requirements may lead to improvements in system performance and fairer market competition. **Outreach programmes:** Clearer guidance on air quality from the governments, feedback to designers about the actual performance of systems, enhanced industrial training for various practitioners involved in construction supply chains, and outreach campaigns to improve the understanding of building administrators and occupants about the benefits of mechanical ventilation especially in the context of low-energy buildings were identified as key outreach measures required to facilitate the use of these systems.

### 3.3.2 Acceptability of MVHR strategy

The acceptability of MVHR in all countries represented in the survey, but Denmark, can be divided in three categories: low – medium (France, China and UK), medium – high (Austria and Estonia) and high (Norway). It is notable that countries with strong financial incentives for MVHR (Austria) or where it is almost mandatory to install MVHR due to strict energy use requirements (Norway and Estonia) show the highest acceptance level.

Regarding the reasons for not using the MVHR in residences, stakeholders mentioned noise as a main reason, followed by running costs, awareness and operation difficulties. In addition, second order problems include draughts, prejudice, complexity and pathogens fear. These issues have not been identified as important as the first set of problems, but point to subtle socio-technical issues that must be considered to overcome the barriers against using mechanical ventilation strategy in low-energy dwellings.

Table 3. Barriers against and problems associated with whole-house mechanical ventilation of low-energy dwellings identified in the survey

<b>Country</b> (interviews)	<b>Design</b> (decision making, concept design & detail design)	<b>Construction</b> (installation & commissioning)	<b>Post-handover</b> (operation & maintenance)
<b>Austria</b> (6)	High capital cost of MVHR systems (4) Spatial requirements & duct routing (3) Implementation in refurbishments particularly challenging (2) Lack of flexibility for flow rates to account for real occupancy (1) Prejudice against MV systems (1)	Lack of up to date training and skills among system installers (1)	Noise especially in decentralised systems (4) System maintenance & access (2) Re-programming the systems (1) No proper support for tenants (1)
<b>China</b> (1)	Lack of control over internal sources of pollution (1)	‘Blank housing’ procurement method (1)	The original ventilation strategy can be compromised when occupants decorate their homes (1)
<b>Denmark</b> (5)	Spatial requirements & duct routing (4) High capital cost of MVHR systems (2) Fire safety requirements for centralized vent. in apartments (1) Stringent energy efficiency requirements (1) Working with architect’s design (2)	Designers are often not involved in commissioning (1) Big centralised systems become too complicated (1)	Maintenance issues (3) Occupants block the inlets distorting the air balance (1) Poor support & aftercare for users (1) No proper support for tenants (1)
<b>Estonia</b> (4)	Spatial requirements & duct routing (1) Challenging frost protection (1) Cost & technical complexity especially in renovating old buildings (1)		Noise (2) Operational failures (2) Cold draughts (1) Smells/odour (1) No proper support for tenants (1)
<b>France</b> (5)	High capital cost of MVHR (2) Maintenance requirements of MVHR (1) Complexity of MVHR compared to humidity-control extract (1) Spatial requirements for MVHR (1) Design acceptability (1) Lack of project-specific design/planning (1)	Poor quality in system installation & commissioning (2) Non-compliance with technical requirements (2)	Lack of maintenance (1)
<b>Norway</b> (7)	Spatial requirements & duct routing (6) Difficult to position the units to minimise noise (1) Difficult to find an appropriate location for air intake (1)	Designers are often not involved in commissioning (1) Systems not balanced (1)	Maintenance issues (3) No follow-up service arrangement (1) Noise (1)
<b>UK</b> (7)	Difficult to position the units to minimise noise (1) Spatial requirements & duct routing (1) Coordination within all design stakeholders (1) No minimum requirements for pollutants in the regulations (1) Costs (1) No control over emission sources introduced by occupants (1)	Installation and commissioning not in accordance with design intent (3) Insufficient skills of installers (1) Balancing the flow rates only, with less attention to pressure drop (1)	Maintenance issues (3) Noise and perceived energy cost (tenants switch the unit off) (2)

## CONCLUSIONS

MVHR systems are dominant even though natural ventilation is allowed by most building codes (if the minimum ventilation rates required are achieved). There is not a minimum efficiency requirement for heat recovery except for Denmark and Norway, and in practice, counter-flow plate heat exchanger is mostly used, followed by cross-flow heat exchanger. Application of DCV is not required by standards and it seems to be rare in practice due to higher costs and complexity. All countries provide a definition of minimum ventilation rate and stakeholders seem to be aware of them. Several stakeholders pointed out that the capital cost required for MVHR systems is notably higher than conventional ventilation systems, which is a barrier for wider implementation. Furthermore, these systems require more space and duct routing can be challenging. Maintenance is also a key consideration and non-compliance with regulatory requirements was raised as a common concern. Finally, noise and the perceived cost of operation, were among other problems identified in the survey. To overcome the previous issues, the main needs identified in the survey were: more flexibility in legislation, codes and building standards, a coordinated approach to energy efficiency and IAQ and control mechanisms to ensure good implementation and operation.

## 4 ACKNOWLEDGEMENTS

The work related to Austria was done within the framework of the IEA-research cooperation funded by the Austrian Federal Ministry for Transport, Innovation and Technology.

## 5 REFERENCES

- Arrêté 24.03.82 (1983). Arrêté du 24 mars 1982 relatif à l'aération des logements. JORF 15 novembre 1983.
- BR15 (2017). The Danish Building Regulations 2015. *Danish Transport, Construction and Housing Authority*.
- CIBSE (2015) Environmental Design CIBSE Guide A. *Chartered Institution of Building Services Engineers*. 8th ed. London.
- DTU 68.32. (2017). Afnor. NF DTU 68.3 Avril 2017. Travaux de bâtiment - Installations de ventilation mécanique.
- Du, Z., Mo, J., Zhang, J. and Xu, Q. (2014). Benzene, Toluene and Xylenes in Newly Renovated Homes and Associated Health Risk in Guangzhou, China. *Building and Environment*, 72, 75–81.
- Estonian legal acts 03.06.2015 nr 55 (2015). Minimum requirements for energy performance of buildings.
- Estonian legal acts 05.06.2015 nr 58 (2015). Methodology for calculating the energy performance of buildings.
- GB/T 18883-2002 (2002). Indoor air quality standard, *Chinese national standard*, Beijing: China Architecture & Building Press.
- JGJ 134-2010 J 116-2010 (2010). Design standard for energy efficiency of residential buildings in hot summer and cold winter zone, *Chinese national standard*, Beijing: China Architecture & Building Press.
- JGJ/T309-2013 J 1638-2013 (2013). The measurement and evaluation for efficiency of building ventilation, *Chinese national standard*, Beijing: China Architecture & Building Press.
- Langer, S., Bekö, G., Bloom, B., Widheden, A. and Ekberg, A. (2015). Indoor Air Quality in Passive and Conventional New Houses in Sweden. *Building and Environment*, 93, 1–9.
- Liu, Q., Liu, Y. and Zhang, M. (2013). Personal Exposure and Source Characteristics of Carbonyl Compounds and BTEXs within Homes in Beijing, China. *Building and Environment*, 61, 210–16.
- McGill, G., Qin, M. and Oyedele, L. (2014). Case Study Investigation of Indoor Air Quality in UK Passivhaus Dwellings. *Energy Procedia*, 62, 190–99.

- Norwegian Building series guideline: <https://www.byggforsk.no/>
- OIB-Richtlinie 3 (2015). Hygiene, Gesundheit und Umweltschutz. *Richtlinien des Österreichischen Instituts für Bautechnik*.
- ÖNORM H 6038 (2014). Ventilation and air conditioning plants - Controlled residential ventilation including heat recovery - Planning, installation, operation and maintenance. *Austrian Standards Institute*. Wien.
- TEK 10 (2010). The Norwegian building regulation 2010. *Directorate for Building Quality*.
- The Building Regulations 2010 (2010). Ventilation. Approved document F. F1 Means of Ventilation (2010 Edition Incorporating 2010 and 2013 Amendments). *HM Government*.
- The Scottish Building Regulations 2015 (2015). Technical Handbook - Domestic. *The Scottish Government*.
- Zhang, Y., Mo, J. and Weschler, Ch.J. (2013). Reducing Health Risks from Indoor Exposures in Rapidly Developing Urban China. *Environmental Health Perspectives*, 121(7), 751–55.

# Numerical analysis of the potential of using light radiant ceilings in combination with diffuse ventilation to achieve thermal comfort in NZEB buildings.

Marie Rugholm Krusaa<sup>\*1,2</sup>, Christian Anker Hviid<sup>1,2</sup>, Jakub Kolarik<sup>1</sup>

*1 Technical University of Denmark, DTU  
Anker Engelundsvej 1  
2800 Kgs. Lyngby, Denmark*

*2 Saint-Gobain Nordic and Baltic A/S  
Robert Jacobsens vej 62 A  
2300 København S, Denmark*

*\*Corresponding author: marrug@byg.dtu.dk*

## ABSTRACT

Renewable energy resources for heating and cooling of buildings have temperatures close to room temperature and therefore a limited convertibility potential, i.e. they are of low value. To exploit low-valued energy sources Low Temperature Heating and High Temperature Cooling (LTH-HTC) systems must be developed.

Hydronic radiant ceiling systems with large surfaces for heat transfer are well suited for the usage of LTH-HTC. In this paper, the aim is to create a system that can be flexible and include ventilation. The system analysed are a suspended capillary tube ceiling placed on top of perforated gypsum ceiling panels. These panels make it possible to combine the heating/cooling ceiling with the diffuse ventilation method. The diffuse ventilation method or leak ventilation use larger surfaces to provide air into the room instead of diffusers.

An office building is investigated and analysed on an annual basis in the dynamic building simulation tool IDA Indoor Climate and Energy (IDA ICE). The office building contains both offices and meeting rooms. Worst-case scenarios are investigated in the office building considering heat gains, solar gains and the temperature offset between supply water temperature and room air temperature.

The studies are carried out to identify the potential of reducing the temperature offset in near-zero energy buildings (NZEB) to the level where temperatures between  $\pm 2-4$  °C becomes possible. The reduction should not compromise on the thermal comfort of the building occupants and comprise energy savings.

The investigations showed that with a NZEB building it was possible to create an adequate thermal comfort with a minimum use of energy. The studies showed that an energy saving of 36-41 % from a fan coil system running with the same temperatures was possible.

## KEYWORDS

Diffuse ventilation, energy saving, radiant ceilings, heating, cooling.

## 1 INTRODUCTION

The building sector is the largest energy-consuming sector and accounts for 40 % of the total energy consumption and 36 % of the CO<sub>2</sub> emission in the EU (Commission 2017). This growing awareness regarding energy use has led to a requirement from the European Union that all new buildings by 2020 must be 'nearly zero energy buildings' (NZEB) (European Union 2010). At the same time, there is an increasing focus on indoor comfort and occupants' productivity, which leads to a higher demand for the heating, cooling and ventilation systems. The energy used in buildings today is mostly produced from fossil fuels, but as the energy system transforms towards renewable sources, low-valued energy sources are explored

(Hepbasli 2012). Low-valued energy for heating and cooling of buildings are sources with temperatures close to room temperature, consequently the term Low Temperature for Heating and High Temperature for Cooling (LTH-HTC) was introduced (Babiak and Olesen 2013).

Of the LTH-HTC systems the hydronic radiant systems show a great potential (Tario and Schmidt 2011). The hydronic radiant systems can be separated into three types: pipes embedded in the main structure (Thermally Active Building Systems, TABS), pipes isolated from the main structure (radiant surface systems), and radiant heating cooling panels or pipes suspended from the building structure (Kazanci, Olesen, and Kolarik 2016). With these radiant systems: floors, walls and ceilings can be used as surfaces that provide heating and cooling.

Other attempts to use LTH-HTC have been explored as well. One study showed potential by using active chilled beams. The active chilled beam supply air to the room and the room air recirculate within the chilled beam, which gives the chilled beam a higher capacity (Butler et al. 2004). In the study, the temperature offset (temperature difference between supply air and room air) was  $\pm 3$  °C (Afshari et al. 2013; Maccarini et al. 2014). This system has been installed in an office building in Jönköping, Sweden. The building has been in operation for a year where the only complaints allegedly has been about the office being too cold during the summer (Kretz 2016).

Other means to supply air to the room is the ventilation concept diffuse ventilation. The system is characterized by the air being supplied to the occupied room through a relatively large perforated surface, often the suspended acoustic ceiling made from perforated metal ceiling tiles or perforated gypsum tiles. The supplied air creates an overpressure in the plenum that diffuses the air through the ceiling (Hviid and Svendsen 2013). One of the advantages of using a large surface is the reduction of inlet velocity and consequently reduction of risk of draught (Yang 2011).

The diffuse ventilation system can be also combined with suspended radiant ceiling panels. By placing the heating/cooling source closer to the room the suspended radiant ceiling have a shorter reaction time than Thermo-active Building Systems (TABS).

In this paper the investigated combination of radiant panels with diffuse ventilation will be gypsum boards with capillary tube mats placed on top. The capillary tubes are produced extruded plastic (PEX) and have a small diameter between 2-5 mm. The tubes are structured in mats, which can be evenly distributed across the ceiling.

The objectives for this paper is

- To investigate if the combination of the capillary tube system and the diffuse ceiling ventilation can provide adequate thermal comfort and yearly energy savings with only a small temperature offset of 2-4 °C
- To investigate how the performance responds to changes in heat gains, circulating water temperature and mass flow, i.e. the sensitivity of the solution

## 2 METHOD

In order to investigate the capillary tube ceiling (CATC) system, a one-room model was constructed in the dynamic building simulation tool, IDA Indoor Climate and Energy (IDA ICE) (Equa 2017).

The approach was to create a base case room-model in a hypothetical office building that could function both as a meeting room and as an office.

The room model had a net floor area of 21.6 m<sup>2</sup>, and a total room height of 3.6 m (Figure 1, left). The office building was simulated to be placed in Copenhagen, Denmark and yearly simulations were conducted with the Danish "Design Reference Year" (DRY) weather file (Wang et al. 2013).

The exterior wall had a U-value of 0.09 W/m<sup>2</sup>K and a thickness of 486 mm. The window was South oriented and had a U-value of 0.8 W/m<sup>2</sup>K, g-value of 31 % and visible light transmittance of 54 %; with a window area of 4.8 m<sup>2</sup> the window to floor ratio was 22 %. Depending if the room model should function as a meeting room or an office the following internal loads were used, see Table 1. The office hours were from 7-17 each weekday, which is also the schedule used for both equipment, occupants, lighting, ventilation, heating and cooling.

Table 1: Simulation input and internal loads during occupancy 7-17

	Office	Meeting room
Occupants	7 m <sup>2</sup> /pers., 80% occupancy 2.5 persons 1.2 MET, 0.75 ± 0.25 clo	2 m <sup>2</sup> /pers., 90 % occupancy 10 persons 1.2 MET, 0.75 ± 0.25 clo
Equipment	3x50 W	150 W
Lighting	4 W/m <sup>2</sup>	4 W/m <sup>2</sup>
Shading	Internal shading	Internal shading
Shading factor	0.65	0.65
Ventilation air flow	47 l/s	127 l/s
Supply air temperature	20 °C	20 °C

## 2.1 Radiant heating and cooling ceiling

To integrate the diffuse ventilation and the CATC system the room model was divided into two zones; an “Office” and a “Plenum” (Figure 1 to the right).

Two types of internal constructions were used. A floor of the office and a ceiling of the plenum was modelled as a 200 mm concrete slab with screed for levelling and floor coating. A suspended ceiling between the office and plenum was modelled as a layer of high-conductive perforated gypsum board with graphite particles ( $\lambda=0.45$  W/m<sup>2</sup>K). On top of the gypsum, approx. 40 mm of insulation batts ( $\lambda=0.037$  W/m<sup>2</sup>K) were placed.

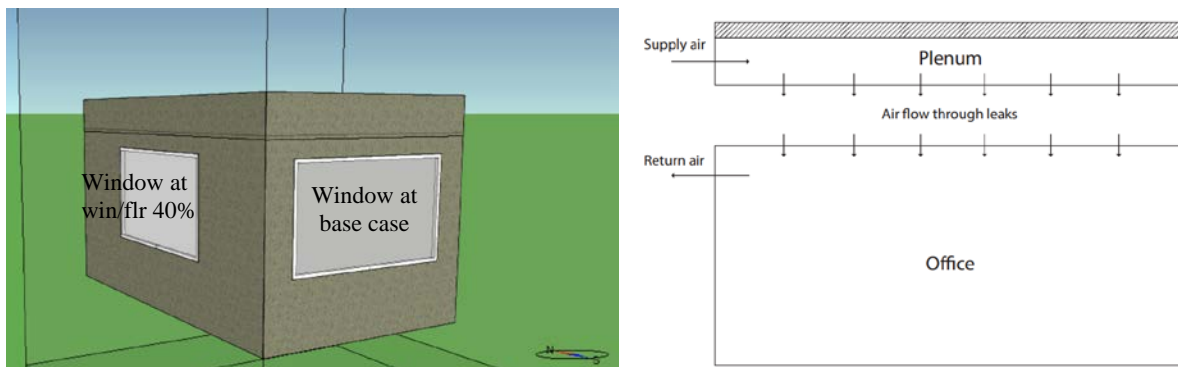


Figure 1: Left: 3D Model from IDA ICE, showing zone model of the office and the plenum with the window and location in the corner of the office building. The window is facing South. Right: Airflow between plenum zone and room zone.

The capillary tubes were modelled using standard IDA ICE component model for embedded heating/cooling systems (EQUA 2013). The IDA ICE component model represents a plane with controllable temperature placed in the building construction (floor/ceiling slab). The model allows for proportional control of heating/cooling output from the plane based on operative temperature. The model was then connected to component models of hydronic heating and cooling in IDA ICE (boiler and chiller component models) and design mass flow through the radiant ceiling system can be set.

Heat transfer between the embedded system and building construction is represented by common heat transfer coefficient according to EN 15377-1 (EN 15377 2008) (replaced by

standard EN ISO 11855). In the present work, the component model for embedded heating/cooling system was used to place an idealized heat conducting layer between the gypsum board and the insulation (Figure 2).

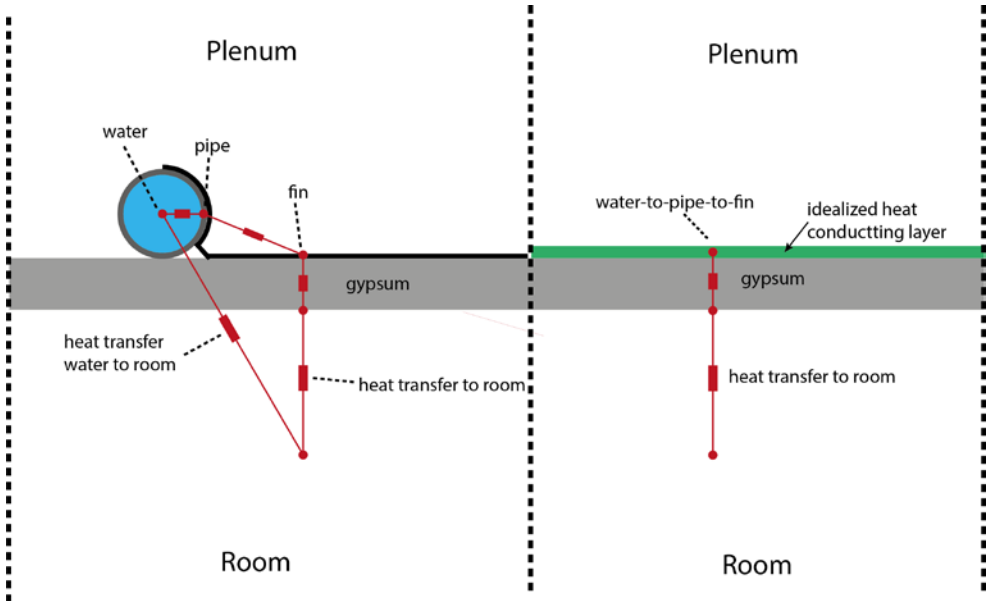


Figure 2: Modeling of heat transfer. Left: EN 15377-1. Right: IDA ICE modelling.

Figure 2 to left shows how EN 15377-1 calculates heat transfer; to the right is the input parameters in IDA ICE. From a preliminary study of a capillary tube ceiling in combination with diffuse ventilation (Onsberg and Eriksen 2014), the power for heating and cooling was found to be 616 W and 698 W, with a temperature difference at 4.8 K (Design Power in IDA ICE). For a room size 21.6 m<sup>2</sup> and 60 % of the ceiling covered with mats. Due to lighting, fire alarms and other installations it designed for 60 % covering of the ceiling. The total heat transfer coefficient from water to room were found by Onsberg & Eriksen to be 7 W/m<sup>2</sup>K. This is divided into a combined transfer from water-to-pipe-to-fin, heat transfer through the gypsum board and heat transfer to the room, shown in Table 2. The simulation of the mats in IDA ICE is by a constant mass flow, which is calculated design power and a temperature offset of 2 °C. This gives a mass flow of 0.083 kg/s.

Table 2: Heat transfer coefficients used in the simulation.

	Resistances [m <sup>2</sup> K/W]	Heat transfer coefficient [W/m <sup>2</sup> K]
Heat transfer to room	0.010	100
Gypsum board	0.022	45
Water-to-Pipe-to-Fin	0.111	9
Sum	0.143	7

## 2.2 Ventilation

The plenum distributes ventilation air from an air handling unit (AHU) to the office below through intentional cracks and leakages. From the office, the air is extracted and returned to the AHU. For the simulations in IDA ICE, the standard AHU is used with a heating coil and a heat exchanger. The heat exchanger had an effectiveness of 85 % and recovers both heating and cooling. The specific fan power for the AHU was 800 W/(m<sup>3</sup>/s). The ventilation rate used in the investigation is Class I from EN 15251 (2007) for the indoor air quality, which states

there should be 10 l/s per person, and 1 l/s per m<sup>2</sup>. The total ventilation rate can be found in Table 1.

The air passage between the plenum and office was modelled in IDA ICE by the leak component. The leak component is built up as a pres flow with the Equivalent Leakage Area (ELA) of 21.6 m. The ELA is defined by the volumetric air flow rate, the discharge coefficient (Cd), which is 1 and the pressure difference, which is set to 4 Pa (Edwards 2006).

### 2.3 Reference

A reference was created for comparison. The reference system is a CAV ventilation system with fan coils as air terminal devices. The fan coils recirculates the air in the room in order to provide sufficient heating/cooling capacity. For easier comparison, the only change introduced in the reference was the removal of the radiant ceiling and introduction of the fan coil as the conditioning source in the room.

The fan coil recirculated with 5.0 l/s per m<sup>2</sup>, and had an estimated pressure drop of 250 Pa with a fan efficiency of 60 %. The system was supplied with the same water temperatures for heating and cooling as the capillary system.

## 3 SIMULATION SCENARIOS

Several investigations have been made, where both the reference system and the capillary tube system was investigated with different supply water temperatures, different window-to-floor area and g-values. In Table 3, the scenarios are listed and commented.

Table 3: Simulated scenarios

Scenario	System	Parameters	Values	Comments
Base case	Capillary	Mass flow $\dot{m}$ [kg/s]	0.083	
		Water temperature $T_w$ [°C]	22	
		Window-to-floor area [%]	22	
		g-value of window [%]	31	
	Fan coil	Mass flow $\dot{m}$ [kg/s]	n/a	
		Water temperature $T_w$ [°C]	22	
		Window-to-floor area [%]	22	
		g-value of window [%]	31	
Mass flow	Capillary	Mass flow $\dot{m}$ [kg/s] of the circulating water	0.035 0.020	The mass flow of the circulating water determines the effective mean temperature of the circulating water and therefore also the heating/cooling capacity.
		Tw	Capillary	The supply temperature of the circulating water $T_w$ [°C] in the radiant ceiling
Fan coil			24	
Win/flr	Capillary	Window-to-floor area [%]	30	The ratio of transparent glazing to thermal mass in the room may cause the solar gains to be non-absorbable, in effect raising the temperature of the room.
	Fan coil		40	
g-value	Capillary	g-value of window [%]	25	The amount of solar heat gains that has been let through the window could, as the window-to-floor area be non-absorbable.
	Fan coil		38	

## 4 RESULTS

Simulations were performed for both office and meeting in corner (two façades) and center configuration (one façade). However, the most critical configurations were corner office and centered meeting room. Consequently, this paragraph reports only these results.

The report results are energy use, which includes lighting, room heating (district), cooling, and fans & pumps along with the thermal indoor comfort. Thermal comfort is evaluated as hours above 26 °C according to EN15251 (2007); with 2610 occupancy hours, the 5 % limit means 130 hours.

The daylight factor in the rooms was checked in accordance to the Danish building regulations standard of a minimum daylight factor of 2 % (“The Danish Building Regulations - 6.5.2 Dagslys” 2017), which is respected in all simulations. This means that the reported window-to-floor ratios and/or g-value combinations (and corresponding visible light transmittances) do not compromise the level of incoming daylight.

In all simulations, the fan coil system used more energy than the capillary system. Figure 3 illustrates that the fan coil system uses approx. three times more energy on the fans and pumps. Figure 4 show that the fan coil spends double the amount for fans and pumps. The fan coil has to be running in order to keep the comfortable temperatures in the room.

In general, the accumulated hours above 26 °C are higher in the simulations with the fan coil system. For both systems, the accumulated hours are highest with the water temperature of 24 °C and is all above the requirement of maximum 130 hours.

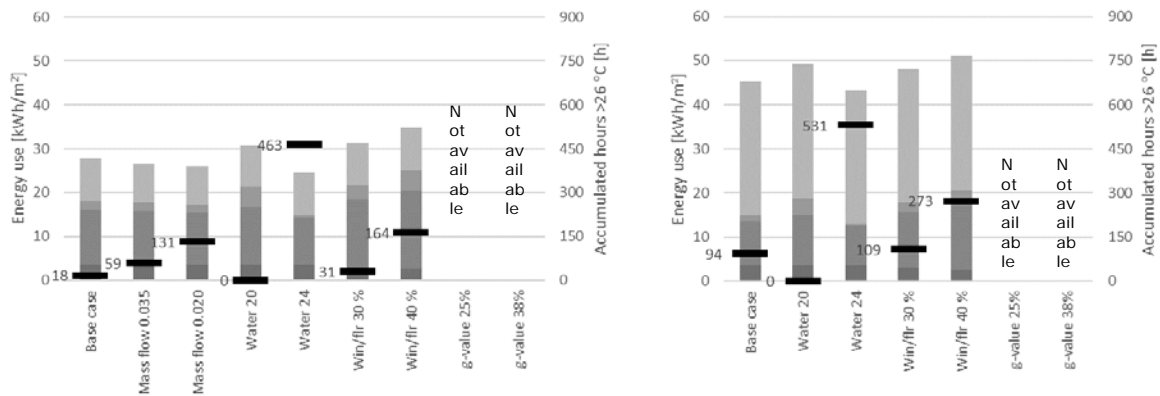


Figure 3: Corner office energy use and overheating. Left: Radiant ceiling system. Right: Fan coil system. Bars of energy use from dark to light grey: Lighting, District heating, Cooling and Fans & Pumps. Solid lines are accumulated hours of operative temperature >26 °C during occupancy

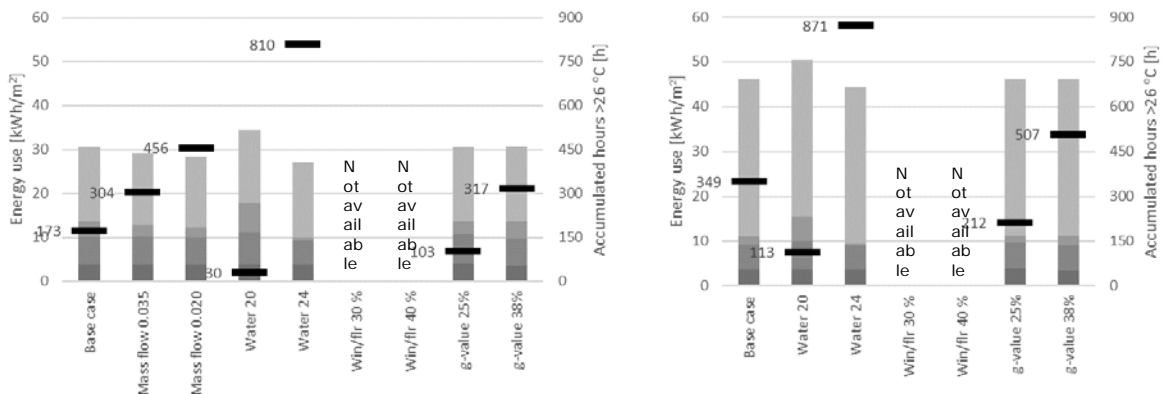


Figure 4: Centered meeting room, energy use and overheating. Left: Radiant ceiling system. Right: Fan coil system. Bars of energy use from dark to light grey: Lighting, District heating, Cooling and Fans & Pumps. Solid lines are accumulated hours of operative temperature >26 °C during occupancy.

For the corner office the base case, the mass flow of 0.035 kg/s, the water temperature 20 °C and the win/flr of 30 % are all within the requirements of maximum 130 hours with temperatures above 26 °C. For the centered meeting room the simulations that fulfil the requirements with a maximum of 130 hours are with the water temperature of 20 °C and the lower g-value.

The energy use for the capillary system only varies slightly. Changing the water temperature to 20 °C make the energy use rise 10 %, though it makes it possible to have comfort in the meeting room. Changing the g-value does not affect the energy, only the amount of overheating hours.

## **5 DISCUSSION**

A conventional fan coil system would operate with a temperature offset of 10 °C. In this investigation, this temperature offset was only 2-4 °C. Consequently, the fan coil system is less effective than expected. If the supply water temperature was lowered to approx. 12-16 °C, the fan coil system would probably out-perform the radiant ceiling in terms of thermal comfort, at the expense of much higher energy use for cooling and probably increased risks of draught.

The simulation of the diffuse ventilation is difficult to simulate in a dynamic simulation program like IDA ICE. There were two different methods; one was the leak model, which ensured that the airflow only was one way. The other methods was large vertical openings where the airflow was both ways and not able to control. The limitations with the leak model is that it is not possible to include the transfer of heating and cooling when the air pass through the surface. With the leak model it is not possible to confirm the residence time of the air in the plenum before supplying to the office.

The resistances were chosen on behalf of the preliminary experimental studies with capillary tube ceiling systems and diffuse ventilation. However, the heat transfer coefficient was in this study only reported as a value from water to the room. An in-depth study of the individual resistances, both convective, conductive and radiative, that make up the total heat transfer of a radiant ceiling in combination with diffuse ventilation, should be conducted to validate the assumptions regarding heat transfer coefficients in this paper.

## **6 CONCLUSIONS**

Simulations have been performed for both a radiant ceiling system in combination with diffuse ventilation and a reference with a more conventional fan coil units; where only a few parameters has been changed even though a fan coil system often is running with higher temperature differences. From these simulations, it can be seen that the radiant system has a higher capacity for heating and cooling. The radiant systems has shown a great potential combined with the diffuse ventilation.

The simulations showed that it was possible to create a system that can provide adequate thermal comfort with a minimal energy use. Significant energy savings were realized in the capillary system compared with the fan coil system.

From the investigations, it can be concluded that a temperature offset of 2 °C for office spaces and 4 °C for meeting rooms is enough to keep the overheating at an acceptable level below 130 hours.

The investigations showed only small changes in the total energy use. The sensitivity was shown at the level of thermal comfort. The meeting rooms was very sensitive to parameter changes and fulfilled only the requirements with the lowest simulated water temperature and

the lowest g-value. The offices are more robust and tolerate higher heat gains and lower mass flows.

## 7 ACKNOWLEDGEMENTS

I would like to acknowledge the financial help from Innovation Fund Denmark and Saint-Gobain Nordic A/S that made this study possible.

## 8 REFERENCES

- Afshari, Alireza, Rouzbeh G Norouzi, Göran Hultmark, and C Niels. 2013. "Two-Pipe Chilled Beam System for Both Cooling and Heating of Office Buildings." *11th REHVA World Congress and 8th International Conference on Indoor Air Quality, Ventilation and Energy Conservation in Buildings*, 16–19 June, 2013, Prague, Czech Republic.
- Babiak, Jan, and Bjarne W Olesen. 2013. *Low Temperature Heating and High Temperature Cooling Federation of European Heating and Air Conditioning Associations*.
- Butler, David, Jonas Gräslund, Jaap Hogeling, Erik L. Kristiansen, Mika Reinikainen, and Gunnar Svensson. 2004. *Rehva 05: Chilled Beam Application Guidebook*. Edited by Maija Virta. *Design*. 2. edition. Vol. 5. REHVA.
- Commission, European. 2017. "Buildings - European Commission." *European Union*. <https://ec.europa.eu/energy/en/topics/energy-efficiency/buildings>.
- Edwards, Rodger. 2006. *Handbook of Domestic Ventilation*. [https://books.google.dk/books?id=xGcABAAAQBAJ&hl=da&source=gbs\\_navlinks\\_s](https://books.google.dk/books?id=xGcABAAAQBAJ&hl=da&source=gbs_navlinks_s).
- EN 15377. 2008. "Varmesystemer I Bygninger – Projektering Af Indstøbte Vandbaserede Systemer Til Overfladevarme Og Overfladekøling – Del 1 : Fastlæggelse Af Dimensionerende Varme- Og Kølekapacitet Heating Systems in Buildings – Design of Embedded Water Base."
- EQUA. 2013. "User Manual IDA Indoor Climate and Energy," no. February.
- Equa. 2017. "IDA Indoor Climate and Energy. EQUA Simulation AB." <http://www.equa.se/en>.
- European Union. 2010. "Directive 2010/31/EU of the European Parliament and of the Council of 19 May 2010 on the Energy Performance of Buildings." <http://eur-lex.europa.eu/legal-content/EN/TXT/PDF/?uri=CELEX:32010L0031&from=EN>.
- Hepbasli, Arif. 2012. "Low Exergy (LowEx) Heating and Cooling Systems for Sustainable Buildings and Societies." *Renewable and Sustainable Energy Reviews* 16 (1). Elsevier Ltd: 73–104. doi:10.1016/j.rser.2011.07.138.
- Hviid, Christian Anker, and Svend Svendsen. 2013. "Experimental Study of Perforated Suspended Ceilings as Diffuse Ventilation Air Inlets." *Energy and Buildings* 56. Elsevier B.V.: 160–68. doi:10.1016/j.enbuild.2012.09.010.
- Kazanci, Ongun B., Bjarne W. Olesen, and Jakub Kolarik. 2016. "Low Temperature Heating

and High Temperature Cooling in Buildings.” DTU. [http://www.rehva.eu/publications-and-resources/eshop/eshop.html?tt\\_products%5BbackPID%5D=6&tt\\_products%5Bproduct%5D=35&cHash=32bd42e0a51e537b90685ebda3d816d4](http://www.rehva.eu/publications-and-resources/eshop/eshop.html?tt_products%5BbackPID%5D=6&tt_products%5Bproduct%5D=35&cHash=32bd42e0a51e537b90685ebda3d816d4).

Kretz, Mark. 2016. “Huset Med Självregerande Klimatsystem.” *Energi & Miljö*. [http://www.energi-miljo.se/sites/default/files/energimilj\\_0010\\_low\\_sid\\_16-20.pdf](http://www.energi-miljo.se/sites/default/files/energimilj_0010_low_sid_16-20.pdf).

Maccarini, Alessandro, Alireza Afshari, Niels Christian Bergsøe, Göran Hultmark, Magnus Jacobsson, and Anders Vorre. 2014. “Innovative Two-Pipe Active Chilled Beam System for Simultaneous Heating and Cooling of Office Buildings.” *Isiaq* 2020.

Onsberg, Rasmus, and Morten Skyum Eriksen. 2014. “Investigations and Development of Capillary Thermal Ceiling Systems with Integrated Ventilation,” 179.

Tario, H., and D. Schmidt. 2011. “Annex 49 - Summary Report.” [http://www.annex49.info/download/summary\\_report.pdf](http://www.annex49.info/download/summary_report.pdf).

“The Danish Building Regulations - 6.5.2 Dagslys.” 2017. Accessed June 16. [http://byggningsreglementet.dk/br15\\_02\\_id102/0/42](http://byggningsreglementet.dk/br15_02_id102/0/42).

Wang, P.G., M. Scharling, K.P. Nielsen, K.B. Witchen, and C. Kern-Hansen. 2013. “2001-2010 Danish Design Reference Year.” Copenhagen.

Yang, Honglu. 2011. “Experimental and Numerical Analysis of Diffuse Ceiling Ventilation.” *Master Thesis*, no. August.

# **Influence of night ventilation on the cooling demand of typical residential buildings in Germany**

**Johannes Schrade<sup>\*1</sup>, and Hans Erhorn<sup>1</sup>**

*1 Fraunhofer Institute for Building Physics  
Nobelstraße 12  
70569 Stuttgart, Germany*

## **ABSTRACT**

The current type of construction preferred for new high energy efficient buildings in Germany, featuring highly insulated building components and an almost completely airtight building shell, raises several new challenges with regard to design, construction and use of these buildings. Cooling, in particular, is an issue that gains importance also in the residential sector, in connection with rising temperatures induced by the climate change.

Increased night ventilation is a cost-effective option to influence the indoor climate such that comfortable conditions are durably ensured, keeping technical expenditure within reasonable bounds. Though the functional principle of night ventilation is well known and its applications are manifold, it is not widely considered by building planners. One of the reasons for lacking attention might be that the potentials of night ventilation with regard to building cooling cannot be sufficiently estimated. The present study investigates the impact of night ventilation on the cooling demand of typical new residential buildings in Germany.

The potentials of night ventilation are examined for two exemplary cases, namely for a single-family home and a multi-family building. Thermal building simulation is used to perform numerical assessments and to discuss functionality and effects of natural ventilation. The study analyses several influences on the indoor thermal comfort including the impact of different types of construction, various designs, thermal insulation standards, ventilation strategies and the use of solar shading devices in combination with or without night ventilation.

The simulation results show that the problem of excess summer temperatures occurring under current climatic conditions in typical, new residential buildings in Germany can be controlled by appropriately adapting the building design and by using solar shading devices. Especially night ventilation can be a very efficient and effective measure to minimize the risk of overheating, irrespective of the type of construction, the use of solar shading systems, the standard of thermal insulation or the building design, thus making the use of an active cooling system superfluous. Even for a worst-case scenario, night ventilation can guarantee comfortable indoor temperatures to a large extent.

## **KEYWORDS**

Ventilative cooling, night ventilation, summer overheating risk, summer heat protection, thermal building simulation,

## **1 INTRODUCTION**

New-built high energy efficient buildings in Germany with highly insulated building components and almost completely airtight building shells raise several new challenges with regard to design, construction and use of these buildings. Cooling, in particular, is an issue that gains importance also in the residential sector, in connection with rising temperatures induced by the climate change.

Alternatively to active cooling, there are also passive and hybrid measures, which minimize the demand of a building for cooling without using mechanical devices. These measures can be grouped in two categories with regard to their impact: (1) passive measures designed to reduce heat gains, (2) measures for activating and discharging structural components that act

as a thermal storage in a building. For instance, measures that contribute to reducing the heat gains include solar shading devices, daylight concepts, energy-efficient appliances or the facade design (bright-coloured paint or planting vegetation). Regarding the thermal activation of building components, the construction of the building plays an important role, and also technical components like phase change materials. The thermal storage is discharged either via hydronic systems (e.g. capillary tube mats) or by means of natural or hybrid ventilation. Increased night ventilation is a particularly cost-effective option to influence the indoor climate such that comfortable conditions are durably ensured, keeping technical expenditure within reasonable bounds. Though the functional principle of night ventilation is well known and its applications are manifold, but it is not widely considered by building planners. One of the reasons for lacking attention might be that the potentials of night ventilation with regard to building cooling cannot be sufficiently estimated. The present study investigates the impact of night ventilation on the indoor climate of typical new residential buildings in Germany.

## 2 METHODOLOGY

In the scope of the study, two typical, newly constructed residential buildings - a single-family home and a multi-family building - are examined with regard to their overall building energy performance and thermal comfort in summer. The energy performance of the buildings is assessed in accordance with the monthly balance method specified in DIN V 18599 [1] with the Fraunhofer software IBP:18599. To evaluate the summer indoor climate, a thermal building simulation is carried out using TRNSYS 17 [2], with a one-hour calculation time step, applying “Multi-Zone Building Type 56“. The simulation model parameters were chosen in conformity to DIN V 18599 default values. In addition, a verification of compliance with summer heat protection requirements according to German standard DIN 4108-2 [3] is done for the critical rooms.

In the scope of a parameter study, several influences on the indoor thermal comfort of both example buildings will be examined, including the impact of different types of construction, various designs, thermal insulation standards, ventilation strategies and the use of solar shading devices in combination with or without night ventilation. In addition, the effects of storage discharge through night ventilation will be illustrated using thermal building simulation.

### 2.1 Building models



Figure 1:3D model of the single-family home

The calculation model for the single-family home is based on typical offers of prefabricated house manufacturer in Germany. It consists of 3 stories including basement, ground floor and top floor. The basement is located entirely below the terrain level; it is partially heated. The

top floor is located beneath a sloped roof with a 45° inclination. The top floor is situated below an unfinished attic. The gable of the pitched roof has an east-west-orientation; the entrance door is placed at the northern facade.

The ground floor includes entrance area, guest room and store room with medium-sized window openings at the northern façade. Living dining room combo and kitchen with large window openings are situated at the south facade. The top floor contains two large bedrooms in the southern part of the sloped roof, and bathroom, smaller bedroom and storeroom in the northern. At each gable side there are two full-height windows, as well as 5 roof windows placed in each room.

Table 1: Building characteristics of the single-family homes

Gross floor [m <sup>2</sup> ]	Net volume [m <sup>3</sup> ]	A/V-ratio [m <sup>2</sup> /m <sup>3</sup> ]	Building envelope [m <sup>2</sup> ]	Window [m <sup>2</sup> ]
271	601	0.64	506	38

A new construction built within the scope of the German research initiative 'EnEff:Stadt' at Lilienstrasse in Munich[4] was selected to serve as the building model for the multi-family building. It consists of 15 residential units on 5 levels, with an average size of 70 m<sup>2</sup>. The upper structure of the building is marked by a slightly inclined roof structure with an inclination of 10°, the bottom of the building is formed by an unheated basement. Contrary to the real building situation, a detached building is being modelled and the balconies at the south facade are not taken into consideration, in order to eliminate the impacts of fixed shading structures.



Figure 2: Southern view of the multi-family building [4]

The floor plan of each story comprises three flats of different sizes, which can be reached via external access balconies and stair cases. In the western part of the building there is a 2-room flat with 55 m<sup>2</sup> living area (Flat 1). Kitchen, entrance and bathroom of flat 1 are facing to north, while living room and bedroom are facing south with full-height windows. In the center part of the story another 2-room flat with a floor area of 48 m<sup>2</sup> is located (Flat 2). Entrance and bedroom of flat 2 are on the northern façade, living room and kitchen with full-height windows are facing south. In the eastern part of the building is a 4-room apartment of 105 m<sup>2</sup> (Flat 3). Entrance, bathroom, kitchen and one bedroom of flat 3 are north facing, while two bedrooms and living room with large window areas are located on the southern façade.

Table 2: Building characteristics of the multi-family building

Gross floor [m <sup>2</sup> ]	Net volume [m <sup>3</sup> ]	A/V-ratio [m <sup>2</sup> /m <sup>3</sup> ]	Building envelope [m <sup>2</sup> ]	Window [m <sup>2</sup> ]
1544	2920	0.43	1554	173

## 2.2 Energy concept

To carry out further investigations, three energy concepts are assumed for different standards of thermal insulation. The reference case is a building concept according to the minimum requirements specified in the EnEV; in addition, one concept for a 'KfW Efficiency House 55' (KfW 55) and one for a 'KfW Efficiency House 40' (KfW 40) are developed. The KfW Efficiency House levels are defined by the Development Loan Corporation. They are used in the loan programs for energy efficient new building and retrofitting. The number indicates how much energy an efficiency house still needs compared to the minimum standard. The heating system consists of a centralized electrical air-to-water heat pump which is used for space heating and DHW. While the concept of the multi-family building implies a mechanical ventilation system with heat recovery, the single-family house is naturally ventilated. Quality of the thermal insulation varies according to the targeted performance standard.

Table 3: Characteristics of building elements featuring different energy performance standards

		EnEV 2016	KfW 55	KfW40
$U_{\text{Wall}}$	[W/m <sup>2</sup> K]	0.28	0.16	0.14
$U_{\text{Roof}}$	[W/m <sup>2</sup> K]	0.20	0.14	0.10
$U_{\text{Floor}}$	[W/m <sup>2</sup> K]	0.35	0.25	0.20
$U_{\text{Win}}$	[W/m <sup>2</sup> K]	1.30	0.95	0.80
$\Delta U_{\text{Thermal bridges}}$	[W/m <sup>2</sup> K]	0.05	0.03	0.02
Air tightness $n_{50}$	[h <sup>-1</sup> ]	1.50	1.00	0.60

In addition to different levels of insulation, it is also examined in which way different types of construction influence the potential of night ventilation. The reference case is a solid construction with reinforced concrete floors/ceilings and masonry internal and external walls. The alternative type of construction provides a timber-post structure with suspended reinforced-concrete floors/ceilings and plasterboard walls as internal walls. A further parameter to be investigated is the influence of the window/facade ratio. Investigations will focus on an increase of the window area by 15% compared to the reference case.

## 2.3 User profiles

### Internal loads

Assumptions for the internal heat loads induced by persons, lighting and electrical equipment are made according to DIN V 18599-10. To create daily profiles, the heat load is divided into hourly values as a function of space usage and time of day, according to the procedure specified in DIN EN ISO 13791 [5].

According to DIN V 18599-10, the net energy need for DHW is assumed to be  $q_{w,b}=11$  kWh/m<sup>2</sup>a in the single-family home and 15 kWh/m<sup>2</sup>a in the multi-family building. For reasons of simplicity, it is assumed that the DHW demand does not change in time. The above described approach is not equivalent to the boundary conditions of DIN 4108-2 for verifying summer heat protection on basis of a thermal building simulation.

### Solar shading

In both residential buildings, external roller shutters are used as flexible solar shading devices. Fixed shading devices provided by structural measures or the environment are not taken into consideration. In the study three different control strategies for solar shading are examined:

- Automatic control using solar sensors (total radiation on façade)
- Manual control during absence (time control with weather forecast)
- Manual control during presence (internal temperature)

## 2.4 Other boundary conditions

For the thermal building simulation, the reference climate for Germany at reference location Potsdam (region 4) is used. The solar radiation on facades and roof is calculated based on the isotropic sky model.

The soil temperature of the ground is represented using Type 501 of the TESS library[6]. The mean surface temperature of the soil is assumed to correspond to the average annual external temperature ( $T_{e,mean} = 9.5^{\circ}\text{C}$ ).

The surrounding of the buildings is assumed to be a dispersed, suburban development. For reasons of simplicity, the infiltration air change is assumed to be constant.

## 2.5 Night ventilation

Increased night ventilation to achieve passive cooling of the building occurs by natural ventilation, no additional fans are used. All operable windows serve as ventilation openings. Depending on the accessibility from the outside (protection against burglary) and the use of the rooms (darkening the bedrooms), different effective ventilation cross-sections are estimated. The calculations are based on the following assumptions:

- Bedroom window: window tilted, shutters closed
- Window accessible from the outside: window tilted
- Other windows: windows half open

The night ventilation is modelled user-controlled and time-dependent, based on the external and internal temperature. If the internal temperature exceeds  $24^{\circ}\text{C}$  while the external temperature is below  $22^{\circ}\text{C}$ , the windows are opened in the period between 11 p.m. and 6 a.m. The windows remain open until the internal temperature falls below  $18^{\circ}\text{C}$  or precipitation occurs.

The effects of natural night ventilation are modelled using the air mass flows balance method. This means that the air mass flow rate, which is conveyed into a zone, will leave the zone in the same time step, thus preventing the occurrence of low-pressure or overpressure.

The air mass flows, which enter the individual rooms through the window openings in each time step, are calculated following Annex 1 of DIN EN ISO 13791. Both, wind and thermal buoyancy induced by a temperature gradient between the interior and the exterior are considered as driving forces.

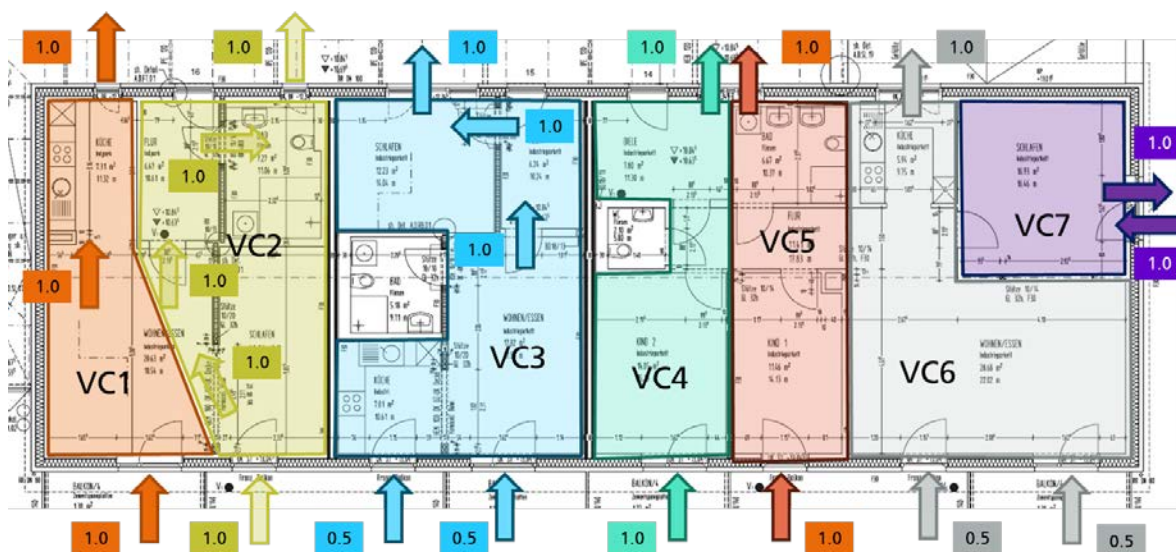


Figure 3: Air flow model for the multi-family building with wind as the driving force

### 3 RESULTS

#### 3.1 Summer heat protection

The most critical rooms in the single-family home are the three bedrooms on top floor and the living room on ground floor. In the multi-family building, the critical rooms are the bedroom in flat1, living room and kitchen in flat 2 and one of the bedrooms in flat3. All these rooms are characterized by high window/façade ratios per unit floor area ( $f_{og}$ ) in combination with either south facing windows or roof windows.

As shown inTable 4, in some rooms sufficient summer heat protection can only be verified in conjunction with increased night ventilation of  $n = 2h^{-1}$ , although the thermal storage mass of the buildings was assumed to be high. If a lightweight construction is used, all other rooms would also tend to overheating.

Table 4: Verification of summer heat protection in critical rooms

	Room	Orientation	$f_{og}$	Construction	Night ventilation
<b>Single Family Home</b>	Bedroom 1	South	0.23	Medium-weight	-
	Bedroom 2	North	0.32	Medium-weight	2.0
	Bedroom 3	South	0.23	Medium-weight	-
	Living room	South	0.40	Heavyweight	2.0
<b>Multi Family building</b>	Bedroom (flat 1)	South	0.25	Heavyweight	-
	Living room (flat 2)	South	0.36	Heavyweight	-
	Kitchen (flat 2)	South	0.20	Heavyweight	2.0
	Bedroom (flat 3)	South	0.25	Heavyweight	-

#### 3.2 Thermal simulation of buildings

The effects of increased night ventilation on the cooling energy demand of buildings are examined by performing thermal building simulations. The single-family home was completely modelled, including basement rooms and attic floor. In the case of the multi-family building, only the top floor was modelled, for which the highest solar gains were expected due to its location. For reasons of simplicity it was assumed that an air exchange taking place between individual rooms will only be examined for the case of night ventilation. The reference case was defined for a building featuring the EnEV standard of thermal insulation, built as a heavyweight construction with normal window sizes and provided with automatically controlled solar shading devices. This reference case equates to the building concept, which was evaluated in chapter 3.1.

The overheating risk is examined using eight variants of the building models (see Table 5). The variants are distinguished in terms of insulation standard,type of building construction,control of the solar shading device and window size.

Table 5: Examined variants with regard to their potential of enhanced night ventilation

Case	Name	Insulation	Construction	Window size	Shading control
Ref	Reference	EnEV	Heavyweight	Normal	Automatic
UCS	User-controlled shading	EnEV	Heavyweight	Normal	User-controlled
TCS	Time-controlled shading	EnEV	Heavyweight	Normal	Time-controlled
NoS	No solar shading	EnEV	Heavyweight	Normal	No shading
KfW55	KfW55	KfW 55	Heavyweight	Normal	Automatic
KfW40	KfW40	KfW 40	Heavyweight	Normal	Automatic
LWB	Lightweight building	EnEV	Lightweight	Normal	Automatic
IWA	Increased window area	EnEV	Heavyweight	Increased	Automatic

**Overheating risk without night ventilation**

The results of the thermal building simulation suggest that the single-family home in the reference case (Ref) is not prone to overheating in summer. As illustrated in Figure 4, the threshold value for excess temperature degree hours acc. to DIN 4108-2 of a maximum of 1200 Kh is not exceeded. The excess temperature degree hours are calculated from the difference between the hourly operative temperature and the reference value for the summer climate region B of 26°C, cumulated across all hours with excess temperature.

Modifications in the control of the solar shading devices (user-controlled (UCS) or time-controlled (TCS)) do not create a risk of overheating. It would, however, make a difference if all solar shading devices were deactivated (NoS). When examining the impacts of the energy concept (KfW55 and KfW 40), excess temperature degree hours are found to increase along with enhanced thermal protection, while remaining clearly below the threshold values. This result meets the expectation that additional insulation even has a rather positive effect on summer heat protection, improved leakage characteristics of the building envelope however prevent the discharge of heat loads by way of infiltration air flows.

The reduced heat storage capacity of a lightweight construction (LWB) results in a significant increase of excess temperature degree hours; however, the values for all rooms of the single-family home remain clearly below the admissible threshold values. The variant with extended window areas (IWA) is not associated with any significant increases in excess temperature degree hours. From this, it can be concluded that the choice of appropriate solar shading devices is of greatest importance for the single-family home.

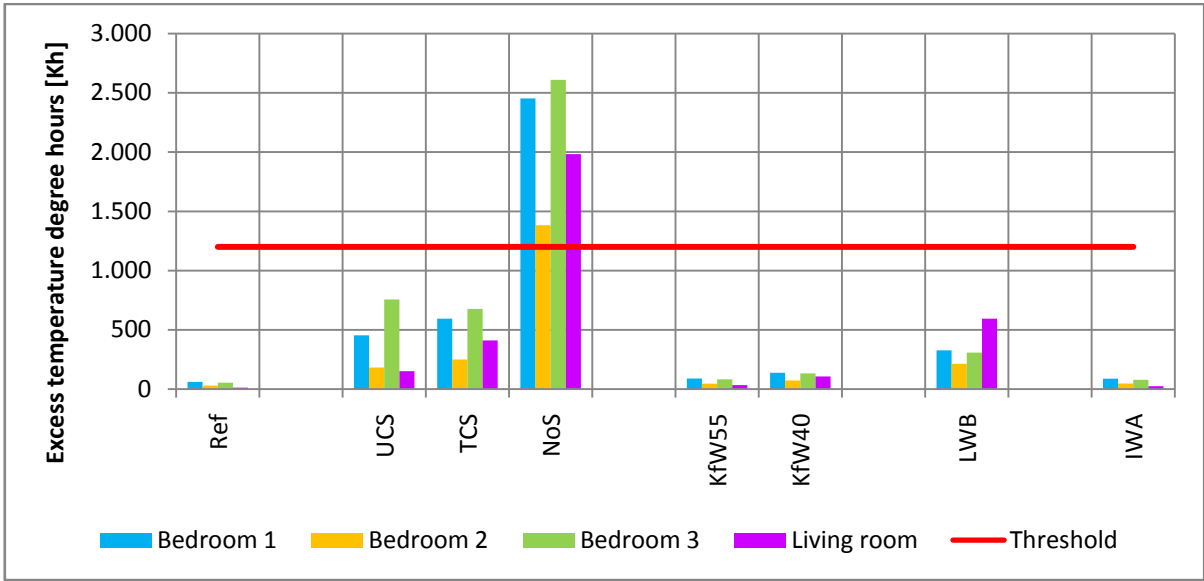


Figure 4: Impact of solar shading, thermal protection, heat storage capacity and size of windows on the excess temperature degree hours in the critical rooms of the single-family home. (Ref = Reference case, UCS = User-controlled shading, TCS = Time-controlled shading, NoS = No Solar shading, KfW55 = KfW Efficiency House 55, KfW40 = KfW Efficiency House 40, LWB = Lightweight building, IWA = increased window area).

Likewise, the reference construction of the multi-family building (Ref) does not tend to overheating as the results of thermal building simulation suggest (see Figure 5). The only critical room featuring a value only just below the maximum admissible excess temperature degree hours is the kitchen of interior flat 2.

A variation of the automatic solar shading control in the reference case would lead to an increase of the overheating risk. The least influence is found for the user-controlled operation (UCS). In the case of time-controlled operation (TCS), the threshold values would exceed in

the living room and kitchen of flat 2. If solar shading is entirely dispensed, excess temperature degree hours will exceed 1200 Kh in all rooms. If the level of thermal insulation is further enhanced, the excess temperature degree hours in the living room and kitchen of flat 2 would exceed the threshold value, while the other rooms would not be affected. Enlarging the window areas (IWA) causes exceedance of the threshold values only in the kitchen of flat 2, in a lightweight construction (LWB) also the living room of flat 2 would exceed the threshold.

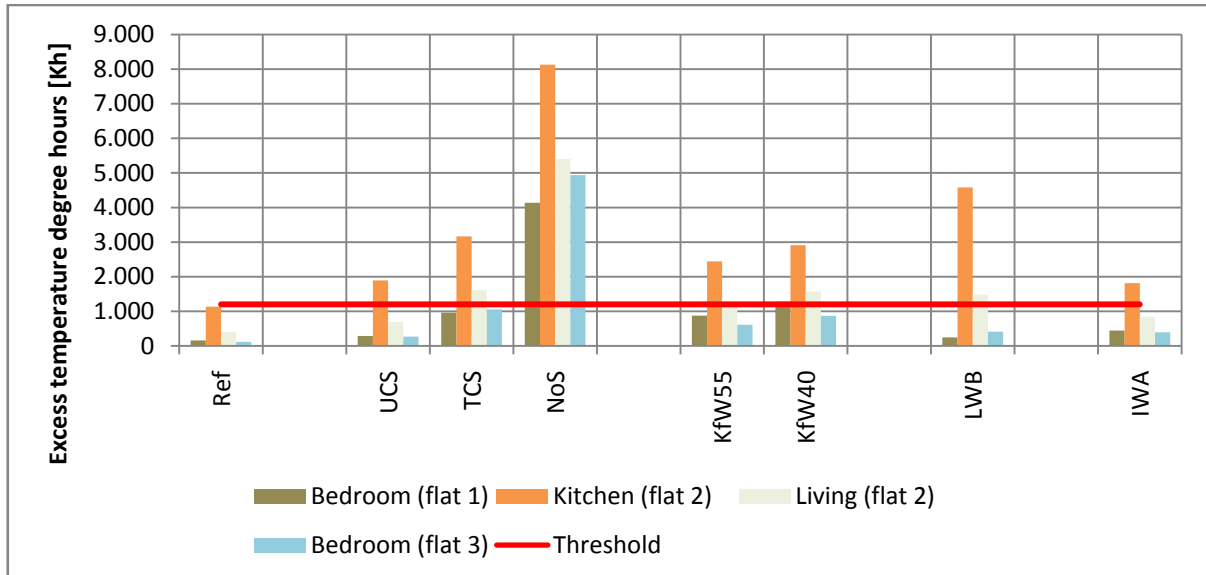


Figure 5: Impact of solar shading, thermal protection, heat storage capacity and size of windows on the excess temperature degree hours in the critical rooms of the multi-family building. (Ref = Reference case, UCS = User-controlled shading, TCS = Time-controlled shading, NoS = No Solar shading, KfW55 = KfW Efficiency House 55, KfW40 = KfW Efficiency House 40, LWB = Lightweight building, IWA = increased window area).

### Effects of night ventilation

Targeted discharge of heat via extended ventilation through windows during night-time hours can substantially reduce daytime indoor temperatures. Figure 6 presents the thermal building simulation results of the living room in the single-family home on the night of 20 to 21 July.

In the evening hours before night ventilation sets in, the indoor air temperature (red line) remains relatively constant above 24°C. The outdoor air temperature (bright blue) drops from 30°C at 8 p.m. to 18°C at 5 a.m. After sunrise, it rises above 20°C. Night ventilation starts as soon as the outdoor temperature falls below the indoor air temperature. Night ventilation remains active until the windows are closed at 7 a.m. in the morning. In the first hour, the force driving the air exchange is the wind acting on the east façade (green column). In the next two hours, the temperature difference between indoor air and outdoor air is the driving force (blue). After four hours the wind velocity augments notably and the wind on the south facade becomes the driving force (orange). In the sixth hour, the wind changes to an eastern direction; hence, the wind on the east facade becomes the driving force.

As expected, the indoor temperature continually declines after night ventilation has begun. In the morning hours, when the wind on the east facade passes through the kitchen into the living room, the indoor temperature rises again until it recovers 23°C at 8 a.m.

At first sight, this course may be somewhat surprising, because the indoor temperature rises at a point in time when the outdoor temperature is still below the indoor temperature and solar gains are not yet expected. The reason for this development becomes evident by looking on the surface temperatures of the enclosing building components (floor, ceiling, and external wall facing south). Due to higher heat storage capacity of building components compared to

that of air, the indoor air is reheated, if the air volume flow passes into the living room is no longer sufficient to discharge the heat dissipated by the building components.

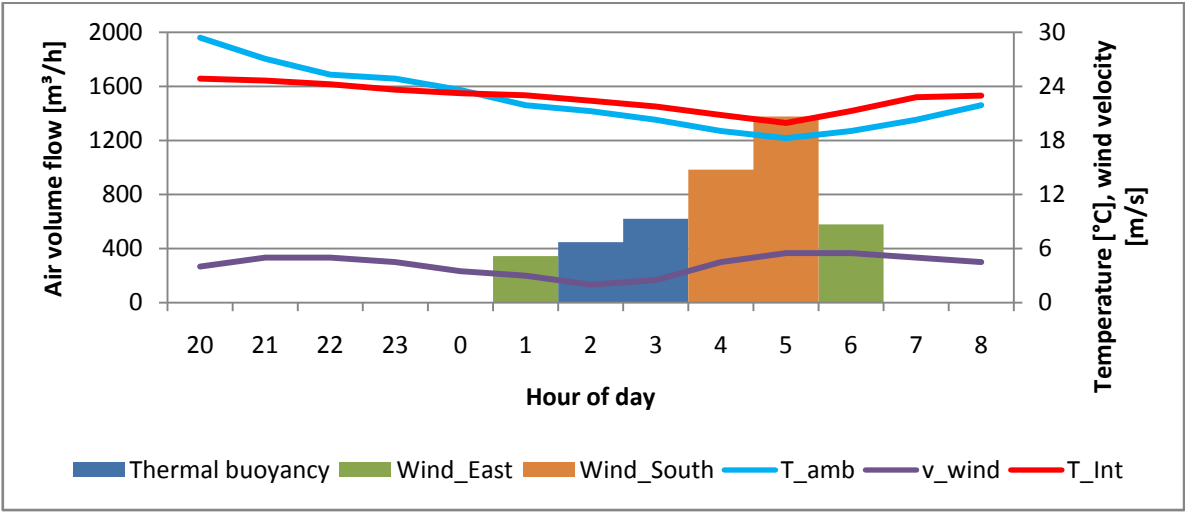


Figure 6: Air volume flow of night ventilation in the living room of the single-family home on 20 July. ( $T_{amb}$  = Outside temperature,  $T_{int}$  = Inside temperature,  $v_{wind}$  = wind velocity)

As the parametric study has shown, there are several variants, which could lead to problems associated with excess temperatures. Particularly in lightweight constructions and the variants without solar shading, a considerable amount of excess temperature degree hours was stated. As shown in Figure 7, these excess temperature problems can be almost entirely eliminated in both cases, by using night ventilation. Only in the kitchen of flat 2 and in the bedroom of flat 3, the simulation results still show minor excess temperature degree hours.

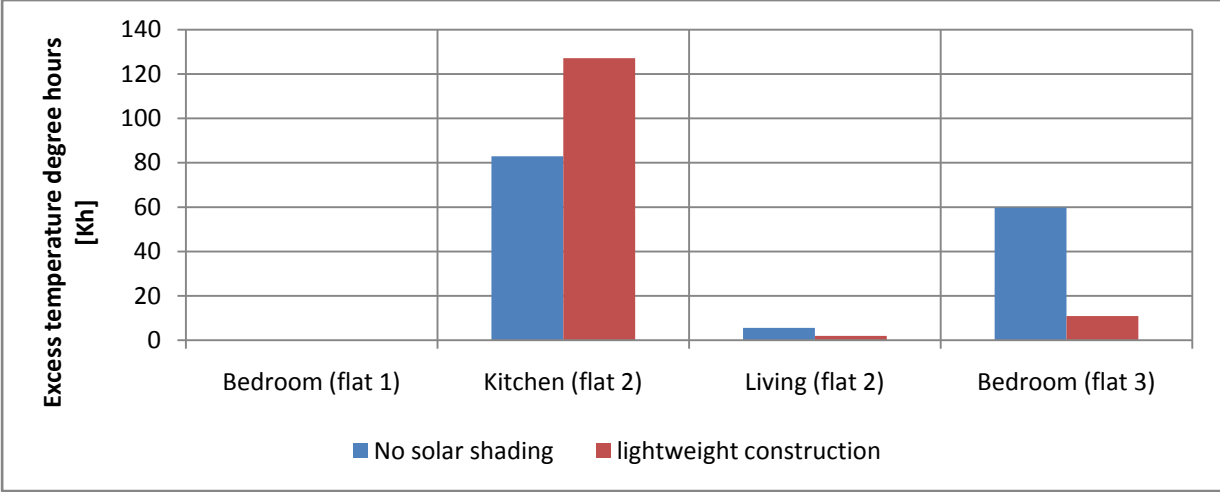


Figure 7: Influence of night ventilation on the excess temperature degree hours in the rooms of the multi-family building for the variant without solar protection.

In a second step, the critical variants with regard to summer overheating were combined. It was examined whether night ventilation suffices to reduce overheating in a combination of 'KfW Efficiency House 40', lightweight construction and no solar shading devices. The simulation results have shown that night ventilation is not quite sufficient to respect the threshold values in all rooms in this absolutely extreme scenario. In the living room and in the bedrooms the threshold value would be exceeded. However, if the lightweight construction is replaced by a solid construction, night ventilation can even compensate a combination of unfavorable parameters.

## 4 CONCLUSIONS

The case study has demonstrated that the problem of excess summer temperatures occurring under current climatic conditions in typical, new residential buildings in Germany can be controlled by appropriately adapting the building design and by using solar shading devices.

In the scope of the present case study, making intelligent use of solar shading systems was identified as the most critical parameter for ensuring thermally comfortable indoor environments in summer. The second influential parameter that was determined is the heat storage capacity of the structural components of the building. The level of thermal insulation was however found to be of minor importance.

The thermal simulation has shown that overheating problems are likely to occur particularly in the multi-family building (namely, due to the higher area-specific internal heat loads).

Here, night ventilation can be a very efficient and effective measure to minimize the risk of overheating, irrespective of the type of construction, the use of solar shading systems, the standard of thermal insulation or the building design. Even for a worst-case scenario combining the least favourable parameters, night ventilation can guarantee comfortable indoor temperatures to a large extent.

Beyond the scope of the present study, future research work will have to deal with further issues. These include investigations of alternative control strategies for night ventilation, such as automated ventilation opening or motor-driven tilting mechanisms. The question which potentials night ventilation holds in other climatic zones receiving higher amounts of global radiation is also left unresolved. Furthermore, an analysis of the effects of a rise in temperature due to global warming could also be an interesting research point.

## 5 ACKNOWLEDGEMENTS

The present study was prepared on behalf of VELUX Denmark and VELUX Germany.

## 6 REFERENCES

- [1] DIN Deutsches Institut für Normung e.V. (2011). Energetische Bewertung von Gebäuden – Berechnung des Nutz-, End- und Primärenergiebedarfs für Heizung, Kühlung, Lüftung, Trinkwarmwasser und Beleuchtung (DIN V 18599), Teil 1 bis 11. Beuth Verlag GmbH, Berlin.
- [2] Transsolar Energietechnik (2010). TRNSYS 17- a transient system simulation program, Volume 5 Multizone building modeling with Type 56 and TRNBuild, Transsolar Energietechnik GmbH, Stuttgart.
- [3] DIN Deutsches Institut für Normung e.V. (2013). *Wärmeschutz und Energie-Einsparung in Gebäuden, Teil 2: Mindestanforderungen an den Wärmeschutz (DIN 4108-2)*. Beuth Verlag GmbH, Berlin.
- [4] Reiß, J., Lyslow, L., Erhorn, H. (2016). EnEff:Stadt: CO<sub>2</sub>-neutrale Energieversorgung der Wohnanlage Lilienstraße Nord in München (IBP-Bericht 187/2016) durchgeführt im Auftrag der Gemeinnützigen Wohnstätten- und Siedlungsgesellschaft mbH (GWG) München, Bericht GWG München, Stuttgart.
- [5] DIN Deutsches Institut für Normung e.V. (2012). *Wärmetechnisches Verhalten von Gebäuden - Sommerliche Raumtemperaturen bei Gebäuden ohne Anlagentechnik – Allgemeine Kriterien und Validierungsverfahren (DIN EN ISO 13791)*. Beuth Verlag GmbH, Berlin.
- [6] Kusuda, T., Achenbach, P.R. (1965). Earth temperature and thermal diffusivity at selected stations in the United States. *Transactions American Society of Heating, Refrigerating and Air-Conditioning Engineers*. (71), 61-75.

# **Affordable and replicable renovation of social housing fulfilling indoor climate and energy targets thanks to seven replicable renovation elements**

Nicolas Galiotto<sup>\*1</sup>, Peter Foldbjerg<sup>1</sup>, Jens Christoffersen<sup>1</sup>, Thorbjørn Færing Asmussen<sup>1</sup>, and Sabine Pauquay<sup>2</sup>

*1 VELUX A/S, Daylight, Energy and Indoor Climate,  
Ådalsvej 99 2970  
Hørsholm, Denmark*

*2 VELUX Belgium  
Boulevard de l'Europe 121, 1300  
Wavre, Belgium*

*\*Corresponding author: nicolas.galiotto@velux.com*

## **ABSTRACT**

RenovActive is a renovation project which took place in Brussels based on the concept of Climate Renovation that implies achieving an excellent indoor climate as well as a high energy performance. The house belongs to a social housing association and is renovated within the financial frame for social housing in Brussels, and renovated using standard solutions and products to facilitate future replications of the result. Seven generic replicable elements were applied; these elements can be used in other renovation projects and are described in the paper. The house is equipped with a mechanical extract ventilation system for winter use, and demand-controlled natural ventilation for warm periods and peak loads during winter. The house is occupied by a family, and physical measurements as well as social scientific enquiries are carried out during a two-year period from June 2017.

## **KEYWORDS**

Renovation; indoor climate; ventilation; replicability, affordability

## **1 INTRODUCTION**

RenovActive House is a single family house of the social housing company Foyer Anderlechtois, located in Brussels, in the garden city of Bon Air in Anderlecht. The renovation is based on the concept of “Climate Renovation”: to renovate houses to create an excellent indoor climate with a good energy performance. Several renovation scenarios were generated and the performance was analysed according to the Active House specifications. RenovActive follows the Model Home 2020 project, for which five single-family houses were built during 2009-2011. The Model Home 2020 project demonstrated that 2020 building performance targets can be achieved with today’s solutions (Feifer et al, 2014). It has previously been found that the Model Home 2020 houses provide good daylight conditions without compromising thermal comfort (Foldbjerg et al., 2014). It is the aim of the present project to extend the good performance in a renovation case that is affordable by using existing standard products and solutions.

A particular focus of the renovation was to identify generic elements that can be replicated in other renovation projects on a large scale. The renovation was completed in May 2016, and

was followed by an open house period for academic and professional studies and visits. Since June 2017 a family has moved in, and the performance of the house is monitored for 2 years.

## **2 METHODS**

The design targets for indoor climate, energy and environmental impact are based on the Active House Specifications (Active House Alliance, 2011). As there was a strict financial frame for the renovation, different renovation scenarios were evaluated according to the Active House radar diagram. The scenario that was selected provided the best overall performance under the three Active House principles and fulfilled the financial frame for social housing in Brussels as well as the requirements for replicability.

### **2.1 Demand-controlled ventilation system and sun screening**

To minimize energy consumption and to maximize thermal comfort during summer, a hybrid ventilation system was developed using both a mechanical ventilation system and natural ventilation with automated window opening. Supported by a study by Holzer (2014), the outdoor temperature is used to identify the most favourable mode of ventilation. Natural ventilation has been identified as the best solution when the climate is mild. During cold periods, the ventilation is a mechanical extract system (type C+). The “+” indicates demand-control based on sensors, a solution based on a product by the company Renson. The house is divided into different zones, each with dedicated sensors of temperature, humidity, CO<sub>2</sub> and VOC installed in the extract ducts.

When the outside temperature exceeds approximately 14°C, the flow through the C+ system is reduced to 25% to minimize electricity use although the sensors are still active. The control system then uses automated windows in each zone to maintain the target of CO<sub>2</sub> levels and prevent overheating thanks to the stack effect. Therefore, the system is a “hybrid” ventilation system, combining the benefits of both mechanical and natural ventilation. The switching between natural and mechanical ventilation modes is limited to once per morning and per evening.

External automatic solar shading is installed on façade and roof windows facing south and west. To ensure a simple and affordable control solution, the solar shading is controlled by pads in each room providing manual control and timer-based control.

### 3 RESULTS

#### 3.1 Replicable elements

The seven generic replicable elements have been identified as the following:

##### 3.1.1 Attic conversion: Growing from within

Utilizing the upper floor's potential; this first densification element identifies idle areas and converts them into first class living areas. For an attic conversion the space is designed with daylight in mind, creating more space with plenty of natural lighting, improved ventilation and heat control. From an energy perspective, an attic conversion is more energy efficient than a building extension, as the attic conversion provides more living area with less building envelope and thus less thermal transmission losses, as seen in Table 1. It is also the cost-optimum solution.

Table 1: Energy performance of different renovation scenarios

	<b>No attic conversion</b>	<b>Attic converted</b>	<b>Extension added</b>	<b>Attic converted + extension</b>
Index of primary energy consumption	100	90	115	104
Primary energy consumption for heating [kWh/m <sup>2</sup> ]	34	31	39	36

##### 3.1.2 Staircase shaft for daylight & ventilation: Respiratory channel

An open stairwell provides enhanced daylight distribution and efficient airing via the stack effect. Daylight is distributed to all floors and central rooms of the home. The stack effect helps to expel humid exhaust air through the roof windows at the top of the staircase, while clean air enters the building via open doors and windows.

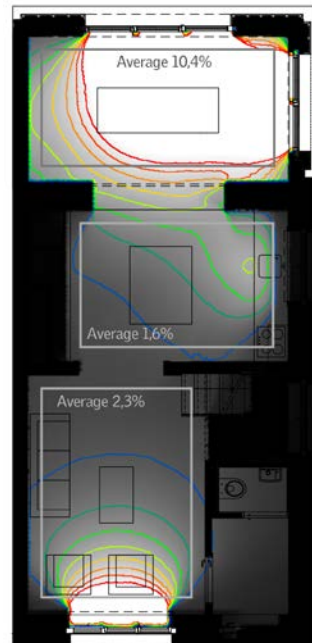
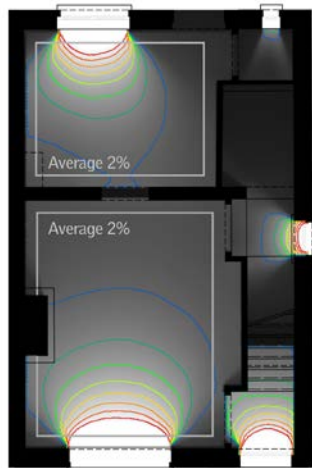
##### 3.1.3 Increased window area: Daylight treatment

Large façade and roof windows increase the level, and in particular the quality, of daylight. A balanced distribution of windows ensures a pleasant and bright indoor environment with plenty of daylight in every room and on every floor. Good daylighting results in less hours of artificial lighting (Christoffersen et al., 2014).

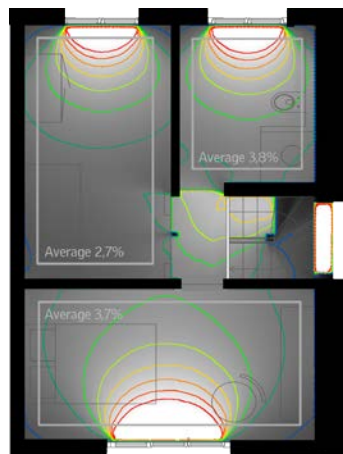
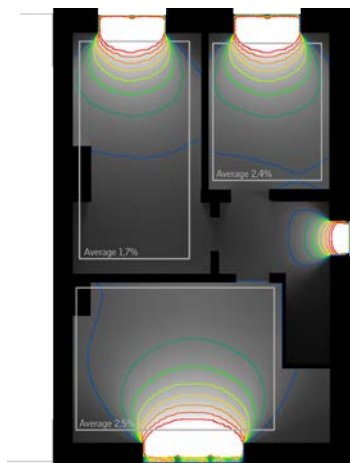
Before renovation

After renovation

Ground floor



First floor



Attic

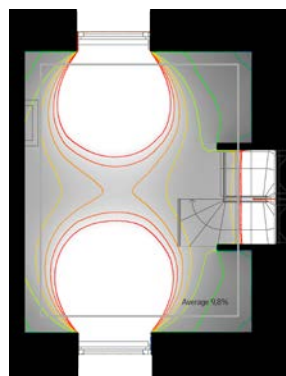
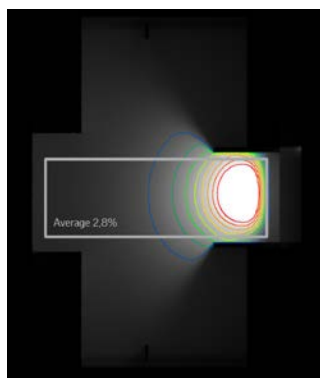


Figure 1. Daylight performance (average daylight factor) for the room on first and second floor in the existing (left) and renovated (right) situations.

### 3.1.4 Building extension: new life space

Building an extension adds precious square meters to the home and creates room for extra people. An extension is subject to the size of the plot and surrounding terrain. A well-daylit extension gives also access to a new living experience and to a space with longer days with daylight and better connected to the outdoor (e.g. to a garden).

### 3.1.5 Dynamic sunscreening: third skin

A dynamic envelope is vital to ensure good indoor comfort with pleasant temperatures day and night as well as during all seasons, particularly in the shoulder seasons. Dynamic external sun screening, e.g. awning blinds, reduces overheating during summer.

### 3.1.6 Hybrid ventilation system: hybrid breathing

The hybrid ventilation system combines mechanical and natural ventilation with automated windows and heating. During the summer, windows and stairwell are used to provide natural cooling in the building, e.g. using the stack effect for efficient air replacement. Natural ventilation can provide high ventilation rates, which results in low CO<sub>2</sub>-concentration in the house, with no use of electricity for fan operation. During the winter, mechanical ventilation helps to maintain good indoor air quality and reduce the risk of draught.

### 3.1.7 Improved thermal envelope

The thermal envelope consists of a façade climate shield and a modern heating system, optimizing energy performance and thermal indoor comfort. Work on the façade comprises extra surface insulation, a new roof construction and new windows. The upgraded heating system includes a new boiler, a floor heating as well as modern radiators on upstairs levels.

The energy cost for heating and ventilating the house would be reduced by 85% after the energy renovation of the house for the same comfort level. But a higher comfort level is expected after renovation, as occupants of poorly insulated houses often reduce the temperature to reduce the energy cost (lower heating set point, only heating of living room, temporary heating of bathroom). After renovation, a “rebound effect” is expected, which could mean that the real energy cost reduction will be in the order of 40–50%. Table 2 presents the indoor climate and energy performance before and after renovation, calculated according to the Belgian PEB software. The energy performance before renovation is a theoretical energy consumption calculated for a whole house at a yearly average temperature of 19°C, and not the measured energy performance.

Table 2. Indoor climate and energy performance before and after renovation

	Before renovation	After renovation
U-values	no thermal insulation double glazing	Improved thermal insulation low-e double glazing, triple glazing on north
Net energy demand for heating	700 kWh/m <sup>2</sup>	25 kWh/m <sup>2</sup>
Primary energy consumption	1300 kWh/m <sup>2</sup>	82 kWh/m <sup>2</sup>
Ventilation	Not ok	Ok
Thermal comfort winter	Not ok	Ok
Thermal comfort summer	Ok	Ok
Energy class	G	B
Energy cost for building services (excluding light and plug loads)	5,000 €/year	800 €/year

Figure 2 illustrates the performance of the house prior to renovation as well as the calculated performance for the renovated house according to Active House specifications.



Figure 2. Performance of the non-renovated house according to the Active House Specification.

The active House Radar shown in Figure 2 is a good tool for displaying the ambition reached before and after renovation. The radar can be a useful tool for monitoring, evaluating and improving the renovation scenarios generated during the design. As communication tool, it can provide clarity and target combinations of three principles: comfort, energy and environment. The comfort principle sits for the indoor air quality, the thermal comfort and daylighting quality. The energy principle includes the energy demand, the energy supply and the primary energy performance. Last but not least the environment principle includes the sustainable construction dimension, the consumption of fresh water and the environmental load for which life cycle assessments of different scenarios are made.

### 3.2 Occupation and post-occupancy evaluation

Since June 2017 the house has been handed to the Foyer Anderlechtois and inhabited by a social housing beneficiary. During the first two years of occupation, the performance of the house is monitored; technically by measuring indoor climate parameters and energy performance, and also by psycho-social techniques including questionnaires and time diary. The monitoring is carried out by researchers from Humboldt University Berlin, Vrije University Brussels and Daidalos Brussels. The technical indoor climate monitoring is undertaken thanks to a room-based system.

## **4 CONCLUSIONS**

The project is an example of an affordable and replicable renovation that not only improves the energy performance of the dwelling and perhaps more importantly, focuses on providing the best possible indoor environment. The seven replicable elements that have been applied are generic and can be replicated easily on a large scale.

## **5 ACKNOWLEDGEMENTS**

The project is financially supported by the VELUX Group. Daidalos and Matriciel have provided engineering consultancy and performance evaluations. Humboldt University Berlin, Vrije University Brussels and Daidalos have contributed to the monitoring setup.

## **6 REFERENCES**

- Active House Alliance (2011) Active House Specification, Active House Alliance, [activehouse.info](http://activehouse.info)
- Feifer, L, Foldbjerg, P, Asmussen, TF and Andersen, PA. 2014. Tomorrows buildings today – results, conclusions and learnings from a cross-european demonstration programme. Proceedings of World Sustainable Buildings 2014, Barcelona.
- Foldbjerg, P, Asmussen, TF and Holzer, P, 2014. Ventilative Cooling of Residential Buildings - Strategies, Measurements results and lessons learned from three Active Houses in Austria, Germany and Denmark, International Journal of Ventilation, September 2014.
- Holzer, P and Foldbjerg, P. 2014. Control of Indoor Climate Systems in Active Houses. Proceedings of World Sustainable Buildings 2014, Barcelona.
- Christoffersen, J.and Foldbjerg, P, 2015. Results from Post-occupancy evaluation in four Single-family Houses. Healthy Buildings Europe 2015, Eindhoven.

# Façade Improvements to Avoid Draught in Cold Climates – Laboratory Measurements

Michael Gruner<sup>\*1</sup>, Maria Justo-Alonso<sup>1</sup>, and Tor Helge Dokka<sup>2</sup>

*1 SINTEF Building and Infrastructure  
Høgskoleringen 7B  
7465 Trondheim, Norway*

*2 Skanska Teknikk  
Lakkegata 53  
0187 Oslo, Norway*

*\*Corresponding author: Michael.Gruner@sintef.no*

## ABSTRACT

With the goal of increasing building flexibility and reducing energy use, yet ensuring IAQ, the feasibility of natural ventilation in a building in Oslo is studied. However, the use of direct outdoor air poses some challenges in the Norwegian cold climate, particularly the risk of thermal discomfort due to draught and low local temperatures. The goal of this paper is to study the most suitable solution to avoid draught in cold climates while maintaining the required airflow rates.

In the presented test these airflow rates are studied to be supplied only by window opening with unidirectional airflow. Experiments are done in a full-scale model of an office for 2 persons in laboratory facilities with a temperature difference between indoor and outdoor of ca. 25 degrees. 16 types of potential improvements are studied at two airflow rates. Principle solutions to reduce the risk of thermal discomfort are presented.

## KEYWORDS

Natural ventilation, full scale experiment, thermal discomfort

## 1 INTRODUCTION

Due to stricter requirements regarding reduction of energy use, airtightness has become the state of the art in new buildings, and therefore the need to ensure minimum airflow rates by ventilation has increased. While mechanical ventilation is the common solution in cold climates, natural ventilation is considered by some as an alternative to mechanical ventilation. Natural ventilation can reduce investment and energy costs. It is space-efficient and provides health, comfort, productivity advantages, and increased control of users over their environment (Emmerich et al., 2001). However, the biggest challenges for natural ventilation in cold climates are linked to supply of low temperature outdoor air, which can cause local discomfort problems linked to draught. For instance, the annual average outdoor temperature in Oslo is 6.3 °C while the limit of outdoor temperature for natural ventilation is stated as 6..10 °C (Fitzner & Finke, 2012). This poses the challenge of feasibility of window opening. EN 15251 with reference to ISO 7730 states the criteria of local discomfort. In Norway, regulations are harmonised to recommended criteria for ISO 7730 category B with a maximum draught rate (DR) of 20 %. Additionally, the Guideline 444 "Climate and Air Quality in the Workplaces" (Arbeidstilsynet, 2016) requires the air velocity to be lower than 0.15 m/s in the occupied zone. The occupied zone is defined according to NS-EN 13779 as virtual space 0.60 m from the walls and between 0.10 and 1.80 m height above floor.

There is scarce literature on how to reduce the risk of discomfort of natural ventilation in cold climate. Heiselberg et al. (Heiselberg et al., 2001) investigated the characteristics of airflow from windows and developed models for the prediction of thermal comfort parameters in the

occupied zone from laboratory experiments. It was concluded that bottom hinged windows located near the ceiling are preferable in cold climate because they increase the distance to the occupied zone. Bjørn et al. (Bjørn et al., 2000) determined 5 possible principal flow patterns from bottom hinged windows, and a relationship with the Archimedes number. They found that at low airflow rates and low supply air temperatures, air will behave similar to draught from a cold wall. Earlier, Heiselberg et al. (Heiselberg et al., 1995) investigated horizontal obstacles to stop draught from fully glazed façades. They found a dependency of the maximum air velocity and the minimum temperature in the occupied zone on the flow characteristic and the size of obstacle. Below a critical width of the obstacle, the airflow reattaches to the wall surface, but in the occupied zone air velocity decreases and temperature increases nonetheless. Above the critical width, the flow is diverted into the room, and comfort depends only on the distance of the lowest obstacle to the floor. However, obstacles were studied only in the context of natural convective flow. Only rectangular obstacles were investigated. Heights over 2 m between obstacles apply for larger multi-storey façade, but can rarely be achieved in normal situations within one floor. Later, Heiselberg et al. (Heiselberg et al., 2002) investigated also the effect of guiding plates, which block the secondary jet through the triangular areas on either side of the bottom hinged window. The effect was judged negative because air velocity increased in the primary jet above the opening sash and at floor level. Field experiments by (Fitzner & Finke, 2012) show the influences of features around windows, such as window sills and heaters, on the characteristics of airflow from the window. It was found that radiators under the window improve comfort as long as they are warm. Mysen et al. (Mysen et al., 2005) documented a low-cost solution for retrofitting. Unfiltered outdoor supply air was supplied via a short insulated duct from the façade with air supply nozzles in each room. Stale air was extracted via a central mechanical fan. In order to reduce the reported draught problems, a more uniform distribution with a continuous row of small nozzles or a continuous narrow slit was suggested, but not tested. Zhang et al. (Zhang et al., 2016) developed a more successful concept for air intake from the façade at ceiling level. Outdoor air is supplied to the space between the suspended ceiling and the floor slab, and supplied to the room through diffuse ceiling panels. Even at supply air temperatures of  $-7\text{ }^{\circ}\text{C}$ , the draught rate was below 10 %.

From the existing research, it can be concluded: a) The preferred solution is a bottom hinged, horizontal vent located near the ceiling; b) In case of low supply air temperature, air will flow down the façade and enter the occupied zone at floor level; c) Horizontal obstacles show potential to reduce discomfort also when the airflow reattaches to the surface; d) Deeper obstacles and larger vertical distances between obstacles are preferable.

The present study takes solutions found in literature, and develops them further with the goal to avoid discomfort in the occupied zone. This is done by testing obstacles with different sizes, shapes and materials in a full-scale model at low outdoor temperatures. This work is linked to the ongoing building project Gullhaug Torg 2A (GT2A) (Snøhetta, 2015), a pilot project of the research project "Naturligvis ("Naturally") – Natural conditioning of office buildings". GT2A is planned as a mixed-use building north of the city centre of Oslo, where floors 3 to 6 are office floors which are envisaged to be exclusively naturally ventilated. Components such as grilles, window ventilators, or active or passive wall ventilators are not considered. The presented work is limited to unidirectional flow and focus is on steady-state condition under continuous ventilation: Other ventilation strategies like intermittent pulse ventilation are not investigated. As the study is linked to a building project, many parameters in the experiments are restrained to the project's specifications. The effects of e.g. varying size and angle of the vent, or airflow rates could not be studied. Furthermore, the available experimental setup with a room height of 2.40 m may not fully represent an office environment, where clear heights of 2.70 m or higher are common.

## 2 EXPERIMENTAL SETUP

The experiments are conducted in a thermally insulated test room with inner dimensions of 7.0 x 3.0 x 2.4 m made of 100 mm PUR-sandwich panels. The room is divided in a cold "outdoor" section, and a warm section representing an office environment with inner dimensions of 3.6 x 3.0 x 2.4 m. XPS insulation was used to model walls, vent, and obstacles due to easy handling. The partition wall is made of 200 mm XPS (U-value 0.17 W/m<sup>2</sup>K). An area of 1.8 x 1.8 m (45 % of the wall area) is made of 30 mm XPS (U-value 0.93 W/m<sup>2</sup>K) in order to represent a glazed façade. Figure 1 shows a photo of the test room and a vertical section of the vent.

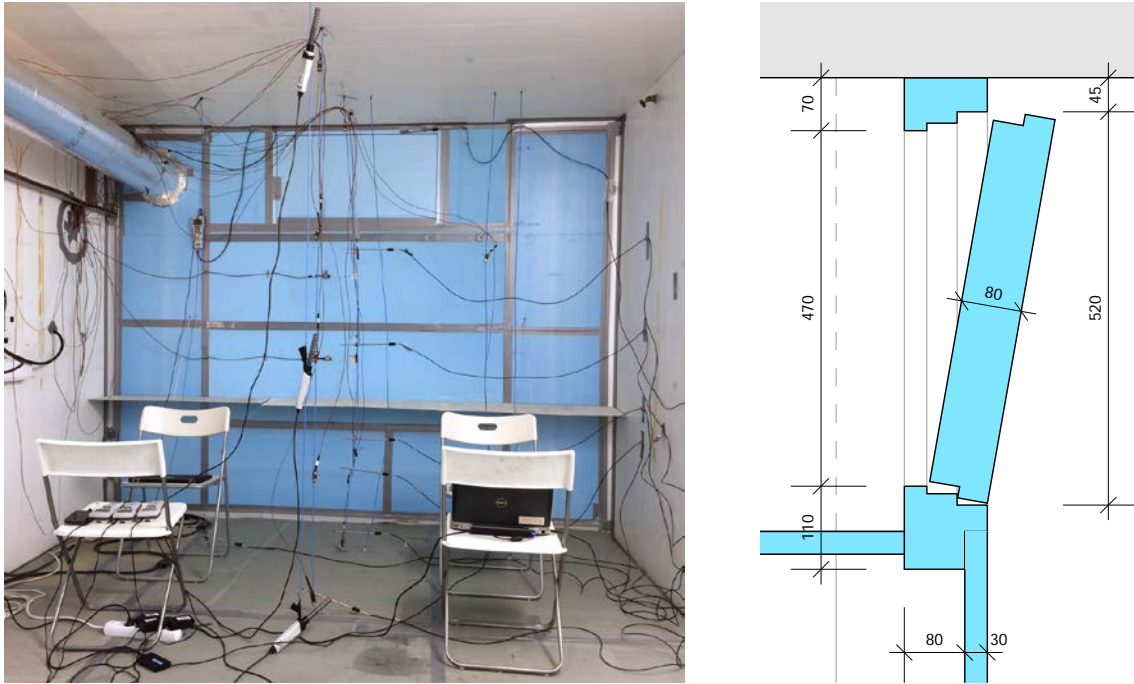


Figure 1: view inside the test room (left), section of the vent (right)

The vent sits flush with the inner surface of the façade and corresponds to a bottom-hinged inward-opening window. The frame profile emulates a typical Norwegian window profile for triple glazing (NorDan, 2017) on all 4 sides. The clear opening is 900 x 470 mm (0.43 m<sup>2</sup>), with the height given by GT2A, and the width chosen in order to measure the airflow rate directly at the vent with a flow hood. A vent opening angle of 10° follows GT2A and is kept constant in all measurements. A settling chamber is mounted in front of the vent on the cold side in order to reduce the influence of turbulences caused by the fan of the cooling system.

The warm section is heated by electric floor heating covering the entire floor. The setpoint temperature of 23 °C is given by measuring point A.2.3 in the middle of the room. Heating is controlled by a simple instantaneous on/off control with a power ca. 550 W with a hysteresis of 0.1 °C. The cold section is conditioned by a JULABO recirculating cooler with a flat plate heat exchanger as emitter in combination with an air to glycol heat pump emitting by an air cooler finned coil heat exchanger. Fans are used to force the flow through the exchangers and to mix the air to a uniform temperature in the cold section. Unidirectional airflow from the cold section through the vent into the warm section is controlled by an extract fan in the wall opposite of the façade (centre of duct ca. 220 cm above the floor) in order to achieve the desired airflow rate. Targeted airflow rates were at 12 and 24 l/s according to the specifications from GT2A and Norwegian building regulations. Airflow was measured with

flow hood Testo 420 both at the window and at the extract inlet in order to determine and adjust airflow rates and adventitious infiltration.

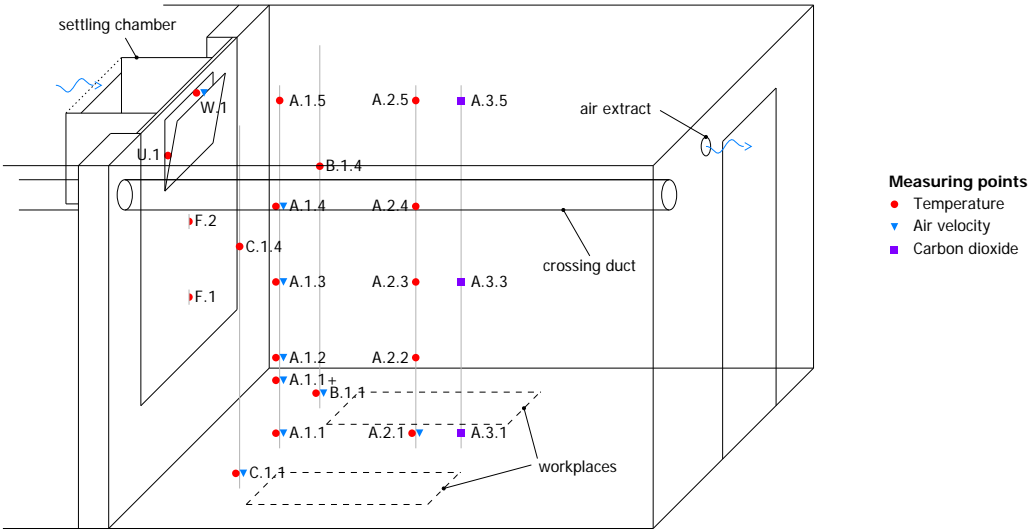


Figure 2: Test room (warm section) with measuring points

Figure 2 shows the measuring points in the test room. Temperature, air velocity were measured at selected points 0.60 and 1.50 m distance from the façade. CO<sub>2</sub> stratification was measured in the centre point of the room at three heights. Table 1 provides an overview over the used devices.

Table 1: Measurement equipment and properties

Parameter	Equipment	Number	Location	Accuracy
Temperature	Thermocouple type T	16	> Poles: 0.10, 0.60, 1.10, 1.60, 2.30 m above floor > Vent: outside (side) and inside (top) of opening > Façade (surface): 1.00, 1.50 m above floor	Accuracy ±0.5 °C
Air velocity	SensoAnemo 5100SF	9	> Poles: 0.10, 0.60, 1.10, 1.60, 2.30 m above floor > Vent: inside (top) of opening	Range(0.05-5.0 m/s) Accuracy ±0.02 m/s
Carbon dioxide	Vaisala M170	5	> Pole A.3: 0.10, 1.10, 2.30 m above floor	Accuracy ±0.035%
Airflow rate	Testo 420	1		Accuracy ±3 %

Figure 3 shows the four different types of obstacles that were investigated – rectangular solid panels, rectangular slotted panels (grille), rectangular perforated panels, and tubular obstacles mounted in a line.

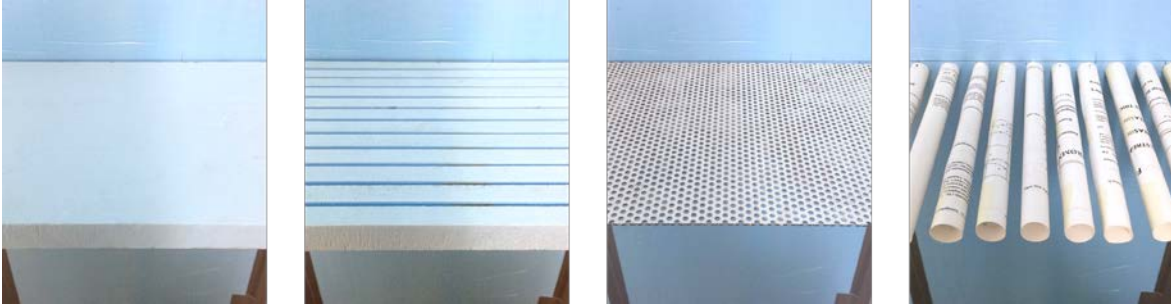


Figure 3: Testes types of obstacles: solid panel, slotted panel, perforated plate, tubes (from left to right)

The intention of the last three types was to slow down and diffuse the supply airflow before entering the occupied zone. The solid and the slotted (5 mm gaps, c/c 25 mm, 20 % openness) panels are made of 30 mm XPS. The perforated panel is a 2 mm thick, perforated steel plate (5 mm holes, 40 % openness). Printing paper was rolled as tubes of 25 mm diameter with 15 mm gaps in between (37.5 % openness). The obstacles stretched over the entire width of the façade. Figure 4 shows the investigated placements of the obstacles – three are mounted on the façade and one on the floor. 0.75 m above floor corresponds to the usual height of window sills. Additionally, obstacle depths of both, 0.15 and 0.30 m were tested in some cases.

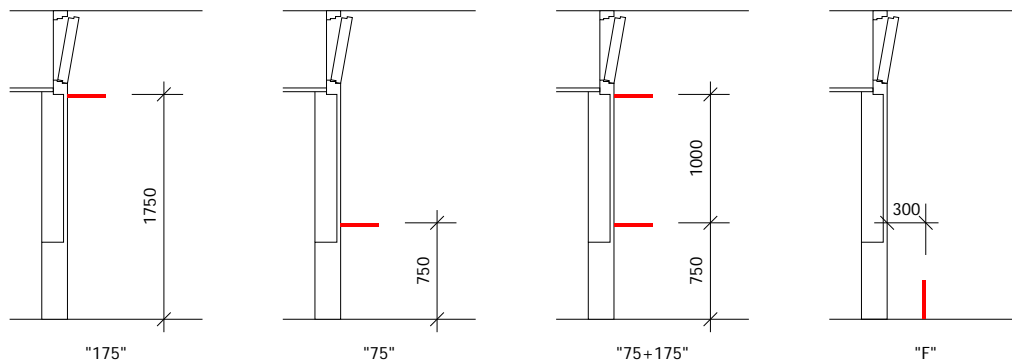


Figure 4: Tested alternative positions of obstacles

Table 2 shows a matrix of the investigated elements. All cases with solid panels were tested. Other test cases were chosen iteratively based on the most promising results.

Table 2: Matrix of test cases

Type	Depth/height	Façade-mounted			Floor-mounted
		1.75 m	0.75 m	0.75 + 1.75 m	
Rect., solid	0.15 m	S.175_15	S.75_15	S.75+175_15	S.F_15
	0.30 m	S.175_30	S.75_30	S.75+175_30	S.F_30
					S.F_30+P.F_30
Rect., grille	0.15 m	–	–	G.75+175_15	–
	0.30 m	–	G.75_30	–	–
Rect., perf.	0.30 m	–	P.75_30	P.75+175_30	P.F_30
					P.F_30+S.75_15
Tubular	0.30 m	–	T.75_30	–	–

In a first stage, the potential of every alternative was studied for an airflow rate of 14 l/s and one person occupancy. The person was sitting still between pole A.3 and the door, and was working on two laptops. In a second stage, the 3 most relevant solutions were studied at two airflow rates under realistic conditions with 2 persons seated close to the border of the occupied zone (to evaluate discomfort subjectively). Consequently, internal heat loads are related to lighting (1 LED light, 1.5 W) in all stages and first one sitting person with 2 laptops (90 W and 65 W) and later two sitting persons with 3 laptops (90 W, 2 x 65 W).

### 3 RESULTS AND DISCUSSION

Table 3 provides the pairs of measured supply and extract airflow rates corrected for standard conditions (21 °C, 1013 hPa).

Table 3: Measured extract and supply airflow rates.

Airflow rate at vent (l/s)	Airflow rate at extract (l/s)
14 (N.N...22)	14 (N.N...22)
24 (15..32)	29 (22..36)

A leakage of ca. 17 % of the extract airflow was estimated for the higher airflow rate. This leakage through gaps and cracks is most likely due to cable passages through walls from outside and the cold section. Its value decreased with smaller airflow rates. During the test with low airflow rates a bidirectional and inconstant flow was observed. 14 l/s represents the average of the measured airflow rates in the 'right' direction. Extract airflow rates were later confirmed by CO<sub>2</sub> measurements. For the second stage the settling chamber was modified yielding the desired airflow rates.

Figure 5 and Figure 6 show the results of the first stage for the relevant measuring points 10 cm above the floor and the different points in pole A.1. Results are an average over 5 min with steady state conditions.

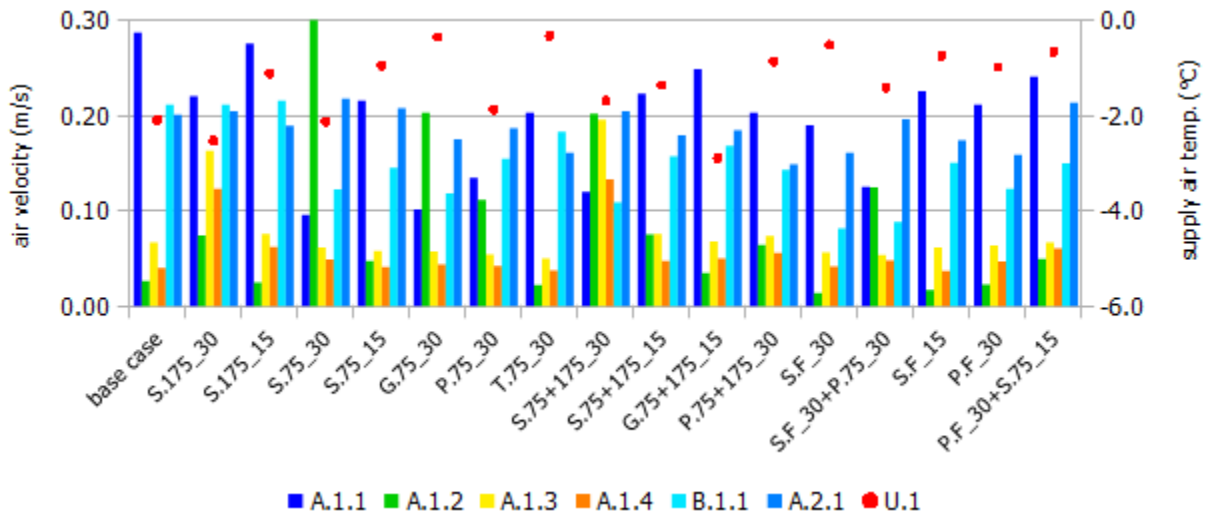


Figure 5: Stage 1, air velocities, and supply air temperature U.1

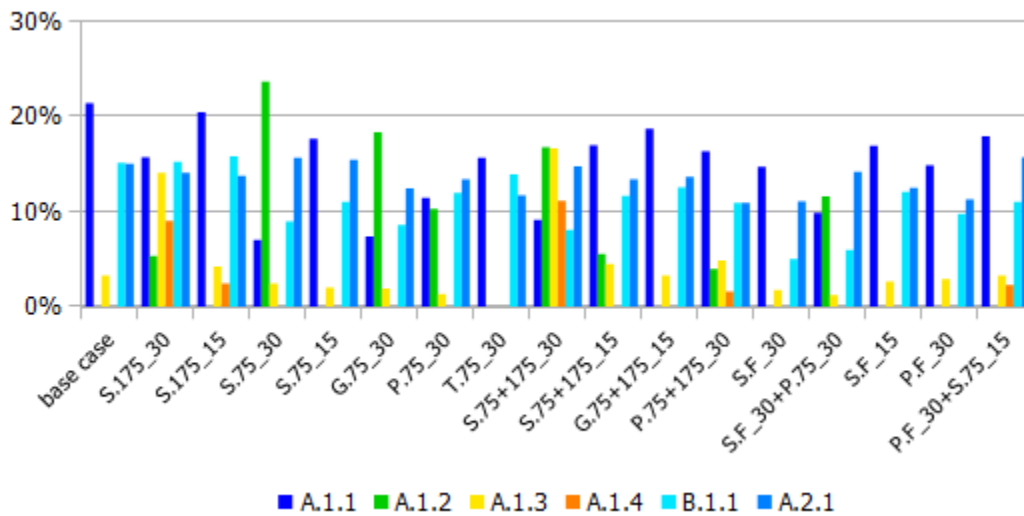


Figure 6: Stage 1, draught rate

In all cases, the lowest measured temperature is less than 2 K below the air temperature at point A.2.3 near the centre of the room. Measured maximum air velocities are expectedly high, particularly found at ankle height at around 0.2 m/s and more. However, the maximum calculated draught rates for the test cases are mostly less lower than 20 % and therefore rather low, probably due to the elevated room temperature of 23 °C and the low turbulence intensities, which were determined based on the logged air velocities.

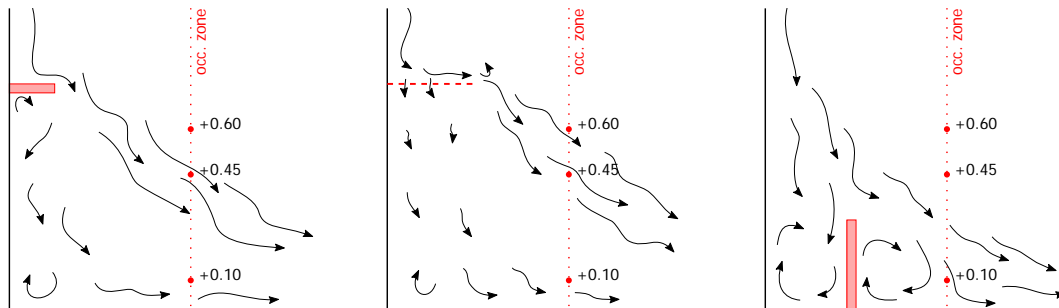


Figure 7: Qualitative visualisation of cases "S.75\_15" (left), "P.75\_30" (centre) and "S.F-30" (right)

High positioned (cases "175") façade-mounted cases do not reduce air velocities effectively. In addition to increased velocities 0.1 m above the floor, they also create problematic elevated velocities at higher points where deflected airflow drops into the occupied zone. Low obstacles (cases "75") reduce the air velocity at ankle height, but in some cases they cause increased velocities at 0.6 m above the floor, where the deflected air enters the occupied zone similar to cases with high positioned obstacles (see Figure 7, left and centre). Combinations of low and high obstacles show no or little improvement. Generally, obstacles with small depth are also less effective.

The permeability of the obstacles affects the velocity distribution at the border of the occupied zone considerably. Depending on the degree of openness, but also of the shape and material of the panel, a characteristic pattern of velocities at different heights develops. This was also visualised with smoke. The cold airflow separates into an airflow that penetrates the panel, where a pressure drop reduces its velocity, and an airflow that is diverted into the room (see Figure 7, centre). Permeability appears to be a promising solution, but requires optimisation of the degree of openness in order to balance the two airflows.

In the floor-mounted cases, the air velocities reduce significantly for case "S.F\_30", but less prominently for the others cases. Visualisations with smoke showed that the panel divides the downstream into two airflows. The stream falling behind the panel creates vortices reducing the velocity and positively affecting the air velocities at low heights (see Figure 7, right).

The test cases "P.75\_30", "S.F\_30", and "S.75\_15" were selected for the second stage. The first two have shown promising performance, "S.75\_15" was chosen as a minimal solution, interfering less with the interior than the other two cases. It may also represent the impact of a window sill on the airflow.

Figure 8 and Figure 9 show the results of the second stage. As a results of the smoke visualisations and reported draught sensation, measuring point A.1.1+ was introduced at 45 cm over floor level as a spot of potentially high velocities.

The lowest temperatures at the border of the occupied zone are found for both airflow rates at ankle height near the façade (point A.1.1) at ca. 2 K below the temperature at point A.2.3 near the centre of the room.

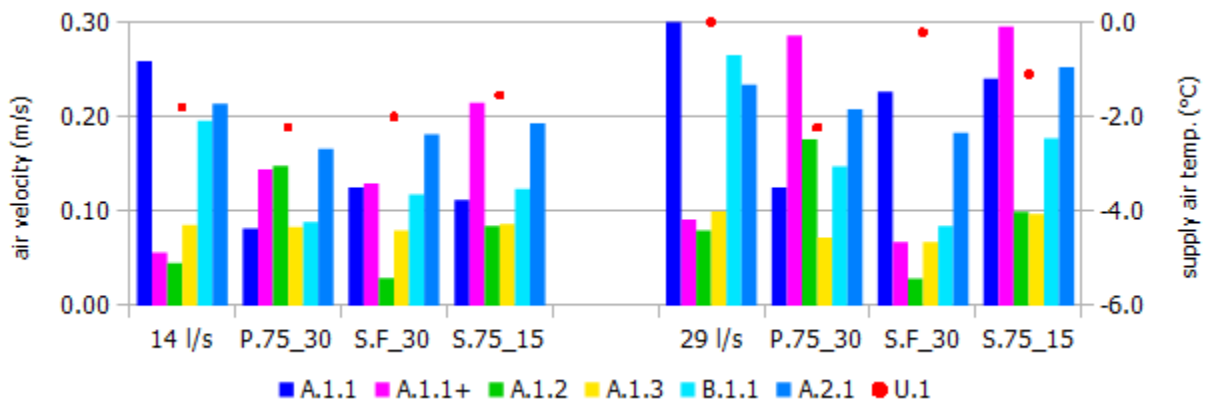


Figure 8: Stage 2, air velocities, and supply air temperature U.1 (cases with 14 l/s left, cases with 29 l/s right)

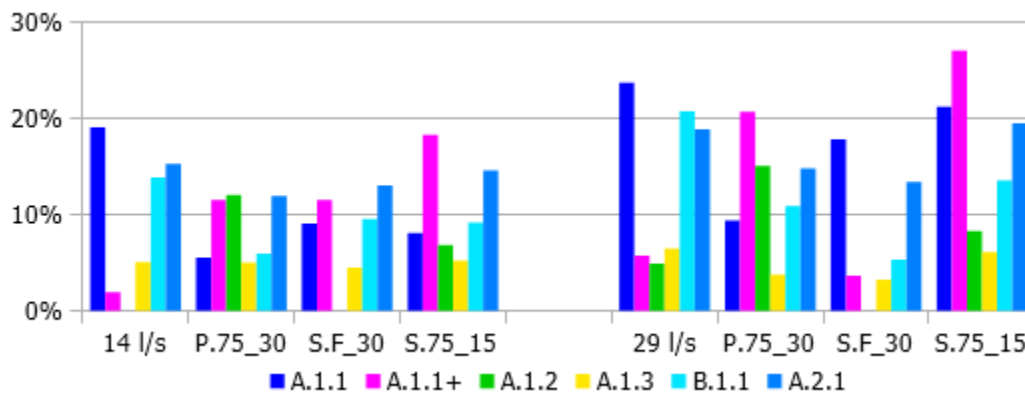


Figure 9: Stage 2, draught rate (cases with 14 l/s left, cases with 29 l/s right)

For airflow rate 14 l/s, the maximum air velocities near the façade are reduced compared to the base case and mostly lower than 0.15 m/s, also with two occupants. Elevated velocities are measured at 0.45 m above the floor, and the highest velocities in the room are measured at point A.2.1, further from the façade. Draught rates are below 20 % in all cases for 14 l/s airflow rate, also for the base case without obstacle.

At the higher airflow rate, air velocities at ankle height are reduced compared to the base case, particularly for case "P.75\_30". However, the maximum velocities remain over 0.20 m/s in all cases and are allocated at point A.1.1+ for the 2 façade-mounted cases. Velocities at point A.2.1 are higher than 0.18 m/s (case "S.F\_30") in all cases. Along with the air velocities, temperatures at point A.2.1 vary slightly between 21 °C (case "S.75\_15") and 22 °C (case "P.75\_30"). Only in case "S.F\_30", the maximum draught rate is below 20 %.

The positioning of the heat sources, people and computer also can show an effect on the airflow distribution in the room. In the second stage the occupants' plume may have affected the results obtained at measuring points at the border of the occupied zone.

CO<sub>2</sub> measurements were conducted during the second stage. Results show similar CO<sub>2</sub> levels at the three measured heights, with corresponding temperatures at points A.2.1, A.2.3, and A.2.5 at ca. 22 °C, 23 °C, and 23.5 ° throughout all cases. While this indicates full mixing in the room, a tendency for stratification is noticeable when persons in the room sat still during tests. However, the duration of tests was short (ca. 15..20 min per test case) and stratification ceased when people moved again.

From the studied examples, case "S.F\_30" shows the larger potential to effectively reduce risk of discomfort both at the lower and the higher airflow rates. However, velocities at ankle height in the central axis of the window, A.1.1 and A.2.1, remain high, particularly for the higher airflow rate. On the other hand, velocity in point B.1.1 75 cm beside the central axis is nearly equal to the velocity in point A.1.1 at 14 l/s, but significantly lower at the higher airflow rate, indicating a change in flow pattern with different airflow rates. This can also be concluded from velocities in points A.1.1 and A1.1+ which show similarities with the base case at the higher airflow rate. It also suggests, that the effectiveness of the obstacle may decrease at increasing airflow rates and/or decreasing outdoor air temperatures.

For all test cases, the impact of the obstacles in air velocities is primarily noticeable close to the façade respectively the location of the obstacle, while regions deeper in the room (e.g. around point A.2.1) seem less affected. There, velocities remain nearly as high as in the base case. This indicates that the effect of elements may be limited to their near vicinity, which suggests that local solutions at the workplace are more suitable.

Moreover, in some cases measured velocities at certain points were higher than in the base case without additional elements, and reached critical values. This raises the issue that solutions that are supposed to reduce draught actually may introduce a new risk of discomfort to the occupants at a different part of the room. The design of the elements must therefore be well considered.

#### **4 CONCLUSIONS**

16 potential solutions to reduce thermal discomfort linked to window opening at cold outdoor supply air temperatures have been studied in a full scale model experiment. All investigated solutions have in common, that they do not reduce the airflow rate through the vent. Horizontal, perforated plates at window sill height and low, vertical elements at the floor between façade and the border of the occupied zone are chosen as the most promising principle solutions. Their presence disturbs the draught flow reducing its velocity and allowing the air to get warmed up before entering the occupied zone. Generally, the solutions found seem more suitable for lower airflow rates, and are mainly effective near the elements.

It was found that these flow deflectors may create discomfort risks at other locations. Careful design and testing is therefore advised. Furthermore, consequences for all points in the room possibly exposed to draught risk need to be evaluated, not only at standard locations at the border of the occupied zone. In addition, although the occupied zone in terms of indoor climate considerations does not stretch until the façade, it is usually desired to use the entire spaces, where obstacles would disturb when protruding into the room. The further development of deflectors should consider this.

The present study uses only a restrained set of parameters. Further studies with a wider range of airflow rates, outdoor temperatures, and types of elements regarding dimensions, material, and placement and integration is necessary.

#### **5 ACKNOWLEDGEMENTS**

This work has been supported by the Research Council of Norway and several partners through the Research and Development project "Naturligvis", grant number 245435.

## 6 REFERENCES

- Arbeidstilsynet. (2016). *Veiledning om klima og luftkvalitet på arbeidsplassen*. Trondheim: Direktoratet for arbeidstilsynet (Arbeidstilsynet).
- Bjørn, E., Jensen, J., Larsen, J., Nielsen, P. V., & Heiselberg, P. (2000). *Improvement of Thermal Comfort in a Naturally Ventilated Office*: Dept. of Building Technology and Structural Engineering Aalborg University.
- Emmerich, S., Dols, W. S., & Axley, J. W. (2001). *Natural Ventilation Review and Plan for Design and Analysis Tools*. Gaithersburg: National Institute of Standards and Technology.
- Fitzner, K., & Finke, U. (2012). *Lüftungsregeln für freie Lüftung*. Dortmund/Berlin/Dresden: Bundesanstalt für Arbeitsschutz und Arbeitsmedizin (BAuA).
- Heiselberg, P. K., Bjørn, E., True, J. P. J., Hagelskjær, S., Darum, J., Andersen, A., & Møller, C. (2002). *Udvikling af brugervenligt styringssystem for naturlig ventilation*: Aalborg Universitet.
- Heiselberg, P. K., Overby, H., & Bjørn, E. (1995). Energy Efficient Measures to Avoid Downdraft from Large Glazed Facades. *ASHRAE Transactions*, 101(Part 2), 1127--1135.
- Heiselberg, P. K., Svidt, K., & Nielsen, P. V. (2001). Characteristics of airflow from open windows. *Building and Environment*, 36(7), 859-869.  
doi:[http://dx.doi.org/10.1016/S0360-1323\(01\)00012-9](http://dx.doi.org/10.1016/S0360-1323(01)00012-9)
- Mysen, M., Schild, P. G., Hellstrand, V., & Thunshelle, K. (2005). Evaluation of simplified ventilation system with direct air supply through the facade in a school in a cold climate. *Energy and Buildings*, 37(2), 157-166.  
doi:<http://dx.doi.org/10.1016/j.enbuild.2004.05.010>
- NorDan. (2017). ND NTech Tilt & Turn. Retrieved from [http://www.nordan.no/media/com\\_products/documents/N010903.pdf](http://www.nordan.no/media/com_products/documents/N010903.pdf)
- Snøhetta. (2015). Gullhaug Torg. Retrieved from <http://snohetta.com/projects/269-gullhaug-torg>
- Zhang, C., Yu, T., Heiselberg, P. K., Pomianowski, M. Z., & Nielsen, P. V. (2016). *Diffuse Ceiling Ventilation: design guide*: Aalborg University Department of Civil Engineering.

# Cool materials in the urban built environment to mitigate heat islands: potential consequences for building ventilation

Carolina de Rezende Maciel<sup>\*1</sup>, Maria Kolokotroni<sup>2</sup>,

*1 School of Architecture and City Planning Mackenzie  
Presbyterian University  
São Paulo, Brazil  
\*Corresponding author:  
arq.carolinamaciel@gmail.com*

*2 Institute for Energy Futures,  
Brunel University London,  
Uxbridge, Middlesex, UB8 3PH, UK*

## ABSTRACT

Urban warming, commonly referred to as the ‘Urban Heat Island’ phenomenon (UHI), is a well-established effect that affects cities all over the world. This occurs due to urban physical characteristics such as urban canyon geometry and vegetation, but mainly to its typical materials. The thermal properties of the materials used for the external walls and roofs of buildings, as well as pavements, can have a major influence on the surface temperature. As a consequence of increased temperature, the UHI has an effect on energy consumption for heating and cooling urban buildings. Cool materials are a cost effective, environmentally friendly and passive technique that uses a coating with high thermal emissivity and solar reflectance properties. At building scale, this technique is recognized for decreasing the amount of heat conducted through the surface and the solar thermal load of the building, reducing its energy requirements for cooling. At urban scale, this strategy contributes to improving the urban microclimate by lowering surface and air temperatures which, in turn, increases the potential for ventilative cooling in the buildings. The goal of this paper is to evaluate the impact of the use of cool materials on the thermal environment of urban spaces and how this can affect ventilative cooling for buildings. The cool materials were evaluated considering the application on roofs and pavements, and the Federal University of Mato Grosso campus, located in Cuiabá, Brazil was used as case study. The study was performed through computer simulations where the 3 scenarios (cool roof, cool pavement and reference scenario) were simulated for the climate of Cuiabá (Aw2 Köppen classification – Tropical wet and dry), considering winter and summer conditions. The methodology consists of three steps: a. preparatory stage (acquisition and compilation of climatic data and physical characteristics of the study area), b. numerical simulation and c. validation of the model and data calibration, for further comparative analysis. As a result, in the scenarios where cool materials were applied, significant differences were found both in the surface temperature and air temperature (height of the pedestrians), up to 7.02°C. The difference was more evident when used as cool pavement than when used as cool roof and this tendency varies in amplitude, considering the locality within the study area and the season analysed. These results allow us to infer that cool materials can increase the potential of the ventilation as strategy for cooling indoor environments, especially by means of stack ventilation which is benefited from greater temperature differences. Thus, it is believed that the wide use of such materials can significantly contribute not only to the mitigation of the heat island effect, but also to reduce overheating risk in buildings by increasing the effectiveness of ventilative cooling and thus reduce the need for air conditioning.

## KEYWORDS

Cool materials; urban heat island effect; cooling ventilation; building ventilation.

## 1 INTRODUCTION

The objective of this paper is to evaluate the impact of the use of cool materials on the thermal environment of urban spaces and their potential consequences for cooling ventilation for buildings. The study was conducted through computational simulations with the ENVI-met

software investigating the case study of the Federal University of MatoGrosso campus, located in Cuiabá, Brazil.

## 2 METHODOLOGY

The method of this work is divided into three main stages, described in the following sections.

### 2.1 Preparatory Stage: acquiring data

The study was conducted in the city of Cuiabá (Figure 1a), capital of the state of Mato Grosso, known as one of the hottest cities in Brazil. According to Koppén classification, its climate is Aw2 type, i.e., Tropical wet and dry or savanna climate, characterized by high temperatures throughout the year, alternating between two well defined seasons, one dry (autumn-winter) and one rainy (spring-summer). For the 10-year period prior to the research (2002-2012), average annual maximum temperature ranges from 28 °C to 38 °C while average annual minimum temperature from 15 to 24 °C. The average relative humidity varied between 52% (August) and 84% (February). (BDMEP/INMET, 2017).

#### 2.1.1 Definition of the study area:

The area to be investigated was partly chosen considering the requirements of the ENVI-met software which needs (a) low topographic variation, (b) dimensions compatible with the software's limits (both surface area and time processing) and (c) to include elements (pavements and roofs) in which cool materials can be applied.

The area chosen is essentially flat (ranging from 165m to 185m). In relation to the size of the area, the version of the software used in this study (v3.1 Beta 5) allows the composition of a horizontal grid up to 250x250 squares. A scale of 2.5x2.5m was used for each grid, which allowed to cover a total area of 600mx600m. Greater grid values (5x5m, for example), would simplify the features and smaller grid values (1x1m, for example) would greatly limit the dimensions of the total area to be simulated.

The Eastern portion of the campus was chosen, since it includes most of the campus buildings as well as large areas of paved surfaces. Thus, considering the three conditions described, the final area selected for the simulation of the scenarios is the Eastern part of the campus, comprising a total of 36ha (figure 1b).

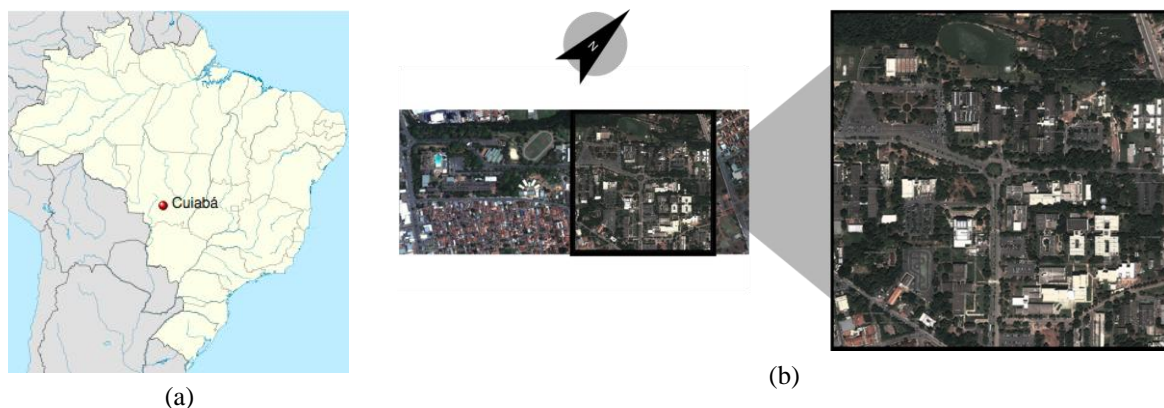


Figure 1: (a) Location of Cuiabá on the map of Brazil; (b) Study area – Federal University of Mato Grosso;

Source: Adapted from Wikipedia (2015) and Google Earth (2014)

### 2.1.2 Microclimatic data acquisition

To configure the Input files of the computational model, we used data from the reference station (83362) - Marechal Rondon Airport, in Várzea Grande, MT, located 6.5 km from the study area. Air temperature data was collected from the Weather Underground (<http://www.wunderground.com>) and the University of Wyoming website (<http://weather.uwyo.edu/uppear>). The reference station at Marechal Rondon Airport provided data (frequency 1h in 1h) of direction and wind speed at 10m height (m/s), atmosphere temperature (K), mixing ratio at 2500m (g/kg) and relative humidity (%) at 2m height.

For the validation of the simulation results, data collected directly in the study area were used, through the Outdoor Weather Station (Onset model U30 Wi-Fi) fixed above the roof to an approximate height of 7.00 m inserted at the Eastern side of the campus. This station provided data, at a frequency of 5 minutes, of the air temperature (°C) used in the data calibration stage. Three months during each season were used, i.e. summer (hot-humid) February, March and April of 2012 and winter (hot-dry), July, August and September of 2012.

### 2.1.3 Spatial characterization of the area

To perform the simulations it is necessary to build an area file that contains the characteristics of the study area. The acquisition of these data was informed by previous work (Maciel, 2011, Silva, 2009), and included the collection of high resolution images of the study area (figure 1b) from Google Earth of dates close to the period in which micrometeorological data were collected. Data such as height of buildings, were identified through on-site visits while definition of albedo values was based on the work of Sailor and Fan (Sailor & Fan, 2002) and Oke (Oke, 1987).

The high-resolution image is inserted into Computer Aided Design (CAD) software in a scale appropriate for the study, allowing detail recognition. Thus, a grid with the defined dimension is drawn (2.5mx2.5m in this case), and the characteristics of the area are identified, such as different ground cover materials, areas occupied by buildings and other elements, resulting in the map of figure 2a. The final step is to insert the categorized information (figure 2a) in the ENVI-met software, shown in figure 2b.



Figure 2: (a) Area attributes categorization in CAD software; (b) Study area inside ENVI-met software;

Table 1 presents information of the characterized areas.

Table 1: Surface areas of the attributes in study area – UFMT campus

Attribute category	Relative area (%)	Absolute area (m <sup>2</sup> )
Water bodies	2,7%	10,068.75
Uncovered soil	3,7%	13,650.02
Sidewalk (concrete)	9,9%	35,645.59
Vegetation - trees	17%	61,355.23
Buildings	18,8%	67,731.25
Vegetation – grass	22,6%	81,364.77
Asphalt	25%	90,184.385

For the specific tree characterization the Scion Image© software as described in (Watkins & Kolokotroni, 2012). The method allows the interpretation of the gray shades of the image (figure 3a and figure 3b). In addition, the concept of the Green Plot Ratio proposed by Ong (Ong, 2003) was considered for the characterization of tree species.



Figure 3: (a) Portion of the study area (with trees); (b) Analysis of gray shades in the Scion Image©;

## 2.2 Numerical Simulation

Three different scenarios were created: Scenario 1 - Cool roof; Scenario 2 –Cool Pavement; and Scenario 3 - Reference (current situation). Each scenario was simulated for summer and winter, totalling 6 simulations.

### 2.2.1 Input files settings

The simulation day and time are defined according to the season of the year to be simulated. It is recommended that the simulations begin at night, minimizing the possibility of convergence errors due to the existence of short-wave radiation in the first few hours of the simulation, (Francisco, 2012). The total simulation time must be at least 48 hours, from which the first 24 hours are the pre-conditioning period. For the present study the simulation was defined the start time at 20h with duration of 48 hours.

The surface roughness value at the reference point was defined according to Oke (1996) and weather data was sourced from Marechal Rondon Airport reference station. Soil temperature and humidity, were sourced from (Rosseti, 2013), both for summer and winter seasons (adjusted for vegetation-irrigated). The values for thermal transmittance (U-value) of walls and roofs were obtained from the Brazilian Standard NBR-15220 (ABNT, 2005).

### 2.2.2 Scenario modelling

The reference scenario was simulated first and then the two hypothetical scenarios according to values usually found for cool roof and cool pavement, described by Gartland (Gartland, 2010). The impact is calculated, therefore, by the temperature difference between the reference scenario and each hypothetical scenario.

a) Scenario 1 – Cool Roof: For this strategy, the attribute responsible for the modifications in the microclimate is the area of roofs, defined by the projection of the buildings contained in the study area, totalling 67,731m<sup>2</sup> or 18.8% of the total surface area. Inside the ENVI-met environment, this strategy is implemented by modifying the albedo values of this element, from 0.15 (reference configuration, described by Oke, 1987), to 0.85 (cool roof configuration).

b) Scenario 2 – Cool Pavement: For this strategy, the attribute responsible for the modifications in the microclimate is the entire area of impervious materials, that is, the sum of the surfaces of pavements and asphalt surfaces, totalling 125,830m<sup>2</sup>, or 34.9% of the total surface area. Inside the ENVI-met environment, this strategy is implemented by modifying the albedo values of the sidewalks, from 0.1 (reference configuration, described by Oke, 1987), to 0.60 (cool surface configuration) and the albedo values for asphalt, from 0.05 (reference configuration, described by Oke, 1987), to 0.80 (cool surface configuration).

### 2.3 Validation of the model and data calibration

To validate the area model, it was necessary to compare the data recorded *in loco* with the data generated by the ENVI-met model for each of the seasons studied winter (hot-dry) and summer (hot-humid).

The data recorded *in loco* were collected by the weather station located inside the study area, while the data generated by the software were registered through 5 sensors arranged in the vicinity of weather station spot, within ENVI-met virtual environment. The average hourly air temperature (°C) of these 5 sensors was calculated for the height of 7m (same as weather station).

Table 2: Data period used for validation and calibration

Season (simulated day)	Validation	Calibration
Summer (26/03/2012)	February + April /2012	March/2012
Winter (25/08/2012)	July + September /2012	August/2012

The indicators presented in Table 3 ( $R^2$  – coefficient of determination, RMSE - Root Mean Square Error, MAE – Mean Absolute Error and, MBE – Mean Bias Error) indicate very good agreement between measurements and predictions

Table 3: Model indicator for validation and calibration steps

Season (step)	$R^2$	RMSE	MAE	MBE
Summer (validation)	0,95125	2,3881	2,0022	1,2923
Winter (validation)	0,95252	2,2088	1,9477	0,3315
Summer (calibration)	0,96002	1,3017	1,1312	0,3701
Winter (calibration)	0,96786	3,3615	3,0531	-0,0050

## 3 RESULTS AND DISCUSSION

The results are displayed using chromatic maps, highlighting the impact of each strategy (cool roof and cool pavement), i.e. the values presented are the difference between the reference

scenario and the scenario with strategy. The periods of times are those that characterize the phenomenon of heat island, recommended by World Meteorological Organization (WMO): 6h for morning, 13h for afternoon and 20h for night.

The results were commented as Areaaverage value andPoint value, already adjusted through the calibration equations, for both periods. The value of the Areaaverage represents the mean value of all the grids present in the study area, at a height of 1.10m from the ground, being therefore a measure of the effect of the strategy on the space as a whole. The Point value represents the value from a single grid, which represents the maximum effect that the strategy reached in a localized way. The colored arrows in blue and red, next to the symbol of the north orientation, represent the predominant direction of the wind for each of the stations, summer (330°) and winter (170°), respectively, counted clockwise from the North.

### 3.1 Scenario 1 – Cool Roof

In the morning period (6h), the thermal maps (figure 4) did not show significant changes in air temperature, registering a Point difference of 0.04 °C for summer and 0.06 °C for winter.

In the afternoon (13h) the impact of Cool Roof strategy is more pronounced, with a decrease in the temperature of Area average value of 0.46 °C for the summer period and 1.05 °C for the winter. At this time, the effect of this strategy at Point value reduce the temperature by up to 3.10 °C for the summer, with its effect spread by the ventilation towards the southern part of the area. For the winter, the temperature is reduced by a factor of up to 3.52 °C, with its effect scattered towards the northeast of the area.

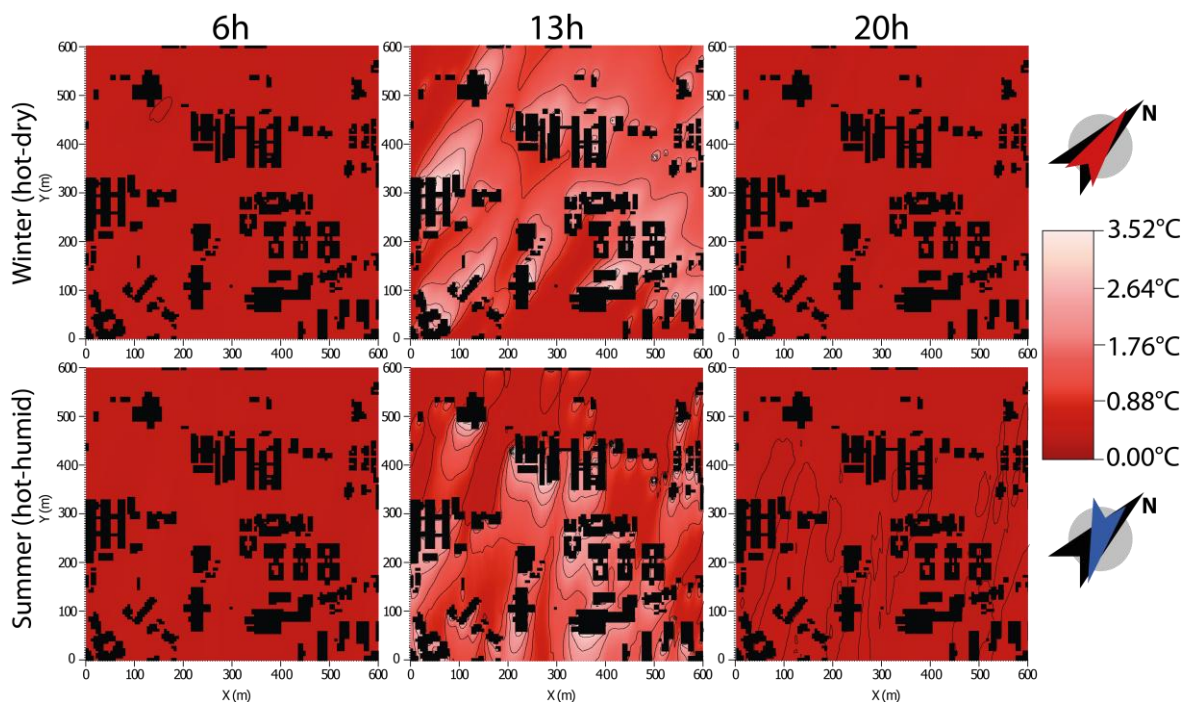


Figure 4: Cool Roof strategy - Difference between air temperature values (°C) for winter and summer, horizontal distribution at 1.10m height

During the night (20h), the cooling effect is not significant, reducing the air temperature by up to 0.09 °C for the summer and up to 0.12 °C for the winter. Ventilation, also at this time, is responsible for spreading the effect along its predominant direction.

This strategy has a maximum effect at afternoon period during the solar peak (between 11h-13h), explained by the lower absorption of thermal energy by the roof material. Due to the albedo, therefore, is expected to have a greater effect at times with higher solar radiation value, in comparison with the reference scenario.

Considering only the interval with solar radiation (7h-17h), the strategy of cool roof resulted in a decrease of 2.02 °C and 2.22 °C in Area average value for the summer and winter periods, respectively. These values are in line with recent numerical studies in temperate climates that have evaluated the impact of applying cool material on roofs. Virk et al (2014) predicted average daily air temperature differences of 0.44 °C at a height of 1.5m above the roof on clear summer days in London with maximum difference of 1.37 °C occurring during the morning with solar radiation of 285W/m<sup>2</sup>. Li et al (2014) also predict reduction of near surface air temperature during the daytime of 0.6 °C for a temperate climate.

### 3.2 Scenario 2 – Cool Pavement

For the Cool Pavement strategy, the thermal maps highlight the effect in the extensive parking areas present on the campus, for the three periods of time.

At morning period (6h), the reduction in the air temperature (Area average value mean) of the space considered reaches 0.04 °C for the summer and 0.08 °C for the winter. At Point value, these values are slightly more expressive, registering reduction of 0.15 °C in the summer and 0.21 °C in the winter.

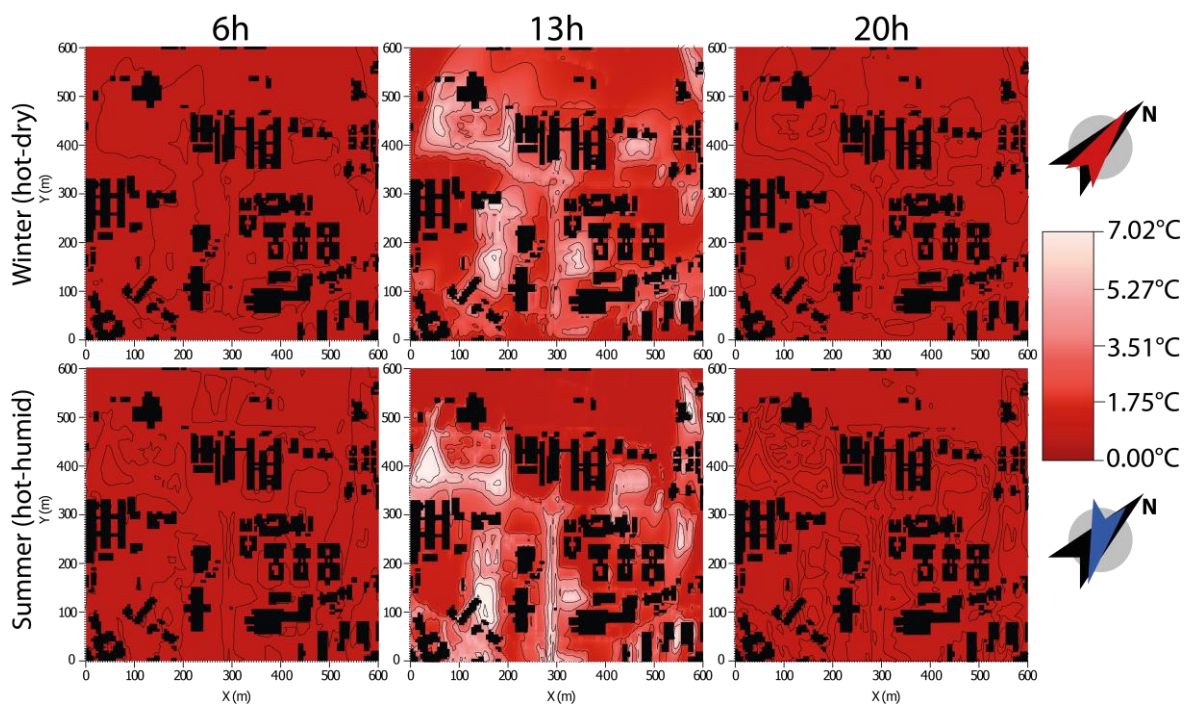


Figure 5: Cool Pavement strategy - Difference between air temperature values (°C) for winter and summer, horizontal distribution at 1.10m height

At afternoon period (13h), the effect is more evident, reaching a reduction in the Area average value meantemperature of 1.20 °C for the summer and 1.94 °C for the winter. At Point value, this effect is higher, reaching a reduction of up to 5.72 °C for the summer and up to 7.02 °C for the winter.

At night period (20h), the effect is also marked in the parking areas. The reduction in Area average value meantemperature reaches 0.11 °C in the summer and 0.21 °C in winter. At

Point value the reduction reaches up to 0.54 °C in the summer and up to 0.66 °C in the winter. Similar to Coof Roof strategy, the effect of the application of cool materials in the form of pavements also has a more evident effect during sun peak times, in response to the variation in the albedo value, which results in greater reflection of the amount of thermal energy.

Shahidan (2012), in a similar study, conducted in Persiaran, Malaysia, found reduction of 2.7 °C in Area average value temperature, using cool pavements (albedo 0.8). Synnefa (2006 and 2011) describes reduction values, during the summer, of up to 4 °C for the daytime period and up to 2 °C for the night period, using reflective material with albedo 0.75. Higher reductions are predicted using CFD modelling by applying a colored thin layer asphalt on pavement with air temperature reduction of 10 °C at 1.5m above the pavement.

The use of cool surfaces in urban areas, evaluated in this paper in form of cool roof and cool pavement strategies, presented a reduction ranging in magnitude, in the average temperature of the study area during both winter and summer seasons (Figure 6). As already mentioned, due to the fact that the cool surfaces have a high albedo value, its effect is proportional to the solar incidence in the area. Thus, the effect starts at sunrise (around 7h), reaching the highest difference soon after the solar peak time (between 12h and 13h), decreasing at the end of the daylight hours (around 18h).

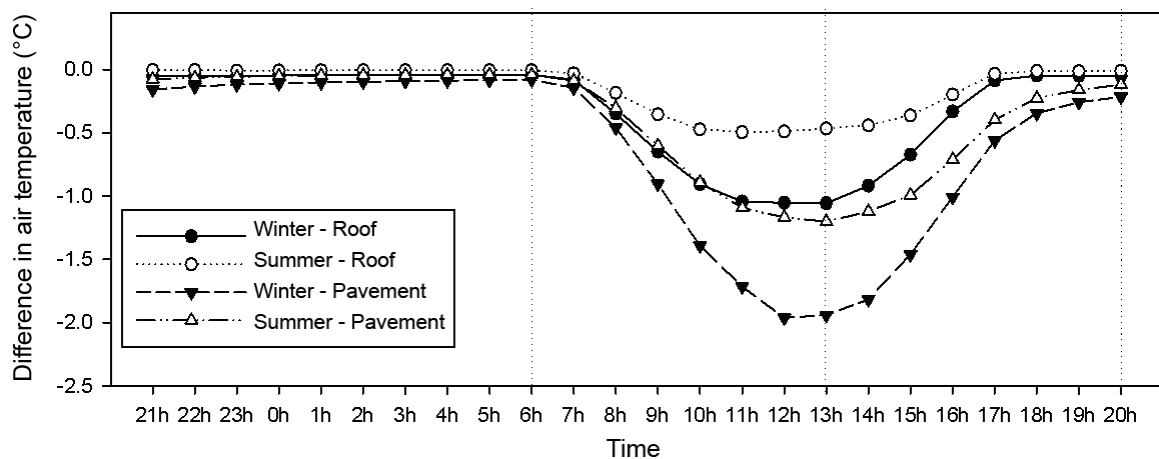


Figure 6: Area average effects of Coof Roof and Cool Pavement strategies during the summer and winter

Between seasons, the highest cooling effect was observed during the winter, with reduction values of 1.94 °C for the cool pavement and 1.05 °C for cool roof strategy. Between strategies, it was observed that the cool pavement (1.94 °C and 1.20 °C) resulted in a higher reduction at Area average value than the cool roof strategy (1.05 °C and 0.46 °C), in the winter and summer seasons, respectively.

It should also be noted that these results are directly influenced by the composition of the study area. In the case of the present paper, the area selected has 34.9% of the surface occupied by impermeable pavements, which may have resulted in a greater effect when compared to the effect of strategy cool roof, which area occupies 18.8% of total surface area.

### 3.3 Potential consequences for building ventilative cooling

The reduction of external air temperature on the roof of the building or in areas surrounding the building has the potential to extend the capacity for ventilative cooling by natural or mechanical means. Cool roofs create lower air temperatures above the roof which will draw cooler air through the ventilating fan if this is located at roof level. It will also be beneficial for air-conditioning plants. An extensive experimental study (Wray and Akbari 2008) has concluded that for high outdoor temperatures (35°C) a 0.3 to 0.5°C reduction in condenser inlet

air temperature will improve Roof Top Air Handling Unit (RTU) capacity about 0.2 to 0.5%, reduce system power consumption about 0.3 to 1.0%, and improve Energy Efficiency Ratio (EER) about 0.6 to 1.1%. The increased capacity also means that the RTU would need to run 0.2 to 0.4% less time to meet a given cooling load. With the run time and power consumption decreases combined, the RTU energy consumption would decrease about 0.3 to 1.0%.

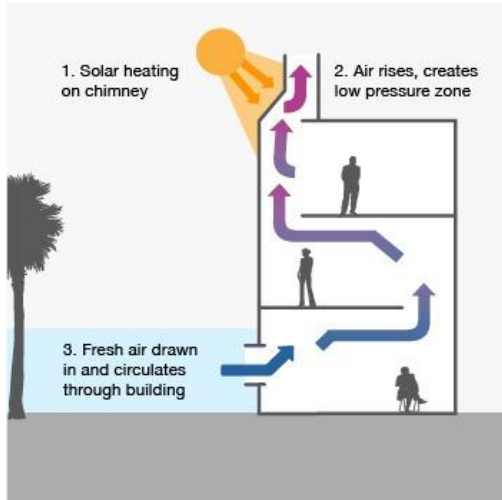


Figure 7: Natural ventilation cooling strategy based on enhancing buoyancy (<http://www.riorenewables.com/efficient-design/ventilation-airflow> study).

Natural ventilation strategies will also benefit from this reduction of the external air temperature, especially in cases where stack ventilation is the design strategy. Many designers prefer to develop natural ventilation strategies based on buoyancy forces for urban buildings because wind patterns are difficult to predict in urban configurations. Therefore, configurations as shown in figure 7 are proposed. Apart from air entering the building at lower temperatures and therefore extending the periods of beneficial natural cooling, pressure drops between inlet and outlet is proportional to density differences and thus temperature differences. An additional air temperature difference of 2 °C will add 1 Pa pressure difference which can be a significant increase considering the low resulting pressure differences during external hot conditions (winter in this case-study).

## 4 CONCLUSIONS

The results presented indicate that cool materials are effective in reducing local temperatures in hot and humid climates, reaching a Point value difference of up to 7.02 °C between the reference scenario and the scenario with cool pavement.

The effect of the cool surfaces is higher during the hours with solar radiation, and the cool pavement strategy was responsible for a greater reduction in the average air temperature during the two simulated seasons. This result was conditioned by the composition of the studied area, formed in 34.9% of pavements, against 18.8% of buildings (cool roof strategy). It can be inferred, therefore, that, availability of surfaces will determine the overall mitigation impact.

The impact on ventilative cooling by natural ventilation will depend on the magnitude of external temperatures; lower air temperatures will enhance buoyancy ventilation and will provide cooler air in cross and single sided ventilation strategies. Finally, cool roofs in addition to establishing significantly lower surface temperatures which reduce heat gains through heat transfer, particularly in less insulated structures, provide energy use reduction by air handling units.

## 5 ACKNOWLEDGEMENTS

The work is supported by the Capes Foundation (BEX: 1462/12-1) and National Council for Scientific and Technological Development (CNPq), Ministry of Education of Brazil.

## 6 REFERENCES

- Alves, E. D. L. (2010). *Caracterização Microclimática do Campus de Cuiabá da Universidade Federal de Mato Grosso*. Cuiabá, 91 f. Dissertação (Mestrado em Física Ambiental) - Instituto de Física, Universidade Federal de Mato Grosso.
- Associação Brasileira de Normas Técnicas (ABNT). (2005) *NBR 15220- 3: Zoneamento bioclimático brasileiro e diretrizes construtivas para habitações unifamiliares de interesse social*. Rio de Janeiro.
- Banco de Dados Meteorológicos para Ensino e Pesquisa. Instituto Nacional de Meteorologia (BDMET/INMET). *Temperatura máxima média, temperatura mínima média e Umidade relativa média 2002/2012 - Cuiabá, MT*. Available at: <<http://www.inmet.gov.br/projetos/rede/pesquisa/>>.
- Francisco, R.C.A. (2012) *Clima urbano: um estudo aplicado a Belo Horizonte, MG*. Dissertação (Mestrado em Arquitetura e Urbanismo), Escola de Arquitetura da UFMG.
- Gartland, L. (2010) *Ilhas de calor: como mitigar zonas de calor em áreas urbanas*. São Paulo: Oficina de textos.
- Li D;Bou-Zeid E; Oppenheimer M (2014). The effectiveness of cool and green roofs as urban heat island mitigation strategies, *Environ. Res. Lett.* 9 (2014) 055002 (16pp).
- Maciel, C. R. (2011) *Análise da relação entre características do ambiente urbano e comportamento de variáveis microclimáticas: Estudo de caso em Cuiabá-MT*. 127f. Dissertação (Mestrado em Física Ambiental), UFMT, Cuiabá.
- Oke, T. R. (1978) *Boundary Layer Climates*. Londres: Metheum.
- Oke, T.R. (1996) *Boundary layer climates*. 2.ed. New York: Routledge.
- Oke, T. R. (2006) Initial Guidance to Obtain Representative Meteorological Observations at Urban Sites. *IOM Report No.81, WMO/TD. No. 1250*. World Meteorological Organization, Geneva, 51p.
- Ong, B. L. (2003) Green plot ratio: an ecological measure for architecture and urban planning. *Landscape and Urban Planning*, v. 63, n. 4, p197-211.
- Rosseti, K.A.C. (2013) *Efeitos do uso de telhados vegetados em ilhas de calor urbanas com simulação pelo software ENVI -Met*. 2013. 273f. Tese (Doutorado em Física Ambiental), Instituto de Física, Universidade Federal de Mato Grosso, Cuiabá.
- Sailor, D.J.; Fan, H. (2002) Modeling the diurnal variability of effective albedo for cities. *Atmos. Environ.*, v.36, p.713-725.
- Silva, C. F. (2009) *Caminhos bioclimáticos - Desempenho ambiental de vias públicas na cidade de Teresina - PI*. Dissertação (Mestrado em Arquitetura), UnB.

- Shahidan, M.F; Jones P.J.; Gwilliam, J.; Salleh, E.(2012) An evaluation of outdoor and building environment cooling achieved through combination modification of ground materials. *Building and Environment*, 58 (0) (2012), pp. 245–257.
- Synnefa, A.; Santamouris, M.; Apostolakis, K. (2006) On the development, optical properties and thermal performance of cool colored coatings for the urban environment. *Solar Energy*, v81, p488-497.
- Synnefa A, Karlessi T, Gaitani Na, Santamouris M, Assimakopoulos D.N. andPapakatsikas C (2011), Experimental testing of cool colored thin layer asphalt and estimation of its potential to improve the urban microclimate, *Building and Environment* 46, pp38-44.
- Virk G, Jansz A, Mavrogianni A, Mylona A,Stocker J and Davies M (2014). The effectiveness of retrofitted green and cool roofs at reducing overheating in a naturally ventilated office in London: Direct and indirect effects in current and future climates, *Indoor and Built Environment*, Vol. 23(3) 504–520
- Watkins R;Kolokotroni M (2012). *The London Urban Heat Island – upwind vegetation effects on local temperatures*, PLEA2012 - 28th Conference, Opportunities, Limits & Needs Towards an environmentally responsible architecture Lima, Perú 7-9 November 2012.
- Wray C; Akbari H, (2008). The effects of roof reflectance on air temperatures surrounding a rooftop condensing unit, *Energy and Buildings*, 40 pp11–28.

# TVOC concentrations measured in Belgium dwellings and their potential for DCV control

Robin De Sutter<sup>1</sup>, Ivan Pollet<sup>2</sup>, Anneleen Vens<sup>2</sup>, Frederik Losfeld<sup>2</sup> and Jelle Laverge<sup>1,\*</sup>

*1 Building Physics, Construction and Services  
Research Group  
Ghent University  
Jozef Plateaustraat 22  
9000 Ghent, Belgium*

*2 Renson Ventilation  
Maalbeekstraat 10  
8790 Waregem, Belgium*

*\*Corresponding author: [jelle.laverge@ugent.be](mailto:jelle.laverge@ugent.be)*

## ABSTRACT

Over the last decade, TVOC sensors have been touted as an interesting alternative to CO<sub>2</sub> and RH sensors in DCV systems. Nevertheless, there is little evidence on the nature and the profile of TVOC concentrations in modern dwellings.

In this project, metal oxide TVOC sensors were installed in the local exhaust ducts in 3-4 bedroom low energy social housing dwellings equipped with a DCV exhaust ventilation system in Belgium. The TVOC and CO<sub>2</sub> concentrations as well as RH levels were measured during operation and 2 control strategies were compared: the DCV was controlled based on the measured CO<sub>2</sub> concentration for 2 weeks and subsequently, the same system was controlled based on the TVOC concentration.

From the observed concentrations, it is shown that, due to occupant activities such as cooking, bathing and cleaning, high, short peaks in TVOC concentrations are a typical feature of residential IAQ. This makes TVOC concentration an especially useful parameter for 'event' related or purge ventilation control. Nevertheless, the relative frequency of these peaks also raises the question whether it is necessary to raise ventilation rates in response to such normal instances such as eating an orange. The average ventilation flow rate during TVOC control is about 50% larger and the system operates at a higher flow rate compared to the CO<sub>2</sub> control 40% of the time on average.

A further observation is that there is only a very weak correlation between the TVOC concentration and the CO<sub>2</sub> concentration at lower concentrations, most likely due to faster secondary reactions of the TVOC compared to the virtually inert CO<sub>2</sub>. This limits the use of TVOC as a control parameter for non-purge related events.

In conclusion, highly peaked TVOC concentrations were observed in low energy dwellings, demonstrating the use of TVOC sensors as a control parameter for purge ventilation in DCV systems.

## KEYWORDS

DCV, TVOC, CO<sub>2</sub>, sensors, control

## 1 INTRODUCTION

Simply reducing ventilation rates, to save energy, deteriorates IAQ, leading to undesirable effects such as productivity loss, increased respiratory problems and susceptibility to allergies (van Holsteijn, 2014). This problem creates conflicts of interest between health and good IAQ on the one hand as energy and cost savings on the other. However, two potential ventilation strategies can provide a possible solution. These energy-efficient ventilation strategies are for example Mechanical Ventilation with Heat Recovery, MHRV, and Demand Controlled Ventilation, DCV. MHRV is primarily used in countries with colder climates. The use and merit of this alternative has already been discussed extensively in literature (eg. Juodis, 2006). The other approach, DCV, possesses the ability to control the ventilation rates by using the concentration levels of pollutants in the occupied space (Haghighat, 1993). Due to well established correlations between the perceived air quality and CO<sub>2</sub> concentration, CO<sub>2</sub> has

been generally embraced as a good indicator for ventilation demand. The continued development of CO<sub>2</sub> sensors over the last decades made this technology find its way into agricultural and industrial application. As a result of this progress, the price of these sensors has already decreased significantly. Recently CO<sub>2</sub> sensors are used as the main detection devices for DCV in residential buildings.

There are, however, important drawbacks with CO<sub>2</sub> sensors from an engineering point of view: they are still rather expensive and energy intensive due to the necessity to heat them for good operation of the most common, NDIR based types. Therefore, researchers are increasingly seeking alternatives to replace conventional CO<sub>2</sub> sensors used in DCV, where VOC detection appears to be promising. Metal oxide VOC sensors are a much more energy efficient and cost effective alternative to NDIR CO<sub>2</sub> sensors, however, their sensor value is non-compound specific and they do not pick up pure CO<sub>2</sub> (Herberger, 2012). Previous studies on the integration of such sensors in demand controlled ventilation systems in an office environment (Kolarik, 2014) and a university classroom (Szcurek, 2015) conclude that the claimed correlation exists but is far from perfect. Since a residential environment has a unique set of pollutants and microenvironments and demand controlled ventilation is widely used in residential ventilation systems in North-Western Europe, further investigations are needed into the potential of replacing traditional CO<sub>2</sub> sensors with VOC sensors for this type of DCV [6].

The aim of this paper is to compare the effect of using either the real CO<sub>2</sub> concentration or an 'equivalent' VOC concentration to control a DCV system in real, occupied dwellings. The observed VOC and CO<sub>2</sub> concentrations will be compared. Additionally, a transformation of the VOC signal will be proposed as a first step in the development of a new approach for control of DCV by VOC detection.

## 2 EXPERIMENTAL SETUP

For the test, 32 newly built or deep-renovated low energy dwellings with recently installed mechanical exhaust ventilation systems with demand controlled dampers in each of the individual exhaust ducts are selected. Carbon dioxide and VOC sensors are installed side by side on the extraction dampers of the kitchens and bedrooms. These are designed to be controlled by either of these sensors in a flexible demand controlled ventilation approach. The system starts with control by CO<sub>2</sub> detection but switches to control by VOC detection after two weeks. In both cases, the damper opening is linearly proportional with the measured concentration, in 7 steps from the minimal flow rate (15%) to the nominal flow rate (100%) in a 200 ppm interval around the setpoint.

The sensor values, as well as the damper position are saved with the internal logging on a 90 seconds interval. Due to the constant pressure ventilation unit, the flow rate through the damper is directly proportional to the valve position. Three such cycles were conducted in every dwelling, corresponding with 12 weeks of measuring. Eventually, due to installation errors, (power) interruptions and sensor errors, only 29 dwellings had at least 2 weeks of data in each mode to make a valid comparison.

## 3 RESULTS

Figure I. shows the CO<sub>2</sub> and VOC concentrations over the course of 2 weeks of measuring for dwelling W27. In the first week, the flow rate through the damper is controlled by adjusting the valve position based on the CO<sub>2</sub> concentration, with a set point of 900 ppm.

As can be seen in the figure, the set point is barely reached and the damper remains closed except one time. During the second week of the figure, the flow rate is controlled by adjusting

the 'valve position' based on the VOC concentration. As can be seen the concentration is more variable and affected by higher peaks and the valve is more intensively opened when occupants are present.

When the CO<sub>2</sub> and VOC concentrations are compared (remember that they are measured at the same point in the damper), the general pattern is rather similar, but the VOC concentration has, as was mentioned above a much higher variability and is affected by higher peaks. This is consistent with the claim of the manufacturers of the sensor that it's calibrated to represent metabolic CO<sub>2</sub> but also reacts to other sources. As has been reported in literature, these other sources may be highly instantaneous, explaining the peaks observed. Another interesting observation is that the slope of the decline in VOC concentrations also seems to be steeper. This can possibly be explained by surface chemistry and secondary reactions, which only very weakly affect the virtually inert CO<sub>2</sub>.

Across all 2-week subperiods and all sensors, on average, the 'equivalent' VOC measured by the metal oxide sensor is 1.52 higher than the average CO<sub>2</sub> concentration measured for the same sub period.

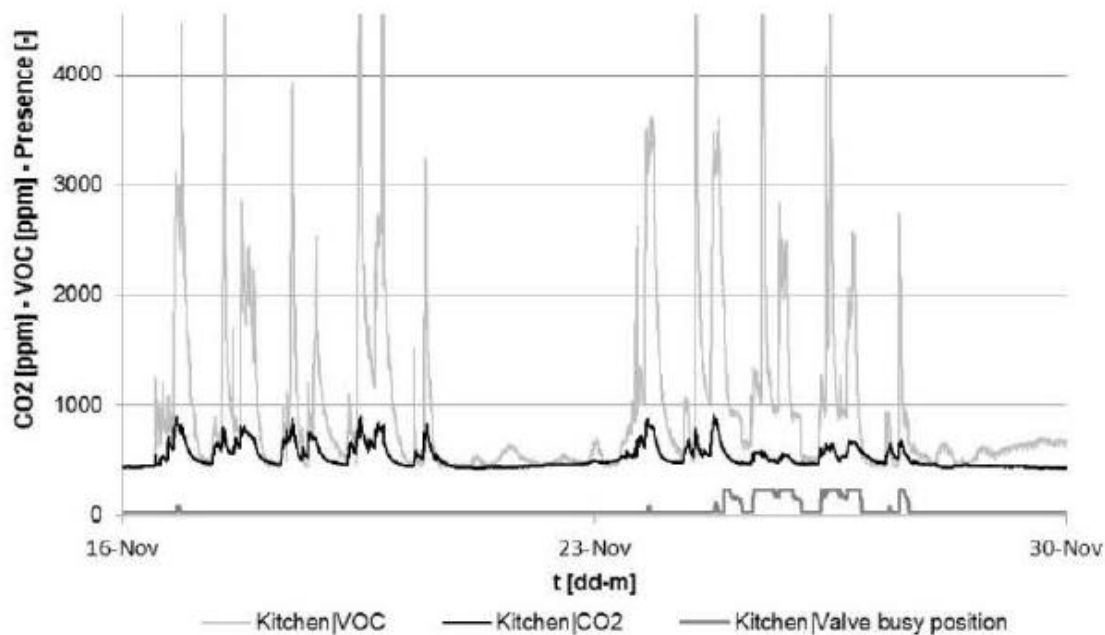


Figure 1: CO<sub>2</sub> and VOC concentrations over 2 weeks  
(week 1: DCV controlled by CO<sub>2</sub>; week 2: DCV controlled by VOC)

The daily concentration profiles for both CO<sub>2</sub> and VOC across the different measurement periods for the bedroom and kitchen sensors for dwelling W33 are shown in figure 2. The occupancy pattern of the spaces is clearly better represented by the CO<sub>2</sub> concentration. Additionally, the ventilation system is able to maintain the set point (900 ppm) quite well for CO<sub>2</sub>, but fails to do so completely for VOC.

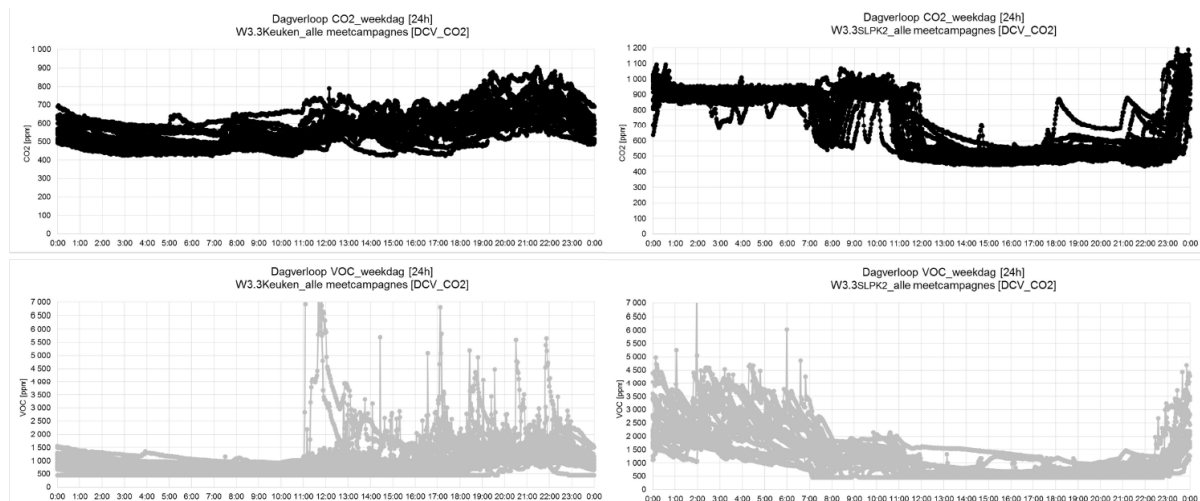


Figure 2. Day profiles of kitchen (left) and bedroom (right) CO<sub>2</sub> (top) and VOC (bottom) concentrations [W33]

Subsequently, to cross compare the 2 weeks of operation, the 'theoretical' valve positions are determined for each damper. This is done following the example of previous studies of Laverge et al. (2015). For each damper the valve position is calculated from the measured VOC concentrations during DCV by CO<sub>2</sub> as if the damper would 'theoretically' be controlled by the VOC concentration. This is also done for the CO<sub>2</sub> concentration during DCV controlled by VOC. Remark that this is only an approximation, because, since the valve does not actually take this position, the subsequent concentrations are not influenced by the theoretical valve position but by the real valve position. In Figure 3, the results for dwelling W27 are given. Actually, the mismatch between the two control signals can be observed. It shows the valve position as a function of both concentrations in case the damper is controlled by the CO<sub>2</sub> concentration (bottom) or the VOC concentration (top). These results are chosen, as this is one of the few dampers that was opened repeatedly during DCV controlled by CO<sub>2</sub>. Other dampers show a high variability between the measured and calculated valve positions, with almost no opening of the damper when controlled by CO<sub>2</sub>.

For all dampers the same results and conclusion, matching the results of the study of Laverge et al. (2015), are seen. The damper is opened 'prematurely' and irrespective of the demand from a CO<sub>2</sub> perspective if the damper is controlled by the VOC concentration, while from a VOC perspective, lots of instances with high concentrations remain unnoticed if the damper is controlled by the CO<sub>2</sub> concentration. Again, we see that the ventilation system is not able to keep the VOC concentration below or around the set point, even if the damper is fully opened. On average, the ventilation flow rate is more than 2 times higher when VOC is used as control parameter. This effect is stronger in the kitchens (average increase 176%) than in the bedrooms (average increase 69%). This is explained by the much higher production of VOC due to occupant activities (e.g. cooking or dishwashing) in the kitchen.

This is also shown in the typical day profiles of the concentrations for both rooms shown in figure 3, where substantially more pronounced peaks that do not match a rise in CO<sub>2</sub> can be seen in the VOC concentration in the kitchen.

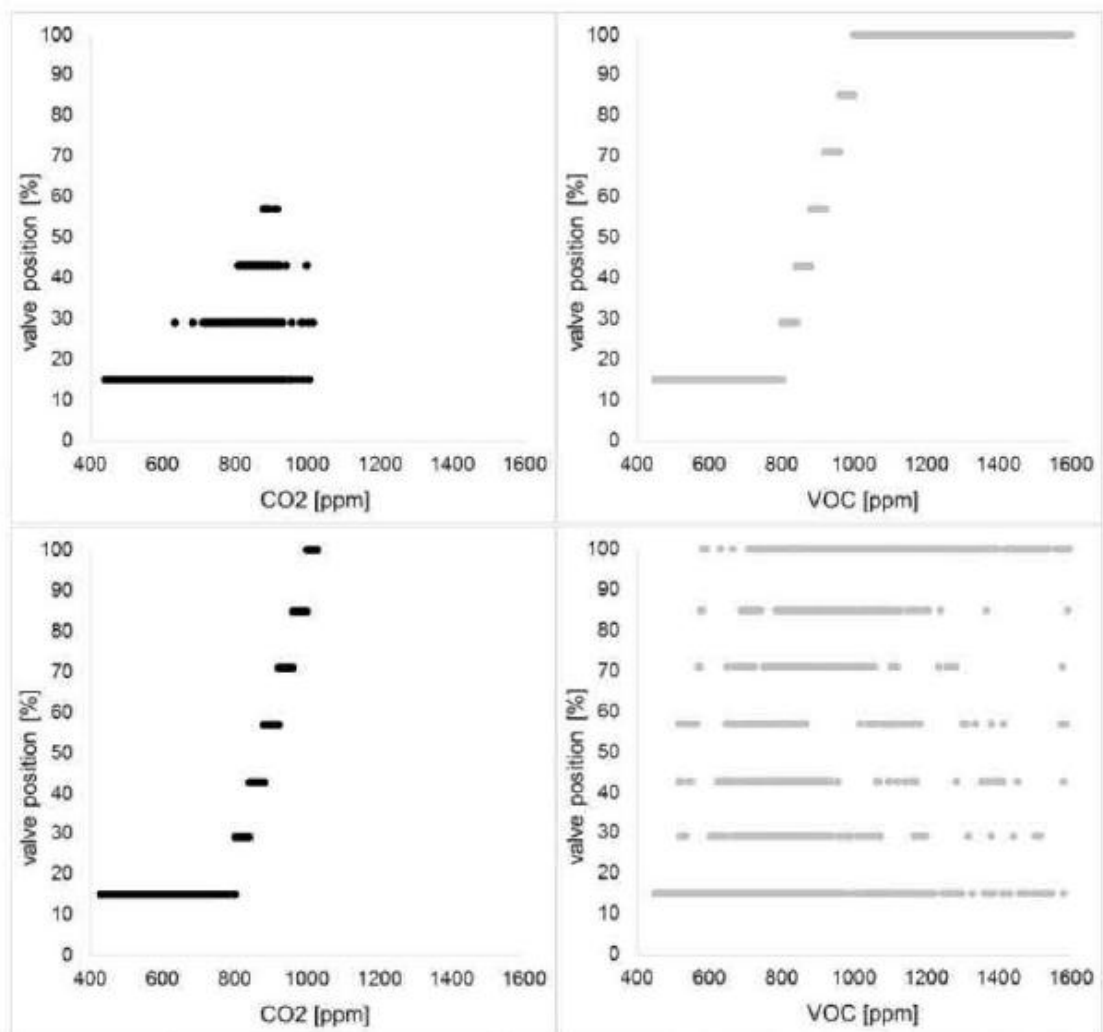


Figure 3: Correlation between the measured CO<sub>2</sub> (left\_top) and VOC (right\_bottom) and the calculated valve position based on measured CO<sub>2</sub> (left\_bottom) and VOC (right\_top) [W2.7Kitchen\_campaign 3]

#### 4 ALTERNATIVE FOR VOC SIGNAL PROCESSING

Considering the results that have been presented above, a new approach to handle the VOC concentration as a DCV control parameter is introduced. The high variability of the VOC concentration is something that can't be left untouched. It's decided to "manipulate" the VOCs signals in such a way the new corresponding valve positions approach the original valve positions that are accessed by DCV CO<sub>2</sub>. The original step control (7 steps, 15 - 100%) and set points (900 or 800ppm +/- 100 ppm) of the considered ventilation system remain the same. This new approach consists of three so-called "manipulations" and is presented below.

The three adjustments that are made to the VOC control signals are: (1) a horizontal stretching of the VOC concentration; (2) a vertical concentration shift; (3) constrain the increases and declines of the VOC-peak concentrations.

##### 4.1 Horizontal stretching

The step control, as described for the determination of the valve position, does not operate using the instantaneous concentration values. It however uses a weighted average. This weighted average, which takes into account the concentration that is previously registered,

ensures a constant sequence of control signals. Depending on a constant k-value, the current weighted average can be affected more or less by the previously determined weighted average. There is a larger horizontal stretching of the VOC control signal as the k-value is higher.

The original formula uses, for the control of DCV by CO<sub>2</sub>, a k-value which is equal to 20. Using the VOC concentration, similar behaviour is obtained for the comparison of the valve positions if one assumes a higher k-value for the determination of the weighted averages. The best results and increasing correlations are received when k=50. Nevertheless, the k-value is considered at 30, as this is the best chosen value when taking the following operations into account.

## 4.2 Vertical shift

The second manipulation is a vertical concentration offset of the VOC signal which is equal to the third quartile, 75<sup>th</sup> percentile, of the observed concentration differences between CO<sub>2</sub> and VOC for each damper. Each damper will be manipulated by a different offset. The universality of this step to obtain an universal control algorithm for DCV by VOC can be questioned since it requires both a startup period (2 weeks of data) and CO<sub>2</sub> concentrations to be measured. The best results are found when using these concentration shifts because they indirectly take into account the user profiles and variability between the dwellings. To avoid that the system becomes insensitive to continuously high concentrations, a maximum value of 600 ppm is allowed for the shift.

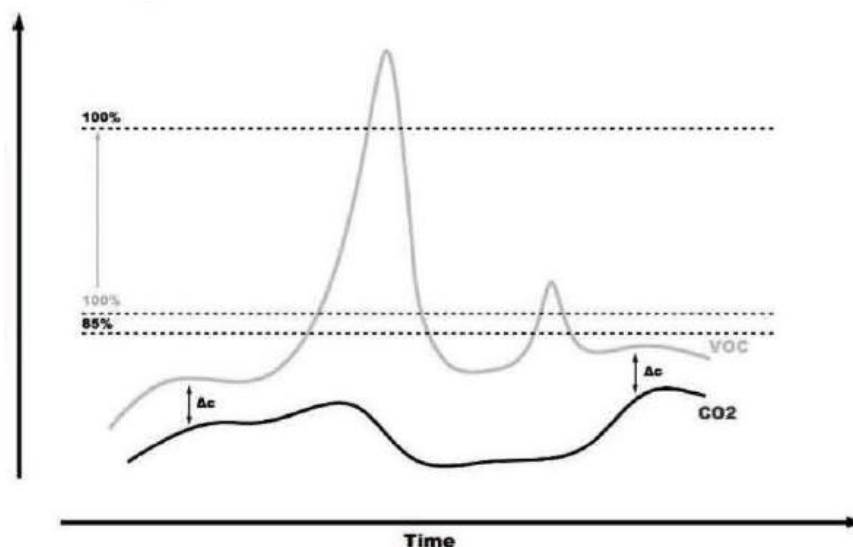


Figure 4: Strategy outline of new approach

## 4.3 Peak shaving

The last manipulation on the VOC concentration is the constraint of so-called "gray areas". These areas represent the slopes of the existing VOC-peaks. This manipulation is shown in the strategy outline in figure 45 below by the dotted lines. In comparison with CO<sub>2</sub>, VOC-peaks show very steep slopes, for which a direct increase in ventilation is not always necessary from a health and comfort perspective. Nevertheless, these sometimes extremely high and damaging VOC-peaks can't be neglected.

VOC concentrations above 2000 - 3000 ppm may have adverse effects on human health. Consequently, an additional requirement is provided. Merely when the average VOC

concentration, expressed in CO<sub>2</sub> equivalents, over a period of 5 min. exceeds the value of 3000 ppm, the damper will be fully opened. Therefore the range of the second to last valve position is expanded in such a way the damper will react more economically, but will be fully opened when the VOC signal reaches values above 3000 ppm regarding comfort and health issues.

Finally, the latter manipulations are performed on the four test cases (8 dampers). The results of this new 'control algorithm' seem to be very promising, as is shown in figure 5. below.

Based on these latest results, an alternative demand controlled ventilation controlled by VOC sensors seems certainly attainable, if one manipulates the VOC signal. However, the dwelling and activity dependency, e.g. the use of different concentration shifts for each dwelling, pose a problem as these make it difficult to assign a universal character to this new approach.

Consequently, one can conclude that the possible replacement of CO<sub>2</sub> sensors by VOC-sensors is 'theoretically' possible. Future research should not focus on achieving similar conducts or correlations between the concentrations, but rather on the way how the VOC signals, and consequently the operation of the system, can be manipulated during DCV controlled by VOC in order to avoid possible over-ventilation and prematurely opening of the damper.

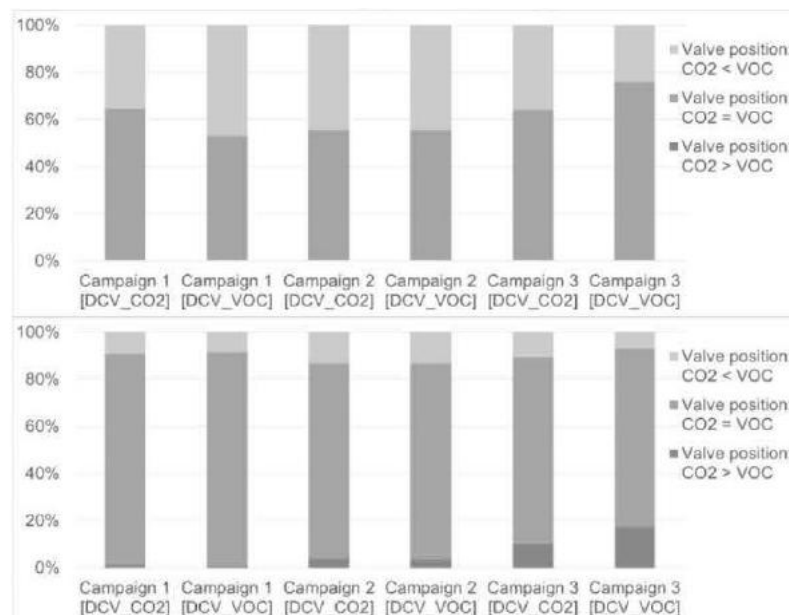


Figure 5: Comparison CO<sub>2</sub> vs VOC valve positions after manipulation of VOC [W2.2Kitchen (top)\_ W2.7Kitchen (bottom)\_ all campaigns]

## 5 CONCLUSIONS

The aim of this paper was to compare the effect of using either the real CO<sub>2</sub> concentration or an 'equivalent' VOC concentration to control a DCV system in real, occupied dwellings. CO<sub>2</sub> and 'equivalent' VOC concentrations were measured simultaneously in 29 dwellings. The observed VOC and CO<sub>2</sub> concentrations were compared and showed that, on average, the VOC concentration was more than 50% higher than the CO<sub>2</sub> concentration and displayed a much more peaked behaviour.

As CO<sub>2</sub> detection is used as the common standard for demand controlled ventilation it seems that the manipulations on the VOC concentration are necessary to avoid over-ventilation when using DCV by VOC. In the observed dwelling, the average ventilation flow rate under VOC based control was double that of CO<sub>2</sub> based control.

Additionally, a transformation of the VOC signal was proposed as a first step in the development of a new approach for control of DCV by VOC detection. The new approach is mainly based on the comparison of valve positions for CO<sub>2</sub> and VOC based control. The results show that achieving similar control behaviour through a manipulation of the VOC signal is possible, but nevertheless, the dependency on dwelling and activity specific data make it difficult to generalise this approach as a control strategy. When using an "overall" value for the concentration shifts acceptable results are recorded, but they appear not always consistent.

In conclusion, a general, obvious choice of CO<sub>2</sub> or VOC detection appears to be difficult, since the different approaches do not always provide straightforward results. Secondary technical and economic interests, as well as health aspects, could possibly be more conclusive in this CO<sub>2</sub> vs VOC debate. DCV controlled by CO<sub>2</sub> detection has repeatedly proven its benefits in various studies. The results obtained in this study also show that CO<sub>2</sub> is a good occupancy related parameter and controls the DCV system quite well if the occupant is the main pollutant of interest, while VOC based DCV will offer better protection against exposure to activity related pollutants. Nevertheless, the highly peaked nature of the exposure to these pollutants severely limits the possibility of the ventilation system to keep the concentrations below the chosen setpoint.

## 6 ACKNOWLEDGEMENTS

The authors would like to thank the occupants of the dwellings and the housing association 'De goedkopewoning' for their support during the measurement campaign.

## 7 REFERENCES

- van Holsteijn, R. C. A., & Li, W. L. (2014). Monitoring the energy & IAQ performance of ventilation systems in Dutch residential dwellings. In 35th AIVC Conference "Ventilation and airtightness in transforming the building stock to high performance" (pp. 467-477). Poznan.
- Juodis, E. (2006). Extracted ventilation air heat recovery efficiency as a function of a building's thermal properties. *Energy and Buildings*, 38(6), 568- 573.
- Haghighat, F., & Donnini, G. (1993). Conventional vs CO<sub>2</sub> demand controlled ventilation systems. *Journal of Thermal Biology*, 18(5-6), 519- 522.
- Laverge, J., Pollet, I., Spruytte, S., Losfeld, F., & Yens, A. (2015). VOC or CO<sub>2</sub>: Are They Interchangeable As Sensors for Demand Control? In *Healthy Buildings Europe 2015* (p. 8). Eindhoven.
- Herberger, S., & Ulmer, H. (2012b). New IAQ sensor for demand controlled ventilation. *REHVA Journal*, 04(August), 37-40.
- Kolarik, J. (2014). CO<sub>2</sub> sensor versus volatile organic compounds (VOC) sensor - Analysis of field measurement data and implications for demand controlled ventilation. In *Indoor Air 2014* (p. 8). Hong Kong: Indoor Air 2014.
- Szczurek, A., Maciejewska, M., & Pietrucha, T. (2015). CO<sub>2</sub> and Volatile Organic Compounds as indicators of LAQ. In 36th AIVC conference: "Effective ventilation in high performance buildings" (pp. 118-127). Madrid.

# Possible UK residential demand-controlled ventilation assessment methodology

Simon Jones<sup>1</sup>, Ivan Pollet<sup>\*2,3</sup>, Frederik Losfeld<sup>2</sup>, Michael Reeves<sup>2</sup>, Pierre Lopez<sup>1</sup>, Elsa Jardinier<sup>1</sup>, and Jelmerde Jong<sup>4</sup>

*1 AerecoLtd.  
483 Green Lanes  
London, UK*

*2 Renson  
Maalbeekstraat 10  
Waregem, Belgium*

*\*Corresponding author: [ivan.pollet@renson.be](mailto:ivan.pollet@renson.be)*

*3 Ghent University  
Department of Biosystems Engineering  
Coupure Links 653  
Ghent, Belgium*

*4 Brink Climate Systems  
Wethouder Wassebaliestraat 8  
Staphorst, The Netherlands*

## ABSTRACT

Demand controlled ventilation (DCV) can improve the energy performance of all kinds of ventilation systems, in residential and non-residential buildings and is already part of the European Lot 6 and Ecodesign regulations and standards. However, the lack of recognition of DCV in SAP (Standard Assessment Procedure) forms a great barrier for the use of this technology in the UK. A methodology was developed to prove the guarantee on good IAQ, with potential saving on heating and auxiliary energy by modulating ventilation rates based on actual demand.

It is generally accepted that a DCV system, with air flow rates lower than UK recommended values, can only be recognised provided that the IAQ is at least as good as the worst performing constant airflow ventilation system in the regulation. Therefore a model, based on UK reference dwellings and systems, was developed and particular attention was paid to dwellings with low air permeabilities.

A representative simulation model was established using the reliable multi-zone simulation tool Contam. Two different dwelling types, a detached house and a flat, were modelled. These dwelling types represent a large part of the UK housing stock.

Hypotheses concerning the dwelling characteristics (detached house and flat), the weather data, the location, the occupancy, the production of contaminants, the user behaviour and the ventilation components were made.

The IAQ achieved with a number of ventilation systems with or without DCV were assessed using (1) relative humidity (RH), (2) (total) volatile organic compounds ((T)VOC) and (3) carbon dioxide (CO<sub>2</sub>), after which the energy saving of hypothetical DCV systems were determined with respect to the four different reference system types in the regulation.

Each ventilation system was modelled at 5 building air permeabilities: 0.6; 2.5; 5; 7.5 and 10 (m<sup>3</sup>/h)/m<sup>2</sup> and for the 2 types of dwellings.

It is found that different configurations of DCV systems can comply with the 3 IAQ criteria, creating equally good or even better IAQ than the reference ventilation systems, while reducing energy consumption for heating and fan power consumption (average reduction factors of 0.83 and 0.93 respectively with the examples taken into account).

## KEYWORDS

Demand controlled ventilation, simulation, IAQ, Energy savings

## 1 INTRODUCTION

Demand controlled ventilation (DCV) can improve the energy performance of all kinds of ventilation systems, in residential and non-residential buildings and is already part of the European Lot 6 and Ecodesign regulations and standards. However, the lack recognition of DCV in SAP forms a great barrier for the use of this technology in the UK. The following study will demonstrate the energy-savings potential in UK dwellings.

It is generally accepted that a DCV system can only be recognised provided that the IAQ is at least as good as the worst ventilation systems 1, 2, 3 or 4 according to Approved Document F (ADF). Therefore, the DCV group developed a model based on UK reference dwellings and systems, and particular attention was paid to dwellings with low air permeabilities.

A representative simulation model was established using the reliable multi-zone simulation tool Contam, as proposed by BRE and supported by PHE (I-VII). Similar to the study of Palmer et al. (I), two different dwelling types, a detached house and a flat were modelled. These dwelling types represent a large part of the UK housing stock.

Hypotheses concerning the dwelling characteristics (detached house and flat), the weather data, the location, the occupancy, the production of contaminants, the user behaviour and the ventilation components were made and are listed in section 2.

The IAQ achieved with a number of ventilation systems with or without DCV were assessed using relative humidity, (total) volatile organic compounds and carbon dioxide, after which the energy saving of a particular DCV system was determined with respect to reference systems 1, 2, 3 and 4.

Three main contaminants affecting the IAQ were modelled:

- Water vapour (H<sub>2</sub>O) with production rates derived from BS5250:2002 (XI) and from references (VIII-X);
- Total volatile organic compounds (TVOC) with an emission rate of 0.3 mg/(h.m<sup>2</sup>) in dry and wet rooms according to ADF;
- Carbon dioxide (CO<sub>2</sub>) with production rates derived from the standard CEN/TR 14788 (XII), EN 15665 (XVII) and from references (II&VII).

## 2 MODEL BUILD-UP

The reference residential ventilation and DCV systems were assessed using the multi-zone airflow modelling software Contam, which was developed by NIST (USA). The software Contam was used in several scientific research dealing with DCV and forms also the basis for the Belgian DCV assessment method (I-VII).

In Contam, each room of the building represents one zone and a simplified humidity buffering model (BLDM) is included. The simulation was run with 5 minutes intervals. Post-processing of the modelling results was done by means of Excel.

Similar to the study of Palmer et al. (I), two houses, a detached one and a flat were modelled. The detached house with a 4-person family was supposed to be situated in a village, while the flat with a couple was located in a city centre. Impact of orientation was taken into account by changing the wind direction every 2 weeks by 90°. Simulations were performed for 5 air

permeabilities: 0.6; 2.5; 5; 7.5 and 10 (m<sup>3</sup>/h)/m<sup>2</sup> and for the 2 types of dwellings (parameters can be found in Table 1).

Fixed simulation parameters were:

- building location: London (Gatwick)
- outdoor climate (temperature, RH, wind speed and wind direction): TRY iwec
- outdoor CO<sub>2</sub>-concentration: 400 ppmv
- indoor air temperature: overall 20°C
- mechanical duct length: 3 or 4 m
- mechanical duct diameter: 125 mm
- inner walls and doors are air tight, with the exception of the transfer openings
- ventilation effectiveness: 1 or perfect mixing as supposed in ADF

The wind pressure coefficients on the different facades and the roof were derived from the “AIVC guide to ventilation” (XIV).

Total air flow rate due to air permeability was derived from the total envelope surface in case of the detached house and only from the vertical external walls in case of the flat. That air permeability was distributed over the vertical external walls, proportionally with the room external wall surface.

The total number of simulations per ventilation systems was 10 (2 houses x 5 air permeabilities). All simulations were run over the typical heating season in UK, which is from 1<sup>st</sup> October to 31<sup>th</sup> May or 243 days (heating period SAP, Table 9D). It corresponds to 5,832 hours. To stabilise simulations, the simulation was starting on 1<sup>st</sup> September. Monthly averaged RH values were calculated on a 30 days basis.

Table 1: Model parameters

Parameter	Detached house	Terraced flat
Terrain roughness	$\alpha = 0.313$ ; $z_{\text{bound}} = 60$ m Obstacles at distances of less than a few times building H	$\alpha = 0.377$ ; $z_{\text{bound}} = 80$ m City centre
Volume	336 m <sup>3</sup>	168 m <sup>3</sup>
Number of floors	2	1
Floor surface	2 x 70 m <sup>2</sup> or 140 m <sup>2</sup>	70 m <sup>2</sup>
Envelope area	303.2 m <sup>2</sup>	269.6 m <sup>2</sup>
Envelope area for permeability	303.2 m <sup>2</sup>	48 m <sup>2</sup> (facades)
Floor to ceiling height	2.4 m	2.4 m
Floor levels	0 and 1	1 (mid floor)

### 3 DCV PERFORMANCE ASSESSMENT

#### 3.1 Performance assessment with respect to IAQ

A DCV system was accepted as being equivalent to the reference residential ventilation systems when the same criteria as described thereafter were fulfilled for the detached house and the flat and for all of the 5 air permeabilities considered. Those criteria are either included in ADF, either derived from Contam simulations performed on the 4 reference ventilation systems.

- **RH:**

The average indoor air RH values per wet room for a certain air permeability  $\leq$  RH values specified in table A2 of ADF:

average per month  $\leq 65\%$

average per week  $\leq 75\%$

average per day  $\leq 85\%$

average over 8 hours  $\leq 90\%$  (additional requirement with respect to ADF as suggested by BRE)

Exceeding the threshold values for up to 58 hours for the whole dwelling ( $< 1\%$  of the heating season) is allowed because high humidity levels during short periods are neither harmful for the building nor for the occupants.

- **TVOC:**

(1) According to ADF, exposure to total TVOC levels should not exceed  $\leq 300 \mu\text{g}/\text{m}^3$  averaged over 8 hours.

Contam simulations revealed that in most cases reference systems don't comply with the above performance criterion.

Therefore, the above criterion was not used. Instead, the following criterion was used to assess the IAQ with respect to TVOC. This new criterion is based on the time which the threshold value was exceeded multiplied by the concentration the threshold value was exceeded. Since the IAQ of system 1 is clearly worse compared to other reference systems and since the TVOC criterion is not applicable to extract ventilation in Part F, System 1 was neglected to set the threshold value.

(2) Cumulative exposure to TVOC-concentration ( $\mu\text{g}/\text{m}^3$ ).h/pers) over  $300 \mu\text{g}/\text{m}^3$  of the DCV system for a certain air permeability  $\leq$  cumulative exposure to TVOC-concentration ( $\mu\text{g}/\text{m}^3$ ).h/pers) over  $300 \mu\text{g}/\text{m}^3$  of the worst reference system taken into account (among systems 2, 3 and 4) which equals  $370,000 (\mu\text{g}/\text{m}^3)$ .h/pers

- **CO<sub>2</sub>:**

Cumulative exposure to CO<sub>2</sub>-concentration (ppm.h/pers) over 1,200 ppm of the DCV system for a certain air permeability  $\leq$

cumulative exposure to CO<sub>2</sub>-concentration (ppm.h/pers) over 1,200 ppm of the worst reference system which equals 1,465,000 ppm.h/pers

The CO<sub>2</sub> threshold was also derived from the Contam simulations for the reference systems 2, 3 and 4 and the results for reference system 1 were also not taken into account following the same reasoning as for TVOC, as there is no threshold mentioned in Part F.

When a DCV system complies with all 3 criteria for all 5 air permeabilities and both types of dwellings, the energy reduction coefficient of the DCV system for lower heat losses and fan consumption can be calculated.

### 3.2 Performance assessment with respect to energy

DCV affects the ventilation heat losses as well as the fan power consumption.

#### Ventilation heat losses

The ventilation heat losses of the DCV system were determined for an air permeability of 0 (m<sup>3</sup>/h)/m<sup>2</sup>, since the effect of infiltration & exfiltration is already taken into account in the SAP calculation (VIII, X). This extrapolation from the 5 modelled air permeabilities to an air permeability of 0 (m<sup>3</sup>/h)/m<sup>2</sup> is done for the 4 reference residential ventilation systems as well as for the DCV systems under investigation. The determination coefficient of this extrapolation must be at least 0.95. When lower than 0.95, non-linear regression must be used.

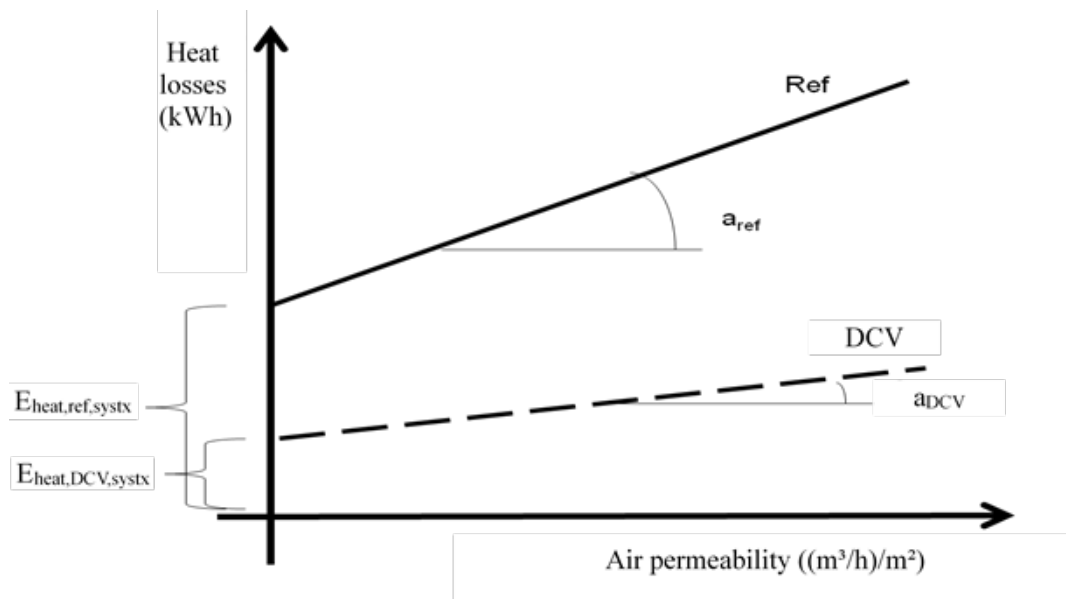


Figure 1: Principle of determination

Consequently, the energy reduction factor of a particular DCV system can be determined as follows:

- The heat losses of the four reference systems is expressed as  $E_{\text{heat,ref,systx}}$  with  $x$  equal to 1, 2, 3 or 4.
- The heat losses of the DCV system is expressed as:  $E_{\text{heat,DCV,systx}}$ .
- The energy performance of the DCV system for the detached house and the flat with respect to heat losses is compared with the energy performance of the same type of reference system to determine the so-called heating reduction factor of the DCV system

$$f_{\text{red,heat,house,DCV,systx}} = \frac{E_{\text{heat,DCV,systx}}}{E_{\text{heat,ref,systx}}} \quad (1)$$

- The heating reduction factors for the detached house and the flat are averaged to become a single heating reduction factor:

$$f_{\text{red,heat,DCV,systx}} = (f_{\text{red,heat,detached house,DCV,systx}} + f_{\text{red,heat,flat,DCV,systx}})/2$$

## Fan consumption

The reduction in fan consumption of the DCV system is derived from the specific fan power values listed in the SAP Product Characteristics Database (PCDB).

For air flow rates lower than 21 l/s, the SFP value is derived as follows:

- The minimum reduced ventilation rate is 1.4 l/s per habitable and wet room. The minimum total reduced ventilation rate at the supply and extract side is found in the flat, i.e. 2.8 l/s (2 wet rooms of 1.4 l/s). Due to the higher number of dry and wet room in the detached house, the total reduced ventilation rate for the detached house is higher than 2.8 l/s. This air flow rate of 2.8 l/s was also considered in Table 2, as an extension of the SAP PCDB values.
- The SFP could be measured at minimum 2.8 l/s within the SAP measurements. When 2,8 l/s is not achievable, the SFP of the lowest air flow rate can be measured. If not measured, **4 x SFP at 21 l/s** is taken, as a common value derived from fan characteristics (see Table 2). Intermediate SFP values are derived from linear interpolation between the power values.

Table 2: SFP as a function of air flow rate

		Kitchen + n wet rooms					
		n=1	n=2	n=3	n=4	n=5	n=6
Air flow rate (l/s)	2.8	21	29	37	45	53	61
SFP (non DCV mode) (W/(l/s))	4*X1	X1	X2	X3	X4	X5	X6
SFP (DCV mode) (W/(l/s))	f*4*X1	f*X1	f*X2	f*X3	f*X4	f*X5	f*X6

The fan consumption (in kWh) in DCV mode is calculated as the sum of the airflows (in l/s) per time step during the heating season multiplied with the corresponding SFP (in W/(l/s)).

The fan power consumption during the heating season is extrapolated to a yearly fan consumption. In the case of DCV systems controlled on RH values, the DCV fan power consumption outside the heating season is considered as equal to the reference system's.

The reduction factor for fan consumption is defined as:

$$f_{red, fan, house, DCV, systx}$$

$$= \frac{\text{fan consumption in DCV mode averaged over the 5 air permeability's (kWh)}}{\text{fan consumption not in DCV mode averaged over the 5 air permeability's (kWh)}}$$

$$= \frac{E_{fan, DCV, systx}}{E_{fan, non DCV, systx}} \quad (2)$$

Then, the fan reduction factors for the detached house and the flat are averaged to become a single fan reduction factor:

$$f_{red, fan, DCV, systx} = (f_{red, fan, detached house, DCV, systx} + f_{red, fan, flat, DCV, systx})/2$$

Finally, the fan reduction factor is used to determine the SFP values of the DCV system as a function of the number of wet rooms, as shown in Table 1:

$$\text{SFP (DCV mode, systx)} = f_{\text{red, fan, DCV, systx}} \text{ SFP (Non DCV mode)}$$

## 4 DCV SYSTEMS MODELLED

Three examples of DCV systems (DCV3a, DCV3b and DCV3c) are modelled to show how the IAQ and energy performance of a DCV system with respect to the reference system is assessed. All three DCV systems are of type 3, which means that the air is supplied naturally and the air is extracted mechanically. Relative humidity detection, presence detection (in toilets) and CO<sub>2</sub> sensors are used to design the following DCV systems.

- DCV3a: natural supply with local humidity controlled mechanical extract
- DCV3b: local humidity controlled natural supply with local humidity controlled mechanical extract
- DCV3c: natural supply with local CO<sub>2</sub> and humidity controlled mechanical extract.

The air supply rates are designed according to a reference system 3 with background ventilators for all air permeabilities (no alternative guidance).

Main characteristics of DCV3a and DCV3b are:

- RH setpoints (30–75% and 30–80 %) are those used in practice (50-65% for air supply)
- Reduced ventilation rates are higher than the minimum reduced rates of 1.4 l/s
- Maximum high rates are higher than minimum high rates of ADF
- The air supply of DCV3b is also controlled on humidity.

The differences between DCV3c and DCV3a are:

- Lower reduced and lower high rates
- Supplementary control on CO<sub>2</sub> in the living room and the master bedroom. These CO<sub>2</sub>sensors impacts on the total extract from all wet rooms.

Results revealed that the three DCV systems comply with the general DCV requirements as set out in §3, and therefore modelling of the DCV system is allowed. A heat and fan power consumption reduction factor can be determined.

## 5 RESULTS

### 5.1 Ventilation heat losses

As for the reference systems, the ventilation heat losses of DCV3a, 3b and 3c were extrapolated to an air tightness of 0 (m<sup>3</sup>/h)/m<sup>2</sup> (see Figure 2) and compared with the corresponding value for reference system 3. The ratio of both gives the heating reduction factor  $f_{\text{red, heat, DCV, syst3}}$ , for the detached house and the flat, which is finally averaged to a value of 0.89; 0.83 and 0.78 for DCV3a, 3b and 3c respectively, as shown in Table 3 and Table 4. This means that the ventilation losses of the proposed DCV3a, 3b and 3c system are 11%, 17% and 22% lower than the reference system 3.

## 5.2 Fan consumption

Based on the assumption of the SFP of the reference system 3 and similar SFP values for DCV3a, 3b and 3c, the fan power consumption was calculated as a function of air permeability, as illustrated in Figure 3 for the detached house and flat.

As all system are controlled on RH, the fan power consumption of the reference system was taken into account for the period outside the heating season.

Based on the average fan power consumption, a fan reduction factor of 0.97; 0.94 and 0.89 can be calculated for DCV3a, 3b and 3c respectively.

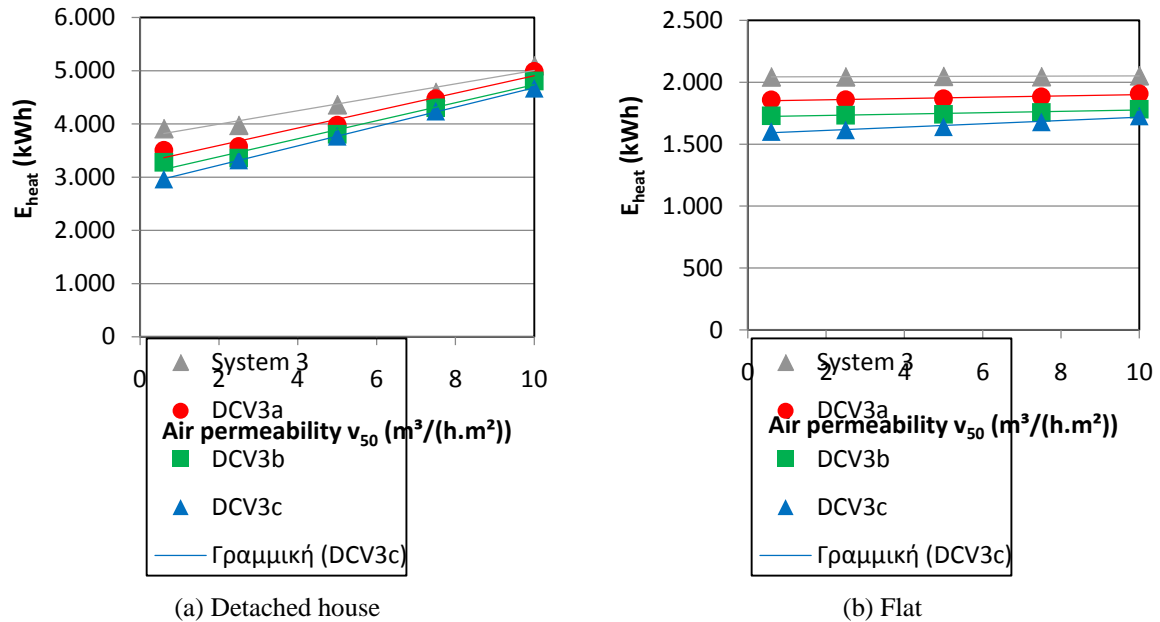


Figure 2: Ventilation heat losses of reference system 3 and DCV3a, 3b and 3c in the detached house

Table 3: Ventilation heat losses of reference system 3, DCV3a, 3b and 3c for the detached house and the flat

	Ventilation heat losses $E_{\text{heat}}(\text{kWh})$	
	Detached house	Flat
System 3	3,744	2,044
DCV3a	3,266	1,859
DCV3b	3,043	1,731
DCV3c	2,849	1,584

Table 4: The heating reduction factor of DCV3a, 3b and 3c for the detached house and the flat and the average values

	Heating reduction factor $f_{\text{red,heat,DCV}}(-)$		
	Detached house	Flat	Average
DCV3a	0.87	0.91	0.89
DCV3b	0.81	0.85	0.83
DCV3c	0.76	0.78	0.77

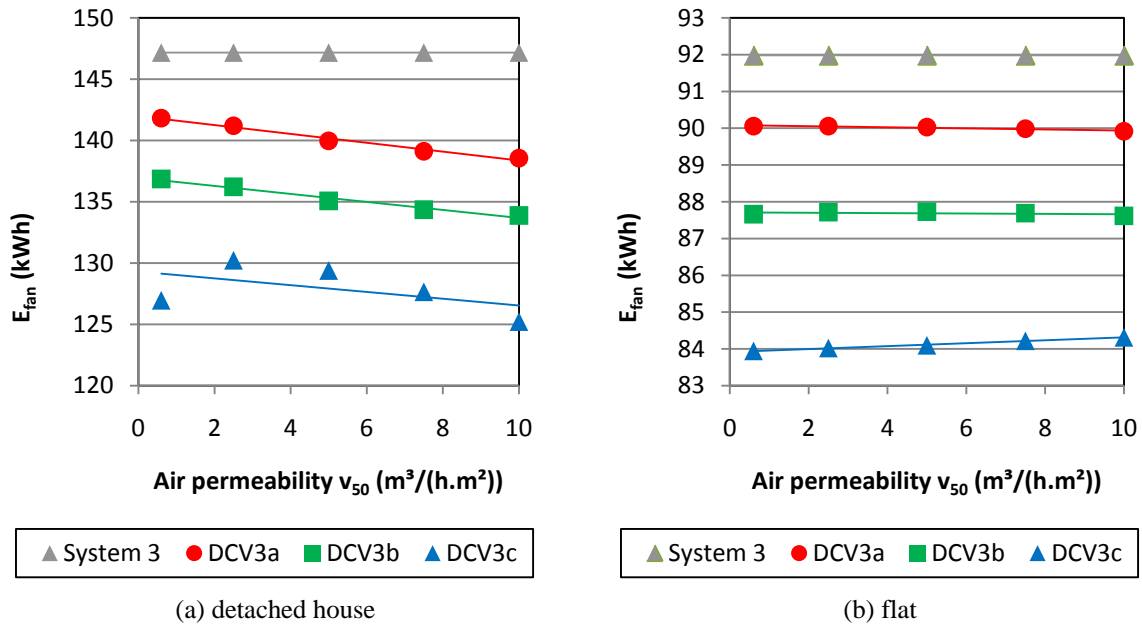


Figure 3: Fan consumption (whole year) of reference system 3 and DCV3a, 3b and 3c

Table 5: Average fan consumption of reference system 3, DCV3a, 3b and 3c for the detached house and the flat

	Fan consumption $E_{fan}$ (kWh)	
	Detached house	Flat
System 3	147	92
DCV3a	140	90
DCV3b	135	88
DCV3c	128	84

Table 6: The fan reduction factor of DCV3a, 3b and 3c for the detached house and the flat and the average values

	Fan reduction factor $f_{red, fan, DCV}(-)$		
	Detached house	Flat	Average
DCV3a	0.95	0.98	0.97
DCV3b	0.92	0.95	0.94
DCV3c	0.87	0.91	0.89

## 6 CONCLUSIONS

- A reliable residential ventilation model and assessment methodology for all 4 reference ventilation systems was built, which can be used to assess all types of ventilation systems using Demand Controlled.
- The energy consumption for heating and fan consumption, expressed as a reduction factor relative to the reference system, are the outputs of the model to be used for the SAP calculation.
- DCV systems can create an equally good or even better IAQ than the reference ventilation systems, while reducing energy consumption for heating and fan power consumption. In that way, DCV has a positive effect to reach EPBD and NZEB goals.
- All 3 example DCV systems modelled comply with the 3 IAQ criteria (relative humidity, TVOC and  $CO_2$ ). Mean reduction factors for heating up to 77% and fan consumption up to 89% were achieved. Further savings can probably be obtained with optimised systems.
- Simulations showed that different configurations of DCV systems can comply with the 3 IAQ criteria, while the energy performance is better than reference systems. One kind of sensor (RH,  $CO_2$ , TVOC, presence in toilets) or a combination of different sensors types allows to ensure IAQ at lower air flow rates, provided the sensors, air flow rates and control setpoints are designed correctly by the manufacturers and

appropriate tests prove their performance and their reliability. Minor site adjustments can be envisaged to adapt to specific layouts when clearly documented in the manufacturers' installation documents. Professional commissioning as per industry and manufacturer's guidelines is essential to ensure proper installation.

- The more advanced the DCV system, the higher the potential to improve the energy performance of the system.
- It is inherent to modelling, that small changes in the DCV characteristics can determine whether the IAQ are fulfilled or not (= high sensitivity) and as a consequence, if the system can be recognised as DCV. However, this small changes will also result in small differences in energy performance (= low sensitivity). This means that the model is robust regarding the energy performance, but sensitive regarding the fulfilment of the IAQ criteria. This latter sensitivity is already limited by the general requirements of a DCV system (as described in section 3) and can further be restricted if needed.
- The energy-saving potential of DCV systems in domestic buildings in the UK can be estimated as follows using the examples of DCV Systems 3 described above:
  - Mean heating and fan reduction factor of the DCV system of 0.83 and 0.93, respectively
  - If 50,000 new homes in the UK have a Demand Controlled Ventilation system
  - Boiler / heat distribution efficiency of 80%
  - CO<sub>2</sub>-emission factors based on secondary energy consumption of 0.202 kg CO<sub>2</sub>/kWh gas and 0.543 kg CO<sub>2</sub>/kWh electricity

⇒ Yearly reduction of heating gas consumption	35.0 GWh
⇒ Yearly reduction of fan electricity consumption	0.46 GWh
⇒ Yearly reduction of CO <sub>2</sub> -emissions	7,311 tons of CO <sub>2</sub>

## 7 REFERENCES

- I. Palmer, J., Orme, M., Pane, G., Ridley, I., Davies, M., Oreszczyn, T., Lowe, R. (2009). Investigation of Ventilation Effectiveness. BD2523, HMSO, 67 p.
- II. Laverge, J., Van Den Bossche, N., Heijmans, N., Janssens, A. (2011). Energy saving potential and repercussions on indoor air quality of demand controlled residential ventilation strategies. *Building and Environment*, 46(7), 1497-1503.
- III. Shrubsole, C., Ridley, I., Biddulph, P., Milner, J., Vardoulakis, S., Ucci, M., Wilkinson, P., Chalabi, Z., Davies, M. (2012). Indoor pm2.5 exposure in London's domestic stock: Modeling current and future exposures following energy efficient refurbishment, *Atmospheric Environment*, vol. 62, pp. 336-343.
- IV. Das, P., Chalabi, Z., Jones, B., Milner, J., Shrubsole, C., Davies, M., Hamilton, I., Ridley, I., Wilkinson, P. (2013). Multi-objective methods for determining optimal ventilation rates in dwellings, *Building and Environment*, vol. 66, pp. 72-81.
- V. Pollet, I., Laverge, J., Vens, A., Losfeld, F., Reeves, M., Janssens, A. (2013). Performance of a demand controlled mechanical extract ventilation system for dwellings: simulations and in-situ measurements. CIBSE Technical Symposium, Liverpool John Moores University, Liverpool, UK, 11-12 April 2013.
- VI. Laverge, J., Pattyn, X., Janssens, A. (2013). Performance assessment of residential mechanical exhaust ventilation systems dimensioned in accordance with Belgian, British, Dutch, French and ASHRAE standards. *Building and Environment*, 59, 177-186.
- VII. Laverge, J. (2013). Design strategies for residential ventilation systems. PhD, 241 p.
- VIII. UBAtc (2012). Goedkeuringsleidraad voor de energetische karakterisatie van vraaggestuurde residentiële ventilatiesystemen. 8 p.
- IX. CSTB (2009). Règles de calculs "Siren" pour l'instruction des avis techniques sur les systèmes de ventilation mécanique hygroréglable. 22 p.
- X. VLA-methodiek (2013). Gelijkwaardigheid voor energiebesparende ventilatieoplossingen in woningen. 57 p.
- XI. BS5250 - Code of Practice for condensation in buildings. (2002).
- XII. CEN/TR 14788. Ventilation for buildings – Design and dimensioning of residential ventilation systems.

- XIII. EN15251 (2007). Indoor environmental input parameters for design and assessment of energy performance of buildings addressing indoor air quality, thermal environment, lighting and acoustics.
- XIV. Liddament, M.W. (1996). A guide to energy efficient ventilation. AIVC, 254 p.
- XV. Law, S., Pane, G., Orme, M., Palmer, J. (2004). Cost effectiveness of mechanical ventilation. C1 71/6/9 BD 2422.
- XVI. Kurnitski, J., Seppänen, O. (2008). Trends and drivers in the Finnish ventilation and AC market. AIVC Ventilation Information Paper 20, 9 p.
- XVII. EN 15665 (2009), Ventilation for buildings. Determining performance criteria for residential ventilation systems
- XVIII. EN 13779 (2007), Ventilation for non-residential buildings. Performance requirements for ventilation and room-conditioning systems

# A novel algorithm for demand-control of a single-room ventilation unit with a rotary heat exchanger

Kevin Michael Smith<sup>\*1</sup>, Anders Lund Jansen<sup>2</sup>, and Svend Svendsen<sup>1</sup>

*1 Technical University of Denmark  
Department of Civil Engineering  
Building 118, Brovej  
2800 KongensLyngby, Denmark*

*2 SustainSolutions ApS  
Rønnegade 1  
2100 Copenhagen, Denmark*

\*Corresponding author: [keys@byg.dtu.dk](mailto:keys@byg.dtu.dk)

## ABSTRACT

Energy renovations seek to improve the airtightness of dwellings and thus require ventilation and heat recovery to maintain or improve energy-efficiency, indoor climate, and durability. These ventilation systems often control the indoor air of an apartment as a single climate zone, which neglects the different demands of individual rooms. Renovations result in greater retention of heat and air inside the building envelope, so rooms become especially sensitive to gains from solar radiation, occupancy, moisture loads and pollutants. Single-room ventilation units are able to provide balanced ventilation with heat recovery in individual rooms. This provides a unique opportunity to meet the demands of each room with an appropriate ventilation rate, supply temperature and drying capacity.

In prior publications, the authors described the development of a single-room ventilation unit with a rotary heat exchanger, which is commercially available in Denmark. The unit includes temperature sensors at the inlet and outlet of the supply and exhaust airflows. At the exhaust inlet, a relative humidity sensor is standard and a CO<sub>2</sub> sensor is optional. Together these sensors detect thermal comfort and air quality in the indoor environment. Based on these values, a demand-control algorithm varies fan speeds to change airflow rates and varies the rotational speed of the heat exchanger to modulate heat and moisture recovery. The algorithm varies airflow rates to provide free cooling and limit CO<sub>2</sub> concentrations and varies the coupled heat and moisture recovery to ensure the appropriate supply temperatures for heating or cooling and to modulate drying capacity. In the default setting, the algorithm is not aware of the heating set-point temperature in each room, so the algorithm decides when to bypass heat recovery without compromising efficiency. Moisture control takes higher precedence in the algorithm and overrides temperature and CO<sub>2</sub> controls. In previous publications, the authors demonstrated that modulating regenerative heat recovery could control relative humidities in 'dry rooms', so the algorithm first attempts to limit moisture recovery by varying the rotational speed and then safely unbalances airflows in a worst-case scenario. In the algorithm, frost protection and minimum supply temperature take the highest priority and override other controls. This paper documents the proposed demand control algorithm and analyses its impacts on compliance of building regulations in Denmark. The paper presents an algorithm that manufacturers can program into their controls. The commercially available single-room ventilation unit with a rotary heat exchanger uses this algorithm coded in the C language. Future work will document the effectiveness of the algorithm and how it behaves in a system.

## KEYWORDS

Demand-control, Single-room ventilation, Heat recovery, Rotary heat exchanger, Energy renovation

## 1 INTRODUCTION

Energy renovations seek to improve the airtightness of dwellings and thus require ventilation and heat recovery to maintain or improve energy-efficiency, indoor climate, and durability. These ventilation systems often control the indoor air of an apartment as a single climate zone, which neglects the different demands of individual rooms. Renovations retain heat and air, so rooms become especially sensitive to gains from solar radiation, occupancy, moisture loads and pollutants. Single-room ventilation units may provide balanced ventilation with heat recovery in individual rooms. This provides a unique opportunity to meet the

demands of each room with an appropriate ventilation rate, supply temperature and drying capacity.

A single-room ventilation unit may exploit the inherent benefits of decentralization. The cost of exploiting this opportunity decreases with the price of sensors, which has dropped for sensors that detect temperature, humidity and CO<sub>2</sub> concentration. Product developers can combine several of these sensors with a programmable controller to operate as a stand-alone demand-controlled unit with the sensors located at its inlets and outlets. The stand-alone aspect would save costs on electronics for communication but could negatively affect overall system performance. Additionally, the manufacturer could opt for further simplicity and lower costs by providing a very simple user-interface, such as a single button or dial to change the airflow setting. Manufacturers selected this design for the default option of a single-room ventilation unit. Smith and Svendsen (Smith, 2015) described the development of this unit, which is now commercially available in Denmark. The unit employs a rotary heat exchanger, filters, and forward-curved centrifugal fans to deliver balanced airflow and heat recovery greater than 80% at nominal flow. The unit includes temperature sensors at the inlet and outlet of the supply and exhaust airflows. At the exhaust inlet, a relative humidity sensor is standard and a CO<sub>2</sub> sensor is optional. Together these sensors detect thermal comfort and air quality in the indoor environment. Based on these values, a demand-control algorithm modulates airflow via the fan signals and modulates heat and moisture recovery via the rotational speed of the heat exchanger. The occupant selects an airflow from four options, but the demand-control algorithm varies that airflow to provide free cooling and limit CO<sub>2</sub> concentrations. The control algorithm modulates heat recovery to ensure the appropriate supply temperatures for heating or cooling. Since the unit does not include wireless communication by default, the manufacturers opted to develop a wireless hub as an optional add-on. Our investigation uses the default stand-alone product for reference. This paper describes the proposed demand-control algorithm and attempts to justify its architecture. With respect to the algorithm, the paper also comments on design requirements, strengths and weaknesses as well as regulatory compliance in Denmark.

## 2 ALGORITHM FOR A SINGLE-ROOM UNIT

This investigation focuses on apartments with newly replaced windows, which effectively seal building envelopes. These apartments have low infiltration heat losses and allow greater degrees of control over the ventilation airflows. Figure 1 shows a proposed demand-control strategy for these units. The diamonds represent conditions and the boxes represent processes. The controls should observe the impact of processes before checking subsequent conditions. This observation may include a built-in delay. The figure just provides an example, so implementations should tune these numbers according to context.  $T$  and  $RH$  represent temperature and relative humidity respectively, while the subscripts *indoor*, *outdoor* and *supply* describe the location of measurement by the sensors. Additionally, the descriptors  $dp_{min}$  and  $t-3h$  respectively represent dew-point, a prescribed minimum and the time three hours prior. The following sections describe these control modes in detail.

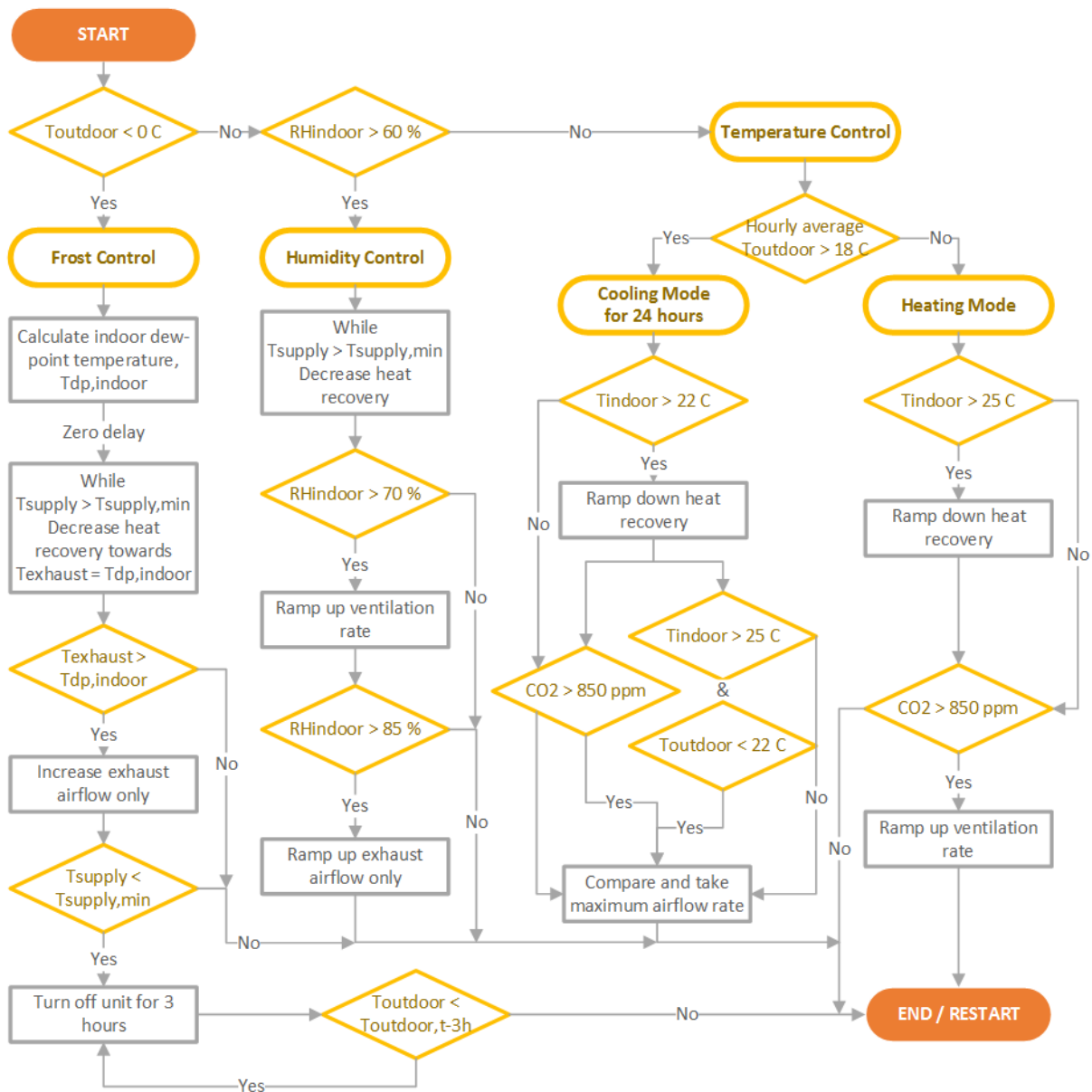


Figure 1. The proposed control algorithm for a single-room ventilation unit with a rotary heat exchanger. The diamonds represent conditions and the boxes represent processes. The controls should observe the impact of processes before checking subsequent conditions.

## 2.1 Main Temperature Control

During the majority of its operation, the demand-control algorithm for the single-room ventilation unit will use measurements of indoor temperatures and optionally indoor CO<sub>2</sub> concentration. This mode is the *Temperature Control* shown in Figure 1. Not included in the figure is the assumption that the occupant chooses a desired room temperature ( $T_{\text{thermostat}}$ ) via a thermostatic radiator valve. The radiator governs the room temperature in typical situations, but improving heat retention reduces the number of hours where heating is necessary. In these hours, the ventilation system will often determine the room temperature. The controls modulate heat recovery to control the room temperature and boost ventilation rates to provide free cooling and prevent over-heating. The occupant can choose to control the room temperature manually by opening and closing windows, but this lacks precision and opens the possibility for wasting heat from radiators. The occupant is less likely to open windows if indoor temperatures remain within their comfort bounds. Bergeet *al.* (Berge, 2016) surveyed

occupants in high performance residential housing, and the need for cooler air was the dominant reason for keeping the windows open.

In the default stand-alone setting, the ventilation control algorithm lacks knowledge of  $T_{\text{thermostat}}$  in each room, so the algorithm attempts to modulate heat recovery without compromising efficiency. The ventilation controls must provide full heat recovery up to an assumed set-point temperature ( $T_{\text{bypass}}$ ). If this temperature is too low, the control algorithm will stop using heat recovery and the thermostat will trigger excessive radiator use. The set value of  $T_{\text{bypass}}$  should be high enough to avoid this situation but not too high that it causes over-heating.

One method to deal with this issue is a conditional set point of  $T_{\text{bypass}}$ . If there is any risk of over-heating, the algorithm chooses a lower value of  $T_{\text{bypass}}$  to limit excessive heat recovery. This was the basis for creating a *Heating Mode* and *Cooling Mode*. The algorithm determines the mode based on recent outdoor temperatures. If the average hourly outdoor temperature rises above 18 °C, the algorithm enacts the cooling mode for the next 24 hours. According to data from the Danish design reference year by Wang *et al.* (Wang, 2012), the cooling mode would operate during approximately 30% of the year in Denmark, but the algorithm could be adjusted for location. In the example in Figure 1, the heating and cooling modes decrease heat recovery above a  $T_{\text{bypass}}$  of 25 °C and 22 °C, respectively. In the *Temperature Control* mode, the rest of the algorithm only adjusts ventilation rates.

The cooling mode raises ventilation rates for excessive indoor temperatures, but it first checks for cooling capacity by comparing the indoor and outdoor temperatures. The temperature difference must be greater than 3 °C to warrant boosting the ventilation. Both control modes also boost ventilation rates if an optional CO<sub>2</sub> sensor detects greater than 850 ppm in the indoor air. This value attempts to prevent CO<sub>2</sub> concentrations from rising above 900 ppm, which is the likely limit for category II air quality in the ISO Standard EN 15251 (European Committee for Standardization, 2007). This standard specifies category II as 500 ppm above ambient, which is approximately 400 ppm in much of Denmark. While the cooling control uses a proportional band of 2 °C to increase airflow, the CO<sub>2</sub> control instead attempts to track a reference value, which is 850 ppm in this case. In the cooling mode, the algorithm compares the resultant fan signals based on temperature and CO<sub>2</sub> measurements and delivers the maximum flow. In the heating mode, the CO<sub>2</sub> concentration solely determines the fan signals.

## 2.2 Moisture Control

Moisture control takes higher precedence in the algorithm and overrides temperature and CO<sub>2</sub> controls. Smith and Svendsen (Smith, 2016) demonstrated that the speed of a rotary heat exchanger could limit relative humidities in ‘dry rooms’ by limiting condensation on its heat transfer surface. As such, the algorithm first attempts to limit moisture recovery by decreasing rotational speeds between 60% and 70% indoor relative humidity while maintaining sufficient supply temperatures for comfort. The standard EN 15251 also prescribes performance categories to assess indoor relative humidity, and the upper limits in categories I and III are 50% and 70% respectively. As such, this interval could start as low as 50% to avoid proliferation of dust mites, but the choice is a balance of priorities. Above 70% relative humidity, the algorithm boosts the signal to both fans. A concern with this decision is the moisture content of indoor and outdoor air, where moisture content is the mass of water per mass of dry air. Denmark has a humid temperate climate, so outdoor moisture content could occasionally exceed indoor moisture content and unnecessarily boost fans. The choice to boost fan speeds between 70% and 85% indoor relative humidity attempts to avoid unnecessary fan power consumption when there is no potential for drying. If the indoor air is 22 °C and has a relative humidity of 70%, then its moisture content is approximately 11.54 g/kg. The outdoor moisture content only exceeds this value for 173 hours in the Danish design

reference year. This decreases to 85 hours, 20 hours and 0 hours for indoor relative humidities of 75%, 80%, and 85% respectively. In Denmark, one could regard these durations as acceptable, but one should be aware of this concern and adjust the limits according to climate zone. A more thorough approach would be the inclusion of another humidity sensor to directly compare indoor and outdoor moisture contents, but this presents an added cost. Above 85%, the algorithm safely unbalances airflows in a worst-case scenario. The unbalance of fan signals never exceeds 15% to avoid excessive under-pressure in the apartment. The unbalancing has a compound effect on drying capacity, since it increases both the exhaust airflow and the exhaust temperature (and thereby less condensation), which increases the drying capacity per volume of airflow.

### **2.3 Freezing Control**

In the control algorithm, frost protection and minimum supply temperature take the highest priority and override other controls. In recuperative heat exchangers, it is common to elevate exhaust temperatures above 0 °C in cold climates since condensation only occurs in the exhaust channels of the heat exchanger. This is not possible in a regenerator, such as an uncoated rotary heat exchanger, because condensation on the exhaust side rotates to the supply side, so it will always encounter outdoor temperatures. Therefore, the only method to deal with freezing is to limit condensation from occurring inside the heat exchanger. An algorithm can achieve this with two methods that use feedback control. The first uses a sensor at the exhaust outlet and tracks a relative humidity less than 100% to avoid condensation. Another method uses a temperature and humidity sensor at the point of extraction and calculates the dew-point temperature of the room air. The algorithm ensures that exhaust temperatures do not drop below this dew-point temperature to avoid condensation. The demand-control algorithm in Figure 1 uses the latter method. It was important to the manufacturers of the unit that supply temperatures never drop below a reference point to secure thermal comfort. Therefore, the algorithm restricted the reduction in heat recovery, which may not be sufficient to avoid condensation. Instead, the algorithm only further boosts exhaust airflow and runs unbalanced. As previously mentioned for the moisture control mode, this increases both the supply and exhaust temperatures. If the algorithm still cannot maintain sufficient supply temperatures, the unit shuts down for three hours. It then checks whether outdoor temperatures increased in this three-hour period before resuming operation.

### **2.4 Variable Heat and Moisture Recovery**

The described controls depend heavily on variable heat and moisture recovery to be effective. It may be uncommon to apply variable heat and moisture recovery in this manner, so it deserves further explanation.

The relationship between rotational speed and heat recovery is non-linear with rotary heat exchangers. Smith and Svendsen (Smith, 2015) plotted this relationship for the aforementioned ventilation unit, and Figure 2 shows new measurements with greater resolution. These new measurements used the same method as described by Smith and Svendsen but with a newer version of the unit. The plot only depicts measurements using 40% fan signals for supply and exhaust.

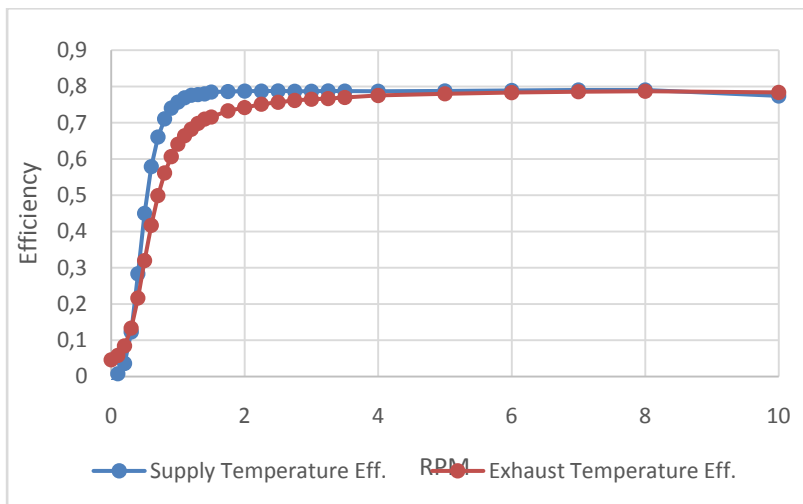


Figure 2. Temperature efficiencies of both the supply and exhaust airflows with various rotational speeds of the rotary heat exchanger in the single-room ventilation unit. The fan signal were 40% for both the supply and exhaust.

Since the relationship between the plotted values is non-linear, it is helpful to create a better gradient for the controls. As the algorithm uses plus-minus control, the impact of each increment or decrement to the rotational speed should be consistent, so the controls will be faster and more stable. The chosen rotational speeds in revolutions per minute for the plus-minus control were 0.0, 0.2, 0.3, 0.4, 0.5, 0.6, 0.7, 1.0, 1.5, 3.0, and 5.0. Figure 3 shows the supply and exhaust temperature efficiencies at these speeds, and it is clear that they have a more consistent increase across each set of adjacent data-points.

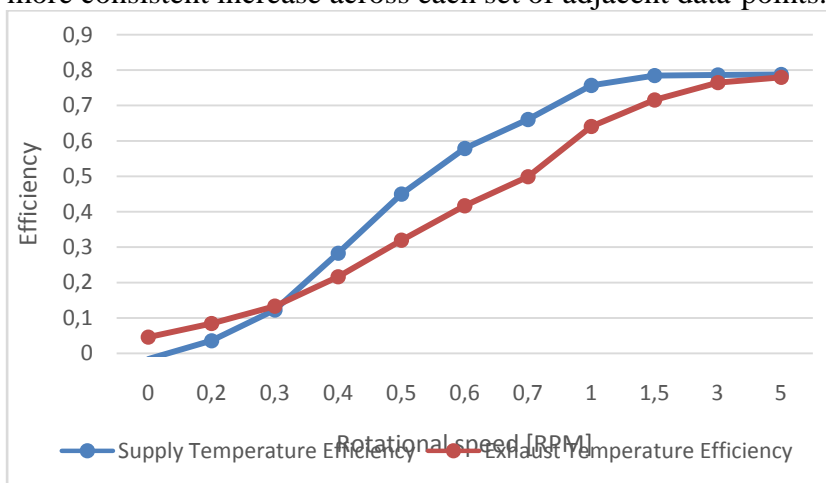


Figure 3. Temperature efficiencies of both the supply and exhaust airflows for various rotational speeds of the rotary heat exchanger. The rotational speeds do not increase linearly in the plot. These were manually selected to improve responsiveness of the controls.

Smith and Svendsen (Smith, 2016) described how an uncoated rotary heat exchanger recovers moisture if there is condensation on its heat transfer surface. That publication provided references and theory to support the claim, but it did not provide any experimental evidence. Table 1 lists the average measurement data for relative humidity, air temperature, dew-point temperature and the calculated moisture content at the inlets and outlets of the supply and exhaust airflows. The ventilation unit used fan signals of 35% and a rotational speed of 10 rpm. The authors described the formula for calculating moisture content based on the three measured quantities in a prior publication (Smith, 2016). Table 2 shows the calculated moisture ratios and temperature efficiencies for the supply and exhaust airflows with the single-room ventilation unit. The moisture ratios and temperature efficiencies are calculated as the respectively change in moisture or temperature as a percentage of the total

potential change during the recovery process. The calculated values include some pressure leakage, which one could also describe as re-circulated air. However, the temperature efficiencies were less than 5% at 0 rpm, as shown in Figure 2, which indicates that very little pressure leakage actually occurred. The authors (Smith, 2015) previously showed analytically that the mass flow ratio of pressure leakage to total leakage is equal to the temperature efficiency with a stationary rotor (i.e. 0 rpm). This indicates less than 5% pressure leakage during the measurements. Table 2 shows that the moisture recovery can be equal to or greater than the temperature efficiency at a high indoor temperature and relative humidity. This single measurement supports the assumption that rotary heat exchangers transfer condensation between airflows.

This assumption was also the basis for the controls and moisture balance equations described by Smith and Svendsen (Smith, 2016). The algorithm described in this paper extends that work into a more practical and explicitly defined algorithm.

Table 1. Measurement data for relative humidity (RH), air temperature (T), dew-point temperature (DP) and the calculated moisture content at the inlets (i.e. Indoor and Outdoor) and outlets (i.e. Supply and Exhaust) of the supply and exhaust airflows.

Air Location	RH [%]	T [°C]	DP [°C]	Moisture Content [g/kg]
Supply	78.2	25.6	21.5	0.157
Indoor	72.6	26.9	21.6	0.158
Exhaust	92.0	9.2	8.0	0.066
Outdoor	87.6	7.4	5.5	0.055

Table 2. Calculated moisture ratios and temperature efficiencies for the supply and exhaust airflows with the single-room ventilation unit. The fan signals were 35% and the heat exchanger rotated at 10 rpm.

Quantity	[%]
Supply Moisture Ratio	100
Exhaust Moisture Ratio	90
Supply Temperature Eff.	93
Exhaust Temperature Eff.	91

## 2.5 Regulatory Compliance

Building regulations commonly focus on centralised ventilation systems, which supply air to dry rooms (i.e. living rooms and bedrooms) and extract air from wet rooms (i.e. kitchens and bathrooms). Building regulations should explicitly include systems based on single-room ventilation units, but in many cases, the designer of these systems requires extra clarification from regulators. The Danish building regulations (Danish Energy Agency, 2015) state that all habitable rooms, as well as the dwelling as a whole, must have ventilation supply of at least 0.3 L/s/m<sup>2</sup> of heated floor area. This is straightforward for single-room ventilation units, which can be set to supply at least this amount based on the floor area of each room. Another provision states that this background airflow must include heat recovery, which single-room units can also satisfy.

The regulations regarding kitchens and bathrooms require more interpretation. A kitchen and bathroom require the capacity to exhaust up to 20 L/s and 15 L/s respectively. There are no regulations for supply, so there is nothing in the text of the building regulations to prevent solutions that use balanced ventilation in each room. One author of the Danish building regulations confirmed this interpretation and noted the restricted spread of moisture from contaminated rooms to other rooms. This is important since the described ventilation unit primarily serves dry rooms, so it should not draw air that is more humid from wet rooms. In the moisture control mode, the unit operates with unbalanced airflows for room relative humidities above 85 %, so it will create an under-pressure in the room that will potentially

draw air from other rooms. However, this unbalance is zero at 85 % and grows proportionally with higher relative humidities. This is in the range of maximum relative humidity, so one could assume that the air in other rooms does not carry significantly more moisture unless it also has a much higher temperature.

The frost control mode in the algorithm also uses unbalanced airflows, and the compliance of this decision is less clear. When outdoor temperatures drop below 0 °C, the controls could have three options to limit frost accumulation. The algorithm could decrease heat recovery to raise the exhaust temperatures above the dew-point temperature of the indoor air. This would avoid condensation and thus freezing in the heat exchanger. However, this could lower supply temperatures below the comfort threshold of the occupant. Another option would be to simultaneously decrease heat recovery and unbalance the ventilation airflows. By increasing the exhaust or decreasing the supply, the algorithm has greater capacity to maintain sufficiently high exhaust temperatures to avoid condensation while also meeting the comfort requirements of the occupant. This is the option applied in the proposed algorithm, but its use of unbalanced airflows may be an issue regarding compliance. The third option is to shut off the unit until temperatures rise above 0 °C, but this does not satisfy the minimum ventilation requirements. It is clear that none of the options is perfect for all situations.

Centralised ventilation systems solve this issue by including a heating coil before or after the heat exchanger on the supply side to satisfy comfort requirements when bypassing heat recovery to avoid freezing. Centralised heating allows the use of a less expensive heat source, such as district heating, but this is not feasible in single-room ventilation units. Electric resistance coils could be an alternative, but the cost of electricity is approximately 5.5 times that of district heating, which prohibits this option. Rather than heat the supply air, it may be possible to lower supply temperatures and still ensure reasonable levels of thermal comfort. Until recently, conventional ventilation systems extracted air from kitchens and bathrooms and supplied air through noise dampening inlets in the façade of dry rooms. Even in newer buildings with relatively airtight envelopes, discomfort due to cold draughts is rarely seen as a problem through these inlets. When it is a problem, the solution is to close the inlets and restrict the exhaust. The inlets do not employ fans, so air velocities are low, but there is no control over diffusion or mixing of airflows, which single-room units could apply. If a unit adequately diffuses ventilation airflow to lower velocities and enhances mixing with room air, there could be less concern of draught from cooler supply temperature. This would be the most compliant option. The necessary change to the algorithm in Figure 1 would be the removal of the statement “while  $T_{\text{supply}} > T_{\text{supply, min}}$ ” and removal of everything from “ $T_{\text{exhaust}} > T_{\text{dp, indoor}}$ ” onwards. An important consideration here is that lower heat recovery has the effect of increasing drying capacity with rotary heat exchangers. As drying capacity increases, the indoor dew-point temperature likely decreases, which increases the allowable heat recovery to avoid condensation. Therefore, the algorithm will likely find an equilibrium at lower indoor relative humidities and thus lower dew-point temperatures.

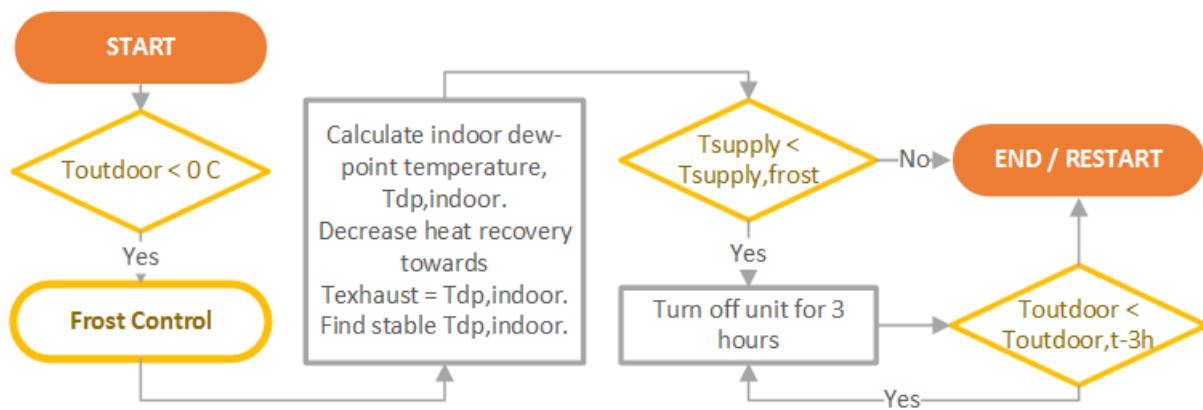


Figure 4. Alternate frost control mode that complies with building regulations but risks causing cool draughts for the occupant. The algorithm introduces a new parameter,  $T_{\text{supply,frost}}$ , which is a lower limit on the minimum supply temperature only in the frost control mode.

### 3 DISCUSSION

This paper demonstrates that it is possible to construct an algorithm for stand-alone operation of a single-room ventilation unit with a rotary heat exchanger. The algorithm targets a range of thermal comfort without compromising heat recovery. The algorithm also targets a range of indoor relative humidities to prevent mould growth. Despite the inherent coupling of heat and moisture recovery in highly effective uncoated rotary heat exchangers, the algorithm attempts to find a balance that satisfies multiple demands (i.e. energy-efficiency and moisture limits). The algorithm also attempts to avoid frost accumulation in the heat exchanger while satisfying a requirement for minimum supply temperatures imposed by the manufacturer of the unit. This paper acknowledges the consequences of this decision with respect to regulatory compliance and proposes an alternative that would improve compliance. This alternative relaxes the constraints on supply temperatures, but this may not be an issue for appropriate designs of the ventilation diffuser. This decision could follow experimental testing, which would produce a different result with every single-room ventilation unit. This paper therefore covers the breadth of issues facing autonomous control of these units and leaves open questions for individual product developers.

Implementation of the proposed algorithm would be different for all developers of single-room ventilation units with rotary heat exchangers. Much of the text refers to set-point temperatures and relative humidities that depend on the local climate to be effective. These may require tuning. Simulations may assist in finding optimal values, but it is likely that some decisions would require experimental testing. For instance, the decision to restrict minimum supply temperatures could impact regulatory compliance, but this decision is unique for each unit based on the inlet airflow. Regardless, documentation of a full case study would provide useful information, and the authors plan to test the algorithm in full-scale experiments. The authors wrote the algorithm shown in Figure 1 in pseudo-code, and control engineers subsequently translated it into C code for implementation in the commercially available unit. Simulations will accompany these tests and may influence the refinement of set points. This work is all very necessary since there is no evidence yet that the proposed algorithm is actually effective. User behaviour is difficult to predict and may have unforeseen consequences. Furthermore, the planned full-scale experiments will include different forms of kitchen exhaust (i.e. balanced or unbalanced, with or without heat recovery) to assess the impact on heat recovery and supply temperatures in each of the single-room units. No ventilation unit operates in isolation from other pressures, so it is very necessary to study the decentralised unit as part of a system. This future work will target successful ventilation systems that include single-room units.

## 4 CONCLUSIONS

This paper documents a proposed demand-control algorithm for a single-room ventilation unit with a rotary heat exchanger. The algorithm uses sensors inside the unit to control air quality and thermal comfort according to the demands of each room. It aims to achieve this by modulating the supply and exhaust airflows and the rotational speed of the rotary heat exchanger. The algorithm protects against frost accumulation and seeks to modulate coupled heat and moisture recovery to achieve a balance between energy efficiency and avoidance of mould risk. The paper discusses its compliance with building regulations in Denmark. Future work will document the effectiveness of the algorithm and how it will behave in a system.

## 5 ACKNOWLEDGEMENTS

This research was funded by The Market Development Fund (Markedsmodningsfonden) and the Technical University of Denmark to research decentralized ventilation for use in renovations of existing residential apartments. Special thanks to LS Control A/S for their contributions.

## 6 REFERENCES

Berge, M., & Mathisen, H. M. (2016). Perceived and measured indoor climate conditions in high-performance residential buildings. *Energy and Buildings*, 127, 1057–1073. <http://doi.org/10.1016/j.enbuild.2016.06.061>

European Committee for Standardization (2007). *EN 15251: Criteria for indoor environment including thermal, indoor air quality, light and noise*. Brussels: European Committee for Standardization

Danish Energy Agency (2015). *Danish Building Regulations 2015*. Danish Transport and Construction Agency. [http://byggningsreglementet.dk/file/591081/br15\\_english.pdf](http://byggningsreglementet.dk/file/591081/br15_english.pdf)

Smith, K. M., & Svendsen, S. (2016). The effect of a rotary heat exchanger in room-based ventilation on indoor humidity in existing apartments in temperate climates. *Energy and Buildings*, 116, 349–361. <http://doi.org/10.1016/j.enbuild.2015.12.025>

Smith, K. M., & Svendsen, S. (2015). Development of a plastic rotary heat exchanger for room-based ventilation in existing apartments. *Energy and Buildings*, 107, 1–10. <http://doi.org/10.1016/j.enbuild.2015.07.061>

Smith, K. M., & Svendsen, S. (2016). Control of Single-room Ventilation with Regenerative Heat Recovery for Indoor Climate and Energy Performance. *Clima 2016 - Proceedings of the 12th Rehva World Congress*.

Wang, P.G., & Scharling, M., Nielsen, K.P. (2012). 2001 – 2010 Design Reference Year for Denmark. *Teknisk Rapport 12-17*. Copenhagen: Danish Meteorological Institute.

# Evaluating the Performance of Island Kitchen Range Hoods

Iain Walker<sup>\*1</sup>, Gabriel Rohas<sup>1</sup>, Jordan Clark<sup>1</sup>, and Max Sherman<sup>1</sup>

*1 Lawrence Berkeley National Laboratory  
MS 90-3074, 1 Cyclotron Road  
Berkeley, CA, USA  
Presenting author: Iain Walker  
\*Corresponding author: iswalker@lbl.gov*

## ABSTRACT

A key aspect of achieving acceptable indoor air quality is source control. Cooking has been recognized as a significant source of pollutants for health impacts (e.g., PM<sub>2.5</sub> and NO<sub>2</sub>) as well as moisture and odour. A common method of controlling this pollutant source is by using a range (or cooker) hood that vents to outside. However, field and laboratory experiments have shown highly variable performance for these devices. We use the capture efficiency metric (the fraction of the pollutants that are exhausted to outside at steady state) to characterize the range hood performance. To address this issue and provide useful information for builders, contractors, designers and home occupants, a laboratory rating method for range hood capture efficiency has recently been developed by LBNL and ASTM. The test method uses standardized emitters to create a heated plume and seed it with tracer gas. The tracer gas measurements in the room, the range hood exhaust and in the ambient air are used to estimate capture efficiency. However, this test method only applies to wall-mounted range hoods. Some range hoods are not wall-mounted: island range hoods are designed to operate over a cooktop in the middle of a room rather than against a wall and downdraft hoods draw air from near the cooktop rather than overhead. This paper discusses the development of a new test apparatus for island and downdraft hoods and presents measured capture efficiency data from example hoods. The results of this work will be used in future revisions to the ASTM standard.

## KEYWORDS

Indoor Air Quality, Kitchen Ventilation, Cooking, Range Hood, Performance Standard

## 1 INTRODUCTION

This work builds on previous studies that developed a test method for capture efficiency of kitchen range hoods that are mounted to a wall above a cooktop. The test method has been published (or shortly will be) as an ASTM Standard (ASTM (2017)) and is likely to be adopted by reference in the near future by building codes and standards. Not all range hoods are wall mounted. Some kitchens have the cooktop in an island, rather than abutting a wall, and the range hood is mounted from the ceiling above the island. There are also downdraft devices that are mounted at the edge of the cooktop rather than above it. These island and downdraft hoods require a different experimental apparatus and testing approach due to the changes in geometry compared to the wall-mount hoods. This study investigates the development of a testing approach suitable for these hoods. So far we only have results for island applications, but the same basic apparatus and procedure will be used in future testing of downdraft hoods.

## 2 OUTLINE OF TEST METHOD

The test method uses the same premise as for the wall-mounted range hoods. The performance of the hood is represented by the capture efficiency (CE) that is the fraction of the plume from the cooking event that is captured by the range hood and exhausted to outside. Burners are operated on the cooktop and the thermal plume above them is tagged with a tracer

gas (in our case CO<sub>2</sub>). The steady-state concentration of tracer gas is measured in air entering the test chamber ( $C_i$ ), in the test chamber ( $C_c$ ) and in the exhaust air stream from the range hood blower ( $C_e$ ). CE is given by:

$$CE = \frac{C_e - C_c}{C_e - C_i} \quad (1)$$

## 2.1 Test Apparatus

The tests are performed in a sealed test chamber (see Figure 1). The dimensions of the test chamber need to be representative of a kitchen with an island cooktop: 4.5 m by 4.6 m (with a ceiling height of 2.4 m). This is larger than the 2.3 m by 4.6 m test chamber used in previous LBNL studies developing the wall-mount hood test procedure (Kim et al (2017), Walker et al (2016), and Simone et al. (2015)). Air enters the test chamber through four 55 cm square air inlets in the corners of the ceiling. The inlets have diffuser plates and are designed to minimize the air velocities entering the test chamber because previous testing for wall-mount hoods found that this was an important factor in testing consistency (Kim et al. (2017) and Walker et al. (2016a and 2016b)). The air inlet velocities are about 0.07 m/s at 100 L/s of exhaust air flow. We expect to have a maximum exhaust air flow of about 300 L/s corresponding to an incoming air velocity of about 0.2 m/s that is substantially below the 0.5 m/s established as a minimum for the previous wall-mount experiments and stated in the ASTM standard. With these air inlets sealed, the air leakage of the test chamber was measured to be 2.5 ACH at 50 Pa. At typical operating air flows and pressures this means that less than 5% of the air entering the chamber does not come through the four inlets. All four inlets are sampled through equal length tubing and brought together in a manifold to measure  $C_i$ .

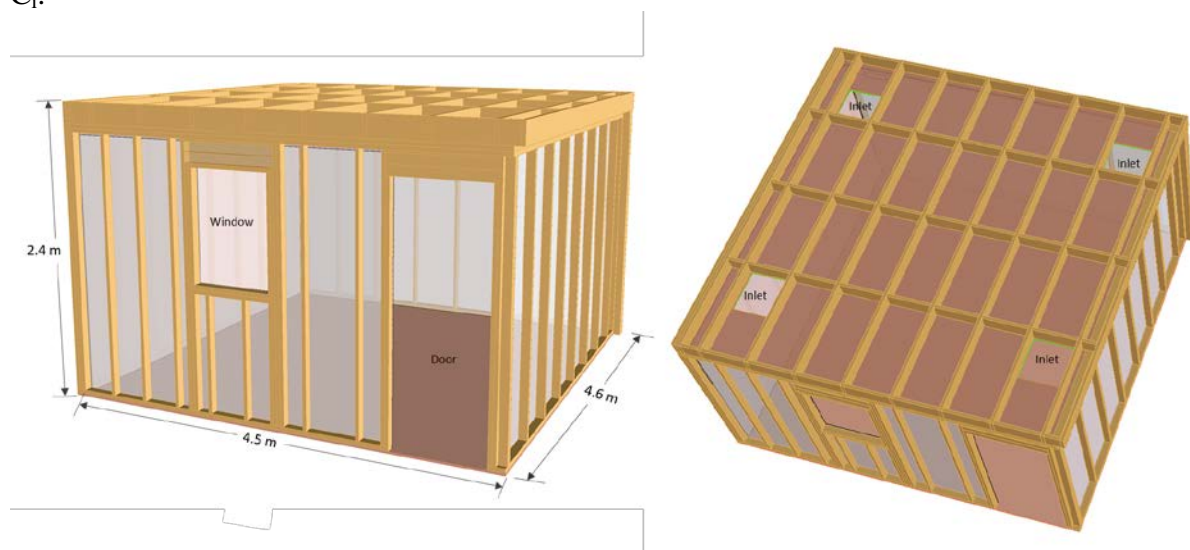


Figure 1a: Test Chamber for Island Hood Testing (Left Image: Front; Right Image: Ceiling)



Figure 1b: Island in test chamber showing cabinets, cooktops and overhead range hood

An island was built in the centre of the test chamber that has a central section containing the cooktop and sections to each side of the cooktop representing typical kitchen work surfaces. The heat sources for the plume are electric resistance cooking elements that are mounted in a custom metal enclosure. This enclosure allows us to precisely place and move the electric resistance elements in the cooktop. The power consumption of the electric elements is monitored using a Continental Control Systems WattNode WNB 3Y-208P. We attempted to meet the same power and temperature specifications as for the wall-mount testing: 1000 W and an upper plate temperature of 200°C. However, the changed air flow geometry of the island configuration meant that we could not simultaneously meet these requirements for all range hood flows. One particular problem was found for higher air flows where more than 1000 W was needed to maintain an upper plate temperature of 200°C, which resulted in unacceptably high emitter plate temperatures.

For this experiment, we investigated using lower plate temperatures and pots with boiling water (that have been used in other cooking experiments (e.g., Singer et al. (2012) and Rim et al. (2012))). These temperatures, however, are lower than cooking events that produce significant cooking contaminants and so may be too low. The following is a list of other relevant temperatures for making such a determination:

300°C	Boiling Temperature of high temperature cooking oils
230°C	Smoking temperature of high temperature cooking oils
200°C	Temperature for frying meat or dry frying
175°C	Smoking temperature of butter and low temperature oils
160°C	Temperature used for frying chicken and vegetables.
100°C	Boiling water

Another problem with using boiling water is that it injects a significant amount of mass into the plume. This mass injection changes the plume dynamics and would need to be carefully controlled/specified for consistent testing. Other types of cooking events (e.g. frying eggs) inject very little mass into the plume, but produce more contaminants (other than water). So boiling water is not representative of the cooking events of interest. It may be appropriate to simulate a typical cooking event by injecting mass into the plume.

The hood to be tested was mounted on the ceiling using an adapter housing that allows the hood to be mounted at different heights above the cooktop. An inline fan and damper are mounted in the exhaust ducting from the range hood outside the test chamber. This allows us to precisely measure and control the range hood exhaust flow.  $C_e$  is measured in the exhaust ducting from the range hood outside the test chamber.  $C_c$  is measured 0.5m horizontally from the centre of the front of the range hood in the test chamber at a height mid-way between the cooktop and the bottom of the range hood being tested (the same as for the wall-mount test method).

## 2.2 Test Procedure

The test procedure is very similar to that for wall-mount hoods. The range hood is turned on and its airflow adjusted to the appropriate level. The electric heating element is turned on and adjusted to achieve either the target power input or emitter plate surface temperature. The tracer gas injection is turned on. The heating element power input, emitter plate temperatures and the tracer gas concentrations are continuously monitored until steady-state conditions are obtained (typically after about 4 chamber air changes). During this development phase we also performed additional measurements that will not be part of a standardized test method, but are useful for troubleshooting the test approach: velocity traverses of the plume, surface temperatures of the cooktop and lower plate.

## 3 RESULTS

### 3.1 Emitter Issues

The standard emitter consists of two plates. A solid metal lower plate in contact with the heating element and an upper plate that is hollow and has many small holes for emitting tracer gas to seed the plume. The two plates are separated by three metal or ceramic standoffs allowing air to flow between the two plates. Preliminary tests in the new test chamber indicated that at 1000 W input to the heating element we could not achieve 200°C upper emitter plate temperatures that is the target in the ASTM standard for wall-mounted hood tests. We experimented with higher power input to maintain the 200°C upper emitter plate temperatures that led to over-heating of one of the emitter plates. To investigate this further we performed some experiments where we measured the temperature of the lower plate and the top surface of the cooktop and performed air velocity traverses of the plume. These tests were carried out in the wall-mount test apparatus as well as the island apparatus to see if we need to re-evaluate the existing test procedure. As well as the standard emitter we used a shallow pan (5 cm high and 22 cm diameter) and a tall pot (23 cm high and 15 cm diameter) both containing water. CO<sub>2</sub> was injected into the water in the pans using a spiral of perforated

copper tube. Figure 2 shows the hot wire anemometer and locations of velocity and temperature measurements.

Figure 3 shows infra-red camera images with superimposed surface temperature measurements (from surface mount thermocouples and thermistors) for a shallow pan containing boiling water and for a standard emitter plate. This illustrates that the emitter plate not only gets much hotter on its lower surfaces but also makes the whole cooktop hotter in a way that could change the air flow and plume dynamics. Figure 4 shows the vertical component of velocity profiles measured above the cooktop with three different hood air flows: off, 76 L/s and 127 L/s for the standard emitter plates, a shallow pan of water and a tall pot of water. The hood used for these tests was a microwave range hood mounted 50 cm above the cooktop. The error bars in the figures indicate the maximum and minimum of 30 measured values over a 30 second averaging time, with the mean of the measurements given by the symbol. The velocities were measured using a thermal anemometer (TA5, Airflow, UK). The velocity profiles show that the emitter plates have the plume shifted away from the centre of the emitter, towards the back of the cooktop compared to the pan of boiling water. As the hood flow increases the plume become more spread out.



Figure 2: Illustration of velocity profile and temperature measurements

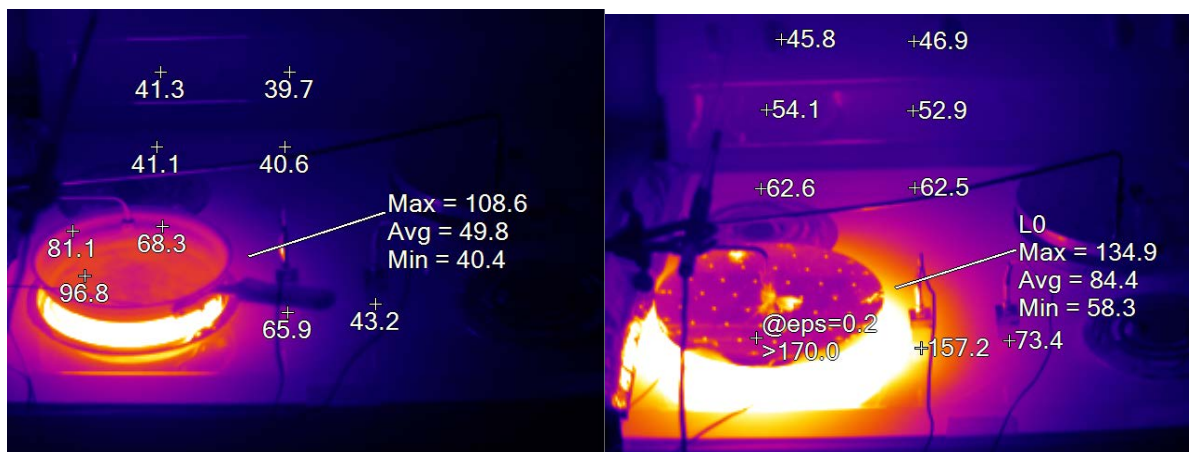


Figure 3: Pan with boiling water (left) and standard Emitter Plate (right) surface temperatures

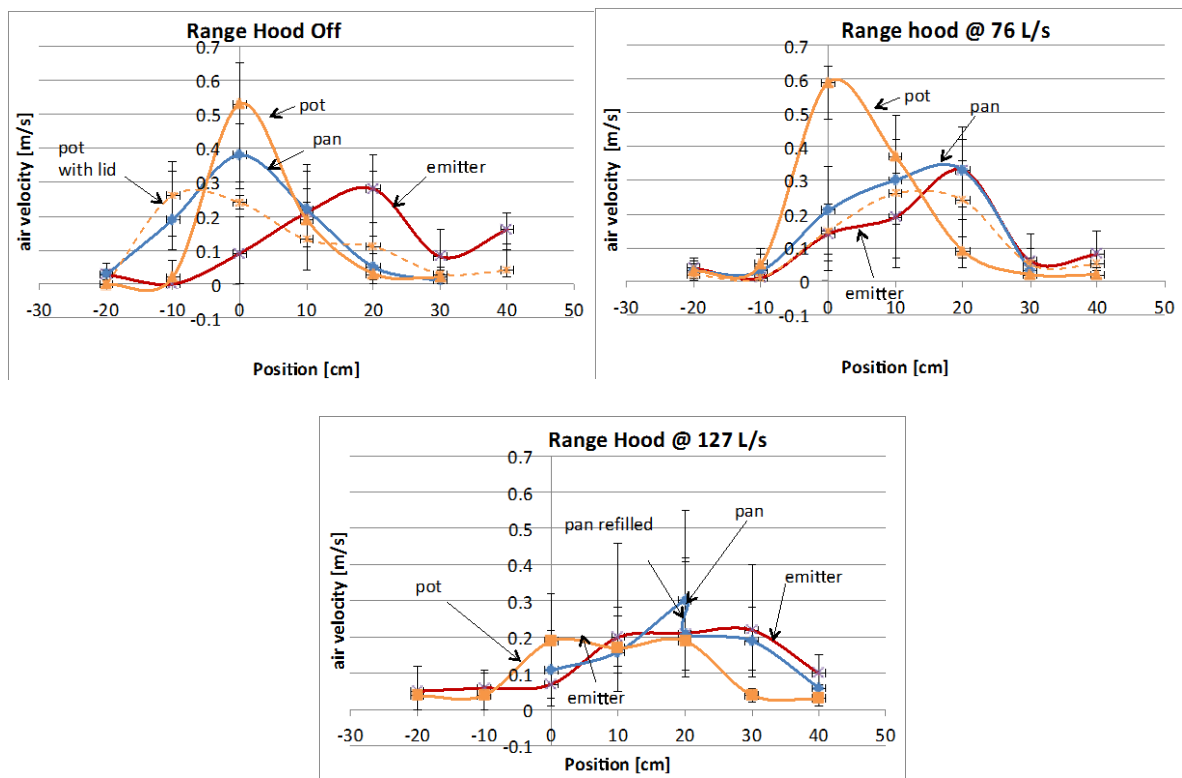


Figure 4: Plume velocity profiles for wall-mount hood – position relative to centre of heating element

For the new test chamber the velocity profiles were measured for the standard emitter plate at three different traverse heights (10, 20 and 30 cm) and the tall pot of boiling water, as shown in Figure 5. The island range hood was mounted 90 cm above the cooktop. These results reveal a complex flow pattern for the emitters. At the low traverse height we see little plume directly above the hot plate with higher velocities towards the middle of the cooktop. The plume gets closer to one from the pot at higher traverse levels as the plume develops. We also released smoke as a visual aid to get a qualitative view of the plume. This confirmed the flow patterns implied by these velocity measurements. There is clearly a flow pattern for the emitters that occurs because of the very high bottom plate temperatures and the air flow between the emitter plates. This air flow tends to be a horizontal flow from the outer edge of the cooktop towards and over the plate and as observed for both the wall-mount and island tests. The large pot filled with water did not exhibit this flow pattern.

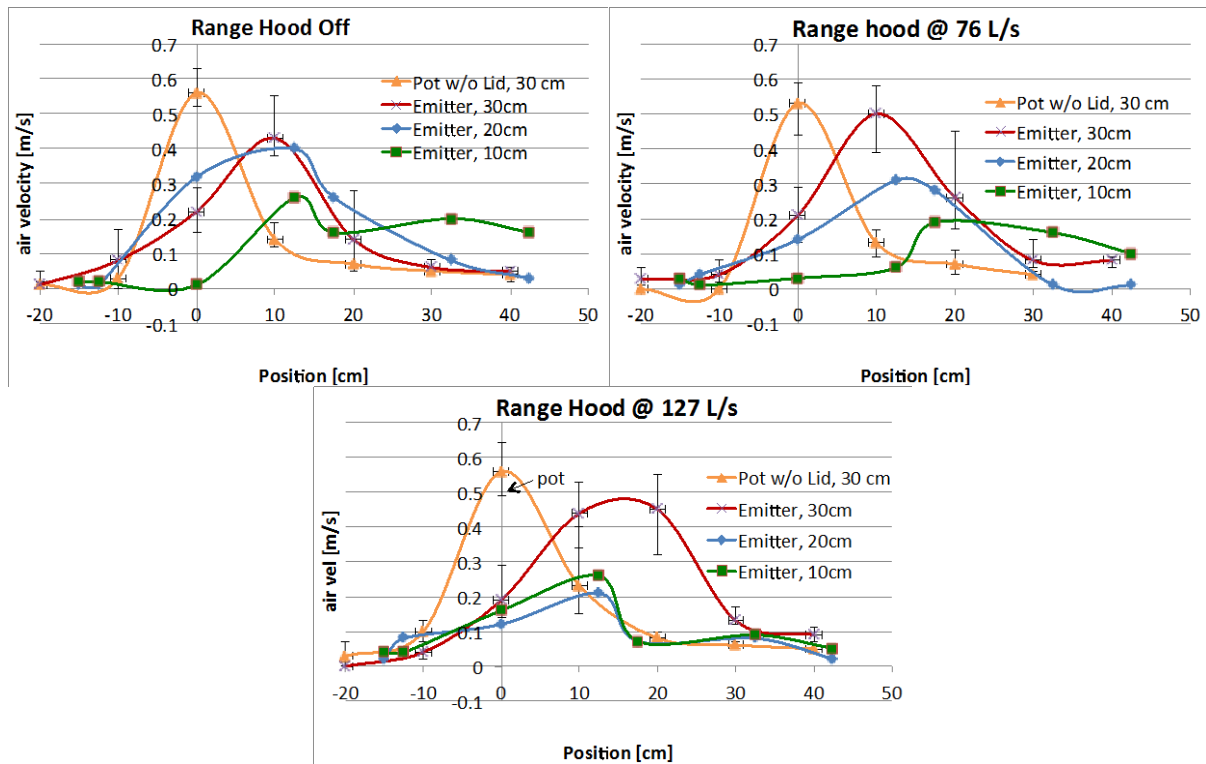


Figure 5: Plume velocity profiles for island hood at three different traverse heights– position relative to centre of heating element

### 3.2 Capture Efficiency for different Emitters in Wall-Mount Configuration

CE was measured in the wall-mounted configuration with a microwave range hood for the different emitters at a single hood exhaust flow of 58 L/s for a range of power inputs. We also included a couple of extra emitter types: the shallow pan dry (without water) and a shallow cast iron skillet. Table 1 summarizes measured capture efficiencies corresponding to the measured profiles in Figure 5.

Table 1: Capture Efficiency (CE) for the Wall-Mount Hood at 58 L/s

Emitter Configuration	Power Input (W)	Emitter Surface or Water Temperature (°C)	CE (%)
Pot with water	170	71	98
Pot with water	590	80	77
Pot with water	930	Data missing	68
Pan with water	170	61	95
Pan with water	640	80	75
Pan with water	940	83	65
Dry Pan, no water	920	>350	73
Skillet	940	343	82
Standard Emitter	220	87	82
Standard Emitter	650	164	79
Standard Emitter	950	199	74

Table 1 shows that the capture efficiencies decline as the power input and surface temperatures increase. The reduced energy plume is easier to capture. This trend is stronger for the water filled pot and pan than for the dry emitters, indicating that water filled emitters are more sensitive to power input. Other observations are that the boiling water containers do not necessarily have water that is uniformly at 100°C. There is also a cooling effect due to the injection of CO<sub>2</sub> into the water. The CO<sub>2</sub> is injected at low temperature due to the CO<sub>2</sub>

cooling upon expansion from the storage cylinder to the room pressure. The single dry plate emitters (the dry pan with no water and the skillet) both have upper surface temperatures much higher than the standard emitter with its dual-plate configuration. These higher temperatures did not lead to significantly reduced CE compared to the standard emitter. This is likely because the lower plate of the standard emitter is also at high temperature and is contributing to the plume due to flow between the two emitter plates. These results indicate that a simplified single plate emitter resembling the dry pan with no water may give similar results to the standard emitter.

### 3.3 Capture Efficiency for different Emitters in Island Configuration

Capture efficiency was also measured for an island range hood at several flow rates with the three emitter types: dry engineered emitter, tall pot with water and shallow pan with water. Tracer gas was bubbled into the water for the pot and pan tests. All tests were conducted at approximately 1000 W. Results are shown below in Figure 6 as a function of range hood flow rate.

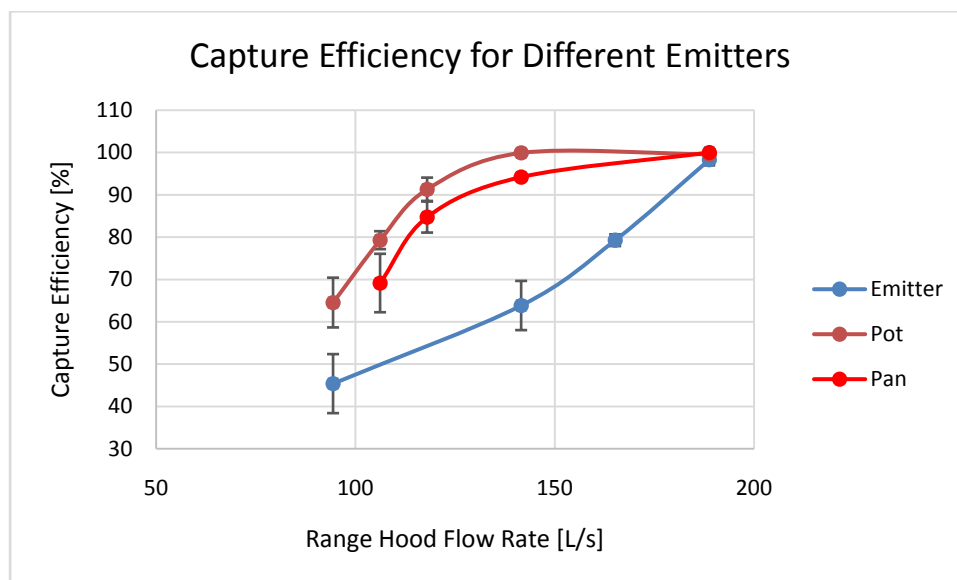


Figure 6: Capture Efficiency as a function of flow rate for different emitter types with an island range hood.

Figure 6 shows that the choice of emitter significantly affects capture efficiency. This is likely due to three differences. First, when water is included, the phase change absorbs a large amount of the energy provided by the burner, causing the air near the heating coil to be much cooler in the wet emitter cases (around 200°C) than in the dry emitter cases (around 500°C), and the surface temperature of the range to be cooler as well (50°C-100°C with water, 100°C-150°C without water). Second the upward injection of mass into the plume by the boiling water creates a plume with a stronger upward momentum in the with-water cases than in the relatively diffuse plume of the dry case. Lastly, the tracer gas is relatively confined when injecting into the water in the pot or pan and all gas leaves the emitter in the portion of the plume with the greatest upward velocity. With the dry engineered emitter, a portion of the gas leaves the emitter with a horizontal velocity, thus spreading out and becoming more difficult for the hood to capture. It is not yet clear which of these cases more closely approximates the emission of combustion products from gas cooking events or ultrafine particles from hot pan or wok surfaces.

## 4 CONCLUSIONS

The experimental results indicate that additional work is needed in the development of a standardized test method. First, we need to determine the plume source/emitter configuration: should we be using machined emitter plates that ensure consistency but may have issues with developing plume dynamics and thermal safety, or using pots of water that might be more difficult to reproduce consistently and may result in a cooler plume that is not representative of other cooking processes. Secondly we need to determine what is a suitable operating condition for the heat source: should it be a fixed temperature plate or a fixed power input pot. Finally we will be investigating appropriate amount of mass injection into the plume.

## 5 ACKNOWLEDGEMENTS

The authors would like to acknowledge the contributions of Woody Delp and Brett Singer of LBNL and the generous donation of range hoods for testing by Mike Moore (Broan). This work was funded by the US Department of Energy Building America Program and the Max Kade Foundation.

## 6 REFERENCES

- ASTM. (2017). Standard Test Method for Capture Efficiency of Domestic Range Hoods (Draft). American Society of Testing and Materials.
- Kim, Y-S, Walker, I.S. and Delp, W.W. (2017). Development of a Standard Capture Efficiency Test Method for Residential Kitchen Ventilation. Submitted to ASHRAE Science and Technology for the Built Environment.
- Rim, D., L. Wallace, S. Nabinger, and A. Persily. 2012. Reduction of Exposure to Ultrafine Particles by Kitchen Exhaust Hoods: The Effects of Exhaust Flow Rates, Particle Size, and Burner Position. *Sci. Total Environ.* 432:350–356
- Simone, A., Sherman, M.H., Walker, I.S., Singer, B.C., Delp, W.W. and Stratton, J.C. (2015). Measurements of Capture Efficiency of Range Hoods in Homes. Proc. Healthy Buildings 2015.
- Singer, B. C., W. W. Delp, P. N. Price, and M.G. Apte. 2012. Performance of Installed Cooking Exhaust Devices. *Indoor Air.* 22(3):223-234
- Walker, I.S., Sherman, M.H, Singer, B.C. and Delp, W.W., (2016a) Development of a Tracer Gas Capture Efficiency Test Method for Residential Kitchen Ventilation. Proc. IAQ 2016.
- Walker, I.S., Stratton, J.C., Delp, W.W. and Sherman, M.H. (2016b). Development of a Tracer Gas Capture Efficiency Test Method for Residential Kitchen Ventilation. LBNL-1004365.

# Efficiency of recirculation hoods

Piet Jacobs<sup>1</sup>, Wouter Borsboom<sup>1</sup>

*1 TNO  
Leeghwaterstraat 44  
Delft, the Netherlands*

## ABSTRACT

Recirculation hoods equipped with carbon and plasma filters are becoming more and more popular. The aim of this study is to determine the effectiveness of recirculation hoods with regard to PM<sub>2.5</sub> and NO<sub>x</sub> removal in a 26 m<sup>3</sup> lab kitchen with a gas furnace. With the carbon filter PM<sub>2.5</sub> is reduced for about 30%. A fresh carbon filter removed about 60% of the NO<sub>2</sub>, dropping within a few weeks of cooking to 20%. With the plasma hood NO<sub>2</sub> concentrations were above the WHO 1-hour limit and the Dutch health council 15 minutes limit. For plasma hoods it is recommended to optimize odor and particulate matter reduction while minimizing the ozone production. As recirculation hoods have favorable properties in terms of applicability and energy conservation it is recommended to add a particulate filter to recirculation hoods and to apply them preferably in combination with electrical cooking.

## KEYWORDS

Cooking emissions, Particulate Matter, activated carbon, plasma filters

## 1 INTRODUCTION

Cooking emissions have long been seen as an odour problem. However recent field studies showed that Particulate Matter (PM) is the main health risk of indoor air (Logue, 2013) and cooking can be a major source of PM<sub>2.5</sub>. In case of cooking on gas aside PM also nitrogen dioxide (NO<sub>2</sub>) is being generated. Dennekamp (Dennekamp, et al., 2001) reported substantial concentrations of NO<sub>x</sub> due to cooking on gas with no extraction and poor ventilation. Using four rings for 15 minutes produced peak concentrations of 1000 ppb NO<sub>2</sub> and 2000 ppb nitric oxide (NO). Expressed in mass this amounts to 2000 µg/m<sup>3</sup> NO<sub>2</sub>. Logue (Logue, 2014) simulated assuming no use of hoods, that in 55 – 70% of the Californian dwellings the NAAQS 1-hour acute standard is exceeded during a typical week in winter. By assuming hoods with an effectiveness of capturing 55% of the emissions, the exceedance percentage is reduced to 18 – 30% of the dwellings. The lower percentage correspond to a deposition rate of 0.5 h<sup>-1</sup> and the higher to a deposition rate of 1,05 h<sup>-1</sup>.

Recirculation hoods equipped with activated carbon and plasma filters are becoming more and more popular. The aim of this study is to study the effectiveness of recirculation hoods with regard to PM<sub>2.5</sub> and NO<sub>2</sub> and to compare the resulting concentrations with existing legal limits and occupational guidelines.

### 1.1 Legal limits and occupational guidelines for PM<sub>2.5</sub>

At the moment there are only guidelines for PM<sub>2.5</sub> outdoor. However, the steering group assisting WHO in designing the indoor air quality guidelines concluded (WHO, WHO guidelines for indoor air quality - selected pollutants, 2010) that there is no convincing evidence of a difference in the hazardous nature of particulate matter from indoor sources as

compared with those from outdoors and that the indoor levels of PM<sub>10</sub> and PM<sub>2.5</sub>, in the presence of indoor sources of PM, are usually higher than the outdoor PM levels. Therefore, the air quality guidelines for particulate matter recommended by the 2005 global update are also applicable to indoor spaces. Other legal limits are listed in Table 1.

Table 1: overview of legal limits and guidelines for Particulate Matter (PM).

	period	PM <sub>10</sub> [µg/m <sup>3</sup> ]	PM <sub>2.5</sub> [µg/m <sup>3</sup> ]
WHO	yearly	20	10
EU	yearly	40	25
	daily	50*	-
US	yearly	50	15**
	daily	150	35

\*Max 35 days higher than 50 µg/m<sup>3</sup>

\*\*3 years average

## 1.2 Legal limits and occupational guidelines NO<sub>2</sub>

WHO (WHO, WHO guidelines for indoor air quality - selected pollutants, 2010) recommends an 1-hour indoor nitrogen dioxide guideline of 200 µg/m<sup>3</sup>, see Table 2. At about twice this level, asthmatics exhibit small pulmonary function decrements. Those who are sensitized may have small changes in airway responsiveness to a variety of stimuli already at this level. An annual average indoor nitrogen dioxide guideline of 40 µg/m<sup>3</sup> is recommended by WHO. WHO states that having a gas stove is equivalent to an increased average indoor level of 28 µg/m<sup>3</sup> compared to homes with electric stoves, and meta-analysis showed that an increase in indoor nitrogen dioxide of 28 µg/m<sup>3</sup> is associated with a 20% increased risk of lower respiratory illness in children. Homes with no indoor sources were estimated to have an average level of 15 µg/m<sup>3</sup>. WHO (WHO, Air Quality Guidelines - Global update 2005, 2005) states that these results support a lowering of the annual nitrogen dioxide guideline value. However, since nitrogen dioxide is an important constituent of combustion-generated air pollution and is highly correlated with other primary and secondary combustion products, it is unclear to what extent the health effects observed in epidemiological studies are attributable to nitrogen dioxide itself or to other correlated pollutants. The current scientific literature, therefore, has not accumulated sufficient evidence to change WHO's 2000 guideline value of 40 µg/m<sup>3</sup> for annual nitrogen dioxide concentration. The Dutch Social and Economic Council (SER, 2007) advises a 15 minutes maximum value of 1000 µg/m<sup>3</sup>.

Table 2: overview of legal limits and occupational guidelines for nitrogen dioxide (NO<sub>2</sub>)

	NO <sub>2</sub> [µg/m <sup>3</sup> ], exposure period			Standard (reference)
	Yearly	8 hourly	hourly	
WHO indoor	40	-	200	WHO (WHO, 2010)
Dutch health council	-	400	1000 (15 min)	SER (2007)
EU ambient	40	200*	-	2008/50/EG (EU, 2008)
US ambient	57	-	339	CAAQS (CAAQS, 2010)
	100	-	188	NAAQS (EPA, 2012)

\*Max 18 hours per year exceedance.

## 2 MATERIALS/METHODS

In the TNO lab a kitchen has been set up with dimensions of 3.65 x 2.66 x 2.68 m. The kitchen setup is according to NEN-EN-IEC 61591 In all experiments room ventilation has been kept constant at 21 dm<sup>3</sup>/s. The air in the room is mixed up with a mixing fan. Frying three hamburgers on a gas furnace for 10 minutes in extra virgin olive (OK, Plus) oil at 220

° C has been used as model dish. This combination of frying of hamburgers olive oil has also been used in a previous research (Jacobs, 2016). A stainless steel 24 cm diameter pan with a soldered temperature sensor has been used. The pan temperature has been kept constant by regulating the gas flow to the furnace. After the frying the hamburgers have been removed from the room.



Figure 1: frying hamburgers in stainless steel pan with temperature sensor.

During the 10 minutes frying and consequently 50 minutes ventilating the room the following components have been measured: PM<sub>2.5</sub>, Elemental Carbon (EC, soot), Polycyclic aromatic hydrocarbon (PAH), ozone, NO and NO<sub>2</sub>. The details of the measuring equipment are mentioned in Table 3.

Table 3: specifications of measurement equipment

PM <sub>2.5</sub>	Grimm 11R
Elemental Carbon (EC)	Multi Angle Absorption Photometer (MAAP) 5012, Thermo Environmental
16 EPA PAHs	Measuring head with particle filter and XAD-2 absorption grains, analysis on the 16 EPA PAHs
NO <sub>x</sub>	Thermo Environmental (model 42i) NO <sub>x</sub> monitor
Ozon	Photometric O <sub>3</sub> Analyzer model 400, API Inc.

Three different situations have been assessed:

1. No exhaust hood;
2. Recirculation hood (ATAG, WS9011QAM) equipped with an fresh carbon filter(ACC928UU) dimensions 28 x 18 x 2 cm, recirculation flow 430 m<sup>3</sup>/hour;
3. An commercial plasma hood (see Figure 2, right).



Figure 2: left positioning of recirculation hood and measurement equipment, right plasma hood.

### 3 RESULTS

Table 4 gives an overview of the experimental results. The  $PM_{2.5}$  emission is strongly dependent on the temperature, increasing the baking temperature from 180 to 220 ° C resulted in a four-fold higher peak concentration. Particulate matter is also formed if only oil is used. Soot makes 0.1 - 1.1% share of the  $PM_{2.5}$  emission. The measured maximum soot concentrations are in the order of magnitude from 0.8 to 3.0  $\mu\text{g}/\text{m}^3$ . There is no set clear relationship with the temperature. The PAH concentrations are not listed as there were no significant increased concentrations found. The concentration of Benzo(a)pyrene (BaP), a PAH, was in all experiments, below 1  $\text{ng}/\text{m}^3$ , the annual averaged EU air standard. Application of the recirculation and plasma hood, respectively, resulted in a reduction of 28% and 31% of the peak  $PM_{2.5}$  concentration. The peak concentration of  $\text{NO}_2$  was by application of the recirculation hood by 67% lower. When using the plasma hood the  $\text{NO}_2$  peak concentration was greatly increased to 667 and 1155  $\mu\text{g}/\text{m}^3$  (duplicate measurements). This can be explained by the fact the plasma hood also generates ozone thereby  $\text{NO}$  is converted to  $\text{NO}_2$  and possibly also nitrogen from the air turnover to  $\text{NO}_2$ . This is supported by the variation in time of the gaseous compounds as shown in Figure 3.

Table 4: cooking emissions per experiment expressed as peak concentrations.

$T_{\text{pan}}$ [° C]	Number of hamburgers	Wasemkap	Ventilation [dm <sup>3</sup> /s]	Max. $PM_{2.5}$ [ $\mu\text{g}/\text{m}^3$ ]	Max. EC (soot) [ $\mu\text{g}/\text{m}^3$ ]	Max. $\text{NO}_2$ [ $\mu\text{g}/\text{m}^3$ ]	Max. $\text{O}_3$ [ppb]
180	3	-	21	194	1.47	-	-
180	3	-	21	195	1.38	274	-
220	3	-	21	894	3.04	-	-
220	3	-	21	615	1.41	350	-
220	3	-	21	808	0.82	358	-
220	Only oil	-	21	751	2.88	222	-
220	3	Recirculation	21	569	2.81	126	-
220	3	Recirculation	21	512	0.64	138	-
220	3	Recirculation*	21	595	0.42	91	-
220	3	Plasma	21	561	6.34	667	69 – 194
220	3	Plasma	21	507	0.76	1155	166 - 441

\* free flow towards ceiling to prevent disturbance of the air flow pattern under the hood.

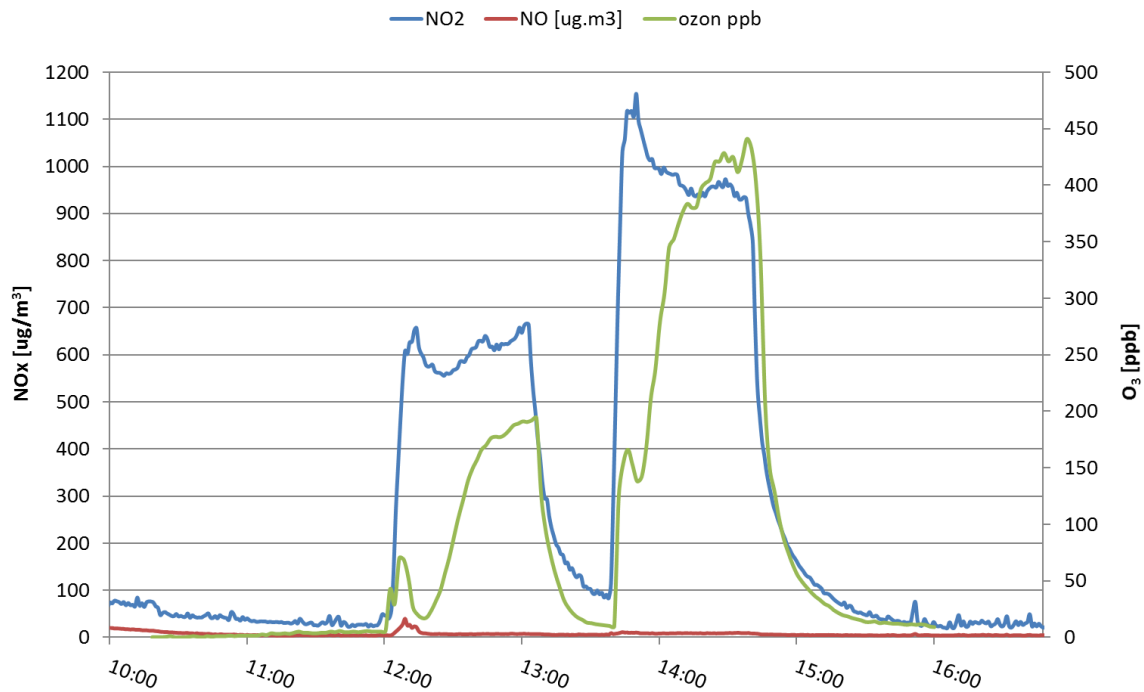


Figure 3: NOx and ozone concentration with plasma hood duplo experiment.

The higher NO<sub>2</sub> and ozone concentration in the second experiment is probably due to the fact that the carbon filter has not been refreshed. An aging test performed on the carbon filter of the recirculation hood simulating 19 days of cooking (20 minutes/day 5 kW) showed an initial NO<sub>2</sub> reduction of 56% and after 19 days only 19%.

## 4 DISCUSSION

### 4.1 PM<sub>2,5</sub>

The measured concentrations are in line with earlier research of Schiavon (Schiavon, 2015) in a 20 m<sup>3</sup> room and Jacobs (Jacobs, 2016). The relatively small PM<sub>2,5</sub> reduction of about 30% by the recirculation hood and the plasma hood can be explained by the fact that carbon filters are very open filters that are designed to absorb gaseous odorants but leave particulate matter almost unobstructed. In air tight dwellings with low ventilation flows this can lead to exposure to relative high PM<sub>2,5</sub> levels. This is supported by the findings in a field study (Jacobs et al., 2016) that a recirculation hood in contrast to its relative high exhaust capacity is not that effective towards PM<sub>2,5</sub> mitigation. As recirculation hoods have favorable properties in terms of applicability and energy conservation it is recommended to add a particulate filter to recirculation hoods.

### 4.2 NO<sub>2</sub>

The peak concentration of NO<sub>2</sub> was by application of the recirculation hood 67% lower. This is higher as measured by Paulin (Paulin, 2014) in an intervention study in homes with unvented gas stoves in Baltimore City. Air purifier placement in that study resulted in an immediate decrease of 27% in the kitchen and 22% in the bedroom, but at 3 months a significant reduction was seen only in the kitchen (20%). This may be caused by the fact that loading the filter reduces the absorption potential as demonstrated by the 19 days aging test. Applying the plasma hood did not decrease but increase the NO<sub>2</sub> concentration towards concentrations which are above the WHO 1-hour limit and the Dutch health council 15

minutes averaged concentration limit. This can be explained by the ozone that almost instantaneously converts the NO towards NO<sub>2</sub>:  $3\text{NO} + \text{O}_3 \rightarrow 3\text{NO}_2$

In figure 3 after stopping the baking the concentration NO<sub>2</sub> remains constant. One would expect a dilution by the ventilation. This can be explained the fact that ozone is still being generated as the hood is still on. Probably NO<sub>2</sub> is generated from N<sub>2</sub> available in the room air. Note that in this study only one burner of the gas furnace has been used. Based on the limited data gained in this study the combination of a gas furnace and a plasma hood seems unfavorable with regard to NO<sub>2</sub> formation. In general ozone production should be avoided. It is recommended to do more research towards optimizing odor and particulate matter reduction while minimizing the ozone production.

#### **4.3 Elemental Carbon (EC) and PAH's**

There is no set clear relationship between the concentrations of Elemental Carbon and PAH's with the temperature and the effect of a recirculation or plasma hood. In the last experiment with the recirculation hood the capture efficiency may be improved due to less disturbance of the air flow pattern under the hood. It may be possible that the carbon filter reduces the concentration Elemental Carbon. In this research no significant increased PAH concentrations were found. A literature review (Abdullahi, 2013) has shown that the cooking method has a large influence on PAHs. Chinese cooking, characterized by frying at high temperatures, can lead to much more PAH's compared to western-style fast food cooking.

### **5 CONCLUSIONS**

This study indicates that recirculation hoods based on carbon and plasma filters remove PM<sub>2.5</sub> for about 30%. A fresh carbon filter removed about 60% of the NO<sub>2</sub>, dropping within a few weeks of cooking to 20%. In case of a recirculation hood based on plasma technology additional NO<sub>2</sub> can be formed leading to concentration which are above the WHO 1-hour limit and the Dutch health council 15 minutes limit. For plasma hoods it is recommended to optimize odor and particulate matter reduction while minimizing the ozone production. As recirculation hoods have favorable properties in terms of applicability and energy conservation it is recommended to add a particulate filter to recirculation hoods and to apply them preferably in combination with electrical cooking.

### **6 ACKNOWLEDGEMENTS**

This project has been financed with TKI toeslag subsidy of the ministry of Economic Affairs for TKI Urban Energy, TopsectorEnergie, [www.tki-urbanenergy.nl](http://www.tki-urbanenergy.nl).

### **7 REFERENCES**

- Abdullahi, K., Delgado-Saborit, J., & Harrison, R. (2013). Emissions and indoor concentrations of particulate matter and its specific chemical components from cooking: a review. *Atmospheric Environment*, 260-294.
- CAAQS. (2010). *California Ambient Air Quality Standards*. Retrieved December 2016, from <https://www.arb.ca.gov/research/aaqs/caaqs/no2-1/no2-1.htm>
- Dennekamp, M., Howarth, S., Dick, C., Cherrie, J., Donaldson, K., & Seaton, A. (2001). Ultrafine particles and nitrogen oxides generated by gas and electric cooking. *Occup. Environ. Med.*, 511-516.

- EPA. (2012). Retrieved from [https://www3.epa.gov/ttn/naaqs/standards/nox/s\\_nox\\_history.html](https://www3.epa.gov/ttn/naaqs/standards/nox/s_nox_history.html)
- EU. (2008). *2008/50/EG*. Retrieved from <http://eur-lex.europa.eu/legal-content/NL/ALL/?uri=CELEX:32008L0050>
- Jacobs, P., Borsboom, W., & Kemp, R. (2016). PM2.5 in Dutch dwellings due to cooking. *AIVC conference Alexandria*.
- Jacobs, P., Cornelissen, H.J.M. ., & Borsboom, W. (2016). Energy efficient measure to reduces PM2.5 emissions due to cooking. *Indoor Air conference*. Gent.
- Logue, J., Klepeis, N., Lobscheid, A., & Singer, B. (2014). Pollutant exposures from natural gas cooking burners; a simulation-based assessment for southern California. *Environment Health Perspectives*, 43-50.
- Paulin, L. (2014). Home interventions are effective at decreasing indoor nitrogen dioxide concentrations. *Indoor Air*, 416 - 424.
- Schiavon, M., Rada, E., Ragazzi, M., Antognoni, S., & Zanoni, S. (2015). Domestic activities and PM generation: a contribution to the understanding of indoor sources of air pollution. *Int. J. Sus. Dev. Plann.*, 347 - 360.
- SER. (2007). *Occupational health values*. Retrieved from SER.nl: <https://www.ser.nl/nl/themas/arbeidsomstandigheden/grenswaarden.aspx>
- WHO. (2005). *Air Quality Guidelines - Global update 2005*. WHO.
- WHO. (2010). *WHO guidelines for indoor air quality - selected pollutants*. WHO.

# Abstract submission form for the 38thAIVC - 6thTightVent&4thventicoolConference, 2017

## PAPER TITLE

Emission source strength of cooking and exposure reduction potential of a typical hood

## MAIN AUTHOR

Catherine O'Leary

## OTHER AUTHORS

Piet Jacobs, Yvonne de Kluizenaar, Wouter Borsboom, Benjamin Jones

## CONFERENCE TOPICS

Ventilation, IAQ, and health relationships – performance of cooker hoods

## PREFERRED TYPE OF PRESENTATION

- Short oral presentation (3 minutes + poster)
- Extended oral presentation (12 minutes + questions)

## PUBLICATION IN SCIENTIFIC JOURNAL

Would you like the scientific committee to consider your paper for publication in a journal?

- Energy and Buildings
- International Journal of Ventilation
- REHVA journal
- No
- I don't know

## ABSTRACT

There is established evidence linking exposure to fine particulate matter (PM<sub>2.5</sub>) to adverse health effects. As people spend the majority of their time indoors, and with the trend towards increasing building air tightness, exposure to PM<sub>2.5</sub> indoors is expected to increase, without additional purpose provided ventilation. Cooking has been identified as a key indoor source of PM<sub>2.5</sub>. Complete source removal is not feasible for cooking, as it is an activity that takes place in most homes, however, the use of cooker hoods which remove emitted pollutants at source can reduce indoor concentrations.

This study investigates the emission source strength of cooking complete evening meals representative for Northern European countries (the Netherlands and the UK), key parameters affecting this source strength, and exposure reduction potential of using a typical cooker hood. Existing studies on indoor emission source strength from cooking mostly investigate components of meals, or individual foods. This study aims to investigate more typical cooking behaviour, by investigating emissions from complete meals. Cooking complete meals may not only have an effect on the source strength but also on the capture efficiency of the cooker hood.

The source strength of 4 representative evening meals ( $PM_{2.5}$  micrograms/second) is determined under controlled laboratory conditions in a test kitchen. Preliminary tests are conducted to establish the laboratory conditions and the repeatability of the tests. All meals are prepared both with and without the use of the installed cooker hood, to establish the exposure reduction potential. Additional tests are conducted using a single test reference meal, to investigate the impact of different parameters on source strength and exposure reduction potential.

Results show the impact of cooking complete meals as an indoor source of particulate matter, and can be used as an input for simulation studies of cooking related exposure in the population. They also indicate exposure reduction potential of interventions, including the use of a typical cooker hood.

### **KEY MESSAGES OF YOUR PRESENTATION**

Give 2-4 key messages of your presentation.

1. Describe  $PM_{2.5}$  emissions of cooking complete meals
2. Identify key factors which impact fine particulate matter emission rates
3. Identify the reduction potential of interventions

# The effect of adjustable cooling jet on thermal comfort and perception in warm office environment – a laboratory study

Henna Maula<sup>\*1,2</sup>, Hannu Koskela<sup>1,2</sup>, Annu Haapakangas<sup>1,2</sup>, and Valtteri Hongisto<sup>1,2</sup>

*1 Finnish Institute of Occupational Health  
Lemminkäisenkatu 14-18 B  
20520 Turku  
Finland*

*2 Turku University of Applied Sciences  
Joukahaisenkatu 3  
20520 Turku  
Finland*

*\*Corresponding author: henna.maula@turkuamk.fi*

## ABSTRACT

The aim was to study how the cooling jet from the ceiling, with individual control over the airflow, is perceived and how it affects the thermal comfort in warm office environment. 32 undergraduate university students participated in the experiment. Two thermal conditions were tested: (1) no cooling jet and (2) adjustable cooling jet from the ceiling. Subjects were able to use a controller with seven different settings to adjust the airflow coming from the nozzles so that the target velocity varied from 0.3 m/s to 1.5 m/s. The cooling jet was directed into the upper body.

The whole experimental session lasted for 110 minutes including acclimatization (30 minutes) and both thermal conditions (40 minutes each). The order of thermal conditions was counterbalanced between participants. Clothing insulation and activity level were controlled. Subjects' work performance was measured with two different tasks: short term memory task and working memory task. Whole body thermal comfort, local thermal comfort, symptoms and subjects perception were assessed with questionnaires.

Most of the subjects adjusted the airflow of the cooling jet. 65% of the subjects adjusted the jet so that at the end of session the target velocity was 1.1-1.3 m/s. Adjustable cooling jet improved thermal comfort, perceived indoor air quality and perception of the work environment. It also reduced symptoms, perceived fatigue, tiredness and subjective workload. Thermal environment with the adjustable cooling jet was perceived to be better for working efficiently for a long time. Condition did not affect work performance.

## KEYWORDS

Individual control, Symptoms, Perception, Perceived indoor air quality, Air velocity

## 1 INTRODUCTION

Too high room air temperature (Maula et al., 2016a) and poor indoor air quality (Maula et al., 2017) can affect negatively on occupant's thermal comfort, perceived indoor air quality and work performance. Local cooling can be provided by increasing air movement. Standards allow elevated air speed to be used to increase the maximum operative temperature for acceptability (ASHRAE 55, 2010; ISO 7730, 2005; EN 15251, 2007).

Increased air movement has been found to reduce the negative impact of increased air temperature, relative humidity, and pollution level on perceived air quality (Melikov and Kaczmarczyk, 2012). The air movement was produced in their study with an air terminal device that was installed on the desk. They noticed that recirculated room air did not reduce the intensity of SBS symptoms, but clean outdoor air did so. Therefore, using clean outdoor air in local ventilation jet applications may be beneficial. However, installing an air terminal unit and ducting providing clean outdoor air into the desk might complicate the layout changes in offices. One solution is to integrate the cooling jet to the HVAC system and place the air terminal unit into the ceiling, which enables layout changes with less effort.

Maula et al. (2016b) studied the effect of cooling jet from the ceiling on thermal comfort and work performance of twenty nine subjects in warm office environment. The airflow rate of fresh air coming from the nozzles was kept constant, so that the target velocity in the facial region was 0.8 m/s, which is according to ASHRAE standard 55 (2010) the upper limit to air speed when sedentary office occupants do not have control over the local air speed. The room air temperature was 29.5 °C and the jet temperature in subject's facial region was 28.5 °C. They found that thermal comfort and perceived working conditions were improved, and indoor air was perceived fresher with the jet. The jet improved the speed of response in a working memory task with increasing exposure time. Self-rated performance was higher with the cooling jet. However, the diverse perception of the jet and the increased eye symptoms showed the need for individual control over the airflow already at the air velocity of 0.8 m/s.

Lipczynska et al. (2014) studied the impact of personalized ventilation combined with chilled ceiling on eye irritation with twenty four subjects in warm office environment. They noticed that the use of individual control of supplied personalized ventilation airflow resulted in acceptable air movement by most of the subjects. Lipczynska et al. (2014) suggested that the use of individual control over the airflow might be one of the main solutions to avoid possible eye symptoms caused by elevated air movement. The personalized ventilation device was installed in to the desk so that the airflow was coming from in front of subject, and therefore results cannot be automatically applied when the airflow is coming from the ceiling.

Our aim was to study the effect of adjustable cooling jet from the ceiling on thermal comfort, symptoms and perception in warm office environment. This study is a continuation of the study by Maula et al. (2016b).

## **2 METHODS**

The study was carried out in the office laboratory (12m<sup>2</sup>) of Finnish Institute of Occupational Health in spring 2015 (Figure 1). Screens of 1.3 metres high were installed between workstations 1 and 2, and next to supervisors' workstation. The room air temperature was 29.4 °C, relative humidity was 15 % and supply air flow rate was 27 l/s per person. Fresh outdoor air was supplied with one terminal unit installed in the middle of the ceiling and with one cooling jet above the other workstation, i.e. workstation 2 (Figure 1). The inlet duct was divided into two branches outside the office laboratory: main branch into terminal unit and secondary branch into workstation 2. A duct fan was installed outside the laboratory into the secondary branch and a remote control was brought into workstation 2 (Figure 2). The cooling jet was produced with seven adjustable nozzles installed symmetrically into the end of secondary branch (Figure 2). Nozzles were adjusted so that the cooling jet was directed towards occupants' chest. Air velocity distributions and target velocities, i.e. maximum velocities in which the cooling jet hits the occupant, for each setting of fan control were

measured separately of the human subject experiments (Figure 3). The direction of the cooling jet was not changed during the experiment. Noise level and lighting conditions met current recommendations for office environment.

Two thermal conditions were tested; (1) no cooling jet and (2) adjustable cooling jet. The cooling jet was isothermal. Participants were advised to adjust the airflow of the cooling jet whenever necessary, with the exception of performing the tasks. Subjects were able to adjust the airflow coming from the nozzles so that the target velocity i.e. maximum velocity on the subjects point, varied from 0.3 m/s to 1.5 m/s (Figure 3). The cooling jet was directed into the upper body.

Altogether, 32 participants (9 male and 23 female) were recruited. The participants were native Finnish speakers and aged between 19 and 38 years (average = 25). The study had a repeated measures design, i.e. each subject was exposed to both thermal conditions and served as their own control minimizing the effect of individual differences on results. Participants were tested one at a time. The order of thermal conditions were counterbalanced between participants to control possible order effects concerning, for example, learning and fatigue.

Clothing insulation and activity level were controlled. The participants were advised to wear trousers, short sleeve shirt, socks and ankle-length shoes. The estimated clothing insulation including office chair (0.1 clo) was 0.71 clo (ISO 7730, 2005). The main activity of the participants during the study was typing. The estimated activity level was 1.1 met (ISO 7730, 2005).

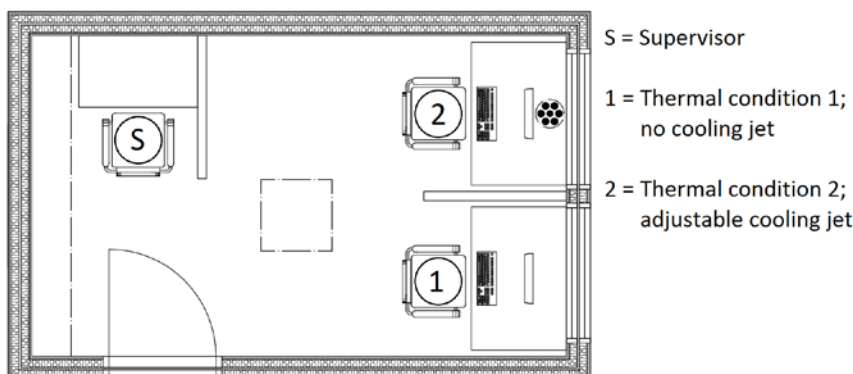


Figure 1: Layout of the office laboratory. Acclimatization was done in workstation 1.

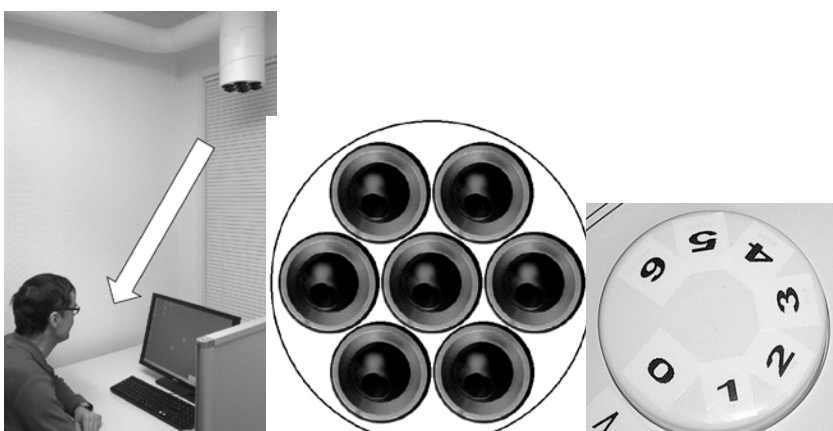


Figure 2: Left: The direction of the cooling jet. Middle: Seven nozzles installed symmetrically into the end of secondary branch of inlet duct. Right: Remote control of the duct fan.

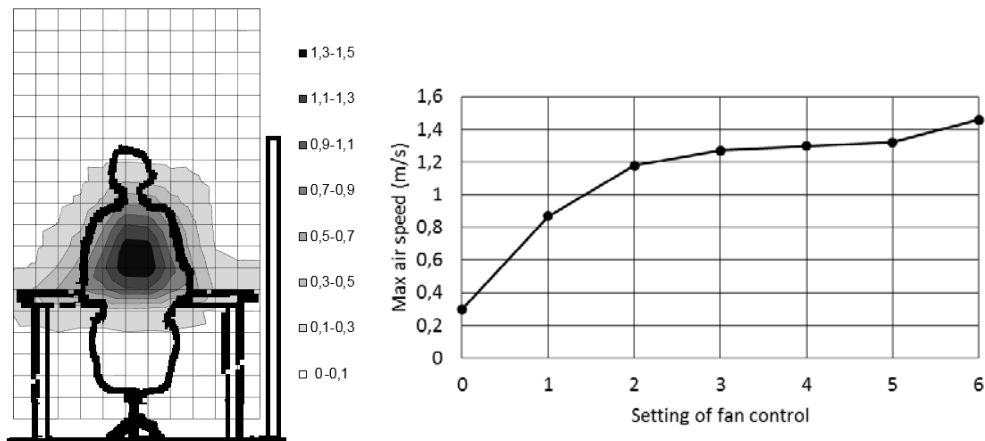


Figure 3: Cooling jet was directed towards occupants' chest as seen from velocity distribution measurements (m/s) with fan control adjusted to maximum (setting 6, left). A 10 x 10 cm measurement grid was used. Right: Target velocities (m/s) of each setting of fan control.

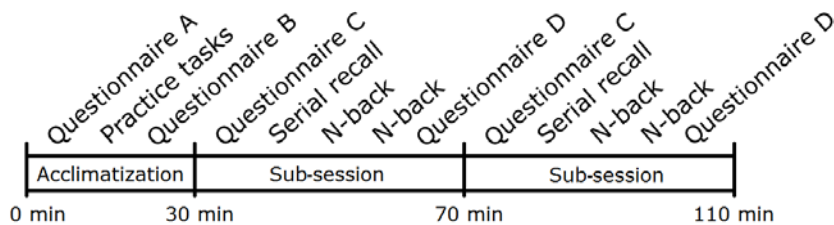


Figure 4: Procedure of the whole experimental session containing both thermal conditions (first sub-session had one thermal condition and the second sub-session had the other thermal condition).

The whole experimental session lasted for 110 min (Figure 4). It included an acclimatization phase (30 min) and both thermal conditions (40 min per sub-session). During acclimatization the participants filled questionnaires and practiced performance tasks. Questionnaires were filled in the beginning and at the end of the acclimation phase and during both sub-sessions. The sub-sessions were carried out right after another without a break.

Participants' performed two different tasks in both sub-sessions: short-term memory task (serial recall task; Maula et al., 2016b) and working memory task (N-back task; Owen et al., 2005). Whole body thermal comfort, local thermal comfort, symptoms, subjective performance ratings and overall experience of the environment were assessed with questionnaires, which were repeated throughout the session. In addition, the perception of cooling jet was assessed in workstation 2. Questions and response scales are presented in Maula et al., (2016b, Table 1).

Statistical analyses were conducted with IBM SPSS Statistics for Windows, Version 20.2 (Armonk, NY: IBM Corp.) with a confidence interval of 95 %. The normality of the data was tested with Shapiro-Wilk test. A repeated measures ANOVA was used when data was normally distributed or when distributions were similarly skewed. The Greenhouse-Geisser correction was applied when Mauchly's test indicated violation of sphericity, and the corresponding p-values are reported. Friedman and Wilcoxon's tests were used for variables that were not normally distributed if they also differed in the direction of skewness. Significant interactions were further analysed with t-test (two-tailed) or Wilcoxon test. Benjamini-Hochberg procedure was used in paired comparisons.

### 3 RESULTS AND DISCUSSION

Most of the subjects adjusted the airflow of the jet. 65% of the subjects adjusted the jet so that at the end of session the target velocity was 1.1-1.3 m/s.

Table 1 shows the results, in which the difference between thermal conditions are statistically significant. The adjustable cooling jet improved thermal comfort (Figure 5), perceived indoor air quality and perceived work environment. The median value of thermal sensation vote at the end of sub-session was +1.9 without the jet, and +0.4 with the adjustable cooling jet, respectively. Response scale was from -3 'cold' to +3 'hot' (Figure 5). Symptoms, subjective workload and cognitive fatigue were decreased with the jet. Eye symptoms were minor and thermal condition had no significant effect on them.

The perception of the jet was slightly diverse between participants. When participants were asked to name body parts where the jet was perceived as pleasant, all body parts under the direct influence of the jet were mentioned, especially the face (69% of participants reported the cooling jet to be pleasant in the face), arms (66%) and torso (41%). Respectively, some participants reported the jet to be unpleasant in the face (38%, including participants who liked the cooling jet in the face but not in the eyes) and front neck (25%). 9% of participants mentioned separately in open questions, that they would have wanted to be able to adjust also the direction of the jet.

No effect of thermal condition was seen on objective or subjective work performance.

Table 1: All results, in which the difference between thermal conditions are statistically significant, and *p*-values. The condition, which was better for occupant, is marked with "X".

Questionnaire		<i>p</i>	No cooling jet	Adjustable cooling jet
Thermal comfort	Whole body thermal sensation	<.001		X
	Local thermal sensation*	<.05		X
Symptoms	Sweating	<.001		X
	Headache	<.01		X
	Nasal symptoms	<.05		X
	Feeling of being unwell	<.05		X
	Difficulties in concentration	<.01		X
Cognitive fatigue	Tiredness	<.05		X
	Lack of energy	<.01		X
	Lack of motivation	<.001		X
Subjective workload	Workload during the most difficult task	<.05		X
	Exertion	<.01		X
Disturbance of performance	Heat	<.001		X
	Draught	<.001	X	
	Stuffiness	<.001		X
Perceived air quality		<.001		X
Perceived work environment	Pleasantness of environment	<.001		X
	Draughtiness	<.001	X	
	Stuffiness	<.001		X
	Overall experience of the environment	<.001		X
	The possibility to work effectively in that temperature	<.001		X

\*All body parts

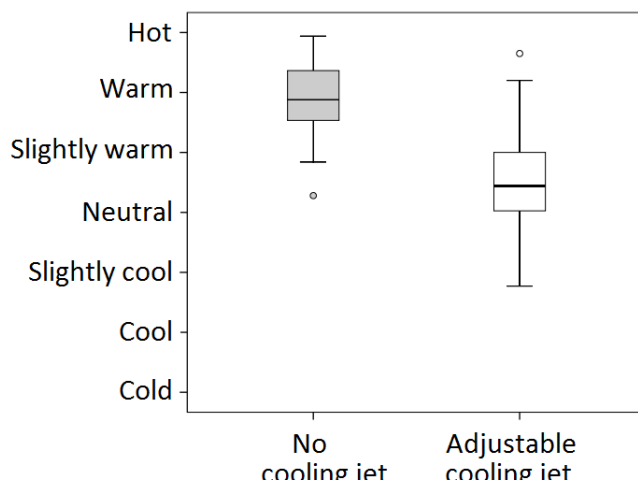


Figure 5: The distribution of whole body thermal sensation at the end of sub-session in both thermal conditions. 72% of participants were dissatisfied with the thermal environment at the end of the sub-session without the jet, while 22% of participants were dissatisfied with the adjustable cooling jet, respectively.

## 4 CONCLUSIONS

The results suggest that providing local cooling with a ceiling based adjustable cooling jet can improve thermal comfort, perceived indoor air quality and perceived working conditions in warm office environment. Additionally, symptoms, subjective workload and cognitive fatigue might be reduced with jet. These findings can be utilized in the development of energy-efficient air conditioning systems for offices where overheating occurs. However, it seems that individual control is needed, not only on airflow, but also on the direction of the jet. In the future, the effect of individual control on both the jet airflow rate and flow direction in otherwise similar conditions should be studied.

## 5 ACKNOWLEDGEMENTS

This work was carried out within the RYM Indoor Environment research program which was financially supported by Tekes and the participating companies. We thank FiSIAQ for travelling grant for AIVC 2017 conference. This study is part of IEA EBC Annex 62 Ventilative cooling.

## 6 REFERENCES

- ASHRAE Standard 55-2010. Thermal Environmental Conditions for Human Occupancy. Atlanta: American Society of Heating, Refrigerating, and Airconditioning Engineers.
- CEN (European Committee for Standardization), EN 15251, Criteria for the Indoor Environment Including Thermal, Indoor Air Quality, Light and Noise, European Committee for Standardization, Brussels, Belgium, 2007.
- ISO 7730, Ergonomics of the Thermal Environment. Analytical Determination and Interpretation of Thermal Comfort Using Calculation of the PMV and PPD Indices

and Local Thermal Comfort Criteria, International Organization for Standardization, Geneva, 2005.

Lipczynska A., Marcol B., Kaczmarczyk J., Zuska L., and Melikov A.K. Impact of personalized ventilation combined with chilled ceiling on eye irritation symptoms, in: Proceedings of Roomvent 2014, 13th SCANVAC International Conference on Air Distribution in Rooms, October 19<sup>th</sup>-22<sup>nd</sup> São Paulo, Brazil, 2014.

Maula, H., Hongisto, V., Östman, L., Haapakangas, A., Koskela, H. and Hyönä, J. (2016a), The effect of slightly warm temperature on work performance and comfort in open-plan offices – a laboratory study. *Indoor Air*, 26: 286–297. doi:10.1111/ina.12209

Maula H., Hongisto V., Koskela H., and Haapakangas A. (2016b). The effect of cooling jet on work performance and comfort in warm office environment. *Building and Environment* 104 (2016) 13-20.

Maula H., Hongisto V., Naatula V., Haapakangas A., and Koskela H. The effect of low ventilation rate with elevated bioeffluent concentration on work performance, perceived indoor air quality and health symptoms. *Indoor Air*. 2017;00:1–13. DOI: 10.1111/ina.12387

Melikov A.K. and Kaczmarczyk J. Air movement and perceived air quality, *Building and Environment* 47 (2012) 400-409.

Owen A.M., McMillan K.M., Laird A.R., Bullmore E., N-back working memory paradigm: a meta-analysis of normative functional neuroimaging studies, *Hum. Brain Mapp.* 25 (2005) 46-59.

# **A Case Study assessing the impact of Shading Systems combined with Night-Time Ventilation strategies on Overheating within a Residential Property.**

Zoe De Grussa<sup>1\*</sup>, Dr Deborah Andrews<sup>1</sup>, Dr Gordon Lowry<sup>1</sup>,  
Dr Elizabeth.J. Newton<sup>1</sup>, Kika Yiakoumetti<sup>1</sup>, Andrew Chalk<sup>2\*</sup> and David Bush<sup>2</sup>

*1. London South Bank University  
103 Borough Road, London  
SE1 0AA, United Kingdom  
\*degrussz@lsbu.ac.uk*

*2. The British Blind and Shutter Association  
PO Box 232, Stowmarket, Suffolk  
IP14 9AR, United Kingdom  
\*andrew@bbsa.org.uk*

## **ABSTRACT**

Overheating in domestic homes, specifically in built up urban areas, has become a pressing problem throughout the UK. It is likely to become a costly energy problem in years to come if passive design strategies are not fully understood and integrated. This research looks to investigate how internal and external solar shading systems impact on operative temperatures when differing blind together with a night time natural ventilation strategy are adopted within a renovated block of flats in North London. Although shading and ventilation were overlooked at the initial stage of the building design, the implementation of solar shading has been found to be beneficial in maintaining thermal comfort within the building when external temperatures were recorded both above and below 20- 25°C.

During the study shading was combined with a night-time natural ventilation strategy which enabled most rooms to cool when external temperatures were at their lowest. However, nighttime ventilation may not be desirable to the occupants due to external traffic noise and security issues in relation to the intended design use of the rooms such as those in this case study. The authors believe lower indoor temperatures could be achieved if the areas of opening were increased in size in the façade design. In two areas of the building natural cross-ventilation was not possible leading to significant overheating issues and the retrofitting of mechanical ventilation. This highlights the need for an effective façade management strategy that considers the inter-relationship between glazing, shading and ventilation collectively at the design stage.

## **KEYWORDS**

Overheating, Night-Time Ventilation, Internal Blinds, External Blinds, Shading.

## **1 INTRODUCTION**

The UK is a predominantly heating reliant nation and it has been identified that the façade, and specifically the glazing system, is the main cause for fabric thermal losses within domestic buildings, improvements of which could lead to substantial energy savings resulting in lower CO<sub>2</sub> emissions (IEA, 2013). The UK government has worked towards energy efficient building standards, Building Regulation - Part L1A, which have reduced unwanted air infiltration and have improved the insulation standard of new homes. Schemes such as the Green Deal in conjunction with Building Regulation – Part L1B have encouraged homeowners to refurbish existing homes to a similar standard. However, through these improvements the number of reported thermal discomfort issues relating to overheating in summer has risen.

The Zero Carbon Hub (2015) has found that up to 20% of the housing stock is subject to overheating alone and in the healthcare sector 90% of hospitals are susceptible to overheating (Seguro and Palmer, 2016). The Good Homes Alliance (2014) identified that urban apartments tend to overheat most frequently. Overall, they identified 90 instances of overheating in domestic buildings in the UK and 73% of these were located in urban locations. 78% (of the 90) of these occurrences were reported in apartments, 48% (of the 90) were new builds (30% had been built post 2000) and 30% were buildings repurposed/refitted into apartments. Within research literature a recent paper by Lomas and Porritt, (2017) reviews 12 studies where overheating has been evidenced across the UK in domestic homes in a mix of building types that vary in age and construction type. However, these studies conducted by different research teams vary in scale, methodologies in defining overheating and data collection procedures which makes comparisons between them problematic.

The term 'overheating' is not clearly defined for post-occupancy evaluations. Recommended operative temperatures for different room purposes are given within CIBSE Guide A (2015), ASHRAE Standard 55 and BS EN 15251:2007 (BSI, 2008). These recommend bedrooms and living areas should remain between 23-25°C in summer and between 17- 19°C in winter. It is important to realise that these temperatures represent the upper and lower limits of thermal comfort and are not representative of long-term temperatures that may cause serious health issues for vulnerable groups. The World Health Organisation (1990) recommended that air temperatures between 18 - 24°C are suitable for healthy sedentary people but for vulnerable groups air temperatures should be maintained at 20°C. The Housing Health and Safety Rating System gives guidance on excess heat and suggests "... temperatures (which) exceed 25°C, mortality increases and there is an increase in strokes" (Department for Communities and Local Government, 2006). This issue was highlighted in 2003, when 2,000 premature deaths occurred in relation to a 10-day heatwave experienced in the UK. These 'heatwave' temperatures are likely to become common summer temperatures as early as 2040 (Public Health England, 2015).

Increased ventilation and solar shading are the recommended strategies for combatting overheating (Zero Carbon Hub, 2015, Seguro & Palmer, 2016, Public Health England, 2015, BRE, 2016, Lomas and Porritt, 2017). However, the barriers to these solutions are those of human behaviour. It has been suggested in the UK Climate Change Risk Assessment 2017 that "... people lack a basic understanding of the risks to health from indoor high temperatures, and are therefore less likely to take measures to safeguard their and their dependents' wellbeing." Natural ventilation in urban areas can be problematic due to issues arising from external noise and security concerns. In a survey given to 89 householders in London windows were also found to be infrequently used with more than half of respondents stating they were unable to open windows due to security reasons and one third asserting they were unable to open them due to high external noises. Furthermore, over the course of a very hot day one in five respondents would not tend to open any windows at night and one in ten would keep all windows closed all day. In total 70% of respondents suggested they would either open one or no windows at night, which limits the potential for night-time ventilation (Mavrogianni et al., 2016).

It is well documented that blinds and shutters are used infrequently and the motivations to instigate blind movements are often related to a number of factors inclusive of lighting conditions, exposure to glare, preference for a view and the associated thermal affects which are then defined by the priorities of the user (Paule et al., 2015, Van Den Wymelenberg, 2012). Within the previously mentioned study conducted in London, even on seemingly hot days one quarter of occupants reported that they did not close blinds during the day (Mavrogianni et al., 2016).

In the UK air conditioning systems are still rarely used within domestic homes however this may change with the increasing frequency of heat waves (BRE, 2016) and

the predicted rise of 5°C in annual average temperature in the South-East of England by the end of the century (Hulme et al., 2002). The Energy Performance Building Directive has identified overheating as a concern across Europe and a cause for increasing energy consumption in relation to air conditioning costs. Passive measures, such as solar shading, are recommended to reduce the need and size of air conditioning units which will subsequently reduce energy consumption (Publications Office, 2010, Wouter et al., 2010).

There is little to encourage the requirement for shading systems to be put in place through Part L building regulations, and compliance tools such as BREEAM are ineffective in capturing the benefits solar shading can offer as they are based on averaged weather data sets that pay little attention to the solar heat gains within a building (Seguro and Palmer, 2016). However as 75- 90% of the buildings have already been built and will still be standing in 2050 (International Energy Agency, 2013), it is also important for industry to understand the impact re-fit options have on the energy consumption, comfort of occupants and the building fabric.

In this study, we aim to investigate the impact that shading and natural ventilation strategies combined can have on a newly refitted, urban apartment taking into consideration user behaviours.

## **2 FIELD STUDY METHODOLOGY**

The case study building is situated in the centre of Camden, London less than a 5-minute walk away from Camden High Street Underground Station. The building was originally constructed for the manufacture of aircraft parts but has now been renovated for residential purposes whilst maintaining the aesthetic of a commercial building. The top part of the building has been transformed from a commercial premises into twenty loft apartments and two penthouse suites on the top floor. The rest of the apartments are spread over three floors above ground and one floor at lower ground (basement) level. The building is south-west orientated (241.58°) with heavily glazed façades on the south-west and north-east face of the building. Overall the building has a medium thermal mass as the walls are constructed from brick with a mix of concrete and timber flooring throughout the building.

The south-west façade of the building is situated on a busy main road in the heart of Camden with a 24-hour use bus stop directly in front of the property. A communal garden area has been created between the front of the building and the pedestrian footpath which consists of a 1.8m wooden fenced surround containing newly planted young evergreen oak trees which will provide privacy from passers-by to the ground floor and provide shading for the ground floor and potentially first floor of the building in years to come (Figure 1.).

In the original building specification, no shading was specified, however during the construction it was reported how some of the apartments appeared to be overheating above acceptable comfort levels. This was causing issues for workers carrying out the re-fit, affecting materials and methods during construction and subsequently created issues with the plumbing system. For example, when the building was left unoccupied for 5-6 weeks, the building manager found that the waste pipe water had evaporated leaving no protection against odour ingress from the sewage system. A member of the British Blind and Shutter Association was approached to give further recommendations of the impact differing shading strategies could have on comfort levels within the building.

The comfort boundaries in this study have been defined by operative temperature recommended by CIBSE Guide A (2015), ASHRAE Standard 55 and BS EN 15251:2007 (BSI, 2008) where bedrooms should remain between 23-25°C in summer and between 17-19°C in winter.

For this case study, we have modelled the real-time behaviour of an occupant who leaves their home vacant between 8am and 4pm, keeping the windows closed for security

reasons during the day whilst assessing the thermal impact of closing a blind either internally or externally for the duration of 24-hours. We examined what effect this has on the operative temperature increase of a room during the day. This is then statistically compared with the operative temperature increase of an almost identical room without solar shading, the control room, to identify and quantify the temperature reduction achieved through the use of internal and external blinds. It is hypothesised that the operative temperature increase will be reduced when shading is used and this would lead to a positive impact on the level of comfort when an occupant returns to the property in the afternoon.



Figure 1. South-West facing building close to Camden High Street Underground Station (Photograph taken with a wide-angled lens).

**2.1 Room Specification**

Four bedrooms in two apartments were identified within the building to be evaluated. All the rooms selected were identical in orientation, finish and the amount of glazed area. The bedrooms within apartments 13 and 18 were chosen to be compared (apartment 13 situated on the 1<sup>st</sup> floor and apartment 18 directly above on the 2<sup>nd</sup> floor). These two units have identical room layouts (see Figure 2.) with each apartment containing a living room, kitchen, bathroom and two rooms designed as bedrooms.

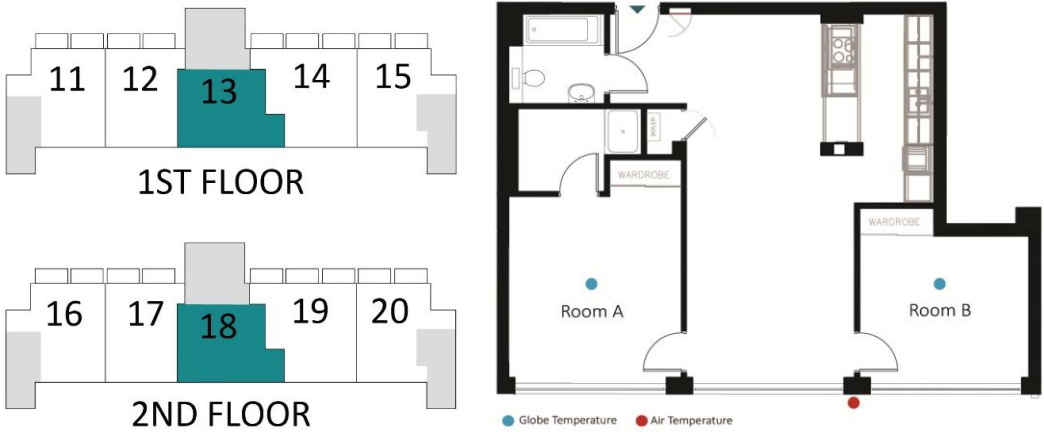


Figure 2. Building floor layout and Unit 13 and 18 layouts with sensor positions.

The bedrooms only differ in room depth; Room A extends to 4.5m and Room B extends to 3.5m. Both Room A and B are 3.5m wide. There was no furniture in either apartment and the walls and floors were finished and painted to the same standard-matt white paint on the walls and oak wood flooring (Figure 3.).

## 2.2 Façade Design

To allow the building to be used for residential purposes, it has been refitted with double low-e argon filled glazing (4-16-4) with a black/grey spacer which fits into steel window mullions. Both bedrooms (Room A and Room B) have a glazed façade on the south-west wall; the glazed areas are of equal size covering 3.2m x 1.85m and each window is split into three columns which is segmented into four rows. There are two areas of opening which are approximately 850mm x 450mm situated in the centre column with the first (from bottom) and third segment (from bottom) openable (Figure 3.) The glazing sits 1.1m above floor level in all rooms and has been specified to have a U-value of 1.1 W/m<sup>2</sup>K. No g-value was given by the building developer but the glazing specifier advised that the glazing alone would be adequate to control the solar gains on all façades.

## 2.3 Solar Shading Selection

We evaluated the impact of three internal and two external solar shading products; an internal 80mm aluminium venetian blind, an internal screen fabric roller blind and an internal reflective screen fabric roller blind. The 80mm aluminium venetian blind and screen fabric roller were also used externally. All types of blinds were tested when fully closed for the period of 8 hours and in addition the external venetian blind was also tested with louvres at an angle of 45°.

The solar properties of each blind type are presented below calculated to BS EN 14501:2005 (BSI, 2005). Even though  $g_{tot}$  could not be calculated due to lack of glazing data, this has not compromised the study as the same type and size of glazing was used in each of the rooms.

Table 1: Blind Fabric Specifications according to BS EN 14501.

Blind Fabric	Material Composition	Solar Transmission (Ts or $\tau_e$ )	Solar Reflectance (Rs or $\rho_e$ )	Solar Absorptance (As or $\alpha_e$ )
Screen Fabric	42% Fibreglass / 58% PVC	0.10	0.20	0.70
Reflective Screen Fabric	36% Fibreglass / 64% PVC	0.05	0.76	0.19
Aluminium Venetian (80mm)	Aluminium	0.00	0.50	0.50
Aluminium Venetian (80mm) at 45° Angle	Aluminium	0.08	0.38	0.55

## 2.4 Data Collection Procedure and Measurements

Before each day of data collection, the windows and joining room doors in all bedrooms and the living area were left open overnight to allow for night-time cooling. Blinds were also installed the day previous and positioned fully closed or closed at a 45° angle, for the Venetian blinds. A different shading strategy was installed in each room except for the control room where no blind was installed. The readings were taken manually which required a researcher to enter each room and record the readings on the sensors; each time this was done in the same way; the door was opened and closed as the individual entered and exited the room being monitored and the instrumentation was left in the same position throughout testing.

The data collection procedure was conducted as follows:

- 8am – Windows and Doors Closed, Measurements Start.
- Measurements taken every 10 minutes.
- 4pm – Windows and Doors Opened, Measurements Stopped.

**Internal Operative Temperature**– A black globe thermometer (40mm Ø) was used with a mercury thermometer as the temperature probe. The sensor was set up on a tripod and positioned 1.8m from the glazed façade and set at 1.2m from floor level within all four rooms being monitored (Figure 3.). The size of the globe used closely correlates with measurements of operative temperature within the indoors, which relates to the temperature humans feel when clothed (Humphreys, 1977).



Figure 3. Room A and B in Unit 18 with sensor

setup.

**External Air Temperature**– An air temperature sensor was situated on the ground floor outside. The handheld air temperature sensor was positioned away from direct solar radiation to prevent the metal probe being affected by radiant heat.

### 3 RESULTS AND ANALYSIS

Data collection took place over a period of twenty days between August and October 2016. Out of these, data from sixteen of the twenty days met the quality requirements and were used for analysis. On six days (of the sixteen) the peak external air temperature was above 25°C. On five days, the external air temperature peaked between 20 - 25°C and on the remaining five days the temperature peaked below 20°C. Overall external wind velocities were considered calm and the weather conditions were considered typical for summer in London.

#### 3.1 Operative Temperature Increase

The operative temperature increase (range - the difference between lowest and highest operative temperature values recorded in one day) was statistically analysed as the starting temperatures in each room were found to fluctuate due to different thermal retention between different rooms (as different blinds were kept closed) and there were potential differences in air leakage. The ranges were calculated for each individual day and the results are presented in Table 2. alongside the minimum (min) and maximum (max) operative temperatures and the external air temperatures (min, max and range).

The peak operative temperature in the non-blind room exceeded 25°C on 13 of the 14 days monitored. Internal blinds were monitored on 21 occasions, on 13 of these occasions the peak operative temperature reached above 25°C. On 18 of the occasions where external blinds were monitored peak operative temperatures rose above 25°C on 5 occasions.

It is also noted that on several occasions the minimum operative temperature exceeded 25°C as the rooms were unable to naturally cool overnight, due to the small area of opening and lack of cross-ventilation. If the minimum operative temperatures were lower then shading would have been able to maintain temperatures within the comfort threshold.

Table2. Data collection of indoor temperatures over 16 days across four rooms between 8am and 4pm. The solar shading specified were fixed in either at closed/ lowered position or at a 45° angle for the entirety of the day.

Testing Day	External Air Temperature (°C)			No Blind			Internal Blind									External Blind								
							Aluminium Venetian			Screen Fabric			Reflective Screen Fabric			Aluminium Venetian			Aluminium Venetian at 45°			Screen Fabric		
	Min	Max	Range	Min	Max	Range	Min	Max	Range	Min	Max	Range	Min	Max	Range	Min	Max	Range	Min	Max	Range	Min	Max	Range
Day 1	22.4	34.2	11.8	26.5*	45.0*	18.5	23.5	31.0*	7.5	-	-	-	-	-	-	-	-	-	-	-	-	-	-	-
Day 2	22.5	31.1	8.6	25.0	40.0*	15.0	-	-	-	28.0*	31.0*	3.0	-	-	-	28.0*	28.0*	0.0	-	-	-	-	-	-
Day 3	20.8	27.9	7.1	27.0*	47.5*	20.5	28.5*	34.5*	6.0	27.0*	32.0*	5.0	-	-	-	-	-	-	27.0*	29.5*	2.5	-	-	-
Day 4	17.3	28.3	11.0	-	-	-	27.5*	34.0*	6.5	27.0*	32.0*	5.0	-	-	-	-	-	-	26.0*	29.0*	3.0	-	-	-
Day 5	16.7	28.4	11.7	-	-	-	26.0*	30.0*	4.0	-	-	-	27.0*	32.0*	5.0	-	-	-	-	-	-	26.0*	28.0*	2.0
Day 6	19.7	25.5	5.8	27.0*	36.0*	9.0	21.0	26.0*	5.0	-	-	-	27.0*	31.0*	4.0	-	-	-	-	-	-	-	-	-
Day 7	14.3	23.2	8.9	23.0	39.0*	16.0	-	-	-	21.5	27.0*	5.5	21.0	26.5*	5.5	-	-	-	-	-	-	-	-	-
Day 8	16.9	20.4	3.5	23.0	33.5*	10.5	-	-	-	-	-	-	22.5	25.0*	2.5	21.0	22.5	1.5	-	-	-	22.0	24.0	2.0
Day 9	13.2	20.1	6.9	22.5	42.0*	19.5	-	-	-	-	-	-	21.0	26.5*	5.5	20.0	21.5	1.5	-	-	-	20.5	23.0	2.5
Day 10	10.5	21.4	10.9	22.0	45.0*	23.0	-	-	-	-	-	-	20.5	28.0*	7.5	20.0	22.5	2.5	-	-	-	19.0	26.0*	7.0
Day 11	13.0	20.5	7.5	23.0	44.0*	21.0	-	-	-	-	-	-	-	-	-	20.0	21.0	1.0	-	-	-	20.0	22.0	2.0
Day 12	13.5	18.7	5.2	22.5	39.0*	16.5	-	-	-	-	-	-	-	-	-	20.0	20.5	0.5	-	-	-	19.5	21.0	1.5
Day 13	9.9	18.2	8.3	19.5	38.0*	18.5	18.5	24.0	5.5	18.0	23.0	5.0	-	-	-	-	-	-	19.5	21.5	2.0	-	-	-
Day 14	12.3	16.4	4.1	21.0	37.0*	16.0	19.5	24.0	4.5	18.5	22.5	4.0	-	-	-	-	-	-	20.0	21.5	1.5	-	-	-
Day 15	11.1	16.0	4.9	20.0	32.5*	12.5	-	-	-	18.0	21.5	3.5	-	-	-	-	-	-	19.0	21.0	2.0	-	-	-
Day 16	4.5	15.3	10.8	20.5	24.5	4.0	-	-	-	19.0	20.0	1.0	-	-	-	-	-	-	20.0	20.5	0.5	-	-	-

\* Operative Temperature higher than 25°C

### 3.2 Impact of Blind Position on Operative Temperature Range

The operative temperature increases between 8am and 4pm were statistically compared using a Paired T-Test in SPSS to observe whether:

- a) Internal blinds have a significant impact on the operative temperature increase in comparison to the control room.
- b) External blinds have a significant impact on the operative temperature increase in comparison to the control room.
- c) Whether there is a significant difference on the operative temperature increase between rooms with internal and external blinds.

Table 3. Paired T-Test of no blind operative increase (range) values vs internal blind and external blind operative temperature increase (range) and internal blind operative increase (range) vs external operative temperature increase (range).

Pair	No. of Paired Samples	Mean (°C)	Std. dev (°C)	95% Confidence Interval of Difference		t - statistic (°C)	Degrees of Freedom	Sig. (2 tailed)
				Lower (°C)	Upper (°C)			
No Blind vs Internal Blind	14	10.71	3.75	8.54	12.88	10.68	13	<0.05
No Blind vs External Blind	10	14.25	5.11	10.60	17.90	8.82	9	<0.05
Internal Blind vs External Blind	12	3.13	1.74	2.02	4.23	6.23	11	<0.05

\* Level of Significance 0.05

Table 3. and Figure 4. represent the findings from the statistical review. These indicate that in all cases there was a significant impact on operative temperature increase when both internal and external blinds were used and compared to the control room. It was found that there was a significant relationship between the operative temperature increase between rooms with internal blinds and rooms with external blinds.

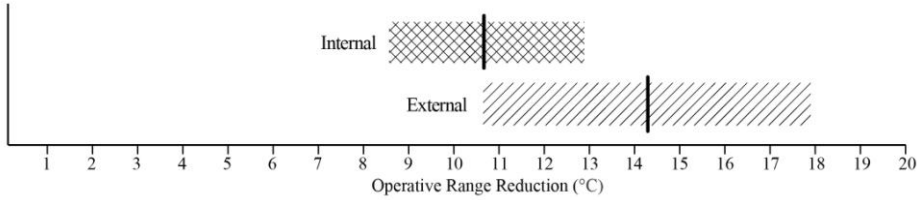


Figure 4. 95% Confidence interval and mean values of internal blind rooms and external blind rooms operative temperature increase (range) compared with a room with no blind.

If the experiment was to be carried out again in the same location, with external conditions within the same parameters and with the same window and blind opening and closing actions, we can say with 95% confidence that:

- a) Internal Blinds will reduce the operative temperature increase by between 8.54°C - 12.88°C. The room with an internal blind would therefore be 8.54°C – 12.88°C cooler than a room without a blind.

- b) External Blinds would reduce the operative temperature increase in the room by between 10.60°C –17.90°C. Theroom with an external blind would therefore be 10.60°C – 17.90°C cooler than a room without a blind.
- c) The difference in operative temperature increase between a room with an internal blind and an external blind installed would be between 2.02°C and 4.23°C. In effect the external blind room would be 2.02°C – 4.23°C cooler than a room with an internal blind.

External blinds, as hypothesised, have been found to reduce operative temperature increase more than internal blinds.

### 3.3 Impact of different blind types on Operative Temperature Range

To understand how different blind types and their properties impact the operative temperature, a paired T-Test was carried out comparing the operative temperature increase of the control room to that of a room with a specific blind type installed at a closed position or in the case of external aluminium venetians with louvres at a 45° angle.

Table 4. Paired T-Test of no blind operative increase (range) values vs specific blind types operative temperature increase (range).

Pair	No. of Paired Samples	Mean (°C)	Std. dev (°C)	95% Confidence Interval of Difference		t - statistic (°C)	Deg. of Freedom	Sig. (2 tailed)
				Lower (°C)	Upper (°C)			
No Blind vs Int. Aluminium Venetian	5	10.30	3.07	6.48	14.12	7.49	4	< 0.05
No Blind vs Int. Screen Fabric	7	10.79	4.01	7.08	14.49	7.12	6	< 0.05
No Blind vs Int. Reflective Screen Fabric	5	10.60	4.29	5.27	15.93	5.52	4	< 0.05
No Blind vs Ext. Aluminium Venetian	6	16.42	4.22	11.98	20.85	9.52	5	< 0.05
No Blind vs Ext Aluminium Venetian at 45°	5	12.60	5.81	5.38	19.82	4.85	4	< 0.05
No Blind vs Ext. Screen Fabric	5	15.10	3.97	10.16	20.04	8.49	4	< 0.05

\* Level of Significance 0.05

The results of the T-Test are presented in Table 4. Once again, all blinds were found to have a statistically significant relationship with the operative temperature increase. The mean, lower and upper confidence intervals vary depending on the properties of the blind type and the location of the products (internal or external).

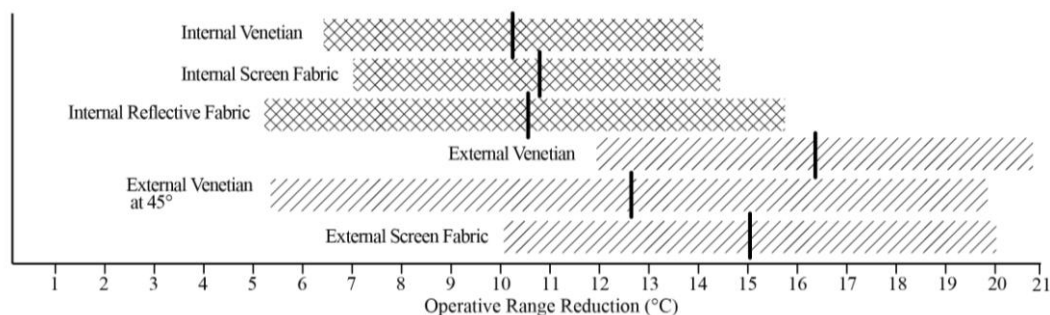


Figure 5. 95% Confidence interval and mean values of all blind types operative temperature increase (range) compared with a room with no blind.

From Figure 5, we observe how the external blinds provide the largest mean difference in operative temperature increase indicating that they limit solar gain effectively.

It is important to recognise the extent of the impact that the internal blinds have on the operative temperature. They have also been able to significantly reduce the operative temperature increase - by 68 - 73% when compared to the operative temperature reduction achieved by external blinds. This means that internal blinds are almost three quarters as effective as external blinds within this building scenario.

#### **4 DISCUSSION**

In the design stage of the building external shading was discouraged by the planning authority on the basis it would not be a necessity and therefore would not justify the impact on the aesthetics of the building. This was further supported by the glazing specifier where the developer was informed the glazing alone would obviate the requirement for solar shading.

This only proves that there are a number of design decisions during the refit of a building that may contribute to issues of overheating which are not fully understood.

Solar shading combined with night-time ventilation in this case has been evidenced to reduce operative temperature increase. There are several other design factors that can also contribute to overheating and these need to be considered and evaluated before construction or re-fit. These are: the location and orientation of the building, ceiling height, room depth, insulation and potential for air leakage, thermal mass of the building, façade design layout, hot water distribution layout and the ability to cross ventilate the building.

#### **5 CONCLUSION**

The study conducted has demonstrated how solar shading when combined with night-time ventilation can be an effective method in reducing operative temperature increase in an urban flat. Although external shading is observed to be most efficient, internal shading in this study demonstrated that it can achieve as much as 73% of the operative temperature reduction as that of an external shading. The use of external shading is not widespread practice in the UK as windows are often outward opening. This would prevent opening of the windows when external shading is extended and situated close to the building façade.

The behaviour behind opening and closing of windows and blinds has been documented to be poorly understood and underutilised. Initiation of movements can be confounded by a number of behavioural factors, particularly in urban areas, where noise pollution, security and availability of daylight are often prioritised over thermal comfort. Within unoccupied rooms changes in solar shading and window opening behaviour could have a beneficial impact on the thermal conditions experienced in a living space later in the day and over a period of time also on the building fabric of a building. The benefits of improved thermal comfort could also considerably reduce the energy requirement from mechanical ventilation systems, especially if users are educated on the best window opening and blind movement strategies and apply these to their daily lives.

Lastly, appropriate specification of glazing systems is vital in combatting the issues of overheating. Increasing the area of openings in a façade design is essential for night-time ventilation of buildings particularly in single aspect designed buildings. Also, clarity is needed on the importance of g-value specification at the design stage to ensure buildings are designed so they do not overheat.

## 6 ACKNOWLEDGEMENTS

The Authors would like to thank Rupert Cain, Alex Gutteridge, Harry Ketley, Diana Csilla Toth, Nick Teixeira and Senez Oznacar from London South Bank University for their support in conducting measurements during such warm conditions.

## 7 REFERENCES

- BRE (2016) *Overheating in dwellings - Assessment protocol*. Available from: <https://www.bre.co.uk/filelibrary/Briefing%20papers/117106-Assessment-Protocol-v2.pdf>
- BRE (2016) *Study on Energy Use by Air- Conditioning: Annex A Literature Search*. Available from: [https://www.bre.co.uk/filelibrary/pdf/projects/aircon-energy-use/A\\_AirConditioningEnergyUseAnnexAFinal.pdf](https://www.bre.co.uk/filelibrary/pdf/projects/aircon-energy-use/A_AirConditioningEnergyUseAnnexAFinal.pdf)
- BSI (2005) *BS EN 14501: 2005 - blinds and shutters Thermal and visual comfort Performance characteristics and classification*. BSI. Available from: <http://shop.bsigroup.com/ProductDetail/?pid=000000000030100403>
- BSI (2008) *BS EN 15251: 2007 Indoor environmental input parameters for design and assessment of energy performance of buildings addressing indoor air quality, thermal environment, lighting and acoustics*. BSI. Available from: <http://shop.bsigroup.com/ProductDetail/?pid=000000000030133865>
- BSI (2014) *BS 8233: 2014 - guidance on sound insulation and noise reduction for buildings – BSI British standards*. Available from: <http://shop.bsigroup.com/ProductDetail/?pid=000000000030241579> [Accessed 26 September 2016].
- CIBSE (2015) *CIBSE Guide A: Environmental design*. 8th ed. CIBSE.
- Department for Communities and Local Government (2006) *Housing health and safety rating system (HHSRS): Guidance for landlords and property-related professionals*. Available from: <https://www.gov.uk/government/publications/housing-health-and-safety-rating-system-guidance-for-landlords-and-property-related-professionals> [Accessed 21 December 2016].
- Good Homes Alliance (2014) *Preventing Overheating*. London. Available from: <http://www.goodhomes.org.uk/downloads/members/gha-preventing-overheating.pdf>
- Hulme, M., Jenkins, G., Lu, X., Turnpenney, J., Mitchell, T. and Jones, R. et al. (2002) *Climate Change Scenarios for the United Kingdom: The UKCIP02 Scientific Report*. p. 120pp. Norwich, UK: Tyndall Centre for Climate Change Research, School of Environmental Sciences, University of East Anglia. Available from: [http://danida.vnu.edu.vn/cpis/files/Papers\\_on\\_CC/CC/Climate%20Change%20Scenarios%20for%20the%20United%20Kingdom.pdf](http://danida.vnu.edu.vn/cpis/files/Papers_on_CC/CC/Climate%20Change%20Scenarios%20for%20the%20United%20Kingdom.pdf)
- Humphreys, M. (1977) The optimum diameter for a Globe Thermometer for use Indoors, *Annals Of Occupational Hygiene*, 20 (2), pp. 135-140. DOI:10.1093/annhyg/20.2.135.

- International Energy Agency (2013) *Technology Roadmap energy efficient building envelopes*. Available from:  
<https://www.iea.org/publications/freepublications/publication/TechnologyRoadmapEnergyEfficientBuildingEnvelopes.pdf>
- Kevin J. Lomas, Stephen M. Porritt. (2017) Overheating in buildings: lessons from research. *Building Research & Information* 45:1-2, pages 1-18.
- Mavrogianni, A., Pathan, A., Oikonomou, E., Biddulph, P., Symonds, P. and Davies, M. (2016) Inhabitant actions and summer overheating risk in London dwellings, *Building Research & Information*, 45 (1-2), pp. 119-142.  
DOI:10.1080/09613218.2016.1208431.
- Paule, B., Boutillier, J. and Pantet, S. (2015) *Global Lighting Performance*. ESTIA. Available from:  
[http://static.wm3.se/sites/45/media/29281\\_ESTIA\\_Study\\_English\\_ver\\_3\\_0.pdf?1426675541](http://static.wm3.se/sites/45/media/29281_ESTIA_Study_English_ver_3_0.pdf?1426675541)
- Public Health England (2015) *Heatwave plan for England*. London.
- Publications Office (2010) *Directive 2010/31/EU of the European parliament and of the council of 19 may 2010 on the energy performance of buildings*. Available from:  
<http://eur-lex.europa.eu/LexUriServ/LexUriServ.do?uri=OJ:L:2010:153:0013:0035:EN:PDF>
- Seguro, F. and Palmer, J. (2016) *Solar Shading Impact Report*. National Energy Foundation.
- Van Den Wymelenberg, K. (2012) Patterns of occupant interaction with window blinds: A literature review, *Energy And Buildings*, 51, pp. 165-176.  
DOI:10.1016/j.enbuild.2012.05.008.
- World Health Organization (1990) *Indoor environment: Health aspects of air quality, thermal environment, light and noise*. Available from:  
<http://apps.who.int/iris/handle/10665/62723> [Accessed 21 December 2016].
- Wouter, W., Dolmans, D., Dutoo, G., Hall, A., Seppänen, O. and Beck, W. (2010) *Solar shading: How to integrate solar shading in sustainable buildings Guidebook No 12*. Brussels, Belgium: REHVA, Federation of European Heating and Air-conditioning Associations.
- Zero Carbon Hub (2015) *Overheating In Homes - The Big Picture*. United Kingdom: Zero Carbon Hub. Available from:  
<http://www.zerocarbonhub.org/sites/default/files/resources/reports/ZCH-OverheatingInHomes-TheBigPicture-01.1.pdf>

# The flow interaction of air distribution with thermal plumes and the effect on the air velocity fluctuation under increased heat load conditions

Sami Lestinen<sup>\*1</sup>, Simo Kilpeläinen<sup>1</sup>, Risto Kosonen<sup>1</sup>, Juha Jokisalo<sup>1</sup>, and Hannu Koskela<sup>2</sup>

*1 Aalto University, School of Engineering  
Sähkömiehentie 4  
02150 Espoo, Finland*

*2 Turku University of Applied Sciences  
Lemminkäisenkatu 14-18 B  
FI-20520 Turku, Finland*

*\*Corresponding author: sami.lestinen@aalto.fi*

*Presenting author: Sami Lestinen*

## ABSTRACT

Flow interaction between thermal plumes and vertical air distribution and the resulting airflow structures were investigated under increasing heat load conditions. The main objective was to investigate the large-scale flow patterns, airflow fluctuation and frequency of the flow field. The flow interaction between thermal plumes and ventilation provides random flow motion and vortical structures that further effect the airflow characteristics such as velocity and temperature fields, turbulence intensity and frequency of the fluctuations. Fourier analysis was conducted in order to observe the energy levels of air speed records. It represents the frequency distribution from the set of discrete values of the given variable over the time-interval by providing the sinusoidal components of original function with certain frequency. The novelty of this study comes from the Fourier analysis of this flow interaction. The flow interaction was investigated in a test chamber of 5.5 m (l) x 3.8 m (w) x 3.2 m (h). Thermal plumes were produced by using 12 symmetrically installed cylindrical thermal loads of 0.4 m x 1.1 m that gave a thermal load range of 40-80 W/m<sup>2</sup>-floor. Omnidirectional anemometers were installed into a measuring mast at the heights of 0.1 m, 0.6 m, 1.1 m, 1.7 m, 2.3 m and 2.9 m. The highest mean air speed was observed near the floor at the height of 0.1 m and the lowest near the top of thermal loads at the height of 1.1 m. The smallest turbulence intensity in turn was near the floor at the height of 0.1 m, whereas the highest intensity was found at the height of 1.1 m. The draught rate *DR* was below 21 %, and it increased with heat load. The highest draught rate was observed near the floor and the smallest at the height of 1.1 m, similarly than in the mean air speed and conversely than in the turbulence intensity. Overall, the results indicate a clear correlation between the thermal load level and the mean air speed as well as the airflow fluctuation. The observations showed that the mean air speed, the airflow fluctuation and the power spectral density increased with thermal load.

## KEYWORDS

Thermal environment, buoyancy flows, convection flow, airflow structure, flow interaction, Fourier analysis

## 1 INTRODUCTION

Thermal comfort is a condition of mind that express satisfaction with thermal environment as represented in EN ISO Standard 7730:2005 (CEN, 2005) and in ASHRAE Standard 55 (ANSI/ASHRAE, 2013). This means that when a person feels thermally neutral or cooler, the increased local heat loss due to higher velocity may cause a local discomfort because of a sensation of draught. Furthermore, the risk of draught increases when the airflow temperature decreases and the mean velocity and the turbulence intensity increase. In an earlier study, Kovanen et al. (1987) found that the energy spectrum is proportional to the mean velocity such that the energy increases with mean velocity. Fanger et al. (1988) proposed that the turbulence

intensity has a significant effect on the sensation of draught. In a subsequent study, Melikov et al. (1997) showed that also temperature fluctuation increase draught sensation.

Indoor airflows are typically turbulent. The mean air speed can be usually 0.05-0.6 m/s with the turbulence intensity of 10-70 % and the significant level of fluctuations are mainly up to 1 Hz frequency with variable air speed, fluctuation and flow direction (Melikov et al., 2007). The turbulent flow is unsteady and random flow motion that is related to a wide range of length and time scales (Tennekes and Lumley, 1972; Etheridge & Sandberg, 1996; Pope, 2000). Turbulent kinetic energy is produced from the mean flow into the largest eddies and the energy is then further transferred to the smaller and still smaller eddies until it is dissipated to the heat mainly from the smallest eddies. The turbulence increases the flow disturbances and the interaction between the vorticity and the velocity gradients in the flow. Turbulence also improves the transform of energy but requires continuous supply of energy against the turbulent stresses (Townsend, 1976).

Also the airflow interaction has an effect on flow structures. The physics of flow interaction may come from the advection, viscous and buoyancy forces, together with static pressure differences and turbulence production, which provide random, transient and vortical flow motion, that can further yield a draught discomfort in an occupied zone. The low-frequency fluctuation can then be closely related to the convection, thus advection and viscous forces. Nielsen (2011) represented that depending on  $Ar$ -number, which describes the ratio between the buoyancy and the inertial forces, the airflows can be classified into the momentum driven or the buoyancy driven flows. The earlier studies also indicate that a plume flow is continuously fluctuating (Kofoed & Nielsen, 1988). In a subsequent study, Kosonen et al. (2010) showed that velocity field is greatly affected by the strength of a heat source and its distribution in a room. Furthermore, Zukowska et al. (2012) emphasized that thermal plumes from low-heat sources are very sensitive to the surroundings and the source itself. In addition, Kandzia (2013) studied a transient flow behavior of detailed flow structures under natural and forced convection, and Müller et al. (2013) demonstrated a significance of flow interaction in an indoor environment. Noteworthy is also that the natural convection flows seem to dominate in the highly occupied enclosures, and the buoyancy-driven convection flows may have a higher effect on the flow field than the previous studies have indicated (Kosonen et al., 2016). In any case, the air distribution can be difficult to control in an occupied zone (Melikov, 2016).

Previous studies have indicated that draught is one of the most challenging thermal comfort problem in buildings with high or moderate level of cooling loads. In practice, the complex interaction of jets and thermal plumes makes the analysis of the air distribution and further the local thermal comfort difficult. It should also be noted that the local thermal comfort index of the draught rate ( $DR$ ) is not able to take into account of turbulent frequency and scales. In this study, the main objective is to analyse the air speed fluctuation and turbulence scales with increasing heat load levels in the case that the low-momentum supply airflow rate is released through a diffused ceiling and when the internal heat loads are installed symmetrically in the occupied zone. The novelty of this study comes from detailed information of airflow fluctuation under high thermal load levels between the thermal plumes and vertical air distribution in a varied thermal environment.

## 2 METHODS

### 2.1 Test chamber

The measurements were carried out in a test chamber of 5.5 m (L) x 3.8 m (W) x 3.2 m (H) (Figure 1). The vertical air distribution was introduced by discharging supply air through a diffused ceiling into the occupied zone. The suspended ceiling was 0.35 m below the ceiling envelope. The suspended ceiling was made of perforated glass-wool-plate elements with the open perforation area of 0.5%. The diameter of drilled holes was 14 mm. The duct-diffuser combination with diameter of 0.2 m extended the entire length of upper chamber and produced rather equal supply air distribution, in which the static pressure difference forces the airflow through the suspended ceiling down to the occupied zone.

### 2.2 Experimental set-up

The experimental set-up was conducted by using 12 cylindrical test dummies (Figure 1). The diameter of the heat source was 0.4 m (Zukowska et al., 2012), and the height of the dummy was 1.1 m (Standard EN 14240:2004). The heat sources were placed evenly on the floor (Figure 2). The thermal load was increased gradually such that specific heat load was 40-80 W/m<sup>2</sup>-floor as shown in Table 1. The effect of supply air temperature was investigated by keeping the target temperature at 26°C in the reference location 9 at the height of 1.1 m (Figure 2). The dummy temperature differences were observed by conducting an infrared camera. The flow field was measured using 6 hot-sphere anemometers and visualised with smoke and low-weight ribbons attached to the suspended ceiling. The anemometers were installed into a measuring mast at the height of 0.1 m, 0.6 m, 1.1 m, 1.7 m, 2.3 m and 2.9 m (EN ISO 7726:2001). The three lowest sensors were the Vivo Draught 20T31 omnidirectional anemometers and the three highest sensors were the Sensoanemo 5100SF omnidirectional anemometers. The readings were between 1 s and 2 s, respectively. Hence, the Vivo Draught anemometers reach the 1 Hz frequency at the region between 0.1 m and 1.1 m. The symmetrical set-up offered a smaller investigation region in which the different locations can be classified as follows. The first group was the locations between the cylindrical thermal loads in a longitudinal direction (L), i.e. locations 3, 4, 7, 9. The second group was the locations between four thermal loads, i.e. locations 2, 8, 10. The third group was the locations between two thermal loads in a wide-wise direction (W), i.e. locations 1 and 5. In addition, one location was 20 cm from the wall at the location 6.

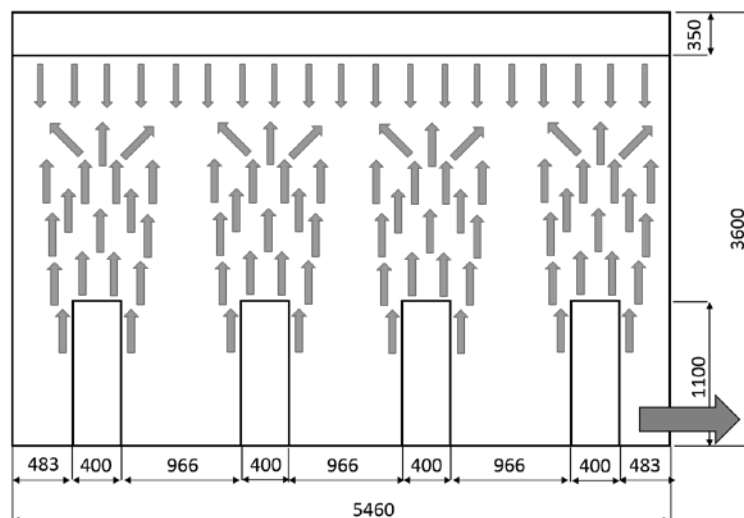


Figure 1: A schematic flow chart (mm) regarding with thermal plumes and vertical air distribution in a simplified thermal environment. The exhaust valve was at the height of 0.4 m (arrow at the right side wall).

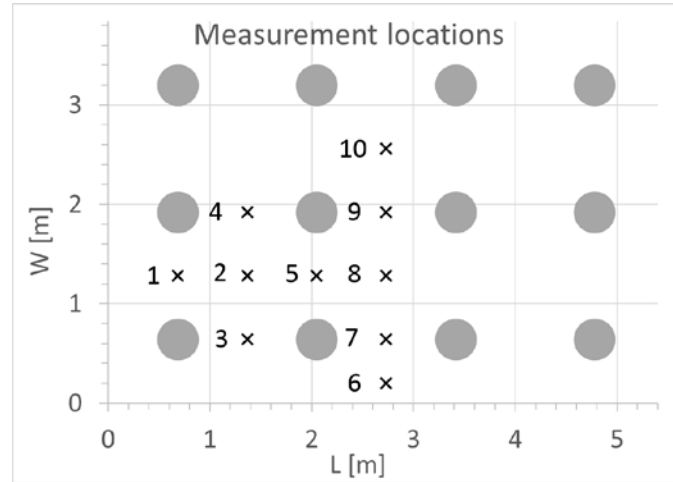


Figure 2: The measurement locations 1-10 and the cylindrical heat sources.

Table 1: The test cases

Test cases	Case 1	Case 2	Case 3	Case 4	Case 5	Case 6	Case 7	Case 8	Case 9
Heat load [ $\text{W}/\text{m}^2$ ]	40	57	80	40	57	80	40	57	80
Supply air [ $\text{l}/\text{s}, \text{m}^2$ ]	3.6	5.2	7.3	2.8	4.2	6.0	4.6	6.8	9.6
Supply air temp [ $^{\circ}\text{C}$ ]	17	17	17	15	15	15	19	19	19
Target temperature	26	26	26	26	26	26	26	26	26

### 2.3 Characterising the flow field

The Reynolds number and the Archimedes number describe the flow conditions and relationships of different forces accelerating the flow. The airflow fluctuation in turn can be investigated by dividing the given variable in a time-averaged component and in a fluctuating component as

$$\phi(x_i, t) = \bar{\phi}(x_i) + \phi'(x_i, t) \quad (1)$$

where  $\phi$  is the variable,  $x$  refers to coordinate system,  $t$  is the time,  $\bar{\phi}$  is the time-averaged component and  $\phi'$  is the fluctuating component, and subscript  $i$  denotes the index notation. The time-averaged component is expressed as

$$\bar{\phi}(x_i) = \lim_{T \rightarrow \infty} \frac{1}{T} \int_0^T \phi(x_i, t) dt \quad (2)$$

where  $T$  is the averaging interval that should be sufficiently large compared to the fluctuating time-scale. Furthermore, the averaging discrete set of records with certain interval  $N$  in a given location  $x_i$  can be expressed by the ensemble average as

$$\bar{\phi}(x_i, t) = \lim_{N \rightarrow \infty} \frac{1}{N} \sum_{n=1}^N \phi(x_i, t) \quad (3)$$

where  $\bar{\phi}(x_i, t)$  is the ensemble-averaged component dependent on both the location and time, and  $N$  is the number of discrete values in the interval that filter more rapid fluctuations. Consequently, the ensemble-averaged component  $\bar{\phi}(x_i, t)$  at Eq. (3) is a sort of moving average of a certain time-interval at the location  $x_i$ , whereas the time-averaged

component  $\bar{\phi}(x_i)$  at Eq. (2) is a mean value of a given time-interval at the location  $x_i$ . The deviation of sample can then be calculated by expressing the sample standard deviation as

$$\phi_{SD} = \sqrt{\frac{\sum_N(\phi_N - \bar{\phi})^2}{N-1}} \quad (4)$$

where  $N$  denotes the number of records in a data series. The turbulence intensity can then be defined as

$$Tu = \frac{u_{SD}}{\bar{u}} \times 100 \quad (5)$$

where  $u_{SD}$  is the standard deviation of air speed records and  $\bar{u}$  is the mean air speed at the same location. The draught rate index in turn can be expressed as

$$DR = (34 - t_{a,l})(\bar{u}_{a,l} - 0.05)^{0.62} (0.37 \cdot \bar{u}_{a,l} \cdot Tu + 3.14) \quad (6)$$

where  $t_{a,l}$  is the local air temperature [ $^{\circ}\text{C}$ ],  $\bar{u}_{a,l}$  is the local mean air velocity [m/s] and  $Tu$  is the turbulence intensity [%]. The Fourier transform of airflow fluctuation represents a frequency distribution from the set of discrete values of a given variable over the time-interval by providing the sinusoidal components of original function with certain frequency (Cochran et al., 1967; Welch, 1967). The Fourier transform can be expressed as

$$\hat{\phi}(\omega) = \int_{-\infty}^{\infty} \phi(t) e^{-i\omega t} dt \quad (7)$$

where  $\omega$  is the angular frequency and  $t$  is the time. The angular frequency can be determined as  $\omega = 2\pi f$  and  $f = 1/t$  where  $f$  is the frequency. The outcome of the Fourier transform is the complex-valued function  $\hat{\phi}(\omega)$ . The frequency distribution can then be shown in real number set by taking the absolute value  $|\hat{\phi}(\omega)|$  from the transformed function, which shows the magnitude spectrum. Furthermore, the power spectrum is determined by  $|\hat{\phi}(\omega)|^2$ . It follows after algebra that the discrete Fourier transform can be defined as

$$\hat{\phi}(f)_k = \sum_{j=1}^N \phi(t)_j e^{(-2\pi i(j-1)(k-1)/N)} \quad (8)$$

where  $j$  and  $k$  denotes the indexes and  $N$  is the sample of the discrete data set e.g. the given discrete time-interval set  $T = N\Delta t$ . The power spectral density describes the distribution of power as a function of frequency that provides the normalized power spectrum. The power spectral density is determined as

$$S(\omega) = \frac{1}{N} |\hat{\phi}(\omega)|^2 \quad (9)$$

where the divisor  $N$  normalize the result.

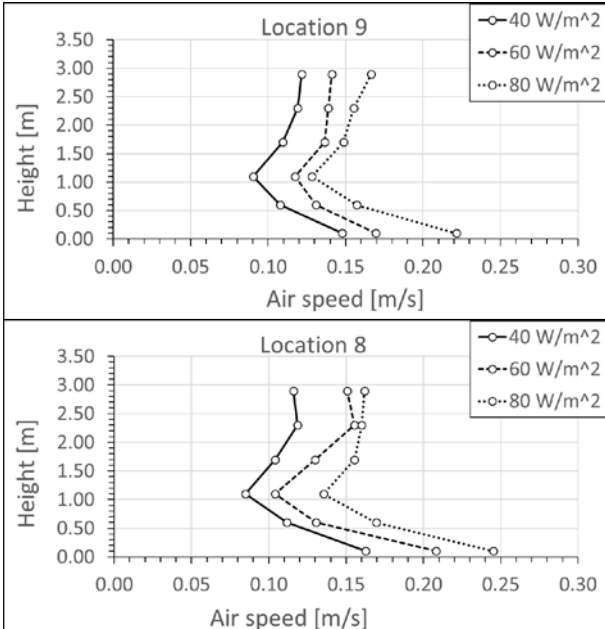
### 3 RESULTS

Thermal load levels in the measurements were produced with several combinations of supply air temperature and supply airflow rates. The given range of supply air temperature provided only 3% deviation on the mean air speed and below 1% on the standard deviation. This small

effect is an outcome from the low-momentum and vertical supply airflow. This means that the effect of air distribution through the diffused ceiling is not significant, and the buoyancy driven convection flows dominated the air distribution in the test conditions. Therefore, the following results include only one combination of supply air temperature and flow rate for each thermal load level (Cases 1-3).

### 3.1 Mean air speed

In the cases 1-3, the mean air speed over the measured locations was generally around 0.15 m/s with the mean standard deviation of 0.045 m/s and with the range of 0.08-0.25 m/s in the region below 1.1 m. At this region, the mean air speed over the measured locations increased around 47 % between the 40 W/m<sup>2</sup> and the 80 W/m<sup>2</sup>. In this case, the range was slightly increased indicating more deviation in the flow field. On the contrary, the mean air speed was reduced about 40 % between the heights of 0.1 m and 1.1 m. The range was slightly decreased towards the top of the heat sources at 1.1 m, i.e. towards the lower air speed levels. Figure 3 shows the mean air speed against the room height at the given locations. Local differences exist but generally, the function characteristics are rather similar such that the mean air speed decrease from 0.1 m up to 1.1 m and increase with thermal load.



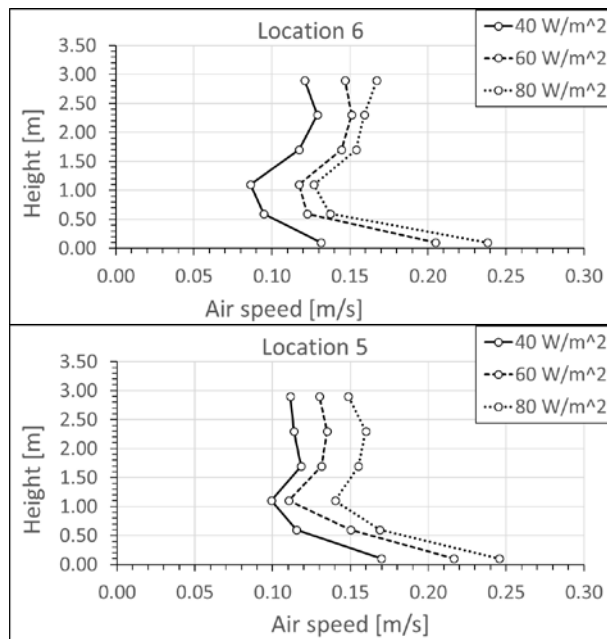


Figure 3: The mean air speed at the locations 5, 6, 8, 9 with the heat loads of 40 – 80 W/m<sup>2</sup>, supply air 17°C, room target temperature below 26°C.

### 3.2 Airflow fluctuation

Figure 4 shows the mean air speed and the standard deviation at the height of 1.1 m in the location 8. The ensemble-averaged function over 60 s interval represents the filtered sinusoidal deviation of the data without faster fluctuation. The slow fluctuation may have a periodical deviation that occur as sinusoidal behaviour while proceeding the time axis further. The mean air speed was 0.085 m/s with the standard deviation of 0.051 m/s under the lowest thermal load of 40 W/m<sup>2</sup>. The mean air speed increased 60 % up to 0.135 m/s towards the highest thermal load 80 W/m<sup>2</sup>. The corresponding standard deviation increased 50 % up to 0.076 m/s, respectively. The increase of standard deviation describes the growing fluctuation that may have a significant effect on the sense of draught and thermal comfort by increasing the heat transfer between the human subject and surroundings. The ensemble-averaged functions seem to have a certain periodicity between the local extrema and the additional information can be produced by conducting the Fourier analysis.

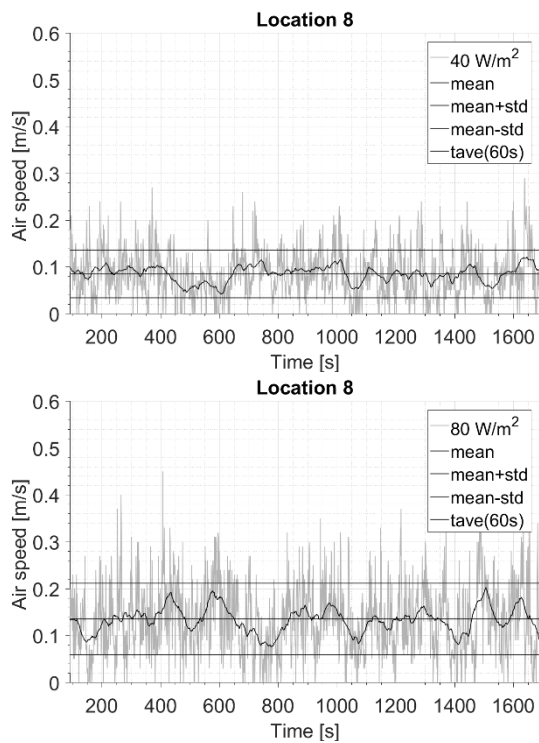


Figure 4: The air speed fluctuation, the mean air speed, the standard deviation and the ensemble time-averaged air speed over 60 s interval with the thermal loads of  $40 \text{ W/m}^2$  and  $80 \text{ W/m}^2$ . Location 8 at the height of 1.1 m, case 1-3.

The turbulence intensity was rather constant regardless of the thermal load level. It seems that the mean velocity level had a bigger effect on the turbulence intensity than the prevailing thermal load level. Consequently, the smallest turbulence intensity was around 40 % near the floor at the height of 0.1 m, and the greatest intensity was about 60 % near the top of the thermal loads at the height of 1.1 m. This is mainly because the turbulence intensity increases towards the smaller mean velocity. The draught rate  $DR$  was below 21 % in the measured locations, and it increased with heat load. Furthermore, the highest draught rate was observed near the floor and the smallest at the height of 1.1 m. It seems that the European Standard EN ISO 7730:2005 (CEN, 2005) classifies this thermal environment mainly into the category B ( $DR$  10-20 %) with the prevailing mean air speed, the air temperature and the turbulence intensity conditions.

### 3.3 Power spectral density

The mean power spectral density over the measured locations was about  $3.9\text{E}-3 \text{ m}^2/\text{s}^2$  with the standard deviation of  $9\text{E}-4 \text{ m}^2/\text{s}^2$  under the thermal load level of  $40 \text{ W/m}^2$  in the considered region below the height of 1.1 m. The corresponding energy level with  $80 \text{ W/m}^2$  was  $6.8\text{E}-3 \text{ m}^2/\text{s}^2$  with the standard deviation of  $1.4\text{E}-3 \text{ m}^2/\text{s}^2$ . Consequently, the mean energy level was 74 % greater with  $80 \text{ W/m}^2$  than with  $40 \text{ W/m}^2$ . This means that the fluctuation generally increased with thermal load. In addition, the standard deviation between the measured locations increased 54 %, which indicates also higher fluctuation in the flow field. The corresponding mean power spectral density was about  $6.1\text{E}-3 \text{ m}^2/\text{s}^2$  with the standard deviation of  $1.4\text{E}-3 \text{ m}^2/\text{s}^2$  at the height of 0.1 m and  $4.5\text{E}-3 \text{ m}^2/\text{s}^2$  with the standard deviation of  $1.4\text{E}-3 \text{ m}^2/\text{s}^2$  at the height of 1.1 m. Consequently, the mean power spectral density decreased 27 % up to the height of 1.1 m. Hence, it seems that the mean power spectral density decreases towards lower mean air speed levels. The standard deviation was almost the same level at both heights. Furthermore, the mean power was non-linearly

dependent on the thermal load level and any specific frequencies were not recognized in the power spectral density function. However, the ensemble-averaged functions were higher with higher thermal loads (Figure 5, left). This means that the fluctuation energy was greater. However, the normalized function (Etheridge & Sandberg, 1996), that is the ratio of the power spectral density over the variance, was at the same level with varying thermal loads (Figure 5, right). In contrast, this also indicates increasing fluctuation with thermal load due to change in variation. Furthermore, the power spectral density decreased relatively gradually towards increasing frequency. The significant energy differences were recognized in the neighboring frequencies and their multiplications while proceeding the frequency axis. The results are summarised in Table 2 and Table 3 where the mean air speeds and power spectral densities are shown with three heat loads levels and at different heights.

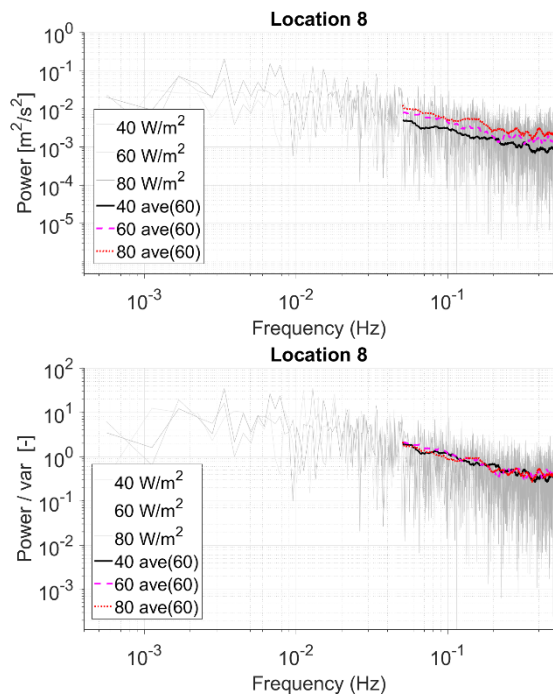


Figure 5: Airflow fluctuation with the different thermal loads: The power spectral density on the left and the normalised function on the right, log-log scales, at height 1.1 m, case 1-3.

Table 2: The statistics of the mean air speed of horizontal plane including locations 1-10 at the certain room height, reading interval 1 s, Cases 1-3.

Mean air speed	0.1 m	0.6 m	1.1 m	0.1 m	0.6 m	1.1 m	0.1 m	0.6 m	1.1 m
Heat load [ $W/m^2$ ]	40	40	40	57	57	57	80	80	80
average	0.16	0.11	0.09	0.20	0.14	0.12	0.23	0.16	0.14
min	0.13	0.09	0.08	0.17	0.12	0.10	0.20	0.13	0.12
max	0.18	0.12	0.11	0.22	0.16	0.16	0.25	0.18	0.18
std	0.017	0.008	0.010	0.020	0.014	0.017	0.015	0.015	0.019
std/range	0.33	0.31	0.36	0.36	0.32	0.30	0.31	0.32	0.32

Table 3: The statistics of the mean power spectral density of horizontal plane including locations 1-10 at the certain room height, reading interval 1 s, Cases 1-3.

Power spectral density	0.1 m	0.6 m	1.1 m	0.1 m	0.6 m	1.1 m	0.1 m	0.6 m	1.1 m
Heat load	40	40	40	57	57	57	80	80	80
average	4.7E-03	3.8E-03	3.2E-03	6.0E-03	5.3E-03	4.5E-03	7.6E-03	6.9E-03	5.7E-03
min	3.7E-03	3.2E-03	2.6E-03	5.4E-03	3.9E-03	3.4E-03	5.9E-03	5.0E-03	4.3E-03
max	5.8E-03	5.1E-03	4.6E-03	6.9E-03	7.6E-03	6.7E-03	1.0E-02	9.1E-03	8.4E-03

std	6.8E-04	6.0E-04	6.8E-04	5.3E-04	1.0E-03	9.3E-04	1.1E-03	1.0E-03	1.3E-03
std/range	3.3E-01	3.2E-01	3.3E-01	3.5E-01	2.7E-01	2.8E-01	2.7E-01	2.5E-01	3.3E-01

## 4 CONCLUSIONS

The mean air speed, the standard deviation and the maximum air speed mainly increased with thermal load. Consequently, also the power of discrete Fourier transform increased. Furthermore, the mean air speed increased 47% from the thermal load level of 40 W/m<sup>2</sup> up to 80 W/m<sup>2</sup>, and reduced 40 % from the height of 0.1 m up to 1.1 m. The mean turbulence intensity was at the same level regardless of the thermal load level. The smallest turbulence intensity was around 40 % at the height of 0.1 m and the greatest intensity was about 57 % at the height of 1.1 m. Therefore, it seems that the current mean air speed level had a greater effect on the turbulence intensity than the prevailing thermal load level. The draught rate (*DR*) was generally below 21 %. The mean power spectral density increased 74 % from the thermal load level of 40 W/m<sup>2</sup> up to 80 W/m<sup>2</sup>. This means that the air speed fluctuation increased towards higher thermal load level. In contrast, the mean power spectral density decreased 27 % from the height of 0.1 m up to 1.1 m in which the mean air speed was lowest. This in turn indicates that the air speed fluctuation decrease with mean air speed. However, the turbulence intensity usually increase towards decreasing mean air speed, thus the significance of fluctuation can be greater in the low velocity regions. Overall, both the mean air speed and the airflow fluctuation increased with thermal load mainly because the internal energy increased locally in the test chamber.

## 5 ACKNOWLEDGEMENTS

The authors wish to acknowledge L.V.Y. foundation, K. V. Lindholms foundation, Finnish Foundation for Technology Promotion (TES) and Sisäilmäyhdistysry (SIY/FiSIAQ) for financial support.

## 6 REFERENCES

- ANSI/ASHRAE (2013). Standard 55-2013 – Thermal Environmental Conditions for Human Occupancy. Ashrae Inc, Atlanta, USA, ISSN 1041-2336.
- CEN (2001). European Standard EN ISO 7726:2001, Ergonomics of the thermal environment. Instruments for measuring physical quantities (ISO 7726:1998).
- CEN (2005). European Standard EN ISO 7730:2005, Ergonomics of the thermal environment — Analytical determination and interpretation of thermal comfort using calculation of the PMV and PPD indices and local thermal comfort criteria. European Standard EN ISO 7730:2005(E), 3rd edition, 2005-11-15, Geneva, Switzerland.
- Cochran, W. T., Cooley, J. W., Favon, D. L., Helms, H. D., Kaenel, R. A., Lang, W. W., ... & Welch, P. D. (1967). What is the fast Fourier transform?. *Proceedings of the IEEE*, 55(10), 1664-1674.
- Etheridge, D., & Sandberg, M. (1996). *Building ventilation: theory and measurement*. Chichester, UK, John Wiley & Sons, ISBN 0-471-96087-X.

- Kandzia, C. (2013). Experimentelle Untersuchung der Strömungsstrukturen in einer Mischlüftung. E. ON Energy Research Center, RWTH Aachen University.
- Kofoed, P., & Nielsen, P. V. (1988). Thermal Plumes in Ventilated Rooms: an experimental research work. Dept. of Building Technology and Structural Engineering, Aalborg University.
- Kosonen R, Lastovets N, Mustakallio P, Carrilho da Graça G, Mateus NM, Rosenqvist M. (2016). The effect of typical buoyant flow elements and heat load combinations on room air temperature profile with displacement ventilation, *Building and Environment*, doi: 10.1016/j.buildenv.2016.08.037.
- Kosonen, R., Saarinen, P., Koskela, H., & Hole, A. (2010). Impact of heat load location and strength on air flow pattern with a passive chilled beam system. *Energy and Buildings*, 42(1), 34-42.
- Kovanen, K., Majanen, A., & Sirén, K. (1987). Huoneilman virtausnopeuden, nopeuden vaihtelutaajuuksien ja turbulenssiasteen kartoitustutkimus. Teknillinen Korkeakoulu, LVI-tekniikan laboratorio, Raportti B17, Espoo, Finland (In Finnish).
- Melikov, A. K. (2016). Advanced air distribution: Improving health and comfort while reducing energy use. *Indoor air*, 26(1), 112-124.
- Melikov, A.K., Hanzawa, H., Fanger, P.O., 1988, Airflow characteristics in the occupied zone of heated spaces without mechanical ventilation. *ASHRAE Transactions*, Vol. 94, Part 1, pp.52-70.
- Melikov, A. K., Krüger, U., Zhou, G., Madsen, T. L., & Langkilde, G. (1997). Air temperature fluctuations in rooms. *Building and Environment*, 32(2), 101-114.
- Melikov, A. K., Popiolek, Z., Silva, M. C. G., Care, I., & Sefker, T. (2007). Accuracy limitations for low-velocity measurements and draft assessment in rooms. *HVAC&R Research*, 13(6), 971-986.)
- Müller, D., Kandzia, C., Kosonen, R., Melikov, A. K., & Nielsen, P. V. (2013). *Mixing Ventilation. Guide on mixing air distribution design*. Federation of European Heating and Air-Conditioning Associations, REHVA, ISBN 978-2-930521-11-4.
- Nielsen, P. V. (2011). The " Family Tree" of Air Distribution Systems. In *Roomvent 2011*. TAPIR Akademisk Forlag. ISBN 978-82-519-2812-0.
- Pope S. B. (2000). *Turbulent flows*, Cornell University, Cambridge University Press, ISBN 0-521-59886-9.
- Tennekes H. and Lumley J. L. (1972). *A First Course in Turbulence*, The MIT Press, ISBN 0 262 20019 8.
- Townsend A. A. (1976). *The Structure of Turbulent Shear Flow*, 2nd edition, Cambridge University Press, ISBN 0 521 29819 9.

Welch, P. (1967). The use of fast Fourier transform for the estimation of power spectra: a method based on time averaging over short, modified periodograms. *IEEE Transactions on audio and electroacoustics*, 15(2), 70-73.

Zukowska, D., Melikov, A., & Popiolek, Z. (2012). Impact of personal factors and furniture arrangement on the thermal plume above a sitting occupant. *Building and Environment*, 49, 104-116.

# Determining the venting efficiency of simple chimneys for buoyant plumes

Henry C. Burridge<sup>\*1</sup>, Gagan Sehmbi<sup>2</sup>, Daniel Fiuza Dosil<sup>3</sup>,  
and Graham O. Hughes<sup>4</sup>

*1 Imperial College London,  
Department of Civil and Environmental Engineering,  
Skempton Building,  
South Kensington Campus,  
London, SW7 2AZ.*

*\*Corresponding author: [h.burridge@imperial.ac.uk](mailto:h.burridge@imperial.ac.uk)*

*2 Imperial College London,  
Department of Civil and Environmental Engineering,  
Skempton Building,  
South Kensington Campus,  
London, SW7 2AZ.*

*3 Imperial College London,  
Department of Civil and Environmental Engineering,  
Skempton Building,  
South Kensington Campus,  
London, SW7 2AZ.*

*Presenting author: [d.fiuza-dosil17@imperial.ac.uk](mailto:d.fiuza-dosil17@imperial.ac.uk)*

*4 Imperial College London,  
Department of Civil and Environmental Engineering,  
Skempton Building,  
South Kensington Campus,  
London, SW7 2AZ.*

## ABSTRACT

We present preliminary results from an examination of the capture and venting of a buoyant plume by a chimney. The aim is to enable improved management of indoor pollutant sources – for instance, the plume rising from a cooking pan in a kitchen or a cooking fire in a hut. Using the principle of dynamic similarity, we precisely and controllably model the behaviour of indoor plumes by using saline solutions ejected into an enclosure containing freshwater. These well-established laboratory analogue techniques enable the location and concentration of tracer in the plume to be easily tracked, reflecting the evolution of pollutants carried in the plume. Focusing on a plume within a room containing a quiescent ambient environment, we identify two physical mechanisms potentially responsible for driving the removal of pollutants. The first, we describe as the *capture* of the plume, a process driven by the direct interaction between the plume and the evacuation opening; the second, we describe as the *draining* flow driven by a buoyant layer of fluid which may accumulate at the ceiling and is then evacuated through the effects of buoyancy. We first demonstrate that the addition of a simple cylindrical chimney that hangs downwards from an opening in the (analogue) ceiling increases the venting efficiency of these potentially polluting plumes. We go on to examine how the capture efficiency of these simple chimneys varies as the relative size of the plume and the chimney are altered, and demonstrate that simple model can provide predictions of the observed variation in capture efficiency.

## KEYWORDS

Cooking smoke plumes, Indoor air quality, Ventilating cooking fumes.

## 1 INTRODUCTION

Indoor air pollution is a serious public health concern affecting the lives of many people in developing regions around the world; especially so, when the degradation of indoor air quality results from combustion for cooking and heating. In India, for example, cooking frequently takes place indoors on inefficient ovens or open fires that burn solid fuels typically comprised of wood, coal, crop residue and cow dung (WHO 2014). When burned, these materials produce dangerous pollutants that are inhaled by those indoors, particularly those doing the cooking – frequently women accompanied by their youngest and most vulnerable children.

Regular exposure to the pollutants from this indoor combustion increases serious health problems such as the risk of young children contracting pneumonia, chronic obstructive pulmonary disease, and further increases the risk of lung cancer and strokes. Issues related to indoor air quality are estimated to lead to 1.7 million premature deaths per annum in South East Asia alone, therefore constituting a major health concern in the developing world (WHO 2014). The pollutants from indoor combustion are carried within plumes of warm smoky air, herein cooking plumes, which rise and develop within the room or hut. We report results from a preliminary investigation of a method to encourage the more efficient evacuation of these cooking plumes.

In more developed regions of the world, cooking on open fires indoors is atypical and any indoor combustion occurs using relatively clean fuels and burners. However, the act of cooking produces odours and particulates that may not only be undesirable but also significantly degrade indoor air quality. The results reported herein have potential application to the cooking plumes rising above pots, pans or burners in more modern kitchens.

In rural parts of the developing world, cooking is frequently carried out relatively centrally within a room or hut and the cooking plume is ultimately evacuated through an opening made by removing a small portion of the ceiling and roof. However, as these cooking plumes rise their mass (or volume) flux increases rapidly due to the entrainment of the room's ambient air and so whilst a portion of the cooking plume may be directly evacuated through the opening in the ceiling there is also potential for a portion of the cooking plume to accumulate at the ceiling forming a layer of warm smoky air within the room – chronic exposure to which is extremely detrimental to human health. We investigate the effectiveness of enhancing the evacuation of these cooking plumes, with a view to reducing the layer of warm smoky air within the room, by the introduction of a thin-walled cylindrical chimney.

For simplicity, we consider cases in which the act of cooking is the only heat source and the effects due to any external wind, or draughts within the room/hut, are negligible. It has long been established that in such cases, the dynamics of buoyant (herein cooking) plumes are self-similar and may be predicted by considerations of the conservation of the fluxes of mass, momentum and buoyancy; with the assumption that the (horizontal) entrainment of ambient fluid at the plume edge occurs at a velocity which is related to the local vertical velocity in the plume by a constant entrainment coefficient,  $\alpha$  (Morton *et al.*, 1956). Utilising this 'plume theory' and the principles of dynamic similarity we create experimental analogues of these cooking plumes and carry out a laboratory study of saline plume in freshwater environments.

The momentum flux (due to the work done by the buoyancy flux) associated with the cooking plume as it reaches the ceiling can be utilised to drive an evacuating flow directly through the opening in the ceiling, a process that we describe as the *momentum capture*. We consider cases where the centre of the plume source is aligned with the centre of the opening, such that the portion of the plume that might be directly captured through this process might be predicted. In the practical example under consideration, illustrated in figure 1a, any portion of the flux of pollutants produced by cooking (the buoyancy flux of the cooking plume) that is not directly evacuated by momentum capture then accumulates at the ceiling, forming a warm upper layer of smoky air within the room – the buoyancy of this warm layer acts to drive a *draining* flow and further contribute to the evacuation of the polluting smoke from the room. In our analogue laboratory experiments, we introduce a chimney, consisting of a thin-walled cylindrical perspex tube, open to flow at both ends that 'hangs' within the space representing the room. The chimney is temporarily fixed to the laboratory analogue of the room's ceiling. We carry out experiments to demonstrate that the polluting cooking plume can be more

effectively evacuated by the addition of a chimney within the room. We develop experiment procedures to measure and the capture efficiency of a chimney in a given set-up and describe these methods in Section 2.

In order to establish an experimental set-up that allows for both the momentum capture and draining of the plume we first introduce a *holed chimney* which had a number of holes drilled in its side walls at a height just within the ceiling of the room. That is, the momentum flux of the plume at the entrance to the holed chimney (closest to the plume source) enabled the buoyancy flux (representing the flux of cooking pollutants) to be ‘captured’, whilst any buoyant fluid accumulating at the (laboratory analogue of the) ceiling could be ‘drained’ through the holes drilled in the chimney side-walls. We discuss the results for these cases in Section 3.1. We then focus on the process of ‘capture’ by the chimney by eliminating the draining process by using a *simple chimney*. We show that a simple model is able to predict the capture efficiency of simple chimneys in Section 3.2. Finally we draw conclusions, discuss their implications and highlight future directions for the research in Section 4.

## 2 EXPERIMENTS AND METHODS

Exploiting the principles of dynamic similarity, we create laboratory analogues of the cooking plumes, of interest to this study, by ejecting saline solution downwards within a clear Perspex visualisation tank. We ensure that density differences between the saline plume and its freshwater environment were relatively small, akin to those arising due to the temperature difference between a cooking plume and the ambient air within a room. Hence, the dynamics were Boussinesq and the physics notionally identical for a cooking plume rising within a room and a dense saline plume falling within a freshwater environment.

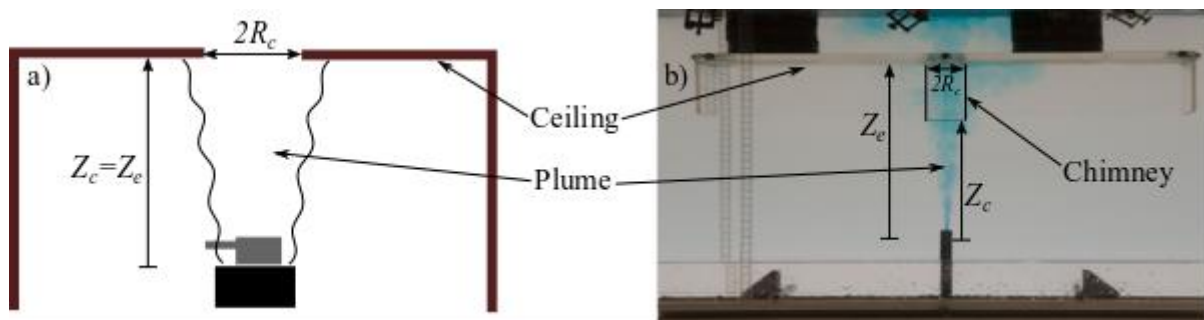


Figure 1: a) Illustration of a cooking plume rising in a room/hut and being evacuated through an opening in the ceiling; b) Experimental image of a saline plume (inverted for ease of comparison) being evacuated through a simple chimney.

To enable visualisation, and ultimately determine the effectiveness of adding a chimney, the saline plume was stained using methylene blue as a dye. The experimental set-up was backlit using a sheet of white perspex to diffuse the light from four halogen spotlights and images were recorded using a Nikon digital SLR camera. Figure 1 shows an illustration of a cooking plume being evacuated from a room or hut, and an experimental image (inverted for ease of comparison) of a saline plume with a simple chimney added. Dyed saline solution (of known density, measured using an Anton Paar densitometer) was pumped (using an Ismatec gear pump) through a circular plume nozzle of radius  $r_0 = 0.25\text{cm}$ . The flow rate was set such that the ratio of inertia to buoyancy attained the invariant ‘pure plume’ balance (Morton *et al.*, 1956) close to source. As such, all vertical distances are measured from a ‘virtual origin’ located a distance  $5 r_0 / (6\alpha)$  behind the source, with  $\alpha = 0.11$  taken throughout as appropriate for a top-hat plume (see Section 2.1).

Following the methods and procedures detailed by Allgayer & Hunt (2012) we used the light attenuation technique, whereby the integral dye concentration along light paths received by the camera sensor can be inferred from the amount of light attenuated by the dye (relative to an image taken in the absence of any dye). Attaching four Perspex walls to the experimental ‘ceiling’ formed a tray in which the dyed saline, that was not directly evacuated, was able to accumulate. By summing the inferred integral dye concentration over light paths representing the viewing area of the tray the total mass of dye in the tray could be estimated and from our calibration data we were able to relate these to estimates of the total buoyancy accumulated within the tray, which denote  $B$ . From this, we could then define the capture efficiency as

$$CE = 1 - \frac{B}{F_0 T}, \quad (1)$$

where  $F_0$  is the plume buoyancy flux (prescribed at the source and physically conserved throughout the plume) and  $T$  denotes the time since the experiment commenced.

It is important to note that throughout, including in equation (1), we make no account for the draining process whereby fluid that accumulates at the ceiling is able to be evacuated due to the action of buoyancy. In Section 3.1, we do report results from a deliberately limited set of experiments in which the draining process is feasible - results that are only included to illustrate the effectiveness of adding a chimney to the application considered herein (figure 1a). Moreover, for the results reported in Section 3.1 the capture efficiency is calculated only for time periods over which the additional evacuation due to the draining process (which requires a meaningful accumulation of buoyant fluid at the ceiling) might be expected to be negligible – we show, in section 3.2, that this is the case for the experiments with the holed chimney.

One would expect that the capture efficiency might vary depending on a number of factors; not least, with the given capture area (determined by the radius,  $R_c$ , of the chimney or the opening in the ceiling) relative to that of the plume. The characteristic radial scale of a plume is known to increase linearly with the distance from the source, such that their (time-averaged) flow envelope forms an expanding cone. Given that the dynamics of plumes are self-similar, one can investigate the effects of the relative size of the chimney simply by using a single chimney, in our case of diameter  $2R_c = 3.4\text{cm}$ , and then varying, for example, the vertical separation between the virtual source and the chimney opening,  $Z_c$  (see figure 1). We denote the height of the chimney  $L$  and examine single chimney of aspect ratio  $L/2R_c = 2.35$ . We denote the vertical distance between the virtual source and the ceiling  $Z_e$ . We choose to express distances from the virtual source in terms of a characteristic radial scale for the plume, defined  $R_T(Z) = (6\alpha/5) Z$ , in so doing we are able to compare the physical scale of the plume (dependent only on the distance from the virtual source) to that of the chimney.

## 2.1 Two models for estimating the capture efficiency

Using plume theory, one can derive simple estimates for the portion of the buoyancy flux in an axisymmetric plume that might pass through a circle, of radius  $R_c$ , positioned a vertical distance  $Z$  from the virtual source. Herein, we consider two simple models, one assuming that the distribution of velocity and buoyancy within the plume follows a uniform distribution – the top-hat plume model; the other assuming that the distribution of velocity and buoyancy within the plume follows a Gaussian distribution – the Gaussian plume model. One can then examine predictions for a top-hat capture efficiency, defined as

$$CE_T = \frac{2\pi \int_0^{R_c} r w_T b_T dr}{F_0}, \quad (2)$$

where  $r$  is the radial coordinate,  $F_0$  is the plume buoyancy flux,  $w_T$  and  $b_T$  are the velocity and buoyancy in the plume assuming top-hat distribution – full analytic expressions for which are presented by Morton *et al.*, (1956). In addition we examine predictions for a Gaussian capture efficiency, which we define as

$$CE_G = \frac{2\pi \int_0^{R_c} r w_G b_G dr}{F_0}, \quad (3)$$

where  $w_G$  and  $b_G$  are the velocity and buoyancy in the plume assuming a Gaussian distribution – full analytic expressions for which are presented by (Baines & Turner, 1969).

### 3 RESULTS

#### 3.1 Demonstrating the effectiveness of adding a chimney

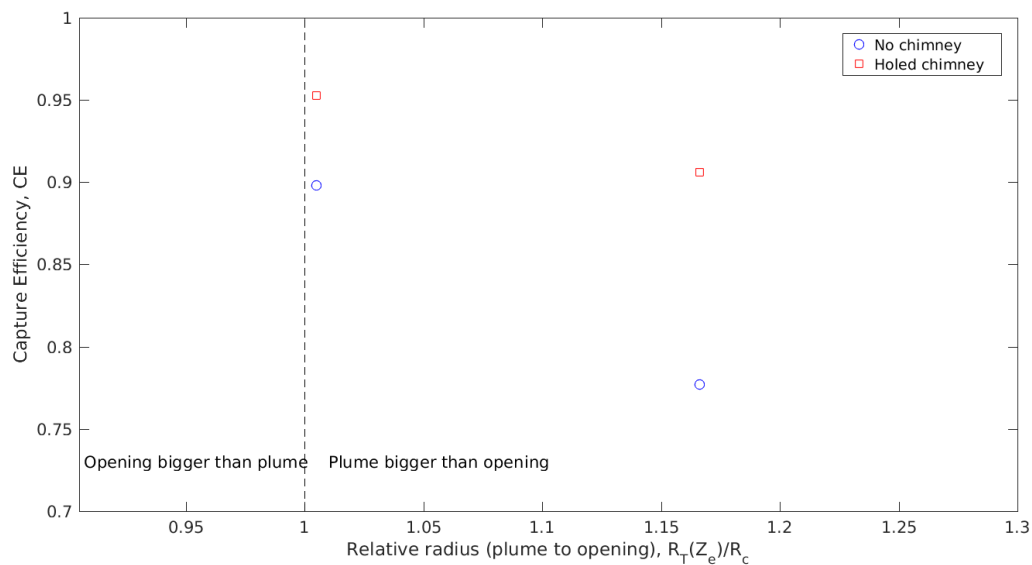


Figure 2: The capture efficiency for two different relative sizes of the chimney and plume. Data is presented without a chimney, typical in current application, and with the addition of a chimney which markedly increases the capture.

To compare situations to those currently found in practice (figure 1a), we ran two experiments in the absence of a chimney and varied the distance between plume source and the ceiling in each – this mimics the effect of changing the radius of the opening in the ceiling. With the radius of the opening approximately equal to the top-hat radius of the plume our data showed around 90% of the buoyancy flux was evacuated by momentum capture. This capture dropped to less than 80% when the radius of the opening was just 15% smaller than the top-hat radius of the plume (figure 2). Crucially, in both cases, figure 2 shows that keeping the distance between the source and the ceiling fixed, and then adding the holed chimney markedly increased the momentum capture of the plume. For our examples, the addition of the chimney approximately halved the buoyancy flux that would accumulate at the ceiling, indicating the potential exposures to any pollutants carried by the plume may be drastically reduced by the addition of a chimney. We note that for these preliminary experiments we tried to minimise the effects due to the draining of buoyant fluid at the ceiling; figure 3 shows that the effects of draining were negligible for the experiments with the holed chimney.

### 3.2 The variation of the capture efficiency with the relative chimney radius

In order to examine the capture efficiency of a chimney we carried out experiments using a simple chimney for which all fluid not directly captured remained within an impermeable tray. We systematically varied the distance between the source and the entrance to the chimney, mimicking the effect of varying the radius of chimney. Chimneys of radius approximately 30% larger than the plume top-hat radius ( $R_T/R_c \sim 0.7$ ) were found to capture almost the entire buoyancy flux of the plume. As one might expect, the capture efficiency decreases as the relative size of the chimney decreases. Crucially, figure 3 shows that predictions of the capture efficiency from the Gaussian model agree relatively well with the experimental data, suggesting that perhaps this simple model can be used to predict the evacuation of a plume by the process of momentum capture.

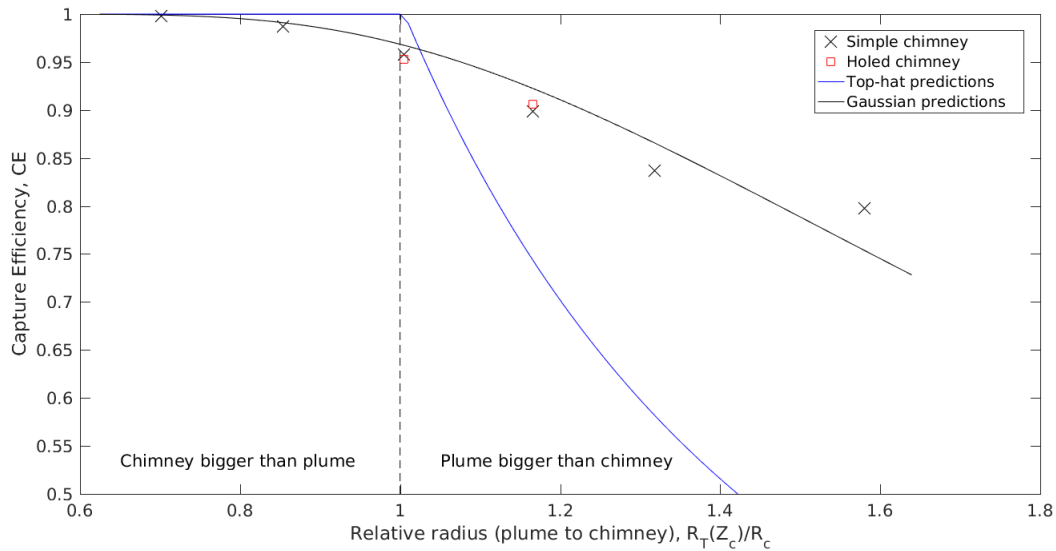


Figure 3: The variation in capture efficiency for different relative sizes of the chimney and plume. Our experimental data is marked at discrete locations and the theoretical predictions of the two models, (2) and (3), are overlaid.

## 4 CONCLUSIONS

The addition of a basic chimney hanging from an opening within a ceiling has been demonstrated to increase the direct capture of buoyant plumes. This suggests that an affordable chimney, which could be simply formed from sheet metal and hung downwards from the opening in the ceiling, offers the potential to reduce exposure to the polluting smoke from cooking and/or heating within rural homes in the developing world. Our experiments further show that the portion of plume fluid evacuated by the mechanism of momentum capture can be simply predicted with a satisfactory degree of accuracy. In so doing, we provide a first step towards being able to reliably predict the exposures to pollutants due to combustion in rural homes both in the absence and presence of a chimney hanging downwards into the room.

That said, we do not underestimate the scale of the work that remains in order to make meaningful predictions in the cases of real application. Thus far, we have not examined the effects of the evacuation due to the buoyancy driven draining of any layer of warm fluid at the ceiling. Moreover, we have not examined the effects that varying the length of the chimney might have, for example potentially reducing the capture due to viscous effects in the presence of the chimney, or enhancing the capture due to the stack effect of the buoyancy. Finally, all of the above neglects the effects of external winds and the resulting internal draughts that are likely to play a significant role in these relatively permeable rural buildings. However, we regard this as a fruitful and rewarding avenue on which to continue future research.

## 5 REFERENCES

Allgayer, D. & Hunt, G. (2012), ‘On the application of the light-attenuation technique as a tool for non-intrusive buoyancy measurements’, *Experimental Thermal and Fluid Science*, 38, 257–261.

Baines, W. & Turner, J. (1969), ‘Turbulent buoyant convection from a source in a confined region’, *Journal of Fluid mechanics*, 37(01), 51–80.

Morton, B. R., Taylor, G. & Turner, J. S. (1956), ‘Turbulent gravitational convection from maintained and instantaneous sources’, *Proceedings of the Royal Society A: Mathematical, Physical and Engineering Sciences*, 234(1196), 1–23.

WHO (2014), ‘World Health Organisation — clean household energy can save people’s lives’, <http://www.who.int/features/2014/clean-household-energy/en/>.

# A comparison of line-sources of buoyancy placed near and far from a wall

David Parker\*<sup>1</sup>, Henry Burridge<sup>2</sup>, Jamie Partridge<sup>1</sup> and Paul Linden<sup>1</sup>

*1 Department of Applied Mathematics and Theoretical Physics, University of Cambridge, Centre for Mathematical Sciences Wilberforce Road, Cambridge CB3 0WA, UK*

*2 Department of Civil Engineering and Environmental Engineering, Imperial College London, London, SW7 2AZ, UK*

*\*Corresponding author: dap58@cam.ac.uk*

## ABSTRACT

Experiments are presented on turbulent buoyant free-line and wall plumes, whereby the buoyancy source is emitted from a horizontal line source, in one case free of the presence of a wall and in the other placed immediately adjacent to a wall. The dynamics of turbulent entrainment, whereby ambient fluid is mixed in to the plume, are explored. The velocity field and scalar edge of the plumes are measured. From this the time-averaged plume-width and volume flux are compared. The spreading rate, and therefore the entrainment, of the wall plume is found to be half that of the free-line plume, indicating that the wall has a significant effect on the entrainment process. Further, the volume flux of the wall plume is found to be half that of the free-line plume, indicating that larger maximum scalar concentrations are present in the wall plume. The effect that the reduced entrainment rate has on a typical heated room, via a line source of buoyancy, is demonstrated by comparing a numerical model of the developing temperature stratification within a sealed enclosure in the case of the line source near a wall and away from a wall, where in particular it is found that higher maximum temperatures are present for the case of the line source near a wall.

## KEYWORDS

Turbulent Convection, Plumes, Ventilation

## INTRODUCTION

Flows driven by line sources of buoyancy often appear within buildings, for example in the case of heating, from radiators, or cooling, from chilled beams. The process of turbulent entrainment in these flows is key to understanding how they evolve and how one might model them. It has been observed that the entrainment is reduced when a line source of buoyancy is positioned immediately adjacent to a wall (Sangras et al. (2000), Grella & Faeth (1975)) and reduced further when the source is vertically distributed along a wall (Cooper & Hunt (2010), McChonnochie & Kerr (2015)). Partly due to the lack of understanding of this effect there remain unanswered fundamental questions regarding the thermal stratification that results from distributed sources placed on the wall within both sealed and ventilated spaces. In order to isolate the effect a wall has on the entrainment process it is instructive to compare two buoyancy driven flows that differ only by the presence of a wall. In our case, this is done comparing line plumes, in the absence of any boundary, and wall plumes, when the line source is adjacent to a vertical boundary. These flows are the obvious choice for this type of study since a vertically distributed buoyancy source without the presence of a wall is not easily achieved.

The study of line plumes has received more recent attention than wall plumes, in particular the work of Paillat & Kaminski (2014) which we outline briefly in the following section. In §2 we introduce the theory and present a review of previous work on free-line and wall plumes. In §3 velocity field and scalar edge data of free-line plumes and wall plumes are presented. The data are compared between the two flows and implications for entrainment are considered. In particular, it is shown how the reduced entrainment due to the wall will affect the developing stratification within a sealed room.

## THEORY AND PREVIOUS WORK

A free-line plume is created from a continuous source of buoyancy released from a horizontal line. A wall plume is created from a continuous source of buoyancy released from a horizontal line which is placed immediately adjacent to an adiabatic wall. Figure 1 shows a simplified diagram of a time-averaged free-line and wall plume.

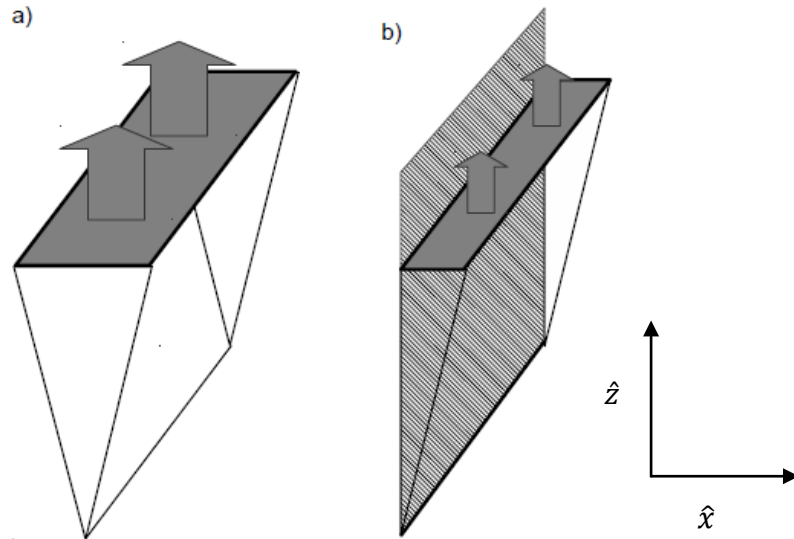


Figure 1: Time-averaged diagram of a free-line plume and a b) wall plume within an environment of constant density.

The fluxes of volume,  $Q$ , momentum,  $M$ , and buoyancy,  $F$ , in the plume per unit width for a free-line plume may be written as follows

$$Q = \int_{-\infty}^{\infty} w dx, \quad M = \int_{-\infty}^{\infty} w dx, \quad F = \int_{-\infty}^{\infty} g \frac{\rho - \rho_a}{\rho_a} w dx, \quad \# (1)$$

where  $\rho(z)$  and  $\rho_a(z)$  are the density of the plume and ambient respectively. For a wall plume they may be written

$$Q = \int_0^{\infty} w dx, \quad M = \int_0^{\infty} w dx, \quad F = \int_0^{\infty} g \frac{\rho - \rho_a}{\rho_a} w dx, \quad \# (2)$$

For a free-line plume the conservation of volume, momentum and buoyancy flux may be written as follows, (Paillat & Kaminski 2014)

$$\frac{dQ}{dz} = 2\alpha_f \frac{M}{Q}, \quad \frac{dM}{dz} = \int_{-\infty}^{\infty} g \frac{\rho - \rho_a}{\rho_a} dx, \quad \frac{dF}{dz} = 0, \quad \# (3)$$

where  $\alpha_f$  is the entrainment coefficient for the free-line plume and for a wall plume the equivalent expressions may be written

$$\frac{dQ}{dz} = \alpha_w \frac{M}{Q}, \quad \frac{dM}{dz} = \int_0^\infty g \frac{\rho - \rho_a}{\rho_a} dx - \epsilon, \quad \frac{dF}{dz} = 0, \quad \#(4)$$

Where  $\alpha_w$  is the entrainment coefficient for the wall plume and  $\epsilon$  is the wall shear stress. Grella & Faeth (1975) find that the wall shear stress is not large compared to the buoyancy force, so we will assume it is negligible in our study. It should be noted, however, that the shear stress does not enter the volume flux balance and so does not affect one of the main purposes of the study, to determine the entrainment coefficient.

We note that in the formulations of (3) and (4) there is no assumption on the shape of the velocity and buoyancy profiles, so it is useful to consider the plume equations in this form since the velocity and buoyancy profiles of the two flows will naturally be different. Self-similarity is found in all studies that measure the velocity and buoyancy profiles in both the free-line and wall plume. In particular, Grella & Faeth (1975) define

$$\frac{\bar{w}}{\bar{w}_m} = W\left(\frac{x}{x - z_o}\right), \quad \frac{\bar{g}}{\bar{g}_m} = G'\left(\frac{x}{x - z_o}\right), \quad \#(5)$$

where  $g' = g \frac{\rho - \rho_a}{\rho_a}$ ,  $W$  and  $G'$  are universal functions far from the source,  $z_o$  is the virtual origin and the overline indicates time-averaged data. For the free-line plume the functions are approximated very well by a Gaussian. The wall plume profiles are more complex due to the lack of symmetry. By assuming power law solutions for  $Q$ ,  $M$  and  $F$  the relations  $dQ^2/dz = 2\alpha$  and  $dQ^2/dz = \alpha$  may be derived for the free-line and wall plume, respectively (Paillat & Kaminski 2014).

By assuming the velocity and buoyancy profiles are Gaussian, Paillat & Kaminski (2014) provide a theoretical framework of entrainment in free-line plumes and determine an expression for the entrainment value depending only on the ratio of the widths of buoyancy and velocity profiles and the self-similar Reynolds stress profile. This is compared to an experimentally determined entrainment coefficient,  $\alpha_g$ , based on the Gaussian width of the time-averaged plume,  $b_w$ , and is defined by  $db_w/dz = 2\alpha_g$  which may be related to  $\alpha$  by  $\alpha = \sqrt{2\pi}\alpha_g$  assuming the Gaussian profiles. Good agreement is found between the experimentally determined  $\alpha_g$  and the model. Ramaprian & Chandrasekhara (1989) focus instead on the entrainment relation  $\alpha_m = \frac{1}{w_m} dQ/dz$ , which makes no assumption of a Gaussian profile but, if imposed, the relation  $\alpha = \sqrt{2}\alpha_m$  may be derived. Most studies on wall plumes also focus on  $\alpha_m$ , although in some cases  $\alpha$  was also calculated. Since the velocity profile of the wall plume is not a known analytic function, a theoretical relation between  $\alpha_m$  and  $\alpha$  has not been derived, however, Grella & Faeth (1975) find that  $\alpha/\alpha_m = 1.43 \approx 2$ . Details of the experiments in previous studies for both free-line and wall plumes are shown in table 1.

Table 1: Experimental data of previous studies of free-line and wall plume. [1] Sangras et al. (2000), [2] Lai & Faeth (1987), [3] Grella & Faeth (1975), [4] Ramaprian & Chandrasekhara (1989), [5] Paillat & Kaminski (2014). \* It is not clear how the average velocity in the plume was calculated for this study and it may differ from the other studies where  $M/Q$  is used. \*\*Explicit  $\alpha$  was not calculated but the relation  $\alpha = \sqrt{2\pi}\alpha_g$  has been used. A dash is placed where data were not made available.

	[1]	[2]	[3]	[4]	[5]
Plume Type	Wall	Wall	Wall	Free	Free
Experiment	Helium and air	CO2 and air	Heated air	Heated water	Ethanol and water
$\alpha_m$	0.068	0.071*	0.067	0.11	-

$\alpha$	-	0.17	0.095	0.158	0.165**
----------	---	------	-------	-------	---------

For the wall plume data presented in the table, the buoyancy flux is that associated with an equivalent free-line plume so that a direct comparison between velocities may be made. From table 1 the studies on wall plumes agree that the entrainment coefficient,  $\alpha_m$ , has a value of  $0.069 \pm 0.02$ . It is also clear that the studies of free-line plumes agree relatively well on the entrainment coefficient,  $\alpha$ , with a value  $\alpha = 0.16$ . It should be noted that Lai & Faeth (1987) calculate the average velocity,  $\bar{w}_a$ , used in the calculation of  $\alpha$ , by the relation

$$\bar{w}_a = \frac{1}{\delta} \int_0^{\delta} \bar{w} dx \quad \#(6)$$

where  $\delta$  is some boundary layer thickness, which is not defined. Therefore, it is not clear, especially given the relatively high value, whether their calculation is equivalent to the top-hat velocity  $M/Q$  used in the other studies. Given that the two flows will have different velocity profiles it seems natural to compare the entrainment rates using the bulk flow properties and not the maximum velocity, i.e. a comparison of  $\alpha$  and not  $\alpha_m$ . It is therefore unfortunate that for the wall plume case less attention has been given to this entrainment coefficient and there is not good consensus about the value. As well as the studies presented in table 1 there have been four other notable previous studies on free-line plumes for which data is presented in Van Den Bremer & Hunt (2014) and entrainment coefficients reported are in the range  $\alpha = [0.14, 0.23]$ . A broad finding among the studies of Grella & Faeth (1975), Lai & Faeth (1987) and Sangras et al. (2000) is an entrainment coefficient, based on the maximum vertical velocity, in the wall plume approximately half that of the free-line case. They largely attribute this reduction in the entrainment coefficient to the wall preventing mixing by inhibiting the meandering motion of the plume centreline which reduces the length scale of the large-scale structures. However, little more is said about the large-scale dynamics beyond this. Given that, at least for an axisymmetric plume, where it is thought that the large-scale structures, in the form of eddies, forming at the edge of the plume are necessary for turbulent entrainment it would be illuminating to study, in more detail, the effect of the wall on these large-scale structures.

## EXPERIMENTS

To study the difference in turbulent entrainment between free-line and wall plume experiments were designed to generate the two flows. The experiments were performed in a tank of horizontal cross-section 100 cm x 80 cm filled with dilute saline solution (of uniform density  $\rho_a$ ) to a depth of 80 cm. Relatively dense source fluid, Sodium Nitrate solution, was supplied to a line source nozzle of width  $b = 0.1$  cm for the free-line plume and  $b = 0.05$  cm for the wall plume and length 15 cm in both cases. The use of Sodium Nitrate allowed for a refractive index match between the ambient and source fluid. This was necessary so that position of the PIV particles were not distorted by refractive index changes. The flow was enclosed by two walls perpendicular to the source, separated by the length of the source, of dimension 60 cm x 60 cm to promote the two dimensionality of the flow. PIV was performed with seeded particles of diameter 50  $\mu\text{m}$ . Videos of the experiments were recorded at a frame rate of 50 Hz with 8000 frames for each individual experiment. Details of the experimental parameters are given in table 2. For both the free-line and wall plume case the data was checked for self-similarity by the independence of maximum vertical velocity with height. Velocity profiles for distances greater than 150b from the source were used and found

to be self-similar, in agreement with Paillat & Kaminski (2014). However, we found that a larger distance than 150b was required, which is not surprising given our smaller source Reynolds number. Sangra et al. (2000) suggest a distance greater than 92b for wall plumes, however they have a significantly higher source Reynolds number because they are using Helium and air for the experiment. It is well established that wall plumes require a greater source distance than for free-line plumes to reach self-similarity, so given our Reynolds number is the same order as Paillat & Kaminski (2014) we expect a distance greater than 150b. For the free-line plume data presented from our study no attempt was made to create a pure plume,  $Ri_0 \approx .14$  (Paillat & Kaminski 2014), at the source. Paillat & Kaminski (2014) and Ramaprian & Chandrasekhara (1989) used only a relatively forced plume,  $Ri_0 = 0.005 - 0.07$ , but using buoyancy field measurements it was found that the plume adjusts to a pure plume in the region of self-similarity. An independent set of experiments were also performed where fluorescein was added to the source fluid for the wall plume and free-line plume. This was purely done to perform analysis on the statistics of the position of the scalar edge of the plume and no attempt was made to infer any buoyancy field data from the images. Test conditions for these experiments were the same, to within experimental uncertainty, as the PIV experiments 1 for the free-line plume and wall plume shown in table 2, therefore we can be confident the plumes are self-similar.

## RESULTS

A virtual origin,  $z_o$ , was first determined for each set of data by assuming a linear growth rate of the plume width and where our measurements imply  $R(z_o) = 0$ , where  $R$  is defined for each flow by (7). Using this correction self-similarity was found in both cases by the scalings in equations (5) for the vertical and horizontal velocities, figure 2 c). In order to directly compare velocity profiles, we non-dimensionalise data for both flows using the physical buoyancy flux,  $F$ , of that associated with wall plume. Profile shapes of the free-line plume agree well with Paillat & Kaminski (2014) and those of the wall plume case agree well with Sangra et al. (2000). Integration of the velocity profiles shows that for a given buoyancy flux,  $F$ , the volume flux,  $Q$ , of a wall plume is half that of a free-line plume. This is a consequence of the wall preventing mixing of the wall plume. From the definition of  $F$  it is clear that if the volume flux is reduced, for the same buoyancy flux, then the wall plume must have higher scalar concentrations within the plume. The effect this will have on the stratification of an enclosed room is shown in the next section.

To aid comparison between the flows we define the plume half-widths as

$$\bar{R} = \begin{cases} \frac{1}{2} \frac{\bar{Q}^2}{\bar{M}} & \text{for the free - line plume,} \\ \frac{\bar{Q}^2}{\bar{M}} & \text{for the wall plume.} \end{cases} \quad \#(7)$$

These may be interpreted as the top-hat plume half-width for the free-line plume and the total width of the flow for the wall plume. The plume widths for all the experiments are shown in figure 3. The data for each flow broadly fit a linear growth rate where, as expected, a lower growth rate is observed in the wall plume. The entrainment coefficients were calculated using this data and were found to be  $\alpha = 0.08 \pm 0.01$  for the wall plume and  $\alpha = 0.15 \pm 0.01$  for the free-line plume. This broadly matches with previous experiments, table 1. The maximum wall plume velocities are on average greater than for the free-line plume by 5%. This is due

to the increased buoyancy close to the wall which is unable to be mixed as effectively as the free-line case (Sangras et al. 2000). Two typical images of the plumes, taken from the experiments where fluorescein was added to the plume fluid, are shown in figure 2. The typical meandering motion of the free-line plume, 2 b), is visible. There are very large regions of ambient fluid between pockets of plume fluid, which can be seen at the top of the image.

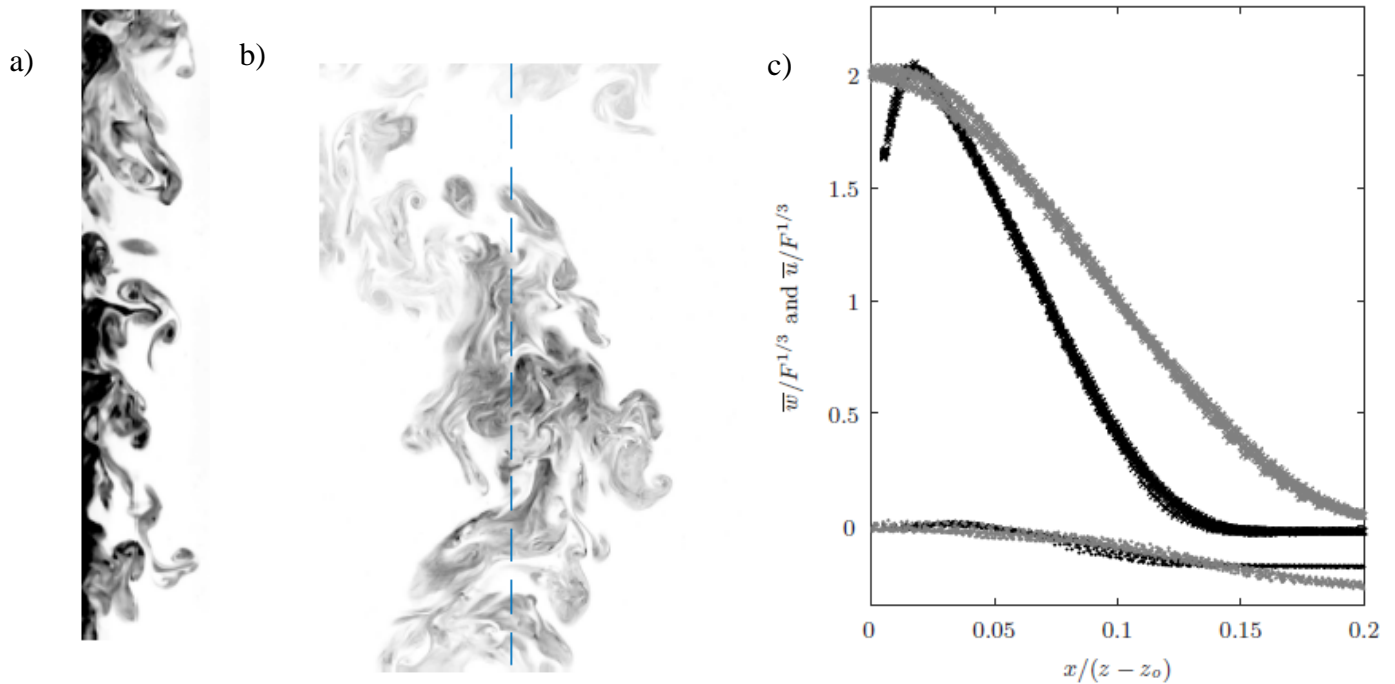


Figure 2: A snapshot of the experiment for a) a wall plume and b) free-line plume. The blue dashed line indicates the position of the source. c) Vertical, crosses, and horizontal, dots, velocity data for free-line, grey, and wall plume, black. Data from experiments 1 are used in both cases and 20 heights are plotted spanning the whole height. For the wall plume case the velocities are scaled using double the physical buoyancy flux in order to make a direct comparison of the velocities.

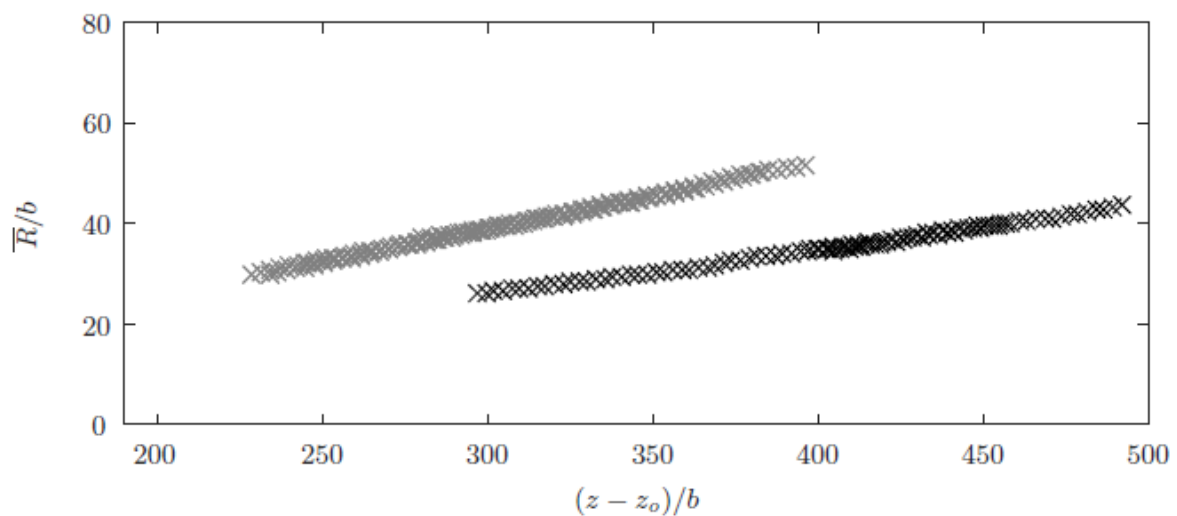


Figure 3: Mean plume widths as defined in (7) for free-line plumes, grey, and wall plumes, black. Both the free-line and wall plume data are scaled on the free-line source width,  $b$ .

At times, ambient fluid is completely transported from one side of the plume to the other, a behaviour which is not typically seen in an axisymmetric plume. Meandering of the scalar edge is also seen in the wall plume. Regions of ambient fluid may be found very close to the wall, again between pockets of plume fluid. The time-averaged position of the scalar edges of the plumes were calculated from the experiments where fluorescein was added to the plume. This was done by using a Canny edge-detection algorithm (Canny 1986) on each snapshot and finding the outer edge of plume.

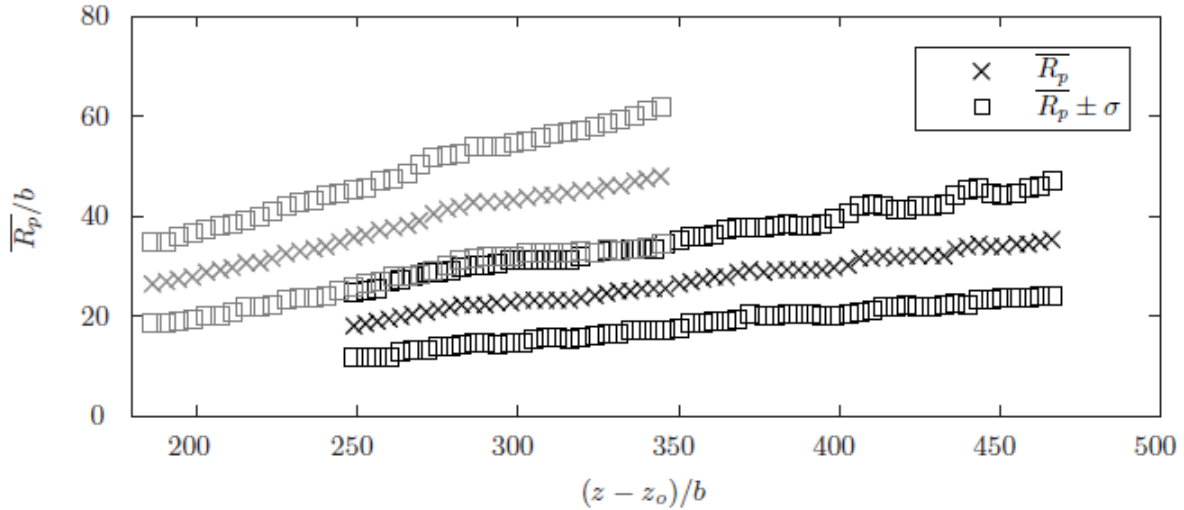


Figure 4: Mean scalar plume widths  $\overline{R_p}$ , crosses, and the variation in scalar plume widths  $R_p \pm \sigma$ , squares, for free-line plumes, grey, and wall plumes, black. Both the free-line and wall plume data are scaled on the free-line source width,  $b$ .

For the free-line plume we define the scalar width,  $R_p$ , as half the distance between the right edge and the left edge of the plume. For the wall plume we define the scalar width as the distance of the outer scalar edge to the wall. The time-averaged position and variation of the plume scalar edge are shown in figure 4. They broadly exhibit linear growth rates with height.

Table 2: Plume experimental data of free line plumes (1F, 2F and 3F) and wall plumes (1W, 2W and 3W)

Parameter	Definition	1F	2F	3F	1W	2W	3W
Buoyancy Flux	$F_0 = Q_0 g'$	13.6	18.1	14.7	10.4	10.4	10.4
Source Richardson number	$Ri_0 = F_0 Q_0^3 / M_0^3$	0.045	0.0097	0.014	0.0206	0.0206	0.0286
Source Reynolds number	$Re_0 = Q_0 / \nu$	67	123	103	50	50	42
Characteristic plume Reynolds number	$\overline{w}_m \overline{R} / \nu$	2900-5200	3080-4650	2900-45900	1470-2070	2000-2350	2000-2500
$\alpha_m$	$\frac{1}{\overline{w}_m} d\overline{Q}/dz$	0.094	0.093	0.090	0.068	0.062	0.063
$\alpha$	$d\overline{R}/dz$	0.156	0.163	0.145	0.087	0.086	0.066
$W_{max}$	$\overline{w}_m / F^{1/3}$	2.04	1.90	2.00	2.05	2.12	2.07

## APPLICATION TO HEATED ROOM

We have shown that the volume flux within a wall plume is significantly reduced and as a consequence, scalar concentrations within the wall plume will be greater than for a free-line plume. We set this in context with a heated room where we compare the developing stratification resulting from a line heat source, with the same heat flux, next to a wall and

away from the wall within a sealed enclosure. We use the model of Baines and Turner (1969) where the plume develops according to the following equations

$$\frac{dQ}{dz} = \alpha \frac{M}{Q}, \quad \frac{dM}{dz} = \frac{FQ}{M}, \quad \frac{dF}{dz} = Q \frac{\partial \Delta_a}{\partial z}, \quad \#(8)$$

where  $\Delta_a = g\beta\Delta T$  is the ambient buoyancy field. Which is assumed to follow an advection model

$$\frac{\partial \Delta_a}{\partial t} = \frac{Q}{L} \frac{\partial \Delta_a}{\partial z}, \quad \#(9)$$

where  $L$  is the width of the room. Initially, it is assumed that the ambient has  $\Delta_a = 0$  everywhere. After each time step, a layer is formed at the top of the enclosure such that the density is given by that in plume at that height. The thickness of the layer is determined by  $Q$  at that height. The layers are advected down according to (9).

We take a typical room of dimension  $H \times L = 4 \times 4m$ , and a heat source of  $100W/m$  with initial temperature  $18^\circ C$ . Figure 5 shows the resulting ambient temperature profiles for different times for both flows. It can be seen that, for a given time, the maximum temperatures for the wall plumes are higher and the falling temperature interface descends at a slower rate. This may be desirable in the case of pollutants that passively trace buoyant fluid. For example, the exit vent may be at the top of the room so as little mixing as possible before the ceiling is reached is desirable. On the other hand, if the sole purpose of the line source is to heat the room then it's more likely a more well-mixed room would be desirable.

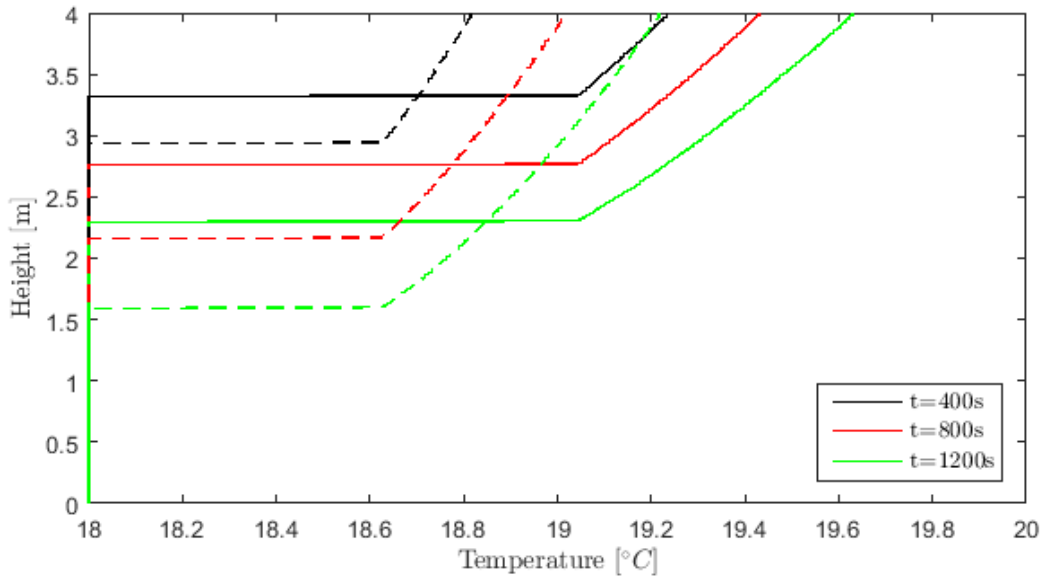


Figure 5: Evolution of the ambient temperature stratification profiles of free-line plume (dashed lines) and wall plumes (solid lines) for times  $t=400s$  (Black),  $t=800s$  (Red) and  $t=1200s$  (Green).

## CONCLUSIONS

In this experimental study of line plumes and wall plumes we have observed the effects that an adiabatic wall has on a line source, which is placed immediately adjacent to it. We have found, in agreement with Sangras et al. (2000) and Grella & Faeth (1975), that the entrainment is significantly reduced and that  $\alpha_f/\alpha_w = 2$ . The velocity profiles of the two flows are presented and compared from which it is found that the spreading rate and volume flux in the wall plume is half that of the free-line plume, for a given buoyancy flux and distance from the source. From this we can conclude that scalar concentrations within the wall

plume are greater than for a line plume, due to the wall preventing mixing with the ambient environment. We show, via a numerical model of a line heat source within an enclosed environment, how the temperature stratification would vary according to whether the line heat source is placed near or far away from a wall. As expected, larger maximum temperatures are found in the case of the heat source near a wall which may or may not be advantageous depending on the application of the source.

## REFERENCES

- Baines, W. D. & Turner, J. S. (1969)*Turbulent buoyant convection from a source in a confined region*. Journal of Fluid Mechanics 37, 51–80.
- Canny, J. (1986)*A computational approach to edge detection*. IEEE Transactions on Pattern Analysis and Machine Intelligence 646, 679–698.
- Cooper, P. & Hunt, G.R. (2010)*The ventilated filling box containing a vertically distributed source of buoyancy*. Journal of Fluid Mechanics 646, 39–58.
- Grella, J. J. & Faeth, G. M. (1975) *Measurements in a two-dimensional thermal plume along a vertical adiabatic wall*. Journal of Fluid Mechanics 71, 701–710.
- Lai, M.-C. & Faeth, G.M. (1987)*Turbulent structures of adiabatic wall plumes*. Journal of Heat Transfer 109 (3), 663–670.
- McConnochie, C.D. & Kerr, R.C. (2015) *The turbulent wall plume from a vertically distributed source of buoyancy*. Journal of Fluid Mechanics 787, 237–253.
- Morton, B. R., Taylor, G. I. & Turner, J. S. (1956)*Turbulent gravitational convection from maintained and instantaneous sources*. Proc. R. Soc. Lond. 234, 1–24.
- Paillat, S. & Kaminski, E. (2014)*Entrainment in plane turbulent pure plumes*. Journal of Fluid Mechanics 755, R2.
- Ramaprian, B. R. & Chandrasekhara, M. S. (1989)*Measurements in Vertical Plane Turbulent Plumes*. Journal of Fluids Engineering 111, 69–77.
- Sangras, R., Dai, Z. & Faeth, G.M. (2000)*Velocity statistics of plane self-preserving buoyant turbulent adiabatic wall plumes*. Journal of Heat Transfer 122 (4), 693–700.
- Van Den Bremer, T. S. & Hunt, G.R. (2014)*Two-dimensional planar plumes and fountains*. Journal of Fluid Mechanics 750, 210–244.

# Effect of human walking on air curtain sealing in the doorway of an airtight building

Narsing K. Jha<sup>\*1</sup>, Daria Frank<sup>1</sup>, L. Darracq<sup>2</sup>, and Paul F. Linden<sup>1</sup>

*1 DAMTP, University of Cambridge  
Wilberforce road  
CB3 0WA, UK*

*2 Mechanical engineering  
Ecole Polytechnique  
France*

*\*Corresponding author: nj299@cam.ac.uk*

## ABSTRACT

Heat and mass flow between cold and warm environments due to the pressure difference between both sides. This exchange causes a loss of energy and human comfort in the buildings. The indoor air quality (IAQ) also reduces because of the passage of dust, odour, insects and bacteria along with the fluid across a doorway. To minimise this heat and mass flux and to maintain IAQ, an air curtain is often used as an artificial separation barrier in public and industrial buildings. Its performance is determined by the sealing effectiveness, defined as the fraction of the exchange flow prevented by the air curtain compared to the open doorway. The controlling parameter for the air curtain is the deflection modulus ( $D_m$ ), which is the ratio of the momentum flux of the air curtain and the transverse forces acting on it due to the stack effect. Although air curtains are used to facilitate the human and the vehicle passage through doorways, the effect of the traffic on the stability and the effectiveness of an air curtain has not yet been studied. In the present study, we conduct laboratory experiments to examine the effect of a person passing through the curtain. The experiments were conducted using fresh water and salt solutions, with dimensions such that they were dynamically similar to the real-scale air curtains installations in the doorways of a building. We find that the effectiveness is decreased by the passage of a person and that the effect increases with the increasing walking speed. We visualised the jet and the wake using dyes of different colours to determine how the air curtain is deflected by the passage of a person.

## KEYWORDS

Air curtain, human passage, effectiveness

## 1 INTRODUCTION

Fluid exchange occurs through open doorways connecting warm and cold environments. It is driven by the stack effect caused by a temperature difference, a wind force or a pressure difference. The fluid transfer also involves the heat and moisture transport, which increases the energy consumption, and also carries substances such as insects, dust, fumes, bacteria, pollutants, which all negatively affect the indoor air quality.

Traditionally, the fluid exchange is reduced using mechanical installations like hinged or sliding doors, vestibules or plastic strip curtains. However, mechanical installations impede the human or vehicle traffic and restrict an easy passage, which can cause problems in the case of an emergency evacuation. Another way to separate the cold and warm environment without affecting the traffic flow is to install an air curtain across the doorway. An air curtain is basically a turbulent jet, which is produced by a fan and is discharged through a nozzle either horizontally or vertically. It can have different design configurations like drawing its primary air supply from either the cold or the warm environment, further being heated or cooled, being discharged at an angle towards the warm or the cold side, or using a recirculation mechanism.

The study of air curtains was started by a patent by *Van Kennel* in 1904 (cf. *Foster 2007*). *Hayes and Stoecker (1969a, b)* first carried out a systematic investigation of air curtains. They developed theoretical models, compared them with the experimental measurements and found the agreement satisfactory. The stability of an air curtain depends on the deflection modulus, which is defined as the ratio of the initial momentum flux and the transverse forces due to the stack effect as shown in equation 1. Here,  $\rho_0$ ,  $T_0$ ,  $b_0$  and  $u_0$  is the density, temperature, width and the velocity of the curtain at nozzle exit, respectively. The height of the doorway is denoted by  $h_b$  and  $g$  is the acceleration due to gravity. The subscripts  $d$  and  $l$  correspond to the properties of dense and light fluid, respectively.

$$D_m = \frac{\rho_0 b_0 u_0^2}{gh_b^2 (\rho_d - \rho_l)}$$

$$= \frac{b_0 u_0^2}{gh_b^2 \left( T_0/T_d - T_0/T_l \right)} \quad (1)$$

$$E = \frac{Q_{open} - Q_a}{Q_{open}} \quad (2)$$

Another important parameter is the effectiveness ( $E$ ), which describes the sealing ability of an air curtain and is defined as the ratio of the volume flow rate stopped by the air curtain and the volume flow rate through an unprotected doorway. This can be expressed as the difference between the volume flow rate through the doorway in the presence of an air curtain ( $Q_a$ ) and the reference value for the open-door situation ( $Q_{open}$ ) when the air curtain is absent, divided by the reference value ( $Q_{open}$ ) as defined in equation 2.

*Guyonnaud et al. (2000)* demonstrated differences between the *Hayes and Stoecker (1969a)* and *Lajos and Preszler (1975)* model. They showed, that knowing the height of the air curtain, jet thickness and jet velocity was not sufficient to completely describe the fluid mechanics of the air curtain. The convection of jet vortices and the height of the impinging zone also affect the effectiveness of the curtain. Later, *Sirén (2003a,b)* presented an overview of possible methods for the technical dimensioning of an upwards blowing air curtain, using momentum balance and moment-of-momentum balance principles.

Full-scale experiments have been carried out for a sealed room with a single opening by *Foster et al. (2006)*, and laboratory scale experiments with multiple openings and with a buoyant curtain have been performed by *Frank & Linden (2014)* and *Frank & Linden (2015)*. There have also been various numerical studies on the performance of air curtains (*Costa, Oliveira & Silva 2006; Foster et al. 2006*) which have shown a good agreement with the experimental data. There have also been some recent studies on the behaviour of air curtains subjected to transversal pressure variations (*Rouaud 2002, Rouaud & Havet 2006*), or when a person is standing in the doorway (*Lu & Fernandez 2008*). However, there remain issues and open questions about the behaviour of an air curtain when a person walks through it, and how this process can affect the air curtain effectiveness. The aim of the present study is to determine how the passage of a person through an air curtain affects its stability and effectiveness.

## 2 EXPERIMENTAL METHODS

Experiments were conducted with water and salt solutions and parameters were chosen such that they were dynamically similar to the real-scale air curtain installations. The kinematic viscosity of water is fifteen times lower as compared to air and thus the length scale can be lowered by a factor of 15 while maintaining the same Reynolds number. Such a substantial reduction in the length scale allowed us to conduct table-top experiments as presented in figure 1.

Experiments were carried out in a Perspex water tank of dimension of 2m X 0.2m X 0.25m. The tank was divided in two equal compartments by a removable vertical gate: one side was filled with fresh water of density  $\rho_l$  and the other side with a salt solution of density  $\rho_d$ . An air curtain device was placed in the fresh waterside of the tank. The water of density  $\rho_0$  was supplied to the curtain from a constant gravity head tank and a valve & a flow meter, which are connected in the supply line, controlled the flow. We used a cylinder pulled at a constant speed by a motor through the air curtain to represent the human walking. The dimensions of the cylinder were chosen such that the process was similar to the real-scale human passage. The speed of the cylinder was varied by a motor controller. For flow visualisations, blue dye was injected in the middle of the air curtain device just below the source. The trajectory of the axis of the cylinder was below this dye injection point. Another red colour dye port was connected at the front stagnation point of the cylinder to visualise the cylinder wake and entrainment. The experimental setup is shown schematically in figure 1.

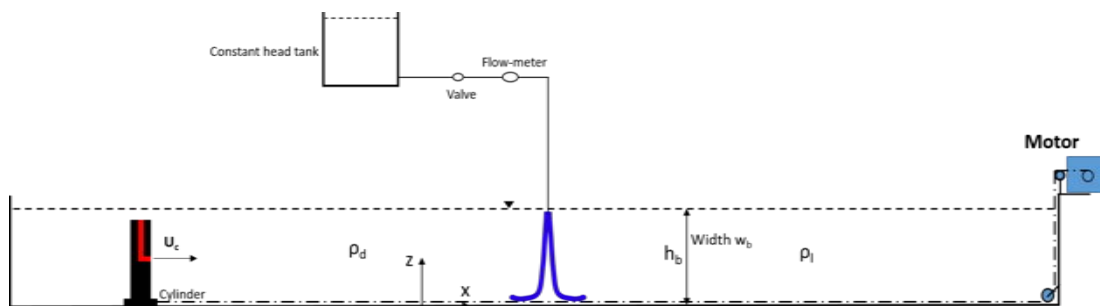


Figure 1: Schematic is showing the gravity current tank with the supply system for the curtain. The cylinder is connected to the motor by a system of pulleys and a flexible thread. The curtain and the cylinder wake are tracked by the blue and red coloured dye, respectively. Supply to the curtain is connected by a valve and a flow meter. Blue coloured jet is separating dense and light environments of density  $\rho_d$  and  $\rho_l$ .

Experiments were started by measuring the densities  $\rho_l$ ,  $\rho_d$  and  $\rho_0$  using the Anton-Paar density meter (DMA 5000) with an accuracy of  $10^{-5}$  g/cm<sup>3</sup>. In the present study, the fluid supplied to the curtain was fresh water, so that  $\rho_0 = \rho_l$ . The flow rate through the curtain was measured using the Omega flow meter (FLR1013) and maintained constant to be about 5 litres per minute (LPM) with an accuracy of  $\pm 3\%$  of full scale. Before the start of the experiment, the water level in the fresh water side with the air curtain device was slightly lower than in the saltwater side. We started the experiment by switching on the flow through the curtain device. Once the flow in the curtain was stabilised and the water level in both sides were equal, we removed the separating gate between the fresh and salt water compartments. Blue and red dye port were opened and the cylinder was dragged at a constant velocity ( $U_c$ ). The separation gate was closed once the cylinder reached the opposite side and the curtain was immediately switched off. Subsequently, we thoroughly mixed the fluid in both sides and measured the new densities in both sides as  $\rho_{l,new}$  and  $\rho_{d,new}$ .

Experiments were carried out for different density differences by changing the density of salt water to vary the deflection modulus ( $D_m$ ). We calculated the entrained volume and the effectiveness from the measured densities. Nikon D3300 was used to capture the colour top and the side-view videos of the experiment at 24 fps. It was used to qualitatively comment on the infiltration, which will help in explaining the observed trend of the effectiveness-deflection modulus curve for different cases.

### 3 RESULTS

In this section, we discuss the effect of the human passage on the effectiveness of an air curtain as shown in figure 2. For the base case without a cylinder, the effectiveness first increases with the deflection modulus ( $D_m$ ) until it reaches a maximum value and then starts to decrease again. The maximum effectiveness is about 0.8, which is similar to the previously observed value by *Frank & Linden (2015)*. At this point, the curtain is stable and reaches the bottom of the tank. With further increase in  $D_m$ , the effectiveness reduces because of the increased mixing in the curtain by the jet entrainment and the impingement.

The cylinder was pulled from the dense fluid to the light fluid side in the present study. As seen in figure 2, the effectiveness of the curtain reduces with the passage of the cylinder and the air curtain becomes progressively less effective for higher cylinder speeds. This reduction in the effectiveness is more prominent at higher deflection modulus values. In the present study, the deflection modulus is varied by changing the density difference while maintaining the same curtain momentum flux. The fluid exchange for the case of a switched-off air curtain device ( $Q_{open}$ ) at higher deflection modulus values is relatively small because of a small density difference. However, the entrained volume by the cylinder ( $Q_{cyl}$ ) is almost constant in all cases as the cylinder velocity is an order of magnitude higher than the gravity current speed. Thus, the influence of the cylinder passage on the effectiveness ( $E_{new} = E_{base} - Q_{cyl}/Q_{open}$ ) increases with the increasing deflection modulus.

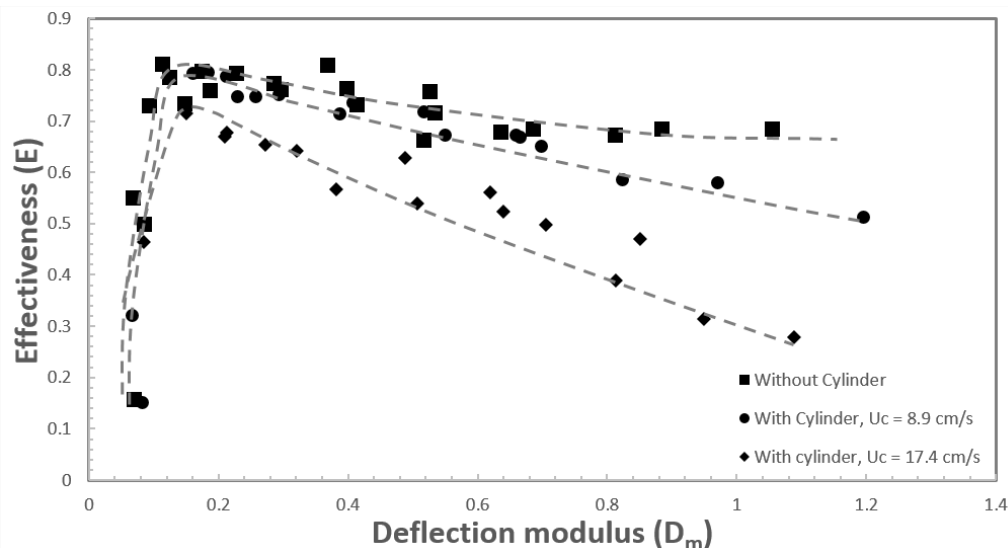


Figure 1: Figure shows the effect of human walking and their speed on the effectiveness of an air curtain. Effectiveness is shown for the cases with and without human/cylinder passage.

At smaller deflection modulus values, the curtain does not reach the bottom of the tank and thus, the cylinder does not have any noticeable effect on the effectiveness. For the deflection modulus values close to  $D_{m,max}$ , the impact of the cylinder passage on the effectiveness is noticeable: the effectiveness is reduced by 10% at the maximum cylinder velocity. As the

deflection modulus increases, the effectiveness further decreases and at  $D_m$  higher than 1, the effectiveness reduces by about 25% compared to the base case for  $U_c=8.9$  cm/s, and by more than 100% for  $U_c=17.4$  cm/s.

Dye visualisations have also been performed to qualitatively study the infiltration by the passage of the cylinder. The blue colour dye was injected at the nozzle exit to track the curtain. In figure 3 (a), the curtain is shown for  $D_m$  of 0.4 when it is undisturbed and the cylinder is far away from the curtain. The jet impinges at the tank bottom and is distributed between both sides of the tank. The cylinder wake and, hence, the entrained dense fluid are visualised using the red dye. The cylinder travels from the dense to the light fluid side as marked by a white arrow in figure 3(b). The interaction can be observed in the figure when the cylinder is just below the curtain. The curtain is blocked by the cylinder passage and the cylinder is followed by a trailing red wake. As the cylinder passes the curtain, the jet is still unestablished and an unhindered fluid exchange between both sides is possible. The fluid flows from the dense fluid to the light fluid side due to the combined effect of the gravity current and the cylinder wake. In figure 3(c), we can see this infiltration while the jet is gradually re-establishing: after the passage of the cylinder, the jet starts to re-establish by penetrating the wake. The jet in the established region starts acting as a separation barrier and thus the available exchange area reduces with time. The time for which the unhindered exchange after the cylinder passage can take place depends on the jet velocity and the opposing force by the cylinder wake and the gravity current. For lower cylinder speeds, the curtain re-establishes faster. The infiltration is lower at lower cylinder speeds because of a lower re-establishment time and a lower infiltration or wake velocity. This is in line with the integral measurement of the effectiveness (figure 2), where the reduction in the effectiveness is lower for a lower cylinder speed. The curtain reaches the bottom of the tank in figure 3d and, as a result, the exchange by the wake is almost stopped.

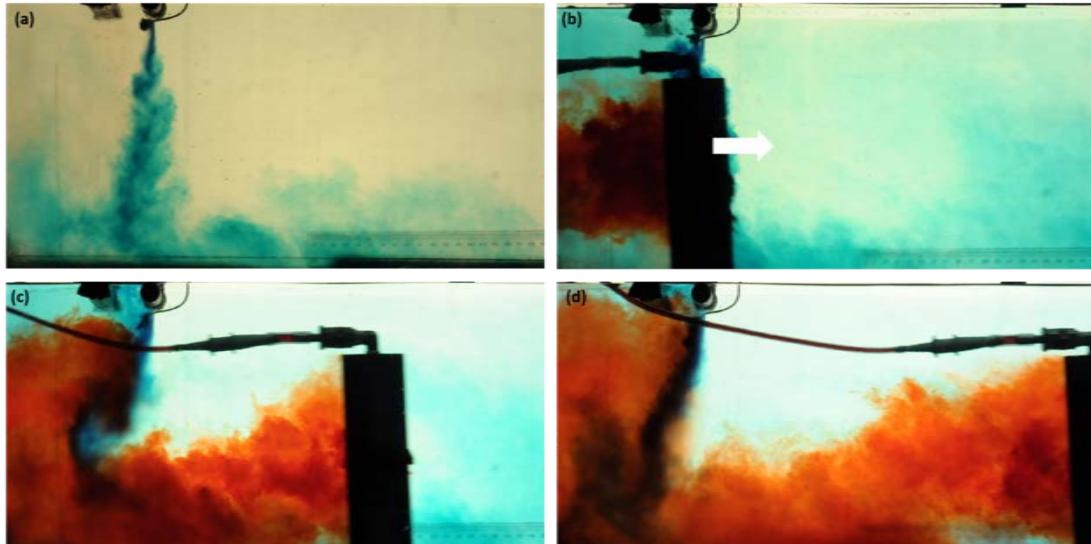


Figure 3: Dye visualisation of the temporal evolution of air curtain and entrainment in human wake is shown from side view. Cylinder is moving from the dense fluid to the light fluid side of the doorways and from left to right in the image as marked in (b). Infiltration across the curtain can be seen in (c).

To gain the three-dimensional perspective of the interaction, we also recorded the top view of the process. In the top view, we see the averaged effect in the vertical direction. In the present study, a classical cylinder wake cannot be expected as the cylinder is not dragged in a quiescent environment. As seen in figure 4, the wake expands radially outwards as it moves

further away from the cylinder. Thus, the exchange width will also increase with time, which will cause increased infiltration along the nozzle length.

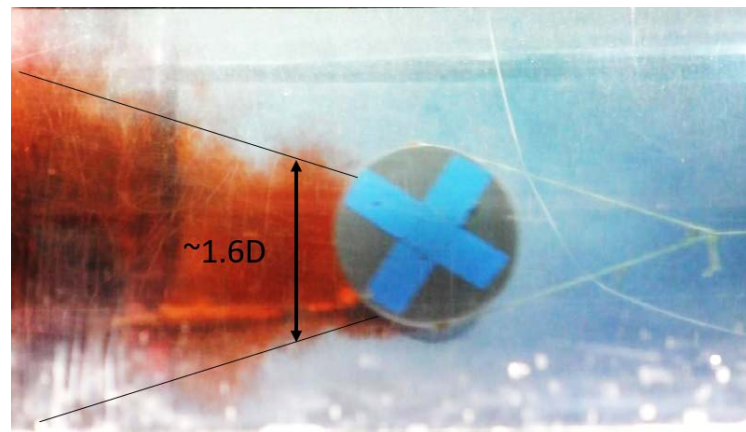


Figure 2: Dye visualisation of the top view of curtain and cylinder wake interaction. Wake expands in radially outward direction away from the cylinder. Image is captured from the bottom and cylinder base is cross marked with blue tape which has 60% larger diameter than cylinder and is 8 mm thick.

#### 4 CONCLUSIONS

We conducted an experimental study to examine the effect of an object passing through an air curtain on its sealing effectiveness. We measured the flow rate through and the density across the doorway with and without the air curtain to calculate the deflection modulus and the effectiveness of the air curtain. We found that the effectiveness is decreased by the passage of a person and that the reduction in effectiveness increases with an increasing walking speed. We visualised the jet and wake using dye to determine how the air curtain is deflected by the passage of a person. Top and side view of dye visualization of jet and wake show that the infiltration of fluid carried in the wake of the person is the reason for the reduction in the curtain effectiveness and that the air curtain takes longer to re-establish at higher walking speeds. The wake width and thus the infiltration in span-wise direction increases with increasing time after the cylinder passage. In the present study, we also observed that the effect is independent of the direction of travel, a result of the relatively fast walking speed compared with the stack-driven exchange flow under normal circumstances. Our study shows that the human or vehicle traffic reduces the effectiveness. To minimize the exchange, we suggest a pause of traffic before the air curtain and then passage across the air curtain with greatly reduced velocity. One other way to reduce the entrainment is to take a 90 degree turn at the entrance. Higher jet velocity reduces the establishment time, which will also help in minimising the entrainment across the curtain.

#### ACKNOWLEDGEMENTS

This research has been supported by the EPSRC and Biddle BV. Lilian Darracq was a summer internship student in the laboratory and received funding from the EPSRC IAA grant. We would like to thank D. Page-Croft for the technical support with the experimental setup.

#### REFERENCES

BROWN, W.G. & SOLVASON, K.R. 1962 Natural convection through rectangular opening in partitions – Part I: vertical openings. *Intl J. Heat Mass Transfer* **5**, 859-868

- COSTA, J.J., OLIVEIRA, L.A. & SILVA, M.C.G. 2006 Energy savings by aerodynamic sealing with a downwards-blowing plane air curtain – a numeric al approach. *Energy build.* **38** 1182-1193
- FOSTER, A.M., SWAIN, M.J., BARRETT, R., D'AGARO, P.D. & JAMES, S.J. 2006 Effectiveness and optimum jet velocity for a plane jet air curtain used to restrict cold room infiltration. *Intl J. Refrig.* **29** 692-699
- FOSTER, A. M., SWAIN, M. J., BARRETT, R., D'AGARO, P. D., KETTERINGHAM, L. P. & JAMES, S. J. 2007 Three-dimensional effects of an air curtain used to restrict cold room infiltration. *Appl. Math. Model.* **31**, 1109–1123.
- FRANK D. & LINDEN, P.F. 2014 The effectiveness of an air curtain in the doorway of a ventilated building *J. Fluid Mech* **756** (2014) 130-164
- FRANK, D. AND LINDEN, P.F., 2015. The effects of an opposing buoyancy force on the performance of an air curtain in the doorway of a building. *Energy and Buildings*, **96**, pp.20-29.
- GUYONNAUD, L., SOLLIEC, C., DE VIREL, M. D. & REY, C. 2000 Design of air curtains used for air confinement in tunnels. *Exp. Fluids* **28**, 377–384.
- HAYES, F.C. & STOECKER, W.F. 1969a Heat transfer characteristics of the air curtain. *Trans. ASHRAE* **75** (2), 153-167
- HAYES, F.C. & STOECKER, W.F. 1969b Design data for air curtains. *Trans. ASHRAE* **75** (2), 168-180
- HUANG, R.F., WU, Y.D., CHEN, H.D., CHEN C.C., CHEN, C.W., & CHANG, C.P., SHIH, T.-S. (2007) Development and evaluation of an air-curtain fume cabinet with considerations of its aerodynamics. *Ann. Occup. Hyg.*, Vol. 51, No. 2, pp. 189–206, 2007
- LAJOS, T. AND PRESZLER, L., 1975. Untersuchung von Türluftschleiranlagen. Heizung, Lüftung, Klimatechnik, Teil, 1(26), pp.171-176.
- LU, F.K. & FERNANDES, J.E. 2008 Visualizing the flow induced by an air curtain over a mannequin using stereo particle image velocimetry. In Proceedings of the 13th *International Symposium on Flow visualization*, 1-4 July 2008, Nice, France.
- ROUAUD, O. 2002 “Etudes numériques et expérimentales de dispositifs de protection contre la contamination aéroportée dans les industries alimentaires” *PhD thesis, Université de Nantes ENITIAA*, Nantes.
- ROUAUD, O. & HAVET, M. 2006 Behaviour of an air curtain subjected to transversal pressure variations. *Journal of Environmental Engineering* **132** (2) 263-270.

# Pollutant loads from materials and assemblies in residential buildings

One obstacle to integrating energy and IAQ strategies for buildings is the lack of reliable method and data for estimating pollutant loads from materials and assemblies in residential buildings in the way heating/cooling loads are routinely estimated. Subtask 2 of IEA EBC Annex 68 focuses on the laboratory measurement of emission of harmful compounds under various temperature, humidity and airflow conditions, since such data under combined exposures generally do not exist today. Formaldehyde, benzene and other harmful volatile organic compounds (VOCs) are of main concern.

## Activities of Subtask 2

First, the Subtask will organize a literature survey and make researcher contacts to gather relevant data and existing knowledge on major pollutant sources and loads in residential buildings, including models. Next, laboratory testing and model setup to provide examples of new types of data, which shall improve knowledge on combined effects that must be taken into consideration in order to achieve new paradigms for energy optimal operation of buildings. It is anticipated that the Subtask will gather data about combined effects describing how temperature and moisture conditions influence the emission and sorption of various pollutants in materials. The experimental tests are ongoing.



Figure 1 the test facilities at Nanjing University, China

## Deliverables from Subtask 2

The Subtask will end with some mechanistic emission source/sink models and IAQ simulation tools for estimating the net loads of pollutions over time under realistic environmental conditions. This will be published in scientific journal articles and in a project report. Furthermore, the Subtask will produce a database of emission and transport properties of materials for use in the models that will be developed and used in the project's Subtask 3. Finally, the Subtask will produce a database of common pollution loads in new and existing buildings.

## Event sponsors

The conference organizers are grateful to the following companies for their support to this event



ISBN : 978-2-930471-51-8  
EAN: 9782930471518